Society of Earth Scientists Series

K.S. Valdiya

The Making of India

Geodynamic Evolution

Second Edition

The Society of Earth Scientists 2008

Springer

Society of Earth Scientists Series

Series editor

Satish C. Tripathi, Lucknow, India

The Society of Earth Scientists Series aims to publish selected conference proceedings, monographs, edited topical books/text books by leading scientists and experts in the field of geophysics, geology, atmospheric and environmental science, meteorology and oceanography as Special Publications of The Society of Earth Scientists. The objective is to highlight recent multidisciplinary scientific research and to strengthen the scientific literature related to Earth Sciences. Quality scientific contributions from all across the Globe are invited for publication under this series.

More information about this series at http://www.springer.com/series/8785

K.S. Valdiya

The Making of India

Geodynamic Evolution

Second Edition

Springer

K.S. Valdiya
Geodynamics Unit
Jawaharlal Nehru Centre for Advanced
Scientific Research (JNCASR)
Bengaluru
India

ISSN 2194-9204 ISSN 2194-9212 (electronic)
Society of Earth Scientists Series
ISBN 978-3-319-25027-4 ISBN 978-3-319-25029-8 (eBook)
DOI 10.1007/978-3-319-25029-8

Library of Congress Control Number: 2015950897

Springer Cham Heidelberg New York Dordrecht London

Printed on acid-free paper

Springer International Publishing AG Switzerland is part of Springer Science+Business Media (www.springer.com)

To My revered teacher
the late Shri Shiva Ballabh Bahuguna
who showed me the path
I have walked on.

Preface from Series Editor

The Indian subcontinent is a coveted destination for geologists owing to its unique geological set-up involving some of the oldest cratonic blocks up to the youngest Quaternary sequences. The oldest cratons—Dharwar, Bastar, Singhbhum and Bundelkhand—represent cratonization process at ~3 Ga and their mosaic forms the Peninsular part of India. The intervening Proterozoic mobile belts and sedimentary basins add another dimension to the varied geology of India. Record of the earliest form of life has been extensively studied. The term "Gondwanaland" has its origin from India. After its break-up, Greater India moved northward rapidly as an island cut-off from rest of the globe supercontinent. The collision and subsequent subsidence of Indian subcontinent with Asia gave rise to the great Himalayan Mountain Ranges—the youngest fold–thrust belt. The vast tract of Indo-Gangetic alluvium as Himalayan foreland basin bears evidence to the voluminous extent of Quaternary fluvial sedimentation. As such, Indian subcontinent offers "food for thought" for geoscientists world over working in different domains.

The book *Making of India: Geodynamic Evolution* by veteran geoscientist and teacher Prof. Valdiya is a wonderful compilation of Indian geology, wherein he has included large number of references including those published but not noticed. The limited published copies of the first edition of the book were sold within a very short span of time, ran out of print and could not meet the demand. Sensing the great demand for the book Prof. Valdiya thoroughly revised and updated the content of the book. When approached, The Society of Earth Scientists immediately accepted to publish it under SES Series with Springer as an International edition for its worldwide circulation. I apologize for delay in bringing this voluminous book to print due to several parallel engagements but hope it will fulfil the need of the students and researchers.

Satish C. Tripathi

Preface to the Second Edition

Within two years of publication of the book *Making of India: Geodynamic Evolution* in 2010, all copies were sold out. Still there was a great demand for the book and I was receiving calls for availability of the book. I felt that my object of distilling substance from stupendous volume of literature published in 65 years after independence, and weaving through the maizes of conflicting contentions of field workers and researchers, and presenting commonly acceptable viewpoints had met with success. So I updated the book, citing additionally more than 350 new works, and corrected mistakes, some inadvertent some my own, related mostly to year of publication of research papers.

The publisher of the first edition of the book M/S Macmillan Publishers India Ltd. discontinued publication of all higher-education text books in science. It took me quite sometime to find a willing publisher—in *The Society of Earth Scientists*. Dynamic and extraordinarily dedicated that he is, Honorary Secretary and Series Editor Dr. Satish C. Tripathi presented me with amazing dispatch a thoroughly reprocessed and altogether reformulated the manuscript.

Hopefully this updated edition will be well received by readers, primarily students, teachers and researchers for whom I have written this book.

I am profoundly grateful to Dr. Satish C. Tripathi, to The Society of earth scientists and to Springer International Publishing Switzerland. But for the crucial and tremendous help of Dr. Kanchan Pande, Professor of Earth Science, Indian Institute of Technology, Mumbai, this edition would not have come out. Dr. Jaishri Sanwal also lent her great help.

K.S. Valdiya

Preface to the First Edition

The seed of the idea of writing a book on the geology and geodynamic evolution of the Indian continent was planted in my mind years ago when Mrs. D.N. Wadia asked me to revise that superb work of D.N. Wadia—*Geology of India*. I had to decline. I wrote back stating that the expansion of geological knowledge has been so vast, and so many advances in our understanding of the geodynamic processes involved in the evolution of the crust had taken place in last few decades that rewriting rather than revision of a book on the geology of India was called for. In 1996, the then President of the Geological Society of India Dr. B.P. Radhakrishna called me telephonically to suggest that I write a text book on the geological history of India. Being inextricably preoccupied with neotectonic study of the Mysore Plateau, I hummed and hawed but waited for a formal letter, which did not come. In early 2003, when the Indian National Science Academy offered, without my asking, the Golden Jubilee Research Professorship, I made up my mind to embark upon the venture of writing an account of the geological setting and tectonic history of the Indian continent. The focus was to be India, but the surrounding regions would have to be brought in the ambit to portray the whole picture of the evolution of the southern part of the Asian continent.

The wonderfully great works of D.N. Wadia, M.S. Krishnan and E.H. Pascoe amply bring out the contributions of pioneers and giants of the pre-Independence time. I have chosen to base my accounts on the works of mainly those who explored the land of India after 1947. Exception has been made in the case of the Himalaya province where comprehensive regional studies started quite late—a decade or a little earlier before India's independence. Endeavour has been made to bring out the works of those silent geologists whose contributions have gone and remain "unhonoured and unsung".

Encompassing broad array of information related to structure and tectonics, stratigraphy and palaeontology, sedimentation and palaeogeography, petrology and geochemistry, geomorphology and geophysics, the book presents in a concise format a simplified and coherent story of the evolution of the Indian continent. Effort has been made to integrate what little I know, desisting, however, from dwelling

on arguments related to controversies (although calling attention to them), curtailing details of methodologies and descriptions, pack no more than is necessary for understanding and avoiding using jargons of stratigraphic nomenclature. Presented in a distilled form, the observations and deductions of workers on different facets of earth science, this book is intended to provide appreciation of the geological developments taken place in the making of India. A comprehensive though selective list of original works would provide lead to those who seek details and wish to go into the depth of problems. No more than an updated guide, this book is meant for readers who wish to enlarge their scientific perception.

Curtailing unnecessary details without making them shallow and updating without being unsympathetic to the past contributions, the diagrams are designed to depict settings and situations rather than precise delineation of geological features.

While writing this book, words of my mentors reverberated in my mind. My college-day teacher Shri Shiva Ballabh Bahuguna used to exhort me to see the world around with wide open eyes and try to know about as many things as possible. "The outcrop is the final court of appeal where all concepts or theories must the tested" wrote Prof. F.J. Pettijohn in 1974. And to have a close look at the outcrops, one must go "out among the rocks" was the message Prof. W.D. West gave me in 1991. Fortunately, I have lived and worked all my life among the rocks in different parts of India—the central sector of the Himalaya, the eastern extremity of the mountain arc, eastern Vindhyachal, northern Bundelkhand, the Mewar region of the Aravali, the Mysore Plateau and the central and southern Sahyadri. The voyages of studies enabled me to carry out "conversation with rocks", which gave me insight and some understanding of the natural phenomena involved in the making of India. I wish to share that understanding with students and teachers of geology and non-specialist readers.

K.S. Valdiya

Acknowledgments

I am deeply grateful to Prof. M.S. Valiathan, the then President of the Indian National Science Academy and to the members of his Council, for enabling me to write this book by offering the Golden Jubilee Research Professorship.

Words cannot express my feeling of gratitude to Jawaharlal Nehru Centre for Advanced Scientific Research for very generous support and immeasurable help to make me pursue the project the way I wanted.

A large number of friends have helped me to prepare the draft of the book, Dr. Anshu Kumar Sinha, then Director of Birbal Sahni Institute of Palaeobotany (Lucknow), Director Dr. V.P. Dimri, Librarian Shri B.M. Khanna, and Scientists Ravi Prakash Srivastava and Ashutosh Chamoli of National Geophysical Research Institute (Hyderabad), and Library Assistant Surendra Singh Bhandari at Wadia Institute of Himalayan Geology (Dehradun) greatly helped me in getting the relevant literature.

Professor Kanchan Pande (Indian Institute of Technology, Mumbai), Dr. Rajeev Upadhyay (Kumaun University, Nainital) and Dr. S.S. Bhakuni (Wadia Institute of Himalayan Geology, Dehradun) extended invaluable help to get the original drafts of diagrams finely redrawn by dedicatedly competent artists Shri S.S. Sawant, Shri G.C. Kothyari and Shri V.N. Ghoshal. Shri C. Vedamurthy ably set the typescript in a proper format and prepared the list of references. Shri Mohan Singh Bisht and Dr. Pradeep Goswami (Kumaun University, Nainital) helped me in innumerable ways. I do not know how to thank these friends.

I am profoundly grateful to Prof. Mallickarjun Joshi (Varanasi), Prof. Kanchan Pande (Mumbai), Prof. R. Vaidyanadhan (Cuddalore), Prof. Vishwas S. Kale (Pune), Dr. D.K. Paul (Kolkata), Dr. U. Raval (Hyderabad), Dr. M. Ramakrishnan (Chennai), Dr. V.N. Vasudev (Bangalore), Dr. M. Jayananda (Bangalore), Prof. C. Srikantappa (Mysore), Prof. R.S. Sharma (Jairpur), Dr. T.M. Mahadevan (Kochi), Dr. S. Sinha-Roy (Jaipur), Prof. N.C. Ghose (Bangalore), Dr. Fareeduddin (Bangalore), Prof. C. Leelanandam (Hyderabad), Prof. Somnath Dasgupta (Kolkata), Dr. T.K. Biswal (Mumbai), Prof. R.K. Lal (Varanasi), Prof. Anand Mohan (Varanasi), Prof. Asru Chaudhuri (Kolkata), Dr. R. Dhana Raju

(Hyderabad), Prof. Naresh Kochhar (Chandigarh), Dr. Jokhan Ram (Dehradun), Dr. V.C. Thakur (Dehradun), Prof. B.N. Upreti (Kathmandu), Dr. O.N. Bhargava (Panchkula), Dr. Anshu K. Sinha (Gurgaon), Prof. S.K. Shah (Secunderabad), Prof. S.M. Casshyap (Noida), Dr. R.C. Tewari (Aligarh), Prof. K.V. Subbarao (Hyderabad), Prof. S.F.R. Sethna (Mumbai), Dr. Hetu C. Sheth (Mumbai), Dr. S.K. Biswas (Mumbai), Prof. Ashok Sahni (Chandigarh), Dr. H.M. Kapoor (Lucknow), Dr. Rajeev Upadhyay (Nainital), Dr. S.K. Acharyya (Kolkata), Prof. S.K. Tandon (Delhi), Dr. A.C. Nanda (Dehradun), Prof. P.K. Saraswati (Mumbai), Dr. A.T.R. Raju (Kakinada), Prof. M.S. Srinivasan (Varanasi), Prof. V. Sharma (Delhi), Prof. Brahm Parkash (Roorkee), Prof. Rajiv Sinha (Kanpur), Dr. D.D. Joshi (Lucknow), Prof. L.S. Chamyal (Vadodara), Prof. Ashok Singhvi (Ahmadabad), Dr. Amal Kar (Jodhpur), Prof. S.M. Ramasamy (Tiruchirappalli), Dr. R.K. Pant (Ahmadabad), Dr. J.R. Kayal (Kolkata), Dr. C.P. Rajendran (Trivandrum), Dr. K.S. Krishna (Dona Paula) and Dr. M.V. Ramana (Dona Paula) for critically and painstakingly going through chapters of the book and making extremely valuable suggestions for improvement.

K.S. Valdiya

Contents

About the Author

Prof. K.S. Valdiya is a distinguished scientist, academics, Author and an active environmentalist. His fields of specialization are tectonics with special reference to active faults and environmental geology. His fundamental studies and research on the Uttarakhand Himalaya serve as a template and a guide for interpreting the structural architecture of the entire Himalaya.

Born at Kalaw in Myanmar, he had his early education in a small town of Pithoragarh in Kumaun Himalaya and higher education at University of Lucknow (UP). After obtaining Ph.D. degree in 1963 from Lucknow University, he studied at Johns' Hopkins University, USA, as a Fulbright Fellow during 1965–1966.

Presently, Prof. Valdiya is Honorary Professor of Geodynamics at Jawaharlal Nehru Centre for Advanced Scientific Research, Bengaluru. He has held several high positions as Additional Director, Wadia Institute of Himalayan Geology, as Professor of Geology, Dean and Vice-Chancellor of Kumaun University, Nainital, as Professor of Geodynamics (1995–1997) and Bhatnagar Research Professor (1997–2002) at Jawaharlal Nehru Centre for Advanced Scientific Research, Bangalore, Golden Jubilee Research Professor of Indian National Science Academy at Jawaharlal Nehru Centre for Advanced Scientific Research, Bangalore for Advance Scientific Research. He has been a Distinguished Guest Professor at Indian Institute of Technology, Mumbai, and a visiting Honorary Professor at Indian Institute of Technology, Rorkee.

Prof. Valdiya has written over 110 research papers, authored 14 books, edited 9 books apart from penning 40 articles in Hindi towards popularization of science. His most referred books are *Geology of Kumaun Lesser Himalaya* (1980); *Aspects of Tectonics: Focus on Southcentral Asia* (1984); *Environmental Geology:*

Indian Context (1987; 2013); *Dynamic Himalaya* (1998); *Saraswati, the River that Disappeared* (2012); *Geology, Environment and Society* (2005); *Ek thi Nadi Saraswati* (2010) and *Geography, People and Geodynamics of India in Puranas and Epics* (2012).

Prof. K.S. Valdiya has been awarded with the prestigious *Padma Bhushan* by Government of India in 2015. He is recipient of the *Padmashri* and the Hindi Sevi Sammaan (*Atmaram Puraskaar*) in 2007, the *G.M. Modi Award* for Science and Environment in 2012, the *National Mineral Award of Excellence* in 1997, the *D.N. Wadia Medal* in 1995, the *National Mineral Award* in 1993, the *S.K. Mitra Award* in 1991, the *Shanti Swarup Bhatnagar Prize* in 1976 and the *Chancellor's Medal* in 1954. He is a Fellow of the Indian National Science Academy, the Indian Academy of Sciences, the National Academy of Sciences, India, Third World Academy of Sciences and Geological Society of India. He is an Honorary Fellow of the Geological Society of America and the Geological Society of Nepal. He has served as a Member, Science Advisory Committee of the Cabinet of the Prime Minister (1983–1988).

Chapter 1
Physiographic Layout of Indian Subcontinent

1.1 Physiographic Divisions

The Indian subcontinent encompasses the mountainous province of Himalaya girdling the northern border, the almost flat expanse of the Indo-Gangetic Plains in the middle, the uplands and plateaus of the Peninsular India, the narrow coastal plains along the seaboards and the alluvial plains of the Irrawaddy River that is flanked eastwards by the Shan–Karen plateaus in Myanmar (Fig. 1.1). Each of these units is a structurally and lithologically contrasted and physiographically distinctive geomorphic province, having altogether different evolutionary history. They seem to make what the ancient literature describes as *Bhâratvarsh* belonging to a mega-island or continent called *Jambudweep*. Within each of these provinces occur many subprovinces of geomorphic units (Chatterjee 1965; Singh 1998; Khullar 1999; Vaidyanadhan 1977, 2002; Tiwari 2003).

Without going into the details of geomorphic characterization, origin and evolution, five major provinces are described briefly (Fig. 1.1, Plate 1.1) in the following pages—(1) the Himalaya, (2) the Indo-Gangetic Plains, (3) the Irrawaddy Plains, (4) the mountains, uplands and plateaus of Peninsular India, and (5) the coastal plains (Figs. 1.1 and 1.2). Interestingly, about 11 % of the geographic area of India comprises high mountains above the 2100 m mean sea level, 18 % area is small mountains and hills of the elevation 900–2100 m, 28 % made up of plateaus in the altitudinal range of 300–900 m, and 43 % area encompasses the plains.

K.S. Valdiya, *The Making of India*, Society of Earth Scientists Series,
DOI 10.1007/978-3-319-25029-8_1

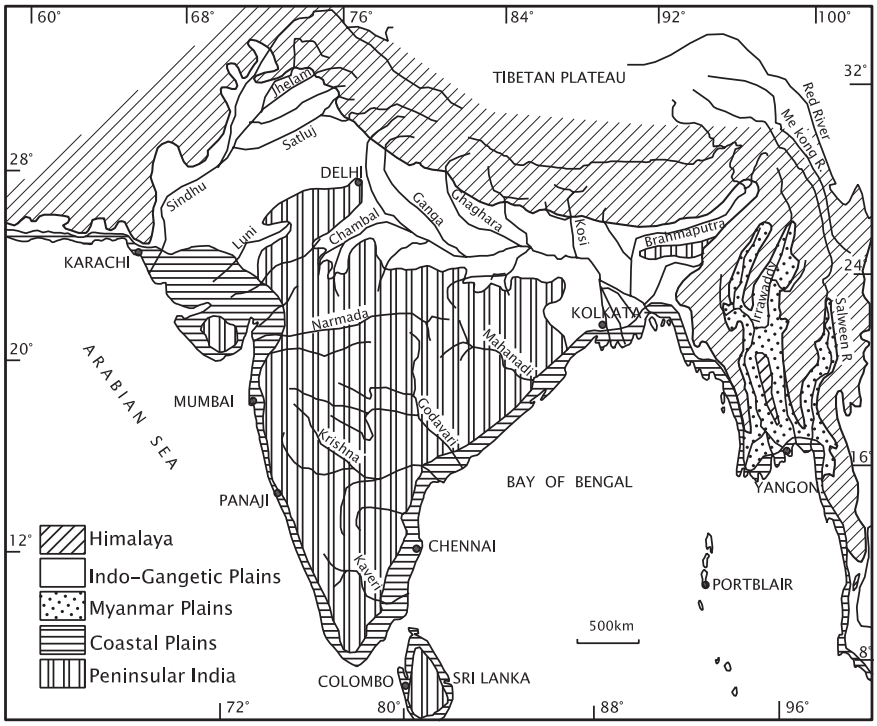

Fig. 1.1 Map of India showing various physiographic provinces of the Indian subcontinent

1.2 The Himalaya

Bordering the Indian subcontinent like a colossal rampart in the north-west, north and north-east, the girdle of the Himalaya mountain isolates India securely from the rest of Eurasia. The mountain province comprises a number of arcuate chains—the Kirthar and the Sulaiman in the west, the main Himalaya in the centre and the Patkai–Naga–Arakan Yoma in the east. Making a festoon of mountains big bulges and inward-pointing acute angles called re-entrants of mountains (Fig. 1.2) inset, these bordering mountain ranges have a common evolutionary history. The arcuate NW–SE-trending 2400-km-long and 300–400-km-wide expanse of the main Himalaya embodies four physiographically contrasted and lithostructurally distinctive terranes, particularly in the stretch between the Ravi in the west and the Arun in the east—the Siwalik, the *Himachal* (Lesser Himalaya), the *Himadri* (Great Himalaya) and the Tethys Himalaya (Fig. 1.2).

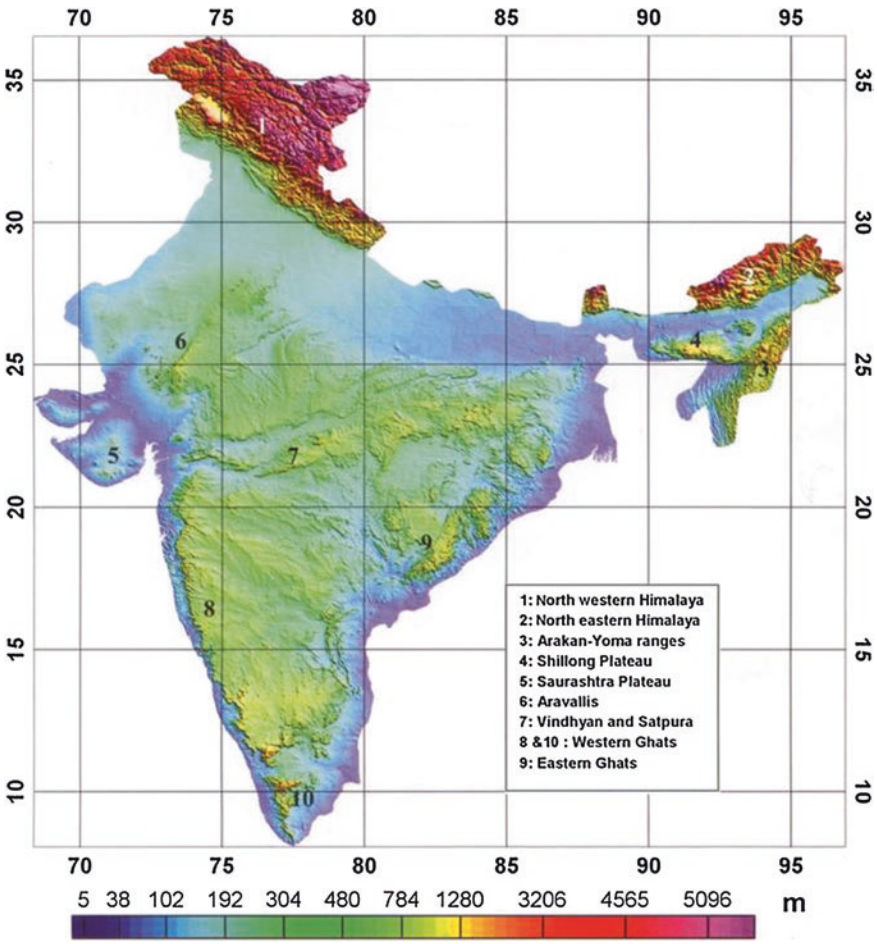

Plate 1 Physiographic map shows the mountains, plateaus, uplands and plains of India (*Courtesy* National Geophysical Research Institute, Hyderabad)

1.2.1 Siwalik

This mountain province abruptly rises above the vast flat expanse of the Indo-Gangetic Plains. The foot of the southern frontal ranges has a discontinuous apron of coalescing fans and cones of gravel or detritus dumped by rivers and streams rushing out of the mountains. The fringe of debris is known as *Bhabhar*.

The 250–800-m-high *Siwalik Ranges* form the southern front of the Himalaya. These are made up of sediments deposited by ancient Himalayan rivers in their channels and floodplains in the last 16–1.5 m year. The rugged Siwalik ranges are commonly broken by south-facing scarps, while on their steepened northern slopes rush down streams through unending cascades and waterfalls as can be seen

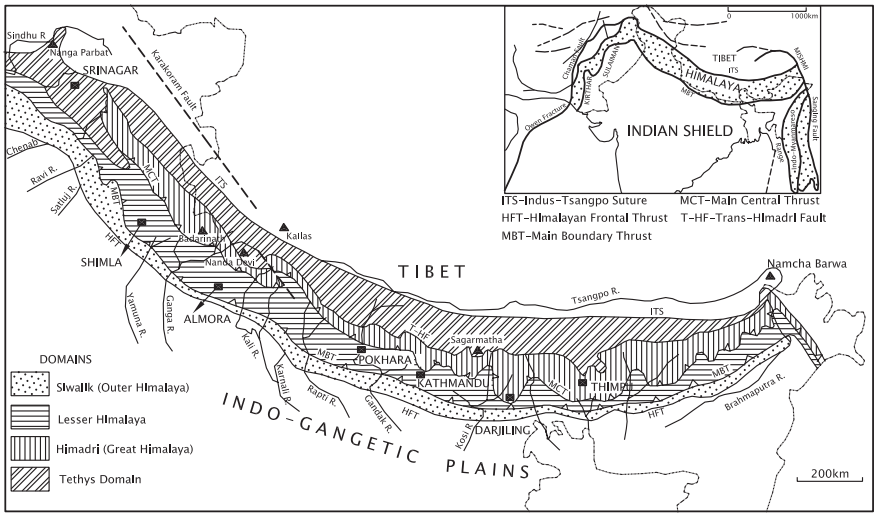

Fig. 1.2 Physiographically distinctive and lithostructurally contrasted four terranes or subprovinces of the Himalaya. *Inset* shows the festoon of arcuate mountain ranges, linked together by syntaxial bends and re-entrants (after Valdiya 1998)

in the central sector. Then, there are long flat stretches within the otherwise rugged Siwalik terrane called the *duns*. The duns represent gravelly deposits within depressions or fillings of now vanished lakes that were formed in the synclinal valleys owing to ponding of rivers and streams or to slackening of current velocity as a result of decrease in gradient following tilting of the ground. Covered densely with forests east of the river Yamuna, the Siwalik is a sparsely populated terrane.

1.2.2 Himachal or Lesser Himalaya

North of the Siwalik rise the formidable ranges of the *Outer Lesser Himalaya*—the Pir Panjal–Dhauladhar–Mussoorie–Nainital–Mahabharat Ranges which are in general higher than 2500 m. In the north-west, the Pir Panjal rises to heights >3500 m. Looking down on the Siwalik, these extremely rugged ranges are thickly forested. North of this lofty rampart in the central sector (Kumaun and Nepal) stretches the beautifully gentle terrain of the 600–2000-m-high *Middle Lesser Himalaya* (Fig. 1.2). The summits of the mountains are rounded, the slopes are gentler, and in the undulating stretches flow streams and rivulets in their winding and wide channels. The valleys of rivers such as Ravi, Satluj, Yamuna, Ganga, Kali, Karnali, Gandaki, Kosi, Arun, and Subansiri—most of which are older than the mountains they cross—are characterized by deep gorges and defiles. These have made extremely rugged landscape characterized by intricate topography with fine drainage networks caused by stream dissection. The land of Lesser

Himalaya was once thickly forested, but present over greater part it is bereft of the sylvan cover. It happens to be the comparatively densely populated terrane of the Himalaya province. This terrane is, by and large, made up of Precambrian rocks—older than 540 m year in age. Sedimentary and volcanic rocks are covered by thick and vast sheets of still older metamorphic and granitic rocks. The rocks wear a mantle of soil over considerable extent.

1.2.3 Himadri or Great Himalaya

Overlooking the Lesser Himalaya terrane, the perennially snow-capped and extremely rugged *Himadri* or *Great Himalaya* rises to elevations of 3000 m to more than 8000 m. It includes the celebrated peaks of Nanga Parbat (8126 m), Nun-Kun (7135 m), Kedarnath (6900 m), Badrinath (7138 m), Nanda Devi (7817 m), Dhaulagiri (8172 m), Sagarmatha or Everest (8848 m), Kanchanjangha (8598 m) and Namcha Barwa (7756 m). The southern face of the Himadri is broken by precipitous high scarps. On the steep northern slopes flow down mountain torrents which churn violently through their deep canyons.

Many of the larger Himalayan rivers had established their drainage trends before local uplift due to crustal movement and continued to cut their channels deeper and deeper, keeping pace with the rate of uplift. These rivers, recognized as *antecedent rivers*, continued to flow in their original channels despite barriers that rose up. The antecedent rivers have cut awesome deep gorges that have vertical to convex walls. Characterized by extremely youthful and forbiddingly rugged topography, the Himadri terrane is made up of thick pile of high-grade metamorphic rocks and gneissic granites which are intruded by 40–20-m-year-old light-coloured granites. This complex has been described by some workers as the "Central Crystalline Axis" of the Himalaya province.

1.2.4 Tethys Himalaya

Beyond the Himadri lies the vast expanse of the *Tethys Himalaya*. This rugged terrain with its fantastically sculptured landscape is made of sedimentary rocks that range in age from the Late Precambrian (>600 m year) to the Cretaceous and Eocene (95–45 m year). Bereft of vegetation on the whole, this desolate domain is a cold desert populated extremely sparsely, that too only in isolated places in valleys where clumps of trees have established their precarious footholds.

The Himalaya province ends up against the zone of docking with Himalaya of India with Asia, now occupied by the rivers Sindhu and Tsangpo. This 50–60-km-wide zone of continental junction is characterized by deep faults and a chain of 60–48-m-year-old volcanic islands caught inextricably in a mixture of deep oceanic trench sediments and seafloor rocks which were squeezed up when the continents

were wedded. Although now 3600–5000 m above sea level, the terrain of the Sindhu and the Tsangpo displays a very gentle topography of river floodways.

North of the Sindhu–Tsangpo valleys, the uplifted plateau of Tibet—belonging to an altogether different landmass of Asia—has been peneplaned out to undulating plains. The southern front of the Tibetan plateau is made up of 90–45-m-year-old granites and granodiorites which make up the Ladakh–Kailas–Gangdese ranges. The granites are associated with 60–48-m-year-old volcanic rocks of a volcanic island arc along the periphery. Some of the volcanoes were active until the Quaternary period about 10,000 years ago.

1.2.5 Syntaxial Bends

Very spectacular features of the Himalaya are the knee-bends in the north-western and north-eastern ends of the main chain. In Kashmir, the entire mountain system turns abruptly southwards from its north-westerly trend, making an acute angle (40°) near Muzzafarabad (Fig. 1.2 *inset*). Along with the mountain ranges bend the whole pile of rock formations and succession of faults and thrust planes, giving rise to what has been described as a *syntaxial bend* recognized and comprehensively described in 1931 by D.N. Wadia. The two flanks of the syntaxial bend characterized by spectacular mountain knots, the Nanga Parbat in the west and the Namcha Barwa in the east, are geologically not exactly similar to each other. The structural architecture and stratigraphic successions on the two sides of the bends are quite different. There is another syntaxial bend down south along the Sibi–Quetta axis between the Sulaiman and Kirthar ranges. After the syntaxis, these ranges gradually bend westwards, forming the E–W-trending ranges of Balochistan, parallel to the Makran Coast.

1.2.6 Eastern Flank

In the east, three different mountain systems, having altogether diverse history of evolution, seem to meet along a deep NW–SE-trending fault (Fig. 1.2 *inset*). The NNE–SSW-oriented *Patkai–Naga–Arakan Yoma* or *Indo-Myanmarese Range* and the ENE–WSW-trending Arunachal Himalaya ranges are sharply truncated by NW–SE-striking Lohit–Mishmi Ranges. The Lohit terrane extends south–southeast into Myanmar, embracing the Kachin–Shan–Tenasserim–Malaysian province belonging to the Asian landmass.

The westward-convex, 1300-km-long series of Patkai Hills–Naga Hills–Kachin Hills and Arakan Yoma—formed of Upper Cretaceous to Tertiary sedimentary rocks along the India–Myanmar border—represents the Himalaya that bends southwards up to the coast of Bay of Bengal. It continues further south for another 1700 km under water, embracing in its sweep the islands of Ramree and Cheduba

(offshore Arakan Coast) and the island arc of Andaman and Nicobar. The height of the Indo-Myanmarese ranges diminishes progressively from north to south. Some peaks of the Patkai and Naga ranges are more than 4000 m high. Mount Victoria in the Chin Hills is 3201 m high, and Mount Padaung in the Arakan Yoma rises to the elevation of 1390 m above the mean sea level.

1.2.7 Himalaya in Pakistan

The Himalaya in Pakistan is not classifiable into the kind of terranes or subprovinces as discernible in India. Not only the structural setting but also the physiographic layout and characteristics are quite different. There is only a broad lithostratigraphic commonality.

West of the Sindhu River in northern Pakistan, the 160-km-long Kohistan, Swat and Dir Ranges trend in the N–S direction, their altitude diminishing from 6000 to 4000 m in the north to 3000 m in the south. There are more than 44 peaks which have elevation above 7300 m. The high mountains have precipitously steep slopes. For example, the western Raikot face of the 8126-m-high *Nanga Parbat* overlooking the Sindhu River is a sheer wall of 7000 m height, and the south-eastern Rupal face is 4500 m high. After the syntaxial bend, the Pir Panjal Range of Kashmir is represented by the *Hazara Ranges* trending NE–SW and comprising a series of hills. The Hazara belt is broadly analogous to the Lesser Himalaya terrane in India. Its E–W-trending Attock–Cherat Range in the south and the N–S-oriented Khyber Pass Range in the west enclose the *Peshawar Plain* of Northwest Frontier Province. South of the Hazara Ranges is the intensely dissected *Kohat–Potwar Plateau*, its southern margin being formed by the 600-m-high *Salt Range*.

The 400-km-long N–S-oriented arcuate *Sulaiman Range* forms the eastern part of Balochistan. The altitude of the Sulaiman peaks varies from 3400 m in the north to 1600 m in the south. Its westward-oriented hill ranges form the Sibi–Quetta Re-entrant around the 3583 m Loesar peak of the NE–SW-trending Zarghun Range. This structural orographic feature separates the Sulaiman Range from the Kirthar Range in the south. The *Kirthar* is an N–S-trending 400-km-long range, the height of which diminishes from 2400 m in the north to 1000 m in the south. Further south, it is represented by the 200-km-long Karachi Arc, 1000–250 m in elevation and extending up to the Arabian Sea.

From the Khuzdar knot emerges the NNE–SSW-trending Las Bela Range associated with the Kalat Plateau. The Bela Range in southern Balochistan gives way to the *Makran Range* that trends E–W parallel to the coast. The altitude of the Makran varies from 2000 m in the north-east to 200–500 m in the south-west. Rivers have cut entrenched valleys across this range. In north-eastern Balochistan, two parallel ranges *Chagai Hills* and *Raskoh Hills* branch off from the N–S-trending Kirthar system. The Chagai is 130 km long, its altitude varying from 2000 to 2400 m. The 230-km-long Raskoh Range has altitude varying

between 1500 and 3000 m. The two are the most conspicuous orographic features of south-western Pakistan. The Chagai Ranges comprise widely separated hills in the midst of wide open flat expanses of sand dunes. West of the Chagai Hills, there is another chain of low hills with extinct volcanoes—Koh-i-Dalel, Damodin and Koh-i-Sultan, running parallel to the Pakistan–Afghanistan border.

Significantly, there are large depressions of Hamun-i-Mashkel and Jaz Murian between the Raskoh–Bazman range in the north and the Makran Range in the south. These depressions have inland drainage of ephemeral rivers and steams.

1.3 The Indo-Gangetic Plains

1.3.1 Extent

In front of the Himalaya mountain arc lies a vast expanse of the world's largest alluvial plains built in the Holocene times by rivers of the Brahmaputra, Ganga and Sindhu systems. The plains extend 3200 km from the southern limit of the Ganga–Brahmaputra delta in the east to the terminal of the Sindhu delta and the Rann of Kachchh in the west (Fig. 1.1, Plate 1.1). The width varies from 150 to 500 km, being widest (550 km) in Panjab and very narrow (90–100 km) in Assam. In the Sindhu basin, the alluvial plain gives way south-eastwards to the arid plain of western Rajasthan and adjoining Sindh—the *Thar Desert*. The Thar domain represents the basin of the legendary Saraswati River that vanished in the Late Holocene time and is presently represented by dry channels of the Ghaghgar Hakra–Nara River in which at present floodwaters flow. The average elevation of the Indo-Gangetic Plains is 150 m, ranging from tide level at the mouths of Ganga and the Sindhu to 291 m at a spot between Ambala in Haryana and Saharanpur in Uttar Pradesh. The underground extension of the Aravali Range towards Haridwar forms the waterdivide between the rivers of the Ganga and Sindhu drainage systems. The gradient of the Ganga Plain is 20 m/km.

1.3.2 Ganga Plain

In the Ganga Basin, the Indo-Gangetic Plains exhibit little variation in relief or landscape for hundreds of kilometres. The monotony of flatness of the *Ganga Plain* is relieved, in limited areas, by bluffs, levees and abandoned channels, oxbow lakes, and ravines or badlands (as seen in the Yamuna–Chambal domain). Mild uplift and subsidence in the deltaic region in Bangladesh and West Bengal are manifest in the formation of *chars* (uplands) and *bils* or *jheels* (marshes and lakes), respectively.

In the 20–100-m-high central Ganga domain in Uttar Pradesh, two distinct physiographical units belonging to different chronological time are

recognizable—the *Older Alluvium* comprising the *Banda*, the *Varanasi* and the *Bhangar* units of rather coarse sedimentary accumulation, and the *Newer Alluvium* consisting of the *Khadar*, the *Bhur* and the *Bhabhar* formations. Made up of gravelly sediments, the Banda terraces and the Varanasi units fringe the Bundelkhand and Vindhyachal uplands in the south. The *Bhabhar* at the foot of the Siwalik in the north is made up of coalescing gravel fans formed in the Late Holocene time. The fans of rivers such as Ganga, Sharada, Gandak and Kosi continue to grow in size and thickness, affecting the drainage pattern considerably. Of these, the Kosi and Gandak rivers migrated to and fro within their fans frequently. The terrains made up of the Bhabhar, Varanasi and Banda formations have uneven topography and a drainage pattern that is characterized by deep incision or cutting by rivers and streams. Where the land is affected by neotectonic uplift, badland topography has developed, as seen in the Yamuna valley in south-western Uttar Pradesh. Forming the larger part of the Indo-Gangetic Plains, the Bhangar and Khadar formations are characterized by nodular concretions of calcium carbonate (*kankar*) as well as encrustation and impregnations of alkali salts (*reh, kallar, usar*). The Bhangar is known as *Rangmati* in West Bengal and Assam, owing to the presence of red-, orange- and yellow-coloured ferruginous concretionary carbonates. In the Bengal–Bangladesh region, the fluvio-deltaic plain is fringed by 30-m-high Pleistocene terraces characterized by these coloured ferruginous concretions. These terraces are called the *Lalmai* in the west, the *Barind* in the north, and the *Madhupur* in the middle between the Brahmaputra and the Meghna rivers. Representing the Bhangar formation, these terraces are considerably affected by neotectonic movements, including faulting, as evident from deep dissection made by rivers and streams.

Rivers have cut 5–20-km-wide and 15–60-m-deep valleys in the Bhangar plain and filled them with sediments forming the *Khadar* flats. The flats are characterized by meandering loops of streams, abandoned channels and oxbow lakes, as seen in the Ganga–Ghaghara interfluve in eastern Uttar Pradesh. In the Bengal–Bangladesh region, the Khadar plain is characterized by innumerable swamps and lakes (called *hoar* or *bil*), occurring in clusters.

1.3.3 Sindhu Plain

The *Sindhu Plain*, 180–210 m above mean sea level in the north and 3–4 m at the delta end, is largely the Khadar expanse which is known as *Chung* in the Panjab interfluve areas. The Sindhu Plain is fringed in the west by a 16–24-km-wide *Piedmont Belt*, the analogue of the Bhabhar in the Ganga domain. Forming an apron of coalescing gravel fans along the foot of the Sulaiman and Kirthar Ranges, the Piedmont belt is characterized by badland topography and braided streams. Within the main Sindhu Plain, rivers and streams are confined to their 6–25-km-wide meandering belts characterized by terraces with a margin of vertical scarp.

1.3.4 Thar Desert

The Luni River has developed an alluvial plain in the arid part of western Rajasthan, known as *Marusthali* or *Marwar*. It is a 650-km-long and 300-km-wide tract along the foot of the Aravali mountain. The plain slopes south-westwards from an altitude range of 300–150 m in the north to mere 20 m in the lower reaches. Wind action coupled with neotectonic activities in the fluvial regime has given rise to anomalous drainage pattern and formation of many saline lakes and playas, including the Sambhar, Didwana, Degana and Lunkaransar lakes. The playas, which turn into water bodies during rainy season, are called *rann*. The biggest one is the *Rann of Kachchh* at the terminal point of the seasonal rivers Luni and Ghaghgar Nara.

The western part of the arid land—*Thar Desert*—is covered with thick mantle of sand dunes of a variety of shapes and sizes. They are longitudinal, transverse, obstacle, parabolic, barchan and shrub coppice. The mean height of the dunes is 8 m in the Jaipur–Sikar region and 30 m in the Barmer belt.

1.4 Irrawaddy Basin

Between the Patkai–Naga–Chin–Arakan Yoma Ranges in the west and the Kachin–Shan–Tenasserim Ranges in the east lie N–S-trending plains built by the Irrawaddy, its tributary Chindwin and the Sittang rivers. The Irrawaddy Basin comprises several plains—the Putao and the Hukawang plains with Indaw Lake in the upper reaches of, respectively, the Irrawaddy and the Chindwin. The Shwebo and Chindwin plains in the middle reaches and the Prome plain in the lower reaches of the Irrawaddy. The Sittang and the Salween have built their own alluvial plains and deltas.

Within the Shan Plateau, there are smaller flood plains—the Lashio plain, the Heho plain with the Inle Lake, and the Namsang plain.

1.5 The Peninsular India

Triangular in shape, the Peninsular India is 1600 km long in the N–S direction and 1400 km wide in the E–W direction. The apex of the triangle is at Kanyakumari at the southern end. It comprises three principal physiographic units—the mountain ranges along its border on three sides, the uplands and plateaus constituting the larger part within the confines of the bordering ranges and the coastal plains along the eastern and western seaboards (Fig. 1.3, Plate 1.1).

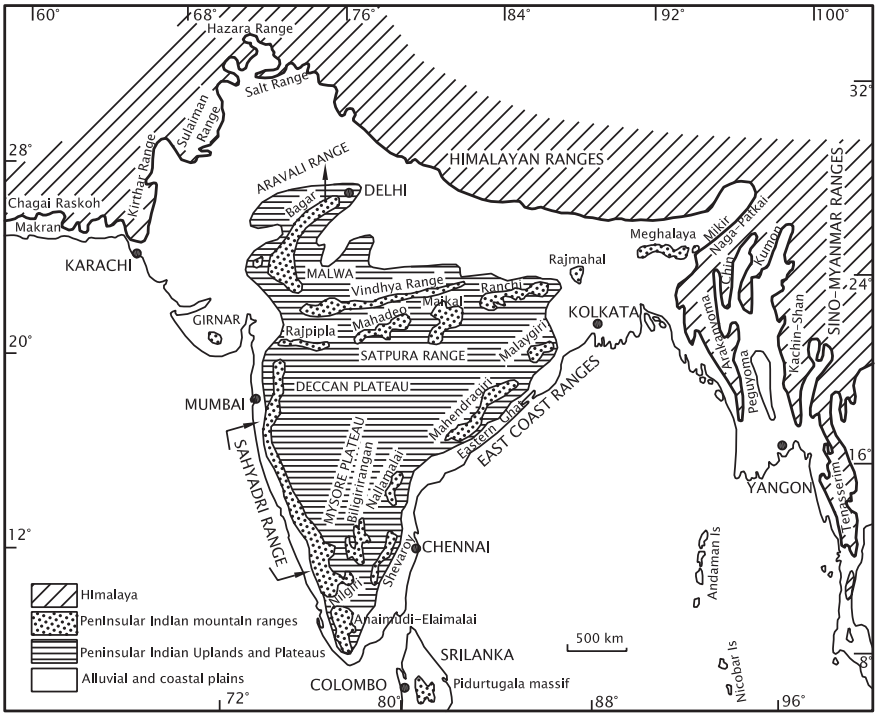

Fig. 1.3 Sketch map shows four principal physiographic units of the Indian continent [based on Dikshi et al. (1994), Khullar (1999) and Tiwari (2003)]

1.5.1 Bordering Mountain Ranges

The NE–SW-trending *Aravali Range* extends more than 800 km from Palanpur in Gujarat to Delhi and beyond undersurface up to Haridwar. Made up of the Proterozoic metasedimentary rocks that are extensively intruded by granites, the Aravali forms the waterdivide between the rivers of the Ganga and Sindhu systems. Significantly, the waterdivide is along the Kailas–Girnar axis—Mount Girnar in Saurashtra and Mount Kailas in south-western Tibet (Valdiya 1998). The general elevation above the mean sea level of the north-eastern part of the Aravali is 400–600 m, while in the south-western segment, the nearly continuous ranges are higher than 1000 m. The high peaks include the 1722-m-high Gurushikhar near Mount Abu, the 1431-m-high Jaga and the 1225 m Bhorat north-west of Udaipur.

South-west of Udaipur, the Aravali bends south-eastwards and seemingly links up with the ENE–WSW-trending Satpura Range, made up of practically similar rock types and of nearly the same age, besides the Deccan Traps. Faulting along the Narmada valley has, however, dismembered and disconnected the two mountain ranges belonging partly to the Proterozoic mobile belt.

The 900–1000-m-high *Satpura Ranges*, as the name implies, consist of a series of seven (*sat*) hill ranges (*pura*). Extending ENE from southern Gujarat to central India and beyond, the Satpura comprises the *Rajpipla Hills* in the west, the *Mahadeo Hills* in the middle, and the *Maikal Hills* in the east. Extending further eastward and embracing the *Ranchi Hills* of Jharkhand, the *Rajmahal Hills* of Jharkhand and the *Meghalaya massif* of eastern India, the Satpura orographic unit is 1600 km long. It abuts against the Patkai–Arakan Yoma along the India–Myanmar border.

The average height of the Satpura is 770 m, the highest peaks being the 1127 m Amarkantak in the Maikal Hills, the 1350 m Dhupgarh in the Mahadeo Hills, and the 1325 m Astambadongar in the western ranges. Interestingly, the Amarkantak massif exhibits a radial drainage—the Narmada flows westwards, the Son takes a northerly course, and the main branch of the Mahanadi goes south-eastwards (Figs. 1.3 and 1.4).

The Satpura extends eastwards embracing the Chhotanagpur terrane made up of Proterozoic gneisses and metamorphic rocks. The terrane is characterized by a series of planation surfaces with laterite covers at different elevation levels, including the 1100 m *Ranchi* and the 600 m *Hazaribagh surfaces*. These planation surfaces have steep slope breaks or scarp faces. The highest point of the Ranchi upland is Goru, 1142 m above the mean sea level. The Hazaribagh surface has the 1366-m-high Parasnath peak. Rivers Koel, Damodar, Subarnrekha and Brahmani emerge from the Ranchi upland, flowing north, east and south, respectively (Figs. 1.3 and 1.4).

Further east in the Sahibganj and Pakaur districts of Jharkhand is the 400–570-m-high *Rajmahal Hills*, made up of Early Cretaceous lavas interbedded with fluvial sediments.

After the gap made by the Ganga and Brahmaputra rivers—the *Rajmahal–Garo Gap*—the Satpura orographic range is represented by the *Meghalaya massif*. Also known as *Shillong Plateau*, the Meghalaya massif consists of the Garo Hills (900 m), Khasi–Jaintia Hills (1500 m) and the Mikir Hills (700 m). The Meghalaya massif is composed of Precambrian gneisses and metasedimentary rocks overlain by Cretaceous to Tertiary sedimentary rock formations. The general elevation varies from 600 to 1800 m, and the massif's highest point is the 1961-m-high Shillong peak. It is this massif which deflects the Brahmaputra westwards to skirt around the upland before joining the Ganga in Bangladesh. The Mikir Hills are detached from the Meghalaya massif and occur as inliers amidst the alluvial sediments of the Brahmaputra. The Rengma peak is 900 m high.

In the east, the Indo-Myanmar Ranges form the border between India and Myanmar. Extending NE–SW, the convex mountain arc is known as the *Patkai Hills* in the north, the *Naga Hills–Chin Hills* in the middle and the *Arakan Yoma* in the south. The highest peaks are as follows: the 3014-m-high Japro in the Naga Hills, the 2164-m-high Blue Mountain in the Chin Hills and the 3053-m-high Mount Victoria in the Arakan Yoma.

The Mishmi Hills of eastern Arunachal (Himalaya) continues south-eastwards and then bends southwards in northern Myanmar, forming the 1700-km-long

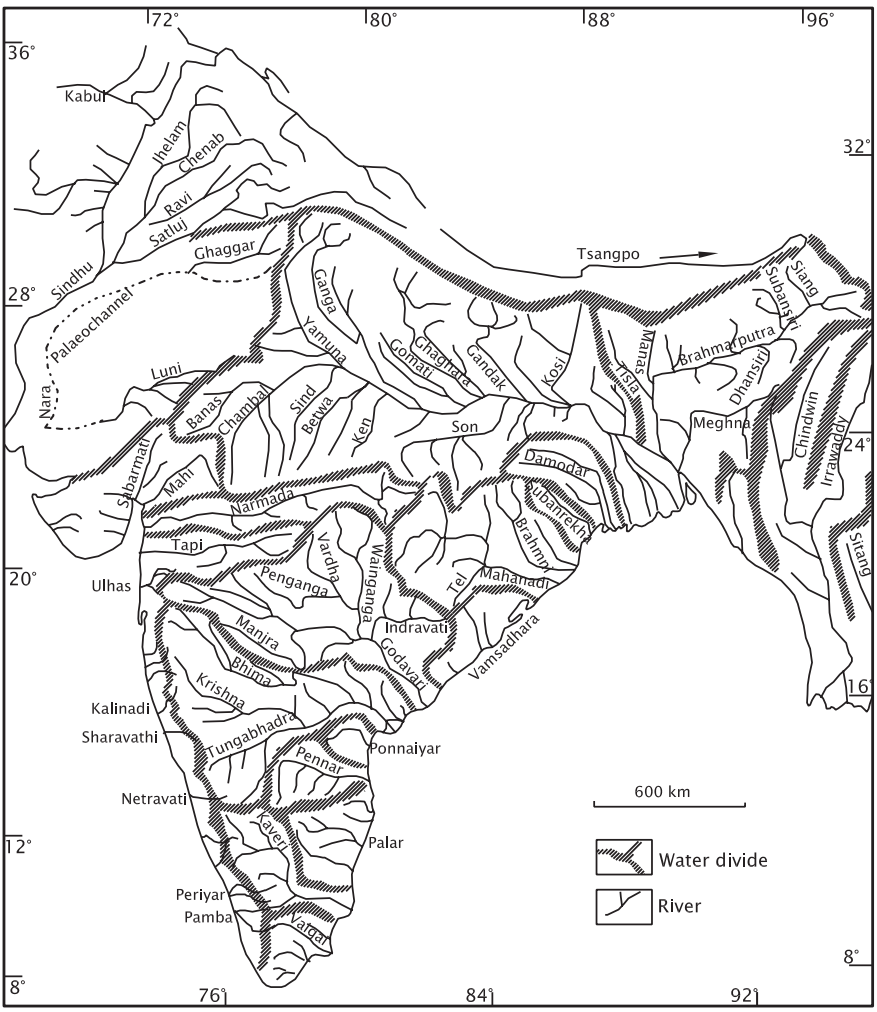

Fig. 1.4 Pattern of drainage of rivers of the Indian subcontinent

Sino-Myanmarese Ranges. These ranges comprise the *Kachin Hills* in the north, the *Shan massif* in the middle and the *Tenasserim Range* in the south. The Tenasserim Range continues south into the Malaysian Peninsula. The average elevation of the Sino-Myanmarese Ranges is 4000 m, the height diminishing from 5885 m Hkakabo Raz in the northern inaccessible part of the country, and 2400 m in Northern Shan States to 2000 m in the Tenasserim Peninsula. One branch of this range turns SSW, forming the Kumon Range in northern Myanmar. All along its length, the Shan massif is sharply defined by a spectacular scarp overlooking the Irrawaddy plain.

The *Sahyadri Ranges* (Fig. 1.3) extend 1600 km south from the Tapi valley to Kanyakumari. These are divided into three sectors—the Northern Sahyadri in Maharashtra is made up of Late Cretaceous basaltic lavas, the Central Sahyadri in Karnataka is constituted of Archaean gneisses and high-grade metamorphic rocks, and the Southern Sahyadri in Kerala is made up of Late Proterozoic charnockites and khondalites. The NNW–SSE-trending fractures and faults defining the ranges forming linear blocks make the Sahyadri a horst mountain of sorts. Its west-facing steep to near vertical flank is characterized by a multiplicity of precipitous escarpments disposed in echelon and alternating with very narrow irregular terraces. These features have given rise to a "landing stair" known as the *Western Ghat*. The mountain range is the Sahyadri and its escarpment the Western Ghat.

The eastern flank of the Northern Sahyadri and the larger part of Central Sahyadri slopes gently eastwards and is drained by the Godavari, Krishna, Tungabhadra and Kaveri rivers. Originating within 50–65 km range of the Arabian Sea, these rivers flow eastward over a long distance to discharge into the Bay of Bengal (Fig. 1.4; Table 1.1). On the other hand, the west-flowing shorter rivers such as the Ulhas, Vaitarni, Kalinadi, Gangavali, Sharavati, Netravati, Payaswini and Valapattan descend through their progressively deepening gorges and drop down the scarps as waterfalls and rapids (such as the 271 m Jog Falls) before emptying themselves in the Arabian Sea. The physiography of the Southern Sahyadri (and the Nilgiri massif) is somewhat different. Both their flanks are broken by scarps or are very steep. While the Noyil and Vaigai rivers flow eastward, the Ponnani, Periyar, Pamba, Achankovil and Kakkad rivers flow westwards to discharge into the Arabian Sea (Fig. 1.4).

The average elevation of the Sahyadri Range is 1000–1200 m. The highest peaks are the Salher 1569 m, Harishchandragarh 1424 m, Mahabaleshwar 1438 m and Kalsubai 1646 m in the Northern Sahyadri, the Kudremukh 1892 m, the Pushpagiri 1714 m and the Tadiannamalai 1745 m in the Central Sahyadri, the Dodabetta 2637 m and Mukurti 2554 m in the Nilgiri, and the Anaimalai 2695 m, and Elaimalai 2670 m, Devarmalai 1922 m in the southern Sahyadri. Between the Nilgiri massif (1500 m) and the Anaimalai Range (2000 m) is the *Palghat Gap*, 25–30 km wide and 75–300 m above the mean sea level.

The *East Coast Ranges* comprise a series of physiographically discontinuous hill ranges which do not have any structural unity. They embrace the *Shevaroy Hills* (1525–1647 m) in Tamil Nadu made up of charnockites of Proterozoic antiquity, the *Nallamalai Hills* (1525–1647 m) marking tectonized margin of the Precambrian Cuddapah Basin of sedimentary rocks in Andhra Pradesh, and the *Eastern Hills* of Proterozoic charnockites and granulites in Odisha. The high peaks of the Eastern Hills include the Deodimunda 1644 m, the Nimgiri 1517 m, the Mahendragiri 1501 m, the Malayagiri 1169 m, the Armakonda 1680 m, the Galikonda 1643 m, and the Sinkramgutta 1620 m. Between the Nallamalai Hills and the Eastern Hills is the vast deltaic plain built by the Godavari and Krishna rivers.

1.5.2 Uplands and Plateaus

Bordered on all three sides by mountain ranges, the central part of the Peninsular India is a composite of plateaus and uplands rising on the average 600–900 m above the mean sea level. The Satpura Range divide the Peninsular India into two parts—the northern part embodying the Malwa, Bundelkhand and Vindhyachal plateaus, respectively, in Maharashtra, Karnataka and Andhra Pradesh, and the southern part comprising the Deccan, Mysore and Telangana plateaus (Fig. 1.3). While the southern part slopes gently eastwards, the rivers of the northern part flow northwards (Fig. 1.4).

Drained by the NE-flowing Banas and Chambal rivers, the *Malwa Plateau* is a 500–600-m-high terrain of flat-topped hills and rolling plains of Late Cretaceous lavas. It embraces the 250–300 m undulating terrain of the Aravali Range in eastern Rajasthan. To the north-east is the *Bundelkhand Upland*, made up of Late Archaean gneisses and granites and 300–600 m above the mean sea level. Through the undulating terrain of the Bundelkhand, the Chambal, Betwa and Dhasan rivers have carved their valleys, cutting deep gorges and developing spectacular ravine land—the *Chambal Badland*—before joining the Yamuna River.

Having a general elevation of 300–650 m, the *Vindhyachal Plateau* in Madhya Pradesh is bordered by 760–1220-m-high hills—*Kaimur* in the north and the *Bhainer* in the south, both characterized by frontal escarpments. The 610-m-high Kaimur scarp overlooks the alluvial plain of the Yamuna and Ganga rivers in south-eastern Uttar Pradesh. Composed of Proterozoic sedimentary rocks, the Vindhyachal Plateau is drained northwards by the Chambal, Sind, Betwa and Ken rivers.

South of the Satpura Ranges and east of the Sahyadri, the *Deccan Plateau* encompasses practically the whole of Maharashtra and adjoining parts of Telangana and Karnataka. The landscape is characterized by flat terraces made up of Late Cretaceous lavas, some with lateritic mantle. The average elevation of the Deccan is 600 m. The Godavari and Krishna rivers drain it east–south-eastwards. In the upland Maharashtra along the foot of the Sahyadri Ranges, the rivers have dissected narrow valleys but become wide with gentle valley slopes in their middle reaches.

Covering the whole of Karnataka and adjoining areas of Tamil Nadu and Telangana, the *Mysore Plateau* is made up of Archaean gneisses, granites and high-grade metamorphic rocks. It comprises two units—the hilly dissected tract adjoining the Sahyadri is known as the *Malnad*, and the rolling to flat topography of the eastern part is called the *Maidan*. The plateau is traversed by a number of NNW–SSE- to N–S-trending linear hills and chains of isolated hillocks such as the Bababudan with 1913-m-high Mullayanagiri Hill, the Ramanagaram with 1255-m-high Madhugiri peak, the Bangalore range with 1467-m-high Nandidurga Hill, the *Chitradurga Range*, the Kolar Range and so on. The Bangalore range of gneissic hills extends southwards with progressive increase in elevation, giving way to the charnockitic *Biligirirangan–Mahadeswaramalai*

Ranges in eastern Tamil Nadu. The highest point of the Biligirirangan is a 1750 m peak, and the summits of the Mahadeswaramalai attain the altitudes of 1487 and 1316 m.

The 900 m Bangalore surface is flanked to the north-east by the 500–600 m planation surface of the *Telangana Plateau* of Andhra Pradesh.

1.6 Coastal Plains

The narrow coastal plains along the seaboards of the Peninsular India (Figs. 1.1 and 1.3; Plate 1.1) are more than 6000 km long, extending from the deltas of the Sindhu and the Saraswati (Ghaggar–Nara) rivers in the west, through the southern tip of the Peninsula, to the delta of the Ganga–Brahmaputra and then along the Arakan Coast to the deltas of the Irrawaddy and the Salween rivers in the east. The island of Sri Lanka has a broad fringe of coastal plains all around.

1.6.1 Makran Coast

In the *Makran Coast*, the margin of the Sindhu deltaic plain is made up of an arcuate zone of older tidal-flat deposits. To the west is the coast of strong emergence characterized by beach deposits, locally tilted and occurring at nine successive levels, indicating uplift of the coast in incremental steps.

East–south-east of the Sindhu deltaic plain is the *Rann of Kachchh*, a salt impregnated and encrusted 350-km-long, 150-km-wide tidal flat which remains inundated by marine waters during the monsoon months. It was once connected to the Gulf of Khambhat through the Nal Sarovar, a shallow brackish water lake east of Saurashtra. The Okhamandal–Dwarka belt in the western part of Saurashtra seems to have sunk northwards along an E–W line. In the southern Saurashtra, pelletal–intraclastic carbonate deposits together with sparse coral reefs and sand dunes form five terraces, at the elevations of 5–7, 15–25, 25–30, 35–45 and 55–60 m above the present sea level.

1.6.2 West Coast

The *West Coast* is mainly a *coast of submergence* characterized by in some sectors by cliff faces and near-shore islands (such as the Mumbai and the Anjdiv (off Goa)) and estuaries, coves, embayments and backwaters, but no deltas in most of the expanse. The coastal plain of Gujarat is the prolongation of the alluvial plains of the Sabarmati and Mahi rivers. The *Gujarat Coast* is marked by strand lines 8–10 m above the present sea level.

Table 1.1 Drainage system of India (Law 1968)

Name of the river	Source	Length (km)	Area drained (km^2)	Volume of average annual flow (million m^3)
Brahmaputra	Lake Konggyu East of Mount Kailas	2900	258,008	627,000
Ganga	Gangotri Glacier at 7010 m	2525	861,404	152,000 at Allahabad 459,040 at Patna 468,700 at Farakka
Yamuna	Yamunotri Glacier at 6330 m	1376	366,223	93,020 at Allahabad
Chambal	Near Mahu (Mhow)	1050	139,468	30,050 at confluence with the Yamuna
Ramganga	Eastern Garhwal at 3110 m	596	32,493	15,258
Ghaghara	Near Gurla Mandhata south of Mansarovar	1080	127,950	94,400
Gandak	Tibet-Nepal border at 7620 m	425 in India	46,300	52,200
Kosi	Sikkim-Nepal-Tibet Himalaya	730 in India	86,900	61,500
Sindhu	Near Mansarovar Lake at 5180 m	2880	1,178,440	110,450 at Kalabagh in Pakistan
Jhelam	Verinag at 4900 m	724	34,775 up to Indo-Pak border	27,890 at Mangla
Chenab	Bara Lacha Pass	1180	26,155 up to Indo-Pak border	29,000 at Marala
Ravi	Near Rohtang Pass	725	14,442	8000 at Madhupur
Beas	Near Rohtang Pass at 4062 m	460	20,303	15,800 at Mandi
Satluj	Mansarovar–Rakas Lakes area at 4570 m	1450	25,900	16,600 at Rupnagar
Mahanadi	Dandakaranya near Sihawa in Raipur district	857	141,600	67,000/66,640
Godavari	Trimbak Plateau near Nasik	1,465	312,812	105,000/118,000
Krishna	Near Mahabaleshwar Northern Sahyadri	1,400	258,948	67,670/62,800
Kaveri	Talkaveri in Central Sahyadri	800	87,900	20,950
Pennar	Kolar district, Karnataka	910	55,213	3238
Narmada	Amarkantak Plateau	1310	98,796	40,700/54,600
Mahi	Aravali Range	560	34,481	11,800

(continued)

Table 1.1 (continued)

Name of the river	Source	Length (km)	Area drained (km^2)	Volume of average annual flow (million m^3)
Tapi	Multai in Betul district	730	65,145	17,980
Sabarmati	Mewar Hills, Rajasthan	320	21,898	3800

Between Vaitarna and Alibagh, the raised beaches are 6 m above the sea level and between Revas and Srivardhan at 3–4 m level. In Maharashtra between Daman and Goa, the 8–24-km-wide lowland known as the *Konkan Coast* is a rocky shore of cliffs, bays, coves with small mudflats and small beaches between seaward projecting NNW–SSE-trending linear ridges or spurs of the Sahyadri Range. Between Goa and Mangalore, the *Kanara Coast* in Karnataka is 30–50 km wide, becoming 70 km wide in the Mangalore tract. The NNW-trending spurs of the Sahyadri progressively diminish in height towards the shore where they disappear under the coastal sediments. The rivers that descend from the Sahyadri Ranges have deeper incised channels, including entrenched meanders, and show anomalous behaviour such as abrupt deflection along lineaments, hairpin geometry of drainage, intimate association of clay flats of palaeolakes and stagnant bodies of river water upstream of the crossing of lineaments. Adjoining the coastal lowlands, the foot belt of the Sahyadri is a 40–120 m high undulating to rugged tract, wearing a thick mantle of laterite.

The 20–100-km-wide *Malabar Coast* in Kerala is physiographically and structurally not different from the Kanara Coast. The lowland along the coast is no more than 5–7 km in width. A 80-km-long and 5–10-km-wide lagoon is barred by a 55-km-long sand spit, giving rise to the Vembanad Lake. The successor to the Tertiary basin between Kollam and Kodungallur, the Vembanad is replenished by the discharges of the Periyar, Muvattupuzha, Manimala, Pamba and Achankovil rivers Pamba and Achankovil rivers (Table 1.1). There are a number of barred lagoons called *Kayals* in coastal Kerala.

1.6.3 East Coast

The 120-km-wide *East Coast* is a *coast of emergence*, characterized by well-defined beaches, sand dunes and sand spits, and many lagoonal lakes associated with backwater swamps. The Pulicat Lake to the north of Chennai is barred by a long sand spit and contains within it the *Sriharikota* island. The 60-km-long Pulicat Lake between the deltas of the Krishna and Godavari rivers is barred by a few sand spits. The Kolleru Lake was once a lagoon but now far inland, implying rapid rate of the growth of deltaic fan. The stretch of the land between

Visakhapatnam and Ganjam is a shore characterized by cliffs. The 70-km-long and 22–7-km-wide Chilka Lake south-west of the Mahanadi delta is the biggest lake in eastern India.

A product of the combined contributions of the Ganga and the Brahmaputra, the *Sundarban Delta* forms part of the coastal plain, forming the head of the Bengal Basin. Not more than 3 to 20 m above the sea level, this deltaic plain is characterized by abandoned channels, lakes and swamps, and by tidal flats. The shoreline has been shifting eastwards and southwards for over 7000 years.

The *Arakan Coast*, a narrow rocky belt for the most part, is characterized by steep rocky shore with overlooking 600-m-high Arakan Yoma. There are innumerable bays and small beaches. Small rivers such as Mayu, Kaladam and Lemro have built their sedimentary fans, making a 70-km-wide coastal plain in the Akyab region.

References

Chatterjee, S. P. (1965). Physiography. In P. N. Chopra (Ed.), *The Gazetter of India* (Vol. I). New Delhi: Ministry of I&B, Government of India.

Dikshit, K. R., Kale, V. S., & Kaul, M. N. (Eds.). (1994). *India: Geomorphological Diversity* (525 p.). Jaipur: Rawat Publication.

Khullar, D. R. (1999). *India: A Comprehensive Geography* (p. 571). Ludhiana: Kalyani Publishers.

Law, B. C. (Ed.). (1968). *Mountains and Rivers of India*. Kolkata: National Committee for Geography.

Singh, A. D. (1998). Late Quaternary oceanographic changes on the eastern Arabian Sea: Evidence from planktonic foraminifera and pteropods. *Journal of Geological Society of India*, *52*, 203–212.

Tiwari, R. C. (2003). *Geography of India* (p. 924). Allahabad: Prayag Pustak Bhavan.

Vaidyanadhan, R. (1977). Recent advances in geomorphic studies in Peninsular India: A review. *Indian Journal of Earth Science*, Ray Volume, 13–35.

Vaidyanadhan, R. (2002). Geomorphology of the Indian subcontinent (29 p). Dehradun: Indian Society of Remote Sensing.

Valdiya, K. S. (1998). *Dynamic Himalaya* (178 p.). Hyderabad: Universities Press.

Chapter 2
Geological Terranes of Indian Continent

In literature and in speaking, India is described as a subcontinent forming the southern part of Asia. Before breaking and drifting away in the Early Permian time, Tibet was a part of Gondwanic India. The microplate of Myanmar separated and moved east towards the Thailand–Malaysia part of the Asian plate sometime later. The geological layouts of Pakistan, Nepal, Bhutan, Bangladesh, Myanmar and Sri Lanka are inseparably linked with the geological framework of India. Forming the periphery of India, the landmasses of these countries have gone through the same evolutionary history as India has. Larger India is, indeed, a continent. This continent comprises as many as nine geological terranes, each having its own lithological–petrochemical characteristics, structural layout and evolutionary history.

2.1 Indian Shield with Archaean Cratons

Peninsular India is a shield embodying four composite, consolidated and rigid blocks evolved during the Archaean era. Remaining practically underformed by compressional tectonism for very long geological periods, these blocks form the cratons—the Dharwar Craton in southern India, the Bastar Craton in central India, the Singhbhum Craton in eastern India and the Bundelkhand Craton in northern India. The cratons have Palaeoarchaean nuclei, 3310–3560 Ma in age, comprising granitic gneisses and basic–ultrabasic rock complexes. Experiencing widespread cratonization or stabilization at about 3000 Ma due to large-scale granite emplacement, the cratons were affected by sagging and rifting along planes of weakness, resulting in the formation of intracratonic elongate basins of sedimentation and basic volcanism. The sedimentation was dominantly ferruginous and siliceous, leading to the making of sedimentary successions that contain very rich deposits

K.S. Valdiya, *The Making of India*, Society of Earth Scientists Series,
DOI 10.1007/978-3-319-25029-8_2

of iron. The emplacement of granite at about 2550 Ma gave rise to large plutonic bodies in all the four cratonic blocks. In many areas, this phenomenon was attended by transformation of high-grade metamorphic rocks into charnockites.

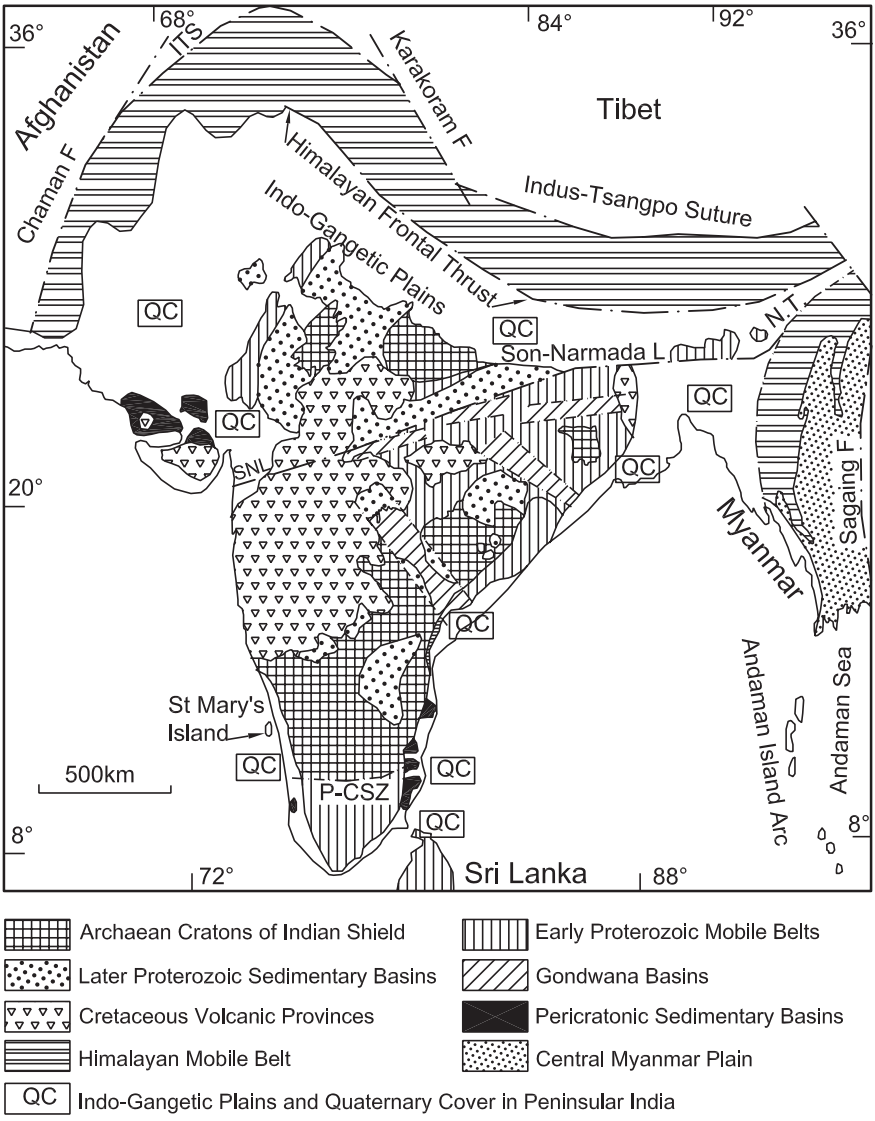

2.2 Early Proterozoic Mobile Belts

The cratons are separated from one another by geodynamically mobile belts of the Early Proterozoic evolution. Shear zones and detachment planes demarcate their boundaries. The Eastern Ghat Mobile Belt borders the Dharwar and

Bastar cratons. The Satpura–Aravali Mobile Belt parabolically embraces the Bundelkhand Craton. And the Chhotanagpur–Singhbhum Mobile Belt forms the northern fringe of the Singhbhum Craton. Made up of metamorphic rocks of grades varying from very high to moderate or even low and comprising voluminous volcanics, and implanted with ultrabasic and alkaline bodies in and near the bordering shear zones, these mobile belts represent Early Proterozoic intracontinental rift basins. The sedimentary successions of these rift basins consist of greywackes and turbidities in the lower part, and quartzarenites with penecontemporaneous basic volcanics in the upper part. Emplacement of granites in some mobile belts marked the end of the Proterozoic era in the Indian Shield.

In common with the Eastern Ghat Mobile Belt that borders the Bastar Craton, the Southern Granulite Terrane in the southern part of Peninsular India is made up of very high-grade metamorphic rocks, including charnockites, khondalites and granulites, intimately associated with granite gneisses. Some of these metamorphic rocks had evolved under very high temperatures and pressures. The Southern Granulite Terrane is separated from the Dharwar Craton by a system of deep shear zones, exhibiting both dip-slip and strike-slip movements, particularly in the time interval 500 ± 25 Ma, when the Pan-African orogeny overwhelmed the continent. It was around this time that there was widespread emplacement of granitic, alkaline and ultrabasic magmas within or in the proximity of shear zones. Simultaneously, there was transformation of high-grade metamorphic rocks into charnockites.

The Southern Granulite Terrane in Tamil Nadu and Kerala is, indeed, a petrochemically reconstituted and tectonically rejuvenated Early Proterozoic Mobile Belt.

2.3 Continent-Interior Later Proterozoic Sedimentary Basins

In front of early Proterozoic Mobile Belts, there are large basins of later Proterozoic sedimentary rocks that have escaped metamorphism, although they are structurally deformed in the proximity of the mobile belts. These basins came into existence in the aftermath of the Eastern Ghat Orogeny in the interval 1600 ± 100 Ma. The Cuddapah and Godavari basins lie to the west of the Eastern Ghat Mobile Belt, and the Vindhyan Basin lies within the arm of the parabolic Satpura–Aravali Mobile Belt.

In all these basins, the thick sedimentary successions are divided into two major groups by unconformities, commonly of the nature of a disconformity. The unconformities date to an event around 1000 ± 50 Ma. The lower part, including the Cuddapah in Andhra Pradesh, the Kaladgi in northern Karnataka, the Pakhal–Penganga in the Godavari Basin and the Semri in the Vindhyan Basin, consists of marine sediments associated with penecontemporaneous volcanics—lavas, agglomerates, tuffs and local ignimbrites. The carbonates at different stratigraphic levels are characterized by stromatolites that indicate their age between

1650 and 1350 Ma. The upper group, comprising the Kurnool (Cuddapah Basin), the Badami–Bhima (northern Karnataka), the Chhattisgarh (central India) and the Upper Vindhyan (Madhya Pradesh and Rajasthan) is made of sediments laid down by rivers and streams. The 1067 ± 31 Ma-old kimberlite pipe intruding the Upper Vindhyan sediments implies that the terrestrial sedimentation commenced well before 1100 Ma. The spectacularly developed stromatolites in the carbonate rocks in the top horizon place it in the time range of 680–570 Ma.

Across the Aravali Ranges in western Rajasthan, the widespread occurrence of granites (Erinpura Granite) and the acid volcanics (Malani Rhyolite) represent strong magmatic activities in the period 900–750 Ma.

2.4 Gondwana Basins

The valleys of the Damodar River in Jharkhand and Bengal, the Mahanadi in Odisha and Chhattisgarh, the Son in southern Uttar Pradesh, the Narmada in Madhya Pradesh and the Pranhita–Godavari in Andhra Pradesh occupy elongate sedimentary basins that evolved as a consequence of formations and eventual filling up with sediments of the grabens and half-grabens. Trending roughly E–W and NNW–SSE, these grabens were formed as a result of rifting of the Gondwanic landmass in the beginning of the Permian. The Gondwana Supergroup of the Gondwana basins comprises glacigene diamictites, in some places associated with marine sediments at the base, the terrestrial coal-bearing fluvial sediments in the middle and the fluvial–aeolian sediments in the upper part. In the southern part of the Pranhita–Godavari domain, there was intercalation of fluvial–deltaic with the marine sediments.

The sagging of the Gondwanaland, which was under cover of continental glaciers, invited marine incursion in the beginning of the Permian. Later, the burial of the forests and plant debris deposited by rivers gave rise to very rich deposits of coal. As the climate grew hot and arid, rivers deposited very ferruginous sediments that were locally reworked by winds into aeolian formations.

2.5 Cretaceous Volcanic Provinces

There are three major volcanic provinces in the Indian Shield which evolved as a result of large-scale volcanic eruptions and explosions during the Cretaceous period. Covering parts of Jharkhand, southern Meghalaya and the Sylhat region of Bangladesh, the Rajmahal Volcanics make the Rajmahal Hills in north-eastern Jharkhand. The lavas and tuffs are intercalated with sediments containing remains of plants of the Upper Gondwana time. The eruption took place in the interval 114–118 Ma.

Offshore north-western Karnataka in southern India, the Saint Mary's Islands are formed of nearly 86-million-year-old acidic lavas. These islands represent a centre of volcanism that preceded the gigantic outpouring of lavas in the land in the later Cretaceous time.

Forming flat-topped stepped plateaus—the Deccan Traps—the stupendous volumes of lavas with tuffs cover practically the whole of Maharashtra, the bordering areas of Karnataka and Telangana, the Malwa division of Madhya Pradesh and the Kachchh–Saurashtra region of Gujarat. The volcanic eruption commenced around 69 Ma and lasted until about 61 Ma, the bulk being emplaced at 65.5 Ma. The dykes, occurring in swarms in the Konkan Coast and in the valleys of the Tapi and Narmada rivers, are believed to have served as feeders of the lavas that flowed 100–300 km from their sources. Reactivation of ancient rift valleys was responsible for the emplacement of these dykes.

The flowing lavas dammed rivers and streams, giving rise to a multitude of lakes and swamps, which became the sanctuaries of animals (including dinosaurs) and plants. The lakes and swamps were eventually filled up with sediments. The sedimentary successions below the lava piles and interbedded with the flows are known as infratrappean beds and intertrappean beds, respectively. These beds contain rich assemblages of remains of the plants and animals that witnessed the tumultuous changes that the Deccan volcanism had brought about.

2.6 Pericratonic Sedimentary Basins of Peninsular India

Sedimentary formations ranging in age from the Upper Jurassic to the Quaternary occur in large discontinuous patches along the periphery of Peninsular India, from Kachchh in the west, through the Malabar and Coromandal coasts in the south, to Odisha in the east. The sedimentary successions represent the pericratonic basins that evolved following subsidence due to faulting of the coastal belts in the Mahanadi, Godavari–Krishna, Palar–Kaveri, Khambhat–Sabarmati and Kachchh sectors of the continental margin. The sedimentation in the fault-basins started in the Middle Jurassic in Kachchh and in the Upper Jurassic in the Coromandal belt. Northern Bangladesh and adjoining southern Meghalaya in the east and the Jaisalmer basins in western Rajasthan also come under the sway of marine transgression, of course at different times. An arm of the sea extended along the Narmada rift valley up to the historical Bagh Caves. The sedimentary deposits of all these basins provide accounts of the history of evolution of the land and life in the India continent.

In all these pericratonic basins, the lower parts of the sedimentary successions are made up of Mesozoic marine sediments intercalated with sediments of deltas of the rivers that brought terrestrial material, including the debris of the plants covering the Gondwanaland. The upper parts of the sedimentary piles are constituted of the Tertiary sediments, which cover much larger areas and form the continental

shelves and continental slopes in eastern and western seaboards. The lower part of the Tertiary successions consists of Palaeogene marine sediments, and the upper part is made up of deltaic sediments grading imperceptibly into fluvial sediments of the Neogene period.

The pericratonic sedimentary formations are of great economic importance as they host commercially productive petroleum fields.

2.7 Himalaya Mobile Belt

The arcuate Himalaya province, forming the wide northern fringe of the Indian continent, is a product of docking of India with Asia—which happened sometime in the time interval 65–55 Ma. In the north, its frontier is defined by the zone of Asia-India welding characterized by squeezed up, strongly deformed, broken fragments of seafloor with sediments of an oceanic trench. The southern boundary is demarcated by a series of reverse faults against the vast plains of northern India.

Between the two tectonic boundaries, the Himalaya Mobile Belt comprises five lithotectonically distinctive and geomorphologically contrasted terranes, each one separated from the other by boundary thrust faults of regional dimension. The northern part, known as the Tethys Himalaya, embodies a thick pile of sedimentary rocks ranging in age from the beginning of the Palaeozoic era to the end of Mesozoic, or locally early Tertiary. There are many long and short gaps in sedimentations, the most important being the one when there was widespread volcanic eruptions in lower Permian on a grand scale, as witnessed in the Pir Panjal in Kashmir and the Abor in eastern Arunachal Pradesh. An arm of the Tethys Sea had also transgressed into the southern border of the Himalaya, leaving behind marine sediments intimately associated with volcanic materials and fluvial sediments containing Gondwana coal with plant fossils.

The Phanerozoic pile of the Tethyan sediments rests (locally discordantly) on the foundation of high-grade metamorphic rocks intruded pervasively by Early Miocene (21 ± 2 Ma) granites. The crystalline rock complexes from the lofty, rugged Great Himalaya or the Himadri terrane. Across a boundary thrust to the south of the Himadri lies the Lesser Himalaya terrane of comparatively milder topography. This subprovince is made up of two parts, the Lower Proterozoic sedimentary pile and the upper imbricating succession of thrust sheets, or nappes, of metamorphic rocks. The sedimentary pile in the lower part comprises Early Proterozoic argilloarenaceous sedimentary rocks, beginning in some places with turbidites and diamictites. The upper part consists of dominant carbonate rocks and argillocalcaceous shales. The carbonate rocks are Later Proterozoic in age, characterized by 1000 ± 50 to 570 Ma-old stromatolites, and locally with rich lenticular deposits of magnesite and talc.

The lower thrust sheet or nappe is made up of low-grade metamorphics invariably associated with mylonitized porphyritic granites and quartz porphyries

belonging to the time interval 1900 ± 100 Ma. In some sectors, a facies variant consisting of quartzarenites interbedded with penecontemporaneous lavas and tuffs with agglomerates forms a disparate independent sheet. The upper nappe is constituted of medium-grade metamorphics penetrated on extensive scale by 500 ± 25 Ma-old Cambro-Ordovician granites.

South of the Lesser Himalaya is a narrow belt of Tertiary sedimentary rocks evolved in the foreland basin that came into existence in front of newly formed mountain as the Lesser Himalaya was thrust southwards and broke along a regional fault. These sediments in Pakistan and Assam hold reserves of petroleum oil and gas. Further southward thrusting of the Himalaya in the Middle Miocene time led to the formation of yet another foreland basin. It was rapidly filled up by great volumes of sediments brought down from the fast rising Himalaya by rivers and streams. The sedimentary pile eventually evolved into the Siwalik terrane.

Further tectonic deformation caused not only the faulting along transverse faults of the Himalaya Mobile Belt, but also the formation of a series of reverse faults parallel to the trend of the mountain which demarcate its southern boundary against the vast plains of northern India.

2.8 Indo-Gangetic Plains and Quaternary Cover of Peninsular India

South of the mountainous Himalaya Mobile Belt, stretching from the Sindhu delta in Pakistan to the Sundarban region in Bengal, are the vast plains of Quaternary sediments known as the Indo-Gangetic Plains. The plains are the outcome of rapid filling up of the foreland basin that was formed in front of the rising Siwalik Ranges. Presently, at the general altitude of 30–100 m above the mean sea level, the Quaternary sediments vary in thickness from less than 10 m in the southern margin to as much as 1500–2500 m in the northern part, in the Bihar–Uttar Pradesh sector. The Indo-Gangetic Plains comprise four major units. The Pleistocene Varanasi terrain, with ferruginous concretions in gravelly coarse sediments from the fringe of the Vindhya Ranges in the south, and the Holocene gravel fans make the Bhabhar apron along the foothills of the Siwalik. In between, the fluvial sediments deposited in the channels, flood plains, lakes and marshes form the Bhangar terraces. The wide, flat valley cuts that the meandering rivers made have been covered thickly with sediments, making the Khadar flats.

The southerly extension of the Sindhu Plains in the western Rajasthan is converted into a desert—the Thar—by the winds that have been blowing ever since aridity set in the later Pleistocene time. The desert domain extends south into Gujarat up to the valley of the Narmada Rivers.

Large parts of the deltaic regions in the riverine regimes of the eastern and western coastal belts have Quaternary covers.

2.9 Andaman Island Arc and Central Myanmar Plain

Constituting the central part of the Indonesia–Myanmar Mobile Belt, the 850-km-long chain of islands between the Bay of Bengal and the Andaman Sea makes the Andaman Island Arc. It comprises two nearly parallel arcuate belts. The western arc is represented by more than 300 islands of the Mentwai, Nicobar and Andaman groups. These islands are made up of successions of Cretaceous to Tertiary sedimentary rocks implanted at various levels with broken-up ocean floor and split up into a multiplicity of steeply dipping rocks of imbricating sheets. The evolutions of these islands are related to the continued underthrusting eastwards of the Indian

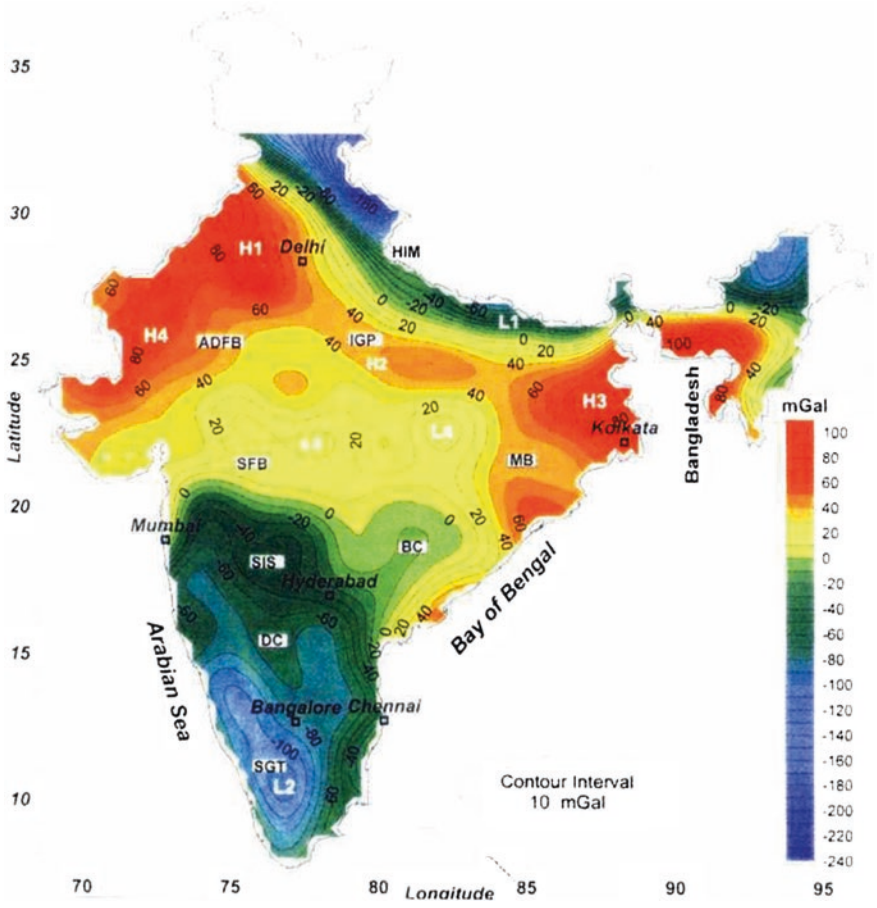

Plate 2.1 Bouguer anomaly (low pass-filtered) map of India with wave number <0.02 corresponding to wavelength of 300 km. L-1 and L-2 gravity lines; H-1 to H-4 gravity highs; *IGP* Indo-Gangetic Plains; *SGT* Southern Granulite Terrane; *DC* Dharwar Craton; *BC* Bastar Craton; *MB*; *SFB* Satpur Belt; *ADFB* Aravali Belt; *HIM* Himalayan Belt (Photo courtesy D.C Mishra NGRI, Hyderabad)

Ocean floor along the Java–Andaman Trench. This trench demarcates the boundary of the Andaman Island Arc. The chain of islands extends north into the land where it is represented by the Indo-Myanmar Border Range, with almost identical structural architecture and lithological setting (Plate 2.1).

The eastern arc embodies seamounts and volcanoes (dormant and active). The volcanoes are related to the actively spreading floor of the Andaman Sea, a back-arc basin. The volcanic island arc extends northwards into the Central Myanmar Plain, characterized by Miocene to Quaternary volcanoes in the alluvial expanse of the Irrawaddy River system.

On the inner (east) side of the volcanic island arc lies the Andaman Sea, the floor of which continues to spread out laterally. The northern part of this back-arc basin is being filled up with terrestrial sediments brought by the Salween, the Sittang and the Irrawaddy rivers. The northern extension into the land of the Andaman Sea basin has been completely filled with sediments delivered by the rivers of the Irrawaddy system and converted into a large alluvial plain—the Central Myanmar Plain.

Chapter 3
Archaean Craton: Southern India

3.1 Indian Shield

South of the Himalaya mountain arc, the Peninsular India is a shield comprising composite, consolidated and rigid crustal blocks of Archaean antiquity. These crustal blocks, which remained undeformed by compressional tectonism for very long geological periods, however, witnessed different degrees of extensional tectonism manifest in sagging down of the crust or its breaking into horsts and grabens. The Indian Shield is thus divided into various number of blocks described as *cratons*, *protocontinents* or *continental nuclei* (Naqvi et al. 1974; Radhakrishna and Naqvi 1986). The four well-defined cratons that constitute the Indian Shield are the *Dharwar Craton* in southern India, the *Bastar Craton* in central India, the *Singhbhum Craton* in eastern India and the *Bundelkhand Craton* in western India (Fig. 3.1).

The cratons contain the oldest granitic rocks of the Indian subcontinent—3.31 Ga in the Bundelkhand Craton, 3.56 Ga in the Singhbhum Craton, 3.01 Ga in the Bastar Craton and 3.20 to 3.40 Ga in the Dharwar Craton. It is inferred that these cratonic blocks have the oldest major components of 3.3 Ga, and which witnessed widespread cratonization events at 3.0 and 2.5 Ga.

The Son–Narmada rift valley demarcates the boundary of the Bundelkhand Craton against the Bastar and Singhbhum cratons. The Singhbhum Craton is separated from the Bastar Craton by the Mahanadi graben. The Godavari rift valley forms the dividing line between the Bastar and Dharwar cratons. The southern boundary of the Dharwar Craton against the Southern Granulite Terrane is formed by a system of shear zones—the Moyar–Bhavani Shear Zone in the north and the Palghat–Cauvery Shear Zone in the south (Fig. 3.2). Within the cratonic domains, slow vertical subsidence later gave rise to a number of intracratonic

K.S. Valdiya, *The Making of India*, Society of Earth Scientists Series,
DOI 10.1007/978-3-319-25029-8_3

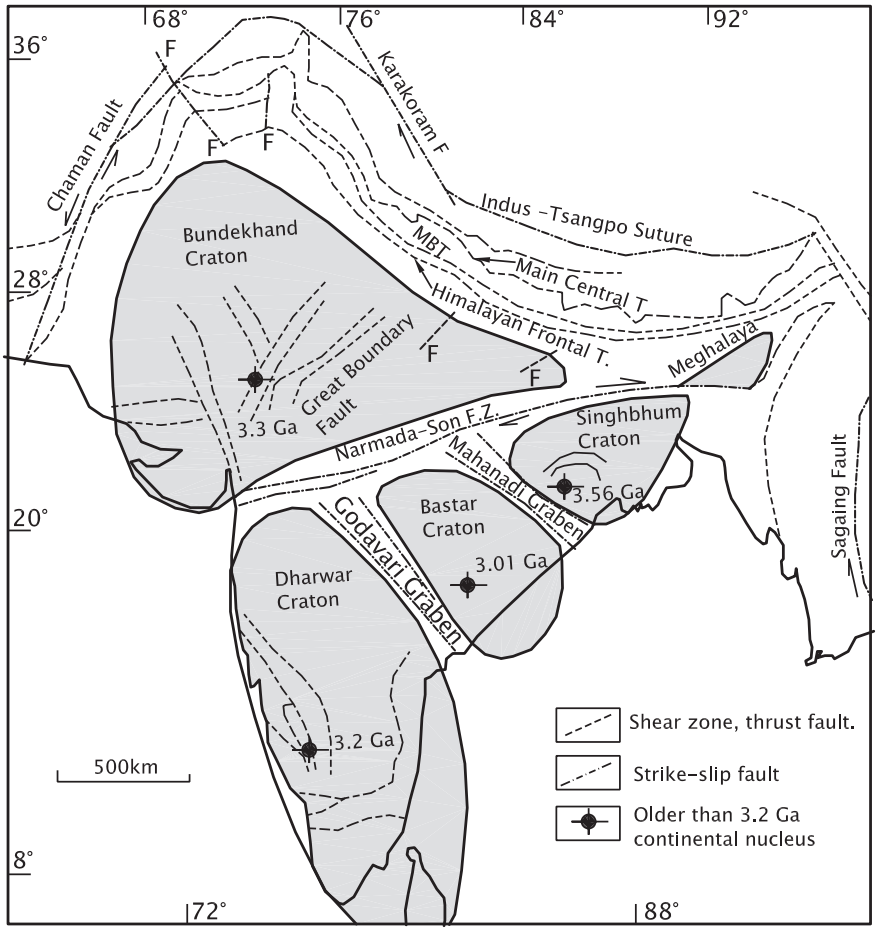

Fig. 3.1 Indian shield comprising four well-defined cratonic blocks made up of various rock complexes of Archaean antiquity. They embody the nuclei of the continental crust

basins of Proterozoic sedimentation such as the Cuddapah, Kaladgi and Bhima in the Dharwar; the Chhattisgarh, Indravati and Abujhmar in the Bastar; and the Vindhyan in the Bundelkhand. Prior to the Proterozoic basin development, there were quite a few events of crustal rifting and sagging or sinking of dismembered blocks, attendant volcanism, followed by transpressional deformation, pervasive metamorphism and plutonism or charnockitization. These processes culminated in the welding of the crustal blocks into composite rigid cratons. The mosaic of these four cratons constitutes the Indian Shield.

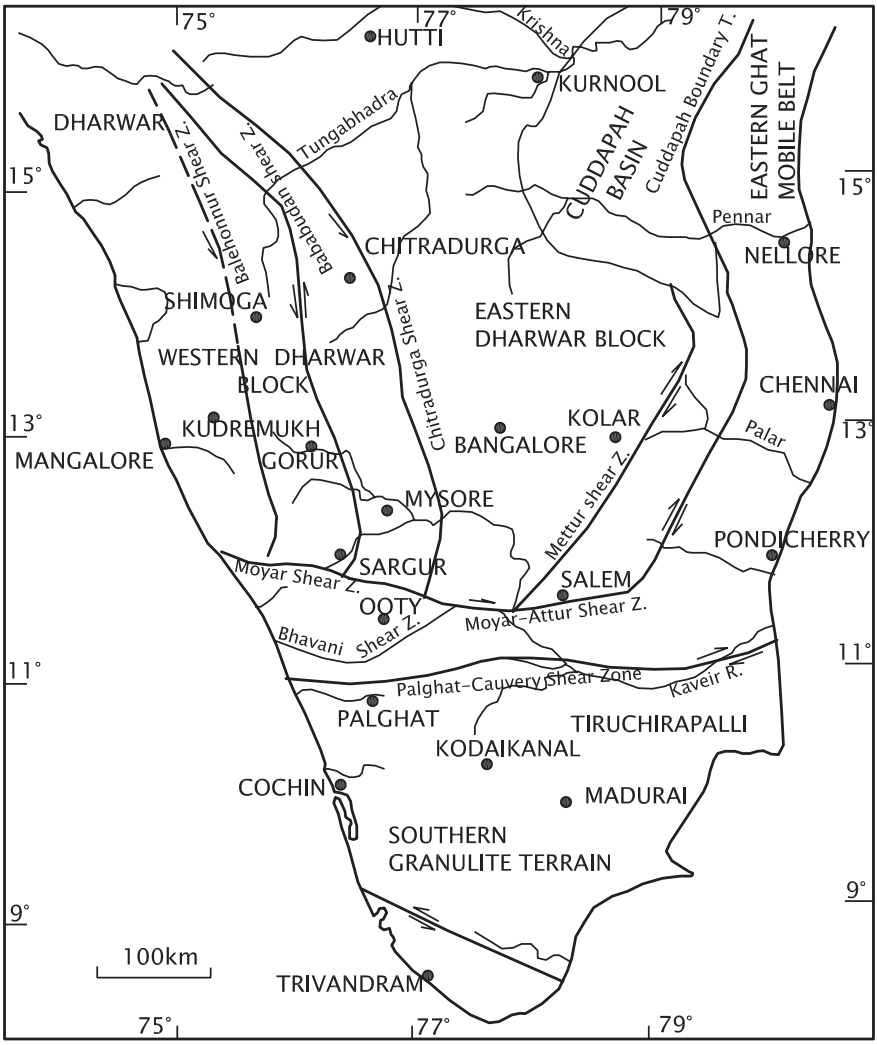

Fig. 3.2 Sketch map of southern India showing the Dharwar Craton and its tectonic boundaries against younger terranes (after Ramakrishnan 2003)

3.2 Dharwar Craton: Crustal Structure

Extending from coast to coast, and covering a vast geographic expanse of Goa, Karnataka, north-western Tamil Nadu and Andhra Pradesh, the Dharwar Craton embodies gneisses and granites of at least three generations, volcanics of two main phases and thick sedimentary successions of two periods, emplaced both on shallow-water platforms and in deep-water basins. The temporal range of these rocks is ~3300–2550 Ma—embracing the entire spectrum of the Archaean era. These

rock successions experienced regional deformation and metamorphism, the intensity of which increases progressively from green schist–lower amphibolite grade in the north to granulite grade in the south.

The cratonic terrane derives its name from the township Dharwar in north-western Karnataka where it was first studied in detail by R.B. Foote in 1882. The seminal contributions of pioneers such as R.B. Foote, W.F. Smeeth, Sampat Iyengar and B. Rama Rao laid the foundation of the geology of this most complex terrane of the Indian subcontinent.

3.2.1 Faulted Terrane

Deep seismic sounding across southern India from Kavali on the east coast to Udupi in the west coast revealed 15 major mantle-reaching faults, 15 intermediate-depth faults or shear zones and two major thrusts within a stretch of about 600 km, dividing the cratonic crust into seventeen linear blocks (Fig. 3.3) (Kaila et al.

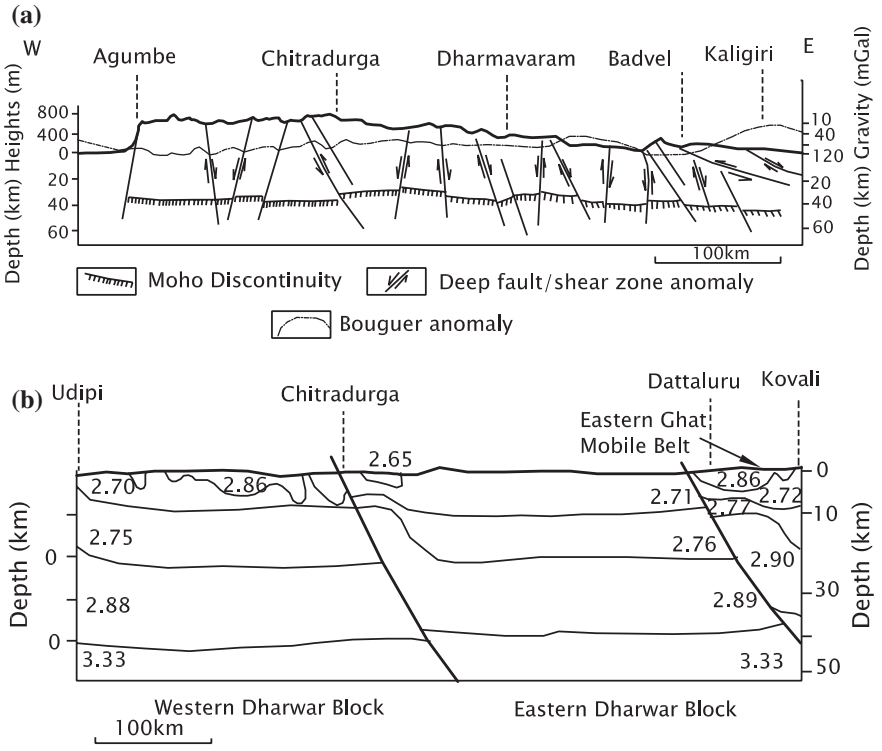

Fig. 3.3 **a** DSS profile across the Dharwar Craton along an east–west line showing the crust broken by faults and thrusts into seventeen blocks (simplified after Kaila et al. 1979). **b** The Dharwar Craton is divided into eastern and western blocks of differing thickness and composition (modified after Singh et al. 2004)

1979). They are responsible for the formation of depressions and uplifted ridges. The development of the present-day 700 -to 900-m-high Mysore Plateau surrounded on three sides by high horst mountains more than 1400, 1800 and 2500 m in elevation is due to the reactivation of these and other faults of Precambrian antiquity (Valdiya 1998, 2001a).

Deep seismic refraction studies demonstrate that of the three prominent N–S to NNW–SSE trending strike-slip faults and thrusts—the one that divides the Dharwar Craton into eastern and western blocks is traceable for about 380 km from SE of Mysore to Gadag in the north. The eastern block is relatively thinner compared to the western block. Two N–S to NNE–SSW trending thrust planes on the eastern margin of the Chitradurga Schist Belt register large-scale westward thrusting of rocks and are responsible for thickening of the crust under the Chitradurga–Shimoga belt. Over this belt, one can see an elongate pattern of gravity high anomaly (Fig. 3.4), and the contact of the schist belt with the surrounding gneisses exhibits steep gravity gradient (Narain and Subrahmanyam 1986).

Significantly, aeromagnetic anomalies and teleseismic receiver function modelling across the Dharwar Craton show that west to east the thickness is variable. Compared to 35 km in the Eastern Dharwar Craton, the crustal thickness in the

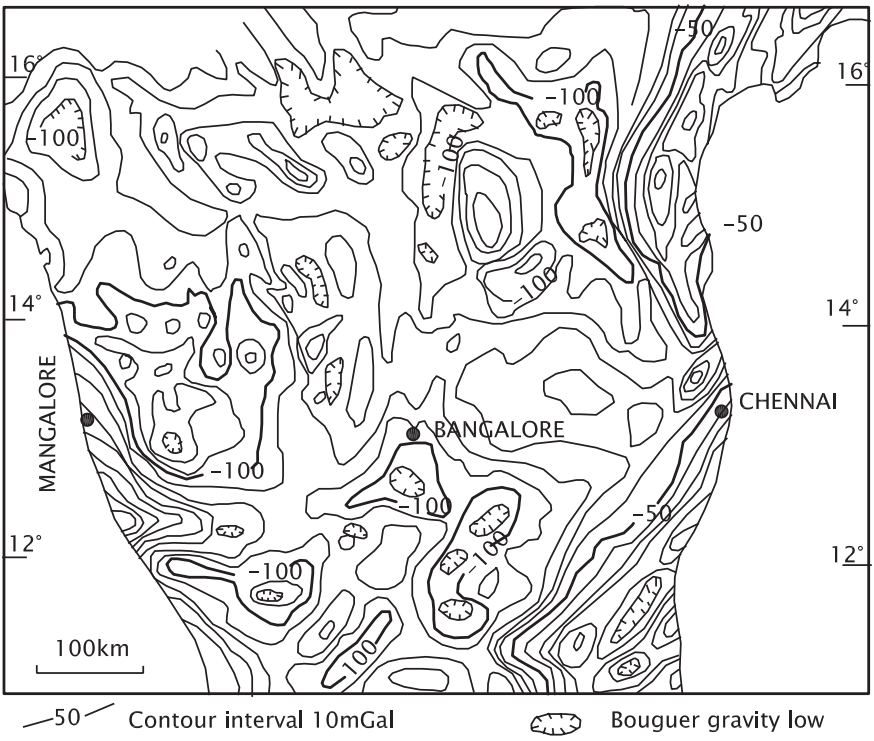

Fig. 3.4 Bouguer gravity anomaly over the Dharwar Craton and adjoining terranes (after Verma 1985)

Western Dharwar Graton is 35–40 km (Reddy et al. 2000; Anand and Rajaram 2002; Prakasam and Rai 2003; Gupta et al. 2003).

The average heat flow in the Western Dharwar Cratonic block is 31 ± 4 mW/m^2 compared to 47 ± 8 mW/m^2 in the Southern Granulite Terrain (Gupta et al. 1991). Immediately north of the Palghat–Cauvery Shear Zone the heat flow is in the range of 28–42 mW/m^2.

3.2.2 Tectonic Boundaries

A large part of the north-eastern Dharwar Craton (Fig. 3.2) is under the cover of Proterozoic sedimentary successions represented by the Kaladgi, the Bhima and the Cuddapah Supergroups. The western margin of the Dharwar Craton is marked by 1000 m to more than 1800-m-high Central Sahyadri Range, characterized by its more than 700-m-high Western Ghat escarpment. The southern margin of the Dharwar Craton is marked by a system of shear zones extending east–west from coast to coast. This 60- to 80-km-wide shear zone system is defined in the north by the *Moyar–Bhavani Shear Zone* and in the south by the *Palghat–Cauvery Shear Zone* (Figs. 3.2 and 3.5). The NNW–SSE trending tracts of aeromagnetic anomalies in the Dharwar Craton (Plate 3.1) are abruptly replaced by the E–W-oriented magnetic anomaly zones of this shear zone system (Rajaram and Harikumar 2001). Between the transcurrent shear zone system contains a number of prominent massifs of rocks very similar in composition and age to those of the southern part of the Dharwar Craton encompassing the Kodagu and Biligirirangan–Mahadeswaramalai Hills.

Taking into consideration a variety of evidence, it seems that the Palghat–Cauvery Shear Zone is the real boundary of the Craton. Some workers believe that the Palghat–Cauvery Shear Zone, like the Moyar–Bhavani Shear Zone, represents an oblique-slip dextral shear system that brought about horizontal displacement of the order of tens of kilometres (Drury et al. 1984; Ramakrishnan 1993, 2003; Chetty and Bhaskar Rao 2006). There is a structural difference in the magnetic crust of the two terranes—in contrast to 36–40 km thickness of the Dharwar crust, the magnetic sources extend up to the depth of only 22 km in the Southern Granulite Terrane (Rajaram et al. 2001).

3.2.3 Intracratonic Shear Zone

The Dharwar Craton is cut by a number of NNW–SSE to N–S trending faults and shear zones. One of these faults divides it into two blocks of slightly different constitution and crustal thickness—the eastern block and the western block (Fig. 3.2). In addition, there are nearly east–west trending lineations which swing from ENE–WSW direction to ESE–WNW orientation (Figs. 3.2 and 3.5). Some of them represent shear zones.

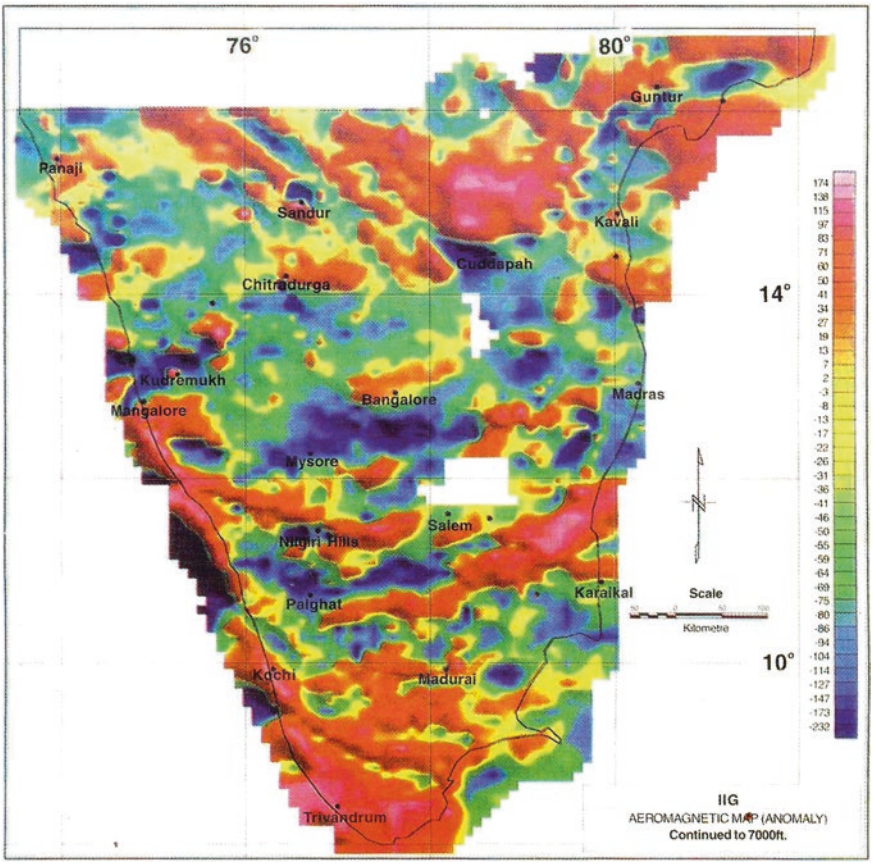

Plate 3.1 Aeromagnetic map of southern Peninsular India bringing our NW-SE to NNW-SSE trending anomaly belts in the Dharwar Craton, in sharp contrast to pronounced E-W-oriented anomaly zones south of the tectonic boundary Mayar-Attur Shear Zone (from Hari Kumar et al. 2000)

The Moyar–Bhavani Shear Zone, continuing eastwards as the Attur Shear Zone in the southern part of the Dharwar Province, is the most prominent one. It is traced westwards through the mouth of the Ponnani River in the western coast, causing sinistral shift of rock formations (Ramasamy 1995). Some of the NNW–SSE to N–S trending faults gently swing westwards and appear to merge with the E–W-oriented Moyar–Bhavani–Attur Shear Zone. The 20-km-wide Moyar Shear Zone (Nair et al. 1981; Drury et al. 1984; Chetty 1996) separating the Nilgiri massif from the Dharwar terrane is marked by 60–80°S-dipping thrust planes. The Bhavani Shear Zone along the southern limit of the Nilgiri is characterized by mylonites and northward-inclined shears recording dip-slip displacement (Srikantappa and Narasimha 1988; Naha and Srinivasan 1996). It seems that the dominantly rock assemblage of the Nilgiri has been thrust up and pushed northwards onto the Dharwar Craton along the steeply dipping imbricate thrust faults,

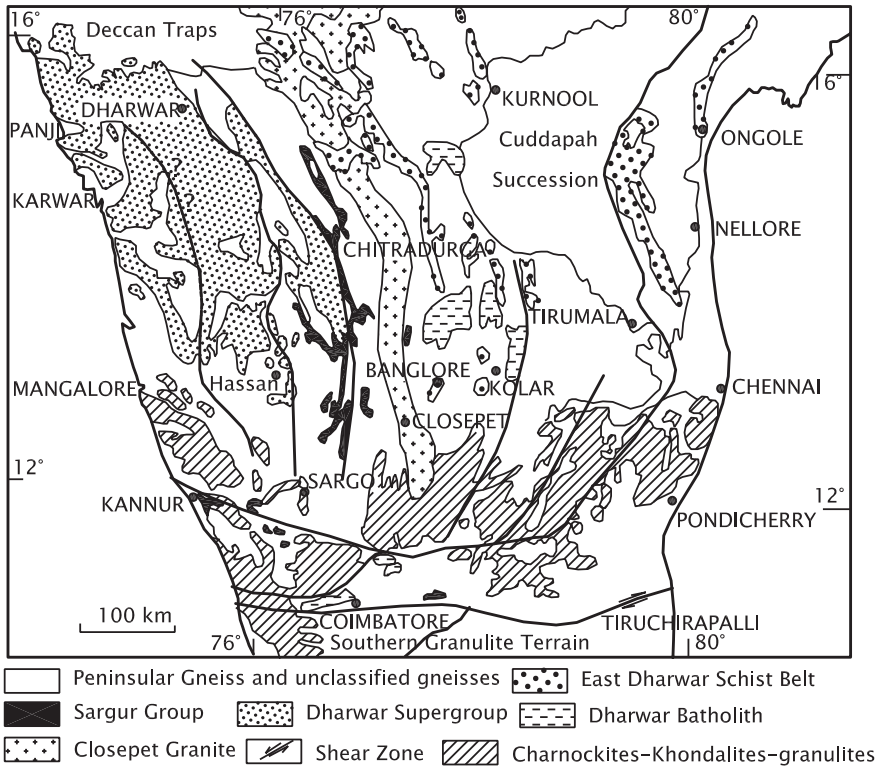

Fig. 3.5 Sketch map showing the geology of the Dharwar Craton and the adjoining terranes (after *Geological Map* of *India* published in 1993 by the Geological Survey of India, Kolkata)

leading to exhumation—exposure on the surface—of deep-seated rocks and the emergence of more than 2500-m-high Nilgiri block (Valdiya 1998, 2001; Raith et al. 1999). Presence of discrete blocks of serpentinized ultrabasic rocks in the Moyar–Bhavani Shear Zone implies that the faults are of crustal scale.

The most prominent NNW–SSE trending intracratonic fault, as already stated, is the one that marks the eastern margin of what is known as the Chitradurga Schist Belt in the north and forms the western boundary of the more than 600-m-high west-facing scarp of the Biligirirangan Hills (Fig. 3.5). This strike-slip sinistral fault is listric and designated as the *Chitradurga Boundary Fault* (Ramakrishnan 1994, 2003; Chadwick et al. 2007). The faults defining the tectonic boundaries of the Bababudan and Shimoga domains are also sinistral strike-slip faults. However, the fault that demarcates the eastern limit of the Closepet Granite (Figs. 3.2 and 3.5) shows dextral strike-slip. As already stated, the Chitradurga Boundary Fault divides the Dharwar Craton into eastern and western blocks. Among many differences, the western block comprises two generations of granitic rocks of the ages 3400 and 3000 Ma in contrast to overwhelmingly 2600–2500 Ma granites in the eastern block. The 3400–3300 Ma

tonalite–trondhjemite–granodiorite complex intimately associated with the 3200 Ma ultrabasic and high-grade metamorphic rocks constitutes what could be described as the *nucleus of the Dharwar Craton* (Naqvi et al. 1974, 2006; Radhakrishna and Naqvi 1986).

The 2- to 3-km-wide ductile shear zone separating the Western Dharwar Craton from the Eastern Dharwar Craton exhibits sinistral transpression movement and is occupied by syntectonic Granite at Bhukkapatna (Sengupta and Ray 2012). Along the shear zone is juxtaposed a terrane of two different structural architecture—the eastern block has a geometry of gently dipping structures in this terrane.

3.2.4 Lithostratigraphy

Notwithstanding tremendous amount of work done, the picture of the lithostratigraphic framework of the Dharwar Craton is baffling. Radiometric dating has, however, helped in removing to some extent the mist of uncertainty. A simplified lithostratigraphy is presented in this chapter without going into the controversies.

Six main lithotectonic units or terranes are recognizable in the Dharwar Craton. All of them have suffered widespread metamorphism, the degree of which varies from unit to unit. On the whole, the grade of metamorphism increases from north to south. The 3300- to 3400-Ma-old *Gorur Gneiss* is intimately associated with basic and ultrabasic rocks locally interleaved with pelitic-siliceous sediments make up the *Sargur Group;* these formations are typically exposed in the Gorur–Holenarasipur belt near Hassan. The 3000 Ma old *Peninsular Gneiss* is made up of tonalite–trondhjemite–granodiorite and forms larger part of the western block of the Craton. The *Dharwar Supergroup* comprises a thick pile of volcanosedimentary rocks resting unconformably on the gneissic basement and occurs in the western block in broad basins, and in the eastern block as narrow elongate N/NNW–S/SSE trending linear belts described as *Greenstone Belt* or *Schist Belt*. The dominantly potassic granites and gneissic granites of the temporal span 2600–2500 Ma forming the bulk of the eastern block of the Dharwar Craton are known as the *Dharwar Batholith*. One of these bodies is the *Closepet Granite* occurring to the east of the Chitradurga Boundary Fault. The granulite–charnockite–gneiss assemblage, associated with banded iron chert-quartzite-marble and amphibolite, dominates the southern part of the Dharwar Craton (Fig. 3.5).

3.3 Gorur Gneiss

The Gorur Gneiss occupies the nucleus of the Dharwar Craton (Naqvi et al. 1974). The low initial strontium ratio varying between 0.7000 ± 0.0004 and 0.7011 ± 0.0006 implies that the igneous precursors of the Gorur were derived from the relatively Rb-depleted source in the mantle and emplaced synkinematically

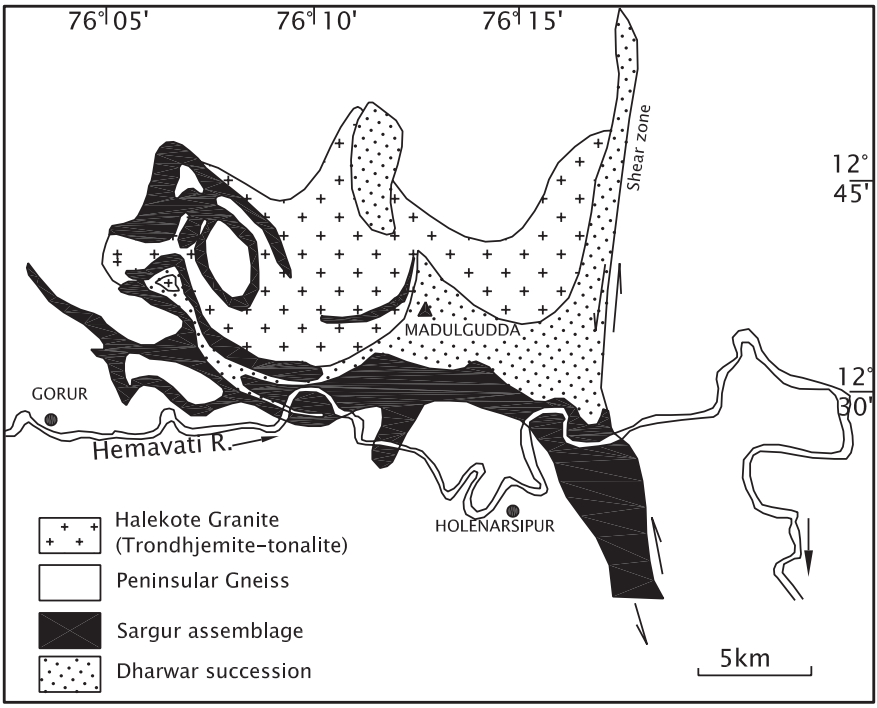

Fig. 3.6 In the Holenarsipur belt in Hassan district, the Gorur Gneiss is intimately associated with basic and ultrabasic magmatic rocks of the Sargur Group. It represents the oldest component of the early sialic crust (after Hussain and Naqvi 1988)

during one of the earliest events of deformation witnessed by the Craton. Intimately associated with the schist belt of Holenarasipur in Hassan district (Fig. 3.6), the Gorur Gneiss is marked by strong E–W gneissosity, parallel to the axial planes of early-formed isoclinal folds. The Gorur is possibly a part of the earliest sialic component in the craton, as evident from its Rb–Sr whole-rock isochron age of 3315 ± 54 Ma and Pb–Pb isochron age of 3305 ± 13 Ma (Beckinsale et al. 1980), 3204 ± 30 Ma (Bhaskar Rao et al. 1992). Far to the north-west, the Anmodghat Gneiss in Goa yields a Pb–Pb age of 3400 ± 140 Ma (Dhaundial et al. 1987).

3.4 Sargur Group

3.4.1 Composition

Identified as an independent oldest lithostratigraphic unit of the Dharwar Craton, the *Sargur Group* is represented by minor linear belts and enclaves of basic–ultrabasic magmatic rocks and pelitic-siliceous-carbonate-rich carbonaceous

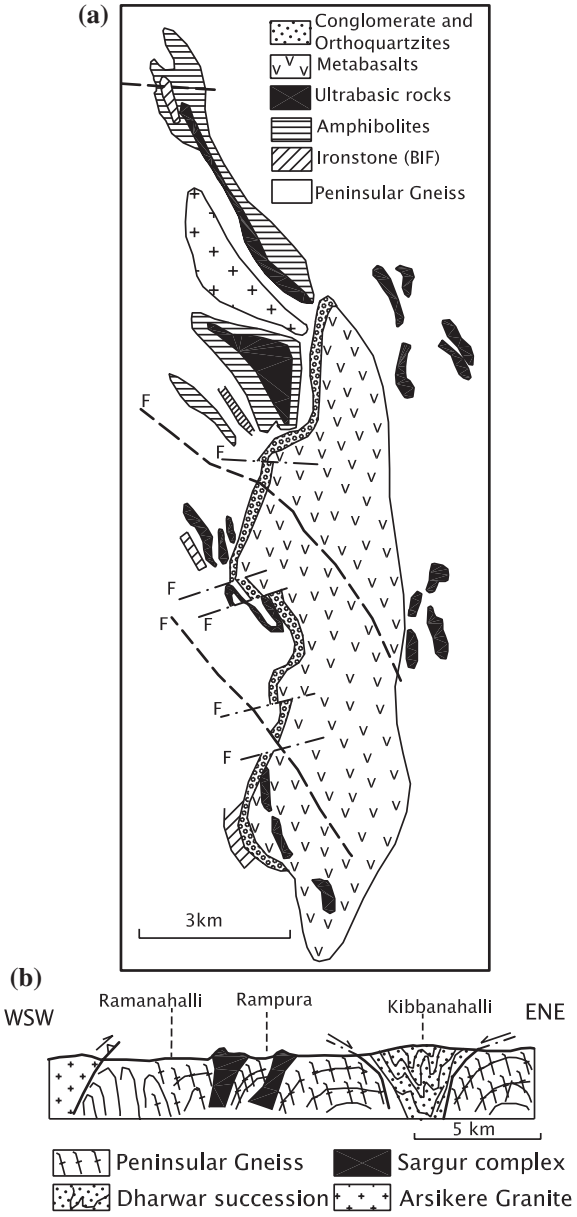

Fig. 3.7 **a** In the Sigegudda belt, the Sargur, the Peninsular Gneiss and the Bababudan Formation of the Dharwar Supergroup (excluding dykes) are clearly distinguishable, the latter two separated from one another by an unconformity (Viswanatha et al. 1982). **b** Interpretative cross section through the Jayachamarajapura area showing the complexity of structure in which the Sargur is caught (after Chardon and Chakroune 1996)

metasediments (Figs. 3.6 and 3.7). They are spread over mainly in the southern part of Karnataka, e.g. Sargur, Dodkanya, Gundlupet and Jayachamarajapura (Viswanatha et al. 1982; Swami Nath et al. 1976; Swaminath and Ramkrishnan 1981; Janardhan et al. 1979; Viswanatha et al. 1982). The Sargur rocks near Hassan are tectonically interleaved with the Gorur Gneiss of the basement, and

elsewhere in the Craton is massively invaded by granitic rocks of the Peninsular Gneiss (Ramakrishnan 1994). The principal igneous components are peridotites, pyroxenites and komatiitic amphibolite with localized occurrence of anorthosite, gabbro and norite interlayered with spinifex-textured komatiite pillow lavas (Hussain and Naqvi 1988). Some workers believe that the Sargur of the Holenarsipur belt (Peucat et al. 1995) (Fig. 3.6) is a product of an accretionary process in an oceanic trench environment (Kunugiza et al. 1996). The basaltic komatiite preserving pillows, ocelli and spinifex texture and the associated peridotite occurring with chert-ferruginous chert quartzite and marble strata in the Jayachamarajapura area (Venkatadasu et al. 1991) corroborate the deduction that the Sargur rocks represent a shallow to deep basin environment.

3.4.2 Metamorphism

The rocks of the Sargur complex have undergone upper amphibolite-grade metamorphism at 700 ± 30 °C and 8.6 ± 0.8 kbar, and its basic–ultrabasic components converted to a schistose assemblage comprising antigorite ± chlorite ± magnetite ± magnesite ± siderite (Srikantappa et al. 1985). The associated volcanosedimentary rocks were metamorphosed to an assemblage of kyanite-staurolite-quartz-plagioclase ± fuchsite ± graphite ± corundum ± sillimanite as seen at Hullahalli, Dodkanya and Satyamangalam where the temperature rose to 767 ± 50 °C and pressure to 8–9 kbar (Janardhan and Gopalkrishna 1983).

3.4.3 Age

The metapelites-associated ultrabasic rocks contain detrital zircon dated 3309 ± 5 Ma by SHRIMP U/Pb method (Bhaskar Rao et al. 1992). In the Nuggihalli area, the chromite-bearing ultrabasic rocks (Varadarajan 1970) are intimately associated with metasediments. The Pb–Pb zircon from the metasediments is dated 3200 Ma (Bidyananda et al. 2003). The stratiform Honnavalli anorthosite complex in Holenarsipur area gave Sm–Nd whole-rock isochron age of 3285 ± 17 Ma (Bhaskar Rao et al. 2000). Komatiites from the Sargur belt define Sm–Nd whole-rock isochron age of 3352 ± 100 Ma (Jayananda et al. 2006). Associated with pillow lavas, the komatiitic mafic rocks of Nagamangala give Sm–Nd whole-rock isochron age of 3352 ± 110 Ma, the time of its eruption (Jayananda et al. 2012). From the available geochronological data, it is evident that there was an unbroken succession of ultrabasic, basic and acidic plutonism in the Sargur Basin where pelitic and siliceous sediments were laid down in a time prior to 3000 Ma.

3.5 Peninsular Gneiss

3.5.1 Composition

West of the Chitradurga Boundary Fault, the larger part of the western block of the Dharwar Craton is made up of gneisses of tonalite–trondhjemite–granodiorite composition. The name was given in 1915 by W.F. Smeeth, who thought the whole of the Peninsular India is made up predominantly of granitic gneisses. Indeed, the *Peninsular Gneiss* is the largest lithological unit of the Southern Indian Shield (Fig. 3.5). The name was given in 1915 by W.F. Smeeth. It is an intriguingly complex assemblage of granitic rocks, possibly formed as a result of more than one process—intrusion, migmatization and granitization in perhaps several phases. This is evident from the diversity of composition and the degree of deformation (Rama Rao 1940; Divakara Rao et al. 1974; Radhakrishna 1974; Chadwick et al. 1981; Bhaskar Rao et al. 1991; Naha et al. 1993).

There is another view that the volcanosedimentary rocks of the Sargur and the Dharwar successions form one unbroken unit, and the Peninsular Gneiss is a younger emplacement (Pichamuthu 1961, 1962; Naha et al. 1990; Srinivasan 1988). Some of workers consider the Gorur Gneiss as a part of the Peninsular Gneiss. This assumption carries the implication that the Peninsular Gneiss constitutes the oldest component of the Dharwar Craton.

3.5.2 Age

Zircon from the Peninsular Gneiss at Kabbaladurga was dated 2963 ± 4 Ma by SHRIMP U/Pb method (Friend and Nutman 1991). Relatively undeformed diapiric trondhjemite at 3000 Ma marks the time of the stabilization of the gneissic terrane (Rogers and Mauldin 1994).

3.5.3 Deformation

The Peninsular Gneiss (Fig. 3.8) is characterized by elongate belts and island-like enclaves of schistose rocks. These schists exhibit shallow to steeply dipping schistosity and lineation. Local domal structures are seen (Bouhallier et al. 1995). The style and sequence of deformation of the gneisses and schists are the same and related to the first-phase isoclinal folding (Naha et al. 1990). The earlier folds were refolded into upright folds.

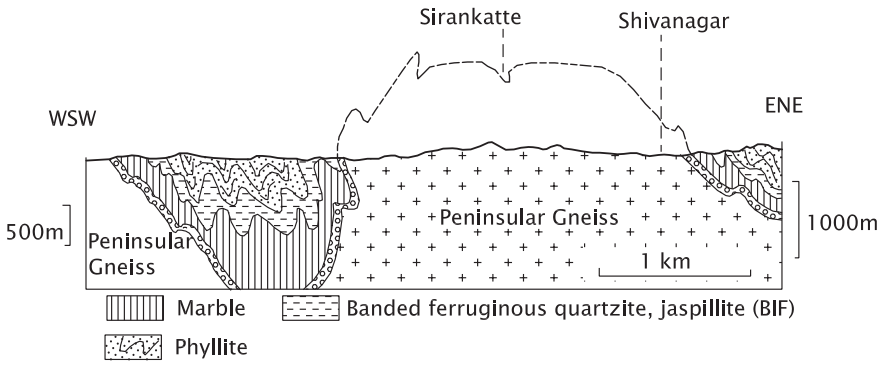

Fig. 3.8 Cross section of a part of the Dharwar Craton in the Chitradurga Basin showing unity of structure of the Peninsular Gneiss with that of the Dharwar succession. This unity is in terms of style and sequence of deformation (modified after Naha et al. 1990)

3.6 Dharwar Supergroup

3.6.1 Basal Unconformity

After a prolonged period of denudation and possible peneplanation, the Dharwar sedimentation commenced in the Kudremukh, Shimoga, Bababudan and Chitradurga basins with widespread emplacement of oligomictic conglomerates (Swami Nath et al. 1976; Radhakrishna and Naqvi 1986; Chadwick et al. 1988, 1992). The Dharwar sediments rest unconformably also on the Sargurs as seen in the Sigegudda belt (Fig. 3.7), and at the base of the Bababudan succession near Karthikere (Fig. 3.9). The metamorphic and structural characteristics change across the unconformity in the Jayachamarajapura area (Viswanatha et al. 1982; Ramakrishnan and Viswanatha 1987). Whereas the Sargur and the Peninsular Gneiss were affected by the first phase of deformation giving rise to dome-and-basin structure, the Dharwars developed a complex geometry of synclines, produced by the second phase of deformation (Chardon and Choukroune 1996). The contact between the two units is discordant.

3.6.2 Lithostratigraphy and Sedimentation

The Dharwar Supergroup (named by Foote in 1882) is divided into the *Bababudan Group* and the *Chitradurga Group* (Fig. 3.10). The two are separated by an unconformity. The Bababudan comprises basal oligomictic conglomerates, overlain by cross-bedded quartz-arenites, stromatolitic carbonates and banded ferruginous chert (described as *Banded Iron Formation* or BIF). The clastic sediments of the Bababudan represent a shallow water platform deposit. In some belts, the

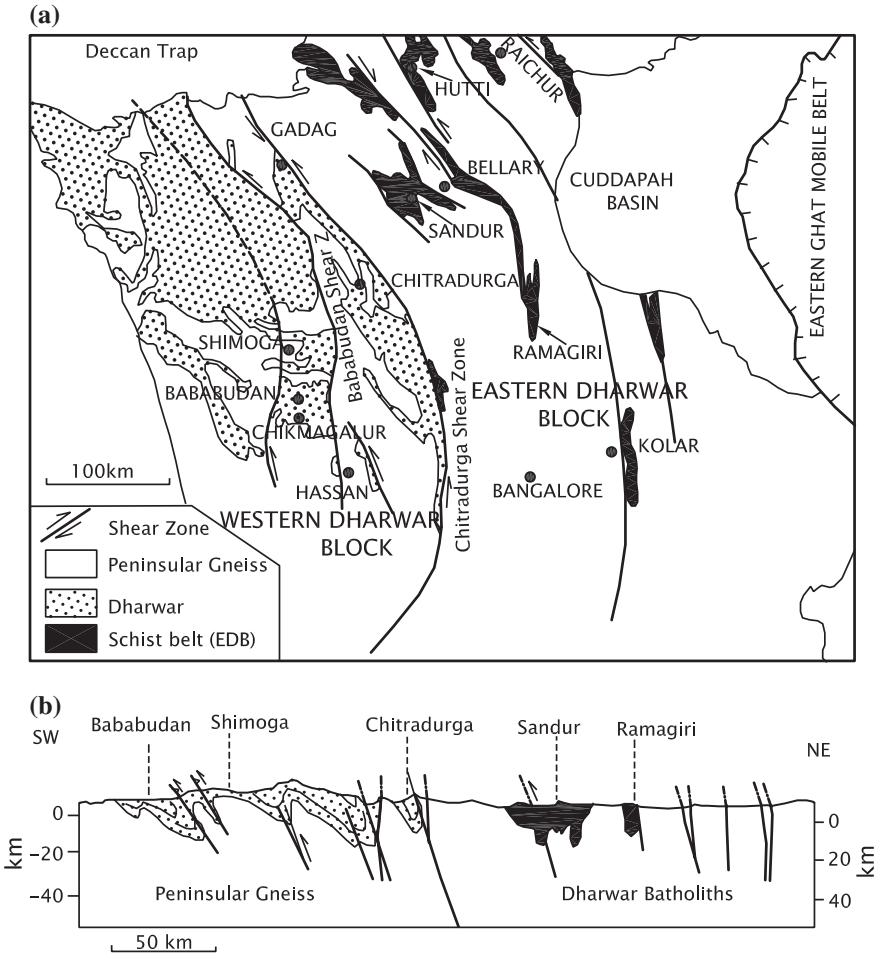

Fig. 3.9 **a** The main lithostratigraphic units of the Dharwar Craton (based on Chadwick et al. 2003). **b** Section across the Dharwar Craton in the NE–SW direction showing relationship between the Peninsular Gneiss and the Dharwar volcanosedimentary succession known as "greenstone belt" or "schist belt" (after Chadwick et al. 2000)

sedimentary strata are interbedded with basic volcanic rocks with pyroxenite and gabbro in the lower part and felsic porphyry, lava and tuff in the upper part of the stratigraphic succession. The *Chitradurga Group* is made up of more than 1000-m-thick succession of polymictic conglomerate at the base; limestones and dolomites and banded ferruginous chert with manganese ore formation in the middle; and greywackes, carbonaceous phyllite and rhythmic alternation of chert and ferruginous silica in the upper part of the sequence. In the Shimoga Basin, the greywackes and banded iron formation are characterized by synsedimentary slump structures, implying tectonic instability in the basin. The instability

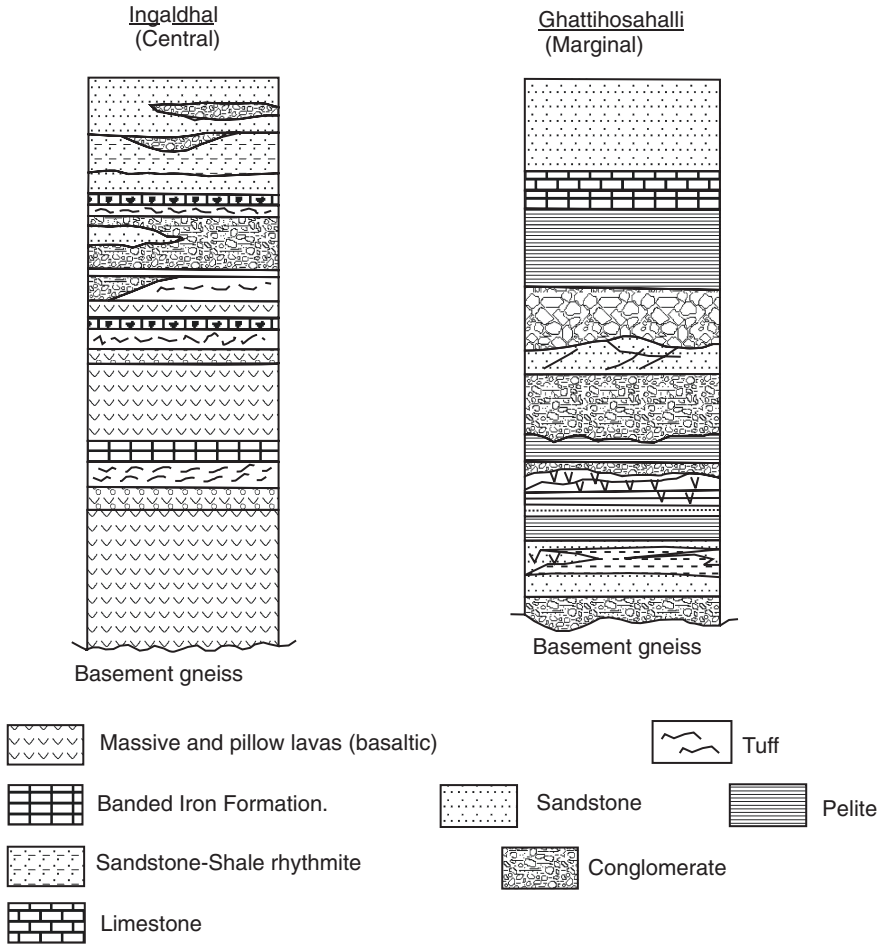

Fig. 3.10 Lithology of the Dharwar Supergroup in the Chitradurga domain (after Bhattacharyya et al. 1988)

manifested itself also in rapid subsidence of the basin floor and debris-flow deposits during the later stage of the Chitradurga sedimentation (Chadwick et al. 1988). Associated with predominant volcanics with some ultrabasics, the Chitradurga succession represents deposit of a deep-water basin. The strongly banded sedimentary succession of the Chiknayakanhalli belt comprising four main facies of oxides, oxides + silicates, oxides + silicates + carbonates and carbonates represents a product of inorganic chemical precipitation (Devaraju et al. 1986).

Associated with current-bedded and ripple-marked quartzites and with conglomerate, the basaltic rocks exhibit pillow structure, first described in 1937 by B.N. Ranganatha Roa from the neighbourhood of Madadakere in the Chitradurga area. The volcanics are characterized by spinifex texture and pillow structure

in lavas, the composition of which varies from basalt to rhyolite as seen in the Kibbanahalli area. The Kudremukh lavas are enriched in LREE and depleted in Sr. The oxidic banded iron formation is characterized by depletion in LREE, Zr, Hf, Cr, Co, Ni, Nb, Ta, V, Sc and Y and enrichment in La, strong positive Eu anomaly. The sulphidic banded iron ore formation exhibits increased LREE–HREE, Hf–Zr, Cr–Zr, Rb–Sr, V–Sc, Nb–Ta and Nd–Fe ratios, implying derivation of their iron from hydrothermal sources related to volcanism under water (Khan et al. 1992; Gnaneshwara Rao and Naqvi 1995). The detrital minerals and the REE pattern of the greywackes of the Chitradurga succession indicate a provenance of gneissic granites in Chitradurga region and of volcanic rocks in the Gadag area in the north (Naqvi 1985; Srinivasan et al. 1989).

The thick sequence of the Dharwar Supergroup between Dharwar and Goa comprises greywackes and conglomeratic greywacke interbedded with banded iron quartzites, carbonates and at the top the mafic volcanic rocks. The volcanic rocks are predominantly tuffaceous, now metamorphosed to chlorite–sericite schists, while the greywackes contain fragments of felsic volcanics embedded in a matrix enriched in Rb, B, Sr, Th, U, Cu, Zr and Ce/Li and depleted in Cr and Ni, indicative of the submarine felsic volcanism playing the prominent role in their emplacement (Devaraju et al. 2010).

3.6.3 Temporal Span

Sm–Nd whole-rock isochron age of the Bababudan volcanics is 2911 ± 49 Ma at Kalasapur and 2848 ± 70 Ma at Santiveri (Anil Kumar et al. 1996). The average is 2700 Ma. The Chitradurga volcanics yielded a Sm–Nd age of 2748 ± 15 Ma (Anil Kumar et al. 1996), whereas the laterally equivalent acidic volcanics of the Daginkatta sequence in the Shimoga Basin gave SHRIMP U/Pb zircon age of 2614 ± 8 Ma (Nutman et al. 1996). The SHRIMP U/Pb age for zircon from the tuff occurring close to the base of the banded iron formation is 2720 ± 7 Ma (Trendall et al. 1997) (Fig. 3.11).

3.7 Structural Architecture of Western Block

Peninsular Gneiss associated with schists and quartzites is characterized by isoclinal structures. The gneisses reacted with ductile deformation and were extensively remobilized, perhaps in different phases. Detailed structural studies in different belts of the Dharwar Supergroup (Mukhopadhyay 1986; Naha et al. 1990, 1993, 1994; Srinivasan et al. 1989; Chadwick et al. 1991, 2000; Mukhopadhyay et al. 1997) demonstrate a structural architecture marked by (1) upright folds having steep axial planes striking N–S and the superposition of folds resulting in the evolution of domal structures; and (2) upwarp along nearly E–W axis. The

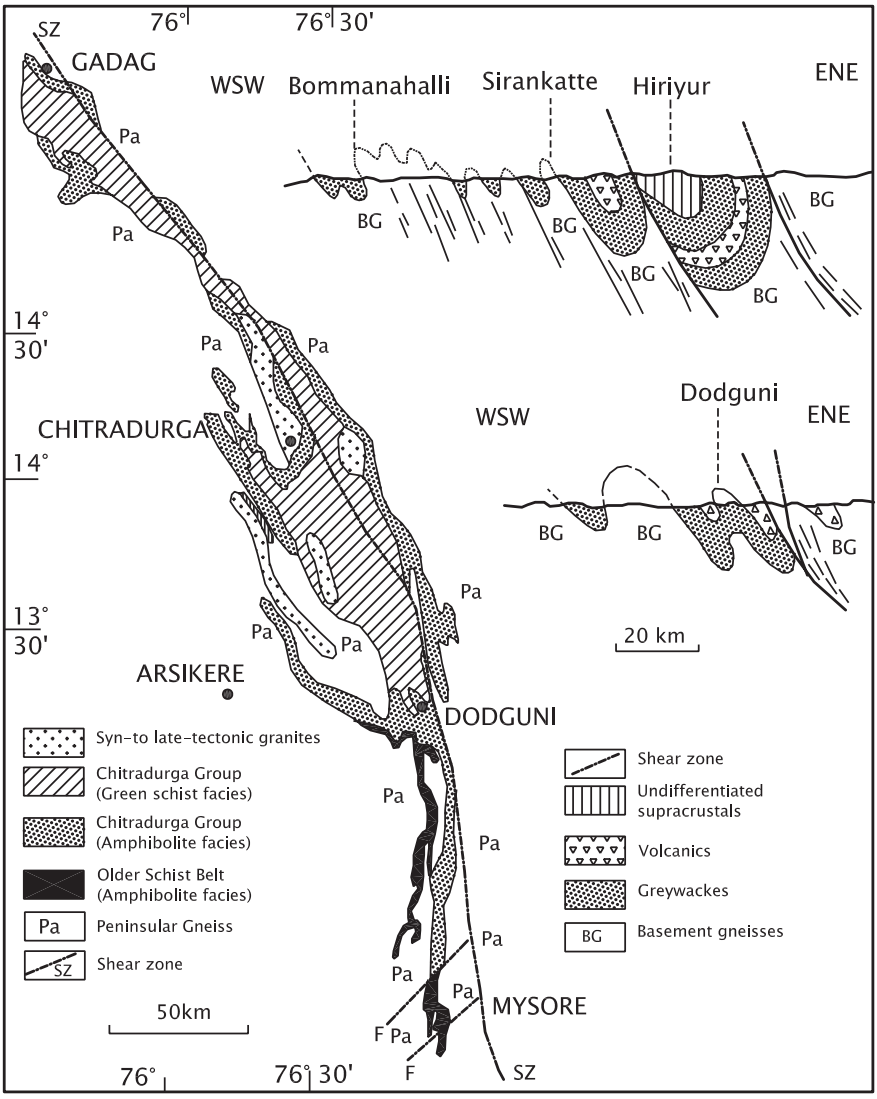

Fig. 3.11 Generalized geological map of the Chitradurga Schist Belt (after Naqvi 1985). *Cross section* showing interpretation of regional structural architecture (after Drury et al. 1984)

deformation along the ENE–WSW axis accentuated the earlier evolved culminations and depressions. Later, strike-slip displacement on steep N–S shear zones modified the earlier formed folds to S-verging structures.

It is inferred that the Sargur attained its peak of metamorphism during the first phase of deformation coinciding with the Dharwar deformation more than 3000 million years ago. The second phase of deformation seems to have reached its closing stage in the 2600 Ma time (Jayanand et al. 2006). The younger phase of

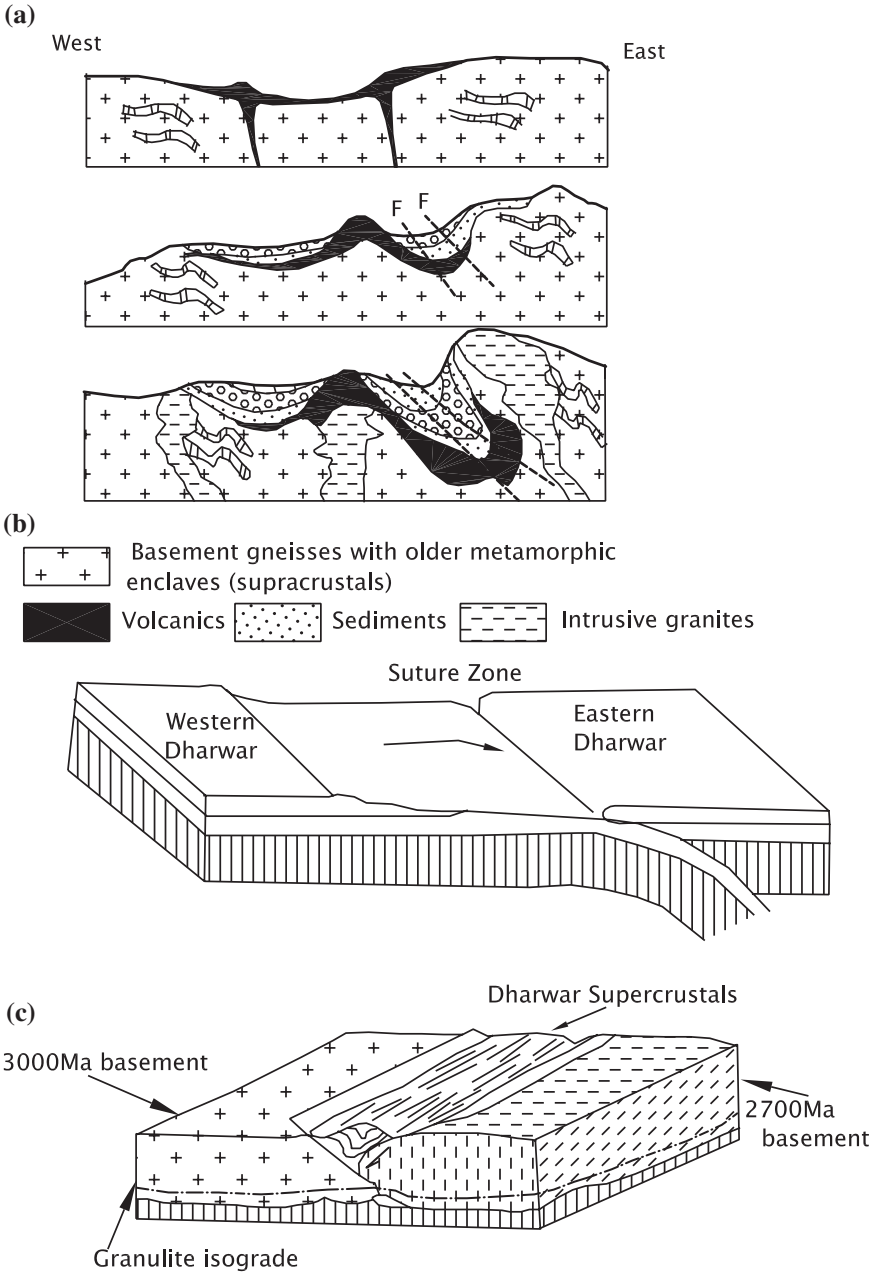

Fig. 3.12 Three different models of the evolution of the Dharwar Craton. **a** Evolution of the Chitradurga Schist Belt epitomizes the evolutionary developments that took place in the Dharwar Craton (after Bhattacharyya et al. 1988). **b** Convergence of the eastern block of the Dharwar Craton towards the western block (after Singh et al. 2004). **c** Development of intracratonic basin of the nature of half graben in the initial stage and magmatic accretion towards the Late Archaean time (after Chardon et al. 2002)

deformation that gave rise to broadly E–W shear zones occurred towards the end of the Archaean and beginning of the Proterozoic (Mukhopadhyay 1986). In the outer margin of the accretionary complex adjacent to the Chitradurga Schist Belt, the granites (SHRIMP U/Pb zircon ages of 2648 ± 40 Ma, 2598 ± 19 Ma and 2600 Ma) occur as steep sheets or wedges emplaced mostly during the southward lasting overturning of folds, resulting in the thickening of the crust. This was the time when there were strike-slip displacements parallel to the trend of the origin (Chadwick et al. 1989, 2007).

The Chitradurga Basin of the Dharwar sedimentation developed as a consequence of strike-slip or oblique-slip movement on a long-lived fault zone in the transcurrent–plate interaction period. The extension or stretching of the basin floor (Fig. 3.12) resulting in the formation of faults provided passage to outwelling lavas (Bhattacharyya et al. 1988). The other view is that it was an oceanic basin and the Chitradurga volcanics represent an island arc (Naqvi et al. 1974).

3.8 Schists Belts in Eastern Block

Adjacent to the Chitradurga Schist Belt, two granite bodies, respectively, 50 and 80 km NW of Chitradurga town, emplaced as sheet-oriented NW–SE, give SHRIMP U–Pb zircon ages of 2648 ± 19 Ma (Chadwick et al. 2007). A mylonitized granite body is dated ~2600 Ma. The aluminous sedimentary rocks occurring in the central part of the Eastern Dharwar Craton were metamorphosed in the temporal interval 2625 ± 26 Ma at temperatures 780–820 °C and pressure nearly 5 kbar (Jayananda et al. 2011). The grains of monazite in the metamorphic rocks have 3161 ± 78 Ma-old core.

Within the granitic gneiss terrane in the eastern block of the Dharwar Craton occur long linear belts of what were earlier described as *greenstone belts* and are known as *schist belts* (Figs. 3.5 and 3.9). The schist belts comprise predominant basic volcanics, including pillow lavas, and felsic volcanics, including pyroclastic rocks with subordinate clastic sediments.

In the north-western part of the eastern block, the *Sandur Schist Belt* comprises six lithostratigraphic units, the volcanics predominating the others in the 3500-m-thick succession of shallow marine sediments (Fig. 3.13). The *Sandur* volcanics comprise tholeiitic pillow basalts and high-Mg basalts, in addition to komatiitic ultrabasic rocks interbedded with sulphide-bearing banded iron formation, argillites, carbonaceous phyllites and carbonates (Manikyamba and Naqvi 1995; Naqvi et al. 2002). The Fe–Mn horizon of the banded iron formation represents a deposit of marine shelf in which Fe and Mn were added by hydrothermal activity related to a spreading ridge or vent. The REE pattern, HFSE content and Nd ratio indicate derivation of the magma of the volcanics from a mantle source, but probably contaminated by crustal material during its upward movement. The SHRIMP U/Pb ages for zircons from the acid volcanics of the Vibhutigudda

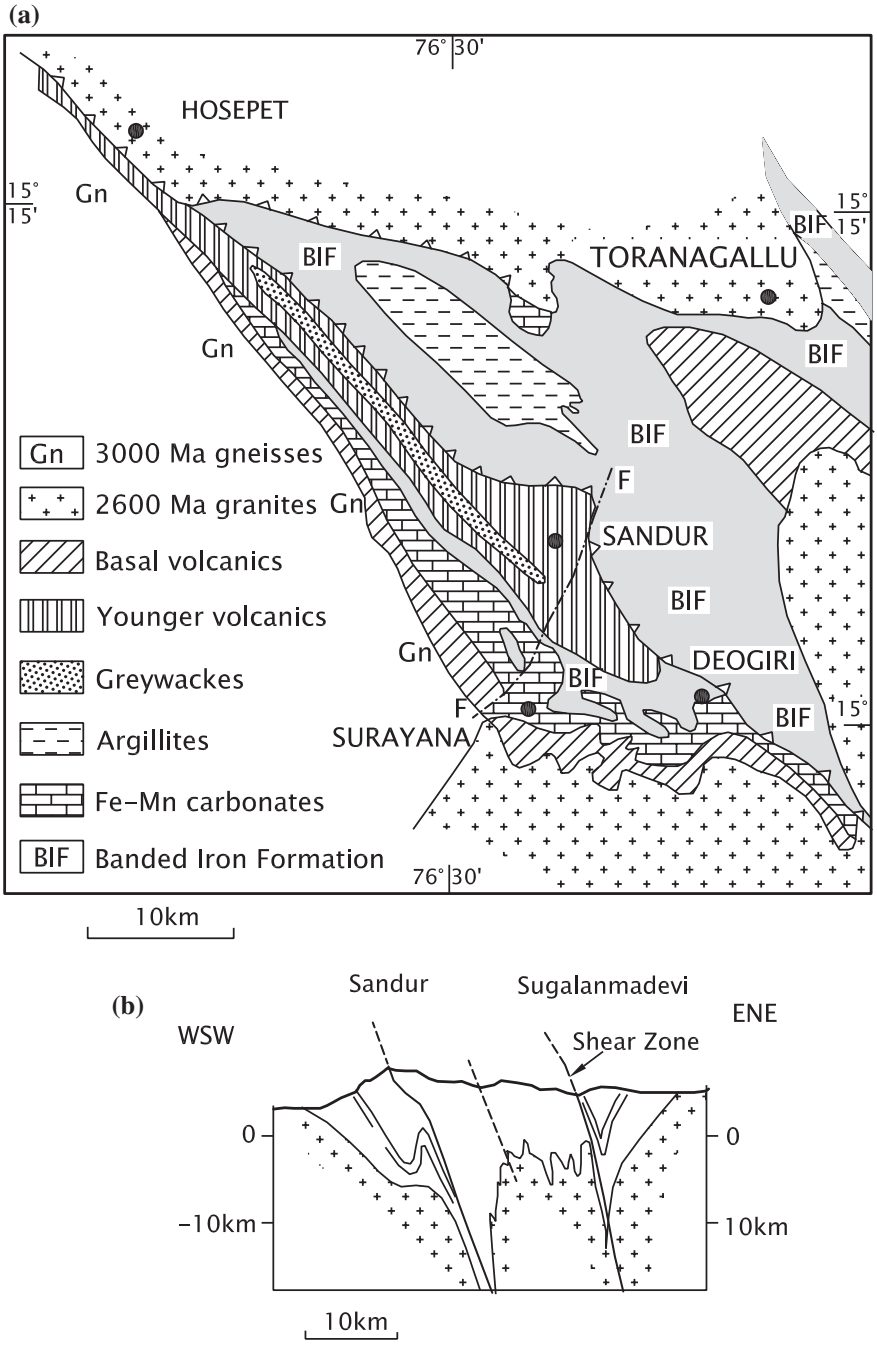

Fig. 3.13 **a** Simplified geological map of the Sandur Schist Belt (Manikyamba and Naqvi 1995). **b** Section across the Sandur Schist Belt illustrating its structural design (after Chadwick et al. 1996)

section are 2658 ± 14 Ma and 2691 ± 18 Ma (Nutman et al. 1996). Significantly, the adjacent granite is dated 2570 ± 60 Ma.

In the Sandur Schist Belt, the deformed margins of the belt (Mukhopadhyay and Matin 1993) were intruded by syntectonic granite of the Late Archaean time when the belt was subjected to sinistral transpression (Chadwick et al. 1996).

The *Hutti Schist Belt* (Fig. 3.14) is made up of predominant metavolcanics, minor felsic volcanics, and polymictite conglomerate (with its 2576 ± 12 Ma old clasts of granodiorite set in the matrix of greywacke) and greyish quartz wacke characterized by convolute structure and graded bedding, indicating emplacement in an environment affected by turbidity currents (Vasudev et al. 2000). The

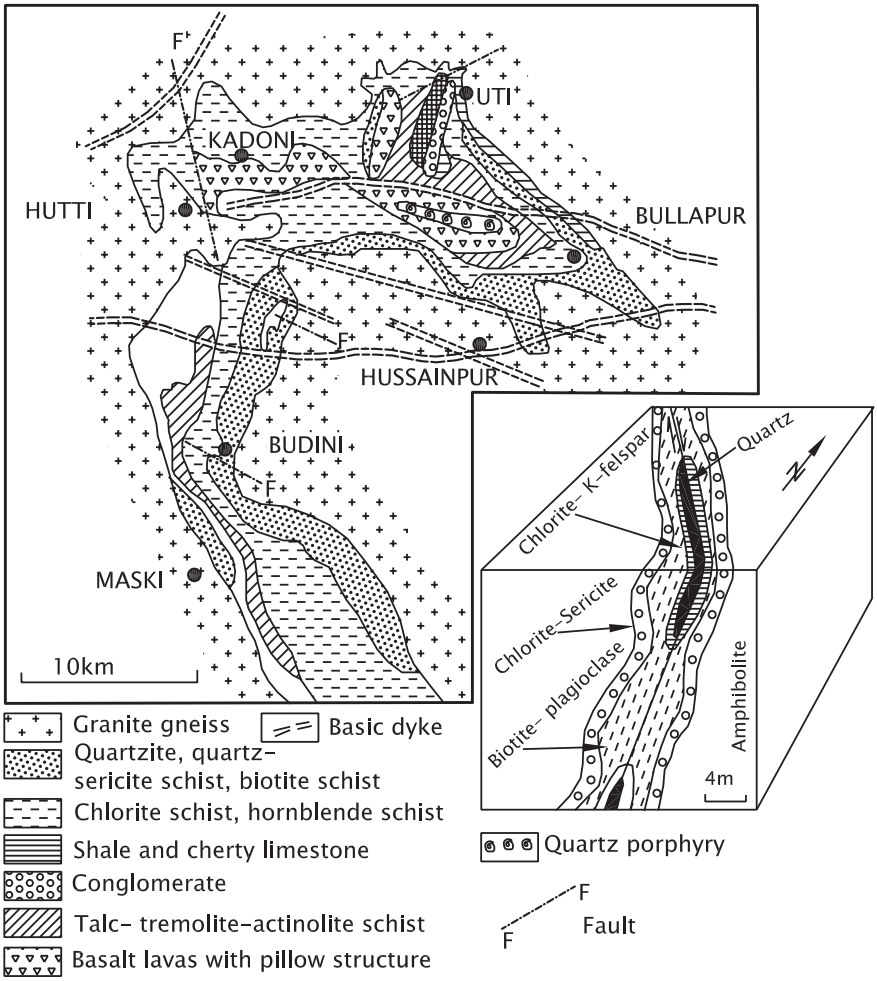

Fig. 3.14 **a** Simplified geological map of the Hutti Schist Belt (after Rajamani 1990). **b** Block diagram exhibiting spatial distribution of laminated quartz veins and alteration zones in the quartz-bearing shear zones (after Kolb et al. 2004)

tholeiitic volcanics, characterized by flat to LREE-enriched REE pattern, were derived from enriched mantle source (Anantha Iyer and Vasudev 1979; Giritharan and Rajamani 1978).

The central block of the *Ramagiri Schist Belt* represents a tectonic melange made up of basaltic and felsic bimodal lavas intermixed with minor amounts of clastic sediments. The tholeiitic volcanics containing sulphide minerals are characterized by higher abundances of Fe and LREE-enrichment and fractionated REE pattern, implying derivation from a mantle source. It has been interpreted as an emplacement in an island-arc setting, the lensoid bodies of serpentinite occurring within the highly sheared gneisses in the western part regarded as slices of the obducted oceanic material (Zachariah et al. 1996).

The Kushtagi–Hungund greenstone belt in the Eastern Dharwar Block comprises high-magnesian-iron basalts, high-magnesian dacites and andesites of boninitic affinity together with felsic rock adakite produced by partial melting of different suites of mantle and slab (Naqvi et al. 2006).

The gold-bearing volcanics of the *Kolar Schist Belt* (Fig. 3.15) are characterized by LILE enrichment and slightly enriched LREE pattern—the compositional characteristics compatible with volcanics of the marginal basin (Anantha Iyer and Vasudev 1979). The emplacement of komatiitic basalts is attributed to rift-related volcanism, possibly associated with plume activity (Rajamani et al. 1985; Rajamani 1990). It is believed that the Eastern Dharwar Block is a terrane resulting from accretion, i.e. addition of rock assemblages. The green belts represent intra-arc basins. The other view is that the basin must have developed due to the sagging of the crust, subjected to horizontal stretching in the N–S direction in an intracratonic setting (Chardon et al. 2002). Granite was emplaced syntectonically along the margin. It seems that the mantle-plume activity at the base of the crust was probably responsible for large-scale magmatism and lateral spreading of the crust.

The 600-km-long and 130-km-wide *Nellore Schist Belt* extending from Nellore to Khammam is sandwiched between the Eastern Ghat Mobile Belt and the Proterozoic Cuddapah Basin. Its boundary is defined by a low-angle fault system (Ramam and Murthy 1997). In the Nellore Schist Belt, amphibolite of tholeiitic composition is characterized by variable incompatible trace-element abundances, relatively constant transition element values and constant ratio of highly compatible elements, and enrichment as well as depletion of LREE. The chemistry implies dynamic melting within a single column of mantle having variable mineralogy and sources (Vijay Kumar et al. 2006).

Forming the eastern margin of the Eastern Dharwar Craton, the *Nellore Schist Belt* includes Kundra gabbro and Damaru gabbroic anorthosite, the former dated (Sm–Nd whole-rock isochron) 1926 ± 110 Ma, and the latter 1882 ± 116 Ma (Ravi Kant 2010). In the eastern extremity along the contact of the Eastern Dharwar Craton with the Eastern Ghat Mobile Belt, the ophiolites occurring at Kandra and Kadur are 1850 Ma old, as the SHRIMP and RG U–Pb zircon dating shows. Furthermore, the geochemistry of these ophiolites recalls that of mid-oceanic ridge basalts (Vijayakumar et al. 2010).

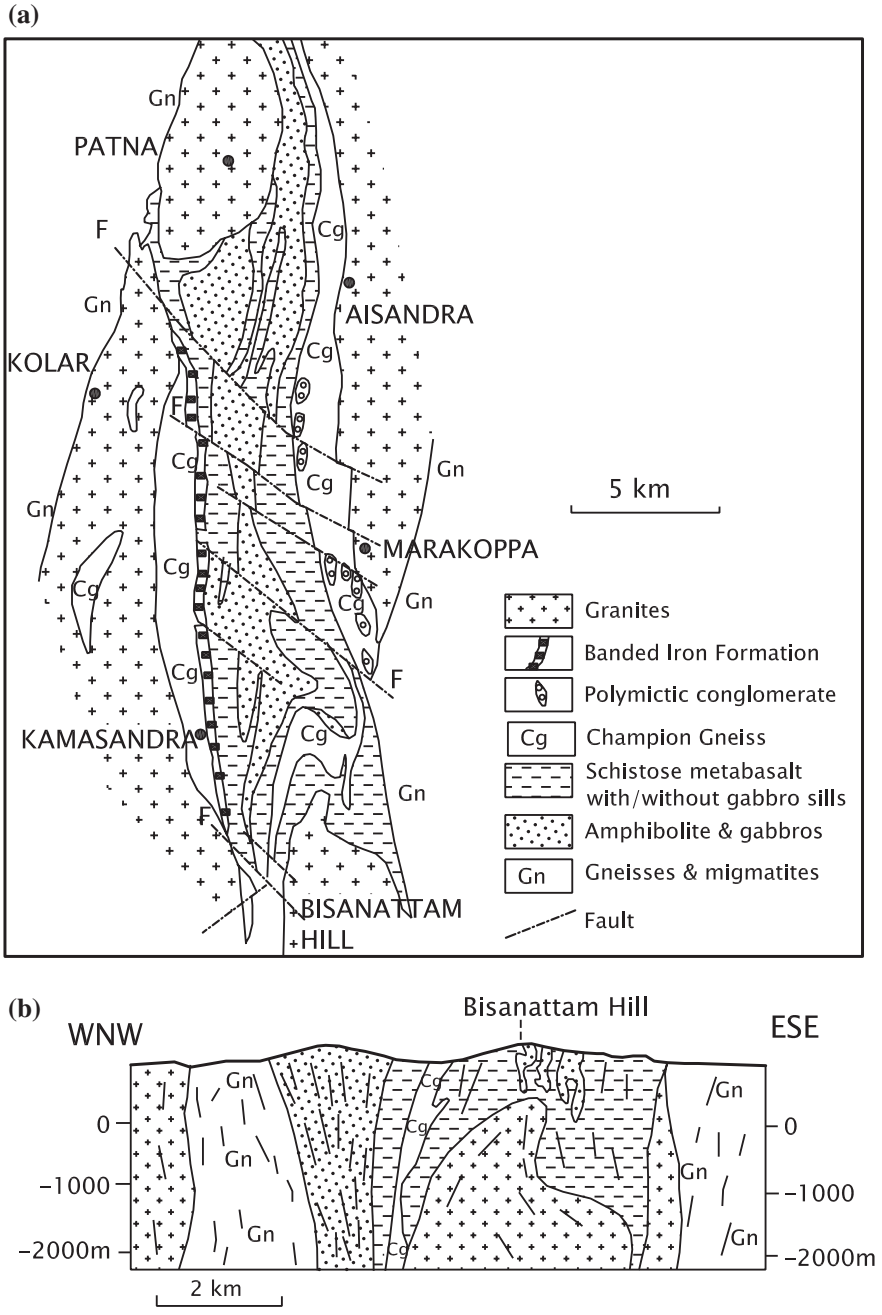

Fig. 3.15 **a** Geological map of the central segment of the Kolar Schist Belt. **b** Cross section of the southern part of the Kolar Gold Field illustrating the structural design of the Kolar Schist Belt (after Chardon et al. 2002)

It may be mentioned that the Sm–Nd and Rb–Sr mineral isochron ages of amphibolites, respectively, at 824 ± 45 Ma and 481 ± 16 Ma imply that there was another metamorphic reconstitution during revival of tectonism in the Proterozoic era and during the Pan-African tectonothermal event at the end of the Neoproterozoic (Okudaira et al. 2001).

The dome-shaped *Inukurti Anorthosite* within the Nellore Schist Belt was deformed and metamorphosed under amphibolite facies conditions at 644–570 °C and 7.6–2.7 kbar, as it followed the decompression path related to exhumation (Narasimha Reddy et al. 2003). In the eastern periphery of the Nellore Schist Belt—and south of Udayagiri—occurs a 40 km by 4 km NW–SE trending body of *Kandra Volcanics*. Represented by amphibolites, schists, pillow lavas including amygdaloidal basalts, and gabbros, the Kandra suite is recognized as an ophiolitic complex (Leelanandam 1990; Leelanandam et al. 2006). However, its magmatic stratigraphy is imperfect and incomplete. More likely, it is a part of the Nellore Schist Belt.

3.9 Closepet Granite

3.9.1 Composition

Typically exposed at Closepet (the old name for Ramanagaram), the Closepet Granite forms 400-km-long and 20- to 30-km-wide linear hill range in the midst of the peneplaned terrane of gneisses (Radhakrishna 1956). The name was given by B. Jayaram in 1912. It extends from Kabbaldurga in the south to beyond Bellary in the north (Figs. 3.5 and 3.16). It shows no substantial effects of deformation (foliation along its margin) and there are no signs of metamorphism. The Closepet Granite is a composite body of predominant potash-rich adamellite, quartz-monzonite and granite. There is considerable variation of composition from north to south, principally because different structural levels of the body from deeper in the northern region to shallower in the southern part are exposed on the surface (Moyen et al. 2003). The occurrence of ductile mylonites and augen gneiss along the margins of the granite plutons and locally well inside the main body indicates shearing during the emplacement of the granite (Jayananda and Mahabaleswar 1991). It is believed that the Closepet batholith was emplaced along a crustal-scale shear zone during the Late Archaean time. It is a sheet-like pluton forming a part of the Dharwar Batholith in the eastern block of the Craton (Friend 1984; Friend and Nutman 1991; Moyen et al. 2003).

3.9.2 Genesis

REE pattern, Ce_N/Yb_N and La_N/Yb_N ratios of the Closepet Granite constituents suggest that the bulk of the pluton is formed of material derived by crustal melting and attendant metasomatism (Divakara Rao et al. 1990). The other view is that

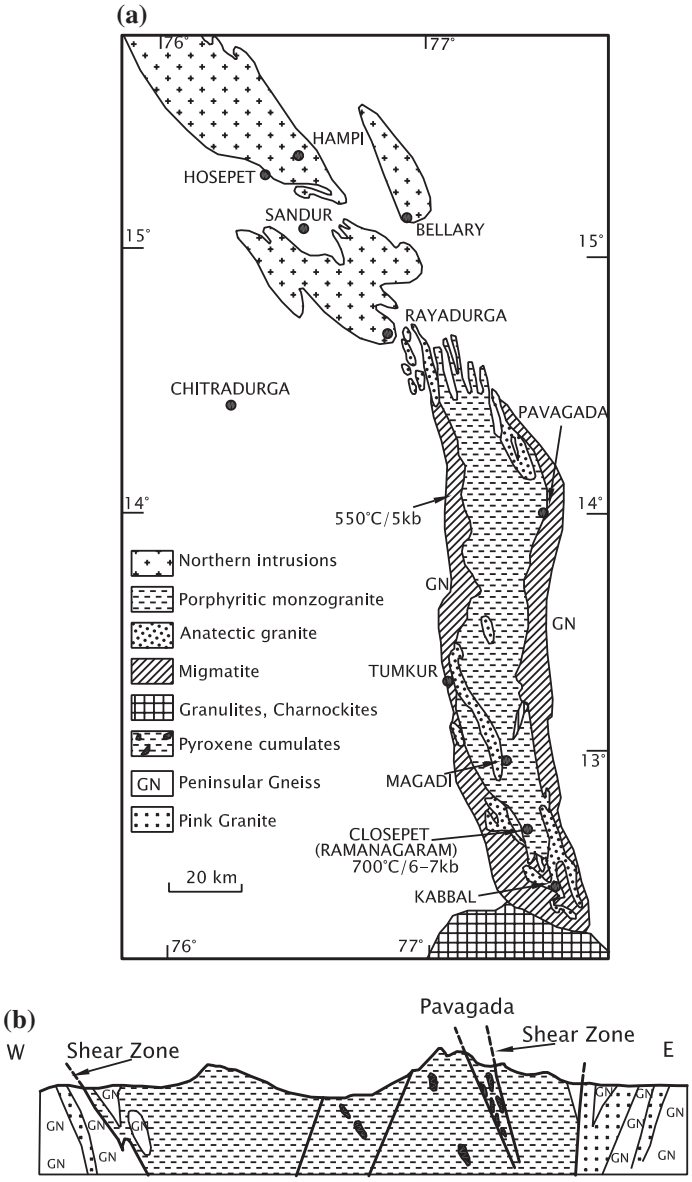

Fig. 3.16 **a** Geological sketch map of the Closepet Granite, a batholithic body more than 400 km long and 20–30 km wide. Figures point to condition of metamorphism experienced by the host rocks. **b** Cross sections along the latitude of Pavagada showing compositional, textural and structural variations in the Closepet pluton (after Moyen et al. 2003)

the composition of the Closepet Granite is a result of interaction between granitic material derived from the enriched mantle and the continental crust of tonalite–trondhjemite–granodiorite composition, the latter from partially melting due to the mantle-derived magma intruding the crust (Jayananda et al. 1995; Jayananda and Mahabaleswar 1991; Moyen et al. 2001).

3.9.3 Age

The Rb–Sr dating of the Closepet Granite was first attempted by Crawford (1969). The SHRIMP U–Pb age of zircon grains in the Closepet Granite at Kabbaldurga is 2513 ± 5 Ma (Friend and Nutman 1991) and the mantle-derived quartz-monzonite is dated 2518 ± 5 Ma (Jayananda et al. 1995). The Rb–Sr whole-rock isochron age at Toranagallu is 2452 ± 50 Ma (Bhaskar Rao et al. 1992). It seems that the Closepet Granite was emplaced towards the close of the Archaean and beginning of the Proterozoic era about 2550 Ma. It thus marks the transition of the two eras.

3.10 Dharwar Batholith

3.10.1 Composition

East of the Closepet Granite is the eastern block of the Dharwar Craton which is made up of 2750- to 2710-Ma-old gneisses of granitic to granodioritic composition. They build N–S trending linear hills of variable length (up to 150 km) and width (15–25 km) (Figs. 3.5 and 3.9) and collectively form the Dharwar Batholith (Chadwick et al. 2000). The boundaries of these sheet-like plutonic bodies with the schist belts are marked by strong shear deformation, tending to mylonitization.

3.10.2 Origin

One of the plutonic bodies of the Dharwar Batholith is the granite of Bangalore. The larger part of the Bangalore Granite, characterized by high negative εNd at 2540 Ma, is made up of material derived from the crust as borne out by higher content of Rb, Th, Y and Nb, very low amount of Ni, Cr, Co and V, and strong negative Eu anomaly, pointing to reworking of the Peninsular Gneiss to form the Bangalore Granite (Jayananda et al. 2006).

The grey granites of the Dharwar Batholith, such as the granite of the Hosekote area in the Kolar Schist Belt, were formed from mixed contributions—granitic melt derived from the mantle and reworked tonalite–trondhjemite–granodiorite of the crust. Possibly, plume activity (Fig. 3.17) played the crucial

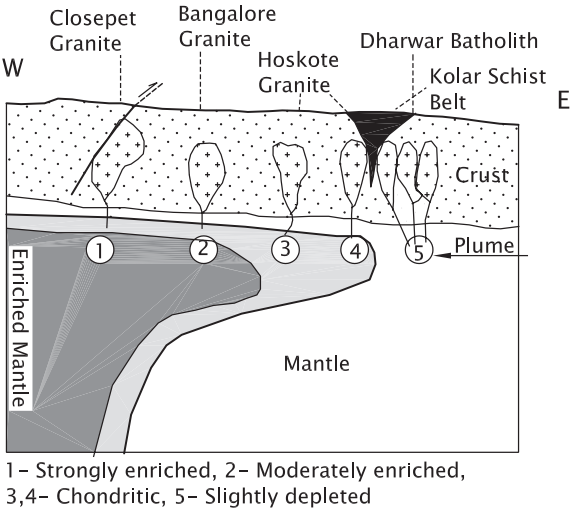

Fig. 3.17 Plume model for explaining the emplacement of the Bangalore granite and Hoskote granite that form parts of the Dharwar Batholith in the eastern block of the Dharwar Craton. Hot spots in the mantle produced high-temperature magmas that penetrated overlying crust and induced partial melting (after Jayananda et al. 2000)

role in the genesis of these granites—Bangalore granite and Hoskote granite—forming parts of the Dharwar Batholith (Jayananada et al. 2006). The 2570- to 2520-Ma-old granitic bodies occurring in these corridors in the EDC correspond to three levels of the crust—the bodies characterized by migmatitic margin represent deeper level and the sharp-margin bodies represent middle and upper levels (Gireesh et al. 2012).

3.10.3 Age

The Chitradurga Schist Belt is intruded by the *Chitradurga Granite* dated 2603 ± 28 and 2452 ± 50 Ma (Bhaskar Roa et al. 1992). It sits in the region of transition between the eastern and the western blocks of the craton. The gneissic granite at Chikballapur and Hulimavu in the Bangalore region yielded Rb–Sr whole-rock isochron ages of 2512 ± 84 and 2730 ± 92 Ma, respectively (Krogstad et al. 1989). The SHRIMP ages for zircon taken from steep elongate wedge of granodiorite that extends for 150 km SE of the schist belt are from 2561 ± 24 Ma to 2590 ± 31 Ma (Vasudev et al. 2000). The granites on the whole have a plateau age of 2550–2534 Ma compared to the plateau age of 2518 Ma of the Closepet Granite (Divakara Rao et al. 1990; Jayananda et al. 2006). It is apparent that the Dharwar Batholith is a near contemporary of the Closepet Granite, emplaced possibly a little earlier during the same phase of tectonothermal event. However, according to some workers, the Closepet Granite is not a separate entity, but a part of the Dharwar Batholith (Chadwick et al. 2007).

3.10.4 Syenites

There are bodies of syenite occurring as elliptical intrusives, such as the one located at Koppal in the western flank of the eastern block of the Dharwar Craton. The NE–SW trending upright asymmetrical *Koppal Syenite*, emplaced in the zone of diffuse banded granite, yielded a SHRIMP U/Pb zircon age of 2528 ± 9 Ma, indicating its contemporaneity with the Closepet Granite (Chadwick et al. 2001).

It is obvious that the 2600–2500 million years old granites described as the Dharwar Batholith were emplaced towards the close of the Dharwar sedimentation in the western block. They are broadly coeval with the 2750–2550 million years old volcanosedimentary assemblages of the linear schist belts in the eastern block of the Dharwar Craton. They can therefore be regarded as near contemporary of the Closepet Granite.

3.11 Granulite–Charnockite Domain

3.11.1 Occurrence

The south-western, southern and south-eastern parts of the Dharwar Craton are made up of granulites and charnockites which are intercalated with minor components of garnetiferous gneisses, banded iron formation, calc-silicate rock, quartzites and amphibolites. Progressive increase in the grade of regional metamorphism from north to south culminated in the formation of high-grade granulite facies rocks in the Kodagu (Coorg) region in the Sahyadri Range, and the Biligirirangan–Mahadeswaramalai Range in south-eastern Karnataka and adjoining western Tamil Nadu (Fig. 3.5).

The transition zone that divides the Sargur–Peninsular Gneiss–Dharwar–Closepet Granite terrane from the granulite-charnockite domain known as *Fermor Line* was first recognized and described by L.L. Fermor in 1936. Significantly, the granulitic rocks that were formed in deeper part of the sialic crust in Archaean time presently form the high mountain ranges of the southern Indian Shield, surrounding the 700- to 800-m-high Mysore Plateau from three sides. The granulites–charnockite rocks form the >1800-m-high Central Sahyadri in the south-west, >2500-m-high Nilgiri in the south, and >1400-m-high Biligirirangan in the south-east (Gopalakrishna et al. 1986; Valdiya 1998, 2001b). It has been suggested (Nautiyal 1966) that the charnockite–granulite mass was thrust up onto the amphibolite facies rocks of the Dharwar Craton, the stratigraphic throw being of the order of several hundred metres. After the Gondwana break-up, the northward tilting of crust of the Peninsular India is responsible for the exhumation or exposure of the deep-seated granulitic rocks (Drury et al. 1984).

3.11.2 Genesis of Charnockites

The charnockites are products of deep-seated metamorphism of gneisses and granites (Pichamuthu 1960, 1961, 1965) intercalated with subordinate sediments and basic–ultrabasics intrusives (Fig. 3.18). The metamorphism took place under strong

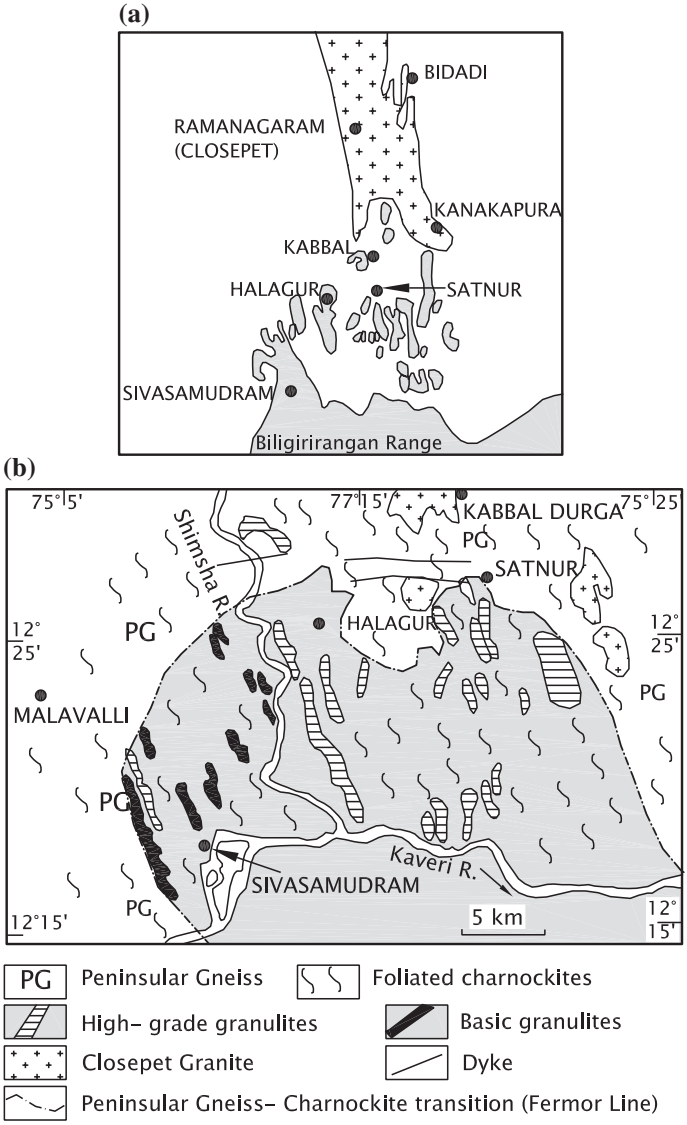

Fig. 3.18 **a** Classical sketch map by Pichamuthu (1961) depicts the transformation of the Peninsular Gneiss into charnockites. **b** Sketch map of the Kabbaldurga area in the line of the Biligirirangan Hills showing patches of charnockite—*incipient charnockite*—in the granitic gneisses of the eastern block of the Dharwar Craton (after Mahabaleswar et al. 1995)

influence of CO_2-rich fluids (Janardhan et al. 1979, 1994; Newton 1990; Newton et al. 1990). In the line of Biligirirangan Hill south of Bangalore at Kabbaldurga, the granitic gneisses of the Dharwar Craton show patches of charnockites of various shape and size, bearing testimony to the transformation of the gneisses to the charnockites. The trace-element chemistry of the charnockites and the granites is the same (Mahabaleswar and Peucat 1988; Mahabaleswar et al. 1995). Fluid rich in CO_2 possibly derived from the mantle or the sedimentary material that was thrust beneath the crustal slabs, removed H_2O from the deep crust, resulting in pervasive dehydration leading to the formation of granulites. A corollary of this phenomenon is that the purged, upward migrating H_2O-rich fluids induced partial melting at intermediate crustal level, culminating in the generation of granitic melt—represented by the Closepet Granite and its coevals. This explains the close similarity of the crystallization age of the Closepet Granite and the time of granulite metamorphism. The granulite metamorphism that gave rise to charnockites occurred around 2500–2500 ± 50 Ma at Chillapur and 2540 ± 17 Ma at Honganuru (Hansen et al. 1997). The pegmatoid veins, cutting across amphibolite of the *Kabbaldurga Charnockite* and dated 2507 and 2520 Ma (Grew and Manton 1984), bear out this conclusion. And the Closepet Granite was emplaced at 2513 Ma.

The pressure–temperature conditions of charnockite-forming metamorphism were 750 °C and 5–6 kbar at Kabbaldurga, 750–900 °C and 6–9 kbar in the Biligirirangan Hill, 678–759 °C and 4.4–5.8 kbar in the Kuppam area, 647–751 °C and 4.0–5.5 kbar in the Karimangalam area (Fig. 3.18), 720–760 °C and 7–8.6 kbar in the Kodagu area of the Central Sahyadri and Hullahalli belt south of Mysore and 850 °C and 6.5 kbar in the Karimnagar area in north-eastern Dharwar terrane (Devaraju and Sadashivaiah 1969; Janardhan et al. 1994; Srikantappa et al. 1994; Mahabaleswar et al. 1995; Bhattacharyya and Sen 2000; Sharma et al. 2003; Jayananda et al. 2003).

The charnockites of the Salem block in Eastern Dharwar Craton host leucocratic granite yielding SHRIMP/U–Pb zircon ages of 2538 ± 6 Ma and 2529 ± 7 Ma (Clark et al. 2009). The metamorphism occurred at 2473 ± 8 Ma and 2482 ± 15 Ma as the $^{207}Pb/^{206}Pb$ dating shows. Mafic granulites of the Kanjamalai Hill in the northern margin of the Palghat–Cauvery Shear Zone and of the Perunndorai in the central domain within the shear zone formed at T 750–800 °C and P 8–12 kbar and 800–900 °C and more than 12 kbar, respectively (Saitoh et al. 2011). The zircon ^{207}Pb–^{266}Pb dates of the associated charnockite and garnetiferous quartzofelspathic gneiss are, respectively, 2477.6 ± 1.8 Ma and 2483.9 ± 25 Ma (Saitoh et al. 2011).

3.11.3 Basic–Ultrabasic Intrusives

The Mehboobnagar *dyke swarm* in the Eastern Dharwar cratonic block, giving Sm–Nd isochron age of 2173 ± 64 (gabbro-dolerite) and 2189 ± 123 Ma (pyroxenite), indicates an event of crustal extension around 2170 Ma, close to

the Cuddapah Basin (Pandey et al. 1997). The Sm–Nd whole-rock isochron ages of N–S trending dykes of a 450-km-long dyke swarm are 2173 ± 43 Ma and 2190 ± 51 Ma, and the U–Pb zircon ages are 2209.3 ± 2.8 Ma, 2220.5 ± 4.9 Ma, and 2210 ± 10 Ma (Anil Kumar el al. 2012). Occurring in close association with dolerite dykes in the eastern margin of the Dharwar cratonic block—at the contact with the Cuddapah Basin, the *kimberlite and lamproite bodies* were emplaced along the NNW–SSE and WNW–ESE oriented faults and fractures. A N–S to NNE–SSW trending broad zone of thin crust provided pathways to the magmas giving rise to kimberlite rocks (Reddy et al. 2000). The lamproites contain glassy vesicles and xenoliths of country rocks and exhibit fragmental pyroclastic texture, indicating their near-surface emplacement at about 1224 ± 14 Ma (Anil Kumar et al. 2001). In contrast to the typical kimberlites and lamproites of Anantpur district, the Mehboobnagar and Krishna district lamproites show high concentration of Ni, Cr, Co, Zr, Hf, Th, U and lower abundances of Ra, Sr and Ba, implying high degree of partial melting of the mantle source.

3.12 Tectonics of Evolution of Dharwar Craton

The history of the evolution of the Dharwar Craton begins with the formation of the Gorur Gneiss, representing a part of the earliest Palaeoarchaean sialic crust. The intimately associated assemblage of ultrabasic–basic magmatic-volcanic rocks with intercalations of pelitic-siliceous sediments constituting the Sargur Group is assumed to be a product of an accretionary or additive process probably in an intracratonic rift basin or possibly in an oceanic trench. The Gorur Gneiss and the Sargur Group together formed the 3400–3200 million years old nucleus of the Dharwar Craton. It was profusely invaded in many phases by gneissic magmas, giving rise to the Peninsular Gneiss around 3000 Ma. After the gneissic terrane had stabilized, the craton experienced extension, resulting in the sagging and rifting along the structural grains of the essentially sialic Mesoarchaean crust. The consequence was the formation of elongate basins of the Dharwar sedimentation and volcanism. The assemblages are represented by the Dharwar Supergroup. The basins had attained the nature and shape of intracratonic grabens. Synsedimentary volcanism dominated the crustal processes in the Dharwar basins.

Towards the close of the Neoarchaean era, there was westward but oblique convergence of the crustal blocks resulting in E–W to NE–SW shortening of the basin in a tectonic regime of thrusting and strike-slip shearing or transpression. The transpression along the N–S line is represented by the Chitradurga Boundary Fault. There was also westward thrusting up of the rocks of the eastern block along steep shears parallel to the Chitradurga Boundary Fault. These phenomena resulted in the south-westward overturning of folds in both the basement (Peninsular Gneiss) and its cover (Dharwar Supergroup). Possibly, mantle plumes

had become active towards the end of the Neoarchaean time. The plumes brought up mantle material through deep shear zones and faults, and melting of the basement rocks, particularly in the region east of the Chitradurga Belt culminating in the emplacement of the Closepet Granite and the Dharwar Batholith in the larger northern part of the Dharwar Province. The granitic activity induced high-temperature–pressure granulite metamorphism, leading to formation of charnockites in the southern part of the Dharwar domain. Quite later, subhorizontal displacement on the N–S and NNW–SSE trending faults and shear zones caused jostling of the crustal blocks within the zones of transpression, aggravating the structural complexity of the Dharwar Craton.

The above-mentioned model of evolution is based on the postulations of Radhakrishna and Naqvi (1986), Chadwick et al. (1989, 2000, 2003, 2007), Chardon et al. (2002), Jayananda et al. (2006) and Ramakrishnan (2003).

3.13 Life in the Archaean Time

Single-celled bacteria without nucleus (*prokaryotes*) had appeared 4.5–4.0 billion years ago and developed into cells with nucleus (*eukaryotes*) during the Late Archaean time. These are represented by biogenic carbon inclusion within minerals and by graphite. Living in communities, the mats of cells trapped and bound sediments in shallow warm waters, building layer after layer of *stromatolites* and oncolites. In course of time, some other non-photosynthetic heteromorphs appeared thriving on organic molecules in dark anoxic environment (Sankaran 2001). In the Indian Shield, life appeared about 3.8 billion years ago. The automorphs produced organic nutrients from inorganic substance. These forms proliferated to multicellular forms in the Late Proterozoic period. During the Archaean–Proterozoic transition period, an oxygen-rich atmosphere was established (Melezhik et al. 2005). The aerobic biosphere promoted vigorous growth of life.

In the world of Dharwar Craton, stromatolites in the carbonate rocks of the Chitradurga Group reveal existence and development of cyanobacterial life (Srinivasan et al. 1989, 1990, 1997). The algal filaments with coccoid and rod-shaped bacteria occur in the stratiform, pseudocolumnar, columnar and branching-columnar stromatolites characterizing dolomites that are interlayered with banded ferruginous chert. In the Donimalai sequence of the Sandur Schist Belt, a microbial trichomes isolated from black chert have been identified as a siderocapsaceous bacterium *Phormidella*, comparable with the sulphur-reducing bacterium *Thiobacillus* recovered from syngenetic pyrite associated with banded ferruginous chert (banded iron formation) of Kudremukh belt (Venkatachala et al. 1990). These forms provide telling evidence of extensive biological activity during the Dharwar time (Fig. 3.19).

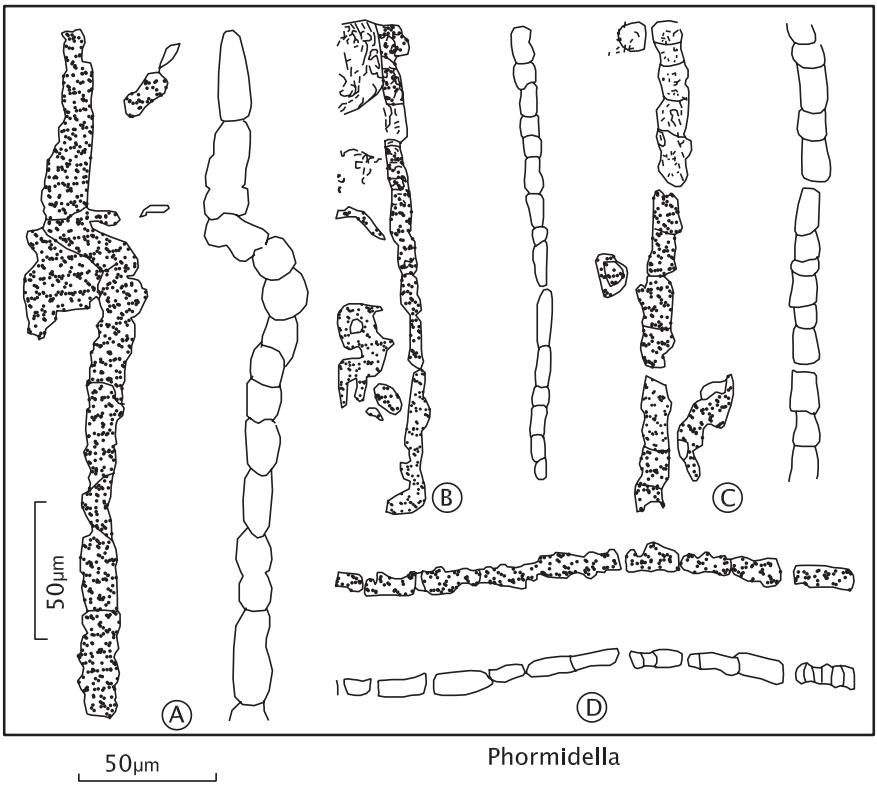

Fig. 3.19 Trichomes *Phormidella* preserved in black chert from the Donimalai sequence in the Sandur Schist Belt, coeval of the Dharwar Supergroup (after Venkatachala et al. 1990)

3.14 Mineral Assets

The most important minerals of the considerable commercial importance are iron ores, manganese ores, copper ores, chromite, magnesite and gold. Closepet Granite, Dharwar Batholith and the Peninsular Gneiss, besides felsite and porphyry dykes, are used on a very large scale as building material. Felspars and quartz are mined from these granites on a substantial scale.

Banded haematite- and magnetite-quartzite of the banded iron formation in the Dharwar Supergroup host *iron ore* deposits of great consequence in the Kudremukh, the Bababudan and the Bellary belts. The iron ore deposits occur in association with greywackes at Ranibennur, Haveri and Gadag, with oxide–carbonate–sulphide deposits in the Chitradurga Group at Chikkanayakanahalli and Chitradurga, in association with volcanics in the Kudremukh and Sandur Schist Belts and as banded magnetite-quartz deposit of the Sargur Group. Residual concentration of iron in the banded iron formation has given rise to rich and large ore

bodies capping the hilltops and plateaus (Devaraju et al. 1986; Bhattacharya and Chatterjee 1990). The proven reserves of iron ores are of the order of 2200 million tonnes, comprising both magnetite and haematite. The main *manganese* minerals are pyrolusite and psilomelane occurring in the schist belts in association with limestones and banded ferruginous cherts of the Dharwar Supergroup in the Shimoga, Chitradurga, Sandur and Uttara Kannada belts (Bhatt et al. 1990; Devaraju et al. 1979; Krishna Rao et al. 1982; Mishra 1982; Sawkar 1981). In the Shimoga area, the manganese-rich bands alternate with phyllites and ferruginous quartzites, and the commercial manganese deposits are the results of reworking of the Precambrian ores. The proven reserve of manganese is of the order of 2,262,000 tonnes.

Copper sulphide occurs together with the sulphides of Pb and Zn forming stratiform deposits within the basic volcanic assemblage consisting of pillow basalt and tuffs as seen in the Jogimardi sequence of the Chitradurga Group (Anantha Iyer and Vasudev 1985). Among the notable deposits of copper are the ones in the Kalyali area in the Sargur Group (Jayaram and Ravindran 1979; Rao and Majumdar 1981) and Nuggihalli Belt (Radhakrishna et al. 1973). The copper sulphide also occurs as vein deposits, the fluid inclusions of which betray a temperature of 350 °C at which it formed under anoxic conditions. In the Ingaldhal area of the Chitradurga belt, the sulphide deposits occur in association with basalts and pyrite-bearing banded chert characterized by high concentration of CO_2 of volcanic origin (Naqvi et al. 1977).

In the Kolar Schist Belt, there is strong structural control on the *gold* mineralization (Narayanswami et al. 1960). Gold occurs in four parallel lodes in stratiform deposits of sulphides associated with amphibolite and banded ferruginous chert. The geochemistry indicates that gold was derived from submarine hydrothermal exhalations. It also occurs in free state as ultrafine particles intergrown with quartz and locally carbonate in quartz veins. The geochemistry of the quartz veins indicates that gold came from the crystallizing granite magma (Siddaiah and Rajamani 1989). In the Hutti Schist Belt, the gold-bearing lodes are associated with basalts and chert beds, being localized in the highly sheared chlorite schist (Vasudev and Naganna 1973; Naganna 1987; Biswas 1990). The closely spaced laminated quartz veins and associated alternations of halos along steeply dipping anastomosing shear zones within amphibolites and chlorite schist show gold mineralization. The fluid inclusions indicate that this development taking place below 280 °C and 1.7 kbar (Pal and Mishra 2002). The Ajjanahalli gold belt in the Chitradurga Schist Belt is hosted by a 100-m-wide antiform in the sulphidic banded ferruginous chert (Sawkar et al. 1995). These rocks suffered peak metamorphism at 300–350 °C, giving rise to gold along with arsenopyrite, pyrite and pyrrhotite due to magnetic fluid infiltration into low-strain areas (Kolb et al. 2004). The Gadag gold is associated with iron-rich tholeiitic basalt and andesite; and its formation is related to deformation and attendant metamorphism of the volcanic rocks (Ugarkar et al. 2000).

Chromite deposits occur in lensoid bodies of serpentinite in the Nuggihalli belt of the Sargur Group (Radhakrishna 1957; Varadarajan 1970, 1975; Jafri et al. 1981; Sahu and Nair 1982). The Byrapur deposit, south-east of Arsikere in the

Hassan district, is one of the major chromite deposits of India. Another important deposit occurs at Sindhuvalli between Mysore and Nanjangud in the form of a lense of chromite within the Sargur ultrabasic rocks. The chromite deposits were formed due to gravity-induced settling of chromite from a crystallizing basaltic magma. The magma was emplaced in the tectonized zones related to possibly an ancient suture.

Magnesite occurs in veins in the serpentinized dunite belonging to the Sargur Group. The deposits are located at Dodkanya, Hullahalli and Karya in the Mysore district. Breakdown of serpentine due to hydrothermal carbonate solutions resulted in the formation of $MgCO_3$ (magnesite) which accumulated in fractures of the host rock (Venkataramana 1983; Krishna Rao et al. 1994).

References

Anand, S. P., & Rajaram, M. (2002). Aeromagnetic data to probe the Dharwar Craton. *Current Sciences, 83*, 162–167.

Anantha Iyer, G. V., & Vasudev, V. N. (1979). Geochemistry of the Archaean metavolcanic rocks of Kolar and Hutti Gold Fields, Karnataka, India. *Journal Geological Society of India, 20*, 419–437.

Anantha Iyer, G. V., & Vasudev, V. N. (1985). Copper metallogeny in the Jogimardi volcanics, Chitradurga greenstone belt. *Journal Geological Society of India, 26*, 580–598.

Anil, K., Pande, K., Venkatesan, T. R., & Bhaskar Rao, Y. J. (2001). The Karnataka Late Cretaceous dykes as products of Marion hotspot at the Madagascar–India breakup event: Evidence from ^{40}AR-^{39}Ar geochronology and geochemistry. *Geophysical Research Letters*, *28*, 2715–2718.

Beckinsale, R. D., Drury, S. A., & Holt, R. W. (1980). 3305-Myr old gneisses from South Indian Craton. *Nature, 283*, 469–470.

Bhaskar Rao, Y. J., Anil, K., Vresky, A. B., Srinivasan, R., & Anantha, Iyer, G. V. (2000). Sm–Nd ages of two metaanorthosite complexes around Holenarasipur: Constraints on the antiquity of Archaean supracrustal rocks of the Dharwar Craton. *Proceedings of Indian Academy of Sciences (Earth & Planetary Science), 109*, 57–65.

Bhaskar Rao, Y. J., Naha, K., Srinivasan, R., & Gopalan, K. (1991) Geology, geochemistry and geochronology of the Archaean Peninsular Gneiss around Gorur, Hassan district, Karnataka, India. *Proceedings of Indian Academy of Sciences (Earth & Planetary Sciences)*, 100, 399–412.

Bhaskar Rao, Y. J., Sivaraman, T. V., Pantulu, G. V. C., Gopalan, K., & Naqvi, S. M. (1992). Rb–Sr ages of late Archaean metavolcanics and granites, Dharwar Craton, South India, and evidence for Early Proterozoic thermotectonic events. *Precambrian Research, 59*, 145–170.

Bhatt, S. S., Dasgupta, D., & Govil, P. K. (1990). Genesis of manganese ore deposits in the volcanosedimentary formations of Sandur Schist Belt, Karnataka. *Indian Journal of Geology, 62*, 48–64.

Bhattacharya, N. N., & Chatterjee, A. B. (1990). Geology of the iron formation of Chitradurga greenston belt, Karanataka. *Indian Minerals, 44*, 141–150.

Bhattacharya, S., & Sen, S. K. (2000). New insights into the origin of Kabbaldurga charnockites, Karnataka, South India. *Gondwana Resarech, 3*, 489–506.

Bhattacharya, P. K., Bhattacharya, H. N., & Mukherjee, A. D. (1988). The Chitradurga greenstone succession in south India, and evolution of the Late Archaean basin. *Geological Magazine, 125*, 507–519.

Bidyananda, M., Deomurari, M. P., & Goswami, J. N. (2003). ^{207}Pb–^{206}Pb ages of zircons from the Nuggihalli schist belt, Dharwar craton, Southen India. *Current Science, 85*, 1482–1485.

Biswas, S. (1990). Gold mineralization in Hutti-Maski schist belt, Karnataka State. *Indian Minerals, 44*, 1–44.

Bouhallier, H., Chardon, D., & Choukroune, P. (1995). Strain patterns in Archaean dome-and-basin structures: The Dharwar Craton, South India. *Earth & Planet Sciences Letters, 135*, 57–75.

Chadwick, B., Hegde, G. V., Nutman, A. P., & Vasudev, V. N. (2001). Syenite emplacement during accretion of the Late Archaean Dharwar Batholith, South India: SHRIMP U/Pb age of structure of the Koppal pluton, Karnataka. *Journal Geological Society of India, 58*, 381–390.

Chadwick, B., Ramakrishnan, M., Vasudev, V. N., & Viswanatha, N. N. (1989). Facies distribution and structure of a Dharwar volcanosedimentary basin: Evidence for late Archaean transpression in southern India. *Journal of Geological Socience London, 146*, 825–834.

Chadwick, Brian, Ramakrishnan, M., & Viswanatha, M. V. (1981). Structural and metamorphic relations between Sargur and Dharwar supracrustal rocks and Peninsular Gneiss in central Karnataka. *Journal Geological Society of India, 22*, 557–569.

Chadwick, B., Vasudev, V. N., & Ahmed, N. (1996). The Sandur Schist Belt and its adjacent plutonic rocks: Implications for Late Archaean crustal evolution in Karnataka. *Journal Geological Society of India, 47*, 37–57.

Chadwick, B., Vasudev, V. N., & Hegde, G. V. (2000). The Dharwar Craton, Southern India, interpreted as a result of Late Archaean oblique convergence. *Precambrian Research, 99*, 91–111.

Chadwick, B., Vasudev, V. N., & Hegde, G. V. (2003). The Chitradurga Schist Belt and its adjacent plutonic rocks, NW of Tungabhadra, Karnataka: A duplex in the Late Archaean convergent setting of the Dharwar Craton. *Journal Geological Society of India, 61*, 645–663.

Chadwick, B., Vasudev, V. N., Hegde, G. W., & Nutman, A. P. (2007). Structure and SHRIMP U/Pb zircon ages of granites adjacent to the Chitradurga Schist Belt: Implications for Neoarchaean convergence of Dharwar Craton, Southern India. *Journal Geological Society of India, 69*, 5–24.

Chadwick, B., Vasudev, V. N., & Jayaram, S. (1988). Stratigraphy and structure of Late Archaean Dharwar volcanic and sedimentary rocks and their basement in part of the Shimoga basin, east of Bhadravati, Karnataka. *Journal Geological Society of India, 32*, 1–19.

Chadwick, B., Vasudev, V. N., Krishna Rao, B., & Hegde, G. V. (1991). The stratigraphy and structure of the Dharwar Supergroup adjacent to the Honnali dome: Implications for Late Archaean basin development and regional structure in the western part of Karnataka. *Journal Geological Society of India, 38*, 457–484.

Chardon, D., & Choukroune, P. (1996). Strain pattern, decollement and incipient sagducted greenstone terrains in the Archaean Dharwar Craton (South India). *Journal of Structural Geology, 18*, 991–1004.

Chardon, D., Peucat, J.-J., Jayananda, M., Choukroune, P., & Fanning, M. (2002). Archaean granite-greenstone tectonics at Kolar (South India): Interplay of diapirism and bulk inhomogenous contraction during juvenite magmatic accretion. *Tectonics, 21*(3), 1016.

Chetty, T. R. K. (1996). Proterozoic Shear zones in Southern Granulite Terrain, In M. Santosh, & M. Yoshida (Eds.), The Archaean and Proterozoic Terrains in Southern India Within East Gondwana. *Memoir, Gondwana Research Group, 3*, 77–89.

Chetty, T. R. K., & Bhaskar Rao, Y. J. (2006). Strain pattern and deformational history in the eastern part of the Cauvery Shear Zone, Southern India. *Journal of Asian Earth Sciences, 28*, 46–54.

Clark, Chris, Collins, A. S., Timms, N. E., Kinny, P. D., Chetty, T. R. K., & Santosh, M. (2009). SHRIMP U-Pb age constraints on magmatism and high grade metamorphism in the Salem block, southern India. *Gondwana Research, 16*, 27–36.

Crawford, A. R. (1969). Reconnaissance Rb–Sr dating of the Precambrian rocks of northern Peninsular India. *Journal Geological Society of India, 10*, 117–166.

Dhaundial, D. P., Paul, D. K., Sarkar, A., Trivedi, J. R., Gopalan, K., & Potts, P. J. (1987). Geochronology and geochemistry of Precambrian granitic rocks of Goa, SW India. *Precambrian Research, 36*, 287–302.

Devaraju, T. C., Anantha Murthy, K. S., & Gamanagatti, S. G. (1979). Mineralogy of the manganese ore from Supa area, North Kanara. *Indian Mineralogist, 20*, 21–27.

Devaraju, T. C., Anantha Murthy, K. S., & Khanadali, S. D. (1986). Iron formation of the Chikkanarayakanahalli greenstone belt, Karanataka. *Journal Geological Society of India, 28*, 201–217.

Devaraju, T. C., & Sadashiviah, M. S. (1969). The charnockites of Satanur-Halagur, Mysore State. *Indian Mineralogist, 10*, 67–88.

Devaraju, T. C., Sudhakar, T. L., Kraukonen, R. J. Viljoen R. P., Alapieti, T. T., Ahmed, S .A. et al. (2010). Petrology and geochemistry of greywackes from Goa, Dharwar sector, western Dharwar Graton: Implications for volcanic origin. *Journal Geology Society of India*, *75*, 465–487.

Divakara Rao, V., Naqvi, S. M., Satyanarayana, K., & Hussain, S. M. (1974). Geochemistry and origin of the Peninsular Gneisses of Karnataka, India. *Journal Geological Society of India, 15*, 270–277.

Divakara Rao, V., Rama Rao, P., Subba Rao, M. V., Govil, P. K., Rao, R. U. M., Walsh, J. N., et al. (1990). Trace and rare earth element geochemistry and origin of the Closepet Granite, Dharwar Craton, India. In S. M. Naqvi (Ed.), *Precambrian continental crust and its economic resources* (pp. 203–227). Amsterdam: Elsevier.

Drury, S. A., Harris, N. B. W., Holt, R. W., Reeves, S. G. J., & Wightman, R. T. (1984). Precambrian tectonics and crustal evolution in South India. *Journal of Geology, 92*, 3–20.

Friend, C. R. L. (1984). The origins of the Closepet Granite and the implications for the crustal evolution of southern Karnataka. *Journal Geological Society of India, 25*, 73–84.

Friend, C. R. L., & Nutman, A. P. (1991). SHRIMP–U/Pb geochronology of the closepet granite and Peninsular Gneiss, Karnataka, South India. *Journal Geological Society of India, 38*, 357–368.

Gireesh, R. V., Sekhamo, Kowete-u, & Jayananda, M. (2012). Anatomy of 2.57 to 2.52 GA granitoid plutons in Eastern Dharwar Craton, southern India: Implications of magma chamber processes and crustal evolution. *Episodes, 35*, 398–413.

Giritharan, T. S., & Rajamani, V. (1978). Geochemistry of the metavolcanics of the Hutti-Maski Schist Belt, South India: Implications to gold metallogeny in the Eastern Dharwar Craton. *Journal of the Geological Society of India*, *51*, 583–594.

Gnaneshwar Rao, T., & Naqvi, S. M. (1995). Geochemistry, depositional environment and tectonic setting of the BIFs of the Late Archaean Chitradurga Schist Belt, India. *Chemistry of Geology, 121*, 217–243.

Gopalakrishnan, D., Hansen, E. C., Janardhan, A. S., & Newton, R. C. (1986). The southern high-grade metamorphic margin of the Dharwar Craton. *Journal of Geology, 94*, 247–260.

Grew, E. S., & Manton, W. I. (1984). Age of allanite from Kabbaldurga Quarry, Karnataka. *Journal Geological Society of India, 25*, 193–195.

Gupta, Sandeep, Rai, S. S., Prakasam, K. S., Srinagesh, D., Chadha, R. K., Priestley, K., & Gaur, V. K. (2003). First evidence for anomalous thick crust beneath mid-Archaean Westen Dharwar Craton. *Current Sciences, 84*, 1219–1225.

Gupta, M. L., Sundar, A., & Sharma, S. R. (1991). Heat flow and heat generation in the Archaean Dharwar cratons and implications for the Southern Indian Shield geotherm and lithospheric thickness. *Tectonophysics, 194*, 107–122.

Hansen, E. C., Stern, R. J., Devaraju, T. C., Mahabaleswar, B., & Kenny, P. J. (1997). Rubidium-strontium wholerock ages of banded and incipient charnockites from southern Karnataka. *Journal Geological Society of India, 50*, 267–275.

Hussain, S. M., & Naqvi, S. M. (1988). Geological, geophysical and geochemical studies over the Holenarasipur schist belt, Dharwar Craton, India. *Memoirs Geological Society India, 4*, 73–95.

Janardhan, A. S., & Gopalkrishna, D. (1983). Pressure-temperature estimates of the basic granulites and conditions of metamorphism in Sargur terrain, southern Karnataka and adjoining areas. *Journal Geological Society of India, 24*, 219–228.

Jafri, S. M., Khan, N., Ahmad, S. M., & Saxena, R. (1981). Geology and geochemistry of Nuggihalli schist belt, Dharwar Craton, Karnataka. *Memoirs Geological Society India, 4*, 110–120.

Janardhan, A. S., Jayananda, M., & Shankara, M. A. (1994). Formation and tectonic evolution of granulites from the Biligirirangan and Nilgiri Hills, S. India: Geochemical and isotopic constraints. *Journal Geological Society of India, 44*, 27–40.

Janardhan, A. S., Ramachandra, H. M., & Ravindra Kumar, G. R. (1979). Structural history of Sargur supracrustal and associated gneisses, southwest of Mysore, Karnataka. *Journal Geological Society of India, 20*, 61–72.

Jayananda, M., (2012). Geochemical constraints on komitiite volcanism from Sargur Group, Nagamangala greenstone belt, Western Dharwar Craton, Southern India: Implications for Mesoarchaean mantle evolution and continental growth, *Geoscience Frontiers*, China University of Geosciences, Beijing, pp. 1–20, http://dox.doi.org/10.1016/j.gf.2012.11.003

Jayananda, M., Banerjee, M., Pant, N.C., Dasgupta, S., Kano, T., Mahesha, N. et al. (2011). The 2.62 Ga high-temperature metamorphism in the central part of the Eastern Dharwar Craton: Implications for the Archaean tectonothermal history. *Geological Journal* (wileyonlinelibrary.com) Doi: 10.1002/gj.1308.

Jayananda, M., Chardon, D., Peucat, J.-J., & Capdevila, R. (2006). 2.61 Ga potassic granites and crustal reworking in the Western Dharwar Craton, southern India: Tectonic, geochronologic and geochemical constraints. *Precambrian Research, 150*, 1–26.

Jayananda, M., Janardhan, A. S., Suvasubramanian, P., & Peucat, J. J. (1995a). Geochronologic and isotopic constraints on granulite formation in the Kodaikanal area, Southern India. *Memoir Geological Society of India, 34*, 373–390.

Jayananda, M., Kano, T., Harish Kumar, S. P., Mohan, A., Swamy, N. S., & Mahabaleswar, B. (2003). Thermal history of the 2.5 Ga juvenile continental crust in the Kuppam-Karimangalam area, Eastern Dharwar Craton, Southern India. *Memoir Geological Society of India, 52*, 255–287.

Jayananda, M., & Mahabaleswar, B. (1991). The generation and emplacement of Closepet Granite during Late Archaean Granulite metamorphism in southeastern Karnataka. *Journal Geological Society of India, 38*, 418–426.

Jayananda, M., Martin, H., Peucat, J. J., & Mahabaleswar, B. (1995b). Late Archaean crust-mantle interaction: geochemistry of LREE-enriched mantle-derived magmas: Examples from Closepet batholith, southern India. *Contributions Mineral Petrology Geochemistry, 119*, 314–329.

Jayananda, M., Moyen, J.-F., Martin, H., Peucat, J.-J., Auvray, B., & Mahabaleswar, B. (2000). Late Archaean (2550–2520 Ma) juvenile magmatism in the Eastern Dharwar Craton, southern India: Constraints from geochronology, Nd–Sr istotopes and wholerock geochemistry. *Precambrian Research, 99*, 225–254.

Jayaram, B. N., & Ravindran, K. V. (1979). Copper deposits in Aladahalli area, Hassan district, Karnataka. *Indian Minerals, 33*, 35–44.

Kaila, K. L., Roy Choudhury, K., Reddy, P., Krishna, V. G., Narain, Hari, Subotin, S. T., et al. (1979). Crustal structure along the Kavali-Udupi profile in the Indian Peninsular Shield from deep seismic sounding. *Journal of Geological Society of India, 20*, 307–333.

Khan, R. M. K., Govi, P. K., & Naqvi, S. M. (1992). Geochemistry and genesis of Banded Iron Formation from Kudremukh Schist Belt, Karnataka nucleus, India. *Journal Geological Society of India, 40*, 311–328.

Krishna Rao, B., Hanuma Prasad, M., Vasudev, V. N., & Sethumadhav, M. S. (1994). Origin of grunerite schist-hosted magnesite mineralization in copper mountain area, Sandur Schist Belt, Karnataka. *Journal Geological Society of India, 44*, 267–274.

Krishna Rao, B., Srinivasan, R., Ramachandra, B. L., & Sreenivas, B. L. (1982). Mode of occurrence and origin of manganese ores of Shimoga district, Karnataka. *Journal Geological Society of India, 23*, 226–235.

Kolb, J., Hellman, A., Rogers, A., Sindern, S., Vennemann, T., Bottcher, M. E., & Meyer, F. M. (2004a). The role of a transcrustal shear zone in orogenic gold mineralization at the Ajjanahalli mine, Dharwar Craton, South India. *Economic Geology, 99*, 743–759.

Kolb, J., Rogers, A., Meyer, F. M., & Vinnemann, T. W. (2004b). Development of fluid conduits in the auriferous shear zones of the Hutti Gold Mine, India: evidence for spatially and temporally heterogeneous fluid flow. *Tectonophysics, 378*, 65–84.

Krogstad, E. J., Balakrishnan, S., Hanson, G. N., & Rajamani, V. (1989). Plate tectonics at 2.5 billion years ago: Evidence from Kolar Schist Belt, South India. *Science, 243*, 1337–1340.

Kumar, Anil, Bhaskar Rao, Y. J., Sivaraman, T. V., & Gopalan, K. (1996). Sm–Nd ages of Archaean metavolcanics of the Dharwar Craton, South India. *Precambrian Research, 80*, 205–216.

Kunugiza, K., Kato, Y., Kano, Y., Takaba, Y., Kuruma, T., & Sohma, T. (1996). An Archaean tectonic model of the Dharwar craton, southern India: the origin of Holenarasipur greenstone belt and reinterpretation of Sargur-Dharwar relationship. *Journal Southeast Asian Earth Sciences, 14*, 149–160.

Leelanandam, C. (1990). Kandra Volcanics in Andhra Pradesh: Possible ophiolite. *Current Science, 59*, 785–788.

Leelanandam, C., Burke, K., Ashwal, L. D., & Web, S. J. (2006). Proterozoic mountain building in Peninsular India: An analysis based primarily on alkaline rock distribution. *Geological Magazine, 143*, 195–212.

Mahabaleswar, B., Jayananda, M., Peucat, J.-J., & Swamy, N. S. (1995). Archaean high-grade gneiss complex from Satanur–Halagur–Sivasamudram area, Karnataka, Southern India, Petrogenesis and crustal evolution. *Journal Geological Society of India, 45*, 33–49.

Mahabaleswar, B., & Peucat, J.-J. (1988). 2.9 b.y. Rb–Sr age of granulite facies rocks of Satanur–Halagur–Sivasamudram area, southern Karnataka. *Journal Geological Society of India, 27*, 282–297.

Manikyamba, C., & Naqvi, S. M. (1995). Geochemistry of Fe–Mn formation of the Archaean Sandur Schist Belt, India—mixing of clastic and chemical processes at a shallow shelf. *Precambrian Research, 72*, 69–95.

Melezhik, V. A., Fallick, A. E., Hanski, E. J., Kump, L. R., Lepland, A., Prave, A. R., & Strauss, H. (2005). Emergence of the aerobic biosphere during Archaean-Proterozoic transition: Challenges of future research. *GSA Today, 15*, 4–11.

Mishra, R. N. (1982). A genetic model for the Sandur manganese ores. *Record Geologyical Survey of India, 114*, 10–18.

Moyen, J.-F., Martin, H., & Jayananda, M. (2001). Multi-element geochemical modelling of crust-mantle interactions during Late Archaean crustal growth: the Closepet Granite (South India). *Precambrian Research, 112*, 87–105.

Moyen, J.-F., Nedelec, A., Martin, H., & Jayananda, M. (2003). Syntectonic granite emplacement at different structural levels: The Closepet Granite, South India. *Journal of Structure Geology, 25*, 611–631.

Mukhopadhyay, D. (1986). Structural pattern in the Dharwar Craton. *Journal of Geology, 94*, 167–186.

Mukhopadhyay, A., Adhikari, S., Roy, S. P., et al. (1997). Eustacy, climate, tectonics, sedimentary environment and the formation of Permian Coal Measures in the Sohagpur Coalfield, Madhya Pradesh. *Special Publication Geological Survey of India, 54*, 305–320.

Mukhopadhyay, D., & Matin, A. (1993). The structural anatomy of the Sandur Schist belt—a greenstone belt in the Dharwar Craton, South India. *Journla of Structure Geology, 15*, 309–322.

Naganna, C. (1987). Gold mineralization in the Hutti mining area, Karnataka, India. *Economic Geology, 82*, 2008–2016.

Naha, K., Mukhopadhyay, D., Dastidar, S., & Mukhopadhyay, R. P. (1994). Basement-cover relations between a granite gneissic body and its metasedimentary envelope: a structural study from the Early Precambrian Dharwar tectonic province, S. India. *Precambrian Research, 72*, 283–299.

Naha, K., & Srinivasan, R. (1996). Nature of the Moyar and Bhavani Shear Zones with a note on its implications on the tectonics of the Southern Indian Precambrian shield. *Proceedings of Indian Academy of Sciences. (Earth & Planet Sciences), 105*, 173–189.

Naha, K., Srinivasan, R., Gopalan, K., Pantulu, G. V. C., Subba Rao, M. V., Vrevsky, A. B., & Bogomolov, Y. S. (1993). The nature of the basement in the Archaean Dharwar Craton of southern India and the age of the Peninsular Gneiss. *Proceedings of Indian Academy of Sciences (Earth & Planetary Sciences), 102*, 547–565.

Naha, K., Srinivasan, R., & Jayaram, S. (1990). Structural evolution of the Peninsular Gneiss—an early Precambrian migmatitic complex from South India. *Sond Geologische Rundschau, 79*, 99–109.

Nair, P. R. K., Prasanna Kumar, U., & Mathai, T. (1981). Structure of the western termination of the Bhavani lineament. *Journal Geological Society of India, 22*, 285–291.

Naqvi, S. M. (1985). Chitradurga Schist Belt—An Archaean suture. *Journal Geological Society of India, 26*, 511–525.

Naqvi, S. M., Divakara Rao, V., & Narain, H. (1974). The protocontinental growth of the Indian Shield and the antiquity of its rift valleys. *Precambrian Research, 1*, 345–398.

Naqvi, S. M., Hanumantha Rao, T., Natarajan, R., Satyanarayana, K., Divakara Rao, V., & Hussain, S. M. (1977). Mineralogy, geochemistry and genesis of the massive base-metal sulphide deposits of Chitradurga (Ingaladhal), Karnataka, India. *Precambrian Research, 4*, 361–386.

Naqvi, S. M., Khan, R. M. K., Manikyamba, C., Ram Mohan, M., & Khanna, T. C. (2006). Geochemistry of the Neoarchaean high-Mg basalts, boninites and adakites from the Kushtagi-Hungund greenstone belt of the Eastern Dharwar Craton: Implications for the tectonic setting. *Journal of Asian Earth Sciences, 27*, 25–44.

Naqvi, S. M., Manikyamba, C., Gnaneshwar Rao, T., Subba Rao, D. V., Ram Mohan, M., & Srinivasa Sarma, D. (2002). Geochemical and isotopic constraints of Neoarchaean fossil plume for evolution of volcanic rocks of Sandur Greenstone Belt, India. *Journal Geological Society of India, 60*, 27–56.

Narain, Hari, & Subrahmanyam, C. (1986). Precambrian tectonics of the South Indian Shield inferred from geophysical data. *Journal of Geology, 94*, 187–195.

Narasimha Reddy, M., Babu, E. V. S. S. K., & Leelanandam, C. (2003). Petrography, mineral chemistry and geothermobarometry of the Inukurti anorthosite complex and associated rocks of the Nellore Schist Belt, Andhra Pradesh. *Journal Geological Society of India, 62*, 413–428.

Narayanaswami, S., Ziauddin, M., & Ramachandra, A. V. (1960). Structural control and localization of gold-bearing lodes, Kolar Gold Field, India. *Economic Geology, 55*, 1429–1459.

Nautiyal, S. P. (1966). Precambrian of Mysore Plateau, Presidential Address, *53rd Indian Science Congress, Part II*, 1–14.

Newton, R. C. (1990). The late Archaean high-grade terrain of south India and the deep Structure of Dharwar Craton. In M. H. Salisbury & D. M. Fountain (Eds.), *Exposed Cross Sections of the Continental Crust* (pp. 305–326). Dordrecht: Kluwer Academy Publishers.

Nutman, A. P., Chadwick, B., Krishna Rao, B., & Vasudev, V. N. (1996). SHRIMP U/Pb zircon ages of acid volcanic rocks in the Chitradurga and Sandur Groups, and granites adjacent to the Sandur Schist Belt, Karnataka. *Journal Geological Society of India, 47*, 153–164.

Okudaira, T., Hamamoto, T., Hari Prasad, B., & Kumar, Rajneesh. (2001). Sm–Nd and Rb–Sr dating of amphibolite from the Nellore-Khammam schist belt SE India: Constraints on the collision of the Eastern Ghats terrane and Dharwar-Bastar Craton. *Geological Magazine, 138*, 495–498.

Pal, Nabarun, & Mishra, B. (2002). Alteration geochemistry and fluid inclusion characteristics of the greenstone-hosted gold deposits of Hutti, Eastern Dharwar Craton, India. *Mineralium Deposita, 37*, 722–736.

Pandey, B. K., Gupta, J. N., Sarma, K. J., & Sastry, C. A. (1997). Sm–Nd, Pb–Pb and Rb–Sr geochronology and petrogenesis of the mafic dyke swarm of Mahabubnagar, South India: Implication for Palaeoproterozoic crustal evolution of the Eastern Dharwar Craton. *Precambrian Research, 84*, 181–196.

Peucat, J.-J., Bouhallier, C., Fanning, C. M., & Jayananda, M. (1995). Age of Holenarsipur greenstone belt, relationship with the surrounding gneisses (Karnataka, South India). *Journal of Geological, 103*, 710.

Pichamuthu, C. S. (1960). Charnockite in the making. *Nature, 188*, 135–136.

Pichamuthu, C. S. (1961). Transformation of Peninsular Gneiss into charnockite in Mysore State. *Journal Geological Society of India, 2*, 46–49.

Pichamuthu, C. S. (1962). Some observation on the structure, metamorphism and geological evolution of Peninsular India. *Journal Geological Society of India, 3*, 106–118.

Pichamuthu, C. S. (1965). Regional metamorphism and charnockitization in Mysore State. *Indian Mineralogist, 6*, 119–126.

Prakasam, K. S., & Rai, S. S. (2003). Crustal thickness and composition in Eastern Dharwar Craton. *Memoirs Geological Society of india, 53*, 115–127.

Radhakrishna, B. P. (1957). The mode of occurrence of chromite at Byrapur, Mysore State, India. *Bulletin Mysore Geological Association, 16*, 1–24.

Radhakrishna, B. P. (1974). The Peninsular Gneissic complex of the Dharwar Craton: A suggested model of its evolution. *Journal Geological Society of India, 15*, 429–454.

Radhakrisna, B. P., & Naqvi, S. M. (1986). Precambrian continental crust of India and its evolution. *Journel of Geology, 94*, 145–166.

Radhakrishna, B. P., Pandit, A. S., & Prabhakar, K. T. (1973). Copper mineralization in the ultramafic complex of Nuggihalli, Hassan district, Mysore State. *Journal Geological Society of India, 14*, 302–322.

Raith, M., Srikantappa, C., Buhl, D., & Kohler, H. (1999). The Nilgiri enderbites, South India: Nature and age constraints on protolith formation, high-grade metamorphism and cooling history. *Precambrian Research, 98*, 129–150.

Rajamani, V. (1990). Petrogenesis of metabasites from the schist belts of the Dharwar Craton: Implications to Archaean mafic magmatism. *Journal Geological Society of India, 36*, 565–587.

Rajaram, M., & Harikumar, P. (2001). *Source field of the aeromagnetic anomalies over Peninsular India, DCS–DST News, January issue 16*. New Delhi: Department of Science & Technology.

Rajamani, V., Shivakumar, K., Hanson, G. N., & Shenoy, S. B. (1985). Geochemistry and petrogenesis of amphibolite, Kolar Schist Belt, south India: Evidence from komatiitic magma derived by low percentage of melting of the mantle. *Journal of Petrology, 96*, 92–123.

Ramakrishnan, M. (1993). Tectonic evolution of the granulite terrains of southern India. *Memoirs Geological Society of India, 25*, 35–44.

Ramakrishnan, M. (1994). Stratigraphic evolution of the Dharwar Craton. In R. M. Ravindra & N. Ranganathan (Eds.), *GeoKarnataka, Karnataka Assist* (pp. 6–35). Bangalore: Geologists' Association.

Ramakrishnan, M. (2003). Craton-mobile belt relations in Southern Granulite Terrain. *Memoirs Geological Society of India, 50*, 1–24.

Ramakrishnan, M., & Viswanatha, M. N. (1987). Angular unconformity, structural unity argument and Sargur-Dharwar relations in Bababudan Basin. *Journal Geological Society of India, 29*, 471–482.

Ramam, P. K., & Murty, V. N. (1997). *Geology of Andhra Pradesh*. Bangalore: Geological Society of India. 245 p.

Ramasamy, S. M. (1995). En echelon faults along West Coast of India and their geological significance. *Current Science, 69*, 811–814.

Rama Rao, B. (1940). Archaean complex of Mysore. *Mysore Geological Department Bulletin*, *17*, 95p.

Rao, M. S., & Majumdar, P. (1981). Ore petrology of the Aladahalli cupriferous pyrite deposit, Hassan district, Karnataka. *Journal Geological Society of India, 22*, 452–458.

Reddy, P. R., Chandrakala, K., & Sridhar, A. R. (2000). Crustal velocity structure of the Dharwar Craton, India. *Journal of Geological Society of India, 55*, 381–386.

Rogers, J. J. W., & ad Mauldin, L. C. (1994). A review of the terranes of Southern India, In K. V. Subbarao (Ed.), *Volcanism*, Wiley Eastern, Hoboken, pp. 157–171.

Sahu, K. C., & Nair, A. M. (1982). The chromite of Byrapur, Karnataka. *Journal Geological Society of India, 23*, 330–337.

Saitoh, Y., Tsunogae, T., Santosh, M., Chetty, T. R. K., & Horie, K. (2011). Neoarchaean high-pressure metamorphism from the northern margin of the Palghat-Cauvery Suture Zone, southern India: Petrology and zircon SHRIMP geochemistry. *Journal of Asian Earth Sciences, 42*, 268–288.

Sankaran, A. V. (2001). Discovery of life in greater than 2.6 billion-year-old terrestrial samples. *Current Science, 80*, 489–491.

Sawkar. R. H. (1981). Geology of the manganese ore deposits of North Kanara district, Karnataka state, In I. M. Varentsov & G. Y. Grasselly (Eds.), *Geology and Geochemistry of Manganese,* (Vol. II, pp. 279–295). Stuttgart.

Sawkar, R. H., Hussain, S. M., & Naqvi, (1995). Gold mineralization in the sulphidic BIFs of Chitradurga schist belt, Karnataka—Possibility of new workable gold deposits. *Journal Geological Society of India, 46*, 91–93.

Sengupta, S., & Roy, A. (2012). Tectonic amalgamation of crustal blocks along Gadag-Mandya shear zone in Dharwar Craton of southern India. *Journal of the Geological Society of India*, *80*, 75–88.

Sharma, I. N., Lal, R. K., & Mohan, A. (2003). Chemographic relationship and metamorphic evolution of orthopyroxene and sillimanite-bearing garnet-cordierite gneisses and saphirine-spinel-corundum granulites from Karimnagar, NE part of the Eastern Dharwar Craton, India. *Memoirs Geologyical Soceity of India, 52*, 195–228.

Siddaiah, N. S., & Rajamani, V. (1989). The geologic setting, mineralogy, geochemistry and genesis of gold deposits of the Archaean Kolar Schist Belt, India. *Economic Geology, 84*, 2155–2172.

Singh, A. P., Mishra, D. C., Gupta, S. B., & Rao, M. R. K. P. (2004). Crustal structure and domain tectonics of the Dharwar Craton (India): Insight from new gravity data. *Journal Asian Earth Sciences, 23*, 141–152.

Srikantappa, C., & Narasimha, K. N. P. (1988). Retrogression of charnockites in the Moyar Shear Zone, Tamil Nadu. *Memoirs Geological Society of India, 11*, 117–124.

Srikantappa, C., Raith, M., & Ackermand, D. (1985). High-grade regional metamorphism of ultramafic and mafic rocks from the Archaean Sargur terrane: Karantaka, S. India. *Precambrian Research, 30*, 189–219.

Srikantappa, C., Venugopal, L., Devaraju, J., & Basavalingu, B. (1994). PT conditions of metamorphism and fluid inclusions characteristics of the Coorg granulites, Karnataka. *Journal Geological Society of India, 44*, 495–504.

Srinivasan, M. S. (1988). Late Cenozoic sequences of Andaman-Nicobar Island: Their regional significance and correlation. *Indian Journal of Geology, 60*, 11–34.

Srinivasan, R., Naqvi, S. M., UdayRaj, B., Subba Rao, D. V., Balaram, V., & Gnaneshwar Rao, T. (1989a). Geochemistry of Archaean greywackes from the northwestern part of the Chitradurga Schist Belt, Dharwar Craton, South India—Evidence for granitoid upper crust in the Archaean. *Journal Geological Society of India, 34*, 505–516.

Srinivasan, R., Naqvi, S. M., & Vasantha Kumar, B. (1990). Archaean shelf-facies and stromatolite proliferation in Dharwar Supergroup, North Kanara district, Karnataka. *Journal Geological Society of India, 35*, 203–212.

Srinivasan, R., Pantulu, G. V. C., & Gopalan, K. (1997). Rare earth element, geochemistry and Rb–Sr geochronology of Archaean stromatolitic cherts of the Dharwar Craton, South India. *Proceedings of Indian Academy of Sciences (Earth & Planet Sci.*), *106*, 369–377.

Srinivasan, R., Shukla, M., Naqvi, S. M., Yadav, V. K., Venkatachala, B. S., UdayRaj, B., & Subba Rao, D. V. (1989b). Archaean stromatolites from the Chitradurga Schist Belt, Dharwar Craton, India. *Precambrian Research, 43*, 239–250.

SwamiNath, J., & Ramakrishnan, M. (1981). Early Precambrian Supracrustals of southern Karnataka. *Memoirs Geological Survey India, 112*, 1–328.

Swami Nath, J., Ramakrishnan, M., & Viswanatha, M. N. (1976). Dharwar stratigraphic model and Karnataka Craton evolution. *Record Geology Survey India, 107*(II), 149–175.

Trendall, A. F., de Laeter, J. R., Nelson, D. R., & Mukhopadhyay, D. (1997). A precise zircon U–Pb age for the base of the BIF of the Mulaingiri Formation, Bababudan Group, Dharwar Supergroup of the Karnataka craton. *Journal Geological Society of India, 50*, 161–170.

Ugarkar, A. G., Panaskar, D. B., & Gowda, G. R. (2000). Geochemistry, petrogenesis and tectonic setting of metavolcanics and their implications for gold mineralization in Gadag Gold field, southern India. *Gondwana Research, 3*, 371–384.

Valdiya, K. S. (1998). Late Quarternary movements on landscape rejuvenation in southeastern Karnataka and adjoining Tamil Nadu in Southern Indian Shield. *Journal of Geological Society of India, 51*, 139–166.

Valdiya, K. S. (2001a). River response to continuing movements and scarp development in central Sahyadri and adjoining coastal belt. *Journal of Geological Society of India, 57*, 13–30.

Valdiya, K. S. (2001b). Tectonic resurgence of the Mysore Plateau and surrounding regions in cratonic southen India. *Current Sciences, 81*, 1068–1089.

Varadarajan, S. (1970). Emplacement of chromite-bearing ultrabasic rocks of Mysore State. *Proceedings of Second Sympossium Upper Mantle Project*, National Geophysical Resarech Institute, Hyderabad, pp. 441–454.

Varadarajan, S. (1975). Mineralogical studies of chromite deposits of Mysore State, India. In V. K. Verma (Ed.), *Recent Researches in Geology* (Vol. 2, pp. 31–40). Delhi: Hindustan Publishing Coporation.

Vasudev, V. N., Chadwick, B., Nutman, H. P., & Hegde, G. V. (2000). Rapid development of the Late Archaean Hutti Schist Belt, northern Karnataka: Implications of new field data and SRIMPT U/Pb ziron ages. *Journal Geological Society of India, 55*, 529–540.

Vasudev, V. N., & Naganna, C. (1973). Mineragraphy of gold-quartz-sulphide reefs of Hutti Gold Mine, Raichur district, Mysore State. *Journal Geological Society of India, 14*, 378–383.

Venkatachala, B. S., Shukla, M., Sharma, M., Naqvi, S. M., Srinivasan, R., & Uday Raj, B. (1990). Archaean microbiota from the Donimalai Formation, Dharwar Supergroup India. *Precambrian Research, 47*, 27–34.

Venkatadasu, S. P., Ramakrishnan, M., & Mahabaleswar, B. (1991). Sargur-Dharwar relationship around the komatiite-rich Jayachamarajapura Greenston Belt in Karnataka. *Journal Geological Society of India, 38*, 577–592.

Venkataramana, P. (1983). Mode of occurrence and origin of magnesite in parts of Mysore district, Karnataka. *Journal Geological Society of India, 24*, 343–355.

Verma, R. K. (1985). *Gravity Field, seismicity and tectonics of the Indian Peninsula and the Himalaya*. New Delhi: Allied Publishers.

Vijaya Kumar, K., Ernst, W. G., Leelanandam, C., Wodden, J. L., & Grove, M. J. (2010). First Palaeoproterozoic ophiolite from Gondwana: Geochronologic-geochemical documentation of ancient oceanic crust from Kandra, SE India. *Tectonophysics, 487*, 22–32.

Vijaykumar, K., Reddy, M. N., & Leelanandam, C. (2006). Dynamic melting of the Precambrian mantle: Evidence from rare earth elements of the amphibolites from the Nellore-Khammam Schist Belt, South India. *Contributions Mineral Petrology, 152*, 243–256.

Viswanatha, M. N., Ramakrishnan, M., & Swaminath, J. (1982). Angular unconformity between Sargur and Dharwar supracrustals in Sigegudda, Karnataka Craton, South India. *Journal Geological Society of India, 23*, 85–89.

Zachriah, J. K., Mohanta, M. K., & Rajamani, V. (1996). Accretionary evolution of the Ramagiri Schist Belt, Eastern Dharwar craton. *Journal Geological Society of India, 47*, 279–291.

Chapter 4
Archaean Cratons in Central, Eastern and Western India

4.1 Introduction

The central, eastern and western parts of the Indian Shield comprise, respectively, the Bastar, the Singhbhum and the Bundelkhand cratons. These three cratons of Archaean antiquity are separated one from the other by Proterozoic mobile belts (Fig. 3.1). The Proterozoic mobile belts have gone through cycles of deformation, metamorphism and granite emplacement. They are bounded by shear zones and thrusts of considerable consequence. In common with the Dharwar Craton in the southern part of the Indian Shield, the early crustal development in these cratonic provinces took place around the nuclei of Palaeoarchaean rocks, and the process of cratonization was completed by the end of the Neoarchaean about 2600–2500 million years ago. The evolution of the Archaean cratons entailed stretching and rifting of sialic crust. This was followed by basic volcanism and attendant intrusion of basic–ultrabasic plutons. After that there was sedimentation in tectonically formed intracratonic linear basins. Finally, there was granite emplacement took place on extensive scales. The granitic magmas that were emplaced 2600–2500 Ma ago represent the finale of the tangled history of the Archaean era in the Indian Shield.

4.2 Bastar Craton

4.2.1 Continental Nucleus

Among the pioneers who laid the foundation of the geology of the Indian Shield in central India, L.L. Fermor and H. Crookshank occupy very exalted positions.

The *Bastar Craton*, also described as *Bhandara Craton*, covers southern Chhattisgarh, north-eastern Maharashtra, south-western Odisha and north-western

K.S. Valdiya, *The Making of India*, Society of Earth Scientists Series,
DOI 10.1007/978-3-319-25029-8_4

Andhra Pradesh (Fig. 4.1). It comprises widespread and preponderant quartzofelspathic gneisses and granites of batholithic dimension. The covering volcano-sedimentary supracrustals form linear belts and islands. Later involved in strong Proterozoic tectonism, both the basement gneisses and the covering volcano-sedimentary rocks were highly deformed and metamorphosed to generally medium-grade metamorphism, but reaching granulite grade in the south-western part. The vestige of 3500-Ma tonalite–trondhjemite–granodiorite in the southern part of the Bastar Craton, and of 3000-Ma orthogneisses enclaves within the vast expanse of the 2600- to 2500-million-year-old granite gneiss, imply that the craton grew around a protocontinental nucleus. The temporal span of the growth must have been of the order of 1000 million years.

4.2.2 Tectonic Boundaries

The south-western and north-eastern boundaries of the Bastar Craton are demarcated by the NW- to SE-oriented Gondwanic grabens, occupied in the present by the Godavari and the Mahanadi rivers, respectively. However, the elongate linear basins became sites of protracted sedimentation but only towards the close of the Palaeozoic era. The faults responsible for the formation of rift basins represent ancient faults that were formed probably at the end of the Neoarchaean time.

East and south-east of the Bastar Craton (Fig. 4.2) lies the Proterozoic *Eastern Ghat Mobile Belt* comprising charnockites, khondalites, granulites and gneisses. The boundary of the Archaean Craton against the Proterozoic Mobile Belt is delineated by a shear zone of the nature of a detachment thrust. This tectonic zone has been described as the *Sileru Thrust* (Chetty and Murthy 1994; Chetty 1995) in the southern sector and as the *Terrane Boundary Shear Zone* in the northern part (Biswal et al. 2000; Biswal and Sinha 2003).

North of the craton a crustal-scale shear zone called the *Central Indian Shear Zone* and oriented broadly ENE–WSW, extends for more than 500 km (Yedekar et al. 1990; Jain et al. 1991; Bandyopadhyay et al. 1995) and is also called Central Indian Tectonic Zone (Roy and Hanuma Prasad 2003). It represents the tectonized boundary of the *Satpura Mobile Belt* of Proterozoic antiquity. The Central Indian Shear Zone is characterized by 2- to 5-km-wide zone of mylonites and northerly dipping steep shears. It extends WSW from Amarkantak to north of Nagpur. Slices of pyroxene granulites exhibiting REE characteristics of ultrabasic rocks associated with ocean-floor basalts occur along the northern margin of the shear zone. This assemblage has been interpreted as closely resembling vestiges of a Precambrian suture between the Bastar and the Bundelkhand cratons (Yedekar et al. 2003; Jain et al. 1991; Raza et al. 1993; Bandyopadhyay et al. 1995). The pattern of Bouguer gravity anomaly shows that it extends east-northeastwards across the Mahanadi Graben into the Singhbhum Shear Zone in the eastern part of the Indian Shield (Jain et al. 1991).

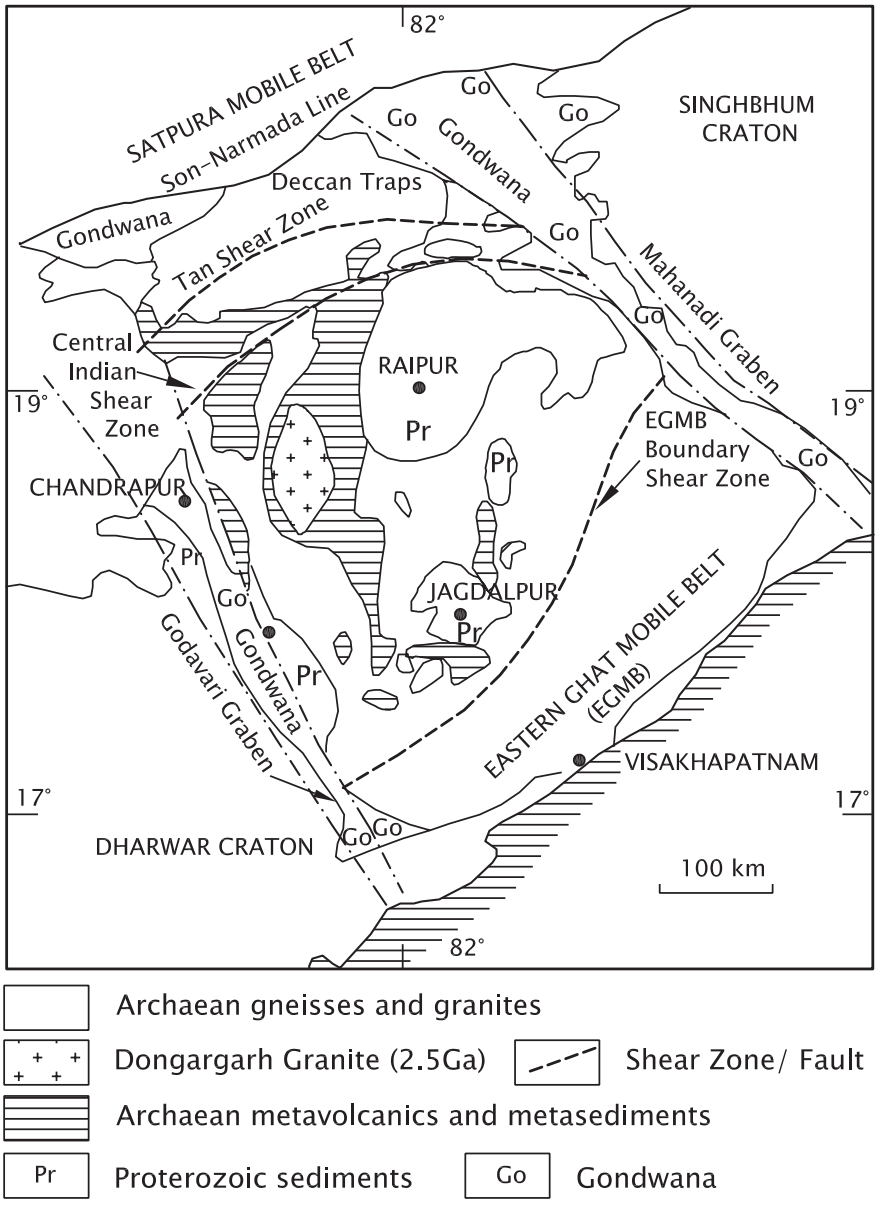

Fig. 4.1 Sketch map showing the position of the Bastar Craton bordered by Proterozoic mobile belts which are themselves defined by deep shear zones and thrusts (based on Ramakrishnan 1990; Roy and Hanuma Prasad 2003)

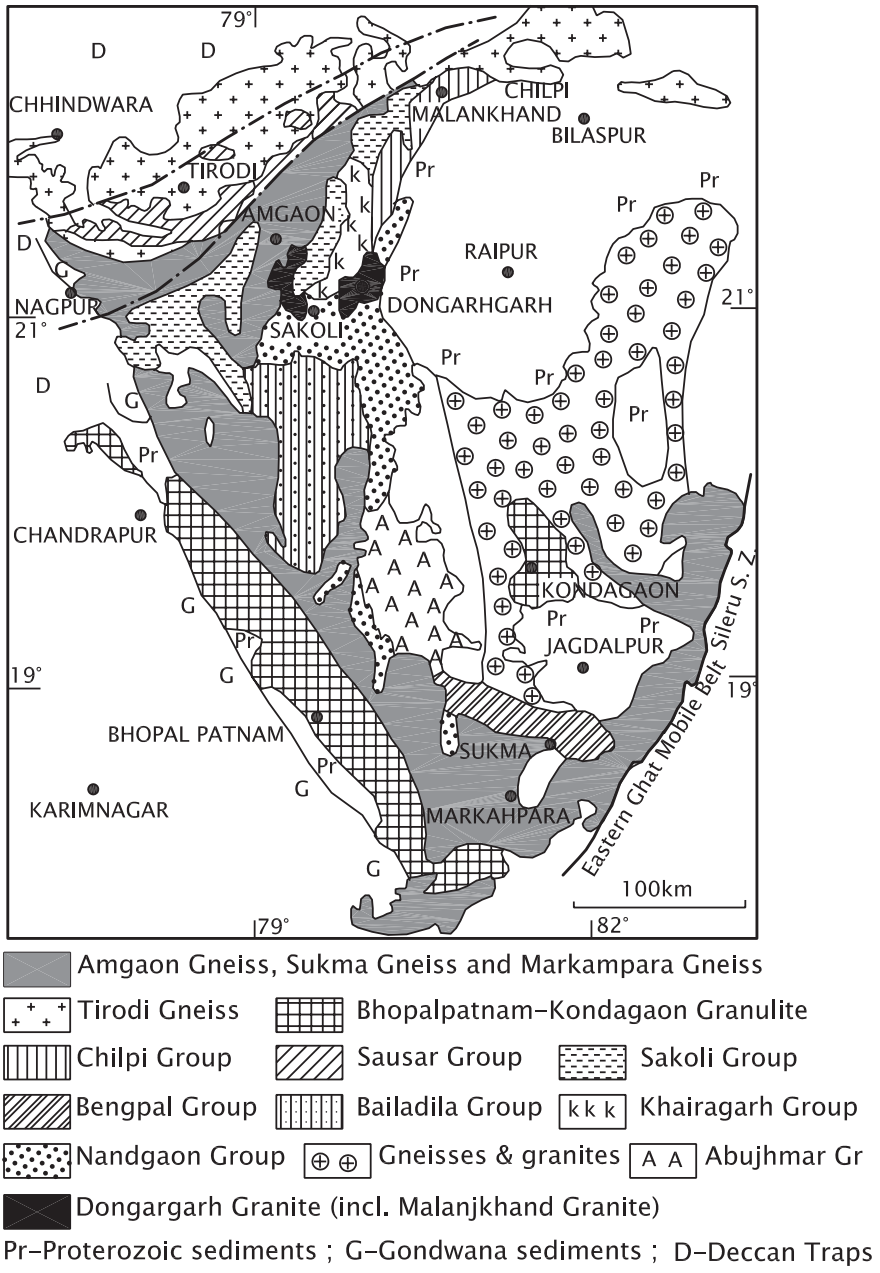

Fig. 4.2 Sketch map shows the lithotectonic units of the Bastar Craton (based on Ramachandra et al. 2001)

4.2.3 Deformation Pattern

The most conspicuous feature of structural architecture of the Bastar Craton (Fig. 4.2) is the intersection of two sets of shear zones associated with mobile belts—the N–S Kotri–Dongargarh belt that evolved in the Proterozoic and the ENE- to WSW-oriented structures of the Satpura Mobile Belt, particularly preponderant in the northern part. The N–S belt associated with Dongargarh Granite marks the terminal phase of the Late Archaean cratonization. The ENE- to WSW-fold belts are of post-Archaean time formed in the period 1500–1200 Ma (Bandyopadhyay et al. 1995) (Fig. 4.3).

4.2.4 Craton Nucleus: Markampara Gneiss

In the southern part of the Bastar district, high-alumina gneiss of tonalite–trondhjemite–granodiorite composition occurs as enclaves within the gneisses and granites that dominate the cratonic terrane. They are variably metamorphosed from middle amphibolite to lower granulite facies. The Markampara Gneiss exhibits initial strontium ratio of 0.7016, strong depletion of P and Ti, enrichment of both LILE and HFSE, and abundance of HREE, well-defined positive Eu anomaly and negative Nb and Ti anomalies. The trace-element chemistry thus implies derivation of the magma by partial melting at the base of an over-thickened continental crust (Wanjari et al. 2005). It could also be a product of melting of a subducted oceanic slab without interaction with mantle wedges (Hussain et al. 2004).

These gneisses have yielded U–Pb zircon age of 3509 ± 14 Ma, indicating the time of primary crystallization of the magma (Sarkar et al. 1993). The tonalite in the central part of the craton is 3560 Ma old (Ghosh 2004). In age and compositional characteristics, the Markampara Gneiss is very similar to the Gorur Gneiss in the Dharwar Craton. However, there is one very significant difference. The Markampara Gneiss is not associated with any suite of basic or ultrabasic rocks, such as discernible in the Holenarsipur Schist Belt in the Dharwar Craton.

4.2.5 Sukma Group

In the nearly 2500-m-thick succession of metamorphic complex (Figs. 4.4 and 4.5) described as the *Sukma Group* (Crookshank 1963; Ramakrishnan 1990), sillimanite-bearing quartzite, calc-silicate gneiss, amphibolite and cordierite–anthophyllite schist, cordierite–biotite–sillimanite–garnet schist, and metamorphosed banded ferruginous quartzite are associated with biotite gneiss and migmatites of tonalite–trondhjemite–granodiorite composition. The Sukma is one among the many gneissic units occurring as enclaves within the younger granites that form the vast expanse

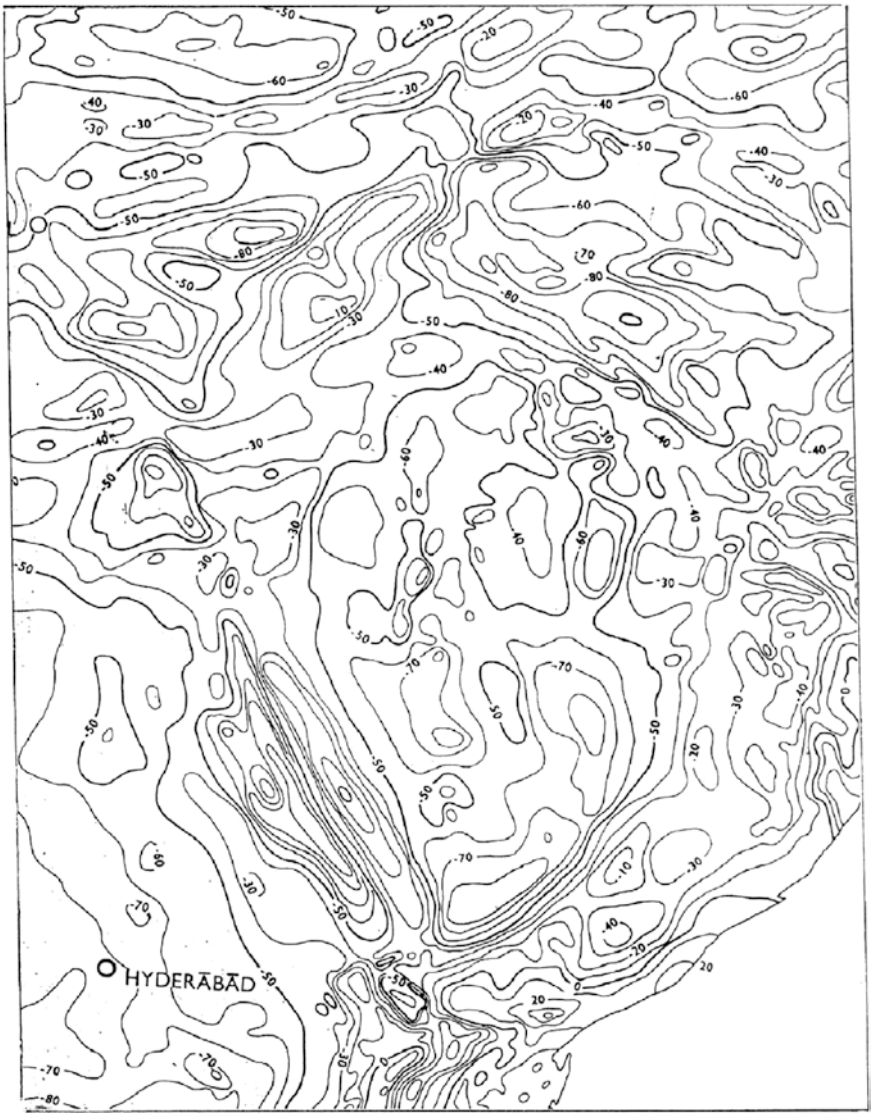

Fig. 4.3 Bouguer gravity anomaly in that part of the Peninsular India which embodies the Bastar and Singhbhum cratonic blocks (after Subrahmanyam 1980, 1985)

of the Bastar terrane. The whole-rock isochron age of the Sukma gneisses is 3081 ± 60 Ma (Sarkar et al. 1990).

It appears that the crust of the Indian Shield in central India was formed and cratonized in the period 3500–3000 Ma. The Sukma and the associated gneisses of the Bastar Craton seem to be coeval with the Peninsular Gneiss of the Dharwar Craton.

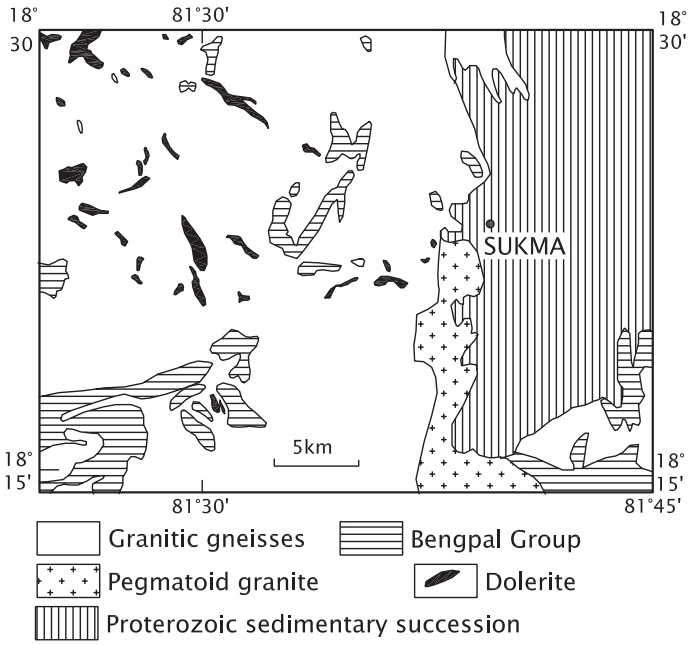

Fig. 4.4 Generalized geological map of the Sukma area showing the relation of the gneissic granites with the volcano-sedimentary units—the supracrustal Sukma and Bengpal groups—in the context of the Proterozoic formations (after Sarkar et al. 1990)

4.2.6 Bengpal Group

Lithologically resembling the Sukma, the *Bengpal Group* (Crookshank 1963) comprises sericite–quartzite interlayered with amygdaloidal basalts and tuffs, ferruginous quartz schist, banded iron-quartzite and conglomerate (Fig. 4.5). These are intimately associated with andalusite–chiastolite schist, andalusite quartzite and chloritoid schist of contact metamorphic origin. Intrusion of younger granites is responsible for the formation of andalusite, chiastolite and chloritoid in the contact zone. The Bengpal rests unconformably on the Sukma (Ramakrishnan 1990). It is described as a younger supracrustal formation belonging to the Neoarchaean time (Ramachandra et al. 2001). Basic volcanics and tuffs form a minor component of the Bengpal. Intercalated with rocks of greenschist facies, they form ESE- to WNW-oriented volcano-sedimentary belt fanning out from the N–S trending Bailadila Belt in the west and Tulsi Dongar in the east.

The assemblage of the Bengpal groups (garnetiferous grunerite schist, banded iron-quartzite and conglomerate) recalls the lithological composition of the lower part of the Dharwar Supergroup in the Southern Indian Shield.

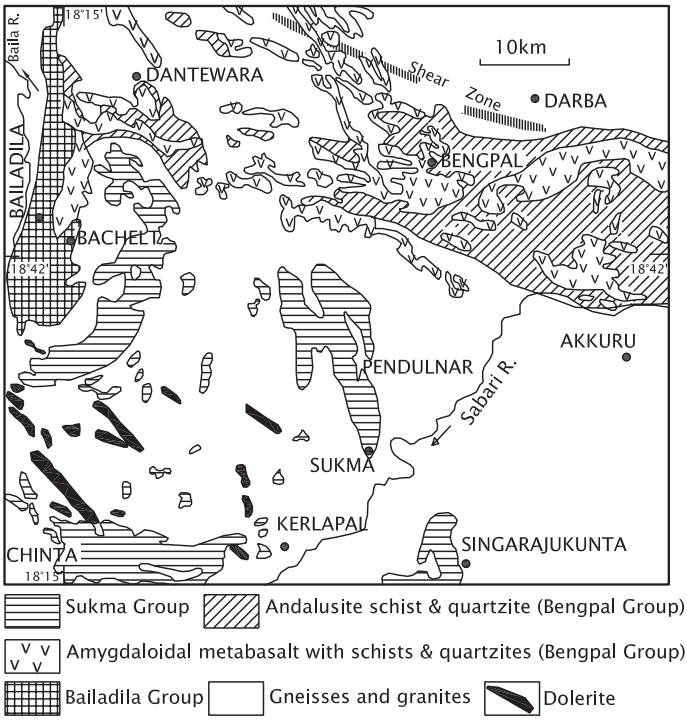

Fig. 4.5 Geological sketch map of southern part of the Bastar Craton showing the Bailadila Group in association with the Sukma and the Bengpal groups (after Ramakrishnan 1990)

4.2.7 Bailadila Group

Unconformably overlying the Sukma and the Bengpal complexes, the 1300- to 2700-m-thick succession of mildly metamorphosed dominantly ferruginous sedimentary rocks (Fig. 4.6) is known as the *Bailadila Group* (Crookshank 1963). It bears striking lithological similarity with the upper part of the Dharwar Supergroup. It may be recalled that the latter also unconformably overlies the older lithological successions of lower group in the Dharwar Craton. In common with the Sukma and Bengpal assemblages, the Bailadila also contains (but in subordinate proportion) grunerite schist, chlorite schist and carbonaceous phyllite. The predominant component is the banded haematite-quartzite. The Bailadila succession comprises five formations (Khan and Bhattacharyya 1993) as given in the Table 4.1.

Before subjected to metamorphism, the original sedimentary succession of the supracrustal or covering Sukma–Bengpal–Bailadala units must have comprised quartzarenites, carbonates and ferruginous shales associated with prominent iron formation and subordinate basic volcanics and ultrabasic rocks. The combined assemblages represent a deposit of a continental-margin setting or a back-arc basin

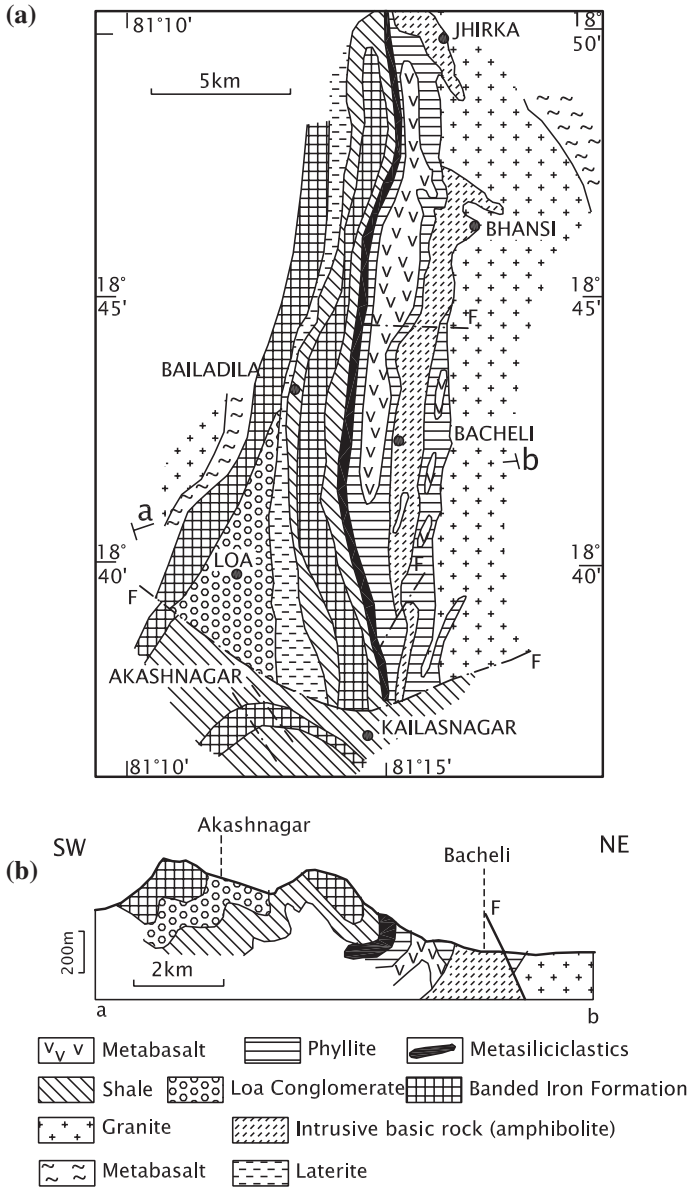

Fig. 4.6 **a** Geological sketch map of the Bailadila Ridge in the Bastar Craton. **b** Cross section, along ENE–WSW line passing by Bacheli and Akashnagar, illustrates the structure of the ridge (**a** and **b** after Khan and Bhattacharyya 1993)

Table 4.1 Lithostratigraphic subdivision of the Bailadila Group (Khan and Bhattacharyya 1993)

Kailashnagar Formation (200-500 m)	Banded haematite-quartzite, banded magnetite-quartzite and pockets of iron ore formed due to supergene alterations
Loa Formation (5–150 m)	*Upper horizon* consists of thinly laminated ferruginous shale that is intensely laterized *Lower horizon* made up of polymictic conglomerate with a matrix of tuffaceous silt and ferruginous sand
---------- *Unconformity* ----------	
East Ridge Formation (206–639 m)	Ferruginous tuffaceous shales interbedded with bedded chert, banded ferruginous chert (jaspillite) and rare carbonaceous phyllite
Bacheli Formation (240–335 m)	Graded bedded wackes and cross-bedded arenite with intercalations of shales
Bhansi Formation (600–1000 m)	Chlorite-mica phyllite with or without porphyroblasts of andalusite, Amygdaloidal basalts
---------- *Unconformity* ----------	
Sukma-Bengpal Groups	

within the continent (Ramakrishnan 1990). Like the Dharwar Supergroup succession, the supracrustal assemblages of the Bastar also represent a deposit of an intracontinental basin in the regime of transpressional tectonism resulting from stretching of the Archaean sialic crust.

4.2.8 Amgaon Gneiss

The granitic gneisses that wholly surround the 3500-million-year-old Markampara Gneiss and the 3100-Ma-old Sukma gneiss represent widespread magmatism heralding the beginning of the Proterozoic era. The *Amgaon Gneiss* is dated 2480 ± 3 Ma by the U–Pb zircon geochronology (Sarkar 1958; Sarkar et al. 1993). The gneiss at Kawadgaon gave an age of 2497 ± 152 Ma (Yamuna Singh and Chabria 1999). It is obvious that the Amgaon Gneiss belongs to the time span 2600–2500 Ma and is therefore a contemporary of the Closepet Granite of the Dharwar Craton.

4.2.9 Bhopalpatnam Granulite

The southern–south-western part of the Bastar Craton forming the north-eastern flank of the Godavari Graben embodies two granulite belts—the Bhopalpatnam and the Kondagoan (Fig. 4.2). The *Bhopalpatnam Granulites* composed of

garnet-bearing enderbitic charnockite and pelitic gneisses which were formed at, respectively, 8–9.5 kbar and 720–800 °C and 4.7–6.5 kbar on 660–720°C (Santosh et al. 2004). The granulites are believed to have been exhumed from the lower crustal level. The granulites contain zoned crystals of zircon that have 1900-Ma-old cores and 1700-Ma-old rims; the grains of monazite define a clear isochron age of 1590 ± 30 Ma. In contrast, the uraninite and monazite in the granulites in the Karimnagar district contain zircon which has 2600-Ma mantle around 3100-Ma core, and show an age peak at 2420 ± 80 to 2470 ± 30 Ma (Santosh et al. 2004). The formation of granulites is thus related to emplacement of Amgaon Gneiss.

4.2.10 Mafic Dykes

Two sets of subalkaline mafic dykes trend in the NW–SE and WNW–ESE directions in the northern part of the Bastar Craton. In the southern part, there is a third set of dykes—occurring in swarms in the granulitic terrane. These dykes have boninitic character, high contents of silica and magnesia and low proportion of titania. The U–Pb, TIMS and EMP U–Th total lead chemical dating of gabbro and dolerite give an age of 1883 ± 114 Ma (Srivastava and Singh 2003).

At the northern margin of the Indravati River Basin the Khadka dykes of lamproites exhibits trace element and rare-earth element geochemistry strikingly similar to those of the 1880-Ma-old Krishna Valley in the Eastern Dharwar Craton (Yellappa et al. 2010).

4.3 Singhbhum Craton

4.3.1 Configuration and Characteristics

The geological framework of eastern part of the Indian Shield embodying the Singhbhum Craton was built on the basis of pioneering works of P.N. Bose in 1904, H.L. Jones in 1934, J.A. Dunn in 1937 and 1940 and J.A. Dunn and A.K. Dey in 1942.

Covering nearly 40,000 km^2 area of Jharkhand, Odisha and adjoining areas in eastern part of the Indian Shield, the *Singhbhum Craton* lies in the embrace of two Proterozoic mobile belts—the Satpura Mobile Belt in the east, north and north-west, and the Eastern Ghat Mobile Belt in the south. It is separated from the Bastar Craton by the Mahanadi Graben of Gondwanic heritage. Characterized by relics of the oldest rocks of the Indian subcontinent, the Singhbhum Craton comprises widespread Palaeoarchaean and Mesoarchaean tonalitic and granodioritic granites and gneisses, and by abundant occurrence of banded iron formation closely associated with basic volcanics and ultrabasic intrusives. All these rocks

have undergone regional metamorphism of the amphibolite facies. The craton is believed to have evolved as a consequence of multiple phases of compressive deformation related to what has been called the *Singhbhum Orogeny* (Saha 1994). It is this terrane that provides India's largest iron ore and chromite deposits.

4.3.2 Tectonic Boundaries

One of the most conspicuous features of the Singhbhum Craton is the curvilinear shear zone that demarcates its northern boundary against the Chota Nagpur Gneiss terrane. This is the *Singhbhum Shear Zone*, also described as the *Copper Belt Thrust* (Figs. 4.7 and 4.8). More than 500 km in length, the deep Singhbhum Shear Zone is represented by a 1- to 5-km-wide zone of fractures. Some of these reached the mantle, providing pathways to outpouring lavas and the locales to ultrabasic plutons (Banerji 1962, 1969, 1977). It originated as a normal fault along which the northern block gradually subsided, giving rise to what is known as the Singhbhum Basin of Proterozoic antiquity. Later reversal of the sense of movement made it a shear zone, later culminated in southwards thrusting of rocks onto the Archaean Singhbhum Craton. It became a zone of magmatism, metasomatism and mineralizing activities on extensive scales (Banerji 1962, 1969, 1977). The shear zone is presently characterized by a multiplicity of thrust planes with variable upward displacement of the northern block. These thrust planes splay out into a number of diverging faults in the south. There are several bands of mylonites formed principally during the first-phase deformation. A strong shear movement related to thrusting is discernible in the Jamshedpur–Mosabani sector (Ghosh and Sengupta 1990). As a product of progressive ductile deformation, the shear zone exhibits reclined folds superimposed by two groups of folds, asymmetric foliation with subhorizontal to gently plunging axes, and gentle upright transverse folds (Sengupta 1972; Mukhopadhyay 1976, 1984; Bhattacharyya and Sanyal 1988).

In the south, the tectonic boundary of the Singhbhum Craton is defined by the *Sukinda Thrust* (Figs. 4.7 and 4.8) which has brought the charnockite–khondalite–granulite assemblage of the Eastern Ghat Mobile Belt against the low-grade metamorphics of the Singhbhum terrane. A number of parallel faults are associated with the Sukinda Thrust. One of them is the Sarapalli–Gundlichanal Fault, extending for 100 km and demarcating the limit of the chromite-bearing ultrabasic horizon. The ultrabasics occur in the core of a WNW-plunging syncline developed along the southern margin of the Singhbhum Craton. They form a body of layered rocks related to a mantle-reaching fault system. From Sarapalli to Kamakhyanagar, the Sukinda Thrust separates the Iron Ore Group of the cratonic terrane from the Gondwana Basin, occupied by the Mahanadi River. The analogue of the Sukinda Thrust further south-west in the Eastern Ghat terrane is known as the *Terrane Boundary Shear Zone* (Biswal and Sinha 2003). The fault zone here is an eastward-dipping (>50º) thrust, and interpreted as a listric fault that acted as the

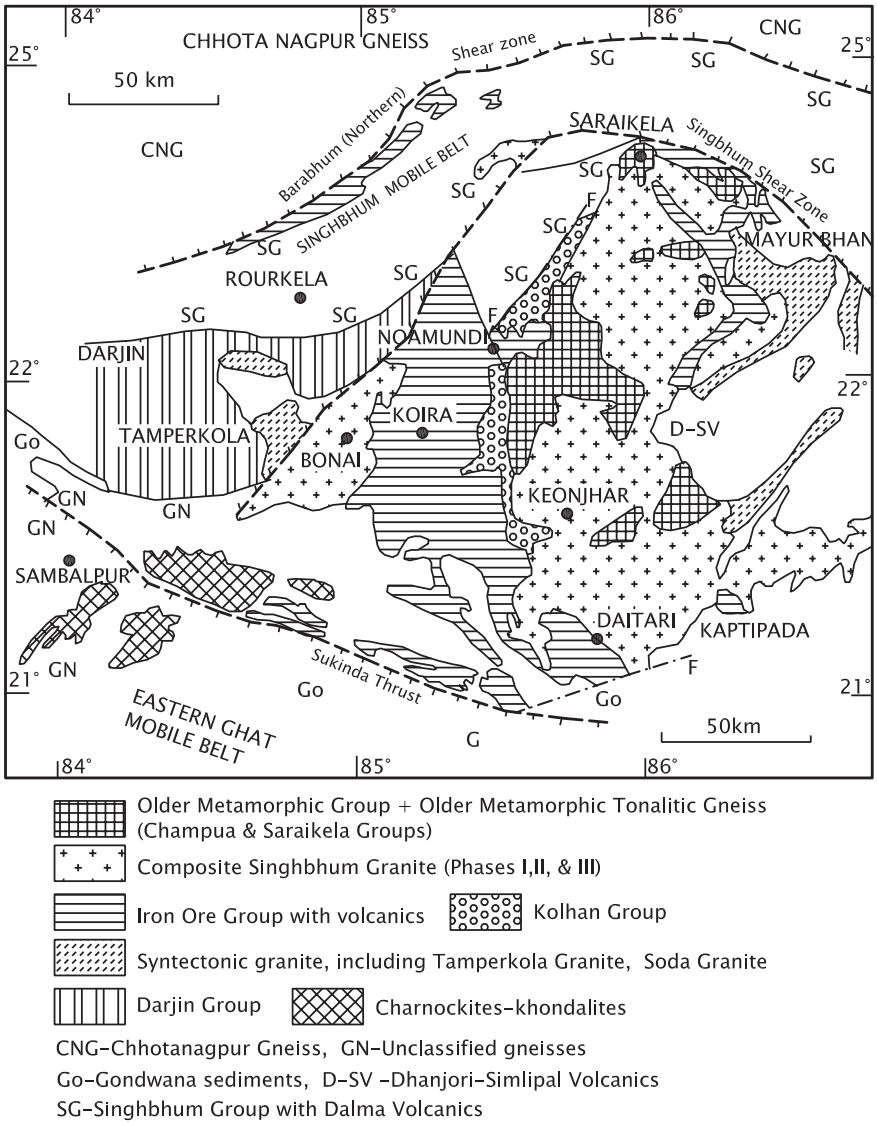

Fig. 4.7 Generalized geological map of the Singhbhum Craton showing the main lithotectonic units of Archaean age (based on Saha 1994; Sarkar 2000; Saha et al. 2004)

sole thrust between the basement (Bastar Craton) and the overthrust charnockite-granulite succession of the Eastern Ghat Mobile Belt. Similar situation is envisaged for the Sukinda Thrust Zone.

The granitoid bodies occurring in the Singhbhum Craton at its tectonic contact with Eastern Ghat Mobile Belt and in the EGMB itself show strong mylonitic

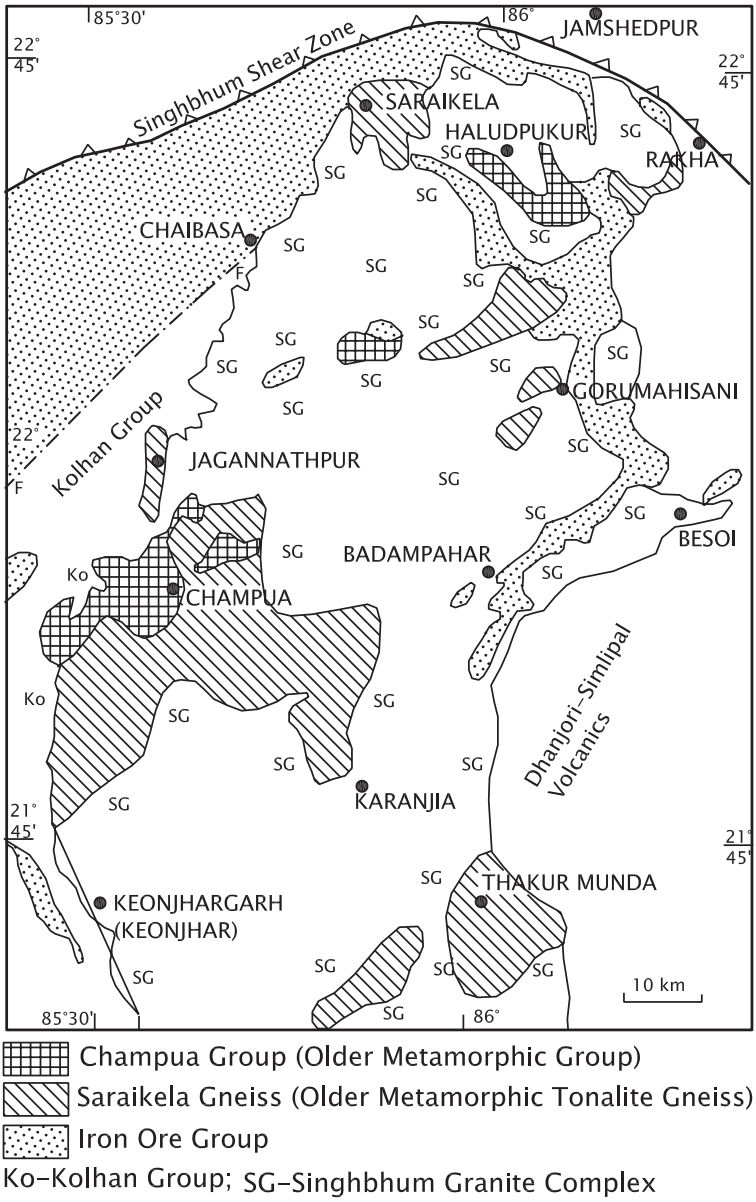

Fig. 4.8 Sketch map shows the Champua Group (Older Metamorphic Group) and the Saraikela (Older Metamorphic Tonalite) Gneiss in the general framework of the Singhbhum Craton (based on Saha 1994)

Table 4.2 Archaean lithotectonic units of the Singhbhum Craton in geochronological order (based on Saha 1994)

Proterozoic Mayurbhanj Granite and Anorthosite-Gabbro Assemblage
---------- *Unconformity* ----------
Tamperkola Granite (2800 Ma)
Darjin Group
---------- *Unconformity* ----------
Singhbhum Granite (Type B, Phase III), Bonai Granite (3160 Ma)
Iron Ore Group
---------- *Unconformity* ----------
Besoi Granite (Singhbhum Granite Type A, Phases I & II) (3200 Ma)
Saraikela Gneiss (Older Metamorphic Tonalite Gneiss) (3440 Ma)
Champua Group (Older Metamorphic Group)

foliation bearing mutual parallelism, implying widespread remobilization accompanying deformation during the last phase of the Eastern Ghat Orogeny (Ghosh et al. 2008).

4.3.3 Lithostratigraphic Layout

In the Singhbhum cratonic province, six major lithotectonic units are recognizable, five of them exhibiting amphibolite-facies metamorphism. The sixth unit is free from deformation and metamorphism and belongs to the Neoarchaean time. These units (Figs. 4.7 and 4.8; Table 4.2) in geochronological order are the Champua Group, the Older Metamorphic Tonalite Gneiss, the Singhbhum Granite Type A, the Iron Ore Group, the Singhbhum Granite Type B and the Darjin Group (Sarkar and Saha 1962, 1983; Saha et al. 1988; Saha 1994; Mukhopadhyay 2001; Bandyopadhyay et al. 2001). These lithostratigraphic units have undergone multiple deformations during the Singhbhum orogeny which occurred late in the Proterozoic time. It is the Singhbhum Granite Type B that forms the larger part of the granite batholithic complex, the Champua Group and the Older Metamorphic Tonalite Gneiss occurring only as minor bodies and enclaves within the batholith. Occurrence of relics of this oldest unit over extensive area within the Singhbhum batholithic complex is suggestive of the fact that the Champua had a large geographic extent. Since the granitic rocks are seen to intrude the amphibolite-facies metasediments of the Champua Group, the gneisses of the latter unit are regarded as the oldest unit—the nucleus of the Singhbhum Craton.

In other words, the Champua is the oldest group in the Singhbhum Craton (Table 4.2).

The Singhbhum Granite Type A forms the basement of the Iron Ore Group and associated volcano-sedimentary cover succession (supracrustals). The Iron Ore

succession unconformably envelopes the Singhbhum batholithic complex. On all sides, the Iron Ore Group is intruded by younger granite described as Singhbhum Granite Type B. This younger granite forms the belonging to the third phase of granitic activity larger central and eastern parts of the batholithic complex.

In the north-western part of the cratonic terrane, a 200-m-thick sediments of the *Darjin Group* is intruded by the 2800-million-year-old Tamperkola Granite.

4.3.4 Champua Group (Older Metamorphic Group)

The oldest lithostratigraphic unit of the Singhbhum cratonic terrane, known as the *Older Metamorphic Group* commonly occurs as minor outcrops ranging in size from a few square kilometres, to several hundred square kilometres and as enclaves in the all-engulfing Singhbhum Granite complex. South-west of Gorumahisani at Champua, the unit typically comprises pelites and sandstones associated with ferromagnesian lithologies. The Older Metamorphic Group can therefore be redesignated as the *Champua Group*. The Champua rocks are transformed by amphibolite-facies metamorphism to an assemblage of muscovite–biotite schist, quartz–sericite schist, sillimanite–quartz schist, quartz–magnetite–cummingtonite schist, calc-silicate schist, hornblende schist and amphibolite, the transformation taking place at 600–650 °C and 5–5.5 kbar (Saha et al. 1984). The orthoamphibolite in the Champua succession represents an original magma of tholeiite affinity, characterized by slight enrichment of LREE, and flat HREE pattern, implying its derivation by partial melting from a mantle depleted in Nd isotopes (Sharma et al. 1994).

Ar–Ar plateau age of hornblende separated from the amphibolite varies between 3286 ± 6 and 3314 ± 4 Ma (Baksi et al. 1987). The Sm–Nd whole-rock isochron age of the orthoamphibolite is 3305 ± 60 Ma—the age of magma crystallization. The sillimanite-bearing schist contains elliptical grains of detrital zircon derived from the provenance of granites. This fact suggests existence of a sialic continental crust older than the Champua, even though its outcrop has not been encountered so far (Basu et al. 1981; Mukhopadhyay 2001). Ion microprobe Pb–Pb single zircon dating yielded ages in the range of 3600–3500 million years, indicating that the crustal formation had begun as early as 3600 Ma (Mishra et al. 1999). The clustering of zircon ages at 3400 and 3200 Ma seems to demonstrate metamorphism during those times. In the U–Pb concordia diagram, the upper intercept age of the zircon grains (taken from the Champua) is 3350 Ma (Basu et al. 1998) and the Pb–Pb dates of the detrital zircon cluster around 3500, 3400 and 3200 Ma (Goswami et al. 1995).

4.3.5 Saraikela Gneiss (Older Metamorphic Tonalite Gneiss)

The Champua succession was affected by widespread intrusion of tonalite, culminating in the evolution of a complex comprising admixture of Champua metamorphics and tonalites. The complex is known as the *Older Metamorphic Tonalite*

Gneiss (Saha et al. 1984; Saha 1994). This complex covers a large part of the Keonjhargarh (renamed Kendujhargarh) region in Odisha. Since another outcrop of similar association occurs north of the Saraikela area in Jharkhand (Fig. 4.8), which is assigned to the Older Metamorphic Tonalite Gneiss (OMTG); it can be given a new name—the *Saraikela Gneiss*. Moderately foliated, the synkinematic Saraikela Gneiss is characterized by a trace-element chemistry that indicates derivation of the tonalite magma by partial melting of amphibolites of the Champua Group and of rocks that are still older (Mukhopadhyay 2001). The age of the Saraikela (Older Metamorphic Tonalite) Gneiss is broadly around 3400 Ma. It was affected by widespread metamorphism about 3200 million years ago.

The Sm–Nd date of one enclave within the Singhbhum batholithic complex is 3775 ± 89 Ma, while the Rb–Sr age of the same suite of rocks is 3200 Ma (Basu et al. 1981). Another enclave in the same area yielded Pb–Pb age of 3378 ± 98 Ma and Rb–Sr isochron age of 3280 ± 130 Ma (Moorbath and Taylor 1988). A tonalite enclave occurring in the Singhbhum body yielded an Ar–Ar age of 3430 Ma (Baksi et al. 1987). The high alumina trondhjemite xenoliths of Saraikeral Gneiss in the *Bonai Granite*—a satellite body west of the Singhbhum batholithic complex around Keonjhargarh—yielded a Pb–Pb isochron age of 3369 ± 57 Ma and a U–Pb age for magmatic zircon of 3380 + 6/−4 Ma and xenocrystic zircon of 3448 Ma (Sengupta et al. 1991, 1996). The Sm–Nd whole-rock age of the tonalite–trondhjemite enclaves in the Bonai is 3288 ± 35 Ma (Sharma et al. 1994) while their Pb–Pb isochron ages are 3664 ± 79 and 3405 ± 53 Ma (Ghosh et al. 1996).

It is also apparent from the trace-element geochemistry, particularly the Sm–Nd isotopic characteristics, that there is a genetic link between the ortho-amphibolite of the Champua Gneiss and the tonalite–trondhjemite components of the Saraikela Gneiss (OMTG). The tonalite of the Saraikela Gneiss was produced possibly by moderate degree of partial melting at 12–18 kbar and 1000 °C of the basement amphibolite (Sharma et al. 1994).

Available geochronological data thus indicate that the bulk of the Champua and Saraikela gneisses—Older Metamorphic Group and Older Metamorphic Tonalite Gneiss—had formed by the time period 3400–3300 million years ago.

4.3.6 Besoi Granite (Singhbhum Granite Type A)

A large batholithic complex elongate in the N–S direction (Figs. 4.7 and 4.9) embodies a number of plutons belonging to three pulses of intrusion, the first two occurring within a short temporal span (Saha et al. 1984, 1988; Saha 1994). The granites of the first two phases are described as the *Singhbhum Granite Type A* (Phases I and II) and of the third phase as *Singhbhum Granite Type B* (Phase III). It is the Type B that forms the larger part of the batholithic complex and should be called sensu stricto the *Singhbhum Granite*. The Singhbhum Granite Type A occurs over a large part of the Keonjhargarh district and has been well dated at Besoi in the Mayurbhanj district. To minimize confusion, it would be better if

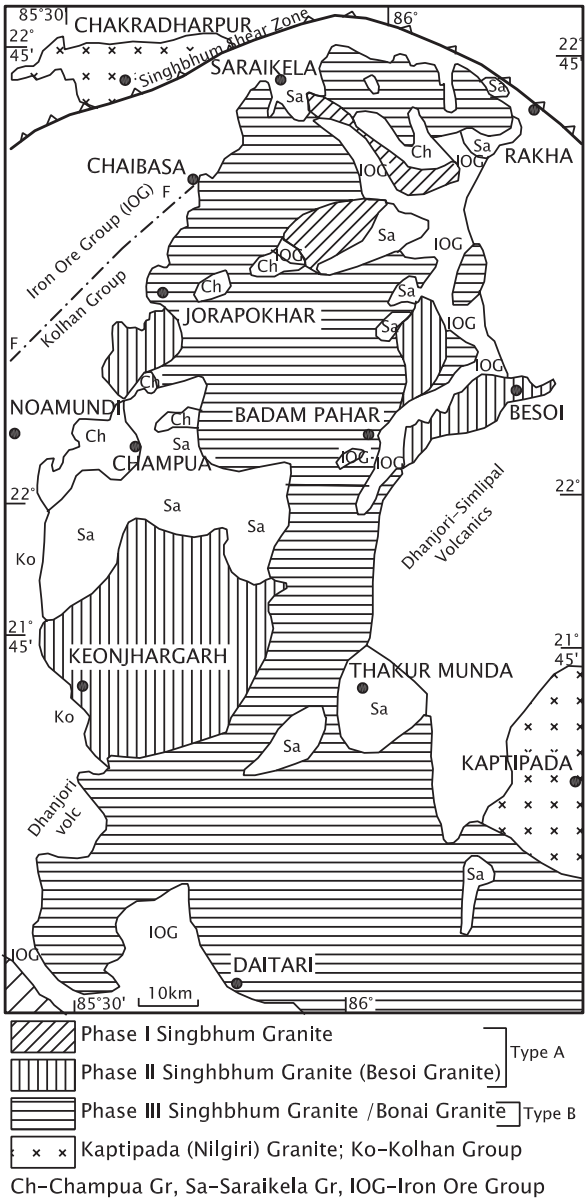

Fig. 4.9 Sketch map shows the extent of the batholithic complex described as the Singhbhum Granite. Saha (1994) identified geochemically distinctive two types of granites—Singhbhum Granite Type A and Singhbhum Granite Type B, belonging to three pulses of emplacement. Type A embodies granites of the first two phases of intrusion (based on Saha 1994)

Type A granite is described as the *Besoi Granite*. The Pb–Pb age of the Besoi Granite is 3442 ± 26 Ma (Ghosh et al. 1996).

The different bodies of granites are separated by partition of metamorphic rocks. One of features of crucial import all over its extent is the occurrence of big and small enclaves or xenoliths of rocks of Champua Group and Saraikela Gneiss. Some of these xenoliths have retained older fold structures and metamorphism, implying emplacement of the Besoi Granite after the deformation and metamorphism of the first two lithotectonic units. In mineralogical composition, the Besoi Granite is a biotite granodiorite, very locally grading to trondhjemite. Its trace-element geochemistry, characterized by gently sloping REE pattern, moderate enrichment in LREE and absence of Eu anomaly, indicates that the Besoi Granite is a product of partial melting (Saha et al. 1988; Saha 1994).

The Pb–Pb isochron age of the Besoi Granite is 3292 ± 50 Ma (Moorbath et al. 1986) and the Rb–Sr whole-rock date is 3300 Ma (Baksi et al., 1987). The Kaptipada (Nilgiri) body has been dated by Rb–Sr whole-rock method at 3369 ± 57 and 3275 ± 8 Ma (Vohra et al. 1991) and the Bonai pluton has yielded Rb–Sr isochron age of 3247 ± 53 Ma (Sengupta et al. 1991). The Bhaura body has given Sm–Nd age of 3298 ± 63 Ma (Ghosh et al. 1996). The ion microprobe Pb–Pb single zircon age is 3328 ± 7 Ma (Mishra et al. 1999). The Besoi body, as already stated, is 3442 ± 26 million years old. It seems likely that the Besoi Granite (that is Singhbhum Granite Type A) was formed contemporaneous with the protoliths of the Saraikela (Older Metamorphic Tonalite) Gneiss (Moorbath and Taylor 1988). Possibly the magma of the two units was derived from the mantle at about the same time or that the temporal interval between the two intrusions was about 150 million years.

The highly fractionated REE pattern with flat HREE, moderate enrichment of LREE, and negative Eu anomaly of the porphyritic *Bonai Granite* is not different from that of the younger Singhbhum Granite Type B (Sengupta et al. 1991). However, in age it is coeval of the Besoi Granite. Possibly the Bonai too has different components belonging to three phases of emplacement.

4.3.7 Iron Ore Group

The Besoi (Singhbhum Type A) Granite forms the basement of a thick succession of mildly metamorphosed, predominantly ferruginous sediments associated with basic volcanics, named the *Iron Ore Group* by H.C. Jones in 1934. It is an unconformable succession upon the Besoi Granite (Murty and Acharya 1975; Mukhopadhyay 1976; Banerji 1977; Iyengar and Murthy 1982). The Iron Ore Group succession occurs in three belts—Noamundi–Jamda–Koira, Gurumahisani–Badampahar, and Tomka–Daitari—forms a north-plunging synclinorium in the Noamundi–Koira belt only (Figs. 4.8 and 4.10; Table 4.3). In all the three belts, the predominant banded iron formation is closely associated with lavas and tuffs.

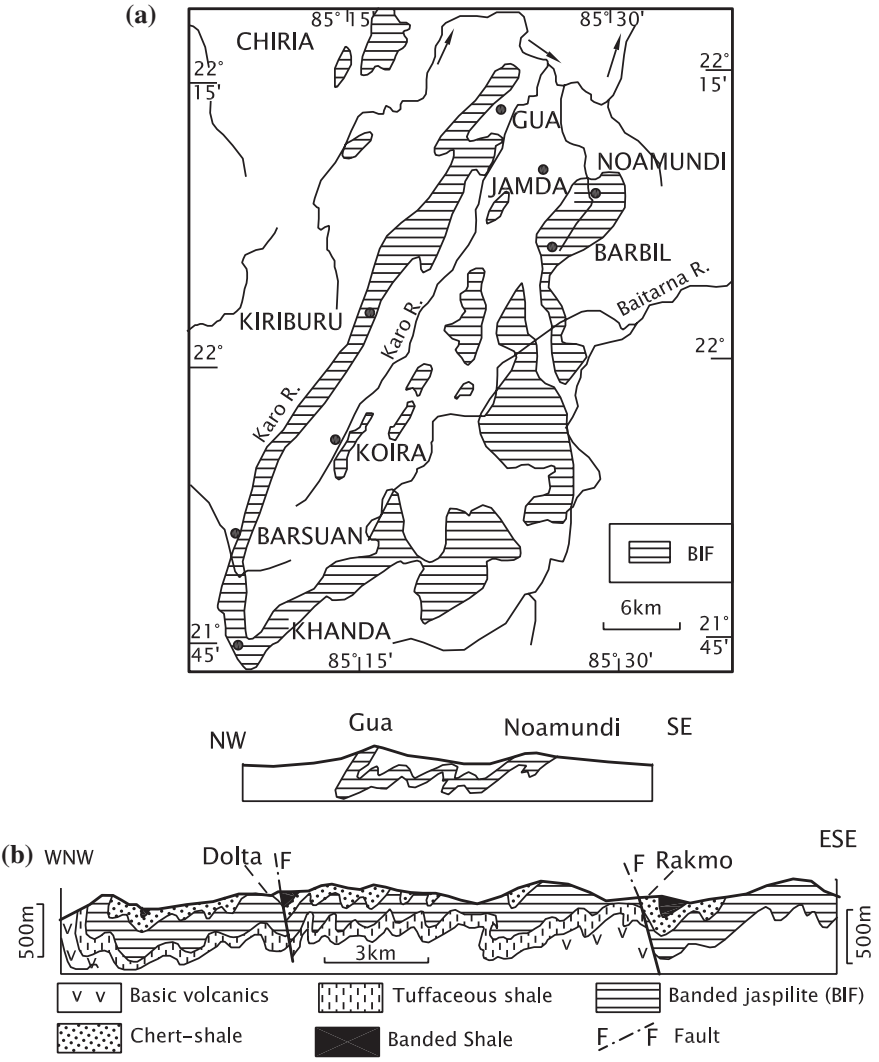

Fig. 4.10 **a** Iron Ore Group forms a synclinorium in the Jamda–Koira valley (after Chakraborty and Majumder 1986). **b** Diagrammatic cross section of the Iron Ore Group in the Koira Valley showing its lithology and structural design (based on Murty and Acharya 1975)

In the Gorumahisani–Badampahar belt, the Iron Ore Group (Fig. 4.12) commences with conglomerates and sandstones at the base. It is followed upsection by ferruginous shale, volcanic tuff, lava and *banded iron formation*. The sandstones include quartzarenite and lithic wacke. The framework of the conglomerate is made up of pebbles of quartz, and the matrix contains sizeable population of detrital zircon derived from the Besoi Granite, that is Singhbhum Granite Type A

(Sinha et al. 1997). The shales are constituted of kaolinite and illite clays, indicating that the detritus was washed down from a granitic provenance (Rao and Dasgupta 1995). Current ripple marks and desiccation cracks with pseudo-conglomerate indicate that the deposition took place in a very shallow-water environment (Rai et al. 1980; Acharya et al. 1982; Chakraborty and Manjumder 1986; Majumder and Chakraborty 1977; Majumder et al. 1982; Murty and Aibarga 1975; Majumder 1991). The banded iron formation, made up of iron-oxide facies sediments, consists of magnetite–chert, magnetite–jasper, haematite–jasper (jaspillite), martite–quartz and magnetite–haematite chert, representing primary precipitation of oxides of Fe and Si. Carbonates are rare, but occur as siliceous dolomite characterized by stromatolites. The stromatolites reveal spheroidal and filamentous organic remain (Avasthy 1980; Sarkar 1989) that grew in shallow-water environment.

The Iron Ore Formation in the Noamundi mines, embodying strata-bound deposits stretching over 3 km in length, was formed as a result of leaching out of silica from the banded iron haematite-quartzite and introduction of iron by hydrothermal fluids of meteoric origin (Beukes et al. 2008). The saprolitic iron ore, on the other hand, is a product of prolonged weathering since Cretaceous.

The interbanded and interlayered pyroclastics and basic volcanics occur sizeably towards the top of the succession in the Jamda–Koira valley. The volcanics form a common component of the Iron Ore Group. The lavas show pillow structure, flow-layering, vesicular-variolitic features, quench structures and in some places spinifex texture (Acharyya 1993; Sengupta et al. 1993). In the Gurumahisani–Badampahar belt, the ultrabasics occurring at the bottom of the sequence show cumulate structures. While the volcanics of the eastern belt have tholeiitic affinity, those of the western belt show calc-alkaline composition. The two types of volcanics are different in their incompatible elemental ratios, and in their REE characters and the Zr/Nb ratio, implying derivation from different sources in the mantle (Sengupta et al. 1997) (Table 4.3).

A granite intruding the banded iron formation in the Deo River section has yielded an errorchron date of 3145 ± 282 Ma, providing evidence of the antiquity of the Iron Ore Group (Paul et al. 1991). The Sm–Nd metamorphic age of the banded iron formation in the Tomka–Daitari belt lies somewhere between 3200 and 2550 Ma. This fact implies that the sedimentation started before the intrusion of the 3120-million-year-old Singhbhum Granite Type B (Chakraborty and Majumder 1986). Analysis of palaeomagnetic polar wanders curve point to the banded haematite–jasper formation belonging to the time span 2900–2600 Ma (Das et al. 1996).

Zircon grains from the dacite lavas in the metamorphosed succession of greenstones give SHRIMP U–Pb age of 3506.8 ± 2.3 Ma, indicating that the greenstone is the oldest reported in India (Mukhopadhyay et al. 2008). If this date is correct, the stratigraphy of the Singhbhum terrane will have to be revised. It is necessary that the geochronologists look at the dating.

Table 4.3 Stratigraphic succession of different iron ore belts in the Singhbhum cratonic terrane (after Chakraborty and Majumder 1986)

Gurumahisani-Badampahar section	Tomka-Daitari section	Jamda-Koira valley
Banded magnetite/martite quartzite with little jasper and iron ore	Banded magnetite/hematite quartzite and jasper with thin interlayered volcanic tuff and enriched iron ore	Upper tuffs and volcanics
Banded cherty quartzite with black chert		Manganese-bearing shale
Interlayered thinly laminated volcanic tuff	Basal quartzite with interlayered banded cherty quartzite and very little thin layers of black chert and intraformational conglomerate	Banded iron formation with iron ore
Banded magnetic/martite cherty quartzite and iron ore		Lower tuffs and greywackes
		Quartzite
Quartzite, fuchsite-quartzite, Cherty quartzite		
Basal conglomerate		
---------- *Unconformity* ----------	Basement not seen	---- *Unconformity* ----
Older Metamorphic Group		Older Metamorphic Group

4.3.8 Singhbhum Granite (Type B)

Making the larger part of the batholithic complex, the geochemically distinctive and geochronologically different granite described as the Singhbhum Granite Type B by Saha (1994), Saha et al. (1984, 1988) is the *Singhbhum Granite* in the strict sense. It represents the third phase of magma emplacement and is seen to intrude the Iron Ore Group in some places. The predominant biotite–granodiorite grades into finer-grained adamellite are characterized by moderate enrichment in LREE, flat HREE pattern and conspicuous negative Eu anomaly, implying derivation of magma by differential melting of low-potash andesitic protolith followed by fractional crystallization.

The oval-shaped *Bonai pluton* that covers 500 km^2 area to the west of the main batholithic complex is made up porphyritic trondhjemite characterized by a chemistry not different from that of the two phases of the Singhbhum Complex. The Pb–Pb age of the Bonai body is 3163 ± 26 Ma (Sengupta et al. 1991). Making the eastern margin of the batholith, the coarse-grained porphyritic granite of the Mayurbhanj pluton is characterized by presence of ferrohastingsite and biotite. The early-phase aplogranite shows granophyrric texture, while the later-phase

granite is leucocratic. The Pb–Pb age of the Mayurbhanj granite at Jhorapokhar is 3050 ± 37 Ma, while the Rb–Sr whole-rock isochron age is 3042 ± 39 Ma (Ghosh et al. 1996). Ion microprobe single zircon data give a well-defined age of 3090 Ma (Mishra et al. 1999). Trace-element geochemistry suggests formation of the *Mayurbhanj Granite* as a consequence of partial melting of the sialic crust. Voluminous emplacement of gabbro along the margin of the plutonic body seems to have provided necessary heat for the partial melting.

4.3.9 Sukinda and Nuasahi Ultrabasic Bodies

In the shear zone related to the terrane boundary Sukinda Thrust occur a number of bodies of ultrabasic rocks, known as the *Sukinda Ultrabasics* and the *Nuasahi Ultrabasics*. The Nuasahi body is very small (3.5 km^2) in dimension. The Sukinda ultrabasic rocks occur in the form of a south-westerly plunging synform, with subvertical southern limb and 40–50º dipping northern limb (Figs. 4.11 and 4.13). The ultrabasic body is flanked on both sides by a gritty micaceous quartzite.

The ultrabasic complex comprises four petrological types: (i) homogeneous gabbro-anorthosite, (ii) peridotite with three layers of chromitite, (iii) pyroxenite exhibiting layering and cumulate texture and (iv) oblong intrusive gabbro (at Bangur), dated 3100 Ma (Auge and Lerouge, 2004a, b). Occurrence of magmatic breccia implies forcible injection. The breccia comprises ultrabasics with clasts of chromitite-wallrock set in a gabbroic matrix. There is a concentration of platinum-group elements in the breccia containing abundant chromitite. The Sukinda body has been metamorphosed to an assemblage of serpentinite, tremolite-talc schist, talc schist and chlorite schist. It has been described as an ophiolite of an ocean basin involved in plate tectonics (Page et al. 1985), the parental melt being of boninite affinity (Pal and Mitra 2004). However, the occurrence of chromitite

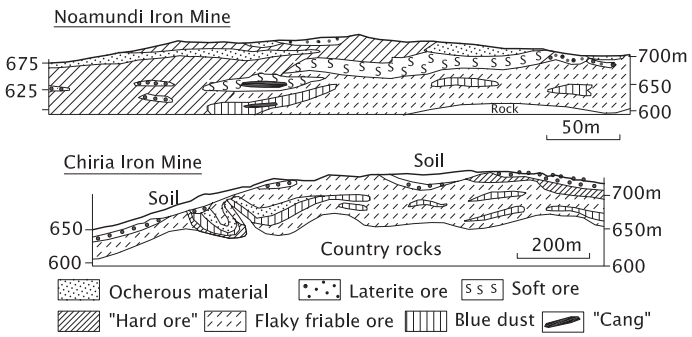

Fig. 4.11 **a** Geological sketch map of the Sukinda Valley showing distribution of the ultrabasic rocks with chromitite bands (Pal and Mitra 2004). *Inset* Nuasahi ultrabasic complex in the southern margin of the Singhbhum Craton (after Mondal et al. 2006)

in six layers in the Sukinda, the Ti-bearing cumulus magnetite deposits in the Baula–Nuasahi body and the layered nature of the ultrabasic bodies rule out their being ophiolites (Sarkar 2000). Interlayered with dunites and clinopyroxenites, the chromitite seams of the Nuasahi Complex testify to its origin from partial melting of siliceous high-magnesian basalts and boninites in the source during the Mesoarchaean period (Mondal et al. 2006).

The Sm–Nd data on the Baula gabbro indicate an age of 3205 ± 280 Ma, and the zircon age of the Bangur gabbro is 3122 ± 5 Ma, while the weighted mean age of mineralization is 3121 ± 3 Ma (Auge et al. 2003).

4.3.10 Darjin Group and Tamperkola Granite

West of the Singhbhum batholithic complex, a 200-m succession of little metamorphosed and undeformed, cross-bedded and ripple marked conglomeratic sandstones, subarkosic sandstones, shales, carbonaceous phyllites and dolomitic limestones, described as the *Darjin Group* (Mahalik 1994), rests unconformably on the Iron Ore Group and the Bonai Granite (Fig. 4.7).

The Darjin succession is intruded by a pink-coloured alkali feldspar-dominant *Tamperkola Granite*. The granite is associated with the acid volcanics that crystallized at 2800 Ma, as indicated by ion microprobe Pb–Pb zircon data (Bandyopadhyay et al. 2001). The Tamperkola Granite was emplaced in an anorogenic environment.

4.3.11 Geodynamic Evolution

The Champua Group and Saraikela Gneiss units forming the lower part of the Archaean lithology were deformed together by two phases of compression in the NW–SE direction (Sarkar and Saha 1962; Saha 1994). This gave rise to early northwards steeply plunging folds and to later moderately plunging folds. The deformation was followed by voluminous emplacement of granite in two major pulses. The first phase gave rise to the Besoi Granite, that is Singhbhum Granite Type A. Subsidence due to sagging or rifting apart formed a NNW-SSE trending depression. It was the repository of iron-rich as well as manganiferous sediments. The Iron Ore Group succession is folded into a synclinorium, oriented in the NNE–SSW direction as clearly discernible in the Jamda–Koira valley. Subsequent rotation around the batholith of the Besoi Granite formed the horseshoe-shaped structure and led to the overturning of folds to the east with gentle plunge northwards. In the Mangtoli sector, superimposition on these broadly NNE–SSW open folds of E–W trending folds with steep axial planes resulted in the development of dome-and-basin structures (Chatterjee and Mukherji 1981).

Saha et al. (1988), Saha (1994) and Mukhopadhyay (2001) have suggested models of evolution of the eastern part of the Indian Shield. A synthesis of the two models of the making of the Singhbhum Craton during the Archaean era is given here. There was a protocontinent in the Palaeoarchaean time. Ascending plumes under the crust of the protocontinent caused tensional stretching and formation of a depression. The sediments that accumulated in this basin are represented by the Champua Group (Older Metamorphic Group). Partial melting of the protocontinental and the underlying sub-crust due to impact of hot plumes generated predominant tonalitic magma. Accreting to the Champua succession, the magma contributed to synkinematic growth by about 3300 Ma of the Saraikela Gneiss (Older Metamorphic Tonalite Gneiss). Continuation of granite magmatism in the period 3300–3200 Ma resulted in the emplacement of the Besoi Granite batholith (Singhbhum Granite Type A). The ensuing thermal perturbation in the subcrustal level and the stretched apart microcontinent gave rise to an elongate NNE- to SSW-oriented basin between the separated granitic bodies. In the shallow water of this basin accumulated dominantly ferruginous and siliceous sediments, much of them as chemical precipitates. At one stage, the emplacement of the banded iron formation in the rift basin was accompanied by voluminous extrusion of basic lavas and the intrusion of gabbro and related ultrabasic magmas, within and outside the basin of the Iron Ore Group.

A period of deformation and attendant metamorphism followed and the structural design of the Iron Ore domain was established in the period 3200–3100 Ma. Further sinking of the sialic crust culminated in more differential melting at the lower level and emplacement of granites on a massive scale, giving rise to the Singhbhum Granite (Type B of Phase III). Renewal of subsidence in the western part of the Singhbhum terrane created a shallow basin of the Darjin sedimentation. And the emplacement of pink alkali feldspar-dominant Tamperkola Granite at 2800 Ma marks the last thermal event of the Neoarchaean era in the eastern part of the Indian Shield.

It may be recalled that the Neoarchaean pink alkali granites were also emplaced towards the termination of the Neoarchaean time in the Bastar and Dharwar cratons, represented by, respectively, the Amgaon Gneiss and the Closepet Granite.

By about 2500 Ma, a stable microcontinent had evolved in the eastern part of the Indian Shield.

4.3.12 Mineral Assets

The reserves of *iron ore deposits*, genetically related to the banded iron formation of the Gurumahisani–Badampahar belt, are of the order of 12 million tonnes, and of the Jamda–Koira valley about 3300 million tonnes (Sarkar 2000). The content of iron varies from more than 40 to 60 %, respectively. Precipitated as hydroxides of Fe^{+3} under condition of photo-oxidation, the iron minerals (magnetite, haematite, jasper) were subjected to intense supergene alteration, resulting in the

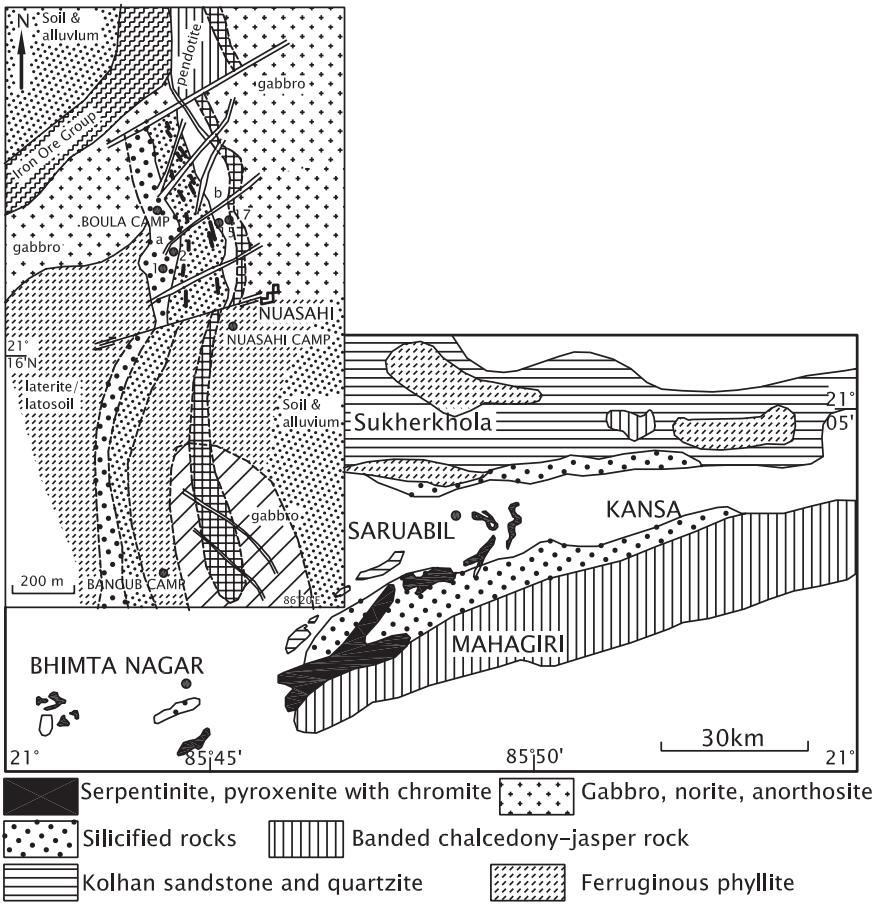

Fig. 4.12 Profiles across the Noamundi and Chiria mines, showing the pattern of supergene enrichment of banded iron formation that hosts rich deposits of iron ore (after Sarkar 2000)

formation of extremely rich iron ore deposits of global importance. The iron ore occurs (Fig. 4.12) as laterite (56–58 % Fe), massive or "hard" ore (64–68 % Fe), laminated ore (72–65 % Fe), recemented "canga" ore (58–60 % Fe) shaly or "soft" ore (61–63 % Fe) and powder or "bluedust" ore (65–68 % Fe).

The *manganese ores* occur in the proximity just below the iron ores in the Jamda–Koira valley. The deposits are located mainly in the shales. The dominant ore is the lateroid type, while the bedded types occur only locally. The minerals of the bedded type include pyrolusite, cryptomelane, manganite and braunite. These minerals were formed in the oxidizing environment of the shallow sea that was subject to regression.

More than 90 % production of chromite of India comes from the Sukinda and Baula-Nuasahi and Jajihatu–Hatgamaria areas of the Sukinda ultrabasic belt in the

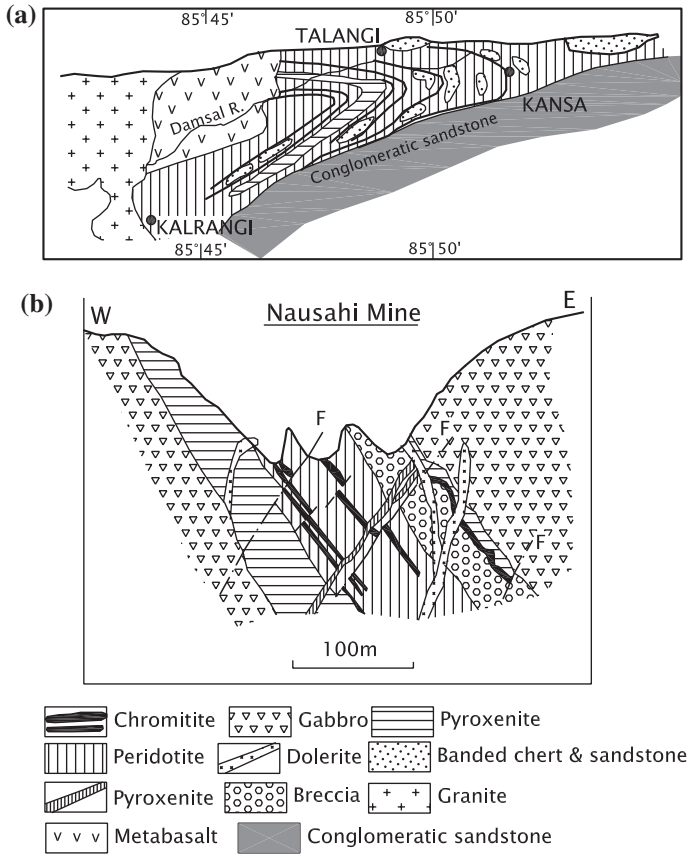

Fig. 4.13 Map and cross section of the Sukinda chromite deposits (after Sarkar 2000)

Keonjhar district. The Sukinda deposit is characterized by intense mineralization. There are six tabular bodies of ores over a length of 7 km and within a thickness of 50 m (Fig. 4.13). The chromium oxide content is more than 42 %.

There are promising indications of mineralization of Pt, Pd, Ir, Os, Rh and Ru in the chromite belt.

4.4 Bundelkhand Craton

4.4.1 Collage of Complexes

Constituting the core of north-western expanse of the Indian Shield, the Archaean *Bundelkhand Craton* is also described as *Aravali Craton* or *Rajasthan Craton*. It lies in the tight embrace of the Early Proterozoic fold-and-fault belts

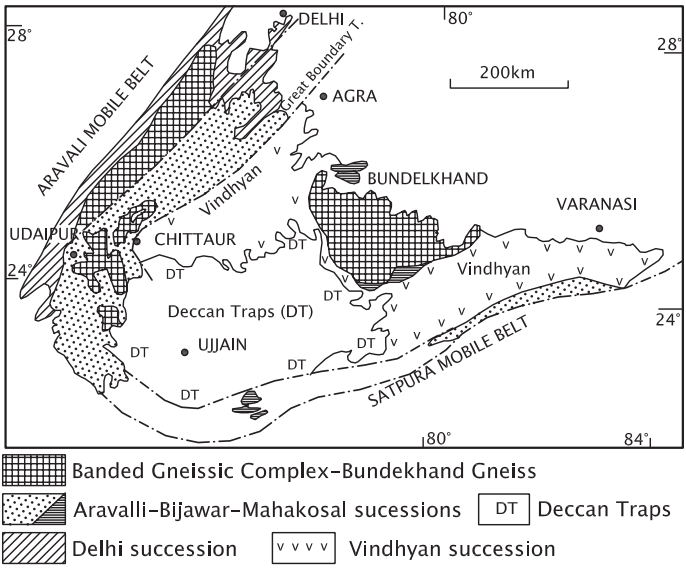

Fig. 4.14 Tectonic setting of the Archaean Bundelkhand Craton occurring within the embrace of the Aravali and Satpura fold-and-fault belts made up of Early Proterozoic rocks. The parabolic cover of the Proterozoic Vindhyan sediments divides it into two parts (based on Soni et al. 1987)

of the NE- to SW-oriented Aravali Range and the ENE–WSW trending Satpura Range (Fig. 4.14). A part of it is entangled with the Early Proterozoic Aravali Mobile Belt. The Bundelkhand Craton covers the geographic areas of eastern Rajasthan, south-western Uttar Pradesh, and north-western Madhya Pradesh. Later Proterozoic Vindhyan sedimentary cover makes a parabolic cover through the middle of the craton. The NE–SW trending Great Boundary Fault demarcating the western limit of the Vindhyas divides the craton into two blocks—the *Bundelkhand block* in the east and the *Mewar block* in the west.

Evolved through multiple episodes of deformation, metamorphism and plutonic–volcanic activities during the Archaean and Proterozoic times, the Bundelkhand Craton is constituted of a number of lithotectonic units or rock complexes that form the basement of the Proterozoic sedimentary successions of the larger Aravali domain. The basement near Udaipur embodies 3500-Ma-old gneissic rocks, representing the nucleus of the Mewar Craton. Multiple phases of ductile deformation, attendant granite magmatism and metamorphism have made the differentiation and delineation of various lithotectonic units very difficult. This has resulted in diverse nomenclature and disagreements. However, there is no denying that within the extent of the Bundelkhand Craton occur (1) Archaean granite–greenstone belts consisting of tonalite–trondhjemite–granite suite is intimately associated with basic volcanics and ultrabasic bodies, the entire assemblage being metamorphosed; (2) granulite–charnockite complex of deep-seated origin; and (3) Late Neoarchaean granites of batholithic dimensions. The

Archaean complexes also occur as isolated inliers within the surrounding fold-and-fault belts of Early Proterozoic rocks. A profound unconformity separates the Archaean basement from the Proterozoic cover or supracrustals. This is seen despite considerable obliteration by shearing and migmatization of rocks in some sectors, especially in the Sarara area, south of Udaipur.

The framework of the geology of the north-western part of the Indian Shield is built on the basis of seminal contributions of pioneers such as A. Hacket in 1881, L.L. Fermor in 1909, A.M. Heron in 1917 and 1953 and B.C. Gupta in 1934. It was Fermor who had given the name Bundelkhand Granite to the gneissic complex.

4.4.2 Geophysical Conditions

Deep seismic sounding across the Aravali domain along a transect from Jhalawar in the south-east to Nagaur in the north-west, together with gravity and magnetic investigations, has revealed the crustal structure below the north-western part of the Indian Shield (Tewari et al. 1995a, b, 1997, 1998; Reddy et al. 1995; Rajendra Prasad et al. 1998; Vijaya Rao et al. 2000; Vijaya Rao and Reddy 2002). A steep-gradient Bouguer gravity anomaly of 70–80 m Gal extends all along the trend of the Aravali orogen with conspicuous lows on the side defined by a 30–km-deep NW-dipping thrust (Figs. 4.14 and 4.16). The presence of divergent reflection fabric implies downwarping of the crust. There is also a high electrical conductivity zone 3 to 6 km in thickness lying at a depth of 3 to 20 km along the Kota–Bundi belt. The total magnetic intensity increases towards north-east, consistent with the thickening of the crust under the Aravali orogen that is characterized by an architecture of folds and faults. There is also an indication of the presence of vertical intrusive bodies in the crustal layer forming the basement of the cratonic province. Interpretation of gravity and magnetic data for depth estimation by application of scaling spectral method shows that the mid-crustal layer has risen up, the uplift-ment being related to a 109-km-wide and 25-km-thick domal structure below the Aravali orogen (Dimri et al. 2003).

4.4.3 Boundaries of Craton

The Archaean Craton is enclosed by Proterozoic Aravali and Satpura mobile belts on the north-western and southern sides, respectively. And both these mobile belts are sharply delimited against the Archaean blocks by deep faults and shear zones. However, parts of the craton complex also occur as large and small inliers within the domain of the Proterozoic supracrustals or cover rocks, which rest unconformably on the basement of Archaean rocks. Involved as it is in the folding, faulting and metamorphism with the supracrustals (Naha and Mohanty 1988) the basement

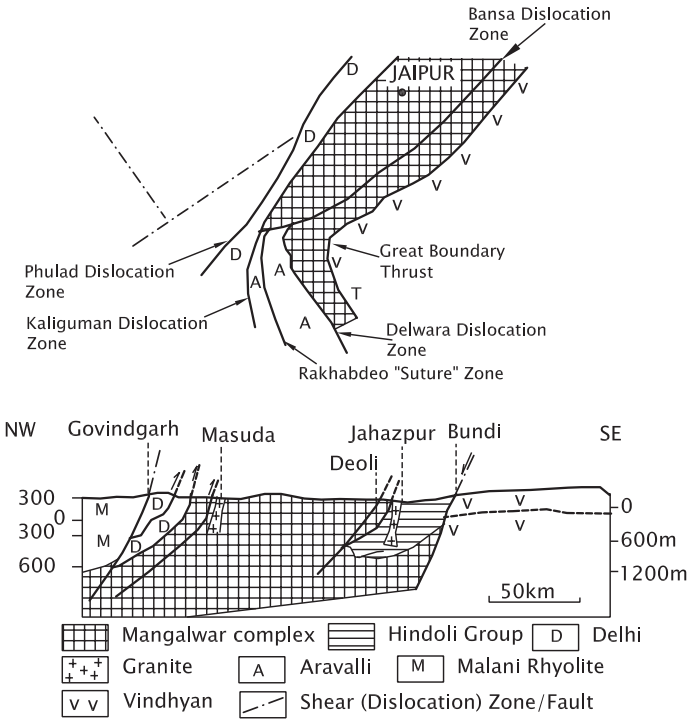

Fig. 4.15 **a** Boundaries of various lithotectonic units within the domain of the Bundelkhand Craton, described as dislocation zones by Sinha-Roy et al. (1995). These are shear zones, some of them are of crustal scale. **b** Cross section brings out the structural design of the Mewar block comprising basement and supracrustals (**a**, **b** after Sinha-Roy et al. 1995)

complex is not easily differentiated from the supracrustal rocks. In some places, later migmatization has obliterated or blurred the contact. In the eastern block of the Bundelkhand region, there is practically no cover rock upon the basement, although it is impersistently fringed along the southern boundary by the Early Proterozoic Bijawar and Later Proterozoic Vindhyan succession.

The Vindhyans occupy 100- to 300-km-wide intervening space between the eastern (Bundelkhand) and western (Mewar) blocks (Fig. 4.14). The limit of the Mewar block against the Vindhyan is demarcated by the *Great Boundary Fault* (Figs. 4.15 and 4.16), which registers an aggregate throw of the order of 500 m (Tewari 1995, 1995). The south-western–western boundary against the early Proterozoic Aravali–Delhi succession is delineated by curvilinear shear zones (Fig. 4.15) described as the Kaliguman and Delwara Dislocation zones. The NE- to SW-oriented Banas Dislocation Zone has split the basement into two unequal parts and truncated the Delwara and Rakhabdeo shear zones (Sinha-Roy 1984; Sinha–Roy et al. 1995).

The structural characteristics and tectonics of the various shear zones are discussed in Chap. 5.

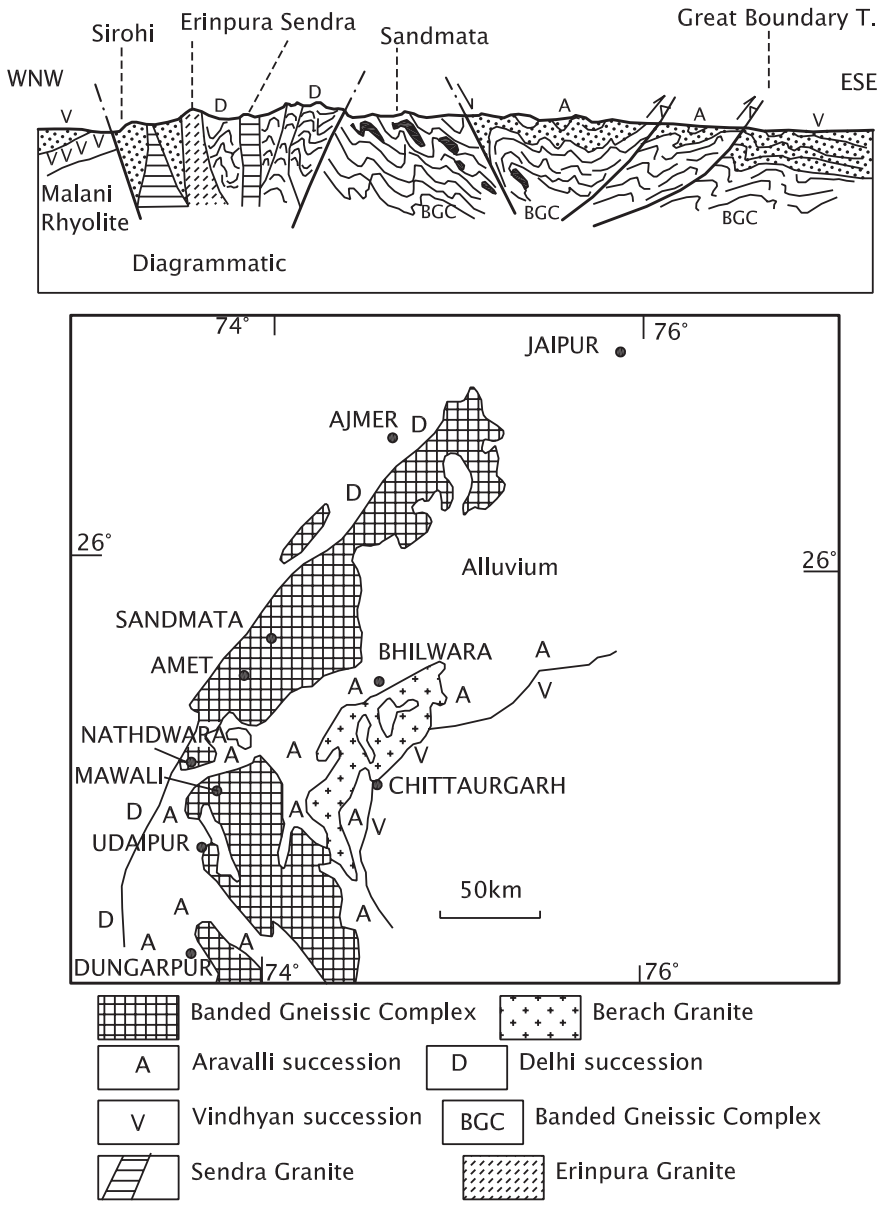

Fig. 4.16 **a** Geological sketch map of the western block of the Bundelkhand Craton encompassing complexes of the Mewar and adjoining terranes. **b** Diagrammatic cross section of the Mewar block of the Bundelkhand Craton (**a**, **b** modified after Sharma 1977)

4.4.4 Lithostratigraphy

Taking the greater Bundelkhand Craton as one whole unit, the Archaean rocks can be grouped into four complexes: (1) tonalitic–granodioritic gneisses intimately associated with enclaves, bands and lenses of metamorphosed volcanic and sedimentary rocks including banded iron formation, chert and greywackes; (2) assemblage of high-grade metamorphic rocks including charnockites, leptynites and pyroxene granulites; (3) intrusive bodies of granites and basic dykes emplaced subsequent to the tectonothermal events that reconstituted the older units; and (4) Undeformed and unmetamorphosed younger granite and adamellite intruding all other older complexes (Figs. 4.16 and 4.17). These four lithotectonic units are clearly identifiable despite bewildering complexity resulting from multiple phases of metamorphism and granite magmatism.

4.4.5 Mawli Gneiss

Within the Mewar terrane intimately associated with metamorphosed basic volcanics and ultrabasic plutonic rocks, there are tonalitic to granodioritic gneisses in the Mawli and Jhamarkotra areas, east and south-east of Udaipur (Fig. 4.16).

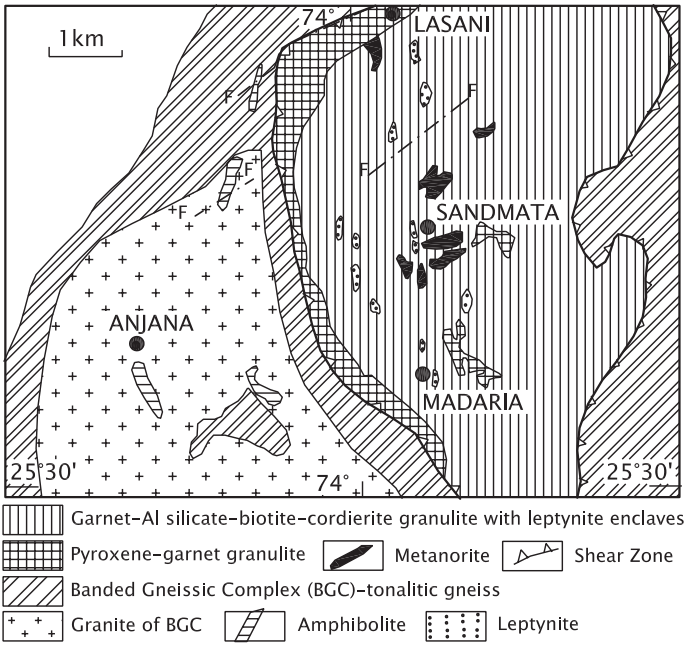

Fig. 4.17 Geological sketch map showing the Sandmata Complex that constitutes a part of the Banded Gneissic Complex of the Mewar block of the Bundelkhand Craton (after Joshi et al. 1993)

The Sm–Nd isochron age of the gneiss is 3310 ± 0.007 Ma (Gopalan et al. 1979). A part of the complex is made up of material coming up from a depleted mantle at 3500 Ma (Macdougall et al. 1983). The Mawli–Jhamarkotra gneiss of tonalite–trondhjemite composition thus represents the nucleus of Heron's (1953) *Banded Gneissic Complex* (BGC) sensu stricto. The Mawli Gneiss seems to be a contemporary of the Champua Gneiss in the Singhbhum Craton, the Markampara Gneiss in the Bastar Craton and the Gorur Gneiss in the Dharwar Craton.

4.4.6 Mangalwar Complex (Western Block)

Within the BGC, there are lenses or enclaves, varying in size from a few centimetres to tens of metres of metamorphosed mafic volcanics, ultramafic plutons, pelites, arenites, carbonates and cherts. Some of these bodies retain their original textures, despite pervasive metamorphism. Widespread metamorphism converted them into an assemblage of amphibolites, paragneisses, mica-chlorite schists, garnet-sillimanite schists, fuchsite quartize, magnesium-rich marbles and graphite phyllite. This assemblage forms the belt from Kankroli to Lawa Sardargarh, which B.C. Gupta in 1934 had described as BGC II, and now recognized by some workers as *Mangalwar Complex* (Gupta et al. 1980; Sinha–Roy 1984, 1985).

Sm–Nd isochron age of amphibolites occurring as lenses within the 3300-Ma-old Mawli Gneiss yielded an age of 2830 ± 0.0005 Ma (Gopalan et al. 1979).

At Jagat, the metabasics are associated with banded iron formation (Sahoo and Mathur 1991). Both the Jagat and the Nathadwara amphibolites bear geochemical signatures analogous to those of the Archaean greenstone belts (Upadhyay et al. 1992; Mohanty and Guha 1995). Showing iron enrichment and limited fractionation, the Tanwan amphibolite of the upper part exhibits tholeiitic affinity (Chauhan 1981; Srivastava 1988). Close to the upper limit of the Banded Gneissic Complex, the mafic enclaves show chondrite-normalized flat REE with pattern with minor, LREE enrichment, negative Sr and Eu anomalies and high Nb/Zr ratio, implying rift-related volcanism in a continental nucleus. The mafic volcanism was probably related to mantle plume impacting a mature subcontinental lithosphere (Ahmad and Tarney 1994). The sedimentary assemblage and the chemical signatures of the metabasic rocks point to extensional tectonic regime in a continental setting (Fig. 4.18).

4.4.7 Mehroni Group (Eastern Block)

Within the large body of granitic gneisses and granite, known as the *Bundelkhand Granite*, occur enclaves and discontinuous bands of metamorphosed volcano-sedimentary rocks. One such band, trending NE–SW in the Lalitpur area, has been

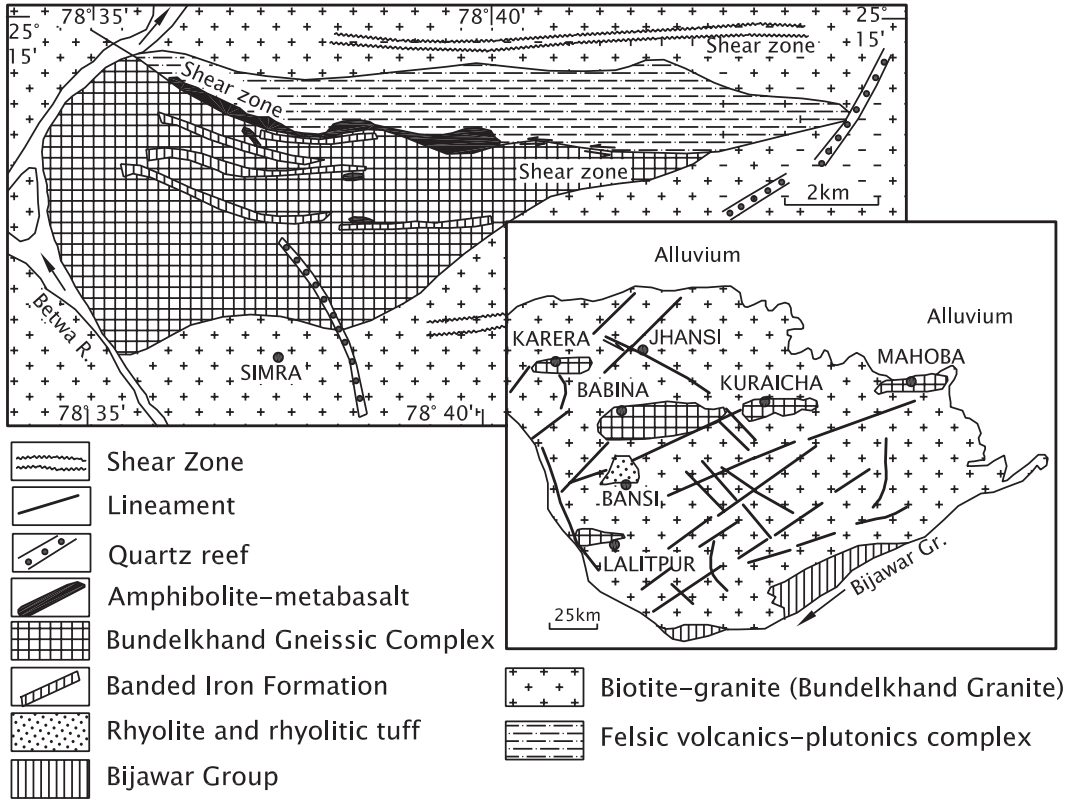

Fig. 4.18 Geological sketch map and cross section of a part of eastern block in Tikamgarh district of the Bundelkhand Craton showing tonalitic–trondhjemitic gneisses in intimate association with metamorphosed volcano-sedimentary assemblage occurring as bands, lenses and enclaves (after Hanuma Prasad et al. 1999). *Inset* shows the extent and tectonic situation of the Bundelkhand Granite characterized by enclaves and discontinuous bands of metamorphosed volcano-sedimentary assemblage (after Mondal et al. 2002)

described as *Mehroni Group* (Prakash et al. 1975; Misra and Sharma 1975). The Mehroni Group comprises two formations. The biotite-felspar orthogneiss, garnet-sillimanite gneiss, chlorite-biotite schist, amphibolite and metabasalt form the lower part named the *Rajaula Formation* or the *Kuraicha Formation*. The upper part of the Mehroni, described as the *Palar,* is made up of conglomerate, fuchsite quartzite, grey–green phyllite, marble and banded iron formation as seen in the Mauranipur–Babina tract. The metamorphosed volcano-sedimentary succession, 15 km by 6 km in dimension, is thicker in the eastern parts. The carbonates are more abundant in the middle and western parts, and the banded magnetite-quartzites are invariably underlain and interbedded by basalts (Basu 1986, 2001). It seems that the Mehroni represents the deposit of a narrow rift basin. In the southern margin of the Bundelkhand Granite, the Mehroni succession is associated discordantly with an assemblage of peridotite, pyroxenite, gabbro and pillow lavas of the *Madaura Formation*. The basic–ultrabasic unit is metamorphosed to an assemblage of serpentinite and talc-actinolite schist.

The Rb–Sr isotopic whole-rock age of a lensoid body of trondhjemitic gneiss within the Bundelkhand Granite at Baghora is 3500 Ma (Sarkar et al. 1984). The Baghora gneiss has geochemical characteristics of a tonalite–trondhjemite–granodiorite suite elsewhere. Ion microprobe Pb–Pb zircon ages from this tonalitic–trondhjemitic gneisses at Mahoba and Kuraicha are, respectively, 3270 ± 3 and 3297 ± 8 Ma, and the associated metabasic rocks is 3249 ± 5 Ma old (Mondal and Zainuddin 1996; Mondal et al. 1998, 2002).

It is obvious that in respect of lithological composition and age, the Mahoba–Baghora Gneiss and the Mehroni assemblage are comparable with the Gorur Gneiss and the Sargur Group of the Dharwar Craton.

4.4.8 Banded Gneissic Complex

The larger part of the western block of the Bundelkhand Craton in the Mewar block is made up of what is known as the BGC (Heron 1953), also described as the Bhilwara Supergroup (Gupta et al. 1980; Sinha-Roy et al. 1995). It is made up of predominant biotite-gneisses, migmatites and granites of more than one pulse of emplacement. The main body of the complex consists of grey tonalitic to trondhjemitic gneisses and the younger components are granites and adamellites. As already stated, the other components of the complex, smaller in proportion but of crucial importance, are the enclaves and bands of the volcano-sedimentary rocks (Ahmad and Rajamani 1988) belonging to the Mangalwar unit (Upadhyay et al. 1992).

There are unfoliated massive pink microcline-granites intruding the BGC in the Mewar region. These bodies are the *Untala Granite* and the *Gingla Granite* associated with felsic veins. Rb–Sr whole-rock age of these bodies is 2860 ± 55 Ma (Choudhary et al. 1984). In the Anasagar area, the granitic plutons intrude the gneisses of the complex—both in the main body and in its inliers. The Sm–Nd

isotopic data on migmatized granite scatter around 2830 Ma (Tobisch et al. 1994). The foliated and lineated nature of the granites, together with the scattering of isotopic ages, indicates effect of remobilization due to some tectonic movements. It is significant that the granite bodies have almost the same age as the lenticular body of amphibolite associated with the Mawli Gneiss near Udaipur—that is 2830 ± 0.0005 Ma (Gopalan et al. 1979). These granites are the products of crustal anatexis.

Several bodies of Palaeoproterozoic granulites within the BGC give U–Pb zircon ages of 1725 and 1621 Ma indicating their formation at about 1900 Ma, the time of the Aravali Orogeny (Roy et al. 2012). The host BGC is 2905 to ~2500 Ma old (Archaean) as single zircon age as well as EA-ICP-MS U–Pb zircon dating confirms (Roy et al. 2012). It is obvious that the BCG embodies rocks of Archaean as well as Palaeoproterozoic rocks.

4.4.9 Sandmata Complex

One of the three major lithotectonic units of the BGC terrane is the *Sandmata Complex* of high-grade metamorphic rocks. Demarcated against the Aravali orogenic belt by a shear zone, called as the Kaliguman Dislocation Zone, the 200-km-long and 25- to 50-km-wide belt extends north-east from Amet to Kishangarh. The granulitic terrain is characterized by enclaves of older gneisses and fine-grained granites. Numerous normal faults characterize the ductile shear zone showing non-coaxial and flattening-type of deformation (Srivastava 2001). The Sandmata Complex is regarded as a tectonic wedge of deep crustal metamorphics brought up by the fault (Sharma 1982, 1988; Sinha Roy et al. 1992; Fareeduddin 1995). It consists of granulites and gneisses of diverse composition, including pelitic granulites, leptynite and pyroxene granulite besides basic intrusives (norite) and calcareous clastics as well as chemogenic sediments. In the Bandanwara area in the Ajmer district, the granulites are associated with charnockites (Pandya and Gyani 1970). Norite dykes, the products of tholeiite magma that crystallized at 1100–1150 °C, were intruded during the waning stages of the granulite metamorphism (Sharma et al. 1987).

The LA-CP-MS U–Pb zircon ages and REE geochemistry of the rocks of the Sandmata Complex indicate that the porphyritic graniodiorite is ~1733 Ma old, while the igneous gneisses are as old as 2750 Ma, and the biotite gneiss 2698 Ma old (Dharma Rao et al. 2011, 2011). The metapelites within the Sandmata Complex give electromicroprobe monazite ages of 1700 ± 3, 1733 ± 15 Ma, ~1597 ± 6 to ~1629 ± 23 Ma, and 882 ± 15 Ma, implying that the Sandmata Complex embodies rocks belonging to Palaeoproterozoic as well as Neoproterozoic (Bhowmik et al. 2010).

The mineral assemblages of the Sandmata Complex indicate polymetamorphism (Fig. 4.19). The earlier amphibolite-facies metamorphics were reworked by second-phase metamorphism resulting in the formation of several anhydrous

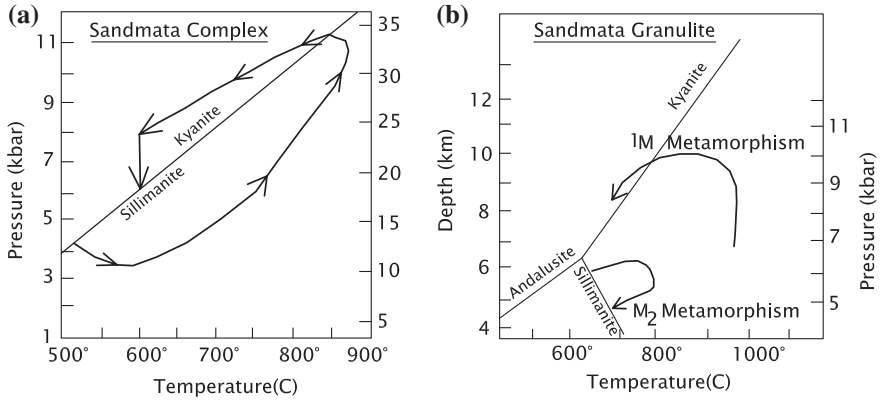

Fig. 4.19 Pressure–temperature conditions under which the high-grade metamorphic rocks of the Sandmata Complex were formed. **a** Anticlockwise P–T path (after Sharma 1988). **b** P–T path (after Guha and Bhattacharyya 1995)

minerals leading to evolution of high-pressure granulites at deeper crustal level. The temperature–pressure conditions varied from 820 °C/7.5 to 870 °C/9 kbar (Sharma 1988; Sharma and Pandit 2003; Sinha-Roy et al. 1992; Guha and Bhattacharyya 1995; Gyani 1997; Fareeduddin et al. 1994; Fareeduddin 1995; Dasgupta et al. 1997). Subsequent reconstitution of minerals was at 650 °C/5–525°C/4 kbar. This fact implies that the granulitic rocks were suddenly exhumed—transported up—from the deeper level of the crust and emplaced at the shallow (15 km) level where the pressure was about 5 kbar (Sharma 1988, 1990). This was accomplished by thrusting up presumably along the Kaliguman Dislocation Zone.

4.4.10 Hindoli Group

In the Mewar block, the grade of metamorphism progressively decreases from west to east. There is an arcuate belt of basic and felsic volcanics and volcaniclastics interbedded with turbiditic greywackes (Raja Rao et al. 1971) mildly metamorphosed to an ensemble (Fig. 4.20) described as the *Hindoli Group* (Sinha-Roy 1985; Sinha-Roy et al. 1992). Some workers do not see justification in giving a name to this low-grade metamorphic assemblage which they believe is coeval with a part of the Aravali Group of the early Proterozoic Aravali Mobile Belt (Heron 1953; Bose and Sharma 1992; Bose et al. 1996; Roy 2001). It is possible that the Hindoli represents less metamorphosed facies of the Mangalwar Complex. The Hindoli succession is intruded by granite plutons in the Berach Valley and in the Jahazpur area, and exhibits Buchanan-type andalusite-forming metamorphism. The Hindoli is unconformably overlain by the Bijawar rocks in the Jhalawar region belonging to the Mesoproterozoic mobile belt (Sinha-Roy and Malhotra 1989).

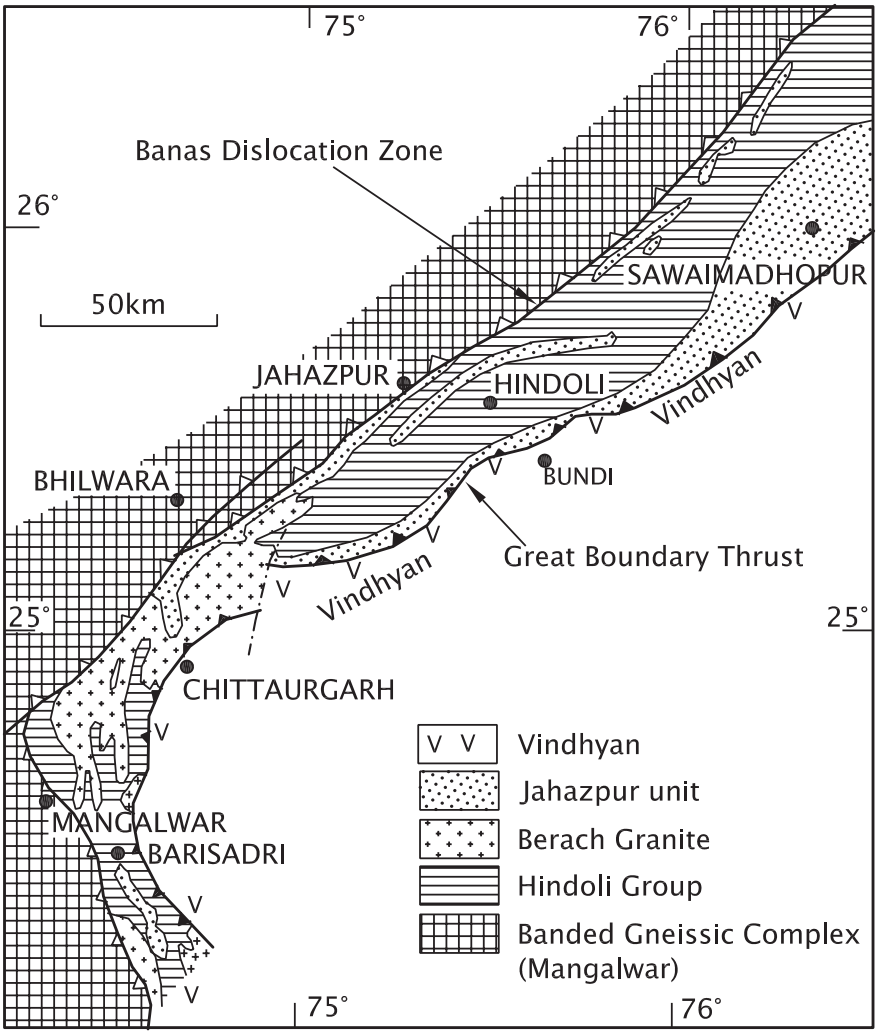

Fig. 4.20 Geological sketch map showing the extent of the Hindoli Group. It is demarcated against the Later Proterozoic Vindhyan Basin by the Great Boundary Fault (after Sinha-Roy and Malhotra 1989)

4.4.11 Dykes

A number of basic dykes intrude the BGC near Anjari area in the Mewar block showing extreme mylonitization in the high strain zone bordering the gneissic complex. The dyke swarms in the Bundelkhand block in the Jhansi–Lalitpur districts trend in the NW–SE direction. However, little is known about their genesis and age.

4.4.12 Berach Granite

In the Mewar block, a batholith covering 300 km^2 area in the valley of Berach River in the Chittaurgarh district is made up of nonfoliated medium-grained pink granite in the east, grading to leucocratic adamellite in the west (Prasad 1987). Rb–Sr dating shows that the Berach Granite is 2585 million years old (Crawford 1969). Zircon geochronology corroborates this age (Sivaram and Raval 1995). There is another pluton in the Vali River valley which gives an age of 2506 ± 4 Ma (Wiedenback et al. 1996). The Berach Granite represents the climactic phase of the development of the Archaean craton in the north-western part of the Indian Shield. It was the cratonization event towards the end of the Archaean (Sinha Roy 1985).

4.4.13 Bundelkhand Granite

Intruding the Mahoba-Baghora tonalite–trondhjemite–gneisses and the Mehroni volcano-sedimentary succession, the *Bundelkhand Granite* is a batholithic body of coarse-grained granite. Its southern margin against the Satpura orogenic belt is gneissose, and the northern margin has a fringe of volcaniclastic rocks. The batholith is by and large undeformed except for the narrow E–W trending dextral shear zones (Hanuma Prasad et al. 1999). One of the most spectacular geomorphic features of the Bundelkhand Granite is a series of NE–SW trending quartz reefs standing high in the eroded terrain. In contrast, the dolerite dykes have NW–SE orientation.

The calc-alkaline Bundelkhand granite (Misra and Sharma 1975) shows moderately fractionated REE pattern and large negative Eu anomaly (Mondal et al. 2002). It may be mentioned that the formation of the larger part of the batholith is attributed by some workers to potash metasomatism. It is this process of granitization that transformed the pelitic metamorphics into granites (Mathur 1954).

The Pb–Pb whole-rock isochron age (Fig. 4.21) of the banded grey granodiorite of Badera in Jhansi district is 2359 ± 53 Ma, while its whole-rock mineral age is 2402 ± 70 Ma, and of Babina–Talbehat is 2246 ± 78 Ma (Sarkar et al. 1984). Ion microprobe ages of zircon grains from the granite at Karera, Panchwara, Mahoba, Lalitpur and Datia fall in the range of 2515 ± 5–2563 ± 6 Ma. While the Babina Gneiss is 2697 ± 3 million years old, the Lalitpur leucogranite is dated 2492 ± 10 Ma, the latter age marking the time of crustal stabilization. Significantly, the rhyolite of Bansi shows the age of crystallization at 2517 ± 7 Ma (Mondal et al. 2002).

It is obvious that the Mewar and Bundelkhand cratonic blocks in the north-western part of the Indian Shield evolved as a single crustal unit, and that the cratonization took place around 2500 Ma.

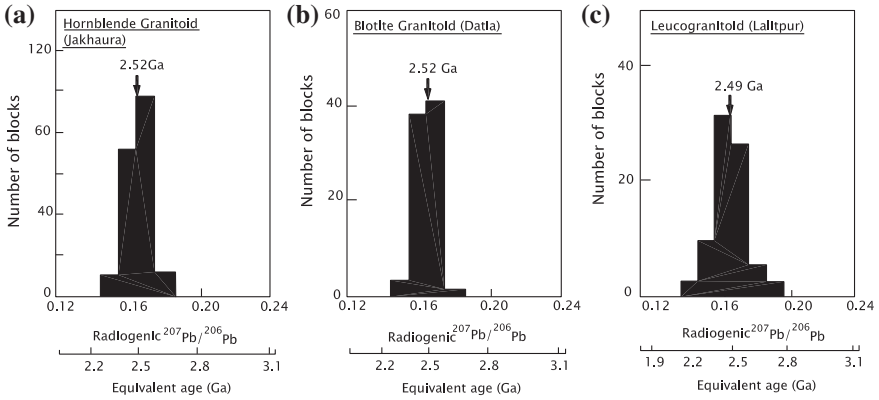

Fig. 4.21 $^{207}Pb/^{206}Pb$ data for zircon grains from different granitic bodies forming the Bundelkhand Granite (Mondal et al. 2002)

4.4.14 Deformation Pattern

Various components of the Archaean craton in Rajasthan were affected by multiple phases of deformation and mineral reconstitution (Sharma and Upadhyay 1975; Sharma 1977). The early structures are tight isoclinal folds overturned south-eastwards and plunging in the NE and SW directions; and the second-phase folds are open, upright with N/NNW- to S/SSE-oriented vertical axial planes, and plunging towards N and NNW. The consequence of the superimposition of later folding on the earlier ones is a structural design characterized by reclined to recumbent folds that have E–W to ESE–WNW axial trend. The folds of the first and second generations of deformation of the basement complex match in entirety with those of the Aravali–Delhi supracrustals, and the granite magmatism was synkinematic with the first-phase deformation (Naha and Mohanty 1988).

The structure of the Bundelkhand block in the eastern part is also characterized by ENE–WSW to E–W trending folds that have steep to moderate dips of their limbs (Basu 2001). The foliation planes of the schists occurring within the gneisses are oriented in the same directions. The first and second of deformation resulted in the formation of isoclinal to reclined folds with steep plunges. The third phase is represented by tight to open folds of variable plunges (Hanuma Prasad et al. 1999).

In the central part of the Budelkhand Craton, an east–west shear zone is characterized by mylonites and vertical to subvertical foliation in the metasediments and metavolcanics (Singh et al. 2010). A Mohar in the south-western part the intersection of E–W, NE–SW and NW–SE trending lineaments has give rise to a circular feature comprising breccias made up of fragments of felsic volcanic (Singh et al. 2010). Obviously, repeated movements along intersecting "lineaments" are responsible for the formation of what has been described as collapse breccia. Interestingly, the structure is overlain by a sedimentary pile equated with the Neoproterozoic Upper Vindhyan.

4.4.15 Evolution of the Craton

The tonalitic gneisses of Mawli and Jhamarkotra in the Mewar block and of Mahoba and Baghora in the Bundelkhand block constitute the nuclei of the north-western Indian Shield formed 3300 million years ago. Due to stretching of the sialic crust, a rift basin came into existence and the volcano-sedimentary material forming the Mangalwar and Mehroni complexes was emplaced in that depression.

There was thickening of the crust due to addition of or underplating of granitic magma (Sharma 1988, 1995) or multiple thrusting and stacking of slabs (Sinha-Roy et al. 1993). It was during the second phase of deformation roughly around 2900 Ma that Untala, Gingla and Sendra granites were emplaced into the complex of older granitic, volcanic and metamorphic rocks. The crust was rifted apart again and the greater Bundelkhand Craton broke into eastern (Bundelkhand) and western (Mewar) blocks. The intervening trough became the site of emplacement of material represented by the Hindoli Complex. Following the closing of this trough, the Hindoli pile underwent metamorphism and the Mewar and Bundelkhand blocks were welded together. The geodynamic evolution of the Bundelkhand Craton was complete with the emplacement of 2550-million-year-old granite in the Berach and Bundelkhand regions. Subsequent rifting in the Early and Later Proterozoic times developed basins for deposition of the Aravali and Delhi successions. Each of them was involved in orogeny, known as the Aravali Orogeny and Delhi Orogeny, respectively. But later in the Proterozoic period at a greater depth where the temperature–pressure conditions were as high as 850º–820º and 9–8 kbar, high-grade metamorphism of parts of the volcano-sedimentary assemblage gave rise to granulites, what is known as the Sandmata Complex. There may have been intrusion of 1723-Ma-old charnockite–enderbite magmas subsequent to metamorphism (Dasgupta et al. 1997). Subsequently, this high-grade metamorphic complex was thrust up to shallower level of the crust.

Some aspects of evolution of the Aravali orogen are discussed in Chap. 5.

4.4.16 Mineralization

Only pyrophyllite and diaspore are commercially mined. Diaspore is found as geodes, veins and dissemination in pyrophyllite (Misra 1947). The deposits are not large. In Jhansi district, it is of the order 2,30,000 tonnes and in Lalitpur about 40,000 tonnes. The deposits occur at the junction of the Kuraicha and Palar formations of the Mehroni Group in the Bundelkhand block. Characterized by higher concentration of Ti, Cr, Zr—comparable with that of the gneisses—the deposits seem to be of the laterite-type products of the Mahoba–Baghora gneisses that were subjected to metamorphism up to 350 °C temperature (Sharma 1979). The deposits are associated with the NE–SW trending quartz reefs.

References

Acharya, S., Amstutz, G. C., & Sarangi, S. K. (1982). Diagenetic crystallization and migration in the Banded Iron Formation of Orissa, India. In G. C. Amstutz, et al. (Eds.), *Ore Genesis—the State-of-the-Art* (pp. 442–450). Berlin: Springer.

Acharyya, S. K. (1993). Greenstones from Singhbhum Craton, their Archaean character, oceanic crustal affinity and tectonics. *Proceedings of the National Academy of Sciences India, 63*, 211–222.

Ahmad, T., & Rajamani, V. (1988). Geochemistry and petrogenesis of mafic inclusions within the Banded Gneissic Complex near Nathadwara: Implications to BGC–Aravali relationship. *Memoirs of the Geological Society of India, 7*, 327–340.

Ahmad, T., & Tarney, J. (1994). Geochemistry and petrogenesis of Late Archaean Aravali volcanics, basement enclaves and granitoids, Rajasthan. *Precambrian Research, 65*, 1–23.

Asish Basu, R., Sharma, M., & Phemo, W. R. (1998). U-Pb age of an Older Metamorphic Group mica schist; earliest terrain of the Eastern Indian Crton. In R. N. Tiwari (Ed.), *Recent Researches in Sedimentary Basins* (pp. 93–102). Dehra Dun: Indian Petroleum Publication.

Auge, T., & Lerouge, C. (2004a). Mineral-chemistry and stable-isotope constraints on the magmatism, hydrothermal alteration, and related PGE (base-metal sulphide) mineralization of the Mesoarchaean Baula-Nuasahi complex, India. *Mineralium Deposita, 39*, 583–607.

Auge, T., & Lerouge, C. (2004b). Mineral-chemistry and stable-isotope constraints on the magmatism, hydrothermal alteration, and related PGE (base-metal sulphide) mineralization of the Mesoarchaean Baula-Nuasahi complex, India. *Mineralium Deposita, 39*, 583–607.

Auge, T., Cocherie, A., Genna, A., Armstrong, R., Guerrot, C., Mukherjee, M. M., & Patra, R. N. (2003). Age of the Baula PGE mineralization (Orissa, India) and its implications concerning the Singhbhum Archaean nucleus. *Precambrian Research, 121*, 85–101.

Avasthy, R. K. (1980). Stromatolites from iron ore formation of Bonai-Keonjhar districts, Orissa, India. *Geological Survey of India Miscellaneous Publications, 44*, 54–56.

Baksi, A. K., Barman, T. R., Paul, K. D., & Farrar, E. (1987). Widespread Early Cretaceous flood basalt volcanism in Eastern India: Geochemical data from the Rajmahal–Bengal–Sylhet Traps. *Chemical Geology, 63*, 133–141.

Bandyopadhyay, B. K., Roy, A., & Huin, A. K. (1995). Structure and tectonics of a part of the Central Indian shield. *Memoirs of the Geology Society of India, 31*, 433–467.

Bandyopadhyay, P. K., Chakrabarti, A. K., DeoMurari, M. P., & Misra, S. (2001). 2.8 Ga old anorogenic granite-acid volcanics association from western margin of the Singhbhum-Orissa Craton. *Gondwana Research, 4*, 465–475.

Banerji, A. K. (1962). Cross folding, migmatization and ore localization along part of the Singhbhum Shear Zone, south of Tatanagar, Bihar, India. *Economic Geology, 57*, 50–71.

Banerji, A. K. (1969). A reinterpretation of the geological history of Singhbhum Shear Zone, Bihar. *Journal of the Geological Society of India, 10*, 49–55.

Banerji, A. K. (1977). On the Precambrian banded iron formation and manganese ores of the Singhbhum region, eastern India. *Economic Geology, 72*, 90–98.

Basu, A. K. (1986). Geology of parts of the Bundelkhand Granite massif, eastern India. *Record Geological Survey of India, 117*, 61–124.

Basu, A. K. (2001). Some characteristics of the Precambrian crust on the northern part of central India. *Special Publication of Geological Survey of India, 55*, 181–204.

Basu, A. R., Ray, S. L., Saha, A. K., & Sarkar, S. N. (1981). Eastern Indian 3800-million year old crust and early mantle differentiation. *Science, 212*, 1502–1505.

Beukes, N. J., Mukhopadhyay, J., & Gutzmer, J. (2008). Genesis of high-grade iron ores of Archaean Iron One Group around Noamundi, India. *Economic Geology, 103*, 365–386.

Bhattacharyya, D. S., & Sanyal, P. (1988). The Singhbhum Orogen—its structure and stratigraphy. *Memoirs of the Geological Society of India, 8*, 85–111.

Bhowmik, S. K., Bernard, H.-J., & Dasgupta, S. (2010). Grenvillian age high- pressure upper amphibolites-granulite metamorphism in the Aravali-Delhi Mobile Belt, northwestern India: New evidence from monazite chemical age and its implication. *Precambrian Research, 178*, 168–184.

Biswal, T. K., & Sinha, S. (2003). Deformation history of the NW salient of the Eastern Ghats Mobile Belt, India. *Journal of Asian Earth Science, 22*, 157–169.

Biswal, T. K., Jena, S. K., Datta, S., Das, R., & Khan, K. (2000). Deformation of the Terrane Boundary Shear Zone (Lakhna Shear Zone) between the Eastern Ghats Mobile Belt and the Bastar Craton, in Bolangir and Kalahandi districts of Orissa. *Journal of the Geology Society of India, 55*, 367–380.

Bose, U., & Sharma, A. K. (1992). The volcanosedimentary association of the Precambrian Hindoli supracrustals in southeastern Rajasthan. *Journal of the Geological Society of India, 40*, 359–369.

Bose, U., Mathur, A. K., Sahoo, K. C., Bhattacharyya, S., Dutt, K., Kumar, A. V., et al. (1996). Event stratigraphy and physicochemical characters of BGC and associated supracrustals in south Marwar plains of Rajasthan. *Journal of the Geological Society of India, 47*, 325–338.

Chakraborty, K. L., & Majumder, T. (1986). Geological aspects of the Banded Iron Formation of Bihar and Orissa. *Journal of the Geological Society India, 28*, 109–133.

Chatterjee, A. K., & Mukherjee, P. (1981). The structural study of a part of the Malangtoli iron ore deposits, Orissa. *Journal of the Geological Society of India, 22*, 121–122.

Chauhan, D. S. (1981). Amphibolites from granitic terrain northwest of Udaipur, Rajasthan. *Indian Journal of the Earth Science, 8*, 35–43.

Chetty, T. R. K. (1995). A correlation of Proterozoic shear zones between Eastern Ghats, India and Ender by Land, East Antarctica on Landsat imagery. *Memoirs of the Geology Society of India, 34*, 205–220.

Chetty, T. R. K., & Murthy, D. S. N. (1994). Collision tectonics in the late Precambrian Eastern Ghats Mobile Belt: Mesoscopic to satellite-scale structural observation. *Terra Nova, 6*, 72–81.

Choudhary, A. K., Gopalan, K., & Shastry, C. A. (1984). Present status of the geochronology of the Precambrian rocks of Rajasthan. *Tectonophysics, 105*, 131–140.

Crawford, A. R. (1969). Reconnaissance Rb-Sr dating of the Precambrian rocks of northern Peninsular India. *Journal of the Geological Society of India, 10*, 117–166.

Crookshank, H. (1963). Geology of southern Bastar and Jeypore from the Bailadila Range to the Eastern Ghats. *Memoirs of the Geological Survey of India, 87*, 1–49.

Das, A. K., Piper, J. D. A., Mallik, S. B., & Sherwood, G. J. (1996). Palaeomagnetic study of Archaean Banded Hematite Jasper rocks from the Singhbhum-Orissa Craton, India. *Precambrian Research, 80*, 193–204.

Dasgupta, Somnath, Guha, D., Sengupta, P., Miura, H., & Ehl, J. (1997). Pressure-temperature-fluid evolutionary history of the polymetamorphic Sandmata granulite complex, northwestern India. *Precambrian Research, 83*, 267–290.

Dharma Rao, C. V., Santosh, M., Purohit, R., Wang, J., Jiang, X., & Kusky, T. (2011a). LA-ICP-MS and U-Pb zircon age constraints on the Palaeoprorterozoic and Neoarchaean history of the Sandmata complex in Rajasthan within the NW Indian Plate. *Journal of Asian Earth Sciences, 42*, 286–305.

Dharma Rao, C. V., Santosh, M., & Wu, Yuan-Bao. (2011b). Mesoproterozoic ophiolitic mélange from SE periphery of the Indian plate: U-Pb zircon ages and tectonic implications. *Gondwana Research, 19*, 384–401.

Dimri, V. P., Bansal, M. R., Srivastava, R. P., & Vedanti, N. (2003). Scaling behaviour of real earth source distribution: Indian case studies. *Memoirs of the Geological Society of India, 53*, 431–448.

Fareeduddin, M. A. (1995). Field setting, petrochemistry and P-T regime of the deep crustal rocks to the northwest of the Aravali-Delhi Mobile Belt, northcentral Rajasthan. *Memoirs of the Geological Society of India, 31*, 117–139.

Fareeduddin, M. A., Shankara, B., Basavalingu, B., & Janardhan, A. S. (1994). P-T conditions of pelitic granulites and associated charnockites of Chinwali area, west of Delhi Fold Belt, Rajasthan. *Journal of the Geological Society of India, 43*, 169–178.

Ghosh, J. G. (2004). 3.56 Ga tonalite in the central part of the Bastar Craton, India: Oldest Indian date. *Journal of Asian Earth Science, 23*, 359–364.

Ghosh, S. K., & Sengupta, S. (1990). The Singhbhum Shear Zone: Structural transition and kinematic model. *Proceedings of Indian Academy of Sciences (Earth & Planet Science), 98*, 229–247.

Ghosh, D. K., Sarkar, S. N., Saha, A. K., & Ray, S. L. (1996). New insights on the early Archaean crustal evolution in eastern India: Re-evaluation of lead-lead, samarium-neodymium and rubidium-strontium geochronology. *Indian Minerals, 50*, 175–188.

Ghosh, G., Bose, S., Guha, S., Mukhopadhyay, J., & Aich, S. (2008). Remobilization of the southern margin of the Singhbhum Craton, Eastern India, during the Eastern Ghat Orogeny. *Indian Journal of Geology, 80*, 97–114.

Gopalan, K., Trivedi, J.R., Merh, S.S., Patel, P.P., & Patel, S.G. (1979). Rb-Sr age of Godhra and related granites, Gujarat. *Proceedings of the Indian Academy of Science* (*Earth & Planet Sciences*), *88A*, 7–17.

Goswami, J. N., Mishra, S., Wiedenbeck, M., Ray, S. L., & Saha, A. K. (1995). 3.55 Ga old zircon from Singhbhum-Orissa iron ore craton, Eastern India. *Current Science, 69*, 1008–1011.

Guha, D. B., & Bhattacharyya, A. K. (1995). Metamorphic evolution and high-grade reworking of the Sandmata complex granulites. *Memoirs of the Geological Society India, 31*, 163–198.

Gupta, S. N., Arora, Y. K., Mathur, R. K., Iqballuddin, P., Sahai, T. N., & Sharma, S. B. (1980). *Lithostratigraphic Map of Aravali Region*. India, Kolkata: The Geological Survey.

Hanuma Prasad, M., Hakim, A., & Krishna Rao, B. (1999). Metavolcanic and metasedimentary successions in the Bundelkhand Granitic complex in Tikamgarh district, M.P. *Journal of the Geological Society of India, 54*, 359–368.

Heron, A. M. (1953). The geology of central Rajputana. *Memoirs of the Geological Survey of India, 79*, 1–389.

Hussain, M. F., Mondal, M. E. A., & Ahmad, T. (2004). Petrological and geochemical characteristics of Archaean gneisses and granitoids from Bastar Craton, central India—Implication for subduction related magmatism. *Gondwana Research, 7*, 531–537.

Iyengar, S. V. P., & Murthy, Y. G. K. (1982). The evolution of the Archaean-Proterozoic crust in parts of Bihar and Orissa, eastern India. *Record Geological Survey of India, 112*, 1–5.

Jain, S. C., Yedekar, D. B., & Nair, K. K. V. (1991). Central Indian Shear Zone: A major Precambrian crustal boundary. *Journal of the Geology Society of India, 37*, 521–531.

Joshi, Mallickarjun, Thomas, H., & Sharma, R. S. (1993). Granulite facies metamorphism in the Archaean gneiss complex from northcentral Rajasthan. *Proceedings of the National Academy of Science India, 63A*, 167–187.

Khan, M. W. Y., & Bhattacharyya, T. K. (1993). A reappraisal of the stratigraphy of Bailadila Group in Bacheli, Bastar District, M.P. *Journal of the Geological Society of India, 42*, 549–562.

MacDougall, J. C., Gopalan, K., Lugmair, G. W., & Roy, A. B. (1983). The Banded Gneissic Complex of Rajasthan, India: Early crust from depleted mantle at 3.5 Ga. *Transactions American Geophysical Union, 64*, 351–360.

Mahalik, N. K. (1994). Geology of the contact between the Eastern Ghats belt and North Orissa Craton. *Journal of the Geological Society of India, 44*, 41–51.

Majumder, T. (1991). Status and origin of magnetite in the Precambrian Banded Iron Formation of eastern India. *Journal of the Geological Society of India, 63*, 98–105.

Majumder, T., & Chakraborty, K. L. (1977). Primary sedimentary structures in the Banded Iron Formation of Orissa. *Sedimentary Geology, 19*, 287–300.

Majumder, T., Chakraborty, K. L., & Bhattacharyya, A. (1982). Geochemistry of Banded Iron Formation of Orissa, India. *Mineralium Deposita, 17*, 107–118.

Mathur, P. C. (1954). A note on the granitization of quartzites in Bundelkhand. *Science and Culture, 20*, 242–243.

Mishra, S., Deomurari, M. P., Wiedenbeck, M., Goswami, J. N., Ray, S., & amd Saha, A. K. (1999). $^{207}Pb/^{206}Pb$ zircon ages and the evolution of the Singhbhum Craton, Eastern India: An ion microprobe study. *Precambrian Research, 93*, 139–151.

Misra, R. C. (1947). Diaspore with pyrophyllite from Hamirpur district, U.P. *Current Science, 16.*

Misra, R. C., & Sharma, R. P. (1975). Petrochemistry of Bundelkhand Granites and associated rocks of central India. *Indian Mineralogist, 15*, 43–50.

Mohanty, M., & Guha, D. B. (1995). Lithostratigraphy of the dismembered greenstone sequence of the Mangalwar Complex, around Lawa-Sardargarh and Parasali areas, Rajasamand district, Rajasthan. *Memoirs of the Geological Society of India, 31*, 141–162.

Mondal, M. E. A., & Zainuddin, S. M. (1996). Evolution of the Archaean-Palaeoproterozoic Bundelkhand massif, cental India: Evidence from granitoid geochemistry. *Terra Nova, 8*, 532–539.

Mondal, M. E. A., Sharma, K. K., Rahman, A., & Goswami, J. N. (1998). Ion microprobe $^{207}Pb/^{206}Pb$ zircon ages for gneiss-granitoid rocks from Bundelkhand massif: Evidence for Archaean components. *Current Science, 74*, 70–75.

Mondal, M. E. A., Goswami, J. N., Deomurari, M. P., & Sharma, K. K. (2002). Ion microprobe 207Pb/206Pb ages of zircons from the Bundelkhand massif, northern India: Implictions for crustal evolution of the Bundelkhand-Aravali protocontinent. *Precambrian Research, 117*, 85–100.

Mondal, S. K., Ripley, E. M., Li, C., & Frei, R. (2006). The genesis of Archaean chromitites from the Nuasahi and Sukinda massifs in the Singhbhum Craton, India. *Precambrian Research, 148*, 45–66.

Moorbath, S., & Taylor, P. N. (1988). Early Precambrian crustal evolution in eastern India: The age of the Singhbhum Granite and included remnants of older gneiss. *Journal of Geological Society of India, 31*, 82–84.

Mukhopadhyay, D. (1976). Precambrian stratigraphy of Singhbhum: The problem and a prospect. *Indian Journal of the Earth Sciences, 3*, 208–219.

Mukhopadhyay, D. (1984). The Singhbhum Shear Zone and its place in the evolution of the Precambrian mobile belt, North Singhbhum. *Indian Journal of the Earth Sciences, CEISM Volume*, 205–212.

Mukhopadhyay, D. (2001). The Archaean nucleus of Singhbhum: The present state of knowledge. *Gondwana Research, 4*, 307–318.

Mukhopadhyay, Joydip, Beukes, N. J., Armstrong, R. A., Zimmermann, U., Ghosh, G., & Medda, R. A. (2008). Dating of oldest greenstone in India : A 3.51 Ga precise U-Pb SHRIMP zircon age for dacitic lava of the southern Iron Ore Group, Singhbhum Craton. *The Journal of Geology, 116*, 449–461.

Murty, V. N., & Acharya, S. (1975). Lithostratigrtaphy of the Precambrian rocks around Koira, Sundargarh district, Orissa. *Journal of the Geological Society of India, 16*, 55–68.

Naha, K., & Mohanty, S. (1988). Reponse of basement and cover rocks to multiple deformation: A study from the Precambrian of Rajasthan, Westen India. *Precambrian Research, 42*, 77–96.

Pal, Tapan, & Mitra, S. (2004). P-T–fO2 controls on a partly inverse chromite-bearing ultramafic intrusive: An evaluation from Sukinda massif, India. *Journal Asian Earth Sciences, 22*, 483–493.

Pandya, M. K., & Gyani, K. C. (1970). Granulitic rocks from the Banded Gneissic Complex of Bandanwara region, Ajmer district, Rajasthan. In *Proceedings of the 2nd symposium: Upper Mantle Project*. Hyderabad: National Geophysical Research Institute, pp 339–348.

Paul, D. K., Mukhopadhyay, D., Pyne, T. K., & Bishoi, P. K. (1991). Rb-Sr age of granitoid in the Deo River section, Singhbhum; and its relevance to the age of the iron formation. *Indian Minerals, 45*, 51–56.

Prakash, Ravi, Swarup, P., & Srivastava, R. N. (1975). Geology and mineralization in the southern part of the Bundelkhand in Lalitpur district, Uttar Pradesh. *Journal of the Geological Society of India, 16*, 143–156.

Prasad, B. (1987). Geochemistry and petrogenesis of Berach Granite, Rajasthan, India. *Indian Minerals, 41*, 1–31.

Rai, K. L., Sarkar, S. N., & Paul, P. R. (1980). Primary depositional and diagenetic features in the Banded Iron Formation and associated iron ore deposits of Noamundi, Singhbhum district, Bihar. *Mineralium Deposita, 15*, 189–200.

Raja Rao, C. S., Poddar, B. C., Basu, K. K., & Dutta, A. K. (1971). Precambrian stratigraphy of Rajasthan: A review. *Record Geological Survey of India, 101*, 60–79.

Rajendra Prasad, B., Tewari, H. C., Vijaya Rao, V., Dixit, M. M., & Reddy, P. R. (1998). Structure and tectonics of the Proterozoic Aravali-Delhi Fold Belt in northwestern India from deep seismic reflection studies. *Tectonophysics, 288*, 31–41.

Ramachandra, H. M., Roy, Abhinaba, Mishra, U. P., & Dutta, N. (2001). A critical review of the tectonothermal evolution of the Bastar Craton. *Geological Survey of India Special Publication, 55*, 161–180.

Ramakrishnan, M. (1990). Crustal development in southern Bastar, central Indian craton. *Geological Survey of India Special Publication, 28*, 144–166.

Rao, V. V. S., & Dasgupta, H. C. (1995). Clay mineralogy of the argillites associated with banded iron formation from the Noamundi basin, eastern India: A clue to its chemical environment of deposition. *Indian Minerals, 49*, 31–44.

Raza, M., Jafri, S. H., Alvi, S. H., & Khar, Shamir. (1993). Geodynamic evolution of the Indian Shield during Proterozoic: Geochemical evidence from mafic volcanic rocks. *Journal of the Geological Society of India, 41*, 455–469.

Reddy, B. M., Janardhan, A. S., & Peucat, J. J. (1995). Geochemistry, age and origin of alkaline and ultramafic rocks of Salem, Tamil Nadu, south India. *Journal of the Geological Society India, 45*, 251–262.

Roy, A. B. (2001). Neoproterozoic crustal evolution of northwestern India Shield: Implications on breakup and assembly of supercontinents. *Gondwana Research, 4*, 289–306.

Roy, Abhinaba, & Hanuma Prasad, M. (2003). Tectonothermal events in Central Indian Tectonic Zone (CITZ) and its implication in Rodinian crustal assembly. *Asian Journal of Earth Science, 22*, 115–129.

Roy, A. B., Kroner, A., Rathore, S., Laul, V., & Purohit, R. (2012). Tectono-metamorphic and geochronological studies from Sandmata Complex, NW Indian Shield: Implications on Exhumation of Late Palaeoproterozoic granulites in an Archaean-Early Palaeoproterozoic granite-gneiss terrane. *Journal of the Geological Society of India, 79*, 323–334.

Saha, A. K. (1994). *Crustal evolution of Singhbhum, North Orissa, Eastern India*. India, Bangalore: Geological Society. 341 p.

Saha, A. K., Ray, S. L., Ghosh, S., Mukhopadhyay, K., & Dasgupta, P. (1984). Studies in crustal evolution of the Singhbhum-Orissa Iron Ore Craton. *Crustal Evolution of Parts of Indian Shield* (pp. 1–74). Kolkata: Indian Society of Earth Scientists.

Saha, A. K., Ray, S. L., & Sarkar, S. N. (1988). Early history of the Earth: Evidence from the eastern Indian shield. In D. Mukhopadhyay (Ed.), *Precambrian of the Eastern Indian Shield* (pp. 13–37). India, Bangalore: The Geological Society.

Saha, A., Basu, A. R., Garzione, C. N., Bandyopadhyay, P. K., & Chakrabarti, A. (2004). Geochemical and petrological evidence for subduction—Accretion processes in the Archaean Eastern Indian Craton. *Earth and Planetary Science Letters, 220*, 91–106.

Sahoo, K. C., & Mathur, A. K. (1991). On the occurrence of Sargur-type banded iron formation in Banded Gneissic Complex of south Rajasthan. *Journal of the Geological Society of India, 38*, 299–302.

Santosh, M., Yokoyama, K., & Acharyya, S. K. (2004). Geochronology and tectonic evolution of Karimnagar and Bhopalpatnam granulite belts, central India. *Gondwana Research, 7*, 501–518.

Sarkar, S. N. (1958). Stratigraphy and tectonics of the Dongargarh system: A new system in the Precambrian of Bhandara–Drug–Balaghat area, Madhya Pradesh. *Journal of Science & Engineering, 1*, 237–268 and 2, 145–160 (IIT, Kharagpur).

Sarkar, Bhagwati. (1989). Algal stromatolites and associated microbiota of the Precambrian Banded Iron Formation in Noamundi basin, eastern India. *Himalayan Geology, 13*, 29–37.

Sarkar, S. C. (2000). Crustal evolution and metallogeny in the Eastern Indian Craton. *Special Publication of the Geological Survey of India, 55*, 169–194.

Sarkar, S. N., & Saha, A. K. (1962). A revision of the Precambrian stratigraphy and tectonics of Singhbhum and adjacent region. *Quaternary Journal of Geology Mining Metallurgy Society of India, 34*, 97–136.

Sarkar, S. N., & Saha, A. K. (1983). Structure and tectonics of the Singhbhum-Orissa iron ore craton, Eastern India. In S. SinhaRoy (Ed.), *Structure and tectonics of Precambrian rocks of India* (pp. 1–25). Delhi: Hindustan Publishing Corporation.

Sarkar, A., Trivedi, J. R., Gopalan, K., Singh, P. M., Singh, B.K., Das, A. K., & Paul, D. K. (1984). Rb-Sr geochronology of the Bundelkhand granitic complex in the Jhansi-Babina-Talbehat sector, U.P. *Indian Journal of Earth Sciences*, *CEISM Volume,* 64–72.

Sarkar, G., Paul, D. K., Laeter, J. R., McNaughton, N. J., & Mishra, V. P. (1990). A geochemical and Pb, Sr isotopic study of the evolution of granite-gneisses from the Bastar craton, central India. *Journal of the Geological Society of India, 35*, 480–490.

Sarkar, G., Corfu, F., Paul, D. K., McNaughton, N. J., Gupta, S. N., & Bishui, P. K. (1993). Early Archaean crust in Bastar craton, central India—a geochemical and isotopic study. *Precambrian Research, 62*, 127–137.

Sengupta, P. R. (1972). Study on mineralization in southeastern part of Singhbhum Copper Belt, Bihar. *Memoirs of the Geological Survey of India, 101*, 1–82.

Sengupta, S., & Ghosh, S.K. (1997). The kinematic history of the Singhbhum Shear Zone. *Proceedings of the Indian Academy of Sciences* (*Earth & Planetary Science*), *106*, 185–196.

Sengupta, S., Paul, D. K., de Laeter, J. R., McNaughton, N. J., Bandyopadhyay, P. K., & Smith, J. B. (1991). Mid-Archaean evolution of the eastern Indian craton: Geochemical and isotopic evidence from the Bonai pluton. *Precambrian Research, 49*, 23–37.

Sengupta, S., Acharyya, S.K., & De Smith, J.B. (1993). Geochemistry of Archaean volcanic rocks from Iron Ore Supergroup, Singhbhum, Eastern India. *Proceedings of the Indian Academy of Sciences* (*Earth & Planetary Science*), *106*, 327–342.

Sengupta, S., Corfu, F., McNutt, R. H., & Paul, D. K. (1996). Mesoarchaean crustal history of the eastern Indian Craton: Sm-Nd and U-Pb isotopic evidence. *Precambrian Research, 77*, 17–22.

Sharma, R. S. (1977). Deformational and crystallization history of the Precambrian rocks in north-central Aravali mountain, Rajasthan, India. *Precambrian Research, 4*, 133–162.

Sharma, R. P. (1979). Origin of pyrophyllite-diaspore deposits of the Bundelkhand complex, central India. *Mineralium Deposita, 14*, 343–352.

Sharma, R. S. (1982). Petrology of a scapolite-bearing rock from Karera, district Bhilwara, Rajasthan. *Journal of the Geological Society of India, 23*, 319–329.

Sharma, R. S. (1988). Pattern of metamorphism in the Precambrian rocks of the Aravali mountain belt. *Journal of the Geological Society of India, 7*, 33–76.

Sharma, C. K. (1990). Geology of Nepal himalaya and adjacent Countries. Sangeeta Sharma: Kathmandu, 479 p.

Sharma, R. S. (1995). An evolutionary model for Precambrian crust of Rajasthan: Some petrological and geochronological considerations. *Memoirs of the Geological Society of India, 31*, 91–115.

Sharma, R. S., & Pandit, M. K. (2003). Evolution of early continental crust. *Current Science, 84*, 995–1001.

Sharma, R. S., & Upadhyay, T. P. (1975). Multiple deformation in the Precambrian rocks to the southeast of Ajmer, Rajasthan, India. *Journal of the Geological Society of India, 16*, 428–440.

Sharma, R. S., Sills, J. D., & Joshi, M. (1987). Mineralogy and metamorphic history of norite dykes with granulite facies gneisses from SandmataRajasthan, NW India. *Mineralogical Magazine, 51*, 207–215.

Sharma, M., Basu, A. R., & Ray, S. L. (1994). Sm-Nd isotopic and geochemical study of the Archaean tonalite-amphibolite association from eastern Indian craton. *Contributions to Mineralogy and Petrology, 117*, 45–55.

Singh, Yamuna, & Chabria, T. (1999). Late Archaean-Early Proterozoic Rb-Sr isochron age of granite from Kawadgaon, Bastar district, Madhya Pradesh. *Journal of the Geological Society of India, 54*, 405–409.

Singh, S. P., Bhattacharya, A. R., Hemraj & Shrivastava, S.K. (2010). Stuctural development of a granite collapse breccias of Mohar, Bundelkhand massif: An evidence of a Precambrian caldera from the Indian shield, *Journal of Ecology, Geology and Georesource Management*, 7, 105–117.

Sinha, K. K., Krishna Rao, N., Shah, V. L., & Sunil Kumar, T. S. (1997). Stratigraphic succession of the Precambrian of Singhbhum: Evidence from quartz-pebble conglomerate. *Journal of the Geological Society of India, 49*, 577–588.

Sinha-Roy, S. (1984). *Precambrian crustal interaction in Rajasthan, NW India* (pp. 84–91). CISM Volume: Indian Journal of Earth Science.

Sinha-Roy, S. (1985). Granite-greenstone sequence and geotectonic development of SE Rajasthan. *Bulletin Geological Mining Metallurgical Society of India, 53*, 115–123.

Sinha-Roy, S., & Malhotra, G. (1989). Structural relations of Proterozoic cover and its basement: An example from the Jahazpur belt, Rajasthan. *Journal of the Geological Society of India, 34*, 233–244.

Sinha-Roy, S., Guha, D. B., & Bhattacharya, A. K. (1992). Polymetamoprhic granulite facies pelitic gneisses of the Precambrian Sandmata complex, Rajasthan. *Indian Minerals, 46*, 1–12.

Sinha-Roy, S., Mohanty, M., & Guha, D. B. (1993). Banas dislocation zone in Nathadwara-Khannor area, Udaipur district, Rajasthan and its significance on the basement-cover relations in the Aravali fold belt. *Current Science, 65*, 68–72.

Sinha-Roy, S., Malhotra, G., & Guha, D. B. (1995). A transect across Rajasthan Precambrian terrain in relaltion to geology, tectonics and crustal evolution of south-central Rajasthan. *Memoirs of the Geological Society of India, 31*, 63–90.

Singh, S. P., Bhattacharya, A. R., Hemraj, & Shrivastava, S. K. (2010). Structural development of a granite collapse breccias of Mohar, Bundelkhand massif: An evidence of a Precambrian caldera from the Indian Shield. Journal of Economic Geology and Geo-resource Management, 7, 105–117.

Sivaraman, T. V., & Raval, U. (1995). U-Pb, isotopic study of zircons from a few granitoids of Delhi-Aravali belt. *Journal of the Geological Society of India, 46*, 461–475.

Srivastava, R. K. (1988). Magmatism in the Aravali Mountain Range and its environs. *Memoirs of the Geological Society of India, 7*, 77–93.

Srivastava, D. C. (2001). Deformation pattern in the Precambrian basement around Masuda, Central Rajasthan. *Journal of the Geological Society of India, 57*, 197–222.

Srivastava, R. K., & Singh, R. K. (2003). Geochemistry of high-Mg mafic dykes from the Bastar Craton: Evidence of Late Archaean boninite-like rocks in an intracratonic setting. *Current Science, 85*, 808–812.

Subrahmanyam, C. (1980). Regional gravity and geological structure in Bastar Province, India. *Geophysics Research Bulletin, 18*, 75–84.

Subrahmanyam, B. (1985). Lonar crater: A crypto-volcanic origin. *Journal of the Geological Society of India, 26*, 326–335.

Tewari, R. C. (1998). Permian Gondwana sedimentation in Yellandu (Singareni) coalfield, Andhra Pradesh, India wih notes on regional palaeogeography and tectonic history. *Journal of the Geological Society India, 52*, 569–578.

Tewari, H. C., Dixit, M. M., & Sarkar, D. (1995a). Relationship of the Cambay rift basin to the Deccan volcanism. *Journal of Geodynamics, 20*, 85–95.

Tewari, H. C., Rao, Vijaya, Dixit, M. M., Rajendra Prasad, B., Madhava Rao, N., Venkateswarlu, N., et al. (1995b). Deep crustal reflection studies across the Delhi-Aravali fold belt: results from the northwestern part. *Memoirs of the Geological Society of India, 31*, 383–402.

Tewari, H. C., Rajendra Prasad, B. R., Vijaya Rao, V., Reddy, P. R., Dixit, M. M., & Madhava Rao, N. (1997). Crustal reflectivity parameters for desciphering the evolutionary processes across the Proterozoic Aravali-Delhi Fold Belt. *Journal of the Geological Society of India, 50*, 779–785.

Tobisch, O. T., Collerson, K. D., Bhattacharyya, T., & Mukhopadhyay, D. (1994). Structural relationships and Sr-Nd isotope systematics of polymetamorphic granitic gneisses and granitic rocks from central Rajasthan, India: Implications for the evolution of the Aravali Craton. *Precambrain Research, 65*, 319–339.

Upadhyay, Rajni, Sharma, B. L, Jr., Sharma, B. L., & Roy, A. B. (1992). Remnants of greenstone sequence from the Archaean rocks of Rajasthan. *Current Science, 63*, 87–92.

Vijaya Rao, V., & Reddy, P. R. (2002). A Mesoproterozoic supercontinent: Evidence from the Indian Shield. *Gondwana Research, 5*, 63–74.

Vijaya Rao, V., Rajendra Prasad, B., Reddy, P. R., & Tewari, H. C. (2000). Evolution of Proterozoic Aravali-Delhi Fold Belt in the northwestern Indian Shield from seismic studies. *Tectonophysics, 327*, 109–130.

Vohra, C. P., Dasgupta, S., Paul, D. K., Bishui, P. K., Gupta, S. N., & Guha, S. (1991). Rb-Sr chronology and petrochemistry of granitoids from the southeastern part of the Singhbhum Craton, Orissa. *Journal of the Geological Society of India, 38*, 5–22.

Wanjari, Nischal, Asthana, D., & Divakar Rao, V. (2005). Remnants of early continental crust in the Amgaon Gneiss, central India: Geochemical evidence. *Gondwana Research, 8*, 589–595.

Yedekar, D. B., Jain, S. C., Nair, K. K. K., & Dutta, K. K. (1990). The central Indian collision suture. *Special Publication of the Geological Survey of India, 28*, 1–43.

Yedekar, D. B., Karmarkar, N., Pawar, N. J., & Jain, S. C. (2003). Tectonomagmatic evolution of central Indian Terrain. *Gondwana Geological Magazine, 7*, 67–88.

Yellappa, T., Chalapathi Rao, N. V., & Chetty, T. R. K. (2010). Occurrence of lampriotic dykes at the northern margin of the Indravati basin, Bastar Craton, central India. *Journal of the Geological Society of India, 75*, 632–643.

Chapter 5
Palaeoproterozoic Mobile Belts in Peninsular India

5.1 Tectonic Perspective

The beginning of the Early Proterozoic era saw rifting of western, central and eastern parts of the Indian Shield, and formation of elongate basins of sedimentation and volcanism (Fig. 5.1). It was ductile extension and rifting of the sialic crust of Archaean antiquity, leading to invasion of sea water. The seawater filled the troughs formed in the NNE–SSW direction in eastern Rajasthan and adjoining Haryana, in the ENE–WSW direction in central India and Singhbhum region of southern Jharkhand and the NNE–SSW direction in north-eastern Maharashtra and adjoining central Chhattisgarh.

These Palaeoproterozoic mobile belts are almost similar in tectonism, igneous activities, metamorphism and sedimentation. The early rift phase was followed by bimodal volcanism, and penecontemporaneous and subsequent deposition of arkose and conglomerate. The sedimentation phase is represented by accumulation of thick sequence of turbidite greywackes and shales. In the third phase, there was compressional deformation with attendant low-to-moderate-grade metamorphism. In some areas, the metamorphism was intense enough to cause differential melting of deeper rocks and generate granitic melt. In all these basins, two facies in three-part packages are discernible: one metamorphosed to moderate grade, the other practically unmetamorphosed. The two facies have been given different formational names by different investigators, despite a common evolutionary history.

Resurgent tectonism invested all these rift-basin successions with characteristics of mobile belts. The Early Proterozoic mobile belts are represented by the *Aravali Range* in north-western India, the *Satpura Range* in central India, the *Singhbhum Terrane* in eastern India and the *Bhandara Triangle* in central Chhattisgarh and adjoining Maharashtra (Fig. 5.1).

The Bouguer anomaly in the Aravali Mobile Belt is 0–80 mGal (Fig. 5.2). The Aravali is characterized by a large linear gravity high of the order of 130 mGal

K.S. Valdiya, *The Making of India*, Society of Earth Scientists Series,
DOI 10.1007/978-3-319-25029-8_5

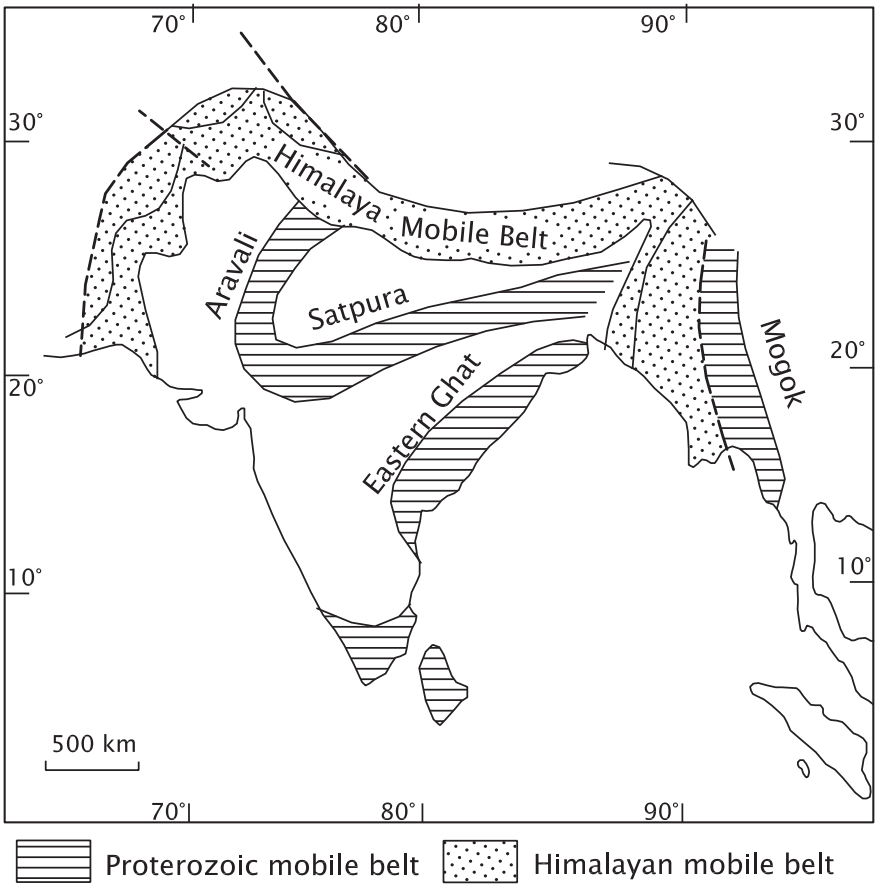

Fig. 5.1 Sketch map shows Palaeoproterozoic mobile belts in the Peninsular India, and the Himalayan Mobile Belt

flanked sharply by two gravity lows of the order of −60 mGal in the west and −70 mGal in the east (Qureshy 1971; Verma 1985). The heat flow is of the order of 56–96 mW/m^2 in the whole mobile belt (Rao et al. 2003). Deeper geophysical probing indicates existence of megathrusts surfacing in the ductile shear zones. There are two sets of oppositely dipping reflection bands in the upper to lower crustal levels together with a stack of dipping reflectors from the top to the Moho level—implying thick-skinned deformation in the Aravali domain (Rajendra Prasad et al. 1998). The processed seismic section in the Satpura Mobile Belt reveals two different blocks dipping towards one another and a recognizable offset of the Moho (Reddy et al. 1995). Seismic profiles and gravity modelling suggest the presence of a 36- to 46-km-thick high-density crust, attributable to upthrusting

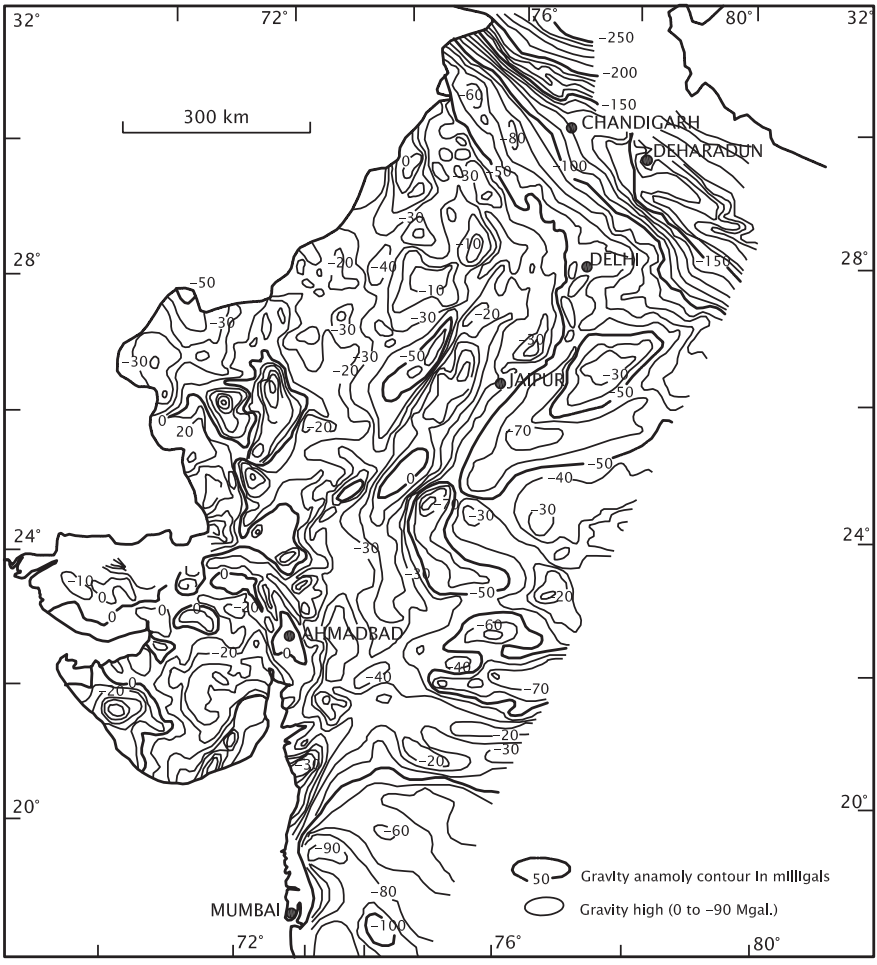

Fig. 5.2 Bouguer gravity anomaly map of north-western India brings out the horst character of the Aravali Mobile Belt (after Raval 1995)

of blocks of granulitic lower crust and the 45° west-dipping reflector, implying westward subduction of the Bundelkhand Craton along the eastern margin of the mobile belt (Mishra et al. 2000). Geomagnetic sounding at the depth of 10–12 km demonstrates existence of an elongate 8- to 10-km-thick conductor along the Satpura, presumably related to an asymmetrical anticlinal structure (Arora et al. 1995). The Satpura conductor anomaly is associated with high heat flow, seismic reflectivity at mid-crustal level and high velocity zone at the middle level of the crust.

5.2 Aravali Domain

5.2.1 Configuration

The pioneering works of A.K. Coulson in 1933, B.C. Gupta in 1934 and A.M. Heron in 1935 and 1953 form the foundation of later studies towards reconstructing the history of tectonic evolution of the Aravali Range. Stretching 700 km from Delhi to Champaner in northern Gujarat, the NNE–SSW trending mountain range developed in the terrane of Bundelkhand Craton.

It is made up of two lithotectonic packages known as the Aravali Supergroup and the Delhi Supergroup. Even though formational interfaces are highly tectonized, there is no doubt that the Aravali and Delhi successions unconformably overlie the Archaean complex (variously named as the Banded Gneissic Complex, the Mewar Gneiss and Bundelkhand Granite) and occur on several belts separated by intervening outcrops of basement rocks (Fig. 5.3). The best development of the Aravali Supergroup is seen in the Nathdwara–Lunavala region (Roy et al. 1988).

5.2.2 Structural Architecture

The Aravali succession, together with the rocks of the underlying basement complex, was involved in three phases of compressional deformation. The early phase of deformation gave rise to ENE–WSW trending isoclinal folds (Fig. 5.4). They were coaxially refolded and quite later deformed again. This resulted in the formation of east- or west-plunging isoclinal folds and NNE- to SSW-oriented upright folds and broad warps. Several ductile shear zones were formed during the early phase of deformation, particularly along the interface of basement and cover rocks, as borne out by wide zones of mylonites and phyllonites (Roy et al. 1988). In the Nathdwara area, the NNE–SSW striking rock-formations take a sharp anticlockwise turn. A little south they swing clockwise, forming spectacular structure resembling a hammer head and a hook. In the Salumbar area, Udaipur district, not only the basal conglomerate of the Aravali succession, but also the rocks of the basement were involved in the deformation, implying mobilization of the basement (Mohanty and Naha 1986). In some areas, the early-phase deformation with attendant mobilization of basement rocks culminated in differential melting of rocks generation of granitic melt and formation of migmatite (Naha and Mohonty 1988). The 2000-million-year-old Darwal and Amet granites represent this phenomenon related to the *Aravali Orogeny* around 1900 ± 100 Ma. The pattern of deformation is the same throughout Mewar and adjoining regions in the Aravali domain (Mookerjee 1965; Naha and Majumdar 1971; Naha and Halyburton 1971; Roy et al. 1981; Paliwal 1998; Sharma 1977, 1988).

In the south-western part of the Aravali Mobile Belt, the deformation changes from brittle–ductile to wholly ductile in the south-western extremity. This fact suggests juxtaposition of three protocontinents—the Aravali, the Dharwar and Singhbhum (Mamtani et al. 2000).

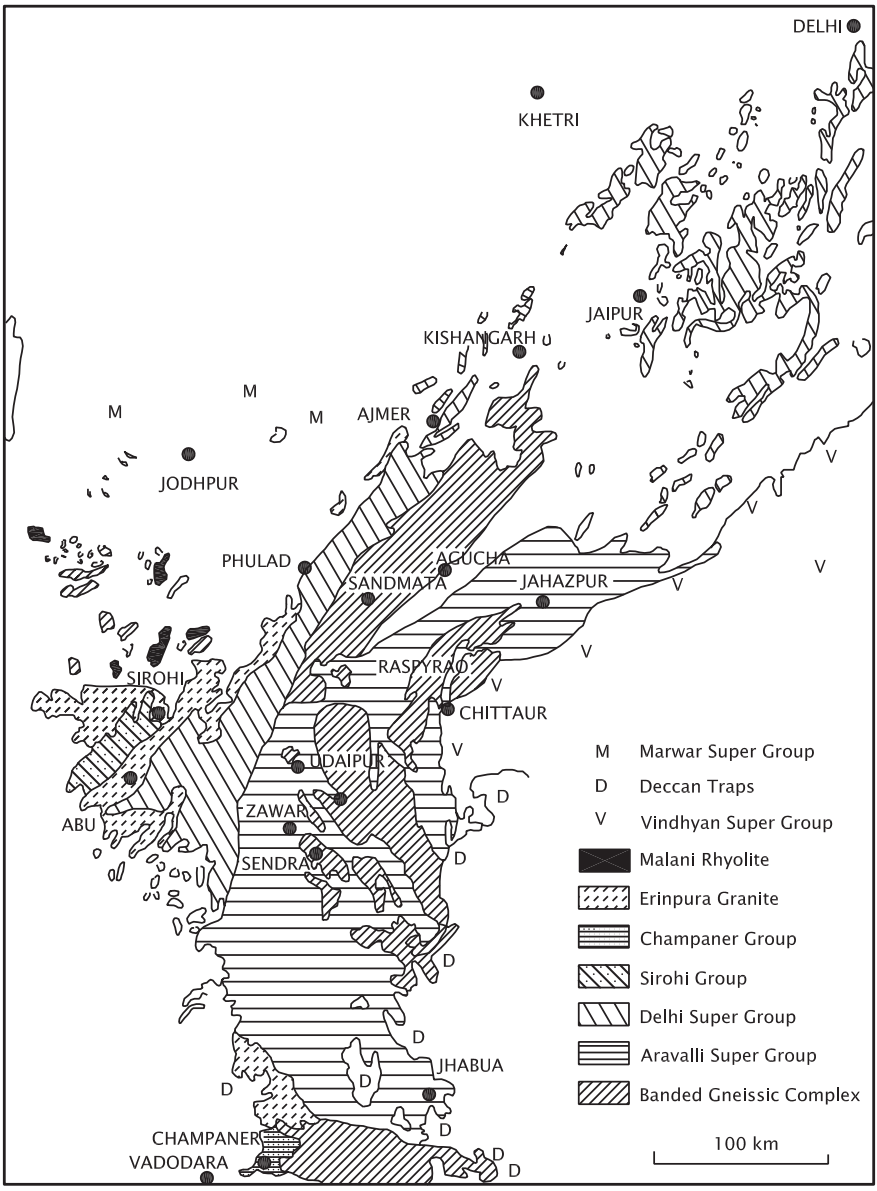

Fig. 5.3 Sketch map of the geology of the Aravali domain, showing the spread of the Aravali and Delhi successions in the terrane of Archaean Gneissic Complex (based on B.C. Gupta in 1934, Heron (1953); Roy et al. 1988)

It may be stressed that the Aravali domain does not exhibit large-scale thrusting and nappe structure such as discernible in the Himalaya (Sharma 1988). Instead, there are deep dislocation zones of crustal scale, marked by ductile shear zones, both at the boundaries and within the domain (Sinha-Roy 1984; Sinha-Roy et al.

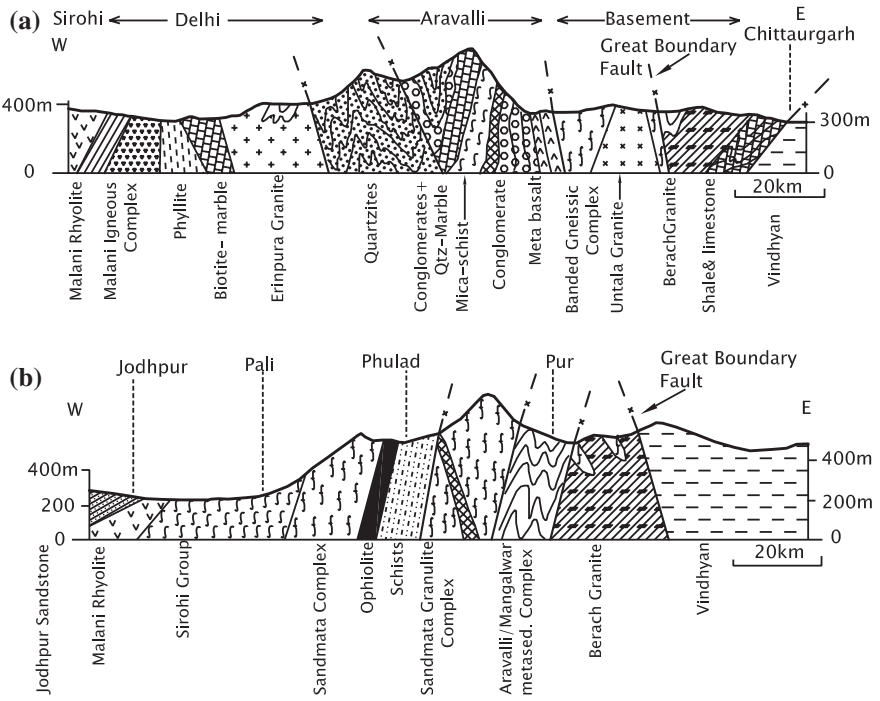

Fig. 5.4 Cross sections illustrate the structure of the Aravali Mobile Belt (based on Sharma 1995)

1995). The basal Aravali succession is juxtaposed against the basement complex along the reworked unconformity. Described as the *Delwara Dislocation Zone* (Fig. 4.15), it is traceable along the interface of the basement and the Aravali succession and has truncated a number of lithofacies. The *Banas Dislocation Zone* forms the eastern boundary of the Aravali terrane. The western boundary of the southern Delhi domain is defined against the basement to the west by the *Phulad Dislocation Zone* and in the eastern part against the Aravali by the *Kaliguman Dislocation Zone*. In its southern part, the Delhi domain is split by imbricating fault zones. The basement rocks have been thrust up and emplaced as wedges within the overlying sedimentary piles. The *Rakhabdeo Suture Zone* comprises tectonized serpentinized bodies of gabbro and ultrabasics, separating the deep water facies from the platform sequence of the Aravali succession.

The *Great Boundary Fault* (Fig. 4.15) defines the eastern limit of the Aravali Mobile Belt against the Vindhyan domain. It is a reverse fault which has time and again registered movements within a hinge located 20 km north of Chittaurgarh. It is a system of parallel faults which at places coalesce to form a single prominent plane. It registers maximum cumulative throw of 1300–1400 m in the Mandalgarh area (Tiwari 1995). Here, the Rewa of the Vindhyan is juxtaposed against the Banded Gneissic Complex, the throw gradually decreasing southwards to merely

150–200 m at Khardeola (Verma 1996). It is thought to have evolved as a normal fault 2500 million years ago, but acquired its reverse geometry during the Delhi orogeny 1400 million years ago.

5.2.3 *Stratigraphy and Sedimentation*

The name Aravali was given by A.M. Heron in 1917. The Aravali succession unconformably overlies the Banded Gneissic Complex (Mewar Gneiss). A horizon at the base of the Aravali Supergroup of conglomerate containing clasts of gneisses, granites, amphibolites and other metamorphic rocks, derived from this basement, is well exposed in the Salumbar area (Fig. 5.5, 5.7). A marker band of

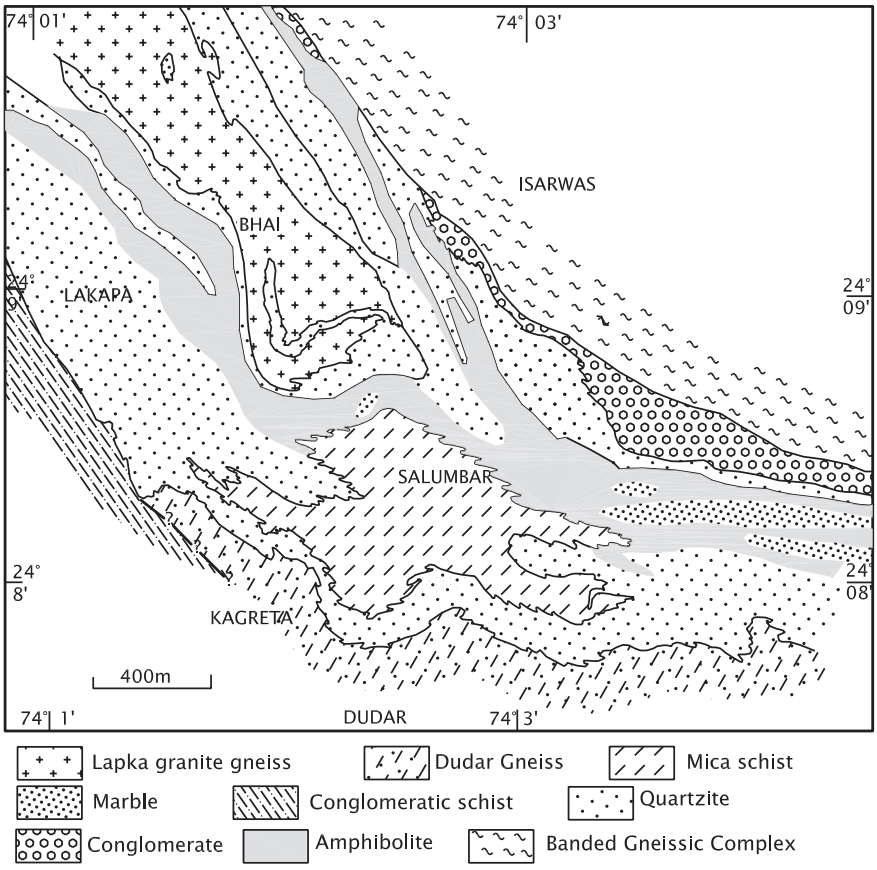

Fig. 5.5 Geological map of the Salumbar area in district Udaipur, showing the horizon of conglomerate at the base of the Aravali Supergroup that rests unconformably on the Archaean Banded Gneissic Complex (after Mohanty and Naha 1986)

quartzite defines the base of the Aravali from east of Udaipur to west of Bhinder (Roy et al. 1981). The conglomerate occurs in patches, and its relationship with the basement is angular. There is a great discordance in the grade of metamorphism across the interface, and in some places, there is palaeosol represented by pyrophyllite (Roy et al. 1988). The occurrence of palaeosol implies a long period of weathering before the commencement of the Aravali sedimentation. The Aravali succession (Table 5.1) comprises two contrasted lithological associations or facies—the sandstone–shale–carbonate assemblage deposited on a shelf in eastern (Udaipur) part, and the flysch assemblage characterized by lithic- and quartzarenites interbedded with shale deposited under deep water in the western (Jharol) part (Poddar 1966; Roy and Paliwal 1981; Roy 1988). It is obvious that the deeper Aravali basin shallowed eastwards where the Banded Gneissic Complex provided detritus to the rivers that flowed westwards.

The shelf sequence is divisible into two groups (Table 5.1). The lower group comprises volcanics–arenites assemblage (*Delwara Formation*) at the base overlain by dolomites, quartzites, carbonaceous phyllites and stromatolitic phosphorite (*Jhamarkotra Formation*). The lower Aravali assemblage of volcanosedimentary rocks was deposited in a number of fault-controlled rift basins formed in the sialic crust (Munshi et al. 1974; Roy and Paliwal 1981). Deep-seated marginal faults evolved during initial stage of basin formation provided passage to mafic magma. The magma came out as lavas and was emplaced as mafic and ultramafic bodies during the deepening of the basin mainly along the margins of the shelf. They were subsequently serpentinized extensively.

Table 5.1 Lithostratigraphic succession of the Aravali Supergroup in the type area (Roy et al. 1988)

Upper Aravali Group	Tide Formation	Slaty phyllite with interbeds of dolomite and quartzite
	Mochiamagra Formation	Quartzite and quartzo-phyllite with local conglomerate
	Zawar Formation	Dolomite, carbonaceous phyllite and quartzite, with sulphide deposits
	Udaipur Formation	Greywacke–slate–phyllite, lithic arenite, local diamictite
	Debari Formation	Conglomerate, arkose, quartzite and phyllite
	Shishmagra–Dantalia Fm.	Conglomerate and quartzite
Unconformity		
Lower Aravali	Jhamarkotra Formation	Dolomite, quartzite, phyllite, carbonphyllite, stromatolitic phosphorite with copper and uranium ore bodies
Group	Delwara Formation	Chlorite schist, amphibolite with interbeds of phyllite, dolomite and quartzite. Basal conglomerate, palaeosol
Unconformity		
Banded Gneissic Complex		

The upper group of the Aravali succession, separated from the lower group by an unconformity, begins with diamictite (as seen at Iswal) and a horizon of ferricrete, silcrete and lateritic shale. Cave breccia occurs atop the carbonate unit and base of the greywacke–shale sequence (Roy et al. 1983). The carbonate unit includes a persistent but thin horizon of prosphorite extending southwest from Jhamarkotra to Dakankotra (Fig. 5.6). Associated intimately with columnar-branching stromatolites, the phosphorite was formed in protected tidal flats under intertidal to supratidal conditions (Barman et al. 1978; Nagori 1988). The algae

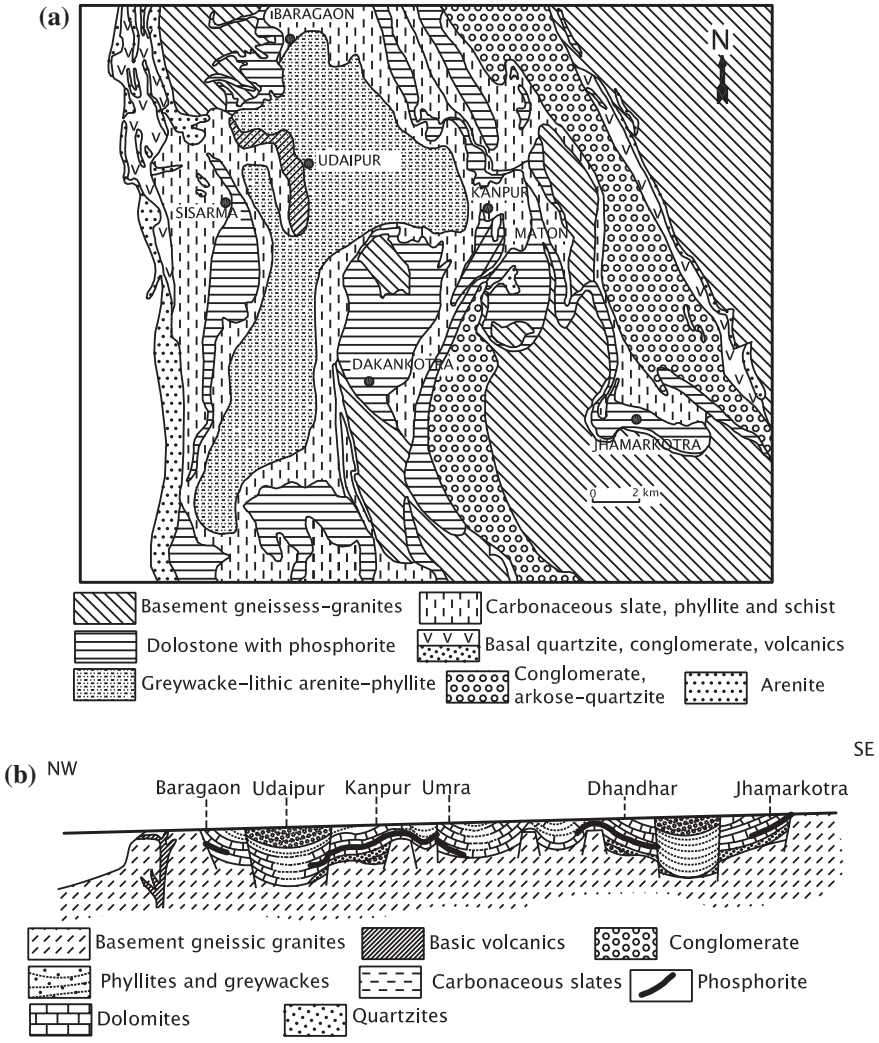

Fig. 5.6 **a** Phosphorite horizon in association with lithostratigraphic units of the Aravali succession. **b** Restored cross section shows the pattern of sedimentation in the fault-controlled basins (**a**, **b** after Nagori 1988)

that constructed the stromatolite edifice of the carbonate bioherms played very crucial role in the genesis of phosphorite under anaerobic conditions (Chaudhuri and Roy 1986; Chauhan 1981, 1989).

Fluvial deposit comprising conglomerate, sandstone, siltstone and shale occurring within the limits of the Udaipur city represents the terminal phase of the Aravali sedimentation in the Late Proterozoic time (Paliwal 1998).

A vast area in the northern part of Gujarat is covered by a thick succession of argillaceous and manganese-bearing calcareous rocks of the *Champaner Group* (Jambusaria and Merh 1967). It represents the upper part of the Aravali Supergroup (Gopinath et al. 1977). A series of NNW–SSE trending folds with steep axial planes characterize this Palaeoproterozoic succession.

5.2.4 Basic Magmatic and Volcanic Activities

Related to lithospheric extension, the volcanics in the basal Aravali succession near Nathdwara, Delwara, Debari, Ghaghri and Sin areas comprise lavas and pyroclastics including tuffs. There are six flows in the 500-m-thick pile of rocks in the Sin area. The lavas belong to tholeiitic to calc-alkaline suite of volcanism, which occured during the early phase of sedimentation. As evident from enrichmet of Fe, Ti and U and depletion of Cr and Ni, greater LREE/HREE fractionation, negative Sr, Eu, P and Ti anomalies, the volcanics are products of a complex process of partial melting, magmatic differentiation and crustal contamination (Deb and Sarkar 1990; Ahmad and Rajamani 1991).

The ultramafic and mafic bodies occupy the deep marginal faults which reactivated towards the close of the Aravali period. Among the ultramafic intrusives, those of Kherwara and Dungarpur are noteworthy (Srivastava 1988). They have been tectonized due to movements along the Rakhabdeo Dislocation Zone.

Associated with the Aravali mafic magmatism are the mafic dyke swarms in the adjoining domain of the Bundelkhand Granite. Intruding the Gneissic Complex in the predominant NW–SE and less common in the NE–SW directions, the tholeiitic dolerite dykes and the pyroxenite and lamproite bodies of the basaltic komatiite suite belong to two generations of emplacement—2115 ± 51 Ma and 2028 ± 22 Ma as Ar–Ar dating demonstrate (Mallikarjuna Rao et al. 2005). However, the NE–SW trending dolerite dykes yield a younger 2000 ± 79 Ma age (Fig. 5.7).

5.2.5 Synkinematic Nepheline Syenites

Forming a hook-shaped pattern owing to involvement in the early phase of Aravali deformation and attendant metamorphism, there is a conformable body of the *Kishangarh Nepheline Syenite* (Fig. 5.8) in the Ajmer region (Sen 1952; Niyogi

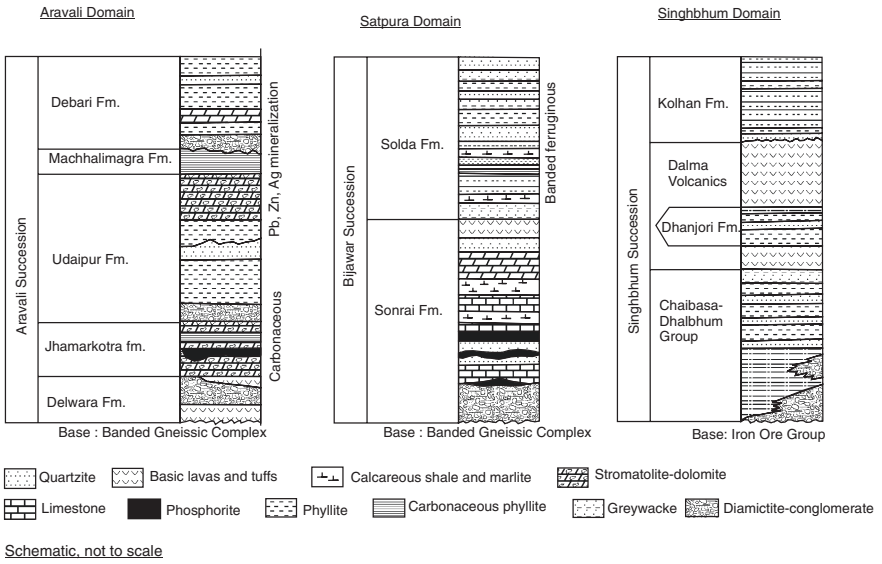

Fig. 5.7 Lithostratigraphic columns of the Palaeoproterozoic successions in Rajasthan, Madhya Pradesh, Jharkhand and Chhattisgarh regions

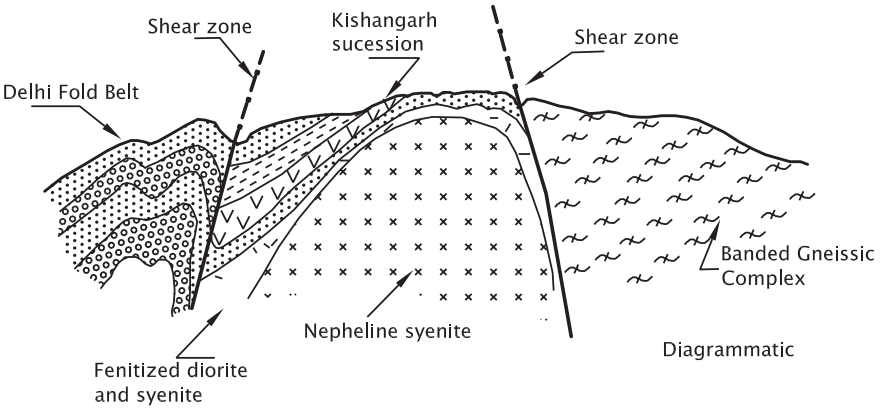

Fig. 5.8 Kishangarh Nepheline Syenite was involved in the first phase of Aravali deformation and emplaced diapirically (Roy and Dutt 1995)

1960, 1966). This essential miaskitic body is intruded by syenitic pegmatite. There is synkinematic fenitization and local partial melting, but no thermal metamorphism. High K/Rb values indicate derivation from the basanitic and alkaline-basaltic source (Srivastava 1988, 1989). It was emplaced diapirically at the katazonal depth, presumably during the closing of the rift basin (Roy and Dutt 1995) sometime between 1900 and 1400 Ma (Crawford 1969).

5.2.6 Regional Metamorphism

The Aravali rocks, on the whole, show very low-grade metamorphism. It increases westwards and northwards—from unmetamorphosed greywacke–shale in the Hindoli belt through greenschist facies in the Jahazpur Belt to amphibolite facies in the Bhilwara–Dariba–Rajpura belt. The 200-km-long and 100-km-wide *Bhilwara Belt* (Raja Rao 1970; Raja Rao et al. 1971) is separated by a tract of migmatized Banded Gneissic Complex or a plane of unconformity from the main Aravali Belt. The Bhilwara assemblage comprises sillimanite–graphite–mica schists in association with magnesian marble and metamorphosed low K-tholeiitic to calc-alkaline basalts characterized by sulphides of copper, zinc and lead, ^{13}C values between −21 and −13 ‰ (Deb 1980). Structural and stratigraphic studies (Roy et al. 1981) and Pb-isotope data (Deb et al. 1989) corroborate A.M. Heron's contention that the rocks of the Bhilwara belt are contemporaneous with those of the Aravali main. In the eastern part of the Bhilwara district in south-eastern Rajasthan, the Archaean basement (Hindoli and Mangalwar) are unconformably overlain by a succession of dolomite, banded iron formation, and tuffaceous–carbonaceous phyllite, described as the *Jahazpur Group* (Sinha-Roy and Malhotra 1989). The Jahazpur succession (of conglomerates, schists and marble) shows significantly negative to near zero values of $\delta^{13}C$—4.8 to +0.9 ‰ V-PDB in the lower part and near zero values in the upper part—in contrast to highly positive values in the Aravali succession in the Delwara–Udaipur area (Pandit et al. 2003). A deposit of rift formed in the sialic crust, the Jahajpur, seems to be homotaxial with or a facies variant of the Aravali Supergroup.

5.2.7 Emplacement of Granites

The mobilization of the basement rocks during severe compressive deformation culminated in the generation of granitic melt, and eventual emplacement synkinematically with the earliest phase of Aravali folding. These granites are represented by plutons at Darwal and Amet. The *Darwal Granite* and the *Amet Granite* are conspicuously porphyritic, characterized by phenocrysts of microcline up to 10 cm by 3 cm in size, and a texture considerably varying from core to periphery. The granites are characterized by higher concentration of LREE and high La/Lu and Ce/Yb ratios (Bhushan and Chittora 2005). The marginal part of the Darwal porphyry is foliated and rich in mafic minerals, and is locally mylonitized. Dated 1900 ± 100 Ma (Choudhary et al. 1984), the Amet granitic suite marks the tectonic upheaval that ended the Aravali sedimentation. That was the time of intense tectonic deformation when the basement along with deep-seated granulitic rocks was brought up (Sinha-Roy 1984), and the development of tension fractures gave rise to another set of intracratonic basins—the Delhi Basin. The Sm–Nd whole-rock age of the Jasrajpur Granite pluton, made up of dominant monzonite, granodiorite and granite of the Andean arc type, is 1800 ± 59 Ma,

while the zircon (evaporation) age is 1821.7 ± 4 Ma—the age of the emplacement (Kaur et al. 2009). The Amet Darwal and Jasrajpur granites strongly recall the 1900 ± 100 million years old Ramgarh Porphyry in Kumaun and the Lingtse Gneiss in Darjiling–Sikkim Himalaya (Valdiya 1981, 1988).

5.2.8 Mineral Deposits

The Rampura–Agucha belt (Fig. 5.9) in the Bhilwara domain hosts deposits of *zinc and lead sulphides*. The mineralization took place along the contact of the Aravali with the basement complex. The mineralization occurred around 1800 ± 40 Ma (Deb et al. 1989, 2001). The deposits occur in the doubly plunging synformal structure made up of sillimanite–graphite–mica schists and amphibolites. The reserve is estimated to be of the order of 61 million tonnes with 13.48 % Zn and 1.57 % Pb (Gandhi et al. 1984). The Rajpura–Dariba belt of siliceous dolomite, calc-biotite schist and iron-rich graphite–mica schist with quartzite and tuff contains blanket-shaped and lensoid bodies of sulphide ores (Deb and Sarkar 1990; Bhattacharya 2004a). The 3.7-km-long Dariba deposit is a product of diagenesis (Poddar 1974; Chauhan 1977). There is vertical zoning of copper, lead and zinc sulphides—the copper sulphides being at the base. The Rajpura–Dariba reserve is estimated to be of the order of 2 million tonnes with 6.7 % Zn and Pb. In the middle part of the Dariba–Bethumbi–Saraswas belt in Rajsamand district, the underground zone of the mineralization in mica schists and carbonaceous schists beneath Sindesar, Khard and Lathiakheri comprises disseminated as well as banded ores of zinc and lead over a stretch of 3.5 km along the strike estimated to be 100 million tonnes (Ameta and Sharma 2008). The primary source of mineralization is believed to be the volcanic rocks of the deeper levels. Lead and zinc deposits occur in the dolomitic carbonates within a succession of phyllites and quartzites in the Mochiamagra–Balaria–Zawarmala and Bororimagra areas. The carbonate-hosted Pb–Zn deposits of the Zawarmala is a banded stratiform body with veins of galena, which were formed at temperature 395 to 290 °C and pressure 1450 bars, as indicated by fluid inclusions (Talluri et al. 2000). The reserve is of the order of 74.3 million tonnes with Pb–Zn content of 5.6 %. The modal age of the mineralization is 1700 ± 40 Ma (Deb et al. 1989).

A low-grade *uranium mineralization* is seen in the carbonates and phyllites of the Umra–Udaipur belt.

The Jhamarkotra Formation of the Udaipur region contains moderately large deposits of *phosphorite*. The phosphorite, intimately associated with columnar-branching stromatolites, was formed in porewater within buried sediments under anaerobic conditions generated by biological activity of algae (Banerjee 1971; Banerjee and Klemm 1985; Nagori 1988). The n-alkane distribution pattern and pristane–phytane data demonstrate that in an overall oxidizing condition of the Aravali Basin, the phosphorite was formed in anoxic pockets generated by microbial communities that constructed stromatolites (Chauhan 1979, 1981, 1989).

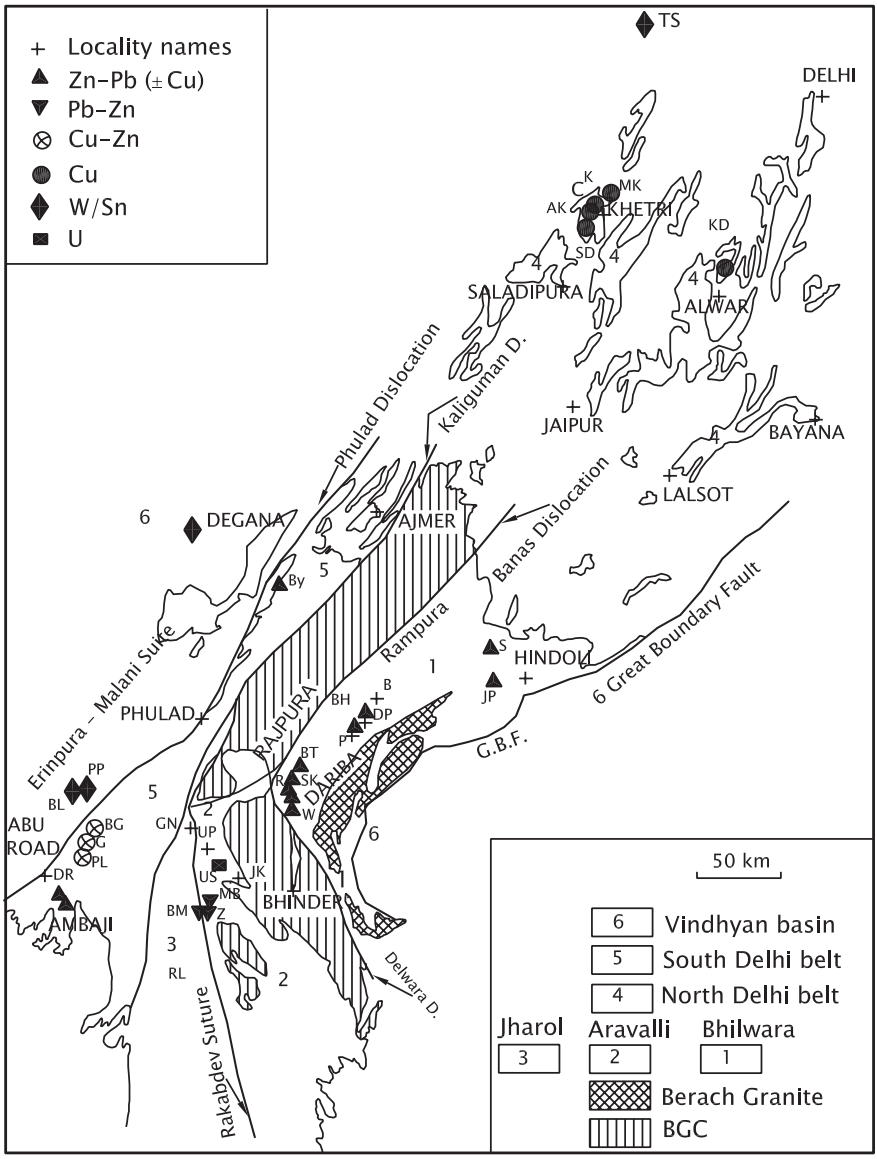

A– Ambaji; AK – Akwali; B – Banera; BG – Basantgarh; BL – Balda; BM – Baroimagra; BT – Bethumni; BY–Birantia; C – Chandmari; D – Degana; DP – Devpura; DR – Devi; G – Golia; Gn – Gogunda; JP – Jahazpuri; JS – Jhamarkotra; K – Kulihan; PL – Pipela; KD – Khoda–Dariba; MB – Mochiamagra–Balaria; MK – Madankudan; P – Pur; PP – Phalwad–Positara; S – Sawar; SD – Satkui–Dhanaole; SK – Sindeswar–Kalan; T – Tiranga; Up – Udaipur; Us–Umra–Udaisagar

Fig. 5.9 Simplified geological map of the Aravali Mobile Belt, showing occurrences of economic mineral deposits (after Deb and Sarkar 1990)

In the Bhukia area, the amphibole-bearing dolomitic marble and the albite-rich quartzofelspathic rock was affected by Na- and Ba-rich fluids channelled through rift-related faults. This phenomena generated hypersaline condition, conducive to precipitation of gold with iron, arsenic and copper sulphides (Golani et al. 2002).

5.3 Delhi Domain

5.3.1 Tectonics

Constituting the main edifice of the mountain range, the Delhi succession of rocks occurs along the western flank of the Aravali Mobile Belt (Fig. 5.3). It stretches from Delhi to Ambaji and beyond, widening to more than 200 km in the Jaipur region. In its widest part, the Delhi domain is represented by a number of practically isolated subbasins. The Delhi Basin evolved as a crustal sag that eventually became the repository of a little less than 10,000-m-thick sedimentary succession. Following the tectonic upheaval that terminated the Aravali sedimentation, the Delhi Basin opened up as a system of grabens and half-grabens (Fig. 5.10) represented by the Khetri, Alwar and Bayana subbasins (Singh 1984, 1988). This development took place initially in north-eastern Rajasthan and adjoining Haryana, and later the Basin extended southwards all along the axial belt of the Aravali Mobile Belt.

There is continuity of the Delhi rocks from NE to SW, as evident from nearly uniform lithostratigraphy (Singh 1984), similar structural history (Naha et al. 1984) and unvarying imprint of metamorphism (Sharma 1988). However, there is marked difference between north-eastern and south-western parts of the Delhi domain with respect to the proportion of volcanic rocks and nature of mafic–ultramafic rocks, the occurrence of carbonate and ferruginous sediments, and the pattern and age of mineralization (Deb and Sarkar 1990). Moreover, the intensity of thermal metamorphism was comparatively strong in the south-western sector (Roy 1988). Therefore, two belts of nearly same age have been identified within the Delhi domain—the *North Delhi Fold Belt* and the *South Delhi Fold Belt*. In the older northern part, shallow water sediments accumulated with volcanics, and in the southern sector, deeper-water carbonates formed along with volcanics and the emplacement of mafic and ultramafic plutons (Sinha-Roy 1988).

5.3.2 Structural History

The Delhi domain was affected by multiple phases of folding (Dasgupta 1964; Gangopadhyay and Sen 1968; Sen 1970; Gangopadhyay and Chatterjee 1971; Gangopadhyay 1972; Ray 1974; Naha et al. 1984; Ranawat et al. 1988). The tight to isoclinal folds with pervasive axial-plane cleavage of the first generation

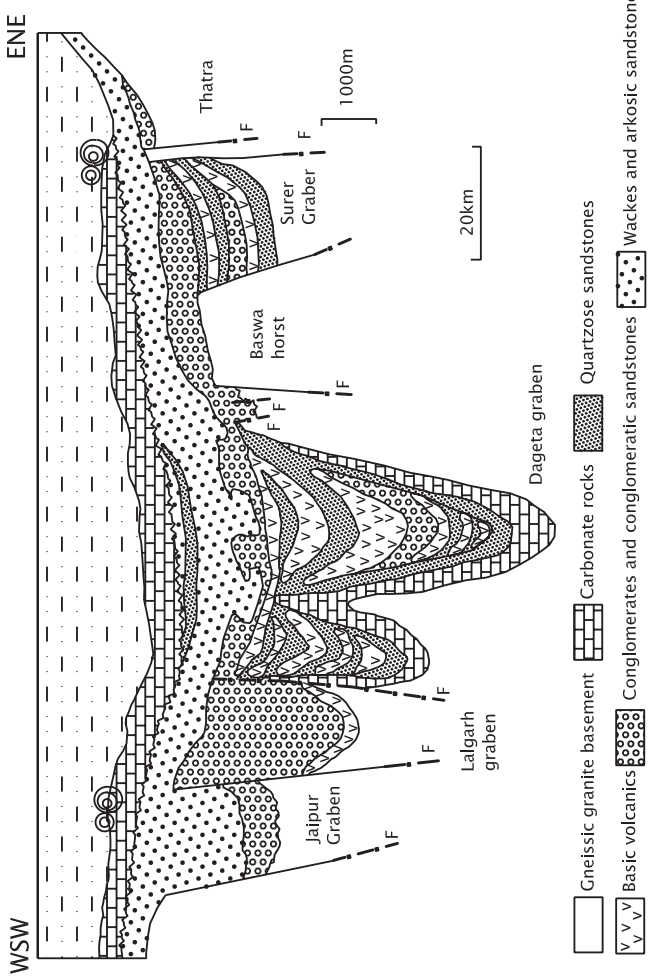

Fig. 5.10 A model portrays the structural peculiarity and sedimentation pattern of the Delhi domain (after Singh 1988)

trend in the NE–SW direction. They were subjected to horizontal squeezing in the NW–SE direction, giving rise to open to tight upright folds oriented NE–SW. The transversely oriented third-generation folds are open to very gentle cross-folds and kinks. In the Khetri region, upright conjugate folds, with their axial plane striking NE and NW, as well as upright chevron folds with axial plane striking E–W, were produced during the fourth phase of deformation. The Ajabgarh structures register buckle shortening in the range of 49–67 % (Bhola et al. 2004).

5.3.3 Stratigraphy and Sedimentation

The Delhi succession is divisible into three groups—the Raialo, the Alwar and the Ajabgarh (Fig. 5.3; Table 5.2). The 3000-m-thick succession in the Delhi graben is an upward-fining assemblage of conglomerates and sandstones. The sediments were laid down by debris flows successively as conglomerates and boulder sheets as proximal fans and longitudinal braid bars in the upper reaches and as alternation of conglomerates and sandstones, characterized by profuse tabular and trough-shaped cross-bedding, megaripples and transverse bars, in the middle and lower reaches of a braided river system (Singh 1984).

Table 5.2 Lithostratigraphy of the Delhi Supergroup (after Singh 1988)

Ajabgarh Group	Kankwari Formation	Quartz–sericite schist, quartzite, thin lenses of marble and felspathic schist with quartzite and slate
	Rajgarh Formation	Quartzite with lenses of schists and phyllites. Quartzite with two thick horizons of conglomerates
---------- *Unconformity*- ----------		
Alwar Group	Pratapgarh Formation	Quartzite and quartz–sericite schist
	Lakhanpur Formation	Sandstone
	Kanawar Formation	Quartzite
	Umraind Formation	Conglomerate
	Mohioni Formation	Conglomerate and quartzite
	Martalab Formation	Quartzite
---------- *Unconformity*- ----------		
Raialo Group	Tehla-Govindpura Formation	Lava flows (including pillow lava), agglomerate and tuff and associated conglomerate, quartzite, phyllite and marble
	Serrate Formation	Quartzite with lenses of oligomictic Conglomerate
	Dogeta Formation	Banded siliceous marble, phyllite, quartzite, dolomitic marble and bands of conglomerate and phyllite
---------- *Unconformity*- ----------		
Banded Gneissic Complex/Aravali Supergroup		

The *Raialo* Group in the type area Rayanhalli comprises dolomite, quartzite, phyllite and oligomictic conglomerate associated with agglomerates and tuffs. There was, thus, volcanism in the beginning of the Delhi sedimentation. The outpouring of the lavas and ejection of volcaniclastics are related to the faults demarcating the boundaries of the basins (Figs. 5.3 and 4.15). In the northern part, the sedimentation commenced with formation of shelf carbonates followed by deposition of coarse clastic and synchronous volcanism. Finally, pelites and semi-pelites were laid down in a multiplicity of lagoons, some of which developed evaporitic conditions (Deb and Sarkar 1990). West of the mountain range in the Sirohi area, the pelite sequence forms a cap on the Raialo succession.

In the *Alwar* times, the sedimentation was affected by a major vertical tectonism, resulting in subsidence of the basin floor and formation of several new grabens and half-grabens in north-eastern Rajasthan (Fig. 5.10). In central and south-western parts, the eastern margins of the Khetri–Ajmer–Pindwara subbasin migrated further east and extended south-westwards up to Gujarat (Singh 1988). Detrital material came from uplifted gneissic blocks lying to the north-west and south-east of the Alwar basin. In the proximal part of the basin, gravel accumulated and formed 1000- to 2800-m-thick fans. The gravels grade basinwards into marginal marine sands that accumulated as estuarine delta plains and tidal flats. The *Barr Conglomerate*, discernible over 35-km stretch, is made up of cobbles and pebbles of quartzite, gneiss, granite, chert and metamorphic rocks. Later deformation and attendant metamorphism converted the unit into an assemblage of felspathic grits and slates (Gangopadhyay and Lahiri 1983).

The *Ajabgarh* time witnessed further downwarping of the crust resulting in submergence of all subbasins and intervening highs. This led to the widening of the area of Delhi sedimentation. There was basin-wide underwater volcanism. Reactivation of basin-margin faults caused generation of coarse clastics which are the preponderant component of the succession. There was rapid variation of thickness and strong overlapping relationship. The synsedimentary volcanism was pronounced (Singh 1988).

The lithostratigraphic unit names such as the Delhi, the Alwar and the Aligarh were given by C.A. Hacket in 1877.

5.3.4 Metamorphism

The amphibolite facies metamorphic rocks occur over extensive areas including the Khetri–Alwar belt. However, in the Lalsot–Bayana and Deri–Ambaji belts, the grade of metamorphism does not exceed the greenschist facies. The early regional metamophism was superimposed by thermal metamorphism related to intrusion of granites. The later metamorphism is manifested in the formation of andalusite-bearing hornfels. In the southernmost part, the thermal metamorphism raised the grade to granulite facies (Gangopadhyay 1972; Sarkar and Dasgupta 1980; Deb 1980; Sinha-Roy and Mohanty 1988).

5.3.5 *Mafic Volcanic Activities*

Mafic volcanic rocks occur all along in three levels—at the top of the Raialo, at the base of the Alwar and at the bottom of the Ajabgarh Group. The aggregate thickness of the Alwar volcanics in the Jahazpur–Govindpura belt of the Bayana subbasin is 1000 m. There are 18 flows of vesicular basalt associated with tuffs (Srivastava 1988). This horizon of the Ajabgarh Group is characterized by lavas that locally show pillow structure and associated pyroclastic material. In the Bayana subbasin, the lavas are interlayered with arkose, conglomerate and minor carbonate rocks (Bhattacharjee et al. 1988). The lavas are tholeiitic in composition and characterized by enrichment in large ion lithophile elements and light rare earth elements and depletion of Nb, P and Sr. They bear close similarity with the low-Ti continental flood basalts derived from enriched mantle source without significant crustal contamination (Raza et al. 2001).

In the western subbasin in the southern part of the Delhi domain, the Ajabgarh contains a significant proportion of basic flows and tuffs, associated with felsic volcanics. This bimodal volcanism in association with shallow water clastic sediments implies ensialic origin within sialic crust of the rifted mobile belt (Gupta et al. 1991).

5.3.6 *Emplacement of Mafic–Ultramafic Bodies*

Layered gabbros and serpentinized ultramafic rocks are associated with pillow basalt, hyaloclastic material and blue schist in the proximity of a belt of greywacke–claystone assemblage in the Phulad area (Figs. 5.4b and 5.11). This suite has been described as the *Phulad Ophiolite*, and its emplacement is attributed to obduction of the material of a rift-related ocean basin following convergence of opposite blocks (Sychanthavong and Desai 1977; Sinha-Roy 1984, 1988; Sinha-Roy and Mohanty 1988). The Phulad suite comprising plastically deformed harzburgite and layered cumulus gabbroic rocks, and structurally overlain by hornblende schist, gabbro, sheeted dykes and pillow basalt, indicates a forearc tectonic regime (Khan et al. 2005). This suite is followed upwards by a pile of rhyolite, andesite and basalts with intercalation of minor cherts and marble. The whole of the mafic–ultramafic assemblage exhibits amphibolite facies metamorphism. In the Phulad–Barr belt, these are characterized by elemental abundances and ratios similar to those of the mid-oceanic ridge basalts; and in the Ranakpur–Desuri belt, the suite shows relatively high Rb, Ba and Sr coupled with low Zr, Nb, Sm and Nd—a chemistry characteristics of ocean-arc basalts (Volpe and Macdougall 1990).

There is another view on the nature and emplacement of the volcanics and basic rocks of the Phulad zone. These have been compared with the continental tholeiite basalts (Gangopadhyay and Lahiri 1984; Srivastava 1988). The configuration and tectonic architecture of the mobile belt tend to support this interpretation.

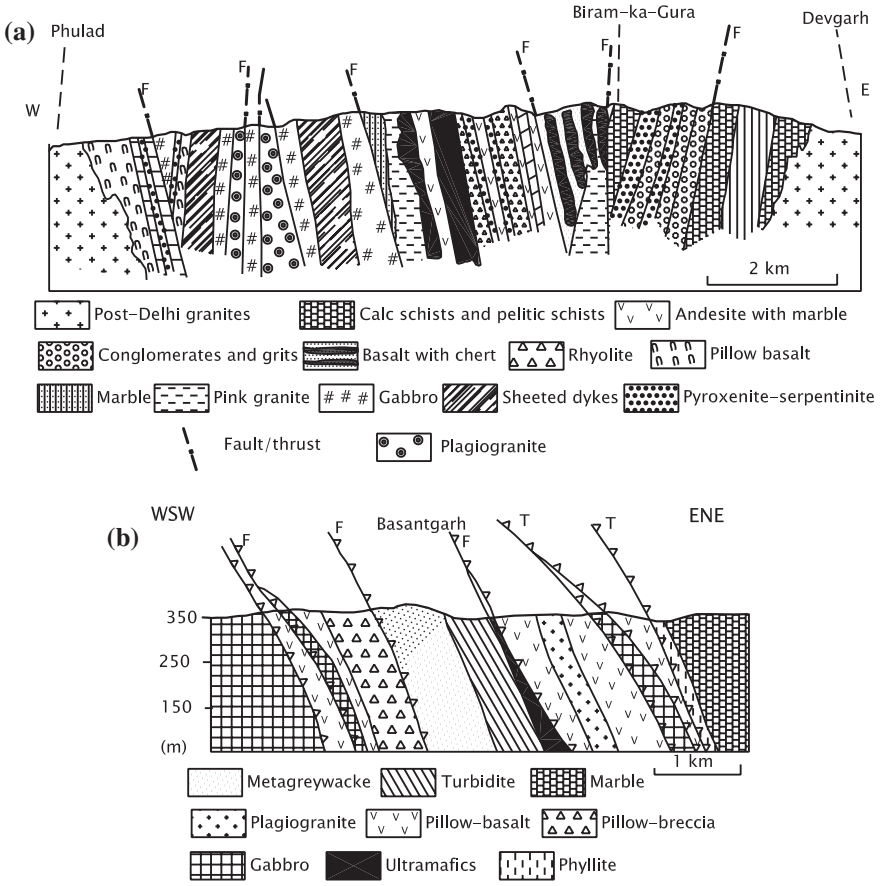

Fig. 5.11 Cross sections show the relationship between different lithotectonic units and their lithological constitution in the **a** Devgarh–Phulad segment, and **b** Basantgarh area (after Sinha-Roy 1984; Sinha-Roy and Mohanty 1988)

5.3.7 Emplacement of Granites

Granites intrude the Alwar succession in the northern part of the Delhi domain. Rb–Sr whole-rock isochron age of the granites ranges between 1450 and 1565 Ma (Choudhary et al. 1984). The 1480 ± 40 Ma-old Khetri Granite and 1450-Ma-old Ajitgarh Granite were emplaced syntectonically with the first phase of folding of the Delhi rocks (Roy and Das 1985). The granitic melt is supposed to have formed in the deeper level of the crust (Bhattacharyya and Dasgupta 1981). In the Khetri Copper Belt in northern part, the Gothara pluton (Fig. 5.12) is a plagiogranite, characterized by granophyric texture, extremely low K_2O, Rb and Ba and high Na_2O and showing a trace and REE geochemistry. This chemistry indicates

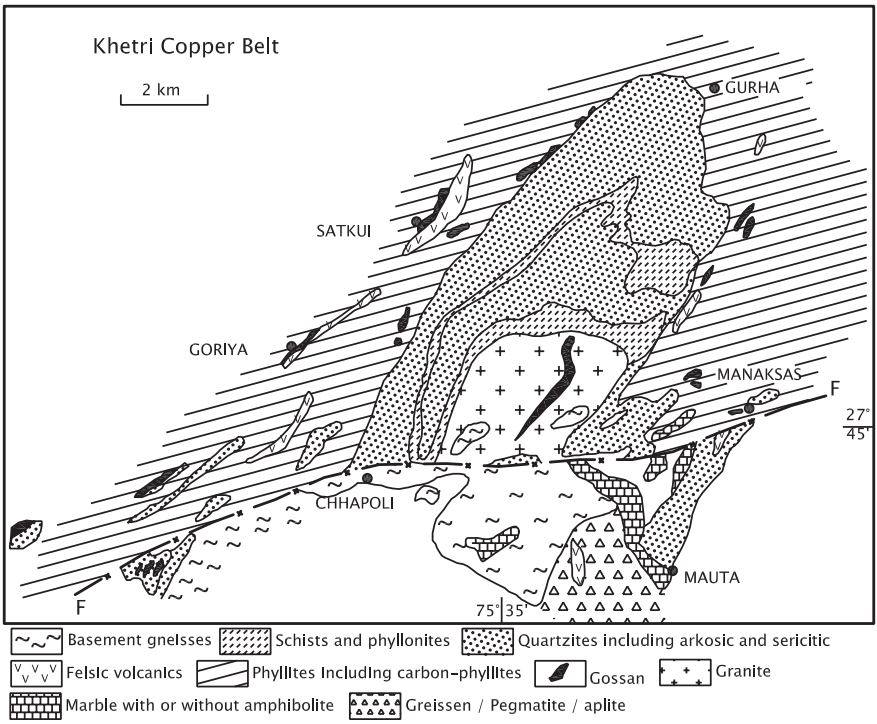

Fig. 5.12 Geological sketch map of the southern part of the Khetri Copper Belt in districts Jhunjhunu and Sikar, Rajasthan, showing sulphide mineralization (after Golani et al. 1992)

derivation of the magma from the mantle in an oceanic ridge setting (Kaur and Mehta 2005). In southern Rajasthan, the Godhra Granite was emplaced syntectonically during the third phase of deformation, the deformation being characterized by oblique simple shearing (Mamtani and Greiling 2005).

The emplacement of granites in the framework of the Delhi Mobile Belt marks the timing of the *Delhi Orogeny*. Taking into consideration the broader aspects, it seems that the tectonic movement that gave rise to the Delhi Mobile Belt occurred at 1600 ± 100 Ma.

5.3.8 Mineralization

In the Khetri Belt (Fig. 5.12; Table 5.3), the sulphide deposits are strata-bound within the garnetiferous chlorite schist and amphibolite that formed at temperature 550–600 °C and pressure 5.5 kbar. The Saladipura deposit of pyrite and pyrrhotite in the *Khetri Copper Belt* occurs along the contact of two lithological units folded into a series of upright to inclined folds, indicating syngenetic primary

Table 5.3 Characteristics of base metal deposits in Rajasthan (Deb and Sarkar 1990)

Deposit	Ore reserve (Mt)	Lithological association	Mode of occurrence	Isotope composition	Transformation	Age (Ma)
Rampura–Agucha	61 (16.1 wt% Zn + Pb)	Graph-sill-mica Schists, Gt-biot-sill gneiss	Sheet-like, deformed into doubly plunging synform	δ^{34}S (Sph); +7 to +10.3 δ^{13}C; −24 to −29	Metamorphosed Upper amphibolite facies Max. $T = 650$ °C Max. $P = 6$ kbar	Model Pb age: 1800
Rajpura–Dariba	152.62 (2.67.38 wt% Zn + Pb + Cu)	Dolomitic marble, chert, Ky-St-bearing Chl-mica schists	Sheet-like/lensoid	δ^{34}S (Py); +9.1 to 6.7 δ^{34}S (Sph); +7.8 to −4.8 δ^{13}C: −21 to −22	Metamorphosed Max. $T = 555$ °C $P = 5.4$ kbar	Model Pb age: 1800
Zawar	74.3 (6.6–6.7 wt% Zn + Pb)	Dolostone, phyllite, quartzite	Transgressive and stratiform	δ^{34}S (Py): +1.5 to 17 δ^{34}S (Gal) −4.4 to +9.2 δ^{13}C: −14 to −22	Low-tempera-ture modification includ-ing remobilization	Model PB age: 1700
Khetri	83 (0.88–1.5 wt% Cu)	Gt-chl schists, banded amphibo-lite, quartzite in the northern part	Lensoid-/sheet-like, peneconcordant with host rocks	δ^{34}S (Py, Po): +7 to +11 δ^{13}C: −28	Metamorphosed Max. $T = 550$–600 °C $P \leq 5.5$ kbar	–
Saladipura	115 (22.5 wt% S)	Amphibolite, qtz-cordortho-amph rock, andl-mica schists, marble	Sheet-like (7 km strike), deformed into a synformal structure	δ^{34}S (Py, Po): +3 to +55 δ^{13}C: −23 to −26	Metamorphosed $T = 600$ °C $P = 5.5$ kbar	Model Pb age: 1780
Ambaji–deri	9.2 (12.1–14.7 wt% Zn + Pb + Cu)	Cord-anth rocks, qtz-chl-trem schists, diopforst marbles	Tabular/lensoid bodies peneconcordant with the host rocks	δ^{34}S (Sulphides): +15.5 to +20.5	Metamorphosed $T = 525$–625 °C $P = 2$–4 kbar	Model Pb age: 1100
Basantgarh	3.5 (2.9 wt% Cu + Zn)	Ch-mus-qtz schists, tholeiitic Metabasalt	Lensoid bodies, accordant with the host rocks	δ^{34}S (Sulphides) +6.8 (mean)	Co-metamor-phosed with the host rocks in the greenschist-amphibolite facies	–

Mineral abbreviations: *Amph* amphibole; *Andl* andalusite; *Anth* anthophyllite; *Biot* biotite; *Chl* chlorite; *Cord* cordierite; *Diop* diopside; *Forst* forsterite; *Gal* galena; *Graph* graphite; *Gt* garnet; *Ky* kyanite; *Mus* muscovite; *Qtz* quartz; *Sill* sillimanite; *Sph* sphalerite; *St* staurolite; *Po* pyrophyllite; *Py* pyrite

origin. The genesis of sulphides is attributed to partly hydrothermal sea water and partly bacteriogenic sulphur in small shallow basins (Sarkar et al. 1980; Sarkar and Dasgupta 1980; Ray 1974; Deb and Sarkar 1990).

The stratiform *zinc–lead–copper sulphides* deposits of the Ambaji–Deri belt, formed 1100 million years ago at temperature 525–625 °C and pressure 2.4 kbar, are related to high-temperature reduction of sea water convecting through multiple sources (Deb and Sarkar 1990). The copper belt containing sphalerite, arsenopyrite, pyrite and galena with minor amount of chalcopyrite is made up of graphite- and sillimanite-bearing quartzofelspathic schists formed at temperature 680 ± 30 °C and pressure 6.2 ± 04 kbar. The copper and zinc mineralization of the Basantgarh–Pipeli belt in the Ajabgarh Group is attributed to different phases of volcanism (Patwardhan and Oka 1988; Ranawat et al. 1988). The lead–zinc deposits of Zawarmala are of epigenetic origin (Talluri et al. 2000).

5.4 Evolution of Aravali Orogenic Belt

As already stated at the outset, the extension of the Indian crust made up of Gneissic Complexes, resulted in the development of elongate basins oriented in the NNE–SSW direction. The depressions were invaded by seawater and became sites of protracted sedimentation. This great thickness of sediments is represented by the Aravali and Delhi made up of sediments and penecontemporaneous volcanics. Later, the sialic crust experienced contraction with attendant deformation and metamorphism of the volcanosedimentary piles. There was partial melting in the deeper level, and anatectic granitic melt was emplaced along the faulted margins of the basins. It was an orogeny involving only the sialic crust (Fig. 5.13) that gave rise to the Aravali Mobile Belt (Roy 1988; Sharma 1988).

There is another view on the evolution of the Aravali Mountain Range (Fig. 5.14). The basin of Aravali sedimentation was an aulacogen. The aulacogen closed at 1800 Ma, and a suture zone, represented by the Antri-Rakhabdeo tectonic line, was formed when the two cratonic blocks collided and the oceanic basin floor was thrust under the continental block (Sychanthavong and Desai 1977; Sinha-Roy 1984, 1988; Sinha-Roy and Mohanty 1988; Deb and Sarkar 1990). In the South Delhi Belt, there was emplacement of basic and ultrabasic material of the seafloor, giving rise to the Phulad Ophiolite along a suture. According to Sinha-Roy's model, the Delhi oceanic crust at an early stage was thrust at shallow angle under the western Rajasthan Craton, culminating in the generation and emplacement of Malani suite of volcanic and granitic rocks.

It may be mentioned that the initial rifting and formation of oceanic basins (in which the Aravali and Delhi sediments accumulated) are attributed to a thermal plume underneath the Bundelkhand Craton.

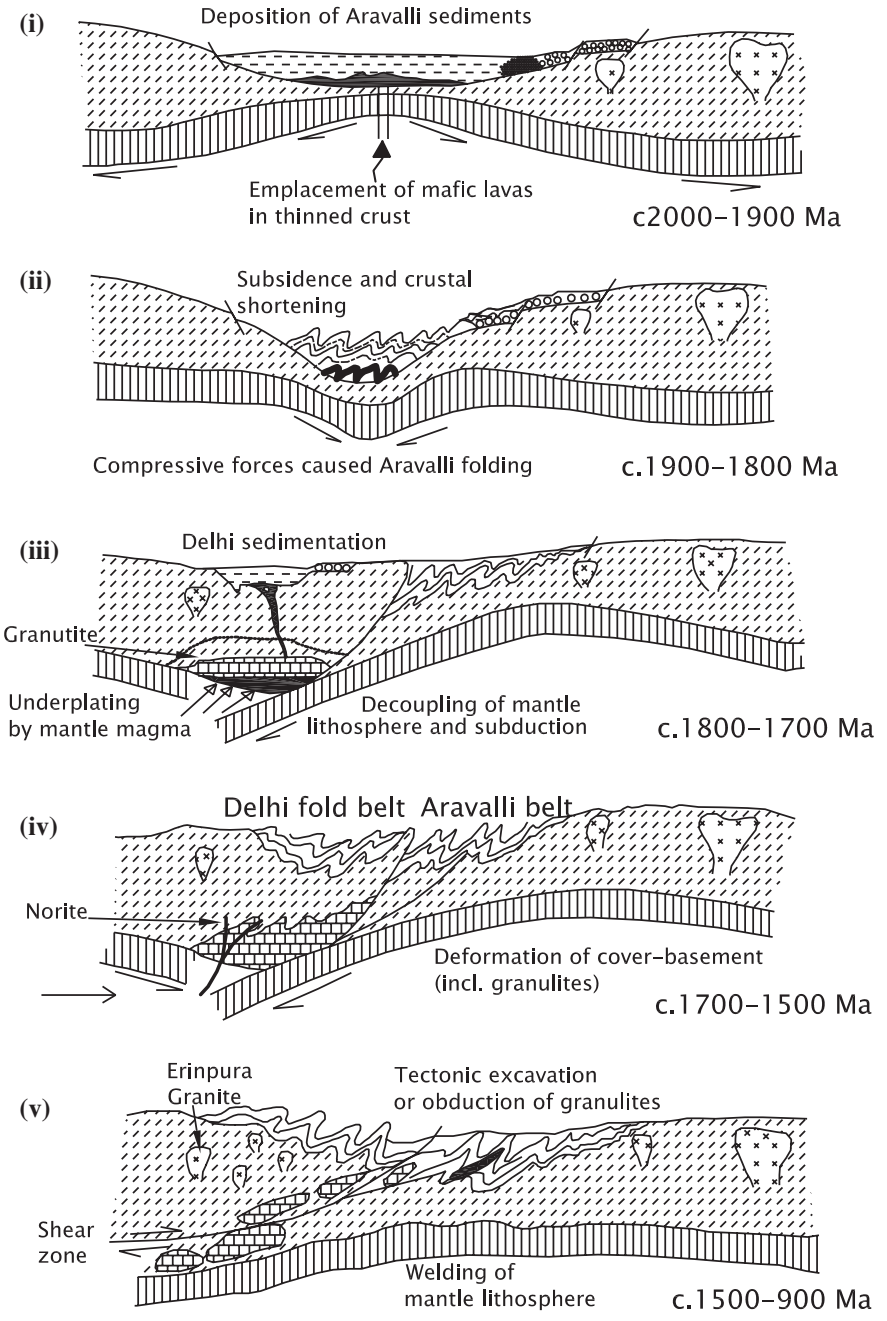

Fig. 5.13 A model of the evolution of the Aravali Mobile Belt. It was an orogeny involving only the sialic crust that gave rise to this Palaeoproterozoic mountain range (after Sharma 1995)

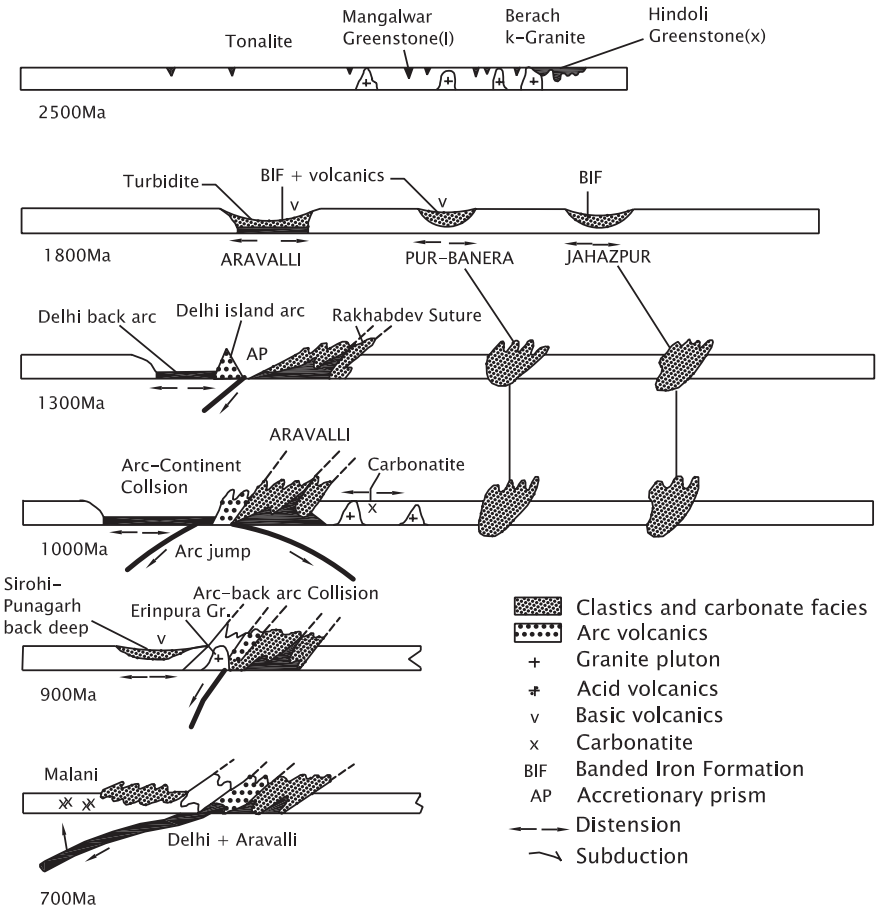

Fig. 5.14 Evolution of the Aravali Mobile Belt is ascribed to plate tectonics (after Sinha-Roy 1988)

5.5 Bijawar Basin

5.5.1 Intracratonic Setting

The Archaean Bundelkhand Gneiss is fringed along its southern periphery by a narrow impersistent group of flyschoid assemblage known as the *Bijawar* in the Chhatarpur district. In the Son–Narmada valleys, the same assemblage forms an important component of the *Satpura Range*. Described as Bijawar by W.T. Blanford in 1869 and by P.N. Bose in 1883–1884, the Palaeoproterozoic belt extends from Dhar in the west through Hoshangabad and Jabalpur in central India to the Rihand valley in the east. The southern equivalent of the Bijawar is described by some workers as the *Mahakoshal Supergroup*. There is little

justification for giving another name to the southern flank of the Bijawar synclinorium, which has admittedly somewhat different lithological sequence, grade of metamorphism and magmatic volcanic activities from those of the northern flank.

The Bijawar succession developed in an elongate depression formed as a consequence of sagging of the crust made up of the Bundelkhand Gneissic Complex and its equivalents. The sagging of the sialic crust is related to rifting of sorts, as evident from early outpouring of lavas contemporaneous with basal terrigenous sedimentation. The 2460- to 2510-million-year-old pillow lavas (Crawford 1969) provide indication of the time when this event occurred.

A broad gravity high exceeding 50 mGal characterizes the Satpura Mobile Belt (Qureshy 1971). The Bouguer gravity anomaly is high (Fig. 5.15) along the axis of the Bijawar Belt (Rao et al. 1990), carrying the implication that the Satpura is a horst mountain associated with the Son–Narmada and Tapi grabens. Deep seismic sounding profile along the Hirapur–Mandla section suggests high-density rocks extending from one kilometre below the Bijawar rocks down into and beyond the Moho (Kaila et al. 1987). In respect of orographic features, gravity anomaly, tectonic design and lithological composition, the ENE–WSW trending Satpura is not different from the NNE- to SSW-oriented Aravali.

5.5.2 Structural Design and History

Like the Aravali succession, the Bijawar rocks were also subjected to triple-phase deformation. The earliest generation of deformation is represented by ENE–WSW to E–W trending tight isoclinal folds all along the belt from Munger in Bihar to south-western Rajasthan (Das 1967; Hasan and Sarkar 1968; Choubey 1971a; Roday and Bhat 1980). The E/ENE–W/WSW-oriented folds are characterized by parallel geometry, syntectonic growth of low-grade metamorphic minerals such as chlorite, biotite and rare garnet, and strong stretching parallel to layers giving rise to a sigmoidal pattern (Bandyopadhyay et al. 1995). The second phase of folding manifested itself in the development to ENE–WSW trending upright to inclined folds with 5°–30° plunge of the axes. The NNW- to SSE-oriented cross-folds were produced during the third phase of deformation.

Significantly, the first phase of deformation gave rise to ENE- to WSW-oriented tight isoclinal folds in the Aravali domain also. It seems that both the Aravali and the Bijawar domains went through the same compression in the NNW–SSE direction. This phase of deformation was accompanied by low-grade metamorphism and emplacement of granites around 1900 ± 100 Ma in many areas.

Just as the Aravali Mobile Belt is sharply delimited against the Vindhyan by the *Great Boundary Fault*, the Bijawar of the Satpura Mobile Belt is faulted against the Vindhyan along the *Son–Narmada Lineament* (Figs. 5.1 and 5.16) (Choubey 1971a, b). The lineament is indeed a series of parallel normal faults. In the Son–Narmada Lineament zone, the rocks have suffered pronounced cataclastic deformation, including brecciation and mylonitization, and variable degree of

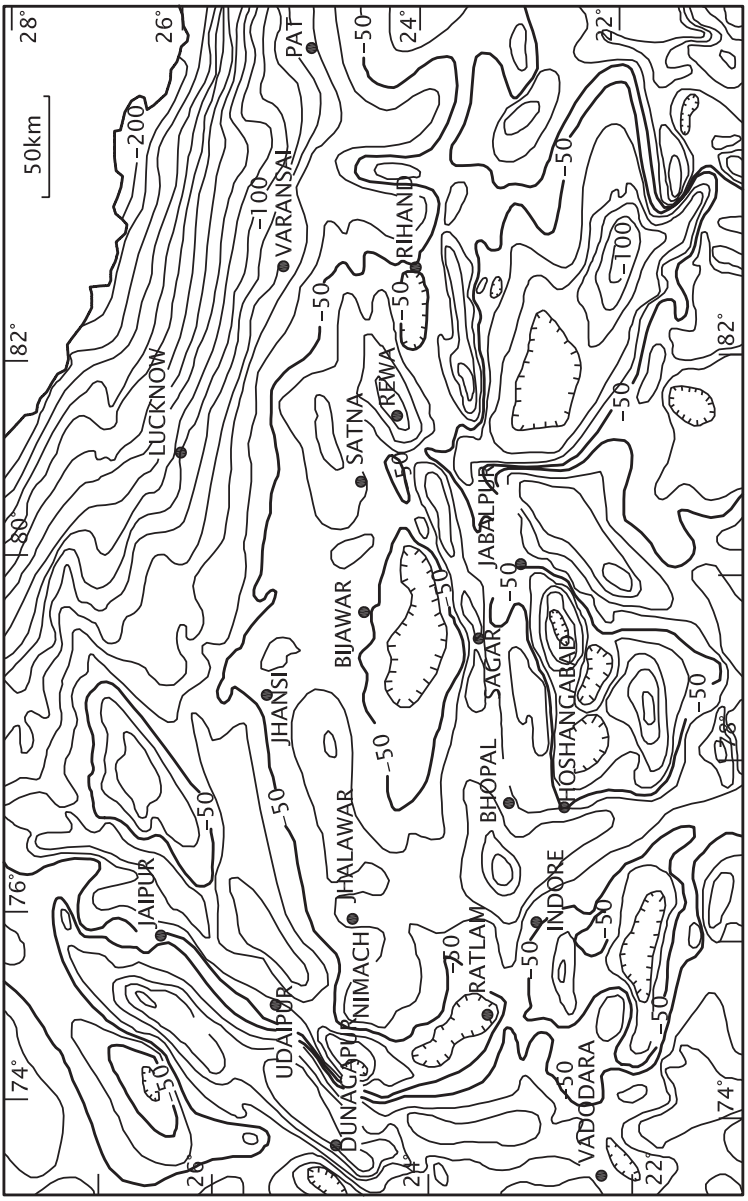

Fig. 5.15 Bouguer gravity map of central India showing the Satpura Mobile Belt (after Qureshy 1971)

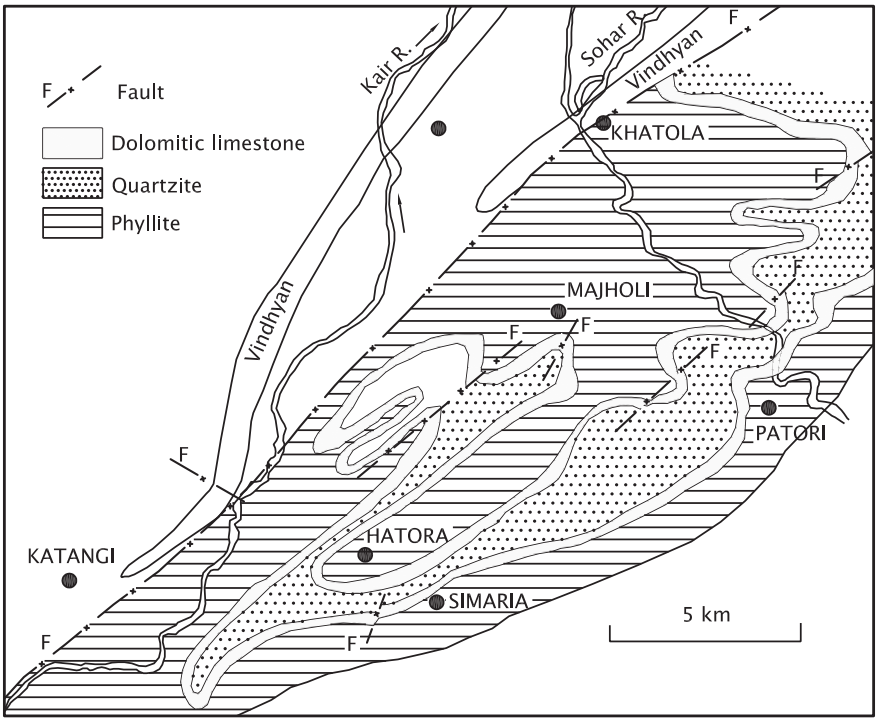

Fig. 5.16 Polyphase deformation of the Bijawar succession adjacent to the Son–Narmada Lineament in the Jabalpur area (after Choubey 1971a)

metamorphism. Locally, the Bijawar rocks override the Lower Vindhyan (Semri) rocks which are inverted, dipping 70°–80° southwards. There was also transcurrent dislocation as observed in the Majholi–Sihora belt in the Jabalpur district. In the Narsipur–Sleemanabad tract, the folds plunge both WSW and ENE, while in the Chitranagar area and further east, they plunge only eastwards (Nair et al. 1995).

5.5.3 Stratigraphy and Sedimentation

Resting unconformably upon the Archaean Gneissic Complex (Bundelkhand Granite), the Bijawar succession is somewhat variable in different sectors owing to overlapping of different lithological units and usual facies variation (Fig. 5.17). The succession broadly comprises conglomerates, greywackes, ferruginous or locally manganiferous quartzites, dolomitic limestones, chert breccia and basic lavas. The lavas occur at different levels. In the type area, it is an upward-fining sequence laid down on the shelf to slope of the basin (Table 5.4). Sandstones and minor conglomerates are interlayered with contemporaneous vesicular basalts and agglomerates. The volcanics (*Chitrangi Formation*) make the dominant component in the 500-km-long, 20-km-wide belt stretching from Barhmanghat to Palamu in

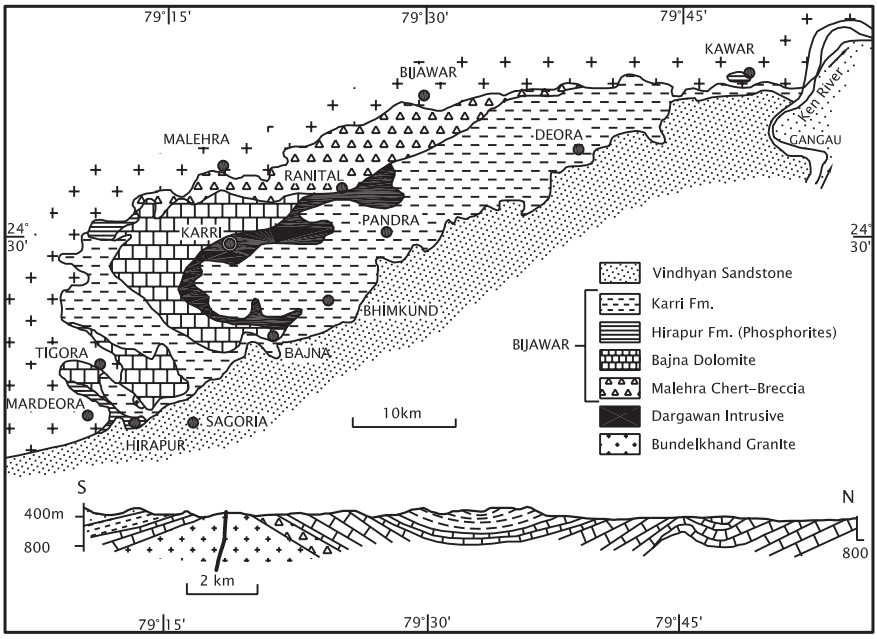

Fig. 5.17 Geological map of the type area of the Bijawar succession. Cross section portrays the structural design of the Bijawar (after Pant and Banerjee 1990)

Table 5.4 Lithostratigraphy of Bijawar Group

Type area (Pant and Banerjee 1990)		Son Valley (Nair et al. 1995)
Vindhyan		
---------- *Unconformity* ----------		
Karri Formation	Ferruginous quartzite and flaser beds	*Parsoi Formation*: Tuffaceous and carbonaceous phyllites, felspathic quartzite, conglomerate with basalt intercalations
Hirapur Formation	Phosphorites	
---------- *Unconformity* ----------		----------
		Agori Formation: Banded haematite quartzite, jaspillite, tuff, impure marble and dolomite with intercalations of calc-chlorite schist, conglomerate with basalt intercalation
Bajna Formation	Dolomites	
Malerhra Formation	Chert breccia	
Kawar Formation	Volcanics–basalts, tuffs and agglomerates	*Chitrangi Formation*: Agglomerate, basalts including pillow lava
---------- *Unconformity* ----------		
Bundelkhand Granite (Gneissic Complex)		

Bihar. Indeed, there were several cycles of volcanism and sedimentation, and in the deposition of chert, each volcanic horizon in the Sidhi district is characterized by pillow lavas, volcanic bomb-agglomerates and tuffs (Tripathi and Mishra 1994).

Chemical sedimentation is represented by formation of chert and jasper followed by carbonates (*Agori Formation*) in broad tidal flats (Pant and Banerjee 1990). The banded iron formation was formed on the shelf and slope of the Bijawar Basin. In the tidal flats, algae grew prolifically, building stromatolitic bioherms as seen in the Joya–Sleemanabad and Barhmanghat belts (Gupta and Verma 1989). Interestingly, pink and white tuff and lenticular basalt flows occur with stromatolitic dolomite, banded haematite-quartzite, jasperite and quartzarenite deposited in a shoal which developed over an extensive area. Mafic dykes cut through dolomite-shale succession, implying synsedimentary magmatic activity.

Emplacement of intraformational collapse breccia was followed by deposition of carbonaceous shales with tuffaceous and felspathic sand (*Parsoi Formation*). There was extensive deposition of ferruginous phosphorite (*Gangau Formation*) along with non-phosphatic ferruginous breccia forming an extensive blanket (Banerjee et al. 1982). The phosphorite, consisting of fluorapatite as the dominant constituent, shows characteristics of shallow water restricted environment in a littoral zone. At Sonrai in the Lalitpur district and Hirapur in the Sagar district, the ferruginous phosphorite is intimately associated with sulphides of Cu, Zn and Pb. Intermittent volcanism, as indicated by intercalations of tuffs and basalts with carbonaceous phyllites of the Parsoi Formation, seems to have provided the ingredients for enrichment of phosphorite.

5.5.4 Volcanic–Magmatic Activities

As already stated, volcanic activities, both eruptive and explosive, occurred during active sedimentation in the submarine environment of the Bijawar. The chemistry of the volcanics conform to iron-rich tholeiite basalt formed in the rift basins, but having some affinity with mid-oceanic ridge basalts (Thakur and Shukla 1990). However, it was a case of platform volcanism in response to crustal thinning and limited rifting as testified by swarms of dykes of diorite and gabbro (Bandyopadhyay et al. 1995). In the Tal area, the Bijawar succession is intruded by a body of peridotite, dunite and gabbro belong to the tholeiitic suite. The peridotite is serpentinized. The ultrabasic intrusives represent early fractionated material from the considerably evolved basaltic magma. The basic and ultrabasic bodies in the Sleemanbad area mark the end phase of the Bijawar magmatic activity (Roy and Bandyopadhyay 1988; Nair et al. 1995).

In the Jungle Valley in Madhya Pradesh, alkaline lamprophyres occur as dykes and plugs as well as flows, and their geochemistry showing that magma emplaced around 1600 Ma was derived from the upper mantle (Srivastava and Chalapathi Rao 2007). Dykes of gabbro and dolerite in the Bijawar succession at Dargawan, which is overlain by the Lower Vindhyan sedimentary pile, are dated by Rb–Sr and Sm–Nd methods at 1967 ± 140 Ma (Pandey et al. 2012). This fact implies that the sedimentation of the lower Vindhyan post-dates ~1900 Ma.

5.5.5 Emplacement of Granites

Towards the end of the Parsoi sedimentation (Table 5.4), there was intrusion of granite—the *Madaura Granite*—in the type area. The stock of granite occurs along the ENE- to WSW-oriented faulted margin of the basin. Associated with quartz porphyry, one of the sheet-like albite granite contains magnetite. The granitic intrusion was followed by emplacement of a series of dykes of trachyte, syenite, minette, kersantite, ijolite, tinguite, alkali gabbro and carbonatite, restricted to the older granitic terrain near the fault contact (Nair et al. 1995). The syenite body near Barr is 1800 million years old, while the mineral age of the alkali gabbro ranges from 1610 to 1760 Ma. Forming a part of migmatitic complex in the Bijawar in the Son Valley, the 1754 ± 166 Ma Dudha Granite is characterized by enrichment of Ni, Cr, Co, V, Zn, Cu, Rb, Ba, Nb, Ce, U and Th and depletion in Sr and Y, pointing to its rift-related anorogenic origin (Dhurandhar et al. 2005).

The Bijawar granites with porphyry seem to be the contemporary of Amet and Darwal granites in the Aravali domain and the 1900 ± 100 Ramgarh Porphyry in the Chail–Ramgarh Nappe in the Lesser Himalayan terrane.

5.5.6 Mineralization

Sphalerite occurs as dissemination in cherty dolomite—the Bajna unit—of the Agori Formation. Phosphorite occuring conspicuously in the Gangau Formation in the upper part of the Bijawar succession is a valuable fertilizer.

5.6 Singhbhum Domain

5.6.1 Tectonic Setting

The seminal works of J.A. Dunn and A.K. Dey, which appeared in 1929, 1941 and 1942, provided the basis of the reconstruction of geological design and history of southern Jharkhand and adjoining Odisha.

The Palaeoproterozoic in eastern India is represented by the *Singhbhum Mobile Belt* (Fig. 5.18; Table 5.5). It abuts against the Chhotanagpur Gneiss in the north and its southern boundary is demarcated by a deep-seated fracture, described as the *Copper Belt Thrust* by Dunn and Dey or *Singhbhum Shear Zone* (Sarkar and Saha 1962; Sengupta and Ghosh 1997). The southern boundary provided passage to basic and alkaline magmas and mineralizing solutions (Banerji 1962; Banerji et al. 1972). Following the tectonic upheaval—to which the emplacement of the Singhbhum Granite is related—a depression is formed between the Singhbhum Granite and Chhotanagpur Gneiss. The development of the depression is probably

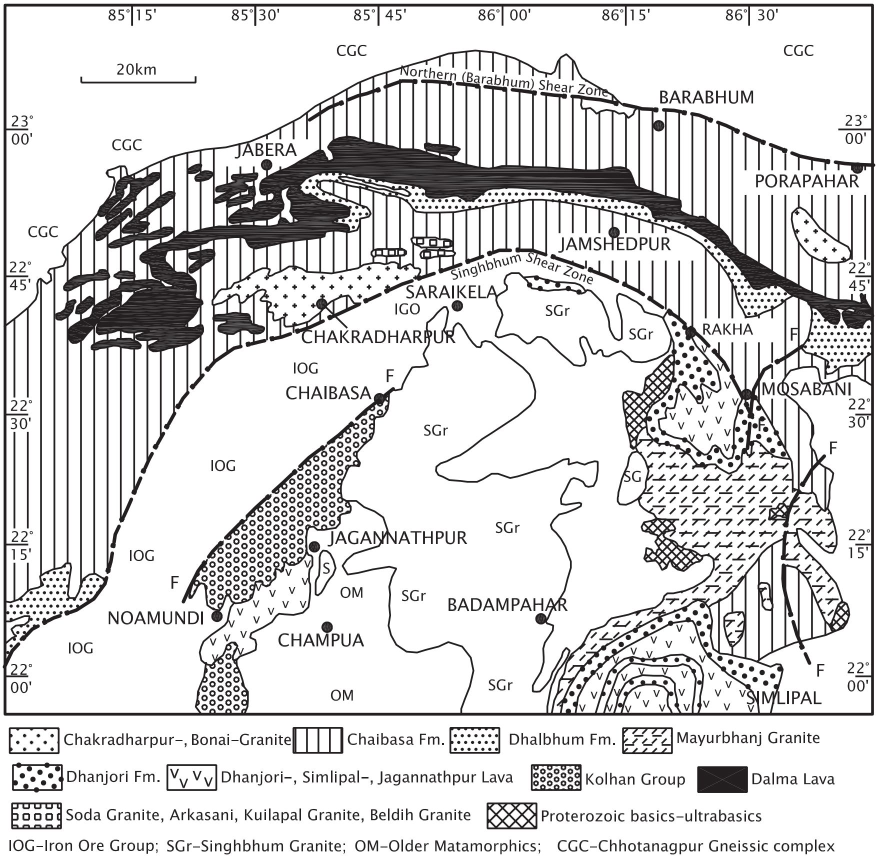

Fig. 5.18 Sketch map showing lithological units of the Palaeoproterozoic Singhbhum Mobile Belt covering the Jharkhand and adjoining states (after Saha 1994)

Table 5.5 Lithostratigraphy of the Singhbhum Mobile Belt (Saha 1994)

	Newer Dolerites (1600–950 Ma)
	Mayurbhanj Granite (2110 Ma)
	Mafic–Ultramafic intrusives
Kolhan Group: (2100–2200 Ma)	Purple sandstones, conglomerates argillites, stromatolitic limestone and phyllites
----------------------- *Unconformity*------------------------------	
Dalma Volcanics (2300 Ma)	Lavas, agglomerates and tuffs
Dhanjori Formation	Sandstones, shales and conglomerate and predominant lavas
Dhalbhum Formation	Phyllites, quartzites and epidiorite sills
Chaibasa Fm. (2300–2400 Ma)	Sandstones–shales with numerous horizons of olistostromes and turbidites
----------------------- *Unconformity*------------------------------	
Singhbhum Granite/Iron Ore Group	

related to the formation of the Singhbhum Shear Zone as a gravity fault. This fault was active time and again all through the history of the mobile belt. The depression became the site of prolonged sedimentation and large-scale volcanism represented by the Chaibasa–Dhalbhum–Dalma–Dhanjori–Kolhan succession. The *Singhbhum Orogeny* converted this pile into a synclinorium, with attendant metamorphism and emplacement of Chakradharpur, Arkasani and Mayubhanj granites, leading to the evolution of the Singhbhum Mobile Belt.

The Singhbhum Mobile Belt lies in the oval-shaped zone of high Bouguer anomaly (Fig. 5.19a), implying the presence of high-density material beneath the

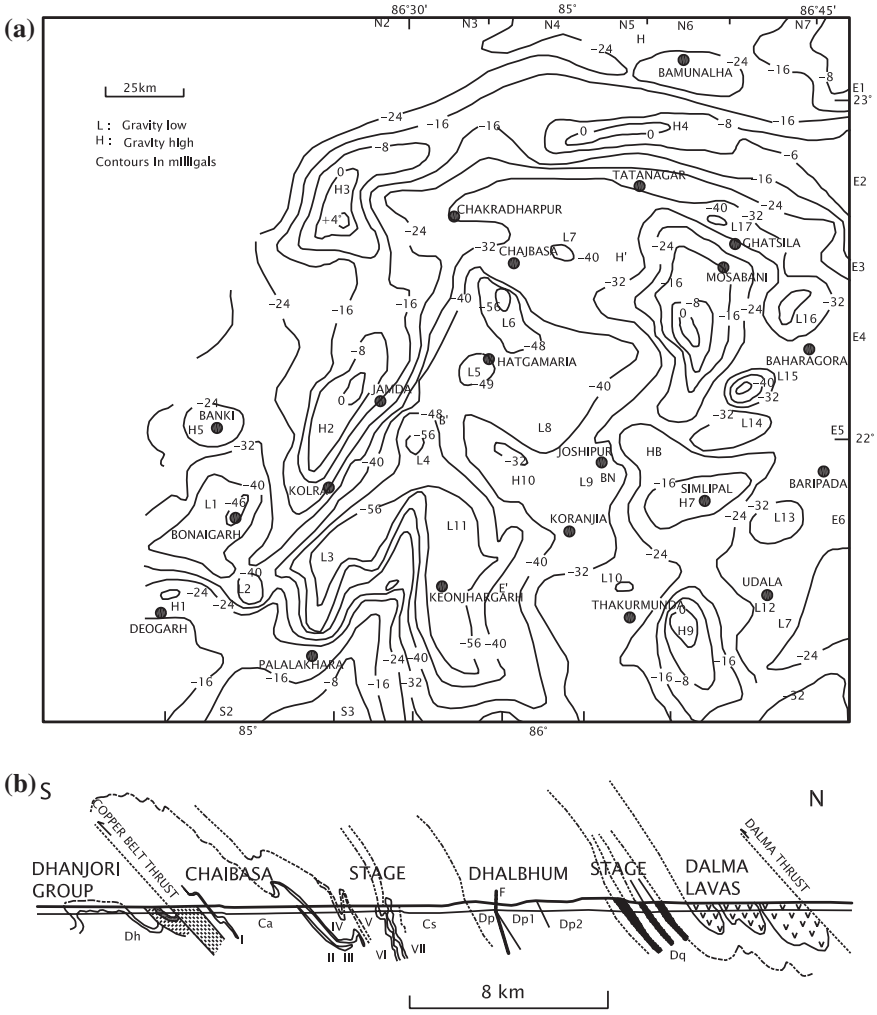

Fig. 5.19 **a** Bouguer anomaly over the Singhbhum Mobile Belt (Verma et al. 1984). **b** Diagrammatic cross section of the Singhbhum domain, showing the structural design and lithological composition of the Singhbhum Mobile Belt (after Saha 1994)

metamorphosed flyschoid assemblages associated with voluminous volcanic rocks (Verma et al. 1984; Verma 1985).

5.6.2 Structural Architecture

The succession of metamorphosed flyshoid sediments and lavas of the Singhbhum domain was deformed into E- to W-oriented folds that are overturned southwards, and are characterized by subhorizontal axis. The E–W trending folds are superimposed by later folds. The axial planes of the folds trend NNE–SSW to NE–SW in the south-eastern part of the Singhbhum domain and E–W in the western sector (Sarkar and Saha 1962). It will be noticed that in respect of the pattern of deformation and orientation of structures, the Singhbhum Mobile Belt bears considerable similarity with the Satpura and Aravali Mobile Belts.

The more than 200-km-long and 1- to 5-km-wide Singhbhum Shear Zone is characterized by multiplicity of thrust planes with variable upward displacement of northern block and then their flaying out into a number of diverging faults in the south. The shear planes show downdip mineral lineation inclined 45°–70° NNE. There are several bands of mylonites formed during the first phase of deformation (Sengupta 1972; Mukhopadhyay 1976, 1984; Bhattacharyya and Sanyal 1988). The mylonites of the Jamshedpur–Mosabani sector exhibit three generations of reclined folds associated with heterogeneous deformation due to N–S and NNE–SSW subhorizontal compression and subsequent strong shear movements related to thrusting (Ghosh and Sengupta 1990).

In the median part of the mobile belt, a thrust has uprooted the pile of the Dalma lavas and abruptly cut the conspicuous V- and U-shaped closures of later-generation cross-folds. There are a number of wrench faults, some dextral and others sinistral, dislocating even the Singhbhum Shear Zone. In the northern part of the Singhbhum domain, the 200-km-long intraformational thrust, known as the *Northern Shear Zone*, has brought high-grade metamorphic rocks of the northern belt upon low-grade metamorphic rocks of the shear zone. The shear zone is characterized by schistose mylonite, reclined folds with axial-plane schistosity showing downdip lineation and rotation of folds in the direction of stretching lineation (Saha 1994; Bhattacharya 2004b).

5.6.3 Stratigraphy and Sedimentation

On the basement of the Archaean Iron Ore Group and Singhbhum Granite rests a succession of mildly to moderately metamorphosed sediments (Fig. 5.18). The succession is divisible into three groups—the *Chaibasa–Dhalbhum* group of flyshoid assemblage (Gaal 1964; Bose 1994), the *Dalma Volcanics*, and the *Kolhan Group* of molasse assemblage (Table 5.5). The Kolhan is separated from

the Dalma by an unconformity, and the Dalma Volcanics are associated with the Dhanjori sediments.

The *Chaibasa* sediments were deposited in the intertidal zone as small overlapping submarine fans along the eastern margin of the craton by rivers that flowed in the NE/NNE direction (Naha 1962). The succession comprises thick sandstones and shales with numerous horizons of turbidites exhibiting slumped structures, sandfilled shallow channels and olistostromes (Das 1997). The sediments were frequently shaken by earthquakes that generated mass movements under water (Bose et al. 1997).

West of the Singhbhum domain in the district of Sundargarh and Sambhalpur M.S. Krishnan in 1937 recognized a succession of rocks very similar to the Chaibasa–Dhalbhum lithology. Resting on the foundation of the Iron Ore Group, the *Gangpur Group* forms a syncline. The southern flank of the syncline is overturned northwards, and the northern flank steeply dips southwards (Kanungo and Mahalik 1972). The eastern closure of the Gangapur synclinorium is characterized by eastward-plunging isoclinal folds and coaxially folded upright folds. Succeeding the Archaean Iron Ore Group without apparent discordance, the Raghunathpalli conglomerate at the base of the group gives way upwards to a succession of carbonaceous quartz–phyllite and banded quartzite (Chaudhuri et al. 1998).

Sand and mud accumulated on the subsiding floor of the Singhbhum Basin. Simultaneously, volcanoes poured out lavas and ejected volcaniclastics on a grand scale, giving rise to a 150-km-long median belt of volcanic rocks—*Dalma Volcanics*—as seen in the Dhanjori, Dalma, Jagannathpur and Simlipal areas. The name Dalma was given by V. Ball in 1881.

Unconformably overlying the Dalma volcanics as well as the Singhbhum Granite, the *Kolhan Group* is a multistoried package of terrigenous sediments (Saha 1948). It comprises purple sandstone and conglomerate at the base, followed upwards successively by thick argillites, stromatolitic limestone and phyllite. There are three parallel sills within the succession. The monotonous grey, current-bedded quartzites are intercalated with shales. The palaeocurrent pattern indicates derivation of detritus from east and southwest. Together with the fining-upward sequence, the vertical and lateral facies variation in the Kolhan implies superimposition of retrograding shorelines on an earlier prograding alluvial fan of a sand complex laid down in an embayment (Ghosh and Chatterjee 1990).

5.6.4 Volcanic Activities

The *Dalma Volcanics* form a 200-km-long and 3–7-km-wide E–W trending arcuate belt practically in the middle of the Singhbhum Mobile Belt. Exhibiting greenschist facies metamorphism, the mafic and ultramafic volcanics of both eruptive and explosive phases are folded into a syncline (Naha and Ghosh 1960; Yellur 1977; Gupta et al. 1980; Bhattacharyya and Dasgupta 1979; Bose and Chakraborti

1994). The volcanic succession is divisible into two units. The lower unit, made up of highly magnesian ultrabasics with actinolite schists, belongs to the picrite suite characterized by low concentration of Na, K, Zr, Y, Ti, P and Sr but higher amounts of Ni and Co and strong LREE depletion. The upper unit comprises pyroclastics and mafic lavas. Lenses of tuffaceous material characterize the sequence of lavas that are vesicular and occasionally pillow-shaped. They belong to the tholeiite suite, mostly depleted in LREE. There is a broad consanguinity of the ultrabasic and basaltic lavas derived from similar sources. The Dalma volcanic activity is related to rifting of the protocontinental crust that allowed tapping of mantle and extrusion of melt (Sarkar 1982, 1988; Saha et al. 1988; Saha 1994). There is another view that the Dalma Volcanics belong to N-type mid-oceanic ridge basalt. Exhibiting geochemical signature of depletion, the Dalma volcanics appear to have evolved in the back-arc setting (Bose and Chakraborti 1994). The gabbro and pyroxenite intrusives of the volcanic assemblage showing depletion of LREE, flat HREE and enrichment in LILE similar to the komatiitic and tholeiitic Dalma lavas originated from a mantle plume that eventually rifted the continental crust and allowed emplacement of magma around 1619 ± 38 Ma (Roy et al. 2003).

The Dalma Volcanics are described by different names in different sectors within the Singhbhum Mobile Belt. The *Dhanjori* lavas, forming an asymmetrical syncline overturned westwards, is associated with sandstones shales and conglomerate. The lavas are petrochemically similar to the contemporaneous Dalma lavas (Saha 1994). It was earlier described as a spilitic suite (Iyengar and Alwar 1965). Ranging in composition from basalt to andesite and showing affinity with the island-arc tholeiites, the iron-enriched volcanics of the Dhanjori Formation were emplaced on the margin of the continent margin (Alvi 1992; Alvi and Raza 1991). The associated conglomerate, coarse sandstone and shale represent a fluvial fan-complex intercalated with volcaniclastic material within the fining-upward fluvial cycle (Mazumder 2005).

The Simlipal Hill is made up of conglomerate and arkosic sandstone overlain by spilitic/mafic volcanics comprising predominant tuffs and lavas and capped at Amjori by a 800-m-thick sill (Iyengar and Banerji 1964). The Amjori sill is a differentiated body of dunite at the base, grading through picrite and dolerite to quartz–dolerite at the top. Sills and dykes of quartz–dolerite intrude the *Simlipal Volcanics*, and intrusive bodies of anorthosite and gabbro occur along the flank of the Simplipal complex. In the western side between Jagannathpur and Noamundi, a pile of metamorphosed basalts, andesite and oligoclase-andesite rests upon the basement of the Iron Ore Group. The *Jagannathpur Lavas* were generated in an essentially continental setting (Alvi and Raza 1991).

5.6.5 Metamorphism

In the Sini area, the Chaibasa rocks exhibit the following zones of metamorphism: (i) chlorite–biotite–phengite, (ii) almandine–chlorite–muscovite, (iii)

staurolite–biotite, and (iv) sillimanite–almandine–biotite (Lal and Singh 1978). In eastern Singhbhum the metamorphism progressed from chlorite grade through biotite, garnet and staurolite to kyanite grade. In the western part of the Singhbhum Mobile Belt, the pattern of metamorphism is quite complex (Bhattacharyya and Sanyal 1988).

5.6.6 Emplacement of Granites

Related to strong deformation along the Singhbhum Shear Zone, synkinematic granites occur as large batholiths in a number of areas within and along the margins of the Singhbhum Mobile Belt. These are the Chakradharpur Granite, the Arkasani Granophyre (Sengupta et al. 1984), the Kuilipal Granite, the Soda Granite and the Mayurbhanj Granite. The Dalma, Dhanjori, Simlipal and Jagannathpur volcanics are intruded by 2200 Ma-old Soda Granite, 2200–2100 Ma-old Mayurbhanj Granite and subjected to metamorphism dated 1629 ± 3 Ma by K–Ar method (Sarkar et al. 1969; Saha 1975, 1994). These bodies range in composition from granite to granodiorite and are characterized by abnormally high initial strontium ratio, flat HREE, enrichment in REE and strong Eu anomaly, indicating their "within-plate" origin as a recycled crustal material. The grey gneissic part of the Chakradharpur body shows highly fractionated REE pattern with a distinct positive Eu anomaly. The younger granite having pegmatitic composition is characterized by less fractionated REE pattern, high HREE abundances and negative europium anomaly (Sengupta et al. 1983).

5.6.7 Dyke Swarms: Newer Dolerite

Spectacular swarm of basic dykes trending dominantly in the NNE–SSW and less commonly in the NW–SE directions traverse the Archaean terrane of the Singhbhum Granite (Saha 1949; Iyengar and Alwar 1965; Saha et al. 1973). The situation is similar to that prevailing in the Bundelkhand Granite terrane. The average spacing is 4 dykes per kilometre, the length varying from a few metres to as much as 20 km, and the width in the range of less than 10 m to more than 1000 m. The composition varies from predominant quartz–dolerite to syenodiorite and norite. The *Newer Dolerite* suite is characterized by high K–Ar ratio, higher Ni and Co and lower Rb, Ba and Sr, implying derivation from picritic magma.

In the 80-km-long belt along the western margin of the Singhbhum Granite between Rajnagar and Champua and also in the north-eastern margin between Malku and Manpur, there are dykes of ultramafic and mafic rocks—harzburgite, lamprophyre and gabbro grading into picrite or pyroxenite (Chatterjee 1955).

5.6.8 Evolution of the Singhbhum Mobile Belt

The evolution of the Singhbhum Mobile Belt (SMB) has been attributed to various phenomena: (1) intracratonic northward subduction of continental plate with Singhbhum Granite along the Singhbhum Shear Zone, (2) collision of the continental blocks represented, respectively, by the Singhbhum Granite and Chhotanagpur Gneiss resulting in obduction along the Dalma, (3) southward subduction of the Chhotanagpur plate and the back-arc zone evolving into the SMB and (4) thermal plume causing rifting of the ensialic crust and emplacement of upper mantle-derived material along deep crustal fractures. One of the models postulates thermal plume causing rifting of the sialic crust and attendant volcanism, followed by delamination and possible limited sinking of the subcrustal lithosphere (Sarkar et al. 1992; Sarkar 2000).

The rifting of the Archaean sialic crust underneath the belt of the Dalma Volcanics (Fig. 5.20) followed by widening of the graben invited sea water that inundated the belts along the periphery of the Singhbhum Granite and Chhotanagpur Gneiss (Mukhopadhyay 1984). Towards the later stage of Singhbhum sedimentation, there was melting of the simatic part of the crust, and the molten basic material came out as lavas, accompanied by explosive volcanism. After the renewal phase of the Kolhan sedimentation, the basin was subjected to compression due to the southern continental plate going down along the Singhbhum Shear Zone. This caused deformation and metamorphism of the rock succession and eventually brought about differential melting of the sialic crust and emplacement of granitic plutons. Immediately following this phenomenon, there was extension of the crust, allowing emplacement of basic and ultrabasic magmas along the fractures, particularly along the eastern margin of the Singhbhum Craton.

5.6.9 Mineralization and Mineral Assets

The Singhbhum Shear Zone hosts mineral deposits of great economic value. The *sulphide deposits* were formed in this shear zone before the third-phase deformation. The original copper mineralization is attributed to hydrothermal activity as indicated by the $\delta^{34}S$ range from 0 to +10 indicates (Sarkar 1982; Sarkar and Deb 1974; Sarkar et al. 1992). The passage of hydrothermal fluids was controlled by faults of the rift zone. Along the shear zone, the deposits of chalcopyrite, pyrite and pyrrhotite are syngenetic with respect to volcanosedimentary phase, predating the main tectonothermal event. The total reserve in the Singhbhum Shear Zone is of the order of 217 million tonnes with 1.36 % Cu. In the Gangpur Basin, the lead and copper deposits of the Sargipali belt are estimated to be 206 million tonnes with 6.73 % Pb and 0.33 % Cu. The Sargipali sulphides are dated 1660 Ma (Vishwakarma 1996).

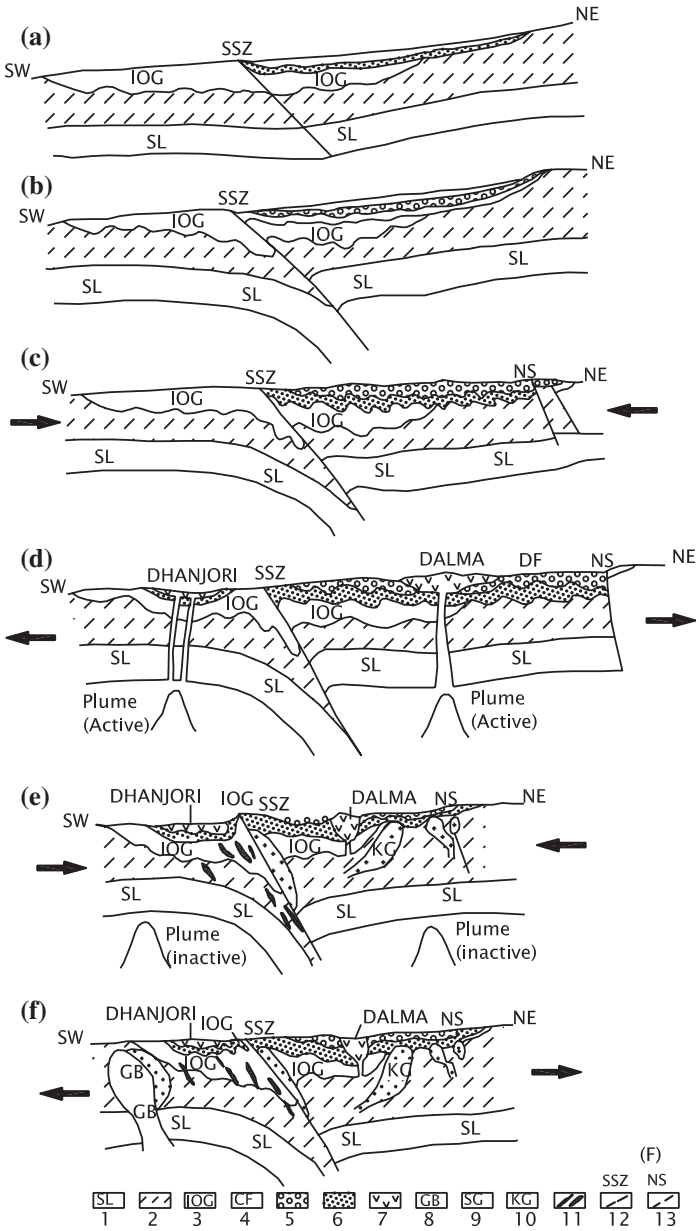

Fig. 5.20 Intraplate subduction model for the evolution of the Singhbhum Mobile Belt (after Saha 1994)

The *uranium mineralization* is confined to mainly quartz–chlorite schist associated with quartzite in the shear zone. The major deposits occur in the Bhatan, Jaduguda and Roam-Rakha areas (Mahadevan 1992b). In the Bagtah-Gohala belt, the uranium mineralization of higher degree is manifested in vein-type occurrences in the Dhanjori amphibolites interbedded with quartzites along shear zone. The Jaduguda uraninite is of hydrothermal origin. The ore bodies are flat concordant corresponding to first-phase metamorphism and dated 1600 Ma (Sarkar et al. 1992). The strata-bound character of the uranium deposits indicates that the uranium source could be syngenetic.

The mineralization in the copper uranium belt in the Singhbhum Mobile Belt took place in the Early Proterozoic time (Bhattacharyya 1992).

5.7 Chhotanagpur Gneiss Complex

5.7.1 Southern Tectonic Boundary

South of the Quaternary expanse of the Indo-Gangetic Plains stretches the 500 km by 200 km E–W terrane of the *Chhotanagpur Gneiss Complex* (Mahadevan 1992a). It is defined along the southern limit by what has been described as the *South Purulia Shear Zone* traceable through Tamar, Porapahar and Khatia. The Gondwanic Mahanadi graben demarcates its western boundary. The Gneissic Complex forms the Archaean core of the Satpura Mobile Belt. Extending in the ENE direction, it stretches east up to the Meghalaya massif.

Comprising granitic gneisses and migmatites with prominent enclaves of metamorphic rocks of amphibolite to granulite facies, the E–W trending Chhotanagpur Gneisse Complex experienced three phases of deformation manifested in tight appressed isoclinal folds (Majumdar 1988). The dominant gneisses belong to the trondhjemite–tonalite–granodiorite suite. Some workers believe that the complex represents a remobilized part of the Indian Shield and forms the basement of the Singhbhum succession. Occurring as enclaves, the charnockites, khondalites and granulites of the Dumka–Mayurakshi belt are associated with schists, banded iron-ore formation, marble and basic–ultrabasic rocks in the Purulia–Bankura belt. Beginning with conglomeratic quartzite, the succession of amphibolite and chlorite schist is intimately associated with aplogranite and mica-pegmatite. The pegmatites and granites occur as phacoliths in open folds in the *Bihar Mica Belt*, as seen at Kodarma, Gaya district (Mahadevan and Maithani 1967). The phacoliths belong to the younger suite of granites. The Bihar Mica Belt succession forms a part of the Palaeoproterozoic Satpura Mobile Belt (Singh 1998). The overlying succession of phyllites and quartzites of the Rajgir–Kharagpur belt represents a Mesoproterozoic formation.

Most significant components of the Chhotanagpur complex are the granite plutons. Phaccolithic to domical in structure, and 2–5 km in dimension, the 1200- to 1000-Ma-old granites are products of partial melting of the Chhotanagpur Gneiss

at temperatures higher than 1000 °C and pressure ~5 kbar (Misra and Dey 2002). There are bands and enclaves of amphibolites and hornblendites which were metamorphosed at 643–781 °C and 3.8–5.4 kbar (Ghose et al. 1973).

Along the South Purulia Shear Zone, that marks the northern boundary of the Singhbhum Shear Zone, occur plutons of granites of the Barabazaar area. These plutons were emplaced into the succession of the Palaeoproterozoic metasediments and felsic rocks of the Singhbhum Group (Dwivedi et al. 2011). The geochemistry of the granites shows that they are rift-related magmatic bodies.

5.7.2 Ultrabasic Body

(1) The ultrabasic rocks are intruded by bodies of gabbro-anorthosite of anorogenic setting. One of the largest anorthosite bodies of the Indian subcontinent is the *Bengal Anorthosite* (Bhattacharya and Mukherjee 1987). This oval-shaped body 35.5 km long and 8 km wide at the centre was first described in detail by S.C. Chatterjee in 1936. It is massive in the central part and banded along the periphery, exhibiting fluxion structure in some limited parts (Ray 1977). The Bengal Anorthosite is a syntectonic body related to the second phase of deformation of the Chhotanagpur Gneiss. It was emplaced along the core of the doubly plunging E–W trending antiform made up of metasediments. The Bengal Anorthosite has yielded U–Pb monazite age of 1550 ± 12 Ma., while the age of metamorphism is 150 to 50 million years more, the metamorphism occurring at temperatures 7750 to 8250 and pressures ranging from 7 to 10.5 kbar (Chatterjee et al. 2008). The anorthosite points to temperature 8500–9000 °C and pressure 8.5–11 kbar. Another dating shows that the Chhotanagpur Gneiss Complex witnessed there magmatic-thermal events—at 2500–2400 Ma, 1200–1000 Ma and 900–800 Ma, the last event being quite widespread (Singh et al. 2007). The first phase of deformation was attended by metamorphism of the ultrabasic rocks, and the second episode of deformation was accompanied by synkinematic emplacement of hydrous gabbroic anorthosite and attendant metamorphism represented by leptynite, garnet–sillimanite gneiss and calc-silicate rock occurring in the country rocks. The retrograde metamorphism that followed resulted in the formation of amphibolite facies and greenschist facies rocks (Ray 1977).

5.7.3 Meghalaya Gneiss Complex

The cratonic Meghalaya massif is a complex of gneisses and granites of different ages. It is characterized by Bouguer gravity anomaly of +40 mGal in contrast to −250 mGal over the Brahmaputra Valley (Verma 1985). The *Dauki Fault* defines

the southern boundary of the Meghalaya massif against the sunken plain of the Bengal Basin. It is of the nature of a normal fault dipping south in the 170-km tract between Dauki and Lieke. The Dauki Fault has also been interpreted as dextral strike-slip fault that abruptly ends against the Haflong Thrust (Evans 1964; Srinivasan 2005). The Haflong Thrust is the south-western extension of the Naga Thrust along the eastern border of the Naga Hills (Ranga Rao and Somanulu 1987). In the Shillong Plateau and the adjoining parts of the Kamrup and Goalpara districts in Assam, the *Sonapahar Group* is a complex of high-grade metamorphics including pelitic gneisses and schists, calc-silicate rocks and banded ferruginous quartzites (Narayana Rao and Chowdhury 1976). The granulite facies metapelites in the Shillong massif indicate peak metamorphism occurring at 7–8 kbar pressure and 850 °C temperature in the time 1596 ± 15 Ma, while the metamorphism of the Garo-Goalpara belt to the north occurred in the interval 1032–1273 Ma (Chatterjee et al. 2007).

Long discontinuous bands and lenses of quartz–sillimanite–corundum schists and cordierite gneisses contain *rich deposits of sillimanite with corundum* at Sonapahar, WNW of Shillong. The mineral deposit is a product of metamorphism of low-iron, high-alumina bauxitic palaeosol (Golani 1989).

The gneissic basement, overlain by a metasedimentary succession, is penetrated by a number of plutonic bodies in the Kyrdem, Milliem, Nongpoh and South Khasi areas. Porphyritic in texture and its composition varies from quartz–monzonite to granite. The *Milliem Granite* is 607 ± 13 Ma old. And the 757 ± 60 Ma-old *South Khasi Granite* is characterized by strontium ratio of 0.7045 to 0.7148792, the $\delta^{18}O$ values of +5.78 to +8.70 ‰ fractionated REE pattern, enrichment in LREE and conspicuous Eu anomaly, indicating derivation of the magma from the lower crust (Ghosh et al. 1991, 2005; Santosh Kumar et al. 2005). Intruding the 1714 to 1150 Ma-old basement gneisses, there are a number of granitic bodies, the Rb–Sr whole-rock ages of which ranges from 881 to 479 Ma (Ghosh et al. 2005).

5.8 Bhandara Triangle

5.8.1 Tectonic Setting

Resting on the Archaean basement made up of Amgaon Gneiss, the Palaeoproterozoic *Sausar*, *Sakoli* and *Dongargarh* lithotectonic belts form a triangle of sorts in the Bastar Craton embracing the Nagpur, Bhandara and Durg districts in central India (Figs. 5.21 and 5.22). The Sausar synclinorium extends east–west in the northern part of the craton. The names Sakoli and Sausar were given by V. Ball in 1877. The Sakoli is a NE–SW trending synclinorium in north-eastern Maharashtra. And the 150-km-long, 90-km-wide NNE- to SSW-oriented Dongargarh Mobile Belt flanks the Sakoli in central Chhattisgarh. The early structures of the Dongargarh belt are oriented ENE–WSW. The third phase of the

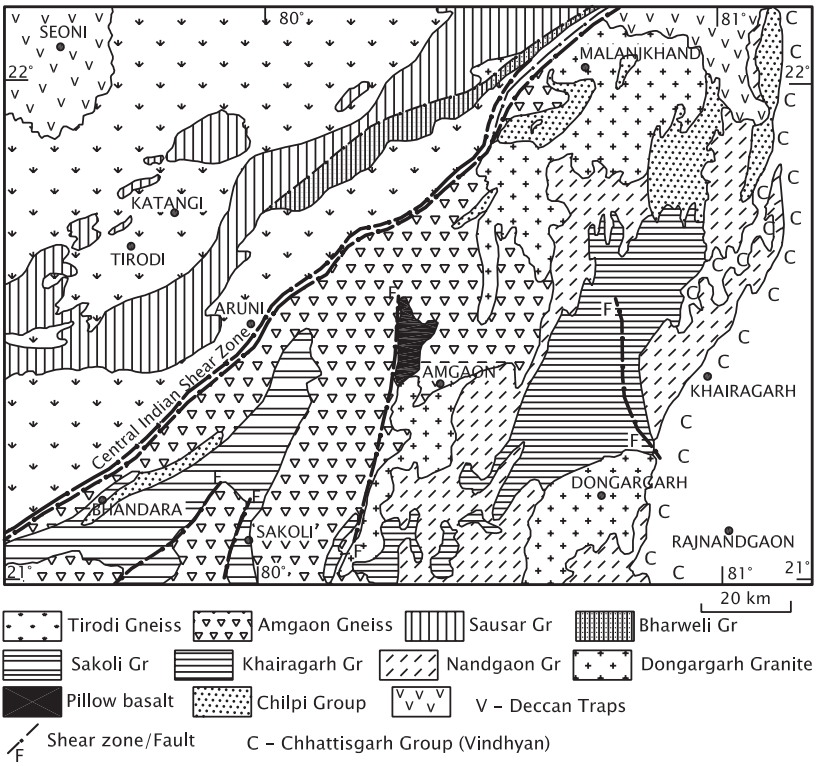

Fig. 5.21 Tectonic setting of the Palaeoproterozoic basins in Central India in the perspective of the Son–Narmada Lineament and the Central Indian Shear Zone (after Yedekar et al. 2003)

Sakoli tectonic upheaval was responsible for the ENE–WSW structural trend of the Sausar Basin (Bandyopadhyay et al. 1995).

It may be recalled that the ENE–WSW Sausar trend is also the structural trend of the Singhbhum Mobile Belt in the eastern part of the Indian Shield, the Satpura domain in central India, the first generation structures of the Aravali Mobile Belt in western India and the strike of the early structures of the Dongargarh basin, the Sausar and the Dongarhgarh thus belongs to the Satpura orogenic cycle.

5.9 Sakoli Basin

5.9.1 Structural Architecture

The northern tip of the Sakoli basin (Fig. 5.21; Table 5.6) forms a large NE-plunging isoclinal synclinorium formed by two phases of deformation (Sarkar 1958). The early phase of deformation generated subvertical isoclinal folds

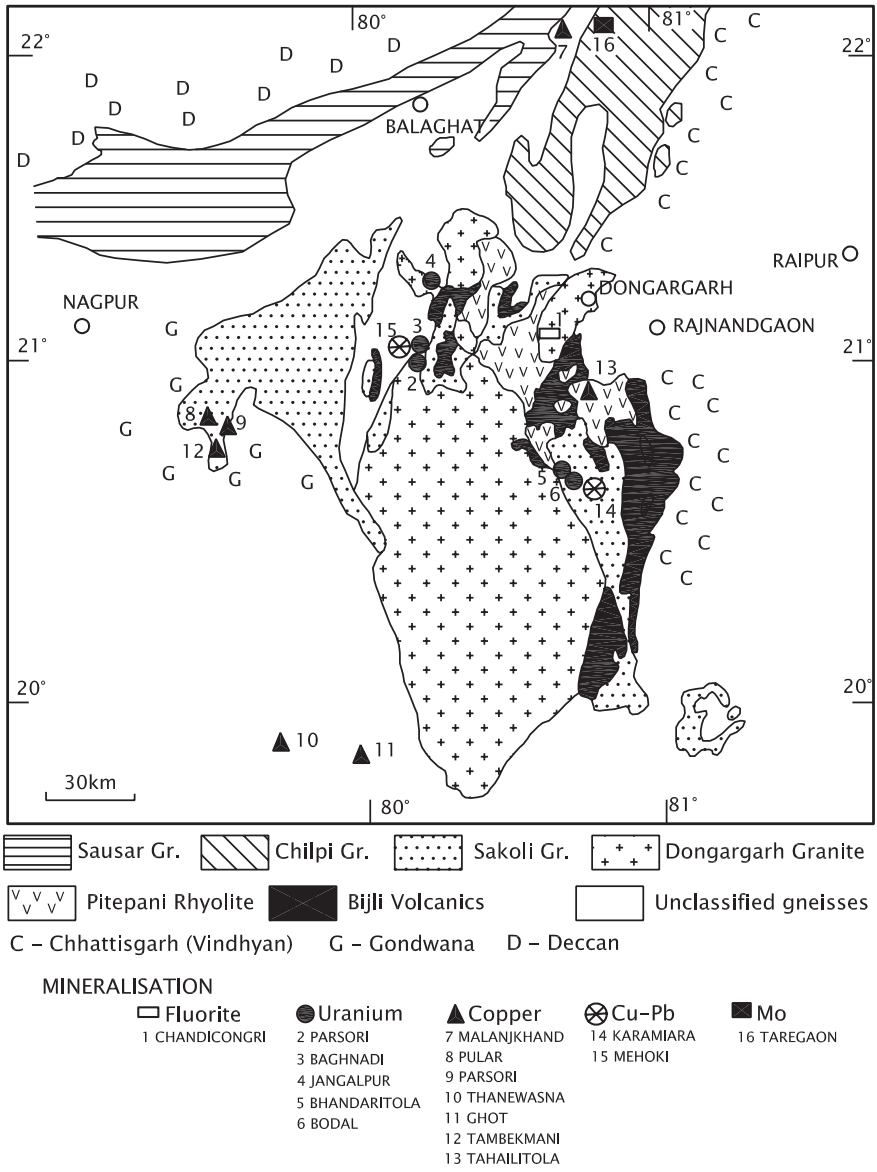

Fig. 5.22 Sketch map of the Bhandara Triangle embracing the Dongargarh–Sausar–Sakoli domains in the Bastar Craton showing occurrence of important mineral deposits of consequence (after Mahadevan 1992b)

trending in the NNE/N–SSW/S directions. Later phase of deformation is represented by ENE- to WSW-oriented upright folds and crumples. Metamorphism is associated with the first phase of deformation represented by overturned reclined folds with NNE–SSW striking subvertical axial planes and steep WNW plunge.

Table 5.6 Lithostratigraphy of the Sakoli domain (Bandyopadhyay et al. 1995)

Gondwana Supergroup		
Fault		
Sakoli Group	Pawni Formation	Slate/phyllite, arkose, quartzite and diamictite
	Bhiwapur Formation	Garnet–staurolite–mica schists with interbands of bimodal volcanics (rhyolite, tuffs, agglomerates and minor basic volcanics)
	Dhabetekri Formation	Metabasalts with minor schists, chert bands and ultramafic rocks (metamorphosed)
	Gaikhuri Formation	Conglomerate, gritty quartzite, arkose, minor carbonaceous phyllite and ferruginous banded quartzite
Tectonized unconformity		
Amgaon Gneiss		

The Rb–Sr whole-rock isochron dates indicate that felsic lavas and tuffs were metamorphosed at 1295 ± 40 Ma (Sarkar 1994; Bandyopadhyay et al. 1995).

5.9.2 Lithostratigraphy

The 6000-m Sakoli succession consists predominantly of metapelitic rocks with banded iron quartzite, arkose and conglomerate resting on the basement of the Archaean Amgaon Gneiss (Table 5.6). In the south-western part of the basin, it is divisible into two parts. The lower Sakoli is essentially a volcanosedimentary sequence dominated by pelites with rhyolite, felsic tuff and basalts. The succession includes (i) gritty quartzite, phyllites and conglomerate with banded ferruginous quartzite; (ii) garnet-amphibolite with chert lenses and basic tuffs metamorphosed to phyllites; (iii) mica schists characterized by garnet, andalusite and chloritoid; and (iv) metamorphosed felsic tuffs and agglomerates, penetrated by dykes of acidic and basic rocks (Chawade and Naik 2003). Obviously, the rocks were mildly metamorphosed and intruded by dykes of gabbro and dolerite, and affected by syntectonic granites along the basin margin.

5.9.3 Mineralization

In the southern part of the Sakoli Basin (Fig. 5.22; Table 5.6) occurs strata-bound sedex-type deposits of copper and zinc. The mineralization took place close to the stratigraphic contact of felsic volcanics and chlorite schists. Chalcopyrite occurs as stringers and disseminations. Stratiform deposits of zinc sulphide—mainly sphalerite—stratigraphically overlie the horizon of chalcopyrite deposits at Kolari. Conformable intercalations of manganese garnets with quartz, biotite and cummingtonite occur within or at the interface of mafic volcanics and underlying the

sequence of chert, carbonaceous phyllite and tuffs (Bandyopadhyay et al. 1995; Chawade and Naik 2003).

5.10 Dongargarh Domain

5.10.1 Lithology

Sarkar (1958) established the supergroup Dongargarh in the district of Durg (Chhattisgarh), resting unconformably on the Archaean Gneissic Complex, the Amgaon Gneiss. The Dongargarh succession comprises volcanosedimentary rocks divisible into two groups—the *Nandgaon* of bimodal volcanic rocks and the *Khairagarh* of arkosic and arenite quartzites interbedded with basalts and agglomerate (Table 5.7). The two groups are separated by an unconformity.

The Dongargarh succession is deformed into NNE–SSW striking folds of an early phase of tectonic upheaval. It is superimposed by E–W- to ENEWSW-oriented later-generation cross-folds (Sarkar 1958; Sensarma and Mukhopadhyay 2003). The Dongargarh domain (Table 5.7) continues southwards into the Bastar district as a N–S trending Kotri Volcanic belt. The two make a 250-km-long, 50-km-wide *Kotri–Dongargarh Mobile Belt* (Bandopadhyay et al. 1995).

5.10.2 Bimodal Volcanism

Early volcanism in the Dongargarh domain is dominated by rhyolites and tuffs (Bijli Formation), followed later by lavas of basalt and andesite (Pitepani Formation).

The *Bijli Rhyolite* is enriched in LREE and Zr, Th and Cr, but depleted in LILE, Sc, Y, Ni, and low in Sr and high in Ce content, implying derivation from

Table 5.7 Stratigraphic succession in the Dongargarh domain (Based on Sarkar 1980, 1994)

Upper Vindhyan		
Unconformity		
Khairagarh Group	Mangikhuta Formation	Basic volcanics
	Karutola Formation	Arkosic and arenitic quartzites
	Sitagota Formation	Basic volcanics and interbedded sediments
	Bortolao Formation	Arkose and arenite with conglomerate
Unconformity		
Nandgaon Group	Pitepani Formation	Basic volcanics
	Bijli Formation	Rhyolite, rhyodacite and tuffs
Unconformity		
Amgaon Gneiss		

partially molten source within the crust (Neogi et al. 1996). The Bijli volcanic assemblage is characterized by high Ba, low Fe, Cr, Ni, moderate Rb, Th and U, high REE and negative Eu anomaly suggestive of anatectic origin (Divakara Rao et al. 2000). The high-grade silicic ignimbrite comprises a variety of welded rheomorphic tuffs produced by plinian volcanism to fissure eruption in a continental setting (Mukhopadhyay et al. 2001). The Bijli Rhyolite of the Nandgaon Group gives Rb–Sr whole-rock isochron age of 2180 ± 25 Ma (Sarkar 1958, 1994) to 2503 ± 35 Ma (Krishnamurthy 1990).

The *Pitepani Volcanics* comprise low-Ti calc-alkaline high-magnesian andesite and high-Ti tholeiitic lavas characterized by high concentration of Ba, K, Rb, Sr, Th and LREE enrichment (Asthana and Sharma 2004).

Having a strong tholeiitic affinity, the Khairagarh Volcanics represent relatively unfractionated, more primitive magma source. These volcanics are characterized by lesser abundances of Ba, Rb, K, Th and Zr and enrichment in Sr, V, Ni, Cr and Sr (Neogi et al. 1996). From the chemical compositions and tectonic setting, it is obvious that the Nandgaon and Khairagarh lavas were erupted in a continental setting along rifts. Faults provided easy passage to the lavas, and there was no significant interaction with the crustal material—and therefore no contamination of the lavas.

The volcanics of the Nandgaon Group are intruded by a granitic batholith characterized by enclaves of rhyolites and basalts. This anorogenic pluton has been dated 2270 ± 90 Ma (Sarkar 1994) to 2465 ± 22 Ma by Rb–Sr method (Krishnamurthy 1990). The *Dongargarh Granite* marks the timing of a tectonic event represented by the unconformity between the Nandgaon and the Khairagarh.

5.11 Sausar Basin

5.11.1 Structural Setup

The 215-km-long and 35-km-wide Sausar Belt (Fig. 5.22; Table 5.8) is an E- to W-oriented arcuate synclinorium first described by L.L. Fermor in 1909. It comprises a succession of thrust sheets, including what W.D. West in 1936 described as the *Deolapar Nappe*. Three phases of deformation are recognizable in the Sausar. The ENE–WSW trending earlier folds, characterized by axial planar schistosity, was coaxially folded into close to tight folds. The third-generation deformation is represented by interference pattern discernible locally (Agrawal 1975).

The Ramkona–Katangi belt to the north of the Sausar Basin is made up of migmatites with granites and rare charnockite–mangerite suite that formed under 10–15 kbar pressure and at 1000 °C temperature and is characterized by mylonitic fabric. It represents the zone of juxtaposition between the Bundelkhand and Bastar cratonic blocks (Roy and Prasad 2003).

The central part of the Sausar Basin is characterized by SE-leaning recumbent folds, and the northern flank is marked by southward thrust isoclines and

Table 5.8 Lithostratigraphic succession of the Sausar Group (Bandyopadhyay et al. 1995)

Bichua Formation	Dolomitic marble, calc gneiss and schist
Junewani Formation	Mica schist, quartzite, biotite gneiss
Charbaoli Formation	Quartizte, felspathic schist–gneiss, autoclastic quartz conglomerate
Mansar Formation	Mica schist–gneiss, graphitic schist, phyllite and quartzite with manganese deposits including gondite
Lohangi Formation	Pink-white calcitic and dolomitic marble calc-silicate gneiss, quartzite and manganese deposits, quartz–biotite schist and gneiss
Sitasaongi Formation	Quartz–mica schist, felspathic schist and gneiss, quartzite and conglomerate
- - - - - - - - - - - - *Unconformity*- - - - - - - - - - - -	
Tirodi Gneiss/Older Metamorphic Group	

recumbent folds. In the eastern part of the domain, the folds plunge eastwards, while in the western part the plunge is south-eastwards. These folds are superimposed by cross-folds that plunge W or WSW. The cores of these cross-folds are occupied by granitic bodies (Straczette et al. 1956). There are NW–SE to NNE–SSW trending sets of cross faults related to the cross-folds (Basu and Sarkar 1966; Basu 1981). The NNW–SSE trending upright folds of third generation, superimposed on earlier phase folds, form the western NNW- to SSE-oriented arm of E–W arcuate Sausar Basin (Mohanty 2002). The E- to W-oriented part of the Sausar Basin is controlled by the folds of the first generation.

5.11.2 Lithostratigraphy

Faulted against the Tirodi Gneiss, the Sausar Group consists of regionally metamorphosed sandstones, shales and carbonate rocks (Fig. 5.21). Dated 1525 ± 70 Ma by the Rb–Sr method, the *Tirodi Gneiss* appears to be the product of granitization of basal Sakoli rocks that had undergone regional metamorphism (Sarkar 1994). Occurrence of clasts of gneiss in the basal conglomerate (Table 5.8) indicates that some other Gneissic Complex formed the basement of the Sausar succession. The metacarbonates are characterized by manganese oxides. Showing facies variation, the Sausar sediments were deposited on a stable shelf in which the environment varied from near-shore intertidal to offshore platform (Basu 1981). The Sausar rocks attained upper amphibolite facies metamorphism under temperature 600–680 °C and pressure of 6 kb (Dasgupta et al. 1984; Bhattacharjee 1988; Phadke 1990). Sr and Nd isotope studies demonstrate that the Sausar rocks underwent two main episodes of metamorphism and the peak metamorphism that gave rise to granulite facies rocks along northern and southern belts and the amphibolite facies metamorphism around 800–900 Ma at, respectively, 1100 Ma and 2670 Ma (Roy et al. 2006).

A suite of felsic and aluminous granulites, intruded by gabbro, norite and pyroxenite along the southern periphery, records ultrahigh-temperature metamorphism taking place during the interval 2040–2090 Ma at ~950 °C and ~9 kbar pressure, as testified by sapphirine and spinels. This event was followed by events that brought about crustal attenuation at ~675 °C and 6.4 kbar pressure. Subsequently, there was near isothermal loading at ~8 kbar pressure during temporal interval 1524–1450 Ma (Bhowmik et al. 2005).

5.11.3 Mineralization

The Sausar hosts large stratiform deposits of *manganese oxides*, the reserve amounting to more than 100 million tonnes. The Mn oxide ore bodies, with or without Mn-silicate-oxide (gondite), occur in three stratigraphic horizons (Roy 1966). It is the Mansar Formation that contains the major deposits of Mn ores. These deposits were formed as a result of metamorphism under temperature as high as 700 °C and pressure 6 kbar (Roy et al. 1986).

The *uranium* mineralization is manifested in dominant epigenetic veins of uraninite. These veins have spatial and temporal relationship with the strata-bound syngenetic ores (Mahadevan 1992b).

5.12 Malanjkhand Granite

5.12.1 Geological Setting

Close to the Central Indian Shear Zone, the *Malanjkhand Granite* is a calc-alkaline plutonic body intruding the Amgaon Gneiss (Fig. 5.21). It comprises tonalite, granodiorite, granite and adamellite. The Malanjkhand Granite has Rb–Sr age of 2362 ± 58 Ma (Ghosh et al. 1996). Enclaves of microgranitic rocks throughout the extent of the pluton seem to represent coeval mafic and felsic magmatism (Santosh Kumar et al. 2004) that affected the Malanjkhand pluton. The granite complex is unconformably overlain by a metasedimentary succession comprising conglomerate, grading upwards to arkosic sandstone and red shales of the *Chilpi Formation*.

5.12.2 Copper Deposit

Characterized by copper mineralization, with Mo, Au, Ag and Co in traces, the Malanjkhand Granite hosts a world-class primary copper deposit, 2.6 km in length, 142 m in width and 900 m deep. It has been described as an Andean-type porphyry copper deposit (Stein et al. 2003) comprising low-grade ores coupled

with large tonnage (5.9 million tonnes up to the depth of −300 m level), mineralized quartz veins in a zone of silicified granite, veinlets and disseminated grains of ore minerals with quartz in granitic rocks, and showing pyrite $\delta^{34}S$ values between −0.38 and +2.9, and zonation of wall-rock alteration (Sikka 1989; Sarkar et al. 1996; Sikka and Nehru 2002; Bhargava and Pal 2000).

The mineralization occurred within the calc-alkaline tonalite–granodiorite pluton; the bulk mineralization occurring in sheeted quartz–sulphide veins and K-silicate alteration assemblages. There are sulphide-bearing stringers and pegmatites that contain suphide disseminations. The main bulk of quartz and sulphides precipitated from a fluid of moderate salinity within a low-temperature range (150–275 °C), and the fluids were derived from the granitic magma which finds its ways through fractures (Panigrahi and Mookherjee 1997).

The age of mineralization seems to be the temporal interval between 1737 ± 49 Ma and 1818 ± 73 Ma (Sikka and Nehru 2002).

References

Agrawal, V. N. (1975). Fold interference patterns in the Sausar Group, northern Nagpur district, Maharashtra. *Journal of the Geological Society of India, 16*, 176–187.

Ahmad, T., & Rajamani, V. (1991). Geochemistry and petrogenesis of the basal Aravali volcanics near Nathadwara, Rajasthan. *Precambrian Research, 49*, 185–204.

Alvi, S. H., & Raza, M. (1991). Nature and magma type of Jagannathpur Volcanics, Singhbhum, eastern India. *Journal of the Geological Society of India, 38*, 524–531.

Ameta, S. S., & Sharma, B. B. (2008). Geology, metallogeny and exploration of concealed lead-zinc deposit in Sindesar-Khurd-Lathiyakheri area, Rajsamand district, Rajasthan. *Journal of the Geological Society of India, 72*, 381–399.

Arora, B. R., Waghmare, S. Y., & Mahashabde, M. V. (1995). Geomagnetic deep sounding along the Hirapur–Mandla–Bhandara profile, central India. *Memoirs of the Geological Society of India, 31*, 519–536.

Bandyopadhyay, B. K., Roy, A., & Huin, A. K. (1995). Structure and tectonics of a part of the Central Indian Shield. *Memoirs of the Geological Society of India, 31*, 433–467.

Banerjee, D. M. (1971). Precambrian stromatolitic phosphorite of Udaipur, Rajasthan, India. *Geological Society of America Bulletin, 82*, 2319–2330.

Banerjee, D. M., Khan, M. W. Y., Srivastava, N., & Saigal, G. C. (1982). Precambrian phosphorite in the Bijawar rocks of Hirapur-Bassia areas, Sagar district, Madhya Pradesh, India. *Mineralium Deposita, 17*, 349–362.

Banerjee, D. M., & Klemm, U. (1985). Organo-geochemical studies of Proterozoic stromatolitic phosphorite and intercolumnar dolomite from the Aravali Group, India. *Journal of the Geological Society of India, 26*, 245–254.

Banerji, A. K. (1962). Cross folding, migmatization and ore localization along part of the Singhbhum Shear Zone, south of Tatanagar, Bihar, India. *Economic Geology, 57*, 50–71.

Banerji, A. K., Sankaran, A. V., & Bhattacharyya, T. K. (1972). Ore genetic significance of geochemical trends during progressive migmatization within part of the Singhbhum Shear Zone, Bihar. *Journal of the Geological Society of India, 13*, 39–50.

Barman, G., Verma, K. K., & Puri, S. N. (1978). Biostratigraphic zonation of stomatolite-bearing horizons in the Aravalis of Udaipur District, Rajasthan. *Journal of the Geological Society of India, 19*, 264–267.

Basu, N. K. (1981). A reassessment of the structure and stratigraphy of the Sausar series as revealed in the Ramtek Tahsil of Nagpur District, Maharashtra. *Special Publication of the Geological Survey of India, 3*, 47–54.

Basu, N. K., & Sarkar, S. N. (1966). Stratigraphy and structure of the Sausar Series of Mahuli–Ramtek–Janawani area of Nagpur district, Maharashtra. *Quarterly Journal of the Geological, Mining and Metallurgical Society of India, 38*, 77–105.

Bhargava, M., & Pal, A. B. (2000). Cu–Mo–Au metallogeny associated with Proterozoic tectonomagmatism in Malanjkhand porphyry copper deposit, Madhya Pradesh. *Journal of the Geological Society of India, 56*, 395–413.

Bhattacaryya, P. K., & Dasgupta, S. (1981). Evolution of massive granites in the Khetri Copper Belt, Rajasthan: Implications in regional correlation. *Indian Journal of Earth Sciences, 8*, 44–53.

Bhattacharjee, P. K. (1988). Petrology of jacobsite-bearing assemblages from Sausar Group, India. *Neues Jahrbuch fur Mineralogie, Abhandlungen, 159*, 101–111.

Bhattacharjee, J., Golani, P. R., & Reddy, A. B. (1988). Rift-related biomodal volcanism and metallogeny in the Delhi fold belt, Rajasthan and Gujarat. *Indian Journal of Geology, 60*, 191–199.

Bhattacharya, H. N. (2004a). Analysis of the sedimentary succession hosting the Paleoproterozoic Zawar zink-lead sulphide ore deposit, Rajasthan, India. In M. Deb & W. D. Goodfellow (Eds.), *Sediment-hosted lead-zinc sulphide deposits: attributes and models of some major deposits in Australia, Canada and India* (pp. 350–361). New Delhi: Narosa Publishing Company.

Bhattacharya, S. (2004b). High-temperature crustal-scale shear zone at western margin of the Eastern Ghats granulite belt, India: Implications for rapid exhumation. *Journal of Asian Earth Sciences, 24*, 281–290.

Bhattacharyya, D. S. (1992). Early Proterozoic metallogeny, tectonics and geochronology of the Singhbhum Cu-U belt, eastern India. *Precambrian Research, 58*, 71–83.

Bhattacharyya, D. S., & Dasgupta, P. (1979). Chemical clues to the origin of basic fragments embedded in a basaltic suite of the Precambrian metamorphic terrane of Singhbhum. *Contributions to Mineralogy and Petrology, 71*, 177–183.

Bhattacharyya, P. K., & Mukherjee, S. (1987). Granulites in and around the Bengal Anorthosite, eastern India; gneises of coronal garnet, and evolution of the granulite-anarthosite complex. *Geological Magazine, 124*, 21–32.

Bhattacharyya, D. S., & Sanyal, P. (1988). The Singhbhum orogen—its structure and stratigraphy. *Memoirs of the Geological Society of India, 8*, 85–111.

Bhola, A. M., Sharma, B. K., & Ghosh, S. K. (2004). Folds in multilayered rocks of Proterozoic age, Rajasthan. *Proceedings of the Indian Academy of Sciences (Earth & Planetary Sciences)*, *113*, 299–311.

Bhowmik, S. K., Basu-Sarbadhikar, A., Spiering, B., & Raith, M. M. (2005). Mesoproterozoic reworking of Palaeoproterozoic ultrahigh temperature granulites in the central Indian Tectonic Zone and its implications. *Journal of Petrology, 46*, 1085–1119.

Bhushan, S. K., & Chittora, V. K. (2005). Proterozoic granitoids of Rajasthan. *Journal of the Geological Society of India, 66*, 741–763.

Bose, M. K. (1994). Sedimentation pattern and tectonic evolution of Proterozoic Singhbhum basin in the Eastern Indian shelf. *Tectonophysics, 231*, 325–346.

Bose, P. K., Banerjee, S., & Sarkar, S. (1997). Slope-controlled seismic deformation and tectonic framework of deposition: Koldaha Shale, India. *Tectonophysics, 269*, 151–169.

Bose, M. K., & Chakraborti, M. K. (1994). Geochemical changes in basalts across the Archaean-Proterozoic boundary—an evaluation of Dalma basalts from Eastern Indian Shield. *Journal of the Geological Society of India, 43*, 281–293.

Chatterjee, S. C. (1955). Peridotites of Manpur, Singhbhum, Bihar and the origin of associated asbestos deposits. *Geological Society of America Bulletin, 66*, 91–104.

Chatterjee, N., Crowley, J. L., & Ghose, N. C. (2008). Geochronology of the 1.55 Ga Bengal Anorthosite and Grenvllian metamorphism in the Chhotanagpur Gneissic Complex, eastern India. *Precambrian Research, 161*, 303–318.

Chatterjee, N., Mazumdar, A. C., Bhattacharya, A., & Saikia, R. R. (2007). Mesoproterozoic granulites of the Shillong-Meghalaya Plateau: Evidence of westward continuation of the Prydz Bay PanAfrican suture into northeastern India. *Precambiran Research, 152*, 1–26.

Chaudhuri, R., & Roy, A. B. (1986). Proterozoic–Cambrian phosphorite deposit: Jhamarkotra, Rajasthan. In P. J. Cook & J. H. Shergold (Eds.), *Phosphate deposits of the World* (Vol. I). London: Cambridge University Press.

Chaudhuri, A. K., Sahoo, M. R., Panda, N. K., & Mahapatra, S. N. (1998). The eastern closure of the Gangpur Group. In B. S. Paliwal (Ed.), *The Indian Precambrian* (pp. 437–444). Jodhpur: Scientific Publishers.

Chauhan, D. S. (1977). The Dariba main load of Rajpura-Dariba zinc-lead-copper deposit, Udaipur district, Rajasthan. *Journal of the Geological Society of India, 18*, 131–140.

Chauhan, D. S. (1979). Phosphate-bearing stromatolites of the Precambrian Aravali phosphorite deposits of the Udaipur region, their environmental significance and genesis of phosphorite. *Precambrian Research, 8*, 95–126.

Chauhan, D. S. (1989). Microbial activities and genesis of Aravali phosphorite, Udaipur, Rajasthan. *Himalayan Geology, 13*, 39–51.

Chawade, M. P., & Naik, K. K. (2003). A reappraisal of tectonostratigraphy of Sakoli fold belt and its implications on mineral occurrences, Central India. *Gondwana Magazine, 7*, 153–168.

Choubey, V. D. (1971a). Superimposed folding in the transitional rocks (Precambrian) and its influence on the structure of southeastern margin of the Vindhyan Basin, Jabalpur district, M.P. *Journal of the Geological Society of India, 12*, 142–151.

Choubey, V. D. (1971b). Narmada-Son Lineament, India. *Nature, 232*, 38–40.

Choudhary, A. K., Gopalan, K., & Shastry, C. A. (1984). Present status of the geochronology of the Precambrian rocks of Rajasthan. *Tectonophysics, 105*, 131–140.

Crawford, A. R. (1969). Reconnaissance Rb-Sr dating of the Precambrian rocks of northern Peninsular India. *Journal of the Geological Society of India, 10*, 117–166.

Das, B. (1967). On the lithological sequence and overall structure of the rocks around Rajgir, Bihar. *Bulletin—Geological Society of India, 4*, 46–49.

Das, S. (1997). Depositional framework of the sandy mid-fan complexes of the Proterozoic Chaibasa Formation, E. Singhbhum, Bihar. *Journal of the Geological Society of India, 50*, 541–557.

Dasgupta, S. P. (1964). Structural evolution of the Khettri Copper Belt, Rajasthan. In *Proceedings of the 22nd International Geological Congress* (Vol. 4, pp. 357–363).

Dasgupta, S., Banerjee, H., & Majumdar, N. (1984). Contrasting trends of mineral reactions during progressive metamorphism in interbanded pelite-manganese oxide sequence: Examples from Proterozoic Sausar Group, India. *Neues Jahrbuch fur Mineralogie, Abhandlungen, 150*, 95–102.

Deb, M. (1980). Genesis and metamorphism of two stratiform massive sulphide deposits at Ambaji-Deri India in the Precambrian of western India. *Economic Geology, 75*, 572–591.

Deb, M., & Sarkar, S. C. (1990). Proterozoic tectonic evolution and metallogenesis in the Aravali-Delhi orogenic complex, northwestern India. *Precambrian Research, 46*, 115–137.

Deb, M., Thorpe, R. I., Cumming, G. L., & Wagner, P. A. (1989). Age, source and stratigraphic implications of Pb-isotope date for conformable, sediment- hosted base metal deposits in the Proterozoic Aravali-Delhi orogenic belt, northwestern India. *Precambrian Research, 43*, 1–22.

Deb, M., Thorpe, R. I., Krstic, D., Corfu, F., & Davis, D. W. (2001). Zircon U-Pb and galena Pb isotope evidence for an approximate I.OGa terrane constituting the western margin of the Aravali-Delhi orogenic belt, northwestern India. *Precambrian Research, 108*, 195–213.

Dhurandhar, A. P., Latha, A., & Krishna, V. (2005). Geochronology and petrochemistry of the Dubha Granite, Sonbhadra district, Uttar Pradesh. *Journal of the Geological Society of India, 65*, 459–467.

Divakara Rao, V., Narayana, B. L., Rama Rao, P., Murthy, N. N., Subba Rao, M. V., Mallikarjuna Rao, J., & Reddy, G. L. N. (2000). Precambrian acid volcanism in central India—geochemistry and origin. *Gondwana Research, 3*, 215–226.

Dwivedi, A. K., Pandey, U. K., Murugan, C., Bhatt, A. K., Ramesh Babu, P. V., & Joshi, M. (2011). Geochemistry and geochronology of A-type Barabazar Granite: Implications on geodynamics of South Purulia Shear Zone, Singhbhum Craton, eastern India. *Journal of the Geological Society of India, 77*, 527–538.

Evans, P. (1964). The tectonic framework of Assam. *Journal of the Geological Society of India, 5*, 80–96.

Gaal, G. (1964). Precambrian flysch and mollase—tectonics and sedimentation around Rakha mines and Jaikan in Singhbhum district, Bihar, India. *Report, International Geological Congress*, Vol. 5, pp. 331–356.

Gandhi, S. M., Paliwal, H. V., & Bhatnagar, S. N. (1984). Geology and ore reserve estimates of Rampura-Agucha zinc-lead deposit, Bhilwara district, Rajasthan. *Journal of the Geological Society of India, 25*, 689–705.

Gangopadhyay, P. K. (1972). Structure and tectonics of Alwar region in NE Rajasthan with special reference to Precambrian stratigraphy. In *Proceedings of the 24th International Geological Congress*, Section I, pp. 118–125.

Gangopadhyay, P. K., & Chatterjee, N. (1971). Structural pattern of rocks around Dariba, Alwar district, Rajasthan with special reference to copper occurrence. *Journal of the Geological Society of India, 12*, 43–50.

Gangopadhyay, P. K., & Lahiri, A. (1983). Barr Conglomerate: Its recognition and significance in the stratigraphy of the Delhi Supergroup in central Rajasthan. *Journal of the Geological Society of India, 24*, 562–570.

Gangopadhyay, P. K., & Lahiri, A. (1984). Earth's crust and evolution of the Delhi Supergroup in Central Rajasthan. *Indian Journal of Earth Sciences*, *CEISM*, 92–113.

Gangopadhyay, P. K., & Sen, R. (1968). Evidence of refolding in Delhi System of rocks near Bairawas, Alwar district, Rajasthan. *Bulletin—Geological Society of India, 5*, 22–25.

Ghose, N. C., Shmakin, B. M., & Smirnov, V. N. (1973). Some geochronological observations on the Precambrians of Chhotanagpur, Bihar. *Geological Magazine, 110*, 481–484.

Ghosh, S., Chakraborty, S., Bhalla, J. K., Paul, D. K., Sarkar, A., Bishui, P. K., & Gupta, S. N. (1991). Geochronology and geochemistry of granite plutons from East Khasi Hills, Meghalaya. *Journal of the Geological Society of India, 37*, 331–342.

Ghosh, S. K., & Chatterjee, B. K. (1990). Palaeoenvironmental reconstruction of the early Proterozoic Kolhan siliciclastic rocks, Keonjhar district, Orissa, India. *Journal of the Geological Society of India*, *35*, 273–286.

Ghosh, S., Fallick, A. E., Paul, D. K., & Potts, P. J. (2005). Geochemistry and origin of neoproterozoic granitoids of Meghalaya, northeast India: Implications for linkage with amalgamation of Gondwana supercontinent. *Gondwana Research, 8*, 421–432.

Ghosh, D. K., Sarkar, S. N., Saha, A. K., & Ray, S. L. (1996). New insights on the early Archaean crustal evolution in eastern India: Re-evaluation of lead-lead, samarium-neodymium and rubidium-strontium geochronology. *Indian Minerals, 50*, 175–188.

Ghosh, S. K., & Sengupta, S. (1990). The Singhbhum Shear Zone: Structural transition and kinematic model. *Proceedings of the Indian Academy of Sciences (Earth & Planetary Sciences), 98*, 229–247.

Golani, P. R. (1989). Sillimanite-corundum deposits of Sonapahar, Meghalaya, India: A metamorphosed Precambrian palaeosol. *Prembrian Research, 43*, 175–189.

Golani, P. R., Gathania, R. C., Grover, A. K., & Bhattacharjee, J. (1992). Felsic volcanics in South Khetri Copper Belt, Rajasthan and their metallogenic significance. *Journal of the Geological Society of India, 40*, 79–87.

Golani, P. R., Pandit, M. K., Sial, A. N., Fallick, A. E., Ferreira, V. P., & Roy, A. B. (2002). B-Na rich Palaeoproterozoic Aravali metasediments of evaporitic association, NW India: A new repository of gold mineralization. *Precambrian Research, 116*, 183–198.

Gopinath, K., Prasad Rao, A. D., Murty, Y. G. K., & Krishnaunni, K. (1977). Precambrian of Baroda and Panchmahal districts, Gujarat: Elucidation of stratigraphy and structure. *Record of the Geological Survey of India, 108*, 60–68.

Gupta, A., Basu, A., & Ghosh, P. K. (1980). The Proterozoic ultramafic and mafic lavas and tuffs of the Dalma greenstone belt, Singhbhum, Eastern India. *Canadian Journal of Earth Sciences, 167*, 210–231.

Gupta, P., Mukhopadhyay, K., Fareeduddin, & Reddy, M. S. (1991). Tectonostratigraphic framework and volcanic geology of the South Delhi Fold Belt in Central Rajasthan. *Journal of the Geological Society of India, 37*, 431–441.

Gupta, S., & Verma, K. K. (1989). Stromatolite biostratigraphy, sedimentary history and age of the Bijawar Group of Central India. *Himalayan Geology, 13*, 53–61.

Hasan, Z., & Sarkar, S. N. (1968). Structural analysis of the Monghyr area, India. *Norsk Geologisk Tidsskrift, 48*, 101–116.

Heron, A. M. (1953). The geology of central Rajputana. *Memoirs of the Geological Survey of India, 79*, 1–389.

Iyengar, S. V. P., & Alwar, M. A. (1965). The Dhanjori eugeosyncline and its bearing on the stratigraphy of Singhbhum Keonjhar and Mayurbhanj district. *D.N. Wadia Commemoration Volume*. Mining, Geological and Metallurgical Institute of India, Kolkata, pp. 138–162.

Iyengar, S. V. P., & Banerji, S. (1964). Magmatic phases associated with the Precambrian tectonics of Mayurbhanj district, Orissa. *Report, International Geological Congress*, Vol. 21, pp. 558–561.

Jambusaria, B. B., & Merh, S. S. (1967). Deformed greywacke conglomerates of Jaban near Sivarajpur, Panchmahal district, Gujarat. *The Indian Mineralogist, 8*, 6–10.

Kaila, K. L., Murthy, P. R. K., Mall, D. M., Dixit, M. M., & Sarkar, D. (1987). A deep sceismic sounding along Hirapur-Mandla profile, Central India. *Geophysical Journal of the Royal Astronomical Society, 89*, 399–404.

Kanungo, D. N., & Mahalik, N. K. (1972). Metamorphism in the eastern part of Gangpur. *Journal of the Geological Society of India, 13*, 122–130.

Kaur, P., Chaudhri, N., Raczek, I., Kroner, A., & Hofmann, A. W. (2009). Record of 1.82 Ga Andeen-type continental arc magmatism in NE Rajasthan, India: Insights from zircon and Sm-Nd ages combined with Nd-Sr isotope geochemistry. *Gondwana Research, 16*, 56–71.

Kaur, G., & Mehta, P. K. (2005). The Gothara plagiogranite: Evidence for oceanic magmatism in a non-ophiolite association North in Khetri Copper Belt, Rajasthan, India. *Journal of Asian Earth Sciences, 25*, 805–819.

Khan, M. Shamim, Smith, T. E., Raza, M., & Huang, J. (2005). Geology, geochemistry and tectonic significance of mafic–ultramafic rocks of Mesoproterozoic Phulad ophiolite suture of South Delhi Fold Belt, NW Indian Shield. *Gondwana Research, 8*, 553–566.

Krishnamurthy, P. (1990). Magmatic rocks of the Dongargarh Supergroup, central India—their petrological evolution and implications on metallogeny. *Special Publication of the Geological Survey of India, 28*, 303–319.

Kumar, S., Pieru, T., Rino, V., & Lyngdoh, B. C. (2005). Microgranular enclaves in neoproterozoic granitoids of South Khasi Hills, Meghalaya Plateau: Field evidence of interacting coeval mafic and felsic magmas. *Journal of the Geological Society of India, 65*, 629–630.

Kumar, S., Rino, V., & Pal, A. B. (2004). Field evidence of magma mixing from microgranular enclosures hosted in Palaeoproterozoic, Malajkhand granitoids, central India. *Gondwana Research, 7*, 539–548.

Lal, R. K., & Singh, J. B. (1978). Prograde polyphase regional metamorphism and metamorphic reactions in pelitic schists at Sini, district Singhbhum. *Neues Jahrbuch fur Mineralogie, Abhandlungen, 131*, 304–333.

Mahadevan, T. M. (1992a). Geological evolution of Chhotanagpur Gneissic Complex in parts of Purulia district, West Bengal. *Indian Journal of Geology, 64*, 1–22.

Mahadevan, T. M. (1992b). Uranium metallogeny in the Proterozoic mobile belts in India in relation to tectonic development. In S. C. Sarkar (Ed.), *Metallogeny related to tectonics of the Proterozoic mobil belts* (pp. 177–208). New Delhi: Oxford & IBH.

Mahadevan, T. M., & Maithani, J. B. P. (1967). Geology and petrology of mica pegmatites in parts of Bihar mica belt. *Memoirs of the Geological Society of India, 93*, 1–114.

Majumdar, S. K. (1988). Crustal evolution of the Chhotanagpur gneissic complex and the mica belt of Bihar. *Memoirs of the Geological Society of India, 8*, 49–83.

Mamtani, M. A., & Greiling, R. O. (2005). Granite emplacement and its relation with regional deformation in the Aravali mountain belt—inferences from magmatic fabric. *Journal of Structural Geology, 27*, 2008–2029.

Mamtani, M. A., Karanth, R. V., Merh, S. S., & Greiling, R. O. (2000). Tectonic evolution of the southern part of Aravali mountain belt and its environment: possible causes and time constraints. *Gondwana Research, 3*, 175–187.

Mazumder, Rajat. (2005). Proterozoic sedimentation and volcanism in the Singhbhum crustal province, India, and their implications. *Sedimentary Geology, 176*, 167–193.

Mishra, D. C., Singh, B., Tiwari, V. M., Gupta, S. B., & Rao, M. B. S. V. (2000). Two cases of continental collision and related tectonics during the Proterozoic period in India—insights from gravity modelling constrained by seismic and magnetotelluric studies. *Precambrian Research, 99*, 149–169.

Misra, S., & Dey, S. (2002). Bihar Mica Belt plutons—an example of post-orogenic granite from Eastern Indian Shield. *Journal of the Geological Society of India, 59*, 363–377.

Mohanty, S. (2002). Structural evolution of Sausar Group around Parseoni, Nagpur district, Maharastra: Its implication for stratigraphy. *Journal of the Geological Society of India, 60*, 309–317.

Mohanty, S., & Naha, K. (1986). Stratigraphic relations of the Precambrian rock in the Salumbar area, southeastern Rajasthan. *Journal of the Geological Society of India, 27*, 479–493.

Mookherjee, A. (1965). Regional structural framework of lead-zinc deposits at Zawar, Rajasthan. *Journal of the Geological Society of India, 6*, 67–80.

Mukhopadhyay, D. (1976). Precambrian stratigraphy of Singhbhum: The problem and a prospect. *Indian Journal of Earth Sciences, 3*, 208–219.

Mukhopadhyay, D. (1984). The Singhbhum Shear Zone and its place in the evolution of the Precambrian mobile belt, North Singhbhum. *Indian Journal of Earth Sciences*, *CEISM*, 205–212.

Mukhopadhyay, J., Ray, A., Ghosh, G., Medda, R. A., & Bandopadhyay, P. P. (2001). Recognition, characterization and implication of high-grade silicic ignimbrite facies from the Palaeoproterozoic Bijli Rhyolites, Dongarhgarh Supergroup, Central India. *Gondwana Research*, *4*, 519–527.

Munshi, R. L., Khan, H. H., & Ghosh, D. B. (1974). The algal structure and phosphorite in the Aravali rocks of Jhabua. *Current Science, 43*, 446–447.

Nagori, D. K. (1988). Palaeogeography and depositional environment of the phosphorite-bearing Early Proterozoic carbonate rocks around Udaipur, Rajasthan. *Memoirs of the Geological Society of India, 7*, 139–152.

Naha, K. (1962). Precambrian sedimentation around Ghatshila in east Singhbhum, eastern India. *Proceedings of the National Institute of Sciences of India, 27A*, 261–272.

Naha, K., & Ghosh, S. K. (1960). Archaean palaeogeography in eastern and northern Singhbhum. *Geological Magazine, 97*, 463–469.

Naha, K., & Halyburton, R. V. (1971). Significance of small-scale deformation structures around Jawad, Udaipur district, Rajasthan. *Journal of the Geological Society of India, 12*, 69–75.

Naha, K., & Majumdar, A. (1971). Reinterpretation of Aravali basal conglomerate at Morchana, Udaipur district, Rajasthan. *Geological Magazine, 108*, 111–114.

Naha, K., Mukhopadhyay, P. K., Mohanty, R., Mitra, S. K., & Biswal, T. K. (1984). Significance of contrast in the early stages of the structural history of the Delhi and Pre-Delhi rock groups in the Proterozoic of Rajasthan, western India. *Tectonophysics, 105*, 193–206.

Nair, K. K. K., Jain, S. C., & Yedekar, D. B. (1995). Stratigraphy, structure and geochemistry of the Mahakoshal greenstone belt. *Memoirs of the Geological Society of India, 31*, 403–432.

Narayana Rao, M., & Choudhury, J. M. (1976). Sonapahar Group; a proposed new lithostratigraphic unit in the Precambrian rocks of the Shillong Plateau. *Journal of the Geological Society of India, 17*, 290–293.

Neogi, S., Miura, H., & Hariya, Y. (1996). Geochemistry of the Dongargarh volcanic rocks, central India: Implications for the Precambrian mantle. *Precambrian Research, 76*, 77–91.

Niyogi, D. (1960). Structural pattern of Kishangarh alkaline rocks. *Quarterly Journal of the Geological, Mining and Metallurgical Society of India, 32*, 27–38.

Niyogi, D. (1966). Petrology of the alkaline rocks of Kishangarh, India. *Geological Society of America Bulletin, 77*, 65–82.

Paliwal, B. S. (1998). The Aravalian fluvial sequence of Udaipur city, India: An excellent example of well-preserved sedimentary structures in complexly deformed Precambrian metasediments. In B. S. Paliwal (Ed.), *The Indian Precambrian* (pp. 142–158). Jodhpur: Scientific Publishers.

Pandey, U. K., Sastry, D. V. L. N., Pandey, B. K., Roy, M., Rawat, T. P. S., Ranjan, R., & Shrivastava, V. K. (2012). Geochronological (Rb-Sr and Sm-Nd) studies on intrusive gabbros and dolerite dykes from parts of northern and central Indian cratons: Implication for the age of onset of sedimentation in Bijawar and Chattisgarh basins and uranium mineralization. *Journal of the Geological Society of India, 79*, 30–40.

Pandit, M. K., Sial, A. N., Malhotra, G., Shekhawat, L. S., & Ferreira, V. P. (2003). C-, O-istotope and whole–rock geochemistry of Proterozoic Jahazpur carbonates, NW India Craton. *Gondwana Research, 6*, 513–522.

Panigrahi, M. K., & Mookherjee, A. (1997). The Malanjkhand copper (+molybdenum) deposit, India: Mineralization from a low-temperature ore-fluid of granitoids. *Mineralium Deposita, 32*, 133–148.

Pant, N. C., & Banerjee, D. M. (1990). Pattern of sedimentation in the type Bijawar Basin of Central India. *Special Publication of the Geological Survey of India, 28*, 156–166.

Patwardhan, A. M., & Oka, S. S. (1988). Characteristics of host rocks and base metal mineralization in the Sirohi district, southern Rajasthan. *Memoirs of the Geological Society of India, 7*, 423–439.

Phadke, A. V. (1990). Genesis of the granitic rocks and the status of the 'Tirodi Biotite Gneiss' in relation to the metamorphites of the Sausar group and the regional tectonic setting. *Special Publication of the Geological Society of India, 28*, 287–302.

Poddar, B. C. (1974). Evolution of sedimentary sulphide rhythmites into metamorphic tectonites in base-metal deposits of Rajpura-Dariba, Rajasthan. *Quarterly Journal of the Geological, Mining and Metallurgical Society of India, 46*, 207–222.

Qureshy, M. N. (1971). Relation of gravity to elevation and rejuvenation of blocks in India. *Journal of Geophysical Research, 76*, 545–557.

Raja Rao, C. S. (1970). Precambrian sequences of Rajasthan. *Miscellaneous Publication of the Geological Survey of India, 23*, 497–576.

Raja Rao, C. S., Poddar, B. C., Basu, K. K., & Dutta, A. K. (1971). Precambrian stratigraphy of Rajasthan: A review. *Record of the Geological Survey of India, 101*, 60–79.

Rajendra Prasad, B., Tewari, H. C., Vijaya Rao, V., Dixit, M. M., & Reddy, P. R. (1998). Structure and tectonics of the Proterozoic Aravali-Delhi Fold Belt in northwestern India from deep seismic reflection studies. *Tectonophysics, 288*, 31–41.

Ranawat, P. S., Bhatnagar, S. N., & Sharma, N. K. (1988). Metamorphic characteristics of Rampura-Agucha lead-zinc deposit. *Memoirs of the Geological Society of India, 7*, 397–410.

Ranga Rao, A., & Samanlu, M. K. (1987). Structural style of the Naga overthrust belt and its implications on explorations. *ONGC Bulletin, 24*, 69–109.

Rao, K. V., SriRama, B. V., & Ramasastry, P. (1990). A geophysical appraisal of Mahakoshal Group of Upper Narmada Valley. *Special Publication of the Geological Survey of India, 28*, 99–117.

Raval, U. (1995). Geodynamics of the tectonomagmatic and geophysical signatures within mobile parts of the transect. *Memoirs of the Geological Society of India, 31*, 37–61.

Ray, S. K. (1974). Structural history of the Saladipura pyrite-pyrrhotite deposit and associated rocks in Khetri Copper Belt, Rajasthan. *Journal of the Geological Society of India, 15*, 227–238.

Ray, Asik, K. (1977). Structural and metamorphic evolution of the Bengal Anorthosite and associated rocks. *Journal of the Geological Society of India, 18*, 203–223.

Raza, M., Casshyap, S. M., & Khan, A. (2001). Accretionary lapilli from the basal Vindhyan volcanic sequence, south of Chittaurgarh, Rajasthan, and their implication. *Journal of the Geological Society of India, 57*, 77–82.

Reddy, P. R., Murthy, P. R. K., Rao, I. B. P., Khare, P., Kesava Rao, G., Mall, D. M., et al. (1995). Deep crustal seismic reflection fabric pattern in central India: Preliminary interpretation. *Memoirs of the Geological Society of India, 31*, 537–544.

Roday, P. P., & Bhat, A. K. (1980). Tectonic history of the Bijawar rocks at the Bramhanghat section of the Narmada Valley. *Journal of the Geological Society of India, 21*, 547–557.

Roy, S. (1966). *Syngenetic manganese formations of India* (p. 219p). Kolkata: Jadavpur University.

Roy, A. B. (1988). Stratigraphy and tectonic framework of the Aravali mountain range. *Memoirs of the Geological Society of India, 7*, 3–31.

Roy, A., & Bandyopadhyay, B. K. (1988). Geology and geochemistry of metabasalt near Sleemanabad in the Proterozoic Mahakoshal belt of central India. *Indian Minerals, 43*, 303–324.

Roy, A. B., & Das, A. R. (1985). A study of time relations between movements, metamorphism and granite emplacement in the middle Proterozoic Delhi Supergroup of Rajasthan. *Journal of the Geological Society of India, 26*, 726–733.

Roy, S., Dasgupta, S., Majumdar, N., Banerjee, H., Bhattacharya, P. K., & Fukuoka, M. (1986). Petrology of the manganese silicate-carbonate oxide rocks of Sausar Group, India. *Neues Jahrbuch fur Mineralogie, Abhandlungen, 12*, 561–568.

Roy, A. B., & Dutt, K. (1995). Tectonic evolution of the nepheline syenite and associated rocks of Kishangarh, district Ajmer, Rajasthan. *Memoirs of the Geological Society of India, 31*, 231–257.

Roy, Abhinaba, & Hanuma Prasad, M. (2003). Tectonothermal events in Central Indian Tectonic Zone (CITZ) and its implication in Rodinian crustal assembly. *Asian Journal of Earth Sciences, 22*, 115–129.

Roy, A., Kagami, H., Yoshida, M., Roy, A., Bandyopadhyay, B. K., Chattopadhyay, A., et al. (2006). Rb-Sr and Sm-Nd dating of different metamorphic events from the Sausar Mobile Belt, central India: Implications for Proterozoic crustal evolution. *Journal of Asian Earth Sciences, 26*, 61–76.

Roy, A. B., & Paliwal, B. S. (1981). Evolution of the lower Proterozoic continental deposits: Stromatolite-bearing Aravali rocks of Udaipur, Rajasthan, India. *Precambrian Research, 14*, 49–74.

Roy, A. B., Paliwal, B. S., Shekhawat, S. S., Nagori, D. K., Golani, P. R., & Bejarniya, B. R. (1988). Stratigraphy of the Aravali Supergroup in the type area. *Memoirs of the Geological Society of India, 7*, 121–138.

Roy, A., Sarkar, A., Jeyakumar, S., Aggrawal, S. K., & Ebihara, M. (2003). Mid-Proterozoic plume-related thermal event in Eastern Indian Craton: Evidence from trace elements, REE geochemistry and Sr-Nd isotope systematics of basic–ultrabasic intrusives from Dalma Volcanic Belt. *Gondwana Research, 5*, 133–146.

Roy, A. B., Somani, M. K., & Sharma, N. K. (1981). Aravali—PreAravali relaltionship: A study from Bhinder region, southern Rajasthan. *Indian Journal of Earth Sciences, 8*, 119–130.

Saha, A. K. (1948). Kolhan Series—Iron Ore Series boundary to the west and southwest of Chaibasa. *Science and Culture, 14*, 77–79.

Saha, A. K. (1949). Dolerite dykes and sills around Chaibasa. *Quarterly Journal of the Geological, Mining and Metallurgical Society of India, 21*, 77–83.

Saha, A. K. (1975). The Mayurbhanj Granite—a Precambrian batholith in Eastern India. *Journal of the Geological Society of India, 16*, 37–43.

Saha, A. K. (1994). *Crustal evolution of singhbhum, North Orissa, Eastern India* (p. 341). Bangalore: Geological Society of India.

Saha, A. K., Ray, S. L., & Sarkar, S. N. (1988). Early history of the Earth: Evidence from the eastern Indian shield. In D. Mukhopadhyay (Ed.), *Precambrian of the eastern Indian shield* (pp. 13–37). Bangalore: Geological Society of India.

Saha, A. K., Sankaran, A. V., & Bhattacharyya, T. K. (1973). Geochemistry of Newer Dolerite suite of intrusions within the Singhbhum Granite. *Journal of the Geological Society of India, 14*, 324–346.

Sarkar, S. N. (1958). Stratigraphy and tectonics of the Dongargarh system: A new system in the Precambrian of Bhandara–Drug–Balaghat area, Madhya Pradesh. *Journal of Science and Engineering Research*, IIT, Kharagpur, *1*, 237–268 and *2*, 145–160.

Sarkar, A. N. (1982a). Precambrian tectonic evolution of eastern India: a model of converging microplates. *Tectonophysics, 86*, 363–397.

Sarkar, S. C. (1982b). Uranium-nickel-cobalt-molybdenum mineralization along the Singhbhum Copper Belt, India, and the problem of ore genesis. *Mineralium Deposita, 17*, 257–278.

Sarkar, A. N. (1988). Tectonic evolution of the Chhotanagpur Plateau and the Gondwana basin in eastern India. *Memoirs of the Geological Society of India, 8*, 127–146.

Sarkar, S. N. (1994). Chronostratigraphy and tectonics of the Dongargarh Supergroup. Precambrian rocks in Bhandara-Drug region, central India. *Indian Journal of Earth Sciences, 21*, 19–31.

Sarkar, S. C. (2000). Crustal evolution and metallogeny in the Eastern Indian Craton. *Special Publication of the Geological Survey of India, 55*, 169–194.

Sarkar, S. C., Bhattacharyya, P. K., & Mukherjee, A. D. (1980). Evolution of the sulphide ores of Saladipura, Rajasthan, India. *Economic Geology*, *75*, 1152–1167.

Sarkar, S. C., & Dasgupta, S. (1980). Geologic setting, genesis and transformation of the sulphide deposits in the northern part of the Khetri Copper Belt, Rajasthan—an outline. *Mineralium Deposita, 15*, 117–137.

Sarkar, S. C., & Deb, M. (1974). Metamorphism of sulphides of the Singhbhum Copper Belt: The evidence from the ore fabric. *Economic Geology, 69*, 1282–1293.

Sarkar, S. C., Gupta, A., & Basu, A. (1992). North Singhbhum Proterozoic Mobile Belt, eastern India: Its character, evolution and metallogeny. In S. C. Sarkar (Ed.), *Metallogeny related to tectonics of the Proterozoic mobile belts* (pp. 271–306). New Delhi: Oxford & IBH.

Sarkar, S. C., Kabiraj, S., Bhattacharya, S., & Pal, A. B. (1996). Nature, origin and evolution of the granitoid-hosted early Proterozoic copper-molybdenum-mineralization at Malanjkhand, central India. *Mineralium Deposita*, *31*, 419.

Sarkar, S. N., & Saha, A. K. (1962). A revision of the Precambrian stratigraphy and tectonics of Singhbhum and adjacent region. *Quarterly Journal of the Geological, Mining and Metallurgical Society of India, 34*, 97–136.

Sarkar, S. N., Saha, A. K., & Miller, J. A. (1969). Geochronology of the Precambrian rocks of Singhbhum and adjacent area, India. *Geological Magazine, 106*, 15–45.

Sen, S. (1952). The genesis of alkaline rocks of Kishangarh, Rajasthan. *Current Science, 21*, 242–243.

Sen, S. (1970). Some problem of Precambrian geology of the central and southern Aravali Range, Rajasthan. *Journal of the Geological Society of India, 11*, 217–231.

Sengupta, P. R. (1972). Study on mineralization in southeastern part of Singhbhum Copper Belt, Bihar. *Memoirs of the Geological Suevey of India, 101*, 1–82.

Sengupta, S., Bandyopadhyay, P. K., & Van den Hul, H. J. (1983). Geochemistry of the Chakradharpur Granite gneiss complex—a Precambrian trondhjemite body from west Singhbhum, eastern India. *Precambrian Research, 23*, 57–78.

Sengupta, S., & Ghosh, S. K. (1997). The kinematic history of the Singhbhum Shear Zone. *Proceedings of the Indian Academy of Sciences (Earth & Planetary Sciences)*, *106*, 185–196.

Sengutpa, S., Bandyopadhyay, P. K., Van del Hul, H. J., & Chattopadhyay, B. (1984). Arkasani Granophyre: Proterozoic intraplate acid magmatic activity on the Singhbhum Craton, eastern India. *Neues Jahrbuch fur Mineralogie, Abhandlungen, 148*, 328–343.

Sensarma, S., & Mukhopadhyay, D. (2003). New insights on stratigraphy and volcanic history of Dungargarh Belt, central India. *Gondwana Geological Magazine, 7*, 129–136.

Sharma, R. S. (1977). Deformational and crystallization history of the Precambrian rocks in north-central Aravali mountain, Rajasthan, India. *Precambrian Research, 4*, 133–162.

Sharma, R. S. (1988). Pattern of metamorphism in the Precambrian rocks of the Aravali mountain belt. *Memoirs of the Geological Society of India, 7*, 33–76.

Sharma, R. S. (1995). An evolutionary model for Precambrian crust of Rajasthan: Some petrological and geochronological considerations. *Memoirs of the Geological Society of India, 31*, 91–115.

Sikka, D. B. (1989). Malanjkhand: Proterozoic porphyry copper deposit, M.P., India. *Journal of the Geological Society of India, 34*, 487–504.

Sikka, D. B., & Nehru, C. E. (2002). Malanjkhand coper deposit: Is it not a porphyry type? *Journal of the Geological Society of India, 59*, 339–362.

Singh, S. P. (1984). Fluvial sedimentation of the Proterozoic Alwar Group in the Lalgarh graben, northwestern India. *Sedimentary Geology, 39*, 95–119.

Singh, S. P. (1988). Sedimentation pattern of the Proterozoic Delhi Supergroup, northeastern Rajasthan, India and their tectonic implications. *Sedimentary Geology, 58*, 79–94.

Singh, S. P. (1998). Precambrian stratigraphy of Bihar—an overview. In B. S. Paliwal (Ed.), *The Indian Precambrian* (pp. 276–408). India: Scientific Publishers.

Sinha-Roy, S. (1984). Precambrian crustal interaction in Rajasthan, NW India. *Indian Journal of Earth Sciences*, *CISM*, 84–91.

Sinha-Roy, S. (1988). Palaeozoic Wilson cycles in Rajasthan. *Memoirs of the Geological Society of India, 7*, 95–108.

Sinha-Roy, S., & Malhotra, G. (1989). Structural relations of Proterozoic cover and its basement. An example from the Jahazpur belt, Rajasthan. *Journal of the Geological Society of India, 34*, 233–244.

Sinha-Roy, S., Malhotra, G., & Guha, D. B. (1995). A transect across Rajasthan Precambrian terrain in relation to geology, tectonics and crustal evolution of south-central Rajasthan. *Memoirs of the Geological Society of India, 31*, 63–90.

Sinha-Roy, S., & Mohanty, M. (1988). Blue schist facies metamorphism in the ophiolitic mélange of the Late Proterozoic Delhi Fold Belt, Rajasthan. *Precambrian Research, 42*, 97–105.

Srinivasan, V. (2005). The Dauki fault in northeast India, through remote sensing. *Journal of the Geological Society of India, 66*, 413–426.

Srivastava, R. K. (1988). Magmatism in the Aravali Mountain Range and its environs. *Memoirs of the Geological Society of India, 7*, 77–93.

Srivastava, R. K. (1989). Alkaline and peralkaline rocks of Rajasthan. *Memoirs of the Geological Society of India, 15*, 3–24.

Srivastava, Rajesh, K., & Chalapathi Rao, N. V. (2007). Petrology, geochemistry and tectonic significance of Palaeoproterozoic alkaline lamprophyres from the Jugel valley, Mahakosal supracrustal belt, Central India. *Mineralogy and Petrology, 89*, 189–215.

Stein, H., Zimmerman, A., Hannah, J. L., & Markey, R. J. (2003). Late Archaean-Early Proterozoic timing for an Andean-style porphyry Cu-Mo deposit and Malanjkhand, Central Indian Tectonic Zone: Implications for a late Archaean supercontinent. *Geophysical Research Abstracts, 5*, 67496.

Straczekett, J. N., Subramanyam, M. R., Narayanaswami, S., Shukla, K. D., Vemban, N. A., Chakravarti, S. C., et al. (1956). Manganese ore deposits of Madhya Pradesh, India. *Report on 20th Interntional Geological Congress*, Vol. 4, pp. 63–96.

Sychanthavong, S. P., & Desai, S. D. (1977). Protoplate tectonics controlling the Precambrian deformation and metallogenic epochs in northwestern India. *Mineralogy Science and Engineering, 9*, 218–236.

Talluri, J. K., Pandalai, H. S., & Jadhav, G. N. (2000). Fluid chemistry and depositional mechanism of the epigenetic, discordant ores of the Proterozoic carbonate-hosted Zawarmala Pb-Zn deposit, Udaipur district, India. *Economic Geology, 95*, 1505–1525.

Thakur, K. S., & Shukla, R. S. (1990). Geochemistry of Early Proterozoic metabasites and associated copper mneralization in Karandia area in Mahakoshal rift basin, Shahdol district, M.P. *Special Publication of the Geological Survey of India, 28*, 512–526.

Tiwari, S. (1995). Extension of great boundary fault of Rajasthan in the Ganga Valley. *Memoirs of the Geological Society of India*, *31*, 311–328.

Tripathi, S. C., & Mishra, M. N. (1994). Cyclic volcanism and sedimentation in the Mahakoshal greenstone belt, district Sidhi, M.P. *Journal of the Geological Society of India, 44*, 167–173.

Valdiya, K. S. (1981). Tectonics of central sector of the Himalaya. In H. K. Gupta & F. M. Delancy (Eds.), *Geodynamics Series: Vol. 3 Zagor–Hindukush Himalaya, Geodynamic Evolution* (pp. 87–110). Washington, D.C.: American Geophysical Union.

Valdiya, K. S. (1988). Tectonic evolution of the central sector of Himalaya. *Philosophical Transactions of the Royal Society of London, A326*, 151–175.

Verma, R. K. (1985). *Gravity field, seismicity and tectonics of the Indian Peninsula and the Himalaya*. New Delhi: Allied Publishers.

Verma, P. K. (1996). Evolution and age of the Great Boundary Fault of Rajasthan. *Memoirs of the Geological Society of India, 36*, 197–212.

Verma, R. K., Sharma, A. U. S., & Mukhopadhyay, M. (1984). Gravity field over Singhbhum; its relationship to geology and tectonic history. *Tectonophysics, 106*, 87–107.

Vishwakarma, R. K. (1996). 1.66 Ga-old metamorphosed Pb-Cu deposit in Sargipali (eastern India): Manifestation of tidal-flat environment and sedex type genesis. *Precambrian Research, 77*, 117–130.

Volpe, A. M., & Macdougall, J. P. (1990). Geochemistry and isotopic characteristics of mafic (Phulad Ophiolite) and related rocks in the Delhi Supergroup, Rajasthan, India: Implication for rifting in the Proterozoic. *Precambrian Research, 48*, 167–191.

Yedekar, D. B., Karmarkar, N., Pawar, N. J., & Jain, S. C. (2003). Tectonomagmatic evolution of central Indian Terrain. *Gondwana Geological Magazine, 7*, 67–88.

Yellur, D. D. (1977). Geochemical clues to the investigations of the tectonic environment of the Dalma greenstones, Bihar, India. *Chemical Geology, 20*, 345–363.

Chapter 6
Mesoproterozoic Eastern Ghat Mobile Belt

6.1 General Layout

The rugged country with discontinuous hill ranges facing the Bay of Bengal is known as the Eastern Ghat. The average altitude is 610 m, and the tallest peak Mahendragiri is 1501 m high. Extending from Brahmani River in Odisha to Ongole in southeastern Andhra Pradesh, the terrane of highly deformed rocks that experienced ultrahigh-temperature granulite facies metamorphism and several invasions of generations of magmas of varied compositional types is recognized as the *Eastern Ghat Mobile Belt* (EGMB). The 1000-km-long terrane is nearly 300 km wide in the northern part (Mahalik 1996), but tapers to merely 30 km in the south, the average width being 100 km (Fig. 6.1). Two Phanerozoic rift valleys, the Mahanadi Graben in the north and the Godavari Graben in the south, break the continuity by hosting Gondwana sediments. It is a Mesoproterozoic terrane that has a very long history of tectonothermal activities including migmatization and charnockitization of supracrustal rocks.

The EGMB has been referred to as a convergent orogen that evolved under NW–SE-directed subhorizontal compression resulting from oblique collision of continental plates (Chetty and Murthy 1994; Ramakrishnan et al. 1998; Bhattacharya 2002).

Gravity modelling (Fig. 6.2) constrained by seismic information suggests that the eastward-inclined 38- to 40-km-thick column of cratonic crust lies 35 km below this mobile belt (Kumar et al. 2004). It will be apparent that the EGMB displays high-gravity anomaly compared to the cratons, implying denser rocks underlying it (Subramanyam and Verma 1986). Building the bulk of the EGMB, the exposed charnockite–khondalite succession represents the thrust-up lower crustal material. The basement Archaean rocks are seen nowhere, but the material forming them occurs in the framework of the mobile belt in a drastically remobilized and reconstituted forms.

K.S. Valdiya, *The Making of India*, Society of Earth Scientists Series,
DOI 10.1007/978-3-319-25029-8_6

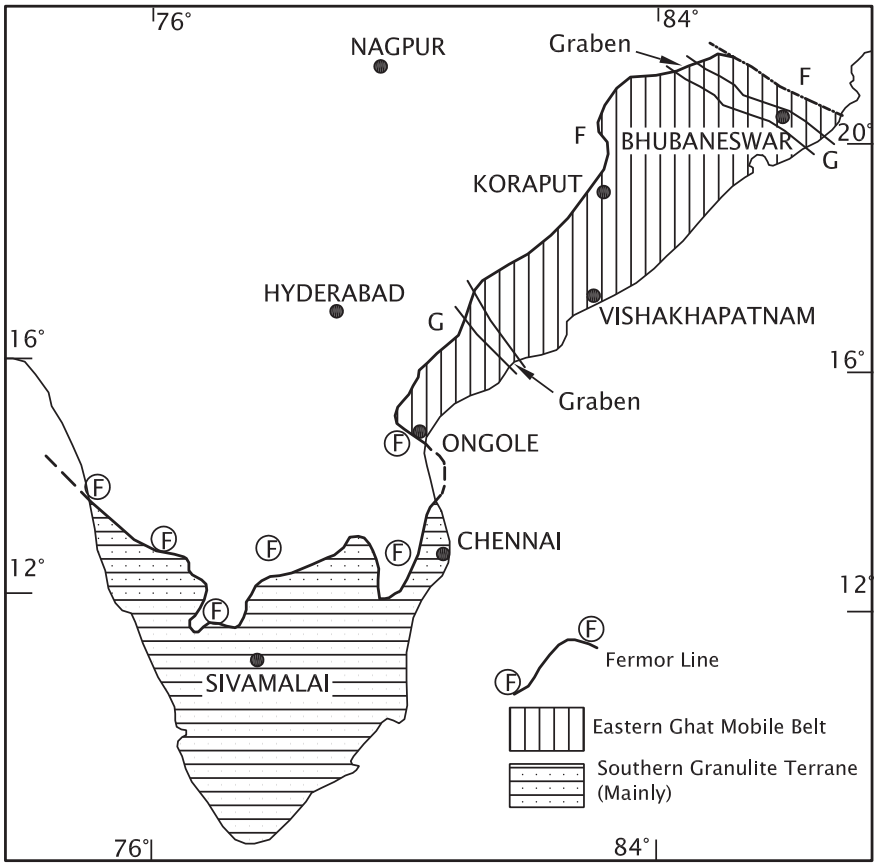

Fig. 6.1 Sketch map shows the position of the Proterozoic Eastern Ghat Mobile Belt adjacent to the cratonic blocks of Archaean antiquity. It is in the line of the Southern Granulite Terrane in southern India

Far away across the Indian Ocean, the terrane of East Antarctica encompasses Napier, Enderby Land and Vestfold Hills (Fig. 6.3), the Raynex Complex bearing some similarity with the EGMB (Upadhyay et al. 2006).

6.2 Structural Architecture and Deformation History

6.2.1 Configuration

The NE–SW-trending EGMB is defined along its western margin against the Archaean Bastar and Dharwar cratons by a prominent shear zone of the nature of a detachment thrust. The thrust is dipping eastwards. Steep gradient in

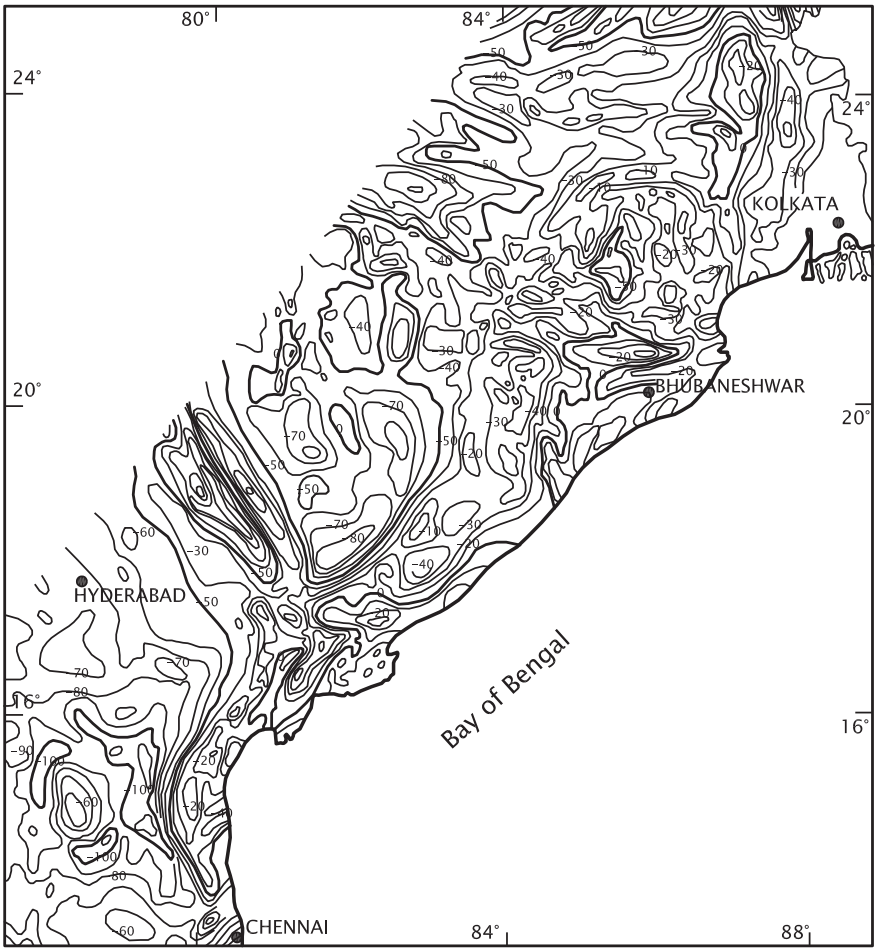

Fig. 6.2 Bouguer anomaly (in m Gal) over the eastern part of southern Peninsular India (after Kumar et al. 2004)

gravity anomaly characterizes the thrust (Subrahmanyam and Verma 1986). The detachment plane has been described variously—West Odisha Boundary Fault (Mahalik 1994), Terrane Boundary Shear Zone (Biswal et al. 2000; Biswal and Sinha 2003), Eastern Ghat Boundary Fault (Crowe et al. 2003) and *Sileru Shear Zone* (Chetty 1995). The fault zone is shown as dipping steeply (50°) eastwards. The tectonic boundary shows a curvilinear geometry. It shows thrust character in the northwestern part, while the movements were dominantly strike slip in the north. It has been interpreted as a listric fault that acted as the sole thrust between basement (Bastar Craton) and overthrust EGMB pile, the thrusting having taken place after the deformation and attendant metamorphism of the succession (Biswal and Sinha 2003). The shear zone is thus marked by disorientation of folds and

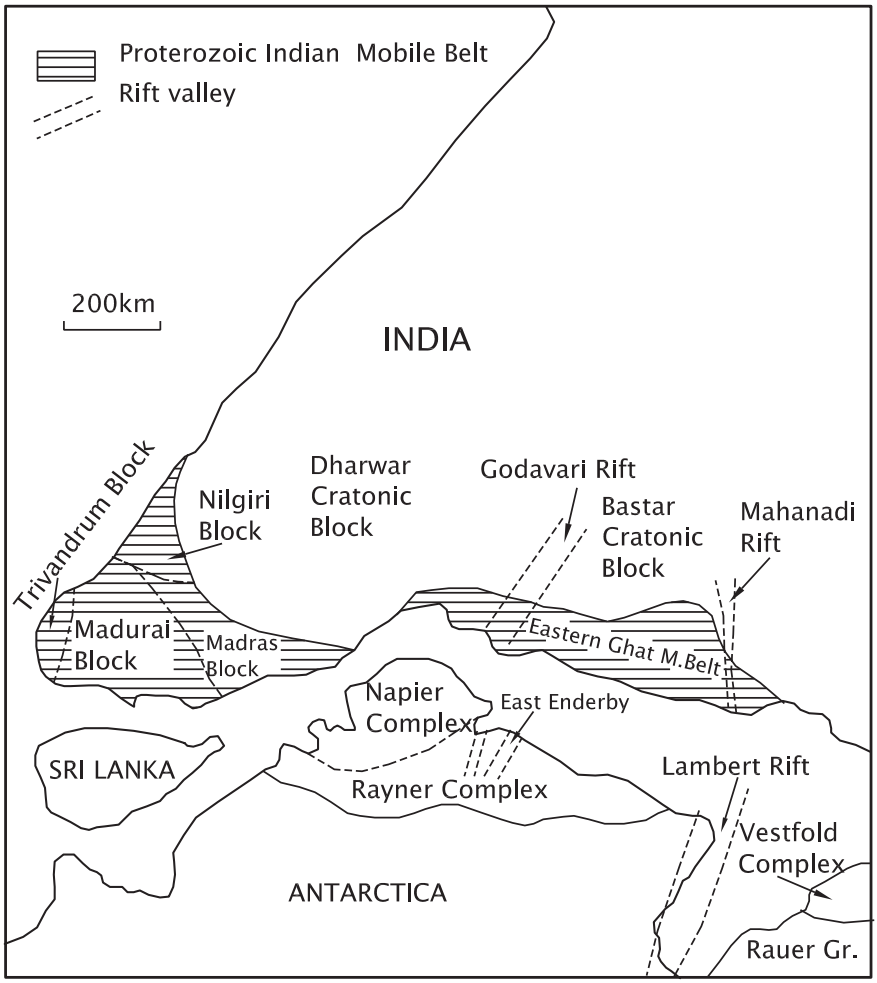

Fig. 6.3 In the Proterozoic era, the Peninsular India lay in juxtaposition with East Antarctica. The adjoining belts have strikingly similar lithotectonic setup and almost the same history of evolution (based on Stein et al. 2004)

retrograde changes of the high-grade metamorphic rocks and their intrusive plutons. Significantly, nearly 1400-million-year-old synkinematic alkaline complexes occupy the shear zone (Sarkar and Paul 1998). However, the thrusting might have continued up to the Neoproterozoic time when the EGMB was amalgamated with the Bastar and Dharwar cratons (Dobmeir and Raith 2003; Upadhyay et al. 2006).

The frontal part of the Nellore Schist Belt comprising folds and thrusts including the Velikonda Thrust accommodates substantially the structures of the upper crust exhibiting inclined transpression (Saha et al. 2010). It may be pointed out that the Maidukur Trust along the western margin of the Nallamalai fold belt has

likewise accommodated upper crust structures of the Cuddapah succession. Along the junction of the Nellore Schist (belonging to the Eastern Dharwar Craton) with the EGMB occur dismembered bodies of ophiolites in a deformed state at Kanigeri, Kandra, Arinanupudu and Gurromkonda. The ophiolite bodies are made up of hornblende metagabbro, massive to pillow metabasalt, sheeted metadolerite and associated metapelites and metapsammite intercalated with metabasalts, the rock sequence strongly recalling the stratigraphy of the oceanic plate (Saha 2011). It seems that the oceanic material was obducted and amalgamated to the Dharwar Craton as the EGMB was welded to it.

The U–Pb zircon age of the plagiogranite within the mélange at Kanigeri is dated nearly 1330 Ma (Dharma Rao et al. 2011).

Interestingly, there is a prominent salient—outward-pointing bend—on the northwestern margin of the EGMB. The granulitic succession is split into thrust sheets—the Lathore nappe and the Turrkela klippe (Fig. 6.5a)—that have moved onto the Bastar Craton (Biswal and Sinha 2003; Bhadra et al. 2004). The basal decollement is characterized by lateral ramps or ridges at Khariar and Paikamal developed along the contacts between granites and gneisses. The northern border is sharply delimited by an E–W- to ESE–WNW-oriented system of strike-slip shear zones of the Mahanadi Valley (Figs. 6.1, 6.4 and 6.5b). The larger terrane is broken by shear zones orthogonal to the trend of the terrane—the Mahanadi, the Vamsadhara, the Nagavalli and the Godavari shear zones (Chetty et al. 2003). The northern and southern shear zones gave rise to grabens of great extent, later to be occupied by the Gondwana sediments of the Phanerozoic eras.

In the Mahanadi domain (Figs. 6.4 and 6.5b), comprising amphibolite facies rocks intercalated with basement gneisses and metavolcanic sediments, the shear zones surround fragments and block of both the Singhbhum Craton and the EGMB (Mahalik 1994). The bounding Kerajang and Barakot shear zones register dextral displacement. The displacement occurred prior to 980 Ma and second-phase folding deformation (Crowe et al. 2003).

6.2.2 Deformation Pattern

A four-phase deformation history is recorded in the structural architecture of the EGMB. The first three phases were dominated by folding, and the last one by shearing and fracturing (Fig. 6.6). The NE–SW to N–S regional trend is defined by the first- and second-generation folds. The second-phase folding was coaxial with the first, and the fold interference produced hook-shaped structures in the khondalites. The third episode of deformation produced asymmetric folds that gently plunge northeastwards in metapelites and upright disharmonic structures in migmatites (Bhattacharya et al. 1994). Pieces of charnockite near the hinge of these third-generation folds represent discontinuous relicts of larger layers that were torn apart and displaced (Fig. 6.6). The generally southeastward- to eastward-dipping rock successions all through their expanse are cut by several ductile and

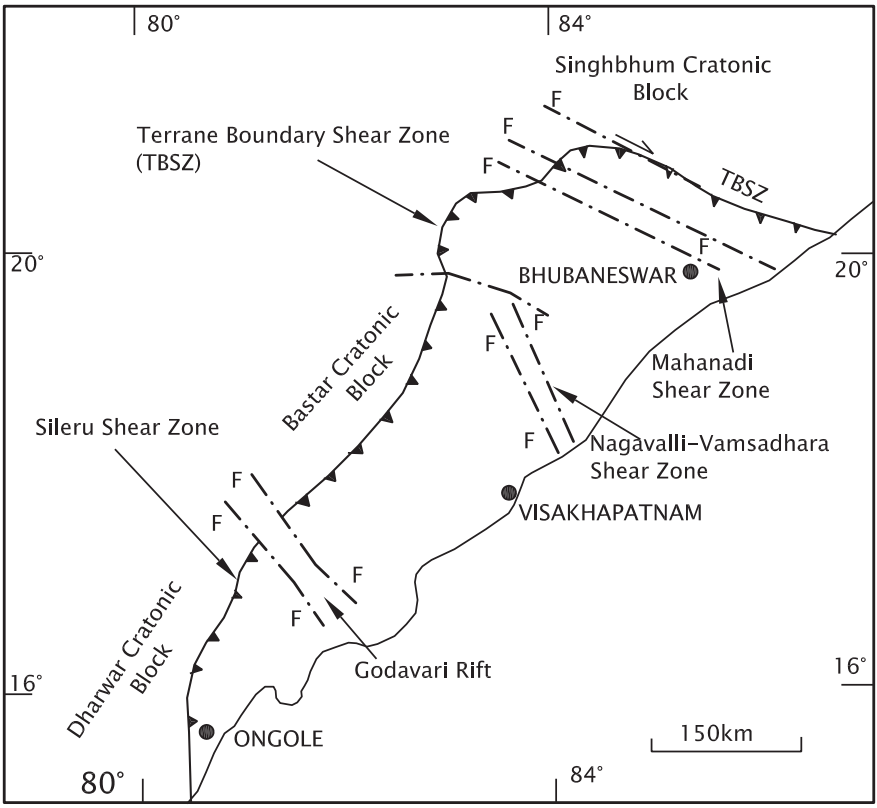

Fig. 6.4 Sketchmap shows the tectonic boundary of the Eastern Ghat Mobile Belt and the transverse rift zones that segment the Proterozoic terrane. There is a salient or outward-pointing bend in the northwestern part. The northern boundary is defined by a system of strike-slip wrench faults (after Biswal and Sinha 2003)

brittle shear zones developed along the early-generation folds. The shear zones are associated with mylonites and pseudotachylites (Chetty and Murthy 1994; Biswal et al. 1998; 2000; Chetty et al. 2003). In some parts of the terrane, dome-and-basin structure of varying scale formed due to the third phase of folding (Natarajan and Nanda 1981).

6.3 Lithological Assemblages and Subdivision

Four lithological zones (Fig. 6.7) have been recognized in the EGMB on the basis of ages of protoliths and constituent minerals (Ramakrishnan et al. 1998). The fifth unit is the zone of transition.

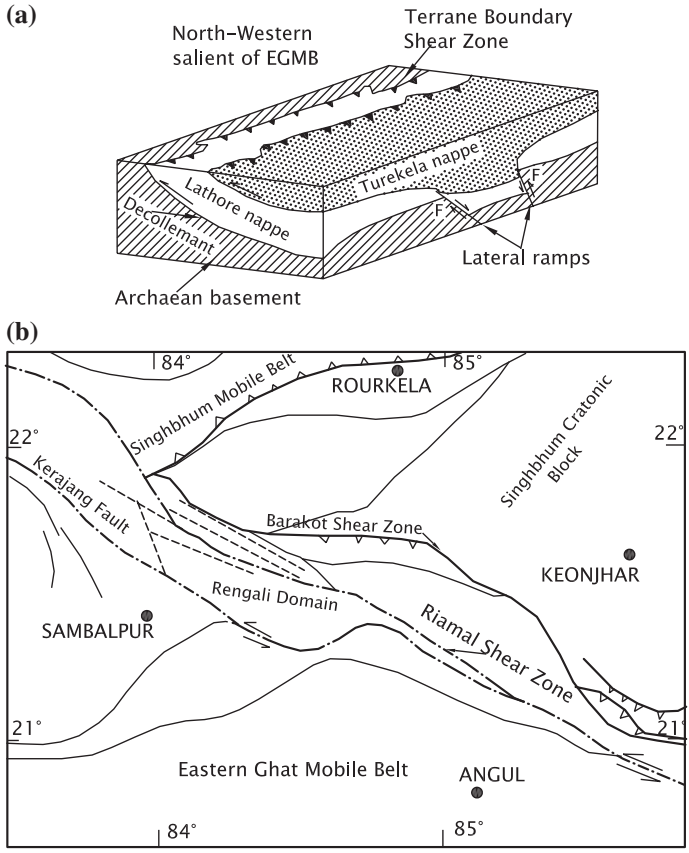

Fig. 6.5 **a** Three-dimensional model of the northwestern part of the EGMB exhibiting nappe structure and lateral ramps on the decollement developed at the contacts of massive granites and gneisses (Biswal and Sinha 2003). **b** Structural map of the Rengali domain in the northern part of the EGMB showing shear zones and interfingering blocks of both the Singhbhum Craton and the Eastern Ghat Mobile Belt (after Crowe et al. 2003)

1. The *Western Charnockite Zone* comprises dominant charnockites and enderbites with lenses of basic and ultrabasic rocks and minor intercalations of metapelite (*khondalite*) and basic granulites. There are several generations of charnockites, the oldest being deformed and gneissose, garnet bearing and concordant in disposition with the khondalite.
2. The *Western Khondalite Zone* is dominated by metapelitic khondalite with intercalations of quartzite, calc silicate gneiss, marble and minor though very significant high Mg–Al granulite characterized by sapphirine. There are intrusive bodies of charnockites and massif-type anorthosite, as seen at Bolangir, Turrkel and Jugsaipatna. Metamorphosed basic sills and lava flows are represented by concordant bodies of basic granulites within the khondalite succession. In many cases, there are plutonic intrusives.

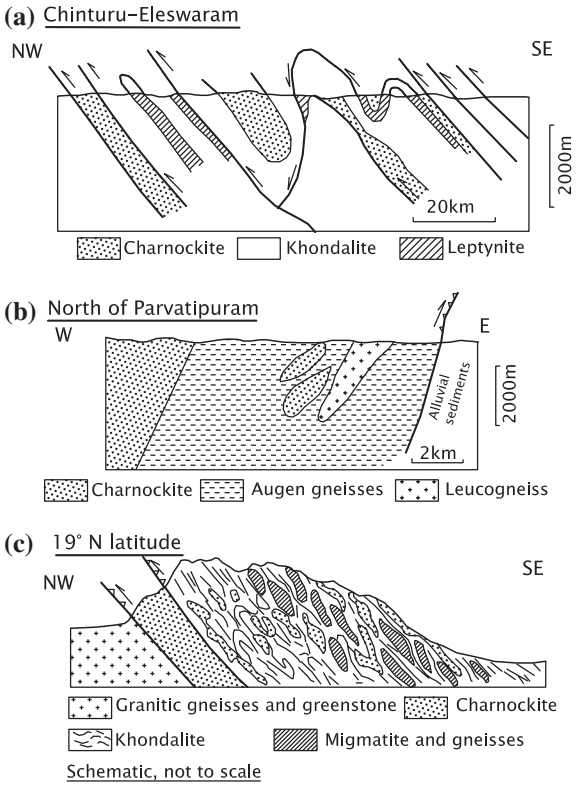

Fig. 6.6 Cross sections of the Eastern Ghat Mobile Belt elucidating its structural architecture. **a** Chinturu–Eleswaram section (after Chetty 1995). **b** Section north of Parvatipuram (after Chetty et al. 2003). **c** Section at about 19°N (after Ramakrishnan et al. 1998)

3. The *Central Migmatite–Charnockite Zone* is made up of dominant migmatites, garnet-bearing diatexites with *leptynites*, high Mg–Al granulite and calc silicate rock intruded by charnockites and porphyritic granites. There are bodies of massif-type anorthosite within the zone. The migmatites owe their origin to high-grade metamorphism with attendant differential melting of siliceous granulites, like the khondalite. The charnockites also show a composition that reveals affinity to tholeiitic to calc-alkaline basalts of the protoliths (Rao et al. 1995). There are patches of charnockite developed *incipiently* on the granulitic gneisses and migmatites. They were supposed to have formed as a result of activity of CO_2-rich fluids and/or through a process of charnockitization of metasediments of appropriate bulk composition (Nanda and Pati 1989; Paul et al. 1990; Rajesham et al. 1992; Mohan et al. 2003).
4. The *Eastern Khondalite Zone* consists of a lithology not different from that of the Western Khondalite Zone, but is devoid of anorthosite bodies. The leptynites that are interlayered with khondalites in the Chilka Lake area represent the granitoids produced by dehydration melting in the metapelites of different composition (Sen and Bhattacharya 1997). The presence of sillimanite trails within garnets suggests that the khondalites were indeed subjected to partial melting.

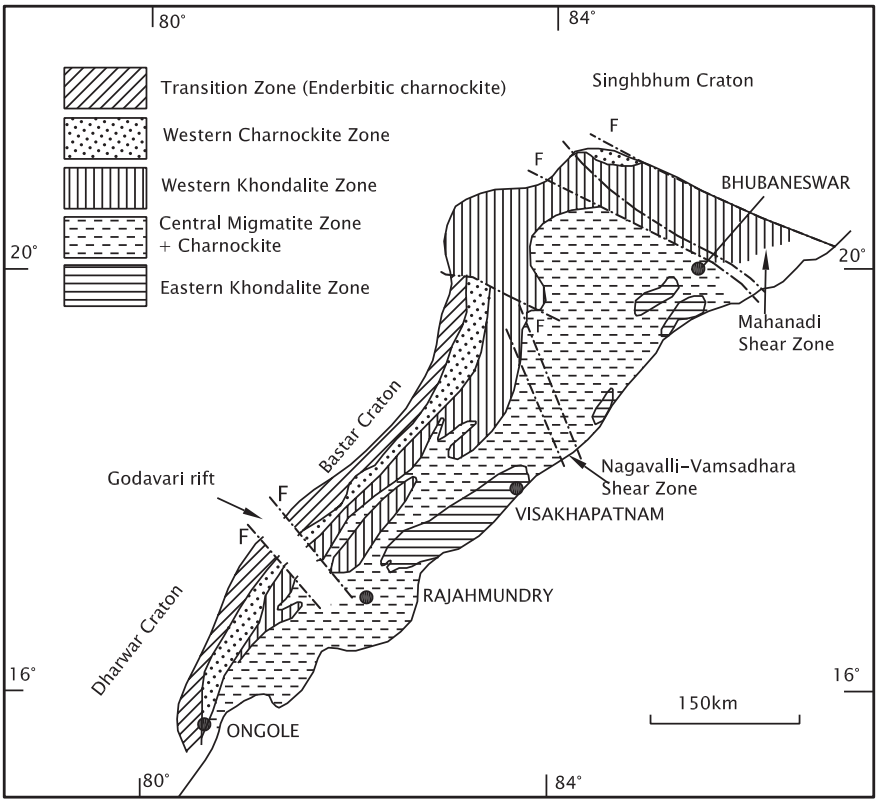

Fig. 6.7 Lithological assemblages, grouped in five longitudinal zones, constitute the terranes of the Eastern Ghat Mobile Belt (based on Ramakrishnan et al. 1998; Dasgupta and Sengupta 2002; Biswal and Sinha 2003)

In the Rengali domain in the northern part of the EGMB, the multiple shear zones seem to have not only served as places for intrusion of alkaline rocks but also provided pathways to fluids that brought about charnockitization and migmatization of granulitic rocks (Mahalik 1994). Understandably, the ultrabasic intrusives occur as boundinaged bodies in the highly deformed masses of khondalites of shear zones (Fig. 6.6c). Closely associated in space, the comagmatic anorthosite occurs as metamorphosed and tectonized layers in the EGMB.

5. *Transition Zone* is present on the western and southwestern margins of the EGMB. It consists of a mixture of lithotypes belonging to the craton and the Western Charnockite Zone. The granulites show retrogression to amphibolite along the shear zone.

6.3.1 Metamorphism: Thermobarometry and Petrogenesis

The rocks building the framework of the EGMB consist of the following mineral assemblages:

(i) Garnet-sillimanite-perthite-plagioclase-quartz ± graphite (*khondalite*)
(ii) Garnet-plagioclase-perthite-quartz (*leptynite*)
(iii) Wollastonite-scapolite-plagioclase-garnet-calcite-clinopyroxene-sphene (*calc silicate granulite*)
(iv) Orthopyroxene-clinopyroxene-plagioclase ± garnet (*basic granulite*)
(v) Sapphirine-spinel-orthopyroxene-garnet-quartz/corundum-cordierite-sillimanite (*high-magnesian-aluminium granulite*)
(vi) Orthopyroxene-plagioclase-quartz-perthite (*enderbite-charnockite*)

The study of chemistry of these mineral assemblages together with interpretation of textural features of constituent grains brings out a coherent picture of thermal history of the terrane. Metamorphism reached the granulite facies at temperatures 950–1040 °C under pressures of 8 to 10 kbar, and then, there was near isobaric cooling (under equal pressure) followed by decompression. Three phases of metamorphism (Fig. 6.8) have been recognized—(i) early ultrahigh-temperature metamorphism with anticlockwise P–T path, (ii) granulite facies reconstitution with

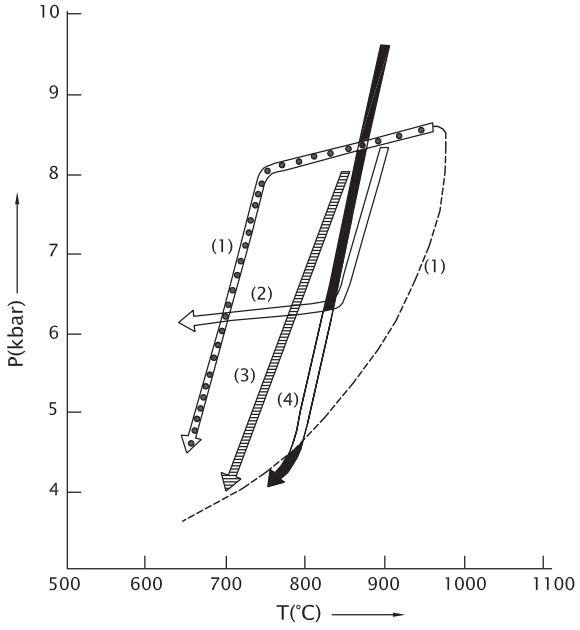

Fig. 6.8 P–T trajectories from different areas of the Eastern Ghat Mobile Belt show the trends of metamorphism (after Dasgupta 1995)

retrograde trajectory of near isothermal decompression and (iii) amphibolite facies metamorphism (Dasgupta 1995; Dasgupta and Sengupta 2002).

The early-stage *ultrahigh-temperature metamorphism* at temperatures higher than 1000 °C and under pressures of 8–10 kbar—representing the peak of the processes—was witnessed by, among other areas, Vijaynagaram (Sarkar et al. 2003) and Chilka Lake (Bhattacharya 2004). The *high Mg–Al granulite* of Visakhapatnam district was formed at temperatures 930–740 °C under pressure of 8.5–5.9 kbar (Lal 1997; Lal et al. 1987; Dasgupta and Sengupta 2002). The orthopyroxene-bearing enderbite rocks associated with basic granulites in the northern part of the terrane has been affected by metamorphism at temperatures in excess of 950 °C and under pressure of 8–9 kbar. The elevated temperature is attributed to emplacement of basic magma (Bose et al. 2003). There was dehydration melting in the Chilka Lake area (Sen and Bhattavcharya 1997). The Gangarajumuduguli charnockites were formed under anhydrous condition generated by influx of CO_2-rich fluids into rocks of lower crustal level where the temperature was 860 °C and pressure of 9 kbar (Mohan et al. 2003). As a matter of fact, ultrahigh-temperature condition prevailed practically all over the Eastern Ghat terrane when thermal perturbation occurred on a lithospheric scale. The cause of exceptionally high heating was the underplating or intraplating of hot basic magma (Dasgupta and Sengupta 2002). The ultrahigh-temperature events were followed by retrograde metamorphism at temperatures 750–800 °C under pressures 6–7 kbar, as deduced from the composition of orthopyroxenes and the coronal garnet which have rims of spinel against quartz (Sarkar et al. 2003). From relict kyanites, a clockwise path with decompression followed by isobaric cooling is witnessed in the Deobhog area (Patel et al. 2001). The mineral assemblages of khondalites and associated felspathic gneisses and porphyritic charnockites of the Araku–Paderu sector indicate a temperature of 750 ± 50 °C and pressure 7.5 ± 0.5 kbar (Divakara Rao and Murthy 1998).

The megacrystic granite widely distributed in the Central Khondalite Zone and Eastern Migmatite–Charnockite zone is characterized by very high strontium ratio (0.7172), negative correlation of Ba, Sr and Zr and positive correlation of REE, Th and Rb with SiO_2. The chemistry betrays their deep-seated origin through melting of the crust at 850°–1000 °C under pressure of 9 kbar (Divakara Rao et al. 2001).

6.4 Multiphase Magmatic Complexes

Intruding the high-grade metamorphic rocks, the NE-SW-trending dykes of a swarm adjacent to the Godavari basin in Karimnagar district have yielded ^{40}Ar–^{39}Ar dates varying from 2400 to 2200 Ma—the time of emplacement of the dyke (Mallikarjuna Rao et al. 2010).

Occurring throughout the length and breadth of the EGMB, there are thirty anorthosite complexes (Fig. 6.9). Deformed and metamorphosed the thirty-odd felspathiodal alkaline complexes are restricted to the western belt, delimited by

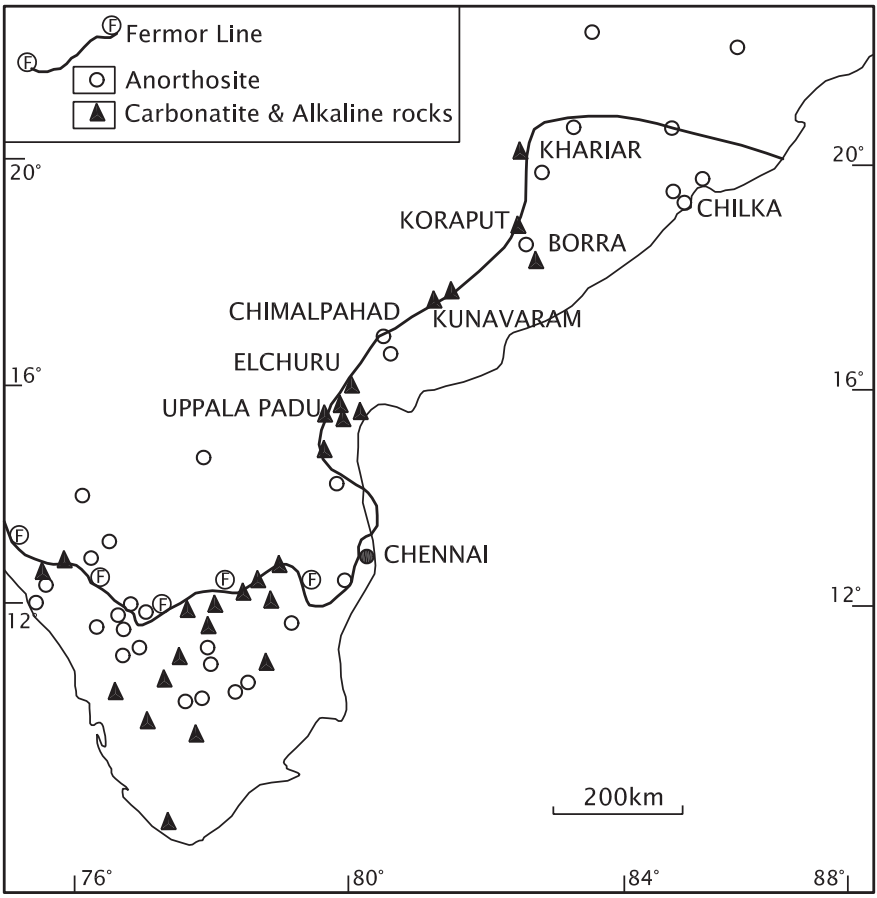

Fig. 6.9 Distribution of ultrabasic and alkaline rock complexes in the five lithological zones of the Eastern Ghat Mobile Belt (Based on Leelanandam 1989, 1993)

the crustal-scale thrust (Leelanandam 1980, 1989, 1993; Leelanandam et al. 1985, 1988, 2006; Ratnakar and Leelanandam 1989; Biswal et al. 2004). The oval or elliptical bodies of ultrabasic and alkaline rocks arranged *en echelon* in the margin of the EGMB resemble morphologically the ring complexes and seem to have been emplaced in a rift-related environment. Together with the alkaline plutons, the *massif-type anorthosite* rocks represent intrusion that has syntectonic to post-tectonic status with respect to the last phase of penetrative deformation (Sarkar et al. 1981). It may be mentioned that belonging to the Neoproterozoic, the dykes and sheets of ferrodiorite at the immediate contact of anorthosite bodies of the Chilka Lake and Bolangir areas yielded U–Pb zircon age of 933 ± 3 Ma and 792 ± 2 Ma, respectively (Krause et al. 2001) in contrast to those of the ~1352-Ma-old ferrosyenites in the Prakasam district (Vijaykumar et al. 2006).

6.4.1 Ultrabasic Layered Complexes

The *Kondapalle complex* exhibits spectacular layering in the dominant gabbro and anorthosite, and subordinate orthopyroxenite, websterite, clinopyroxenite, dunite and harzburgite (Nanda and Natarajan 1980; Leelanandam and Narasimha Reddy 1985; Leelanandam 1997, 2005; Leelanandam et al. 2006). They occur as discontinuous stratiform bodies enveloped by charnockites and gneisses. The pyroxenes from the coexisting ultrabasic rocks and charnockites indicate a P-T condition of 830–950 °C and 6.8 kbar, when the Kondapalle complex was emplaced in dry country rocks at lower- to middle-crustal level probably in the period immediately following metamorphism. The Kondapalle body is cut by 851 ± 28 Ma old dyke of metadolerite. The Kandra represents a volcanic phase (Leelanandam 1990). At Pangidi (close to Kondapalle), there is a small body of magmatically layered anorthosite complex emplaced in the high-grade supracrystal rocks similar in setting, composition and origin to the Kondapalle. Emplaced within the high-grade metamorphic rocks of the EGMB, the nearly 1634-Ma-old-layered Kondapalle magmatic suite has geochemistry strongly recalling that of rocks occurring in the subduction of an oceanic lithosphere in a "long-lived convergent margin" (Dharma Rao and Santosh 2011). The zircon 207Pb/206Pb age of the Kondapalle rocks is 1693 ± 110 Ma and of the Pangidi 1634 ± 18 Ma (Dharma Rao et al. 2012).

Its strikingly low εNd value (−14.4 ± 3.7) indicates that crustal contamination affected the magma emplaced at 1739 ± 270 Ma as Sm–Nd isochron whole-rock dating shows (Dharma Rao et al. 2004).

6.4.2 Alkaline Complexes

As already stated, the deformed alkaline complexes (Fig. 6.9) occur preponderantly in the western tectonized margin of the EGMB (Leelanandam et al. 2006). They evince apparent preferred emplacement in the shear zone between Archaean basement and Proterozoic supracrustal rocks. Ranging in length from 30 m to 30 km, the deformed bodies of gneissose nepheline syenite and carbonatite in the EGMB and Southern Granulite Terrane are concentrated within a few tens of kilometres of what may be a single suture, namely the Sileru Shear Zone (Leelanandam et al. 2006). These bodies mark sites of intracontinental rifting, and plutons of calcic anorthosite suggest peaks of petrotectonic events at 1000, 750 and 550 Ma.

The nepheline syenite bodies in Elchuru, Purimetta and Uppalapadu and the syenite-quartz syenite pluton at Settupalle belong to the category mentioned above (Leelanandam 1989, 2006; Ratnakar and Leelanandam 1989). They also occur in the belt between the Western Charnockite Zone and Western Khondalite Zone (Ramakrishnan et al. 1998). The *Koraput complex* in northern part occurs within

the Western Khondalite Belt (Bose 1970; Nanda and Pati 1989). Interestingly, strain partitioning in the Koraput Complex ensured preservation of igneous textures in its gabbroic core (Gupta et al. 2005). There is another view that this complex was emplaced synkinematically due to hotspot activity in a pull-apart structural basin far from the EGMB boundary (Bhattacharya and Kar 2005). In the Prakasam district, fayalite–quartz-bearing ferrosyenite, characterized by eulite, ferrosilite and inverted pigeonite resulting from high-temperature (~1000 °C) initial crystallization from a melt that was tholeiitic (not alkalic) in character—was genetically unrelated to normal nepheline syenite (Leelanandam 1993; Vijaykumar et al. 2006). The ferrosyenites of Errakonda and Gokanakonda are composed of eulitic and ferro-silicic orthopyroxenes and almandine garnet plus exceptionally iron-rich olivine. Spatially associated with gabbro-anorthosite masses, the ferrosyenites probably represent a highly evolved and fractionated parental magma at 660–810 °C temperature and 6.2–7.6-kbar pressure.

The Elchuru body was emplaced at ~1321 Ma (Upadhyay et al. 2006) in the NE–SW-trending fault of the western marginal zone. It is a suite of rocks having miaskitic affinity varying in composition from ultrabasic to felsic. The Rb–Sr isochron age of the complex is 1242 ± 33 Ma (Subba Rao et al. 1989). Northeast of the Elchuru complex occurs the Kunavaram complex in the same setting, thus showing similar petrochemical evolution (Subbarao 1971). While the nepheline syenite was derived from an Rb-depleted and Sr–Ba-enriched source, the syenite came from Ba-enriched and Rb–Sr-depleted magma. Near Borra in the Vishakhapatnam district, an *ultrapotassic rock* is composed of leucite, K-felspar, graphite, apatite together with diopside, meionite and phlogopite. It occurs in thin veins and veinlets within pyroxenites associated with calc silicate granulites and dolomitic marble (Bhowmik 2000). Emplaced after the early phase of ultrahigh-temperature metamorphism along late ductile shear zone at mid-crustal level, the Borra veins betray lamproitic affinity.

The *Khariar complex* in Odisha occupies the two-km-wide SE-dipping shear zone of the terrane boundary thrust (Biswal et al. 2004). Characterized by foliation, strong mineral lineation and fold fabric, this concordant body is surrounded by mylonites. Emplaced in the riftogenic setting along the tectonic junction between the EGMB and the Bastar Craton, the Khariar alkaline complex is dated 1480 ± 70 Ma (Upadhyay et al. 2006). The zircon grains from the nepheline syenites show crystallization age (U–Pb) of 1500 ± 3/4 Ma (Aftalion et al. 2000).

6.5 Evolution of Continental Crust

On the basis of interpretation of isotopic geochemistry of minerals and whole-rock age data, a model of evolution of the EGMB has been suggested. Older rocks were reworked, and a new crust formed and accreted onto the mobile belt (Sarkar and Paul 1998). The generation of charnockitic suite under granulite facies conditions took place nearly 3000 million years ago as borne out by Sm–Nd and

Rb–Sr whole-rock systematics and Pb–Pb zircon dating (Fig. 6.10). The Pb–Pb prismatic zircon age of 3000 Ma and the Sm–Nd model dates between 3400 Ma and 3500 Ma with negative epsilon values imply incorporation of Archaean continental material in the making of the EGMB lithology (Bhattacharya al. 2001). The Nd model ages between 3200 and 3400 Ma for the orthogneisses north of the Godavari Graben (Rickers et al. 2001) provide support for this deduction. The other view is that the Archaean material represented by protoliths was wholly recycled during the Mesoproterozoic (Dasgupta 1995).

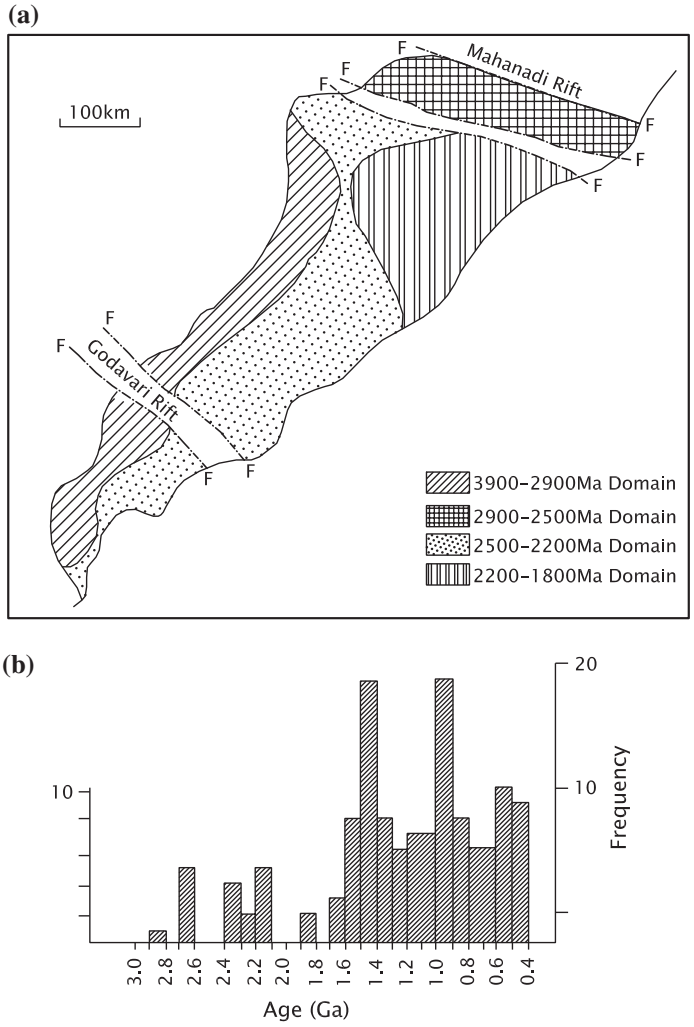

Fig. 6.10 **a** Isotopic age domains in the Eastern Ghat Mobile Belt (Dasgupta and Sengupta 2002). **b** Age peaks of rocks of the EGMB at 1500, 900 and 500 Ma (Sarkar and Paul 1998)

In the Mesoproterozoic time, a new crust was formed. It embodied differentiated suite of charnockites and massif-type anorthosites, alkaline rocks and genetically connected ultrabasic bodies. The new crust was accreted onto the terrane of the Eastern Ghat (Sarkar and Paul 1998). Rounded grains of ziron having Pb–Pb age of 2600 Ma may be taken as indicators of the time of recrystallization or reprecipitation (Bhattacharya and Kar 2004). The Nd model ages between 2300 and 2500 Ma for orthogneisses, between 2600 and 2800 Ma for metasediments in the Western Charnockite Zone—south of the Godavari Graben—between 1800 and 2200 Ma for rocks of the Migmatite–Charnockite Zone and Western Khondalite Zone and between 1800 and 3200 Ma for orthogneisses of the transitional belt between the above two zones (Ricker et al. 2001)—unequivocally show that the bulk of the EGMB is made up of Mesoproterozoic rocks. The U–Pb age of 1600 Ma for monazite, allanite and zircon, and $^{40}Ar/^{39}Ar$ age of hornblende from rocks of all over the Western Charnockite Zone indicate that there was indeed a thermal event towards the close of the Mesoproterozoic era (Mezger and Cosca 1999). Monazite from spinel granulite has also been dated (Rao et al. 1998).

The EGMB was later affected by Grenvillian deformation and charnockitization as borne out by dates between 800 and 1100 Ma for sapphirine granulites and charnockites of the Visakhapatnam area (Grew and Menton 1986) and the pegmatites (Sarkar and Paul 1998). Concordant 516 ± 1 Ma U–Pb zircon age for apatite-magnetite veins in plutons and the hornblende age from the central zone (Kovach et al. 1997) show that the EGMB was overtaken also by Pan-African geodynamic development. The 500-million-year-old Vishakhapatnam Granite stands testimony to the Cambro–Ordovician upheaval.

6.6 Mineral Deposits

Constituting the most important mineral asset of the EGMB, *bauxite* occurs as a red and yellow blanket, forming mesa-type plateaus in the western and southern parts of the granulitic terrain. Low in silica, the bauxite deposits consist of gibbsite, goethite and haematite, produced by protracted weathering of rocks.

Medium- to high-grade ores of *graphite* occur in bedded form in the khondalite succession associated with quartzites and migmatites, such as seen at Tumudibend in Kalaherds district, Bolangir and Sambalpur district. Pure coarsely flaky graphite occurs in pegmatites also.

Silicates, oxides and carbonates of *manganese* form small deposits within banded quartzite and at the contacts of quartzites and calc-granulites near Vishakhapatnam, Srikakulam, Vijayanagaram and Koraput. The Garbham–Koduru manganese deposit, known as *Kodurite* that is equated with the *Gondite* in the Bastar cratonic block, is a product of metamorphism of syngenetic oxides at.

Low-grade *sillimanite* deposits of restricted distribution occur in the sillimanite–quartz schist as seen near Palasama in the Sambalpur district.

There are insignificant occurrence of *precious and semi-precious minerals* such as aquamarine, yellow beryl, sapphire, and amethyst, in nepheline syenites and aegirine syenite along the western tectonic border of the EGMB. There are veins bearing fluorapatite and magnetite in ultrabasic bodies at Kasipatna, near Borra.

References

Aftalion, M., Bower, D. R., Dash, B., & Fallick, A. E. (2000). Late Pan-African thermal history in the Eastern Ghats terrane, India, from U-Pb and K-Ar isotopic study of the Mid-Proterozoic Khariar alkali syenite, Orissa. *Geological Survey of India Special Publication, 57*, 26–33.

Bhadra, S., Gupta, S., & Banerjee, M. (2004). Structural evolution across the Eastern Ghats Mobile Belt-Bastar Craton boundary, India: Hot over cold thrusting in an ancient collision zone. *Journal of Structural Geology, 26*, 233–245.

Bhattacharya, S. (2002). Nature of crustal trijunction between the Eastern Ghats Mobile Belt, Singhbhum Craton and Bastar Craton around Paikmal, Western Orissa: Structural evidence of oblique collision. *Gondwana Research, 1*, 53–62.

Bhattacharya, S. (2004). High-temperature crustal-scale shear zone at western margin of the Eastern Ghats granulite belt, India: Implications for rapid exhumation. *Journal of Asian Earth Sciences, 24*, 281–290.

Bhattacharya, G. C., Chaubey, A. K., Murty, G. P. S., Srinivas, K., Sarma, K. V. L. N. S., Subrahmanyam, V., & Krishna, K. S. (1994). Evidence for seafloor spreading in the Laxmi Basin, northeastern Arabian Sea. *Earth and Planetary Science Letters, 125*, 211–220.

Bhattacharya, S., Kar, R. (2004). Alkaline intrusions in a granulite ensemble in the Eastern Ghats belt: Shear zone pathway and a pull-apart structure. *Proceedings of the Indian Academy of Sciences* (*Earth and Planetary Sciences*), *113*, 37–48.

Bhattacharya, S., & Kar, R. (2005). Petrological and geochemical constratints on the evolution of the alkaline complex of Koraput in Eastern Ghats Granulite Belt, India. *Gondwana Research, 8*, 596–602.

Bhattacharya, S., Kar, R., Misra, S., & Teixeira, W. (2001). Early Archaean continental crust in the Eastern Ghats Granulite belt, India: Isotpic evidence from a charnockite suite. *Geological Magazine, 138*, 609–618.

Bhowmik, S. K. (2000). Ultrapotassic rocks along late ductile shear zones from the Eastern Ghats belt, India. *Gondwana Research, 3*, 55–63.

Biswal, T. K., Ahuja, H., & Sahu, H. S. (2004). Emplacement kinematics of nepheline syenites from the Terrane Boundary Shear Zone of the Eastern Ghats Mobile Belt, West of Khariar, NW Orissa: Evidence from meso-and micro-structures. *Proceedings of Indian Academy Science* (*Earth and Planetary Science*), *113*, 785–793.

Biswal, T. K., Jena, S. K., Datta, S., Das, R., & Khan, K. (2000). Deformation of the Terrane Boundary Shear Zone (Lakhna Shear Zone) between the Eastern Ghats Mobile belt and the Bastar Craton, in Bolangir and Kalahandi districts of Orissa. *Journal of Indian Geophysical Union, 55*, 367–380.

Biswal, T. K., Sanjeevan, G., & Nayak, B. P. (1998). Deformational history of Eastern Ghats Mobile Belt around Lathore, Bolangir district, Orissa. *Journal of Indian Geophysical Union, 51*, 219–225.

Biswal, T. K., & Sinha, S. (2003). Deformation history of the NW salient of the Eastern Ghats Mobile Belt, India. *Journal of Asian Earth Sciences, 22*, 157–169.

Bose, M. K. (1970). Petrology of the intrusive alkalic suite of Koraput, Orissa. *Journal of Indian Geophysical Union, 11*, 99–126.

Bose, S., Pal, S., & Fukuoka, M. (2003). Pressure-temperature-fluid evolutionary history of orthopyroxene-bearing quartzofelspathic and mafic granulites from northern parts of the Eastern Ghats belt, India: Impliciations for Indo-Antarctica correlation. *Journal of Asian Earth Sciences, 22*, 81–100.

Chetty, T. R. K. (1995). A correlation of Proterozoic shear zones between Eastern Ghats, India and Enderby Land, East Antarctica on Landsat imagery. *Memoirs-Geological Society of India, 34*, 205–220.

Chetty, T. R. K., Bhaskar Rao, Y. J., & Narayana, B. L. (2003a). A structural cross section along Krishnagiri-Palani corridor, Southern Granulite Terrain of India. *Memoirs-Geological Society of India, 50*, 255–277.

Chetty, T. R. K., & Murthy, D. S. N. (1994). Collision tectonics in the Late Precambrian Eastern Ghats Mobile Belt: Mesoscopic to satellite-scale structural observation. *Terra Nova, 6*, 72–81.

Chetty, T. R. K., Vijay, P., Narayana, B. L., & Giridhar, G. V. (2003b). Structure of the Nagavalli shear zone, Eastern Ghats Mobile Belt: Correlation in the East Gondwan reconstruction. *Gondwana Research, 6*, 215–229.

Crowe, W. A., Nash, C. R., Harris, L. B., Leeming, P. M., & Rankin, L. R. (2003). The geology of the Rengali Province: Implications for the tectonic development of northern Orissa, India. *Journal of Asian Earth Sciences, 21*, 697–710.

Dasgupta, S. (1995). Pressure-temperature evolutionary history of the Eastern Ghats Granulite province: Recent advances and some thoughts. *Memoirs-Geological Society of India, 34*, 101–110.

Dasgupta, S., & Sengupta, P. (2002). Ultra-high temperature metamorphism in the Eastern Ghats belt, India: evidence from high Mg-Al granulites. *Proceedings of the Indian National Science Academy, 68A*, 21–34.

Dharma Rao, C. V., Santosh, M., & Dong, Y. (2012). U-Pb zircon chronology of the Pangidi-Kondapalle layered intrusion, Eastern Ghats belt, India, Constraints on Mesoproterozoic arc magmatism in a convergent margin setting. *Journal of Asian Earth Sciences, 49*, 362–378.

Dharma Rao, C. V., Santosh, M., Purohit, R., Wang, J., Jiang, X., & Kusky, T. (2011). LA-ICP-MS and U-Pb zircon age constraints on the Palaeoprorterozoic and Neoarchaean history of the Sandmata complex in Rajasthan within the NW Indian Plate. *Journal of Asian Earth Sciences, 42*, 286–305.

Dharma Rao, C. V., Vijaya Kumar, T., & Bhaskar Rao, Y. J. (2004). The Pangidi anorthosite complex, Eastern Ghats granulite belt, India: Mesoproterozoic Sm-Nd isochron age and evidence for significant crustal contamination. *Current Science, 87*, 1614–1618.

Divakara Rao, V., & Murthy, N. N. (1998). Thermobarometry and mineral chemistry of granulite-facies rocks from Eastern Ghats, India. *Gondwana Research, 1*, 267–274.

Divakara Rao, V., Narayana, B. L., & Murthy, N. N. (2001). Time-space relation between the megacrystic granites and leptynites in the Eastern Ghats Granulite belt: Evidence for peak-metamorphic anatectic melting. *Gondwana Research, 4*, 219–222.

Dobmeier, C. J., & Raith, M. M. (2003). Crustal architecture and evolution of the Eastern Ghat Granulite Belt and adjacent regions of India, Geological Society of London Special Publication No. 6, pp. 145–168.

Grew, E. S., & Manton, W. I. (1986). A new correlation of sapphire-granulite in the Indo-Antarctica metamorphic terraine, Late Proterozoic dates from the Eastern Ghats. *Precambiran Research, 33*, 123–139.

Gupta, S., Nanda, J., Mukherjee, S. K., & Santra, M. (2005). Alkaline magmatism versus collision tectonics in the Eastern Ghat belts, India: Constraints from structural studies in the Koraput Complex. *Gondwana Research, 8*, 403–419.

Kovach, V. P., Salnikova, E. B., Kotov, A. B., Yakova, S. J., & Rao, A. T. (1997). Pan-African U-Pb zircon age from apatite-magnetite veins of Eastern Ghats granulite belt, India. *Journal of Indian Geophysical Union, 50*, 421–424.

Krause, O., Dobmeier, C., Raith, M., & Mezger, K. (2001). Age and emplacement of massif-type anorthosites in the Eastern Ghats Belt, India: Constraints from U-Pb zircon dating and structural studies. *Precambrian Research*, 25–38.

Kumar, N., Singh, A. D., Gupta, S. B., & Mishra, D. C. (2004). Gravity signature, crustal architecture and collision tectonics of the Eastern Ghats Mobile Belt. *Journal of Indian Geophysical Union, 8*, 97–106.

Lal, R. K. (1997). Internally consistent calibrations for geothermobarometry of high-grade Mg-Al rich rocks in the system MgO-Al_2O_3-SiO_2 and their applications to sapphirine-spinel granulites of Eastern Ghats, India and Enderby Land, Antarctica. *Proceedings of the Indian Academy of Sciences* (*Earth and Planetary Sciences*), *106*, 91–113.

Lal, R. K., Ackermand, D., & Upadhyay, H. (1987). P-T-X relationship deduced from corona textures in sapphirine-spinel-quartz assemblages from Paderu, Southern India. *Journal of Petrology, 28*, 1139–1168.

Leelanandam, C. (1980). Some observations on the alkaline provinces in Andhra Pradesh. *Current Science, 50*, 799–802.

Leelanandam, C. (1989). The Prakasm Alkaline Province in Andhra Pradesh, India. *Journal of Indian Geophysical Union, 34*, 25–45.

Leelanandam, C. (1990). Kandra Volcanics in Andhra Pradesh: Possible ophiolite. *Current Science, 59*, 785–788.

Leelanandam, C. (1993). Eulitic and ferrosilitic orthopyroxenes from ferrosyenitic of South India: Evidence for a high-temperature crystallization and tholeiitic parentage. *Current Science, 64*, 729–735.

Leelanandam, C. (1997). The Kondampalli layered complex, Andhra Pradesh: Synoptic overview. *Gondwana Research, 1*, 95–114.

Leelanandam, C., Burke, K., Ashwal, L. D., & Web, S. J. (2006). Proterozoic mountain building in Peninsular India: An analysis based primarily on alkaline rock distribution. *Geological Magazine, 143*, 195–212.

Leelanandam, C., & Narasimha Reddy, M. (1985). Petrology of the Chimalpahad anorthosite complex, Andhra Pradesh, India. *Neues Jahrbuch fur Mineralogie-Abhandlungen, 153*, 91–119.

Leelanandam, C., Ratnakar, J., & Narasimha Reddy, M. (1988). Anorthosites and alkaline rocks from the deep crust of Peninsular India. *Journal of Indian Geophysical Union, 31*, 66–86.

Mahalik, N. K. (1994). Geology of the contact between the Eastern Ghats belt and North Orissa Craton. *Journal of Indian Geophysical Union, 44*, 41–51.

Mahalik, N. K. (1996). Lithology and tectonothermal history of the Precambrian rocks of Orissa along the Eastern coast of India. *Journal of Asian Earth Sciences, 14*, 209–219.

Mallikarjuna Rao, J., Poornachandra Rao, G. V. S., Widdowson, M., Yellappa, T., & Kelley, S. P. (2010). Tectonic history and occurrence of 2.4 Ga mafic dyke swarms adjacent to Godavari Basin, Karimnagar. *Current Science, 98*, 1472–1478.

Mezger, K., & Cosca, M. A. (1999). The thermal history of the Eastern Ghats Belt (India) as revealed by U-Pb and 40Ar/39Ar dating of metamorphic and magmatic minerals: implications for SWEAT correlation. *Precambrian Research, 94*, 251–271.

Mohan, A., Singh, P. K., & Sachan, H. K. (2003). High-density carbonic fluid inclusions in charnockites from Eastern Ghats, India: Petrologic implications. *Journal of Asian Earth Sciences, 22*, 101–113.

Nanda, J. K., & Natarajan, V. (1980). Anorthosites and related rocks of the Kondampalli Hills, Andhra Pradesh. *Records of the Geological Survey of India, 113*, 57–67.

Nanda, J. K., & Pati, U. C. (1989). Field relations and petrochemistry of granulites and associated rocks in the Ganjam-Koraput sector of the Eastern Ghats belt. *Indian Minerals, 43*, 247–264.

Natarajan, V., & Nanda, J. K. (1981). Large-scale basin and dome structures in the high-grade metamorphics near Visakhapatnam, South India. *Journal of Indian Geophysical Union, 22*, 548–592.

Patel, S. C., Behra, S., Mohanty, A., Singh, A. K., & Patel, S. K. (2001). Metamorphic history of sapphirine-and relict-kyanite bearing Mg-Al rich rocks at Hatimunda Hill near Junagarh, Kalahandi district, Orissa. *Journal of Indian Geophysical Union, 57*, 417–428.

Paul, D. K., RayBarman, P., McNaughton, N. J., Fletcher, I. R., Potts, P. J., Ramakrishnan, M., & Augustine, P. F. (1990). Archaean-Proterozoic evolution of Indian charnockites: Isotope and geochemical evidence from granulites of the Eastern Ghats belt. *Journal of Geology, 98*, 253–263.

Rajesham, T., Bhaskar Rao, Y. J., & Murti, K. S. (1992). The Karimnagar granulite terrane—a new sapphirine-bearing granulite province, South India. *Journal of Indian Geophysical Union, 41*, 51–59.

Ramakrishnan, M., Nanda, J. K., & Augustine, P. F. (1998). Geological evolution of the Proterozoic Eastern Ghats Mobile Belt. *Geological Survey of India Special Publication, 44*, 1–21.

Rao, A. T., Divakara Rao, V., Yoshida, M., & Asima, M. (1995). Geochemistry of charnockites from the Eastern Ghats granulite belt—evidence for possible linkage between India and Antarctica. *Memoirs-Geological Society of India, 34*, 273–291.

Rao, A. T., Fonarav, V. I., Konilov, A. N., & Romeanenko, M. (1998). Electron microprobe dating of monazite from spinel granulite in the Eastern Ghats belt, India. *Journal of Indian Geophysical Union, 52*, 345–350.

Ratnakar, J., & Leelanandam, C. (1989). Petrology of alkaline plutons from the eastern and southern Peninsular India. *Memoirs-Geological Society of India, 15*, 145–176.

Rickers, K., Mezger, K., & Raith, M. M. (2001). Evolution of the continental crust in the Proterozoic Eastern Ghats Belt, India and new constraints for Rodinia reconstruction: Implications from Sm-Nd, Rb-Sr and Pb-Pb isotopes. *Precambrian Research, 112*, 183–210.

Saha, D. (2011). Dismembered ophiolites in Palaeoproterozoic nappe complexes of Kandra and Gurramkonda, South India. *Journal of Asian Earth Sciences, 42*, 158–175.

Saha, D., Chakraborti, S., & Tripathy, V. (2010). Intracontinental thrusts and inclined transpression along eastern margin of the East Dharwar craton, India. *Journal of the Geological Society of India*, *75s*, 323–337.

Sarkar, A., Bhanumati, L., & Balasubramanyan, M. N. (1981). Petrology, geochemistry and geochronology of the Chilka Lake igneous complex, Orissa, India. *Lithos, 14*, 93–111.

Sarkar, A., & Paul, D. K. (1998). Geochronology of the Eastern Ghats mobile belt—a review. *Geological Survey of India Special Publication, 44*, 51–86.

Sarkar, A., Sarangi, S., Bhattacharya, S. K., & Ray, A. K. (2003a). Carbon isotope across the Eocene-Oligocene boundary sequence of Kutch, western India: Implications to oceanic productivity and CO_2 change. *Geophysical Reseach Letters, 30*, 1–4.

Sarkar, A., Yoshioka, H., Ebihara, M., & Naraoka, H. (2003b). Geochemical and organic carbon isotope studies across the continental Permo-Triassic boundary of Raniganj basin, eastern India. *Palaeogeography, Palaeoclimatology, Palaeoecology, 191*, 1–14.

Sen, S. K., & Bhattacharya, S. (1997). Dehydration melting of micas in the Chilka Lake Khondalites: The link between the metapelites and granitoids. *Proceedings of the Indian Academy of Sciences* (*Earth and Planetary Sciences*), *106*, 277–297.

Stein, H. J., Hannah, J. L., Zimmermann, A., Markay, R. J., Sarkar, S. C., & Pal, A. B. (2004). A 2.5 Ga porphyry Cu-Mo-Au deposit at Malanjkhand, central India: Implications for Late Archaean continental assembly. *Precambrian Research, 134*, 189–226.

Subba Rao, T. V., Bhaskar Rao, Y. J., Sivaraman, T. V., Gopalan, K. (1989). Rb-Sr age and petrology of the Elchuru alkaline complex: Implication to alkaline magmatism in the Eastern India. *Memorial Geological Society of India*, *15*, 207–223.

Subbarao, K. V. (1971). The Kunavaram series—a group of alkaline rocks, Khammam district, Andhra Pradesh, India. *Journal of Petrology, 12*, 621–641.

Subrahmanyam, C., & Verma, S. K. (1986). Gravity fields, structure and tectonics of the Eastern Ghats. *Tectonophysics, 126*, 195–212.

Upadhyay, D., Raith, M. M., Mezger, K., Bhattacharya, A., & Kinny, P. D. (2006a). Mesoproterozoic rifting and Pan-African continental collision in SE India: Evidence from the Khariar alkaline complex. *Contributions to Mineralogy and Petrology, 151*, 434–456.

Upadhyay, D., Raith, M. M., Mezger, K., & Hammerschmidt, K. (2006b). Mesoproterozoic rift-related alkaline magmatism at Elechuru, Prakasam Alkaline Province, SE India. *Lithos, 89*, 447–477.

Vijaykumar, K., Reddy, M. N., & Leelanandam, C. (2006). Dynamic melting of the Precambrian mantle: Evidence from rare earth elements of the amphibolites from the Nellore-Khammam Schist Belt, South India. *Contributions to Mineralogy and Petrology, 152*, 243–256.

Chapter 7
Southern Granulite Terrane of Pan-African Rejuvenation

7.1 Two Geological Domains

South and south-east of the Archaean Dharwar Craton, across a prominent terrane-defining shear zone, the southern part of the Peninsular India (Fig. 7.1) is known as the *Southern Granulite Terrane* (SGT). It embodies two lithotectonically contrasted domains or subprovinces that have undergone different tectonothermal upheavals. The larger southern part, embracing Tamil Nadu and central and southern Kerala, is made up of high-grade metamorphics and predominant charnockites. Two blocks—Madurai and Trivandrum—separated by a shear zone make up this part of the SGT. The terrain is dominated by lofty the Palni (~2100 m), Anaimalai (2695 m) and Elaimalai (2670 m) mountain ranges of the southern Sahyadri.

The northern part of the SGT is more than 100 km wide domain of shear zones with blocks of the Nilgiri (2670 m), Kollimalai–Pachaimalai (1525 m) and Shevaroy (1647 m) massifs entangled with strongly deformed and radically reconstituted rocks of Archaean antiquity and penetrated by Neoproterozoic to Cambro–Ordovician plutons. The Nilgiri, Kollimalai–Pachaimalai and Shevaroy blocks bear very strong resemblance with the rocks and structural styles of the domains of the Dharwar Craton and seem to represent its dismembered and displaced parts (Fig. 7.2). The northern shear zone, occupied by the Moyar River, separates the northern block of the SGT from the Dharwar Craton. And the southern shear zone constitutes the boundary between the Madurai Block and the Palakkad–Tiruchirapalli Belt along the foothills of the Palni Range. Between these two terrane boundaries runs from east to west the transition terrane of mixed rocks, belonging to both the Dharwar and the SGT. It is characterized by high-grade metamorphic rocks penetrated by ultrabasic and alkaline complexes of Proterozoic ages, geophysical peculiarities of its lithospheres, higher-than-normal heat flow, and mild to low seismic activities.

K.S. Valdiya, *The Making of India*, Society of Earth Scientists Series,
DOI 10.1007/978-3-319-25029-8_7

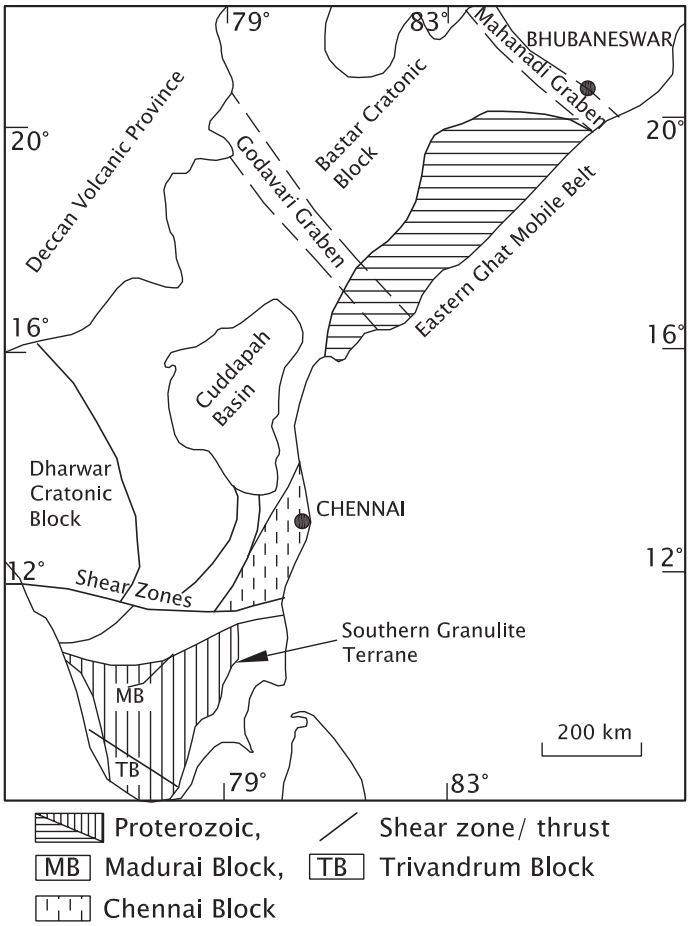

Fig. 7.1 Sketch map shows the Southern Granulite Terrane with respect to the Dharwar Craton, the Cuddapah Basin of Proterozoic sedimentation and the Eastern Ghat Mobile Belt of proterozoic antiquity (based on Satyanarayana et al. 2003; Ramakrishnan 2003)

7.2 Geophysical Characteristics

Aeromagnetic survey indicated that the SGT comprises discrete crustal blocks separated by planes of vertical movements and that crustal thickness increases northwards and eastwards (Reddi et al. 1988). This crust is cut by a profound structural dislocation along the Palakkad–Kaveri line designated as the Palghat–Cauvery Shear Zone (P–CSZ). Magnetotelluric apparent resistivity data indicate a heterogeneous nature of the lithosphere in this belt of P–CSZ. The highly resistive crust is underlain by a thick conducting layer with relatively uniform average structure stretching north from the foothills of the Kodaikanal Range to the P–CSZ

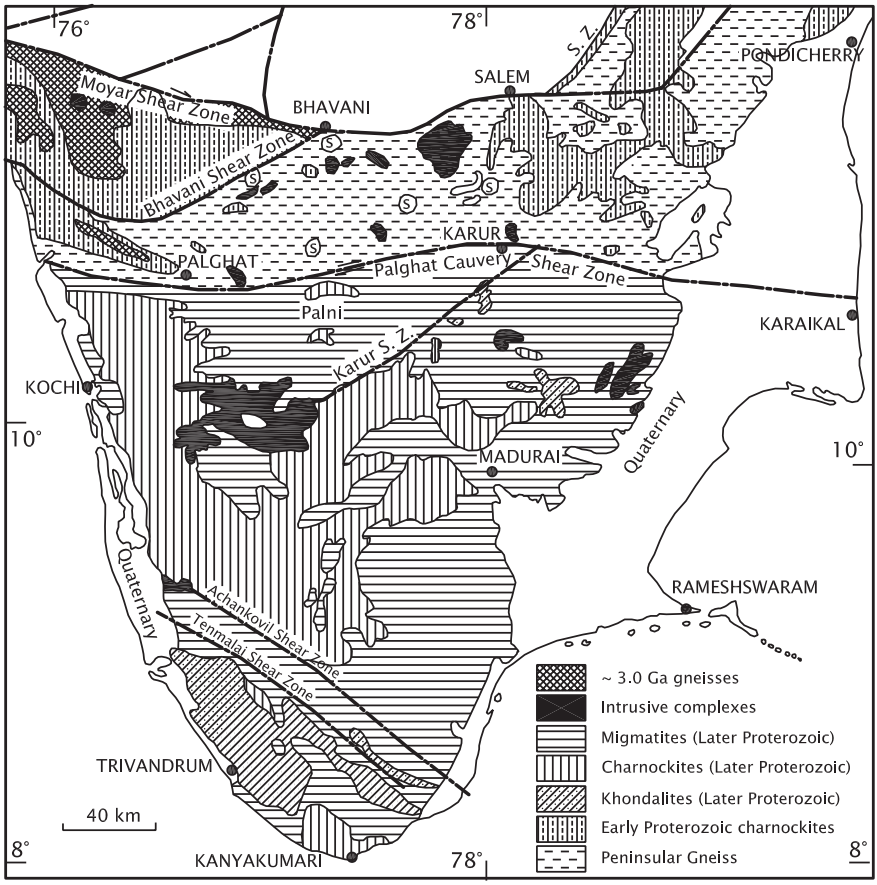

Fig. 7.2 Sketch map shows the structural framework and lithological assemblages of the Southern Granulite Terrane (after generalized geological map: Project Vasundhara, Geol. Surv. India, Kolkata, 1994)

(Manglik 2005). This is in contrast to a drastically different subcrust having high conductivity and 60-km extension up to the P-CSZ. This contrast is interpreted to indicate existence of a steeply dipping fault reaching a depth greater than 60 km.

The composite airborne, total intensity map plus gravity anomaly modelling with seismic constraints suggest (i) presence at the depth 6–8 km of high-density mafic rocks along the P–CSZ (ii) the thickening of the crust to 44–46 km south of it and (iii) the northward thrusting of the lower crustal granulites with ultrabasic bodies (Mishra and Vijaya Kumar 2005). There is relatively higher amount of heat flow and mild to low seismic activity along this zone (Roy and Rao 2000). The seismic structure indicates presence of, as stated above, a southward-dipping interface in the crust that has thinned to 38–40 km in the P–CSZ (Mishra and Rao 1993). In the Kuppam–Kodaikanal transect, the low-velocity mid-crust lies at the

depth between 20 and 30 km (Reddy et al. 2003) and paired or bipolar gravity lows and highs (Fig. 7.3) indicate subcrustal inhomogeneity (Singh et al. 2003). Based on tonometry, it is inferred that the crust is 4–5 km thicker south of the Moyar–Attur Shear Zone (M–ASZ) compared to that of the Dharwar domain and that the low-velocity (−3 %) zone in the upper mantle in the Palni Range is a product of N–S compression (Srinagesh and Rai 1996). The N–S compression must have caused crustal upwarping along pre-existing weak zones, faults or thrusts and given rise to the shear zones.

It is evident that the pattern of geophysical variations in the lithosphere the style and intensity of deformation, the distribution of ultrabasic and alkaline plutonic bodies in the granulitic assemblages, and the isotopic age data collectively point to the presence of three lithotectonic subdivisions in the Southern Granulite Terrane (SGT)—(i) the Nilgiri–Pachaimalai Belt of Late Archaean rocks having NE–SW structural trends and delimited by the E–W-oriented M–ASZ in the north and the P-CSZ in the south, (ii) the Pollachi–Tiruchirapalli Belt defined by the P–CSZ in the north and the Karur–Oddanchatram Shear Zone in the south and (iii) the Madurai–Trivandrum Block constituting what is also described as Pandyan mobile province (Ramakrishnan 2003).

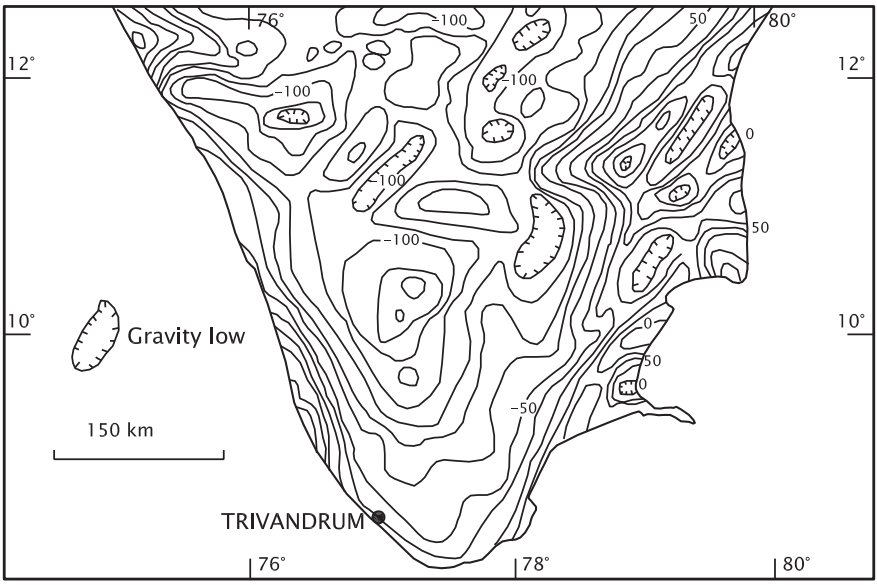

Fig. 7.3 Bouguer gravity anomaly map of the southern part of the Peninsular India (based on Verma 1985)

7.3 Structural Framework

As already adumbrated, the southern part of the Peninsular India is characterized by wide, long and deep shear zones separating the SGT (Fig. 7.1) into disparate domains or subprovinces (Vemban et al. 1977; Drury et al. 1984). These shear zones cut across the crust as evident from pronounced geophysical anomalies. And they provided pathways to magmas in their ascent and to the flow of heat coming from depth. Moreover, they evince continuing tectonic movement albeit of mild intensity. The most important shear zones are described in the following pages.

7.3.1 Moyar–Attur Shear Zone

Curvilinear in trend, the E–W-oriented steeply dipping shear zone demarcates the northern boundary of the northern block of the SGT against the Dharwar Craton. The nearly 200-km-long and 10-km-wide shear zone is followed by the Moyar River in its western segment, and its eastern part follows the Attur tract (Chetty 1996). It is linked to another arcuate shear zone that defines the southern foothills of the Nilgiri massif and is occupied by the Bhavani River (Fig. 7.2). The faults of M–ASZ (Fig. 7.4), registering predominant dip-slip movements (Naha and Srinivasan 1996), are responsible for exhumation or bringing up to the surface of lower crustal charnockitic and granulitic rocks. Repeated dip-slip movements on it also caused their northward thrusting up to form the lofty Nilgiri mountain presently more than 2500 m in elevation (Valdiya 1998; Chetty et al. 2003). Simultaneously, there was dextral strike-slip displacement of the order of 70 km (Drury et al. 1984; Jain et al. 2003; Chetty et al. 2003). The intensity and recurrence of movements on this fault system is reflected in the widespread nature of structural deformation and retrogressive changes in the rock assemblages, including basic granulite, enderbitic granite and mafic plutons (Srikantappa and Narasimha 1988). It may be mentioned that the Nilgiri massif is made up of metamorphic rocks that evolved under high temperatures and pressures—720–880 °C and 6.7–9.5 kbar (Janardhan et al. 1988; Raith et al. 1997; Srikantappa 1993). The E–W *Attur Shear Zone* is a 1–1.5 km wide zone of phyllonites, resulting in ductile shearing and attendant mylonitization of rocks that dip 80–70°. These facts imply relative vertical uplift of adjacent blocks in addition to their dextral sliding (Chetty 1996; Bhadra 2000; Jain et al. 2003). The Attur Shear Zone—regarded as the eastward extension of the Moyar–Bhavani Shear Zone—is characterized by occurrence of 10-m-thick zone of low-angle thrust of foliated mylonites, the foliation dipping gently southwards. The thrust is inclined southwards (Biswal el al. 2010). The thrust zone is associated with recurrent shear folds. The thrust is responsible for upliftment of the charnockites of the upper crust (Biswal et al. 2010). South-east of the Cauvery Shear Zone, the Manamedu Complex, involved in the imbrications of thrust sheets, comprises pyroxene–actinolite hornblendite,

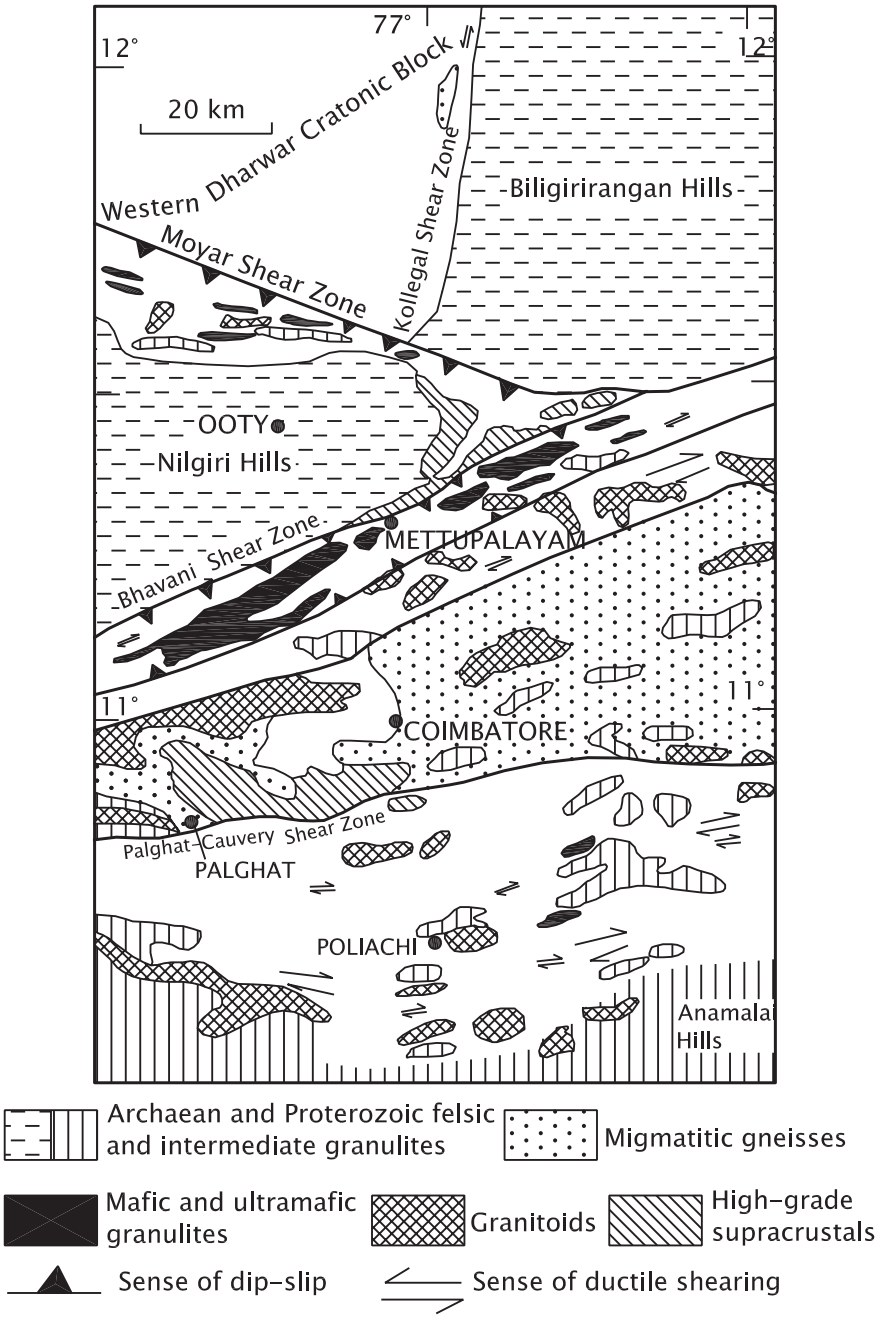

Fig. 7.4 Moyar–Bhavani Shear Zone related to other shear zones which collectively define the northern margin of the Southern Granulite Terrane (after Braun and Kriegsmann 2003)

gabbronorite, gabbro, anorthosite, amphibolites, mafic dykes and pelagic sedimentary rocks including chert and magnetite schist (Chetty et al. 2011). The imbricated package is related to a south-verging back thrust (Chetty et al. 2011). From Salem to the upper reaches of the Moyar River, in the Moyar Shear Zone, there is a systematic rotation of NNE–SSW-oriented structures of the Late Archaean Nilgiri–Pachaimalai domain, implying large-scale strike-slip displacement (Jain et al. 2003) under essentially transpressional regime (Valdiya 1998).

The nature of the M–ASZ is a matter of divergent opinion. It is regarded as a zone of amalgamation of the SGT with the Dharwar Craton, the welding having taken place synchronously with the regional metamorphism at 2480 Ma in the Dharwar Craton (Raith et al. 1997). The *Bhavani Shear Zone* (BSZ) that branches off from it evolved quite later, possibly during the Pan-African upheaval. It has brought about decoupling of the Nilgiri massif from the SGT. The BSZ seems to be a detachment fault. The other view is that there was thrusting of the Late Archaean rocks of the SGT during the Paleoproterozoic, but there was no crustal accretion (Chetty et al. 2003). The widespread shearing related to transpressional regime occurred during the Neoproterozoic when the Nilgiri massif was thrust up against the Dharwar terrane. The Nilgiri is thus an allochthonous—uprooted, displaced and thrust up—mass and the M–ASZ does not represent a zone of collision or amalgamation of two continents (Valdiya 1998; Jain et al. 2003).

North-east of the Moyar Valley, there is the *Bavali Zone* in northern Kerala. It is manifested in spatially filled gravity anomaly and is characterized by northward thinning by 2 km of the 34–41-km-thick SGT crust (Ramakrishnan 2003). Dipping steeply southwards, the shear zone extends deep into the lithosphere, affecting even the Moho, albeit slightly. Eastwards in the Wynad plateau, it is less prominent. The westward extension of the Bavali Zone in the mouth of the Ponnani River is evident from sinistral shifting of the coast (Ramaswamy 1995).

7.3.2 Palghat–Cauvery Shear Zone

Passing through the physiographic gap at Palakkad (Palghat) in the high Sahyadri Mountain Ranges and following the upper reaches of the Noyil River (a tributary of the Kaveri) and through Chinimalai, the *Palghat–Cauvery Shear Zone* (Figs. 7.2 and 7.5) is a southward-dipping boundary between the Archaean and Proterozoic terranes (Drury et al. 1984; Chetty 1996; Chetty et al. 2003). The eastern segment of the Cauvery–Palghat Shear Zone is characterized by a flower structure resulting from interlinking of sigmoidal shear belts that developed during the Neoproterozoic tectonism (Bhaskar Rao et al. 2003; Chetty and Bhaskar Rao 2006). Its southern splay extends eastward along the Kaveri River, affecting the Sittampundi Complex. The northern splay follows the Sweta River and has caused the formation of rootless folds, fold sheaths and ductile shearing dominated by dip-slip movements indicating that the P–CSZ resulted from N–S compression (D'Cruz et al. 2000). Within the P–CSZ, there are numerous bodies of granites

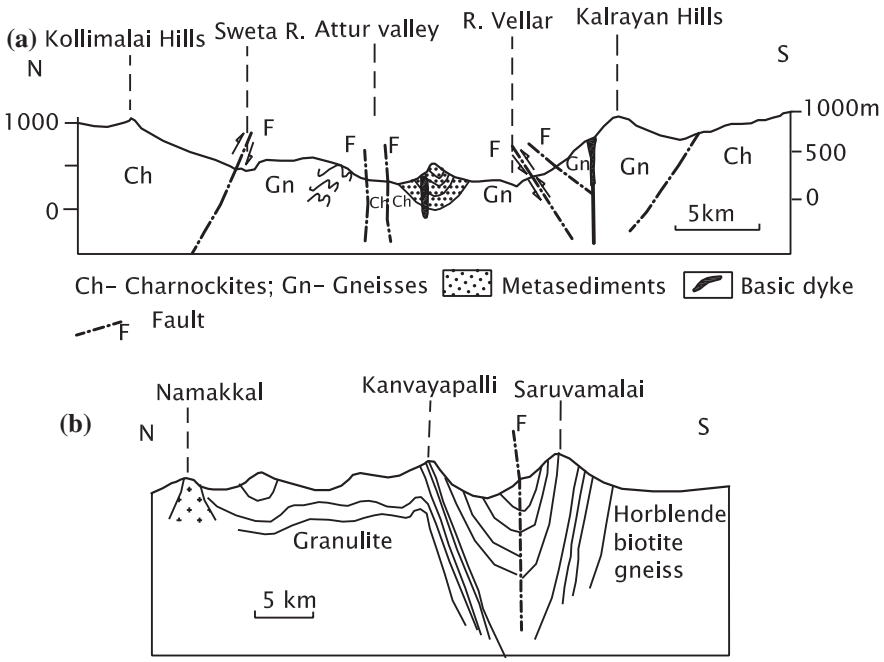

Fig. 7.5 **a** North–south cross section shows the structural design of the Attur Shear Zone in the terrane of granulitic–charnockitic rocks (After Srinivasan 1974). **b** Section depicts the structural architecture of the Cauvery Shear Zone in the Namakkal area (after Mukhopadhyay et al. 2003)

and gneisses containing 2900-Ma-old protoliths, interbanded with quartzofeldspathic gneiss and metasediments. These bodies testify to later dextral shearing that was highly penetrative. The formation of granitic bodies within the shear zone is attributed to melting during exhumation. The second phase of metamorphism was responsible for the development of *incipient charnockites*. In the Palakkad area (Fig. 7.6), the ENE-plunging folds in calc gneisses interbedded with marble and sillimanite schists represent second-generation deformation. This deformation folded the axial planes of earlier isoclinal folds, resulting in their reclining on the hinge zone and buckling and flattening of layers. The ENE-plunging folds could not have evolved by reorientation of the N–S structures of the Dharwar trend but seem to be related to dip-slip movement on steep reverse faults of the shear zone (Naha et al. 1994). In the Namakkal area in the eastern sector of the P–CSZ, the fold pattern in the granulite facies rocks suggests shortening across the zone rather than due to single transcurrent motion (Mukhopadhyay et al. 2003). Significantly, in contrast to complex metamorphism under temperature 730 °C and pressure 8.6 kbar, the northern block (the Kaveri Shear Zone rocks) records metamorphism under high temperature (850 °C) and high pressure (9.6 kbar), followed by

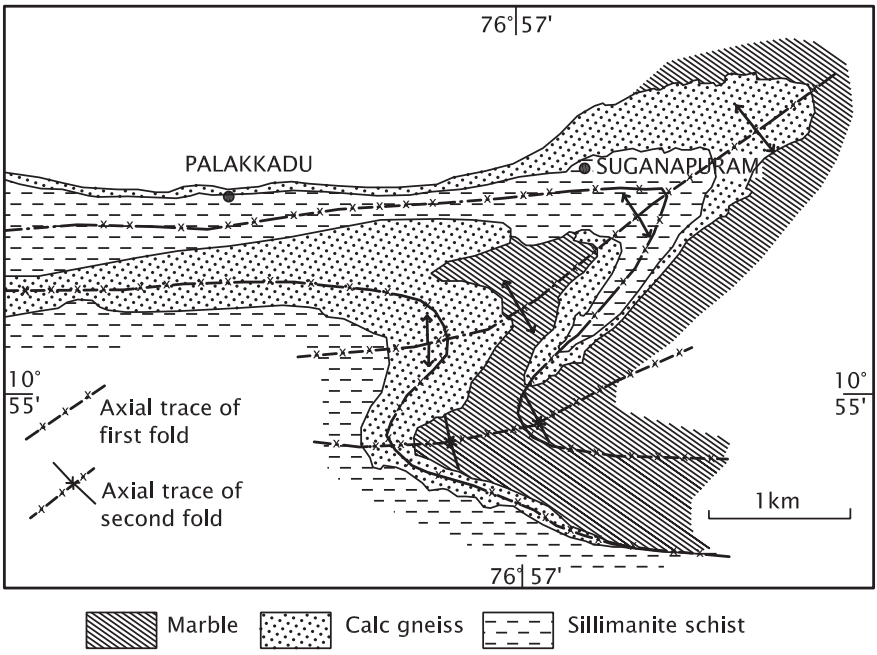

Fig. 7.6 Structural peculiarity and lithological components of the Palghat–Cauvery Shear Zone (based on Naha et al. 1994)

isothermal decompression (John et al. 2005). This fact carries an implication that the Kaveri SZ represents juxtaposition of two contrasted domains.

In the Saint Thomas Mount–Pallavaram area—the type area of the charnockites—axial planes of tight isoclinal folds in basic granulites swerve from NNE–SSW orientation in the southwest through E–W in the central part to N–S in the southern area (Subramanian 1959; Merh 1962; Sen et al. 1970).

7.3.3 Karur–Oddanchatram Shear Zone

The shear zone that passes through Karur and is traceable north of Kodaikanal on the northern slope of the Palni Hills defines the northern tectonic boundary of the Madurai Block. It represents the actual boundary of the Archaean–Neoproterozoic terranes (Janardhan 1996, 1999). Massif-type Oddanchatram Anorthosite (Janardhan and Wiebe 1985) and the Kadavur Complex occupy the shear zone comprising a sequence of quartzites, metapelites and local banded iron formation—the metasediments representing continental margin deposits. This setting is reminiscent of lithotectonic framework of the Eastern Ghat Mobile Belt.

7.3.4 Achankovil Shear Zone

In the south-western part of the Peninsular India, the Madurai–Periyar Block is separated from the Trivandrum–Nagercoil Block by a shear zone occupied by the Achankovil River. This 20–25 km wide NW–SE trending shear zone (Fig. 7.7) shows evidence of early dextral movement in the eastern part but overprinted by sinistral movement which become dominant towards north-west (Sachs et al. 1997). Defined by the NW–SE trending foliation fabric with steep dip due SW, S-shaped folds and shear bands, the Achankovil Shear Zone (ASZ) corroborates strike-slip movement (Rajesh and Chetty 2006). The many-time deformed and metamorphosed rocks, gneisses, cordierite–gneisses, khondalites, charnockites and basic granulites of the ASZ display isoclinal folds trending WNW/NW–ESE/SE, and hading 50°SW, subsequently appressed to form rootless folds and hook-shaped structures (Radhakrishna et al. 1990). The ASZ is believed to have resulted from crustal extension followed by its collapse (Santosh and Yoshida 2001). The intimately associated Tenmalai Shear Zone, containing post-tectonic alkali granites and discontinuous strands of cordierite-bearing gneisses, shows several peaks of high-pressure metamorphism—the highest being under 8.5–9.5 kbar and

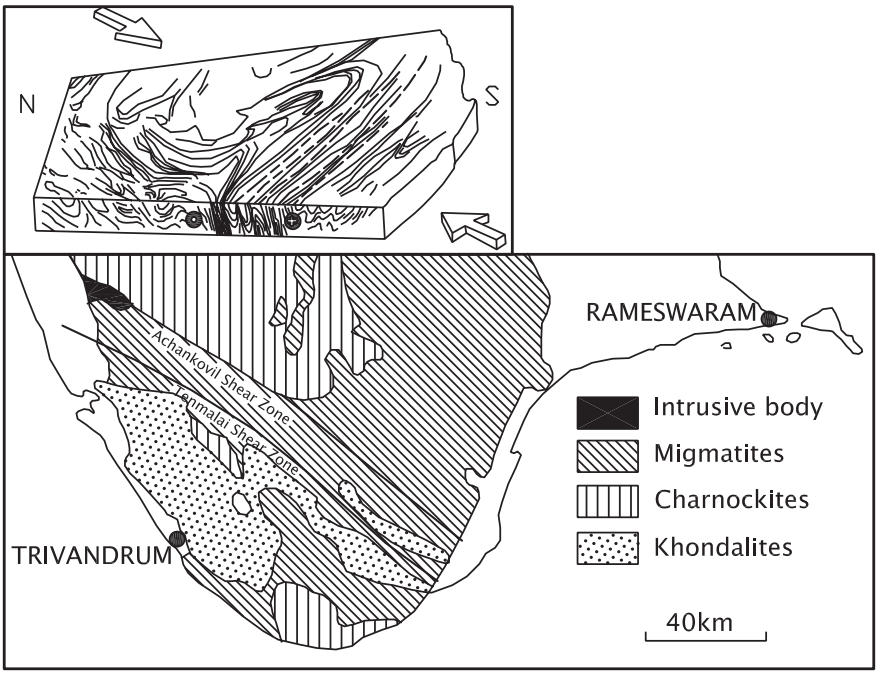

Fig. 7.7 The Achankovil Shear Zone separates the Madurai Block from the Kerala Khondalite Belt (After Ramakrishnan 2003) (*Inset* after Chetty 1996)

940–1040 °C PT conditions. This is in contrast to the high-temperature metamorphism in the Madurai and Trivandrum blocks. The isotope systematics provides valuable insight into the evolutionary history of the shear zones. The testimony of plutonic bodies within the shear zone is of critical importance. The Pathanapuram Granite in the ASZ has yielded zircon ages varying from 1149 to 961 Ma of their cores and 560–540 Ma of their overgrowth rims and monazite ages of 574–526 Ma of their cores and 539–506 Ma of their rims (Santosh et al. 2005). It is obvious that the latest imprint at 515 ± 15 Ma indicates that the rocks of the ASZ were overtaken by the Pan-African tectonothermal upheaval.

7.4 Tectonics of Southern Granulite Terrane

In the northern part of the SGT, there are two isolated, displaced or uprooted segments in the zone of low strain, between the B–ASZ and the P–CSZ. Caught up in this maize of sheared rocks, these blocks have yielded Nd model ages that indicate that the protoliths are of Late Archaean antiquity—2900–2600 Ma for the Shevaroy massif, 2800–2350 Ma for the Madras Block and 2900–2600 Ma for the Nilgiri massif (Bernard-Griffiths et al. 1987; Peucat et al. 1989). The Nilgiri rocks are characterized by garnets that also yield Sm–Nd age of 1705 Ma, and the maduKarai supracrustal rocks have model Nd age older than 1900 Ma, in addition to 600–550 Ma age of metamorphism (Meisner et al. 2002). In common with the Madurai Block, the maduKarai segment experienced Pan-African reconstitution of rocks. The alkali granites and pegmatites of the Ambalavayal area in northern Kerala yielded rhenium–osmium ages of 567 ± 28 Ma and 466 ± 77 Ma, respectively (Santosh et al. 2003).

In the Moyar Shear Zone, reverse faulting was accompanied and/or followed by channelling of metamorphic fluids through rock partings, leading to retrogression of granulite rocks to amphibolites at 521 ± 8 Ma. In the P–CSZ, the metamorphism was followed by non-coaxial deformation under amphibolite facies conditions (Meisner et al. 2002).

Subject to extension, the Peninsular Indian crust broke along the M–ASZ (Fig. 7.8), owing to its lithospheric peculiarity (thickening by 4–5 km along that belt). The southern block was thrust up against the Dharwar Craton along the steeply southward-dipping plane (Valdiya 1998), and the hanging-wall block was dismembered, followed by displacement of the broken blocks culminating in the detachment of the southern block from the SGT along the Bhawani Shear Zone (Fig. 7.8). There is no evidence for collision of two continental blocks—no subduction zone characterized by trench turbidites–siliceous pelagic clays-bedded cherts, no island-arc basalts, no ophiolites with sheeted dykes, no Andean-type arc of granite–granodiorite plutons along the flank and no suggestion of Benioff-type sinking of crust beneath the Dharwar Craton or the SGT.

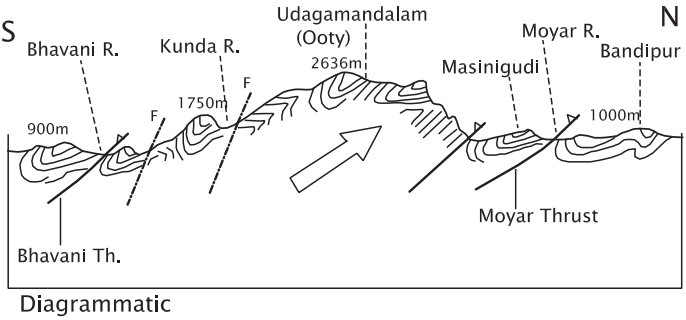

Fig. 7.8 Subject to strong compression, the Peninsular Indian crust buckled and broke up along the Moyar–Attur Shear Zone. The Nilgiri–Pachaimalai Belt of Late Archaean was thrust northwards against the Dharwar cratonic blocks. Subsequently, the Nilgiri Block was detached from the Southern Granulite Terrane along a fault on its southern flank. The Bhavani Shear Zone thus represents a detachment fault (after Valdiya 1998)

7.5 Metamorphism in Madurai Block

7.5.1 Lithology

The Madurai Block comprises predominant charnockite of intermediate composition and of tonalitic to granitic affinity. Despite strong metamorphism, the original igneous nature of their protoliths is preserved. Furthermore, they show intrusive contacts in places and have xenoliths in other locations. The greenish and greenish yellow colour of the charnockite is due to alteration and attendant fracture fillings in felspar. The predominant garnet-free charnockites consisting of hypersthene, biotite, plagioclase, perthite and quartz make the high mountain ranges of the Palni, the Anaimalai, the Elaimalai and the Varushnad of the southern Sahyadri.

7.5.2 Metamorphic Mineral Assemblages

The charnockites making the Kollimalai and Pachaimalai hills give Rb–Sr whole-rock isochron age of about 2900 Ma—the age of granulite facies metamorphism—while the Sm–Nd data show their age in the range 2980 ± 3 Ma (Choudhary et al. 2011). An upper age limit of ~3280 Ma is assigned to the crustal accretion of the protolith of all the rocks.

The charnockites are intimately associated with broad strips of metapelites and metapsammites and calc granulites interbanded with pyroxene granulites. Four major mineral assemblages are identifiable in the expanse of the Madurai Block (Lal et al. 1987; Lal 2003)—(i) garnet–cordierite–biotite–spinel–sillimanite–potash–felspar; (ii) garnet–cordierite–orthopyroxene–biotite–plagioclase–potash–felspar–quartz; (iii)

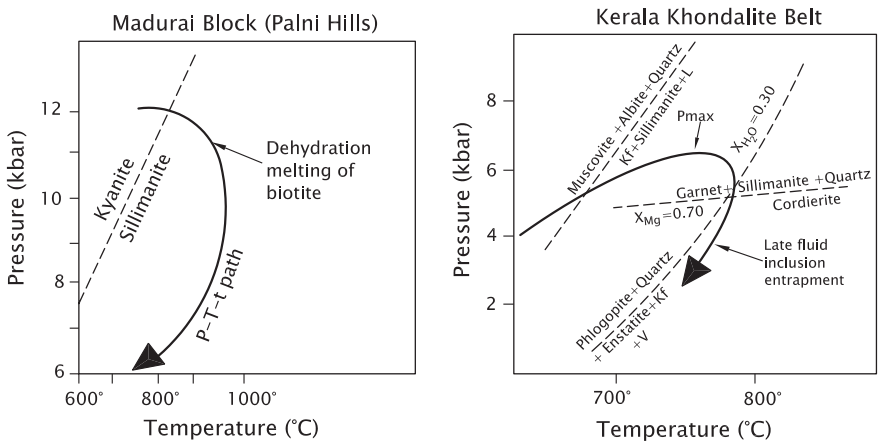

Fig. 7.9 Clockwise pressure–temperature–time (P-T-t) paths of rocks of the three blocks within the Southern Granulite Terrane along with main metamorphic reactions (after Mohan and Jayananda 1999)

sapphirine–cordierite–orthopyroxene–biotite–plagioclase–spinel, and (iv) cordierite–biotite–plagioclase–potash–felspar. The first two assemblages dominate the Madurai lithology and occur as bands of varying width and length (up to 5 km). The calc silicate bands (the thickness of which does not exceed a few decimetres) are made up of calcite, scapolite, wollastonite, clinopyroxene, garnet, plagioclase, K-felspar, sphene and quartz. These rocks are intimately associated with pyroxene granulites. The Rajapalayam and Perumalmalai sapphirine-bearing quartzofeldspathic and pelitic gneisses indicate temperature as high as 1040–1060 °C and pressure of 8–12 kbar (Brown and Raith 1996; Raith et al. 1997; Tateishi et al. 2004; Prakash et al. 2006). The sapphirine–orthopyroxene–sillimanite–spinel-bearing granulites of Ganguvarpatti, Kiranur and Palni areas exhibit prograde clockwise pressure–temperature–time (P-T-t) path with notable decompression history (Fig. 7.9) as temperature declined to 850° and pressure dropped to 5 kbar (Mohan and Jayananda 1999; Mohan et al. 2003; Lal 2003). The sapphirine-bearing massive granulites occurring with garnet–cordierite gneiss north-west of Madurai have yielded SHRIMP U–Pb zircon age of 550 ± 18 Ma and 530 ± 50 Ma as the age of their metamorphic overprint and the ages of 2509 ± 12 Ma and 2509 ± 30 Ma correspond to the timing of protolith formation in sapphirine-bearing granites and cordierite–garnet gneisses, respectively (Prakash 2010).

The charnockites of the Palni Range evolved at temperatures 750–900 °C and pressure 5–9 kbar (Janardhan 1999; Janardhan and Wiebe 1985). The intermediate charnockite of the SGT in general is characteristically enriched in Rb and Ba and depleted in HREE, with positive Eu anomaly (Rajesh and Santosh 2004). The charnockite magma crystallized within the temperature range of 750 and 940 °C under pressures that varied between 4 and 6.3 kbar. This happened in an event of low water activity but high influx of CO_2 with just traces of CH_4 and N_2 in later

stages. This is testified by fluid inclusions in garnets formed during the peak of metamorphism (Harris et al. 1982; Chacko et al. 1992, 1996; Raith et al. 1997; Santosh et al. 2003). The CO_2 is supposed to have come from magmatic sources beneath the lithosphere and transferred through deep-seated shear zones. Presence of ultrabasic and alkaline rocks in the proximity tends to support the proposition that there was basaltic underplating with ponding of alkaline and mafic magmas. This was followed by partial melting of the lower crust, giving rise to charnockitic magma (Rajesh and Santosh 2004).

7.6 Dynamothermal History of Trivandrum Block

The Trivandrum Block embodies what is known as the *Kerala Khondalite Belt* (KKB) and the *Nagercoil Block*. It is made up of gneisses of varied kind, principally the *khondalite* characterized by mineral assemblage garnet–biotite ± graphite, and the *leptynite* consisting of garnet, mica and quartz. These gneisses are associated with garnetiferous charnockites, cordierite gneiss and subordinate, calc silicate rocks and basic granulites. The assemblage represents an original psammitic to pelitic sediments which were metamorphosed to amphibolite to granulite facies. An outstanding feature of the KKB is the *arrested charnockite* that resulted from partial isochemical in situ conversion of many or most of the quartzofeldspathic gneisses, the transformation having been prompted by influx of CO_2-rich fluids (Ravindra Kumar et al. 1985; Ravindra Kumar and Chacko 1986, 1994; Hansen et al. 1997; Ravindra Kumar and Srikantappa 1995; Ravindra Kumar and Sukumaran 2003; John et al. 2005). The REE pattern, weak or no Eu anomaly, marked depletion of HREE and textural characteristics of various types of *arrested charnockites* indicate that this development took place in the temperature range of 780–880 °C at pressures 9–10 kbar and under the intervention of CO_2 influx. They were formed in structurally controlled zones in the melt portions of the migmatite gneisses, particularly along the margins of invading alkaline dykes.

The pegmatites occurring within the KKB record cooling down of temperature to 400–500 °C, the rate of cooling being extremely slow—3–6 °C per million years (Cenki et al. 2004).

There is an interesting suite of metacarbonates in the Ambasamudram area in the KKB near Tirunelveli. Associated with calc silicate rocks, the marble exhibits carbonate and oxygen isotope ratios ($\delta^{13}C$ nearly 0.0 % and $\delta^{18}O$–20 %) typical of Middle to Late Proterozoic marine carbonates (Satish Kumar et al. 2001).

7.7 Age of Metamorphic Rejuvenation

Dating of zircon crystals recovered from the Kodaikanal charnockites (Fig. 7.10) indicates that initial crustal formation occurred at 2118 ± 8 Ma, and the Sm–Nd garnet and whole-rock isochron ages suggest that the peak metamorphism took place at 553 ± 15 Ma (Jayananda et al. 1995). In other words, there was remobilization and reworking of older rocks during the Pan-African geothermal event. This deduction is further supported by the U–Pb zircon dating of the Elaimalai Hills charnockites, yielding an age of nearly 585 Ma, and by the 512 Ma age of the Melankode pegmatite within the KKB (Miller et al. 1996). There is no doubt that the charnockites of Kerala were formed during the Pan-African tectonothermal upheaval as borne out by the Sm–Nd mineral ages of incipient charnockites at Ponmudi (Choudhary et al. 1992). The cores of the zircon and monazite crystals in the khondalites at Nedumpara of the Trivandrum Block give a date of 3534 Ma, while regression of age data for several spot analysis in single zircon shows the range from 3193 ± 72 to 2148 ± 94 Ma, indicating derivation from multiple provenances of detrital grains from rocks of Archaean ages (Santosh et al. 2006). The basement rocks of the Nagercoil area in the southern extremity of the SGT contain monazite and zircon of sedimentary origin, ranging in age from 2800 to 590 Ma. The massive charnockites are characterized by 2500–500 Ma zircon grains, the majority belonging to the time span of 1530–2200 Ma (Santosh et al. 2006). However, there is clear evidence for Pan-African metamorphism throughout the Madurai Block as borne out from Rb-Sr mineral isochron and Kober zircon overgrowth ages of 500–550 Ma (Bartlette et al. 1995). The Sm–Nd systematics on mineral separates from the KKB yielded an age of 534 ± 26 Ma for leptynite and 537 ± 27 Ma for khondalite (Unnikrishnan-Warier 1997). The Th-U-total Pb isochron dating of monazite from gneissic rocks at Nellikala in the KKB yielded an age of 527 ± 10 Ma (Bindu et al. 1998). SHRIMP U-Pb zircon and titanite ages for metapelites, migmatites and calc silicate rocks are, respectively, 530.2 ± 4.4 Ma, 525 ± 4.5 Ma and 520 ± 4.7 Ma (Shabeer et al. 2005). The Puttetti alkali syenite pluton dated 508 ± 2.5 Ma was emplaced during final phase of amalgamation of the Gondwana supercontinent (Santosh et al. 2005, 2006). The K-Ar ages of glimmerite and phlogopite separated from an ultrabasic body in the ASZ are, respectively, 470.5 ± 9.3 Ma and 465 ± 9.2 Ma, indicating that the influx of highly potassic CO_2-rich melt happened during the Pan-African orogeny. The granitic gneisses and granites of the KKB have yielded wide range of U–Pb monazite ages—between 590 and 520 Ma (Fig. 7.10a, b).

These dates have been interpreted as the time of high-grade metamorphism at 750–800 °C rather than the time of magmatic emplacement (Braun and Brocker 2004). The Pan-African dates of overgrowth rims of zircon crystals in both the Madurai and Trivandrum blocks confirm this inference (Santosh et al. 2003). It is evident that the high-grade metamorphism in the KKB represents a Neoproterozoic development closely related in time to the intrusion of plutonic bodies, alkaline and granitic in composition.

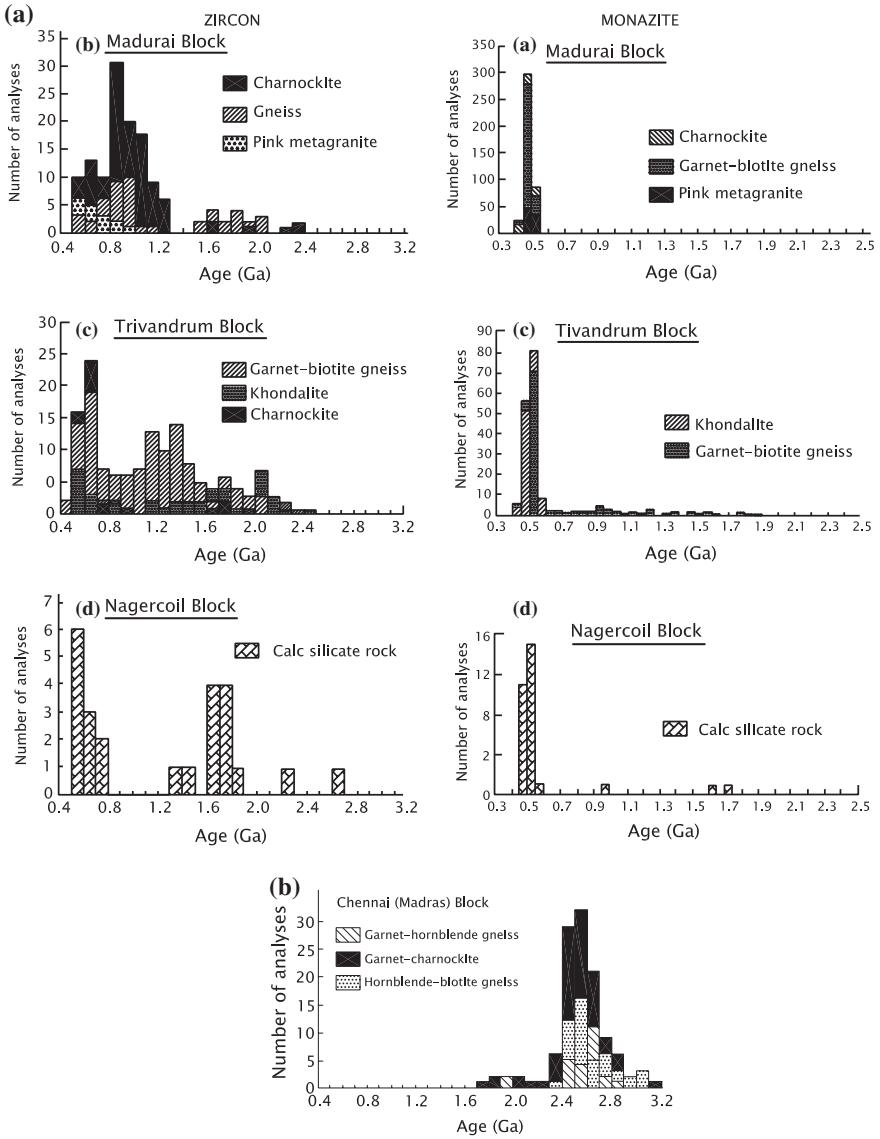

Fig. 7.10 **a** and **b** Combined histograms showing age data on zircons and monazites from various granulitic blocks in southern India (from Santosh et al. 2003)

7.8 Felsic Magmatic Activity

Overwhelmingly, large part of magmatic bodies of granitic composition (Figs. 6.9 and 7.2) were emplaced in the period 520–590 Ma. The U–Pb zircon dates represent the times of crystallization—585 Ma in the Elaimalai massif, 555 Ma in

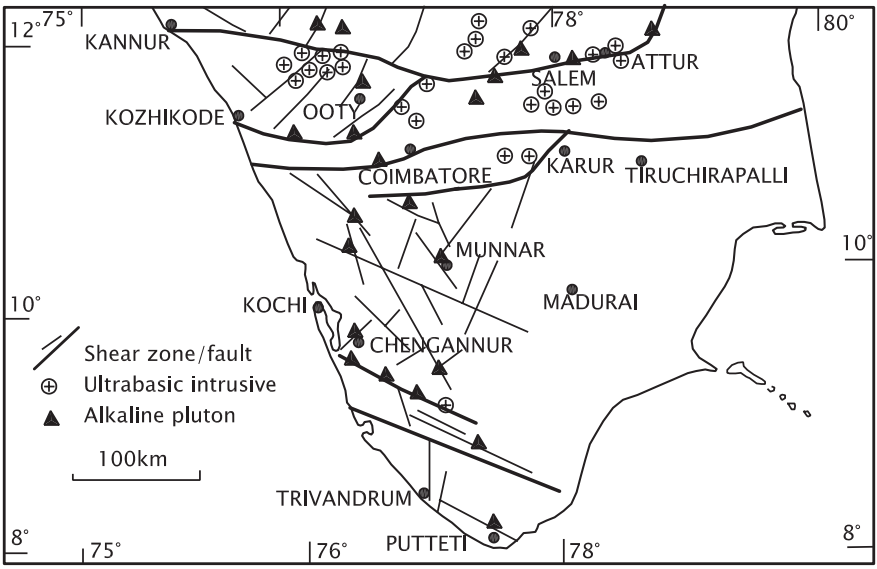

Fig. 7.11 Spatial distribution of ultrabasic and alkaline rock complexes in the southern part of the Peninsular India (based on Ratnakar and Leelanandam 1989; Santosh 1989)

the Kalpatti area and 560 Ma in the Peralimalai hills (Miller et al. 1996). These massifs lie north and south of the P-CSZ. The magmas were derived from porphyritic granite intrusive into basic granulite. The country rocks were deformed and metamorphosed at 750–800 °C over an extended period of nearly 50 Ma (Braun and Brocker 2004). Nearly contemporary of these granites are the pegmatites, such as the 512 Ma Melankode pegmatite in the KKB and the 566 ± 77 Ma intrusives in the Ambalavayad Complex in northern Kerala. In the Wynad area, the 567 ± 28 Ma molybdenum-bearing pegmatites are spatially associated with and genetically related to 595 ± 20 Ma alkali granite. The Vattamalai Granite in the P-CSZ (Fig. 7.11) has been dated by electron microprobe of zircons at 693 ± 139 Ma—the cores of zircons yielding isochron age of 517 ± 67 Ma and of rims 506–539 Ma (Santosh et al. 2003).

7.9 Ultrabasic and Alkaline Rock Complexes

The ultrabasic and alkaline rocks occur together in the form of complexes, located preferentially along faults of Precambrian age (Fig. 7.11). They constitute the earliest manifestation of magmatic activities, particularly in the Pollachi–Tiruchirapalli Belt of the SGT. The faults and fractures that cut across the sialic crust provided pathways to the magmas derived from upper mantle.

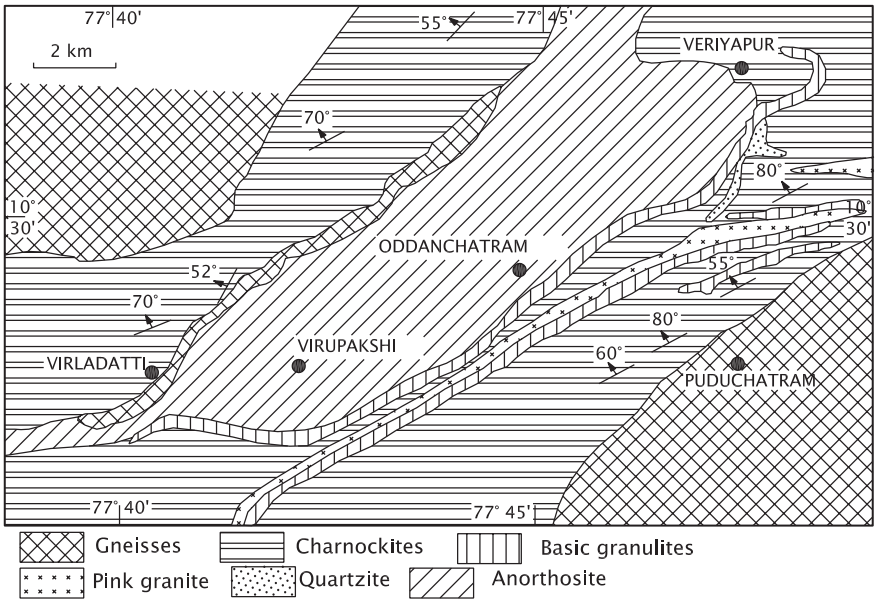

Fig. 7.12 Oddanchatram Anorthosite is a massif-type ultrabasic body occurring in the charnockite terrane cut by a regional shear zone defining a tectonic boundary (after Janardhan 1999)

U-Pb zircon ages of plagiogranite and gabbro of the ophiolitic complex at Manamedu located along the southern periphery of the P-C Shear Zone are 737 ± 23 Ma and 782 ± 24 Ma, respectively (Santosh et al. 2012). The ages of the xenocryst entrained in the plagiogranite during the ascent of the magma are 2278 and 2527 Ma, with intercept to age of 2418 ± 65 Ma (Santosh et al. 2012).

The dismembered ophiolites along the valleys of Moyar–Bhavani rivers give SHIRMP U–Pb zircon ages of 2528 ± 61 Ma and 2545 ± 56 Ma (Yellappa et al. 2012). It is deduced that the material forming the ophiolite complex was derived from the depth of 100–180 km.

The largest of the plutonic complexes, the *Oddanchatram Anorthosite* is associated with the high-grade metamorphic assemblage comprising cordierite-bearing pelites and calc silicate rocks with pyroxene granulites of the Palni Range. They occupy the area (Figs. 7.11 and 7.12) in the proximity of the Karur–Oddanchatram Shear Zone (Janardhan and Wiebe 1985; Janardhan 1996). The anorthosite pluton is made up of 90 % plagioclase of the composition An_{55} along with a few pods rich in Fe–Ti oxides, having highly variable igneous texture. The pods escaped metamorphism and foliation in the contact zone. The primary pyroxenes indicate a temperature range of 960–1000 °C and a pressure of 5.3 kbar (Janardhan 1996, 1999). The location of its palaeomagnetic pole is compatible with the palaeomagnetic poles of the rocks of the 1000–1100 Ma period, and the pole for the second component fits well with the pole for the 550 Ma time (Satyanarayana et al. 2003).

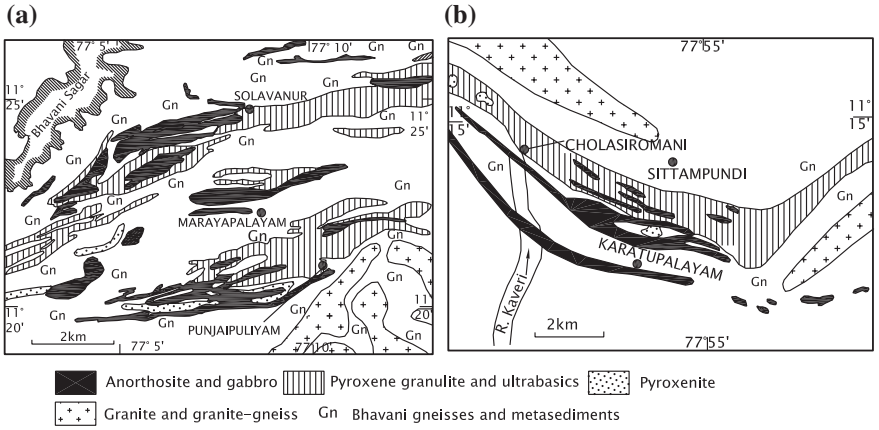

Fig. 7.13 **a** Layered anorthosite complex in the Bhavani Shear Zone. **b** Sittampundi ultrabasic layered complex in the Palghat–Cauvery Shear Zone (**a**, **b** after Bhaskar Rao et al. 1996)

It is evident that the Neoproterozoic Oddanchatram body bears stamp of the Pan-African geothermal upheaval.

East of the Oddanchatram pluton occurs the Tirupattur Carbonatite (Fig. 7.12) associated with alkali syenites and located in a NE–SW trending rift valley of sorts (Borodin et al. 1971). To the north-west is the Bhavani Layered Anorthosite in the tectonized area of the BSZ (Fig. 7.13). To the north-east is located the Sittampundi Complex in the Cauvery Shear Zone. The Sittampundi Complex comprises from bottom upwards (i) gabbro with pyroxenite inclusions, (ii) chromite-layered hornblende-bearing anorthosite, and (iii) clinozoisite-rich anorthosite (Subramanian 1956). The ultrabasic body with quartzofelspathic gneisses is folded into isoclinal folds. Late deformation was accompanied by the second phase of high-grade metamorphism. Garnet granulite (earlier described as eclogite) formed at temperatures 850 °C and pressure 10 kbar (Janardhan and Leake 1975). The Sittampundi suffered two episodes of metamorphism—one at 2900 Ma (Sm–Nd isochron rock age) and the other at 730 Ma, the latter related to a transpressional tectonic event that culminated in the shearing along the P–CSZ (Bhaskar Rao et al. 1996). The U-Pb zircon geochemistry and Hf isotope data show that the Sittampundi anorthosite complex crystallized at 2541 ± 13 Ma and 2461 ± 15 Ma, the high-grade metamorphism that affected the country rock occurring at 715 ± 18 Ma (Rammohan et al. 2013). The *Sivamalai Syenite* (Fig. 7.11) is a lensoid body of ferrosyenite which is tilted north-eastwards (Bose 1971). Derived from the upper mantle, the syenitic magma was emplaced around 623 ± 21 Ma (Subba Rao et al. 1994). The emplacement of the *Sevattur*, *Yelagiri* and *Samalpatta* complexes was controlled by the NE–SW trending lineaments (Udas and Krishnamurthy 1970; Krishnamurthy 1977; Viladkar and Subramanian 1995). The plutons intrude epidote–hornblende–gneiss and represent highly differentiated magmas derived from the source that was characterized by pronounced LILE enrichment and large Nb anomaly. They were

emplaced at 757 ± 32 Ma in the Yelagiri area and at 756 ± 11 Ma at Sevattur (Anil Kumar and Gopalan 1991; Miyazaki et al. 2000, 2003). Presence of boudinaged xenoliths and strongly strained constituent minerals in these elongated bodies of anorthosites and carbonatites testify to forcible injection of their magmas.

The *Samalpatti Carbonatite*, associated with syenites, lamprophyres, pyroxene granulites and dunites, represents a magma characterized by evolved Sr and Nd isotopic composition and enrichment in LILE and HFSE. This body was affected by liquid immiscibility and attendant segregation of carbonate and silicate melts. The complex was subjected to metamorphism at 650–756 °C at low pressures (Srivastava 1998; Srivastava et al. 2005). The Hogenakal Complex is dominated by carbonatites with pyroxenites occurring as important component. The carbonatite bodies, occurring in a discontinuous series between two pyroxenite dykes trending NNE–SSW, have yielded Rb-Sr whole-rock isochron ages of 1984 ± 78 and 1994 ± 76 Ma (Natarajan et al. 1994). These are the oldest known carbonatite body in the Indian subcontinent.

7.10 Proterozoic Terranes of Sri Lanka

7.10.1 Lithotectonic Subdivision

Nearly 90 % of the land of Sri Lanka is made up of Proterozoic rocks developed under high-temperature and high-pressure conditions. Extensive isotope studies have established a new geochronological framework for subdividing the lithologies. Four complexes are identifiable—the Highland, the Wanni, the Vijayan and the Kadugannawa (Fig. 7.14). These constitute NNE–SSW trending subprovinces or terranes of Proterozoic antiquity (Cooray 1984, 1994). The boundary between the Highland Complex and the Vijayan Complex is defined by a thrust. The thrust zone is occupied over a large stretch by the River Mahaweli, the longest river of Sri Lanka. The thrust zone is also marked by occurrence of a few serpentinite bodies. The boundary between Highland Complex and Wanni Complex in the western side is not manifested in any structural discordance, except for a 30-km-long shear zone in the Digana segment in the Kandy region. Geochemical studies have demonstrated contrasted characteristics of these four complexes—their distinct crustal ages, but all having undergone petrological rejuvenation due to Late Neoproterozoic tectonothermal upheaval. It may be emphasized that isotope data preclude a common premetamorphic history of the four terranes (Milisenda et al. 1994).

7.10.2 Lithostratigraphy and Petrogenesis

Running NNE–SSW through the middle of the island, the *Highland Complex* comprises mainly charnockites and granulite-grade enderbitic rocks of igneous

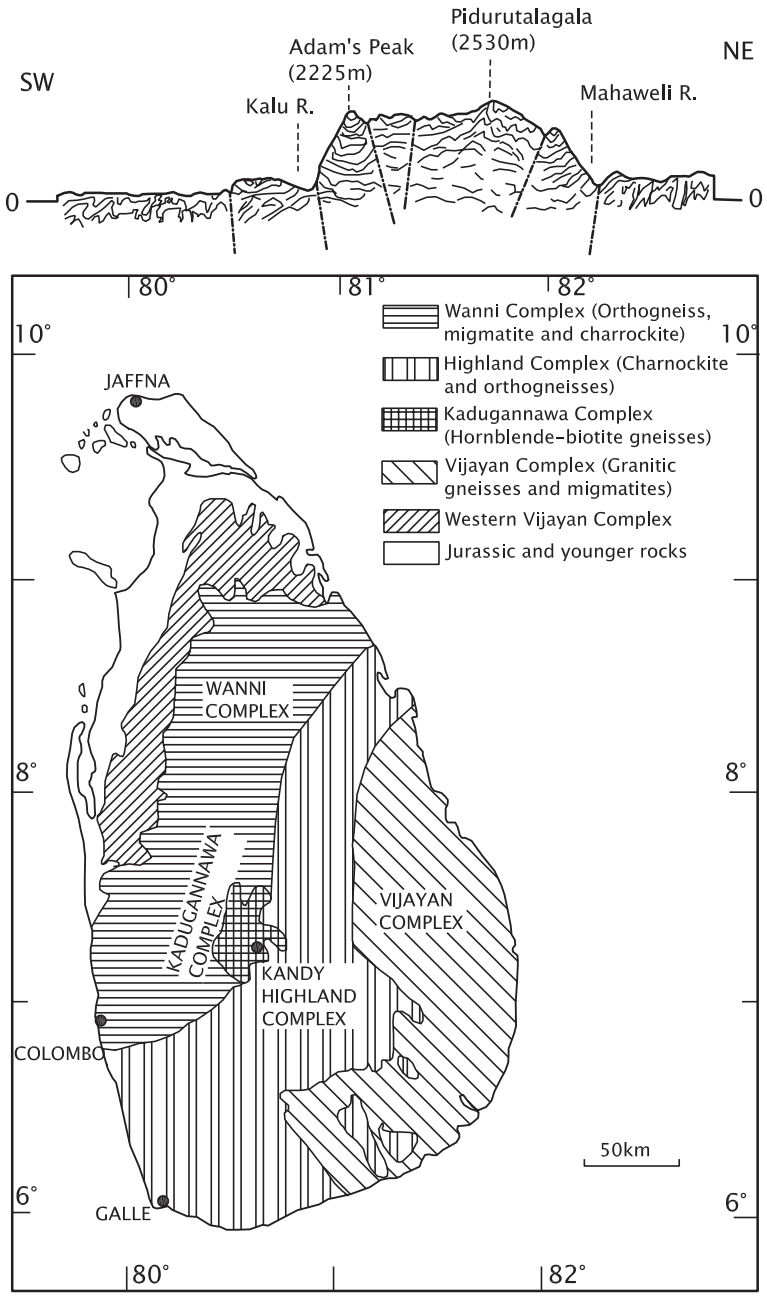

Fig. 7.14 Four geochronologically contrasted complexes constituting four lithotectonic terranes of Sri Lanka (based on Mathavan et al. 1999)

parentage and metasediments including quartzites, marbles, calc silicate rocks and sapphirine-bearing high-magnesian granulites. Nd model ages in the range of 2000 and 3400 Ma reflect a long crustal history before metamorphism (Cooray 1994; Milisenda et al. 1994; Mathavan et al. 1999). Occurring as stratabound dissemination in granulites in the form of pods and lenses within pegmatites, and as booklets in calc silicate rocks, graphite shows $\delta^{13}C$ values of −17.5 to −32.1, indicating its biogenic origin (Radhika et al. 1995). The metamorphism took place under high-temperature and high-pressure granulite facies conditions in the period 610 and 550 Ma (Braun and Kriegsmann 2003). The Palaeoproterozoic metasediments of the Highland Complex represent sedimentary deposits of rifted continental margin that later evolved into a stable shelf region (Dissanayake and Munasinghe 1984; Kroner et al. 2003). The 1850–1950-Ma-old granites intruding these rocks (Baur et al. 1991; Holzl et al. 1994) indicate that, as in the Aravali and Satpura mobile belts and the Himalaya province, this part of the Indian subcontinent also was overtaken by events which manifested itself in the emplacement of 1900 ± 100 Ma porphyritic granites and porphyries. Most of these granites are now charnockitic gneisses and granulites, occurring along with basaltic sills and dykes and forming conformable bands or layers within metasediments. These rocks have suffered intense and multiple deformation and granulite facies metamorphism. There is a 170–300 m thick *layered basic intrusive* of original cumulate consisting of gabbro–amphibolite–ultrabasics forming a synformal body (Kleinschrodt et al. 1991). The Highland terrane shares some similarities with the Madurai Block and the KKB of the SGT.

To the west of the Highland Complex lies the subprovince of *Wanni Complex* (Fig. 7.14). It consists of migmatized gneisses of both igneous and sedimentary parentage. The igneous-category migmatites have granitic, granodioritic and tonalitic composition. The sedimentary rock is represented by garnet, sillimanite and often cordierite-bearing gneisses. Nd model ages range from 2000 to 1000 Ma—within the temporal spectrum of the Mesoproterozoic and Neoproterozoic times. A single zircon crystal from the Vavuniya orthogneiss suggests the date of crystallization at 1100–1000 Ma (Holzl et al. 1994). Comparing the lithologies, the Nd model ages, tectonic style and degree of metamorphism, the Wanni Complex is similar to the ASZ, both having a common Pan-African evolutionary history (Braun and Kriegsmann 2003).

The calc alkaline granitic magma was emplaced in both the Wanni and Vijayan complexes in the period 1100–880 Ma. Evidently, these terranes were affected by tectonothermal upheaval broadly contemporaneous with the Grenville orogeny. It seems that sedimentation took place in the period 1500–1000 Ma in the Wanni domain compared to 2000–1900 Ma interval in the Highland subprovince.

Forming the eastern flank of the island, the *Vijayan Complex* consists of mainly granitic and basic gneisses, with minor quartzite and calc silicate rock (Kehelpannale et al. 2001). The granitic gneisses show calc alkaline affinity, their composition ranging from leucogranite to tonalite. The zircon and monazite dating has yielded crystallization ages of 1023 ± 8 Ma, 1016 ± 28 Ma and

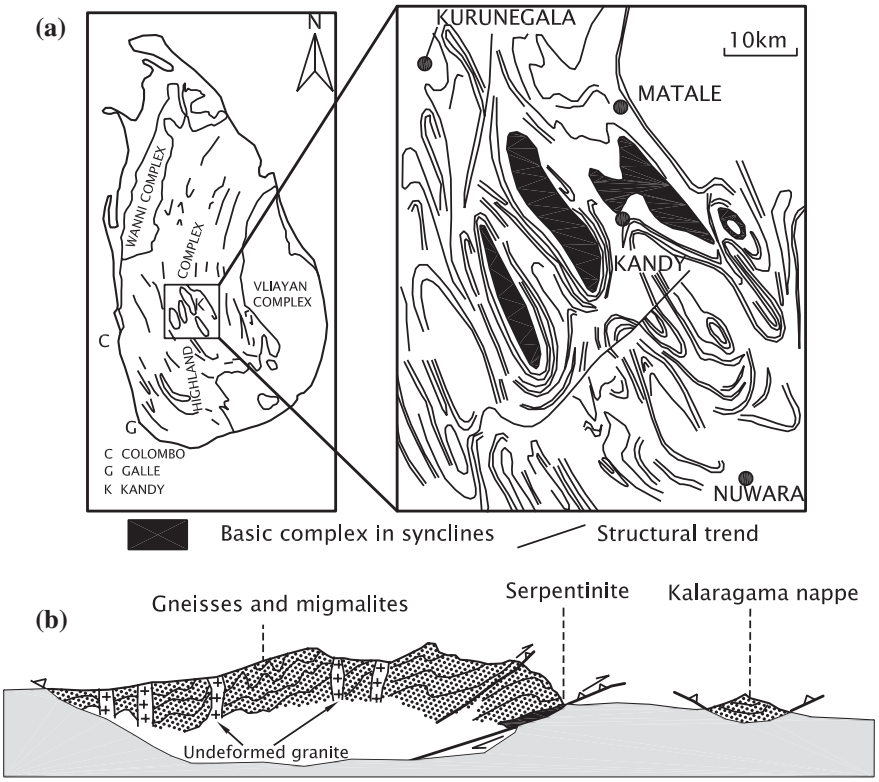

Fig. 7.15 **a** Structural trend lines and folds developed in central Kandy area of the Highland Complex (After Kleinschrodt 1994). **b** Structural section across the Highland Complex (after Munasinghe and Dissanayake 1982)

1133 ± 121 Ma (Holzl et al. 1994; Milisenda et al. 1994). The Vijayan rocks exhibit metamorphism of the amphibolite facies. They are locally affected by late stage development, culminating in the charnockitization of gneisses (Jayawardane and Carswell 1976).

The *Kadugannawa Complex* is of restricted occurrence in the central part of Sri Lanka (Fig. 7.14). It comprises metamorphosed magmatic rocks ranging in composition from gabbro through diorite to granite. Metasediments (marble and calc silicate rock and quartzites) occur sparsely (Perera 1983; Cooray 1984). The magmatic rocks occur in the cores of doubly plunging later generation folds (Fig. 7.15) near Kandy (Munasinghe and Dissanayake 1980). Underlying the thin sequence of metasedimentary rocks, there is an elongate lense of amphibolite within the calc silicate assemblage representing highly deformed pillow lava (Kriegsmann 1994). Single zircon evaporation age and Nd systematics of dioritic to granodioritic gneisses of the Kadugannawa Complex suggest magmatism in the interval 1006–881 Ma (Kroner et al. 2003). Zircon evaporation Pb–Pb age indicates that its

emplacement took place between 1010 and 890 Ma (Kroner and Williams 1993). Directly underneath the basic rock is a pink granite locally becoming gneissic. This body marks the lower limit of the Kadugannawa Complex.

7.10.3 Tectonic Framework and Structural History

Interpretation of geophysical characteristics of Sri Lanka and SGT rules out the possibility of intracratonic rift between the two (Agrawal and Pandey 1999), even though there is evidence for small-scale translational and rotational movements (Yoshida et al. 1999). India and Sri Lanka seem to have travelled together to the present position after their break-up from the Gondwana supercontinent (Fig. 7.16).

As already stated, the boundaries of the four terranes of Sri Lanka are defined by tectonic planes that have placed in just a position four contrasted complexes. However, they exhibit a common trend of structures—NNE–SSW orientation in north-eastern part, swinging to NW–SE, then E–W and finally ENE–WSW in the south-western part of the island. This trend is possibly the product of the last phase of deformation which also caused formation of upright folds. The folding was simultaneous with eastward thrusting of the granulite facies rocks of the

Fig. 7.16 Gondwana assembly of continents showing the position of Sri Lanka during the Pan-African period (after Santosh and Yoshida 2001)

Highland Complex (Fig. 7.15) onto the amphibolite facies terrane of the Vijayan Complex. There is another notable structural feature—the syntaxial bending of fold structures (Fig. 7.14). It is attributed to a corner effect produced by westward indenting basement underneath the eastern Sri Lanka. This happened after E–W shortening and simultaneous strike-slip movement along a N–S fault, supposed to lie west of the island (Braun and Kriegsmann 2003).

Kilometric-scale upright folds dominate central part of Sri Lanka (Fig. 7.15). Towards the boundary between the Highland and Vijayan complexes, the axial planes of these folds become more inclined even as folds become overturned asymmetrically eastward and end up in thrusting upon the eastern terrane (Kleinschrodt 1994). The situation in southern Sri Lanka is more complicated where the structural trend is highly variable. The Wanni and Kadugannawa domains have been interpreted as fold nappes, emplaced atop the Highland Complex (Kriegsmann 1994). The main deformation occurred during the peak of metamorphism as testified by the garnet plasticity (Braun and Kriegsman 2003). The overturning of asymmetric folds together with sheath folds parallel to a strong NNW–SSE lineation in the Kadugannawa Complex indicates a top to NNW displacement.

7.10.4 Metamorphism and Petrological Rejuvenation

The peak metamorphism at more than 9 kbar and 830 °C in the Highland Complex implies sinking of the constituent rocks to the depth of nearly 30 km. The P-T path of these rocks is characterized by early isobaric cooling at 800 °C, followed by near isothermal decompression accompanied by cooling (Braun and Kriegsmann 2003). This phenomenon was attended by uplift of the terrane. The high pressure of more than 9 kbar in the central part of the island dropped to 5–6 kbar towards the south-western edge. There was sudden increase in the rate of cooling of the Highland rocks at 480 Ma. This was possibly related to thrusting of the Highland rocks onto the Vijayan domain, with attendant retrograde metamorphism. The entire cycle of changes was completed in the period 610–500 Ma (Baur et al. 1991; Holzl et al. 1994; Braun and Kriegsmann 2003). In the Wanni Complex, the garnet–sillimanite–biotite gneiss of the Eppawala area indicates a temperature range 770–730 °C and pressure varying from 6.6 to 7.8 kbar, while the migmatites testify to the P-T condition of 780–750 °C and 5.6–6.4 kbar (Weerakoon et al. 2001).

As already stated, the regional metamorphism to amphibolite and granulite facies occurred in the period 610–550 Ma, falling in the temporal span of the Pan-African orogeny. This tectonothermal event is dated by granite plutons, which occur in many places. The U–Pb zircon dates firmly constrain the time of peak metamorphism between 610 and 550 Ma when granitic magmas were formed and emplaced (Holzl et al. 1994; Kroner and Williams 1993).

7.10.5 Magmatic Activity

The granite pluton at Kurunegala in the Wanni Complex is dated 790 to 750 Ma (Milisenda et al. 1994; Baur et al. 1991). The little deformed Tonigala Granite and the Galgamuwa Granite in the western part of the Wanni Complex yield dates 558 ± 14 Ma and 552 ± 8 Ma, respectively (Holzl et al. 1994). The Tangalla Granite in southern Sri Lanka is 550 ± 3 Ma old. It is evident that there was extensive magmatism leading to emplacement of high-Ba, high-Sr granites at 550–560 Ma interval in both the Wanni and Highland subprovinces.

There are intrusives of syenite and pegmatite occurring in small shear zones oriented roughly E–W. These are 570 to 500 m.y. old. Some of the shear zones were responsible for charnockitization of some gneisses (Kehelpannala 1997; Kehelpannala et al. 2001). The *Eppawala Carbonatite* in the Wanni Complex was emplaced in the interval earlier than 493 ± 5 Ma, but after 610–550 Ma (Weerakoon et al. 2001).

References

Agrawal, P. K., & Pandey, O. P. (1999). Was there an intracontinental rift between India and Sri Lanka? *Journal Geological Society India, 54*, 237–249.

Bartlette, J. M., Harris, N. B. W., Hakesworth, C. J., & Santosh, M. (1995). New isotope constraints on the crustal evolution of South India and Pan-African granulite metamorphism. *Memoir Geological Society India, 34*, 391–397.

Baur, N., Kroner, A., Todt, W., Liew, T. C., & Hofmann, A. W. (1991). U-Pb isotopic systematics of zircons from prograde and retrograde transition zones in high grade orthogneisses, Sri Lanka. *Journal Geology, 99*, 527–545.

Bernard-Griffiths, B. J., Jahn, B. M., & Sen, S. K. (1987). Sm-Nd isotopes and REE geochemistry of Madras granulites, India: An introductory statement. *Precambrian Research, 37*, 343–355.

Bhadra, B. K. (2000). Ductile shearing in Attur Shear Zone and its relation with Moyar Shear Zone, South India. *Gondwana Research, 3*, 361–369.

Bhaskar Rao, Y. J., Chetty, T. R. K., Janardhan, A. S., & Gopalan, K. (1996). Sm-Nd and Rb-Sr ages and P-T-history of the Archaean Sitampundi and Bhavani layered meta-anorthosite complexes in Cauvery shear zone, south India: Evidence for late proterozoic reworking of Archaean crust. *Contributions to Mineralogy and Petrology, 125*, 237–250.

Bhaskar Rao, Y. J., Janardhan, A. S., Vijaya Kumar, T., Narayana, B. L., Dayal, A. M., Taylor, P. N., et al. (2003). Sm-Nd model ages and Rb-Sr isotopic systematics of charnockites and gneisses across the Cauvery shear zone, Southern India: Implication for the Archaean-Neoproterozoic terrane boundary in Southern granulite terrain. *Memoir Geological Society India, 50*, 297–317.

Bindu, R. S., Suzuki, K., Yoshida, M., & Santosh, M. (1998). The first report of CHIME monazite age from the South Indian granulite terrain. *Current Science, 74*, 852–858.

Biswal, T. K., Thirukumaran, V., Ratre, K., Bandopadhyay, K., Sundaralingam, K., & Mondal, A. K. (2010). A study of mylonites from parts of the salem-Attur Shear Zone (Tamilnadu) and its tectonic implications. *Journal Geological Society India, 75*, 128–136.

Borodin, L. S., Gopal, V., Moralev, V. M., Subramanian, V., & Poni Karov, V. (1971). Precambrian carbonatites of Tamil Nadu, south India. *Journal Geological Society India, 12*, 101–112.

Bose, M. K. (1971). Petrology of the alkaline suite of Sivamalai, Coimbatore, Tamil Nadu. *Journal Geological Society India, 12*, 241–261.

Braun, I., & Brocker, M. (2004). Monazite dating of granitic gneisses and leucogranites from the Kerala Khondalite Belt, southern India: Implications for late proterozoic crustal evolution in East Gondwana. *International Journal Earth Science (Geology Rundsch..)*, *93*, 13–22.

Braun, I., & Kriegsmann, L. (2003). Proterozoic crustal evolution of southernmost India and Sri Lanka. In M. Yoshida, B. F. Windley & S. Dasgupta (Eds.), Proterozoic East Gondwana: supercontinent assembly and breakup (Vol. 206, pp. 169–202), Geological Society London.

Brown, M., & Raith, M. (1996). First evidence of ultrahigh-temperature decompression from the granulite province of southern India. *Journal Geological Society London, 153*, 819–822.

Cenki, B., Braun, I., & Bröcker, M. (2004). Evolution of the continental crust in the Kerala Khondalite Belt, southernmost India: Evidence from Nd isotope mapping, U-Pb and Rb-Sr geochronology. *Precambrian Research, 134*, 275–292.

Chacko, T., Lamb, M., & Farquhar, J. (1996). Ultra-high temperature metamorphism in the Kerala Khondalite Belt. In M. Santosh., & M. Yoshida (Eds.), *The Archaean and proterozoic terrains in southern India within East Gondwana* (Vol. 3, pp. 157–165). Memoir, Gondwana Research Group

Chacko, T., Ravindra Kumar, G. R., Meen, J. H., & Rogers, J. J. (1992). Geochemistry of high-grade supracrustal rocks from the Kerala Khondalite Belt, and adjacent massif charnockites, South India. *Precambrian Research, 55*, 469–489.

Chetty, T. R. K. (1996). Proterozoic shear zones in Southern Granulite Terrain, In M. Santosh & M. Yoshida (Eds.), *The Archaean and proterozoic terrains in Southern India within East Gondwana*, (Vol. 3, pp. 77–89). Memoir, Gondwana Research Group.

Chetty, T. R. K., & Bhaskar Rao, Y. J. (2006). Strain pattern and deformational history in the eastern part of the Cauvery shear zone, southern India. *Journal Asian Earth Science, 28*, 46–54.

Chetty, T. R. K., Bhaskar Rao, Y. J., & Narayana, B. L. (2003). A structural cross section along Krishnagiri-Palani corridor, Southern granulite terrain of India. *Memoir Geological Society India, 50*, 255–277.

Chetty, T. R. K., Yellappa, T., Nagesh, P., Mohanty, D. P., Venkatasivappa, V., Santosh, M., & Tsunogae, T. (2011). Structural anatomy of a dismembered ophiolite suite from Gondwana : The Manamedu complex, Cauvery Suture zone, southern India. *Journal Asian Earth Science, 42*, 176–190.

Choudhary, A. K., Harris, N. B. W., Van Calsteren, P., & Hawkesworth, C. J. (1992). Pan-African charnockite formation in Kerala, South India. *Geological Magazine, 129*, 257–264.

Choudhary, A. K., Jain, A. K., Singh, S., Manickavasagam, Rm, & Chandra, K. (2011). Crustal accretion and metamorphism of Mesoarchaean granulites in Palghat-Cauvery Shear Zone, Southern India. *Journal Geological Society India, 77*, 227–238.

Cooray, P. G. (1984). *An introduction to the geology of Sri Lanka (Ceylon)* (2nd ed.). Colombo: National Museum of Sri Lanka Publication.

Cooray, P. G. (1994). The Precambrian of Sri Lanka: A historical review. *Precambrian Research, 66*, 3–18.

D'Cruz, E., Nair, P. K. R., & Prasanna Kumar, V. (2000). Palghat gap—a dextral shear zone from the South Indian granulite terrain. *Gondwana Research, 3*, 21–31.

Dissanayake, C. B., & Munasinghe, T. (1984). Reconstruction of Precambrian sedimentary basin on the granulite belt of Sri Lanka. *Chemical Geology, 47*, 221–247.

Drury, S. A., Harris, N. B. W., Holt, R. W., Reeves, S. G. J., & Wightman, R. T. (1984). Precambrian tectonics and crustal evolution in South India. *Journal Geological, 92*, 3–20.

Hansen, E. C., Stern, R. J., Devaraju, T. C., Mahabaleswar, B., & Kenny, P. J. (1997). Rubidium-strontium wholerock ages of banded and incipient charnockites from southern Karnataka. *Journal Geological Society India, 50*, 267–275.

Harris, N. B. W., Holt, R. W., & Drury, S. A. (1982). Geobarometry, geothermometry and the Late Archaean geotherms from the granulite facies terrain in South India. *Journal Geology, 90*, 509–527.

Holzl, S., Hofmann, A. W., Todt, W., & Kohler, H. (1994). U-Pb geochronology of the Sri Lankan basement. *Precambrian Research, 66*, 123–149.

Jain, A. K., Singh, Sandeep, & Manickavasagam, R. M. (2003). Intercontinental shear zones in the Southern Granulite Terrain, their kinematics and evolution. *Memoir Geological Society India, 50*, 225–253.

Janaradhan, A. S., & Leake, B. E. (1975). The origin of the metaanorthositic gabbros and garnetiferous granulites of the Sittampundi Complex, Madras, India. *Journal Geological Society India, 6*, 391–408.

Janardhan, A. S. (1996). The Oddachatram anorthosite body, Madurai Block, southern India. *Memorial Gondwana Research Group, 3*, 385–390.

Janardhan, A. S. (1999). Southern granulite terrain, south of the Palghat-Cauvery shear zone: Implications for India-Madagascar connection. *Gondwana Research, 2*, 463–469.

Janardhan, A. S., & Wiebe, R. A. (1985). Petrology and geochemistry of the Oddanchatram anorthosite and associated basic granulites, Tamil Nadu, South India. *Journal Geological Society India, 26*, 163–176.

Jayananda, M., Janardhan, A. S., Suvasubramanian, P., & Peucat, J. J. (1995). Geochronologic and isotopic constraints on granulite formation in the Kodaikanal area, Southern India. *Memoir Geological Society India, 34*, 373–390.

Jayawardane, D. E., & Carswell, D. A. (1976). The geochemistry of "charnockites" and their constituent ferromagnesian minerals from the Precambrian of southeast Sri Lanka. *Mineralogical Magazine, 40*, 541–554.

John, M. M., Balakrishan, S., & Bhadra, B. K. (2005). Contrasting metamorphism across Cauvery shear zone, South India. *Journal Earth Systems Science, 114*, 143–158.

Kehelpannala, K. V. W. (1997). Deformation of a high-grade Gondwana fragment, Sri Lanka. *Gondwana Research, 1*, 47–68.

Kehelpannala, K. V. W., & Ratnayake, R. M. J. W. K. (2001). Polyphase migmatization of layered basic rocks in the Wanni Complex of Sri Lanka. *Gondwana Research, 4*, 174–178.

Kleinschrodt, R. (1994). Large-scale thrusting in the lower crustal basement of Sri Lanka. *Precambrian Research, 66*, 39–57.

Kleinschrodt, R., Voll, G., & Kehelpannala, W. (1991). A layered basic intrusion deformed and metamorphosed in granulite facies of the Sri Lanka basement. *Geologische Rundschau, 80*, 779–800.

Kriegsmann, L. M. (1994). Evidence for fold nappe in the high-grade basement of central Sri Lanka: Terrain assembly in Pan-African lower crust. *Precambrian Research, 66*, 59–76.

Krishnamurthy, P. (1977). On some geological aspects of the Sevattur carbonatite complex, North Arcot district, Tamil Nadu. *Journal Geological Society India, 18*, 265–274.

Kroner, A., Kehelpannala, K. V. W., & Hegner, F. (2003). Ca 750–1100 Ma magmatic events and Grenville-age deformation in Sri Lanka: Relevance for Rodinia supercontinent formation and dispersal and Gondwana amalgamation. *Journal Asian Earth Science, 22*, 279–300.

Kroner, A., & Williams, I. S. (1993). age of metamorphism in the high-grade rocks of Sri Lanka. *Journal Geology, 101*, 513–521.

Kumar, A., & Gopalan, K. (1991). Precise Rb-Sr age and enriched mantle source of the Sevattur carbonatites, Tamil Nadu, South India. *Current Science, 60*, 653–654.

Lal, R. K. (2003). Metamorphic evolution of granulites from southern Indian shield. *Memoir Geological Society India, 52*, 61–108.

Lal, R. K., Ackermand, D., & Upadhyay, H. (1987). P-T-X relationship deduced from corona textures in sapphirine-spinel-quartz assemblages from Paderu, Southern India. *Journal Petrology, 28*, 1139–1168.

Manglik, A. (2005). Variations in lithospheric structure in the vicinity of Palghat-Cauvery shear zone, Southern Indian Shield: Inferences from magneto-telluric data. *Current Science, 88*, 497–501.

Mathavan, V., Prame, W. K. B. N., & Cooray, P. G. (1999). Geology of the high grade proterozoic terrains of Sri Lanka and the assembly of Gondwana: An update on recent developments. *Gondwana Research, 2*, 237–250.

Meisner, B., Deters, P., Srikantappa, C., & Kohler, H. (2002). Geochronological evolution of the Moyar, Bhavani and Palghat shear zones of southern India: implications for East Gondwana correlation. *Precambrian Research, 114*, 149–175.

Merh, S. S. (1962). Structural aspects of the charnockitic rocks of Pallavaram, Madras State. *Journal M.S University Baroda, 11*, 123–138.

Milisenda, C. C., Liew, T. C., Hofmann, A. W., & Kohler, H. (1994). Nd isotopic mapping of the Sri Lanka basement: Update and additional constraints from Sr isotopes. *Precambrian Research, 66*, 95–110.

Miller, J. S., Santosh, M., Pressley, R. A., Clements, A. S., & Rogers, J. W. (1996). A Pan-African thermal event in southern India. *Journal Asian Earth Science, 14*, 127–136.

Mishra, D. C., & Rao, M. B. S. V. (1993). Thickening of crust under the granulitic province of South India and associated tectonics based on gravity-magnetic study. *Memoir Geological Society India, 25*, 203–219.

Mishra, D. C., & Vijaya Kumar, N. (2005). Evidence for Proterozoic collision from airborne magnetic and gravity studies in Southern Granulitic Terrain, India and signatures of recent tectonic activity in the Palghat Gap. *Gondwana Research, 8*, 43–54.

Miyazaki, T., Kagami, H., Ram Mohan, V., Shuto, K., & Morikiyo, T. (2003). Enriched sub-continental lithospheric mantle in the northern part of the South Indian Granulite Terrain: Evidence from Yelagiri and Sevattur syenite plutons, Tamil Nadu, South India. *Gondwana Research, 6*, 585–594.

Miyazaki, T., Kagami, H., Shuto, K., Moriyoko, T., Ram Mohan, V., & Rajasekaran, K. C. (2000). Rb-Sr geochronology, Nd-Sr isotopes and Sevattur syenites, Tamil Nadu, south India. *Gondwana Research, 3*, 39–53.

Mohan, A., & Jayananda, M. (1999). Metamorphism and isotopic evolution of granulites of southern India: Reference to Neoproterozoic crustal evolution. *Gondwana Research, 2*, 251–262.

Mohan, A., Singh, P. K., & Sachan, H. K. (2003). High-density carbonic fluid inclusions in charnockites from Eastern Ghats, India: Petrologic implications. *Journal Asian Earth Science, 22*, 101–113.

Mukhopadhyay, D., Senthil Kumar, P., Srinivasan, R., & Bhattacharya, T. (2003). Nature of the Palghat-Cauvery lineament in the region south of Namakkal, Tamil Nadu: Implications for the terrane assembly in the South Indian granulite province. *Memoir Geological Society India, 50*, 279–296.

Munasinghe, T., & Dissanayake, C. B. (1980). Pink granites in the highland series of Sri Lanka—A case study. *Journal Geological Society India, 21*, 446–452.

Munasinghe, T., & Dissanayake, C. B. (1982). A plate tectonic model for the geological evolution of Sri Lanka. *Journal Geological Society India, 23*, 369–380.

Naha, K., Mukhopadhyay, D., Dastidar, S., & Mukhopadhyay, R. P. (1994). Basement-cover relations between a granite gneissic body and its metasedimentary envelope: a structural study from the early Precambrian Dharwar tectonic province, S, India. *Precambrian Research, 72*, 283–299.

Naha, K., & Srinivasan, R. (1996). Nature of the Moyar and Bhavani shear zones with a note on its implications on the tectonics of the Southern Indian Precambrian shield. *Proceedings of Indian Academy Science (Earth & Planet Sci.)*, *105*, 173–189.

Natarajan, M., Bhaskar Rao, B., Parthasarathy, R., Kumar, Anil, & Gopalan, K. (1994). 2.0 Ga-old proxyenite–carbonatite complex of Hogenakal, Tamil Nadu, South India. *Precambrian Research, 65*, 167–181.

Perera, L. R. K. (1983). The origin of the pink granites of Sri Lanka—Another view. *Precambrian Research, 20*, 17–37.

Peucat, J.-J., Vidal, P., Bernard-Griffiths, J., & Condie, K. C. (1989). Sr, Nd and Pb isotope systematics in the Archaean low- to high-grade transition zone of southern India: Syn-accretion vs post-accretion granulites. *Journal Geology, 97*, 537–550.

Prakash, D. (2010). New SHRIMP U-Pb zircon ages of the metapelitic granulites from NW of Madurai, Southern India. *Journal Geological Society India, 76*, 371–383.

Prakash, D., Asima, M., & Mohan, A. (2006). Ultrahigh-temperature metamorphism in the Palni Hills, South India: Insights from felspar thermometry and phase equilibria. *International Geological Review, 48*, 619–638.

Radhakrishna, T., Mathai, J., & Yoshida, M. (1990). Geology and structure of the high grade rocks from Punalur-Achankovil sector, Souh India. *Journal Geological Society India, 35*, 263–272.

Radhika, U. P., Santosh, M., & Wada, H. (1995). Graphite occurrences in southern Kerala: Characteristics and genesis. *Journal Geological Society India, 45*, 653–666.

Raith, M., Karmakar, S., & Brown, M. (1997). Ultra-high-temperature metamorphism and multistage decompressional evolution of sapphirine granulites from the Palani Hills Ranges, southern India. *Journal Metamorphic Geology, 15*, 379–399.

Rajesh, K., & Chetty, T. R. K. (2006). Structure and tectonics of the Achankovil shear zone, southern India. *Gondwana Research, 10*, 86–98.

Rajesh, H. M., & Santosh, M. (2004). Charnockitic magmatism in southern India. *Proceedings of Indian Academy Science (Earth & Planet. Sci.)*, *113*, 565–585.

Ram Mohan, M., Satyanarayanan, M., Santosh, M., Paul, J. S., Tubrett, M., & Lam, Rebecca. (2013). Neoarchaean suprasubduction zone arc magmatism in southern India : Geochemistry, zircon U-Pb geochronology and Hf isotopes of the Sattampundi Anorthosite complex. *Gondwana Research, 23*, 539–557.

Ramakrishnan, M. (2003). Craton-mobile belt relations in Southern Granulite Terrain. *Memoir Geological Society India, 50*, 1–24.

Ramasamy, S. M. (1995). En echelon faults along West Coast of India and their geological significance. *Current Science, 69*, 811–814.

Ratnakar, J., & Leelanandam, C. (1989). Petrology of alkaline plutons from the eastern and southern Peninsular India. *Memoir Geological Society India, 15*, 145–176.

Ravindra Kumar, G. R., & Chacko, T. (1986). Mechanisms of charnockite formation and breakdown in southern Kerala: Implications for the origin of the southern Indian Granulite Terrain. *Journal Geological Society India, 28*, 277–288.

Ravindra Kumar, G. R., & Chacko, T. (1994). Geothermobarometry of mafic granulites and metapelites from Palghat region of south India: Evidence for isothermal uplift and rapid cooling. *Journal Metamorphic Geology, 12*, 479–492.

Ravindra Kumar, G. R., & Srikantappa, C. (1995). Arrested charnockite formation in Palghat region, south India. *Journal Geological Society India, 45*, 147–164.

Ravindra Kumar, G. R., Srikantappa, C., & Hansen, E. C. (1985). Charnockite formation at Ponmudi, southern India. *Nature, 313*, 207–209.

Ravindra Kumar, G. R., & Sukumaran, S. (2003). Petrology and geochemistry of gneisses, charnockites and charnoenderbites of Palghat region, south India. *Memoir Geological Society India, 50*, 409–434.

Reddi, A. G. B., Mathew, M. P., Singh, Baldev, & Naidu, P. S. (1988). Aeromagnetic evidence of crustal structure in the granulitic terrane of Tamil Nadu-Kerala. *Journal Geological Society India, 32*, 368–381.

Reddy, P. R., Rajendra Prasad, B., Vijay Rao, V., Sain, Kalachand, Prasada Rao, P., Khare, P., & Reddy, M. S. (2003). Deep seismic reflection and refraction/wide-angle reflection studies along Kuppam-Palani Transect in Southern Granulite Terrain of India. *Geological Society India Memoir, 50*, 79–106.

Roy, S., & Rao, R. U. M. (2000). Heat flow in Indian shield. *Journal Geophysics Research, 105*, 25587–25604.

Sachs, P. E., Nambiar, C. G., & Walters, L. J. (1997). Dextral Pan-African shear along the southwestern edge of the Achankovil shear belt, south India: Constraints of Gondwana reconstruction. *Journal Geological, 105*, 275–284.

Santosh, M. (1989). Alkaline plutons, decompression granulites and Late Proterozoic CO_2 influx in Kerala, south India. *Memoir Geological Society India, 15*, 177–188.

Santosh, M., Morimoto, T., & Tsutsumi, Y. (2006). Geochronology of the khondalite belt of Trivandrum Block, southern India: Electron microprobe ages and implications for Gondwana tectonics. *Gondwana Research, 9*, 261–278.

Santosh, M., Tanaka, K., Yokoyama, K., & Collins, A. S. (2005). Late Neoproterozoic-Cambrian felsic magmatism along transcrustal shear zones in southern India: U-Pb electron microprobe ages and implications for the amalgamation of the Gondwana supercontinent. *Gondwana Research, 8*, 31–42.

Santosh, M., Xiao, W. J., Tsunogae, T., Chetty, T. R. K., & Yellappa, T. (2012). The Neoproterozoic subduction complex in southern India: SIMS zircon U-Pb ages and implications for Gondwana assembly. *Precambrian Research, 192–195*, 190–208.

Santosh, M., Yokoyama, K., Biju-Sekhar, S., & Rogers, J. J. W. (2003). Multiple tectonothermal events in the granulitic blocks of southern India revealed from EPMA dating: Implications on the history of supercontinent. *Gondwana Research, 6*, 29–63.

Santosh, M., & Yoshida, M. (2001). Pan-African extensional collapse along the Gondwana suture. *Gondwana Research, 4*, 188–191.

Satish-Kumar, M., Wada, H., & Santosh, M. (2001). Contrasting carbon and oxygen isotopic evolution in metacarbonates from the Kerala Khondalie Belt, Southern India. *Gondwana Research, 4*, 377–386.

Satyanarayana, K. V. V., Arora, B. R., & Janardhan, A. S. (2003). Rock magnetism and palaeomagnetism of the Oddanchatram anorthosite, Tamil Nadu, south India. *Internal Geophysics Journal, 155*, 1081–1092.

Sen, D. P., Bhattacharya, S. C., & Ray, S. K. (1970). Turbidite deposits around the Simla Hills: A study from the Simla Series, H.P. (India). *Sedimentary Geology, 3*, 317–329.

Shabeer, K. P., Satish-Kumar, M., Armstrong, R., & Buick, I. S. (2005). Constraints on the timing of Pan-African granulite-facies metamorphism in the Kerala Khondalite Belt of southern India. *Journal Geology, 113*, 95–106.

Singh, A. P., Mishra, D. C., Vijaya Kumar, V., & Rao, M. B. S. V. (2003). Gravity magnetic signatures and crustal architecture along Kuppam-Palani geotransect, South India. *Memoir Geological Society India, 50*, 139–163.

Srikantappa, C. (1993). High-pressure charnockites of the Nilgiri Hills, southern India. *Memoir Geological Society India, 25*, 95–110.

Srikantappa, C., & Narasimha, K. N. P. (1988). Retrogression of charnockites in the Moyar Shear Zone, Tamil Nadu. *Memoir Geological Society India, 11*, 117–124.

Srinagesh, D., & Rai, S. S. (1996). Teleseismic tomographic evidence for contrasting crust and upper mantle in south Indian Archaean terrain. *Physics Earth Planetary Interior, 97*, 27–41.

Srivastava, R. K. (1998). Petrology of the Proterozoic alkaline carbonatite complex of Samalpatti, district Dharmapuri, Tamil Nadu. *Journal Geological Society India, 51*, 233–244.

Srivastava, R. K., Heaman, L. M., Sinha, A., & Shihua, S. (2005). Emplacement, age and isotope geochemistry of Sung Valley alkaline carbonatite complex, Shillong Plateau, northeastern India: Implications for primary carbonate melt and genesis of the associated silicate rocks. *Lithos, 81*, 33–54.

Subba Rao, T. V., Narayana, B. L., & Gopalan, K. (1994). Rb-Sr age of the Sivamalai alkaline complex, Tamil Nadu. *Proceedings of Indian Academy Science (Earth & Planetary Science)*, *103*, 425–437.

Subramanian, A. P. (1956). Mineralogy and petrology of the Sittampundi complex, Salem district, Madras State, India. *Bulletin Geological Society America, 67*, 317–390.

Subramanian, A. P. (1959). Charnockites of the type area near Madras—a reinterpretation. *American Journal Science, 257*, 321–353.

Tateishi, K., Tsunogae, T., Santosh, M., & Janardhan, A. S. (2004). First report of sapphirine + quartz assemblage from southern India: Implications for ultrahigh temperature metamorphism. *Gondwana Research, 7*, 899–912.

Udas, G. R., & Krishnamurthy, P. (1970). Carbonatites of Sevattur and Jokipatti, Madras State, India. *Proceedings Indian National Science Academy, 36*, 331–343.

Unnikrishnan-Warrier, C. (1997). Isotopic signature of Pan-African rejuvenation in the Kerala Khondalite Belt, Southern India: Implications for East Godavari Assembly. *Journal Memoir Geological Society India, 50*, 179–190.

Valdiya, K. S. (1998). Late Quarternary movements on landscape rejuvenation in southeastern Karnataka and adjoining Tamil Nadu in Southern Indian Shield. *Journal Geological Society India, 51*, 139–166.

Vemban, N. A., Subramanian, K. S., Gopalakrishnan, K., & Venkata Rao, V. (1977). Major faults, dislocations and lineaments of Tamil Nadu. *Geological Survey India Misc Publication, 31*, 53–56.

Verma, R. K. (1985). *Gravity field, seismicity and tectonics of the Indian peninsula and the himalaya*. New Delhi: Allied Publishers.

Viladkar, S. G., & Subramanian, V. (1995). Mineralogy and geochemistry of the carbonatites of the Sevattur and Samalpatti complexes, Tamil Nadu. *Journal Geological Society India, 45*, 505–517.

Weerakoon, M. W. K., Miyazaki, T., Shuto, K., & Kagami, H. (2001). Rb-Sr and Sm-Nd geochronology of Eppawala metamorphic rocks and carbonatite, Wanni Complex, Sri Lanka. *Gondwana Research, 4*, 409–420.

Yellappa, T., Santosh, M., Chetty, T. R. K., Kwon, S., Park, C., Nagesh, P., et al. (2012). A Neoarchaean dismembered ophiolite complex from southern India: Geochemical and geochronological constraints on its suprasubduction origin. *Gondwana Research, 21*, 246–268.

Yoshida, M., Santosh, M., & Dissanayake, C. B. J. (1999). Proterozoic events in East Gondwana, progress in 1998. *Geological Research, 2*, 665–667.

Chapter 8
Intracratonic Purana Basins in Peninsular India: Mesoproterozoic History

8.1 Introduction

In the wake of the Eastern Ghat orogenic movements when a large part of India was affected by tectonic upheaval and attendant magnetic activities, a number of shallow but subsiding basins developed in the active parts in front of the older orogenic belts. The Cuddapah Basin in Andhra Pradesh evolved immediately west of the Eastern Ghat Mobile Belt, and the Vindhyan Basin developed in front of the parabolic Satpura–Aravali orogenic belts (Fig. 8.1 inset). The continental margin in the north, likewise, subsided progressively to give rise to the Himalaya Basin of the Precambrian time. The Mesoproterozoic–Neoproterozoic sedimentary basins are known as the *Purana* (from the Sanskrit word *Purān* or Hindi *Purānā*, meaning ancient). The name was given by Thomas H. Holland in 1907. The term has no stratigraphic connotation; it merely represents shallow-water platform sediments that escaped metamorphism and structural deformation over larger parts excepting the margins of basins. The Purana succession is broadly contemporaneous with what the Russians call *Riphean* and *Vendian* spanning the temporal period from 1650 ± 50 Ma to 570 Ma.

It may be stressed that the Purana basins span both the Mesoproterozoic and the Neoproterozoic periods. It is not easy to separate the two groups of rock successions. In this chapter, only the Mesoproterozoic successions are discussed.

The successions of sedimentary rocks of the Purana basins vary in thickness from less than 200 m to more than 10,000 m and comprise predominant sandstones with minor lenses of conglomerate and shale and subordinate limestones–dolomites. The successions in various basins (Fig. 8.1) preserve records of two major cycles of sedimentation, each punctuated by multiple marine transgression and recessions, volcanic and magmatic activities, and episodes of tectonic disturbance. The earlier tectonic disturbance coincides broadly with the end of the Palaeoproterozoic era when sedimentation commenced at 1600–1700 Ma the

K.S. Valdiya, *The Making of India*, Society of Earth Scientists Series,
DOI 10.1007/978-3-319-25029-8_8

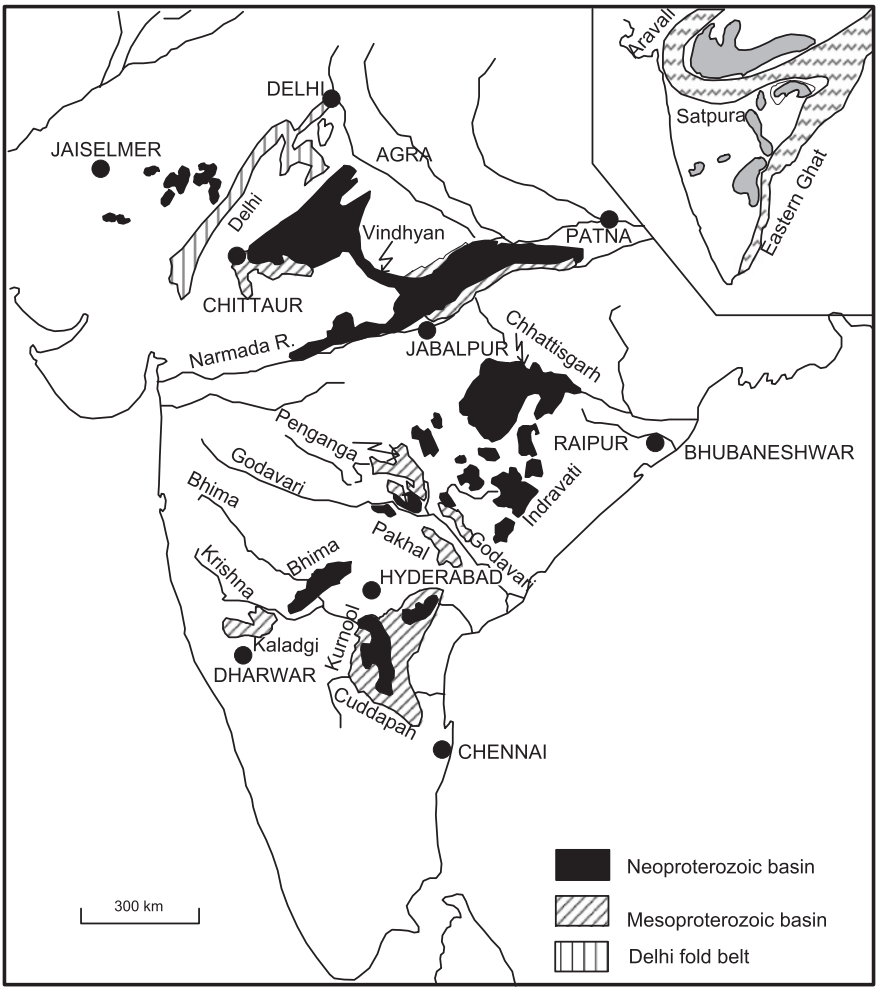

Fig. 8.1 Purana basins in the Peninsular India. While the Mesoproterozoic era witnessed development of intracratonic basins in the Cuddapah, Kaladgi, Godavari and Vindhyan regions, in the following Neoproterozoic time many more areas became sites of sedimentation. *Inset* shows the proximity of the Purana basins with the Proterozoic mobile belts, affected by 1600 ± 100 Ma crustal movements

middle one around 1000 ± 50 Ma, when there was interruption, and the later one marks the termination of the protracted Purana sedimentation sometime between 500 and 600 Ma.

Among the many events that happened during the evolutionary history of India, one was the formation of the fault along the eastern boundary of the Cuddapah Basin, and of the Great Boundary Fault separating the Aravali orogenic belt from the Vindhyan. The Son–Narmada Lineament was reactivated pronouncedly, as evident from severe deformation witnessed along the belt.

8.2 Twofold Subdivision of Purana Succession

The Purana successions are divided into two major groupings (Fig. 8.2). A regional unconformity separates the two. Overlying the Cuddapah, the Kurnool is a Neoproterozoic succession. It implies a tectonic upheaval of consequence. Later tectonic movements, contemporaneous with the Pan-African Orogeny of Africa and the Adelaide Orogeny of Australia (Valdiya 1995), brought about the end of sedimentation in all the Purana basins. The earlier tectonic movement manifested itself in significant tectonic mobility disturbance and attendant magmatic activity in the Eastern Ghat Mobile Belt, as evident from (1) clustering of

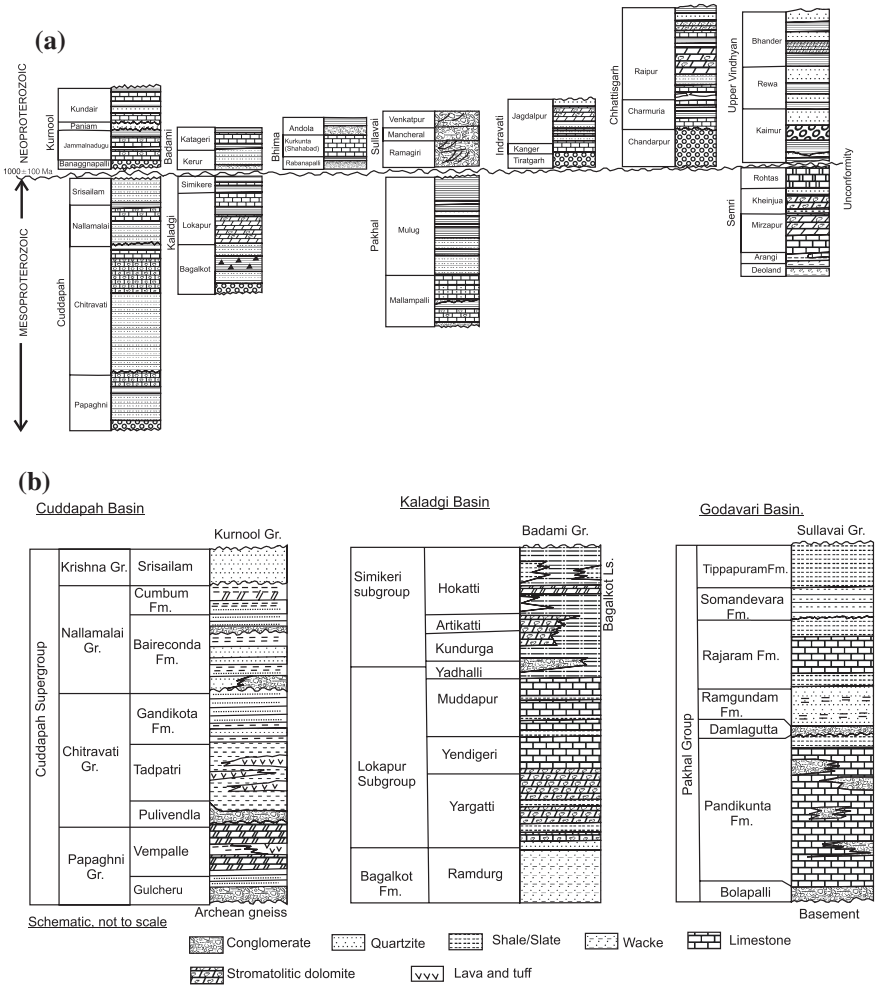

Fig. 8.2 Twofold subdivision of the Purana successions, represented by lithological columns—one set of the Mesoproterozoic successions and another of the Neoproterozoic

U–Pb and Ar–Ar dates (Mezger and Cosca 1999); (2) strong folding and thrusting of Mesoproterozoic rocks along the margins of the Cuddapah, Godavari and Vindhyan basins; and (3) granitic activity close to the eastern margin of the Vindhyan Basin in Bihar. The emplacement of kimberlite in a number of places in the Vindhyan, Indravati and Cuddapah basins at 1067 Ma seems to be related to this tectonic event. The Pan-African orogeny is represented by emplacement of charnockites in the Southern Granulite Terrane and widespread granitic activity in the Himalaya province (Valdiya 1993).

8.3 Cuddapah Basin

8.3.1 Tectonics

The crescent-shaped basin is 440 km in length along its eastern margin and 145 km across in its widest part. It is a foreland basin in front of the Eastern Ghat Mobile Belt (Figs. 8.1 and 8.3). It was W. King who in 1872 brought to the notice of earth scientists this great pile of Precambrian sedimentary rocks resting on the foundation of Archaean gneisses and granulites. Practically without any sign of metamorphism, the sedimentary pile forms the Nallamalai Range parallel to Eastern Ghats. The basin is characterized by a steep gravity anomaly in and gentle gradients on all other sides (Narain 1987; Mishra et al. 1987; Ram Babu 1993). The basin shows elliptical pattern of aeromagnetic anomaly in the south-western part (Fig. 8.3 inset), implying subsurface presence of highly magnetic material—in addition to known basic lavas and sills. Deep seismic sounding demonstrated that the basin floor is cut by a number of deep faults, producing step-like configuration of the Cuddapah Basin (Kaila et al. 1979; Kaila and Tewari 1985). It seems that the Cuddapah Basin evolved through formation of a series of subbasins—the Papaghni in the south-west, the Nallamalai in the east, the Srisailam in the north-west and the Kurnool in the north-east and west (Ram Babu 1993).

8.3.2 Structural Architecture

The Cuddapah Basin is an arcuate north-plunging, low-amplitude asymmetrical synclinorium. Its western limb dips gently with little disturbance, but the eastern flank is intensely deformed—characterized by overfolds and overthrusts (Narayanaswamy 1966). The intensity of deformation increases eastwards (Fig. 8.4). The open normal folds of the western and central parts give way to tight isoclinal, overthrust folds, in the east. The deformed eastern part of the Cuddapah makes the *Nallamalai Range*. There is thrusting over of the Eastern Ghat rocks upon the Cuddapah sedimentary rocks (Lakshminarayana 2002b). Mylonites mark the zone of thrusting described as *Velikonda Thrust* (Matin and Guha 1996).

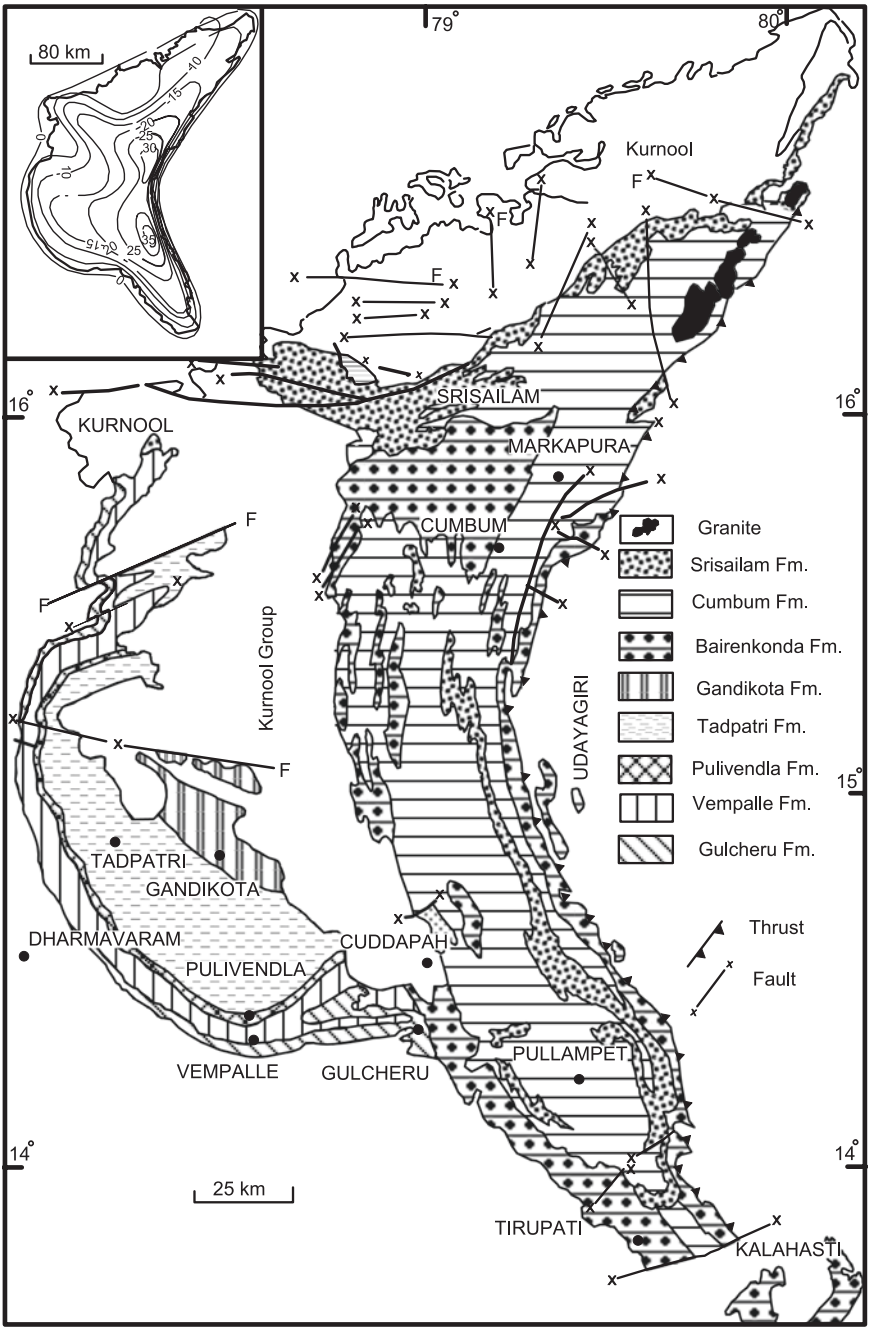

Fig. 8.3 Sketch map of the geology of the Cuddapah Basin showing distribution of the Meso-proterozoic rock formations (After Nagaraja Rao et al. 1987) *Inset* shows aeromagnetic anomaly pattern in the Cuddapah Basin (After Babu Rao et al. 1987)

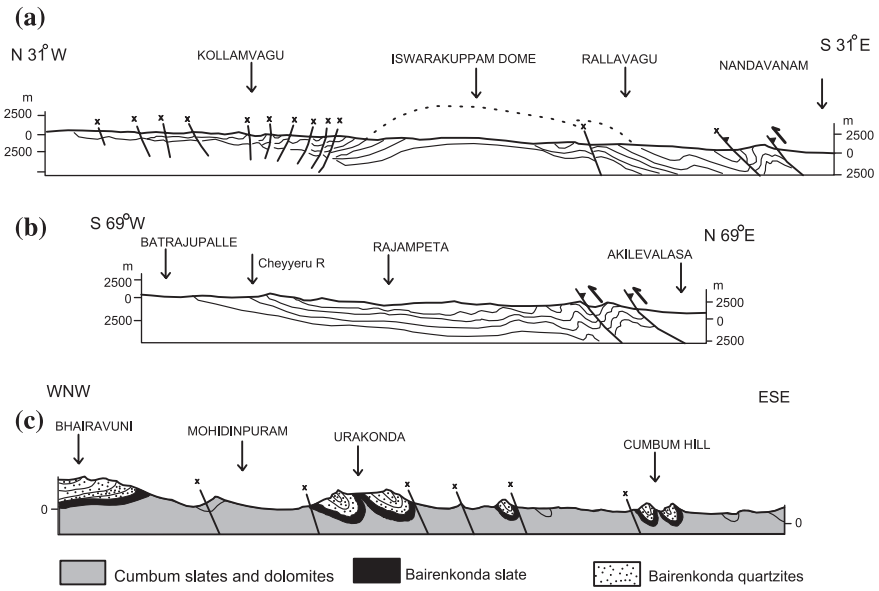

Fig. 8.4 Structural architecture of the Cuddapah Basin as revealed by transverse cross sections. It may be noticed that the intensity of deformation progressively increases eastwards, leading to overfolding and overthrusting of the Eastern Ghat Mobile Belt (After Nagaraja Rao et al. 1987)

Higher gravity anomaly over the Eastern Ghat terrane in contrast to low anomaly over the Cuddapah clearly brings out the crustal-scale nature of the east-dipping shear zone (Mishra et al. 1987; Singh and Mishra 2002). In the line of this shear zone to the north, there are Lakhena and Sileru shear zones, characterized by ophiolites (Leelanandam et al. 1990; Leelanandam 1993). This fact seems to imply that the tectonic plane that separates the Eastern Ghat Mobile Belt from the Cuddapah sedimentary domain—the Velikonda Thrust—is a terrane boundary of considerable geodynamic importance. Strong compression, presumably later in the history of Cuddapah evolutionary history, pushed the Cuddapah rocks upon the Eastern Ghat Mobile Belt is one place in the middle sector (Fig. 8.3) as eloquently borne out by klippen such as at Udayagiri (Narayanaswamy 1966; Nagaraja Rao et al. 1987).

In the middle part of the Cuddapah Basin, there are large domal upwarps (Fig. 8.4a) associated with shear zones and ENE–WSW trending wrench faults. Even the unconformably overlying Kurnool Group of rocks are affected by deformation, giving rise to flexures and doubly plunging folds (Natarajan and Rajgopalan Nair 1977).

8.3.3 Stratigraphy and Sedimentation

The Cuddapah succession comprises predominant arenites and argillites with carbonate rocks forming very crucial horizons, geodynamically as well as economically. Divided into four groups (Table 8.1; Figs. 8.2 and 8.3), each unit begins

Table 8.1 Lithostratigraphical subdivision of the Cuddapah supergroup (after Nagaraja Rao et al. 1987)

	Kurnool Group	
	Unconformity	
Krishna Group	Srisailam Fm (300 m)	Quartzites and shales
	Unconformity	
Nallamalai Group	Cumbum (Pullampet) Fm (2000 m)	Phyllites, slates, quartzites, shale, dolomites
	Bairenkonda (Nagari) Fm (1500–4000 m)	Quartzites, shales, conglomerates with intrusives
	Unconformity	
Chitravati Group	Gandikota Fm (300 m)	Quartzites and shales
	Tadpatri Fm (460 m)	Shales, tuffs, quartzites, dolomites and intrusives
	Pulivendla Fm (1–75 m)	Conglomerates and quartzites
	Disconformity	
Papaghni Group	Vempalle Fm (1900 m)	Stromatolitic dolomites, chert-breccia, quartzite, lavas and pyroclastics
	Gulcheru Fm (28–210 m)	Conglomerates, arkose uartzites and shales
	Unconformity	
	Dharwar gneisses and granites	

characteristically with quartzites and ends up with dolomites or limestone–shale alternations. The sediments were deposited in a shallow-water environment along the shore and the shelf, the latter deepening eastwards. The carbonates represent platform deposits on the shelf of the Proterozoic sea. In the Palnad Basin, the Banaganapalli quartzite represents littoral to infraneritic environment under stable-shelf condition. The Narji Limestone was laid down in infraneritic to neritic zone. The Auk Shale was emplaced in the quiet-water environment, the Panian witnessed mild tectonic instability and the Kundair Limestone was deposited in the neritic environment where reducing condition prevailed (Vijayan, personal communication). Analysis of palaeocurrent pattern indicates that the currents sweeping the coast flowed in the north-easterly direction. Significantly, when the Cuddapah sediments accumulated on the shelf, the Eastern Ghat Mobile Belt had not emerged above the sea level to form a provenance of the detritus. This is evident from the lack in the Cuddapah rocks of such heavy minerals as garnet, kyanite and sillimanite, which are so characteristic of the Eastern Ghat rocks. The detritus was derived from the gneisses and granites of the Dharwar Craton on which

the Cuddapah succession rests. Greater enrichment in respect of K_2O and REE, more fractionated nature, larger Eu-anomaly and depletion of ferromagnesian elements corroborate derivation of the Cuddapah sediments from an evolved crust dominated by tonalities–granodiorites of the Dharwar Craton (Weightman 1986 in Radhakrishna and Naqvi 1986).

8.3.4 Igneous Activity

The upper part of the Papaghni Formation (Table 8.1; Fig. 8.5) comprises a sequence of seven lava flows associated with agglomerates and tuffs, described as *Kuppalapalle Volcanics* (Srikantia 1984). The volcanism commenced towards the close of the Vempalle epoch and continued into the Tadpatri time (Bhaskar Rao et al. 1995). Lavas of andesite and basalt, together with ignimbrite and crystal tuff, were emplaced subaerially. In the western part of the Cuddapah Basin, the Vempalle and the Tadpatri formations comprise sills of dolerite, gabbro and picrite, in addition to basalt flows. In the Nallamalai succession, the Cumbum Formation at Mangampeta includes synsedimentary deposit of siliceous tuffs associated with bedded chert.

NW–SE trending dykes of mafic rocks occur in the Cuddapah Basin as well as in the adjoining southern part of the Bastar Craton, encompassing over

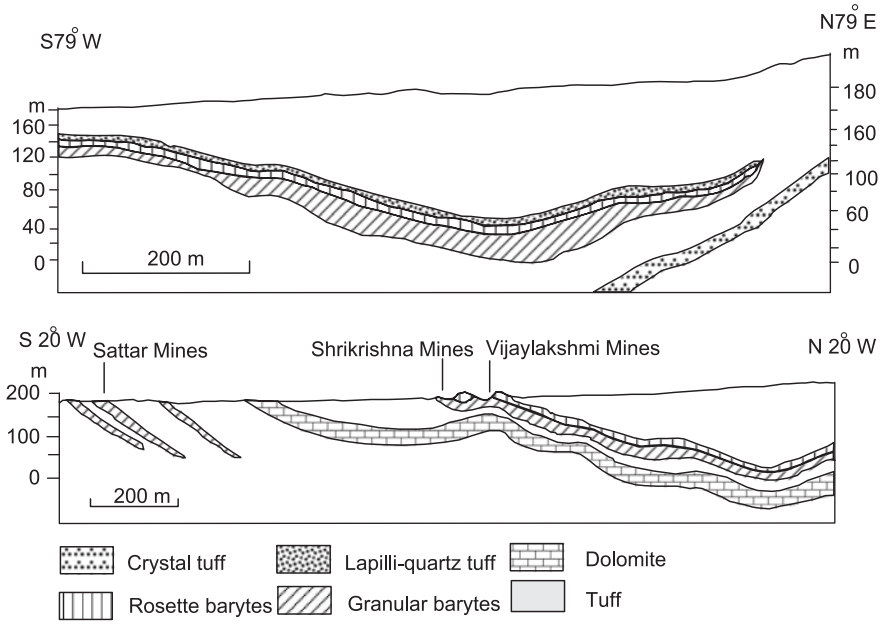

Fig. 8.5 Lensoid deposits of granular and rosette-type barytes are intimately associated with volcanic tuffs (Modified after Neelakantam 1987)

90,000 km^2 area. These dykes, seemingly belonging to a large mafic gneissic province, are dated (U–Pb) 1830 ± 1.4 Ma and 1891.1 ± 0.90 Ma (French et al. 2008). The dykes are believed to be related to the rifting of the continent in this part of southern India.

Significantly, there are intrusive bodies of kimberlite penetrating the succession in the Chelima–Giddaluru area (Leelanandam 1980) and in a number of places towards the western margin. While the kimberlite bodies have ε Nd value of +0.5 to +4.68 implying origin in the depleted mantle magma, the associated lamproite at Chelima and Ramannapet is characterized by εd Nd value of −6.43 to −8.29, suggesting derivation from an enriched source in the mantle (Chalapathi Rao et al. 1998). It seems that the upper mantle beneath the Cuddapah domain was isotopically heterogeneous. Analysis of Rb–Sr of leached phlogopite macrocrysts from four kimberlite plugs at Wajrakarur, Lattavaram, Venkatapalli and Mulligiripalle give a concordant age of 1090 Ma (Anil Kumar et al. 1993).

8.3.5 Life in the Cuddapah Time

Along the western margin of the Basin, Vempalle and Tadpatri formations are characterized by rich development of stromatolites of cyanobacterial origin (Srinivasa Rao 1944; Vaidyanadhan 1961). The Cumbum dolomite of the Nallamalai Group is likewise stromatolitic. Each formation has its specific assemblage exhibiting time-controlled variations in morphology over wide geographical extent. The Vempalle stromatolite assemblage includes what have been described as *Kussiella, Anabaria* and *Inzeria* and the Tadpatri suite is characterized by *Jurusania*, *Gymnosolen*, *Omachtenia*, besides *Conophyton, Colonella* and *Jacutophyton*. The two assemblages strongly recall Lower to Late Riphean stromatolites of the erstwhile USSR (Gururaja and Chandra 1987). The Cumbum stromatolites exhibit laterally linked hemispheroids and vertically stacked columns belonging to the conophytonida supergroup (Raha and Sastry 1982). The digitate and laminated stromatolites are dominated by clotted and bushy spongiostromate calcified microfabrics (Riding and Sharma 1998).

8.3.6 Age of the Cuddapah

A mafic sill that intrudes the Tadpatri succession at Pulivendla is dated 1899 ± 20 Ma by Ar–Ar method (Kumar et al. 2003) and the U–Pb age of baddelyte in the sill is 1881 ± 31 Ma. These dates of intrusives indicate that the Cuddapah sedimentation commenced prior to 1800 Ma. The Zangamrajupalle galena in the Pullampet horizon (Nallamalai Group) gave Pb–Pb age of 1400–1470 Ma (Aswathanarayana 1962, 1964). The amygdaloidal basalt in the Vempalle

and the dolerite sill in the Pulivendla gave Rb–Sr ages of 1359 ± 110 Ma and 980 ± 110 Ma, respectively (Bhaskar Rao et al. 1995).

The 1090 Ma kimberlite plugs intruding the Cuddapah succession leave little doubt as to the Mesoproterozoic age of this supergroup. Palaeomagnetism of 171 samples of the Cuddapah quartzites delineates the Precambrian polar wandering curve, suggesting a time span of 1700–1250 Ma for the Cuddapah (Prasad et al. 1987). Viewing sedimentation in the perspective of all the Purana basins in the Indian subcontinent, it may be inferred that the Cuddapah sedimentation commenced in the interval 1700–1800 Ma.

8.3.7 Mineral Assets

Barytes occur as vein deposits, formed in fractures, shear zones and faulted rocks, and also in bedded forms. Granular and rosette forms of barytes with $BaSO_4$ content as high as 85 % constitute India's 90 % (and world's 25 %) deposits. These deposits are largely confined to the Vempalle belt extending from Guvvalacheruvu to Bolaram. The lenticular deposit at Mangampeta is the single largest deposit of its kind. The grey, granular barytes is intimately associated with lapilli-tuffs (Fig. 8.5) in the upper carbonaceous part of the Cumbum Shales (Karunakaran 1976). The granular variety is a product of exhalative volcanism, the lapilli-hosted barytes is related to a pyroclastic phase, and the vein-type deposit is attributed to hydrothermal replacement (Neelakantam 1987).

Uranium minerals with U_3O_8 concentration up to 1.44 % form lensoid bodies in a 2-km-long belt near Bandi within the Gulcheru Quartzite of the Papaghni Group. There are disseminations of uraninite and coffinite in chlorite–sericite matrix of the fractured quartzite cut by E–W trending faults (Umamaheshwar et al. 2001). The overlying phosphatic-siliceous dolomites of the Vempalle Formation are likewise mineralized, giving rise to low-grade but large-tonnage strata-bound deposits. In the Tummalapalle–Rachakuntapalle–Giddapalle sector, pitchblende and coffinite constitute the main uranium minerals (Raju et al. 1993). In the western part of the basin at Lambapahar occur uranium mineralizations above and below the unconformity separating the Precambrian basement from the Srisailam quartzites (Sinha et al. 1995). An unconformity-related subsurface horizon persistently extending 4.4 km in the east–west direction and 2.7 km across in the Srisailam subbasin in the Chitral area, district Nalgonda, comprises veins of pitchblende and uraninite developed in microfractures of granitoids below (Verma et al. 2009). The mineralization horizon holds reserve of promise.

Asbestos of crysotile variety occurs in a 14-km-long Pulivendla belt between Lingale and Brahmapalle. The deposits are confined to narrow zone of serpentinization of dolerite sills within the Vempalle dolomites. Steatite occurs with asbestos.

Copper sulphides with minor lead and zinc sulphides occur as disseminations, stringers, pockets and veins in the brecciated dolomite of the Vempalle, Tadpatri

and Cumbum formations. The Cumbum dolomite is the principal host of the copper deposits in the Agnigundala belt. The 50-km stretch of the belt, affected by ENE–WSW-oriented faults, shows structurally controlled mineralization, such as seen at Bandalamottu and Dhukonda. The mineralization is confined to very steep dipping discordant quartz reefs in the Tadpatri unit (Ramam and Murty 1997).

In the 50-km-long Zangamrajupalle belt along the eastern margin of the Nallamalai Range, syngenetic *stratiform deposits of lead and zinc* are confined to the top of the horizon of cherty dolomite and bedded chert. Copper sulphide occurs in the lower member made up of dolomites.

8.4 Kaladgi Basin

8.4.1 Structural Setting

In northern Karnataka and adjoining Maharashtra, the Kaladgi Basin (Figs. 8.1 and 8.6) evolved as a consequence of crustal extension. Resting on the basement of the Archaean gneisses (and underlying the Deccan Traps), the Kaladgi

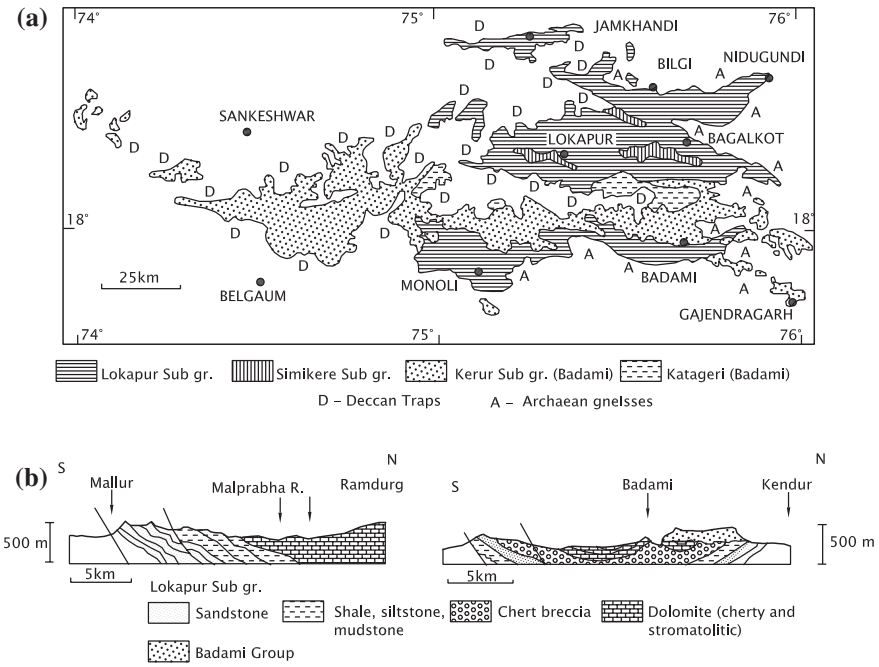

Fig. 8.6 **a** Geological sketch map of the Kaladgi Basin in northern Karnataka (Modified after Jayaprakash et al. 1987). **b** Cross sections illustrate the structural design of the Kaladgi Basin (After Kale and Phansalkar 1991)

succession is more than 4500 m thick. The Kaladgi sedimentary pile is folded into a series of anticlines and synclines on E–W to ESE–WNW axes. These folds have been superposed by later-generation cross-folds producing doubly plunging structures (Jayaprakash et al. 1987). In the eastern part of the Basin, the basal formation is faulted. The associated chert breccia indicates that growth faults remained active all through the duration of the Kaladgi sedimentation even as the basin floor sagged in the western part (Kale and Phansalkar 1991).

8.4.2 Stratigraphy and Sedimentation

The Kaladgi succession is divided into two groups—the *Bagalkot* belonging to the Mesoproterozoic and the *Badami* of the Neoproterozoic. An angular unconformity separates the two assemblages (Table 8.2; Fig. 8.2a). Only the Bagalkot (Jayaprakash et al. 1987) is discussed here. The basin floor sagged rapidly, and conglomerates were emplaced as lenses within the sandstone-dominated siliciclastic succession. Most important among the sand-size clasts are felspars and rock fragments. The quartzwacke and arkose grade upwards into purple and brown argillite (*Ramdurg Formation*) of the *Lokapur* succession. The succeeding succession (*Yargatti Formation*) comprises cherty stromatolitic dolomite of blue grey colour associated with siliceous–ferruginous argillite representing a platform deposit. Continued movement on growth faults generated chert breccia in the basal part of the formation and then followed the deposition of limestones, dolomites

Table 8.2 Lithostratigraphic subdivision of Bagalkot Group in the lower part of Kaladgi succession (after Jayaprakash et al. 1987)

Badami Group	
---------- *Unconformity* ----------	
Simikeri Subgroup	Hokatti Formation (702 m) Arlikatti Formation (168 m) Kundarga Formation (277 m)
---------- *Disconformity* ----------	
Lokapur Subgroup	Yadhalli Formation (58 m) Muddapur Formation (566 m) Yendigeri Formation (259 m) Yargatti Formation (853) Ramdurg Formation (475 m)
---------- *Unconformity* ----------	
Archaean Gneisses	

and shales (*Yendigeri, Muddapur* and *Yadhalli* formations) on the shelf. The limestone at Chiksellikeri is extensively mined for cement-making. A 15-m-thick conglomerate horizon marks a disconformity between the Lokapur and the overlying the *Simikeri* succession of quartzites, chert breccia, ferruginous shale, and dolomite. Towards the close of the Bagalkot time, pegmatite and quartz veins (*Mallapur* intrusives) were emplaced when the Mesoproterozoic sedimentation ended. An upheaval seems to have overtaken the Kaladgi Basin.

Repeated reactivation of basement faults is represented by seismites, and penecontemporaneous deformational structures including tectonic breccia, in the Bagalkot succession. The shallow marine sediments attain a maximum thickness of 4000 m. Evidently, the basin floor continuously subsided with the growing pile of sediments (Kale, personal communication 2008).

8.4.3 Bagalkot Stromatolites

In the lower part of the Lokapur succession (in the Chitrabhanukot area) occurs a horizon of stromatolitic limestone testifying to prolific growth of cyanobacteria. Besides cumulate and hemispheroidal forms, there are columnar forms with conical tops described as *Conophyton* and *Colonella* (Viswanathaiah et al. 1964; Viswanathaiah and Sreedhara Murthy 1979; Viswanathaiah 1977; Govind Rajulu and Gowda 1968; Chandrasekhar Gowda and Govind Rajulu 1980). The stromatolites are comparable with the Middle Riphean stromatolites of the erstwhile USSR.

8.5 Godavari Basin

8.5.1 Tectonics

The Indian Shield was dismembered by rifting apart into the Dharwad and Bastar cratonic blocks along NW–SE trending, presumably pre-existing, weak zones. Rivers Godavari and Pranhita now occupy the terrain over the graben that was formed in the Mesoproterozoic time. The sedimentary succession of the Godavari Basin is represented by what W. King in 1881 named the *Pakhal* and the *Penganga*. They occur in the southern and northern parts of the elongate basin that deepened south-eastwards (Figs. 8.1 and 8.7). The Pakhal and Penganga successions occur independently in different fault-controlled subbasins, characterized by varying degree of tectonism (Chaudhuri 1985, 2003; Chaudhuri et al. 1989; Sreenivasa Rao 1987).

The Pakhal and Penganga groups are both overlain unconformably by the *Sullavai* succession belonging to the Neoproterozoic era (Figs. 8.2 and 8.7). In the northern part, the Godavari successions are hidden under the lava pile of the Deccan, and in the south-eastern side the Basin is terminated by the NE–SW

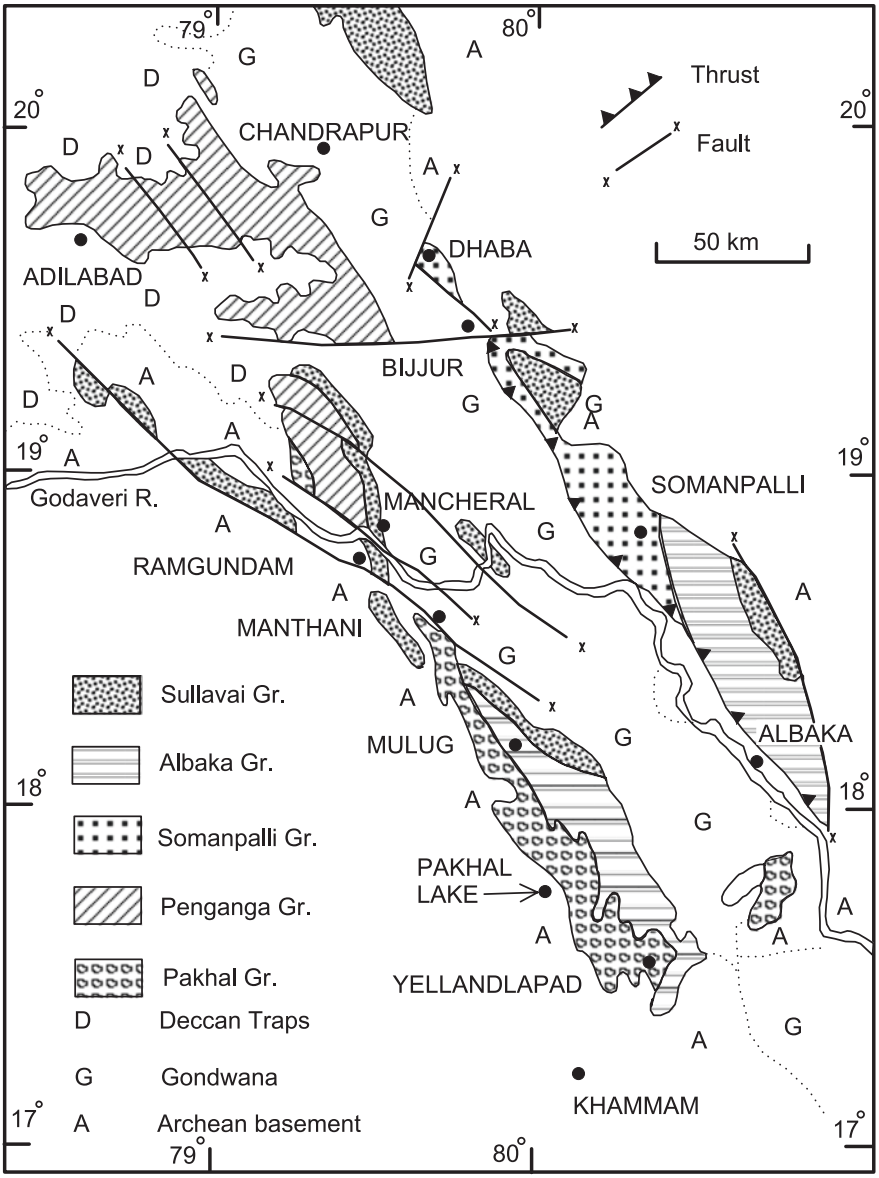

Fig. 8.7 Sketch map shows the Mesoproterozoic–Neoproterozoic geology of the Godavari Basin developed in the NW–SE trending graben of Precambrian antiquity (based on Chaudhuri 2003 and Kale and Phansalkar 1991)

trending Bapatla Ridge of the Eastern Ghat terrane. Tectonic convergence of the Eastern Ghat Mobile Belt against the Godavari succession caused considerable deformation of the Mesoproterozoic succession (Saha and Chaudhuri 2003).

8.5.2 Structural Design

Subjected to strong compression, the Godavari rocks suffered large-scale penetrative deformation resulting in folding and imbricate thrusting (Fig. 8.8). The deformation occurred before the Sullavai sediments of the Neoproterozoic were laid down (Ramamohana Rao et al. 1994; Saha 1990; Mukhopadhyay and Chaudhuri 2003; Saha and Chaudhuri 2003). Two major thrusts are recognized in the Adilabad area. There was southerly propagation of thrust sheets as evident from southwards transportation of the northern packages of rocks. In the Bijjur area, the Godavari sedimentary rocks are truncated against the uplifted basement complex. In the Somanpalli area, the ENE–WSW-oriented cross-folds, superposed on the NW–SE trending folds, were formed due to strike-slip sinistral faulting during the main contractional deformation (Ghosh and Saha 2003).

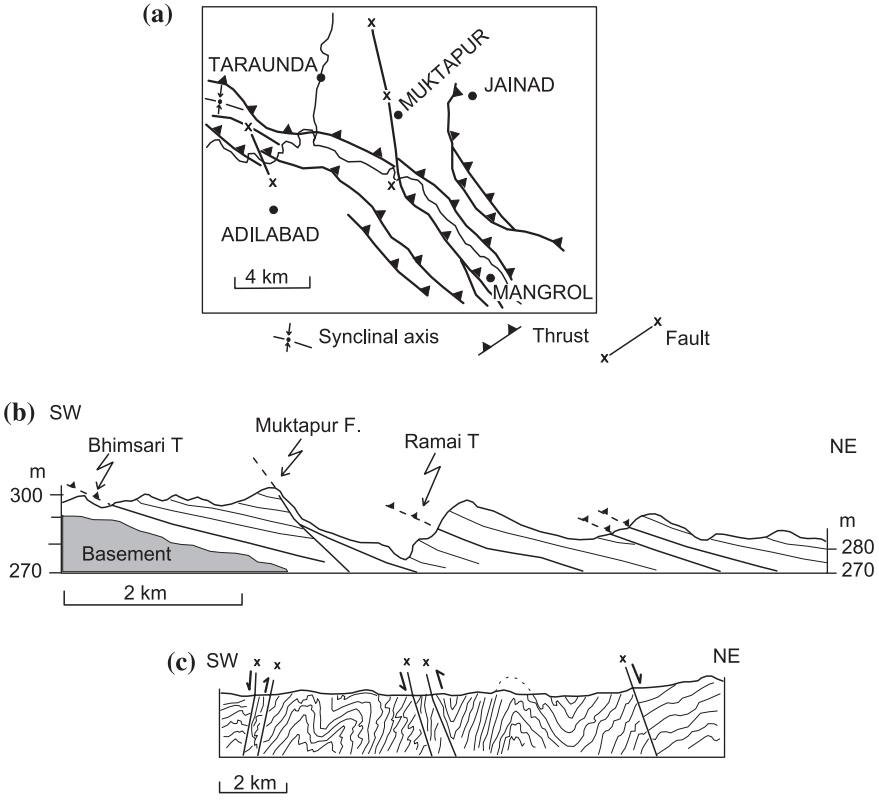

Fig. 8.8 **a** Simplified structural map of the northern and central parts of the Godavari Basin. **b** Cross section illustrates the structural architecture of the northern part. **c** Severe deformation in the east-central part of the Godavari Basin (**a** and **b** after Mukhopadhyay and Chaudhuri, 2003; **c** after Ghosh and Saha 2003)

8.5.3 Stratigraphy and Sedimentation

The lithostratigraphic subdivision of the Mesoproterozoic Pakhal and Penganga (Fig. 8.2) is given in Table 8.3. As already stated, the two groups belong to two separate, fault-controlled subbasins having different pattern of sedimentation (Basumallick 1967). The Pakhal succession of conglomerates, arkosic and quartzarenitic sandstones and shales (*Jonalarasi* Formation) was laid down in settings varying from alluvial fan, braided plain, foreshore and shoreface to offshore environments. The *Pandikunta Limestone*, comprising stromatolitic dolomites and microbial laminites (Chaudhuri 1970), formed on the offshore platform. Glauconite of the interbedded sandstone, dated 1330 ± 53 Ma by the K-Ar method, was formed due to authigenic change of felspar in the tide-influenced high-energy zone of sediment reworking (Chaudhuri et al. 1994). Thick wedges of conglomerate within cross-bedded, ripple-laminated arkosic sandstone (*Damlagutta Formation*) and wave-built shoal bars and outer bar fillings of sandstone (*Ramgundam Sandstone*) were deposited as a series of fault-controlled fans and delta-fan sequences. The sandstones give way to a tidal-flat carbonates, recognized as the *Rajaram Limestone* (Chaudhuri and Howard 1985).

The *Penganga* is a predominant lithographic limestone with minor shales that formed carbonate ramp in relatively deeper water environment below the base of storm waves. During marine transgression, basin-wide anoxic conditions caused precipitation of black carbonates, forming the middle level of the Chanda Formation (Mukhopadhyay and Chaudhuri 2003). The genesis of manganese carbonates in the Penganga succession, characterized by spherical to oval-cylindrical, microconcretions and tubular to irregular elongate film-like microstructures closely resembling microbial extra-cellular polymeric substance. It is attributed to the control of or inducement provided by organotemplates in early diagenetic environment (Mukhopadhyay et al. 2005).

Table 8.3 Lithostratigraphic subdivision of the Pakhal and Penganga groups (after Chaudhuri 2003)

Sullavai Group		
---------- *Unconformity* ----------		
	Rajaram Limestone (735 m) Ramgundam Sandstone (120 m) Damlagutta Conglomerate (90 m)	Satnala Shale
Pakhal Group ---------- *Disconformity* ----------		Penganga Group
	Pandikunta Limestone (340 m) Jonalarasi Formation (50 m)	Chanda Limestone
---------- *Unconformity* ----------		
Archaean Basement Complex		

8.5.4 Volcanic Activity

The Somanpalli area witnessed volcanic activity, testified by volcanic cones and felsic ash beds with pyroclastics occurring within sedimentary succession at different stratigraphic levels. The explosive volcanism is attributed to a common magma chamber which was activated repeatedly throughout the period of basin-filling (Patranabis-Deb 2003). It implies that the Godavari Basin experienced extension repeatedly.

8.6 Vindhyan Basin: Semri Time

Our understanding of the geology and evolutionary history of the Vindhyan Basin (Figs. 8.1 and 8.10) is based on the seminal works of pioneers like H.B. Medlicott in 1859, F.R. Mallet in 1869, R.D. Oldham in 1900, T.H.D. Latouche in 1902, A.M. Heron in 1922 and 1936, A.L. Coulson in 1927 and J.B. Auden in 1933. It was R.D. Oldham who in 1876 gave the name *Vindhyan System* to the 1800–2400-m-thick succession of the making the Vindhya Hill Range. The Vindhyan rocks figure prominently in the Indian history. Bearing the lion cap that is adopted as the national emblem, the Ashok Pillar at Sarnath near Varanasi was carved out of the Vindhyan Sandstone. The temples of Khajuraho were built of the

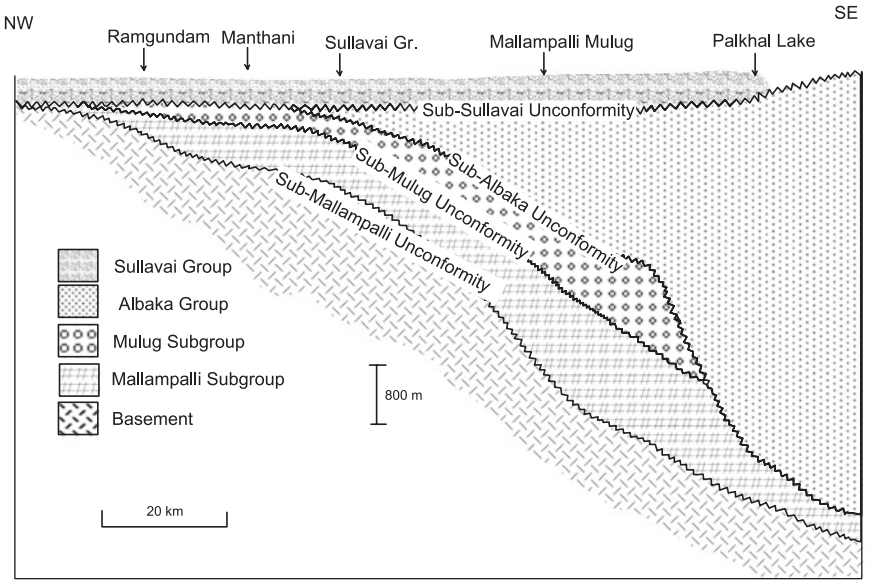

Fig. 8.9 Sedimentation in the Godavari Basin was affected by marine transgression and regression, and tectonic disturbances in the basin floor (After Chaudhuri and Howard 1985)

Vindhyan Sandstones and the Mughal forts at Agra and Delhi and the Fatehpur Sikri complex were all constructed with the Upper Vindhyan Sandstones.

8.6.1 Tectonic Setting

Parabolically enclosing the Archaean domain of the Bundelkhand Granite (Roy and Bhattacharya 1982), the Vindhyan Basin (Figs. 8.10 and 8.11) lies in the embrace of the Satpura and Aravali orogenic mobile belts. It exhibits characteristics of both an intracratonic (continent-interior) basin as well as a peri-continental depression in front of the Satpura orogenic belt. The basin evolved from cumulative consequences of (i) rifting of continental crust, (ii) flexing of foreland basin and (iii) thermal cooling and contraction that caused crustal

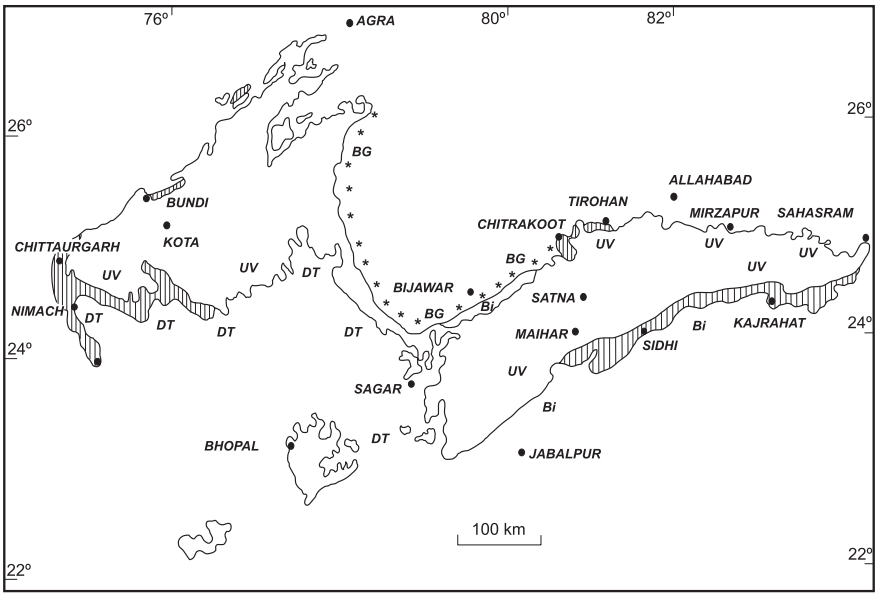

DT- Deccan Traps

UV- Upper Vindhyan

Semri Group (Lower Vindhyan)

Bi- Bijawar

BG- Bundelkhand Granite

Fig. 8.10 Sketch map shows the exposed parts of the Semri Group—the so-called Lower Vindhyan—at the base of a 1800- to 2400-m-thick succession of largely undisturbed sedimentary rocks of Precambrian age (based on Soni et al. 1987)

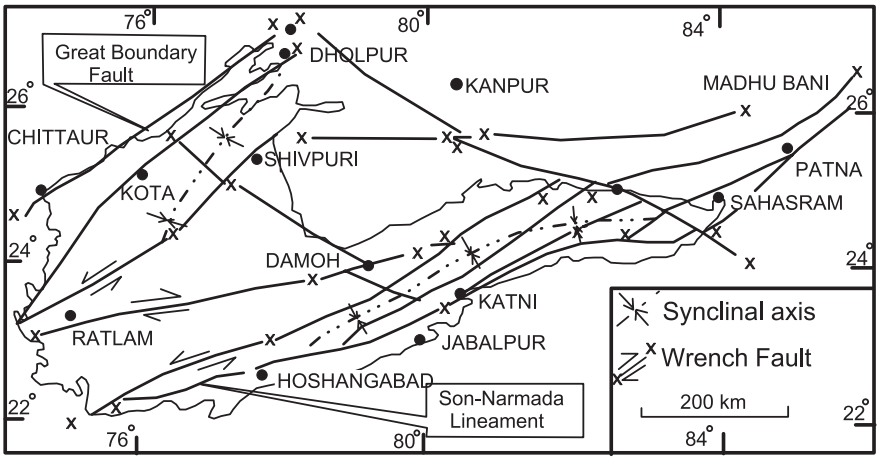

Fig. 8.11 Vindhyan Basin is demarcated by the Son–Narmada "Lineament" along its southern margin and by the Great Boundary Fault along its western flank. A number of faults—some of which wrench faults—divide the Basin into subbasins of the nature of half-grabens (after Ram et al. 1996)

sagging and reactivation of older faults due to thrust loading (Chakraborty and Bhattacharya 1996). Seismic profiles and isopach maps indicate northward extension of the Vindhyan sedimentary pile beneath the Indo-Gangetic alluvial sediments. The Bundelkhand–Faizabad subsurface ridge divides it into two subbasins (Narain and Kaila 1982).

The western, south-western and southern margins of the Vindhyan Basin are demarcated by arcuate faults, forming a parabolic system of thrusts against the Aravali and Satpura orogenic belts (Tewari 1968). Isopach map suggests opening up of the Vindhyan Basin in the west (Ahmad 1958; Banerjee 1974) and in the north as inferred from the occurrence of 1000- to 4300-m-thick succession of the Vindhyan rocks in the Indo-Gangetic domain (Krishnan and Swaminath 1959; Krishnan 1966).

8.6.2 Structural Architecture

The Vindhyan succession is by and large a flat-lying pile of sedimentary rocks. However, along the southern and western margins against the Satpura–Aravali Mobile Belt, the rocks are folded and faulted, and characterized by strong shearing and attendant brecciation (Fig. 8.12). In the Narmada Lineament zone, strong deformation gave rise to overfolds and isoclinal folds with nearly vertical beds (Choubey 1971a). In the Chittaurgarh–Jhalrapatan belt in south-western Rajasthan—where the tectonic boundary swerves from NW–SE to NE–SW—the axes of tight folds dip steeply (50°–70°) westwards (Krishnan and

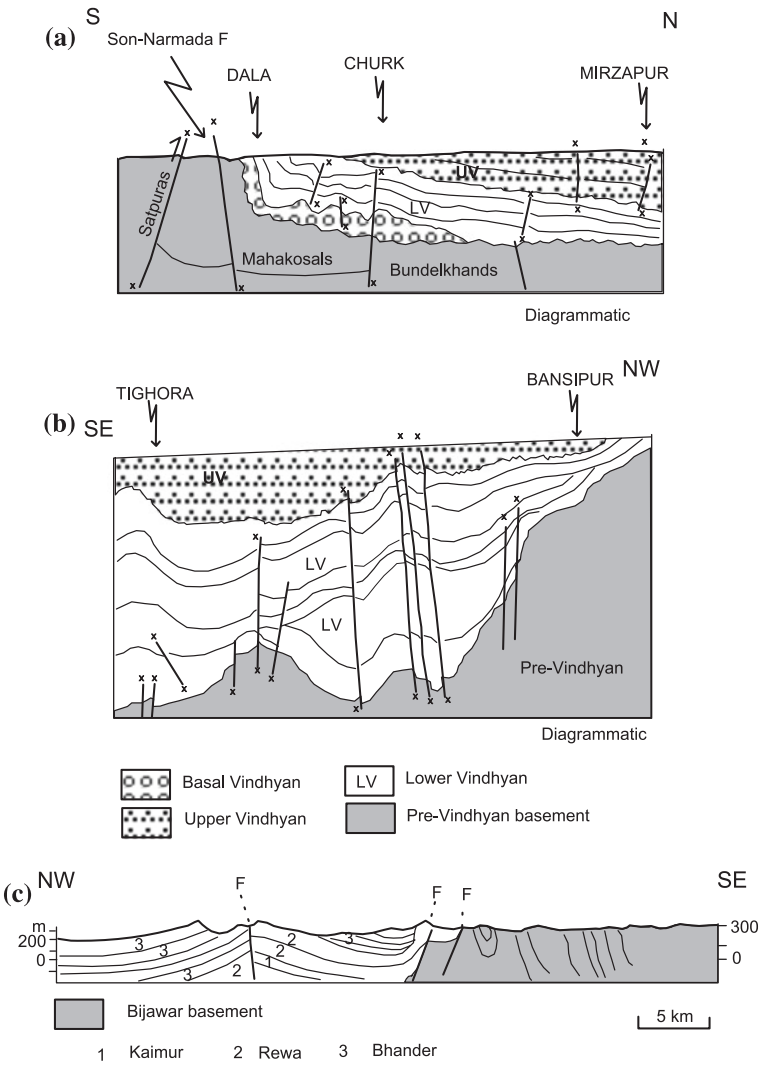

Fig. 8.12 Cross sections illustrate the structural development along the margin of the Vindhyan Basin. **a** Eastern part in the Son Valley (after Chakraborty and Bhattacharyya 1996). **b** Northern margin in northern Madhya Pradesh (after Ram et al. 1996). **c** Western margin in SW Rajasthan (after Soni et al. 1987)

Swaminath 1959). The deformation of the marginal Vindhyan is related to the transpressional *Great Boundary Fault*, traceable from Mewar to Fatepur Sikri near Agra (Fig. 8.11).

The Vindhyan Basin is segmented into smaller elongate subbasins by multiplicity of faults, some of which are wrench faults (Ram et al. 1996; Das et al. 1990). The subbasins are of the nature of half-graben tilting northwards. The structural

architecture of the domain is attributed to combined influence of rifting and dextral shearing (Bose et al. 2001).

The existence of the basin-wide unconformity separating the Semri Group of the Lower Vindhyan (Mesoproterozoic) from the Kaimur–Rewa–Bhander successions of the Upper Vindhyan (Fig. 8.2a) carries an implication that the Vindhyan domain was affected by a tectonic upheaval before commencement of Neoproterozoic sedimentation. While the Semri sediments in the northern margin of the Vindhyan Basin are confined to their present limit, the Upper Vindhyan extends far northwards into the Indo-Gangetic domain. Thus, much larger area came under the sway of the Vindhyan sea during the Neoproterozoic time. This fact is further borne out by development of many Neoproterozoic basins in the Peninsular India to the south (Fig. 8.1).

8.6.3 Semri Sedimentation and Stratigraphy

The Mesoproterozoic sedimentary rocks in the Vindhyan Basin (Misra 1969) are represented by the *Semri Group* (Fig. 8.10). It was a laterite-capped terrain of Palaeoproterozoic Bijawar that formed the floor of the Vindhyan Basin. The east–west-oriented basin in the Mirzapur–Lalitpur belt sank rapidly even as immature sediments accumulated at a brisk rate. This is evident from a 3-m-thick lenticular horizon of diamictite—described in 1933 as the *Basal Conglomerate* by J.B. Auden—well-developed in the valley of the Patherwa, a rivulet near Hardi (Fig. 8.13; Table 8.4). The *Patherwa Conglomerate* (Prakash 1967) has wider extent and has been named the *Deoland Formation* in the Mahanadi Valley (Chakraborty and Bhattacharyya 1996). The diamictite at Gangau, described by some investigators as glacial tilloids (Ahmad 1955; Mathur 1981), was formed by debris flows, originating from ferruginous and locally silicified regolith (Williams and Schmidt 1996; Schmidt and Williams 1999). The Gangau diamictite point to tectonic instability of the terrain at the commencement of the Semri sedimentation. The diamictite is intimately associated with an assemblage of flysch rocks (*Arangi Shale*) comprising shales with coaly matter, and muddy, wacke sandstones. In the Son Valley, the Arangi succession is made up of vertically stacked facies of upward-fining fan-delta sediments and of turbidites, characterized by graded bedding, flute marks, sole marks, and ripple laminations formed under deep water slope-to-basin environment (Chakraborty and Bhattacharyya 1996). The chert breccias interbedded with platform sediments in the Vindhyan Basin in the Dhar Forest (Madhya Pradesh) and the Kaladgi Basin (Karnataka) have been reinterpreted as transporated debris deposit of chert material resulting from synsedimentary faulting within the basin (Kale and Shilpa 2011).

In the Chitrakoot area in south-central Uttar Pradesh, the Bundelkhand gneisses are overlain directly by shallow-water, intertidal to peritidal sediments (Fig. 8.14). The succession consists of pelletal limestones and sandstones, characterized by abundant glauconite and stromatolitic siliceous dolomite as seen in the Lodhwara,

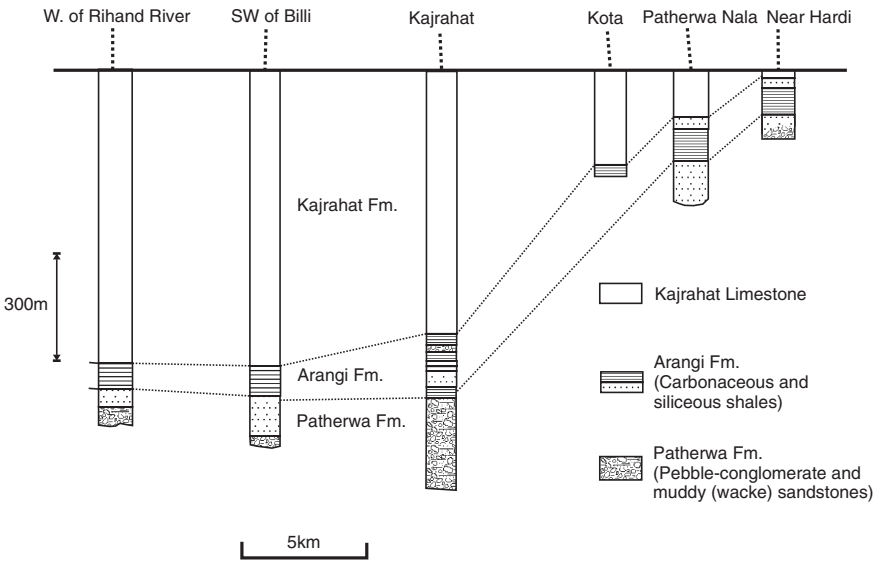

Fig. 8.13 Lithologs showing the position of the diamictite body in relation to the lower part of the Semri succession in the Son Valley in south-eastern Uttar Pradesh (after Prakash 1967)

Table 8.4 Lithostratigraphy of the Lower Vindhyan Semri Group in Son Valley and Rajasthan

Son Valley		Rajasthan
Auden, J.B. (1933)	Bhattacharyya, A.K. (1996)	Coulson, A.L. (1927)
Kaimur Group		Kaimur Group
Unconformity		
Banded Shale-Limestone	Bhagwar Shale	Suket Shale
Nodular Limestone	Rohtasgarh Limestone	Nimbahera Limestone
Glauconite Beds	Rampur Formation	Bari Shale
Fawn Limestones	Salkhan Limestone	Binota Shale + Kalmia Sandstone
Olive Shales	Koldaha Shale	
Porcellanite Beds	Deonar Formation	Palri Shale + Sawa Sandstone
Kajrahat Limestone	Kajrahat Limestone Arangi Formation	Bhagwanpura Limestone Khardeola Sandstone
Basal Conglomerate	Deoland Formation	Khairmalia Volcanics
Unconformity		
Bijawar		Aravalli/Pre-Aravalli

Kamtanath, Sangrampur and Muradnagar hillocks (Anbarasu 2001). Elsewhere in the Son Valley, the Patherwa–Arangi succession is followed upwards by platform deposits, comprising dominant carbonates with shales (*Kajrahat Limestone*). While some parts of the Semri Basin subsided rapidly, accumulating immature

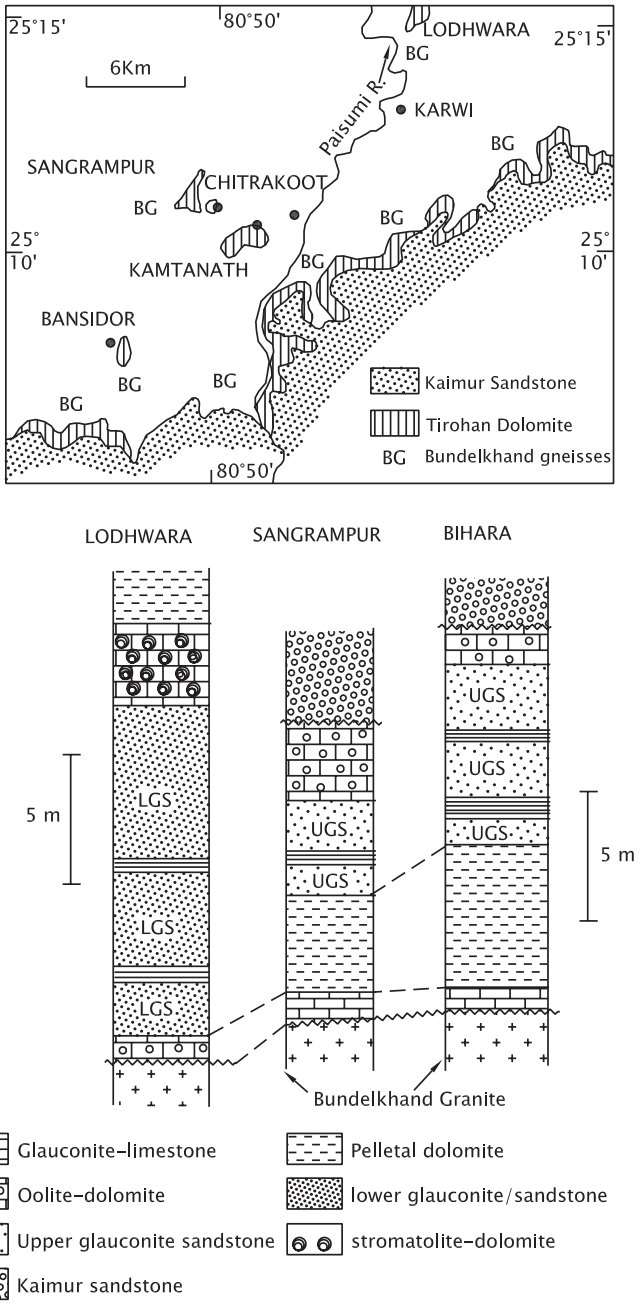

Fig. 8.14 Early Semri sedimentation in the Chitrakoot area in south-central Uttar Pradesh on the exposed Bundelkhand Granite basement (modified after Anabarasu 2001)

sediments as fan-delta and slope-edge clastic fans, other parts remained a shallow shelf where sedimentation took place slowly, giving rise to carbonate ramps on the seaward side. After an interregnum due to acid volcanism, shales and limestones–dolomites were deposited for a long period. The olive-coloured *Koldaha Shale* records synsedimentary deformation, discernible in the belt between Chorhat and Shikarganj, as testified by boudinage features, small-scale conjugate faults and bi-directional joint planes resulting from ENE–WSW extension and attendant reactivation of older faults in the basin floor (Bose et al. 1997). There was a concentration of large fans of mineralogically immature sediments, deposited by southerly flowing streams along the northern fringe of the Semri Basin.

The carbonate–shale sequence developed below the wave-base in the marine environment. Towards the later part of the Semri time, there was extensive formation of dolomitic bioherms (*Salkhan Limestone*, *Rohtas Limestone*). These are characterized by stromatolites, microbial laminites and thrombolites, formed in the shallow shelf. Significantly, the dominating carbonate formations also contain lenticular deposits of debris flows below the base of storm waves represented by intraformational carbonate breccia. This assemblage (*Bhagwar*) is associated with sediments characterized by ripple-cross-laminations, climbing ripples and Bouma sequence of turbidites (Chakraborty and Bhattacharya 1996). In the Rajasthan sector, the lower 200-m part of the Khardeola succession, made up of shale, siltstone, mudstone and showing parallel to wavy lamination, ripple marks and desiccation crack, represents a deposit in back-barrier lagoon and tidal flat. The upper 40- to 150-m-thick sequence of subarkose, sublitharenite and quartz-arenite of the Khardeola was emplaced as a barrier-island sequence in an environment swept by east–west flowing currents (Casshyap et al. 2001).

It seems that towards the close of the Semri time, the Vindhyan Basin in the Son Valley was overtaken by tectonic instability. This situation heralded the onset of a regional tectonic upheaval, putting to end the Mesoproterozoic sedimentation in the entire Peninsular India (Table 8.4).

8.6.4 Volcanic Activity

The Semri time witnessed volcanic activity at a number of places, at least twice during the Mesoproterozoic time span. It is represented in Rajasthan by the *Khairmalia Volcanics* comprising andesitic lavas and accretionary lapilli-tuff formed from "ash-charged volcanic clouds produced by repeated volcanism" (Raza et al. 2001). The volcanism is related to a N–S trending zone of faults along the western margin of the Vindhyan Basin. In the Sonbhadra district in the Son Valley, volcanism occurred after the deposition of the Kajrahat Limestones. It was an explosive volcanism, penecontemporaneous with sedimentation on land and in water in a tidal flat. The acidic volcanics at Chopan consist of rhyolitic tuff, vesiculated and accretionary lapilli, ignimbrite (Srivastava et al. 2001) and agglomerate with fragments of pumice and volcanic bombs up to 80 cm in length (Bose et al. 2001). This volcanic

assemblage associated with chert (*Deonar Formation*) was earlier described as *Porcellanite beds* (Srivastava 1977). It is speculated that the Deonar volcanism started as a fissure eruption in the marine environment and ended up in the subaqueous to terrestrial setting.

8.6.5 Life in the Semri Time

The Kajrahat Limestone in the Son Valley and the Bhagwanpura Limestone in Rajasthan exhibit development of stromatolites of the types *Kussiella* together with domal and laminated forms (Valdiya 1969). In the Chitrakoot area (Fig. 8.14), passive branching and upward swelling columns showing marked protuberances and prominent projecting edges of convex laminae represent early forms of Lower Riphean (1650–1350 Ma) stromatolites of the *Kussiella* assemblage (Valdiya 1969). In the younger Salkhan Limestone occur conical stromatolites recognized as *Conophyton* and *Maslowviella* (Mathur et al. 1958; Valdiya 1969). In the Chorhat area, this horizon is characterized by burrows formed by triploblastic animals, identified as worm-like metazoan (Seilacher et al. 1998). In the Rohtas Limestone in the upper part of the Semri succession, the bedding planes of shales show carbonaceous discs and filaments, variously described as *Chuaria, Tawula, Sekwia* (Sahni and Shrivastava 1954; Misra 1969; Maithy and Babu 1988; Kumar 1995; Sharma 1996). The filaments have been identified as *Grypaenia spiralis*, an eucaryote (Sarangi et al. 2004).

8.6.6 Age of Lower Vindhyan Semri Group

Vinogradov et al. (1964) first attempted radiometic dating by potassium-argon method of the Vindhyan sediments. The glauconites of the basal Semri at Chitrakoot in south-central Uttar Pradesh (Figs. 8.10 and 8.15) gave Rb–Sr ages of 1449 ± 15, 1461 ± 15, 1504 ± 15 and 1531 ± 15 Ma (Kumar et al. 2001). The Kajrahat Limestone has given Pb–Pb age of 1729 ± 110 Ma (Sarangi et al. 2004). The zircon crystals from the Deonar porcellanite bed has been dated 1631 ± 5 Ma by SHRIMP (Ray et al. 2002). Zircon crystals in siliceous tuff bounding the Chorhat Sandstone (≡Salkhan) that bears burrows of triploblastic animal have been dated by sensitive high-resolution ion probe method at 1628 ± 8 Ma and 1599 ± 8 Ma (Rasmussen et al. 2002).

The stromatolite assemblage of the Salkhan Limestone is characterized by Lower Riphean (1650–1350 Ma) stromatolites (Valdiya 1969). The *Grypaenia*-bearing Rohtas Limestone in the upper part of the Semri Group gives Pb–Pb isochron age of 1599 ± 48 Ma (Sarangi et al. 2004). It is obvious that the Semri sedimentation started sometime in the temporal span from 1600 to 1700 Ma (Valdiya 1995).

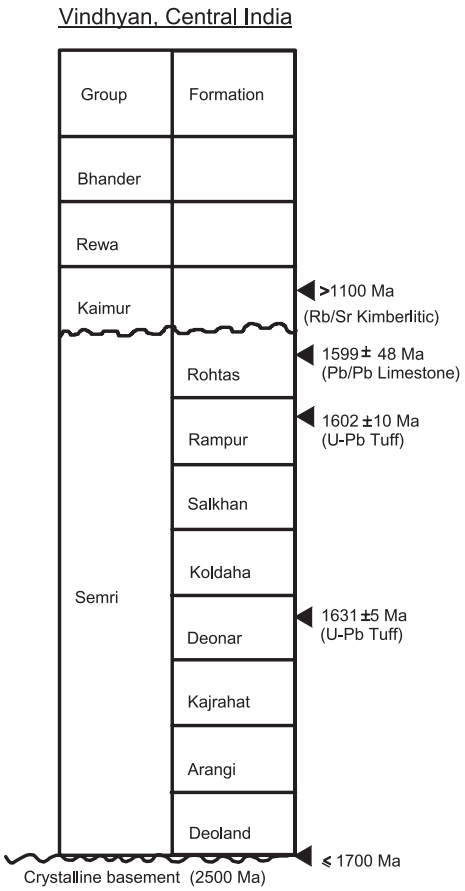

Fig. 8.15 Radiometric dates of crucial horizons of the Semri succession (Sarangi et al. 2004)

Presence of annulated coccoidal and microbial fabric resulting from *Girvanella* and *Renalcis* in the Semri sediments places the Lower Vindhyan in the time span of the Palaeoproterozoic (Bengston et al. 2009). In a horizon of the Fawn Limestone in the Semri Group have been found cuniform columnar stromatolites identified as *Calypso*, *Thyssagetes, Siren Ephyalites, Cyathotes,* etc., belonging to the period 1800–1600 Ma (Misra and Kumar 2005).

References

Ahmad, F. (1955). Glaciation in the Vindhyan system. *Current Science, 24*, 231.

Ahmad, F. (1958). Palaeogeography of central India in the Vindhyan period. *Record Geology of Survey India, 87*, 513–548.

Anbarasu, K. (2001). Facies variation and depositional environment of Mesoproterozoic Vindhyan sediments of Chitrakut area, central India. *Journal-Geological Society of India, 58*, 341–350.

Aswathanarayana, U. (1962). Age of the Cuddapah, South India. *Nature, 193*, 470.

Aswathanarayana, U. (1964). Istopic ages from the Eastern Ghats and Cuddapahs of India. *Journal of Geophysical Research, 69*, 3479–3486.

Auden, J. B. (1933). Vindhyan sedimentation in the Sone valley, Mirzapur district. *Memorial Geological Society of India*, *62*,147–250.

Babu Rao, V., Atchuta Rao, D., Rama Rao, Ch., Sarma, B. S. P., Bhaskara Rao, D. S., Veeraswamy, K., & Sarma, M. R. L. (1987). Some salient results of interpretation of aeromagnetic data over Cuddapah Basin and adjoining terrain, South India. *Memorial Geological Society of India, 6*, 295–312.

Banerjee, I. (1974). Barrier coastline sedimentation model and the Vindhyan example. *Geological, Mining and Metallurgical Society of India, Quarterly Journal, 46*, 101–127.

Basumallick, S. (1967). Problems of the Purana stratigraphy of the Godavari valley with special reference to the type area in Warangal district, Andhra Pradesh, India. *Geological, Mining and Metallurgical Society of India, Quarterly Journal, 39*, 115–127.

Bengston, S., Belivanova, V., Rasmussen, B., & Whitehouse, M. (2009). The controversial "Cambrian" fossils of the Vindhyan arc real but more than a billion years older. *Proceedings of the National Academy of Sciences USA, 106*, 7729–7734.

Bhaskar Rao, Y. J., Pantulu, G. V. C., Damodara Reddy, V., & Gopalan, K. (1995). Time of early sedimentation and volcanism in the Proterozoic Cuddapah Basin, South India: Evidence from the Rb-Sr age of Pulivendla mafic sill. In T. C. Devaraju (Ed.), *Mafic Dykes, Swarms of Peninsular India,* (pp. 329–338). Bangalore: Geological Society of India.

Bose, P. K., Banerjee, S., & Sarkar, S. (1997). Slope-controlled seismic deformation and tectonic framework of deposition: Koldaha Shale, India. *Tectonophysics, 269*, 151–169.

Bose, P. K., Sarkar, S., Chakrabarty, S., & Banerjee, S. (2001). Overview of the Meso- to Neoproterozoic evolution of the Vindhyan basin, central India. *Sedimentary Geology, 141–142*, 395–419.

Chakraborty, C., & Bhattacharya, A. (1996). The Vindhyan Basin: An overview in the light of current perspectives. *Memorial Geological Society of India, 36*, 301–312.

Chalapathi Rao, N. V., Gibson, S. A., Pyle, D. M., & Dickin, A. P. (1998). Contrasting isotopic mantle sources for Proterozoic lamproites and kimberlites from the Cuddapah Basin and Eastern Dharwar Craton: Implications for Proterozoic mantle heterogeneity beneath southern India. *Journal-Geological Society of India, 52*, 683–694.

Chandrasekhar Gowda, M. J., & Govinda Rajulu, B. V. (1980). Stromatolites of the Kaladgi Basin and their palaeoenvironmental significance. *India Geological Survey Miscellaneous Publication, 44*, 220–239.

Chaudhuri, A. K. (1970). Precambrian stromatolites in the Pranhita-Godavari valley (south India). *Palaeogeography, Palaeoclimatology, Palaeoecology, 7*, 309–340.

Chaudhuri, A. K. (1985). Stratigraphy of the Purana Supergroup, Andhra Pradesh. *Journal-Geological Society of India, 26*, 301–314.

Chaudhuri, A. K. (2003). Stratigraphy and palaeogeography of the Godavari Supergroup in the southcentral Pranhita-Godavari valley, South India. *Journal of Asian Earth Sciences, 21*, 595–611.

Chaudhuri, A. K., Chanda, S. K., & Dasgupta, S. (1994). Proterozoic glauconitic peloids from South India: Their origin and significance. *Journal of Sedimentary Research, A64*, 765–770.

Chaudhuri, A. K., & Howard, J. P. (1985). Ramagundam Sandstone—A middle Proterozoic shoal-bar sequence. *Journal of Sedimentary Research, 55*, 392–397.

Choubey, V. D. (1971). Superimposed Folding in the Transitional Rocks (Precambrians) and its Influence on the Structure of South Eastern Margin of the Vindryan Basin, Jabalpur District, Madhya Pradesh. *Journal-Geological Society of India, 12*, 142–151.

Coulson, A. L. (1927). Geology of Bundi State, Rajasthan. *Records of the Geological Survey of India*, *50*, 185–199.

Das, L. K., Mishra, D. C., Ghosh, D., & Banerjee, B. (1990). Geomorphotectonics of the basement in a part of upper Son valley of the Vindhyan Basin. *Journal-Geological Society of India, 35*, 445–458.

French, J. E., Heaman, L. M., Chako, T., & Srivastava, R. K. (2008). 1891–1883 Ma southern Basta-Cuddapah mafic igneous events: A newly recognized igneous province. *Precambrian Research, 160*, 308–322.

Ghosh, G., & Saha, D. (2003). Deformation of the Proterozoic Somanpalli Group, Pranhita-Godavari valley, South India—Implication for a Mesoproterozoic basin inversion. *Journal of Asian Earth Sciences, 21*, 623–631.

Govinda Rajulu, B. V., & Gowda, M. J. C. (1968). Algal stromatolites from the southwestern part of the Kaladgi basin, Lokapur, Mysore State, India. *Journal of Sedimentary Research, 38*, 1059–1064.

Gururaja, M. N., & Chandra, A. (1987). Stromatolites from the Vempalle and the Tadpatri formations of Cuddapah Supergroup (Proterozoic), Andhra Pradesh and their significance. *Memorial Geological Society of India, 6*, 399–428.

Jayaprakash, A. V., Sundaram, V., Hans, S. K., & Mishra, R. N. (1987). Geology of the Kaladgi-Badami basin Karnataka. *Memorial Geological Society of India, 6*, 201–255.

Kaila, K. L., Roy Choudhury, K., Reddy, P., Krishna, V. G., Narain, H., Subotin, S. T., et al. (1979). Crustal structure along the Kavali-Udupi profile in the Indian Peninsular Shield from deep seismic sounding. *Journal-Geological Society of India, 20*, 307–333.

Kaila, K. L., & Tewari, H. C. (1985). Structural trends in the Cuddapah basin from deep seismic sounding and their tectonic implications. *Tectonophysics, 115*, 69–86.

Kale, V. S., & Phansalkar, V. G. (1991). Purana basins of Peninsular India: a reveiw. *Basin Research, 3*, 1–36.

Kale, V., & Pillai, S. (2011). A reinterpretation of two breccias from the Proterozoic basins of India. *Journal-Geological Society of India, 78*, 429–445.

Karunakaran, C. (1976). Sulphur isotopic composition of barite and pyrite from Mangampeta, Cuddapah district, Andhra Pradesh. *Journal-Geological Society of India, 17*, 187–195.

Krishnan, M. S. (1966). *Geology of India and Burma*. Chennai: Higginbothams. 604 p.

Krishnan, M. S., & Swaminath, J. (1959). The great Vindhyan Basin of southern India. *Journal-Geological Society of India, 1*, 10–30.

Kumar, S. (1995). Megafossils from the Mesoproterozoic Rohtas Formation (the Vindhyan supergroup) Katni area, central India. *Precambrian Research, 72*, 171–184.

Kumar, A., Dayal, A. M., & Padmakumari, V. M. (2003). Kimberlite from Rajmahal magmatic province: Sr-Nd-Pb isotopic evidence for Kerguelen plume derived magma. *Geophysical Research Letters, 30*, 9–11.

Kumar, A., Padma Kumari, V. M., Dayal, A. M., Murthy, D. S. N., & Gopalan, K. (1993). Rb-Sr ages of Proterozoic kimberlites of India: evidence for contemporaneous emplacement. *Precambrian Research, 62*, 227–237.

Kumar, A., Pande, K., Venkatesan, T. R., & Bhaskar Rao, Y. J. (2001). The Karnataka Late Cretaceous dykes as products of Marion hotspot at the Madagascar-India breakup event: Evidence from ^{40}Ar-^{39}Ar geochronology and geochemistry. *Geophysical Research Letters, 28*, 2715–2718.

Lakshminarayana, G. (2002). Sedimentary facies and stratigraphic significance of Cumbum and Bairenkonda type sections of Nallamalai fold belt, Cuddapah Basin, Andhra Pradesh. *Journal-Geological Society of India, 59*, 167–177.

Leelanandam, C. (1980). Some observations on the alkaline provinces in Andhra Pradesh. *Current Science, 50*, 799–802.

Leelanandam, C. (1990). Kandra volcanics in Andhra Pradesh: Possible ophiolite. *Current Science, 59*, 785–788.

Leelanandam, C. (1993). Eulitic and ferrosilitic orthopyroxenes from ferrosyenitic of South India: Evidence for a high-temperature crystallization and tholeiitic parentage. *Current Science, 64*, 729–735.

Maithy, P. K., & Babu, R. (1988). The mid-Proterozoic Vindhyan microbiota from Chopan, southeast Uttar Pradesh. *Journal-Geological Society of India, 31*, 584–590.

Mathur, S. M. (1981). The Middle Proterozoic Gangau tillite, Bijawar Group, central India. In M. J. Hambrey & W. B. Harland (Eds.), *Earth's pre-pleistocene glacial record* (pp. 424–427). Cambridge: Cambridge University Press.

Mathur, S. M., Narain, K., & Srivastava, J. P. (1958). Algal structure from the Fawn Limestone, Semri Series (lower Vindhyan) in the Mirzapur district, Rec. *Geological Survey of India, 87*, 819–822.

Matin, A., & Guha, J. (1996). Structural geometry of rocks of the southern part of the Nallamalai fold belt, Cuddapah Basin, Andhra Pradesh. *Journal-Geological Society of India, 47*, 535–545.

Mezger, K., & Cosca, M. A. (1999). The thermal history of the Eastern Ghats Belt (India) as revealed by U-Pb and 40Ar/39Ar dating of metamorphic and magmatic minerals: implications for SWEAT correlation. *Precambrian Research, 94*, 251–271.

Mishra, D. C., Babu Rao, V., Laxman, G., Rao, M. B. S. V., & Venkatarayudu, M. (1987). Three-dimensional structural model of Cuddapah basin and adjacent eastern part from geophysical structures. *Memorial Geological Society of India, 6*, 313–330.

Misra, R. C. (1969). *The Vindhyan system*. Presidential Address 56th Indian Science Congress, Kolkata, pp. 1–32.

Misra, Y., & Kumar, S. (2005). Coniform stromatolites and Vindhyan Supergroup, central India: Implications for basinal correlation and age. *Journal of the Palaeontological Society of India*, *50*, 153–167.

Mukhopadhyay, J., & Chaudhuri, A. K. (2003). Stratigraphy of the Chanda Limestone of the Proterozoic Penganga Group, Adilabad, Andhra Pradesh: New light on depositional setting and palaeogeography. *Journal-Geological Society of India, 62*, 356–368.

Mukhopadhyay, J., Gutzmer, J., & Beukes, N. J. (2005). Organotemplate structures in sedimentary manganese carbonates of the Neoproterozoic Penganga Group, Adilabad, India. *Journal of Earth System Science, 114*, 247–257.

Nagaraja Rao, B. K., Rajurkar, S. T., Ramalingaswamy, G., & Ravindra Babu, B. (1987). Stratigraphy, structure and evolution of the Cuddapah basin. *Memorial Geological Society of India, 6*, 33–86.

Narain, H. (1987). Geophysical constraints on the evolution of Purana basins of Peninsular India (Middle to Late Proterozoic). *Memorial Geological Society of India, 6*, 5–32.

Narain, H., & Kaila, K. L. (1982). Inferences about the Vindhyan Basin from geophysical data. In K. S. Valdiya, S. B. Bhatia, & V. K. Gaur (Eds.), *Geology of Vindhyachal* (pp. 183–192). Delhi: Hindustan Publishing Corporation.

Narayanaswamy, S. (1966). Tectonics of the Cuddapah basin. *Journal-Geological Society of India, 7*, 33–50.

Natarajan, V., & Rajagopalan Nair, S. (1977). Post-Kurnool thrust and other structural features in the northeast part of the Palnad basin, Krishna district, Andhra Pradesh. *Journal-Geological Society of India, 18*, 111–116.

Neelakantam, S. (1987). Mangampeta barytes deposit, Cuddapah district, Andhra Pradesh. *Memorial Geological Society of India, 6*, 429–458.

Prakash, R. (1967). On the stratigraphy of the Basal Formations, Semri Group (Vindhyan System). *Journal of Mining and Geological Institute of India, 64*, 55–64.

Prasad, C. V. R. K., Pulla Reddy, V., Subbarao, K. V., & Radhakrishnamurthy, C. (1987). Palaeomagnetism and the crescent shape of the Cuddapah Basin. *Memorial Geological Society of India, 6*, 331–347.

Radhakrisna, B. P., & Naqvi, S. M. (1986). Precambrian continental crust of India and its evolution. *Journal Geology, 94*, 145–166.

Raha, P. K., & Sastry, M. V. A. (1982). Stromatolites and Precambrian stratigraphy in India. *Precambrian Research, 18*, 293–318.

Raju, R. D., Roy, M., Roy, M., & Vasudeva, S. G. (1993). Uranium Mineralisation in the South-Western Part of Cuddapah Basin: A Petromineralogical and Geochemical Study. *Geological Society of India*, *42*, 135–149.

Ram Babu, H. V. (1993). Basement structure of the Cuddapah Basin from gravity anomalies. *Tectonophysics, 223*, 411–422.

Ram, J., Shukla, S. N., Pramanik, A. G., & Varma, B. K. (1996). Recent investigations in the Vindhyan Basin: Implication for the basin tectonics. *Memorial Geological Society of India, 36*, 267–286.

Ramam, P. K., & Murty, V. N. (1997). *Geology of Andhra Pradesh*. Bangalore: Geological Society of India. 245 p.

Rasmussen, B., Bose, P. K., Sarkar, S., Banerjee, S., Fletcher, I. R., & McNaughton, N. J. (2002). 1.6 Ga U-Pb zircon age for the Chorhat Sandstone, Lower Vindhyan, India: Possible implications for early evolution of animals. *Geology, 30*, 103–106.

Ray, J. S., Martin Mark, W., Veizer, J., & Bowring, S. A. (2002). U-Pb zircon dating and Sr isotope systematics of the Vindhyan Supergroup, India. *Geology (Boulder), 30*, 131–134.

Raza, M., Casshyap, S. M., & Khan, A. (2001). Accretionary lapilli from the basal Vindhyan volcanic sequence, south of Chittaurgarh, Rajasthan, and their implication. *Journal-Geological Society of India, 57*, 77–82.

Riding, R., & Sharma, M. (1998). Late Proterozoic (1800–1600 Ma) stromatolites, Cuddapah Basin, southern India: Cyanobacterial or other bacterial microfabrics. *Precambrian Research, 92*, 21–35.

Roy, A. K., & Bhattacharya, A. (1982). Regional geomorphology of Vindhyachal. *Geology of Vindhyachal* (pp. 9–22). Delhi: Hindustan Publishing Corporation.

Saha, D. (1990). Internal geometry of a thrust sheet, eastern Proterozoic belt, Godavari valley, South India. Proceedings of the Indian Academy of Sciences-Earth and Planetary Sciences 99:339–355.

Saha, D., & Chaudhuri, A. K. (2003). Deformation of the Proterozoic succession in the Pranhita-Godavari basin, South India—A regional perspective. *Journal of Asian Earth Sciences, 21*, 557–565.

Sahni, M. R., & Shrivastava, R. N. (1954). New organic remains from the Vindhyan system and the probable systematic position of *Fermonia* Chapman. *Current Science, 20*, 289–304.

Sarangi, S., Gopalan, K., Kumar, S. (2004). Sr and Pb isotope systematics of carbon sequences of the Vindhyan Supergroup, India, *Precambrian Research*, *123*.

Schmidt, P. W., & Williams, G. E. (1999). Palaeomagnetism of the Mesoproterozoic Gangau Formation, Basal Vindhyan Supergroup, Madhya Pradesh. *Memorial Geological Society of India, 44*, 75–85.

Seilacher, A., Bose, P. K., & Pfluger, F. (1998). Triploblastic animals more than 1 Billion years ago: Trace fossils evidence from India. *Science, 282*, 80–83.

Singh, A. P., & Mishra, D. C. (2002). Tectonosedimentary evolution of Cuddapah basin and Eastern Ghats Mobile Belt (India) and Proterozoic collision: Gravity, seismic and geodynamic contraints. *Journal of Geodynamics, 33*, 249–267.

Sreenivasa Rao, T. (1987). The Pakhal basin—A perspective. *Memorial Geological Society of India, 6*, 161–180.

Srikantia, S. V. (1984). Kuppalapalle volcanics—A distinct Upper Papaghni volcanic activity in the Cuddapah Basin. *Journal-Geological Society of India, 25*, 775–779.

Srinivasa Rao, M. R. (1944). Algal structures from the Cuddapah Limestone (Precambrian), south India. *Current Science*, 13–75.

Srivastava, V. K. (1977). Environmental significance of some depositional structures in banded porcellanites (Lower Vindhyan) of Mirzapur district, U.P. *Journal of Indian Association of Sedimentologists, 1*, 45–51.

Srivastava, R. N., Srivastava, A. K., Singh, K. N., & Radcliffe, R. P. (2001). Precambrian acidic volcanism in the lower Vindhyan Basin of the Sonbhadra district and adjoining areas of Uttar Pradesh: A review. *Special Publication Series–Geological Survey of India*, *55*, 205–218.

Soni, M. K., Chakraborty, S., & Jain, V. K. (1987). Vindhyan Supergroup: A review. *Geological Society of India, Memoir*, *36*, 257–265.

Tewari, A. P. (1968). A new concept of palaeotectonic setup of parts of northern Peninsular India with a special reference to Great Boundary Fault. *Geologie en Mijnbouw, 47*, 21–27.

Umamaheswar, K., Basu, H., Patnaik, J. K., Ali, M. A., & Banerjee, D. C. (2001). Uranium mineralization in the Mesoproterozoic quartzites of Cuddapah Basin in Bandi area, Cuddapah district, A.P.: A new exploration target for uranium. *Journal-Geological Society of India*, *57*, 405–409.

Vaidyanadhan, R. (1961). Stromatolites in Lower Cuddapah limestone (Precambrian) in Cuddapah Basin. *Current Science, 30*, 221.

Valdiya, K. S. (1969). Stromatolites of the Lesser Himalayan carbonate formations and the Vindhyan. *Journal-Geological Society of India, 10*, 1–25.

Valdiya, K. S. (1993). Evidence for Pan-African–Cadomian tectonic upheaval in Himalaya. *Journal of the Palaeontological Society of India, 38*, 51–62.

Valdiya, K. S. (1995). Proterozoic sedimentation and Pan-African geodynamic development in the Himalaya. *Precambrian Research, 74*, 35–55.

Verma, M. B., Maithani, P. B., Chaki, A., Nageshwar Rao, P., & Kumar, P. (2009). Srisailam subbassin and uranium province of unconformity-related deposits in Andhra Pradesh—Case study of Chitral uranium exploration, Nalgonda district. *Current Science, 96*, 588–591.

Vinogradov, A., Tugarinov, A., Zhykov, C., Stapnikova, N., Bibikova, E., & Khorre, K. (1964). *Geochronology of Indian Precambrian*. Reports of Twentysecond International Geological Congress (Vol. 11, pp. 553–567), New Delhi.

Viswanathiah, M. N. (1977). Lithostratigraphy of the Kaladgi and Badami groups, Karnataka. *The Indian Mineralogists, 18*, 122–132.

Viswanathiah, M. N., & Sreedhara Murthy, T. R. (1979). Algal stromatolites from Kaladgi Group around Bilgi, Bijapur district, Karanataka. *Journal-Geological Society of India, 20*, 1–6.

Williams, G. E., & Schmidt, P. W. (1996). Origin and palaeomagnetism of the Mesoproterozoic Gangau tilloid, basal Vindhyan Supergroup, central India. *Precambrian Research, 79*, 307–325.

Chapter 9
Neoproterozoic Intracratonic Basins in Peninsular India

9.1 Beginning of Neoproterozoic Era

There was a pronounced interruption of sedimentation in the Purana basins of Cuddapah, Kaladgi, Godavari and Vindhyan in the period 1000 ± 50 Ma. This interruption is represented by, as already stated, a regional unconformity above the Mesoproterozoic sedimentary successions in all these basins. It was a result of the tectonic upheaval. Both the Aravali–Satpura orogenic belt and the Eastern Ghat Mobile Belt were overtaken by tectonothermal developments in the period 1050 and 950 Ma. This development had an impact on the Purana basins. The Somanpalli, Penganga and Yellandapad areas of the Godavari basin were subjected to folding and thrusting. Sedimentation halted in all basins and then followed a period of pronounced erosion before its resumption. Much larger areas came under the sway of sedimentation as new regions sank, giving rise to the Bhima, Indravati and Chhattisgarh basins. In the north, the sedimentation expended beyond the limits of the Vindhyan Basin (Fig. 9.1) and encompassed parts of the Indo-Gangetic domain.

There was a marked change in the environment of sedimentation—the marine environment of the Mesoproterozoic gave way to a dominantly terrestrial environment in the Neoproterozoic time—rivers playing very dominant role, and wind reworking the fluvial sediments in some regions.

9.2 Vindhyan Basin

9.2.1 Tectonic Setting

As already stated, the Semri succession ended in an unconformity. Structural discordance between the Semri and the succeeding piles indicates that the Upper

K.S. Valdiya, *The Making of India*, Society of Earth Scientists Series,
DOI 10.1007/978-3-319-25029-8_9

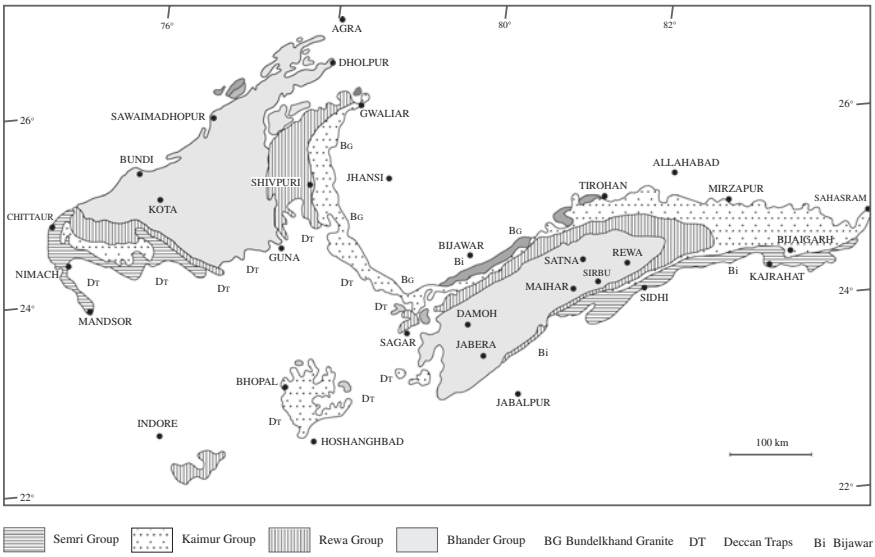

Fig. 9.1 Vindhyan Basin lying in embrace of arms of Satpura and Aravali mobile belts. The sketch map shows distribution of the Kaimur, Rewa and Bhander successions in addition to the Semri making up the Upper Vindhyan (after Soni et al. 1987)

Vindhyan sedimentation was preceded by a tectonic upheaval. The overlying fluvial sediments begin with a horizon of conglomerates (*Kaimur Group*), which developed in full force in the Rajasthan sector. The region north of the Vindhyan Basin (Fig. 9.1) subsided, giving rise to Upper Vindhyan sedimentary succession in the Indo-Gangetic domain.

9.2.2 Stratigraphy and Sedimentation

The Upper Vindhyan succession is divided into three groups: the Kaimur, the Rewa and the Bhander (Fig. 9.1; Table 9.1).

In the *Kaimur* time, the environment of deposition in a terrestrial setting fluctuated from alluvial fan, braided-plain, fan-delta to lacustrine facies. In the large lacustrine basin that developed in the floodplain of the Kaimur rivers, strong wave action resulted in formation of brecciated detritus (*Susnai Breccia*) in the assemblage of vertically stacked shallowing-upward facies (Bhattacharya 1996). Prevalence of anoxic conditions in an environment charged with profuse organic matter gave rise to black carbonaceous, pyrite-rich fine sediments (*Bijaigarh Shale*) (Pandalai and Chandra 1986). Locally the concentration of pyrite is very high such as at Amjhor. Later, the lake opened out and sediments deposited in the deeper part were affected by density underflows as borne out by Bouma Sequence

Table 9.1 Stratigraphic succession of Upper Vindhyan

Son valley* (Bhattacharya 1996)		Rajasthan (Coulson 1927)
Bhander Group	Shikaoda Sandstone (Upper Bhander Sandstone) Sirbu Shale Bundi Hill Sandstone (Lower Bhander Sandstone) Lakheri Limestone (Bhander Limestone) Ganurgarh Shale	Bhavpura Shale Balwan Limestone Bundi Hill Sandstone Lakheri Limestone Ganurgarh Shale
---------- ? ----------		
Rewa Group	Govindgarh Sandstone (Upper Rewa Sandstone) Drammondganj Sandstone Jhiri Shale Asan Sandstone (Lower Rewa Sandstone) Panna Shale	Taragarh Fort Sandstone Jhiri Shale Indergarh Sandstone Panna Shale
---------- ? ----------		
Kaimur Group	Dhandraul Sandstone (Dhandraul Quartzite) Mangesar Formation (Scarp Sandstone) Bijaigarh Shale Ghaghar Sandstone (Upper Quartzite) Susnai Breccia Sasaram Formation (Lower Quartzite)	Kaimur Sandstone
---------- *Unconformity* ----------		
Semri Group		

*Names within brackets were given by J.B. Auden in 1933

and various sole markings (Misra and Awasthi 1962). The lacustrine environment then changed back to fluvial, and ephemeral braided streams, characterized by network of channels, deposited their loads (Bhattacharya and Morad 1993). Wind blew strongly, forming curved and straight-crested aeolian dunes and transverse bars on the marginal shorelines. Thus evolved a 30- to 150-m-thick succession of the *Dhandraul Sandstone* that today forms high spectacular scarp overlooking the Indo-Gangetic Plains in the north (Chakraborty 1996; Chakraborty and Bhattacharya 1996a, b).

During the Kaimur period, there were three reversals of geomagnetic field (Poornachandra Rao et al. 1997). On the basis of palaeomagnetic data, the sandstone at Baghain of the Upper Kaimur has been correlated with the Banaganapalli quartzites of the Cuddapah Basin.

In the *Rewa time, there* were deposited shale and marl (*Panna Shale*) in an environment dominated by storms on the north-eastward-sloping shelf. As the extent of sedimentation enlarged, fluvial sands (*Asan Sandstone*) accumulated on the floodplain that sloped westwards. The overlying *Jhiri Shale* is a shallowing-upward deposit in the offshore zone below the storm-wave base. Fluctuation of sea level resulted in stacking of several coarsening-upward and fining-upward sequences formed as near-shore sandbars. These are characterized by cross-bedding and parallel lamination (*Drammondganj Sandstone*). The overlying succession of sandstones (*Govindgarh Sandstone*) was laid down by a river system

on a laterally extensive flat erosional surface (Chakraborty and Chaudhuri 1990; Chakraborty et al. 1996). By this time, weathering of kimberlite bodies had yielded diamonds, which were washed down by streams and emplaced in the proximal conglomerates of the Rewa succession.

The *Bhander Group* represents deposits in a shallow basin embracing lagoons, tidal flats with channels and beaches along which longshore and storm currents were active (Chakraborty 2001). Finely laminated algal mats and cyanobacterial stromatolites formed bioherms (*Lakheri Limestone*) in the supratidal to subtidal environment in the Rajasthan sector (Akhtar 1976, 1978, 1996). In the Maihar area in the eastern part of the basin, multiple tidal sediments (*Bundi Hill Sandstone*) were formed in the tidal flat-and-lagoon complex affected by storms. This is evident from the alternation of ripple-drift lamination in sheet sandstones and the presence locally of shale–pebble conglomerates (Bhattacharya et al. 1980; Basumallick et al. 1996).

9.2.3 Palaeocurrents

The floor of the Vindhyan Basin sloped north-westwards in some parts and westwards in others. The currents operating at some periods of its life flowed broadly north-westwards, changing to west or north locally (Fig. 9.2). The terrigenous siliciclastic sediments were derived from a low-relief provenance. Lying to the south of the basin, this provenance was occasionally uplifted and supplied detritus but not coarser than granules (Bose et al. 1997). Possibly, tidal and shore currents

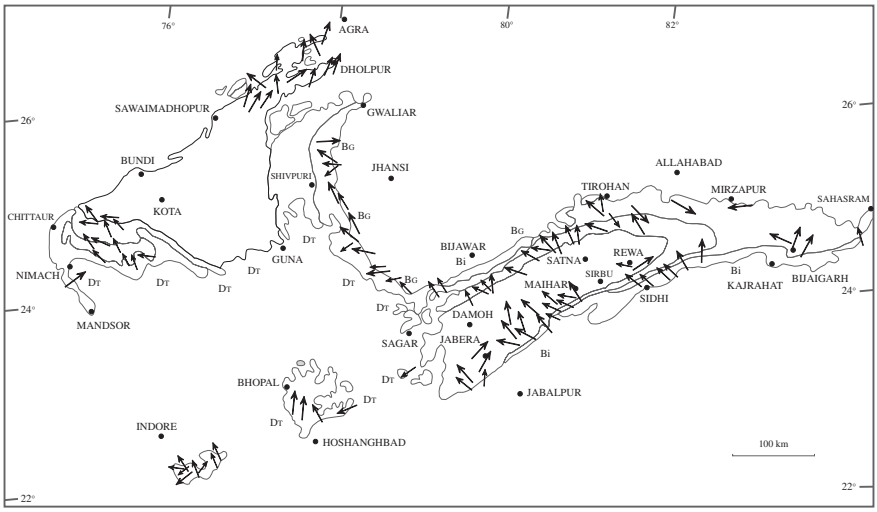

Fig. 9.2 Palaeocurrent pattern of the Vindhyan Basin during the Neoproterozoic era (after Misra 1969 and Soni et al. 1996)

were induced by winds. This is inferred from the consistency of north-westerly direction of palaeocurrent (Chanda and Bhattacharya 1982). In the Rajasthan sector, the currents flowed W or NW during the Kaimur and Rewa times but northwards in the Lower Bhander epoch (Akhtar 1978).

9.2.4 Igneous Activities

Towards the close of the Kaimur time, there was widespread volcanic activity resulting in deposition of nearly 10-m-thick volcaniclastic sediments over a large area (Chakraborty et al. 1996).

The Kaimur strata at Majhgawan and Hinota in Panna district (Fig. 9.3) are intruded by kimberlite and lamproite, the latter characterized by diamond and phlogopite. Covering 500-m by 320-m ground surface, the carrot-shaped Majhgawan plug is made up of olivine–lamproitic lapilli tuffs of the crater facies and characterized by high amount of TiO_2, Ba, Sr and La, K and Th (Paul 1979, 1991; Chatterjee and Rao 1995). The diamond distribution is concentric within the body. Weathering of the plugs released the diamond that occurs in the conglomeratic horizons of the Rewa succession.

9.2.5 Life in the Bhander Time

The Lakheri Limestone of the Bhander Group in the Maihar area comprises a bioherm built by stromatolites described as *Baicalia* and *Tungussia*, exhibiting characteristic branching of their tall columns (Valdiya 1969). In the Sawai Madhopur–Kota Bundi belt in Rajasthan, the stromatolite assemblage comprises *Baicalia, Tungussia, Minjaria, Maslowviella* and *Linella* (Prasad 1980). Confined as they are to definite stratigraphic levels, the Bhander stromatolites are morphologically distinct from those of the Semri, and evince time-controlled variations in their shapes and structures but are unaffected by facies variation.

9.2.6 Age of Upper Vindhyan

The Lakheri stromatolites strongly compare with the Middle Riphean (1350–1000) to Upper Riphean (1000–680 Ma) stromatolites of the erstwhile USSR (Valdiya 1969). It seems that the Lower Bhander represents a period transitional between Middle Riphean and Upper Riphean, and the Upper Bhander belongs to Upper Riphean to Vendian (680–570 Ma) time. The isotopes of carbon and oxygen ($\delta^{13}C$ and $\delta^{18}C$) values of carbonaceous material in the Upper Vindhyan

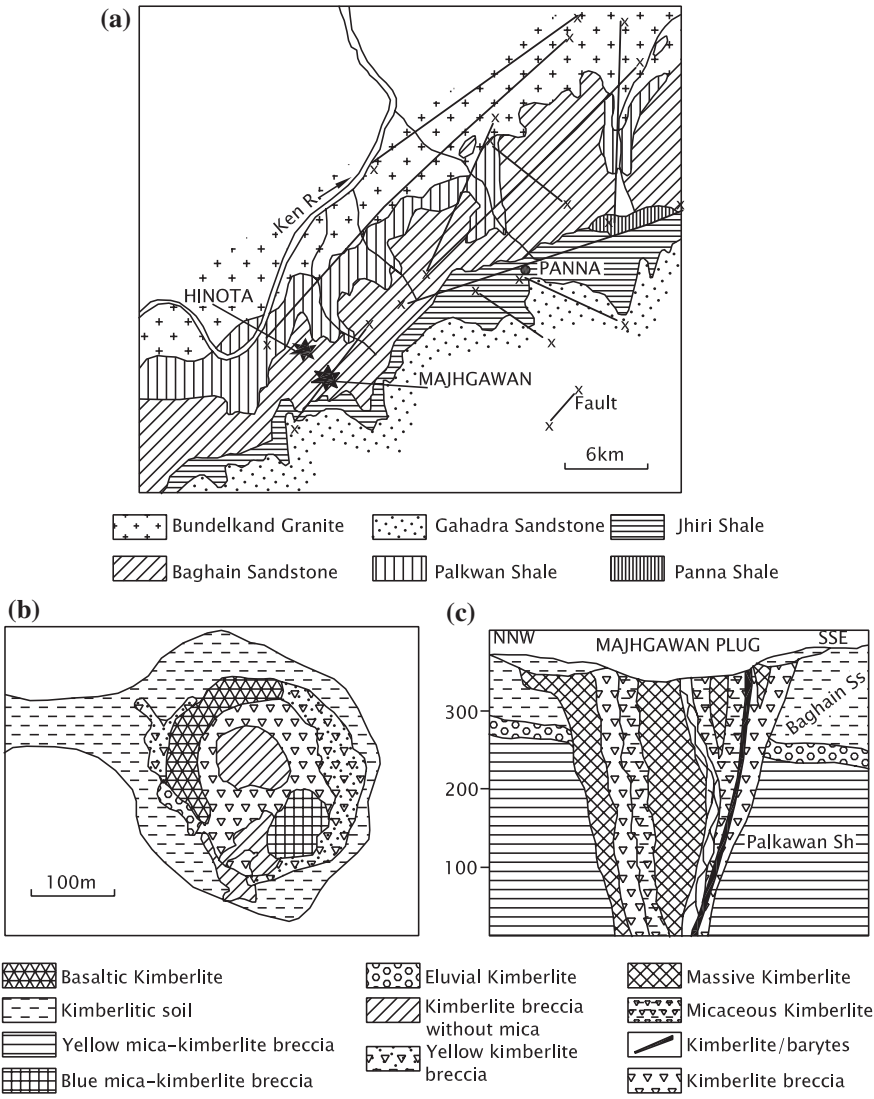

Fig. 9.3 **a** Geological sketch map of a part of Vindhyan showing the setting of the kimberlite plugs (after Chatterjee and Rao 1995). **b** Petrological types making the Majhgawan pipe. **c** Section shows the structure and compositional characteristics of the Majhgawan body (**b**, **c** after Soni et al. 1987)

sediments show that the Lakhera Limestone of Rajasthan is older than the Bhander Limestone in the east—the two are not coeval as commonly believed (Kumar et al. 2005).

The K–Ar age of the phlogopite of the Majhgawan pipe is 1140 ± 112 Ma (Paul et al. 1975). The Rb–Sr isochron age of lamproite body is 1067 ± 31 Ma

(Kumar et al. 1993). However, the plug has contributed diamond to the conglomerates in the Rewa succession. It may safely be deduced that that the Upper Vindhyan sedimentation commenced well before 1100 Ma. The palaeomagnetic pole position suggests the age of the Lower Bhander *not* younger than ~1200 Ma (J.G. Meert, *per. com*. 2008) as testified by the stromatolites placing the Upper Bhander in the interval 1000–900 Ma (Valdiya 1969). Palaeomagnetic study and dating of detrital zircon from the sediments in the Son Valley in the east and Rajasthan in the west show that the Rewa–Bhander succession belongs to the time range 1000–1070 Ma (Malone et al. 2008).

It seems that the lower part of the Upper Vindhyan succession extends down into the Upper Mesoproterozoic.

9.2.7 Mineral Resources

The Bijaigarh Shale of the Kaimur Group contains rich deposits of pyrite and *copper sulphide*.

The Bhander Sandstones and Kota Limestones have provided fine-quality building stones since historical times.

In the south-western part of the Sidhi district in Madhya Pradesh, *uranium mineralization* (0.088 % U_3O_8) has been detected in brecciated ferruginous shale, porcellanite and tufaceous rocks along the Kubari–Semariya–Marwa fault zone (Roy et al. 2009).

With source reservoir and cap rock present and favourable hydrogeological conditions prevailing in the Vindhyan succession, the prospect of finding oil is rated fair to good (Fuloria 1996). Formation waters with dissolved petroleum gas were encountered in most of the wells drilled for exploration in the Indo-Gangetic Plains. Discovery of hydrocarbon gases in the Jabera well drilled through the Vindhyan succession in central Madhya Pradesh lends support to the speculation on the prospects of oil and gas in the Vindhyan domain. Recent discovery of oil and gas in the homotaxials of the Vindhyan in the Jaisalmer–Bikaner region in north-western Rajasthan further strengthens the prospect.

9.3 Trans-Aravali Igneous Activities

9.3.1 Emplacement of Erinpura Granite

During the Neoproterozoic era, the south-western flank of the Aravali Mobile Belt and the terrane west of it witnessed emplacement of granites and felsic volcanism on a grand scale over large part of the continental margin. Plutonic bodies giving nearly concordant dates between 750 and 900 Ma are known as the *Erinpura Granite* (Fig. 9.4). Anorogenic in origin, the Erinpura Granite is extremely variable

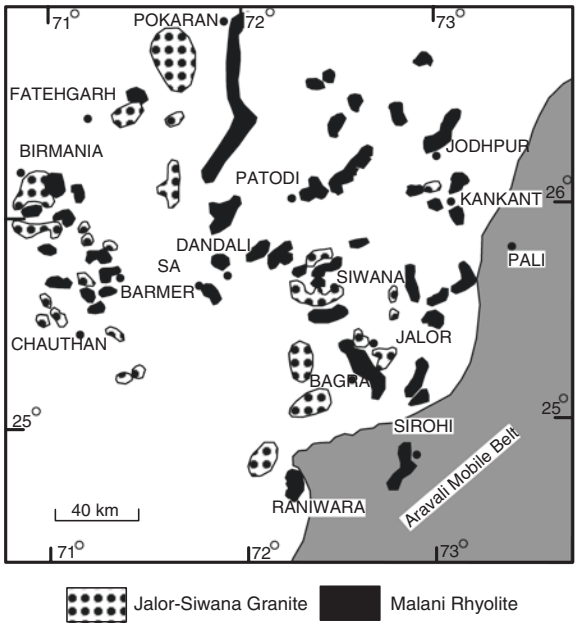

Fig. 9.4 Sketch map showing the distribution of granitic bodies known as the Erinpura Granite and the distribution of the Malani Rhyolite (after Roy 2001)

in colour and texture—some are massive, others foliated. The composition ranges from granodiorite to adamellite. Brecciation of the country rocks (Delhi phyllites) and granite porphyry in some places demonstrate forcible injection of magma (Pandian and Varma 2001).

East of the Phulad Ophiolite Belt, these granites are spatially associated with metagabbro characterized by the presence of scapolite and ferrian zoisite indicating influence of metamorphic fluids. They show LREE depletion, low K and low initial strontium. Significant negative europium anomaly and straight HREE indicate many pulses of inclusion (Bhushan and Chittora 2005).

The granite in the Godhra area is dated 900 Ma (Gopalan et al. 1979). The U–Pb zircon data on the tonalitic to granitic plutons cutting through the Delhi rocks in the Sendra area yield weighted whole-rock isotope age of 967.8 ± 1.2 Ma while the Rb–Sr whole-rock isotope data show regression of 906 ± 6.1 Ma (Pandit et al. 2003a). The emplacement of the Godhra–Sendra granites marks the culmination of the orogeny that shaped the Aravali Mobile Belt.

The U–Pb dating, with electron microprobe method, of monazite of the protolith in the Erinpura Granite crystallized at 863 ± 23 Ma, and along the shear zone it was recrystallized at 775 ± 26 Ma (Just et al. 2011). Associated with 1700- to 1720-Ma-old granites, the metasomatized mafic rocks at Dosi in the Khetri belt give Sm–Nd whole-rock isochron age of 831 ± 15 Ma, implying that the mafic rocks of Desi were emplaced synchronously with the Erinpura Granite (Kaur et al. 2013).

The monazite grains in metamorphic rocks of the Mangoli Complex are dated by electromicroprobe method at 946 ± 6.9 and 865 ± 10 Ma, while the granite intruding the metamorphic rocks are ~978 ± 18 Ma old (Bhowmik et al. 2010).

9.3.2 Malani Rhyolite

The volcanic domain of the *Malani Rhyolite* stretches south-west from Tusham in Haryana to Churu–Jhunjhunu in Rajasthan and west up to Barmer and Kirana hills in Panjab and Nagarparkar in Sindh (Pakistan). The volcanic succession was given this name by W.T. Blanford in 1877. Resting unconformably upon the basement, the Malani rhyolites occur at the base with conglomerate and coarse sandstone at Sandreth, Diri and Kankani in the Sirohi district (Sharma and Bhola 2004). Significantly, the 680- to 780-million-year-old lavas are free from all deformation features. Intimately associated with the lavas are agglomerates, ignimbrites and tuffs. The volcanics were derived by fractional crystallization from a crustal magma (Pandit et al. 1999). The alignment of rhyolite hills from east of Jodhpur to west of Barmer is parallel to the Aravali Range. It possibly represents a line of weakness in the continental crust—in the Rajasthan Shelf—that developed as an aftermath of the Delhi Orogeny.

Four chemically distinct associations, widely spaced in time, are recognizable in the Malani Volcanic domain (Srivastava 1988). These assemblages are: (i) basalt–andesite–dacite–rhyolite, the oldest assemblage, (ii) commendite–pantellerite–soda trachyte, (iii) trachybasalt–trachyandesite–trachyte–alkali rhyolite and (iv) alkali pyroxenite–micromelteigite–ijolite–essexite–basanite–felspathoidal syenite–nephelinite–phonolite and carbonatite of the Mundwara, Sarnu–Dandoli and Barmer areas. In the Kundal area near Sinwa (Singh and Valliyagam 2004), the glomeroporphyritic basalt and gabbro intrusives closely associated with the Malani rhyolites are both enriched in the Fe, Ti, incompatible elements (LREE) but slightly depleted in HREE and show slight positive Eu anomalies, implying derivation from primitive mantle source and emplacement in an anorogenic setting (Bhushan and Chittora 1999). The U–Pb age of rhyolite emplacement is between 751 and 771 Ma (Torsvik et al. 2001). The ultrapotassic rhyolite represents the youngest activity at 681 ± 20 Ma. The peralkaline granites and associated peralkaline rhyolite (pantellerite) at Manihari in the Pali district are coeval and cogenetic (Rathore et al. 1999a). Associated with the Siwana Granite are rhyolitic dykes, related to magma source fairly enriched in Rb, K, La, Ce, Nd, Sm, Zr, Y and Yb (Kochhar et al. 1985). The dykes date the time of rifting of the lithosphere in north-western India—750 Ma. Associated with the rhyolite dykes is another ring dyke of alkali granite forming the *Siwana Ring Complex*. This complex is characterized by high Zr, Nb, Y and low Sr with significant absolute abundances of trace elements and REE, indicating derivation from a primary mantle magma that was subsequently modified by crustal contamination (Vallinayagam and Kochhar 1998).

9.3.3 Granites of Malani Suite

Intimately associated with the Malani volcanics are ring complexes of granitic composition, such as the *Tosham Granite* and *Siwana Granite*. The peralkaline *Jalor Granite*, and the peraluminous Jhunjhunu Granite and *Tosham Granite* are associated with cogenetic carapase of welded tuffs, rhyolites, trachyte breccia, etc. This suite forms a *ring complex* and radial dykes (Kochhar 1983). The hypabyssal complexes are located in areas of crustal upwarp and are related to rifting of the continental crust and attendant caldera subsidence, as evident from the elliptical ring of quartz-porphyry associated with explosion breccia all along the length (Kochhar 1983). The Jhunjhunu Granite is characterized by a rather flat REE pattern with slight enrichment of LREE and marked Eu anomaly (Kochhar 2000). The Tosham Hill (Fig. 9.5) is made up of rhyolitic plug associated with potassic porphyritic granite dated 745 ± 20 Ma by Rb–Sr method (Kochhar et al. 1985; Eby and Kochhar 1990). The Jalar Granite is dated 727 ± 8 Ma (Dhar et al. 1996).

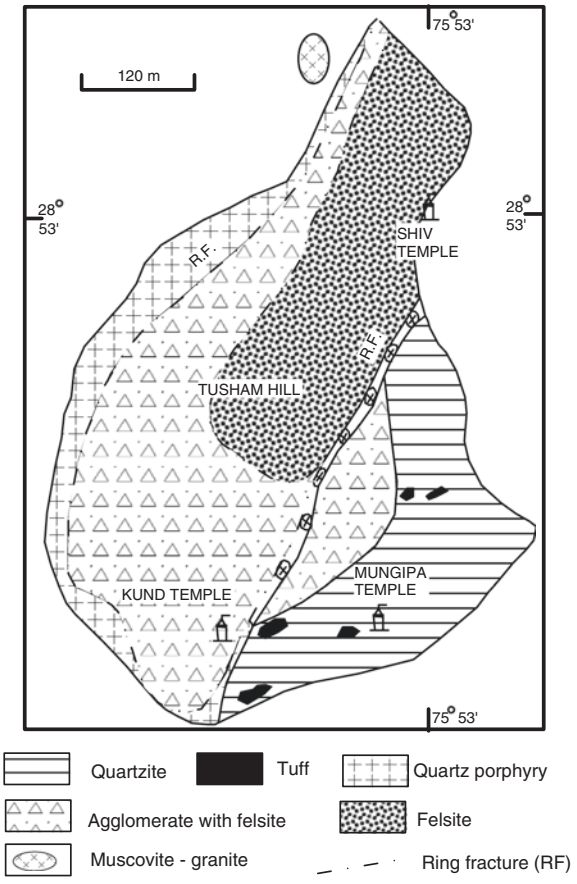

Fig. 9.5 Sketch map of the Tosham Hill in Haryana showing distribution of Malani Rhyolite and associated granites. Tosham is located 200 km WNW of Delhi (after Kochhar 1983)

In the area of Barmer horst, peralkaline granite bodies forming the Siwana ring structure are associated with extensive flows of rhyolite–commendite.

The batholithic *Mount Abu Granite* is intruded by a dyke of rhyolitic composition and characterized by enrichment in Rb, Nb, Zr, Y, Ga, Th and Zr, and depletion in Ba and Cr, implying genetic connection with "within-plate" anorogenic granite of rift-related setting (Singh and Joshi 2005; Singh 2007).

9.3.4 Mineralization

The Degana Granite is characterized by *tin* and *tungsten* mineralization in the form of cassiterite and wolframite as seen in the Degana, Sewariya Baldi, Phalwad and Positara areas. The tin mineralization is noticed along the rhyolite–metasediments and rhyolite–granite contacts, forming a linear zone about one kilometre long and 30 m wide. The porphyries carry minor veins of cassiterite (Deb and Sarkar 1990). The tungsten mineral deposit at Degana is associated with the Jalor Granite intruding the Ajabgarh metasediments. The mineralization is manifested in quartz veins in the marginal parts of the granitic body. The Tosham deposits of tin and tungsten with copper in the Malani Igneous Suite were formed in the temperature range of 150–450 °C as a result of action of hydrothermal fluids of high to low salinity (Kochhar et al. 1985; Somani 2006).

Most of the uranium deposits in India are of medium to low grade, with average grade ranging from 0.03 % to 0.01 U_3O_8, and the source of the majority of these uranium occurrence is peraluminous granites and granite-gneisses of Archaean to Proterozoic ages (Maithani 2011).

9.4 Greater Marwar Basin

9.4.1 Nature of Basement

South-east of Sargodha in the alluvial plain of the Panjab rivers, there are 36 inliers (such as of Kirana, Chiniot, Shahkot and Buland) made up of Precambrian crystalline rocks. The Kirana hill rises 330 m above the alluvial plain. The inlier complex consists of quartzites and slates or phyllites, interbedded with rhyolitic lavas, welded tuffs and agglomerates of the Malani suite, and sills and dykes. The volcanic rocks are bimodal and dated 870 ± 40 Ma (Crawford and Davies 1975). North-east of the Rann of Kachchh in south-eastern Sindh is the NagarParkar Complex made up of amphibolite, rhyolite, quartz-trachyte, acidic dykes and pink–grey granites, (Butt et al. 1994), forming a fringe around the Thar desert. The granites represent the extension of the Jalor–Siwana Granite, west of the Aravali region, and the lavas belong to the Malani suite. This complex is intruded by undeformed dykes of dolerite and lamprophyres (Kazmi and Khan 1973).

9.4.2 Marwar Group

West of the Aravali Mobile Belt, the basement rocks comprising predominant Malani Rhyolite–Siwana Granite suites are covered by what was named *Marwar Group* (Fig. 9.6a) by A.M. Heron in 1932. Resting unconformably on the Malani Rhyolite, the Marwar succession begins with the Jodhpur Sandstone, an assemblage of mature sandstones with shales, and the evaporites (anhydrite and gypsum) forming the middle part (Pareek 1983, 1984). The Jodhpur sediments were deposited in a shallow basin that was subjected to a number of transgression and regression (Awasthi and Parkash 1981). On a regional scale, the *Jodhpur Formation* comprises *Pokaran Conglomerate* and *Sonia Sandstone* (Dasgupta and Bulgauda 1994). The clasts of the Pokaran boulder beds were derived from the Malani

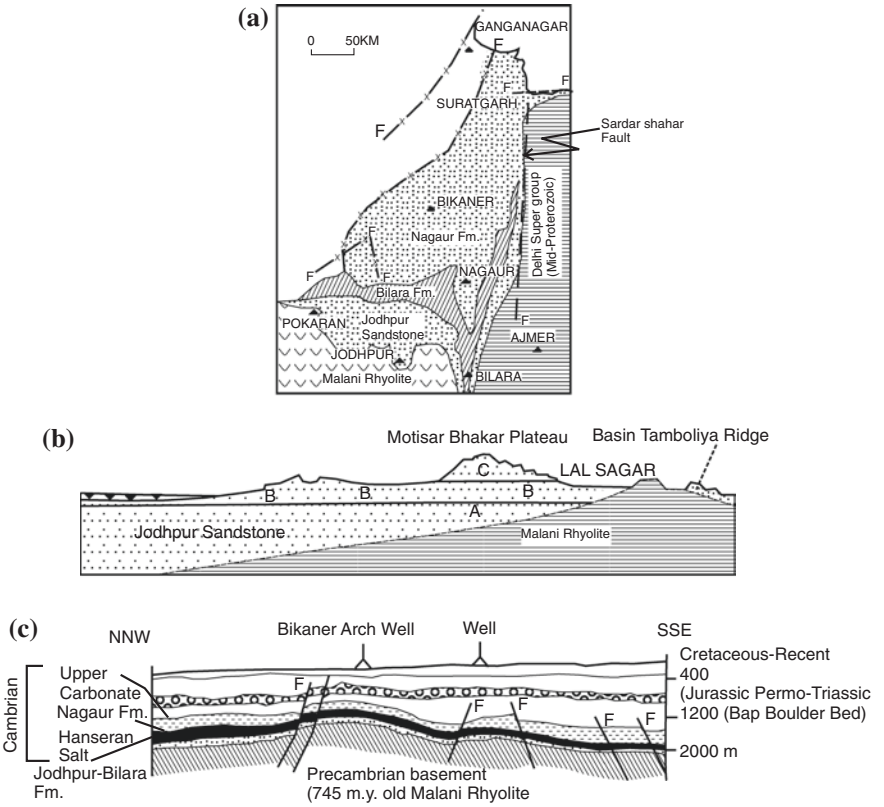

Fig. 9.6 **a** Geological sketch map of western Rajasthan showing the exposure of the Neoproterozoic–Early Cambrian rocks amidst the Thar Desert (after Dasgupta 1996). **b** Section shows the geological set-up of the Jodhpur area—the Jodhpur Sandstone unconformably overlying the Malani Rhyolite (after Chauhan et al. 1992). **c** Cross section of the western Rajasthan and Sindh plain demonstrating the lithological units extending north-westward towards the Salt Range in Pakistan (after Dasgupta and Bulgauda 1994)

Rhyolite and the Siwana Granite. The stratified upper part of the conglomerate is regarded as a product of Neoproterozoic glaciation (Chauhan et al. 2001). A coarsening-upward sequence of arkose, the *Sonia Sandstone,* is characterized by calcareous concretion in purple and green shale interbedded with subordinate dolomitic limestone. It is characterized by profuse wave ripple marks and trough- and tabular cross-beddings, particularly in the upper part. It is a deposit of a braided river system that built a plain with a delta (Chauhan et al. 1992).

The Baghewala well showed that in the Bikaner Basin, oil occurs in the reservoirs of the Proterozoic Jodhpur Sandstone. Prognostic assessment indicates that the probable resource of hydrocarbon is of the order of 90 MMT, of which only 2.15 MMT constitutes the geological reserve and mere 1.3 MMT is the recoverable reserve.

Overlying the Jodhpur is the Bilara Formation. The Bilara succession is seen in the southern and eastern margins of the basin while the Hanseran Formation in the northern margin is exposed amidst the desert sands. There is a horizon of purple-red to white gritty to pebbly sandstone, implying a hiatus between the Jodhpur and the Bilara formations. The *Bilara Formation* is a succession of cherty dolomite, ashgrey-coloured laminated dolomitic limestone, and stromatolitic limestone with intercalation of shale and siltstone. The carbonates of the lower part of the sequence show marked oscillation and broadly $\delta^{13}C$ characteristics, with the negative anomalies as low as or even less than—4.3 ‰ but the upper part exhibiting gradual shift towards positive characteristics (Pandit et al. 2001). It may be pointed out that this signature is correlated with the Neoproterozoic–Early Cambrian transition. The unit of the Bilara is characterized by stromatolites of the type *Stratifera* and *Weedia* besides a few cumulate and pseudocolumnar types (Barman 1980) recalling Vendian stromatolites.

The *Hanseran Formation* is an assemblage of evaporites—halite, polyhalite and anhydrite with intercalations of red sandstone and siltstone and shale. Presence of collapse breccia and slump structures in different units of the Hanseran succession indicates synsedimentary tectonic movements along the fault that demarcates the eastern boundary of the Marwar Basin (Dasgupta 1996). It is possible that the collapse breccia could be of non-tectonic origin related to ground subsidence. Reefs built by stromatolites were possibly responsible for development of a barred basin with restricted circulation of water conducive for evaporite precipitation under hot dry climate conditions. The aggregate thickness of the evaporite is 60 m. The rhythmic alternation of anhydrite and halite, and the occasional polyhalite lamellae within halite indicate microcycles in evaporite precipitation system—due to ingress of open sea water in the restricted environment (Dey 1991).

The *Nagaur Formation* is made up of brick red claystone, siltstone and gritty to pebbly sandstone. The pebble beds consist of clasts of chert, dolomite, quartzite and Malani rhyolites. The *Birmania succession* is a formation of cherty limestone overlain by calcareous ferruginous sandstone, phosphatic limestone and dolomite. The grey, yellow cherty limestone and dolomite alternate with sandstone and variegated to black shale. There are layers of phosphorite with shale and limestone in the middle part of the succession. The phosphorite consists of carbonate fluorapatite (Hussain and Banerjee 1986). In the upper part of the Nagaur Sandstones, trace

fossils attributable to trilobites suggest that the Marwar succession extends up to the Lower Cambrian. The Nagaur Sandstone of the Marwar Supergroup at Dulmera contains well-preserved trace fossils *Cruziana*, *Diamorphicus*, *Rusophycus*, etc., produced by Lower Cambrian trilobites (Kumar et al. 2009). It is apparent that the Precambrian–Cambrian boundary ties within the Bilara Group at the top of the Marwar Supergroup (Kumar 2012).

9.5 Chhattisgarh Basin

9.5.1 Structural Set-up

Located in the Bastar Craton, the Chhattisgarh Basin developed as a continental-interior depression south of the Satpura Orogenic Belt and west of the Eastern Ghat Mobile Belt (Figs. 8.1 and 9.7). While its northern and western parts are largely undistributed, the eastern margin in the Sambhalpur district in Odisha is deformed into a N–S trending the Barapahar Hill fold belt—characterized by faulting (Mishra et al. 1987a). The sedimentary successions in the neighbouring Khariar, Abujha and Ampani outliers are likewise folded along their eastern margin. In the case of the Ampani outlier, the Neoproterozoic overfolded rocks are faulted against the uplifted basement complex in the eastern side (Balakrishnan and Mahesh Babu 1987).

9.5.2 Stratigraphy and Sedimentation

The Chhattisgarh succession (Fig. 9.7; Table 9.2) is divided into two groups—the Chandarpur and the Raipur (Murti 1987, 1996; Deb 2000). An unconformity separates the two groups in the south-western part of the basin, and two more unconformities are recognizable in the northern part (Schnitzer 1971). The Chhattisgarh succession shows signatures of sea-level fluctuation as reflected in the cyclic deposition of sediments on different scales.

The lower part of the Neoproterozoic succession (*Lohardih Formation*) is a fan-delta complex consisting of quartzo-felspatic deposit laid down when the basin evolved after rifting of the crust. At Sukda in the north-eastern part of the Chhattisgarh Basin, welded felsic tuffs and ignimbrite characterized by high Sr/Y and La/Ybw ratios indicate volcanism during sedimentation (Subba Rao et al. 2006). Contorted bedding and slump- and load-structures indicate tectonic pulsation afflicting the basin during the commencement of the Chhattisgarh sedimentation (Patranabis-Deb and Chaudhuri 2007). The detritus of polymictic conglomerate and pebbly sandstones of arkosic to subarkosic composition in the *Chandarpur Group* were derived from the upthrown basement blocks, presumably along a fault. There was reworking of the earlier fluvial sediments in the wave- and tide-dominated near-shore environment, as testified by megaripples in sandstones.

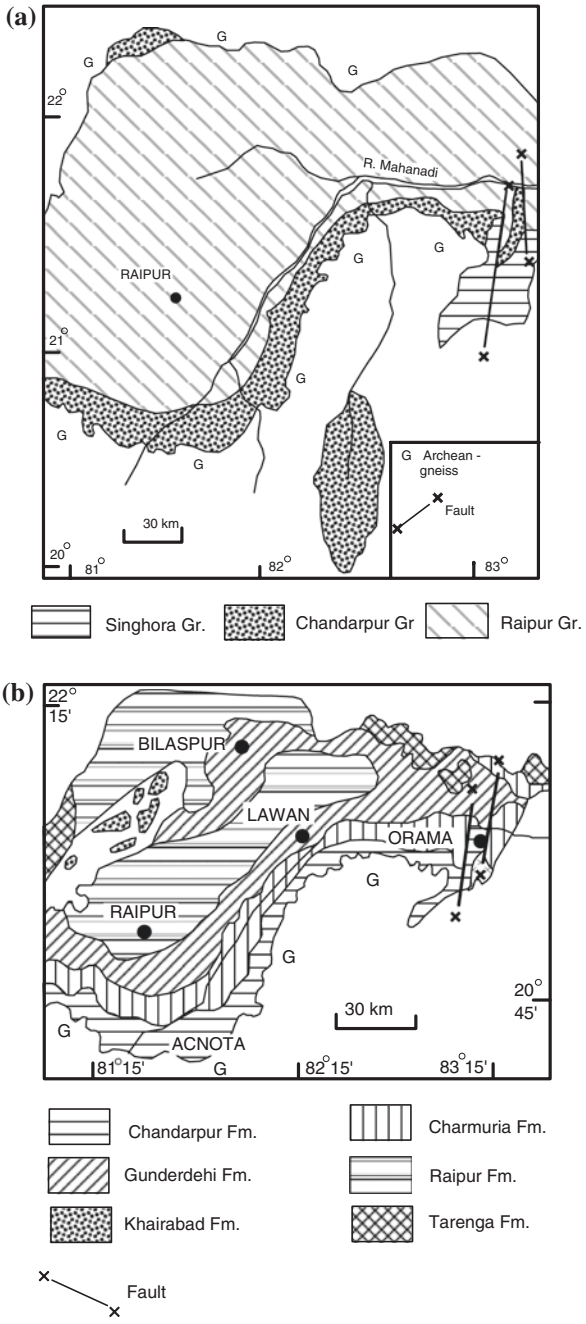

Fig. 9.7 **a** Geological sketch map of the Chhattisgarh Basin (after Murti 1987). **b** Details of geology of the south-eastern part of the Chhattisgarh Basin (after Patranabis-Deb and Chaudhuri 2002)

Table 9.2 Lithostratigraphy of the Chhattisgarh succession

South-central part (Murti 1996)		Northern part (Schnitzer 1969)
Raipur Group	Tarenga Formation (180 m)	Maniari Shale (100 m)
		Hirri–Kharkhera Dolomite (50–100 m)
	Chandi Formation (670 m)	Behla Limestone (80 m)
		Patharia–Umaraya Shale (50 m)
	Gunderdehi Formation (430 m)	Nandini Limestone (80-100 m)
		Bhatapara Dolomite (50 m)
	Charmuria Formation (490 m)	Lilagarh Shale (50 m)
		Akaltara Dolomite (40 m)
	- - - - - - - - - - - - - - - - - - - *Unconformity* - - - - - - - - - - - - - - - - - - -	
Chandarpur Group	Kansapathar Formation (125 m)	Karuid Shale (100–150 m)
		Karuid Limestone (50 m)
	Chapordih Formation (15 m)	Seorinaryan Shale (100 m)
		Sarangarh Limestone (30–50 m)
	Lohardih Formation (240 m)	Chandarpur Quartzite (200 m)
		Chandarpur Conglomerate (300 m)
- *Unconformity* -		
Archaean basement complex		

The thick mud sequence (*Chapordih Formation*) is followed upwards by a pile of quartzarenite (*Kansapathar Formation*) formed during regression as fluvial conditions prevailed once again. In the neighbouring Khariar Basin at Panduka, the lower part of the Neoproterozoic is represented by alluvial fan and braided-plain deposit. This deposit developed as a prograding succession pinching out downslope towards south and south-east, where it is represented by basal conglomerate (Datta 1998).

The *Raigarh* succession comprises argillocalcareous offshore slope deposits of grey, pink and purple shales intercalated with phosphorite. The Raipur sediments were laid down in a storm-dominated shallow platform which deepened following marine transgression, leaving behind a horizon of black limestone formed under anoxic condition all over the basin (Deb 2004). The dolomites (*Chandi Formation*) are characterized by prolifically developed stromatolites and prokaryote algae that grew in tidal flats (Schnitzer 1971; Moitra 1995). Towards the end of the Raipur time, climate had become arid, and in the sabkha-type environment the evaporite gypsum cyclically precipitated with carbonates (Das et al. 1990) forming the rhythmite of the *Tarenga Formation*.

9.5.3 Age of Chhattisgarh Succession

The turbinate columns of stromatolites of the Raipur Group are characterized by active branching with constriction at the base of branches, resembling Tungussids of the Bhander Group of the Vindhyan Basin. Stromatolite assemblage places the

Chandi Limestone in the Neoproterozoic. Palaeomagnetic study of the Gunderdehi rocks of the approximately middle of the Chhattisgarh succession (Table 9.2) places it in the time span of 1250–1300 Ma (Krueger et al. 1977).

In the Chhattisgarh Basin, diabasic intrusions into the succession at Singhora have been dated 1420 Ma, thus placing the Chhattisgarh Supergroup into the Mesoproterozoic—1500–1000 Ma (Das et al. 2011). In the Damdami area, dolerite dykes yield Rb–Sr isochron age of 1641 ± 120 Ma, and the rhyolite tuffs at Sukhada is dated ~1000 Ma, the two dates thus indicating that the Chandarpur and Rajpur groups together span the period 1600–1000 Ma (Das et al. 2011).

9.6 Indravati Basin

9.6.1 Configuration

The Indravati, a tributary of the River Godavari, traverses the succession of the Neoproterozoic succession (Figs. 8.1, 8.2 and 9.8; Table 9.3) designated the *Indravati Series* by Dutt (1963). The Indravati succession rests on the basement

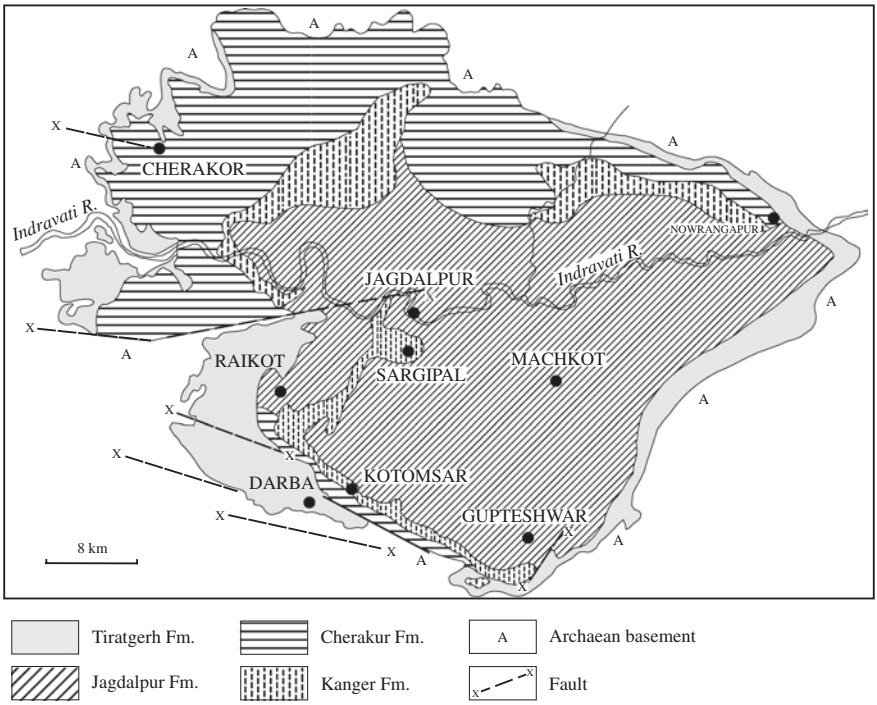

Fig. 9.8 Geological sketch map of the Indravati Basin located in the Bastar cratonic block (after Ramakrishnan 1987)

Table 9.3 Stratigraphic classification of the Indravati Group (Dutt 1963 and Ramakrishnan 1987)

Indravati Group	Jagdalpur Formation (200–250 m) Kanger Limestone (150–200 m) Cherakur Formation (50–60 m) Tiratgarh Formation (50–-60 m)
- - - - - - - - - - - - - - - - - *Unconformity* - - - - - - - - - - - - - - - - -	
Archaean basement complex	

of Archaean complex in the Chhattisgarh state. Its eastern margin is folded into NE–SW trending tight anticlines and synclines that are faulted along the boundary with the Eastern Ghat Mobile Belt. This deformation is attributed to tectonic reactivation in the Eastern Ghat Mobile Belt (Ramakrishnan 1987). South of the Chhattisgarh there is an outlier in the Sukma region.

9.6.2 Stratigraphy and Sedimentation

The 500-m-thick Indravati succession is divided into four formations (Table 9.3). The lower part of the group is an assemblage of conglomerates and arkosic sandstones (*Tiratgarh Formation*), with purple and green shales (*Cherakur Formation*) exhibiting shoreline facies. The laminated limestones (*Kanger*) represent a tidal-flat deposit on a shallow shelf. The uppermost part of the sequence (*Jagdalpur*) is a mud-carbonate facies, characterized by lenticular horizons of stromatolite bioherms associated with flat–pebble chert conglomerate. The stromatolites have been described as *Gymnosolen, Conophyton, Colonella, Tungussia*, *Baicalia* and *Anabaria* (Ramakrishnan 1987) (Table 9.3).

9.6.3 Igneous Activity

Fifteen kilometres south-east of Jagdalpur, there is a plug of kimberlite penetrating through the Kanger–Jagdalpur boundary. The proximal Indravati succession includes a sequence of volcanic tuff and agglomerate. The plug comprises a feeder dyke or a vent. The proximal extra-crater pyroclastics were formed by flow and surge and the pyroclastic material forms a 2-km-wide apron of lapilli, tuff and agglomerate. It was trapped between the sedimentary formations.

9.6.4 Mineral Resources

The thinly laminated *limestone* with paper-thin shale partings of the Kanger Formation is characterized by 35–45 % CaO and 5–10 % insolubles. It is a valuable source of raw material for cement making.

Table 9.4 Lithostratigraphic subdivision of the Sullavai in the Godavari Valley (Chaudhuri Asru 2003)

Gondwana succession	
- - - - - - - - - - - - - - *Unconformity* - - - - - - - - - - - - - -	
Sullavai Group	Venkatapur Sandstone (20 m) Mancheral Quartzite (23 m) Ramagiri Formation (250 m)
- - - - - - - - - - - - - - - -*Unconformity* - - - - - - - - - - - - - - - -	
Pakhal/Penganga Group/Basement Complex	

Six areas of significant *uranium mineralization* are associated with the unconformity between the gneissic basement and the Chhattisgarh succession. The uranium minerals (pitchblende, betauranophane, autunite and breunnerite) are attributed to hydrothermal solutions and later adsorption on iron oxide material within microfractures (Bhattacharjee et al. 2005).

9.7 Sullavai Group

Resting on gneissic complex of the Bastar cratonic block and unconformably upon the Pakhal and Penganga successions in the Godavari Basin (Fig. 8.7; Table 9.4), the *Sullavai* succession is divided into three units—the Ramagiri, the Mancheral and the Venkatapur.

The coarse-grained pebble to conglomeratic sandstone of arkosic and quartzose composition, purple to red colours, is characterized by trough-shaped as well as planar cross-bedding. These were deposited by a braided river receiving detritus from both flanks and flowing SE to SSE. Towards the close of the Sullavai time, the climate had become semi-arid, and riverine sediments were reworked pronouncedly by strong winds that shifted finer material into dunefields within a well-developed erg (Chakraborty 1991, 1994). In the extreme south-east, there was alternation of aeolian sands with marine sediments—making the termination of the sandsea in the direction of palaeowinds.

9.8 Bhima Basin

9.8.1 Stratigraphy and Sedimentation

Developed in a terrane of Archaean gneisses and granites of the Dharwar cratonic block in north-eastern Karnataka and adjoining part of Andhra Pradesh, the *Bhima Basin* is 160 km long and 40 km wide (Figs. 8.1, 8.2 and 9.9; Table 9.5). The 250-m-thick succession (Janardhan Rao et al. 1975) begins with 1- to 2-m-thick conglomerate associated with gritty felspathic cross-bedded sandstone with interbedded shale showing ripple marks (*Rabanapalli Formation*), deposited in a near-shore

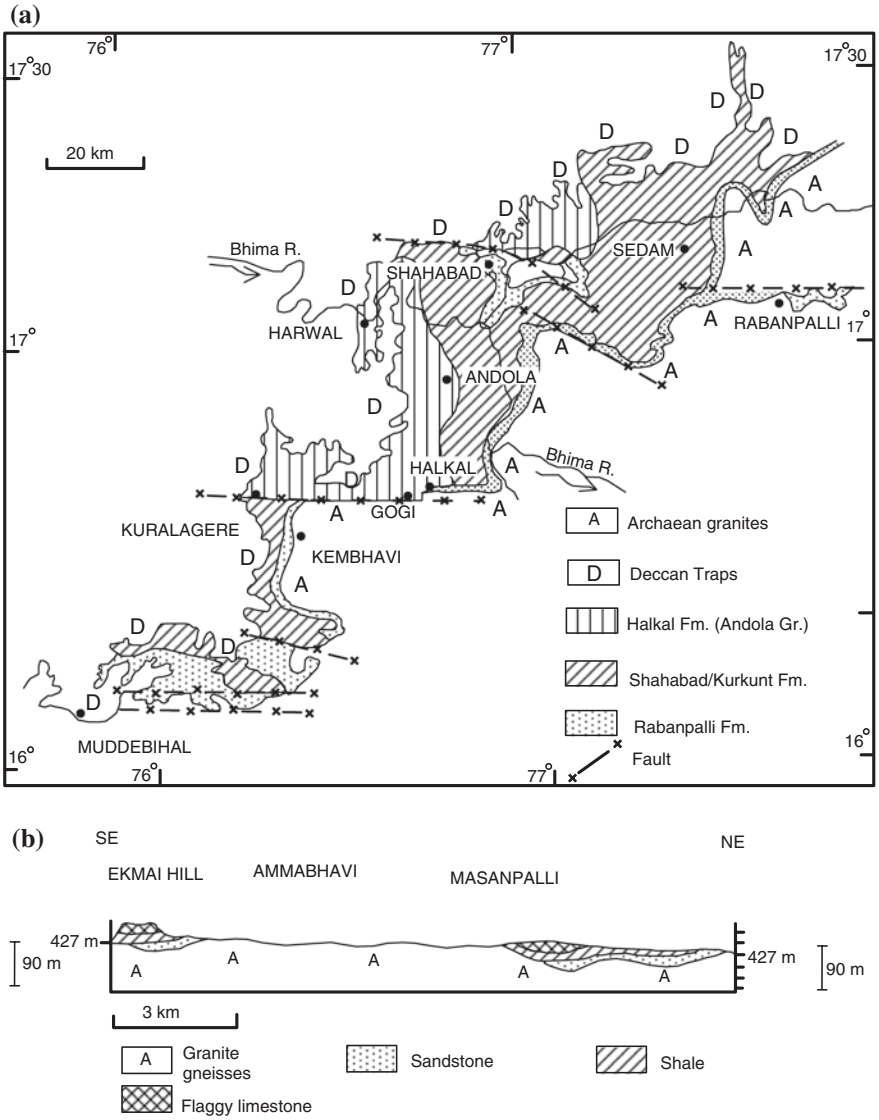

Fig. 9.9 **a** Sketch map of the geology of Bhima Basin in north-eastern Karnataka and adjoining Andhra Pradesh (after Mishra et al. 1987b). **b** Cross section shows the structural design of the Bhima succession (after Kale Vivek and Peshwa 1995)

environment. The basin was occasionally affected by reactivation of faults. The tectonic disturbance is indicated by penecontemporaneous deformation features in the basal part of the Bhima succession (Kale et al. 1990; Kale Vivek and Peshwa 1995). The succeeding sequence of flaggy to massive bluish grey limestones with grey shales and local cherty layers (*Kurkunta Limestone/Shahabad Formation*) represents

Table 9.5 Lithostratigraphy of the Bhima Group (Mishra et al. 1987b)

Deccan Traps	
- - - - - - - - - - - - - - - - *Unconformity* - - - - - - - - - - - - - - - -	
Bhima Group	Harwal Formation (5–10 m)
	Katamdevarahalli Formation (10–40 m)
	Halkul Formation (16–18 m)
	Kurkunta/Shahabad Formation (46–129 m)
	Rabanapalli Formation (16–76 m)
- - - - - - - - - - - - - - - - *Unconformity* - - - - - - - - - - - - - - - -	
Archaean basement complex	

a carbonate platform in tidal-flat environment. Marine transgression and regression were also responsible for the formation of chert pebble conglomerate associated with shale–quartzite sequence of the *Halkul Formation* (Malur and Nagendra 1994). Dark grey siliceous limestone (*Katamdevarahalli Formation*) and red shale (*Harwal Formation*) were deposited in the tectonically pulsating environment towards the close of the Bhima time (Mishra et al. 1987b).

9.8.2 Mineral Resources

The Kurkunta *Limestone* is remarkably uniform in its chemical composition—40–50 % CaO, trace MgO and 10–20 % insolubles. The 1500 million tonnes of valuable carbonate reserve is utilized on an extensive scale. The dark grey siliceous limestone of the Katamdevarahalli Formation hosts deposits of *barytes* (Table 9.5).

9.9 Badami Group

As stated in the previous chapter, the Neoproterozoic era in the Kaladgi Basin in northern Karnataka commenced with the deposition of *Badami Group* sediments unconformably over the Bagalkot succession (Table 9.6) and onlapping onto the Archaean basement (Jayaprakash et al. 1987). The spread of sedimentation had thus become larger than it was in the earlier period (Fig. 9.6). The *Kerur* Conglomerate, best seen at Kandur, is associated with white buff and red-coloured quartzarenites and shales, forming a 130-m-thick pile in which are located the historical caves of Badami. The shales and limestones (*Katageri Formation*) were deposited in the shallow shelf of the Badami Basin during the close of its life (Table 9.6).

Table 9.6 Lithostratigraphic succession of the Badami Group in northern Karnataka (Jayaprakash et al. 1987)

Deccan Traps	
- - - - - - - - - - - - - - - *Unconformity* - - - - - - - - - - - - - - - - -	
Badami Group	Katageri Formation (152 m)
	Kerur Formation (250 m)
- - - - - - - - - - - - - - - *Unconformity* - - - - - - - - - - - - - - - - -	
Archaean basement	

9.10 Kurnool Group

9.10.1 Tectonics

The tectonic unrest that the Cuddapah Basin experienced sometime between 1100 and 900 Ma is reflected in the end of sedimentation. There was an interval of erosion represented by the angular unconformity between the sediments of the *Kurnool Group* and the Cuddapah successions. Compared to the Cuddapah, the Kurnool sedimentation took place in a shrunken basin restricted to northern and western parts. The Kurnool sediments overstep onto several units of the Cuddapah succession (Figs. 8.1 and 9.10).

9.10.2 Stratigraphy and Sedimentation

Resting unconformably on the Srisailam quartzites of the Upper Cuddapah succession and overstepping on other units elsewhere, the Kurnool comprises quartzites (with basal conglomerate), limestones and shales deposited in the shallow shelf of the Cuddapah Basin (Fig. 9.10; Table 9.7). The environment of deposition varied from beach through littoral to tidal flats and lagoons. The most important unit of the Kurnool is the impersistent 10- to 15-m-thick horizon of the conglomerate at the base (*Banaganapalli Formation*). Load structures such as convolute lamination and bedding, slump structure and gravity fault-folds related to synsedimentary deformation occur in the sequence of quartzite–grey shale and shale–siltstone of the Banaganapalli Formation (Gupta et al. 2010). Associated with coarse-grained to gritty felspathic sandstones, the conglomerate is characterized by detrital diamond derived from the kimberlite pipes of the Cuddapah Basin and the surrounding terrane. It is evident that the Kurnool sedimentation commenced quite after the emplacement of the kimberlite bodies 1090 million years ago.

9.10.3 Mineral Resources

Diamond mining in the Krishna Valley dates back to fifth-century B.C. World-famous *Kohinoor* and *Regent* diamonds were recovered from the alluvial gravel

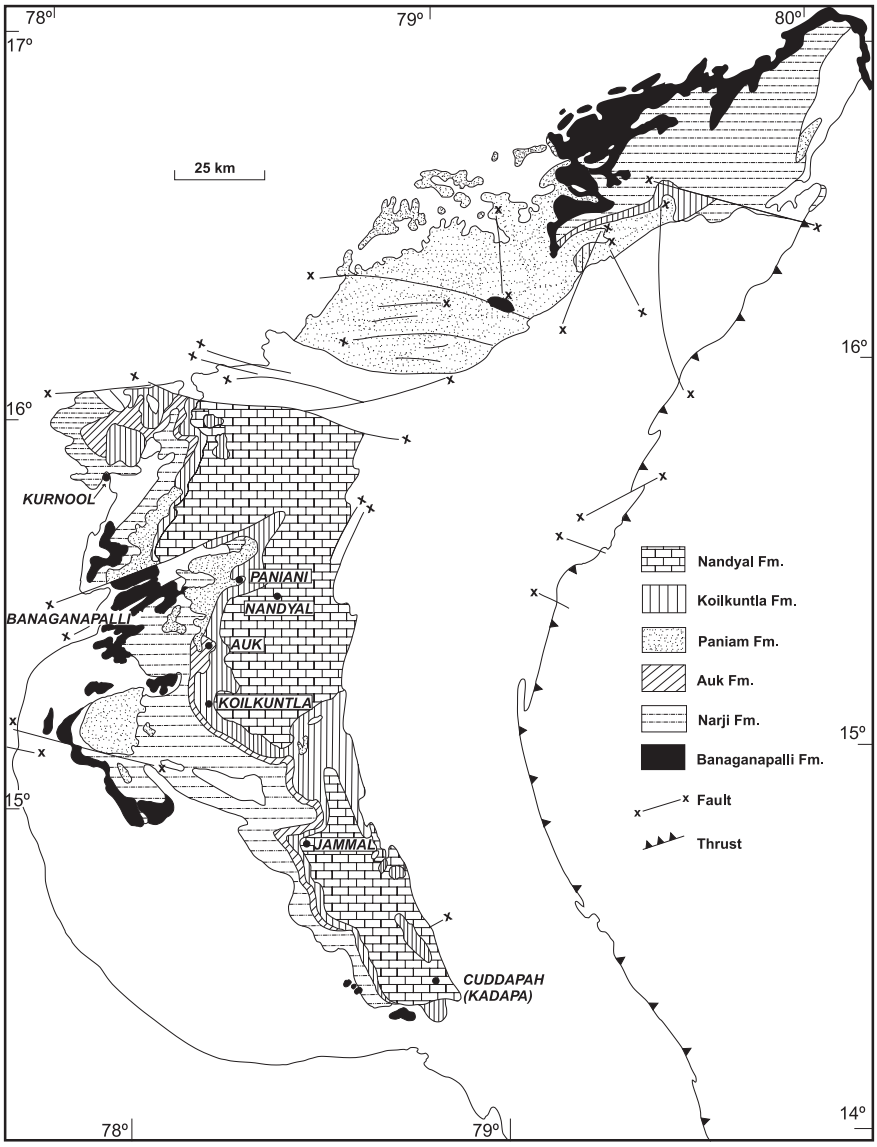

Fig. 9.10 Sketch map of the geology of the Cuddapah Basin showing the extent and lithostratigraphic units of the Kurnool succession (after Ramam and Murty 1997)

of the river between Kolluru and Ustapalle. The Banaganapalli Conglomerate also contains diamond. In the Koppunuru area in the Palnad sub-basin uranium minerals pitchblende and coffinite occur as veins, in fractures, as cavity fillings in the quartzites of the Banaganapalli Formation, as well as in the underlying granitoids of the basement (Jeygopal et al. 2011). The association of uranium minerals with biogenic

Table 9.7 Lithostratigraphy of the Kurnool Group of the Cuddapah Basin (after Nagaraja Rao et al. 1987)

Kurnool Group	Nandyal Shale (50–100 m) Koilkuntla Limestone (15–50 m) Paniam Quartzite (10–35 m) Auk Shale (10–15 m) Narji Limestone (100–200 m) Banaganapalli Formation (10–50 m)
- - - - - - - - - - - - - - *Unconformity* - - - - - - - - - - - - - -	
Cuddapah: Srisailam Quartzite	

sulphide and carbonaceous matter seems to suggest that these played an important role in the precipitation of uranium. In the Srisalam sub-basin, uranium mineralization (0.01–0.017 % U_3O_8) of significance occurs in the marginal part of the basin in the unconformity as well as 11–17 m below in the Kottapullareddypuram–Achchammagunta–Rachchamapadu area (Banerjee et al. 2012).

The siliceous *Narji Limestone* of pink, purple and blue colours is used extensively as building material and for the manufacture of cement.

9.11 Summing up

It is evident from the accounts of sedimentation history in different Neoproterozoic basins that sedimentation commenced with the influx of voluminous detritus, including gravels, from the uplifted basement complexes, made up of dominant gneisses and granites. At the very beginning, there was tectonic disturbance. The sediments were deposited as delta–fan deposits in the initial stage and as braided-plain deposit subsequently. In many areas, tectonic movements continued and caused synsedimentary deformation of soft sediments. The terrestrial sediments gave way to shallow water deposits on shelf parts of the Purana Basin. Towards the close of the Neoproterozoic time, in the northern part of the Purana Province, climate had become semi-arid and the wind reworked the fluvial sediments, giving rise to aeolian deposits. In the subaqueous shallow environment evaporitic conditions developed and in association with carbonates and shales the evaporites (gypsum and salts) formed in the Sabkha-like setting. The end of the Neoproterozoic era is marked by aridity on land and evaporitic conditions under water in the basins that were to dry up soon after.

References

Akhtar, K. (1976). Facies analysis and depositional environment of the Bhander Limestone, southeastern Rajasthan and adjoining M.P. *Sedimentary Geology, 16*, 299–318.

Akhtar, K. (1978). Palaeogeography and sediment dispersal patterns of the Proterozoic Bhander Group, Western India. *Palaeogeography, Palaeoclimatology, Palaeoecology, 24*, 327–357.

Akhtar, K. (1996). Facies, sedimentation processes and environments in the Proterozoic Vindhyan Basin, India. *Memoir Geological Society of India, 36*, 127–136.

Awasthi, A. K., & Parkash, B. (1981). Depositional environments of microfossiliferous sediments of the Jodhpur Group, western India. *Sedimentary Geology, 30*, 15–42.

Balakrishnan, P., & Babu, M. (1987). Geology of the Ampani outlier, Kalahandi, Koraput district, Orissa. *Memoir Geological Society of India, 6*, 281–286.

Banerjee, R., Bahukhandi, N. K., Rahman, M., Achar, K. K., Ramesh Babu, P. V., Umamaheswar, K., & Parihar, P. S. (2012). Lithostratigraphic and radiometric appraisal of deeper parts of Srisailam and Palnad sub-basin in Kottapullareddipuram-Achchammagunta-Rachchamallepadu area, Guntur district, Andhra Pradesh. *Exploration and Research for Atomic Minerals, 22*, 55–69.

Barman, G. (1980). An analysis of the Marwar Basin in the light of stromatolite study. *Miscellaneous Publication, Geological Survey of India, 44*, 292–302.

Basumallick, S., Sarkar, B. C., & Banerjee, S. (1996). Tidal cyclicity in Lower Bhander Sandstone Maihar, Madhya Pradesh. *Journal of Geological Society of India, 47*, 189–194.

Bhattacharjee, I., Mukundhan, A. R., Sachan, A. S., Tiwary, K. N., Sinha, R. M., & Gupta, R. K. (2005). Proterozoic unconformity related uranium mineralization around Chitakhol, Korba district, Chhattisgarh. *Journal of Geological Society of India, 65*, 619–622.

Bhattacharya, A. (1996). Advances in Vindhyan Geology. *Geological Society of India, Memoir*, *36*, VIII–XI.

Bhattacharya, A., & Morad, S. (1993). Proterozoic braided ephemeral fluvial deposits: an example from the Dhandraul Sandstone Formation of the Kaimur Group. *Son Valley, Central India, Sedimentary Geology, 84*, 101–114.

Bhattacharya, A., Sarkar, S., & Chanda, S. K. (1980). Storm deposits in the late proterozoic lower Bhander sandstone of Vindhyan supergroup around Maihar, Satna district, M.P., India. *Journal of Geological Mines, Metal Society of India, 34*, 175–181.

Bhowmik, S. K., Bernard, H.-J., & Dasgupta, S. (2010). Grenvillian age high- pressure upper amphibolites-granulite metamorphism in the Aravali-Delhi Mobile Belt, northwestern India: New evidence from monazite chemical age and its implication. *Precambrian Research, 178*, 168–184.

Bhushan, S. K., & Chittora, V. K. (1999). Late Proterozoic bimodal volcanic assemblage of Siwana subsidence structure, western Rajasthan. *Journal of Geological Society of India, 53*, 433–452.

Bhushan, S. K., & Chittora, V. K. (2005). Proterozoic granitoids of Rajasthan. *Journal of Geological Society of India, 66*, 741–763.

Bose, P. K., Majunder, R., & Sarkar, S. (1997). Tidal sandwaves and related storm deposits in the transgressive Protoproterozoic Chaibasa Formation, India. *Precambrian Research, 84*, 63–81.

Butt, K. A., Jan, M. Q., & Karim, A. (1994). Late Proterozoic rocks of Nagar Pahar, southeastern Pakistan: Preliminary petrologic account. In R. Ahmed & A. M. Sheikh (Eds.), *Geology in South Asia-1, Hydrocarbon Develop* (pp. 106–109). Islamabad: Institute of Pakistan.

Chakraborty, T. (1991). Sedimentology of a Proterozoic erg: the Venkatapur Sandstone, Pranhita-Godavari valley, South India. *Sedimentology, 38*, 301–322.

Chakraborty, T. (1994). Stratigraphy of the Late Proterozoic Sullavai Group, Pranhita-Godavari valley, A.P. *Indian Journal of Geology, 66*, 124–147.

Chakraborty, C. (1996). Sedimentary records of erg development over a braided plains, Proterozoic Dhandraul Sandstone, Vindhyan Supergroup, Son Valley. *Memoir Geological Society of India, 36*, 77–99.

Chakraborty, C. (2001). Lagoon-tidal flat sedimentation in an epeiric sea: Proterozoic Bhander Group, Son valley, India. *Geological Journal, 36*, 125–141.

Chakraborty, C., & Bhattacharya, A. (1996a). The Vindhyan Basin: An overview in the light of current perspectives. *Memoir Geological Society of India, 36*, 301–312.

Chakraborty, C., & Bhattacharya, A. (1996b). Fan-delta sedimentation in a foreland moat: Deoland formation, Vindhyan supergroup, son valley. *Memoirs-Geological Society of India, 36*, 27–48.

Chakraborty, T., & Chaudhuri, A. K. (1990). Stratigraphy of the late Proterozoic Rewa Group and palaeogeography of the Vindhyan basin in central India during Rewa sedimentiation. *Journal of Geological Society of India, 36*, 383–402.

Chakraborty, T., Sarkar, S., Chaudhuri, A. K., & Dasgupta, S. (1996). Depositional environment of Vindhyan and other purana basins: A reappraisal in the light of recent findings. *Memoir Geological Society of India, 36*, 101–126.

Chanda, S. K., & Bhattacharya, Ajit. (1982). Vindhyan sedimentation and palaeogeography of post-Auden developments. In K. S. Valdiya, S. B. Bhatia, & V. K. Gaur (Eds.), *Geology of Vindhyachal* (pp. 95–100). Delhi: Hindustan Publishing Corporation.

Chatterjee, A. K., & Rao, K. S. (1995). Majhgawan diamondiferous pipe, Madhya Pradesh, India—A review. *Journal of Geological Society of India, 45*, 175–189.

Chaudhuri Asru, K. (2003). Stratigraphy and palaeogeography of the Godavari Supergroup in the southcentral Pranhita-Godavari valley, South India. *Journal of Asian Earth Sciences, 21*, 595–611.

Chauhan, D. S., Dubey, J. C., & Ram, B. (1992). Geological analysis of part of Nagaur basin in the vicinity of Jodhpur city. In S. K. Tandon, C. C. Pant, & S. M. Casshyap (Eds.), *Sedimentary basins of India: Tectonic context* (pp. 63–75). Nainital: Gyanodaya Prakashan.

Chauhan, D. S., Mathur, K. M., & Ram, N. (2001). Geological nature of the Pokaran Boulder Bed: Palaeoenvironmental, palaeoclimatic and stratigraphic implications. *Journal of Geological Society of India, 58*, 425–433.

Crawford, A. R., & Davies, R. G. (1975). Ages of Pre-Mesozoic formations of the Lesser Himalaya, Hazara district, northern Pakistan. *Geological Magazine, 112*, 509–514.

Das, N., Das, M. G., & Arora, Y. K. (1990). Microfacies assemblage of gypsum from Chhattisgarh Basin—a sabkha model of evaporite formation. *Special Publication of Geological Survey of India, 28*, 639–647.

Das, P., Das, K., Chakraborty, P. P., & Balakrishnan, S. (2011). (The) 1420 Ma diabasic intrusive from the Mesoproterozoic Singhora Group, Chhattisgarh Supergroup, India: Implications towards non-plume intrusive activity. *Journal of Earth System Sciences, 120*, 1–14.

Dasgupta, S. P. (1996). Marwar supergroup evaporites, Rajasthan. *Memoir Geological Society of India, 36*, 49–58.

Dasgupta, U., & Bulgauda, S. S. (1994). An overview of the geology and hydrocarbon occurrences in the western part of Bikaner-Nagaur basin, Indian Jour. *Petrolum Geology, 3*, 1–17.

Datta, B. (1998). Stratigraphic and sedimentologic evolution of the Proterozoic siliciclastics in the southern part of Chhattisgarh and Khariar, central India. *Journal of Geological Society of India, 51*, 345–360.

Deb, S. P. (2004). Lithostratigraphy of the Neoproterozoic Chhattisgarh sequence, its bearing on the tectonics and palaeogeography. *Gondwana Research, 7*, 323–337.

Deb, M., & Sarkar, S. C. (1990). Proterozoic tectonic evolution and metallogenesis in the Aravali-Delhi orogenic complex, northwestern India. *Precambrian Research, 46*, 115–137.

Dey, R. C. (1991). Trans-Aravali Vindhyan evaporites under the semidesertic plain of western India—Significance of depositional features. *Journal of Geological Society of India, 37*, 136–150.

Dhar, S., Frei, R., Kramers, J. C., Nägler, T. F., & Kochhar, Naresh. (1996). Sr, Pb and Nd isotope studies and their bearing on the petrogenesis of the Jalor and Siwana complexes, Rajasthan, India. *Journal of Geological Society of India, 48*, 151–160.

Dutt, N. V. B. S. (1963). Stratigraphy and correlation of the Indravati Series (Purana) of Bastar district (MP). *Journal of Geological Society of India, 4*, 35–48.

Eby, G. N., & Kochhar, Naresh. (1990). Geochemistry and petrogenesis of the Malani Igneous Suite, north Peninsular India. *Journal of Geological Society of India, 36*, 109–130.

Fuloria, R. C. (1996). Geology and hydrocarbon prospects of the Vindhyan sediments in Ganga valley. *Memoir Geological Society of India, 36*, 235–256.

Gopalan, K., Trivedi, J. R., Merh, S. S., Patel, P. P., & Patel, S. G. (1979). Rb-Sr age of Godhra and related granites, Gujarat. *Proceedings of Indian Academic Sciences (Earth & Planet Sciences), 88A*, 7–17.

Gupta, S., Vimal, R., Banerjee, R., Ramesh Babu, P. V., & Maithani, P. B. (2010). Sedimentation pattern and depositional environment of Banaganapalle Formation in southwestern part of Palnad sub-basin, Guntur district, Andhra Pradesh. *Gondwana Geological Magazine, 12*, 59–70.

Husain, V., & Banerjee, D. M. (1986). Birmania phosphorites: petro-mineralogical characters and palaeogeological implications. *Journal of Geological Society of India, 27*, 450–455.

Janardhana Rao, L. H., Srinivasa Rao, C., & Ramakrishna, T. L. (1975). Reclassification of the rocks of Bhima basin, Gulbarga district, Karnataka State. *Miscellaneous Publication, Geological Survey of India, 23*, 177–184.

Jayaprakash, A. V., Sundaram, V., Hans, S. K., & Mishra, R. N. (1987). Geology of the Kaladgi-Badami basin Karnataka. *Memoir Geological Society of India, 6*, 201–255.

Jeyagopal, A. V., Deshpande, M. S. M., Gupta, S., Ramesh Babu, P. V., Umamaheswar, K. & Maithani, P. B. (2011). Uranium mineralization and association of carbonaceous matter in Koppunuru area, Palnad sub-basin, Cuddapah Basin, Andhra Pradesh, *The Indian Mineralogist, 45*, 100–111.

Just, J., Schultz, B., de Wall, Helga, Jourdan, F., & Pandit, M. K. (2011). Monazite CHIME/EMPA dating of Erinpura granitoid deformation: Implications for Neoproterozoic tectonothermal evolution of northwest India. *Gondwana Research, 19*, 402–412.

Kale, Vivek, S., Mudholkar, A. V., Phansalkar, V. G., & Peshwa, V. V. (1990). Stratigraphy of the Bhima Group. *Journal of Palaeontological Society of India, 35*, 91–103.

Kale, Vivek, S. & Peshwa, V. V. (1995). *Bhima basin* (p. 142). Bangalore: Geological Society of India.

Kaur, P., Chaudhri, N., Hofmann, A. W., Raczek, F., & Okrush, M. (2013). Geochemistry and Sm–Nd geochronology of the metasomatised mafic rocks in the Khetri Complex, Rajasthan, NW India: Evidence of Early Cryogenian metasomatic event in the northern Aravali Orogen. *Journal of Asian Earth Sciences, 62*, 401–413.

Kazmi, A. H., & Khan, R. A. (1973). The report on the geology, mineral and water resources of Nagar Parkar, Pakistan. *Geological Survey of Pakistan, Information Release, 64*, 1–33.

Kochhar, N. (1983). Tusham ring complex, Bhiwani, India. *Proceedings of Indian National Society of Acadamy, 49A*, 459–490.

Kochhar, N. (2000). Attributes and significance of the A-type Malani magmatism, NW Peninsular India. In M. Deb (Ed.), *Crustal Evolution and Metallogeny in the NW Indian Shield* (pp. 158–188). New Delhi: Narosa Publishing Company.

Kochhar, N., Pande, K., & Gopalan, K. (1985). Rb-Sr age of Tosham ring complex, Bhiwani, India. *Journal of Geological Society of India, 26*, 216–218.

Krueger, H., Karre, W., Krustein, M., Schnitzer, W. A., Murti, K. S., & Srivastava, N. K. (1977). K/Ar dates of glauconites from the Chandrapur Series (Chhattisgarh Basin, Central India). *Geologisches Jahrbuch B, 28*, 23–36.

Kumar, S. (2012). Stratigraphy and correlation of the Neoproterozoic deposits of central and Western India: An overview. *Special Publication Geological Society of London*, *366*, http://dx.doi.org/10.1144/S (P 366.9).

Kumar, S., Misra, P. K., & Pandey, S. V. (2009). Ediacaran megaplant fossils with Vaucheriacean affinity from the Jodhpur Sandstone, Marwar Supergroup, Western Rajasthan. *Current Sciences, 97*, 701–705.

Kumar, A., Padma Kumari, V. M., Dayal, A. M., Murthy, D. S. N., & Gopalan, K. (1993). Rb–Sr ages of Proterozoic kimberlites of India: Evidence for contemporaneous emplacement. *Precambrian Research, 62*, 227–237.

Kumar, S., Schindowski, M., & Joachimisky, M. M. (2005). Carbon isotope stratigraphy of the Palaeo-Neoproterozoic Vindhyan Supergroup, central India: Implications for basin evolution and interbasinal correlation. *Journal of the Palaeontological Society of India, 50*, 65–81.

Maithani, P. B. (2011). Targeting felsic volcanic rocks in India as potential source for uranium mineralization with a special emphasis on Malari magmatic province—A review. *The Indian Mineralogist, 45*, 1–8.

Malone, S. J., Meert, J. G., Banerjee, D. M., Pandit, M. K., Tamrat, L., Kamenov, G. D., et al. (2008). Palaeomagnetism and detrital zircon geochronology of the Upper Vindhyan sequence. *Son Valley and Rajasthan, India, Precambrian Research, 162*, 424–440.

Malur, M. N., & Nagendra, R. (1994). Lithostratigraphy of the Bhima Basin (central part), Karnataka, southern India. *Journal of Palaeontology Society of India, 39*, 55–60.

Mishra, V. P., Datta, N. K., Ramchandra, H. M., Bhattacharya, P., Das, D. P., Kumaran, K., et al. (1987a). Geological history of the Abujhmar basin, Bastar district, Madhya Pradesh. *Memoir Geological Society of India, 6*, 189–199.

Mishra, R. N., Jayaprakash, A. V., Hans, S. K., & Sundaram, V. (1987b). Bhima Group of Upper Proterozoic—A stratigraphic puzzle. *Memoir Geological Society of India, 6*, 33–86.

Misra, R. C. (1969). The Vindhyan system. *Presidential Address 56th Indian Science Congress* (pp. 1–32), Kolkata.

Misra, R. C., & Awasthi, N. (1962). Sedimentary markings and other structures from Son Valley and Maihar-Rewa area. *Journal of Sedimentary Petroleum, 32*, 775–782.

Moitra, A. K. (1995). Depositional environmental history of the Chhattisgarh basin, M.P., based on stromatolites and microbiota. *Journal of Geological Society of India, 46*, 359–368.

Murti, K. S. (1987). Stratigraphy and sedimentation in Chattisgarh basin. *Memoir Geological Society of India, 6*, 239–260.

Murti, K. S. (1996). Geology, sedimentation and economic mineral potential of the southcentral part of Chhattisgarh Basin. *Memoir Geological Survey of India, 125*, 90–116.

Nagaraja Rao, B. K., Rajurkar, S. T., Ramalingaswamy, G., & Ravindra Babu, B. (1987). Stratigraphy, structure and evolution of the Cuddapah basin. *Memoir Geological Society of India, 6*, 33–86.

Pandalai, H. S., & Chandra, D. (1986). Textural studies on the ores of Amjhore pyrite deposit, Rohtas district, Bihar. *Journal of Geological Society of India, 27*, 527–530.

Pandian, M. S., & Varma, O. P. (2001). Geology and geochemistry of topaz granite and associated wolframite deposit at Degana, Rajasthan. *Journal of Geological Society of India, 57*, 297–307.

Pandit, M. K., Carter, L. M., Ashwal, L. D., Tucker, R. D., Torsvik, T. H., Jamtreit, B., & Bhushan, S. K. (2003). Age, petrogenesis and significance of IGa granitoids and related rocks from the Sendra area, Aravali craton, NW India. *Journal of Asian Earth Sciences, 22*, 363–381.

Pandit, M. K., Shekhawat, L. S., Ferreira, U. P., Sial, A. N., & Bohra, S. K. (1999). Trondhjemite and granodiorite assemblages from west of Barmer: Probable basement for Malani magmatism in western India. *Journal of Geological Society of India, 53*, 89–96.

Pandit, M. K., Sial, A. N., Jamrani, S. S., & Ferreira, V. P. (2001). Carbon isotopic profile across the Bilara Group rocks of Trans-Aravali Marwar Supergroup in western India: Implications for Neoproterozoic-Cambrian transition. *Gondwana Research, 4*, 387–394.

Pareek, H. S. (1983). Stratigraphy of northwestern India and its correlation with that of Indus basin. *Pakistan, Malagasy and South Africa, Geophytology, 13*, 1–21.

Pareek, H. S. (1984). Pre-Quaternary geology and mineral resources of northwestern Rajasthan. *Memoirs-Geological Society of India, 115*, 1–99.

Patranabis-Deb, S., & Chaudhuri, A. K. (2002). Stratigraphic architecture of the Proterozoic succession in the eastern Chhattisgarh Basin, India: tectonic implications. *Sedimentary Geology*, *147*, 105–125.

Patranabis Deb, S., & Chaudhuri, A. K. (2007). A retreating fan-delta system in the Neoproterozoic Chattisgarh rift basin, central India: Major controls in its evolution. *American Association of Petroleum Geologists, 91*, 12–24.

Paul, D. K. (1979). Isotopic composition of strontium in Indian kimberlite. *Geochimica et Cosmochimica Acta, 43*, 389–394.

Paul, D. K. (1991). Indian kimberlites and lamprophyres: Mineralogical and chemical aspects. *Journal of Geological Society of India, 37*, 221–238.

Paul, D. K., Rex, D. C., & Harris, P. G. (1975). Chemical characteristics and K-Ar ages of Indian kimberlites. *Geological Society of America Bulletin, 86*, 364–366.

Poornachanra Rao, G. V. S., Mallikarjuna Rao, J., Chako, S. T., & Subrahmanyam, K. (1997). Palaeomagnetism of Baghain Sandstone formation, Kaimur Group. *Journal of Indian Geophysical Union, 1*, 41–48.

Prasad, B. (1980). A review of the Vindhyan Supergroup in southeastern Rajasthan. *Miscellaneous Publication, Geological Survey of India, 50*, 31–40.

Ramakrishnan, M. (1987). Stratigraphy, sedimentary environment and evolution of the Late Proterozoic Indravati basin, Central India. *Memoir Geological Survey of India, 6*, 139–160.

Ramam, P. K., & Murty, V. N. (1997). *Geology of Andhra Pradesh*. Bangalore: Geological Society of India. 245 p.

Roy, A. B. (2001). Neoproterozoic crustal evolution of northwestern India Shield: Implications on breakup and assembly of supercontinents. *Gondwana Research, 4*, 289–306.

Roy, M. K., Banerjee, R., Agarwal, M., & Maithani, P. B. (2009). Uranium mineralization associated with Mesoproterozoic Semri sediments of Vindhyan Supergroup along Kubari-Semariya-Marwa Fault, Sidhi district, Madhya Pradesh. *Journal of Indian Association Sedimentalogists, 28*, 53–71.

Schnitzer, W. A. (1969). Zur Stratigraphic and Lithologie des nordlichem Chhattisgarh-Beckens (zentral-Indiens) Unter besonderer Beruksichtigung von Algenriff Komplexentz district. *Geology Gesellschaft, 1966*(118), 290–295.

Schnitzer, W. A. (1971). Distribution of stromatolites and stromatolitic reefs in the Precambrian of India. In E. Fugel (Ed.), *Fossil Algae* (pp. 107–112). Heidelberg: Springer.

Sharma, B. K. & Bhola, A. M. (2004). Kink bands in the Chamba region, Himalaya, India. *Journal of Asian Earth Sciences, 25*, 1–16.

Singh, B. N. (2007). Petrology and geochemistry of the Mount Abu granites, SW Rajasthan. *Journal of Geological Society of India, 69*, 247–252.

Singh, B. N., & Joshi, M. (2005). Occurrence of rhyolitic dykes within the Mount Abu batholith, southwestern Rajasthan. *Journal of Geological Society of India, 65*, 309–316.

Somani, R. C. (2006). Evolution of tin-tungsten and copper-bearing hydrothermal solutions associated with Tosham Igneous Complex, Tosham, Bhiwani district, Haryana: A fluid study. *Journal of Geological Society of India, 67*, 379–386.

Srivastava, R. K. (1988). Magmatism in the Aravali Mountain Range and its environs. *Memoir Geological Society of India, 7*, 77–93.

Subba Rao, D. V., Mukherjee, A., Khan, M. W. Y., & Sridhar, D. N. (2006). New occurrence of intrabasinal ignimbrites and welded tuffs from NE part of Neoproterozoic Chhattisgarh Basin, Bastar Craton. *Journal of Geological Society of India, 68*, 589–592.

Torsvik, T. H., Carter, L. M., Ashwal, L. D., Bhushan, S. K., Pandit, M. T., & Jamtveit, B. (2001). Rodinia refined or obscured: Palaeomagnetism of the Malani igneous suite (NW India). *Precambrian Research, 108*, 319–333.

Valdiya, K. S. (1969). Stromatolites of the lesser Himalayan carbonate formations and the Vindhyan. *Journal of Geological Society of India, 10*, 1–25.

Vallinayagam, G., & Kochhar, N. (1998). Geochemical characterization and petrogenesis of A-type granites and associated acid volcanics of Siwana Ring Complex, north Peninsular India. In B. S. Baliwal (Ed.), *The Indian Precambrian* (pp. 460–481). Jodhpur: Scientific Publishers.

Chapter 10
Early Proterozoic in the Himalaya: Rocks, Metamorphism and Igneous Activities

10.1 Tectonic Setting

Within the 2400 km long and 300 to 400 km wide expanse of the Himalaya province, four physiographically distinctive and geologically contrasted subprovinces or terranes are recognizable, particularly between the rivers Ravi and Arun (Fig. 10.1). Each of these four terranes has its own structural layout, near similar stratigraphic pattern over large expanse and almost the same physiography. The middle latitudinal domain, known as the *Lesser Himalaya*, is tectonically separated from southern terrane of the Siwalik by the Main Boundary Thrust and northern subprovince of the *Great Himalaya* or *Himadri* by the Main Central Thrust. It is in the 600- to 2600-m-high Lesser Himalaya subprovince and the lower part of the 3000–8000-m-high Great Himalaya *geographical* terrane that the Early Proterozoic rock formations are developed in full force.

It may be relevant to point to the tomographic imaging carried out in the central sector of the Himalayan arc showing that the thickness of the crust is 60 km in the Lesser Himalaya and 70–80 km in the Great Himalaya and Tethys Himalaya (Huang et al. 2009). From the combination of isotropy and seismic wave spread, it is inferred that possibly eclogite occurs in the lowermost crust and uppermost mantle beneath the Great Himalaya and Tethys Himalaya (Huang et al. 2009).

The Lesser Himalayan terrane comprises autochthonous to parautochthonous sedimentary succession thrust over by sheets or nappes of metamorphic rocks associated with granitic rocks occurring as prominent components all through the length and breadth of thrust sheets (Fig. 10.1). As the allochthonous sheets comprise rocks that have travelled far from their roots and were involved in later folding with underlying autochthonous sedimentary pile, it is difficult to reconstruct a commonly acceptable stratigraphic model of their evolution.

Barren of fossils, affected by metamorphic transformation to various degrees, and structurally lying in a tangled confusion, the Lesser Himalayan sedimentary

K.S. Valdiya, *The Making of India*, Society of Earth Scientists Series,
DOI 10.1007/978-3-319-25029-8_10

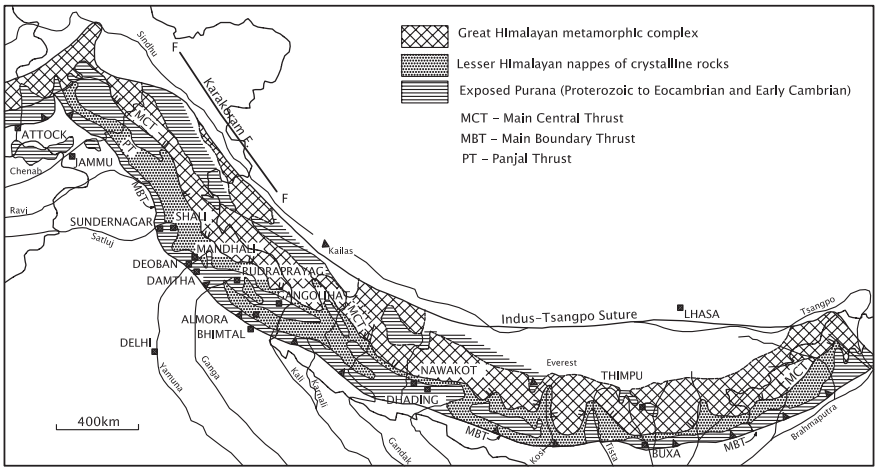

Fig. 10.1 Sketch map of the Himalaya province showing the Early Proterozoic rock formations occurring in the autochthonous zone and as thrust sheets, one overlapping another. Only some parts of the Lesser Himalayan sedimentary zone and the basal part of the Great Himalayan metamorphic complex belong to the Early Proterozoic (after Valdiya 1998)

rocks are like an unpaged historic manuscript. Significantly, they are so similar to the corresponding sedimentary–metasedimentary successions of the Proterozoic Peninsular India that T.H. Holland was constrained to regard them as the northern outliers of the Peninsular Puranas, which were continuous and connected before the separation of the Himalaya and the Peninsula. Pascoe (1950) summarized the situation admirably—"much of the Lesser Himalaya would appear to belong stratigraphically to the Peninsula".

10.1.1 Triple Division of Early Proterozoic Succession

Thrusting on regional scale all through the expanse of the Himalaya from northern Pakistan to eastern Arunachal Pradesh has brought about subdivision of the Lesser Himalayan Early Proterozoic into an autochthonous sedimentary succession at the base and two (locally three) disparate thrust sheets or nappes. The nappes are made up of, respectively, epimetamorphic and mesometamorphic rocks, successively resting on the autochthonous pile and overlapping one another. There are thus three packages or units: (1) flysch and flyschoid assemblages of sedimentary rocks making the lower part of the autochthonous succession, the foundation of which is nowhere seen. This unit has been designated as the *Damtha* in Uttarakhand (Valdiya 1980a, 1988a) where it consists of flysch grading upwards and laterally into flyschoid facies. (2) Low-grade epimetamorphic rocks comprising metaflysch, almost invariably associated with 1900 ± 100 million-year-old

porphyritic granites and quartz porphyries which have overwhelming presence through the length and breadth. The thrust sheet may be described as the *Chail–Ramgarh Nappe*. Within its expanse, this nappe shows pronounced facies variation—from predominant sublitharenite to subgreywacke and shale to quartzarenite interbedded with basic volcanics. In the Uttarakhand–Himachal sector, the unit comprising predominant quartzarenite, with basic volcanics constitute an independent nappe—a separate thrust sheet known as the *Berinag Nappe*—below the larger epimetamorphic Chail–Ramgarh nappe. (3) Medium-grade or mesometamorphic rocks intruded by 500 ± 25 million-year-old granodiorite–granite bodies constituting what may be called the *Jutogh–Almora–Munsiari Nappe*. The mesograde metamorphic rocks include garnetiferous mica schists, micaceous quartzites, carbonaceous/graphitic schists or phyllites, marble and amphibolites. Underneath the Great Himalayan domain in the inner belt, the augen gneisses make the predominant component of this mesometamorphic nappe, split into a multiplicity of imbricating sheets. This tectonized unit may be described as the *Munsiari Formation*.

There are many points of commonality between the Early Proterozoic rocks of Peninsular India and the Lesser Himalaya. In the initial stage of sedimentations, there was deposition of turbiditic flysch in basins formed as a result of continental rifting. This was followed by outpouring contemporaneous with sedimentation of basic lavas and emplacement of tuffs and agglomerates as seen in the Lesser Himalaya, the Aravali, the Bijawar and the Chaibasa domains. In both the provinces, metamorphism has affected the sedimentary successions variably so that different parts of the same lithological unit evince different grade of metamorphism. In the Lesser Himalaya, while the Bhowali Formation of the Berinag sheet in southcentral Kumaun shows prehnite–pumpellyite–metagreywacke facies, the rocks of Chail–Ramgarh sheet were metamorphosed to greenschist facies metamorphism, and the Jutogh–Almora nappe is characterized by epidote–amphibolite facies metamorphism. In the Aravali Mobile Belt, the Aravali domain shows no or mild metamorphism in contrast to the Bhilwara unit characterized by higher grade metamorphism.

Related to this metamorphism is the earliest phase of deformation. This phase of deformation gave rise to ENE–WSW-trending isoclinal folds in the Aravali, Bijawar and Singhbhum mobile belts, as well as in the two thrust sheets of the Lesser Himalaya. The early deformation and attendant metamorphism in many parts of the Peninsular India culminated in the generation and emplacement of granites, exemplified by the nearly 2000-million-year-old Amet Granite, the Darwal Granite in the Aravali Mobile Belt, the Rihand Granite in the Bijawar Basin and the Chakradharpur–Mayurbhanj Granite in the Singhbhum domain. In the Lesser Himalaya terrane, the 1900 ± 100 million-year-old porphyritic granites and quartz porphyries have predominant presence in the two metamorphic thrust sheets, particularly in the Chail–Ramgarh nappe. In some areas, these granites are associated with high-grade metamorphic rocks occupying the cores of early-generation folds of Precambrian antiquity (Chakrabarti 1985, 1996). Early Proterozoic deformation with attendant metamorphism and granite intrusion at

2174 m and 1850 Ma are indicated by U–Pb zircon dating of rocks of north-western Pakistan (DiPietro and Isacsen 2001).

10.2 Autochthonous Zone

10.2.1 Tectonic Configuration

A very large part of the middle latitudinal Lesser Himalayan subprovince comprises thick pile of unmetamorphosed sedimentary succession exposed in tectonic windows cut by rivers in the crystalline thrust sheets. Thrown into asymmetric folding, the basal part of this pile is made up of Early Proterozoic rocks, the foundation of which is seen nowhere (Figs. 10.2 and 10.3). In rare cases, concordant bodies of porphyritic granite are seen. As of now, there is no reliable information available to date, the beginning of the Proterozoic cycle of sedimentation.

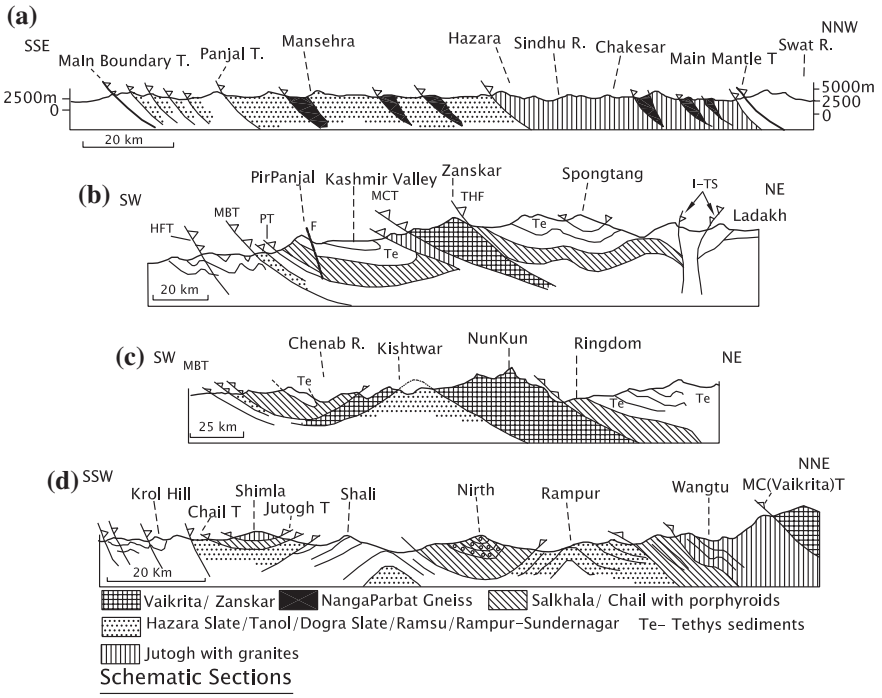

Fig. 10.2 Cross sections across the Himalaya province illustrate triple to quadruple subdivision of the Early Proterozoic rock formations in the western part of the Lesser Himalayan terrane. **a** Pakistan (after Tahirkheli 1982). **b** Kashmir (after Thakur 1987). **c** Western Himachal (after Thakur et al. 1990). **d** Eastern Himachal (after Auden 1934; Berthelsen 1951)

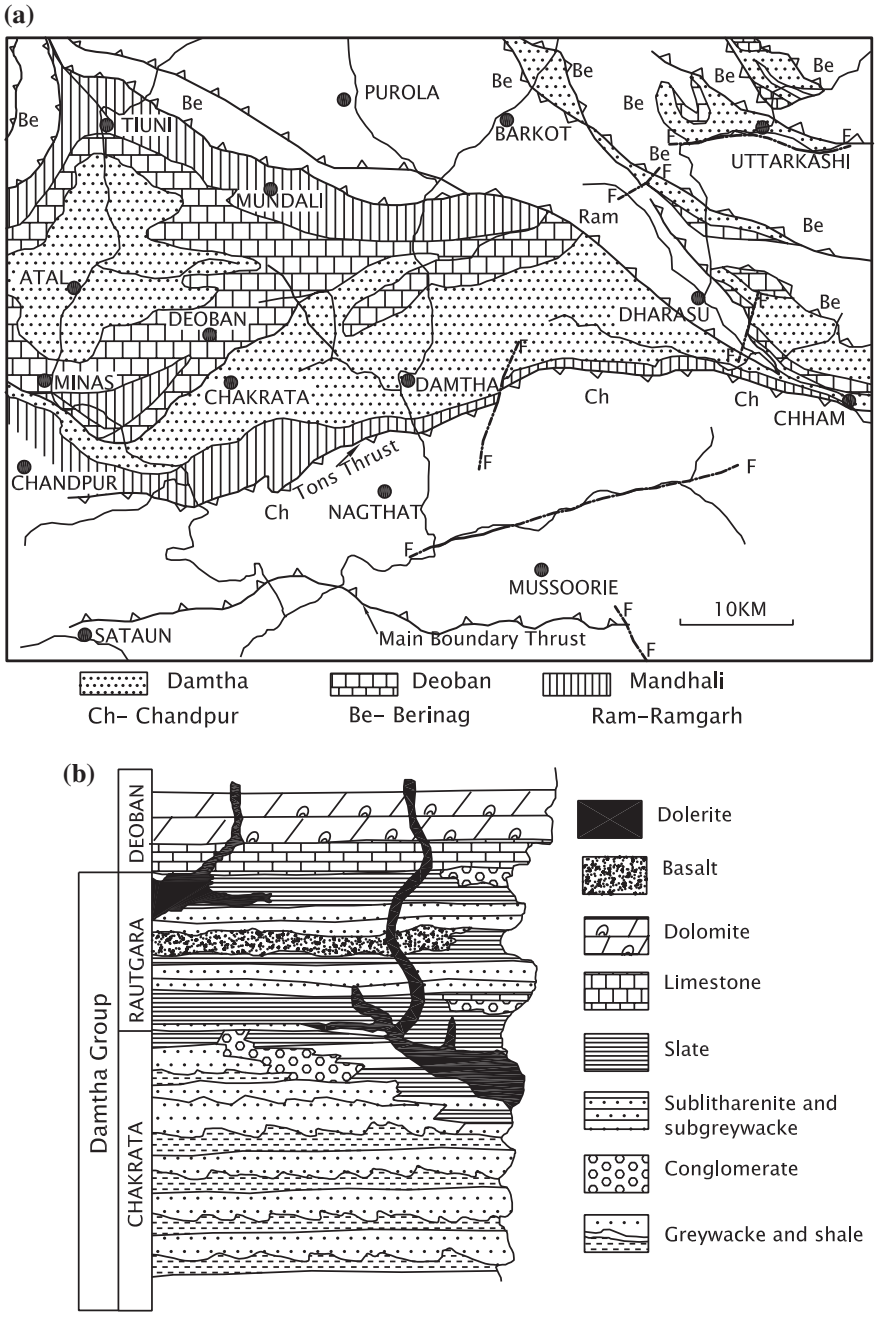

Fig. 10.3 **a** Proterozoic sedimentary succession seen in the window cut by the Yamuna and Tons rivers in western Uttarakhand. **b** The Damtha Group, comprising the Chakrata and Rautgara formations, make up the Early Proterozoic. Note the occurrence of dolerite sills and dykes (after Valdiya 1980b)

10.2.2 Lithology and Depositional Environment

The lowermost part of the autochthonous sedimentary succession in western Uttarakhand (Table 10.1), described as the *Damtha* (Rupke 1974; Valdiya 1980b), comprises turbiditic flysch (*Chakrata Formation*), grading upwards and laterally into a flyschoid assemblage (*Rautgara Formation*) (Valdiya 1980b). The Chakrata consists of maroon, purple and pink shales and greywackes and related turbidites with or without diamictites such as discernible north of Chakrata in Uttarakhand (Fig. 10.3) and in the Tanakki area in northern Pakistan. The greywackes show small-scale cross-bedding and ripple marks, graded bedding, flute casts and spectacular convolution of lamination in the middle level of individual beds. Subordinate pebbly conglomerate at the base grade upwards into dark grey-green greywackes is characterized by graded bedding, ball-and-pillow structures, load casts, flute casts and related tool marks and ending at the top with impersistent beds of boulder conglomerate. The flysch was laid down on the continental slope by presumably turbidity currents flowing N, NNE, NE and ENE (Valdiya 1970). The deposition took place rapidly under rather unstable tectonic conditions. Discernible over long distance of 100 km, such features as dropstones, pseudonodules, ball-and-pillow structure and cusps described earlier as synsedimentary deformation structures formed by turbidity currents (Valdiya 1970, 1980b) have been identified as palaeoseismites. The seismicity is attributed to rifting of the basin (Ghosh et al. 2011, 2012).

The rhythmic alternation of sublitharenite–subgreywacke with shale/slate and very minor stromatolitic limestone and basic sills and dykes, and lentiform horizons of diamictite make up the Rautgara Formation. The pelites of the Rautgara in the Garhwal sector show enrichment in LREE, depletion in HREE and a large Eu anomaly (Rashid 2005). This horizon occurs over vast region from one end of the Himalaya to another. The fawn, pink and purple quartzarenites and granular quartzite in southern Kumaun are interbedded with amygdaloidal vesicular basaltic lavas and tuffs and locally agglomerate (Shah and Merh 1976, 1978; Valdiya 1980b, 1988b). The basic volcanics of the Bhimtal–Bhowali area, the *Bhimtal Volcanics*, show prehnite–pumpellyite–metagreywacke facies metamorphism (Varadarajan 1974).

The eastern extension of the *Damtha* in Nepal is represented by the *Kuncha* (Bordet et al. 1971). It succeeded by quartzites (Fagfog), phyllites (Dandagaon) and limestones (Nourpul) (Stocklin 1980; Jaisi et al. 2008). Its extension in Bhutan has been described as the *Phuentsholing* (Nautiyal et al. 1964; Jangpangi 1974) and in western Arunachal Pradesh as the *Bichom* (Das et al. 1976; Bhushan et al. 1991). In southcentral Himachal, the *Sundernagar Formation* (Fig. 10.4a) of the Mandi Hills (Srikantia and Sharma 1971; Srikantia 1977) represents the north-westerly extension of the Rautgara. Across the Sindhu River in Pakistan (Figs. 10.2a and 10.5), the *Hazara Slate*, also described as *Attock Slate* (Calkins et al. 1975; Latif 1970), bears striking lithological resemblance with the Chakrata Formation (Lower Damtha). The Hazara consists of green-grey to black slates, sillstones, and subgreywackes occurring in cyclic units and showing various

Table 10.1 Correlation of the Early Proterozoic lithotectonic units of the Lesser Himalayan subprovince (Valdiya 1998)

Period	Northern Pakistan	Jammu and Kashmir	Himachal Pradesh	Kumaun	Nepal	Sikkim and Bhutan	Arunachal Pradesh
Mesoproterozoic	Sirban Ls. Abbottabad Fm.	Jammu Ls. (O)	Shali Fm. (I)	Deoban Fm. (I) Blaini Fm. (O)	Dhading Fm.	Buxa Fm. (O)	Dedza Fm.
Palaeoproterozoic	Hazara Slate/ Attock Slate	Ramban Fm. (O) Dogra Slate (I) With Sauni Volcanics	Sundernagar Fm. (O) with Mandi Volcanics	Damtha Fm. (I) Jaunsar Fm. (O) with Bhimtal Volcanics (O)	Kuncha Fm. (I)	Jainti/Phuentsholing Fm. (O)	Bichom/ Tenga Fm.
Base not seen anywhere							

I Inner (Northern) belt, *O* Outer (Southern) belt, *Fm*. Formation, *Ls*. Limestone

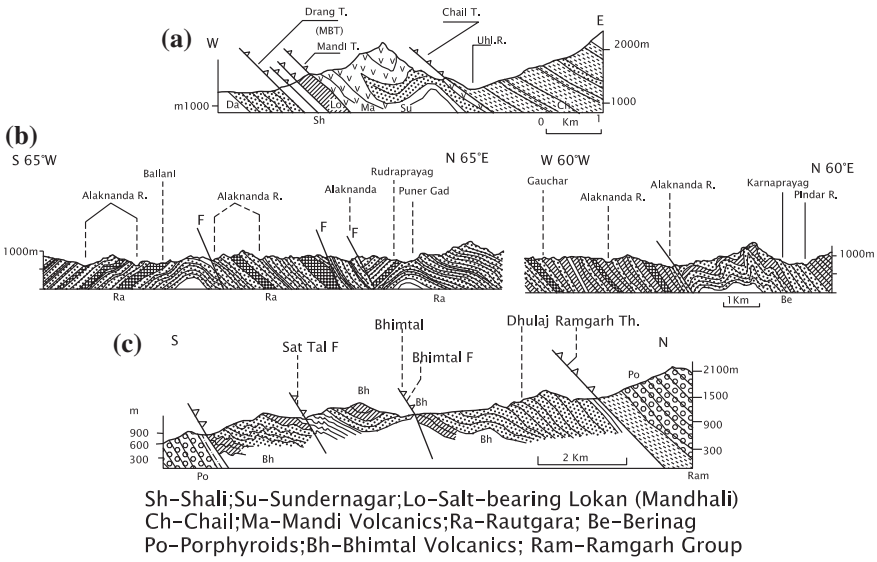

Fig. 10.4 Cross sections show the occurrence of basic lavas and volcaniclastics in the Proterozoic succession. **a** Sundernagar Formation in southcentral Himachal (after Srikantia 1977). **b** Rautgara Formation in the Rudraprayag area in the Alaknanda Valley (after Valdiya 1980b). **c** Bhowali–Bhimtal area in southcentral Kumaun (after Valdiya 1980b)

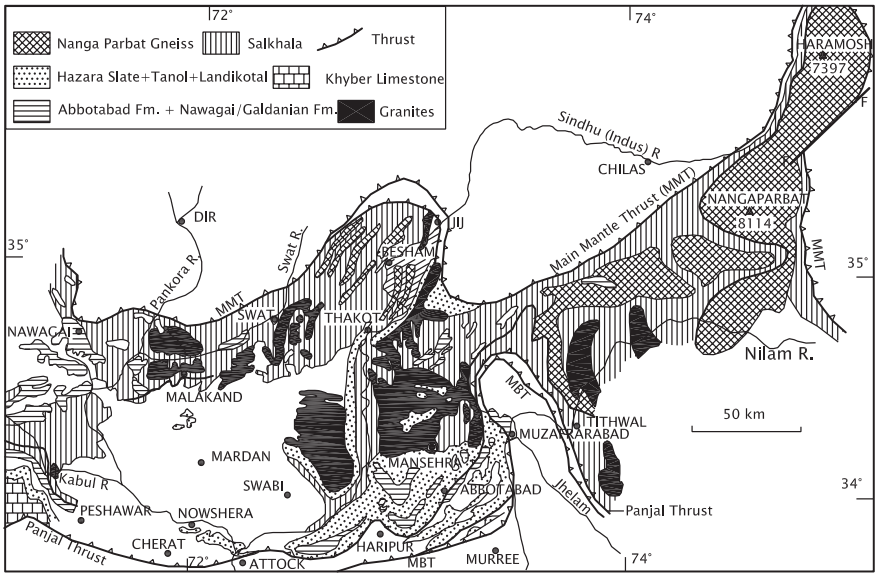

Fig. 10.5 Geological sketch map of northern Pakistan showing distribution of the Proterozoic and Lower Cambrian rocks (based on Tahirkheli 1996)

turbidite features such as flute casts, graded bedding, tool marks, convolute bedding, ball-and-pillow structures, cross-bedding and ripple marks. The overlying *Kakul* Formation, comparable with the Rautgara, begins with a horizon of boulder conglomerate and consists of red shale, cross-bedded, ripple-marked quartzites and muddy sandstone with basic sills and dykes and intercalations of conglomerates.

10.2.3 Volcanic Activities

In the Ladhiya Valley–Bhimtal Belt in southern Kumaun, the Alaknanda Valley in Garhwal and the Mandi–Darla Belt in southcentral Himachal, the Rautgara succession includes sizeable volumes of penecontemporaneous volcanics—amygdaloidal and vesicular basalts, tuffs and sparse agglomerates (Fig. 10.4). The *Darla Volcanics* are aphyric, representing an evolved quartz-tholeiite characterized by SiO_2 abundances, and enrichment in FeO, TiO_2, incompatible trace and rare elements (Bhat 1987; Ahmad and Bhat 1987). The Darla volcanism is related to rifting of the sialic crust in the Lesser Himalayan subprovince. The area of volcanic activities lies in the line of the Aravali Mobile Belt which was also affected by volcanism in the initial stage of its evolution. The Rb–Sr whole-rock isochron age of the Darla lavas is 1487 ± 45 Ma (Kakar 1986). Intriguingly, the Sm–Nd whole-rock isochron age of the equivalents of the Darla Volcanics in the Rampur window is 2510 ± 90 (Bhat and Le Fort 1992). The volcanics of the Rudraprayag–Karnaprayag area in the Alaknanda Valley and the Bhowali–Bhimtal area in southcentral Kumaun have also yielded Sm–Nd age of 2510 ± 80 Ma (Bhat et al. 1998). However, the zircon crystals in the Rampur Volcanics near Jakhri in the Satluj Valley give the zircon age of 1800 ± 13 Ma, and there is a good correlation between 1/Nd and $^{143}Nd/^{144}Nd$ ratio in the metabasalts (Miller et al. 2000). According to Miller and others, it seems that 2510 ± 90 Ma Sm–Nd array determined by Bhat and Lefort "is an errochron and an artefact of mixing between depleted mantle-melts generated at 1.8 Ga and an older enriched lithospheric component". Moreover, the 1840-million-year-old Bandal Granite in the Satluj Valley is intruded by mafic rocks that yield single zircon $^{207}Pb/^{206}Pb$ age of 1800 Ma (Miller et al. 2000). Significantly, the gabbroic body within the Chail Nappe is dated 1907 ± 91 Ma, and it is one among the many amphibolite bodies that show low-Ti tholeiitic characters, enrichment in LREE and LILE and distinct negative Nb, Sr, P and Ti anomalies (Ahmad et al. 1999). Representing metamorphosed lavas and hypabyssals, the amphibolites belong to the suite of the 1800-million-year-old mafic intrusives and volcanics that were emplaced in the aftermath of large-scale regional invasion of porphyritic granite in the period 1900 ± 100 Ma—marking a major event of lithospheric evolution. It seems that the 2500 Ma date of the Rampur and Rudraprayag and Bhimtal Volcanics interbedded with Berinag quartzites (Bhat and Le Fort 1992; Bhat et al. 1998) is **not** the age of the volcanic assemblage in eastern Himachal and in Uttarakhand.

10.2.4 Occurrence of Porphyritic Granite

One of the most striking and stratigraphically a critical feature of the autochthonous zone is the occurrence of remarkably fresh, pink porphyritic 1900 ± 100 million-year-old granite in the Rautgara succession near Jauljibi in the Gori Valley, north-eastern Kumaun (Trivedi et al. 1984). There is no suggestion of intrusive contact and no indication of its tectonic implantation. In far eastern Nepal, the Taplejung window reveals a succession of the Kuncha embodying lenticular granite of per-aluminous composition (Fig. 10.6). A granite body 6–7 km in length and 2 km in width is undeformed in its core and slightly sheared and mylonitized along the periphery (Upreti 1999; Upreti et al. 2003) There is a postulation of tectonic implantation or tectonization of the contact of the two disparate bodies. This granite body is characterized by xenoliths of metasedimentary rocks and has caused

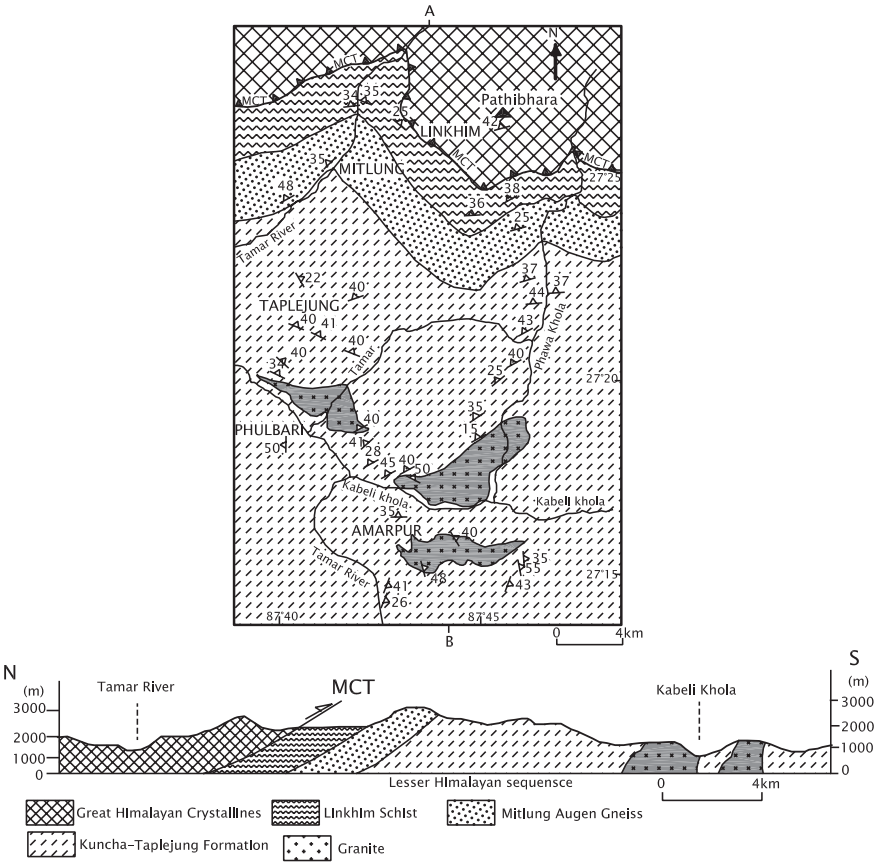

Fig. 10.6 Taplejung window in eastern Nepal reveals Early Proterozoic part of the Kuncha Group, characterized by lensoid bodies of porphyritic granite (after Upreti 1999)

baking of the country rocks in the Kabeli Khola. There are a number of such bodies concordant with the Kuncha rocks, showing no significant contact metamorphism, except 1–2-m-thick hornfels in some places.

10.3 Nappe of Epimetamorphic Rocks

10.3.1 Lithology

Low-grade metamorphic rocks comprising phyllites/shales, sericite–quartzite, sericite–quartz schists with marble and talcose phyllite were identified in the Shimla region (Fig. 10.2c) as the *Chail* by G.E. Pilgrim and W.D. West in 1928 and described as *Ramgarh* in southern Kumaun (Fig. 10.7a) by A. Heim and A. Gansser in 1939. The Chail–Ramgarh succession represents a metamorphosed flyschoid assemblage—a deposit of deeper water continental slope. It seems that

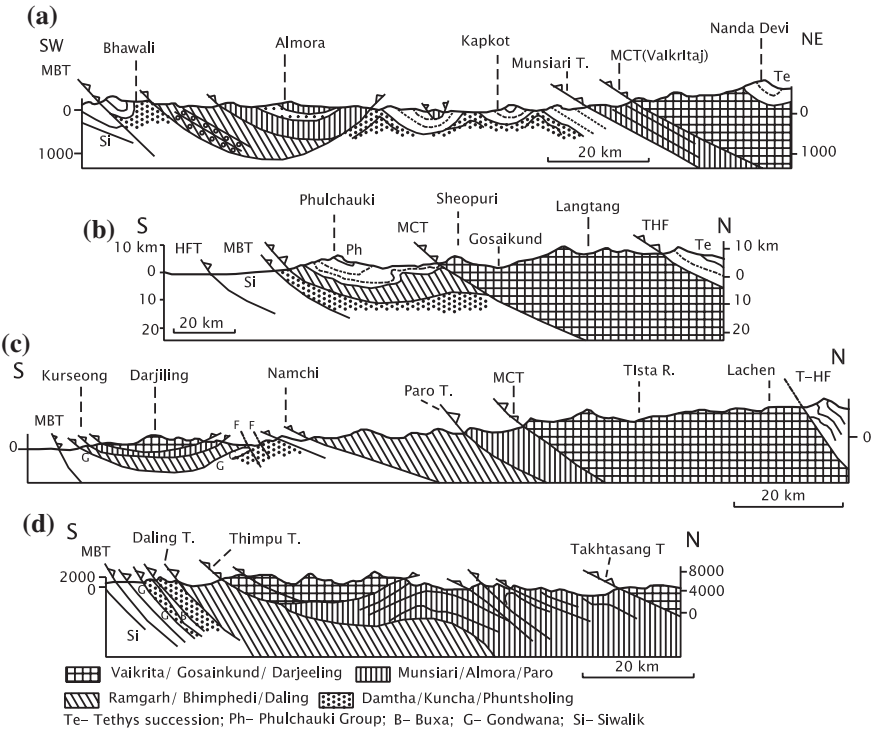

Fig. 10.7 The autochthonous and two allochthonous thrust sheets comprising Early Proterozoic rock formations in the eastern part of the Himalaya province, Kumaun (after Gansser 1964; Valdiya 1981), central Nepal (after Upreti and Le Fort 1999; Rai 2001), Darjeeling Hills (after Acharyya 1971) and Bhutan (after Gansser 1964)

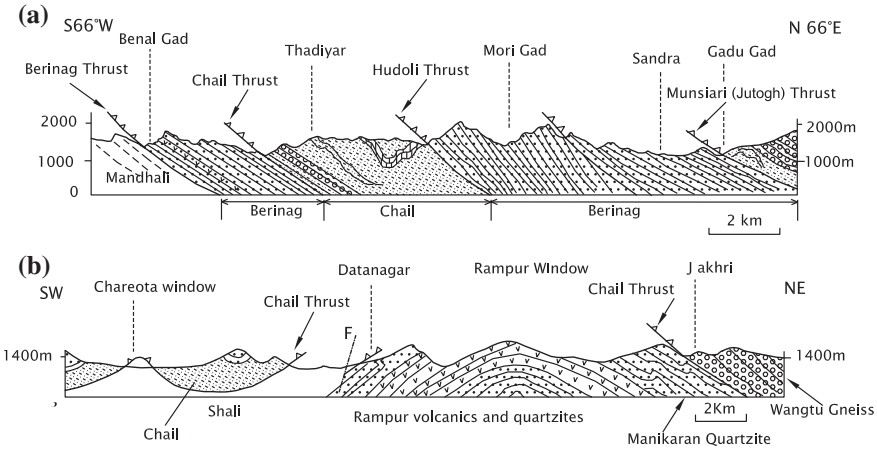

Fig. 10.8 Cross sections show the lithological sequences of the epimetamorphic nappes with special reference to the position of the Berinag facies and nappe and the occurrence of mylonitized porphyritic granites and quartz porphyries, 1900 ± 100 million years in age. **a** Uttarakhand Himalaya (after Valdiya 1980b). **b** Eastern Himachal (after Pandey et al. 2003)

the Chail–Ramgarh assemblage represents the metamorphosed uprooted and overthrust part of the Damtha–Kuncha succession (Valdiya 1978, 1988a). This sheet covers vast areas in Himachal including the Shimla Hills, the Dhauladhar Range and the Kullu region in the Beas Valley (Das and Srikantia 1972; Sharma 1976; Frank et al. 1973; Bhargava 2000). In Kumaun, the Ramgarh is a thick sheet below the Almora Nappe and its klippen (Fig. 10.8a) and in the root zone beneath the Great Himalaya. The root zone is split into a multiplicity of imbricating sheets forming a duplex of sorts. In Nepal (Fig. 10.7), the extension of the Ramgarh has been described as the Chail (Fuchs 1967, 1975; Fuchs and Frank 1970; Arita et al., 1984). In southcentral Nepal, the Ramgarh has been recognized as a distinct unit (DeCelles et al. 2001; Gehrel et al. 2006); in western Nepal, it is variously described as Ranimatta (Sharma 1980, 1990), Birethanti, etc. In the Darjeeling Hills and Sikkim the *Daling* (Auden 1935) and in Bhutan the *Samchi* (or Shumar) (Nautiyal et al. 1964; Jangpanji 1974) represent the Chail–Ramgarh sheet. The *Tenga* in western Arunachal Pradesh (Das et al. 1976) and the *Siang* in eastern Arunachal (Jain et al. 1974; Kumar and Singh 1980) are the homotaxials of the Chail–Ramgarh unit.

The Daling of the Darjeeling–Sikkim sector records pumpellyite–prehnite–metagreywacke facies of metamorphism at temperature 300–400 °C and pressure 5–7.5 kbar (Sinha-Roy 1976). In Kumaun, the Bhimtal Volcanics within the Berinag sheet of the Ramgarh Nappe, at Bhowali, show the same metamorphic grade (Varadarajan 1974).

Bands of sericite schist occur almost invariably at the base of all Lesser Himalayan thrust sheets or nappes. These are commonly believed to be the product

of retrograde metamorphism and are intimately associated with mylonitized granites. On the basis of geochemical composition, the 2–3-m-thick sericite schist seen overlying the 1866 ± 100 Million year old Wangtu Gneiss at Karcham in the Satluj Valley has been reinterpreted as a metamorphosed palaeosol (Bhargava et al. 2011). This postulation is not sustainable by facts observed elsewhere in the whole of Lesser Himalaya.

10.3.2 Berinag Unit: Facies, Nappe and Volcanism

In the central sector of the Lesser Himalaya province embracing Uttarakhand and Himachal Pradesh, a thick succession of white, fawn, pink and purple quartzarenite with very subordinate shale and prominent basaltic lavas and related volcaniclastics represent a special facies of the Chail–Ramgarh nappe. Named the *Berinag* in Kumaun (Valdiya 1962, Valdiya 1980b), the orthoquartzite assemblage constitutes a disparate sheet underneath the Chail–Ramgarh Nappe. The quartzites also occur as large and small lenses within the Chial–Ramgarh epimetamorphic rock succession. The Berinag sheet extends into Himachal and is described as the *Rampur Quartzite* in the Satluj Valley, the *Manikaran Quartzite* in the Beas Valley and the *Shalimar Quartzite* in the Chenab Valley in Kishtwar area (Das and Srikantia 1972; Thakur 1980; Bhargava 2000). Further north-west in the Jammu Himalaya, it is known as the *Sauni Formation*. The quartzarenites represent the sands deposited in shallow water intertidal to supratidal environment of the platform swept by waves and currents. Tidal channels laid down shoestring-shaped oligomictic conglomerate in some places within the succession of clean sands. The bulk geochemistry of the pelites shows depletion in Sr and Ba, the $(La/Yb)_N$ ratio ranging from 8.8 to 18.6, highly fractionated REE pattern, slightly fractionated HREE and large negative Eu anomaly, implying derivation of detritus from felsic sources (Bhat and Ghosh 2001).

As already stated, the Berinag quartzites are intimately associated with basaltic lavas (amygdaloidal, vesicular and compact) and tuffs (Valdiya 1980a, b). The volcanism was penecontemporaneous with sedimentation in shallow-shelf platform (Fig. 10.9). The chemistry and mineralogy of the Rampur Volcanics in the Satluj Valley and the Berinag Volcanics in the Alaknanda Valley are not much different from those of the Darla Volcanics in the Mandi Belt. The volcanics are characterized by low Nb, P, Ti, Nb/La, Ti/Y, Ti/Zr and Sm/Nd and high SiO_2 and Fe_2O_3 values (Ahmad and Bhat 1987; Bhat and Le Fort 1992). The volcanics of the Karnaprayag and Rampur areas have composition consistent with tholeiitic basalts subjected to both crystallization and crustal contamination of the magma derived from variably enriched mantle source, as evident from uniformly high $\in$Nd value and depletion of LREE. The lava eruption is related to rifting of the sialic crust (Fig. 10.9).

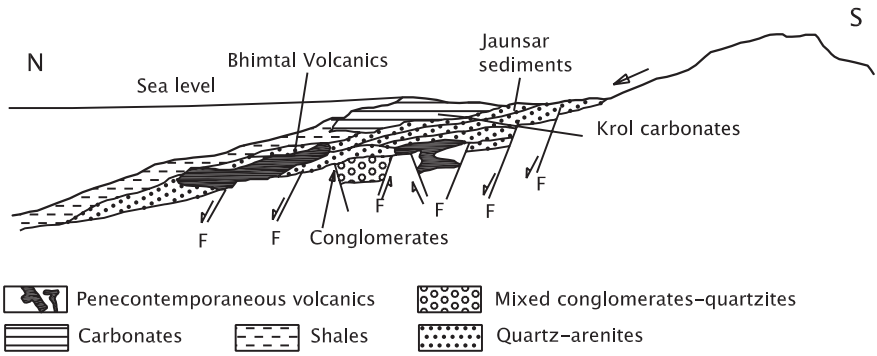

Fig. 10.9 Basaltic volcanics of the Berinag–Bhowali domain were poured out through faults and fissures related to continental rifting (after Valdiya 1998)

10.3.3 Emplacement of Porphyritic Granites

The most striking feature of the Chail–Rampur Nappe and its klippen is the predominant occurrence of porphyritic granites and quartz porphyries within the epimetamorphic succession. Commonly, the granitic rocks are intensely mylonitized and sheared, leading to formation of streaky gneiss, particularly in the proximity of boundary thrusts, such as the Ramgarh thrust in Kumaun (Pande 1950; Merh et al. 1971) and its extension in western Nepal (Arita 1983; Upreti 1990).

Involved in the strong tectonic movements of the duplex of imbricating thrust sheets underneath the Main Central Thrust in the inner zone in Garhwal, the porphyritic granites and porphyries have undergone wholesale mylonitization, and with phyllonites make overwhelming presence, as seen in the Bhatwari area between the Bhagirathi and Alaknanda rivers (Bahuguna and Saklani 1988; Bist and Sinha 1980, 1990; Saklani et al. 1991; Valdiya 1978, 1980b, 1981; Saklani 1972a, b, 1993), in the Ulleri area and Ramechhap–Okhaldhunga Belt (Arita 1983; Arita and Sharma 1992; Upreti et al. 2003) in central Nepal and in the Tamar region in eastern Nepal (Maruo and Kizaki 1983; Schelling and Arita 1992). The *Ulleri Gneiss* in northcentral Nepal, shown imperceptibly grading into the low-grade metamorphic rocks, is believed to have resulted from strong deformation and attendant metamorphism of felsic magmatic and volcaniclastic rocks at temperature 300–350 °C (Pecher and Le Fort 1977; Lefort and Rai 1999).

The detrital zircon age of the porphyritic granite–augen gneiss within the Ramgarh nappe in the Kusma, Ranimatta and Ulleri areas in Nepal is dated, respectively, 1866 Ma, 1943 Ma and 1831 ± 17 Ma (DeCelles et al. 2001). The sheared *Lingtse Gneiss* occurs in the basal part of the Daling in the Darjeeling Hills, thrown into tightly appressed and locally rootless flexural slip folds (Sinha-Roy 1976, 1980). The Lingtse Gneiss is a tabular body of peraluminous granite characterized by variable isotopic composition (due to presumably different tectonothermal events) and showing fractionated REE pattern and an age that varies from

Rb–Sr age of 1678 ± 44 Ma and Pb–Pb age 1792 ± 45 Ma (Paul et al. 1996) to 2034 ± 21 Ma (Bhanot et al. 1977, 1980; Pandey et al. 1980; Raju et al. 1982; Singh et al. 1986). The Ramgarh porphyroids in Kumaun, likewise, have variable isotopic composition, and a 10-point whole-rock isochron yielded a date of 1875 ± 90 Ma (Trivedi et al. 1984). In the Bhatwari–Naitwar Belt below the Main Central Thrust in north-western Garhwal, the mylonitized porphyritic granite is 1900 ± 100 million years old (Singh et al. 1986). The *Wangtu Gneiss* in the Satluj Valley is dated by Rb–Sr method at 2025 ± 86 Ma (Bhanot et al. 1980; Kwatra et al. 1986). However, SHRIMP U–Pb zircon ages of mylonitized porphyritic granites in the Satluj Valley indicate that the Wangtu Granite contains elements (zircon cores) as old as 3000 Ma, which were reworked in the period 2100–1800 Ma when there was extensive ensialic rifting and emplacement of anorogenic granites (Singh et al. 2007). The *Bandal Gneiss* in the Beas Valley is dated 1904 ± 70 million years old (Frank et al. 1977). The Wangtu–Bandal is a peraluminous granite formed from water-deficient melt at pressures 3–4 kbar (Sharma and Rashid 2001). The granite is characterized by enrichment in LREE, moderate depletion of HREE, pronounced negative Eu anomaly, negative Ba, Nb, Sr, P and Ti anomalies, and relatively high level of Rb, Th and U (Islam et al. 2003). Across the Sindhu River, the gneisses of *Besham* in northern Pakistan have been dated 1920 ± 24 Ma by Ar–Ar method, while the Pb–Pb isotopic ratios suggest that the Pb–Zn mineral deposit was formed 2120–2200 million years ago and the reequilibrium having occurred at 1950 Ma (Shah et al. 1997). U–Pb zircon isotopic ages of metamorphic rock in north-western Pakistan indicate two cycles of deformation, intrusion and regional metamorphism—one at 2174 Ma manifested in the granulite facies rocks of the Nanga Parbat and the other at 1850 Ma associated with low-grade metamorphism and widespread intrusion (DiPietro and Isachsen 2001). It is quite obvious that the porphyritic granites were emplaced around 1900 ± 100 Ma.

10.3.4 Origin of the Ramgarh Nappe

There are remarkably strong lithological similarities of the Ramgarh–Chail unit (and its analogues) with the Early Proterozoic sedimentary succession described as the Rautgara (of the Damtha Group) in Uttarakhand, the Sundernagar in Himachal, the Kuncha in Nepal and the Phuentsholing in Bhutan. The flyschoid sedimentary pile beneath the Main Central Thrust is tightly folded and repeatedly split along their axial planes, giving rise to a schuppen zone with duplex structure. Involved in the imbricate pile of tectonic slabs, the porphyritic granites are strongly tectonized and considerably altered. In other words, the 1900 ± 100 million-year-old mylonitized porphyroids represent slabs and sheets of granite implanted in the imbricated pile of Early Proterozoic flyschoid sediments. The parts that were uprooted and travelled far south gave rise to the nappes and klippen of the epimetamorphic rocks with mylonitized granites such as the Chail, the Ramgarh, the Bhimphedi and the Daling (Valdiya 1978, 1988a).

10.3.5 Mineralization

Uranium mineralization is manifested in uraninite filling veins in joints and fractures and occurring as disseminations in the Berinag quartzites that are intimately associated with basic volcanics (amphibolites and chlorite schists). This is seen in the Chhinjra–Manikaran–Kasha Belt in Himachal Pradesh (Narayandas et al. 1979; Kaul et al. 1991), particularly in areas characterized by shear zones along branching thrusts as seen in the Munish–Kaladi area in the Shimla district (Yadav 1995) and in the Loharkhet area immediately beneath the Main Central Thrust in Kumaun (Nanda et al. 1995). In the Loharkhet area, the uraninite occurs **also** around quartz grains and in intergranular space, implying epigenetic concentration along weak zones. The carbonaceous phyllites associated with carbonates in a Bhatwari triangle bear uranium minerals in sheared rocks, comprising quartz–talc–chlorite–sericite assemblage in the Tungi–Pokhri Belt (Negi 1967).

The stratiform *galena* deposit with *pyrite* and *pyrrhotite* occurs over 1275-m tract in the Daling succession of phyllites, metagreywackes, carbonaceous phyllite and subordinate basic volcanics (Mukherjee and Dhruba Rao 1974).

10.4 Nappe of Mesometamorphic Rocks

10.4.1 Lithology

The medium-grade metamorphic rocks comprising garnetiferous sericite–biotite schists interbedded with garnet–mica–quartzite, carbonaceous/graphitic schist, marble and amphibolite in the Shimla Hills (Fig. 10.2c) are known as the *Jutogh* (Pilgrim and West 1928; Berthelsen 1951; Srikantia and Bhargava 1984; Bhargava 2000; Bhargava and Bassi 1994). The Jutogh extends south-westward into Uttarakhand (Fig. 10.7a) where it has been described as the *Almora* (Heim and Gansser 1939) in the outer zone and as the *Munsiari* (Valdiya 1980b) in the inner zone below the Main Central Thrust. In Kumaun, the Nd values in the Lesser Himalayan Munsiari rocks are of −23 to 28, nearly the same as in the metasedimentary lithologies from the inner Lesser Himalayan belt. This fact indicates that the two assemblages of sediments were partially homogenized at about the same time (Ahmad et al. 2000). It is inferred that the sediments that now form the Munsiari, Ramgarh and related overthrust successions in the inner belt of the Lesser Himalaya were deposited between 2300 and 1800 Ma (Parrish and Hodges 1996). In the Chaur Massif in Himachal and in the Dudhatoli–Ranikhet–Champawat Range in Uttarakhand, the mesometamorphic succession is intruded by 500 ± 25 million-year-old granitic batholiths of trondhjemitic suite. The bulk of its klippen and the root (the Munsiari) is made up of preponderant augen gneisses of the Palaeoproterozoic age. In far-western Nepal, the Jutogh–Almora Nappe has been recognized in the Dadeldhura Range (Upreti 1996; DeCelles et al. 2001), in western Nepal is described as Lower Crystalline Nappe (Fuchs 1967, 1975; Frank and Fuchs 1970), in central Nepal as Upper Midland Formation (Hashimoto et al. 1973; Arita 1983) or the *Kathmandu* (*Bhimphedi*) (Gehrel et al. 2006), in eastern

Nepal as *Arun Gneiss* (Jaros and Kalvoda 1978), in Sikkim–Bhutan (Fig. 10.7c, d) as the *Paro* (Nautiyal et al. 1964; Jangpangi 1974), and in western Arunachal as the *Dirrang* in the Bomdila district (Das et al. 1976; Verma and Tandon 1976; Bhushan et al. 1991). Across the Brahmaputra river, the NW–SE-trending Mishmi Hills are made up of metamorphic rocks and gneisses comparable with the Jutogh in Himachal Pradesh (V.C. Thakur, 2007, personal communication).

In the north-west Himalaya, the mesometamorphic succession (Figs. 10.1 and 10.10) is known as the *Salkhala* (Wadia 1928, 1934; Ibrahim Shah 1977; Bhargava 2000). In some areas, the grade of metamorphism is locally elevated to kyanite–sillimanite grade as seen in the proximity of the Piparan Granite in the Kishtwar region (Srivastava 1982). Across the Sindhu River (Fig. 10.5), mica schist and graphitic schist with quartzite and amphibolite (*Kaghan*) lie below the Great Himalayan of the Sharda Group (Chaudhry and Ghazanfar 1987; Greco et al. 1989; Chaudhry et al. 1974). Still further west, the *Besham* succession of quartzofelspathic gneisses and schists (Butt 1983) with metamorphosed basic sills and pillow lava of komatiitic affinity (Baig and Snee 1991) represents the Salkhala. West of Dargai, the schists with interbeds of subordinate calcareous and carbonaceous arenite are characterized by negative Eu values, high ∈REE and LREE/HREE ratio, and a mineralogy of sediments deposited on a passive

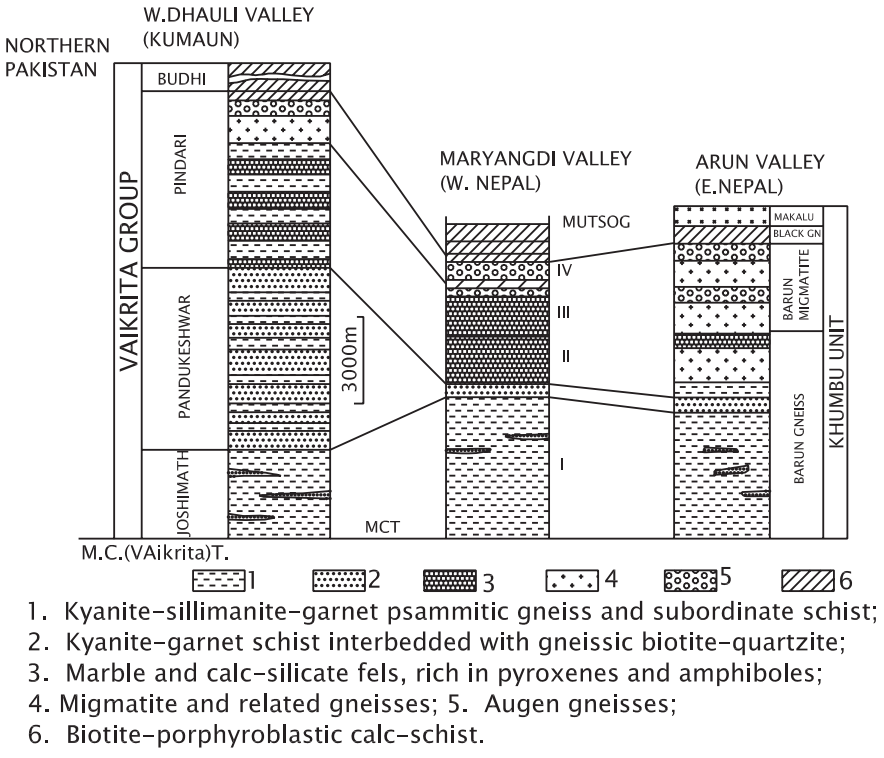

Fig. 10.10 Statigraphic columns illustrating the lithologies of the Vaikrita and its homotaxials in three sectors of the central Himadri terrane (based on Valdiya and Goel 1983; Bordet et al. 1971)

continental margin (Ahmed 1990). In the Hazara region (Fig. 10.5), the Salkhala is discernible around the apex of the syntaxis and it thins out to a few hundred metres at Balakot from 1800 to 3000 m thicker slab. The Salkhala occupies both sides of the Sindhu Valley from Tarbela to Kandhar (Calkins et al. 1975).

10.4.2 Structural Characteristics

The Jutogh of the type area was subjected to three phases of deformation (Pande and Virdi 1970; Naha and Ray 1971; Kumar 1977). The earliest isoclinal recumbent to reclined folds generated by southward transportation was coaxially refolded and flattened due to overthrusting. This development gave rise to upright open to tight folds that are overturned northwards. They were subsequently overprinted by N/NNW–S/SSE-trending conjugate and chevron folds due to compression that also gave rise to axial culminations and depressions.

Similar is the structural situation in the synclinal Almora Nappe and its klippen in Kumaun (Valdiya 1963; Merh and Vashi 1965; Gairola 1967; Misra and Sharma 1967; Powar 1970; Sharma 1971; Merh et al. 1971; Merh 1977; Gairola and Joshi 1980) where the isoclinal recumbent to reclined NNE/NE–SSW/SW-oriented earlier folds are superimposed with NW/WNW–SE/ESE-trending open asymmetric to slightly overturned second generation folds. The second-generation folds are regarded as shortening structures (Schwan 1980). In the basal part in the proximity of the delimiting thrust, porphyritic granites are converted into augen gneiss, bearing strong impress of mylonitization. Within the nappe, the granitic bodies have gneissic or foliated margin in contrast to undeformed core. In the root zone (the Musiari), there is strong deformation of practically the whole mass.

In Nepal, the pronounced NNE–SSW-oriented mineral lineation was attributed to Precambrian deformation (Hashimoto et al. 1973). The Early Proterozoic metamorphic rocks in Himachal Pradesh and the Darjeeling Hills are folded along NNE–SSW-trending axes and characterized by pronounced mineral lineation parallel to this fold axis of the first phase of deformation which occurred in the Precambrian time (Chakrabarti 1985, 1993). The cores of these first-generation anticlines are occupied by high-grade metamorphics, migmatites and granites, and the intensity of metamorphism decreases progressively towards the outer part of the fold limbs. Subsequently, the large-scale folding gave rise to culminations and depressions, the latter occupied by the Tethyan Basins of Kashmir, Lahaul-Spiti, Kumaun, Nepal and Bhutan.

10.4.3 Metamorphism

The rocks of the Jutogh–Almora Nappe show greenschist facies metamorphism in the lower part (Das 1971, 1973; Das and Pande 1973), epidote–amphibolite facies in the middle level (Pande and Powar 1968) and local development

of kyanite–sillimanite grade in the upper part intruded by granite as seen in the Dhunaghat and Almora areas in Kumaun (Singh et al. 1991; Joshi and Tiwari 2004). At Dhunaghat, the Champawat Granodiorite has caused contact metamorphism as evidenced by andalusite, fibrolite and chloritoid-bearing hornfels facies rocks (Valdiya 1963) that developed at temperature 600–650 °C and pressure 3 kbar (Joshi et al. 1994). The metamorphic and granitic rocks of the Almora Nappe exhibit four sets of folding (Joshi and Tiwari 2007). The accompanying metamorphism gave rise to green schist facies at ~450 °C and 4–7.9 kbar and to the amphibolites facies rocks at 500–700 °C (Joshi and Tiwari 2009). The structural and fabric data of the Almora Thrust match with the magnetic susceptibility data of the crystalline rocks in both the North Almora Thrust and South Almora Thrust (Agrawal et al. 2010). Veins of dark pseudotachylite identified in the zone of South Almora Thrust imply that there was recrystallization resulting from strong movements along the thrust (Agrawal et al. 2011).

In the Kameng district in western Arunachal Pradesh, the metamorphic and granitic rocks of the Great Himalayan succession were subjected to four phases of deformation in the ductile and brittle-ductile regimes, the sense of movement on the Tawang and Sela thrusts being SSW (Srivastava et al. 2011). In the Kullu region in Himachal Pradesh, the grade of metamorphism increases from the chlorite to sillimanite grade, the isograds showing inversion of succession (Thakur 1993). In the Kishtwar succession, polyphase metamorphism is manifested in medium- to high-pressure regional metamorphism of pelitic schist (Das 1978).

In the Munsiari unit, just below the Main Central Thrust, the mineral assemblages indicate metamorphic temperatures of the order of 450–500 °C and pressure of 4 kbar in the Kumaun region (Valdiya and Goel 1983) and 500–600 °C temperature and 3–6 kbar pressure in the Garhwal region (Metcalfe 1993; Singh et al. 1997). To the south-east in the Marsyangdi Valley in west-central Nepal, the chlorite-grade rocks at the base gradually pass upwards to garnet–staurolite and rarely kyanite grade just under the Main Central Thrust (Upreti 1999). This anomalous situation, described as *inverted metamorphism,* is a result of juxtaposition of units of normal metamorphic condition by out-of-sequence thrusting (Harrison et al. 1998)—thrusting without normal order of displacement—particularly in the zone of imbricate thrusting under the Main Central Thrust as seen in the Alaknanda–Bhagirathi triangle in Garhwal (Valdiya 1980b, 1981) and in the Langtang area in Nepal (Macfarlane et al. 1992).

10.4.4 Mineralization

Sulphides of copper, zinc and lead form stringers and dissemination in the chlorite–sericite–muscovite–biotite schists of the Almora Group in the Askot klippen in the valley of Gunji Gad, near the village Askot. The mineralization taking place at temperatures 350–500 °C was controlled by structures (Farooq and Hasan 1994). The sulphides in the Askot klippe are being mined.

Occurring as pocket, lenses and bands, the mineral graphite in the metamorphic rocks of the Almora Nappe succession exhibits under microscope tiny nodular and circular features pointing to biogenic origin of carbon, as substantiated by $\delta^{13}C$ values, and the Raman Shifts (Rawat and Sharma 2012).

10.5 Great Himalayan Vaikrita Group

10.5.1 Tectonic Setting

Delimited at the base by the Main Central Thrust and cut at the top by the Trans-Himadri Detachment Fault, the Great Himalaya or Himadri terrane is a 6000- to 10,000-m-thick lithotectonic slab squeezed up as a consequence of continued India–Asia convergence (Fig. 10.11). It forms the 3000- to 8000-m-high ever-snowy rampart that controls the atmospheric circulation and climate of Asia. The Great Himalaya terrane is made up of high-grade metamorphic rocks intruded by Early Miocene granites of anatectic origin. The *crystalline complex of uncertain age* formed the floor of the Tethys Basin in which the Phanerozoic sediments ranging in age from the Cambro–Ordovician to the Eocene were laid down. It has been described as the *Central Gneiss*, the *Central Crystalline Zone* (Heim and Gansser 1939) or the *Central Crystalline Axis* (Saxena 1971).

It may be emphasized at the outset that the crystalline rocks (metamorphic and granitic) of the Great Himalaya are distinctly different from those of the Lesser Himalayan nappes. In the Garhwal section in Uttarakhand, the contrast between the Lesser Himalayan and Great Himalayan metamorphic and associated granitic

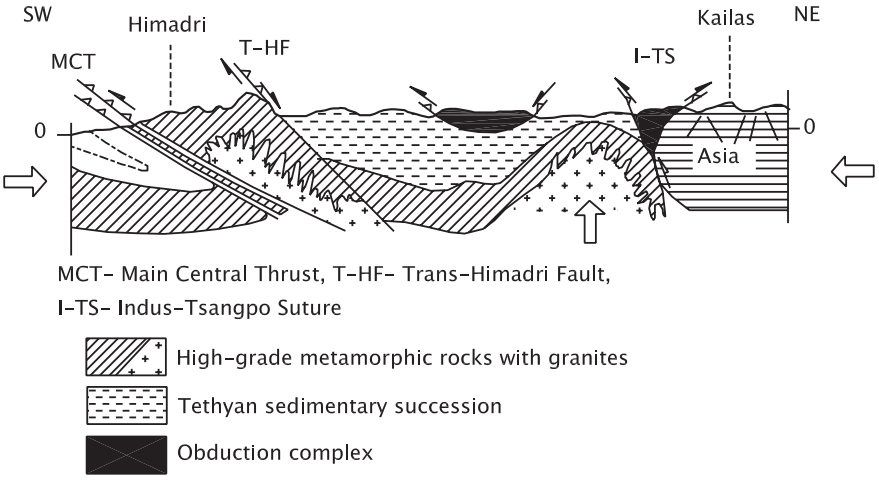

Fig. 10.11 Diagrammatic cross section of the Himadri subprovince portraying its structural design—a thick lithotectonic slab squeezed up to great height as a result of continental convergence. Plane area is Lessesr Himalayan Proterozoic sedimentary rocks (after Valdiya 1988a)

rocks is quite sharp—while the Lesser Himalayan crystalline rocks yield ziron U–Pb ages varying from 1614 ± 14 to 2679 ± 14 (the age spectra at 1870 Ma) and the C Hf values of zircon from 1 to 8, the crystalline rocks of the Great Himalaya have much varied age from 841 ± 10 to 2560 ± 8 Ma and the C Hf values of zircon from 13 to 21 (Spencer et al. 2012). In the Satluj Valley (Himachal Pradesh), the mylonitized gneisses of the wangtu done in the Lesser Himalaya, garnet is dated 7.9 ± 0.9 Ma (Sm–Nd) and muscovite-biotite 5.5 ± 0.1 Ma (Rb–Sr). In contrast, the Sm–Nd age of garnet in the Haimanta succession belonging to the bottom of the Great Himalayan pile and intruded by the Leo Pargial Granite is 19 ± 1, and the Rb–Sr ages of muscovite–biotite are 16.4 and 11.6 Ma (Thoni et al. 2012). The garnet mineral in the pegmatites within the Great Himalayan Vaikrita rocks is 40.5 ± 1.3 Million year old, while the whole-rock isochron age of the leucosome is 29 ± 1 Ma (Thoni et al. 2012). These age variations show that the Lesser Himalayan and Great Himalayan domains have distinctly different thermal history.

The *Main Central Thrust*, defining the base of the Great Himalaya terrane, has brought the high-grade metamorphic rocks upon the Lesser Himalayan low-grade metamorphics with 1900 ± 100 million-year-old porphyroids and/or upon the medium-grade metamorphics with 500 ± 25 million-year-old anatectic granites. The steeply dipping *Trans-Himadri Detachment Fault* is a gravity fault that has detached the Phanerozoic sedimentary cover of the Tethys terrane from the Himadri basement complex (Fig. 10.11). Both the tectonic boundaries are of regional dimension, extending from end to end and reaching great depth.

10.5.2 Structural Characteristics

The thick homoclinal terrane is split up by a number of intraformational thrust planes. This is evident from thick zones of shearing and mylonitization within the Vaikrita succession. No large-scale structures are seen—there are only intrafolial folds of lesser dimension resulting from internal deformation characterized by polyphase folding and transpositional foliation (Roy and Valdiya 1988). In Kumaun, two broad orientations of folds in relation to dominant lineation are recognized—(i) folds subparallel to NNE/NE–SSW/SW-oriented lineation that marks the direction of tectonic transport and (ii) folds with hinges at high angles to the lineation. A large majority of folds of early-generation plunging downdip have a reclined geometry. They appear as appressed isoclines with thickened hinges and attenuated and/or unequal limbs. The mineral lineation is invariably parallel to the fold hinges. The later generation of folds is upright, and their axes are oriented at high angles to the general WNW–ESE strike. They vary in shape from sharp-hinge arrowhead folds through conjugate links to round-hinge folds. All gradations between these categories of folds are discernible. There is rotation of axial surfaces of folds due to movements on shear planes, clearly reflecting progressive nature of deformation during thrust movements **quite later in the Tertiary period**. Continued movements resulted in the elimination of fold limbs along shear planes, giving rise to rootless

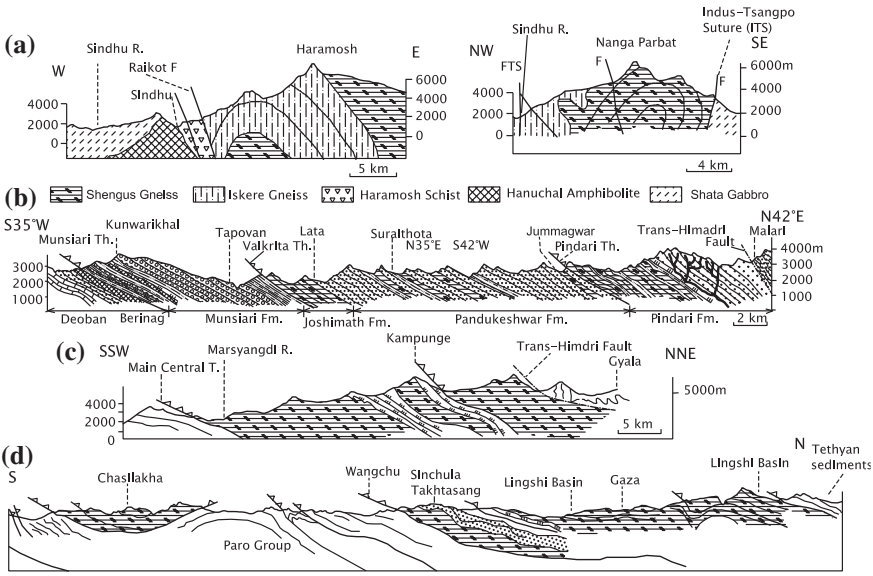

Fig. 10.12 Cross sections show the lithological succession of the Great Himalayan Vaikrita Group in different sections. **a** Haramosh–Nanga Parbat massif in northern Pakistan (based on Butler et al. 1992, 2000). **b** Kumaun Himalaya along the valley of western Dhauli River (after Valdiya and Goel 1983). **c** Nepal along the Marysandi River (after Pecher 1989). **d** Bhutan (after Gansser 1964)

isoclines occurring in rows (Roy and Valdiya 1988). The resulting feature mimics streaky augen gneiss that is the hallmark of the underlying Munsiari unit of the Lesser Himalayan subprovince.

What looks like a uniform lithology, the Vaikrita indeed comprises a number of slabs each with different thermal history (Fig. 10.12).

10.5.3 Lithology

The succession of kyanite–sillimanite–garnet-bearing psammitic gneisses and schists, kyanite–garnet schist interbedded with garnetiferous biotite–quartzite, calc silicate rock and marble and biotite porphyroblastic calc-schist (Fig. 10.12) in Kumaun and eastern Himachal was designated as the *Vaikrita* by C.L. Greisbach in 1891. The high-grade metamorphic succession is penetrated and extensively migmatized by anatectic granites. The Vaikrita Group is divisible into four formations in Uttarakhand (Heim and Gansser 1939; Gansser 1964; Valdiya and Goel 1983; Valdiya et al. 1999).

The 6- to 10-km-thick Vaikrita succession is traceable north-west through Kinnar Kailas massif into the Zanskar Range in Ladakh. It is described as the *Suru* (Nanda and Singh 1977), the *Higher Himalayan Crystallines* (Fuchs 1977,

1987; Thakur 1987; Baud et al. 1984), the *Padar* (Jangpangi et al. 1978) and the *Zanskar Crystallines* (Thakur et al. 1990). Further north-west, the Nanga Parbat–Haramosh Massif is all migmatites and anatectic granites caught in the syntaxial bend. The Vaikrita Complex occurs in the form of an anticlinal structure (Wadia 1928; Coward and Butler 1985; Coward et al. 1988). The high-grade basement complex comprises 500-m-thick mica gneisses with subordinate amphibolites and calc silicate rocks (*Shengus Gneiss*) underlain by 2500 m of biotite schists with marble and calc silicate gneiss with subordinate amphibolite (Kazmi and Qasim Jan 1997). The Nd data show that the core of the Nanga Parbat is made up of protoliths of the age range 2800–2300 Ma, with εNd −18 to −30, indicating their strong affinity with the Lesser Himalayan gneisses that have average protolith age of 2640 ± 220 Ma and T_{DM} 2300 to 3400 Ma with εNd −18 to −27 (Whittington 1996). However, the covering metamorphic rocks of the Nanga Parbat Massif are characterized by T_{DM} 1600–1800 Ma with εNd −10 to −14, which is not different from that of the Great Himalayan (Himadri) complex—1940 ± 270 Ma (1700–2000 Ma), having εNd −6 to −16. Across the Sindhu River syntaxis, the *Sharda* succession in the Kaghan Valley comprises garnetiferous calc schists and marble with amphibolite intracalated with metapsammites and pelites characterized by sillimanite and the occurrence of porphyritic and non-porphyritic granites associated with migmatites (Chaudhry and Ghazanfar 1987).

In western Nepal, the Vaikrita has been described as the *Tibetan Slab* (Lombard 1958; Bordet 1961, 1973; Bordet et al. 1971; Colchen et al. 1986), the *Upper Crystalline Nappe* (Fuchs 1967, 1975; Fuchs and Frank 1970; Frank and Fuchs 1970), the *Annapurna Gneiss Complex* (Bodenhausen and Egeler 1971), the *Himalayan Gneiss* (Hashimoto et al. 1973) and in eastern Nepal as the *Khumbu–Lumbasumba Nappe* (Hagen 1958, 1969) and the *Barun Gneiss* (Jaros and Kalvoda 1978). In the Darjeeling Hills, the Vaikrita is known as the *Darjeeling Gneiss* comprising kyanite–sillimanite–garnet–quartz gneisses and schists associated with calc silicate rocks and migmatites (Ray 1947; Acharyya 1975). It extends eastwards as the *Thimphu* in Bhutan (Nautiyal et al. 1964) or *Takhtasang–Chasilakha Gneiss* (Gansser 1964, 1983) and in the Arunachal Pradesh as the *Sela* (Das et al. 1976; Bhushan et al. 1991).

Significantly, the Vaikrita metamorphic assemblage in Nepal is characterized by εNd(o) values of −19 to −12 with detrital zircon age peak at 1050 Ma, in sharp contrast to the Lesser Himalayan metamorphic complex which have εNd(o) values between −20 and −26 (−21.5) with detrital zircon age peak at 1550 Ma (Robinson et al. 2001; Martin et al. 2005). It is abundantly clear that the Great Himalayan metamorphic complex is younger than the metamorphic succession covering large parts of the Lesser Himalaya. It turns out that in contrast to 1870–2600 Million year old zircons in the metamorphics of the Lesser Himalayan nappes, the Vaikrita metamorphics of the Langtang region in Nepal contain 800–1000 Million year old zircons, implying presence of Late Proterozoic sedimentary protoliths in the Great Himalayan succession (Parrish and Hodges 1996). This means that the Vaikrita does not constitute the basement upon which the Tethyan sediments were laid. It is possibly the Lesser Himalayan Crystalline Complex

embodying 1900 ± 100 Ma prophyritic granites and porphyries that served as the basement. However, this is a debatable subject.

The Great Himalayan complex of crystalline rocks in Bhutan includes mafic granulites and amphibolites in the Masang Kang area, their SIMS data suggesting an age of 1742 ± 32 Ma for the mafic magmatic rocks that were metamorphosed granulite (Chakungal et al. 2010). It is quite obvious that the granulites point to a Late Palaeoproterozoic thermal event. In the Arun Valley in north-eastern Nepal, eclogite has been recognized in association with amphibolites. The Lu–Hf data of garnet separated from eclogite indicate that it is 20.7 ± 0.4 Million year old and that granulite metamorphism occurred at ~780 °C and ~12 kbar and at 14 Ma was retrogressed to amphibolites at ~675 °C and 6 kbar (Corrie et al. 2010).

The Great Himalaya crystalline rocks in the Kameng district in western Arunachal Pradesh were intruded by leucocratic granite below the Trans-Himadri Detachment Fault, above the Main Central Thrust and south of the Indus-Tsangpo Suture Zone. While those that occur above the MCT and below the T-HDF are 19 million years old, those that occur intruding the Tethyan sedimentary pile above the T-HDF as far north as the I-TSZ are 44.1 ± 1.2 and 42 ± 5 Ma, respectively (Aikman et al. 2012), implying different thermal history of the two domains.

10.5.4 Metamorphism

The metamorphism of the Vaikrita and its equivalents all through the expanse of the Great Himalaya subprovince was coeval with deformation, which occurred over a long period of time. Practically in all sections of the Vaikrita, the regional metamorphism is prograde. However, towards the top of the succession, the impact of tectonothermal events related to large-scale emplacement of anatectic granite is manifested itself in the increase of the metamorphic grade.

In the Kumaun sector, the metamorphism took place at temperatures 600–650 °C and pressure 5–5.7 kbar (Valdiya and Goel 1983). The presence of cordierite and saffire in the sillimanite–biotite–plagioclase subfacies rocks in the Badrinath area and the occurrence of diopside in calc silicate rock indicate that the grade of metamorphism had locally risen up to the pyroxene–granulite facies in the uppermost unit, the Pindari Formation (Valdiya and Goel 1983; Valdiya et al. 1999). In the Garhwal sector, the thermodynamic condition of metamorphism was more or less similar −980°K and 523–317 Mpa (Hodges and Silverberg 1988), 645 ± 50 °C and 7.5 ± 0.5 kbar (Gairola and Ackermann 1988), 650–670 °C and 5.5–6.5 kbar, 700–800 °C and 9 kbar (Singh et al. 1997) and 550–640 °C to 770 °C and 8–9 to 12 kbar (Metcalfe 1993). Annealing textures and presence of staurolite and locally cordierite in and around granite bodies imply contact metamorphism as seen in the Bhagirathi Valley (Stern et al. 1989; Searle et al. 1993).

In Nepal, the Great Himalayan metamorphic rocks show upper amphibolite to lower granulite facies metamorphism at temperature 754 ± 40 °C and pressure 890 ± 260 Mpa (Rai et al. 1998; Upreti 1999). The metamorphic assemblages

of the Darjeeling Gneiss in Sikkim–Darjeeling sector indicate temperature of 580–770 °C and pressure of 5.0–7.7 kbar (Mohan et al. 1989). In the Thimphu of Bhutan, the grade of metamorphism conforms to almandine amphibolite facies (Gokul et al. 1982).

10.6 Proterozoic Mogok Complex in Myanmar

10.6.1 Tectonic Setting and Structure

Myanmar is divided into three geomorphologically, structurally, stratigraphically and geochronologically contrasted terranes by transcontinental strike-slip faults (Fan and Koko 1994). The eastern terrane comprising Sino-Myanmar Ranges is delimited in the east by the *Chiang Rai Suture* and in the west by the strike-slip *Sagaing Fault* (Fig. 10.13). Within the subprovince of the China–Myanmar Border Ranges, there are three subterranes, separated by regional faults. Proterozoic rock complex occurs in the middle subterrane embracing the *Mogok Belt*. Making a 1400-km-long uplifted terrane in eastern Myanmar and embracing East Kachin, Shan States, Kayah State, Karen State, and the Tenasserim division, the *Mogok Complex* makes the mountainous belt that was uplifted as a consequence of combined strike-slip displacement and dip-slip movements on the faults of the Sagaing fault system. In the Bhamo district in the north, the uplifted block forms mountains as high as 4000 m. In the belt east of Shwebo–Sagaing–Mandalay, the high-grade metamorphic rocks of the Mogok Complex are thrown into folds oriented in the E–W direction (Bender 1983). An elongate horst-like narrow hill range occurs along with west bank of the Irrawaddy. It is represented by the Mandalay Hill and the Boywa Mountain.

10.6.2 Lithology

The Mogok Complex comprises pelitic and semipelitic biotite-bearing gneisses and schists with quartzites, giving way upwards to calc silicate rocks and marbles intercalated with gneisses, schists and quartzites. The complex is intruded by bodies of acid, intermediate, basic and ultrabasic rocks including peridotite, pyroxenite, nepheline-, aegirine-syenite, hornblend/tourmaline-granites (Iyer 1953). In the Shan States, the grade of metamorphism increases from amphibolite facies in the east to granulite facies in the west and north-west, where the metamorphic rocks are intruded by the *Kabaing Granite* (Searle and Haq 1964). Attendant contact metamorphics of calc silicate rocks have given rise to the formation of corundum and spinel in calciphyres and calc granulites. The rock assemblage recalls the Great Himalayan high-grade metamorphic rocks (Mitchell 1989).

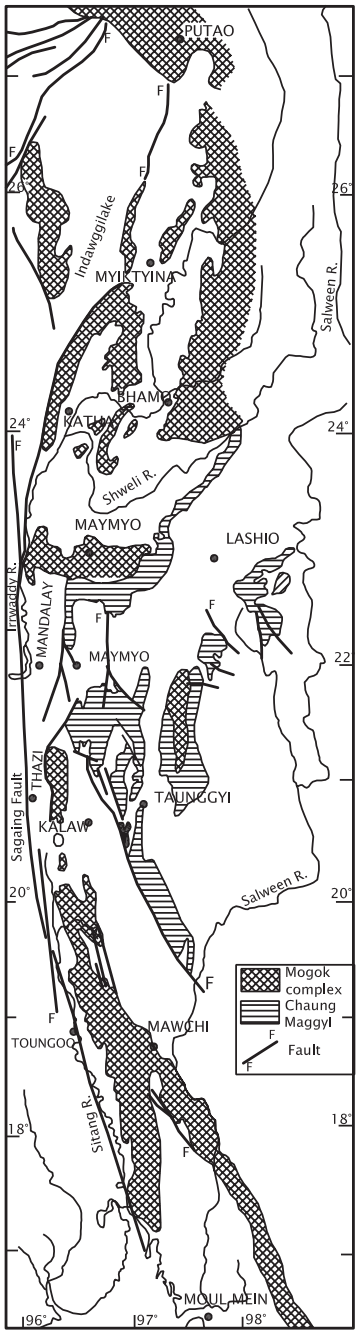

Fig. 10.13 Proterozoic Mogok Belt (predominantly gneisses) and younger Chaung Magyi Group occur in the East Kachin–Shan States subterrane of the China–Burman border terrane (after Morley 2004)

10.6.3 Mineralization

World's finest *rubies* occur in the Mogok Belt. The ruby occurs with spinel at the contact of nepheline syenite and alaskite (Fan and Koko 1994). Most rubies from the weathered horst rocks have been carried by streams to alluvial sediments of low valleys where they occur as placer deposits (Table 10.1).

References

Acharyya, S. K. (1971). Ranjit Pebble: State—A new formation from the Darjeeling hills. *Indian Minerals, 25*, 61–64.

Acharyya, S. K. (1975). Structure and stratigraphy of the Darjeeling frontal zone, Eastern Himalaya. *Geological Surey of India Miscellaneous Publications, 24*(II), 71–90.

Agrawal, K. K., Jahan, N., & Agarwal, A. (2010). Modification of fold geometry in Almora Crystalline Shear Zone, Lesser Himalaya, India. *Journal of the Geological Society of India*, *75*, 411–414.

Agrawal, K. K., Bali, R., Patil, S. K., & Nawaz Ali, S. (2011). Anisotropy of magnetic susceptibility in the Almora Crystalline Zone, Lesser Himalaya, India: A case study. *Asian Journal of Earth Sciences*, ISSN 1819–1886.

Ahmad, T., & Bhat, M. I. (1987). Geochemistry and petrogenesis of Mandi-Darla Volcanics, NW Himalaya. *Precambrian Research, 37*, 231–256.

Ahmad, T., Harris, N., Bickle, M., Chapman, H., Burnbury, J., & Prince, C. (2000). Isotopic constraints on the structural relationships between the Lesser Himalayan series and the High Himalayan crystalline series, Garhwal Himalaya. *Geological Society of American Bulletin, 112*, 467–477.

Ahmad, T., Mukharjee, P. K., & Trivedi, J. R. (1999). Geochemistry of Precambrian magmatic rocks of western Himalaya, India: Petrogenetic and tectonic implications. *Chemical Geology, 160*, 103–119.

Ahmed, Z. (1990). Geochemical characterization of Proterozoic upper crustal metamorphic terrain in southern Malakand Agency, Pakistan. *Precambrian Research, 46*, 181–194.

Aikman, A. B., Harrison, T. M., & Hermann, J. (2012). Age and thermal history of Eo- and Neo-Himalayan Granitoids, eastern Himalaya. *Journal of Asian Earth Sciences*, *51*, 85–97.

Arita, K. (1983). Origin of the inverted metamorphism of the Lower Himalayas, central Nepal. *Tectonophysics, 95*, 43–60.

Arita, K., & Sharma, M. P. (1992). Chemical characteristics of some granitic rocks in Central Nepal. *Bulletin Geological Publications, Tribhuvan University, 2*, 1–9.

Arita, K., Sharma, T., & Fujii, Y. (1984). Geology and structure of the Jajarkot-Piuthan area, central Nepal. *Journal of Nepal Geological Society, 4*, 5–27.

Auden, J. B. (1934). The geology of the Krol belt. *Records of Geological Survey of India, 67*, 357–454.

Auden, J. B. (1935). Traverses in the Himalaya. *Records of Geological Survey of India, 69*, 123–167.

Bahuguna, V. K., & Saklani, P. S. (1988). Tectonics of the main central thrust in Garhwal Himalaya. *Journal of Geological Society of India, 31*, 197–209.

Baig, M. S., & Snee, L. W. (1991). A discovery of late Archean to early Proterozoic komatite from northwestern margin of the Indian plate: Besham area, northwest Himalaya, Pakistan. *Kashmir Journal of Geology, 8&9*, 19–23.

Baud, A., Gaetani, M., Garzanti, E., Fois, E., Nicora, A., & Tintori, A. (1984). Geological observation in southeastern Zanskar and adjacent Lahaul area (northwestern Himalaya). *Eclogae Geologicae Helvetiae, 77*, 171–197.

Bender, F. (1983). *Geology of Burma*. Berlin: Gebruder Borntraeges. (293 p).

Berthelsen, A. (1951). A geological section through the Himalaya. *Meddelelser Dansk Geologisk Forening, 12*, 102–104.

Bhanot, V. B., Pandey, B. K., Singh, V. P., & Kansal, A. K. (1980). Rb–Sr ages for some granitic and gneissic rocks of Kumaun and Himachal Himalaya. In K. S. Valdiya & S. B. Bhatia (Eds.), *Stratigraphy and correlations of the Lesser Himalayan formations* (pp. 139–144). Delhi: Hindustan Publishing Corporation.

Bhanot, V. B., Singh, V. P., Kausal, A. K., & Thakur, V. C. (1977). Early Proterozoic Rb–Sr whole-rock age for central crystalline gneiss of Higher Himalaya, Kumaun. *Journal of Geological Society of India, 18*, 90–91.

Bhargava, O. N. (2000). The Precambrian sequences in the western Himalaya. *Special Publication of the Geological Survey of India, 55*, 69–84.

Bhargava, O. N., & Bassi, U. K. (1994). The crystalline thrust sheet in the Himachal Himalaya and the age of amphibolite-facies metamorphism. *Journal of Geological Society of India, 43*, 343–352.

Bhargava, O. N., Frank, W., & Bertle, R. (2011). Later Cambrian deformation in the Lesser Himalaya. *Journal of Asian Earth Sciences, 40*, 201–221.

Bhat, M. I. (1987). Spasmodic rift reactivation and its role in the pre-orogenic evolution of the Himalayan region. *Tectonophysics, 134*, 103–127.

Bhat, M. I., Claesson, S., Dubey, A. K., & Pande, K. (1998). Sm–Nd age of the Garhwal-Bhowali Volcanics, western Himalaya: Vestiges of the Late Archaean Rampur flood basalt province of the northern Indian craton. *Precambrian Research, 87*, 217–231.

Bhat, M. I., & Ghosh, S. K. (2001). Geochemistry of the 2.51 Ga old Rampur group (pelites) western Himalaya: Implication for their provenance and weathering. *Precambrian Research, 108*, 1–16.

Bhat, M. I., & Le Fort, P. (1992). Sm–Nd age and petrogenesis of Rampur metavolcanic rocks, NW Himalaya: Late Archaean relics in the Himalayan belt. *Precambrian Research, 56*, 191–210.

Bhushan, S. K., Bindal, C. M., & Aggarwal, R. K. (1991). Geology of Bomdila Group in Arunachal Pradesh. *Journal of Himalayan Geology, 2*, 207–214.

Bist, K. S., & Sinha, A. K. (1980). Some observations on the geological and structural setup of Okhimath area in Garhwal Himalaya. *Himalayan Geology, 10*, 467–475.

Bist, K. S., & Sinha, A. K. (1990). Imbrication of main central thrust and its tectonic implication in the central sector of the Himalaya. In S. P. H. Saychanthavong (Ed.), *Crustal evolution and orogeny* (pp. 293–302).

Bodenhausen, J. W. A., & Egeler, C. G. (1971). On the geology of the upper Gandaki valley, Nepalese Himalaya. *Koninklijke Nederlandse Akademie van Wetenschappen, 74*, 526–546.

Bordet, P. (1961). *Recherches Geologiques den l'Himalaya due Nepal region du Makalu*. Paris: Centre Nationale Recher, Scientifique. (275 p).

Bordet, P. (1973). On the position of the Himalayan main central thrust within Nepal Himalaya. *Proceedings of the Seminar Geodynamics* (pp. 148–155). Hyderabad: NGRI.

Bordet, P., Colchen, M., Krummenacher, D., Le Fort, P., Mouterde, R., & Remy, M. (1971). *Recherches Geologiques dans l'Himalaya du Nepal Region de la Thakkola*. Paris: Centre Nationale Recher, Scientifique. 279 p.

Butler, R. W. H., George, M., Harris, N. B. W., Jones, C., Prior, D. J., Treloar, P. J., & Wheeler, J. (1992). Geology of the northern part of the Nanga Parbat massif, northern Pakistan, and its implications for Himalayan tectonics. *Journal of Geological Society of London, 149*, 557–567.

Butler, R. W. H., Wheeler, J., Treloar, P. J., & Jones, C. (2000). Geological structure of the southern part of the Nanga Parbat massif, Pakistan Himalaya and its tectonic implications. In M. A. Khan, P. J. Treloar, M. P. Searle, & M. Q. Jan (Eds.), *Tectonics of the Nanga Parbat Syntaxis and the Western Himalaya* (pp. 123–136). London: Geological Society.

Butt, K. A. (1983). Petrology and geochemical evolution of Lahor pegmatoid granite complex, northern Pakistan, and genesis of associated Pb–Zn–Mo and U mineralization. In F. A. Shams (Ed.), *Granites of Himalaya, Karakoram and Hindukush* (pp. 309–324). Lahore: Institute of Geology, Punjab University.

Calkins, J. A., Offield, T. W., Abdullah, K. M., & Ali, S. T. (1975). Geology of the southern Himalaya in Hazara, Pakistan and adjacent area. *United States Geological Survey of Professional Papers, 716C*, 29.

Chakrabarti, B. K. (1985). Role of Precambrian megastructures in solving the problems of stratigraphy and tectonics of the Simla Himalaya. *Bulletin Geological Mining Metallurgical Society of India, 53*, 27–55.

Chakrabarti, B. K. (1996). Precambrian deformation signatures on the Himalayas. *Indian Minerals, 50*, 259–270.

Chakungal, J., Dostal, J., Grujic, P., Duchene, S., & Ghalley, K. S. (2010). Provenance of the great Himalayan sequence: Evidence from mafic granulites and amphibolites in NW Bhutan. *Tectonophysics, 480*, 198–212.

Chaudhry, M. N., & Ghazanfar, M. (1987). Geology, structure and geomorphology of upper Bhaghan valley, northwest Himalaya, Pakistan. *Geological Bulletin Punjab University, 22*, 13–57.

Chaudhry, M. N., Jaffrey, S. A., & Saleemi, B. A. (1974). Geology and petrology of Malakand Granite and its environment. *Geological Bulletin Panjab University, 10*, 43–58.

Colchen, M., Le Fort, P., & Pecher, A. (1986). *Recherches Geologiques dans l' Himalaya due Nepal Annapurna, Manaslu, Ganesh Himal*. Paris: Centre Nationale Recherche Scientifique. (136 p).

Corrie, S. L., Kohn, M. J., & Vervoort, J. D. (2010). Young eclogite from the greater Himalayan sequence, Arun Valley, eastern Nepal: P-T-t path and tectonic implications. *Earth & Planet Science Letters, 289*, 406–416.

Coward, M. P., & Butler, R. W. H. (1985). Thrust tectonics and deep structure of the Pakistan Himalaya. *Geology, 13*, 417–420.

Coward, M. P., Butler, R. W. H., Khan, M. A., & Knipe, R. J. (1988). Folding and imbrication of the Indian crust during Himalayan collision. *Philosophical Transactions of the Royal Society of London, A326*, 89–114.

Das, B. K. (1971). Petrology of pelitic schists and gneisses of Chaubatia-Ranikhet area, Almora district, U.P. *Geologische Rundschau, 60*, 552–568.

Das, B. K. (1973). Green schist facies of the Almora Nappe, Kumaun Himalaya. *Geological Magazine, 110*, 59–66.

Das, B. K. (1978). Polyphase medium- to high-pressure regional metamorphism of the pelitic rocks around Kishtwar, Jammu and Kashmir State, India. *Neues Jahrbuch für Geologie und Paläontologie-Abhandlungen, 132*, 73–90.

Das, A. K., Bakliwal, P. C., & Dhaundial, D. P. (1976). A brief outline of the geology of parts of Kameng District, Nefa. *Geological Survey of India Miscellaneous Publications, 24*, 115–127.

Das, B. K., & Pande, I. C. (1973). Zone of progressive metamorphism in Dudhatoli-Syncline, Garhwal Himalaya. *Himalayan Geology, 3*, 190–208.

Das, A. S., & Srikantia, S. V. (1972). The Larji window, Panjab and Himachal Pradesh. *Miscellaneous Publication of Geological Survey of India, 15*, 97–100.

DeCelles, P. G., Robinson, D. M., Quade, J., Ojha, T. P., Garzione, C. N., Copeland, P., & Upreti, B. N. (2001). Stratigraphy, structure and tectonic evolution of the Himalayan fold-thrust belt in western Nepal. *Tectonics, 20*, 487–509.

DiPietro, J. A., & Isachsen, (2001). U–Pb zircon ages from the Indian plate in northwest Pakistan and their significance to Himalayan and pre-Himalayan geologic history. *Tectonics, 20*, 510–525.

Fan, P.-F., & Koko, (1994a). Accreted terranes and mineral deposits of Myanmar. *Journal of Southeast Asian Earth Sciences, 10*, 95–100.

Farooq, S., & Hasan, N. (1994). Base-metal mineralization along the Gurji stream near Askote, Kumaun Himalaya. *Journal of Geological Society of India, 44*, 513–525.

Frank, W., & Fuchs, G. R. (1970). Geological investigations in west Nepal and their significance for the geology of the Himalaya. *Geological Rundschau, 59*, 552–580.

Frank, W., Gansser, A., & Trommsdorff, V. (1977). Geological observations in the Ladakh area, a preliminary report. *Schweizerische Mineralogische und Petrographische Mitterling, 57*, 89–113.

Frank, W., Hoinkes, G., Miller, C., Purtschellere, F., Richter, W., & Thoni, M. (1973). Relations between metamorphism and orogeny in a typical section of the Indian Himalayas. *Tschermaks mineralogische und petrographische Mitteilungen, 20*, 303–332.

Fuchs, G. R. (1967). *Zum Bau des Himalaya*. Wien: Denkschriften der Obterreichischer Akademie Wiss. 211 p.

Fuchs, G. R. (1975). On the geology of the Karnali and Dolpho region, West Nepal. *Sound Mitteilungen der Geologischen Gesellschaft, 66–67*, 21–32.

Fuchs, G. R. (1977). Traverse of Zanskar from the Indus to the valley of Kashmir—A preliminary note. *Jahrbuch der Geologischen Bundesanstalt, 120*, 219–229.

Fuchs, G. R. (1987). The geology of southern Zanskar (Ladakh)—Evidence for the autochthony of the Tethys zone of the Himalaya. *Jahrbuch der Geologischen Bundesanstalt, 130*, 465–491.

Fuchs, G. R., & Frank, W. (1970). The geology of west Nepal between the rivers Kali Gandaki and Thulo Bheri. *Jahrbuch Geologische Bundesanstalt, 18*, 1–103.

Gairola, V. K. (1967). Refolding in the tectonites of Kausani area district Almora. *Publications of the Centre Advanced Study in Geology, Panjab University, 3*, 101–106.

Gairola, V. K., & Ackermann, D. (1988). Geothermobarometry of the central crystallines of the Garhwal Himalaya, U.P. *Journal of Geological Society of India, 31*, 230–242.

Gairola, V. K., & Joshi, M. (1980). Structure of a part of Dudhatoli-Almora crystalline thrust sheet around Thalisen, district Pauri, Garhwal. *Himalayan Geology, 8*(1), 379–398.

Gansser, A. (1964). *Geology of the Himalayas* (p. 289). London: Interscience Publishers.

Gansser, A. (1983). *Geology of the Bhutan Himalaya*. Basel: Birkhauser. (181 p).

Gehrel, G. E., DeCelles, P. G., Ojha, T. P., & Upreti, B. N. (2006). Geologic and U–Pb geochronological evidence for early Paleozoic tectonism in the Kathmandu thrust sheet, central Nepal Himalaya. *Bulletin Geological Society of America, 118*, 185–198.

Ghosh, S. K., Islam, R., Roy, Y., & Sinha, S. (2011). Palaeoproterozoic seismites in Damtha Group, Lesser Himalaya, India. *Himalayan Geology, 32*, 43–55.

Ghosh, S. K., Pandey, A. K., Prabha, P., Ray, Y., & Sinha, S. (2012). Soft-sediment deformation structures from the Palaeoproterozoic Damtha Group of Garhwal Lesser Himalaya, India. *Sedimentary Geology*, *261–262*, 76–89.

Gokul, A. R., Mulay, V. V., Pasayat, S., & Devadu, G. R. (1982). The contact relationship between the Thimphu Gneissic complex and the Paro Group in west central Bhutan. *Miscellaneous Publications of the Geological Survey of India, 41*(II), 172–175.

Greco, A., Martinotti, G., Papritz, K., Ramsay, J. G., & Rey, R. (1989). The crystalline rocks of the Kaghan valley. *Eclogae Geologicae Helvetiae, 82*, 629–653.

Hagen, T. (1958). Uber den Geologischen Bau des Nepal Himalaya. *Jarhbuch St-Gallishcen Naturforschende Gesellschaft, 76*, 3–48.

Hagen, T. (1969). Report on the geological survey of Nepal-1, preliminary reconnaissance. *Denkschriften der Schwieizerishen Naturforschenden Gasellschaft, 86*, 1–159.

Harrison, T. M., Grove, M., Lovera, O. M., & Catlos, E. J. (1998). A model for the origin of Himalayan anatacxis and inverted metamorphism. *Journal of Geophysics Research, 103*, 27017–27032.

Hashimoto, S., Ohta, Y., & Akiba, C. (1973). *Geology of the Nepal Himalayas*. Sapparo, Japan: Committee of Hokkaido University. 284 p.

Heim, A., & Gansser, A. (1939). Central Himalaya: Geological observations of the Swiss expedition 1936. *Denkschriften der Schwieizerishen Naturforschenden Gasellschaft, 32*, 1–245.

Hodges, K. V., & Silverberg, D. S. (1988). Thermal evolution of the great Himalaya, Garhwal, India. *Philosophical Transactions of the Royal Society of London, A326*, 257–280.

Huang, G.-C. (Dino), Wu, F. T., Roecker, S. W., & Sheehan, A. (2009). Lithospheric structure of the central Himalaya from 3-D tomographic imagery. *Tectonophysics, 475*, 524–543.

Ibrahim Shah, S. M. (Ed.). (1977). *Stratigraphy of Pakistan*. Quetta: Geological Survey of Pakistan (138 p).

Islam, R., Ahmand, T., & Rawat, B. S. (2003). Geochemistry and petrogenesis of the Phe volcanics, Zanskar, western Himalaya: Bearing on the Neotethys. *Memoires Geological Society of India, 52*, 339–357.

Iyer, L. A. N. (1953). The geology and gemstones of the Mogok tract, Burma. *Memoires Geological Survey of India, 82*, 1–100.

Jain, A. K., Thakur, V. C., & Tandon, S. K. (1974). Stratigraphy and structure of the Siang district, Arunachal Pradesh (NEFA). *Himalayan Geology, 4*, 28–60.

Jaisi, D., Dhital, M. R., & Pantlee, S. (2008). Geology of the Kusma-Behadi fold belt area Lesser Himalaya, central west Nepal. *Himalayan Geology, 29*, 119–126.

Jangpangi, B. S. (1974). Stratigraphy and tectonics of parts of Eastern Bhutan. *Himalayan Geology*, *4*, 117–136.

Jangpangi, B. S., Dhaundial, D. P., Kumar, G., & Dhaundiyal, J. N. (1978). On the geology of Sumcham sapphire mine area, Doda District, J & K. *Himalayan Geology, 8*(II), 837–849.

Jaros, J., & Kalvoda, J. (1978). *Geological structure of the Himalayas, Mt. Everest-Makalu Section*. Praha: Academia, Nakladalelsti Cesk. Acad. Ved. (69 p).

Joshi, M., Singh, B. N., & Goel, O. P. (1994). Metamorphic conditions of the aureole rocks from Dhunaghat area, Kumaun Lesser Himalaya. *Current Science, 67*, 185–188.

Joshi, M., & Tiwari, A. N. (2004). Quartz C-axes and metastable phases in the metamorphic rocks of Almora Nappe: Evidence of pre-Himalayan signatures. *Current Science*, *87*, 995–999.

Joshi, M., & Tiwari, A. N. (2007). Folded metamorphic reaction isograds in the Almora Nappe, Kumaun Lesser Himalaya: Field evidence and tectonic implications. *Neues Jahrbuch für Geologie und Paläontologie-Abhandlungen, 244*(2), 215–225.

Joshi, M., & Tiwari, A. N. (2009). Structural events and metamorphic consequences in Almora Nappe during Himalayan collision tectonics. *Journal of Asian Earth Sciences, 34*, 326–335.

Kakar, R. K. (1986). Rb–Sr radiometric ages of the Darla volcanics and amphibolites from the Jutogh area near Shimla Hills, H.P. *Bulletin Indian Geological Association, 19*, 97–101.

Kaul, R., Singh, R., Sen, D. B., & Gupta, R. K. (1991). Uranium exploration in the Proterozoic rocks of northwestern Himalaya. *Exploration and Research for Atomic Minerals, 4*, 1–12.

Kazmi, A. H., & Qasim Jan, M. (1997). *Geology and Tectonics of Pakistan*. Karachi: Graphic Publishers. (554 p).

Kumar, R. (1977). Structural and metamorphic history of the Lesser Himalayan rocks of Arki–Jutogh area, Shimla Hills, H.P. *Recent researches in geology* (Vol. 3). Delhi: Hindustan Publishing Corporation, pp. 425–449.

Kumar, S., & Singh, T. (1980). Tectono-stratigraphic set up of the Subansiri District, Arunachal Pradesh. In K. S. Valdiya & S. B. Bhatia (Eds.), *Stratigraphy and correlations of the Lesser Himalayan formations* (pp. 267–282). Delhi: Hindustan Publishing Corporation.

Kwatra, S. K., Bhanot, V. B., Kakar, R. K., & Kansal, A. K. (1986). Rb–Sr radiometric ages of the Wangtu Gneissic complex, Kinnaur district, Himachal Himalaya. *Bulletin Indian Geological Association, 19*, 127–130.

Latif, M. A. (1970). Explanatory notes on the geology of southeastern Hazara. *Jahrbuch der Geologischen Bundesanstalt, Sonderband, 15*, 5–20.

Lefort, P., & Rai, S. M. (1999). Pre-Tertiary felsic magmatism of the Nepal Himalaya: Recycling of continental crust. *Journal of Asian Earth Sciences, 17*, 607–628.

Lombard, A. (1958). Un itineraire geologique dan l' est due Nepal (massif du Mont Everest). *Denkschriften der Schweizerishen Naturforschenden Gasellschaft*, *82*, 108.

Macfarlane, A., Hodges, K. V., & Lux, D. (1992). A structural analysis of the main central thrust zone, Langtang National Park, Central Nepal Himalaya. *Geological Society of the American Bulletin, 104*, 1389–1402.

Maruo, Y., & Kizaki, K. (1983). Thermal structure of the nappes of the eastern Nepal Himalaya. In F. A. Shams (Ed.), *Granites of Himalaya, Karakoram and Hindukush* (pp. 271–286). Lahore: Institute of Geology, Panjab University.

Merh, S. S. (1977). Structural studies in the parts of Kumaun Himalaya. *Himalayan Geology, 7*, 26–42.

Merh, S. S., & Vashi, N. M. (1965). Structure and metamorphism of the Ranikhet area of Almora District, Uttar Pradesh. *Indian Mineralogist, 6*, 55–66.

Merh, S. S., Vashi, N. M., & Patel, J. P. (1971). On the nature of the Ramgarh Thrust in Kumaun Himalaya. *Journal of Geological Society of India, 11*, 380–382.

Metcalfe, R. P. (1993). Pressure, temperature and time constraints on the metamorphism across the main central thrust zone and High Himalayan slab in Garhwal Himalaya. In P. J. Treloar & M. P. Searle (Eds.), *Himalayan Tectonics* (pp. 485–509). London: Geological Society.

Miller, C., Klotzb, U., Frank, W., Thoni, M., & Grasemann, B. (2000). Proterozoic crustal evolution in the NW Himalaya (India) as recorded by 1.80 Ga mafic and 1.84 Ga granitic magmatism. *Precambrian Research, 103*, 191–206.

Misra, R. C., & Sharma, R. P. (1967). Geology of the Devidhura area, district Almora, U.P. *Journal of Geological Society of India, 8*, 110–118.

Mitchell, A. H. G. (1989). The Shan Plateau and Western Burma: Mesozoic-Cenozoic plate boundaries and correlation with Tibet. In A. M. C. Sengor (Ed.), *Tectonic evolution of the Tethyan region* (pp. 567–583). Netherlands: Kluwer.

Mohan, A., Windley, B. F., & Searle, M. P. (1989). Geothermobarometry and development of inverted metamorphism in the Darjeeling-Sikkim region of the eastern Himalaya. *Journal of Metamorphic Petroleum, 7*, 95–110.

Morley, C. K. (2004). Nested, strike-slip duplexes and other evidence for Late Cretaceous-Paleocene transgressional tectonics before and during India-Eurasia collision in Thailand, Myanmar and Malaysia. *Journal of Geological Society of London, 161*, 799–812.

Mukherjee, N. K., & Dhruba Rao, B. K. (1974). Geology of the Bhotang sulphide deposits, Rangpo, Sikkim. *Journal of Geological Society of India, 15*, 65–74.

Naha, K., & Ray, S. K. (1971). Evidence of overthrusting in the metamorphic terrane of the Simla Himalaya. *American Journal of Sciences, 270*, 30–42.

Nanda, L. K., Saxena, S. K., Chhabra, J., Gupta, R. K., & Singh, R. (1995). Geological control of uranium mineralization in Loharkhet area, Almora district, U.P. *Journal of Atomic Science, 3*, 11–16.

Nanda, M. M., & Singh, M. P. (1977). Stratigraphy and sedimentation of the Zanskar area Ladakh and adjoining parts of the Lahul region of Himachal Pradesh. *Himalayan Geology, 6*, 367–388.

Narayandas, G. R., Parthasarathy, T. N., Taneja, P. C., & Perumal, N. V. A. S. (1979). Geology, structure and uranium mineralization in Kulu, Himachal Pradesh. *Journal of Geological Society of India, 20*, 95–102.

Nautiyal, S. P., Jangpangi, B. S., Singh, P., Guha Sarkar, T. K., Bhate, V. D., Raghavan, M. R., et al. (1964). A preliminary note on the geology of Bhutan Himalaya. *Report of 22nd International Geological Congress*, Vol. 11, pp. 1–14.

Negi, B. S. (1967). Uranium mineralization in Pokhri-Tunji area Chamoli district, Quart. *Journal of Geological Mining Metallurgical Society of India, 39*, 93–97.

Pande, I. C. (1950). A geological note on the Ramgarh area, District Nainital, U.P. *Quarterly Journal of Geological Mining Metallurgical Society of India, 27*, 15–23.

Pande, I. C., & Powar, K. B. (1968). Petrology and emplacement of the Almora Granite. *Bulletin India Geological Association, 1*, 57–64.

Pande, I. C., & Virdi, N. S. (1970). On the Chareota window structure, District Mahasu, H.P. *Journal of Geological Society of India, 11*, 275–278.

Pandey, B. K., Singh, V. P., Kwatra, S. K., & Bhanot, V. B. (1980). Rb–Sr isotopic studies on the granitic and gneissic rocks of Baijnath crystallines, Kumaun Himalaya. *Himalayan Geology, 10*, 256–263.

Pandey, A. K., Virdi, N. S., & Gairola, V. K. (2003). Evolution of structural fabrics and deformation events in the Kulu-Rampur and Larji window zones, NW Himalaya, India. *Himalayan Geology, 24*, 1–21.

Parrish, R. R., & Hodges, K. V. (1996). Isotopic constraints on the age and provenance of the Lesser and Greater Himalayan sequences, Nepalese Himalaya. *Geological Society of American Bulletin, 108*, 904–911.

Paul, D. K., McNaughton, N. J., Chattopadhyay, S., & Ray, K. K. (1996). Geochronology and geochemistry of the Lingtse Gneiss, Darjeeling-Sikkim Himalaya: Revisited. *Journal of Geological Society of India, 48*, 497–506.

Pecher, A. (1989). The metamorphism in the central Himalaya. *Journal of Metamorphic Geology, 7*, 31–41.

Pecher, A., & Le Fort, P. (1977). Origin and significance of the Lesser Himalayan augen gneisses. In C. Jest (Ed.), *Ecologie et Geologie de l'Himalaya* (pp. 319–329). Paris: CNRS.

Pilgrim, G. E., & West, W. (1928). The structure and correlation of the Simla rocks. *Memoires Geological Survey of India, 53*, 140.

Powar, K. B. (1970). Multiphased mesoscopic folding in the metasediments of Almora area, Kumaun Himalaya. *Publications of the Centre Advanced Study in Geology, Panjab University, Chandigarh, 7*, 61–67.

Rai, S. M. (2001). Geology, geochemistry and radio-chronology of the Kathmandu and Gosainkund crystalline nappes, central Nepal Himalaya. *Journal of the Nepal Geological Society, 25*, 135–155.

Rai, S. M., Guillot, S., LeFort, P., & Upreti, B. N. (1998). Pressure-temperature evolution in the Kathmandu and Gosainkund region, central Nepal. *Journal of Asian Earth Sciences, 16*, 283–298.

Rashid, S. A. (2005). The geochemistry of Mesoproterozoic clastic sedimentary rocks from the Rautgara Formation, Kumaun Lesser Himalaya: Implications for provenance, mineralogy and weathering. *Current Science, 88*, 1832–1836.

Rawat, R., & Sharma, R. (2012). Features and characterization of graphite in Almora Crystallines and their implications for the graphite formation in Lesser Himalaya, India. *Journal of Asian Earth Sciences, 42*, 51–64.

Ray, S. (1947). Zonal metamorphism in the eastern Himalaya and some aspects of local geology. *Quarterly Journal of Geological Mining Metallurgical Society of India, 19*, 117–140.

Robinson, D. M., DeCelles, P. G., Patchet, P. J., & Garzione, C. N. (2001). The kinematic evolution of the Nepalese Himalaya interpreted from Nd isotopes. *Earth & Planet Science Letters, 192*, 507–521.

Roy, A. B., & Valdiya, K. S. (1988). Tectonomorphic evolution of the Great Himalayan thrust sheet in Garhwal region, Kumaun Himalaya. *Journal of Geological Society of India, 32*, 106–124.

Rupke, J. (1974). Stratigraphic and structural evolution of the Kumaun Lesser Himalaya. *Sedimentary Geology, 11*, 81–265.

Saklani, P. S., Nainwal, D. C., & Singh, V. K. (1991). Geometry of composite main central thrust in the Yamuna valley, Garhwal. *Neues Jahrbuch für Geologie und Palaeontologie: Monatshefte, 6*, 364–380.

Schwan, W. (1980). *Shortening structures in eastern and northwestern Himalayan Rocks*. New Delhi: Today & Tomorrow's. (62 p).

Searle, D. L., & Haq, B. T. (1964). *The Mogok Belt of Burma and its relationship to the Himalayan orogeny* (Vol. 11, pp. 133–161). Report 22nd International Geological Congress.

Searle, M. P., Metcalfe, R. P., Rex, A. J., & Norry, M. J. (1993). Field relations, petrogenesis and emplacement of the Bhagirathi leucogranite, Garhwal Himalaya. In P. J. Treloar & M. P. Searle (Eds.), *Himalayan Tectonics* (pp. 429–444). London: Geological Society.

Saxena, M. N. (1971). The Crystalline Axis of the Himalaya: The Indian shield and continental drift. *Tectonophysics*, *12*, 433–447

Shah, O. K., & Merh, S. S. (1976). Spilites of the Bhimtal-Bhowali Area, District Nainital, U.P. *Himalayan Geology, 6*, 423–448.

Shah, O. K., & Merh, S. S. (1978). Structural geology and stratigraphy of Bhimtal-Bhowali area in Kumaun Himalaya—A reinterpretation. *Journal of Geological Society of India, 19*, 91–105.

Sharma, R. P. (1971). Structural study of Mornaula area, district Almora, U.P.—A part of the Almora Nappe. *Journal of Geological Society of India, 12*, 387–391.

Sharma, V. P. (1976). Stratigraphy and tectonics of the southeastern part of the Jammu Himalaya—A new approach. *Miscellaneous Publication of Geological Survey of India, 34*(I), 185–216.

Sharma, C. K. (1980). Stratigraphy of Lesser Himalayan formations of western and far western Nepal. In K. S. Valdiya & S. B. Bhatia (Eds.), *Stratigraphy and correlation of Lesser Himalayan formations* (pp. 174–179). New Delhi: Hindustan Publishing Company.

Sharma, C. K. (1990). *Geology of Nepal Himalaya and adjacent countries*. Kathmandu: Sangeeta Sharma (479 p).

Sharma, K. K., & Rashid, S. A. (2001). Geochemical evolution of peraluminous Palaeoproterozoic Bandal orthogenesis, NW Himalya, Himachal Pradesh, India: Implication for the ancient crustal growth in the Himalaya. *Journal of Asian Earth Sciences, 19*, 413–428.

Singh, B. N., Geol, O. P., & Joshi, M. (1991). Chemical mineralogical classification of granitoid rocks: A case study from Dhunaghat area of Kumaun Lesser Himalaya. *Bulletin Indian Geological Association, 24*, 101–108.

Singh, S., Jain, A. K., & Barby, M. E. (2007). SHRIMP U–Pb ~1860 Ma anorogenic magmatic signatures from NW Himalaya: Implications for Palaeoproterozoic assembly. In *Palaeoproterozoic supercontinent and global evolution*. London: Geological Society of London.

Singh, R. P., Singh, V. P., & Bhanot, V. B. (1986). Rb–Sr ages of gneissic rocks of Rhee-Gangi, Bhatwari, Hanumanchatti and Naitwar areas of the central crystallines zone of Kumaun Himalaya, U.P. *Indian Journal of Earth Sciences, 13*, 197–208.

Singh, S. P., Singh, V. K., & Saklani, P. S. (1997). Metamorphism in the central crystallines of Higher Himalaya in Kedarnath valley, Garhwal Himalaya. *Himalayan Geology, 18*, 119–133.

Sinha-Roy, S. (1976). Tectonic elements in the eastern Himalaya and geodynamic model of evolution of the Himalaya. *Miscellaneous Publication of Geological Survey of India, 34*(I), 57–74.

Sinha-Roy, S. (1980). Terrace systems in the Tista valley of Sikkim-Darjeeling Himalayas and the adjoining piedmont region. *Indian Journal of Earth Sciences, 7*, 146–161.

Spencer, C. J., Harris, R. A., & Dorais, M. J. (2012). Depositional provenance of the Himalayan metamorphic core of Garhwal region, India: Constrained by U–Pb and Hf isotopes in zircon. *Gondwana Research, 22*, 26–35.

Srikantia, S. V. (1977). The Sundernagar Group: Its geology, correlation and significance as stratigraphically deepest sediment in Lesser Himalaya. *Journal of Geological Society of India, 18*, 7–22.

Srikantia, S. V., & Bhargava, O. N. (1984). The Jutogh klippen of the Simla area of the Himachal Himalaya; its geology and structural evolution. *Journal of the Geological Society of India*, *25*, 218–230.

Srivastava, G. S. (1982). Geology of Kishtwar region, Jammu and Kashmir State. *Miscellaneous Publications of the Geological Survey of India, 41*(II), 259–271.

Srivastava, A. K., Krassilov, V. A., & Agnihotri, D. (2011). Peltasperma in the Permian of India and their bearing on Gondwanaland reconstruction and climatic interpretation. *Palaeogeography, Palaeoclimatology, Palaeoecology, 310*, 392–399.

Stern, C. R., Kligfield, R., Schelling, D., Virdi, N. S., Futa, K., Peterman, Z. E., & Amini, H. (1989). The Bhagirathi leucogranite of the Higher Himalaya (Garhwal): Age, petrogenesis and tectonic implication. *Geological Society of American Special Paper, 232*, 33–45.

Stocklin, J. (1980). Geology of Nepal and its regional frame. *Journal of Geological Society of London, 137*, 1–34.

Tahirkheli, R. A. K. (1982). Geology of the Himalaya, Karakoram and Hindukush in Pakistan. *Geological Bulletin, Peshawar University, 15*, 1–51.

Thakur, V. C. (1987). Development of major structures across northwestern Himalaya. *Tectonophysics, 135*, 1–13.

Thakur, V. C. (1993). *Geology of western Himalaya*. Oxford: Pergamon Press. (366 p).

Thakur, V. C., Rawat, B. S., & Islam, R. (1990). Zanskar crystallines—Some observations on its lithostratigraphy, deformation and metamorphism and regional framework. *Journal of Himalayan Geology, 1*, 11–25.

Thoni, M., Miller, C., Hager, C., Grasemann, B., & Horschinegg, M. (2012). New geochronological constraints on the thermal and exhumation history of the Lesser and Higher Himalayan Crystalline units in the Kulu-Kinnaur area of Himachal Pradesh, India. *Journal of Asian Earth Sciences*, *52*, 98–116.

Trivedi, J. R., Gopalan, K., & Valdiya, K. S. (1984). Rb–Sr ages of granite rocks within the Lesser Himalayan nappes, Kumaun, India. *Journal of Geological Society of India, 25*, 641–654.

Upreti, B. N. (1990). An outline geology of far-western Nepal. *Journal of Himalayan Geology, 1*, 93–102.

Upreti, B. N. (1996). Stratigraphy of the western Nepal, Lesser Himalaya: A synthesis. *Journal of Nepal Geological Society, 13*, 11–28.

Upreti, B. N. (1999). An overview of the stratigraphy and tectonics of the Nepal Himalaya. *Journal of Asian Earth Sciences, 17*, 577–666.

Upreti, B. N., & Le Fort, P. (1999). Lesser Himalayan crystalline nappes of Nepal: Problems of their origin. *Geological Society of the American Special Papers, 328*, 225–238.

Upreti, B. N., Rai, S. M., Sakai, H., Koirala, D. R., & Takigami, R. (2003). Early Proterozoic granite of the Taplejung window, far-eastern Lesser Nepal Himalaya. *Journal of Nepal Geological Society, 28*, 9–18.

Valdiya, K. S. (1962). An outline of the stratigraphy and structure of the southern part of the Pithoragarh District, U.P. *Journal of Geological Society of India, 3*, 27–48.

Valdiya, K. S. (1963). The stratigraphy and structure of the Lohaghat subsdivision, District Almora, U.P. *Quarterly Journal of Geological Mining Metallurgical Society of India, 35*, 167–180.

Valdiya, K. S. (1970). Simla Slates, the Precambrian flysch of Lesser Himalaya; its turbidites, sedimentary structures and palaeocurrents. *Geological Society of American Bulletin, 81*, 451–468.

Valdiya, K. S. (1978). Extension and analogues of the Chail Nappe in the Kumaun Himalaya. *Indian Journal of the Earth Sciences, 5*, 1–19.

Valdiya, K. S. (1980a). The two intracrustal boundary thrusts of the Himalaya. *Tectonophysics, 66*, 323–348.

Valdiya, K. S. (1980b). *Geology of Kumaun Lesser Himalaya*. Dehradun: Wadia Institute of Himalayan Geology. (291 p).

Valdiya, K. S. (1981). Tectonics of central sector of the Himalaya. In H. K. Gupta & F. M. Delancy (Eds.), *Zagor–Hindukush Himalaya, geodynamic evolution, geodynamics series* (Vol. 3, pp. 87–110). Washington D.C.: Publication of the American Geophysical Union.

Valdiya, K. S. (1988a). Tectonic evolution of the central sector of Himalaya. *Transactions Philosophical of the Royal Society of London, A326*, 151–175.

Valdiya, K. S. (1988b). *Geology and Natural Environment of Nainital Hills*. Nainital: Gyanodaya Prakashan. (155 pp).

Valdiya, K. S. (1998). *Dynamic Himalaya*. Hyderabad: Universities Press. (178 p).

Valdiya, K. S., Paul, S. K., Chandra, T., Bhakuni, S. S., & Upadhyay, R. (1999). Tectonics and lithological characterization of the Himadri (Great Himalaya) between Kali and Yamuna rivers, Central Himalaya. *Himalayan Geology*, *20*, 1–17.

Valdiya, K. S., & Goel, O. P. (1983). Lithological subdivision and petrology of the Great Himalayan Vaikrita Group in Kumaun. *Proceedigns of the Indian Academic Sciences (Earth & Plantation Science*), *92*, 141–163.

Varadarajan, S. (1974). Prehnite-Pumpellyite metagreywacke facies of metamorphism of the metabasites of Bhimtal-Bhowali area, Nainital District, Kumaun Himalaya, India. *Himalayan Geology, 4*, 581–599.

Verma, P. K., & Tandon, S. K. (1976). Geological observations in a part of the Kameng District, Arunachal Pradesh. *Himalayan Geology, 6*, 259–286.

Wadia, D. N. (1928). The geology of the Poonch State (Kashmir) and adjacent portions of Panjab. *Memoires Geological Survey of India, 65*, 189–371.

Wadia, D. N. (1934). The Cambrian-Trias sequence of NW Kashmir. *Record of Geological Survey of India, 68*, 121–167.

Whittington, A. G. (1996). Exhumation over-rated at Nanga Parbat, northern Pakistan. *Tectonophysics*, *206*, 215–226.

Yadav, R. S. (1995). Uranium-gold mineralization around “horse” structure in the Proterozoic rocks of Rampur Group in Munish-Kaladi area, Shimla district, Himachal Pradesh. *Journal of Himalayan Geology, 6*, 17–22.

Chapter 11
Later Proterozoic and Early Cambrian in the Himalaya

11.1 Tectonic Layout

The Late Proterozoic to Early Cambrian sedimentary formations of the Purana spectrum occur in three lithotectonic zones of the Himalaya province (Fig. 11.1; Table 11.1). The windows and half windows carved by rivers in the thrust sheets of epimetamorphic and mesometamorphic rocks expose Proterozoic sedimentary succession. The larger part of this succession belongs to the Upper Mesoproterozoic–Neoproterozoic period, extending up to the Early Cambrian. In the central sector of the Himalaya province, the outer Lesser Himalayan part was uprooted and thrust 4–23 km southward during the Tertiary revolution, forming parautochthonous Krol Belt. This belt is made up of preponderant Neoproterozoic to Early Cambrian rocks. The third zone encompasses the transition from the Great Himalaya to the Tethys subprovince and embodies rocks of the Neoproterozoic and Early Cambrian times.

It may be recapitulated that the Proterozoic rocks of the Himalaya represent a thick and extensive deposit on the distal part of the passive continental margin of the Indian plate. Experiencing occasional tectonic unrest in the early stage, the lower part of this succession comprises argilloarenaceous sediments of the time extending from Late Palaeoproterozoic to Early Mesoproterozoic. They have been discussed in Chap. 10. These sediments pass upwards to preponderant calcareous and argillocalcareous sediments laid down in shallow-shelf platforms and lagoons under tectonically tranquil conditions. Except for intrusion of basic sills and dykes, there were no tectonothermal events of consequence to leave imprints in the geological record of the Lesser Himalaya in the Late Proterozoic era.

However, as the Neoproterozoic era closed, the situation changed. The change was drastic in some sectors. As the direction of earth's spin axis changed during the Vendian–Cambrian period, there was shifting of continental plates followed by

K.S. Valdiya, *The Making of India*, Society of Earth Scientists Series,
DOI 10.1007/978-3-319-25029-8_11

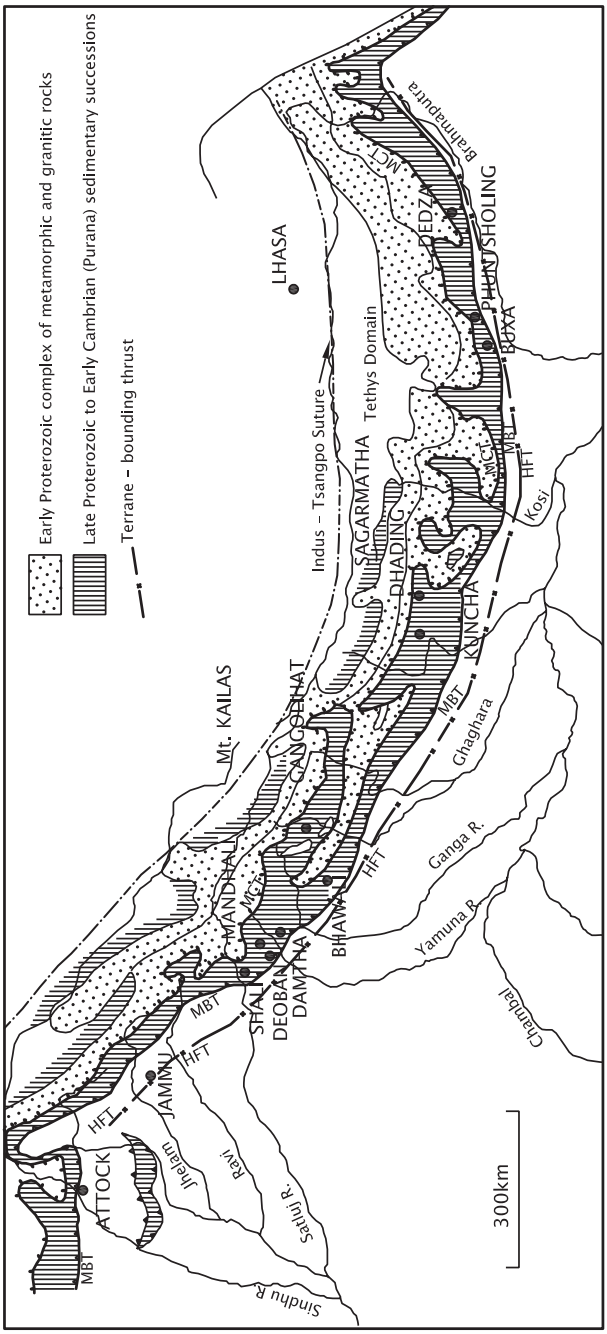

Fig. 11.1 Sketch map shows the Purana succession in the Himalaya province. The upper part of the succession belongs to the Late Proterozoic–Lower Cambrian time (Valdiya 1995)

Table 11.1 Later Proterozoic and Early Cambrian succession in different sectors of the Himalaya (Valdiya 1998a)

Age	Northern Pakistan	Jammu–Kashmir	Himachal Pradesh	Outer Lesser Himalaya in Himachal-Kumaun	Kumaun	Nepal	Sikkim–Bhutan	Arunachal Pradesh
Early Cambrian	Jhelam Fm.	Sincha Fm./Zilant Fm. (I)		Tal (O)		?		
Late Proterozoic	Hazira Fm. Salt Range Fm.	Baila Fm. Gamir Fm. (O)	Basantpur (I)	Krol (O)	Mandhali (I)	Robang (I) Malekhu (I) Benighat (I)		Saleri
	Shahkot/Sirban Limestone	Jammu Limestone (O)	Shali (I)	Blaini (O)	Deoban (I)	Dhading (I)	Buxa (O)	Dedza
Early Proterozoic	Hazara Slate/Attock Slate	Ramban Fm. (O) Dogra Slates (I)	Sundernagar (O)	Jaunsar (O)	Damtha (I)	Kuncha (I)	Phuntsholing (O)	Bichom

I Inner (northern) belt, *O* Outer (southern) belt, *Fm.* Formation, *Ls.* Limestone, *Lr.* Lower

their rifting and eventual separation between 850 and 750 Ma (Sankaran 2004). These geodynamic developments resulted in shifts of climate zones, disruption of ecosystems and isolation of organic communities, leading to diversification of life on earth. The period of tectonic turmoil and attendant developments in the Lesser Himalayan terrane is manifested in the variable sedimentary sequences, their rapid facies variation and the appearance of life in varied forms in the newly developed ecological niches.

11.2 Carbonate Sedimentation: Autochthonous Zone

11.2.1 Deoban Lithostratigraphy

Overlying the siliciclastic assemblage of the Ramban–Sundernagar–Damtha–Kuncha–Phuntsholing groups (Figs. 11.2 and 11.4), the carbonates form an extensive succession of cherty dolomites intercalated with bands and beds of blue limestones and grey slates. R.D. Oldham in 1883 recognized and named this succession as the *Deoban Limestone* after the Deoban peak north of Chakrata. It extends south-east (Fig. 11.1) into Kumaun and is described as the *Gangolihat Dolomite* in the Pithoragarh district (Valdiya 1962a, 1980b). The most notable and characteristics feature of the Deoban are algal bioherms made up of columnar-branching stromatolites (Misra and Valdiya 1961; Valdiya 1969). The carbonates comprise, in addition to predominant chemically precipitated dolomite and limestone of a wide variety, minor detrital calcarenites (pelletal, oolitic) and calcrudites (intraformational conglomerate) associated with stromatolitic bioherms. The stromatolites have a wide variety of shape and size, predominantly columnar branching in nature. An outstanding feature of the Gangolihat Dolomite is the occurrence of large and small lentiform deposits of crystalline magnesite between the Kali and Mandakini rivers (Misra and Valdiya 1961; Valdiya 1962a, 1968, 1980b). Associated with talc and steatite, the magnesite deposits have considerable economic importance. There are sporadic disseminations, pockets and veins of copper and lead sulphides in magnesite and associated dolomites. The Deoban extends north-west and is known as the *Shali* in Himachal Pradesh, the *Jammu Limestone* in the Vaishnodevi massif in Riasi district, and the *Sirban* or *Shahkot* in northern Pakistan. Towards east, the equivalents of the Deoban have been described as the *Dhading* in Nepal, the *Buxa* in the Darjiling–Sikkim–Bhutan sector and the *Dedza* in western Arunachal Pradesh (Table 11.1).

Distribution of zircon ages and whole-rock neodymium isotope composition demonstrates that the Gangolihat Dolomite in Uttarakhand is correlative with Rohtas Formation of Semri Group of nearly 1600 Ma depositional age in the Vindhyan Basin (Cawood et al. 2007). This implies that the whole Damtha–Gangolihat succession of the Lesser Himalaya belongs to the Palaeoproterozoic time span. Significantly, the detrital zircon age distribution for the sedimentary

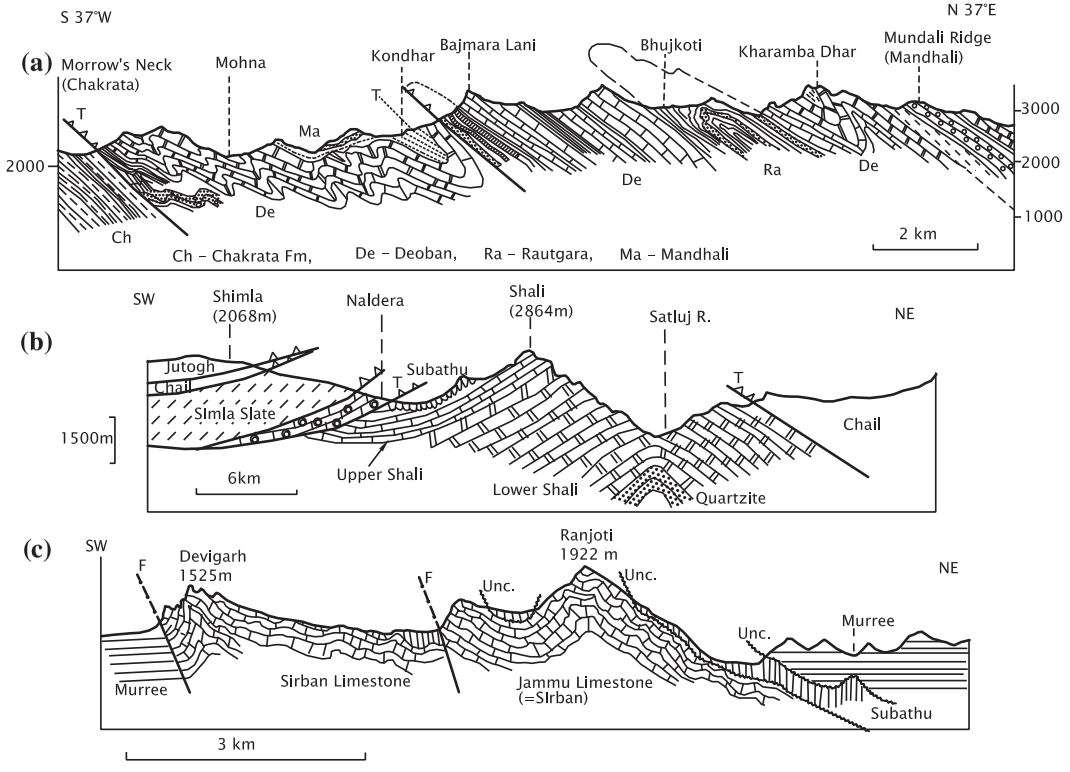

Fig. 11.2 Cross sections showing the stratigraphic positions of the Late Proterozoic carbonate formations in the Lesser Himalaya. **a** Deoban Limestone in western Uttarakhand (After Valdiya 1980b). **b** Shali Formation in eastern Himachal Pradesh (After West 1939). **c** Jammu Limestone in Ranjoti Peak in the Riasi district, Jammu (After Wadia 1937)

succession of the cratonic in northern India is remarkably similar to the distributions in the depositional coeval sedimentary rocks of the Lesser Himalaya, suggesting that both the regions shared similar detrital sources and that they are not separated (Cawood et al. 2007). This is exactly what was proposed long ago by Krishnan and Swaminathan (1959) and Valdiya (1964, 1970, 1976).

These findings negate the postulation that the Gangolihat Dolomite belongs to the Neoproterozoic on the basis of presence of microscopic features described as hexactinellid and monaxon sponge spicules (Tiwari 2008; Tiwari and Pant 2009).

11.2.2 Life in the Deoban Time

South of Rawalpindi in the Shahkot Limestone (≡Sirban) of the Gandgarh Range, R.D. Oldham had noticed "pseudo-organic structures resembling closely chambered heads", which he linked in 1883 to the structures discernible in the Deoban. The Deoban features were identified as cyanobacterial stromatolites (Misra and Valdiya 1961; Valdiya 1962a, 1969). The dominant type is the columnar-branching *Baicalia* of Middle Riphean (1350 ± 50 to 950 ± 50 Ma). The other types are *Minjaria*, *Kussiella* and *Maslowviella*, the first one being a typical Upper Riphean (950 ± 50 to 680 ± 50 Ma) form. On the basis of collective testimony of the stromatolites, the Deoban (Gangolihat) is placed in the transitional period between Middle Riphean and Upper Riphean, that is around 1100–900 Ma (Valdiya 1969, 1980b). At Chhera near Pithoragarh and near Ultrora south-west of Kapkot in the Pithoragarh district, an uppermost horizon of the Gangolihat has yielded isolated hexactinellid and monaxon sponge spicules of Lower Vendian age (Tiwari et al. 2000), implying that the temporal range of the Gangolihat carbonate formation extends up to Lower Vendian in the Neoproterozoic. The Shali in the Satluj Valley is, likewise, characterized by such stromatolites as *Colonella*, *Conophyton*, *Tungussia*, *Newlandia* and *Kussiiela* (Sinha 1977). The Jammu Limestone has an assemblage of *Colonella*, *Conophyton* and *Baicalia* (Raha and Sastry 1973; Raha and Das 1989). Coccoid and crustose cyanobacterial mats entombed in cherts of the Jammu Dolomite around Bidda indicate warm shallow hypersaline marine water in which these stromatolites proliferated (Venkatachala and Kumar 1997). Galena occurring in the top quartzite bed at Garan and Sarsenda give a Pb/Pb age of 967 Ma (Raha et al. 1978).

The Buxa Dolomites at Chillipam, Rupa and Dedza in the Kameng district and at Menga in the Subansiri Valley in Arunachal Pradesh show development of stromatolites characterized by vase-shaped microfossils suggesting Terminal Proterozoic–Lower Cambrian transition, and, significantly, $\delta^{13}C$ value in the Menga Dolomites ranges from +3.7 to +5.45 ‰ PDB and $\delta^{18}C$ value from −8.9 to −7.2 ‰ PBD (Tewari 2003).

11.2.3 Depositional Environment

Benthic algae flourished in abundance in the clear warm waters and formed stromatolites, building bioherms and biostromes. The formation of algal reef created protected environment like enclosed lagoons in the intertidal zones. Agitated waves and tides lashing the bioherms produced pelletal and oolite calcarenite and flat-pebble conglomerate consistently associated with the stromatolites (Valdiya 1980b). Locally in the enclosed lagoons of the subtidal zone developed conditions propitious for increase in phosphorous content, leading eventually to partial phosphatization of stromatolites and associated dolomites (Valdiya 1972). As the climate grew warmer and evaporation exceeded supply of water, concentration of $MgCO_3$ in the shallow barred basin increased, and magnesite was formed by late synsedimentary diagenetic replacement (Valdiya 1968). A good portion of magnesium might have been contributed by blue-green algae themselves which held footholds here and there.

11.2.4 Vendian Time: Mandhali Sediments

The dominant carbonate sediments of the Deoban gave way to a very thick argillocalcareous succession known as the *Mandhali Formation* (Figs. 11.2, 11.3 and 11.4). Locally dominated by euxinic facies, the assemblage consists of shale and slate interbedded with marlites and argillaceous limestones and large and small lenticular horizons of limestones and cherty-dolomitic limestones or dolomites. Locally, there are lense-shaped units of diamictites occurring at several levels. Occurring in the shallow water quiet environment of argillites, the diamictites represent debris flows, presumably triggered by tectonic disturbances. The tectonic disturbances were precursors of the impending tectonic upheaval that eventually terminated protracted Proterozoic sedimentation.

This variable succession was described by R.D. Oldham as *Mandhali* after a place Mundali in the Deoban massif. In Kumaun, Heim and Gansser in 1939 included the sequence in the upper part of what they called Calc Zones of Tejam and Badolisera. The Mandhali is a succession of olivegreen, grey and black carbonaceous and locally pyritic shale, interbedded with variegated marble and marlite. The basal conglomerate at Mundali is made up of clasts derived from the Deoban and the older Rautgara and embedded in the matrix of black limestones and shales. Elsewhere, the transition from the Deoban to the Mandhali is gradational. In the larger Mandhali spectrum, three units have been identified in Kumaun—the calcareous slates interbedded with argillaceous limestone and marlite with carbonaceous shales making the *Sor Slate*, the large lentiform horizon of dolomitic limestone constituting the *Thalkedar Limestone* (Valdiya 1962a), and the upper succession of grey-brown slates interbedded with fine-grained sandstone and siltstone forming the *Patet Slate* in the Pipalkoti–Tejam zone in the inner Lesser Himalaya (Kumar et al. 1976).

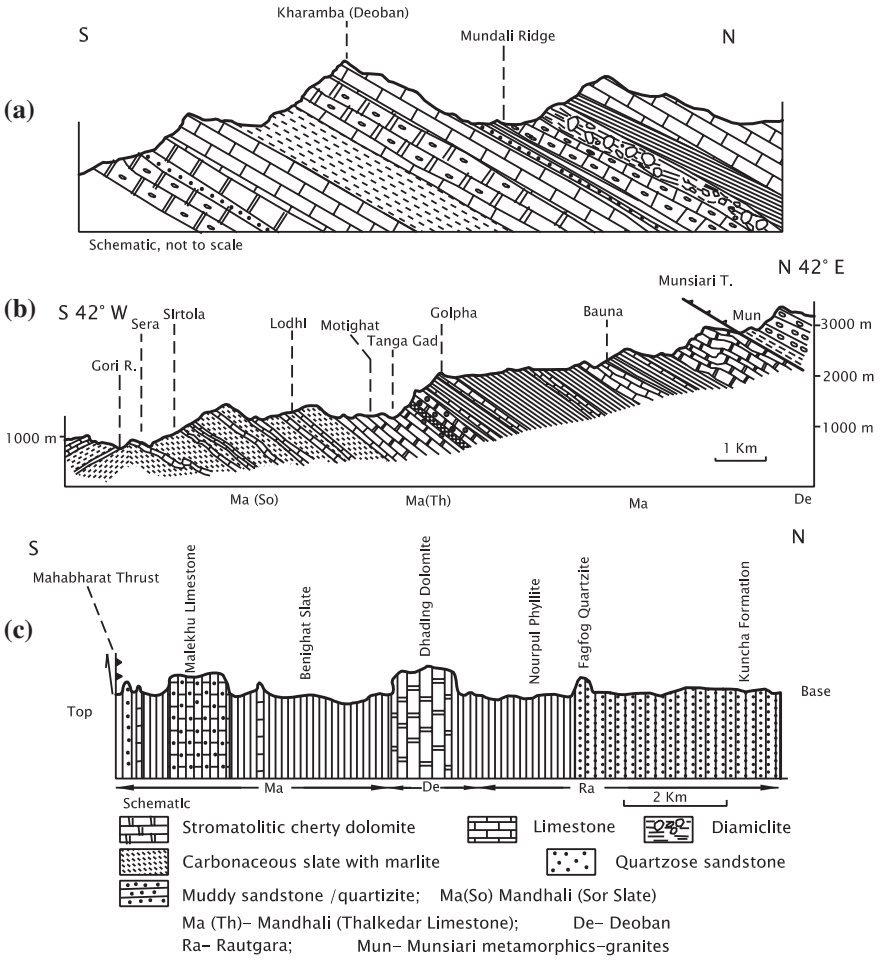

Fig. 11.3 Cross sections showing the stratigraphic positions and lithology of the Mandhali in different transects. **a** Type area Bawar in western Uttarakhand (After Valdiya 1980b). **b** Tanga Valley, Tejam zone, in Kumaun (After Valdiya 1980b). **c** Toppled column of Upper Nawakot in central Nepal (After Stocklin 1980)

The Mandhali extends into Himachal Pradesh as the *Basantpur Formation* which is thrust southwards (Srikantia and Sharma 1976). In northern Pakistan, the equivalent is known as the *Hazira Formation* and in the Gandgarh–Cherat–Attock Ranges described as the *Uttchkhattak* (Tahirkheli 1970; Yeats and Hussain 1987).

In Nepal, the Kali Gandaki, Budhi Gandaki and Trisuli rivers have exposed 5000-m-thick succession of the *Upper Nawakot* comprising the *Benighat Slate*, the *Malekhu Limestone* and the *Robang Formation* (Stocklin 1980), lithologically

comparable and correlatable with the Sor, the Thalkedar and the Patet. The Upper Nawakot Formations are units of Kumaun. In western Arunachal Pradesh, the Mandhali is represented by the *Saleri* (Das et al. 1976).

11.2.5 Life During the Vendian Transition

The Naldera Limestone of the Mandhali succession in Himachal Pradesh contains Late Precambrian *Osagia tenuilamellata* (Nalivkin 1966). The carbonate contains a suite of Upper Riphean to Vendian stromatolites, including *Jusussania Irregularia*, *Stratifera*, *Tungussia*, *Acaceilla* and *Inzeria* (Valdiya 1969) and *Jurusania* (Sinha 1977, 1989) very similar to those of the Thalkedar Limestone in Kumaun. This age assignment of the Thalkedar at Naldera places the younger Patet in the Late Vendian to Early Cambrian. Significantly, at Lameri, near Rudraprayag in the Alaknanda Valley, carbonaceous shale overlying the equivalent of Thalkedar Limestone yielded acritarchs of very Early Palaeozoic affinity (Agarwal 1974). In the Deoban mountain top, a tectonic slice representing the Mandhali contains *Illictica*, a Lower Cambrian stromatolite (Sinha 1977). Interestingly in Paristan in south-eastern Kashmir, the *Zilant* Formation (made up of chert, black shale with limestone cap) is characterized by Lower Cambrian microfossils (Raina et al. 1988). Overlying the Abbotabad Formation, the *Hazira* is made up of 150-m-thick ferruginous siltstone–shale with ferromanganese ores, phosphorites with barytes and thickly bedded reddish brown siltstones (Shah and Moon 2004). In the Hazira were found Lower Cambrian archiasters and calyptomids (Fuchs and Moestler 1972).

On the other side towards east, the upper succession of the south-easterly extension of the Tejam in western Nepal has been consistently described as Tal (of the parautochthonous Krol Belt) by Fuchs (1967, 1975, 1977; Fuchs and Frank 1970). In northcentral Nepal in the Kathmandu–Sagarmatha section, the sparry magnesite associated with carbonates—presumably the Thalkedar equivalent—exposed on the slope of the Magar-ko-danda revealed sporocysts' palaeobasidiospores of Late Proterozoic to Early Cambrian age (Brunel et al. 1985).

It seems that the upper part of the Mandhali extends into the Lower Cambrian time.

11.2.6 Mandhali Environment of Deposition

The Mandhali sediments (Fig. 11.4) were deposited in shallow water littoral environment. Under humid climate condition, development of semi-isolated basins due to the reefs built by prolifically growing algae promoted sedimentation in oxygen-deficient condition (Valdiya 1980b). The abundant carbonaceous shales and limestones testify to the existence of euxinic or anoxic environments in the Mandhali time. In northern Pakistan, geochemical analysis of the Hazira demonstrates

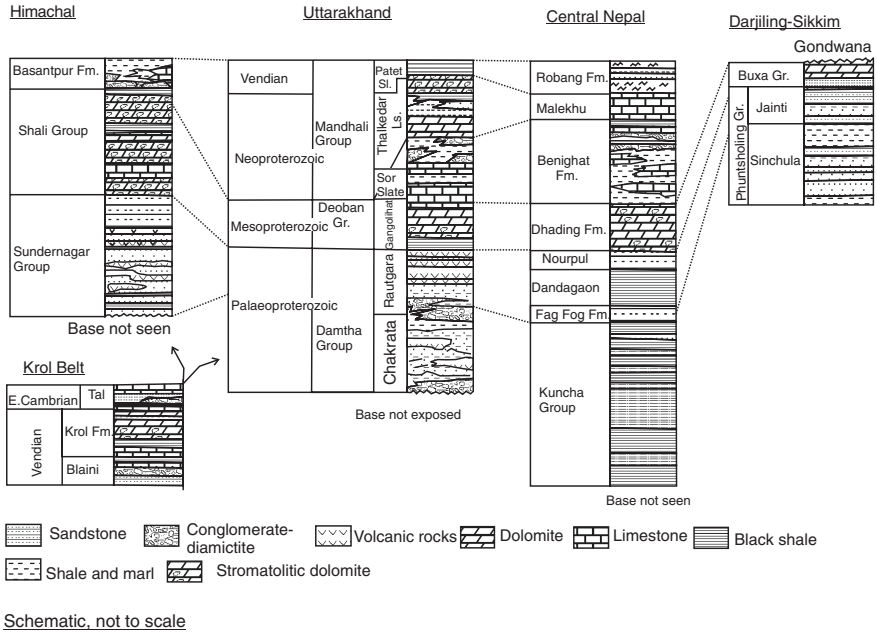

Fig. 11.4 Lithological columns of the Lesser Himalayan sedimentary succession in Larji window in the Beas Valley and the Dhauladhar Range (combined); Yamuna and Kali sections (combined) in Kumaun Himalaya; Trisuli–Mahabharat section in west central Nepal; and Sikkim–Bhutan in the east

"a line of descent from LREE to HREE with a small positive Ce-anomaly", the petrochemical characters suggesting the formation in shallow water on the continental shelf environment due to upwelling of anoxic deep-seated water (Shah and Moon 2004).

The Mandhali represents a time of tectonic disquiet manifested in submarine mass movements and formation of diamictites. These events, as already stated, were precursors to the orogenic upheaval that eventually brought about cessation of sedimentation all over in the Lesser Himalaya subprovince.

11.3 Parautochthonous Krol Belt

11.3.1 Tectonic Setting

As stated at the outset, the second zone of Proterozoic sedimentary rocks occurs in the southern part of the central sector of the Himalayan arc. Extending for 300 km from Solan in Himachal Pradesh to Nainital in Uttarakhand, the Krol Belt is named after the mountain peak south of Shimla by J.B. Auden in 1934. It comprises a chain of five en echelon basins (Figs. 11.4 and 11.5) constituting a doubly plunging

synclinorium defined by the Krol Thrust (Auden 1934, 1937; Hukku et al. 1974; Fuchs and Sinha 1974; Pande 1974; Valdiya 1980a, 1981, 1988). Thrusting along the Krol Thrust is responsible for 4–23 km of horizontal southward dislocation of the Krol Belt succession. The Krol Nappe in its southern flank is split by a multiplicity of faults and is truncated against the Siwalik terrane by the Main Boundary Thrust.

11.3.2 Lithostratigraphy

The Krol Nappe is made up of two groups of sedimentary rocks (Fig. 11.5)—the *Jaunsar Group* comprising the *Chandpur* and the *Nagthat* formations, and the *Mussoorie Group* consisting of the *Blaini*, the *Infrakrol,* the *Krol* and the *Tal* formations.

The *Chandpur* in the Bhumiadhar section of the Nainital Hills comprises lithicwacke and sublitharenite laterally grading into siltstone and shale that are characterized by ubiquitous limonite stain. Lenticular horizon of diamictite is intimately associated with greywackes (Valdiya 1988). The Chandpur sediments were deposited in a storm-dominated progradational shelf affected by a major transgression (Pant and Goswami 2002). In Himachal Pradesh, the tectonic situation has been variously interpreted by different workers. North of the Krol Hill syncline, the lower part of the Shimla Hill syncline is made up of a succession of the *Simla Slates* and the *Jagas Quartzite* (Pilgrim and West 1928), under the thrust sheets of epimetamorphic Chail and mesometamorphic Jutogh rocks. The Simla Slates is a shaly flysch facies consisting of greywackes and pelites. Characterized by such sedimentary features as graded bedding, load cast, ball-and-pillow structure, longitudinal microridges with transverse wrinkles, torose load cast, furrow and groove casts, flute cast and small-scale ripple cross-lamination (Valdiya 1980b), the Simla sediments were deposited by the north-westward-flowing turbidity currents in the distal part of the basin that was simultaneously swept by indigenous bottom currents flowing consistently in the easterly direction across the basin slope (Valdiya 1970). It seems that the detritus was derived from the northern edge of the then high Aravali Mobile Belt of the Peninsular India. Another view is that the Simla Slate represents a prograding muddy delta built by collapse of a carbonate shelf that formed in the basal part of the succession (Kumar and Brookfield 1987). Floods from distributaries and shelf storms caused very rapid deposition, mostly above wave base.

Over the Simla Slates, the *Jagas* is an attenuated horizon of pink and white quartzarenite with subordinate purple and maroon phyllites. In the Krol Belt, the Chandpur is overlain by a thick succession of the *Nagthat Formation* made up of white, fawn, pink and purple quartzite interbedded with subordinate variegated slates and locally associated with shoe-string-like body of oligomictic conglomerate. Three lithofacies are identifiable in the Nagthat succession in Mussoorie Hills: (i) cross-bedded (tabular and trough types) sandstones with lenses of conglomerate and erosional surfaces, (ii) medium-grained siliciclastics characterized

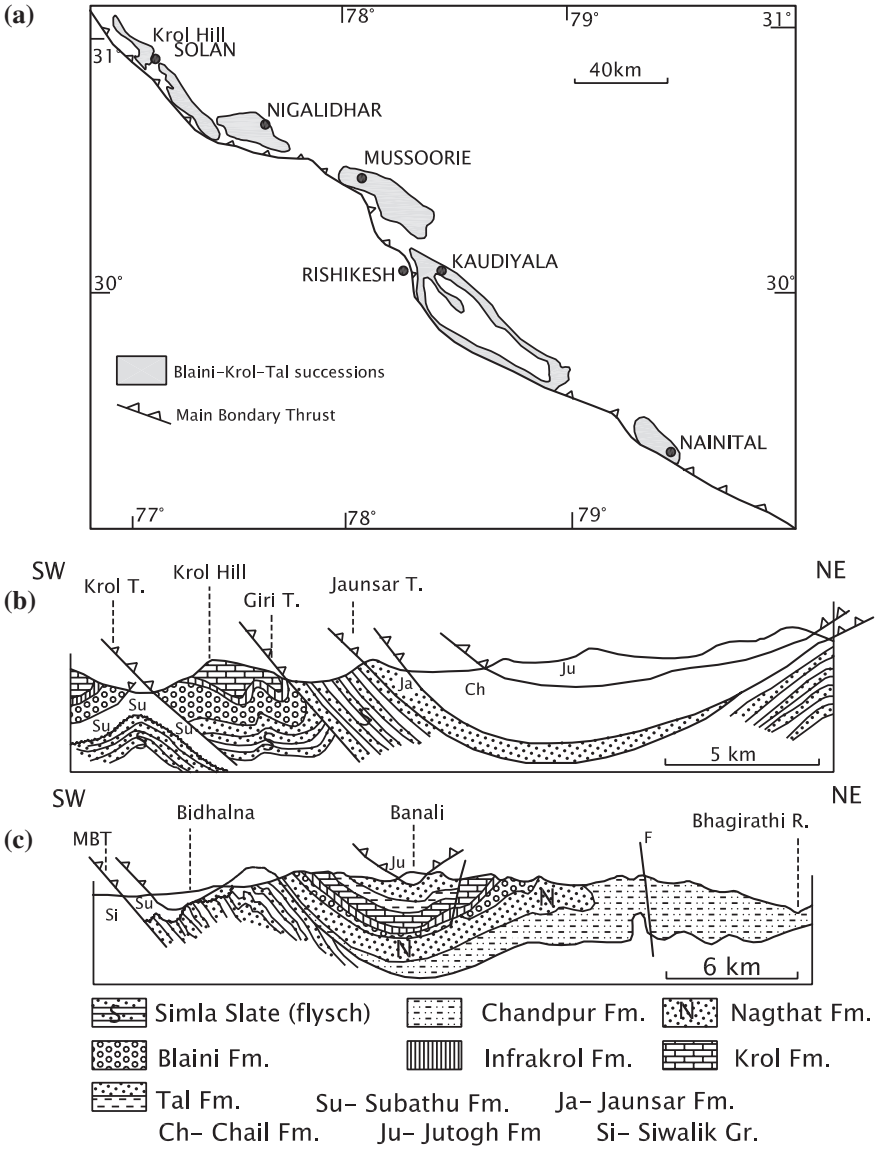

Fig. 11.5 **a** Krol Belt is a doubly plunging synclinorium comprising a chain of five basins. **b** Section shows the structure of the Krol Belt in Himachal Pradesh (After Auden 1934). **c** Lithostratigraphy and structure in the Mussoorie Hills (After Auden 1937)

by alternation of subarkose and quartzwacke showing herringbone-type cross-lamination and (iii) fine-grained siliciclastics showing parallel to cross-lamination in silty sandstone and shale (Ghosh 1991a, b). The multistoried sedimentary complex

of the Nagthat is a shoreface to proximal inner shelf deposit representing a prograding delta developed under dominant influence of tides and occasional storms. In the Nainital Hills, the Nagthat succession is a deposit laid down by currents that flowed in the NE, E and SW directions along shallow shore in the Nainital part of the basin (Valdiya 1988). Lateral and vertical distributions of various lithofacies demonstrate deposition in a progradational barrier-island system in subtidal upper shoreface and channels, subtidal longshore bars, foreshore beachface, tidal channels, intertidal sandflat channel and mixed flat environments (Shukla and Pant 1996; Pant and Shukla 1999).

The *Blaini Formation* begins with polymictic conglomerate intimately associated with greenish brown sandstone, calcareous sandstone, purple shale and deep pink or red dolomitic limestone. While the purple siltstones are characterized by flutecasts and small-scale cross-stratifications, the pink limestone locally exhibits algal mats. Rounded, subrounded clasts of quartzites, phyllites and marble are embedded in sandy matrix of the conglomerates characterized by imbrication of clasts, pointing to NNE direction of palaeocurrents in the Kilberry–Pangot belt of the Nainital Hills (Valdiya 1988). The Blaini diamictites are believed to be glacial tillites (Gaur and Dave 1971; Bhargava 1972; Niyogi and Bhattacharya 1971; Jain and Varadaraj 1978) as first suggested by R.D. Oldham in 1883. The tillites can be related to the global event within the period 900–540 Ma. The warmer climate that followed resulted in the melting of ice in a very short geological time, giving rise abruptly to precipitation of ferruginous red and pink dolomitic limestones. In the Nainital Hills, imbrication of rounded to subrounded clasts in Blaini sandstones and sedimentary features like cross-bedding indicate that the sediment deposition took place in a supratidal to intertidal environment under warmer climate condition (Tangri and Singh 1982; Valdiya 1988). The NE, NNW and less common SE and SW palaeocurrent directions indicate dominant tidal dispersal, in addition to longshore currents at an earlier stage (Pant and Goswami 2003). The other view is that the diamictites were produced by submarine slides in an environment of tectonic instability (Rupke 1968, 1974; Valdiya 1980b). The uppermost unit of the Blaini Formation, known as *InfraKrol*, is a succession of ashgrey and black carbonaceous shales, locally containing pyrite and nodules of phosphate. In the InfraKrol time, it was deposition as tidal-flat sediments in the lagoonal environment characterized by euxinic conditions.

The InfraKrol is succeeded by the *Krol Formation*. A sequence stratigraphic study backed up by carbon isotope analysis (Fig. 11.6) reveals existence of a regional stratigraphic discontinuity marked by less than 60-m-deep incised valleys and irregular relief, regional flooding surfaces and subaerial dissolution and weathering calcrete and breccia filling fissures and cavities, all through the 300-km expanse of the Krol Belt (Jiang et al. 2002, 2003). The Krol consists of calcareous limestone with minor gypsum in some places and carbonaceous shale at the base (*Krol A*). This is overlain by red and purple ferruginous shale interbedded with biohermal stromatolitic dolomite (*Krol B*). Still higher up, massive dark grey and blue dolomite characterized by pervasive brecciation and such structures as fenestral, shrinkage and pinch-and-swell structures and cross-bedding in

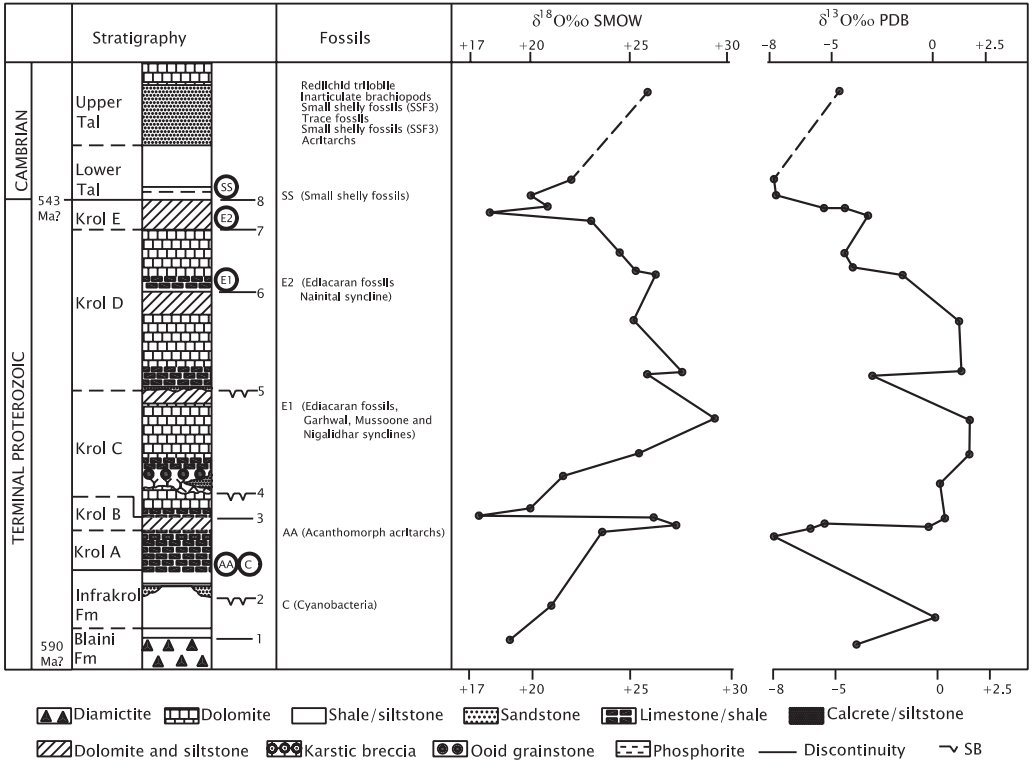

Fig. 11.6 Lithological succession of the InfraKrol–Krol and Tal formations showing reported fossil finds, interpreted stratigraphic discontinuities and carbon isotope excursion (Jiang et al. 2002; Mathur et al. 1997)

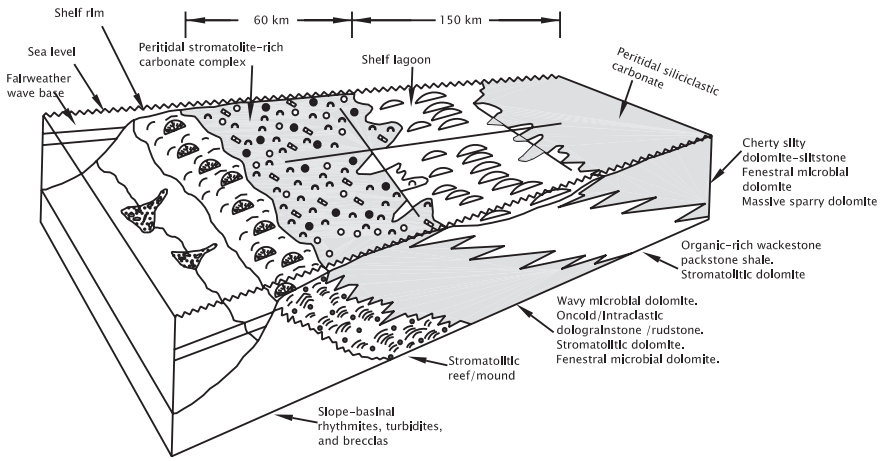

Fig. 11.7 Model portraying the geometry and facies distribution of a peritidal shelf of the Krol platform (After Jiang et al. 2003)

calcarenite form the *Krol C*. This unit is succeeded by a horizon made up of rhythmic alternation of thinly bedded black shale with marlite and carbonaceous limestone showing convolution and pinch-and-swell structure (*Krol D*). The uppermost horizon (*Krol E*), well-developed in the Sherwood College campus in the Nainital Hill, is a sequence of cherty dolomite which is locally phosphatic. The dolomite is characterized by short columnar branching, domal, plumose, oncidal and laminated stromatolites, associated with pelletal and oolitic calcarenite (Fuchs and Sinha 1974). The Krol carbonates were deposited in shallow lagoons along the coast—behind barrier beaches, which later changed to tidal flats (Awasthi 1970; Niyogi and Bhattacharya 1971; Kharkwal and Bagati 1974), which were evaporitic in parts during the mid-Krol time (Gundu Rao 1970). It seems that the intertidal conditions of the Middle Krol (Fig. 11.7) time became lagoonal towards the later period when formation of bioherms gave rise to pockets of restricted water circulation and resulted in the development of euxinic condition in the peritidal belt (Valdiya 1988).

The *Tal Formation* (Auden 1934; Bhargava 1975; Shanker 1975; Valdiya 1988) is made up of two members. The lower member comprises carbonaceous–pyritic black shale with subordinate black limestone showing stromatolites and penecontemporaneous deformation structures. Characterized by phosphatic nodules and lamine, it becomes a prominent chert–phosphorite horizon in the Mussoorie Hills. The upper member is made up of ripple-marked sandstone–siltstone interbedded with purple brown and grey shales. Towards the end of the Krol time, the chemistry of sea water had changed. The carbon isotopes show marked negative excursion, and there was concentration of such trace elements such as Ba, Cu, Zn, Ni, U and V and increase in the contents of phosphorous and organic carbon across the Krol–Tal boundary (Banerjee et al. 1997). The Tal Basin was shallow, and algal

reefs caused restriction in the circulation of water, so that lagoons and enclosed embayments had anoxic environment in the back-shelf side (Valdiya 1980a, b). Possibly, basin upwellings moved the organic-rich anoxic water to the coastal flats, leading to widespread episodic deposition of black shale, organic-rich chert and dark grey phosphorite It may be pointed out that chemostratigraphy of the Blaini–Krol–Tal succession demonstrates that the Neoproterozoic–Cambrian transition lying in the Lower Tal is characterized by $\delta^{13}C$—4 ‰ PDB (Tewari and Sial 2007).

11.3.3 Lithostratigraphical Comparison of Krol Belt and Autochthonous Zone

It is apparent that the Jaunsar Group made up of Chandpur and Nagthat formations of the Krol Nappe is comparable in lithology with the Damtha Group comprising Late Palaeoproterozoic to Mesoproterozoic Chakrata and Rautgara formations of the autochthonous zone. In the autochthonous zone, the Damtha succession is overlain by Deoban and Mandhali formations of the Tejam Group, while in the Krol Belt, the Jaunsar Group made up of the Chandpur and the Nagthal is succeeded by Mussoorie Group of the Krol Belt which is made up of the Blaini–Krol–Tal succession. The testimonies of stromatolites, acritarchs and other microbiota favour placing the Mandhali in the temporal range of Upper Vendian (680–570 Ma) to Lower Cambrian (542–513 Ma). The Tal is characterized by definite Lower Cambrian fauna. It seems that the autochthonous Tejam Group of the Deoban and Mandhali formations, correlatable with the parautochthonous to allochthonous Mussoorie Group of the Blaini, Krol and Tal formations, is a Neoproterozoic to Lower Cambrian succession.

11.3.4 Life in the InfraKrol–Krol Time

The chert nodules and shales of the InfraKrol in the Nainital and Nigalidhar areas contain prokaryotic and eucaryotic organic-walled and multicellular microfossils comprising cyanobacterial filaments, coccoids, large acanthomorphic acritarchs and thallophytic algae (Tiwari and Azmi 1992; Tiwari and Knoll 1994; Tiwari 1996; 1999; Tiwari and Pant 2004). The Krol stromatolites have been identified as *Stratifera*, *Irregularia* and *Conophyton* of Vendian/Yudomian age (Tewari 1984). In the uppermost horizon—including the Sherwood Member in the Nainital Hills—the occurrence of small shelly fossils such as *Caleoloids typicalis*, *Olivooides alveus*, *Spiellus columnorus* and *Anabarites trisulitos* (Bhatt and Mathur 1990; Bhatt 1996) indicates the first appearance of preservable life forms.

11.3.5 Appearance of Shelly Fauna in Tal

The marked negative excursion of carbon isotope ratio ranging from −8.4 ‰ to −2.6 ‰ together with high proportion of organic carbon buried in the phosphorite and black shale in the basal Tal was accompanied by the first appearance of small shelly fossils in the Nigalidhar, Mussoorie and Nainital subbasin (Azmi 1983; Azmi and Pancholi 1983; Bhatt et al. 1983; Brasier and Singh 1987; Bhatt and Mathur 1990; Bhatt 1996). The appearance of the shelly fauna heralded the coming of a variety of organism that had preservable body parts, such as conodonts; trilobites *Redlichia noetlingi;* and brachiopods *Obolus*, *Obolella and Lingulella* (Rai and Singh 1983; Kumar et al. 1983; Tripathi et al. 1984; Joshi et al. 1989; Bhargava et al. 1998), hexactinellid and siliceous sponge spicules (Mazumdar and Banerjee 1998) and a variety of microscopic biota (Tiwari and Azmi 1992; Tiwari 1996). The trilobites and brachiopods place the Tal Formation in the Lower Cambrian (Tommotian) epoch.

Far west in the Salt Range, the Early Cambrian trilobite *Neobolus* suddenly appeared in shales overlying the magnesian sandstone of the Jhelam Formation (Tahirkheli 1982; Gee 1989).

11.3.6 Sudden Diversification

It is obvious that towards the end of the Neoproterozoic suddenly around 550 Ma, the cyanobacteria-dominated sea was swarmed by diverse type of complex multicellular life forms, including sponges, trilobites and brachiopods. And they evolved rapidly, culminating in what has been described as *Cambrian Explosion of Life* or *Evolutionary Big Bang*. There was maximum diversification globally during 550–543 Ma interval (Shields 1999).

This biological event of great moment is attributed to burst of voluminous methane and/or emplacement of flood basalts, particularly in submarine environment which provided nutrients and materials for building of preservable skeletons of the organisms. There must have been climate shift that changed the regional ecosystems and created, among other things, isolated communities of organisms. This isolation prompted natural selection and diversification of life. There is also a suggestion that increase in oxygen level (by 5–15 % of the present level) that took place in the Neoproterozoic may have sparked a biological revolution.

11.4 Transition in the Salt Range

Along the north-western flank of the Sindhu Basin, a Neoproterozoic succession known as the *Salt Range Formation*—earlier described as the Saline Series (Gee 1989)—forms the hills of the Salt Range (Fig. 11.8). The 800–2000-m-thick

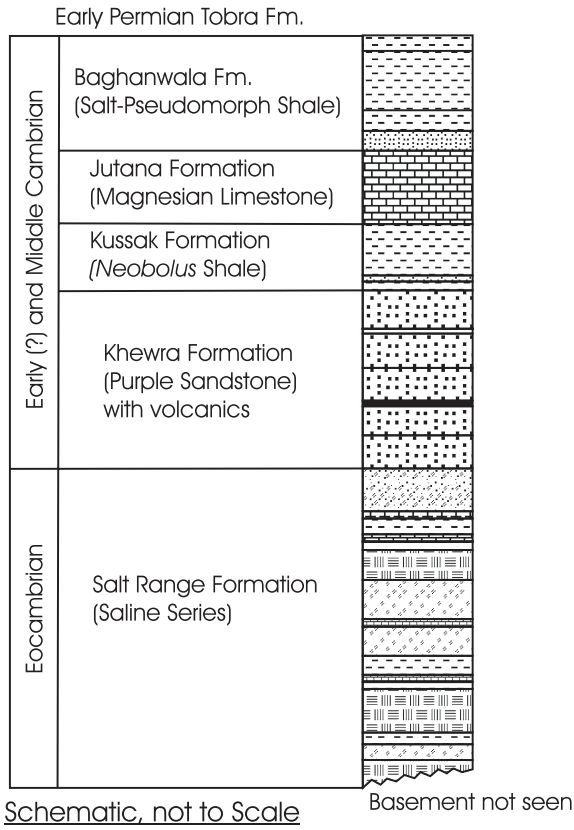

Fig. 11.8 Lithology shows the transition from Neoproterozoic to Lower Cambrian in the Salt Range (After Gee 1989)

alternation of gypsum and red clay is capped by ultrapotassic porphyritic lava known as the *Khewra Traps*. It occurs widely—under the cover of the alluvial deposits of the Sindhu River including the foredeeps in front of Kohat–Potwar and Sulaiman ranges (Kazmi and Qasim Jan 1997). The Salt Range evaporite formation is succeeded without break by the *Jhelam succession* (Tahirkheli 1982) of magnesian sandstone and shale, the latter characterized by Lower Cambrian *Neobolus* (Gee 1989). The Jhelam Formation marks the end of the Purana sedimentation.

11.4.1 Time of Desiccation

Evaporites occur widely in north-west India at the terminal stage of the Neoproterozoic era—the Ropri–Mandi belt in Himachal Pradesh (Srikantia and Sharma 1972), in the Sincha area in the Ramban belt in Kashmir (Virdi 1990), the

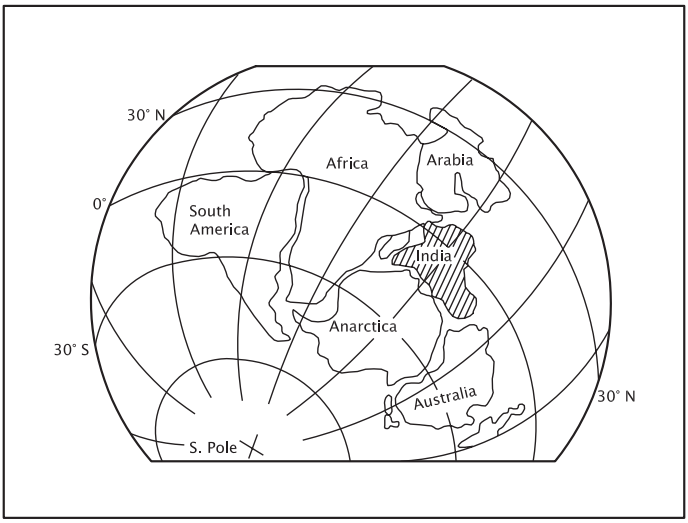

Fig. 11.9 India was close to the equator towards the end of Neoproterozoic and beginning of the Early Cambrian when quite a part of the subcontinent was affected by dessication (After Virdi 1990)

Salt Range in Pakistan (Gee 1989) and the Hanseran belt in Marwar (Dasgupta et al. 1988). These occurrences imply desiccation just before the advent of the Phanerozoic era that was full of life. In the Vindhyan Basin of the Peninsular India, evaporitic condition had begun a little earlier as evident from salt pseudomorph in shales of the Upper Bhander (Misra 1969). The desiccation occurred in the period 570–525 Ma when India was near the equator (Fig. 11.9). It was but natural that in some parts of the continental marginal sea where evaporation exceeded precipitation, there was concentration of salts in the waters of barred basin.

11.5 Proterozoic–Lower Cambrian Transition in Tethys Domain

Overlying the crystalline complex of the Great Himalaya, the 10–12-km-thick sedimentary succession of the Tethys domain occurs in a number of basins (Fig. 12.1). Putting a boundary between the crystalline basement and the covering sedimentary pile is beset with difficulty in view of transitional passage in some areas and tectonic detachment or faulting in other sectors (Berthelsen 1951, 1953).

In Himachal Pradesh, the high-grade metamorphics of the Vaikrita Group are transitionally succeeded by metamorphosed muddy flysch described by H.H. Hayden in 1904 as the *Haimanta* or as the *Batal* by S.V. Srikantia in 1981. The transition zone Batal gives way gradationally through greywacke–slate assemblage

the *Kunzumla* (Bhargava 1991) to what Hayden had called the Parahio series. The *Parahio Formation* consisting of more than 1350 m of dominantly siliciclastic sediments is characterized by numerous medium-scale shallowing cycles in deltaic lobes (Myrow et al. 2006). The palaeocurrents suggest northward prograding fluvial–deltaic depositional system. The Parahio is characterized by Early Cambrian trilobite *Olenus*. In north-eastern Kumaun, Heim and Gansser (1939) showed the Vaikrita passing gradually into slightly metamorphosed *Martoli* flysch. In the flyschoid maroon phyllite rhymically alternating with siltstone, representing the north-western extension of the Martoli Fm of Kumaun and south-eastern continuation of the Kunzumla Formation of Himachal Pradesh, well-preserved trace fossils produced by trilobites such as *Cruziana*, *Dimorphicnus and Rusophycus* along with worm tracks have been found at Lal Devata Temple in the Jadhganga Valley, NNW of Gangotri (Upadhyay and Parcha 2012). In the Tsarap Valley in Ladakh, the Zanskar Crystallines are overlain by mildly trace metamorphosed argillites and siltstones of the *Phe Formation* (Nanda and Singh 1976; Baud et al. 1984; Gaetani et al. 1985; Fuchs 1987). The Phe is a succession of massive to laminated wacke–sandstone that are locally micaceous and conglomeratic greywacke characterized by clay galls, groove cast, flute casts, load cast convolutions and scour marks. The horizon contains trace fossils including *Cruziana* (Srikantia 1981; Bhargava and Srikantia 1985). The Kunzumla/Phe (Lower Haimanta) bears strong lithological resemblance with the Salkhala of Kashmir. The *Salkhala* in the Pir Panjal Range (Thakur et al. 1990) is made up of metamorphic rocks which imperceptibly grade into the flysch assemblage described as the *Dogra Slate* by Wadia (1934). The Dogra Slate comprises argillites and wacke–sandstones with lenticular beds of diamictites (*Machhal*) giving way up to the Cambrian Formation the *Lolab* in the Hundwara–Kupwara belt and the *Nutunus* in the Liddar Valley (Shah 1982, 1991) and Redlichid trilobites (Shah et al. 1980). In the Pohru Valley, the Precambrian–Cambrian boundary sequence contains sponge spicule with an assemblage of small shelly fossils (Tiwari 1997).

In Nepal, the Annapurna Gneiss of the Vaikrita complex is succeeded with a sharp break by an attenuated horizon of phyllites, greywackes and acidic tuff of the *Sanctuary Formation* (Colchen et al. 1986). Similar is the situation in the Dolpho–Dhaulagiri massif (Fuchs 1967). In the Marsyangdi Valley, the augen gneiss of the Great Himalayan complex gives way to the geochemically similar *Larjung Formation*, made up of the carbonates in the Chame–Mustog belt and the latter overlain by the Ordovician Nilgiri Limestone (Upreti 1999). In the TangChu–WachuLa area in Bhutan, the high-grade Thimpu is succeeded by the low-grade Chekha Formation, and the latter passes upwards through metamorphosed amygdaloidal andesite–dacite volcanics (Singhi) and quartzarenite–conglomerate sequence (*Deshichiling*) to fine-grained quartzite–slate succession (*Maneting*) containing Early Cambrian trace fossils in the lower part and brachiopod *Lingulella* and Lower Cambrian trilobites in the upper part (Tangri et al. 2003).

11.6 Chaung Magyi Group

Overlying the basement of the Mogok complex, the *Chaung Magyi* is a 3000-m-thick succession of mildly metamorphosed flysch (Fig. 10.13. It has been assigned to the Late Proterozoic period (Searle and Haq 1964). Between the Shan States and the Salween River in the east, the Chaung Magyi rocks form about 2000-m-high mountain ranges trending N–S. Its arched up parts occur as inliers within the terrane of the Plateau Limestone. In the Ye-ngan area in Southern Shan States, the Chaung Magyi comprises in the lower part a sequence of greywacke, felspathic subgreywacke, mudstone and shale. There are intercalation of dolomite and green limestone. The siliciclastics are characterized by graded bedding, flute and groove casts, giving way upwards to cross-bedded sandstone and shale with burrows, indicating deposition in the delta-top and delta-slope under shallow water (Garson et al. 1976).

11.7 Pan-African Tectonism

11.7.1 Manifestation

After life had diversified in various forms, and proliferated in the Himalaya province, and sedimentation had continued in environments varying from open shelf to anoxic lagoons, there was a tectonic upheaval. The tectonic movements resulted in wholesale cessation of sedimentation in the entire Lesser Himalaya subprovince and in the whole of Peninsular India and caused pronounced interruption in basin-filling in the Tethys domain (Valdiya 1993a, 1995). This interlude of non-deposition varied in temporal span from sector to sector. The tectonism manifested itself in (i) deformation of rocks, including tilting and folding; (ii) widespread granitic activity; and (iii) cessation of sedimentation in the Lesser Himalaya and its interruption in the Tethys domain.

11.7.2 Deformation

In the Rohtang Pass in Himachal Pradesh, the Vaikrita rocks under the Tethyan sedimentary pile show NE–SW trending folds and NE/ENE–SW/WSW-oriented upwarps associated with Shyarma Fault—the fault that exercised control on emplacement of sediments and transverse pattern of their facies variation (Bhargava 1991). About 20 km south of Muth in the Pin Valley, the pre-Ordovician rocks below an unconformity are deformed into mesoscopic upright folds with their axial planes dipping 30°NW (Grassemann et al. 1997). A well-marked

unconformity between the Kunzumla (Haimanta) and the younger Thango conglomerate in the Zanskar–Lahaul region argue strongly for the tectonic upheaval and attendant marine regression in the Cambro–Ordovician interval.

Manifestation of Early Palaeozoic tectonism was, in addition to moderate- to high-grade metamorphism, a large-scale southward thrusting as witnessed in the Kathmandu sector where there was folding of garnet-grade metamorphic rocks and offsetting along faults *prior to* the emplacement of the 476.3 ± 3.4 m.y. old Palung Granite (Stocklin and Bhattarai 1979; Stocklin 1980). In the Kinnar Kailas area in eastern Himachal Pradesh, the 488-million-year-old Kinnar Kailas Granite intrudes the regionally folded kyanite–sillimanite schist (Marquer et al. 2000). In the Zanskar area in the Tethyan strata, the Middle Ordovician conglomerate contains sediments representing a foreland basin of a thrust belt that was active during the Late Cambrian through Middle Ordovcian time (Garzanti et al. 1986). And in the Koraikhola in far-western Nepal, a 30-m-thick conglomerate sequence at Damagad comprises clasts of *pre-Ordovician metamorphic rocks* along with 530–480 Ma detrital zircon in the sediments (Gehrels et al. 2006).

Along the border of Uttarakhand–Himachal Pradesh, in the Tons Valley, the Proterozoic sedimentary succession rests as pile of sheets upon the Middle Cambrian Chilar Formation which also occurs as tectonic slices within the thrust sheets (Bhargava et al. 2011). Taken in conjunction with the existence of a distinct unconformity between the Cambrian and the overlying Ordovician in the Tethys domain, Early Palaeozoic metamorphism and widespread emplacement of Early Palaeozoic granites, there is a strong case for Late Cambrian deformation in the Lesser Himalaya (Bhargava et al. 2011).

11.7.3 Volcanism

Volcanic explosion and eruption in many areas were precursors to the tectonic upheaval that overtook the Himalaya in the Cambro–Ordovician time. In Pakistan, the Salt Range Formation is capped by a thin sheet of ultrapotassic porphyritic lavas described as the *Khewra Traps* (Jan and Faruqi 1995). The Khewra underlies the Cambrian fossil-bearing Jhelam Formation. In the Suran Valley in Punch district (Kashmir) between the Dogra Slate and the Tanawal of the Cambrian spectrum, ichnofossil-bearing slates are interbedded with dominant spilitic lavas, tuffs and associated keratophyre dykes which constitute the *Bafliaz Volcanics* (Wakhaloo and Shah 1968; Sharma and Gupta 1972). To the south-east in the Spiti Basin, the greywackes and slates of the Kunzumla are interbedded with basaltic tuffs (Fuchs 1982, 1987). In Kinnaur in north-eastern Himachal Pradesh, the Hilap succession contains acid tuffs (Bhargava and Bassi 1998; Bhargava 2000). In the Kali Valley in north-eastern Kumaun, chlorite schist and K-bentonite representing an altered basic tuffs occur in the lower part of the Garbyang Formation (that succeeds the flyschoid Martoli–Ralam sequence) (Gansser 1964). In the Annapurna

massif in Nepal, acid tuffs and lavas occur in the *Yellow Formation* (≡Larjung) of the probable Cambrian age (Colchen et al. 1986). Between the Precambrian Chekha and Late Precambrian Deshichiling in the Black Mountain in Bhutan occurs nearly a hundred metre thick horizon (the Singhi) of amygdaloidal andesite and dacite interbedded with quartzarenite (Tangri and Pande 1995a, b) (Table 11.2, Fig. 11.10).

11.7.4 Granitic Activity

Strikingly leucocratic, the 500 ± 25 million-year-old granites occur extensively in the upper part of the low- and medium-grade metamorphic nappes of the Lesser Himalaya, in the lower part of the high-grade metamorphic rocks of the Vaikrita, and in the domal upwarp in the proximity of the Indus–Tsangpo Suture (Fig. 11.10; Table 11.2). The suture represents the junction of India and Asia. These granites belong to the 10,000-km-long girdle of the Cambro–Ordovician granites embracing Afghanistan, the Himalaya, Australia, and Antarctica (Le Fort et al. 1986)—the landmass that once formed a supercontinent. The granites are products of anatexis of the continental crust that was rifted and attenuated. The thermal events were not restricted to the Himalaya province, the south-western part of Rajasthan also witnessed the granitic activity during nearly the same period, as testified by the 510 ± 10 Ma Sendra Granite (Gangopadhyay and Lahiri 1984). In the distant Kerala, the 550 ± 15 Ma Ponmudi Charnockite (Choudhary et al. 1992), representing widespread charnockite emplacement in the Southern Granulite Terrane, shows that even South India did not escape the Pan-African granitic activity.

The Cambro–Ordovician peraluminous granites are identical in petrological and geochemical characters all through the expanse of the Himalaya—quartz + felspar + plagioclase + biotite + muscovite ± garnet ± tourmaline ± cordierite ± andalusite ± sillimanite. Granitic bodies of all sizes, including batholithic dimension such as the *Badarinath Granite* in Uttarakhand, occur extensively in the Vaikrita succession, particularly in the upper part. They have thrown out a network of dykes and veins of adamellite, aplite and pegmatite. There was a large-scale permissive layer-by-layer injection of granitic melt formed at depth of 15–20 km due to differential melting of high-grade metamorphics (Powar 1972). This resulted in the formation of migmatites on an extensive scale around granitic bodies (Valdiya and Goel 1983; Valdiya et al. 1999). The anatectic origin of granite is borne out by sillimanite, garnet and cordierite present in the granites and is corroborated by high strontium ratios of 0.743–0.784. The highly variable strontium ratios and the low REE imply involvement of a variety of metasediments in the differential melting of rocks that gave rise to the granitic melt. In the Nanga Parbat massif in the north-western part of the Himadri domain, there was wholesale granitization of the high-grade metamorphic rocks (Misch 1949;

Table 11.2 Rb–Sr whole-rock isochron dates from granites from the Chail, the Jutogh and the Haimanta formations and the Tso–Morari Crystallines (Modified after Islam et al. 1999)

Locality	Tectonic unit	Age (Ma)	Initial Sr isotope ratio	Authors
Almora	Almora (≡Jutogh)	560 ± 20	0.710 ± 0.001	Trivedi et al. (1984)
Ranikhet	Almora	485 ± 55	0.735 ± 0.009	Pandey et al. (1981)
Champawat	Almora	565 ± 22		Trivedi et al. (1984)
Chaur	Jutogh	530 ± 40	0.7326	Kwatra (1986)
Kulu	Jutogh	518 ± 8	0.719	Mehta (1977)
Mandi	Chail (Salkhala)	545 ± 12		Mehta (1977)
Mandi	Chail	500 ± 100/ 518 ± 100/ 545 ± 12		Jaeger et al. (1971)
Dalhousie	Chail	472 ± 50/ 456 ± 50		Bhanot et al. (1974)
Manikaran	Chail/Jutogh	467 ± 45	0.719	Bhanot et al. (1979)
Lahaul	Haimanta	495 ± 16		
Jispa	Lower Haimanta	512 ± 16	0.720	Frank et al. (1977)
Akpa-Rakcham	Haimanta	477 ± 29	0.7201	Kwatra (1986)
Rohtang	Central crystallines	601 ± 19/ 581 ± 9	0.711	Mehta (1977)
Kade	Tso Morari Gneiss	472 ± 9/–6 460 ± 8		Stutz and Thoni (1987)
Nanga Parbat	Shengus Gneiss	400–500 (U–Pb, zircons)		Zeitler et al. (1989)
Kazinag	Salkhala	477 ± 24		Trivedi et al. (1985)
Kagan	Salkhala	470 ± 11	0.7216 ± 0.0023	Trivedi et al. (1985)
Mansehra	Tanol (Chail/Haimanta)	516 ± 16	0.7189	Le Fort et al. (1980)
Nimaling	Tanglang La of Tso–Morari Crystallines	460 ± 8		Stutz and Thony (1987)
Polokong La	Tso–Morari Crystallines	487 ± 25	0.7154 ± 0.0067	Trivedi et al. (1986)
Korzok	Tso–Morari Crystallines	487 ± 14	0.7113 ± 0.0036	Trivedi et al. (1986)
Palung		486 ± 10		
Dudh Kosi		550 ± 32		
Kangmar		485 ± 6/ 484 ± 14/ 435 ± 37		References in Lefort et al. (1986)
Thimpu		508 ± 15		

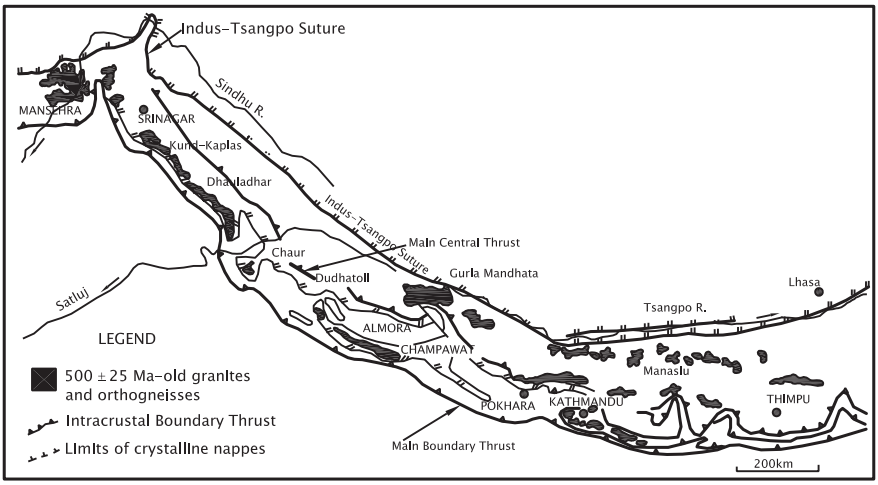

Fig. 11.10 Cambro–Ordovician (500 ± 25 Ma) granites in the Himalaya province occurring preponderantly in the epimetamorphic nappes of the Lesser Himalaya, the lower part of the Vaikrita, and in the northern upward edge of the Indian plate along the India–Asia junction (Based on Le Fort et al. 1986)

Shams 1983). In eastern Himachal Pradesh, the *Kinnar Kailas Granite* is a discordant body penetrating the Vaikrita metamorphic rocks that were affected by four phases of deformation. The granite contains xenoliths of paragneiss characterized by deformational features developed under amphibolite facies conditions (Marquer et al. 2000). This fact has profound implication—the first three phases of deformation suffered by the Vaikrita occurred prior to the emplacement of the 488-million-year-old Kinnar Kailas Granite. Thus, there was pre-Cambrian deformation in the Himachal Himalaya. U–Th–Pb dating of zircon and monazite crystals establishes the age of Kade Granite in the Himadri domain at 472 ± 9/−6 Ma (Pognante et al. 1990). The Nyimaling Granite in the TsoMorari complex is dated by Rb–Sr method at 460 ± 8 Ma (Stutz 1988). In the Tethyan terrane, the Puga gneiss at Kiagarla is 499 ± 8 Ma old and the granites of the Polokongkla and Tso–Morari areas in the setting of the Puga gneisses and schists have yielded U–Pb zircon age of 479 ± 2 Ma (Rameshwar Rao and Rai 2002). The age data together with similarity of petrochemical compositions of the gneisses and granites imply their derivation from similar or the same magma generated by partial melting of crustal-derived pelitic rocks.

The calcalkaline Hant Granite in north-west Kashmir, syntectonically emplaced in the Salkhala and the Dogra Slate, crystallized from anatectic magma generated in the Precambrian continental crust (Rameshwar Rao et al. 1990). The 553 ± 2 Ma Kund Kaplas Granite (Miller et al. 2001) and the intrusive peraluminous Dalhousie Granite in the Chail are depleted in REE (Sr, Zr, Th, P) and somewhat enriched in U (Mukherjee et al. 1998). The crustally derived 477 ± 29 and

453 ± 9 Ma Akpa-Rakcham Granite in the Satluj Valley is characterized by higher Sr, Ba, Zr, Ni, Th and Y and total REE contents pronounced Eu anomaly, and low Rb content and lower Rb/Sr ratio (Islam and Gururajan 2003; Singh and Kumar 2005). Hornfels is formed around the Dalash Granite in the Satluj Valley due to contact metamorphism and at the base of the Mandi–Karsog Granite (Gururajan and Islam 1991; Islam and Gururajan 2003). Compositionally, the *Champawat Granodiorite* is a quartzdiorite–granodorite–adamellite–granite suite, it evolved in an environment charged with moisture or water, and was subsequently involved in the folding of the host rocks (Valdiya 1962b). The granodiorite–granite assemblage is characterized by enrichment of Y, Zr, Th, U, Nb, La, Ce, Pr and Nd (Singh et al. 1991). The Rb–Sr whole-rock isochron age of the Champawat pluton is 560 ± 20 Ma (Trivedi et al. 1984; Trivedi 1990). The age of the *Chaur Granite* is 526 ± 46 Ma or near about (Kwatra et al. 1986; Singh 2003). The Champawat Granodiorite within the mesometamorphic succession of the Dadeldhura Range in far-western Nepal has yielded concordant U–Pb zircon age of 492 ± 6 Ma, while the associated augen gneiss of granitic composition gave U–Pb zircon age of 478 ± 10 Ma (Upreti 1996; DeCelles 2000, 2001). The biotite–quartz-rich Champawat Granodiorite body is intruded by sills, dykes and veins of leucocratic adamellite, aplogranite and pegmatite which are compositionally and texturally indistinguishable from the granite plutons intruding the Chail Nappe in the Dhauladhar and Pir Panjal Ranges. The Mandi, Dalhousie and Kazinag granites have been dated, respectively, 545 ± 12 Ma (Mehta 1977), 456 ± 50 and 477 ± 24 Ma (Bhanot et al. 1980). The origin of the *Mandi Granite* is attributed to partial melting of heterogeneous crustal material under water-deficient condition (Gupta 2001).

In northern Pakistan, the polymetamorphic Tanol assemblage enveloped by the Salkhala is intruded along the contact by granitic bodies (Shams 1983). One of them, the *Mansehra Granite,* is dated 516 ± 16 Ma (Lefort et al. 1980). It is derived from old crustal material. The *Ambela Granite* and the Lower *Swat Granite*, showing alkaline affinity (Ahmad and Ahmad 1974; Shams 1980a, b; Jan et al. 1983; Kempe and Jan 1970; Kempe 1983), belong to the same generation of granites—the 500 ± 25 m year old Cambro–Ordovician granites.

In the east, the Palung (485 ± 20 Ma), the Dudhkosi (550 ± 32 Ma), (Decelles et al. 2000), the *Thimpu Granite* (508 ± 15 Ma) and the *Bomdila Granite* (530 ± 75 Ma) (Dikshatulu et al. 1995) represent this event of global significance.

SHRIMP U–Pb zircon dates of peralkaline Lesser Himalayan granites in the Kathmandu region with xenoliths showing deformation structures truncated by host granite and their signature inherited detrital zircon ages ranging from Archaean to Palaeozoic (~500 Ma)—with prominent peaks of Late Proterozoic and Neoproterozoic ages—there is little doubt that the Himalaya was strongly affected by Cambro–Ordovician Pan-African orogeny (Cawood et al. 2007) as earlier suggested among others by Valdiya (1995).

These are the few of the many anatectic granites showing distinctive petrochemical characteristics of the Pan-African granites.

11.8 Mineralization

The Neoproterozoic rocks of the Lesser Himalaya are very valuable in terms of mineral deposits of economic value and genetic significance. Among the important mineral deposits, those of magnesite, talc, phosphorite, barytes and copper sulphides are quite important.

The Gangolihat Dolomite is the mineralised facies of the Deoban. It is characterized by lentiform deposits of coarsely crystalline to spathic *magnesite* interbedded with cherty dolomite and dolomitic–stromatolitic limestones. Locally, the relationship is discordant, marked by interdigitation of magnesite and dolomite. Generally, the contact is sharp. The thickness of the deposits vary from a fraction of a metre to as much as 30 m (the average 5–25) and the length ranges from less than a kilometre to several kilometres. The deposits occur at a definite stratigraphic level in the Deoban succession that is mineralized between Kali and Mandakini rivers in Uttarakhand. The important deposits are located at Jhirauli in the Almora district and Chandaak in the Pithoragarh district.

The origin of magnesite is attributed to hydrothermal metasomatism of dolomites, the magnesian solution supposedly derived from basic intrusives being the agent of transformation (Nautiyal 1953; Nath and Wakhaloo 1962). The other view is that synsedimentary diagenetic volume-for-volume replacement of dolomite sediment gave rise to the magnesite deposits (Misra and Valdiya 1961; Valdiya 1968, 1980b). Interestingly, the Kumaun magnesite deposits strongly resemble in shape and textural character of the magnesite deposits of Asturettes in the Spanish Pyrenees. The Asturette magnesite was formed by diagenesis at ~150 °C in the basin which had high primary concentration of Mg-rich sedimentary carbonate, resulting in the transformation into magnesite with minor ulterior metamorphic remobilization (Velasco et al. 1987). In Kumaun, the algae that built the stromatolite structures must have played a vital role in the genesis of magnesium carbonate, particularly in creating an environment conducive to the concentration of $MgCO_3$ in barred basins (Valdiya 1968). There is also a suggestion that magnesite was initially precipitated as nesquehonite and later converted to magnesite (Tewari 1973). South-east of the Jhiroli magnesite mine in Almora district, the Bauri magnesite deposit shows correlation between salinity and temperature, indicating formation of magnesite through diagenetic replacements of dolomite at 90–160 °C (Sharma and Joshi 1997). Significantly, not only the magnesite and dolomite minerals show the same range of oxygen isotope ratios, but also are characterized by fluid inclusion of nearly the same characters. The magnesite deposits in the Chamba district in western Himachal Pradesh, localized below the Chamba Thrust between Jiuni in Bharmauer and Bindrabani in the Pangi Valley, are supposedly products of reaction of hot (200–275 °C) saline waters with dolomite and limestone, a process prompted by the tectonics of the Chamba Thrust (Singh and Sharma 1997).

Intimately associated with magnesite occur lentils, pockets and veins of *talc and steatite*, and the latter intercalated with dolomite in a bedded form. They are extensively mined. The origin of talc is attributed to reaction during mild metamorphism of $MgCO_3$ with silica that occurs abundantly in magnesite and

dolomite. The reaction was promoted by CO_2-rich groundwaters (Valdiya 1968). In the Rema area, irregular patches and pockets of talc within magnesite were formed at the expense of magnesite by silica as borne out by the common presence of fluid inclusions in talc, magnesite and dolomite associated with it. The fluids within inclusions are $H_2O + NaCl + KCl + MgCl_2CaCl_2$—representing the fluids of the sedimentary basin (Sharma et al. 2008).

The lower part of the Tal Formation in south-eastern Himachal Pradesh and the Mussoorie Hills in Uttarakhand is made up of *phosphorite* with chert, black limestone and carbonaceous shale (Shanker 1975). The thickness of the deposit varies from less than a metre to over 150 m in some places. Phosphorite of Maldeota, Chamsari, Paritibba and Chaunpa–Kumali occurs predominantly in a laminated or platy form and less commonly as granular (pelletal and nodular) deposits. The finely laminated phosphorite laterally grades into cherty limestones, implying their formation due to concentration of phosphorous brought up by upwelling currents (Patwardhan and Ahluwalia 1973).

Copper and lead sulphides occur as disseminations, small veins and lentils in dolomites and magnesite of the Gangolihat facies of the Deoban Formation. In Kumaun, the sulphide mineralization shows preference for contact between the Gangolihat Dolomites and overthrust Berinag quartzites (Valdiya 1980b). There seem to be a stratigraphic control on the base metal localization and their syngenetic remobilisation in structurally weak zones. South-west of Bageshwar, in the Sisakhani–Chhanapani–Bhaldeo belt, lead sulphide (galena) occurs in *en echelon* bodies of cherty dolomite, magnesite and talc, as dissemination, minute veins and tiny streaks or patches. The model Pb–Pb age of the lead sulphide mineralization is 1550–1700 Ma (Sarkar 2000). In the Jammu Limestone, the sphalerite mineralization is confined to two carbonate units, the mineral initially occurring as a stratabound deposit later altered and remobilised by hydrothermal solution (Sharma and Nayak 1991). Near Askot in the Pithoragarh district, deposits of copper sulphide (along with other sulphides) in the basic schists within the Berinag are being mined.

In eastern Arunachal Pradesh, in the NNE–SSW trending Siang Group, the iron formation is associated with muscovite–quartz schist and brecciated quartzite in a 30-km-long and 30-m-wide belt and the *sulphides* associated with the *uranium minerals* occur as disseminations, stringers, veins and vug fillings along fractures in sericite–quartzites and garnetiferous amphibolite (Bisht et al. 2005). The sulphide–uranium mineralization is attributed to hydrothermal solutions, possibly derived from the Cambro–Ordovician granites of the terrane.

The Krol–Tal contact in the Mussoorie Hills and the Nigalidhar belt contain pockets of *barytes* in the phosphorite zone. In the Nigalidhar Hills in south-east Himachal Pradesh, the barytes deposits occur below the phosphorite zone. It occurs as veinlets, nodules, lentils and stringers in limestones. Near Khairasen in the Nayar Valley, the barytes deposit is 500 m long and 1–1.5 m thick in the basal part of the Nagthat quartzite (Sharma et al. 2003). In the Jammu Limestone, barytes occurs as veins, nodules and stringers in cherty and dolomitic limestones, and in the brecciated carbonates of the Jangalgali, Kherikot and Sersandhu areas. The origin of these stratabound deposits is attributed to synsedimentary processes.

References

Agarwal, N. C. (1974). Discovery of bryozoan fossils in the calcareous horizon of Garhwal Group, Pauri Garhwal district. *Himalayan Geology, 4*, 600–618.

Ahmad, S., & Ahmed, Z. (1974). Petrochemistry of the Ambela granites, northern Swat district, Pakistan. *Pakistan Journal of Science and Research, 26*, 63–69.

Auden, J. B. (1934). The geology of the Krol belt. *Records Geological Survey of India, 67*, 357–454.

Auden, J. B. (1937). The structure of the Himalaya in Garhwal. *Records Geological Survey of India, 71*, 407–433.

Awasthi, N. (1970). Some aspects of the Krol Formation of the Himalaya, India. *Contri. Mineral. Petrol., 28*, 192–220.

Azmi, R. J. (1983). Microfauna and age of Lower Tal phosphorite of Mussoorie syncline, Garhwal Lesser Himalaya. *Himalayan Geology, 11*, 373–409.

Azmi, R. J., & Pancholi, V. P. (1983). Early Cambrian (Tommatian) conodonts and other shelly microfauna from the Upper Krol of Mussoorie syncline, Garhwal Lesser Himlaya, with remarks on the Precambrian boundary. *Himalayan Geology, 11*, 360–372.

Banerjee, D. M., Schindowski, M., Siebert, F., & Brasier, M. D. (1997). Geochemical changes across the Proterozoic-Cambrian transition in the Durmala phosphorite mine section, Mussoorie Hills, Garhwal Himalaya, India. *Palaeogeography, Palaeoclimatology, Palaeoecology, 132*, 183–194.

Baud, A., Gaetani, M., Garzanti, E., Fois, E., Nicora, A., & Tintori, A. (1984). Geological observation in southeastern Zanskar and adjacent Lahaul area (northwestern Himalaya). *Eclogae Geologicae Helvetiae, 77*, 171–197.

Berthelsen, A. (1951). A geological section through the Himalaya. *Meddelelser Dansk Geologisk Forening, 12*, 102–104.

Berthelsen, A. (1953). On the geology of the Rupshu District, N.W. Himalaya. *Meddelelser Dansk Geologisk Forening, 12*, 350–414.

Bhanot, V. B., Pandey, B. K., Singh, V. P., & Kansal, A. K. (1980). Rb–Sr ages for some granitic and gneissic rocks of Kumaun and Himachal Himalaya. In K. S. Valdiya & S. B. Bhatia (Eds.), *Stratigraphy and correlations of the Lesser Himalayan Formations* (pp. 139–144). Delhi: Hindustan Publishing Corporation.

Bhargava, O. N. (1972). A reinterpretation of the Krol Belt. *Himalayan Geology, 2*, 47–81.

Bhargava, O. N. (1975). The lithostratigraphy and sedimentation of the Tal Formation, Nigalidhar Syncline, Himachal Pradesh. *Geological Survey of India Misc Public, 24*, 27–33.

Bhargava, O. N., Frank, W., & Bertle, R. (2011a). Later Cambrian deformation in the Lesser Himalaya. *Journal of Asian Earth Sciences, 40*, 201–221.

Bhargava, O. N., Kaur, G., & Deb, M. (2011b). A Palaeoproterozoic palaeosol horizon in the Lesser Himalaya and its regional implication. *Journal of Asian Earth Sciences, 42*, 1371–1380.

Bhargava, O. N., Singh, I., Hans, S. K., & Bassi, U. K. (1998). Early Cambrian trace and trilobite fossils from the Nigalidhar syncline (Sirmur District, Himachal Pradesh), Lithostratigraphic correlation and fossil contents of the Tal Group. *Himalayan Geology, 19*, 89–108.

Bhargava, O. N., & Srikantia, S. V. (1985). Trilobites and other trace fossils from the Kunzumla Formation, eastern Lahaul, Himachal Pradesh. *Journal of Geological Society of India, 26*, 880–886.

Bhargava, O. N., Srivastava, R. N., & Gadhoke, S. K. (1991). Late Proterozoic-Palaeozoic Spiti basin. In S. K. Tandon, S. M. Casshyap, & C. C. Pant (Eds.), *Sedimentary basins of India: Tectonic context* (pp. 236–260). Nainital: Gyanodaya Prakashan.

Bhaskar Rao, Y. J., Anil Kumar, Vresky, A. B., Srinivasan, R., & Anantha Iyer, G. V. (2000). Sm-Nd ages of two metaanorthosite complexes around Holenarasipur: Constraints on the antiquity of Archaean supracrustal rocks of the Dharwar Craton. *Proceedings of the Indian Academy of Sciences (Earth & Planet Science), 109*, 57–65.

Bhatt, D. K. (1996). The end phase of sedimentation of Krol Belt in Nainital syncline—Stratigraphic analysis and fossil levels. *Current Science, 70*, 772–774.

Bhatt, D. K., Mamgain, V. D., Misra, R. S., & Srivastava, J. P. (1983). Shelly microfossils of Tommatian age (Lower Cambrian) from the Chert-Phosphorite member of Lower Tal Formation, Maldeota, Dehradun District, U.P. *Geophytology, 13*, 116–123.

Bhatt, D. K., & Mathur, A. K. (1990). Small shelly fossils of Precambrian-Cambrian boundary beds from the Krol-Tal succession the Nainital syncline, Lesser Himalaya. *Current Science, 59*, 218–222.

Bisht, B. S., Ali, M. A., Pande, A. K., & Pavanagaru, R. (2005). Geological characteristics of iron-uranium mineralization in the Lesser Himalayan region of Arunachal Himalaya. *Journal of Geological Society of India, 66*, 185–202.

Brasier, M. P., & Singh, Pratap. (1987). Microfossils and Precambrian-Cambrian boundary stratigraphy at Maldeota, Lesser Himalaya. *Geological Magazine, 124*, 323–345.

Brunnel, M., Chaye, de'Albissin, M., & Locquin, M. (1985). The Cambrian age of magnesite from east Nepal as determined through the discovery of palaeobasiospores. *Journal of Geological Society of India, 26*, 255–260.

Cawood, P. A., Johnson, M. R. W., & Nemchin, A. A. (2007). Early Palaeozoic orogenesis along the Indian margin of Gondwana: Tectonic response to Gondwana assemblage. *Earth & Planet Science Letters, 255*, 70–84.

Choudhary, A. K., Harris, N. B. W., Van Calsteren, P., & Hawkesworth, C. J. (1992). Pan-African charnockite formation in Kerala, South India. *Geological Magazine, 129*, 257–264.

Colchen, M., Le Fort, P., & Pecher, A. (1986). *Recherches Geologiques dans l'Himalaya due Nepal Annapurna, Manaslu, Ganesh Himal*. Paris: Centre Nationale Recherche Scientifique. (136 p).

Das, A. K., Bakliwal, P. C., & Dhaundial, D. P. (1976). A brief outline of the geology of parts of Kameng District, Nefa. *Geological Survey of India Misc Publication, 24*, 115–127.

Dasgupta, S. P., Kumar, V., Ramachandra, & Jairam, M. S. (1988). A framework of the Nagaur-Ganganagar evaporite basin, Rajasthan. *Indian Minerals, 42*, 57–64.

DeCelles, P. G., Gehrels, G. E., Quade, J., LaReau, B., & Spurlin, M. (2000). Tectonic implications of U–Pb zircon ages of the Himalayan orogenic belt in Nepal. *Science, 288*, 497–499.

DeCelles, P. G., Robinson, D. M., Quade, J., Ojha, T. P., Garzione, C. N., Copeland, P., & Upreti, B. N. (2001). Stratigraphy, structure and tectonic evolution of the Himalayan fold-thrust belt in western Nepal. *Tectonics, 20*, 487–509.

Frank, W., Gansser, A., & Trommsdorff, V. (1977). Geological observations in the Ladakh area, a preliminary report. *Schweizerische Mineralogische und Petrographische Mitteilungen, 57*, 89–113.

Fuchs, G. R. (1967). *Zum Bau des Himalaya*. Wien: Denkschriften der Kaiserlichen Akademie der Wissenschaften. (211 p).

Fuchs, G. R. (1975). On the geology of the Karnali and Dolpho region, West Nepal. *Sond Mitteilunger Geologischen Gessellschaft, 66–67*, 21–32.

Fuchs, G. R. (1977). Traverse of Zanskar from the Indus to the valley of Kashmir—a preliminary note. *Jahrbuch Geologische Bundesanstalt, 120*, 219–229.

Fuchs, G. R. (1982). The Geology of the Pin valley in Spiti India. *Jahrbuch Geologische Bundesantalt, 125*, 325–359.

Fuchs, G. R. (1987). The geology of southern Zanskar (Ladakh)—Evidence for the autochthony of the Tethys zone of the Himalaya. *Jarhbuch Geologische Bundesanstalt, 130*, 465–491.

Fuchs, G. R., & Frank, W. (1970). The geology of west Nepal between the rivers Kali Gandaki and Thulo Bheri. *Jahrbuch Geologische Bundesanstalt, 18*, 1–103.

Fuchs, G. R., & Moestler, H. (1972). Der erste Nachweis von Fossilien (Kambruschen Alters) in der Hazira Formation, Hazara, Pakistan. *Geology Palaeontographica Mitteilungen, 2*, 1–2.

Fuchs, G., & Sinha, A. K. (1974). On the geology of Nainital (Kumaun Himalaya). *Himalayan Geology, 4*, 463–580.

Gaetani, M., Raffache, C., Fois, E., Garzanti, E., Jadoul, F., Nicora, A., & Tintori, A. (1985). Stratigraphy of the Tethys Himalaya in Zanskar Ladakh. *Rivista Italiana Palaeontology & Stratigraphy, 91*, 443–478.

Gangopadhyay, P. K., & Lahiri, A. (1984). Earth's crust and evolution of the Delhi Supergroup in Central Rajasthan. *Indian Journal of Earth Sciences, CEISM*, 92–113.

Gansser, A. (1964). *Geology of the Himalayas*. London: Interscience Publishers, p. 289.

Garson, M. S., Amos, B. J., & Mitchell, A. H. G. (1976). The geology of the area around Neyaunagga and Ye-ngan, Southern Shan States, Burma. *Oversees Memoires Interational Geological Sciences, London, 2*, 1–70.

Garzanti, E., Casnedi, R., & Jadoul, F. (1986). Sedimentary evidence of a Cambro-Ordovician orogenic event in the northwestern Himalaya. *Sedimentary Geology, 48*, 237–265.

Gaur, G. C. S., & Dave, V. K. S. (1971). Blaini tillites near Rishikesh and their origin. *Journal of Geological Society of India, 12*, 164–172.

Gee, E. R. (1989). Overview of the geology and structure of the salt range with observation on related areas of northern Pakistan. In L. L. Malinconico & R. J. Lillie (Eds.), *Tectonics of western Himalaya* (pp. 95–112). Boulder: Geological Society of America.

Gehrel, G. E., DeCelles, P. G., Ojha, T. P., & Upreti, B. N. (2006). Geologic and U–Pb geochronological evidence for early Paleozoic tectonism in the Kathmandu thrust sheet, central Nepal Himalaya. *Bulletin Geological Society of America, 118*, 185–198.

Ghosh, S. K. (1991a). Source rock characteristics of the late Proterozoic Nagthat Formation, NW Kumaun Lesser Himalaya. *Journal of Geological Society of India, 38*, 485–495.

Ghosh, S. K. (1991b). Palaeoenvironmental analysis of the late Proterozoic Nagthat Formation, NW Kumaun Lesser Himalaya, India. *Sedimentary Geology, 71*, 33–45.

Grasemann, B., Miller, Ch, Frank, W., & Draganits, E. (1997). Structural evidence of Pre-Ordovician deformation in the Pin Valley. *Special Publication of 12th Karakoram Himalaya–Tibet Workshop Abstract*, pp. 143–144.

Gundu Rao, C. (1970). A note on the oolites of the Krol series and their age significance. *Publication Centre Advanced Study of Geology, Panjab University, 7*, 127–129.

Gupta, L. N. (2001). Petrochemistry and origin of the Mandi granitoids, NW Himalaya. In L. N. Gupta, R. Kumar, & G. S. Gill (Eds.), *Structure and Tectonics of Indian plate* (pp. 19–34). Chandigarh: Indian Geological Association.

Gururajan, N. S., & Islam, R. (1991). Petrogenesis of the Khab leucogranite in the Higher Himalayan region of Himachal Pradesh (Satluj Valley), India. *Journal of Himalayan Geology, 2*, 31–37.

Heim, A., & Gansser, A. (1939). Central Himalaya: Geological observations of the Swiss expedition 1936. *Denkschriften der Schwieizerishen Naturforschenden Gasellschaft, 32*, 1–245.

Hukku, B. M., Srivastava, A. K., & Jaitli, G. N. (1974). Evolution of lakes around Nainital and the problem of hillside instability. *Himalayan Geology, 4*, 516–531.

Islam, R., & Gururajan, N. S. (2003). Geochemistry, petrogenesis and tectonic setting of Akpa-Rakcham Granites, Satlej valley, Himachal Pradesh. *Himalayan Geology, 24*, 63–76.

Islam, R., Upadhayay, R., Ahmad, T., Thakur, V. C., & Sinha, A. K. (1999). Pan-African magmatism and sedimentation in the NW Himalaya. *Gondwana Research, 2*, 263–270.

Jain, A. K., & Varadaraj, N. (1978). Stratigraphy and provenance of late Palaeozoic diamictites in parts of Garhwal Lesser Himalaya, India. *Geologische Rundschau, 5*, 469–478.

Jan, M. Q., & Faruqi, (1995). Khewra trap: An unusual ultrapotassic rock in the salt range of Pakistan. *Journal of Nepal Geological Society, 11*, 237–252.

Jiang, G., Christie-Blick, Banerjee, D. M., Kaufmann, A. J., & Rai, V. (2003). Carbonate platform growth and cyclicity at a Terminal Proterozoic passive margin, Infrakrol Formation and Krol Group, Lesser Himalaya, India. *Sedimentology, 50*, 921–952.

Jiang, G., Christie-Blick, N., Kaufman, A. J., Banerjee, D. M., & Rai, V. (2002). Sequence stratigraphy of the Neoproterozoic Infrakrol Formation and Krol Group, Lesser Himalaya, India. *Journal of Sedimentary Research, 72*, 524–542.

Joshi, A., Mathur, V. K., & Bhatt, D. K. (1989). Discovery of Redlichiid trilobites from arenaceous member of Tal Formation, Garhwal Syncline, Lesser Himalaya. *Journal of Geological Society of India, 33*, 338–345.

Kazmi, A. H., & Qasim Jan, M. (1997). *Geology and Tectonics of Pakistan*. Karachi: Graphic Publishers. 554 p.

Kempe, D. R. C. (1983). Alkaline granites syemites and assocated rocks of the Peshawar Plain Alkaline Igneous Province, NW Pakistan. In F. A. Shams (Ed.), *Granites of Himalaya, Karakoram and Hindukush*. Lahore: Institute of Geology, Panjab University, p. 143.

Kempe, D. R. C., & Jan, M. Q. (1970). An alkaline igneous province in the NW Frontier Province, West Pakistan. *Geological Magazine, 107*, 395–358.

Kharkwal, A. D., & Bagati, T. N. (1974). Mineralogy and origin of red shales of the Krol Formation. *Himalayan Geology, 5*, 469–478.

Krishnan, M. S., & Swaminath, J. (1959). The great Vindhyan basin of southern India. *Journal of Geological Society of India, 1*, 10–30.

Kumar, R., & Brookfeld, M. E. (1987). Sedimentary environments of the Simla Group (upper Precambrian), Lesser Himalaya and their palaeotectonic significance. *Sedimentary Geology, 52*, 27–43.

Kumar, G., Raina, B. K., Bhatt, D. K., & Jangpanji, B. S. (1983). Lower Cambrian body and trace fossils from the Tal Formation, Garhwal synform, Uttar Pradesh, India. *Journal of Palaeontology Society of India, 28*, 106–111.

Kumar, G., Safaya, H. L., & Prakash, G. (1976). Geology of the Berinag-Mansiari area, Pithoragarh District, Kumaun Himalaya, U.P. *Himalayan Geology, 6*, 81–110.

Kwatra, S. K., Bhanot, V. B., Kakar, R. K., & Kansal, A. K. (1986). Rb–Sr radiometric ages of the Wangtu Gneissic Complex, Kinnaur district, Himachal Himalaya. *Bulletin Indian Geological Association, 19*, 127–130.

Le Fort, P., Debon, F., Pecher, A., Sonet, J., & Vidal, P. (1986). The 500-Ma magmatic event in Alpine-Southern Asia: a thermal episode at Gondwana scale. *Science de Terre, 47*, 191–209.

Lefort, P., Debon, F., & Sonet, J. (1980). The Lower Himalaya cordierite-granite belt: Topology and age of the pluton of Mansehra, Pakistan. *Geological Bulletin University of Peshawar, 13*, 51–62.

Marquer, D., Chawla, H. S., & Challandes, N. (2000). Pre-alpine high-grade metamorphism in High Himalaya crystalline sequences: Evidence from Lower Palaeozoic Kinnar Kailas Granite and surrounding rocks in the Satluj valley (Himachal Pradesh, India). *Eclogae Geologica Helvetica, 93*, 207–220.

Mazumdar, A., & Banerjee, D. M. (1998). Siliceous sponge spicules in Early Cambrian chert-phosphorite member of the Lower Tal Formation, Krol belt, Lesser Himalaya. *Geology, 26*, 899–902.

Mehta, P. K. (1977). Rb–Sr geochronology of the Kullu-Mandi belts: Its implications for the Himalaya. *Sond Geological Runds, 66*, 186–195.

Miller, C., Thoni, M., Frank, W., Grassemann, B., Klotzb, U., Guntli, P., et al. (2001). The early Palaeozoic magmatic event in the Northwest Himalaya, India: Source, tectonic setting and age of emplacement. *Geological Magazine*, *138*, 237–251.

Misch, P. (1949). Metasomatic granitization of batholithic dimension. *American Journal of Sciences, 247*, 209–245, 372–406, 673–705.

Misra, R. C. (1969). *The Vindhyan system*. Kolkata: Presidential Address 56th Indian Science Congress, pp. 1–32.

Misra, R. C., & Valdiya, K. S. (1961). The Calc Zone of Pithoragarh, with special reference to the occurrence of stromatolites. *Journal of Geological Society of India, 2*, 78–90.

Mukherjee, P. K., Purohit, K. K., Rathi, M. S., Khanna, P. P., Saini, N. K., & Islam, R. (1998). Geochemistry and petrogenesis of a supercrustal granite from Dalhousie, Himachal Himalaya. *Journal of Geological Society of India, 52*, 163–180.

Myrow, P. M., Thompson, K. R., Hughes, N. C., Paulsen, T. S., Sell, B. K., & Parcha, S. K. (2006). Cambrian stratigraphy and depositional history of the northern Indian Himalaya, Spiti Valley, northcentral India. *Bulletin Geological Society of America, 118*, 491–510.

Nalivkin, V. D. (1966). Geological structure of the southern Himalayas in Simla region. In Problems of geology at the XXII session of the International Geological Congress Publishing House, "Nauka", Moscow, pp. 281–285.

Nanda, M. M., & Singh, M. P. (1976). Stratigraphy and sedimentation of the Zanskar area, Ladakh and adjoining parts of Lahaul region of H.P. *Himalayan Geology, 6*, 365–388.

Nath, M., & Wakhaloo, G. L. (1962). A note on the magnesite deposits of Almora district, U.P. *Indian Minerals, 16*, 116–123.

Nautiyal, S. P. (1953). The reconnaissance geological report of a part of the copper belt of Almora district, Kumaun Himalaya. *Record Geological Survey of India, 89*, 341–358.

Niyogi, D., & Bhattacharya, S. C. (1971). A note on the Blaini boulder beds of lower Himalaya. *Himalayan Geology, 1*, 111–122.

Pande, I. C. (1974). Tectonic interpretation of the geology of Nainital area. *Himalayan Geology, 4*, 532–546.

Pant, C. C., & Goswami, P. K. (2002). The Proterozoic bhumiadhar member (Blaini Formation), Nainital Hills: an example of storm-dominated regressive offshore sedimentation in Krol Belt, Kumaun Lesser Himalaya. In C. C. Pant & A. K. Sharma (Eds.), *Aspects of geology and environment of Himalaya* (pp. 112–127). Nainital: Gyanodaya Prakashan.

Pant, C. C., & Goswami, P. K. (2003). Tide-storm-dominated shelf sequence of the Neoproterozoic Blaini Formation and its implications on the sedimentation history of Krot Belt, Kumaun Lesser Himalaya, India. *Journal of Nepal Geological Society, 28*, 19–39.

Pant, C. C., & Shukla, U. K. (1999). Nagthat Formation: An example of a progradational, tide-dominated Proterozoic succession in Kumaun Lesser Himalaya, India. *Journal of Southeast Asian Earth Sciences, 17*, 353–368.

Patwardhan, A. M., & Ahluwalia, A. D. (1973). A note on the origin of Mussoorie phosphorite in the Lower Himalaya, India and its palaeogeographic implications. *Minerals Deposita, 8*, 379–389 and *10*, 261–318.

Pilgrim, G. E., & West, W. (1928). The structure and correlation of the Simla rocks. *Memories Geological Survey of India, 53*, 140 p.

Pognante, U., Castelli, D., Benna, P., Genovese, G., Oberli, F., Meier, M., & Tonarini, S. (1990). The crystalline units of the High Himalayas in the Lahaul-Zanskar region (NW India): Metamorphic tectonic history and geochronology of the collided and inbricated Indian plate. *Geological Magazine, 127*, 101–116.

Powar, K. B. (1972). Petrology and structure of the Central crystalline Zone, Northeastern Kumaun. *Himalayan Geology, 2*, 34–46.

Raha, P. K., Chandy, K. C., & Balasubramanyan, (1978). Geochronology of the Jammu Limestone, Udhampur district, Jammu. *Journal of Geological Society of India, 18*, 221–223.

Raha, P. K., & Das, D. P. (1989). Correlation of stromatolite-bearing Upper Proterozoic basins of India and palaeogeographic significance. *Himalayan Geology, 13*, 119–142.

Raha, P. K., & Sastry, M. V. A. (1973). Stromatolites from the Jammu Limestone, Udhampur district, Jammu and Kashmir state and their stratigraphic and palaeogeographic significance. *Himalayan Geology, 3*, 135–147.

Rai, V., & Singh, I. B. (1983). Discovery of trilobite impression in the arenaceous member of Tal Formation. *Journal of Palaeontology Society of India, 28*, 114–117.

Raina, B. K., Bhatta, D. K., & Gupta, B. K. (1988). Discovery of skeletal microfossils of the Precambrian-Cambrian boundary beds in Paristan, Doda district, J & K. *Memoires Geological Survey of India, 16*, 33–40.

Rameshwar Rao, D., & Rai, H. (2002). Rb–Sr isotopic studies of Puga gneiss and Polokongka La Granites from Tso Morari region of Ladakh, J&K. *Current Science, 82*, 1077–1079.

Rameshwar Rao, D., Sharma, K. K., Sivaraman, T. V., Gopalan, K., & Trivedi, J. R. (1990). Rb/Sr dating and petrochemistry of Hant Granite (Baramulla area), Kashmir Himalaya. *Journal of Himalayan Geology, 1*, 57–63.

Rupke, J. (1968). Note on the Blaini boulder bed of Tehri Garhwal, Kumaun Himalaya. *Journal of Geological Society of India, 9*, 31–133.

Rupke, J. (1974). Stratigraphic and structural evolution of the Kumaun Lesser Himalaya. *Sedimentary Geology, 11*, 81–265.

Sankaran, A. V. (2004). Methane fuse for Cambrian mass evolution, volcanism for mass extinction: Proponents review their hypotheses. *Current Science, 86*, 257–260.

Sarkar, S. C. (2000). Crustal evolution and metallogeny in the Eastern Indian Craton. *Special Publications of Geological Survey of India, 55*, 169–194.

Searle, D. L., & Ba Than, H. (1964). *The Mogok Belt of Burma and its relationship to the Himalayan orogeny*. Report 22nd International Geological Congress (Vol. 11, pp. 133–161).
Shah, S. K. (1982). Cambrian stratigraphy of Kashmir and its boundary problems. *Precambrian Research, 17*, 87–98.
Shah, S. K. (1991). Stratigraphic setting of the Phanerozoic rocks along the northern boundary of the Indian plate. *Physics and Chemistry of the Earth, 18*, 317–328.
Shah, M. T., & Moon, C. J. (2004). Mineralogy, geochemistry and genesis of the ferromanganese ores from Hazara area, NW Himalaya, northern Pakistan. *Journal of Asian Earth Science, 23*, 1–15.
Shah, S. K., Raina, B. K., & Razdan, M. L. (1980). Redlichiid fauna from the Cambrian of Kashmir. *Journal of Geological Society of India, 21*, 511–517.
Shams, F. A. (1980a). Origin of the Shangla blue schist, Swat Himalaya, Pakistan. *Geological Bulletin of University of Peshawar, 13*, 67–70.
Shams, F. A. (1980b). An anatectic liquid of granitic composition from the Hazara Himalaya, Pakistan, its petrogenetic importance. *Rendiconti Atti della Accademia Nazionale dei Lincei, 68*, 207–215.
Shams, F. A. (1983). Granites of the NW Himalaya in Pakistan. In F. A. Shams (Ed.), *Granites of Himalayas, Karakorum and Hindukush* (pp. 75–113). Lahore: Institute of Geology, Panjab University.
Shanker, R. (1975). Stratigraphic analysis of chert member of Lower Tal Formation in Dehradun and Tehri districts, U.P. *Record Geological Survey of India, 106*, 54–74.
Sharma, T. R., & Gupta, K. R. (1972). On the spilite-keratophyre rocks of Thanamandi area, Kashmir Himalaya. *Himalayan Geology, 2*, 452–467.
Sharma, R., & Joshi, M. N. (1997). Fluid of magnesitization: Diagenetic origin of Bauri magnesite, Kumaun Lesser Himalaya. *Current Science, 73*, 789–792.
Sharma, R., Joshi, P., & Pant, P. D. (2008). The role of fluids in the formation of talc deposits of Rema area, Kumaun Lesser Himalaya. *Journal of Geological Society of India, 73*, 237–248.
Sharma, R., & Nayak, B. K. (1991). Ore petrology and origin of lead-zinc deposits in Great Limestone, Riasi, District Udhampur (J & K). *Journal of Himalayan Geology, 2*, 103–110.
Sharma, R., Verma, P., & Joshi, M. N. (2003). Barite mineralization in western Himalaya: Distribution and depositional trends. *Himalayan Geology, 24*, 75–82.
Shields, G. (1999). Working towards a new stratigraphic calibrations scheme for the Neoproterozoic-Cambrian. *Eclogae Geologicae Helvetiae, 92*, 221–233.
Shukla, U. K., & Pant, C. C. (1996). Facies analysis of the late Proterozoic Nagthat Formation, Nainital Hills, Kumaun Lesser Himalaya. *Journal of Geological Society of India, 47*, 431–445.
Singh, S. (2003). Conventional and SHRIMP U–Pb zircon dating of the Chor granitoid, Himachal Himalaya. *Journal of Geological Society of India, 62*, 614–626.
Singh, B. N., Geol, O. P., & Joshi, M. (1991). Chemical mineralogical classification of granitoid rocks: A case study from Dhunaghat area of Kumaun Lesser Himalaya. *Bulletin Indian Geological Association, 24*, 101–108.
Singh, B., & Kumar, Santosh. (2005). Petrogenetic appraisal of early Palaeozoic granitoids of Kinnaur district, High Himachal Himalaya. *Gondwana Research, 8*, 67–76.
Singh, K., & Sharma, R. (1997). Magnesite mineralization along the Chamba Thrust, Himachal Himalaya: Structural control and depositional environment using fluid inclusions. *Journal of Geological Society of India, 49*, 289–296.
Sinha, A. K. (1977). Riphean stromatolites from western Lower Himalaya, Himachal Pradesh, India. In E. Flugel (Ed.), *Fossil Algae* (pp. 86–100). Berlin: Springer.
Sinha, A. K. (1989). *Geology of higher central Himalaya*. Chichester: Wiley. (236 p).
Srikantia, S. V. (1981). Lithostratigraphy, sedimentation and structure of Proterozoic–Phanerozoic formations of Spiti basin in Higher Himalaya of Himachal Pradesh. In A. K. Sinha (Ed.), Contemporary geoscientific researches in Himalaya (Vol. I). Dehradun: Bishensingh & Mahenderpalsingh, pp. 31–48.
Srikantia, S. V., & Sharma, R. P. (1972). The Precambrian salt deposit of the Himachal Pradesh Himalaya—Its occurrence, tectonics and correlation. *Himalayan Geology, 2*, 222–238.

Srikantiah, S. V., & Sharma, R. P. (1976). Geology of the Shali belt and the adjoining areas. *Memoires Geological Survey of India, 106*, 31–116.

Stocklin, J. (1980). Geology of Nepal and its regional frame. *Journal of Geological Society of London, 137*, 1–34.

Stutz, E. (1988). Géologie de la chaine de Nyimaling aux confins du Ladakh et du Rupshu (NW Himalaya, Inde)—évolution paléogéographique et tectonique d'un segment de las marge nord-indienne. *Memoires de géologie de l'Universite de Lausanne, 3*.

Tahirkheli, R. A. K. (1970). The geology of the Attock-Cherat Range, West Pakistan. *Geological Bulletin University of Peshawar, 5*, 1–26.

Tahirkheli, R. A. K. (1982). Geology of the Himalaya, Karakoram and Hindukush in Pakistan. *Geological Bulletin Peshawar University, 15*, 1–51.

Tangri, S. K., Bhargava, O. N., & Pande, A. C. (2003). Late Precambrian-Early Cambrian trace fossils from Tethyan Himalaya, Bhutan and their bearing on the Precambrian-Cambrian boundary. *Journal of Geological Society of India, 62*, 708–716.

Tangri, S. K., & Pande, A. C. (1995a). Tectonostratigraphy of Tethyan sequence. *Geological Survey India Special Publications, 39*, 109–142.

Tangri, S. K., & Pande, A. C. (1995b). Tethys sequence. In O. N. Bhargava (Ed.), *The Bhutan Himalaya: A geological account* (pp. 109–141). Kolkata: Geological Survey of India.

Tangri, A. K., & Singh, I. B. (1982). Palaeo-environment of Blaini Formation, Lesser Himalaya. *Journal of Palaeontology Society of India, 27*, 35–48.

Tewari, D. N. (1973). Nesquehonite—A possible precursor in the origin of Himalayan magnesite. *Himalayan Geology, 3*, 94–102.

Tewari, V. C. (2003). Sedimentology, palaeobiology and stable isotope chemostratigraphy of the Terminal Neoproterozoic Buxa Dolomite, Arunachal Pradesh, NE Lesser Himalaya. *Himalayan Geology, 24*, 1–18.

Tewari, V. C., & Sial, A. N. (2007). Neoproterozoic-Early Cambrian isotopic variation and chemostratigraphy of the Lesser Himalaya, India, Eastern Gondwana. *Chemical Geology, 237*, 84–108.

Thakur, V. C., Rawat, B. S., & Islam, R. (1990). Zanskar crystallines—Some observations on its lithostratigraphy, deformation and metamorphism and regional framework. *Journal of Himalayan Geology, 1*, 11–25.

Tiwari, M. (1996). Precambrian-Cambrian boundary microbiota from the Chert-Phosphorite member of Tal Formation in Korgai Syncline, Lesser Himalaya. *Current Science, 71*, 718–719.

Tiwari, M. (1997). Nabaviella acanthomorpha n.sp., a sponge spicule from the Precambrian-Cambrian boundary interval in the Tethys sequence of northwestern Kashmir. *Journal of Geological Society of India, 50*, 655–658.

Tiwari, M. (1999). Organic-walled microfossils from the Chert-Phosphorite member of Tal Formation, Precambrian-Cambrian boundary, India. *Precambrian Research, 97*, 99–113.

Tiwari, M. (2008). Additional Neoproterozoic sponge specules from Gangolihat Dolomite, Kumaun Lesser Himalaya. *Himalayan Geology, 29*, 49–55.

Tiwari, M., & Knoll, A. H. (1994). Large acanthomorphic acritarchs from the Infrakol Formation of the Lesser Himalaya and their stratigraphic significance. *Journal of Himalayan Geology, 5*, 193–201.

Tiwari, M., & Pant, C. C. (2004). Neoproterozoic silicifed microfossils in Infrakrol Formation, Lesser Himalaya, India. *Himalayan Geology, 25*, 1–21.

Tiwari, Meera, & Pant, I. (2009). Microfossils from the Neoproterozoic Gangolihat Formation, Kumaun Lesser Himalaya: Their stratigraphic and evolutionary significance. *Journal of Asian Earth Science, 35*, 137–149.

Tiwari, M., Pant, C. C., & Tewari, V. C. (2000). Neoproterozoic sponge spicules and organic-walled microfossils from the Gangolihat Dolomite, Lesser Himalaya, India. *Current Science, 79*, 651–654.

Tripathi, C., Jangpanji, B. S., Bhatt, D. K., Kumar, G., & Raina, B. K. (1984). Early Cambrian brachiopods from Upper Tal, Mussoorie Syncline, Dehradun district, U.P. *Geophytology, 14*, 221–227.

Trivedi, J. R. (1990). *Geochronological studies of Himalayan Granites*. Unpublished Ph.D. Thesis, Physical Research Laboratory, Ahmedabad, 170 p.

Trivedi, J. R., Gopalan, K., & Valdiya, K. S. (1984). Rb–Sr ages of granite rocks within the Lesser Himalayan nappes, Kumaun, India. *Journal of Geological Society of India, 25*, 641–654.

Upadhyay, R., & Parcha, S. K. (2012). Ichnofossils from the Jadhganga (Nelang) Valley, Uttarkashi district, Garhwal Tethys Himalaya, India. *Himalayan Geology, 33*, 83–88.

Upreti, B. N. (1996). Stratigraphy of the western Nepal, Lesser Himalaya: A synthesis. *Journal of Nepal Geological Society, 13*, 11–28.

Upreti, B. N. (1999). An overview of the stratigraphy and tectonics of the Nepal Himalaya. *Journal of Asian Earth Sciences, 17*, 577–666.

Valdiya, K. S. (1962a). An outline of the stratigraphy and structure of the southern part of the Pithoragarh District, U.P. *Journal of Geological Society of India, 3*, 27–48.

Valdiya, K. S. (1962b). A study of the Champawat Granodiorite and associated metamorphics of the Lohaghat subdivision, district Almora, U.P., with special reference to petrography and petrogenesis. *Indian Mineralogist, 3*, 6–37.

Valdiya, K. S. (1968). Origin of the magnesite deposits of southern Pithoragarh, Kumaun Himalaya. *Economic Geology, 63*, 924–934.

Valdiya, K. S. (1969). Stromatolites of the Lesser Himalayan carbonate formations and the Vindhyan. *Journal of Geological Society of India, 10*, 1–25.

Valdiya, K. S. (1970). Simla Slates, the Precambrian flysch of Lesser Himalaya; its turbidites, sedimentary structures and palaeocurrents. *Geological Society of American Bulletin, 81*, 451–468.

Valdiya, K. S. (1972). Origin of phosphorite of the Late Precambrian Gangolihat Dolomite of Pithoragarh, Kumaun Himalaya, India. *Sedimentology, 19*, 115–128.

Valdiya, K. S. (1976). Himalayan transverse faults and folds and their parallelism with subsurface structures of North Indian plains. *Tectonophysics*, *32*, 353–386.

Valdiya, K. S. (1980a). *Geology of Kumaun Lesser Himalaya*. Dehradun: Wadia Institute of Himalayan Geology. (291 p).

Valdiya, K. S. (1980b). The two intracrustal boundary thrusts of the Himalaya. *Tectonophysics, 66*, 323–348.

Valdiya, K. S. (1981). Tectonics of central sector of the Himalaya. In H. K. Gupta & F. M. Delancy (Eds.), *Zagor–Hindukush Himalaya, geodynamic evolution, geodynamics series* (Vol. 3). Washington D.C.: Publications of American Geophysics Union, pp. 87–110.

Valdiya, K. S. (1988). *Geology and Natural Environment of Nainital Hills*. Nainital: Gyanodaya Prakashan. (155 pp).

Valdiya, K. S. (1993). Evidence for Pan-African–Cadomian tectonic upheaval in Himalaya. *Journal of Palaeontology Society of India, 38*, 51–62.

Valdiya, K. S. (1995). Proterozoic sedimentation and Pan-African geodynamic development in the Himalaya. *Precambrian Research, 74*, 35–55.

Valdiya, K. S., Paul, S. K., Chandra, T., Bhakuni, S. S., & Upadhyay, R. (1999). Tectonics and lithological characterization of the Himadri (Great Himalaya) between Kali and Yamuna rivers, Central Himalaya. *Himalayan Geology*, *20*, 1–17.

Valdiya, K. S., & Goel, O. P. (1983). Lithological subdivision and petrology of the Great Himalayan Vaikrita Group in Kumaun. *Proceedings of the Indian Academy of Sciences (Earth & Plant Sciences*), *92*, 141–163.

Velasco, F., Pesquera, A., & Olmedo, F. (1987). A contribution to the ore genesis of the magnesite deposit of Eugui, Navassa (Spain). *Mineralium Deposita, 22*, 33–41.

Venkatachala, B. S., & Kumar, A. (1997). Cyanobacterial mats from the Neoproterozoic Vaishnodevi Limestone, Jammu and Kashir. *Current Science, 73*, 83–87.

Virdi, N. S. (1990). Vendian-Lower Cambrian dessication along the southern margin of the Palaeotethys. *Journal of Himalayan Geology, 1*, 103–114.

Wadia, D. N. (1934). The Cambrian-Trias sequence of NW Kashmir. *Record Geological Survey of India, 68*, 121–167.

Wadia, D. N. (1937). Permo-Carboniferous limestone inliers in the subHimalayan Tertiary Zone of Jammu, Kashmir Himalaya. *Records Geological Survey of India, 72*, 162–173.

Wakhloo, S. N., & Shah, S. K. (1968). A note on the Bafliaz Volcanics of western Pir Panjal. *Publication Centre Advanced Studied Geology, Panjab University, 5*, 53–64.

West, W. D. (1939). Structure of the Shali window near near Simla. *Records Geological Survey of India, 74*, 133–163.

Yeats, R. S., & Hussain, A. (1987). Timing of structural events in the Himalayan foothills of northwestern Pakistan. *Bulletin Geological Society of America, 99*, 161–175.

Chapter 12
Himalaya Province Between Pan-African and Hercynian Tectonic Upheavals

12.1 Disturbed Beginning of Palaeozoic Era

The beginning of the Palaeozoic era witnessed complete cessation of sedimentation in the Lesser Himalaya subprovince and in the Peninsular India. And there was pronounced interruption in basin-filling in the Tethyan realm (Valdiya 1993, 1995). The duration of interruption varied from sector to sector, but lasted until about the Middle Ordovician over larger parts. It seems that the Indian continental plate with its Tethyan margin had gradually risen up, forcing the sea to retreat from its many parts. Only the northern continental margin continued to remain under the sway of the sea (Fig. 12.1).

Indisputable evidence of tectonic movement towards the end of the Neoproterozoic era and beginning of the Palaeozoic is seen in some parts of the Tethyan subprovince as already discussed in Chap. 11. The mildly metamorphosed rocks of the Hazara Slate are characterized by axial planar cleavage and yielding 951 ± 20 Ma, 752 ± 20 Ma and 728 ± 20 Ma ages (Crawford and Davies 1975). They are overlain unconformably by sedimentary succession of the Abbotabad Formation beginning with the Tanakki Conglomerate (Fig. 12.2), containing clasts derived from the mildly metamorphosed Hazara rocks. And the upper part of the Abbotabad is made up of carbonates that contain Cambrian fossils (Baig et al. 1988). It may be recapitulated that this tectonic disturbance was followed 500 ± 25 million years ago by invasion of granitic magma over a large region (Fig. 10.5). Indeed, the granite was emplaced over a vast belt stretching from Mansehra in northern Pakistan to Manaslu and beyond in north-eastern Nepal (Fig. 11.10). The granitic activity was preceded by volcanism in some parts of the Himalaya—the Khewra in the Salt Range, the Bafliaz in Poonch, the Hilap in Kinnaur, the Mandi in Himachal Pradesh, the Ganesh Himal in Nepal and the Singhi in central Bhutan.

K.S. Valdiya, *The Making of India*, Society of Earth Scientists Series,
DOI 10.1007/978-3-319-25029-8_12

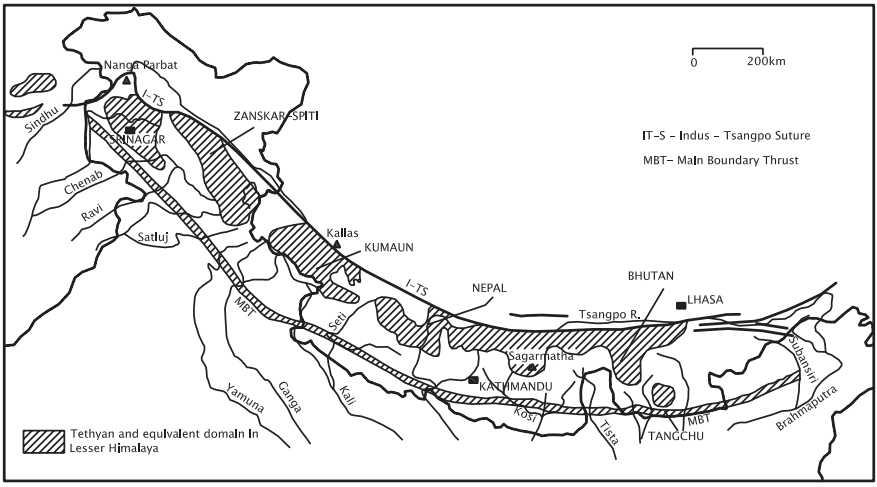

Fig. 12.1 Tethyan subprovince of the Himalaya comprises a number of basins which record a chequered history of sedimentation from the beginning of the Lower Cambrian up to the Eocene, with many big and small interruptions (after Valdiya 1998)

In south-central Nepal (Fig. 12.3), the Tistung sediments of the Palaeozoic Phulchauki succession south of Kathmandu rest unconformably upon the metasedimentary rocks of the Precambrian Bhimphedi Group, which show foliation and deformation one phase more than the younger sediments in the Tistung–Kulikhani section (Kumar et al. 1978). And the clasts of the Basal Conglomerate of younger unit are derived from the Bhimphedi.

This tectonic event was not an isolated occurrence, but global in dimension. This is evident from the dramatic change in the palaeogeography world over, related possibly to the reorganization of continental plates, and making and unmaking of a supercontinent. Simultaneously, there was profound change in the climate during the Late Precambrian–Cambrian interval, and the world witnessed explosive evolution of the biosphere (Brasier 1992). This biological event was manifest in the biomineralization of skeletons—the formation of phosphatic and silicious shells of invertebrate organisms in the initial stage of adaptive radiation. This implies that the sea water had become enriched in nutrients, at least in some niches of its environment.

12.2 Cambrian Canvas of Biostratigraphy

12.2.1 Haitus

In northern Pakistan, the Late Proterozoic Abbotabad is capped by a 20–150-m-thick sequence of iron-rich chert and siltstone grading into brown and red siltstones and shales that are locally phosphatic and glauconitic known

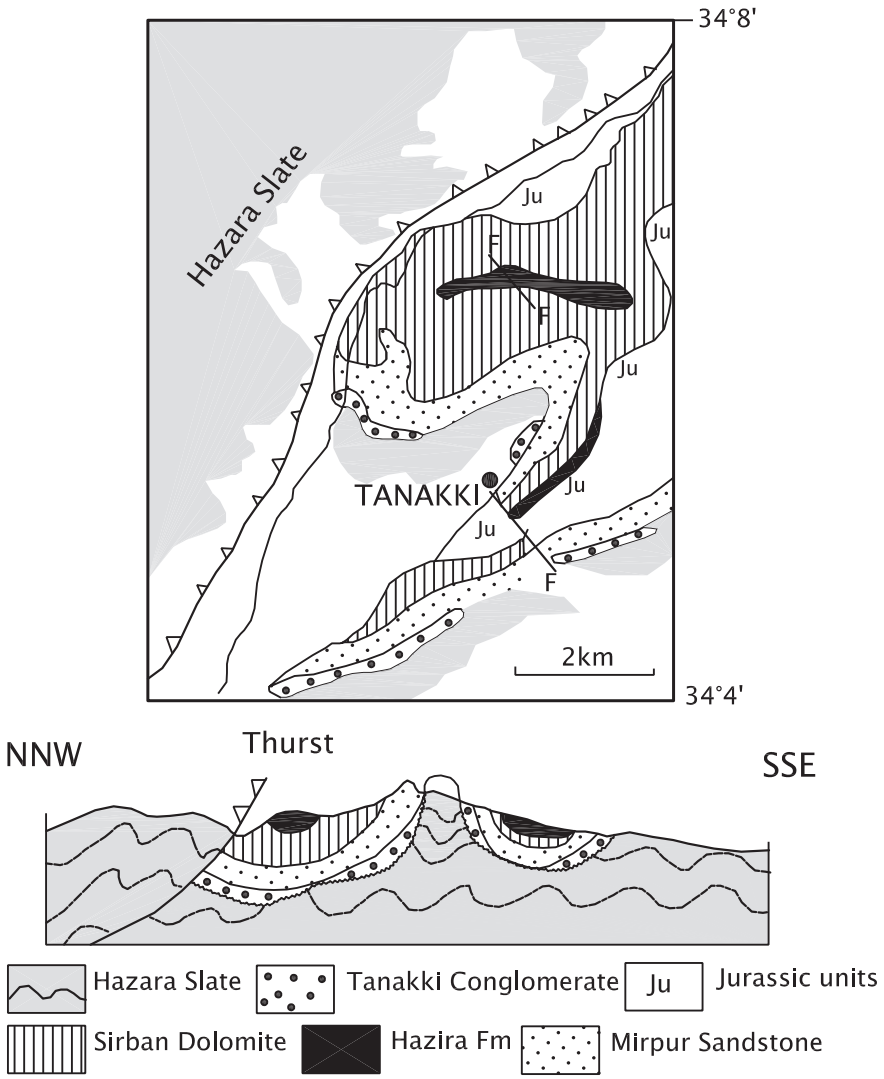

Fig. 12.2 Geological sketch map and cross section of the Tanakki area in the Hazara district, northern Pakistan, showing an angular unconformity between the mildly metamorphosed Hazara Slate and the Tanakki Conglomerate. The latter belongs to the Cambrian Abbotabad Formation (after Baig et al. 1988)

as the *Hazira Formation*. The Hazira shales contain Lower Cambrian *Hyolithes* and *Chancelloria* (Latif 1970, 1972) and archiasters and calyptomids (Fuchs and Moestler 1972). There is an attenuated horizon of the Cambrian succession east of Mardan at Ambar (Tahirkheli 1970, 1992).

Across the Sindhu River in Kashmir, the Later Proterozoic *Dogra Slate* (also described as the *Machhal* or *Ramsu*) is conformably overlain by an almost

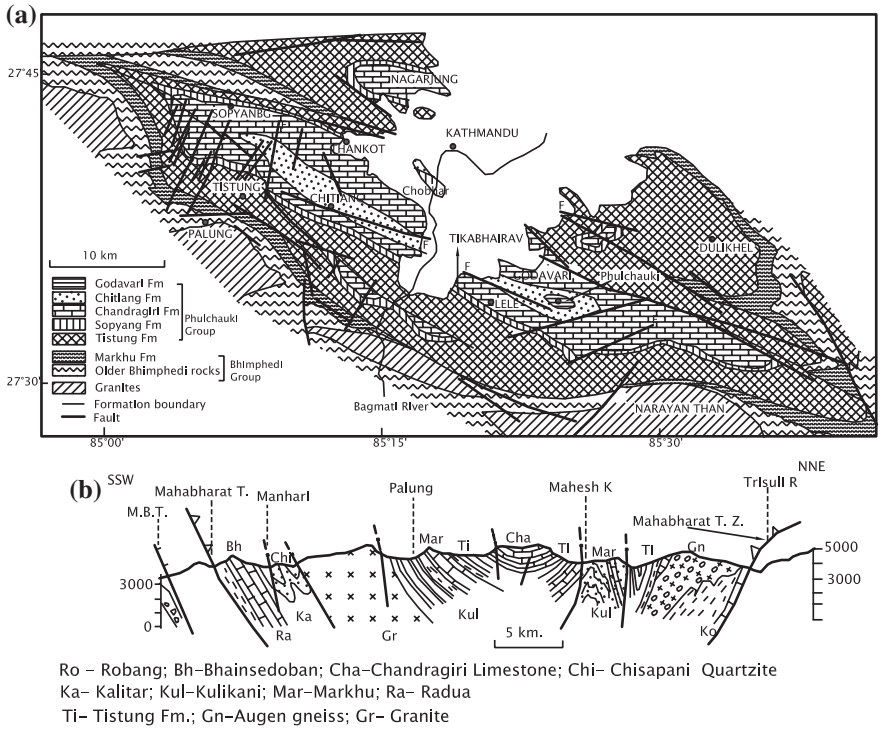

Fig. 12.3 Geological sketch map and cross section of the Chandragiri Hills in Nepal showing Palaeozoic succession (based on Stocklin 1980)

complete succession of the Cambrian *Pohru Group* (Shah 1982). Despite continuity of sedimentary succession (Fig. 12.4; Table 12.1), there are a number of biostratigraphic gaps, and the fossil-bearing horizons have restricted extent. Consisting of dark grey slates with bands of greywackes and greyish green sandstones and subordinate limestones, the Pohru is divided into the *Lolab*, *Nutunus* and *Trahagam* formations in the Kupwara–Hundwara region in north-western Kashmir and into the *Khaiyar* and *Karikul* units in the Liddar Valley, Anantnag district. The Lolab (Khaiyar) sequence contains Lower Cambrian trilobite *Redlichia* and primitrive brachiopod *Obolus* along with prolific trace fossils that represent annelid markings. The Nutunus unit is characterized by early Middle Cambrian *Ptychoparia–Tonkinella* fauna together with *Trilagnostus, Diplognostus* and *Pagetia* (Shah 1982; Shah and Sudan 1987; Parcha 1999, 2005). The micritic bluish limestone with bands of oolitic and pisolitic limestones of the Trahagam has yielded early Upper Cambrian *Damesella* and *Blackwelderoides*.

In the Zanskar–Lahaul–Spiti basins (Figs. 12.5 and 12.6), the Haimanta metaflysch (*Batal* Fm) gives way upsection to a 800–1000-m succession of greywackes and dark grey green shales (*Kunzumla* Fm) characterized by *Cruziana* trace fossils and *Redlichia* trilobite (Srikantia 1981; Bhargava and Srikantia 1985). The

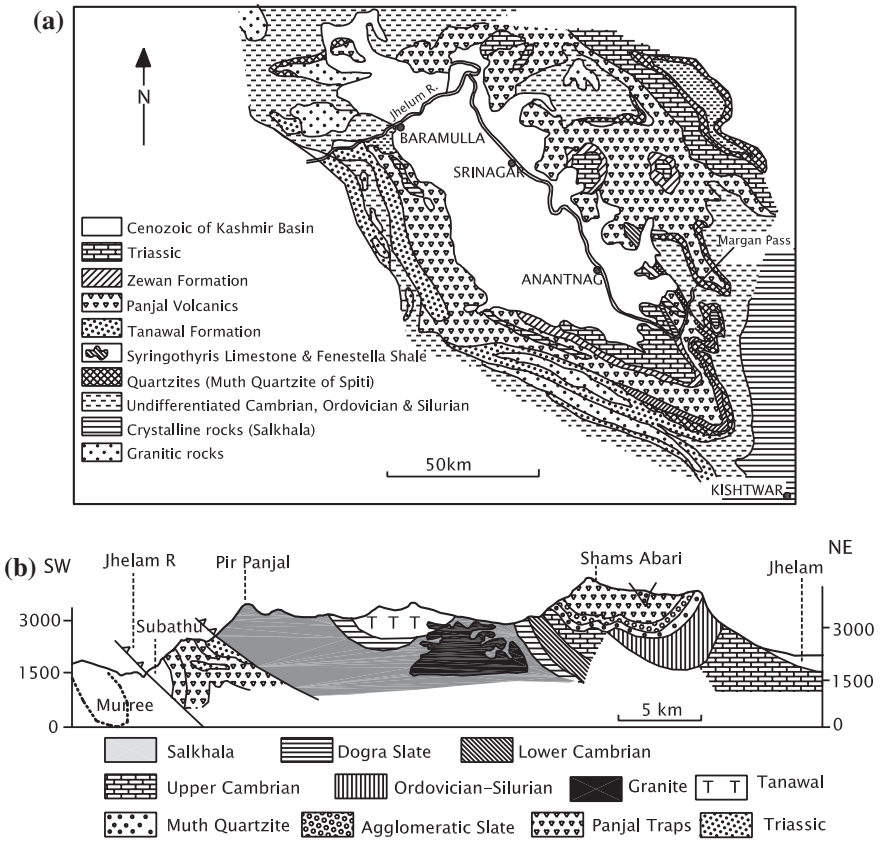

Fig. 12.4 **a** Sketch map showing the spread of the Palaeozoic formations in the Kashmir Valley between the PirPanjal and the Zanskar ranges (after Shah 1982). **b** Section across the Shams Abari Peak shows the structural design and stratigraphic succession of the Pir Panjal range (after Wadia 1934)

Kunzumla grades upwards into dolomitic limestone characterized by domal stromatolites, and the associated shales contain *Neobolus, Lingulella* and *Ptychoparia*. This unit is described as the *Karsha* in the Zanskar Belt (Nanda and Singh 1976) and as the *Parahio* in the Spiti region (by H.H. Hayden in 1904). The Karsha has been assigned a possible Early Cambrian age (Baud et al. 1984; Fuchs 1977). In the Kurgiakh section, probably Upper Cambrian bioturbated pelites showing mudcracks and cross-bedding are associated with nodular dolomite and basaltic tuffs in the lower parts (Gaetani et al. 1985). Basic volcanics occur in the Batal in Himachal (Bhargava 1991). Seven assemblages of trilobites recognized along the Pin and Parahio valleys in Spiti Basin place the succession in the temporal range from late early Lower Cambrian to early Upper Cambrian (Parcha 1999). There are no sediments of the temporal span Middle–Upper Cambrian to Lower Ordovician in this sector, implying a hiatus (Shah 1991, 2005).

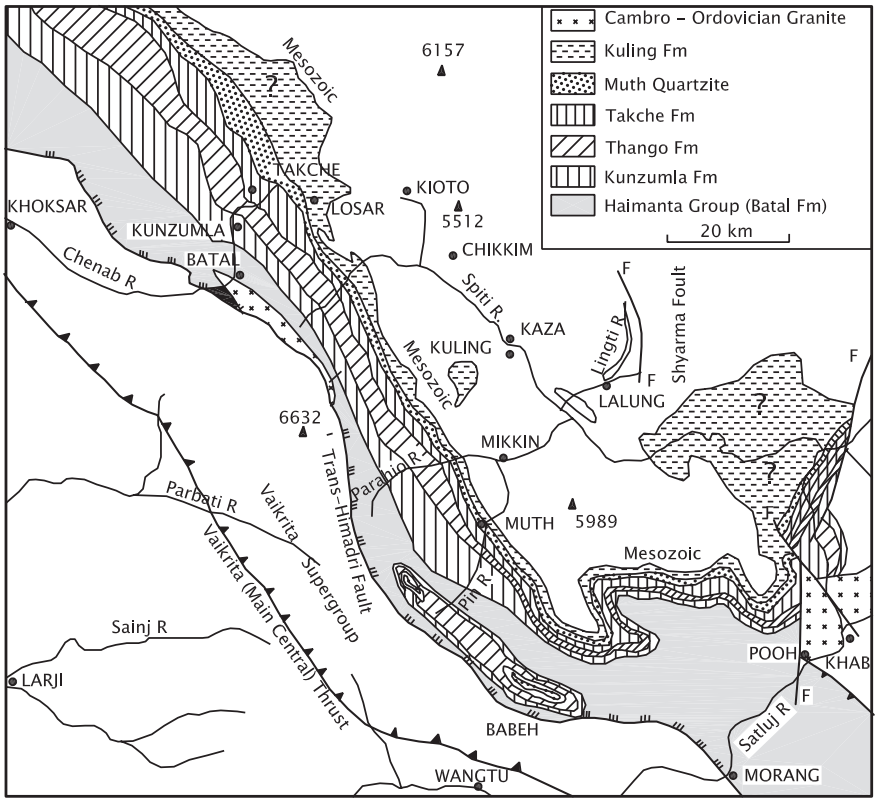

Fig. 12.5 Geological sketch map of the Spiti Basin showing the spread of the Palaeozoic formations (after Sinha 1989)

In the central sector embracing Kumaun and Nepal (Fig. 11.6), the Cambrian is intriguingly absent, and the Late Precambrian metasediments are succeeded directly by the carbonates bearing Middle Ordovician fauna. In central Bhutan, the Precambrian metamorphic succession Chekha is unconformably overlain by a thick suite of volcanic rocks—amygdaloidal–aphyric andesitic flows and pyroclastics with sedimentary intercalation (*Singhi* Fm). In the Chendebji area, the volcanics are acidic in composition. The Singhi is succeeded by the quartzite–conglomerate sequence described as the *Nakechu* (Chaturvedi et al. 1981) and the *Deshichiling*. The phyllitic partings contain ichnofossil. Covering large parts of the Black Mountains, the overlying *Maneting* Formation, is a sequence of shale, greywacke, micaceous–ferruginous arenite and quartzarenite with subordinate thin-bedded limestone. The upper horizon contains, besides trace fossils, a rich assemblage of Early Cambrian fauna—brachiopods *Glossella* and *Lingulella* and lamellibranchs *Ctenodonta* and *Palaeoneilo* (Tangri and Pande 1995).

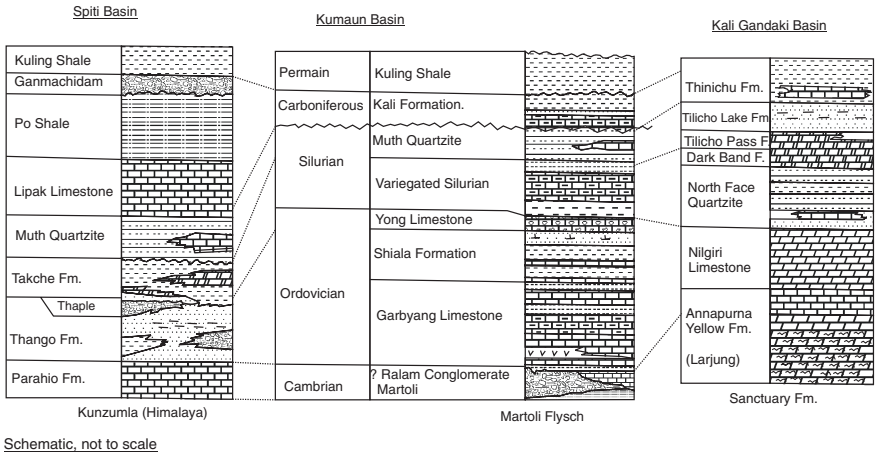

Fig. 12.6 Lithological columns illustrating the lithostratigraphy of the Palaeozoic formations and the intervening hiatuses in the Tethys subprovince

12.2.2 Situation in Eastern Myanmar

J.C. Brown and V.P. Sondhi in 1933 provided detailed account of the geology of the Southern Shan States between Kalaw and Taunggyi. Unconformably overlying the Neoproterozoic metamorphics of the Chaung Magyi Group, there is a thick succession of ripple-marked red purple and violet sandstones intercalated with red shale and siltstone—the *Pangyun* in Northern Shan States and the *Molohein* in Southern Shan States (Bender 1983). In the Yadanatheingyi and Kyaukme–Longtawkno areas, the purple sediments include polymictic conglomerate and intercalations of dolomite and limestone of the shelf environment. In the Pindiya Range, the top of this succession has yielded Upper Cambrian trilobites *Saukiella*, *Eusaukia* and *Dalminella* (Thein 1973a). A sequence of conglomeratic sandstone and crystalline dolomite forming peaks of the Bawsiang and Heho ranges has been assigned an Upper Cambrian to Early Ordovician age—on the basis of the concordantly overlying Naungkangyi succession containing Middle Ordovician fauna.

12.2.3 Cambrian Volcanism

There was explosive volcanic activity in a part of the Shan States in eastern Myanmar, emplacing more than 1000-m-thick deposits of acid tuffs and agglomerates known as the *Bawdwin Volcanics*. Significantly, these volcanic rocks are characterized by deposits of lead, zinc and silver sulphides and veins of barytes. The ~100-m-thick basaltic lava-pyroclastic cycles of potassium–calc alkaline volcanics of the Singhi–Rachau–Nobding areas in Bhutan underlay the Early Cambrian

succession (Tangri and Pande 1995). The volcanics exhibit strong enrichment in LREE and comparatively less HREE fractionation. Basic volcanic rocks occur in the Batal in the Spiti region (Bhargava 1991).

In the Zanskar region, the Upper Cambrian sequence in the Kurgiakh section includes basaltic tuffs with bioturbated pelites in the lower part (Gaetani et al. 1985).

12.3 Ordovician Period

12.3.1 Central Sector

The central sector of the Tethys subprovince embracing Kumaun and Nepal saw initiation of Palaeozoic sedimentation in the Middle Ordovician time. North of Sagarmatha in the Arun Valley, the *Chiatsung* succession overlying the Late Precambrian Rouquiecum Fm contains Early Ordovician *Aporthophyllum, Eucalymene* and *Didoceras*. To the east in central Bhutan, the Lower Cambrian Maneting comprises deposits of debris flows (Bandyopadhyay and Gupta 1990). It is overlain by a 75-m-thick succession of cross-bedded grey white and brown quartz arenites with shales (Chaturvedi et al. 1981) are characterized by Middle Cambrian fauna (Bhargava 1995). To the west in the Kali Gandaki Valley, the 3000–4000-m-thick succession of the *Nilgiri Limestone* includes the Llavirnian brachipod-bearing blue to light grey limestones with intercalations of sericitic pelites resting on the low-grade metamorphics (Colchen et al. 1986). Similar situation obtains across the river in the Dolpho–Dhaulagiri region (Fuchs 1975). In the Kali Valley in Kumaun (Fig. 12.7), the Budhi Schist is succeeded by a thick succession of limestones and dolomitic limestones, rhythmically interbedded with marlite and calcareous shale (*Garbyang Fm*). The upper part of the Garbyang has revealed a badly preserved Middle Ordovician gastropod (Heim and Gansser 1939). The Garbyang succession of calcilutite, showing rainprints and mudcracks in ferruginous slates, was laid down in a shallow platform. The Garbyang imperceptibly passes upwards into the *Shiala Formation* made up of olivegreen shales and siltstones interbedded with blue grey crinoidal limestone and marlite with maroon and light grey limestone–shale rhythmite. Towards the top of the Shiala succession occurs a biostromal horizon.

In south-central Nepal, the Chandragiri Hills of the Mahabharat Range (Fig. 12.3) is made up of very thick Palaeozoic succession known as the *Phulchauki Group* (Bordet et al. 1960). Resting on the metamorphic rocks of the Bhimphedi, the Phulchauki succession begins with grey argillaceous to arenaceous limestone, locally containing crinoids (*Chandragiri Fm*). It is succeeded by purple siltstone alternating with sandstone, shale and sandy limestone (*Chitlang Fm*). It is this Chitlang that has yielded *Caryocrinites*, the trilobite *Pterogometopus* and some brachipods. The uppermost part of the Phulchauki is an assemblage of variegated limestone with intercalations of shale (*Godavari Fm*) containing Ordovician trilobite *Illaenus* (Funakawa 2001) together with brachiopods, orthoceratids and cephalopods.

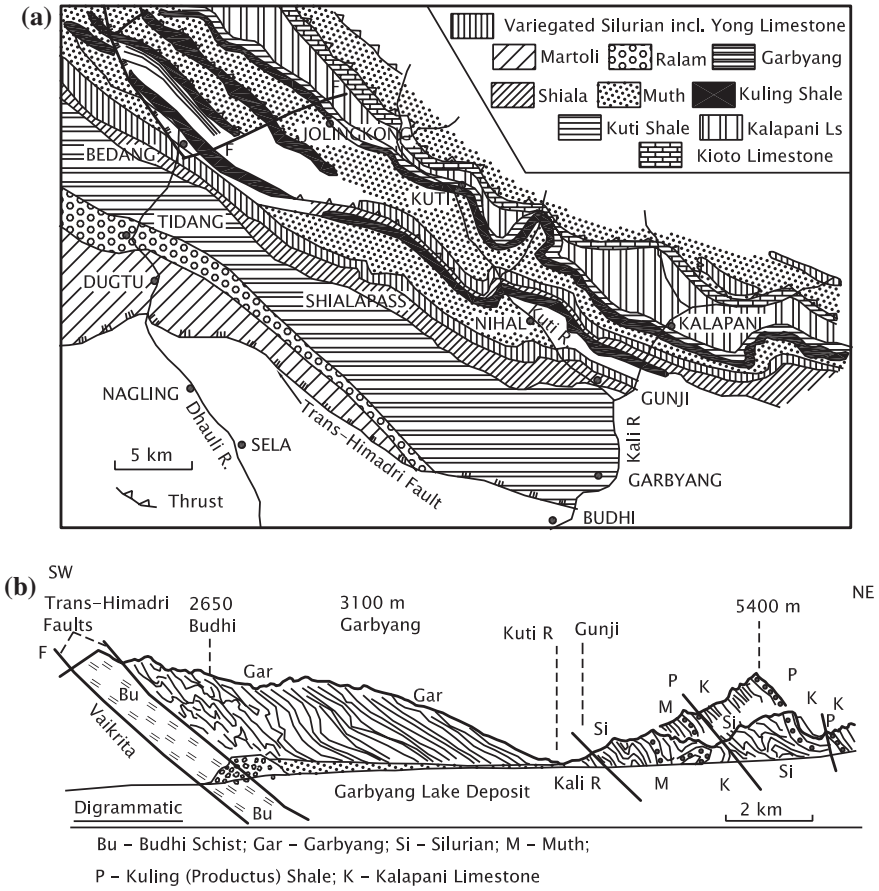

Fig. 12.7 **a** Sketch map of the geology of Tethyan domain in the Kali Valley, NE Kumaun, showing the Palaeozoic succession (after Sinha 1989). **b** Cross section illustrates the structural design of the Palaeozoic formations (after Heim and Gansser 1939)

12.3.2 Short-Lived Fluvial Regime

The Middle Ordovician in the Spiti–Lahaul basins (Fig. 12.5) commenced with deposition of gravelly sediments by streams and rivers that flowed in the northerly direction. The 600–900-m-thick fluvial conglomerate and sandstone described variously as the *Thaple* (Nanda and Singh 1976), the *Thango* (Srikantia 1981) and the *Shian Quartzite* (Bagati et al. 1991) is a multistoried assemblage of sub-litharenites with minor mudstone. The sandstones are characterized profusely by cross-bedding—planar as well as trough-shaped and herringbone type—pointing to deposition in an environment affected by tides. Remains of a plant *Rhaecopteris* in some places indicate that these streams drained the land clothed with vegetation. Significantly, in the Yunamchu area SW of Sarchu, the Thaple

is intruded by Early Permian—(U–Pb) 284 ± 1 Ma—dykes of alkaline-granitic composition, depleted in Al_2O_3 and with higher values of Th, Nb, REE, Y and Zr (Spring et al. 1993).

In Kashmir, the *Marhaum–Margan* formations, consisting of conglomerates and quartz arenites with argillite intercalations, contain abundant orthids, strophominids, trilobites and corals of the Ordovician age (Wadia 1934; Shah 1982). In northern Pakistan, the *Shahkotbali* succession of yellow brown sandstones and marble resting on the Abbotabad contain the Ordovician–Silurian bryozoans *Rhombopora* and *Bathopora* in the Hazara–Cherat Range (Tahirkheli 1970), and the Ordovician to Middle Ludlow conodonts in the lower part of the Khyber Pass succession (Shah et al. 1980).

12.3.3 Eastern Myanmar

Concordantly overlying the Pangyun–Molohein formations, the *Naungkangyi* succession (Fig. 12.8) in Northern Shan States comprises fine-grained clastics with variegated carbonates and marls that contain Ashgillian to Llandoverian (Silurian–Devonian) echinoderms, tribolites, brachiopods, and less common graptolites. The orthoceratids and conodonts place the Naungkangyi in the Ordovician time span. In Southern Shan States, the thickly bedded micacaceous siltstone and multicoloured mudstone with marl of the *Ngwetaung* and *Lokepyin* units together with the 1600–2000-m-thick succession of limestone and dolomite with siltstone intercalations (*Doktoye–Wunbye* formations) are succeeded by the 100–150 m of buff claystone, marl and calcareous siltstone (*Kinle–Na on* horizons), capped by calcareous sandstone and red-purple shale (*Linwe Fm*) representing the Ordovician period in eastern Myanmar. It may be mentioned that the Linwe Shale at the top of the succession contains *Monograptus* and *Glycograptus* that have temporal range up to the Silurian (Thein 1973a). The *Biya Limestone* in the Mawchi area in the Kayah state and a part of the *Mergui Series* in the Tenasserim division are assumed to have Ordovician elements (Bender 1983).

12.3.4 Volcanism

In the Bawsaing–Baweetaung sector, the lower part of the Naungkangyi succession includes rhyolitic lavas and tuffs. The volcanics are associated with deposits of Pb, Zn, and Ag sulphides and veins of barytes, as seen near Maymyo. The *Bawdwin Volcanics* comprise about 1000-m-thick succession of rhyolite, rhyolitic tuff, common tuff and agglomerate intercalated with felspathic sandstones. The fossils in the sedimentary intercalation range in age from Ordovician to Silurian (Bender 1983).

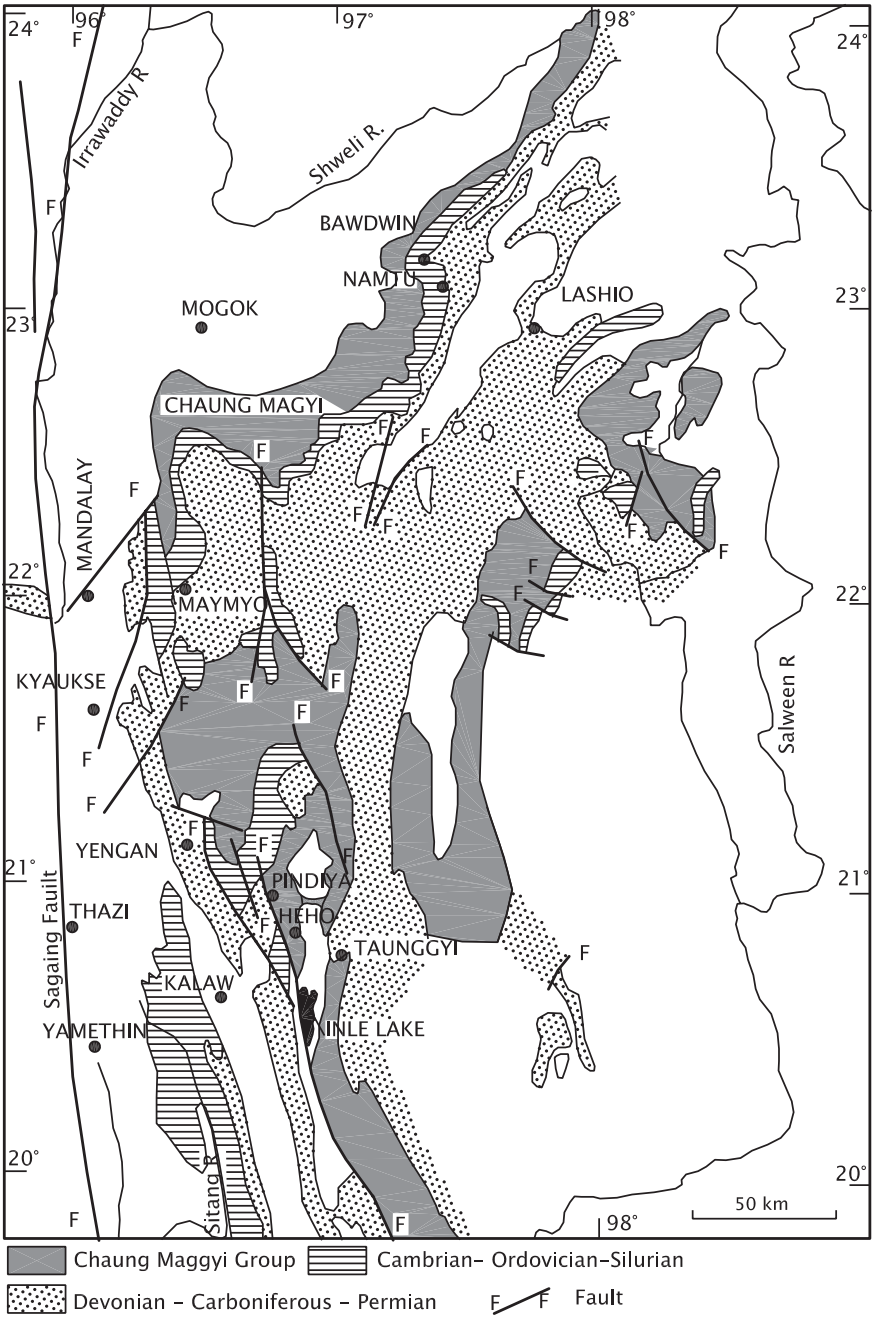

Fig. 12.8 Sketchmap of eastern Myanmar showing distribution of the Palaeozoic formations studied in the Shan States and adjoining Kayah and Karen states (after Thein 1973a)

12.4 Silurian Scenario

12.4.1 Eastern Myanmar

A 60-m-thick grey-to-black siltstone and 500-m-thick white cross-bedded sandstones becoming pink buff and red sandstone with marlite at the top—the *Pangshapye–Namhsin* formations—represent the variegated Silurian in the Northern Shan States (Figs. 12.8 and 12.9). Their equivalents in the Southern Shan States are known as the *Wabye* and the *Taungmingyi*. The Taungmingyi contains graptolite-bearing black shale intercalated with rhyolitic tuffs. The Pangshapye is characterized by *Monograptus, Orthograptus, Diplograptus* and *Climacograptus* of the early Llandovery (Silurian) time. The Namhsin contains Wenlock (Silurian) graptolites and Late Llandovery to Ludlow (Silurian) shelly fauna. The Wabye forms a part of the Pindiya Range, where the Llandovery graptolites were found. In the Kayah State deep red mudstone and mottled shale, the *Loikaw Beds*, are characterized by *Monograptus, Climacograptus* and *Diplograptus,* as reported by Coggin Brown and V.P. Sondhi in 1933.

12.4.2 Main Himalaya

Resting on the Nilgiri Limestone, the 400–700-m-thick succession of white, green, grey and pink calcareous arkosic sandstones with intercalations of dolomite and limestone forms a prominent horizon described as the *North Face Quartzite* (Bodenhausen and Egeler 1971). Clay galls are quite common in phyllitic layers sandwiched between variegated sandstones and calcareous shale containing brachiopods and crinoids. The succeeding *Dark Band Formation*, made up of calcareous siltstone and crystalline limestone, is rich in crinoids and graptolites.

In north-eastern Kumaun (Fig. 12.7), algal bioherms characterized by Early Silurian stromatoporoids form a part of the *Yong Limestone* (Shah and Sinha 1974; Khanna et al. 1983). The Yong laterally grades into what Heim and Gansser (1939) and described as the *Variegated Silurian* made up of chocolate brown and deep red siliceous limestones, rhythmically alternating with ashgrey and pink red shale. In the upper part, the dolomites and black carbonaceous shales form the top of this prominent horizon. In the Spiti area (Fig. 12.5), the Silurian succession consists of clastic limestone passing up into reddish brown dolomite described as the *Pin Dolomite* (Goel and Nair 1977) or the *Takche Formation* (Srikantia 1981). At Mikkin in the Pin Valley, the upper part of this succession has yielded Llandoverian (Lower Silurian) conodonts (Talent and Bhargava 2003). The basal part contains Late Ordovician conodonts. The Takche represents a deposit of a transgressive cycle which caused build-up of a carbonate reef in the lagoons within upper foreslope setting (Bhargava and Bassi 1998). The regressive cycle that followed left behind sands on the beaches. East of Anantnag in Kashmir, rusty brown calcareous and sandy shales with minor coral build-up contain Ashgillian to Llandoverian fauna.

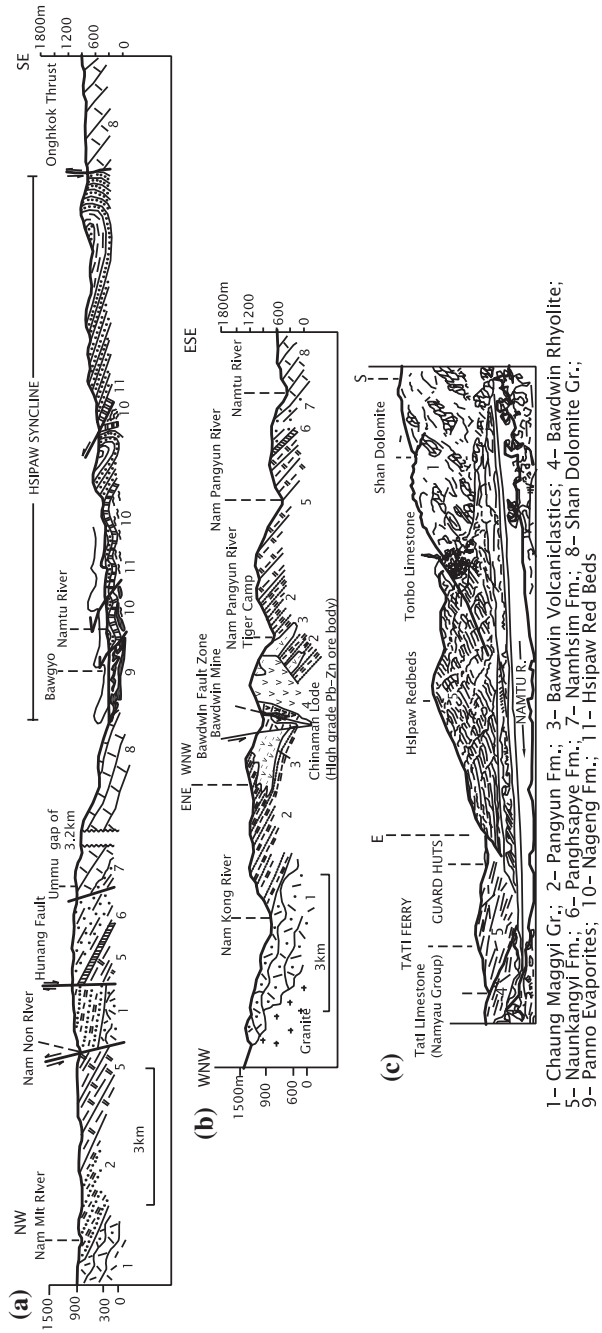

Fig. 12.9 Generalized cross sections of the Northern Shan States in eastern Myanmar. **a** Across the Namtu River showing Palaeozoic formations (after Bender 1983). **b** Relationship of the Palaeozoic units with the basement Chaung Magyi succession (after Bender 1983). **c** Relationship of the Palaeozoic with the Mesozoic succession near Tati Ferry, 5 km NNE of Hsipaw (after Brunnschweiller 1970)

As mentioned above, the Devonian marked a major break in the Himalayan sequence. In Pakistan and Kashmir, this break extends from Late Cambrian onwards. There was only shallow-water deposition during the Middle Silurian to Early Devonian in certain sectors such as western Kashmir and Nowshera. East of the Sindhu river in the western part of Kashmir (Fig. 12.4a) 300–600-m-thick band of strikingly snow-white quartzite overlying the Cambrian succession is known as the *Muth Quartzite*, lucidly described by Wadia (1939). At the base on the western slope of the Shams Abari (Fig. 12.4) occurs a unit of purple conglomerate which marks an unconformity between the Cambrian and the Devonian. In Kashmir, Zanskar, Spiti, Kumaun and north-western Nepal, the *Muth Quartzite* forms a blanket of quartzarenite (Fig. 12.5). The name Muth Quartzite was given by Franz Stoliczka in 1865 after a village in the Pin Valley (Fig. 12.5). The Muth is one of the very conspicuous datum lines in the stratigraphic history of the Himalaya. This formation was time-transgressive unit that ranged in age from Middle to Late Silurian (Shah 2005). The sediments were deposited very rapidly in a short span of time in a coastal environment. The Muth sediments represent offshore elongate bars and shoal complex (Bagati 1990; Bagati et al. 1991). Conspicuous domal structures up to 80 cm wide and 30 cm high in the quartzarenite in the Pin Valley are attributed to ascending gases produced by decomposing organic matter that was buried in the lower supratidal zone affected by tidal flushing in a wave-dominated environment (Draganits and Noffke 2004). Near Mikkin, giant trackways of arthropods in sandstone corroborate supratidal environment of the Muth (Draganits et al. 1998).

In Kumaun, the Muth is an attenuated horizon of quartzarenite with intercalations of chocolate-coloured dolomitic limestone containing brachiopods. The Muth in Nepal is represented by the *Tilicho Lake Formation*, characterized by rill marks, tool marks and flute-casts in sandstones, and the conodonts (Bodenhausen and Egeler 1971; Fuchs 1975; Fuchs et al. 1988).

The Muth marks an epoch of tectonic stability during the Later Silurian period when practically the whole of the Tethyan domain stretching from Tanawal in the west to northern Nepal became a site of shallow-water deposition of well-sorted clean sands.

12.4.3 Northern Pakistan

In the Nowshera–Khyber Pass belt (Fig. 12.10), reefal limestone with partings of quartzite and phyllite of greenish grey colour (*Kandar Phyllite*) is succeeded by a sequence of crinoidal limestone (*Misri Banda Fm*) which in the Chingalet synclinorum has yielded Llandovery to Wenlock (Early Silurian) fauna (Pogue et al. 1992). The *Landikotal* succession of limestone and slate has been assigned a Silurian age (Shah et al. 1980). The *Panjpir* succession of argillite and siltstone with lenses of conglomerate contains conodonts *Polygnathoides, Ozarkodina* and *Kockelella* of Ludlow–Pridoli (Later Silurian) age (Hussain et al. 1990; Barnett et al. 1966).

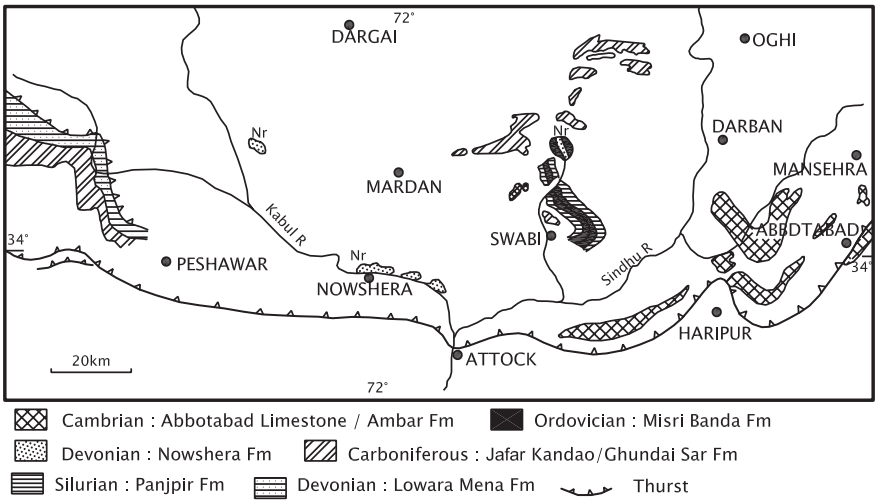

Fig. 12.10 Sketch map of the geology of northern Pakistan showing Palaeozoic formations in the midst of preponderant Precambrian metamorphics and Cambro–Ordovician granites (after Tahirkheli 1982)

12.5 Devonian Development

12.5.1 Northern Pakistan and Kashmir

The Devonian marks an important break in the Himalayan setting, as no undoubted Devonian rocks are known anywhere in the Himalaya region, except in Chitral in northern Pakistan (Shah 2005). Here, isolated pockets of Devonian rocks occur over the dominant Silurian sediments. In the Nowshera area, the Silurian sedimentation extended into the Early Devonian time (Talent and Bhargava 2003).

The 120-km-long E–W trending ridge south-east of Peshawar is a reef complex embodying biohermal core enveloped by breccia and calcarenite (*Nowshera Formation*). The complex contains Lower Devonian stromatoporoid and rugose and branching corals such as *Favosites, Thamnopora, Heliolites, Cladopora, Alveolites*, brachiopods such as *Ambocoelia, Atrypa* and *Gypidale* and the conodont *Lachkovi* (Teichert and Stauffer 1965; Teichert 1966; Barnett et al. 1966; Ali and Anwar 1969). Above the Nowshera is a 500-m-thick sequence of light grey to pink sandstones with lenticular dolomite containing Devonian fossils. The Nowshera extends westwards into the Khyber Pass region where it is represented by the *Ghundaisar* succession of variegated limestone with partings of quartzite and slate (Tahirkheli 1996). In the Lowaramena area, the Devonian consists of slates and sandstones with conglomerate lenses.

12.5.2 Eastern Myanmar

In Northern Shan States (Fig. 12.8), the succession of the *Zebingyi Beds*, the *Padaukpin Limestone* and the *Wetwin Shale*—the so-called *Maymyo Dolomite* (Brunnschweiller 1970)—comprise Devonian complex of carbonates. Along the Maymyo–Mandalay road, the Zebingyi Shale revealed Lower Devonian graptolite *Monograptus*, brachipods *Strophaedonta, Pentamerus* and *Merstella*, lamellibranchs *Modiolopsis* and *Vlasts* and trilobite *Dalmantis* (Anderson et al. 1969; Berry and Boucot 1972). The biostromal Padaukpin Limestone contains Eifelian (Middle Devonian) rugos coral *Phacellophyllum* and *Phillipsastrea* and *Peripaedium*, *Dolmophyllum, Temnophyllum* and *Puanophyllum* (Aung, 1995). The *Wetwin Shale* has been assigned to the Givetian (Mid Devonian) temporal span.

In the Karen State, the Devonian is represented by the *Loikaw Beds*.

12.6 Carboniferous Time

12.6.1 Haitus in Eastern Myanmar

The Maymyo Dolomite in the Kayah and Karen states is overlain disconformably by the Carboniferous succession of mudstones with intercalations of sandy limestones (*Mawchi/Lebyn* Fm) and greywacke with agglomerates in shale (*Taungnyo/Mergui* Fm). Among the fauna in the Taungnyo are the Later Carboniferous brachipods *Dictyoclostus, Mesolotus, Spirifer* and *Squamularia* (Brunnschweiller 1970). Significantly, the Mergui succession in the archipelago of the Tenasserim division includes intercalations of tuffs and agglomerates, the latter comprising pumice, volcanic bombs and glass porphyry (Bender 1983). The Twangpang area in Northern Shan States was intruded by 340 ± 34 Ma porphyritic granites (Mitchell et al. 1977), forming a NE–SW trending ridge parallel to the mountain range that extends from Namhsin to Yunnan in China (Fig. 12.8).

12.6.2 North-eastern Nepal

In the Sagarmatha–Shishpagma belt in north-eastern Nepal, the Neoproterozoic crystalline complex is overlain directly by a horizon of diamictite characterized by glacigene clasts—faceted, trapezoidal in shape and as large as 1000 m^3 in size (Garzanti and Sciunnach 1997). The intercalated Tournasian (early Lower Carboniferous) limestone and Fenestella-bearing Bashkirian (Middle Carboniferous) shale imply that glaciation had set in quite early in this part of the Tethyan domain.

12.6.3 Kumaun and Spiti Basins

In Kumaun pink and grey siliceous limestone, dolomite and sandstone (*Kali Fm*) contain Lower Carboniferous *Linoproductus* and *Chonetes* (Valdiya et al. 1972;

Mamgain and Mishra 1989). In the Spiti–Lahaul basin, as in Kumaun (Figs. 12.5, 12.6 and 12.7), restriction of water circulation caused development of anoxic conditions as reflected in the accumulation of thick black carbonaceous shale and black limestone, described by H.H. Hayden in 1904 as the *Lipak Limestone* and the *Po Shale*, respectively. The crinoidal black limestone in the upper reaches of the Lingti Valley contains Tournasian (early Lower Carboniferous) fossils. It was a time when gypsum was precipitated under sabkha-like conditions in lagoons. During the Visian time, the neighbouring land supplied erosional debris that contained, among other fossils, *Rhaecopteris* flora. The Po succession contains, besides the plant remains, such taxa as *Productus, Syringothyris, Linoproductus* and *Fenestella*.

The Lipak has been described as the *Syringothyris Limestone* in Kashmir and the Po as the *Fenestella Shale*. The latter unit contains Lower Carboniferous plants such as *Archaeosigillaria, Lepidosigillaria, Lepidodendropsis, Cyclostigma, Rhaecopteris, Triphyllopteris, Rhodea* and *Palmatopteris* (Singh et al. 1982).

12.6.4 Northern Pakistan

The 1000-m *Khyber Limestone* of the E–W trending axial belt comprises white limestone and dolomite with argillite partings and minor limonite-rich sandstone intruded by basic sills and dykes (Shah et al. 1980; Tahirkheli 1970). The upper member of the Khyber in the Saknali area contains Carboniferous fossils, including foraminifers.

12.7 Permian Panorama

12.7.1 New Cycle of Transgression

The Salt Range, the Khisor Range and the Kohat–Potwar belt in Pakistan witnessed return of the sea at the beginning of the Permian period. It may be recalled that in this region the sea had retreated in the beginning of the Middle Cambrian. The Permian transgression is represented by the *Nilawan* and the *Zaluch* succession (Tichert 1966; Teichert and Stauffer 1965). The *Nilawan* succession begins with diamictite made up of rafted clasts embedded in mudstone (*Tobra Conglomerate*). The Tobra unit grades upwards into marine sandstone alternating with siltstone and shale containing cold water-loving bivalve *Eurydesma* and *Conularia*, together with freshwater ostracodes and land-derived plants *Glossopteris*. The succeeding olivegreen shale (*Dandot*) contains Lower Permian brachiopods (*Discina, Martiniopsis Chonetes*), bivalves (*Eurydesma* and *Conularia*) and bryozoans. The overlying sequence of cross-bedded red-and-purple-speckled *Wardha Sandstone* includes bright pink shale with plant remains. The *Sardhari* Fm is made up of bluish–greenish sandstones and dominant brown-and-lavender-coloured shales containing *Anastomopora, Fenestella, Athyris* and

Spirifer. The *Zaluch* comprises a 300-m-thick succession of platform carbonates deposited on the edge of the continental margin with intercalation of minor calcareous sandstones and shales with phosphatic nodules. The carbonates are characterized by abundant brachiopods such as *Productus, Derbya, Neospirifer, Marginifera, Dictyoclostus, Ortholinis, Strophalosia, Dielasma, Waagenoconfra, Richthofena, Oldhamia, Linoproductus* and *Spirigerella* (Teichert 1966) together with some trilobites and plants such as *Glossopteris* and *Gangamopteris*. The fauna and flora collectively place the Zaluck in the Upper Permian time.

12.7.2 Magmatic Activity

Northern Pakistan witnessed widespread magmatic activity when the Salt Range domain was inundated by marine waters. The Shewa and Warsak areas were intruded by porphyries and the Koga area by syenites (Pogue et al. 1997). This magmatic activity is regarded as coeval with the basic volcanism that overwhelmed large parts of the Himalaya province in the Permian period.

12.7.3 Widespread Volcanism

The volcanic activities, which began with the explosive phase, are represented by agglomerates and tuffs. The volcaniclastics are intercalated with marine sediments forming the *Agglomerate Slate* (Figs. 12.1, 12.12). It was R. Lyddeker who gave this name in 1883. The pyroclastics of acid to intermediate composition (Pareekh, 1976) interfinger with and pass laterally and vertically into basaltic to andesitic lavas which C.S. Middlemiss in 1910 has named the *Panjal Traps*. The Panjal lavas show ropy structure and porphyritic to glomeroporphyritic texture and build up a pile more than 2500 m in thickness. Associated with the lavas are dolerite dykes, showing glomeroporphyritic texture. They seem to have served as feeders of the Panjal volcanics (Papritz and Rey 1989). In northern and north-eastern Kashmir, the massive lavas are aphyric tholeiites to mildly alkaline in composition (Honegger et al. 1982) and affected by metamorphism of zeolite to upper greenschist facies, but to amphibolite facies in the Suru Valley in Ladakh. The Panjal volcanics of the Zanskar region are both low-Ti tholeiite basalts showing enrichment in LREE, LILE, Fe and Ti, and depletion in Nb, P and Cr, and high Ti tholeiites exhibiting pronounced positive anomalies with respect to Nb, P and Ti in addition to the above-mentioned constituents, implying derivation from a variably enriched mantle source (Islam et al. 2003).

The volcanism lasted longer in the western Kashmir than in eastern part (Fig. 12.12). Between Tragbal and Gurais, the volcanics are intercalated with Mushelkalk and Lower Triassic limestones, and in the Erin Valley between Bandipura and Gurais, the lava flows are interbedded with the basal part of the

Upper Triassic sediments (Wadia 1934). Similar development took place in northern Pakistan (Calkins et al. 1975). Interpretation of the virtual geomagnetic pole positions assigns the Phe Volcanics an age of Upper Carboniferous to Lower Permian (Poornachandra Rao et al. 2003). In northern Lahul, the *BaralachaLa dyke swarms* show clear spatial association with Lower Carboniferous tension-related synsedimentation faults. These are genetically unrelated to the Panjal Volcanics, and belong to an altogether different suite of tholeiitic to alkaline basalts that evolved by fractional crystallization (Vannay and Spring 1993).

12.7.4 Occurrence of Terrestrial Plants

The limestones–shale succession above the Panjal Traps is described as the *Zewan Beds* in the Vihi district, upper Sind and Liddar valleys (Fig. 12.11). The sediments are characterized by abundance of *Productus.* While the lower part of the succession is rich in bryozoan *Protoretepora,* the upper calcareous part abounds in brachiopods (*Linoproductus, Productus, Dielasma, Martinia, Spiriferina, Spirigerella, Neomarginifera, Marginifera, Lyttonia, Chonetes, Derbya*), the coral *Zaphrentis* and the ammonite *Xenaspis* of the Middle Permian age. Significant is the occurrence of plant fossils, both above and below the lava pile (Fig. 12.12). The shales at Nishatbagh and Mamal contain *Gangamopteris, Glossopteris, Parasphenophyllum, Ginkgophyllum, Lobatannalaria, Rhepidosis* and *Rajahia* of undoubted Gondwana domain. But this floral assemblage also contains elements such as *Lobatannularia, Rajahia, Sphenophyllum, Rhipidopsis* of the *Cathaysian affinity*, indicating link with the vegetation that flourished in the Sino-Tibetan landmass (Singh et al. 1982; Bajpai and Maheshwari 1995).

12.7.5 Interruption in Sedimentation in Spiti Basin

At Phukad in the Zanskar–Lahaul belt, a horizon of 8- to 10-m-thick conglomerate and quartzite with partings of black shale—the *Ganmachidam Conglomerate* (Srikantia 1981)—overlies the Po. It presumably indicates a large hiatus in the Lower Permian time when pyroclastics were being deposited below and above the lavas in the Kashmir sector. Above the Ganmachidam there is a persistent and prominent horizon (Fig. 12.5) of black shale, black sandstone and black bioclastic limestone with randomly dispersed phosphatic nodules—the *Kuling Shale*, a name given by F. Stoliczka in 1865. The fauna includes *Eurydesma* in the lower part of the succession and *Cyclolobus oldhami, Neospirifer, Spirigerella, Camnimargus* and *Aaloster* of Djulfian age (Garzanti et al. 1998) in the upper part.

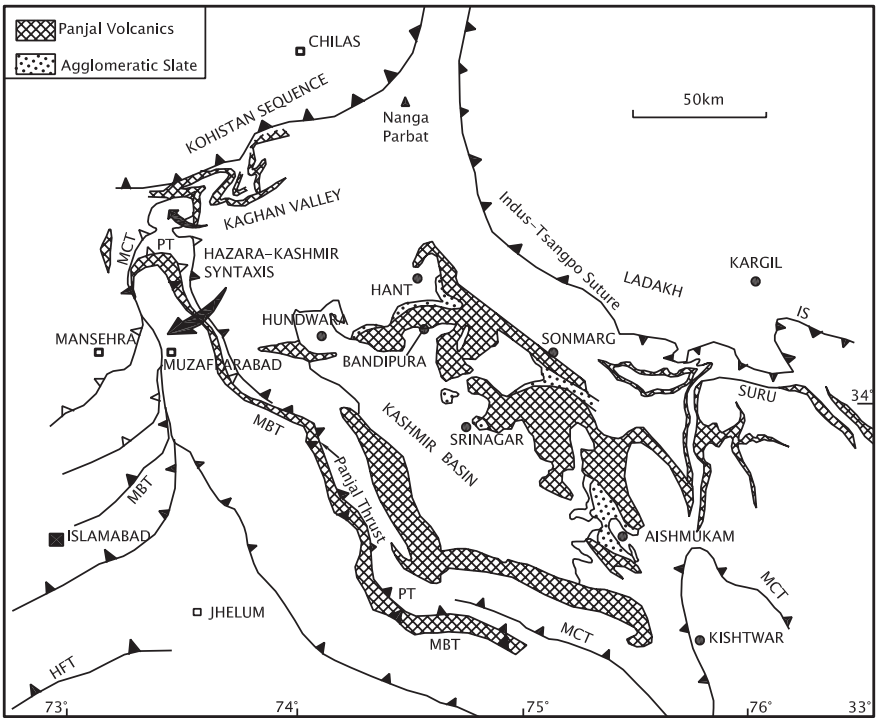

Fig. 12.11 Sketch map shows the distribution of the Permian volcanics in association with other Palaeozoic formations in the Kashmir Valley (after Papritz and Rey 1989)

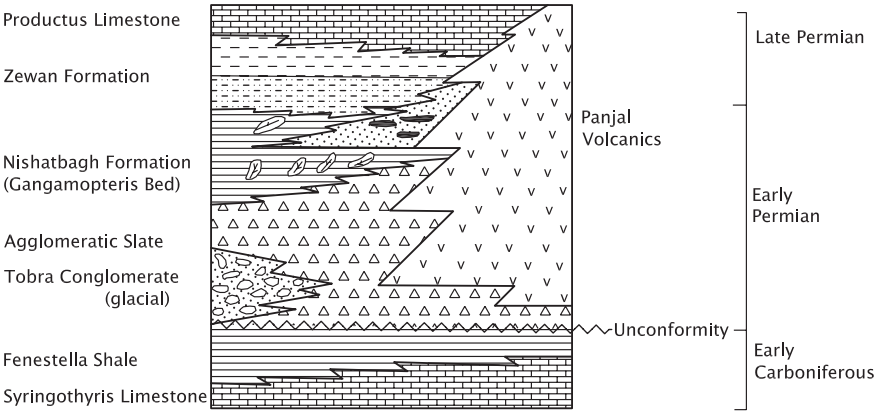

Fig. 12.12 Litholog shows vertical and lateral facies variation in the Permian succession of Kashmir (after Valdiya 1998)

12.7.6 Northern and North-eastern Nepal

The Kuling Shale is known as the *Thinichu Formation* in north-central Nepal (Egeler et al. 1964) and described by Wager (1939) as the *Lachi* in the Sagarmatha region. This Upper Permian formation, developed over a large area north of the Nilgiri–Shishpagma–Sagarmatha belt, is characterized by cosmopolitan brachiopods of Lopingian age. The conodont *Mesogondolella* and the bivalve *Atomodesma* in the topmost part of the succession are comparable with those of the Zewan in Kashmir and of the Zaluch in the Salt Range (Shu-Zhong et al. 2003). Close to the India–Tibet tectonic boundary in the north, the Qubu–Selong succession of micaceous sandstone and shale has yielded *Glossopteris,* and its upper limestone unit is characterized by ammonite *Cyclolobes* that built seamounts and carbonate reefs on the outer shelf (Shu-Zhong et al. 2003). By then, the water had become warm enough to promote carbonate precipitation (Singh 1987).

12.7.7 "Gondwana Fringe" in Lesser Himalaya

A remarkable association of marine, fluvial, glacial and volcaniclastic sediments forms an impersistent narrow fringe all along the outer belt of the Lesser Himalaya in the proximity of its junction with the Siwalik subprovince (Figs. 12.1 and 12.13). It is seen in patches from the Brahmaputra Valley in Arunachal Pradesh (Singh 1993), throughout Bhutan and southern Sikkim (Singh 1973; Acharyya 1971, 1975), southern Nepal (Bashyal 1980; Sakai 1984, 1991; Dhital 1992), southern Garhwal in Uttarakhand (Ganesan 1971; Valdiya 1975) to the southern flank of the PirPanjal in Kashmir (Wadia 1934).

Commonly described as the Gondwana element in the Himalaya province, the succession consists of two units. The lower one is made up of diamictite interbedded with greywacke and black shale bearing marine fauna including *Fenestella, Acathocladus* and *Polypora*, and the upper part comprises an upward-fining sequence of limonite stained arkosic sandstone, and carbonaceous shale with coal seams. The sediments were laid down by braided and meandering rivers in their flood plains. In the Tansen Hills in south-central Nepal (Fig. 12.14), the lower unit is named as the *Sisne Formation*, and the upper part the *Taltung* (Sakai 1984, 1985, 1991). In the Barahshetra area in south-eastern Nepal, phosphatic nodules occur in black shale of the coal-bearing succession characterized by Gondwanic Barakar plants (Bashyal 1980). The bioturbated, mudstone and shale bear bryozoans *Fenestella, Polypora* and *Acathocladus*.

Extremely significant is the occurrence of rifting-related trachytic lavas with keratophyre and tuff and tuffaceous sediment forming a 200-m-thick assemblage in the Tansen Hills (Sakai 1991) (Fig. 12.14).

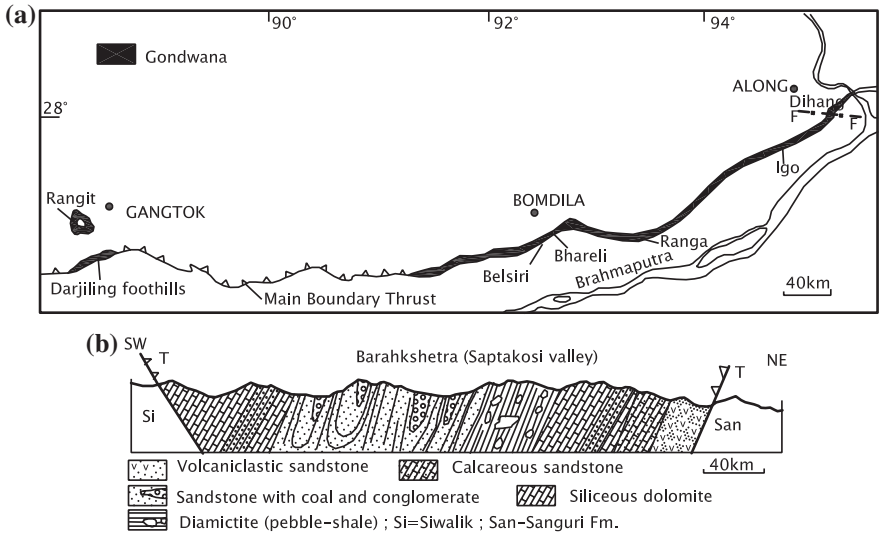

Fig. 12.13 **a** Sketch map showing the remarkable association of volcanics with marine, fluvial, glacial and volcaniclastic sediments of the Early Permian along the southern periphery of the Lesser Himalaya subprovince. This remarkable association represents the Gondwana element in the Himalaya (Based on Jain et al. 1974). **b** Section across the Barahkshetra Hills in south-eastern Nepal, illustrating the lithology of the "Gondwana element" (After Bashyal 1980)

In the Tista Valley in southern Sikkim and the Bhareli area in western Arunachal Pradesh, the *Rangit* succession (Acharyya 1971) comprises massive polymictic tillite associated with ferruginous sandstone and mudstone locally characterized by concretionary nodules and coal balls, and such plants as *Glossopteris*, *Vertebraria* and *Phyllotheca*. In the Garu succession in the south-central Arunachal Pradesh, the marine black shale contains *Deltopecten, Aviculopecten, Plateteichun, Warthia, Linoproductus, Tomiopis, Uratoceras, Tivertonia* and *Trigonotreata* of Sakmarian to Artinskian age (Singh 1981, 1993).

In the southern part of Pauri district in Uttaranchal, a narrow belt of fossiliferous formation described in 1885 by C.S. Middleman as the *Volcanic Breccia* is traceable from near Dugadda to Lamdhar, north-west of the Jim Corbett National Park (Fig. 12.15). The succession comprises two units—the lower unit *Jogira* is made up of diamictites with profuse clasts of volcanic rocks embedded in mudstone, carbonaceous shale and greywacke, and the upper *Maskhet* consists of sandstone intercalated with red and maroon siltstone and shale showing mudcracks and cross-bedding as discernible in deposits of paralic environment (Valdiya 1975). The Jogira has yielded Artinskian to Sakmarian fauna including *Fenestella, Spirifer, Strophalosia, Spiriferina, Productus, Neospirifer, Eomarginifera, Chonetes* and *Eurydesma* (Ganesan 1971).

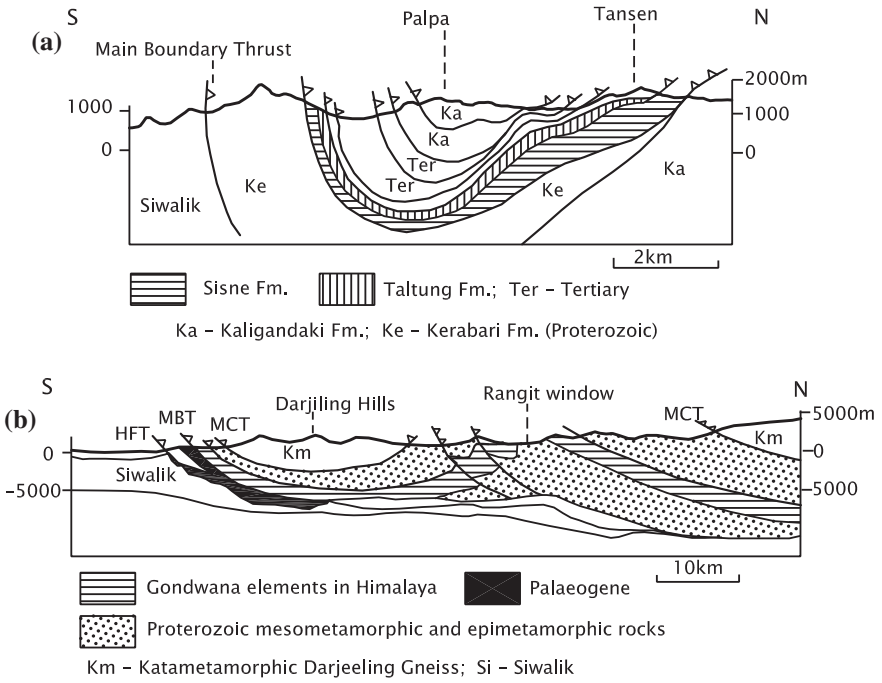

Fig. 12.14 **a** Structure and lithotectonic succession in the Tansen Hills in south-central Nepal, showing the position of the Gondwana element (after Sakai 1991). **b** Gondwana sediments caught in the tangle of the structure of the Darjiling Hills (after Acharyya 1975)

12.7.8 Abor Volcanics

A strong manifestation of volcanism in the Lesser Himalayan Gondwana Belt was witnessed by the Dihang (Siang) Valley in eastern Arunachal Pradesh. Coggin Brown in 1912 described the Dafla Hills—lavas and pyroclastics of this sector as the *Abor Volcanics*. In the Yingkiong, Dalbuing and Miriyong areas, the volcanics are intimately associated with penecontemporaneous quartzose sediments (Jain and Thakur 1975; Acharyya and Sengupta 1998). The sediments of the succession have yielded trilete and monolete microspores, radial monosaccates and striated and non-striated disaccate pollens of Early Permian age (Prasad et al. 1989). The volcanics are characterized by Fe and Ti abundances and relatively high values of incompatible elements, greater LREE enrichment, high (La/Yb)N and high Nb/Zr ratios, implying that the magma experienced CO_2-metasomatism as it moved to shallow level from the deeper source (Bhat 1984; Bhat and Ahmad 1990).

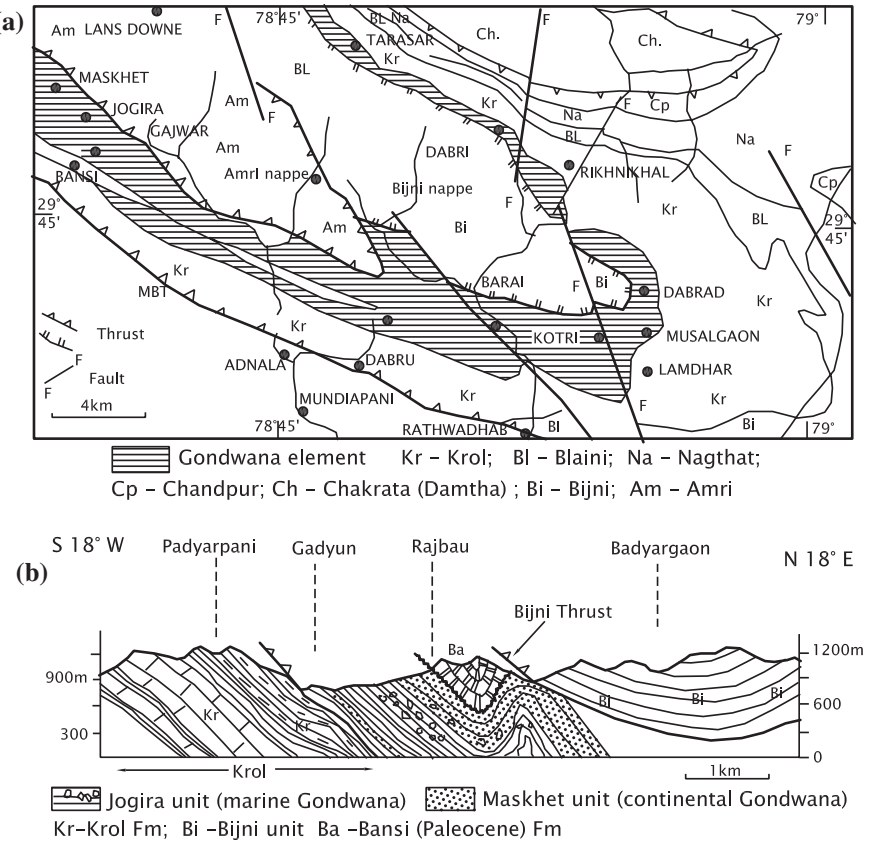

Fig. 12.15 Sketch map and a cross section of southern Lansdowne Hills in south-eastern Garhwal showing a Permian succession comprising marine Jogira and terrestrial Maskhet succession, the former characterized by volcaniclastic sediments with marine diamictites (after Valdiya 1975)

12.7.9 Eastern Myanmar

Resting unconformably on the Devonian Zebyingyi Shale and the Carboniferous Mawchi Formation, the Permian succession comprises the *Thitsipin Limestone* and the *Nwagangyi Dolomite* in the Shan States (Fig. 12.8) and the *Moulmein Limestone* and the *Martaban Beds* in the Tenasserim division (Fig. 12.16 *inset*). The Thitsipin, which has also been described as the *Dattawtaung Limestone* in Northern Shan States, comprises cherty micrite and cross-bedded calcarenite containing Lower to Upper Permian foraminifers (*Pseudoschwagerina, Pseudofusulinella, Pseudofusulina Parafusulina, Neoschwagerina, Verbeekina, Yangchienia*, etc.); brachiopods such as *Productus, Chonetes*; and bryozoans such as *Polypora* and *Fenestella*. A part of the carbonate succession is biohermal

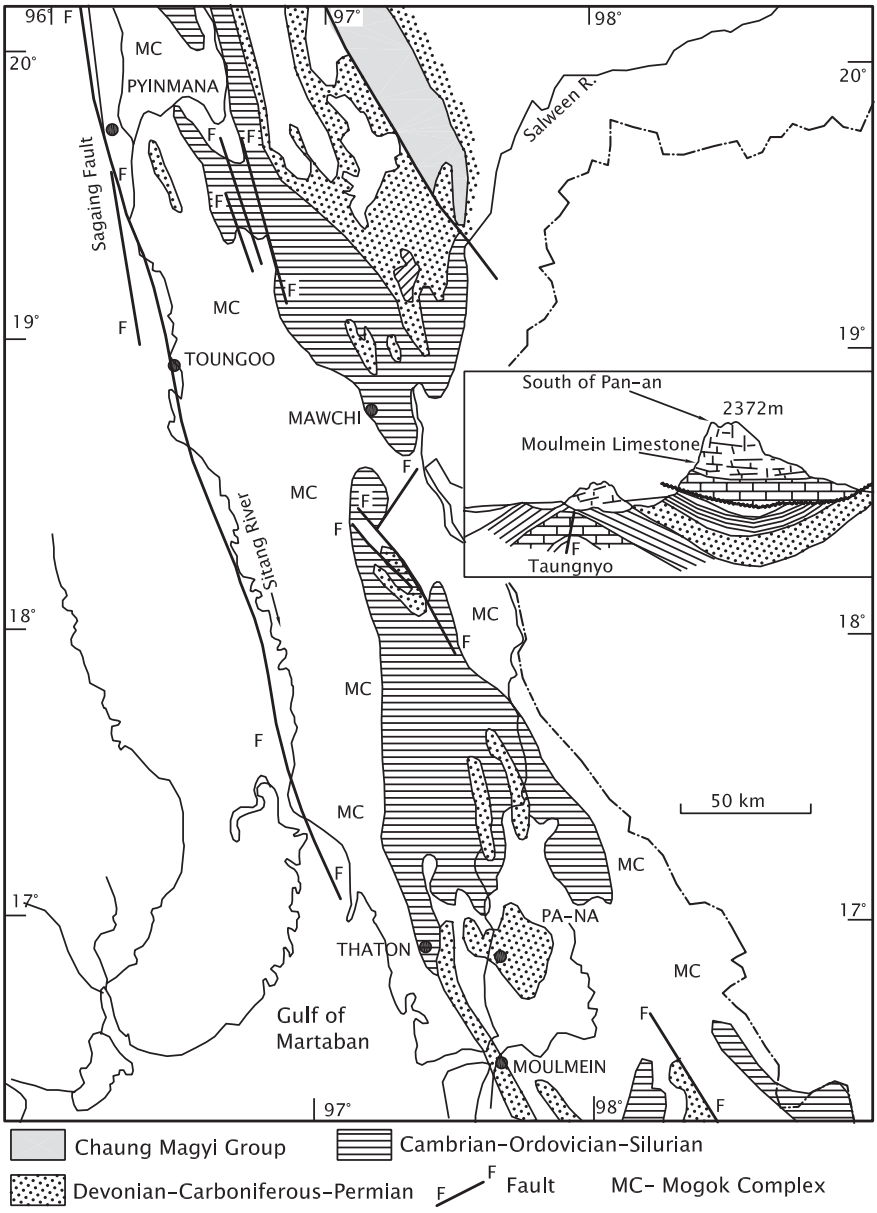

Fig. 12.16 Sketch map of the geology of southern part of eastern Myanmar embracing Kayah, Karen and Shan States and the Tenasserim division (after Thein 1973b). Cross section *Right Centre inset* shows the Permian biohermal–biostromal complex (Moulmein Limestone) showing karstic features (Brunnschweiller 1970)

in nature, its top containing Late Permian fauna (Garson et al. 1976). It passes upwards without break into the Nwabangyi Dolomite made up of intraformational oligomictic conglomerate and lithic packstone, floatstone, dolomitic wackestone and thinly bedded turbiditic dolomitic packstone–grainstone containing fossils in the upper parts that range up to Early Triassic (Oo et al. 2002). The Permian carbonates of Shan States are metamorphosed and locally intensely brecciated.

The *Moulmein Limestone* is a 1000-m succession of Artinskian biohermal–biostromal carbonate complex, making the mountain ranges characterized by karstic landscape and deranged drainage (Fig. 12.16). In the southern Tenasserim division, the crystalline limestones make up islands of the Mergui archipelago. These carbonates contain Upper Permian foraminifer *Schwagerina* and corals *Lonsdaleia* and *Lithostrotian*, and productids (Corbett 1973). The overlying shales and limestones with marls (*Martaban Beds*) contain nearly the same fauna plus *Palaeoanodonte* gastropod of the range Upper Permian to lowermost Triassic (Brunnschweiller 1970).

12.8 Palaeozoic Stratigraphy of Karakoram

We owe a great deal to Ardito Desio and Eric Norin for our understanding of the geology of the Karakoram and adjoining regions.

In the Karakoram domain resting *unconformably* on the crystalline basement occur Ordovician–Silurian shales with carbonate intercalations. This sequence is overlain by widespread peritidal platform deposits of the Early Devonian age (Juyal 2006; Juyal and Mathur 1996; Gaetani 1997). In the Middle Devonian to earliest Carboniferous time, there was rifting of the continental margin where Carboniferous *Brangsa Formation* was deposited unconformably on the floor of the depression. It consists of dominant carbonates with shales and sandstones. The Permian *Agtash Formation* comprises volcanics associated with diamictites and shales. The Agtash contains plant fossils. Black shales, siltstone, calcareous sandstone and dark argillaceous limestone overlying a pillow lava, known as the *Chhongtash Formation* in the upper Shyok Valley, contains abundant fossils of plant and polymorphs that bear remarkably strong similarity with those of the Gondwanic Salt Range and central India (Upadhyay et al. 1999).

A large prism of alluvial to transitional marine sediments represents onset of Permian upheaval (Gaetani 1997). The Early Permian upheaval resulted in the rifting of the Karakoram Basin, triggering the opening of the *NeoTethys Ocean*, and attendant extensive basic volcanism, eventually leading to drifting away of the Karakoram block to form the Lhasa–Iran–Turkey microcontinent (Fig. 12.18).

12.9 Palaeozoic Stratigraphy of Tibet

In the Lhasa area, the Upper Devonian carbonates are overlain disconformably by a sequence of limestones, shales and sandstones betraying their Lower Carboniferous age. The overlying succession, known as the *Yongdzu Formation*,

comprises pebbly sandstone and diamictite of the Artinskian age, and the Yongdzu is capped by a sequence of dark shale with fine clastics and limestone of the *Angui Formation* (Xiaochi 2002). The Angui is characterized by the presence of *Spirifer*, *Martina*, and *Parmirina* (fusulinids) along with bryozoans and crinoids. In the Boashan, Lhasa and southern Quiangtang regions, the Permo–Carboniferous sequence contains plant remains, including *Glossopteris*, *Stenophyllum* and *Dichotomopteris* of the Gondwana affinity indicating that Tibet was a part of the Gondwanic India during the Permocarboniferous times (Xiaochi 2002).

12.10 Progression of Palaeozoic Life

12.10.1 Evolutionary Radiation

The Palaeozoic era witnessed evolutionary radiation of nearly all invertebrate phyla—the appearance of vertebrate animals in the form of bony fish without jaw, the colonization of land by plants, and the evolution of reptiles from the amphibians that were derived from one of the branches of fish. While there was extremely diverse evolutionary radiation in the Cambrian, Ordovician and Silurian periods, there was, ironically, large-scale extinction of most of the major invertebrates towards the end of the Palaeozoic (Kummel 1961; Wicander and Monroe 2000).

12.10.2 Development of Chitinous and Phosphatic Shells

During the Cambrian period, almost all the major invertebrate phyla evolved, experimenting in developing new body plans and moving into new niches (Wicander and Monroe 2000). The trilobites that had shells of horn-like organic material called chitin were by and large the most conspicuous elements of the marine invertebrate community. First appearing in the Early Cambrian, these creatures crawled on muddy seafloor or swam across the waters and showed wide range of adaptation as they rapidly diversified. However, towards the end of the Cambrian a large number of them met with their end. Secreting chitinophosphatic shells, the brachiopods were inarticulate—without tooth and socket arrangement along the hinge line. The bottom-dwelling sessile sponge-like archaeocyathids built reef-like structures in shallow waters in narrow belts close to coasts. Sponges, coelenterates and gastropods were other animals that peopled the Cambrian sea. There was little specialization among these invertebrates, and most phyla were represented by only a few species.

During the Ordovician and Silurian periods, the trilobites continued to dominate the invertebrate community. Arthropods with scorpion-like bodies and impressive pincers were abundant in brackish and fresh waters. Many new groups of nautiloids, corals brachiopods, pelecypods, echinoderms and gastropods appeared in

the ocean. The nautiloids grew in size, feeding on possibly the trilobites. Tabulate as well as branching (rugose) corals together with calcareous algae and stromatoporoids built reefs, particularly during the Middle Silurian. In the Early Ordovician appeared the first articulate brachiopods and radiated rapidly. The echinoderms with long cup-like bodies and "feathers" (cystoids and crinoids) were important rock builders in the Middle Palaeozoic time. The dendroid graptolites that secreted chitinous material to make cup-like and tube-like branches, lived on the sea bottom of shallow well-oxygenated water. Graptoloids floated on the surface, attaching to their floats or to seaweeds. They lived a cosmopolitan life and evolved rapidly.

12.10.3 Appearance of Fish

In the Late Silurian appeared the first fish—a jawless, armoured (bony skin) creatures, living in estuaries, lakes and freshwater streams. Apparently conditions favourable to preservation of non-marine life had developed towards the close of the Silurian period.

12.10.4 Colonization of Land by Plants

In the Upper Silurian also appeared the first plant on land, coming presumably from the marine realm. Acquiring a foothold on land during the Devonian time the plants rapidly colonized the coasts, the swamps and the river courses. They were rootless vascular plants, having specialized tissues for conduction of water and nutrients. The early plants were characterized by naked stems without or with but a few small leaves and spore-bearing organs occurring at the end of the main shoot or its branches. Adaptive radiation taking place in the Late Silurian and early Devonian resulted not only in the great diversity of the flora but also in the *evolution of seed*. This development freed the plants from their dependence on moist conditions and allowed them to spread over all parts of the land (Kummel 1961; Wicander and Monroe 2000). By the Middle Devonian, real forests had grown all over the land near water bodies.

Among the invertebrate animals, the cephalopod ammonoids evolved from the nautiloids in the Early Devonian and diversified rapidly. In contrast, there was near total decimation of the marine reef builders, primarily due to reduction of shelf environment perhaps as a result of global cooling.

12.10.5 The Coming of Land-Living Amphibians

The armoured fish became diverse and abundant all over the oceanic realm. The fish developed jaws that ensured "an evolutionary future" for the placoderms. Adapting themselves to a variety of conditions of environment, the bony fish became the most successful of all vertebrate animals. The shark had also appeared and grew along with the bony fish. One of the fish types *Osteolepis* characterized by two dorsal fins

and very different kind of scales seems to have evolved into land-living amphibian—the pair of lobed fins containing bone developing into limbs of the quadrupeds (Kummel 1961). As arid conditions developed in the Devonian time, shallower pools and streams dried up, forcing the fish to go across the country looking for pools and for supply of food. Undergoing adaptive radiation, the marine fauna evolved into the amphibians during the Devonian. Insects, millipedes, spiders and snails invaded the land before the amphibians became successful in occupying the land.

The Late Carboniferous time witnessed the zenith of plant evolution. The abundance of carbonaceous material in sediments and the formation of coal seams bear testimony to the high point in the floral history, when thick forests occupied swampy plains and coastal strips.

12.10.6 Amniote Eggs and Evolution of Reptiles

One of the most significant developments in the organic evolution was the appearance of large-yolked shelled eggs with characteristic embryonic membrane—the *amniote eggs*—of land-living amphibians. This development heralded the transformation in the Late Carboniferous from the amphibians to the reptiles. One of the reptiles that evolved was *Seymouria*, belonging to the group cotylosaurs. This group underwent an elaborate evolutionary radiation, leading to emergence of nearly all major reptile groups. By the Permian time, the reptile became very diverse and abundant. Unaffected by any crisis of extinction, the land-living amphibians and reptiles continued to evolve and proliferate towards the end of the Palaeozoic—in the land covered with plants.

Among the invertebrates, there was renewed adaptive radiation and rediversification. The brachiopods and ammonoids recovered quickly and soon became important members of the animal community. Bryozoans and crinoids showed greatest diversity and contributed skeletal material for making bedded limestones and built reefs with the help of calcareous algae, and fusulinid foraminifers. Before meeting their doom, the trilobites and nautiloids showed evolutionary diversity (only a few dendroid graptolites had persisted into the Carboniferous). In the Permian, there was considerable shrinkage of the areal extent of distribution of marine fauna. Constituting an important part of reef complexes, the odd-shaped spiny productids dominated the brachiopod community. The spindle-shaped foraminifer fusulinids greatly diversified, and some types of bryozoans, sponges and calcareous algae became very common among the Permian fauna just before the great event towards the end of the Permian end.

12.10.7 Decimation of Fauna

Towards the end of the Permian period, there was considerable decimation of fauna—the mass extinction that wiped out more than 90 % of all invertebrate species of the oceans. Among those which disappeared forever were trilobites, rugose

and tabulate corals, fusulinid foraminifers and several orders of brachiopods and bryozoans. The cataclysmic events did not spare the land-dwelling animals. More than 65 % of all amphibians and reptiles as well as 33 % insects on land became extinct (Wicander and Monroe 2000). It may be mentioned that the mass extinction took place over a long interval of 8 million years at the end of the Permian.

12.11 Disturbed End of the Palaeozoic Era

12.11.1 Rifting of Continental Margin

Towards the end of the Palaeozoic era, a number of geodynamic development of far-reaching consequence took place. While there was interruption of sedimentation over large parts of the Tethys subprovince (Fig. 12.17), the southern part peripheral to what is today the Lesser Himalaya–Siwalik boundary came under the sway of seawaters for the first time after the Middle Cambrian retreat. The return of the seawater in the Lesser Himalaya is linked to marine transgression along sunken tracts in the Peninsular India—the Bap–Badhaura arm in Rajasthan and the Rajahara–Umaria course in Jharkhand–Madhya Pradesh (Figs. 12.1 and 13.4). The sedimentary assemblages with Gondwanic elements of southern Garhwal, south-central Nepal, southern Sikkim and southern Arunachal Pradesh represent that transgression of the Gondwanic sea. Significantly, the outer Lesser Himalayan Permian units are associated intimately with lavas and pyroclastics. It seems that the deposition of sediments in the new cycle took place in an elongate basin

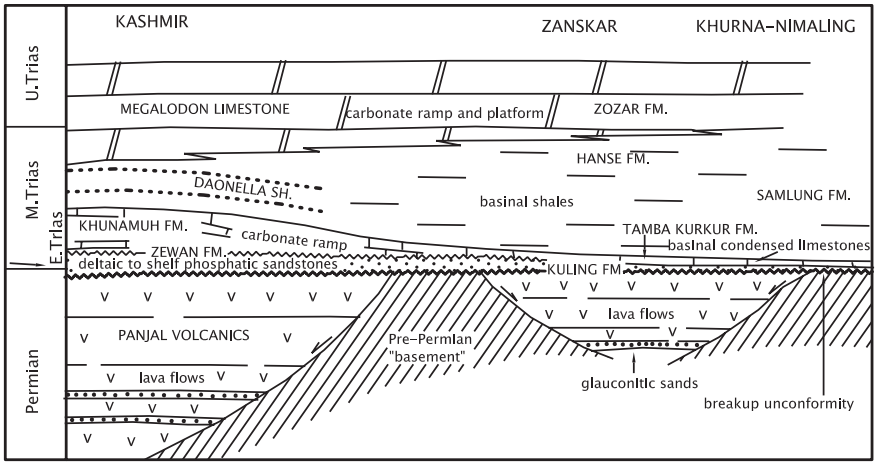

Fig. 12.17 One of the major unconformities in the Himalaya province is the one that marks the tectonic disturbance towards the close of the Permian. It was an event correlated with the breakup of the Indian plate and opening up of the NeoTethys Ocean (after Gaetani and Garzanti 1991)

formed due to sagging or rifting down of the crust along the southern periphery of the Lesser Himalayan subprovince. The basin extended from the Salt Range in Pakistan to Garu and beyond in Arunachal Pradesh (Fig. 12.1).

12.11.2 Widespread Volcanism

All along the southern part of the Himalaya from the Sindhu Valley in the west to the Brahmaputra Valley in the east, volcanoes became very active, pouring out lavas and ejecting pyroclastics. The volcanics are represented by the *Panjal Traps* in the north-west and by the *Abor Volcanics* in eastern Arunachal Pradesh. Across the Sindhu in northern Pakistan, contemporary igneous activity is represented by Shewa–Shahbazganj suite of intrusives. Some of the volcanic islands were covered with forests of *Glossopteris, Gangamopteris, Waagenophyllum,* etc. that grew luxuriantly in the mainland, the Gondwanaland. In the islands nestled freshwater lakes peopled by, among others, fish such as *Amblypteris* and *Labyrinthodon*.

12.11.3 Separation of Tibetan Microcontinent

The fissuring of the Indian continental margin (within the Himalaya province) with attendant volcanism and marine incursion along a depression implies that the Gondwanic India was overtaken by a powerful crustal movement—the *Hercynian diastrophism*. The impact of this tectonic movement reached the climax in the northern part of the continental margin, resulting in the breaking away in the Late Permian of the Karakoram–Tibetan landmass along with Iran and Turkey (Fig. 12.18). A new seaway known as the *NeoTethys* was formed between the Indian plate and the Cimmerian microcontinent that drifted away. The newly formed sea was connected to the Mediterranean Tethys that extended up to Portugal in the periphery of Europe.

The abrupt shift of the $^{12}C/^{13}C$ ratios in the marine sediments in the Later Permian indicates greater abundance suddenly of biogenic carbon isotope (^{12}C), resulting from increased influx and burial of terrestrial plants. The resultant oxidation (decomposition) of the buried plant material caused depletion of oxygen and excess of carbon dioxide in the ocean water as well as in the atmosphere. The increase in CO_2 due to this process was over and above the very high influx of volcanogenic carbon dioxide. This had an adverse effect on the environment. The increase in the quantity of CO_2 and deficiency of oxygen in water caused development of anoxic conditions, leading to snuffing out of life from the areas experiencing extreme conditions. That explains the mass extinction of fauna living in the marine environments and decimation of plants on land (Fig. 12.19; Table 12.1).

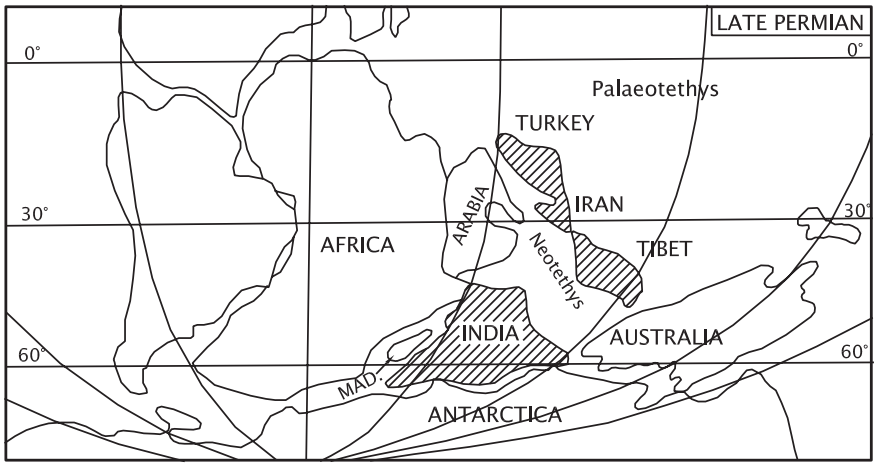

Fig. 12.18 Opening up of the NeoTethys ocean between Indian plate and Tibetan microcontinent that broke away from India in the Late Permian (after Sengor 1984)

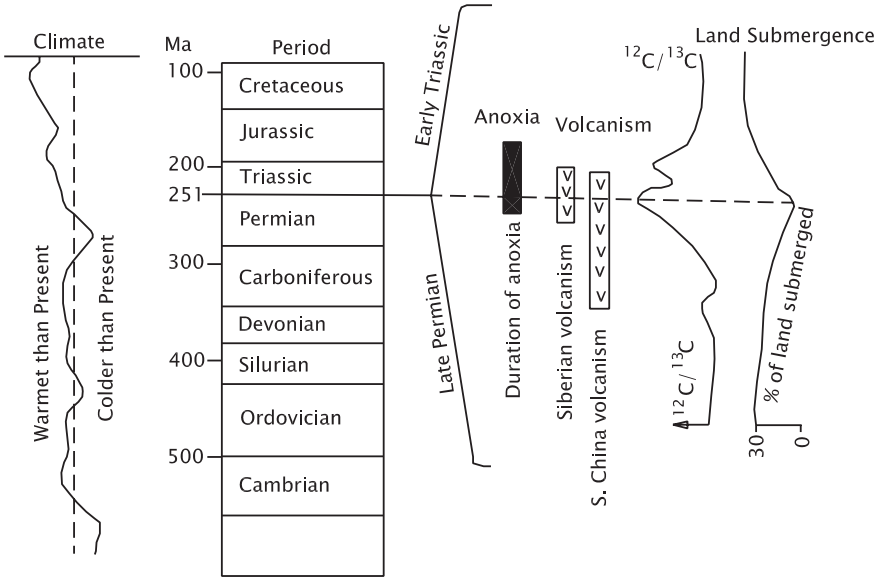

Fig. 12.19 Abrupt shift of carbon isotope ratios in the marine sediments, land submergence and mass extinction in the later part of the Permian period (after Sankaran 1997)

Table 12.1 Palaeozoic sedimentary formations in the Tethys domain of the Himalaya and Myanmar

Age		Kashmir	Himachal	Kumaun	Nepal	Sikkim	Bhutan	Shan States	Karen–Tenasserim Belt
Permian	L	Zewan Fm.	Kuling Shale	Kuling Shale	Thinichu Fm.	Lachi Fm.		Nwabangyi Dolomite	Martaban Beds
	M	Panjal Volcanics	Panjal Volcanics	----------	*Unconformity*	----------		Thitspin Limestone	Moulmein Limestone
	E	Agglomeratic Slate	Ganmachidam Conglomerate						
Carboniferous	L	----------						Sitha Limestone	Taungnyo Group/ Mergui Series
	M	Fenestella Shale	Po Shale					Ohn-hne Limestone	
	E	Syringothyris Limestone	Lipak Limestone	Kali Fm.				Maymyo Dolomite (Devonian)	Loikaw Beds (Devonian)
----------					*Unconformity*	----------			
Silurian		Muth Quartzite	Muth Quartzite	Muth Quartzite	TilichoLake Fm				
			Takche/Pin Fm.	Veriegated Silurian	Dark Band Fm.			Namhsin Fm. Panghsapye Fm.	
Ordovician	L	Marhaum/ Margam Fm.	Thango/Thaple Fm.	Shaila Fm.	North Face Quartzite			Naungkangyi Fm.	Biya Limestone
	M	----------		Garbyang Fm.	Nilgiri Ls.	Everest Ls.	Wachila	Taunkyun Fm.	
	E					Everest Pelites		Pangyun Fm.	Pangyun Formation
Cambrian	L	----------							
	M	Trahagam Fm.	Parahio/Kurgiakh	Ralam Conglomerate			Maneting	Bawdwin Volcanics	
	E	Nutunus/Karikul	Karsha Limestone				Nakechu	Chaung Magyi Group	Chaung Magyi Group
		Loab/KhaiyarFm.	Kunzumla Fm.	Martoli Fm.			Singhi Fm.		

Unconformity; Fm.= Formation; Gr.= Group; Qz.= Quartzite; Congl.= Conglomerate; Ls.= Limestone

References

Acharyya, S. K. (1971). Ranjit Pebble. State—a new formation from the Darjeeling hills. *Indian Minerals, 25*, 61–64.

Acharyya, S. K. (1975). Structure and stratigraphy of the Darjeeling frontal zone, Eastern Himalaya [Miscellaneous Publication]. *Geological Survey of India, 24*(2), 71–90.

Acharyya, S. K., & Sengupta, S. (1998). The structure of the Siang Window; its evolution and bearing on the nature of eastern syntaxis of the Himalaya. *National Academy Science Letters, 21*, 178–192.

Ali, K. A., & Anwar, J. (1969). Stratigraphic studies of the Nowshera reef complex, Nowshera Tahsil, West Pakistan. *Geological Bulletin of the University of Peshawar, 4*, 33–43.

Anderson, M. M., Boucot, A. J., & Johnson, J. G. (1969). Eifelian brachiopods from Padaukpin, Northern Shan States, Burma. *Bulletin of the British Museum (Natural History) Geology, 18*, 107–163.

Aung, A. K. (1995). New Middle Devonian (Eifelian) rugrose corals from Myanmar. *Journal of Asian Earth Sciences, 11*, 23–32.

Bagati, T. N. (1990). Lithostratigraphy and facies variation in Spiti basin (Tethys) Himachal Pradesh, India. *Journal of Himalayan Geology, 1*, 35–47.

Bagati, T. N., Kumar, Rohtash, & Ghosh, S. K. (1991). Regressive-transgressive sedimentation in the Ordovician sequence of the Spiti (Tethys) basin, Himachal Pradesh, India. *Sedimentary Geology, 73*, 171–184.

Bhargava, O. N. (1991). Late Proterozoic-Palaeozoic Spiti basin. In S. K. Tandon, S. M. Casshyap, & C. C. Pant (Eds.), *Sedimentary Basins of India: Tectonic Context* (pp. 236–260). Nainital: Gyanodaya Prakashan.

Baig, M. S., Lawrence, R. D., & Snee, L. W. (1988). Evidence for later Precambrian to early Cambrian orogeny in northwest Himalaya, Pakistan. *Geological Magazine, 125*, 83–86.

Bajpai, U., & Maheshwari, H. K. (1995). Late Palaeozoic plant geography of the Perigondwana evolution of the Kashmir Basin. *Journal of the Geological Society of India, 46*, 303–308.

Bandyopadhyay, B. K., & Gupta, A. (1990). Submarine debris-flow deposits from the Ordovician Maneting Formation in Tethyan Black Mountain basin, Central Bhutan. *Journal of the Geological Society of India, 36*, 277–289.

Barnett, S. G., Kohul, J. J., Rust, C. C., & Sweet, W. C. (1966). Conodonts from Nowshera reef limestones (uppermost Silurian or lowermost Devonian), West Pakistan. *Journal of Palaeontology, 40*, 435–438.

Bashyal, R. P. (1980). Gondwana-type of formation with phosphatic rocks in SE Nepal. *Journal of the Geological Society of India, 21*, 484–491.

Baud, A., Gaetani, M., Garzanti, E., Fois, E., Nicora, A., & Tintori, A. (1984). Geological observation in southeastern Zanskar and adjacent Lahaul area (Northwestern Himalaya). *Eclogae Geologicae Helvetiae, 77*, 171–197.

Bender, F. (1983). *Geology of Burma* (p. 293p). Berlin: Gebruder Borntraeges.

Berry, W. B. N., & Boucot, A. J. (1972). Correlation of the Southeast Asian and near eastern Silurian rocks [special papers]. *Geological Society of America, 137*, 1–65.

Bhargava, O. N. (1995). The Bhutan Himalaya: A geological account [special publication]. *Geological Survey of India, 39*, 191–214.

Bhargava, O. N., & Srikantia, S. V. (1985). Trilobites and other trace fossils from the Kunzumla Formation, eastern Lahaul, Himachal Pradesh. *Journal of the Geological Society of India, 26*, 880–886.

Bhat, M. I. (1984). Abor Volcanics: Further evidence for the birth of the Tethys ocean in the Himalayan segment. *Journal of the Geological Society of London, 141*, 763–775.

Bhat, M. I., & Ahmad, T. (1990). Petrogenesis and the mantle source characteristics of the Abor volcanic rocks, eastern Himalaya. *Journal of the Geological Society of India, 36*, 227–246.

Bodenhausen, J. W. A., & Egeler, C. G. (1971). On the geology of the upper Gandaki valley, Nepalese Himalaya. *Koninklijke Nederlandse Akademie van Westenchappen, 74*, 526–546.

Bordet, P., Cavet, P., & Pillet, J. (1960). La faune de Phulchauki, près des Kathmandu (Himalaya du Népal). *Bulletin de la Société Géologique de France, 7*, 3–14.

Brasier, M. P. (1992). Global ocean-atmosphere change across the Precambrian-Cambrian transition. *Geological Magazine, 129*, 161–168.

Brunnschweiller, R. O. (1970). Contributions to the post-Silurian geology of Burma (Northern Shan States and Karen State). *Journal of the Geological Society of Australia, 17*, 59–79.

Calkins, J. A., Offield, T. W., Abdullah, K. M., & Ali, S. T. (1975). Geology of the southern Himalaya in Hazara, Pakistan and adjacent area. U.S. Geological Survey professional paper, 716C, 29p.

Chaturvedi, R. K., Mishra, S. N., & Mulay, V. V. (1981). On the Tethyan Palaeozoic sequence of Black Mountain Region, central Bhutan. *Himalayan Geology, 11*, 224–249.

Colchen, M., Le Fort, P., & Pecher, A. (1986). *Recherches Geologiques dans l' Himalaya due Nepal: Annapurna, Manaslu, Ganesh Himal* (p. 136p). Paris: Centre Nationale Recherche Scientifique.

Corbett, D. J. (1973). Carboniferous and Permian correlation in Southeast Asia. *Bulletin of the Geological Society of Malaysia, 6*, 131–142.

Crawford, A. R., & Davies, R. G. (1975). Ages of Pre-Mesozoic formations of the Lesser Himalaya, Hazara district, northern Pakistan. *Geological Magazine, 112*, 509–514.

Dhital, M. R. (1992). Lithostratigraphic comparison of three diamictite successions of Nepal Lesser Himalaya. *Journal of the Nepal Geological of Society, 8*, 43–54.

Draganits, E., Grasemann, B., & Braddy, S. J. (1998). Discovery of abundant arthropod trackways in India: Implications for the depositional environment. *Journal of Asian Earth Sciences, 16*, 109–118.

Draganits, E., & Noffke, (2004). Siliclastic stromatolites and other microbially induced sedimentary structures in an early Devonian barrier island environment (Muth Formation, NW Himalayas). *Journal of Sedimentary Research, 74*, 191–202.

Egeler, C. G., Bodenhausen, J. W. A., DeBooy, T., & Nijhuis, H. J. (1964). *On the geology of central west Nepal*. Report 22nd international geological congress, Part 10, New Delhi, pp. 101–122.

Fuchs, G. R. (1975). On the geology of the Karnali and Dolpho region, West Nepal. *Mitteilungen der Geologischen Gesellschaft in Wien, 66–67*, 21–32.

Fuchs, G. R. (1977). Traverse of Zanskar from the Indus to the valley of Kashmir—a preliminary note. *Jahrbuch der Geologischen Bundesanstalt, 120*, 219–229.

Fuchs, G. R., & Moestler, H. (1972). Der erste Nachweis von Fossilien (Kambrischen Alters) in der Hazira Formation, Hazara, Pakistan. *Geologisch-Paläontologische Mitteilungen Innsbruck, 2*, 1–2.

Fuchs, G. R., Widder, R. W., & Tuladhar, R. (1988). Contributions to the geology of the Annapurna Range (Manang area) Nepal. *Jahrbuch der Geologischen Bundesanstalt, 131*, 593–607.

Funakawa, Satoshi. (2001). Lower Palaeozoic Tethys sediments from the Kathmandu Nappe, Phulchauki area, central Nepal. *Journal of Nepal Geological Society, 25*, 123–134.

Gaetani, M. (1997). The Karakoram block in central Asia, from Ordovician to Cretaceous. *Sedimentary Geology, 109*, 339–359.

Gaetani, M., & Garzanti, E. (1991). Multicyclic history of northern India continental margin (NW Himalaya). *American Association of Petroleum Geologists Bulletin, 75*, 1427–1446.

Gaetani, M., Raffache, C., Fois, E., Garzanti, E., Jadoul, F., Nicora, A., & Tintori, A. (1985). Stratigraphy of the Tethys Himalaya in Zanskar Ladakh. *Rivista Italiana di Paleontologia e Stratigraphia, 91*, 443–478.

Ganesan, T. M. (1971). Note on the first record of the fenestellid bryozoan in the 'Volcanic Breccia' of Garhwal. *Indian Minerals, 25*, 257.

Garson, M. S., Amos, B. J., & Mitchell, A. H. G. (1976). The geology of the area around Neyaunagga and Ye-ngan, Southern Shan States, Burma. *Oversees Memoir International Geological Sciences, London, 2*, 1–70.

Garzanti, E., Angiolini, L., Brunton, H., Sciunnach, D., & Balini, M. (1998). The Bashkirian "Fenestella Shales" and the "Muscovian Chaetid Shales" of the Tethys Himalaya (S. Tibet, Nepal and India). *Journal of Asian Earth Sciences, 16*, 119–126.

Garzanti, E., & Sciunnach, D. (1997). Early carboniferous onset of Gondwanian glaciation and Neotethyan rifting in South Tibet. *Earth and Planetary Science Letters, 148*, 359–365.

Goel, R. K., & Nair, N. G. K. (1977). The Spiti–Ordovician–Silurian succession. *Journal of the Palaeontological Society of India, 18*, 47–48.

Hayden, H. H. (1904). Geology of Spiti with parts of Bashar and Rupshu. *Memoirs of the Geological Survey of India, 36*(1), 1–21.

Heim, A., & Gansser, A. (1939). Central Himalaya: Geological observations of the Swiss Expedition 1936. *Denkschriften der Schweizerischen Naturforschenden Gesellschaft, 32*, 1–245.

Honegger, K., Dietrich, V., Frank, W., Gansser, A., Thoni, M., & Trommsdroff, W. (1982). Magmatism and metamorphism in the Ladakh Himalaya (The Indus Tsangpo Suture Zone). *Earth and Planetary Science Letters, 60*, 253–292.

Hussain, A., Yeats, R. S., & Pogue, K. R. (1990). *Geological map of Attock-Cherat Range and adjoining areas, NWEP and Panjab, Pakistan*. Quetta: Geological Survey of Pakistan.

Islam, R., Ahmand, T., & Rawat, B. S. (2003). Geochemistry and petrogenesis of the Phe Volcanics, Zanskar, Western Himalaya: Bearing on the Neotethys. *Memoirs of the Geological Survey of India, 52*, 339–357.

Jain, A. K., & Thakur, V. C. (1975). Stratigraphic and tectonic setting of the Eastern Himalayan Gondwana Belt with special reference to the Permo-Carboniferous Rangit Pebble Slate. *Bulletin of the Indian Geological Association, 8*(2), 50–70.

Jain, A. K., Thakur, V. C., & Tandon, S. K. (1974). Stratigraphy and structure of the Siang district, Arunachal Pradesh (NEFA). *Himalayan Geology, 4*, 28–60.

Juyal, K. P. (2006). Foraminiferal biostratigraphy of the Early Cretaceous Hundriri Formation, lower Shyok area, eastern Karakoram India. *Current Science*, *91*, 1096–1101.

Juyal, K. P., & Mathur, N. S. (1996). Stratigraphic status and age of the Tethyan sedimentary sequence of the eastern Karakoram. In J. Pandey, R. J. Azmi, A. Bhandari, & A. Dave (Eds.), *Contributions to the XV Indian Colloquium on Micropalaeont, Stratig* (pp. 765–775). Dehradun: KDMIPE and WIHJ.

Khanna, A. K., Sinha, A. K., & Sah, S. C. D. (1983). Yong Limestone of Tethys Himalaya: Its stratigraphic status and palynological fossils. *Journal of the Geological Society of India, 26*, 191–198.

Kumar, R., Shah, A. N., & Bingham, D. K. (1978). Positive evidence of a Precambrian tectonic phase in Central Nepal Himalaya. *Journal of the Geological Society of India, 19*, 519–522.

Kummel, B. (1961). *History of the Earth: An introduction to historical geology* (p. 610). Delhi: Eurasia Publishing House.

Latif, M. A. (1970). Explanatory notes on the geology of southeastern Hazara. *Jahrbuch der Geologischen Bundesanstalt, Sonderband, 15*, 5–20.

Latif, M. A. (1972). Lower Palaeozoic (Cambrian) hyolithids from the Hazara Slates, Pakistan. *Nature, 138*, 124–125.

Mamgain, V. D., & Mishra, R. S. (1989). Biostratigraphical studies of the Palaeozoic and Mesozoic sediments of the Tethyan facies in U.P. Himalaya. *Records of the Geological Survey of India, 122*, 296–299.

Mitchell, A. H. G., Marshall, T. R., Skinner, A. C., Amos, B. J., & Bateson, (1977). Geology and exploration geochemistry of the Adanatheingyi and Kyaukone-Lonataukno areas, Northern Shan States, Burma. *Overseas Geology and Mineral Resources, 51*, 1–35.

Nanda, M. M., & Singh, M. P. (1976). Stratigraphy and sedimentation of the Zanskar area, Ladakh and adjoining parts of Lahaul region of H.P. *Himalayan Geology, 6*, 365–388.

Oo, T., Hlaing, T., & Htay, N. (2002). Permian of Myanmar. *Journal of Asian Earth Sciences, 20*, 683–689.

Papritz, K., & Rey, R. (1989). Evidence for the occurrence of Permian Panjal Trap basalts in the Lesser and Higher Himalayas of the Western Syntaxis, NE Pakistan. *Eclogae Geologicae Helvetiae, 82*, 603–627.

Parcha, S. K. (1999). Cambrian biostratigraphy in Tethyan sequences of the Spiti Valley, Himachal Himalaya, India. *Newsletters on Stratigraphy, 37*, 177–190.

Parcha, S. K. (2005). Biostratigraphic studies and correlation of the Middle Cambrian successions of northwestern Kashmir Himalaya. *Journal of the Geological Society of India, 65*, 183–196.

Pogue, K., DiPietro, J. A., Rahim Khan, S., Hughes, S. S., Dilles, J. H., & Lawrence, R. D. (1992). Late Palaeozoic rifting in northern Pakistan. *Tectonics, 11*, 871–883.

Poornachandra Rao, G. V. S., Someswara Rao, M., Prasanna Lakshmi, K. J., & Srinivasa Rao, B. (2003). Palaeomagnetism and age Phe Volacanics from Zansakar Valley, Ladakh. *Himalayan Geology, 24*, 103–111.

Prasad, B., Dey, A. K., Gogoi, P. K., & Maithani, A. K. (1989). Early Permian plant microfossils from the intertrappean beds of Abor Volcanics, Arunachal Pradesh, India. *Journal of the Geological Society of India, 34*, 83–88.

Sakai, H. (1984). Stratigraphy of Tansen area in the Nepal Lesser Himalaya. *Journal of the Nepal Geological of Society, 4*, 41–52.

Sakai, H. (1985). Geology of the Kali Gandaki Supergroup of the Lesser Himalaya in Nepal. *Memoirs of the Faculty of Science, Kyushu University, Series D, 27*, 337–397.

Sakai, H. (1991). The Gondwanas in Nepal Himalaya. In S. K. Tandon, S. M. Casshyap, & C. C. Pant (Eds.), *Sedimentary Basins of India: Tectonic context* (pp. 204–217). Nainital: Gyanodaya Prakashan.

Sankaran, A. V. (1997). Polar wander and the Cambrian biological leap. *Current Science, 73*, 636–639.

Sengor, A. M. C. (1984). The Cimmeride orogenic system and the tectonics of Eurasia [special paper]. *The Geological Society of America, 195*, 74.

Shah, S. K. (1982). Cambrian stratigraphy of Kashmir and its boundary problems. *Precambrian Research, 17*, 87–98.

Shah, S. K. (1991). Stratigraphic setting of the Phanerozoic rocks along the northern boundary of the Indian plate. *Physics and Chemistry of the Earth, 18*, 317–328.

Shah, S. K. (2005). Phanerozoic stratigraphy of Himalaya: Some recent advances and future challenges. *Himalayan Geology, 26*, 299–307.

Shah, S. K., & Sinha, Anshu K. (1974). Stratigraphy and tectonics of the Tethyan zone in a part of western Kumaun Himalaya. *Himalayan Geology, 4*, 1–27.

Shah, S. M. I., Siddiqui, R. A., & Talent, J. A. (1980). Geology of the eastern Khyber Agency, Northwestern Frontier Province, Pakistan. *Records of the Geological Survey of Pakistan, 44*, 1–31.

Shah, S. K., & Sudan, C. S. (1987). Trace fossils from the Cambrian of Kashmir and their stratigraphic significance. *Journal of the Geological Society of India, 24*, 194–202.

Shu-Zhong, S., Chang-Qun, C., Shi, G. R., Xiang-Dong, W., & Shi-Long, M. (2003). Lopingian (Late Permian) stratigraphy, sedimentation and palaeogeography in southern Tibet. *Newsletters on Stratigraphy, 39*, 159–179.

Singh, P. (1973). A note on the fossiliferous formation in the Lesser Himalaya of Nepal and Bhutan. *Himalayan Geology, 3*, 372–380.

Singh, T. (1981). Age and faunal affinity of the Garu Formation, Arunachal Pradesh. *Himalayan Geology, 11*, 271–286.

Singh, T. (1987). Palaeoclimatic significance of fauna and microflora of the Garu Formation (Permion), Arunachal Pradesh, Eastern Himalaya. In I. Mackenzie & D. Garvy (Eds.), *Gondwana 6* (pp. 141–194). Washington: American Geophysical Union.

Singh, T. (1993). Gondwana sediments (Permian) of Arunachal Himalaya: Stratigraphic status and depositional environment. *Gondwana Eight* (pp. 345–354). Rotterdam: Balkema.

Singh, G., Maithy, P. K., & Bose, M. N. (1982). Upper Palaeozoic flora of Kashmir Himalaya. *Palaeobotanist, 30*, 185–232.

Sinha, Anshu K. (1989). *Geology of Higher Central Himalaya* (p. 236p). Chichester: Wiley.

Spring, L., Bussy, F., Vannay, J. C., Huon, S., & Cosca, M. A. (1993). Early Permian granitic dykes of alkaline affinity in the Indian High Himalaya of Upper Lahul and SE Zanskar: Geochemical characterization and geotectonic implications. In P. J. Treloar & M. P. Searle (Eds.), *Himalayan Tectonics* (pp. 251–264). Boulder: Geological Society of America.

Srikantia, S. V. (1981). Lithostratigraphy, sedimentation and structure of Proterozoic–Phanerozoic formations of Spiti basin in Higher Himalaya of Himachal Pradesh. In A. K. Sinha (Ed.), Contemporary geoscientific researches in Himalaya (Vol. I, pp. 31–48). Dehradun: Bishensingh & Mahenderpalsingh.

Stocklin, J. (1980). Geology of Nepal and its regional frame. *Journal of Geological Society of London, 137*, 1–34.

Tahirkheli, R. A. K. (1970). The geology of the Attock-Cherat Range, West Pakistan. *Geological Bulletin University of Peshawar, 5*, 1–26.

Tahirkheli, R. A. K. (1982). Geology of the Himalaya, Karakoram and Hindukush in Pakistan. *Geological Bulletin of the University of Peshawar, 15*, 1–51.

Tahirkheli, R. A. K. (1992). Geology of the Himalaya, Karakoram and Hindukush in Pakistan. *Geological Bulletin, University of Peshawar*, *15*, 1–51.

Talent John, A., & Bhargava, O. N. (2003). Silurian of the Indian subcontinent and adjacent regions. In E. Landing & M. E. Johnson (Eds.), *Silurian lands and seas: Palaeogeography outside Laurentia* (pp. 221–239). : Univ. of the State of New York.

Tangri, S. K., & Pande, A. C. (1995). Tectonostratigraphy of Tethyan sequence [special publication]. *Geological Survey of India, 39*, 109–142.

Teichert, C. (1966). Stratigraphic nomenclature and correlation of the Permian "Productus Limestone" of Salt Range, West Pakistan. *Records of the Geological Survey of Pakistan, 15*, 1–19.

Teichert, C., & Stauffer, K. W. (1965). Palaeozoic reef discovery in Pakistan. *Records of the Geological Survey of Pakistan, 14*, 1–3.

Thein, M. L. (1973a). The Lower Palaeozoic stratigraphy of western part of the Southern Shan States, Burma. *Geological Society of Malaysia, 6*, 143–163.

Thein, M. (1973b). A preliminary synthesis of the geological evolution of Burma, with special reference to the tectonic development of Southeast Asia. *Bulletin of the Geological Society of Malaysia, 6*, 87–116.

Upadhyay, R., Chandra, R., Rai, H., Jha, N., Chandra, S., Kar, R. K., & Sinha, A. K. (1999). First find of the Early Permian Lower Gondwana plant remain and palynomorphs from the Chhongtash Formation (Upper Shyok valley) eastern Karakoram. *Palaeobotanist, 48*, 7–18.

Valdiya, K. S. (1993). Evidence for Pan-African–Cadomian tectonic upheaval in Himalaya. *Journal of the Palaeontological Society of India, 38*, 51–62.

Valdiya, K. S. (1995). Proterozoic sedimentation and Pan-African geodynamic development in the Himalaya. *Precambrian Research, 74*, 35–55.

Valdiya, K. S. (1998). *Dynamic Himalaya* (p. 178p). Hyderabad: Universities Press.

Vanny, J.-C., & Spring, L. (1993). Geochemistry of continental basalts with the Tethyan Himalaya of Lahaul-Spiti at SE Zanskar, NW India. In P. J. Treloar & M. P. Searle (Eds.), *Himalayan Tectonics* (pp. 237–250). Boulder: The Geological Society of America.

Wadia, D. N. (1934). The Cambrian-Trias sequence of NW Kashmir. *Records of the Geological Survey of India, 68*, 121–167.

Wager, L. R. (1939). The Lachi series of N. Sikkim and the age of the rocks forming Mount Everest. *Records of the Geological Survey of India, 74*, 171–188.

Wicander, R., & Monroe, J. S. (2000). *Historical geology: Evolution of earth and life through time* (4th ed., p. 427 p). Thompson, USA: Books/Cole.

Xiaochi, J. (2002). Permo-Carboniferous sequences of Gondwana affinity in southwest China and their palaeogeographic implication. *Journal of Asian Earth Sciences, 20*, 633–646.

Chapter 13
Gondwana Tectonics, Inland Sedimentation and Life

13.1 Hercynian Crustal Upheaval

Late in the Palaeozoic era, the Indian landmass was overwhelmed by strong tectonic tension. The supercontinent *Gondwanaland* was beginning to split into smaller cratonic blocks, and the Indian plate started moving northwards. The shear zones, faults and rift valleys of the Precambrian antiquity were reactivated, and a number of elongate depressions were formed as a result of ground subsidence and downfaulting of the cratonic blocks. These depressions were represented by grabens and half-grabens. They were subsequently filled up with sediments brought by rivers, giving rise to the Gondwana basins (Fig. 13.1). Waters of the surrounding seas rushed in along some of the grabens and inundated the floodplains and lakes that had formed in the depressions. In the northern margins of the Indian landmass, lavas came out through deep faults, forming a chain of volcanoes that stretched east–west from the Siang Valley in Arunachal Pradesh to the Pir Panjal and beyond in Kashmir.

It may be recapitulated that the ultimate outcome of the tectonic and volcanic activities in the Early Permian along the northern margin was the breaking away of a microcontinent comprising Tibet, Iran and Turkey and opening up of a new sea, known as the *NeoTethys* (Fig. 12.18). This sea was linked with the Mediterranean Tethys of Europe. Later in the Middle and Late Permian time, another microcontinent embracing Eastern Myanmar, Thailand, Malaysia and Sumatra rifted away from the north-eastern margin of the Gondwanaland. These events in the Indian subcontinent were contemporaneous with the large-scale crustal disturbances in Eurasia that had given rise to the *Hercynian mountain system*.

K.S. Valdiya, *The Making of India*, Society of Earth Scientists Series,
DOI 10.1007/978-3-319-25029-8_13

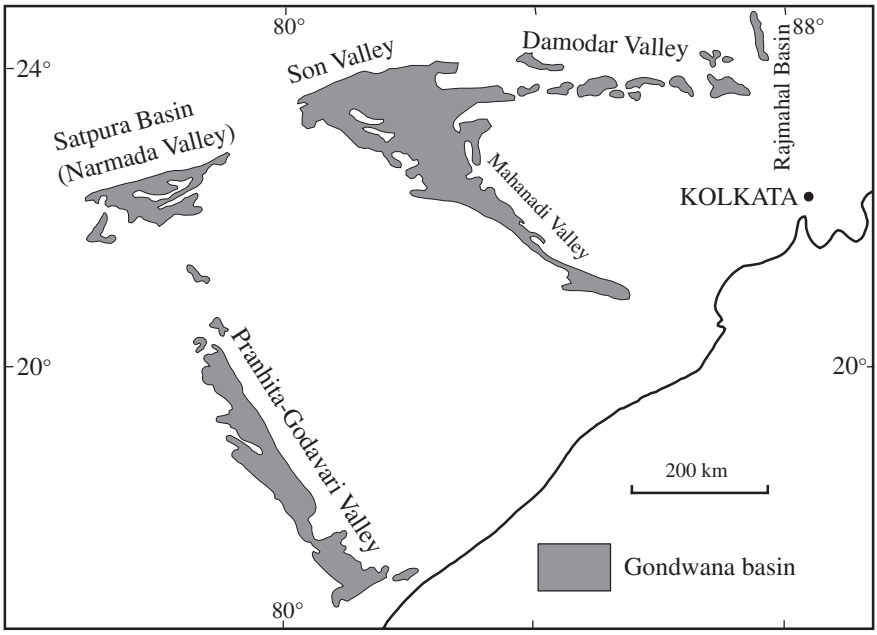

Fig. 13.1 Gondwana basins, developed in tectonically formed depressions and rift valleys in the continental shield (modified after Ghosh et al. 2004)

13.2 Formation of Continent-Interior Basins

As stated above, reactivation of ancient shear zones, passive rifts, older faults and tectonic contacts of Precambrian protocontinental blocks during the Early Permian resulted in the formation of grabens, half-grabens and crustal depressions (Figs. 13.2 and 13.3). Sedimentation in the grabens—and resulting distribution of Gondwana rocks—is the consequences of the activities on the faults demarcating the boundary of depression (Chakraborty et al. 2005). The reactivation of ancient faults and shear zones was a result of the northward movement of the Indian plate subsequent to its splitting from the West Gondwanaland. There are other views on the formation of some Gondwana basins. On the basis of disposition, shape and structural architecture, the origin of the Satpura Basin in central India is attributed to left-lateral displacement along ENE–WSW-trending, left-stepping strike-slip faults—the southern fault of the Son–Narmada Fault System and the northern fault of the Tapi system (Chakraborty and Ghosh 2005). It is also attributed to passage of the Indian plate over hot spots, which have been resurgent time and again (Raval 1993, 1995; Raval and Veeraswamy 2003).

The elongate Gondwana basins trending ENE–WSW and NW–SE (Fig. 13.1) are occupied by the rivers Damodar, Son, Narmada, Mahanadi, Pranhita with Godavari. The depressions formed in the subsurface Rangpur Saddle in northern Bangladesh and adjacent Bengal lie concealed under thick pile of the

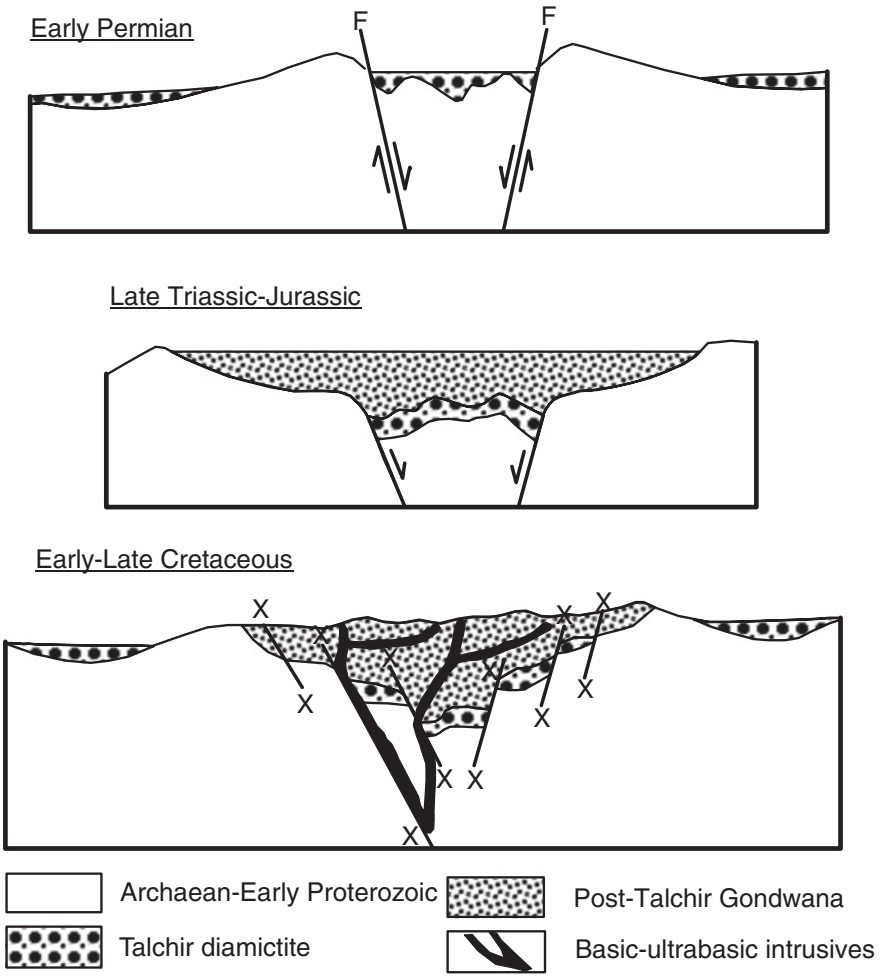

Fig. 13.2 Formation of the Gondwana basin is due to renting apart of the Indian Shield and sinking of crustal blocks between parallel normal faults. The faults have been active all through the time (based on Cashhyap et al. 1993b)

Indo-Gangetic sediments. The continent-interior grabens, half-grabens and crustal depressions in the Indian Shield became sites of vigorous fluvial, alluvial, lacustrine and deltaic sedimentation from the Early Permian to the Late Jurassic or Early Cretaceous. This sedimentary succession in different basins is known as the *Gondwana Supergroup*.

There are two views on the mode of the Gondwana sedimentation. First, the sediments were laid down by rivers in linear depressions formed by rifting as borne out by fan- or cone-shaped conglomeratic deposits in lines parallel to the bounding faults (Ahmad 1960). Second (Fig. 13.2), the growing load of accumulating sediments initiated movements on faults and progressive deepening of the

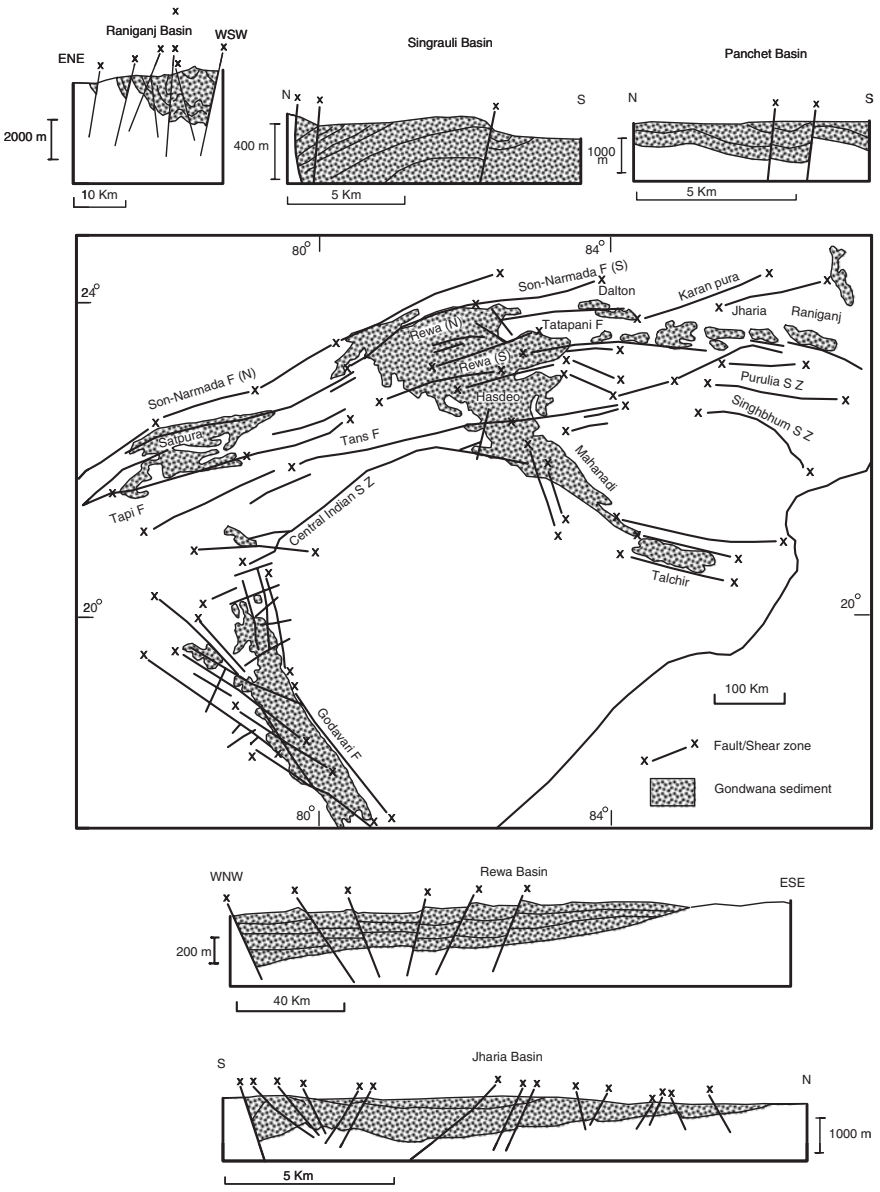

Fig. 13.3 Major faults and lineaments that demarcate the Gondwana basins (after Chakraborty 1996) *Inset* cross sections illustrate structural architecture of these basins (after Veevers and Tewari 1995)

basin floor, resulting in the expansion of the basin of deposition as time progressed (Casshyap and Srivastava 1987; Srivastava et al. 1993). In other words, the lower

part of the Gondwana succession represents sediments accumulated in sag basins, which had developed over ancient rift sites and the upper sequence is the accumulation in rift basin (Biswas 2003). In short, there was sedimentation synchronous with fault-controlled subsidence, which was relatively more in places of differently oriented structural discontinuities (Chakraborty 1996).

13.3 Land of Continental Glaciers

In the Early Gondwana time, when these things were happening, a large part of the land was in the grip of severe refrigeration and under thick cover of ice (Fig. 13.4). Glaciers descended down the valleys and deposited their loads in depressions and in their water bodies. These deposits are known in the Peninsular India as the *Talchir Boulder Beds* (Table 13.1). Some of the glaciers were very long as evident

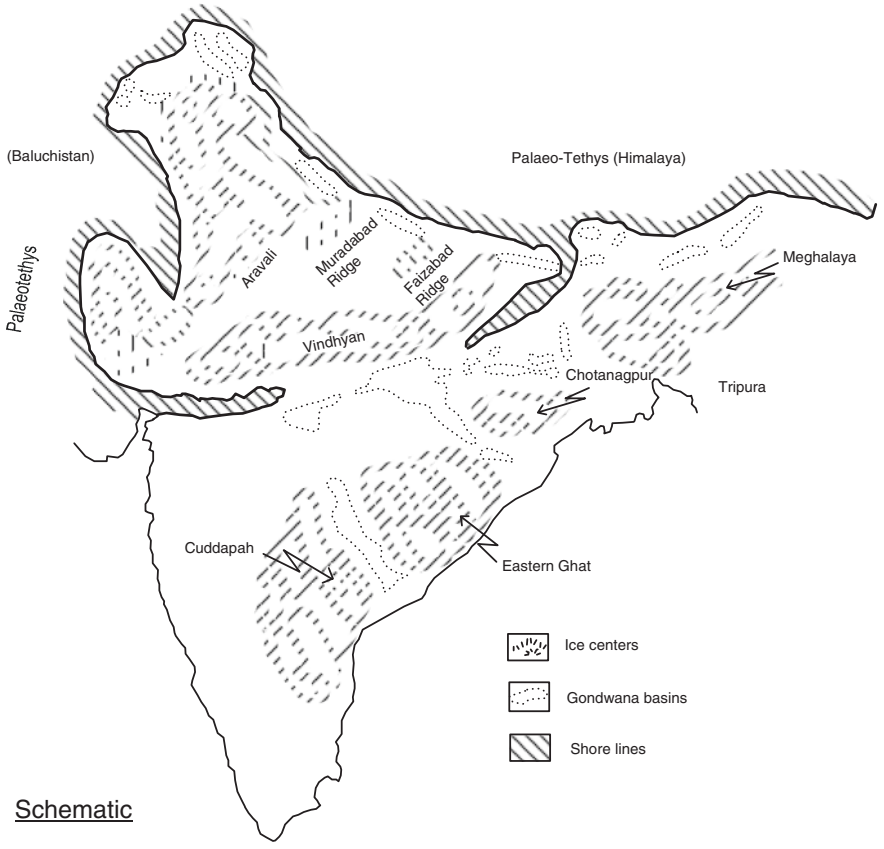

Fig. 13.4 A large part of India was glaciated in the Early Permian when the Gondwana basins developed. Marine incursion in the Early Permian linked parts of central India with the seas around the Gondwanic India (after Chatterjee and Hotton 1986)

Table 13.1 Integrated lithostratigraphy of the Gondwana succession

Age		Formation	Basin			
			Damodar	Son–Mahanadi	Satpura	Pranhita–Godavari
Cretaceous	Lower	Rajmahal		Bansa		
Jurassic	Upper					Gangapur
	Middle	Jabalpur	Dubrajpur		Jabalpur	Chikala
	Lower					Kota
Triassic	Upper	Mahadev	Mahadev	Parsora	Bagra	Dharmaram
	Middle	Denwa		Pali/Tiki	Denwa	Maleri/Bhimavaram
	Lower	Panchet	Panchet		Pachmarhi	Gollapalli/Yerrapalli
Permian	Upper	Raniganj	Raniganj	Kamthi	Bijori	Kamthi/Chintalapudi
	Middle	Barren Measures	Kulti		Motur	Kundaram
	Lower	Barakar	Barakar	Barakar	Barakar	Barakar
		Karharbari	Karharbari	Umaria	Karharbari	
		Talchir	Talchir	Talchir	Talchir	Talchir

from the occurrence within the Talchir units of rock clasts of rhyolite, felsite and granite of the Malani–Erinpura areas of the Aravali Range—in the Bap and Badhaura beds in the Marwar region of Rajasthan and in the Tobra boulder bed in the Salt Range, Pakistan, the latter nearly 600 km away from the source. In a number of places, striations made on hard rocks delineate the directions in which the continental glaciers moved.

13.4 Drainage Pattern

The Gondwanic India sloped north-westwards, and rivers and streams flowed in the northward directions. This is evident from sediment dispersal pattern unravelled from isopach maps and palaeocurrent pattern of various Gondwana basins (Fig. 13.5). Take the case of the Pranhita–Godavari domain in South India. The rivers flowed in the north-westerly direction all through the Triassic and Early Jurassic times, but changed westwards in the Middle Jurassic, following the tilting of ground closer to the coast (Tewari 1998; Lakshminarayana 2002). The same north-westerly flow during the Triassic is witnessed in the Satpura basin in the Narmada Valley. In the Upper Triassic, the Bagra basin was drained by rivers that flowed southwards, of course locally in a limited region (Casshyap et al. 1993).

In the Damodar domain (Figs. 13.5 and 13.6), the palaeocurrent directions varied from NE in the Lower Permian to NW during the Upper Permian

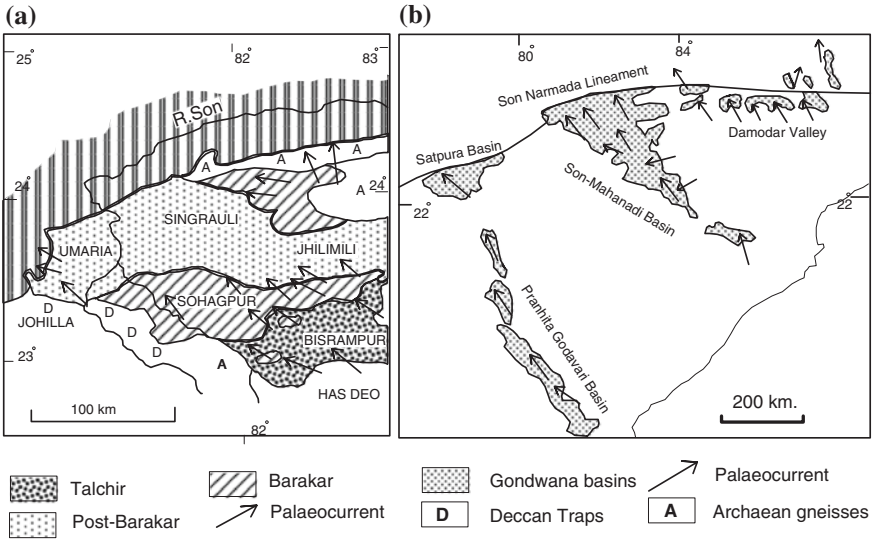

Fig. 13.5 **a** Palaeocurrent directions in the Son Valley Gondwana basin (after Casshyap 1982). **b** North-westerly palaeocurrents in all the Gondwana basins imply that the Gondwanic India sloped northwards (after Casshyap et al. 1993)

(Casshyap 1973). In the Giridih and Bokaro basins, the streams that flowed WNW/NW during the Early Lower Permian changed direction to N during the Late Lower Permian (Tewari and Casshyap 1982; Casshyap and Kumar 1987). In the Son Valley, the Gondwana rivers drained the terrain north-westwards but shifted to WNW along the margin of the basin (Casshyap 1982).

The uniformity of northerly flow directions in all the Gondwana basins seems to imply existence of a unified master drainage basin opening towards north-west (Veevers and Tewari 1995). These rivers of Gondwanic India emptied themselves in the *Palaeotethys* and ocean stretched north of the Indian landmass. They originated in and brought their sediment loads from the upland that lay beyond the present-day East Coast of India. During that time, India was an integral part of the East Gondwanaland and lay next to Antarctica and Australia (Fig. 12.18). The highlands of the Enderby-Wilkies Lands in Antarctica were the source of the Gondwanic Godavari, Mahanadi and Damodar rivers.

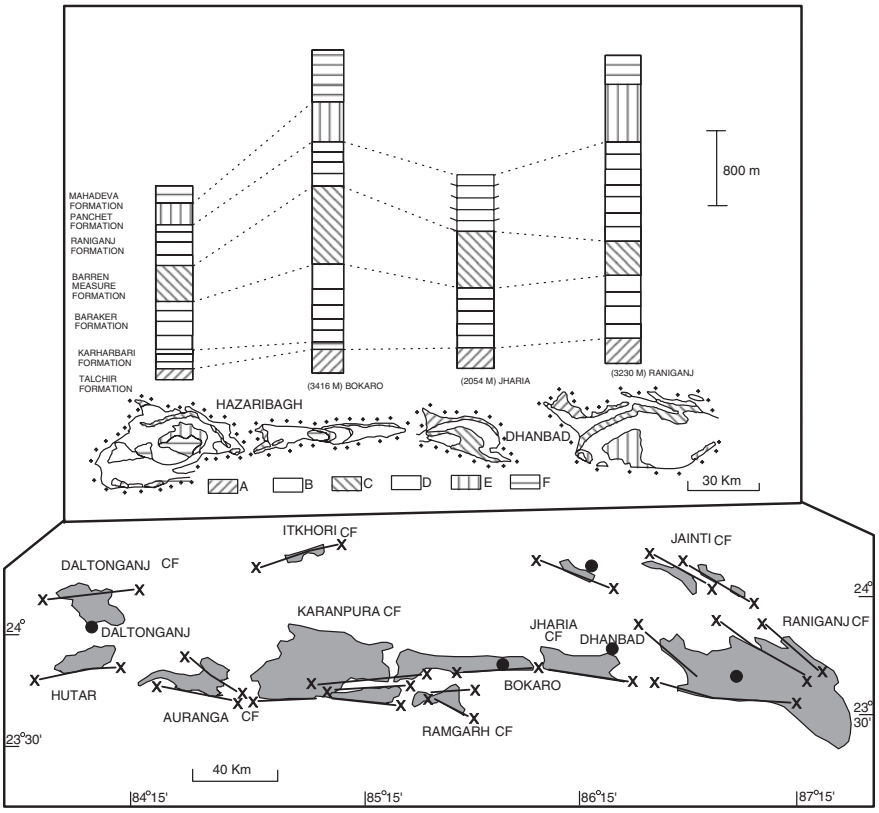

Fig. 13.6 Gondwana formations in the Damodar Valley domain (after Casshyap and Kumar 1987)

13.5 Early Permian Marine Incursion

The continued sagging or subsidence of the continental crust invited marine waters to inundate Gondwanic basins in the Early Permian time. The marine incursion through Deoghar and Rajmahal linked the Tethys Sea in the Subansiri (Arunachal Pradesh) with the low-lying tracts in central India including Daltonganj, Manendragarh and Umaria (Fig. 13.4). On the other side, the sea in the Salt Range (Pakistan) transgressed over to Badhaura and Bap areas in western Rajasthan. And the Arabian Sea waters found a pathway to Rajahar through an elongate depression. An analysis of sedimentary facies of the Arunachal Gondwana indicates marine transgression giving rise to development of marginal swamps and lagoons under fluctuating colder and warmer climate conditions and underwater basic volcanism, followed by regression that left its signs in the deltaic deposits (Singh 1993).

The marine incursion left behind deposits. The *Umaria Marine Beds* of grey claystone, shale, siltstone and limestone are characterized by phosphatic nodules. Such fossils such as *Productus, Eurydesma, Deltopecten and Consularia*, together with *Spirifer, Spiriferina* and *Derbyia*, and leiosphaerid polymorphs assign Early Permian age to the event (Misra et al. 1961; Ranga Rao et al. 1977; Dickins and Shah 1979; Venkatachala and Tiwari 1987).

13.6 History of Sedimentation

13.6.1 General

The sedimentary succession of the Gondwana Supergroup provides a record of a continuous history of sedimentation and of the climate change that occurred from the earliest Permian to the Early Cretaceous (Figs. 13.1 and 13.11; Table 13.1). The thick sedimentary deposits in the intracratonic inland basins were given the name *Gondwana System* by H.B. Medlicott in 1872 after an ancient kingdom of Gond tribe inhabiting central India. It is truly a stratigraphic term without any connotation of geographic location or biotic assemblages.

At the base, the Gondwana succession, there is a glacigene unit recognizable in all the basins. The time of glacial activities was followed over a prolonged period by deposition by rivers in their channels and floodplains which were characterized by marshes and lakes. The basins of deposition grew in size and soon became broad, as evident from overlaps and onlaps of younger sediments on older ones and their resting directly on Precambrian basement (Casshyap 1977). Then, the climate became dry and semi-arid as testified by red sediments of the alluvial plains. There was a spell of non-deposition before fluvial–alluvial sedimentation gave way to deltaic deposition in the Late Jurassic (Table 13.1). It is noteworthy that while the Permian rocks are extensively exposed in all the Gondwana basins, the Triassic and Jurassic strata have restricted occurrence. Moreover, while the

Permian and Early Triassic rocks exhibit uniform facies and mode of occurrence in all Gondwana basins, the Middle and Late Triassic formations have variable characters and different mode of occurrence in different basins.

13.6.2 Detritus from Glaciated Land

It was an undulating country of Precambrian rocks, predominantly gneisses and granites in central and eastern India and Proterozoic sedimentary rocks in Andhra Pradesh. Glaciers carved their courses down the slopes to north-west and dumped their detritus in depressions and lakes in the floodplains. The glacigene deposits were named *Talchir* by W.T. Blanford and W. Theobold in 1856 after the Talchar Coalfied in Odisha. The *Talchir Formation* comprises muddy massive and laminated diamictite and rhythmite, characterized locally by rafted pebbles in shales, convolute bedding and slump structures. In some places, the pebbles are faceted and striated, indicating their transportation in frozen ice of the glaciers. As the proximal part of the basins was filled up with sediments and converted into floodplains, in the distal delta-front parts (Fig. 13.7), there were inflowing streams and turbidity currents which triggered slumping and debris flows. This was the scenario of the Damodar Valley (Fig. 13.6) domain (Das and Sen 1980; Sen 1991; Sen and Banerji 1996; Casshyap and Kumar 1987). In the Son–Mahanadi and Satpura basins, the conditions and pattern of sedimentation were much the same as in the Damodar domain. Features such as beachface sand, storm-laid sand sheets, rip current, channel fills, hummocky cross-bedding in siltstones, deep and wide palaeochannels in peat-forming environment, mutually perpendicular sets of gutter casts trending NW–SE, polymodal groove marks and bounce marks, and bimodal prod marks have been interpreted as products of interplay of unidirectional currents and oscillating waves during storms along shores (Mukhopadhyay and Bhattacharya 1994; Mukhopadhyay et al. 1997; Dutt and Mukhopadhyay 1997; Bhattacharya et al. 2004). Clearly, the upper part of the Talchir bears marine influence. Alternatively, there was a large body of water often swayed by storms and wave action.

13.6.3 Fluvial–Alluvial Sedimentation

By middle of the Early Permian, the Damodar Valley moors were surrounded by forests, and the terrains subjected intermittently to moderate to high floods (Gupta et al. 1999). This is testified by bituminous coal, rich in inertinite and the quantitative relationship of macerals microlithotypes and mineral matters (Singh et al. 2003). The fluvial sedimentation began with what was recognized as the *Karharbari Formation* by W.T. Blanford in 1878 after a village in the Giridih district. It comprises pebbly conglomerate and pebbly sandstone representing

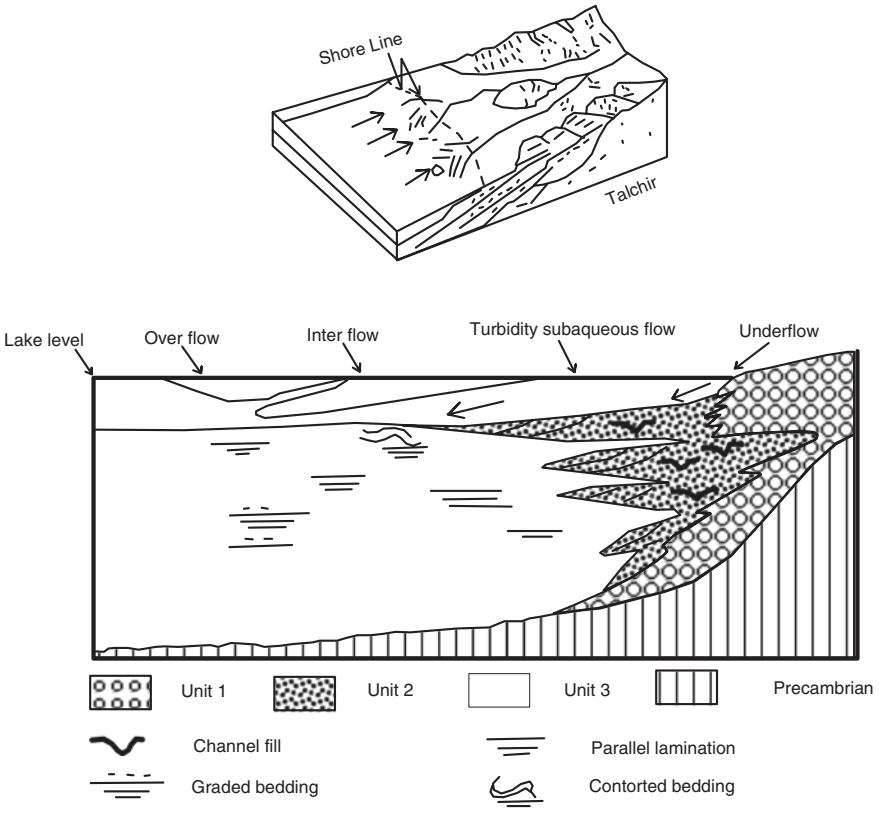

Fig. 13.7 Mode of emplacement of the sediments of the Talchir Formation in the Jainti basin (after Sen and Banerji 1996; *Inset* after Veevers and Tewari 1995)

channel fills, planar cross-bedded sandstone characterized by small and large coalescent channels, and shales with coal beds (Tewari and Casshyap 1982). In the Pranhita–Godavari domain, the Karharbari comprises sandstone characterized by pronounced cross-bedding, sandstone body of the shape of a shoestring body and sandstone interfingering with laminated argillite of the floodplain in which the channels shifted in space and time (Sengupta 2003).

The succeeding fluvial–alluvial deposit comprising conglomerate, multistoried sandstones, siltstones and shales with thick beds of coal is known as the *Barakar Formation*. It was named by T. Oldham in 1867 after the Barakar River in the Raniganj Coalfield in Jharkhand. The lower part of the Barakar succession represents a deposit of braided rivers, the middle part of the meandering streams with oxbow lakes and cut-off meanders, and the upper part of the deltas affected by storms and tides (Fig. 13.8). In the Pench Valley (Satpura domain), the floodplains of the Barakar streams were characterized by extensively vegetated marshland and lakes. Certain features described as tidal bundles and tidal rhythmites in the

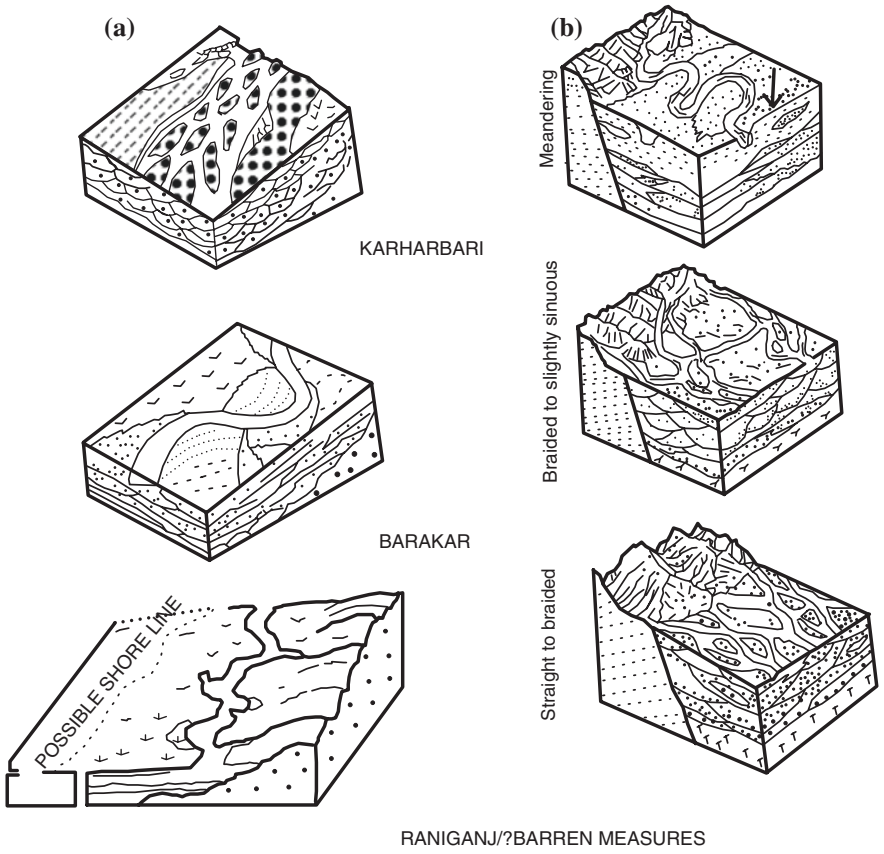

Fig. 13.8 Schematic diagrams illustrate the changing scenario of river regime in the Damodar domain in the Permian time (after Casshyap and Khan 1993; Veevers and Tewari 1995)

delta-type deposits have been interpreted as indicators of tidal activities (Ghosh et al. 2004). It is evident that towards the close of the Early Permian epoch, the braided streams had given way to meandering rivers flowing on large plains characterized by marshes and lakes (Cashhyap and Khan 1993; Tewari et al. 2012). In these lakes, developed deltas of fluvial architecture are affected by storms and tides.

Overlying the Barakar are the *Barren Measures* (also called Kulti Formation). The formation is made up of lensoid massive beds of pebbly sandstone emplaced by flows during flood events (Dasgupta 2002) interbedded with variegated claystones and siltstones of the alluvial plain. In the Satpura and Pranhita–Godavari domains, the time equivalent of the Barren Measures is the *Motur Formation*,

comprising red mudstone with calcareous nodules and sheets or lenses of cross-bedded sandstone representing channel fills in a floodplain of an anastomosing river system (Ray and Chakraborty 2002). Sandstone contains silicified wood. The calcareous nodules represent a palaeosol formed under semi-arid conditions. The Barren Measures are followed up by what W.T. Blanford in 1861 named the *Raniganj* in the Damodar Valley. Its time equivalents are the *Bijori Formation* in the Satpura domain, the *Kamthi Formation* in the Wardha Valley and the *Chintalapudi Sandstone* in the Pranhita–Godavari domain. The Kamthi in the Talcher Coalfield in Odisha contains Triassic plant fossils (Bhattachary et al. 1997). Characterized by abundant wave ripples, hummocky and swaley cross-stratifications, hydromorphic palaeosols, local folding surfaces and temnospondyl vertebrate fossils, the Bijori represents a lacustrine sequence in the alluvial plain made up of channel fills and delta-front bar sediments (Chakraborty and Sarkar 2005). The shore of the lake was oriented in the ENE–WSW direction, while the rivers flowed in the north and north-west directions. As a matter of fact, all these Upper Permian formations are made up of cross-bedded sandstones interbedded with shales, carbonaceous shale and coal beds. The cross-bedded sandstone represents migrating dunes in pointbar deposits. While the upper part of the succession consists of planar cross-bedded sandbars in floodplains, the top is made up of fine-grained sediments characterized by flaser bedding and ripple cross-lamination (Casshyap and Kumar 1987). Evidently, the sediments were deposited in an extensive floodplain drained by a system of WNW-flowing streams whose sinuosity increased progressively westwards. The Chintalapudi Sandstone, comprising conglomeratic ferruginous sandstone interbedded with pink- to buff-coloured siliceous shale, was deposited by streams that drained the Dharwar terrain (Ramamohana Rao et al. 1994).

13.6.4 Prevalence of Dry Climate

The Panchet Hill in the Raniganj Coalfield is made up of coarse-grained feldspathic sandstones with thin greenish brown shale and red claystone with a few beds of impure limestone in the upper part and conglomerate with laterite nodules at the base of the *Panchet Formation*. Floral assemblage places the Panchet in the Early Triassic. Estherids recovered from red sediment in the Singrauli Coalfield of the South Rewa Basin confirm Early Triassic age of the Panchet (Datta and Ghosh 1997). In the Pachmarhi Hill (Fig. 13.9) in the Satpura domain, the vertically stacked sheets of coarse-grained and pebbly sandstone, multistoried sandstone and minor red claystone indicate fluvial–alluvial regime of the Early Triassic time (Peters and Singh 2001). The homotaxial formation in the Pranhita–Godavari domain is known as the *Yerrapalli Sandstone*. It is constituted of red and green claystones containing rich assemblage of vertebrate fossils.

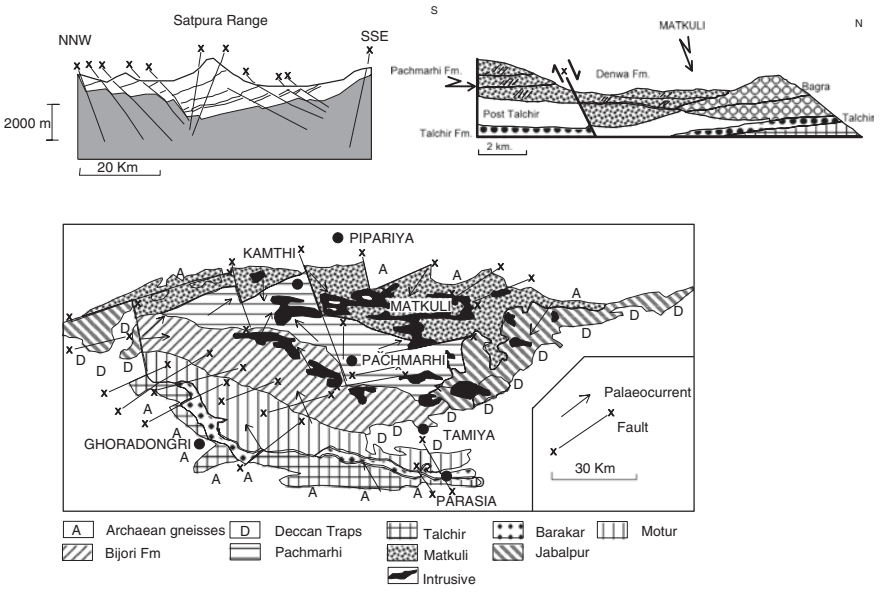

Fig. 13.9 Sketch map of the Gondwana formations in the Satpura Basin in Madhya Pradesh showing, among others, palaeocurrent direction (modified after Peters and Singh 2001). *Left inset* shows the structure of the Satpura Hills (after Veevers and Tewari 1995) *Right inset* demonstrates the Bagra sedimentary succession (after Casshyap et al. 1993)

The variegated claystone interbedded with white arkosic, locally conglomeratic sandstone makes up the *Denwa Formation* in the Satpura domain (Fig. 13.9 *inset*). Calcareous red sediment at the base represents palaeosol formed under semi-arid condition, and the overlying sandstone–claystone alternation was laid down by streams that changed from braided to meandering mode (Malik et al. 2000). In the South Rewa Basin, the homotaxial *Tiki (Pali) Formation* is made up of arkosic sandstone and red shales–mudstone. In the Pranhita–Godavari domain (Fig. 13.10), the *Maleri Formation* associated with the *Bheemaram Sandstone* is a red-bed unit comprising claystone with a few sheets of channel-fill sandstone and pedogenic peloidal calcirudite–calcarenite at the base (Sarkar 1988). The formation has revealed an assemblage of interesting flora (conifer woods) and fauna (fish, amphibians, reptiles including dinosaurs) that throw light on the evolution of life in the Gondwanic India. The muddy polymictic conglomerate and cross-bedded sandstone intercalated with shale represent a fluvial fan complex that prograded northwards in the Satpura basin (Casshyap et al. 1993; Peters and Singh 2001). It was described as the *Bagra* by H.B. Medlicott in 1873 in the Tawa gorge in the Hoshangabad district. In the Auranga Coalfields in the Damodar

domain, the pile of cross-bedded red sandstones of the homotaxial *Mahadev Formation* has been interpreted as aeolian dunes with wadi sand between them (Sen and Sinha 1985). The wind blew from SE to NW. In the Johilla River section in the Son–Mahanadi domain, the coarse- to medium-grained cross-bedded sandstones interbedded with ripple-marked mottled mudstones (Parsora Beds) are characterized by typical Late Triassic plant fossils.

13.6.5 Terminal Phase of Gondwana Sedimentation

Resting directly on the Archaean gneisses, a sequence of the sandy conglomerate and white clay is known as the *Jabalpur Formation* in the Satpura domain. It was named by T. Oldham in 1871. In some areas, the Jabalpur unconformably overlies the Denwa or the Bagra (Fig. 13.11). The sandy conglomerate is characterized by class of jasper, and there are a few beds of coal in the succession. It is overlain in turn by the Lameta Formation of the Deccan Volcanic Province. The Jabalpur contains an assemblage of Middle Jurassic plant fossils.

In the Jharkhand–Bengal border, the *Rajmahal Formation* is essentially a pile of basaltic lavas with intertrappean sedimentary strata of the Gondwana spectrum. T. Oldham had given it the name in 1860. At the base of the Rajmahal Formation occurs a 55-km-long persistent horizon of cherty oolitic ironstone and sideritic claystone that is locally phosphatic (Ray and Jodha 2001). The intertrappean beds contain rich suite of plant fossils suggesting an age between Middle Jurassic and Early Cretaceous. The $^{40}Ar/^{39}Ar$ ages 114–118 Ma of the basalt, place the Rajmahal in the Aptian (Lower Cretaceous) epoch (Baksi et al. 1987).

Eruption of lavas on a large scale over a vast stretch of land extending from Rajmahal to Sylhet region in north-eastern Bangladesh and adjoining Meghalaya marks the end of the Gondwana era in eastern India.

13.7 Subsurface Gondwana Formations in Bangladesh

Geophysical surveys and deep drilling have revealed existence under the thick pile of Indo-Gangetic sediments of grabens and half-grabens on northern and southern slopes of the so-called *Rangpur Saddle*. It is the shelf of the continental margin lying in the Rajmahal–Garo Gap between the Jharkhand Hills and the Meghalaya–Mikir Plateau. The subsurface Rangpur Saddle is 16–40 km wide (Reiman 1993) and bound by N–S-trending faults and lineament (Khan et al. 1994; Nehaluddin 1994). The grabens contain the Gondwana succession—the Talchir, the Barakar, the Raniganj and the Rajmahal. While the northern group of the Gondwana

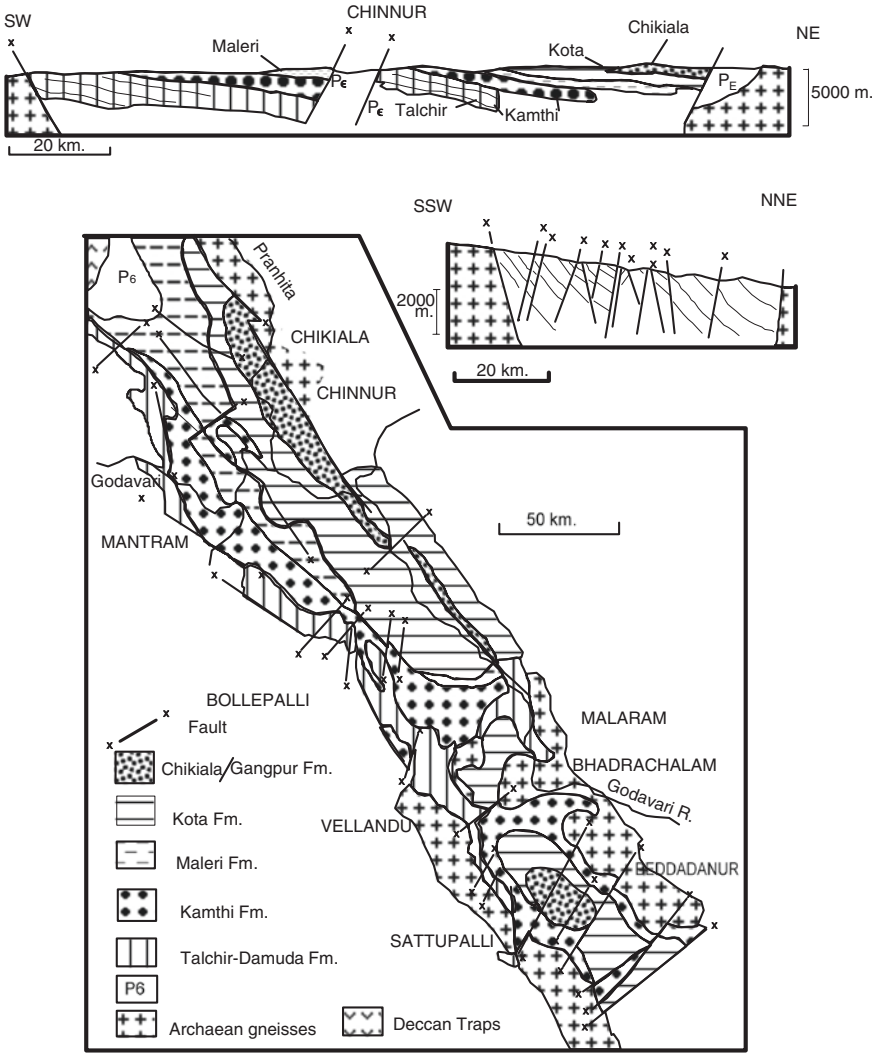

Fig. 13.10 Gondwana formations in the Pranhita–Godavari Valley, Andhra Pradesh (Based on Lakshminarayan 2002; Ramamohana Rao et al. 1994). *Insets* illustrate the structural design of the basin (after Veevers and Tewari 1995)

grabens is in the line of the Satpura–Damodar domains, the southern group is comparable with the Gondwana units of the Pranhita–Godavari and Mahanadi domains. The important Gondwana basin of the Rangpur Saddle includes the Bogra Graben and the Jamalgarh half-graben (Reiman 1993).

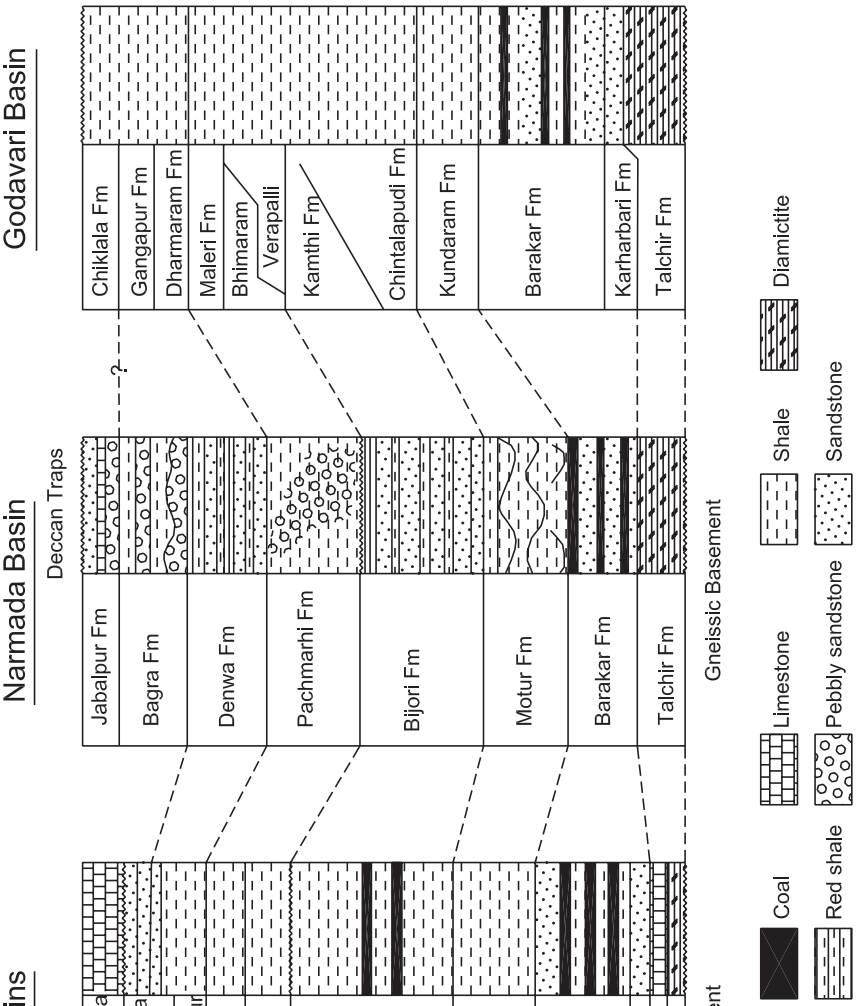

Fig. 13.11 Integrated and simplified lithostratigraphic column of the Gondwana succession

13.8 Igneous Activities in Grabens

The E–W-trending zone of the Damodar Valley grabens has been the places of magmatic activity since the Palaeoproterozoic, ending up with the eruption of the Rajmahal lavas 114–118 Ma ago. Dyke swarms of tholeiitic dolerite and ultrapotassic lamprophyres and lamproite in the Bokaro, Raniganj, Jharia and Giridih basins indicate that deep-seated basement dislocation provided pathways to the magma (Mukherjee and Ghose 1999). Among the intrusions, the 265-million-year-old hornblende–peridotite dyke at Richuguta and the 185-million-year-old body at Latehar occur close to southern margin of the Damodar Graben. The lamprophyres are calc-alkaline in nature, and the composition of the 105–115 Ma lamproites varies from olivine lamproite through olivine-leucite lamproite to calc-alkaline minette, implying their derivation by partial melting from metasomatically enriched zones in the mantle (Paul 1993; Basu et al. 1997). The Salma dolerite dyke in the Raniganj basin, characterized by chondrite-normalized REE pattern similar to that of the Deccan dykes of the Son–Narmada rift zone, is dated (by Ar–Ar whole-rock method) suggesting its genetic relation to the late phase of the Deccan Volcanism 65 Ma (Paul 2005).

13.9 Plant Life of the Gondwana Floodplains

13.9.1 Age of Seed-Bearing Gymnosperms

The wetter parts of floodplains of the Gondwanic India were lush with forest of seedless vascular vegetation in the Early Permian. These were reduced to creeping forms by the end of the Permian. Higher and drier areas were covered by forests of diverse seed-bearing but not flowering *gymnosperms* plants—*Glossopteris* and *Cordiates*. The *Cordiates* trees were as tall as 50 m during their heyday, but became extinct by the Raniganj (Late Permian) time. The Permian flora included *Glossopteris indica, Gangamopteris cyclopteroid, Schizoneura gondwanensis, Noeggerathiopsis hislopi, Neuropteris, Sphenopteris, Phyllotheca and Paranocladus* (conifer). The plant *Glossopteris* that grew in cool climate when the land was going through rigours of glaciation invests the Gondwana with an individuality and uniformity. By the Late Permian Barakar time, the climate had become warm and there was abundance of water. New species of *Rhabdotaenia* and *Walkomielli* appeared in place of older ones and there was manifold increase in the diversity in species of pteridophytes and gymnosperms (Venkatachala 1977). The numerous thick coal seams testify to rich growth of plants on the floodplains during the Permian period. In the Satpura Basin, the Barakar Formation contains along with Glossopteris other plant fossils belonging to the peltasperma group, indicating that there was exchange of flora between the Indian landmass and Eurasia in the Early Permian times (Srivastava et al. 2011).

The climate became dry and warm in the Triassic time. Only a few pools of water were left in the wasteland which the floodplains had become. The vegetation impoverished—their extent shrank and the composition changed. New floral assemblage comprised ferns, horsetails, rushes and club mosses. A study (Fig. 13.12) shows that there was 9 % drop in the organic carbon $^{13}\delta C$ in the Early Triassic of the Raniganj basin indicating that the humid climate had given way to warm, semi-arid conditions (Sarkar et al. 2003). Large trees of seed ferns became extensive by the end of the Triassic. One of the very common conifers was the fair-sized *Schizoneura*.

The *Glossopteris–Vertebraria* assemblage of the Late Permian gave way to the *Dicrodium–Lepidopteris* assemblage in the Triassic, as testified by the Raniganj and the Kamthi flora—particularly the Late Assinian to Ladinian *Dicrodium* assemblage in the Kamthi of the Hingir Valley in Mahanadi domain (Pal et al. 1992; Bhattacharya et al. 1997). Estherids made their appearance in the Triassic assemblage. The Triassic flora includes *Schizoneura gondwanesis, Glossopteris, Rhabdotaenia, Lepidopteris, Recopteris, Trizygia* and *Speciosa*. The proliferation of *Cycadeoides* and other cycads in the Upper Triassic was a major development. A new type of gymnosperm evolved during the Triassic—*Williamsonia.* It had slender 1- to 2.5-m-long trunk with marked spiral rows of leaf scars and a crown bearing long slender palm-like leaves. Remains of *Williamsonia sewardiana* are found in the Cretaceous Rajmahal intertrappean beds. The Upper

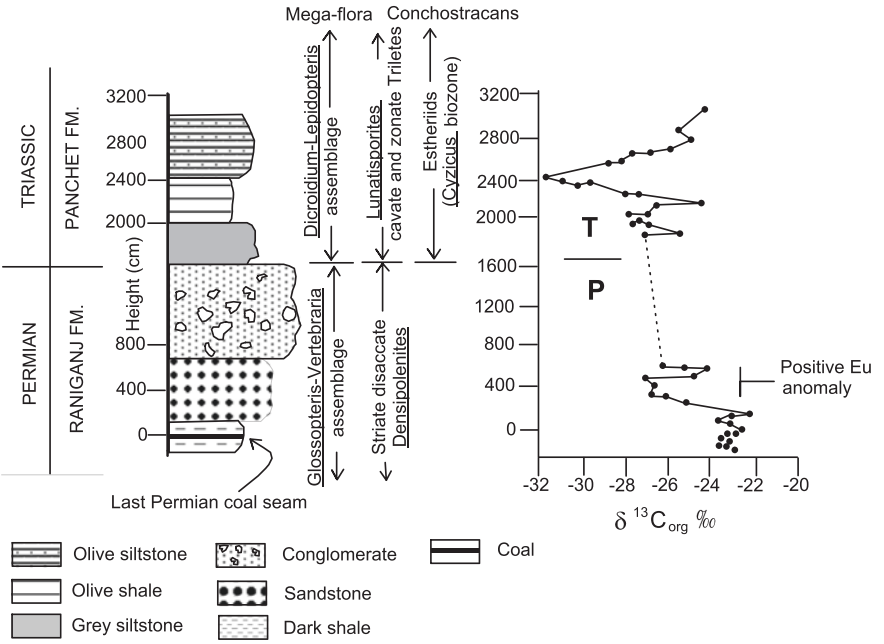

Fig. 13.12 Change of vegetation as the Permian gave way to the Triassic period. There was a large drop of $^{13}\delta C$ in the Early Triassic (Sarkar et al. 2003)

Triassic Tikri Formation (Satpura Basin) is found to be extraordinarily rich in the vertebrate assemblage which is characterized by the presence of low-diversity, monodominant, multitaxic rhynchosaurs (Mukherjee and Roy 2012).

13.9.2 Advent of Flowering Angiosperms

The Late Jurassic witnessed a marked change in the plant community. The seed-bearing gymnosperms gave way to the flowering *angiosperms* plants, marking the most significant development in the evolution of the plant life. The angiosperms proliferated very rapidly and became the most abundant during the Cretaceous. The Rajmahal flora, representing the Cretaceous plant assemblage of the Gondwanic India, comprises *Phyllopterides leavis, Equisites, Pachyopteris indica, Thinnfeldia indica, Ptilophyllum acutifolia, Brachyphyllum, Otozamites, Dictyozamites, Nilssonia, Podozamites, Ginkgopites, Taenopteris spatulata, Elatocladus confertus, Aurocarites cutchensis* and *Coniferocaulon indica* (Banerji and Jana 1998).

13.10 Animal Communities

13.10.1 Predominance of Reptiles

The Mesozoic era is regarded as the *Age of Reptiles*. They were abundant and very diverse, dominating all other animals living on land (Fig. 13.13). It was the evolutionary process in the reptiles that led to the development of mammals in the Triassic and of birds in the Jurassic. The dinosaurs were the most spectacular of the reptiles that reigned supreme in the Mesozoic until their demise towards the close of the Cretaceous (Jain 1974, 1996; Jain et al. 1964, 1974, 1975). Nine vertebrate faunal assemblages have been identified in the Gondwana of the Kundaram and the Yerrapalli of the Pranhita–Godavari Valley—seven families of fish, twenty six of reptiles and five of mammals (Table 13.1), the Denwa and Tiki of the Satpura basin, the Maleri and the Dharmaram of the Pranhita–Godavari Valley (Bandyopadhyay, Saraswati 1999).

In the Late Permian appeared early amphibian *Gondwanosaurus*, which lived up to the Early Triassic Pachmarhi time. It was accompanied by labyrinthodont crocodiles *Archaegosaurus* and *Actinodon* in the Gondwanic Kashmir Himalaya (Prasad 1974). In freshwater lived *Amblypteris* fish. In the uninterrupted Gondwana succession of the Pranhita–Godavari Valley (Jain 1974, 1996; Jain et al. 1964; Ray 2000; Ray et al. 2003) occur, besides fish such as *Saurichthys, Ceratodus, Xenacanthus*, *Lepidotes*, *Paradapedium*, *Tetragonolepsis*

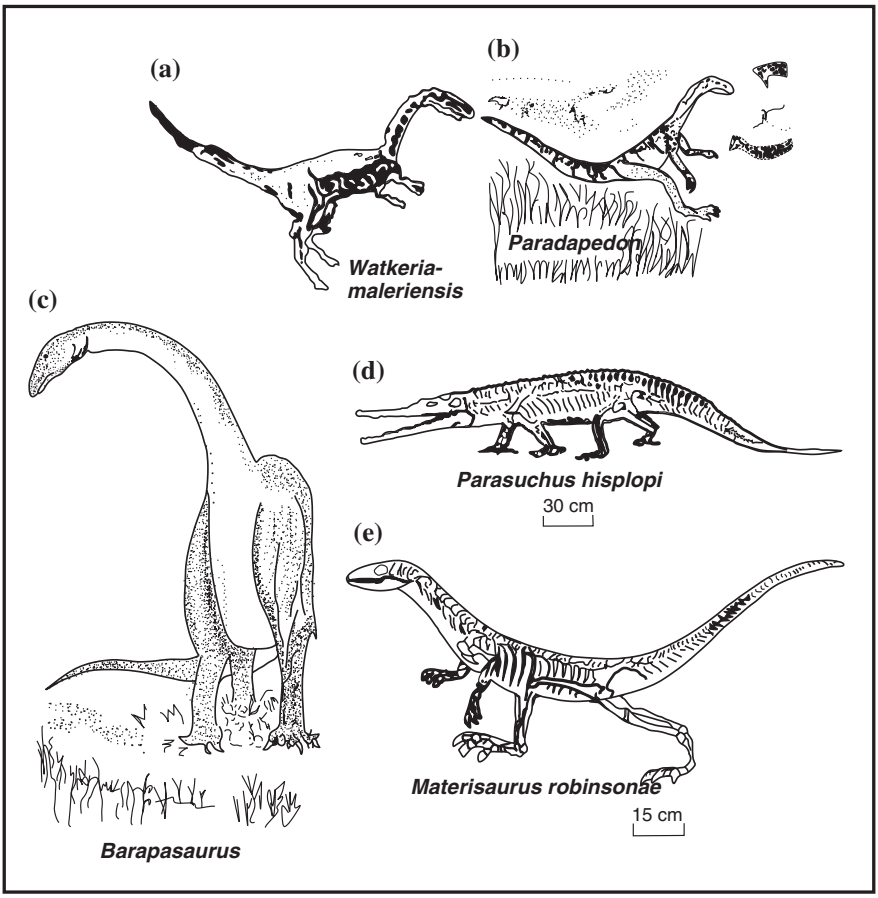

Fig. 13.13 Some reptiles that lived in the Gondwana domain (after Chatterjee and Hotton 1986; Bandyopadhyay 1999)

and *Pholidophous*, a wide variety of reptiles including *Wadiasaurus indicus*, *Rechnisaurus*, *Mesodapedon, Paradapedon huxleyi*, *Parasuchus hislopi*, *Walkeria maleriensis* and *Campylognathoides indicus*. Living on the floodplains of the Pranhita–Godavari domain, the *Parasuchus* was nearly 2.7 m long and its body covered with two rows of elongated paramedian scrubs, as dermal armour (Fig. 13.13). It was a formidable carnivore that lived like crocodiles. In the Denwa Valley, near Pachmarhi, lived crocodile-like *Capitosaurus* and the crocodile *Mastodonsaurus* with eyes far backwards and possessing tusk-like teeth, and in the Maleri sediments of the Godavari Valley were found remains of crocodile *Metoposaurus* and crocodile-like *Compsocerops* (Prasad 1994; Jain 1996).

13.10.2 Evolution of Mammals

The mammal-like *Dicynodon* recovered from the Kamthi Formation in the Damodar basin which had flat head and a pair of elongated tusk-like teeth in the anterior part was a marsh-loving herbivore (Jain 1996). *Lytosaurs* that found in the Panchet beds in Madhya Pradesh had mammal-like characters (Prasad 1994). *Exaeretodon* that found in the Maleri Formation in the Pranhita–Godavari domain had mammal-like attributes and a complex dentition that was well differentiated for various junctions. It was the most prolific of all mammal-like reptiles in the Triassic time (Jain 1996).

The mammals had evolved from the reptiles by the Late Triassic. They were warm-blooded animals with hair or fur to maintain the body temperature. They had mammary glands and gave birth to their young. The transitions is reflected in the differentiation of dentition—formation of distinctive teeth for grinding, chewing and tearing. Most of the early mammals were small—of the size of a mouse. They diversified early into two distinct branches—those that laid eggs (triconodonts) and those that gave birth to the young (symmetrodonts). The descendents of the latter branch evolved as marsupials and palcentals. In the Early Jurassic Kota Formation were found a number of symmetrodont mammals such as *Kotatherium, Trishulitherium* and *Indotherium* (Yadagiri 1984). The divergence into the marsupial and placental forms occurred in the Early Cretaceous.

In the early stage of evolution, the mammals were small insignificant animals, and many became extinct by the Middle Cretaceous. However, one group, pentotheres (before becoming extinct), gave rise to two orders that dominated the land fauna in the Cenozoic era. They had become quite common and widespread by the Late Cretaceous.

13.10.3 Evolution of Birds

The fast moving theropods that leaped into the air with their arms outstretched to catch insects, or to avoid predators, evolved into birds. It is also possible that those theropods which climbed trees and glided down learnt to fly like birds. The first animal to accomplish flight was *Pterosaurs*, which evolved from the archosaur during the Triassic (Wicander and Monroe 2000). The earliest pterosaurs were small in built and had long tail, light hollow bones and a bony structure on the breastline for flight. Related to the pterosaurs, remains of *Pteradon* were found in the Lower Jurassic Kota Formation of the Pranhita–Godavari Valley at Yemnapalli in the Adilabad district. It must have glided close to ground surface and picked up fish from water by its beak. The biped pterosaurid *Campylagnathiodes indica* from the same Kota Formation was a small creature with slender neck, small head and forelimbs half the size of the back pair, resembling a bird but had teeth like those of reptiles (Jain et al. 1974).

13.10.4 Dinosaurs, the Ruling Group

Taking adaptive line of existence, the *thecodonts* not only became a very important group of animals in the Mesozoic but also gave rise to dinosaurs. Two quite distinct groups evolved from the thecodonts—those with bird-like pelvis (ornithischians) and those that had lizard-like hipbones (saurischians). The saurischians comprised two branches, the carnivorous *theropods* and the plant-eating *sauropods*. Varying in size from 24 m in length to a size of a chicken, the dinosaurs showed a strong tendency of general increase in size, culminating in the evolution of mighty formidable creatures. The carnivore *Tyrannosaurus* stood 6 m tall, 15 m long from the tip of nose to end of tail and weighed 8 to 10 tonnes. The plant-eating *Brontosaurus* was 24 m long from tip to tip and *Brachiosaurus* weighed 75 tonnes (Kummel 1961).

The dinosaurs were gregarious animals, living in herds as evident from their trackways, bone beds, and nesting sites in floodplains of the Gondwanaland. These warm-blooded animals, which were capable of maintaining a rather constant body temperatures regardless of the outside temperature, successfully adapted themselves to varied environmental conditions—from those of humid rainforest to dry desert. There are 15–20 genera of dinosaurs known in India, and they survived 165 million years world over (Sahni 2003). The dinosaurs first appeared in the Triassic in India, and diversified and radiated in the Jurassic and Cretaceous periods (Chatterjee and Scotese 1999). The earliest known dinosaur found in the Panchet Formation in Bengal is *Epicampodon*, an archosaur carnivore of small size with elongate neck, small head and serrated sharp teeth (Prasad 1994). Another predaceous primitive dinosaur was *Walkeria maleriensis*, a saurischian theropod found at Nannial in the Adilabad district (Chatterjee 1987). *Walkeria* was a small biped with elongate neck and long forearm. The contemporary *Plateosaurus* and *Thecodontosaurus* lived in the Dharmaram area (Table 13.1).

The Early Jurassic sauropod *Barapasaurus* from the Kota Formation in the Pranhita–Godavari domain was a giant (Jain et al. 1975). In the Narmada Valley of the Early Cretaceous time near Jabalpur roamed *Celiosaurus and Titanosaurus indicus* (having whip-like tail that dragged on the ground. The *Jabalpuria* was a slightly built animal with long neck, very sharp teeth and front legs longer than hind pairs) and possibly *Tyrannosaurus* also lived there (Prasad 1994). And *Indosuchus raptorious* was a giant carnivore that inhabited the Cretaceous floodplains of the Jabalpur region (Tripathi and Mamgain 1987). In the Balasinor taluka, Kheda district, in Gujarat, lived *Titanosaurus indicus, Antarctosaurus septentrionalis* and *Megalosaurus* (Mathur and Pant 1986).

The dinosaurs met with their doom towards the close of the Mesozoic era. It was a case of mass extinction. Chapter Fourteen deals with this aspect.

Table 13.2 Gondwana coal reserve (Chandra et al. 2000)

State	Total reserve (million tonnes)	Proven reserve (million tonnes)
West Bengal	25,892 (12.5 %)	10,315
Jharkhand	67,997 (33 %)	33,983
Madhya Pradesh	42,116 (20 %)	11,388
Uttar Pradesh	1062 (0.5 %)	575
Maharashtra	6779 (3.3 %)	3810
Odisha	48,376 (23.4 %)	7678
Andhra Pradesh	13,127 (6.4 %)	6988
Arunachal Pradesh	90 (0.04 %)	31

13.11 Mineral Deposits

The Gondwana coals were formed from the old forests and marshes that were buried under thick blankets of riverine sediments. This is testified by (i) upright tree trunks, (ii) fossil roots and (iii) underlying clay depleted of alkalies (nutrients) due to extraction by plants. The clay is used as the *fire clay* on an extensive scale for making fire-proof tiles and bricks. Parts of coal deposits are products of burial of plant material transported by rivers and streams and dumped in subsiding basins. It took nearly a million years for the conversion of plant debris into bituminous coal.

The dominant horizons that have yielded coal are the Lower Permian Karharbari and Barakar formations, and the Upper Permian Raniganj Formation (Table 13.2). Some coals occur in the Upper Jurassic Rajmahal, Chikala and Kota formations. The total resource of the Gondwana coals is of the order of 205,352 million tonnes (Chandra 1992; Chandra et al. 2000).

Of the total 213 billion tones of re-estimated coal reserve in the Gondwana succession, about 149 billion tones coal of shallow deposits are mineable and the remaining 64 billion tones of deeper deposits being are presently not amenable to mining.

The Gondwana coal seams at shallow depths contain *clean fuel gas* having properties similar to that of the natural gas. The estimated reserve of this gas at 16 places in central India is of the order of 820 billion cubic metres, and the expected production would be 23 million cubic metres per day for almost 20 years (Sibal et al. 2006). Coal-bed gas (methane) reserve in 26 identified blocks amounts of 8.39 trillion cubic feet, while the prognosticated resource in all the blocks in India is of the order 52 trillion cubic feet.

References

Ahmad, F. (1960). Gondwana basin of sedimentation in India. *Records of the Geological Survey of India, 86*, 523–536.

Baksi, A. K., Barman, T. R., Paul, K. D., & Farrar, E. (1987). Widespread Early Cretaceous flood basalt volcanism in Eastern India: Geochemical data from the Rajmahal–Bengal–Sylhet Traps. *Chemical Geology, 63*, 133–141.

Bandyopadhyay, S. (1999). Gondwana vertebrate faunas of India. *Proceedings of the National Academy of Sciences, 65A*, 285–313.

Banerji, J., & Jana, B. N. (1998). Early Cretaceous megafossils from Balidih, Rajmahal basin, India. *Geophytology, 27*, 35–38.

Basu, A., Bhattacharya, A. K., & Paul, D. K. (1997). Petrology and geochemistry of the lamprophyric rocks from the Bokaro Coalfield, Bihar and their economic potential. *Journal of Geological Society of India, 50*, 255–266.

Bhattacharya, H. N., Bhattacharya, B., Chakraborty, I., & Chakraborty, A. (2004). Sole marks in storm event beds in the Permo-Carboniferous Talchir Formation. *Raniganj Basin, India, Sedimentary Geology, 166*, 209–222.

Bhattacharya, A., Nandi, A., & Dutta, A. (1997). Triassic mega- and micro-plant fossils from the Kamthi Formation of Talchir coalfield, Orissa, with chronological significance. *Special Publication of Geological Survey of India, 54*, 123–126.

Biswas, S. K. (2003). Regional tectonic framework of the Pranhita-Godavari basin, India. *Journal of Asian Earth Sciences, 21*, 543–551.

Casshyap, S. M. (1973). Palaeocurrents and palaeogeographic reconstruction in the Barakar (Lower Gondwana) sandstones of Peninsular India. *Sedimentary Geology, 9*, 283–303.

Casshyap, S. M. (1977). Patterns of sedimentation in Gondwana basins. In *Proceedings of Fourth International Gondwana Symposium, Kolkata* (Vol. 2, pp. 525–551).

Casshyap, S. M. (1982). Palaeodrainage and palaeogeography of Son-Valley Gondwana basin, M.P. In K. S. Valdiya et al. (Eds.), *Geology of Vindhyachala*. Delhi: Hindustan Publishing Corporation, –142.

Casshyap, S. M., & Khan, A. (1993). Palaeohydrology of Permian streams in Bokaro Basin, Bihar. *Journal of Geological Society of India, 23*, 419–430.

Casshyap, S. M., & Kumar, Ajay. (1987). Fluvial architecture of the Upper Permian Raniganj Coal Measures in the Damodar basin, eastern India. *Sedimentary Geology, 51*, 181–213.

Casshyap, S. M., & Srivastava, V. K. (1987). Glacial and proglacial Talchir sedimentation in Son–Mahanadi Gondwana basin: Oakaeigeigraoguc recibstruction, *American Geophysical Union*, 167–182.

Casshyap, S. M., Tewari, R. C., & Khan, A. (1993). Alluvial fan origin of the Bagra Formation (Mesozoic Gondwana) and tectonostratigraphic implications. *Journal of Geological Society of India, 42*, 269–279.

Chakraborty, C., & Ghosh, S. K. (2005). Pull-apart origin of the Satpura Gondwana basin, central India. *Journal of Earth System Science, 114*, 259–273.

Chakraborty, T., & Sarkar, S. (2005). Evidence of lacustrine sedimentation in the upper Permian Bijori Formation, Satpura Gondwana basin: Palaeogeographic and tectonic implications. *Jour. Earth Syst. Sci., 114*, 303–323.

Chakraborty, T., Sarkar, S., Chaudhuri, A. K., & Dasgupta, S. (1996). Depositional environment of Vindhyan and other Purana basins: A reappraisal in the light of recent findings. *Memoir Geol. Soc. India, 36*, 101–126.

Chandra, D. (1992). *Jharia Coalfield*. Bangalore: Geological Society of India. 149 p.

Chandra, D., Singh, R. M., & Singh, M. P. (2000). *Text Book of Coal (Indian Context)*. Varanasi: Tata Book Agency. 402 pp.

Chatterjee, S. (1987). A new theropod dinosaur from India, with remarks on the Gondwana-Laurasia connection in the Late Triassic. In G. D. McKenzie (Ed.), *Gondwana Six: Stratigraphy, Sedimentology and Palaeontology, Amer* (pp. 183–189). Washington: Geophysical Union.

Chatterjee, S., & Hotton, N. (1986). The palaeoposition of India. *Journal of Southeast Asian Earth Science, 1*, 145–189.

Chatterjee, S., & Scotese, C. R. (1999). The breakup of Gondwana and evolution of biogeography of the Indian plate. *Proceedings of the National Academy of Sciences, 65A*, 397–425.

Das, S. N., & Sen, D. P. (1980). Depositional history of Permo-Carboniferous tillites and associated sediments in W. Bokaro Gondwana basin, Bihar. *Journal of Geological Society of India, 21*, 30–38.

Dasgupta, P. (2002). Architecture and facies pattern of a sublacustrine fan. *Jharia basin, India, Sedimentary Geology, 148*, 373–387.

Datta, D. R., & Ghosh, S. C. (1997). A new find of estherid from Singrauli Coalfield of South Rewa Gondwana Basin and its bearing on Gondwana stratigraphy. *Special Publication of Geological Survey of India, 54*, 233–246.

Dickins, J. M., Shah, S. C. (1979). Correlation of the Permian marine sequences of India and Western Austrlia. In B. Laskar & C. S. Raja Rao (Eds.), *Proceedings of Fourth Interne National Gondwana Symposium* (Vol. 11, pp. 384–408). Delhi: Hindustan Publishing Corporation.

Dutt, A. B., & Mukhopadhyay, S. K. (1997). Research advances in knowledge of near-shore signatures within fluvial Lower Gondwana (Early Permian) sequences in parts of Satpura Basin, Central India. *Special Publication of Geological Survey of India, 54*, 69–86.

Ghosh, S. K., Chakraborty, C., & Chakraborty, T. (2004). Combined tide and wave influence on sedimentation of Lower Gondwana coal measures of central India: Barakar Formation (Permian), Satpura Basin. *Journal of the Geological Society, 161*, 117–131.

Gupta, A. (1999). Early Permian palaeoenvironment in Damodar valley coalfields, India: an overview. *Gondwana Research, 2*, 149–165.

Jain, S. L. (1974). Jurassic pterosaur from India. *Journal of Geological Society of India, 15*, 330–335.

Jain, S. L. (1996). Aspects of vertebrate fossils from Pranhita-Godavari Valley, with emphasis on dinosaur discoveries. *Journal of the Palaeontological Society of India, 41*, 1–16.

Jain, S. L., Kutty, T. S., Roychowdhury, T., & Chatterjee, S. (1975). The sauropod dinosaur from the Lower Jurassic Kota Formation of India. *Proceedings of the Royal Society of London, A188*, 221–228.

Jain, S. L., Robinson, P. L., & Roychowdhury, T. L. (1964). A new vertebrate fauna from the Triassic of the Deccan, India. *Quarterly Journal of the Geological Society, 120*, 115–124.

Jain, S. L., Robinson, P. L., Roychowdhury, T. K., & Chatterjee, S. (1974). The sauropod dinosaur from the Lower Jurassic Kota Formation of India. *Transactions of the Royal Society of London, A188*, 221–228.

Khan, A. A., Sattar, G. S., & Rahman, T. (1994). *Tectogenesis of the Gondwana Rifted Basins of Bangladesh in the So-called Garo-Rajmahal Gap and Their Pre-drift Gegional Tectonic Correlation* (pp. 647–655). Oxford-IBH, New Delhi: Proc. Ninth International Gondwana Symposium.

Kummel, B. (1961). *History of the Earth: An introduction to historical geology* (p. 610). Delhi: Eurasia Publishing House.

Lakshminarayana, G. (2002). Evolution in basin-fill style during the Mesozoic Gondwana continental breakup in the Godavari triple junction, southeastern India. *Gondwana Research, 5*, 227–244.

Malik, P. K., Chakraborty, C., Ghosh, P., & Rudra, D. (2000). Meso- and macroscale architecture of a Triassic fluvial succession: Denwa Formation, Satpura Gondwana Basin, M.P. *Journal of Geological Society of India, 56*, 489–504.

Mathur, U. B., & Pant, S. C. (1986). Sauropod dinosaur from Lameta Group (Upper Cretaceous–Paleocene) of Kheda District, Gujarat. *Journal of Palaeontological Society of India, 31*, 22–25.

Misra, J. S., Srivastava, B. P., & Jain, S. K. (1961). Discovery of marine Permo-Carboniferous in western Rajasthan. *Current Science, 30*, 262–263.

Mukherjee, D., & Ghose, N. C. (1999). Damodar graben: A case of contrasting magmatism in the eastern Indian shield margin. In A. K. Sinha (Ed.), *Basement Tectonics* (pp. 179–202). Amsterdam: Kluwer Academic Publishers.

Mukherjee, D., & Ray, S. (2012). Taphonomy of an Upper Triassic vertebrate bone bed : A new rhynochosarus (*Reptilia Archaosauromorph*) accumulation from India. *Palaeogeography, Palaeoclimatology, Palaeoecology, 333–334*, 75–91.

Mukhopadhyay, A., Adhikari, S., & Roy, S. P. et al. (1997). Eustacy, climate, tectonics, sedimentary environment and the formation of Permian Coal Measures in the Sohagpur Coalfield, Madhya Pradesh. *Special Publication of Geological Survey of India*, *54*, 305–320.

Mukhopadhyay, G., & Bhattacharya, H. N. (1994). Facies analysis of Talcher sediments (Permo–Carboniferous), Dudhi Nala, Bihar—a glaciomarine model. In *Proceedings of Ninth International Gondwana Symposium* (pp. 737–755). New Delhi: Oxford-IBH.

Nehaluddin, Md. (1994). *Structure and Sedimentation in Gondwana Basins in Bangladesh* (pp. 805–826). Oxford-IBH, New Delhi: Proc. Ninth Intern. Gondwana Symposium.

Pal, A. K., Chaudhuri, P. N., Bose, S., & Ghosh, R. N. (1992). A Middle Triassic age for the Kamthi (Hingir) Formation of the Lower Gondwana Ib-Hingir basin, Odisha: New palaeobotanical evidence. *Newsletters on Stratigraphy, 27*, 33–39.

Paul, D. K. (1993). Mid-Cretaceous basalt and lamprophyre magmatism in eastern India: Petrogenetic perspectives. *Proceedings of the National Academy of Sciences India, 63A*, 33–44.

Paul, D. K. (2005). Petrology and geochemistry of Salma dyke, Raniganj coalfield (Lower Gondwana) eastern India: Linkage with Rajmahal or Deccan volcanic activity. *Journal of Asian Earth Sciences, 25*, 903–913.

Peters, J., & Singh, S. K. (2001). Satpura basin—An example of pre-rift, syn-rift and post-rift-Gondwana sedimentation in India. *Journal of Geological Society of India, 57*, 309–320.

Prasad, K. N. (1994). *An Introduction to Earth Science*. New Delhi: Vikas Publishing House. 168 p.

Ramamohan Rao, T., Venkateswara Rao, Y., Prasad, G. J. S., & Thirumala Rao, P. (1994). Tectonics of Chintalapudi and adjoining subbasins of Gondwanas of Godavari Valley and the East Coast of India. In *Proceedings of Ninth International Gondwana Symposium* (pp. 155–781). New Delhi: Oxford-IBH.

Ranga Rao, A., Dhar, C. L., & Obergfell, F. A. (1977). *Badhaura Formation of Rajasthan—its stratigraphy and age* (pp. 481–490). Geological Survey of India, Kolkata: Proc. Fourth Intern. Gondwana Symposium.

Raval, U. (1993). Rift and basin tectonics of the Indian subcontinent within a possible rheological waveguide. In S. M. Casshyap, S. K. Tandon, & C. C. Pant (Eds.), *Rift Basins And Aulacogens* (pp. 47–72). Nainital: Gyanodaya Prakashan.

Raval, U. (1995). Geodynamics of the tectonomagmatic and geophysical signatures within mobile parts of the transect. *Memoirs-Geological Society of India, 31*, 37–61.

Raval, U., & Veeraswamy, K. (2003). India-Madagascar separation: Breakup along a pre-existing mobile belt and chipping of the craton. *Gondwana Research, 6*, 467–485.

Ray, S. (2000). Endothiodont dicynodonts from the Late Permian Kundaram Formation, India. *Palaeontology, 43*, 375–404.

Ray, S., & Bandyopadhyay, S. (2003). Late Permian vertebrate community of the Pranhita-Godavari Valley, India. *Journal of Asian Earth Sciences, 21*, 643–654.

Ray, S., & Chakraborty, T. (2002). Lower Gondwana fluvial succession of the Pench-Kanhan Valley, India's stratigraphic architecture and depositional control. *Sedimentary Geology, 151*, 243–271.

Ray, A., & Jodha, B. S. (2001). Occurrence of oolites in the intertrappean beds of Rajmahal Formation – its environmental implications. *Coal and Lignite Basins of India* (pp. 247–254). Calcutta: Geological Survey of India.

Reimann, K.-U. (1993). *Geology of Bangladesh*. Berlin: Gebrüder Borntraeger. 160 p.

Sahni, A. (2003). Indian dinosaurs revisited. *Current Science, 85*, 904–910.

Sarkar, A. N. (1988). Tectonic evolution of the Chhotanagpur Plateau and the Gondwana basin in eastern India. *Memoirs Geological Survey of India, 8*, 127–146.

Sarkar, A., Yoshioka, H., Ebihara, M., & Naraoka, H. (2003). Geochemical and organic carbon isotope studies across the continental Permo-Triassic boundary of Raniganj basin, eastern India. *Palaeogeography, Palaeoclimatology, Palaeoecology, 191*, 1–14.

Sen, D. P. (1991). Sedimentation patterns of the Talchir Group in the Giridih Gondwana basin, India: A case of multiple glacial advance and retreat. *Palaeogeography, Palaeoclimatology, Palaeoecology, 86*, 339–352.

Sen, D. P., & Banerji, T. (1996). Talchir sedimentation in Jainti Gondwana basin: a case of glaciolacustrine low-slope prograding delta sedimentation. *Journal of Geological Society of India, 47*, 365–374.

Sen, D. P., & Sinha, T. C. (1985). Triassic aeolian sedimentation in the Auranga Gondwana basin, Bihar, India. *Sedimentary Geology, 43*, 277–300.

Sengupta, S. (2003). Gondwana sedimentation in Pranhita-Godavari Valley: a review. *Journal of Asian Earth Sciences, 21*, 633–642.

Sibal, V. K., Raju, S. V., Mondal, M. E. A., & Nauroz Ahmad, M. (2006). CO2 storage in coal mines. *Current Science*, *91*, 405–406.

Singh, T. (1993). Gondwana sediments (Permian) of Arunachal Himalaya: Stratigraphic status and depositional environment. *Gondwana Eight* (pp. 345–354). Rotterdam: Balkema.

Singh, M. P., Singh, P. K., & Singh, A. K. (2003). Petrography and depositional environments of the Permian coal deposits of Deogarh basin, Bihar. *Journal of Geological Society of India, 61*, 419–438.

Srivastava, V. K., Ahmad, A., & Casshyap, S. M. (1993). Control of basin-floor configuration in sedimentary evolution of Talcher sediments in parts of Son-Mahanadi Gondwana Basin belt, M.P. In S. M. Casshyap, S. K. Tandon, & C. C. Pant (Eds.), *Rifted Basin And Aulacogens* (pp. 39–49). Gyanodaya Prakashan: Nainital.

Srivastava, H. B., Srivastava, V., Srivastava, R. K., & Singh, C. K. (2011). Structural analyses of the crystalline rocks between Dirang and Tawang, West Kamang district, Arunachal Himalaya. *Journal of Geological Society of India, 78*, 45–56.

Tewari, R. C. (1998). Permian Gondwana sedimentation in Yellandu (Singareni) coalfield, Andhra Pradesh, India wih notes on regional palaeogeography and tectonic history. *Journal of Geological Society of India, 52*, 569–578.

Tewari, R. C., & Casshyap, S. M. (1982). Palaeoflow analysis of Late Palaeozoic Gondwana deposits of Giridih and adjoining basins and palaeogeographic implications. *Journal of Geological Society of India, 23*, 67–79.

Tiwari, R. C., Hota, R. N., & Maejima, W. (2012). Fluvial architecture of Early Permian Barakar rocks of Korba, Gondwana basin, eastern-central India. *Journal of Asian Earth Sciences, 52*, 43–52.

Veevers, J. J., & Tewari, R. C. (1995). *Gondwana Master Basin of Peninsular India*. Boulder: Geological Society of America. 72 p.

Venkatachala, B. S. (1977). Fossil floral assemblage in the east coast Gondwana—Critical review. *Journal of Geological Society of India, 18*, 378–379.

Venkatachala, B. S., & Tiwari, R. S. (1987). Lower Gondwana marine incursion: Periods and pathways. *The Palaeobotanist, 36*, 24–29.

Wicander, R., & Monroe, J. S. (2000). *Historical geology: Evolution of earth and life through time* (4th ed., p. 427 p). Thompson, USA: Books/Cole.

Yadagiri, P. (1984). New symmetrodonts from Kota Formation (Early Jurassic). *Journal of Geological Society of India, 25*, 514–521.

Chapter 14
Cretaceous Volcanism

14.1 Cretaceous Scenario

The beginning and the end of the Cretaceous period in India witnessed voluminous outpouring of lavas and stupendous volcanic explosions. In the Early Lower Cretaceous (114–118 Ma), nearly 20,000 km^2 area of eastern India embracing the Rajmahal Hills in Jharkhand and the Sylhet region in Meghalaya was affected by volcanism. Towards the close of the Cretaceous (61–69 Ma) more than 500,000 km^2 land in western and central India was inundated by extensive floods of lavas. The eastern theatre of volcanism is known as the *Rajmahal Volcanic Province* and the western domain as the *Deccan Volcanic Province* (Fig. 14.1). The Deccan Volcanism was preceded by eruption of lavas 91–95 Ma ago in offshore north-western Karnataka, giving rise to the *Saint Mary's Islands*. In the Rajmahal Volcanic Province, the lava pile was nearly 244 m thick, while the lava succession is more than 2500 m in the Nasik district in Maharashtra in the Deccan Volcanic Province.

The Deccan lavas are believed to have flowed 100–300 km from their sources along the Western Ghat and in the Narmada Valley before they froze to form stepped plateaus. Evidently, the lavas must have been very mobile and therefore spread far and wide, overcoming topographic impediments, filling depressions and valleys, damming rivers and streams and burying forests and grasslands. The result of the lava floods was the evolution of flat-topped plateaus, with step-like landform called the *Deccan Traps*. The Deccan Volcanic Province covers Maharashtra and adjoining regions in Gujarat, Madhya Pradesh, Telangana and Karnataka.

That was the time of the Gondwana era when rivers and streams were depositing their detrital loads in their channels, floodplains and lakes. The climate was semi-arid, but the forests and grasslands in the well-watered alluvial tracts abounded in small-sized mammals, reptiles (including dinosaurs) and many

K.S. Valdiya, *The Making of India*, Society of Earth Scientists Series,
DOI 10.1007/978-3-319-25029-8_14

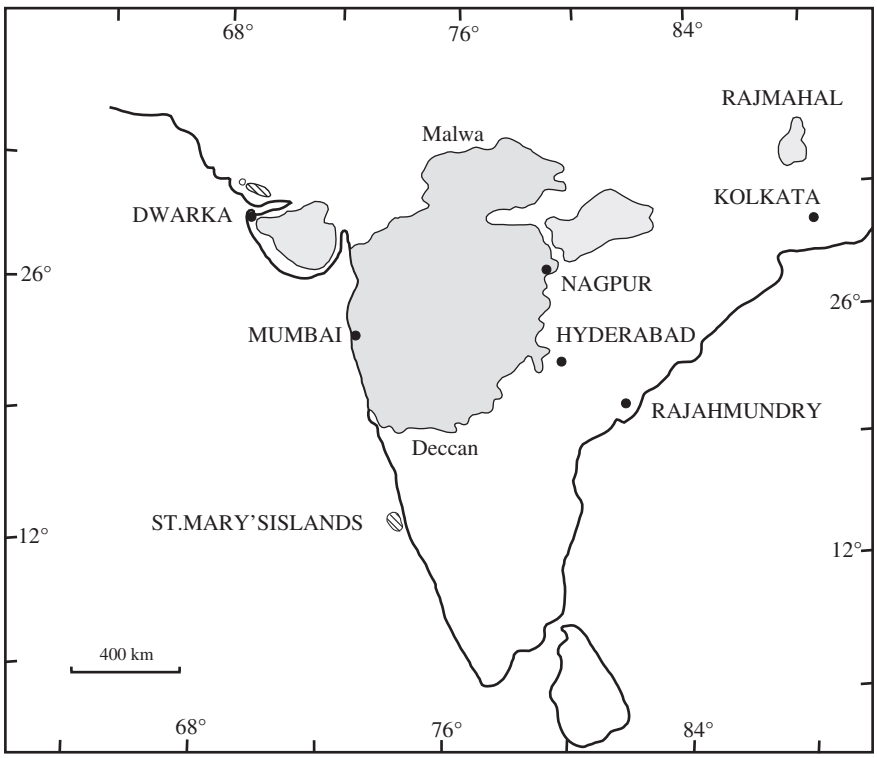

Fig. 14.1 Theatres of stupendous volcanic activities during the Cretaceous

aquatic animals. And conifers and palms grew prolifically. The fiery floods of lavas must have taken heavy toll of animals that could not run away from their preferred habitats. Blockages in rivers due to lava dams gave rise to multitudes of shallow lakes and swamps, which became sanctuaries for aquatic fauna and oasis for dinosaurs, mammals and plants. The lakes and swamps were eventually filled up with sediments. The sedimentary succession of these lakes and marshlands preserves the remains of plants and animals and records the geological history of the time.

The Cretaceous was a period of global warmth—the world being warmer than what it is at present. In the Lower Cretaceous when climate was quite warm, the concentration of greenhouse gas carbon dioxide in the atmosphere was of the order of 1500–3000 ppm (Andrews et al. 1995). However, in the Late Cretaceous (Maastrichtian), the CO_2 concentration dropped to less than 1300 ppm, implying cooling down of the atmosphere. The decline in temperature commenced in the Cenomanian–Turonian time.

Against this global scenario, the eruption of lavas in India released enormous volumes of gases, including CO_2 and SO_2. The atmosphere must have become thick with greenhouse gases. Its temperature rose appreciably enough to cause

changes in the flora and fauna. There was a dramatic biotic turnover at the end of the Cretaceous, culminating in the extinction of a large number of animal taxas at the Cretaceous–Tertiary Boundary time. This was an event that marks the end of the Mesozoic era and the beginning of the Cenozoic time.

14.2 Eastern Theatre of Volcanism—Rajmahal Volcanic Province

14.2.1 Areal Extent

In the Upper Lower Cretaceous time, a large part of eastern India encompassing parts of Jharkhand, northern Bengal, Bangladesh and southern Meghalaya was engulfed in volcanic activities. Nearly 244-m-thick lava pile makes up the *Rajmahal Hills*, the type area (Fig. 14.2). The lavas of the 608-m-high Rajmahal Hills dip 2°–5° eastwards and northwards, and form a steep scarp face in the west. The individual flows vary in thickness from less than 1 m to more than 70 m. Isolated outcrops of the lavas occur along western margin of the Bengal Basin and in southern part of the Meghalaya plateau and adjoining Bangladesh. To the north-east and east, basaltic rocks have been encountered in deep drill holes in the Bengal Basin.

14.2.2 Lithostratigraphy

The Rajmahal lavas comprise predominantly tholeiitic basalts, quartz-tholeiite, olivine-tholeiite and alkali basalt with minor amounts of trachyandesite, andesite, dacite, rhyolite and agglomerates with tuffs (Baksi 1995; Ghose et al. 1996; Ghose and Kent 2003). The lavas alternate with siltstone, claystone and shale. The sedimentary rocks contain rich assemblage of Lower Cretaceous plant fossils towards the middle and upper part of the succession. The floral assemblage includes *Cladophlebis indica, Dictyozamites indicus, Taeniopteris spatulata* and *Brachyphyllum rhombium*, which grew in humid semitropical climate. The subsurface occurrence of lavas at Punagarh in Bengal is interbedded with sediments containing spores of Berriasian–Hautervian age (Vijaya and Bhattacharji 2002).

14.2.3 Genesis

Petrochemical data obtained from studies of the Rajmahal Volcanics suggest two types of parental magmas, the tholeiites bearing strong similarity with the lavas of the Kerguelen Plateau in the Indian Ocean. The Rajmahal Volcanics (Fig. 14.3)

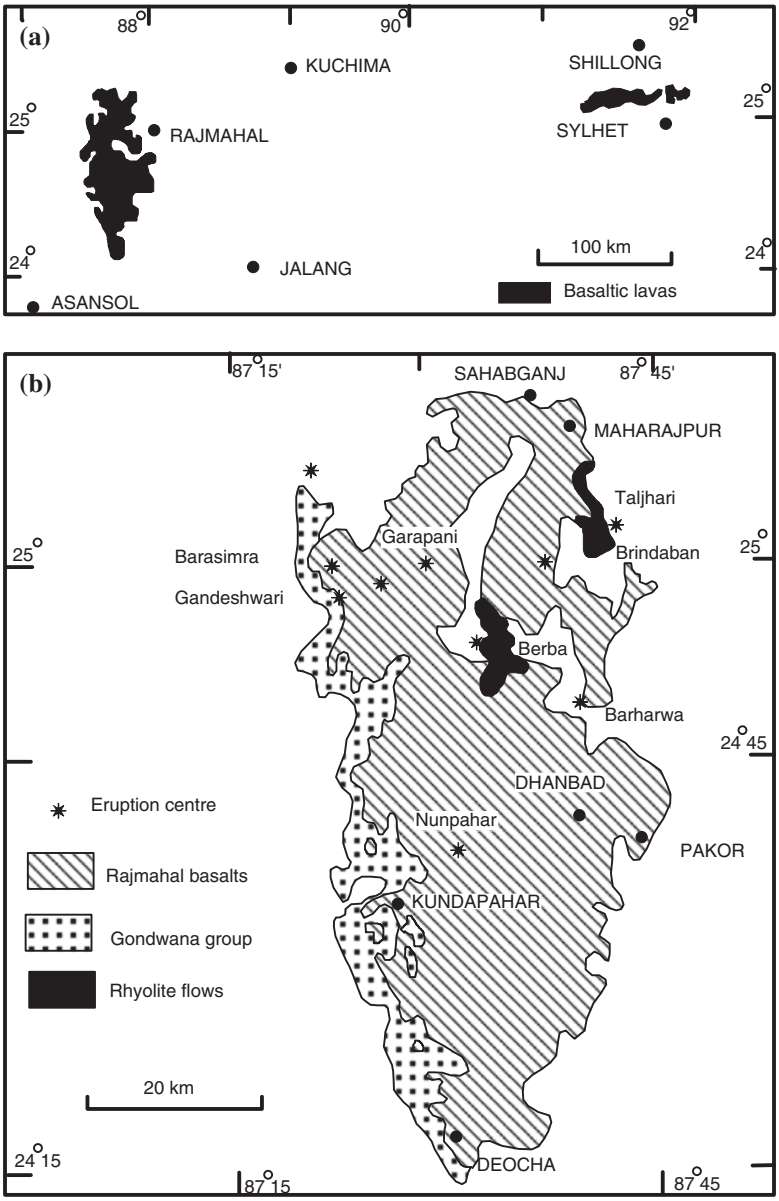

Fig. 14.2 Extent of the Rajmahal Volcanic Province in eastern India (after Ghose and Kent 2003)

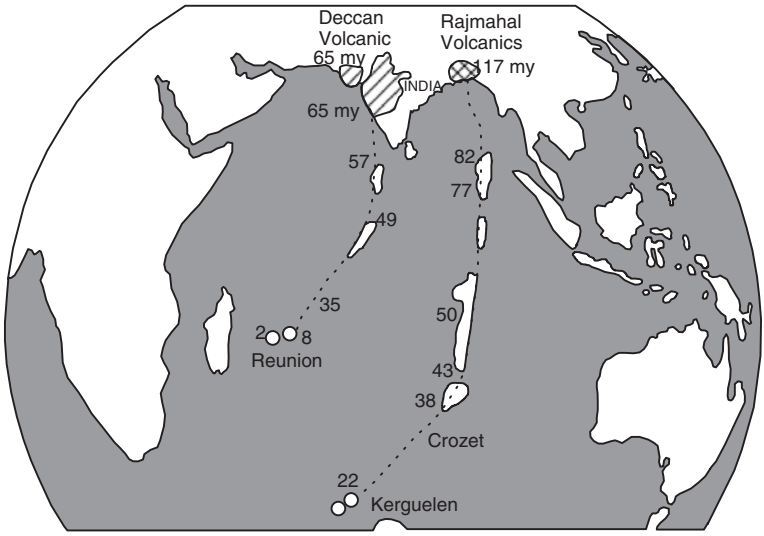

Fig. 14.3 As the Indian plate rode over the Kerguelen Hotspot in the Indian Ocean, molten material derived from the mantle poured out through the fissures developed in the lithospheric plate (after Ghose et al. 1996)

have understandably been related to the Kerguelen Hotspot (Baksi et al. 1987; Baksi 1995; Kent et al. 2002; Ghose and Ken 2003). The chemistry of kimberlite in the Rajmahal Volcanics tends to corroborate its Kerguelen connection (Kumar et al. 2003). It is also inferred that there was very little crustal contamination of the mantle-derived magma.

The main body of the Rajmahal lava was emplaced 114–118 million years ago (Baksi 1995). Palaeomagnetic study confirms the Early Cretaceous age of the Rajmahal (Poornachandra Rao et al. 1996). Associated with the basaltic lavas are tholeiitic and alkaline intrusives emplaced in the Gondwanic Damodar rift. Dykes occurring south-west of the Rajmahal Hills are 2–3 million years younger than the lavas. At the southern edge of the Meghalaya Plateau, the Sylhet Traps are characterized by rare earth and multiple trace-element geochemistry, demonstrating their similarity not only with the Rajmahal Traps in Jharkhand but also with the Burnberg basaltic lavas of the Kerguelen Plateau in the Indian Ocean (Ghatak and Basu 2011).

14.3 Volcanism in South-west India: St. Mary's Island

Four islands aligned in the NNW–SSE direction in offshore Udupi, north-western Karnataka (Figs. 14.1 and 14.4) are made up of rhyolite, rhyodacite and dacite. The lavas are characterized by spectacular columnar jointing and a

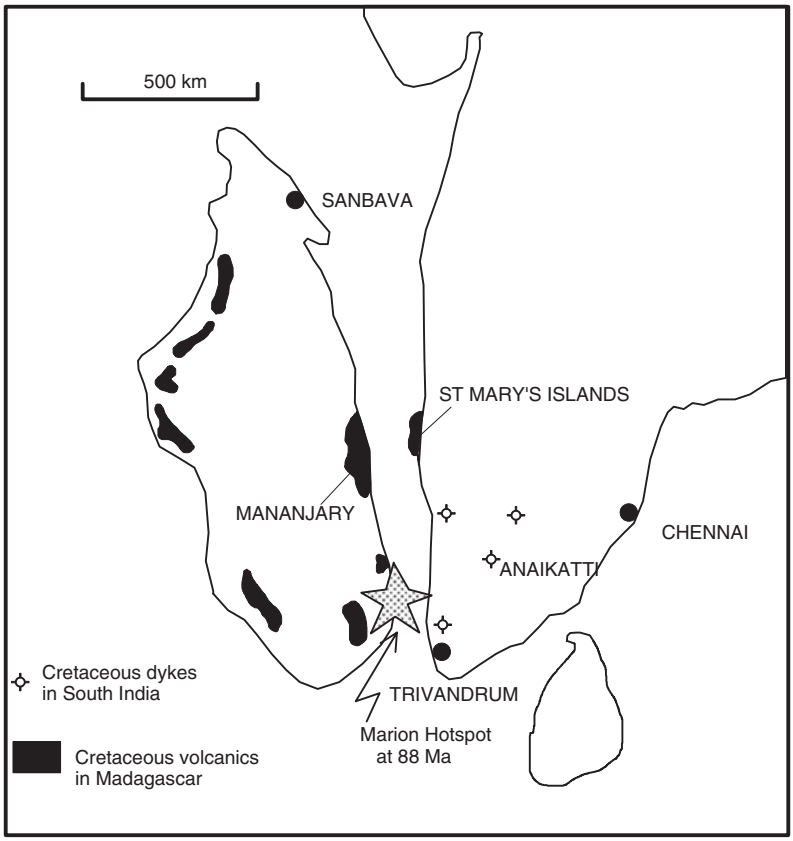

Fig. 14.4 Marion Hotspot-related volcanic activity and intrusives (after Kumar et al. 2001a, b)

chemistry quite similar to that of the Deccan rhyolite–dacite of the mainland (Subbarao et al. 1993). The chemistry indicates crystallization at shallow depth of parent magma for a short duration. The lavas are associated with granophyre intrusives. The acid volcanic rocks of the St. Mary's Islands have been identified as rhyolites characterized by phenocrysts of zoned plagioclase and locally hypersthenes or augite, their trace-element geochemistry indicating their continental setting (Bhushan et al. 2010).

The lavas give K–Ar date of 93.1 ± 2.4 Ma (Valsangkar et al. 1981), and Ar–Ar age of 85.6 ± 04 Ma (Pande et al. 2001). Significantly, the ENE–WSW trending dolerite dykes of inland north-western Karnataka are 90.0 ± 1.0 and 87.5 ± 0.9 million years old (Kumar et al. 2001a, b). Down south in Kerala, the leucogabbro and felsite dykes are nearly 85 million years in age (Radhakrishna et al. 1999). The volcanic episode and the emplacement of dykes are events related to the *Marion Hotspot*, over which India rode after its separation from Madagascar.

14.4 Deccan Volcanic Province

14.4.1 Extent and Topographic Peculiarity

One among the most remarkable volcanic provinces on earth, and one of the very prominent terranes of the Indian subcontinent, the *Deccan Volcanic Province* (DVP)—also known as the *Deccan Traps* by E. Vrendenburg, 1908—encompasses Maharashtra and adjoining regions in Gujarat, Madhya Pradesh, Andhra Pradesh and Karnataka. Outcrops of the DVP in distant Rajahmundry in Andhra Pradesh and in Kachchh and Saurashtra in Gujarat indicate that the extent of the DVP was much larger in the past. Offshore drilling west of the Konkan Coast revealed subsurface extension of the Deccan lavas in the Arabian Sea. In some places, the top of the lavas lie nearly 1500 m below the sea level, pointing to the foundering by faulting of the western part of the DVP.

14.4.2 Nature of Deccan Lavas

The bulk of the Deccan lavas are tholeiite basalts of simple type. In addition to basalts, the other rock types of the DVP are alkali basalts (basanite and picrite), nephelinites, carbonatites and rhyolite, occurring in minor amounts in the rifted western margin of the domain and in the Narmada Valley. In the Sahyadri Range, the lava build-up comprises dominant pahoehoe flow fields. These are aggregates of many flow lobes, each of which grew by thickening through injection of melt under solidified crust (Sen 2001). Thin irregular flows with ropy surfaces dipping in different directions and piled up into chaotic masses are quite common in western Maharashtra (Agashe and Gupte 1971). The Borghat section along the Pune–Mumbai tract provides a portrait (Fig. 14.5) of the variable morphology, structure and texture—thick extensive flows of compact basalt, tabular flows of amygdaloidal basalt, thin irregular flows of amygdaloidal basalts and thin irregular flows of vesicular basalt (Karmarkar 1978). It seems that in the early stage, viscous lavas erupted in small quantities, and later, there was fissure eruption in the Mumbai–Pune region. East of Pune near Daund, a hummocky flow with toes, lobes tumulus and lava tubes characterize the terminal part of the Thakurwadi Formation (Duraiswami et al. 2002).

In the western part of the Deccan Province lava tubes and channels within lava flows form an arterial system of sorts (Misra 2002). In the Khadri Dam, north-east of Nasik, resting over a pile of pahoehoe lava has been discovered a 120-m-wide lava channel lined with plagioclase-phyric basalt and containing angular fragments of basalts. Characterized by a pair of levees made up of breccias, the channel indicates that the lava discharge and lava flow velocity were high (Sen et al. 2012).

Between the lava flows occur red *boles*—a product of weathering during major hiatuses. The boles are indeed palaeosols formed subsequent to the lavas they cap

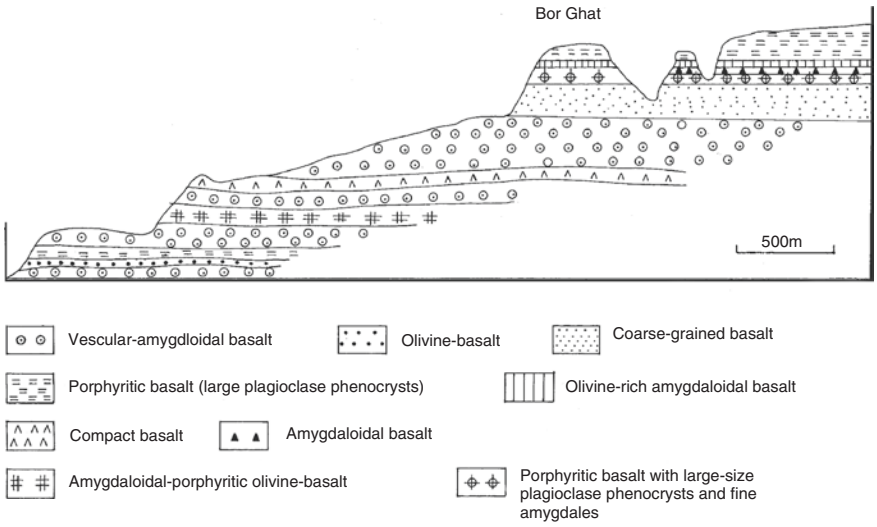

Fig. 14.5 Profiles of the Deccan Traps along the Borghat section in the Mumbai–Pune tract. (Modified after Karmarkar, 1978)

(Ghosh 1997). Others appear to be altered tuffaceous airfall deposits. They are rich in iron and aluminium and deficient in calcium and silica. The study of clays forming the red boles between lava flows that make the Mandla Plateau indicate that the montmorillonite component in the lower part was formed in of wet climate alternating with long dry season, and the kaonite clay in the upper part under tropical to subtropical climate during the main phase of deccan lava outpouring (Ahmad and Srivastava 2008).

The lateral extent of individual flows is of the order of 20–40 km to 80–120 km in Maharasthra (Beans et al. 1986) and 100–160 km in Madhya Pradesh (Choubey 1973).

14.4.3 Lithostratigraphy–Magnetostratigraphy

On the basis of detailed studies in the Mahabaleshwar–Nasik region in Maharashtra, involving interpretation of measured sections, palaeomagnetism, analyses of major and trace elements in rocks and determination of isotopic ratios of rare earths and strontium, a standard stratigraphy of the DVP has been established (Beans et al. 1986; Khadri et al. 1999a, b; Sethna 1999). The DVP lava succession is divisible into four subgroups comprising fifteen formations (Table 14.1; Fig. 14.7), each distinctive in its chemical types. The younger formations have wider spread—the *Poladpur Formation* lavas extending 800 km north-westwards to Gujarat and northwards to Madhya Pradesh, and the *Mahabaleshwar* lavas

reaching as far south as Belgaum in Karnataka (Figs. 14.7 and 14.8). It may be stressed that the lava flows are not continuous—there is pinching and swelling along their spread. There is also southward overstepping of successive units such as the *Bushe Formation* tapering out near Lonikhind, and the *Khandala Formation* resting directly under the Poladpur. The upper *Wai Subgroup* makes up the entire southern part of the DPV (Fig. 14.6), overstepping all older formation southwards, the Mahabaleshwar Formation overstepping the Precambrian rocks of Belgaum (Mitchell and Widdowson 1991), and so on.

The *Malwa Plateau* in Madhya Pradesh is made up of lava succession that represents petrochemically and palaeomagnetically the Bhimshankar, Khandala, Bushe formations (Table 14.1), the first 75-m sequence exhibiting normal polarity and the upper 400-m thickness in the Migrali area (district Dhar), showing reversed polarity (Khadri et al. 1999a, b; Khadri 2003). Between the Deccan and the Malwa, the Satpura succession of lavas exhibits contrasting magnetic polarity across the Narmada graben—550-m-thick succession of normal–reversed-normal polarity south of the Narmada and 666-m-thick pile of normal and reversed polarity in the north (Sreenivasa Rao et al. 1985).

The Nagpur–Bidar region in the eastern part of the DVP (Fig. 14.8) comprises Bhimshankar, Khandala, Poladpur and Ambenali formations. The younger formations overstep the older ones eastwards. In the eastern outskirts of Rajahmundri, a 30–60-m-thick succession of Deccan lavas is exposed over a stretch of 60 km across the Godavari River. While the lavas of the east bank show normal magnetic polarity and have a chemistry identical to that of the Mahabaleshwar Formation,

Table 14.1 Lithostratigraphic subdivision of the Deccan Volcanic Province. (Based on Khadri et al. 1999a and Sethna 1999)

Subgroup	Formation	Thickness (m)	MgO%	Polarity
Salsatte	Manori			Normal
	Madhutan			
	M umbai			
Wai	Desur		5–6	
	Panhala	>150	6.3 –6.8	
	Mahabaleshwar	280	5–6.7	
	Ambenali	500	5–7	
	Poladpur	370	6–9	
Lonavala	Bushe	325	5–12	Reverse
	Khandala	140	4.2 –9.4	
Ka lsubai	Bhimshankar	140	5–6.5	
	Thakurwadi	400	5–10	
	Neral	100	5–11	
	Igatpuri	150	5–10	
	Jawhar	>200	5–10	

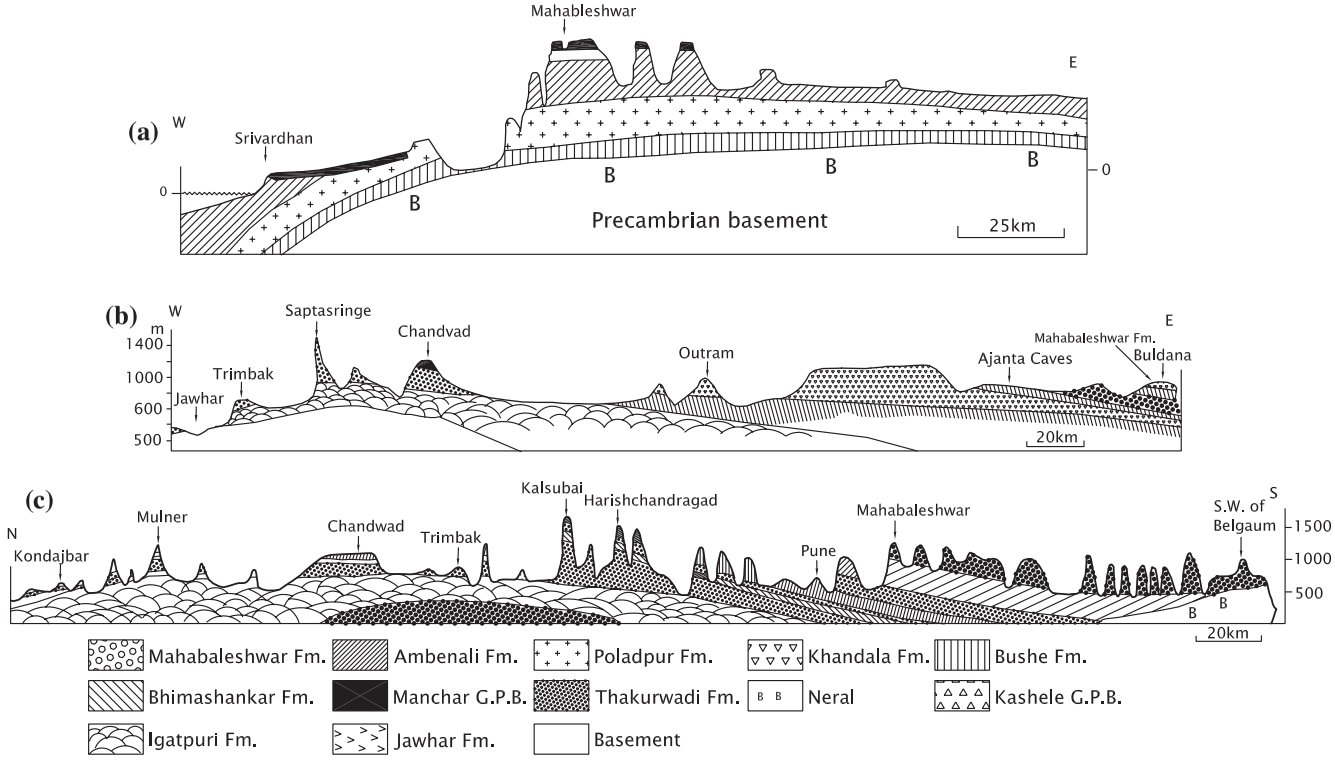

Fig. 14.6 Schematic north–south and east–west cross sections portray the structural architecture and lithostratigraphic succession of the Deccan Volcanic Province (DVP) (after Khadri et al. 1999a)

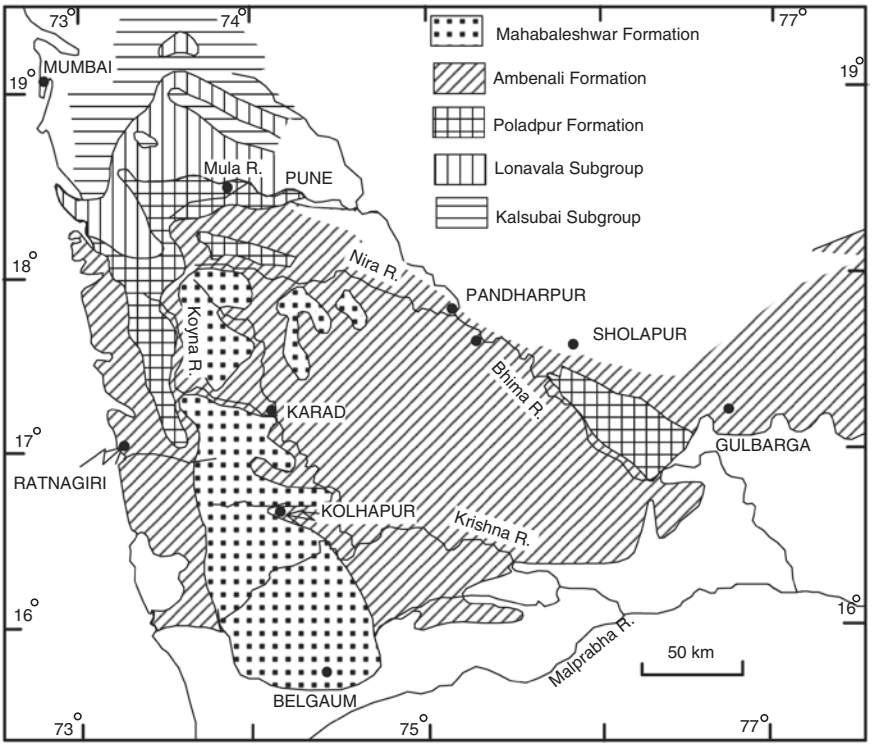

Fig. 14.7 Spread of different formations of the Deccan Volcanic Province in western and southern Maharashtra (after Mitchell and Cox 1988)

the west-bank lavas exhibit reversed polarity below the intertrappean beds and normal polarity above them, the chemistry and polarity being like those of the Ambenali Formation (Subbarao and Pathak 1993).

14.4.4 Structural Design

The lava flows forming the Deccan Plateau in the Sahyadri domain are not always flat-lying. The western limb of the structure is steeper than the eastern flank. The 10–20° westward dip is presumably due to foundering or faulting down of the continental margin (Fig. 14.6a). Over vast stretches in eastern and northern parts of the DVP, the lava flows are horizontal, forming flat tableland.

Along the Tapi and Narmada valleys, the Deccan succession is conspicuously affected by reactivation of the graben-defining faults. This has resulted in the formation of scarps that face the rivers. In Gujarat plain, the N–S faults of the

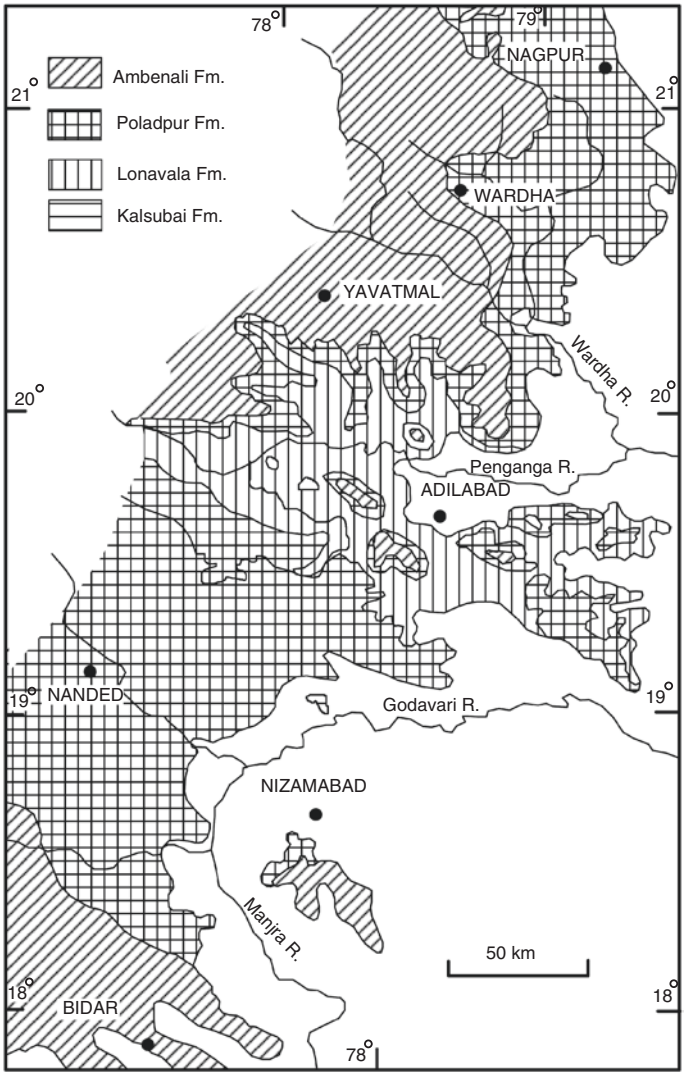

Fig. 14.8 Lithological units of the middle part of the Deccan succession occur in the eastern part of the Deccan Volcanic Province (after Bilgrami, 1999)

Sabarmati Graben have pushed down the lavas in the depression. In the Mumbai peninsular, the lava plate is broken by parallel faults. Southwards along the offshore Konkan Coast, the lavas have, likewise, sunk to great depths—in some places as much as 1500 m. They now lie underneath a thick pile of Tertiary and Quaternary sediments.

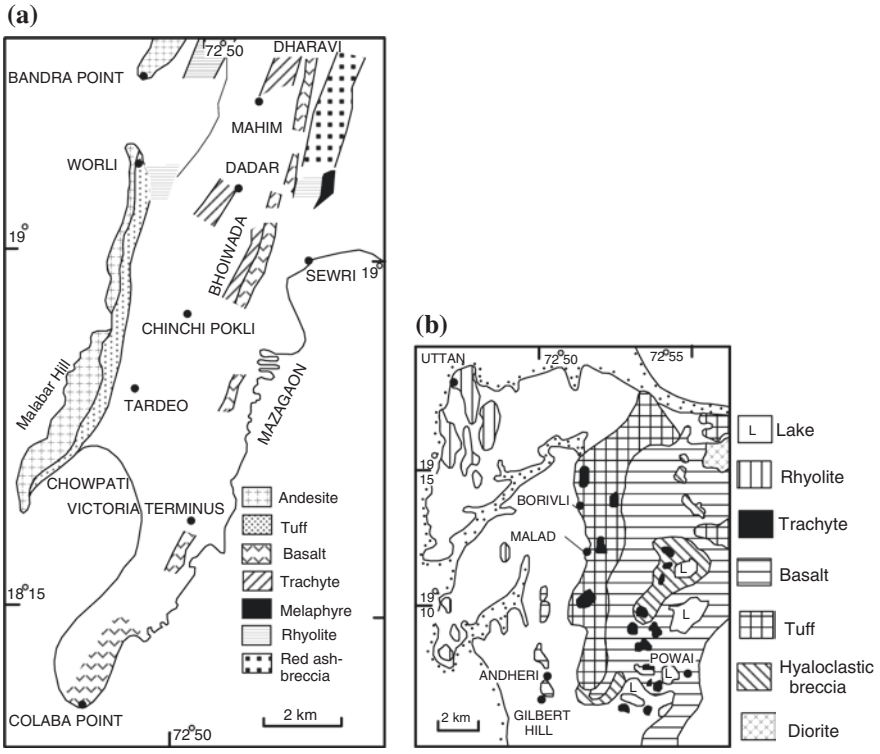

Fig. 14.9 Types of the Deccan lavas seen in the Mumbai area. **a** Based on Sukeshwala and Poldervaart 1958. **b** After Sheth et al. 2001a and Sethna 1999

14.4.5 Petrochemistry and Petrogenesis

The *Kalsubai* unit at its northern end comprises basalts with phenocrysts of olivine and locally clinopyroxene at the base, and their concentration varied as the flows spread over the land surface (Beans and Hooper 1988). The concentration of phenocrysts represents cumulates towards the base of individual flows. In some places, the phenocrysts are extraordinarily large in size (Karmarkar et al. 1972). The *Jawhar* and *Igatpuri* lavas are characterized by identical chemical and mineralogical compositions, constituting a continuous sequence with no real compositional gap, and have been derived from the same or similar source in the enriched mantle (Subbarao et al. 1988). The mineralogy and chemistry of the lavas of the Bhiwandi–Igatpuri and Poladpur–Mahabaleshwar sections show that the tholeiitic magma that gave rise to the lavas was a product of fractional differentiation of parental picrite basalt magma (Sethna and Sethna, 1990).

In the Mumbai area (Fig. 14.9), the volcanics are represented by an assemblage of basaltic lavas with subordinate intrusive and extrusive bodies of highly mafic

rocks—monchiquite, ankaramite and oceanite together with rhyolite and rhyodacite. The magma must have cooled rapidly, and the diffusion of volatiles gave rise the rhyodacite and rhyolite lavas (Sukeshwala and Poldervaart 1958; Sakeshwala and Sethna 1962). In the Bhoiwada sector, there are pillow lavas, showing albitization as a result of eruption of lavas in shallow marine water (Sukeshwala 1974). The spilitization of basaltic lavas is also attributed to reaction with a complex fluid having identical Sr isotopic composition (Subbarao 2000). The spilitic lavas with pillow structure are also associated with hyaloclasites and rhyolite lavas (Sethna 1999).

The 10–20° west-dipping basalts are interbedded with carbonaceous shale containing fossils of frogs and turtles.

In the Rajpipla Hills, the Narmada is flanked by lavas comprising alternation of potassic basalt and intruded by tholeiite dykes. The Nd–Sr isotopic compositions indicate that the two types of lavas were erupted concomitantly from the same parental magma but from different vents or fissures (Mahoney et al. 1982). In the Satpura domain, a thick succession of lavas exposed in the 1150-m-high Toranmal Hill includes porphyritic basalts with phenocrysts of olivine, augite and plagioclase. The lavas show large range of isotopic ratios of Nd, Sr and Pb (Chandrashekharam 2003).

In the 829-m-high *Pavagarh Hill* (Fig. 14.10) in the Vadodara district in Gujarat, an outlier of the DVP comprises a unique succession beginning with ankaramite at the base, followed upwards successively by mugearite, hypersthene-basalt, olivine-basalt, andesite with rhyolite and tuffs at the top (Chatterjee 1961). The bulk of the lava succession indicates differentiation of primary magma in the upper part of the crust long before its outpouring. Characterized by phenocrysts of three minerals, the Pavagarh basalts constitute one of the most primitive basalts of the Deccan Volcanic Province, derived as it was from the lherzolite zone of an undepleted mantle at a depth of nearly 85 km where the pressure must have been around 27 kbar (Furuyama et al. 2001). Atop the Pavagarh Hill occurs a group of 50- to 80-m wide sauser-shaped depressions having rims that gently slope away from the rims, identified as rootless cones that formed when the lava flow entered a surface water body in a wet ground (Sheth et al. 2004). The spectacular main hill of Pavagarh is surrounded by smaller hills, representing satellite vents. These are made up of rhyolite and volcanic breccia deposited with quaquaversal dips.

Characterized by uniformity of chemical composition, the picritic lavas of the Ahmadabad and Saurashtra regions are the products of differentiation of garnet-peridotite (eclogite) magma in the upper mantle. The magma of varied composition that was thus generated poured out earlier as picrite basalt with rhyolite and later as mildly alkaline lavas (West 1958). The differentiation of picritic parental material was the main process through which the entire basalt types evolved. In the north-western extremity of the DVP, six flows of typical tholeiite basalt are overlain by the seventh flow of olivine-tholeiite basalt belonging to a different batch of magma (De 1981). Interestingly, there is not only a close temporal association of the two types, but they also have a common source as indicated by their Sm–Nd isotopic composition (Pande et al. 1988). Occurrence of small nodular xenoliths of spinel-peridotite and dunite in the flat-lying alkali basalt

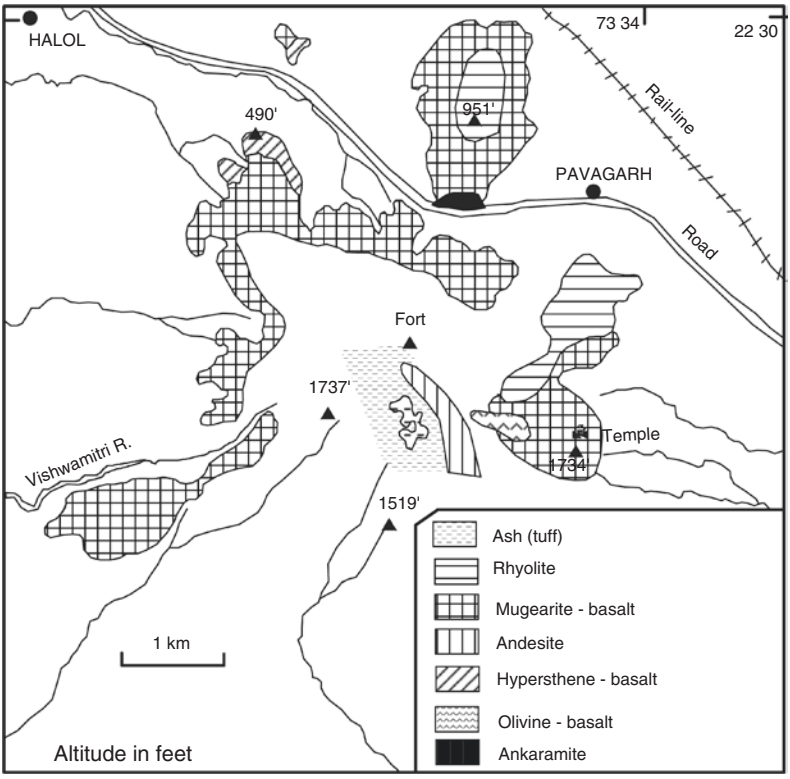

Fig. 14.10 Pavaragh Hill in the Vadodara district is an outlier of the Deccan Volcanic Province or probably an independent centre of volcanism. (Modified after Chatterjee 1961)

(melanephelinite and basanite) points to the derivation of the lavas from the upper mantle and that the parental magma underwent polybasic and polyphase fractionation together with mixing up of primitive and slightly evolved magmas and attendant contamination in the crustal level (Krishnamurthy et al. 1988, 1999).

In the northern margin of the DVP, the lavas of the *Malwa Plateau* consist of olivine-tholeiite, quartz-tholeiite and low-calcium tholeiite, evolved by open-system fractional crystallization of olivine tholeiitic melt in shallow-level magma chamber (Srivastava et al. 1988). Along the eastern margin of the Malwa plateau, there are low potassic basalts characterized by low absolute REE abundance, less fractionated chondrite normalized REE pattern and lower Ce/Yb ratios, implying genesis at later stage of magmatism and attendant metasomatism. In the Chhindwara–Jabalpur–Piparia region, the chemistry of the lavas indicates multiple sources (Shrivastava and Pattanayak 2002).

Far north-west at Tavidar in the desertic western Rajasthan, a group of lavas with subordinate pyroclastic rocks show highly divergent composition—from basaltic to rhyolitic. Their ^{40}Ar–^{39}Ar isochron and inverted isochron ages are 67–65 Ma (Sen et al. 2012). The Tavidar volcanic succession is thus

contemporaneous with the Mahabaleshwar and Panhale formations of the western Maharashtra. In the eastern extremity of the Deccan Volcanic Province, the Mandla Plateau comprises 900-m-thick pile of volcanics characterized by small-scale inflated pahoehoe lavas exhibiting elliptical to spheroidal features that vary in the size from 0.5 to 2 m (Kashyap et al. 2010).

In the Rajahmundry outcrops, the Deccan lavas are interbedded with fossiliferous sedimentary rocks. The lowermost lava flow is characterized by rootless cones, tumuli and dykelets, implying explosive volcanic activity in hydrous environment, followed by subaerial eruption as the middle and upper flows testify (Lakshminarayana et al. 2010).

This fact is not surprising. In the offshore submarine Krishna–Godavari Basin, the basaltic lavas are interbedded with sediments that contain Danian foraminifers, as ten deep wells have revealed (Keller et al. 2008).

14.4.6 Origin of Acid and Alkaline Rocks

The rhyolitic lava flows and intrusive trachytes in the Mumbai area show characteristics including (Sm, Nd and Pb) chemistry similar to the Deccan basalts and were generated due to decompression partial melting of the gabbroic layer below the crust (Lightfoot et al. 1987). During crustal thinning, along the West Coast there was development of a crustal monocline and sagging giving rise to the Panvel Flexure (Auden 1949). The consequent rise of the still-hot underplating gabbro within the crust would have given rise to about 10 % decompression partial melt of trachytic composition. This, in turn, would have generated rhyolitic differentiates during its rise within the crust (Sethna 2003). A number of rhyolitic lava flows, such as those in the north-western part of Salsette Island, together with intrusive trachytes (e.g. Manori–Gorai areas) that lie directly over this upwarp of the underplating basaltic layer (Negi et al. 1992). The rise of the asthenosphere could have been responsible also for minor quantities of decompression melting to form alkaline basic magmas, such as essexite (Sethna 2003) and their differentiated variants which include nepheline syenite of Girnar (Bose 1973). The Chogat–Chamardi hills in western Saurashtra are made up of plutons of microgranite, granophyres and gabbro, as well as plugs of rhyolite and dykes of basaltic and andesitic rocks (Seth et al. 2011).

14.5 Geodynamics of Deccan Volcanism

Palaeomagnetic evidence adduced from Deccan Volcanics and intrusives suggest India drifting northwards from south of the equator. The alkaline olivine-basalt and olivine-nephelinite of Saurashtra show close compositional similarity with the rock types associated with the *Reunion Hotspot* (Fig. 14.3), that is the mantle

plume in the Indian Ocean (De 1981). As the northward moving India rode over the hotspot, lavas came out along its western margin (Cox 1989).

The passage of the lithosphere over the mantle plume or the magmatic underplating along the N–S geofracture caused doming up of the western part of the Indian landmass, and resultant thinning, stretching and rifting of the crust. There was decompression melting, leading to eruption of a large volume of lavas from the fissures developed. The volume of lavas is estimated to be of the order of 3 million km^3 (Sen 2001). Significantly, there is an unusual oval-shaped positive gravity anomaly over the Mumbai coastal zone, and the analysis indicates the presence of two subsurface structures at depths of 4.5 ± 0.5 km and 18 ± 2 km, corresponding to, respectively, the top of the crustal basalt layer and an upwarped Moho discontinuity (Negi et al. 1992).

14.6 Feeders of Deccan Lava Flows

There are meagre evidence of the passage of lava flows into dykes. In many places, dykes cut across the lava flows. The dyke swarms of the Konkan Coast and the Narmada–Tapi valleys (Fig. 14.11) are considered to have served as the feeders of the Deccan lava flows (Auden 1949). It was the rifting or the reactivation of faults of ancient rifts or crustal weak lines that was responsible for the emplacement of the dykes. Significantly, some of the lamprophyre dykes representing the waning phase of the Deccan volcanism in the coastal belt contain xenoliths of mafic and felsic granulites and ultrabasic pyroxenites, wehrlite and websterite (Dessai et al. 2004).

The average width of the Deccan dyke is 15 m. There are 7 dykes per kilometre along the Konkan Coast, and 20–35 dykes per kilometre in the Narmada–Tapi Belt (Deshmukh and Sehgal 1988) compared to 185–370 dykes per kilometre in the Hawaii Island. This fact implies that the emplacement took place from a shallow crustal magma chamber (Bhattacharji et al. 1996). The aggregate thickness of 71 dykes is 1470 m within a distance of 29 km in the Rajpipla Hills in the Tapi–Narmada domain. The dyke swarm that intrudes the Deccan lavas in the Nandurbar–Dhule belt in Maharashtra comprises as large as 79-km-long dykes, their individual thickness varying from 3 to 62 m (Ray et al. 2007). The source of the dykes is believed to be shallow magma chambers, some of which spreading laterally. The majority of the dykes have the same Sr isotopic composition and magnetic polarity as the associated lavas, but the dykes that intrude lava flows have different magnetic polarity (Subbarao et al. 1999). Among the intrusives younger than the Deccan lavas are radial dykes related to the Girnar complex in Saurashtra (Figs. 14.11a and 14.12). North of Amreli, the dykes are enriched in fresh olivine and are associated with dykes of ankaramite and stock-like bodies of essexite, while south of Amreli, the dykes penetrate southward-plunging anticline and are olivine-poor and associated with quartz-porphyry (Sethna et al. 2001). The *Girnar Complex* is a laccolith made up of olivine-gabbro along the periphery and

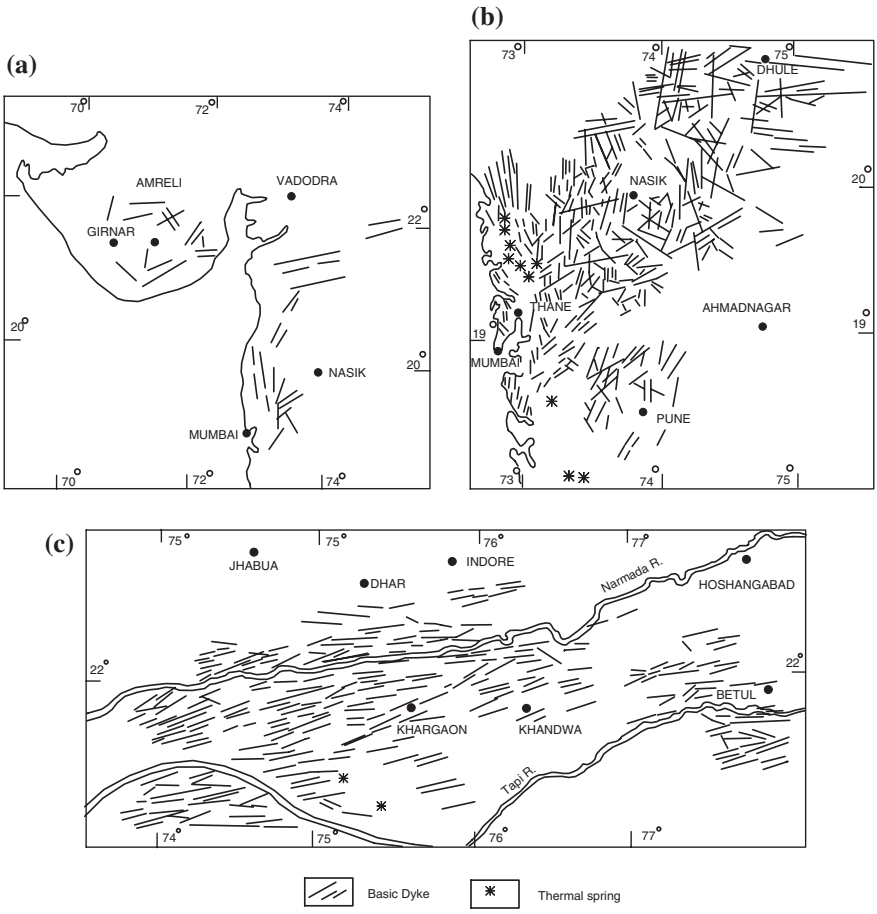

Fig. 14.11 **a** Dominant trends of dyke clusters and network (after Auden 1949). **b** N/NNW–S/SSE dyke swarms of the Konkan Coast and north-western Maharashtra. **c** E/ENE–W/WNW-oriented dyke swarms of the Tapi–Narmada valleys. (**b** and **c** modified after Deshmukh and Sehgal 1988)

diorite–monzonite in the core. The petrogenesis of the complex was first explained by K.K. Mathur, V.S. Dubey and N.L. Sharma in 1926. It is intimately associated with nepheline syenite and granophyre that form ring dykes in the domed up lava flows dipping in all directions (Sukeshwala 1982). Trace elements variations indicate that the rhyolite and trachyte dykes, around Rajule in southern Saurashtra, are associated and coeval with the Deccan volcanics. They contain two populations of zircon and monazite—one that crystallized from the felsic melt, and the other that contains inherited material of the crust that was heated to nearly 900 °C by the intruding Deccan magma (Chatterjee and Bhattacharji 2004).

About 200 km east of the eastern margin of the Deccan Volcanic Province (DVP), there are mafic dykes intruding the Mesoproterozoic Chhattisgarh

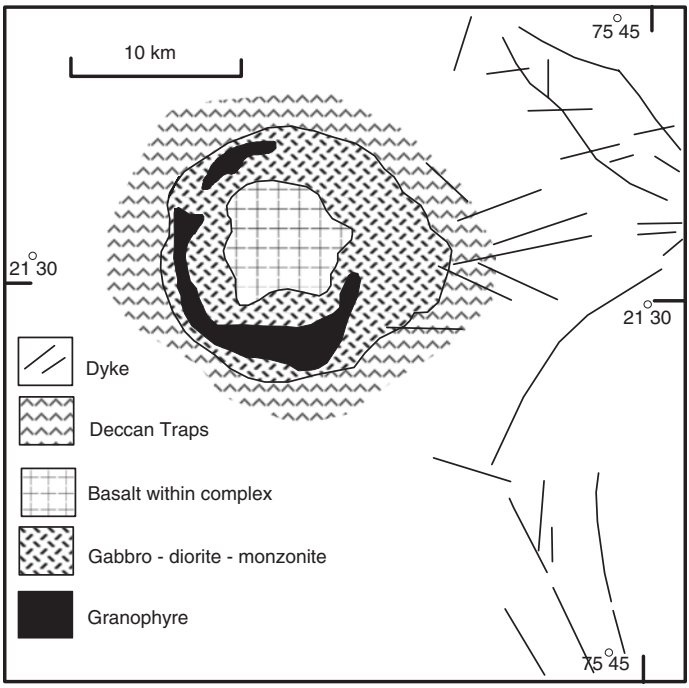

Fig. 14.12 Sketch map of the Girnar complex in the Deccan Volcanic Province, Saurashtra. (Based on Auden, 1949)

succession. These dykes give ^{40}Ar–^{39}Ar whole-rock ages of 63.7 ± 2.7 Ma and 66.6 ± 2.2 Ma—the same time range as of the Deccan lavas (Chalapathi Rao et al. 2010). The geochemical composition of these dykes is similar to those of the Ambeni and Poladpur formations of the main DVP. In the Gondwanic Pachmarhi and Rewa subbasins of the Satpura domain, the mafic dykes at the basin margin have Sr–Nd isotopic compositions similar to those of the Upper Cretaceous Rajmahal Volcanic Province in far east. It seems that the Deccan magma travelled subsurface over long distance—as far as 500 km—along the Narmada "lineament" and was emplaced along the intrabasinal faults in the Gondwana basins, including the Rewa subbasin (Lala et al. 2011).

14.7 Terminal Phase of Deccan Volcanism

The last phase of the Deccan Volcanism is represented by nepheline syenite, alkali trachyte and carbonatite. They occur as intrusive bodies in the form of dykes, sheets and plugs, cutting across the Deccan lavas of the main phase. This is discernible in the Denodhar Hill in Kachchh, at Junagarh, Osham, Chamardi,

Chogat and Bhavnagar in Saurashtra, and Phenaimata, Ambadongar, Netrang and Barwaha in the Narmada rift valley. In *Ambadongar Complex* (Fig. 14.13), nepheline syenite dykes form a ring of 1.6 km diameter around a plug of carbonatite. The plug penetrates the Deccan lavas which are overlain by the Bagh Beds of the Upper Cretaceous age (Sukeshwala and Udas 1963; Yellur 1968). After their intrusion, there was another phase of volcanic activity. The central depression of the ring complex is occupied by basalt that post-dates the carbonatite–nephelinite activity. Significantly, stratified tuffs with components of both carbonatite and nephelinite occur at Mongra, west of the ring complex (Viladkar et al. 2005).

A modelling of trace elements contents suggests that the carbonatites and coeval alkaline silicate rocks are the products of fractional crystallization of two separate parental magmas (Ray and Pande 1999; Ray et al. 2003). Carbon and oxygen isotope study of the Ambadongar complex indicates that magmatic differentiation was characterized by a distinctive isotope trend, having a moderate rise in ^{13}C couple with increase in ^{18}O, and the whole complex having deep-seated primordial carbon derived from the upper mantle (Viladkar and Schidlowski 2000). Both the carbonatite and its associate alkali rocks were derived from a common perental magma through liquid immiscibility as testified by abundance of rare elements (Ray et al. 2000). Judging from the low contents of Sr, Ba and ∑REE in the dolomitic and ankeritic carbonates at Newania, it has been postulated that a part of the carbonatite complex formed due to selective metasomatism of magnesiocarbonate that was affected by ferruginous solutions (Pandit and Golani 2001). The carbonatite of Ambadongar hosts a rich *deposit of fluorite* of economic importance.

Thirty kilometres west of Mount Abu, the *Mundwara Complex* comprises three laccolithic intrusives—Musala, Mer and Toa. These are made up of calcalkaline and subalkaline rocks including pyroxenite and felspathoidal syenites associated with radial and concentric dykes of olivine–dolerite, alkaline-dolerite, tinguaite and carbonatite. The complex is characterized by the presence of annular fractures. There is an arcuate shatter zone with breccia in the outer Mer pluton, indicating upwarping and later intrusion of carbonatite (Narayandas et al. 1982). The $^{40}Ar/^{39}Ar$ whole-rock date indicates that the igneous activity commenced around 70 Ma and the differentiation of the magma continued until about 64 Ma (Rathore et al. 1996). The Toa pluton is a layered suite, varying in composition from felspathic peridotite to gabbro and gabbroic anorthosite and characterized by olivine-bearing cumulophyric rocks formed as a result of rapid crystallization and settling of crystals (Subrahmanyam and Leelanandam 1991).

Recently discovered *ultrabasic diamondiferous kimberlite plugs* in central India give ^{40}Ar–^{39}Ar ages around 66 Ma, implying their emplacement almost at the same time as when the bulk of Deccan lavas was erupted (Lehmann et al. 2010). In the Narmada valley rift zone in the Chhota Udepur area, the E–W trending dykes of lamprophyres intruding the basement gneiss exhibit rare earth geochemistry that places the dykes in the spectrum of alkaline rocks of the Deccan Volcanic Province (Chalapathi Rao et al. 2012).

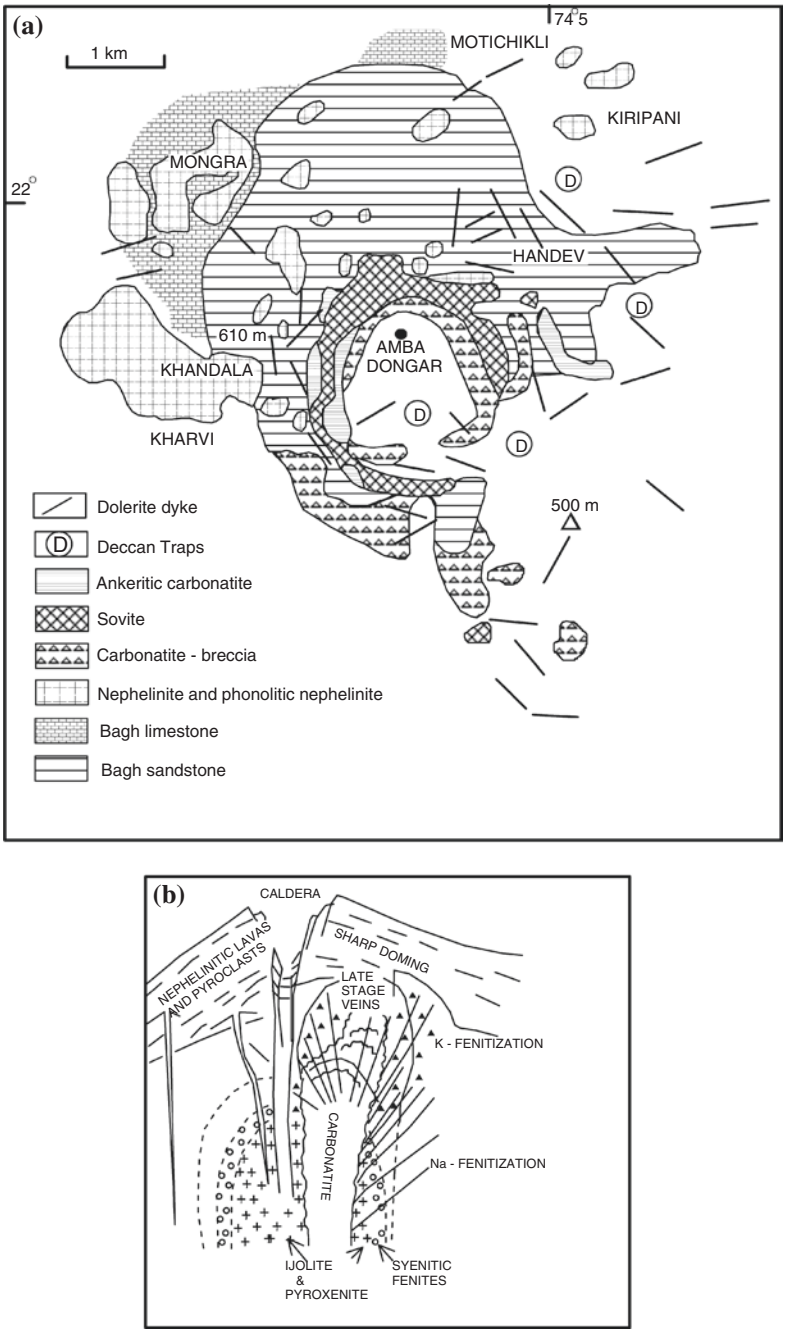

Fig. 14.13 At Ambadongar in the Narmada graben, a plug of carbonatite penetrates the Deccan lavas and the overlying Bagh Beds. Around the plug, there is a ring of nepheline syenite dykes. (Modified after Sukeshwala and Udas, 1963; Viladkar and Schidlowski, 2000). *Inset*: Mode of emplacement of the Ambadongar carbonatite. (Ray et al. 2000)

14.8 Temporal Span of Deccan Volcanism

On the basis of stratigraphic relation, West (1981) had concluded that the Deccan Volcanism was a short-term phenomenon. Nine basalt samples from the bottom to top of the 2500-m-thick succession, comprising Igatpuri to Mahabaleshwar formations in the Sahyadri, showed no difference in age from the stratigraphically oldest to the youngest lavas, implying very rapid emplacement over perhaps a million years at 67.5 ± 0.3 Ma (Duncan and Pyle 1988). A suite of basaltic rocks shows Re–Os isochron age of 65.6 ± 0.3 Ma (Allegre et al. 1999).

However, the Deccan lava succession embraces three magnetic chrons—30 N, 29 R and 29 N that span the time from 73.8 million years to 60.6 million years (Courtillot et al. 1986). The 68.5 Ma age of the alkali basalt in central India, the 60.5 ± 1.2 ma age of the Gilbert Hill lava, the 60.4 ± 0.6 Ma of trachyte at Manori and 61.8 ± 0.6 Ma of basalt at Saki Naka in Mumbai (Lightfoot et al. 1987; Sheth et al. 2001b) show that the temporal span of the Deccan Volcanism was of the order of nearly 8 million years (Pande 2002; Chandrashekharam 2003).

The basalt flows at Anjar in Saurashtra overlying and underlying the lacustrine shale are remarkably enriched in iridium and iron (Bhandari et al. 1995) and belonging to chron 29 R (Shukla et al. 2001) are dated 65.2 ± 06 Ma and 64.9 ± 08 Ma by ^{40}Ar–^{39}Ar method (Venkatesan et al. 1996). The plagioclase separates of the Rajahmundri lavas in Andhra Pradesh give ^{40}Ar–^{39}Ar age of 64.7 ± 05, 64.5 ± 0.8 and 65.0 ± 0.1 Ma (Knight et al. 2003). The reversely magnetized tholeiitic lava flow of the Bhimashankar Formation has yielded $^{40}Ar/^{39}Ar$ age of 66.0 ± 0.9 Ma, implying that the basal part of the 1800- to 2000–m-thick lava succession of the Western Ghat was extruded very close to 67.4 Ma (Pande et al. 2004). Significantly, the dolerite dykes of West Coast have been dated 62 Ma (Kaneoka et al. 1996) and 62.8 ± 0.2 Ma (Widdowson et al. 2000). The terminal phase of the Deccan Volcanism is represented by the alkali rocks and carbonatites, as already stated. The $^{40}Ar/^{39}Ar$ ages of these rocks in Kachchh are 64 and 67 Ma, respectively (compared to 66.8 ± 0.3 Ma of the tholeiite basalt of the same area), define the time boundary (Pande et al. 1988). The Ambadongar carbonatite is dated 65.2 ± 0.7 Ma by $^{40}Ar/^{39}Ar$ method and the basalt which the plug penetrates is 68.5 ± 0.9 Ma in age (Ray et al. 2003).

In the Mandla Plateau, in the eastern part of the DVP, the 900-m-thick succession of 21 lava beds have red horizons of boles made up a of variety of clays. On calculating the aggregate time for the formation of clays due to the weathering, it turns out that it is 7 million years, carrying the implication that the volcanic activity started much earlier than the Late Maastrichtian, that is 65 Ma (Shrivastava et al. 2012). In other words, the volcanism was not a short-duration event, but quite longer as Pande (2002) demonstrated.

In the Rajahmundry Deccan Volcanic sequence, the sedimentary rocks containing marine planktic foraminifers indicate Danian (basal Palaeocene) age, and the immediately underlying lava beds show magnetic polarity Chron 20 n, that is the Cretaceous–Tertiary Boundary (Keller et al. 2008). Far to the north-west in the Jhilmili area in district Chhindwara, the Deccan lavas are interbedded with sedimentary rocks containing *marine* planktic foraminifers of Danian (basal Palaeocene) age indicating that a marine seaway had extended as far inland as the Chhindwara region during the Cretaceous–Tertiary Boundary time (Keller et al. 2009).

To the south-east in the offshore submarine Krishna–Godavari Basin, ten deep wells dug for exploration of oil and gas revealed that interbedded with sedimentary rocks bearing Danian planktic foraminifers, there are lava flows. Importantly, nearly 50 % foraminifers became extinct at or near the Cretaceous–Tertiary Boundary, implying that volcanic activity related to Deccan Volcanic Province (Fig. 14.14) must have caused the extinction (Keller et al. 2008, 2012).

It seems that the Deccan eruption commenced some 69 million years ago and lasted until about 61 million years, the bulk of the lavas having erupted around 65.5 million years ago. The terminal phase of the Deccan Volcanism, marked by emplacement of carbonatites, coincides with the Cretaceous–Tertiary boundary.

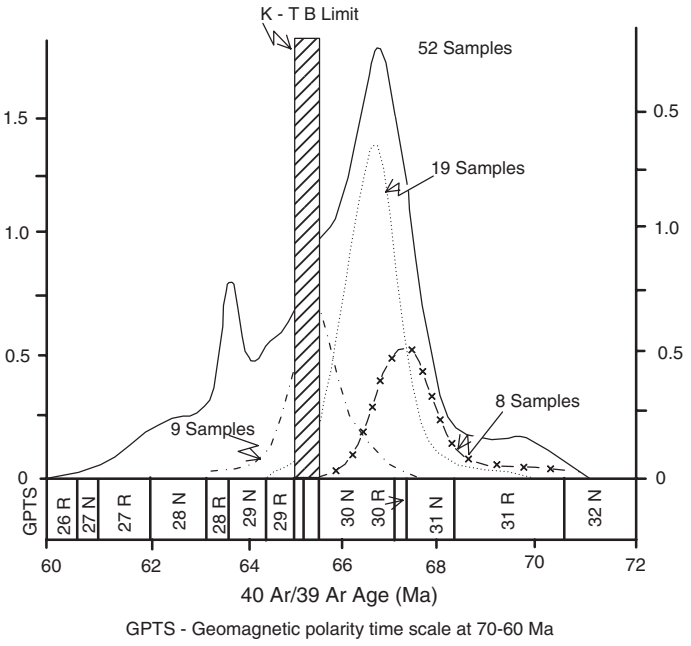

Fig. 14.14 Radiometric dates of the Deccan lavas and intrusives. The summary of the plots of dates from various rocks and places was prepared by S. Chatterjee and Rudra in 1992 (after Sen 2001)

14.9 Testimony of Lacustrine Fossils

The lava flows of the Deccan succession are interbedded with sedimentary rocks including limestones (Bhattacharya et al. 1997) formed in lakes (Figs. 14.15 and 14.16). These lakes had originated due to damming up of rivers and streams by lava flows. The lacustrine sediments underlying the lava succession are known as the *Infratrappean Beds*, and (in some places) those that are interbedded with the lava flows are called the *Intertrappean Beds*. The Intertrappean and Infratrappean sediments are indeed facies variants of one and the same horizon (Fig. 14.17). At Bamansar near Wankaner, the two are seen interfingering with each other (Chiplonkar 1987). Palaeontologically the two are indistinguishable, characterized as they are by remarkably similar floral and faunal remains (Sahni and Bajpai 1988; Prasad and Khajuria 1995).

Fossil assemblages in the Intertrappean Beds of the upper part of the Deccan succession provide evidence on the upper age of volcanism. It is remarkable that, as already stated, there is strong similarity of the biota of Infratrappean and Intertrappean beds (Fig. 14.17). It seems that there was no change in the life before and during the later phase of Deccan Volcanism.

The palynomorphs of the intertrappean *Lameta Formation* at Jabalpur, *Aquilapollenites indicus* and *Proxapertites crassimurus,* indicate Maastrichtian age (Dogra et al. 1994). The Naskel intertrappean beds near Hyderabad have also yielded Maastrichtian polymorphs (Venkatachala 1977). The associated *Deccanolestes hislopi* was a Late Cretaceous placental mammal (Prasad 1989; Prasad and Khajuria 1995, 1996). Along the eastern periphery of the DVP in the Nand, Dongargaon, Asifabad, Naskel, Morepalli and Timsapalli areas (Fig. 14.15), both the infratrappean and intertrappean beds contain rich assemblages of large vertebrate and microvertebrate animals of Upper Cretaceous age (Rana 1990; Mohabey et al. 1993; Mohabey and Udhoji 2000).

In the Krishna–Godavari basin in the Pangadi area (West Godavari district), the intertrappean sediments contain estuarine–marine foraminifers that have been identified as Early Eocene forms (Bhalla 1968). The planktonic foraminifers, nannoplanktons and dinoflagellate cysts from marine sediments (sandwiched between basalts) suggest that the volcanism started in the latest Maastrichtian at 66.6–67 Ma and the youngest lava flow was erupted just before the 64.3-million-year-old nannoplankton-bearing sediment was deposited (Raju et al. 1995).

The intertrappean beds at Anjar in Kachchh (Fig. 14.15) have yielded profuse therapod dinosaur eggshells associated with the Late Cretaceous ostracodes (Bajpai et al. 1990; Bajpai and Prasad 2000) and with the Maastrichtian microflora including *Aquilopollenites indicus* (Dogra et al. 2004). The chocolate-coloured limonitic shale intercalated with marl and cherty limestone of the Anjar intertrappean horizon is characterized by anomalously high 1300–700 pg/g value of iridium, siderophiles (Bhandari et al. 1993), fullerene (Parthasarthy et al. 2000), and high-temperature cristobalite silica of volcanic origin (Sant et al. 2003), implying that the horizon coincides with the Cretaceous–Tertiary Boundary.

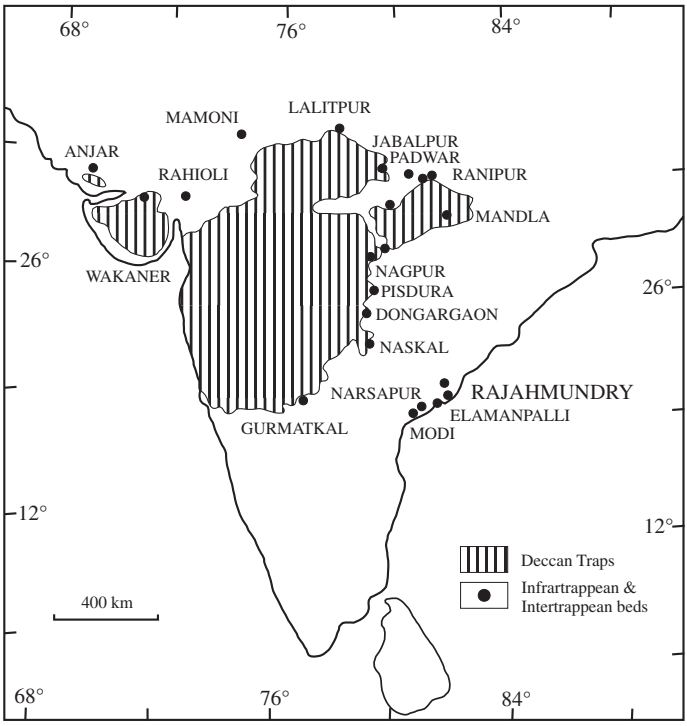

Fig. 14.15 Major Infratrappean and Intertrappean fossiliferous localities around the periphery of the Deccan Volcanic Province. These localities are the sites of dinosaur fossil (after Prasad and Khajuria 1995)

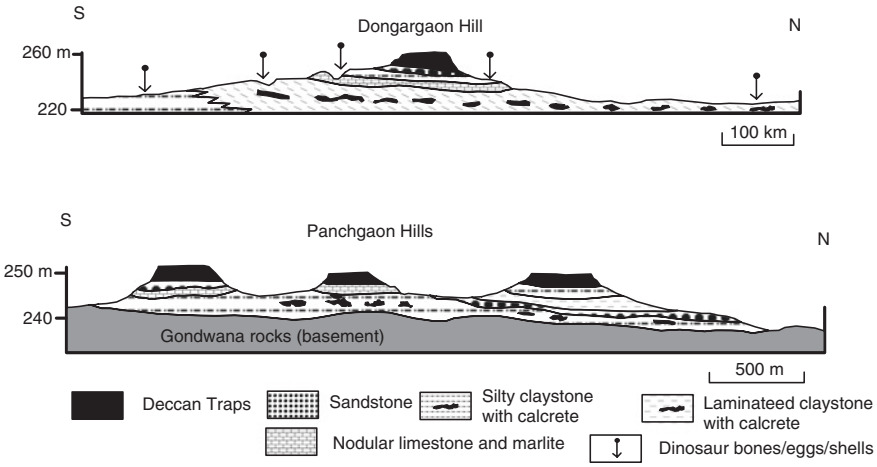

Fig. 14.16 Cross sections of the Lameta Formation in the Dongargaon and Pachgaon areas (after Mohabey, 1996)

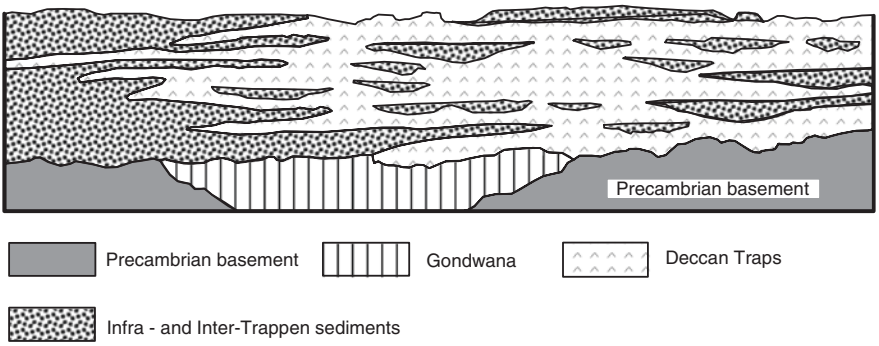

Fig. 14.17 Pattern of sediment deposition of the Infratrappean and Intertrappean Beds in relation to the Deccan lavas (after Sahni et al. 1994)

Using ^{40}Kr–^{40}Ar Cassignol–Gillot technique the dating of the 3500-m-thick Deccan Trap succession demonstrated that the mean age of the Jawhar Formation at the bottom is 64.8 ± 0.6 Ma, and of the Ambeni and Mahabaleshwar formations at the top is 64.5 ± 0.6 Ma, implying very short duration of eruption *in the main theatre of volcanism* (Chenet et al. 2007). However, this finding is at variance from the conclusion derived from other evidence, collected from many places.

14.10 Environment and Life During the Deccan Time

14.10.1 Sedimentation in River Impoundments

Remains of animals and plants entombed in the Intertrappean and Infratrappean beds tell a great deal about the climate and the ecological conditions in lakes, swamps and floodplains of the time.

As the lava floods froze, their frontal lobes created blockages in streams and rivers. These lakes became sites of sedimentation. The sedimentary succession comprises not only the regolith material but also resulting lacustrine and paludal claystone, marlite and limestone. The resulting intertrappean beds, as already stated, are collectively known as the *Lameta Formation*—a name given by H.D. Medlicott in 1860. They occur in a large number of places around the periphery of the DVP (Fig. 4.15). In the type locality Lametaghat on the Narmada River and at Jabalpur in Madhya Pradesh, the Lameta Formation comprises calcareous sandstone, calcified sandstone, mottled nodular limestone, and sandstone characterized by multiple horizon of calcrete (Fig. 14.18). The basal *Green Sandstone* represents a deposit of ephemeral braided stream (Tandon et al. 1995; Tandon 2002), containing material derived from regolith of the basaltic lavas and the clays characterized by dominant smectic, chlorite, a little kaolinite, illite and volcanic calcedonite—earlier described as glauconite (Salil and Shrivastava 1996). It is apparent that there was volcanic

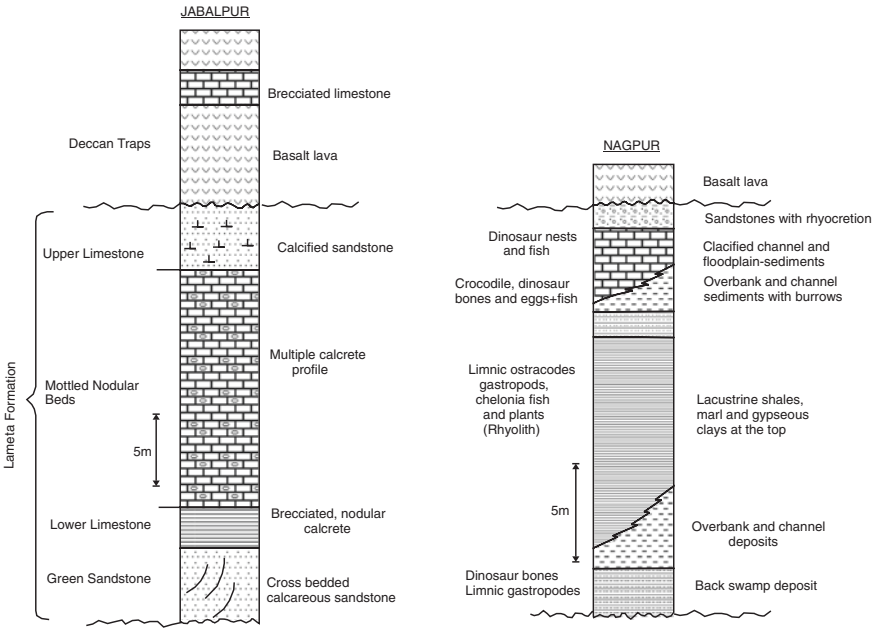

Fig. 14.18 Lithology of the Lameta Formation at Jabalpur and near Nagpur. (Modified after Tandon 2002 and Mohabey and Udhoji, 2000, respectively)

activity when the Lameta sedimentation commenced. The succeeding limestone is a palustrine carbonate, subaerially exposed and affected by desiccation-related shrinkage cracks. The *Mottled Nodular Beds*, comprising variable range of calcrete fabrics and morphology including shrinkage cracks, root casts and concretionary modules, is a sheet wash deposit of a semi-arid alluvial plain. And the *Upper Limestone* represents a sheet flood deposit that was pedogenically modified before burial under the Deccan Lavas (Tandon et al. 1990, 1995).

The Lameta is thus a regionally extensive deposits, exhibiting evidence of drainage disruption, formation of subaerial paludal flats and development of a floodplain affected by sheet floods. The carbonate palaeosol and the profusely occurring calcrete indicate prevalence of semi-arid climate (Brookfield and Sahni 1987; Tandon et al. 1995, 1998; Ghosh 1997; Mohabey et al. 1993; Mohabey 1996; Tandon 2002; Shrivastava et al. 2000; Tandon 2002).

14.10.2 Dinosaurs of the Lameta Time

Around the lakes and swamps in the floodplains of rivers of the lava world lived a variety of animals amidst profusion of vegetation. The biota was dominated by dinosaurs (Fig. 14.19). In 1828, Capt. W.H. Sleeman discovered at Jabalpur a fossil, named *Titanosaurs indicus* by R. Lyddeker in 1877. Another taxa dug out in

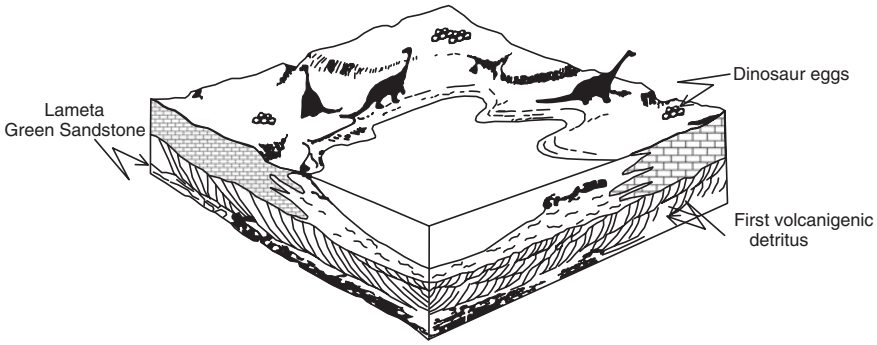

Fig. 14.19 Landscape during the Upper Cretaceous Lameta time, when dinosaurs lived around lakes (after Sahni et al. 1994)

the Bara Simla Hills near Jabalpur turned out to be *Indosuchus raptorious* of the Upper Santonian to Maastrichtian age. *Indosuchus* was a giant carnivore. Rahioli in Balasinor taluka in Kheda district in Gujarat (Fig. 14.15) is another locality where rich assemblage of dinosaur remains has been found within the intertrappean beds (Mohabey 1984). The skeletal remains are of sauropod *Titanosaurus indicus* and *Antarchosaurus septentroinalis* and therapod *Megalosaurus* (Mohabey 1987; Mathur and Pant 1986). The eggshells recovered near Dohad in Panchmahal district indicate affinity with the Campanian–Maastrichtian sauropods (Mohabey and Mathur 1989). Near Pavna in the Nand–Dongargaon area clutches of small oblong eggs indicate avian (bird) affinity of the dinosaurs (Sarkar et al. 1991; Mohabey et al. 1993). Coprolites (dungs) of titanosaurian dinosaurus at Pisdura (Nagpur) contained tissues, cuticles, pollens of angiospermous plants and water-ingested microorganism including bacteria and fungal and algal material, indicating that the dinosaurs were herbivores and ate C^3 plants (Ghosh et al. 2003).

Intertrappean beds bearing dinosaur remains are known from several places in the periphery of the DVP (Fig. 14.15) including at Dikang, West Khasi Hills and Meghalaya (Mishra and Sen 2004). It was during the Lameta time that the dinosaurs diversified and spread far and wide. This is evident from the sauropod nesting sites having eggs as long as 15–20 cm in diameter. These represent the largest hatchery known worldwide from a single lithological unit, the calcareous sandstone of the Lameta Formation (Sahni et al. 1994; Sahni 2003). The dinosaur chose their nesting sites in topographic highs, usually marshy or sandy soft sediment (Fig. 14.19). Isotopic analysis of eggshell carbonate suggests that the food of the sauropod dinosaurs was C^3 plants.

14.10.3 Demise of Dinosaurs

Towards the end of the Cretaceous, many plants and animals suddenly disappeared. Over 65–70 % species of animals, including the dinosaurs, perished. Two-thirds of marine species also vanished. The disappearance was not a catastrophic

event, but a gradual phenomenon (Mohabey and Udhoji 2000). The Deccan Volcanic activities contributed excessive amount of CO_2 to the atmosphere, leading to temperature rise. Carbon and oxygen isotopic studies of the Lameta carbonates indicate hot to semi-arid climate in the Late Cretaceous time (Devey and Lightfoot 1986; Ghosh et al. 1995). Large quantities of CO_2 and other noxious volatiles released by Deccan volcanoes must have caused deterioration of the biosphere, proving fatal to most of the dinosaurs and other animals. It has also been postulated that atmospheric cooling (Andrews et al. 1995) could have been too much for the dinosaurs. Only a few species endured the environmental stresses engendered by Deccan volcanism and survived into the Palaeocene.

The age of the dinosaurs, which lasted 165 million years, came to an end by 65 Ma, the Cretaceous–Tertiary Boundary.

In the intertrappean beds near Kisalpuri in Dindori district, Madhya Pradesh, are found well-preserved lower molars of a shrew-size mammal *Deccandestes narmadaensis*, correlatable with the *Afrodon* of the family Adapisoriculidae from the Late Palaeocene of Africa and Europe (Prasad et al. 2010). This is the first find of a mammal in the Late Cretaceous of India and suggests that the *Deccandestes* represents an ancestral morphotype from which the African–European adapisoriculid *Afrodon* may have been derived (Prasad et al. 2010; Smith et al. 2010).

14.10.4 Connection with Eurasian Landmass

The non-marine ostracode assemblages of the intertrappean beds at Asifabad and Takli show remarkable identity at the specific level with the Maastrichtian fauna of Central Asia, Mongolia and China (Bhatia et al. 1996). It seems that the northward drifting India had established connection with the Asian continent by the Maastrichtian time, allowing migration of fauna.

Several other taxas belonging to mammals, crocodiles and frogs occurring in the Upper Cretaceous formation of central India show remarkably strong affinity with the contemporary forms of Mongolia, China, Central Asia and Europe. Of particular significance is the existence of small-sized palaeryctid mammals which bear remarkable affinity with the those of Central Asia (Sahni and Bajpai 1991). The pelepatid frogs and alligators and the charophytes such as *Nemegtichara* together with ostracodes bear close similarity with those of Mongolia and China (Bhatia and Rana 1984; Bhatia et al. 1990). The close faunal and floral similarity bordering on identity of the central Indian forms with those of Eurasia provide impelling evidence for existence of a land bridge between the two landmasses in the Upper Cretaceous time (Jaegar et al. 1989; Sahni and Bajpai 1991).

Probably, the leading edge of the northward moving India had touched Asia, forming a bridge between the two continents and opening the gates of faunal migration.

References

Agashe, L. V., & Gupte, R. B. (1971). Mode of eruption of Deccan Traps basalts. *Bulletin of Volcanology, 35*, 591–601.

Ahmad, M., & Shrivastav, J. P. (2008). Compositional studies on clays associated with the intra-volcanic bole horizons from the eastern Deccan Volcanic Province : Environmental implications. *Memoirs-Geological Society of India, 74*, 299–321.

Allegre, C. J., Birch, J. L., Capmas, F., & Courtillot, V. (1999). Age of the Deccan Traps using ^{187}Re–^{189}/Os systematics. *Earth & Planetary Science Letters, 170*, 197–204.

Andrews, J. E., Tandon, S. K., & Dennis, P. F. (1995). Concentration of carbon dioxide in the Late Cretaceous atmosphere. *Journal of the Geological Society of London, 152*, 1–3.

Auden, J. B. (1949). Dykes in western India—a discussion of their relationship with the Deccan Traps. *Transactions of the Indian Institute of Metals, 3*, 123–157.

Bajpai, S., & Prasad, G. V. R. (2000). Cretaceous age for ir-rich Deccan intertrappean deposits, palaeontological evidence from Anjar, Western India. *Journal of the Geological Society of London, 157*, 257–260.

Bajpai, S., Sahni, A., Jolly, A., & Srinivasan, S. (1990). Kachchh Intertrappean biotas: affinities and correlation. In A. Sahni & A. Jolly (Eds.), *Cretaceous Event Stratigraphy and the Correlation of the Non-marine Strata* (pp. 101–105). Chandigarh: Geology Department, Panjab University.

Baksi, A. K. (1995). Petrogenesis and timing of volcanism in the Rajmahal flood basalt province, northeastern India. *Chemical Geology, 121*, 73–90.

Baksi, A. K., Barman, T. R., Paul, K. D., & Farrar, E. (1987). Widespread Early Cretaceous flood basalt volcanism in Eastern India: Geochemical data from the Rajmahal–Bengal–Sylhet Traps. *Chemical Geology, 63*, 133–141.

Beans, J. E., & Hooper, P. R. (1988). A note on the picrite-basalts of the Western Ghats, Deccan Trap, India. *Memoirs-Geological Society of India, 10*, 117–134.

Beans, J. E., Turner, C. A., Hooper, P. R., Subbarao, K. V., & Walsh, J. N. (1986). Stratigraphy, composition and form of the Deccan basalts, Western Ghats, India. *Bulletin of Volcanology, 48*, 61–83.

Bhalla, S. N. (1968). Palaeoecology of the Raghavapuram Shale (Early Cretaceous), east coast Gondwana, India. *Palaeogeography, Palaeoclimatology, Palaeoecology, 3*, 345–357.

Bhandari, N., Shukla, P. N., & Cini Castagnoli, G. (1993). Geochemistry of some K/T sections in India. *Palaeogeography, Palaeoclimatology, Palaeoecology, 104*, 199–211.

Bhandari, N., Shukla, P. N., Ghevariya, Z. G., & Sundaresan, S. M. (1995). Meteorite impact did not trigger Deccan volcanism: Evidence from Anjar K/T boundary intertrappean sediments. *Geophysical Research Letters, 22*, 433–436.

Bhatia, S. B., Prasad, S. V. R., & Rana, R. S. (1996). Maastrichtian non-marine ostracodes from Peninsular India: Palaeogeographic and age implications. *Memoirs-Geological Society of India, 37*, 297–311.

Bhatia, S. B., & Rana, R. S. (1984). Palaeogeographic implications of the Charophyta and Ostracoda of the intertrappean beds of Peninsular India. *Memoir of the Geological Society of France, 147*, 29–35.

Bhatia, S. B., Riveline, J., & Rana, R. S. (1990). Charophyta from the Deccan intertrappean bed near Rangapur, A.P., India. *The Palaeobotanist, 37*, 316–323.

Bhattacharya, A., Nandi, A., & Dutta, A. (1997). Triassic mega- and micro-plant fossils from the Kamthi Formation of Talchir coalfield, Orissa, with chronological significance. *Special Publication of Geological Survey of India, 54*, 123–126.

Bhattacharji, S., Chatterjee, N., Wampler, J. M., Nayak, P. N., & Deshmukh, S. S. (1996). Indian intraplate and continental margin rifting, lithospheric extension, and mantle upwelling in Deccan flood basal volcanism near the K/T Boundary: Evidence from mafic dyke swarms. *Journal of Geology, 104*, 379–398.

Bhushan, S. K., Rao, K. N., & Vidyadharan, K. T. (2010). Petrography and geochemistry of St. Mary's Islands, nearly Malpe, Dakshina Kannada District, Karnataka. *Journal of the Geological Society of India, 76*, 155–163.

Bilgrami, S. A. (1999). A reconnaissance geological map of the eastern part of the Deccan Traps (Bidar–Nagpur). *Journal of the Geological Society of India, 43*, 219–232.

Bose, M. K. (1973). Petrology and geochemistry of the igneous complex of Mount Girnar, Gujarat, India. *Contributions to Mineralogy and Petrology, 39*, 247–266.

Brookfield, M. E., & Sahni, A. (1987). Palaeoenvironments of the Lameta Beds, Late Cretaceous at Jabalpur, Madhya Pradesh, India: Soils and biotas of a semi-arid alluvial plain. *Cretaceous Research, 8*, 1–14.

Chalapathi Rao, N. V., Dharma Rao, C. V., & Das, S. (2012). Petrogenesis of lamprophyres from Chhota Udepur, Narmada rift zone, and its relation to Deccan magmatism. *Journal of Asian Earth Sciences, 45*, 24–39.

Chalapathi Rao, N. V., Dongre, A., Kamde, Srivastava, G., Rajesh, Sridhar, M., & Kaminisky, F. V. (2010). Petrology, geochemistry and genesis of newly discovered Mesoproterozoic highly magnesian calcite-rich kimberlites from Siddanpalli, Eastern Dharwar Craton, south India. *Mineralogy and Petrology, 98*, 313–328.

Chandrashekharam, D. (2003). Deccan flood basalts. *Memoirs-Geological Society of India, 53*, 197–214.

Chatterjee, S. C. (1961). Petrology of the lavas of Pavagad hill, Gujarat. *Journal of the Geological Society of India, 2*, 61–77.

Chatterjee, N., & Bhattacharji, S. (2004). A preliminary geochemical study of zircons and monazites from Deccan felsic dykes, Rajula, Gujarat, India: Implications for crustal melting. *Proceedings of the Indian Academy of Sciences (Earth & Planetary Sciences)*, *113*, 533–542.

Chenet, A. L., Quidelleur, X., Fluteau, F., Courtillot, V., & Bajpai, S. (2007). $^{40}K/^{40}Ar$ dating of the main Deccan large igneous province: Further evidence of KTB age and short duration. *Earth and Planetary Science Letters, 263*, 1–15.

Chiplonkar, G. W. (1987). Three decades of invertebrate palaeontology and biostratigraphy of marine Cretaceous rocks of India. *Special Publication of Geological Survey of India, 2(1)*, 305–339.

Choubey, V. D. (1973). Long-distance correlation of Deccan basalt flow, central India. *Journal of Geological Society of America, 84*, 2785–2790.

Courtillot, V., Besse, J., Vandamme, D., Montigny, R., Jaeger, J. J., & Cappeta, H. (1986). Deccan flood basalts and the Cretaceous-Tertiary Boundary. *Earth & Planetary Science Letters, 80*, 361–374.

Cox, K. G. (1989). The role of mantle plumes in the development of continental drainage patterns. *Nature, 343*, 873–877.

De, A. (1981). Late Mesozoic-Lower Tertiary magma types of Kutch and Saurashtra. *Memoirs-Geological Society of India, 3*, 327–339.

Deshmukh, S. S., & Sehgal, M. N. (1988). Mafic dyke swarms in Deccan Volcanic Province of Madhya Pradesh and Maharashtra. *Memoirs-Geological Society of India, 10*, 323–340.

Devey, C. W., & Lightfoot, P. C. (1986). Volcanological and tectonic context of stratigraphy and structure in the Western Deccan Traps. *Bulletin of Volcanology, 43*, 125–126.

Dogra, N. N., Singh, R. Y., Kulshreshtha, S. V. (1994). Palynostratigraphy of intratrappean Jabalpur and Lameta Formation (Lower and Upper Cretaceous) in Madhya Pradesh, India. *Cretaceous research*, *15*, 205–215

Dogra, N. N., Singh, Y. R., & Singh, R. Y. (2004). Palynological assemblage from the Anjar intertrappeans, Kutch district, Gujarat: Age implications. *Current Science, 86*, 1596–1597.

Duncan, R. A., & Pyle, D. G. (1988). Rapid eruption of the Deccan flood basalts at the Cretaceous-Tertriay Boundary. *Nature, 333*, 841–843.

Duraiswami, R. A., Bondre, R., Dole, G., & Phadnis, V. (2002). Morphological structure of flow-lobe tumuli from Pune and Dhule areas, Western Deccan Province. *Journal of the Geological Society of India, 60*, 57–65.

Furuyama, K., Hari, K. R., & Santosh, M. (2001). Crystallization history of primitive Deccan basalt from Pavagarh Hill, Gujarat, western India. *Gondwana Research, 4*, 427–436.

Ghatak, A., & Basu, A. R. (2011). Vestiges of the Kerguelen plume in the Sylhet Traps, northeastern India. *Earth & Planetary Science Letters, 308*, 52–64.

Ghose, N. C., & Kent, R. W. (2003). The Rajmahal basalts: A review of their geology, composition and petrogenesis. *Memoirs-Geological Society of India, 53*, 167–196.

Ghose, N. C., Singh, S. P., Singh, R. N., & Mukherjee, D. (1996). Flow stratigraphy of selected sections of the Rajmahal basalts, Eastern India. *Journal of Southeast Asian Earth Sciences, 13*, 83–93.

Ghosh, P. (1997). Geomorphology and palaeoclimatology of some Upper Cretaceous palaeosols in Central India. *Sedimentary Geology, 110*, 25–49.

Ghosh, P., Bhattacharya, S. K., & Jani, R. A. (1995). Palaeoclimate and palaeovegetation in Central India during the Upper Cretaceous based on stable isotope composition of the palaeosol carbonates. *Palaeogeography, Palaeoclimatology, Palaeoecology, 114*, 285–296.

Ghosh, P., Bhattacharya, S. K., Sahni, A. K., Kar, R. K., Mohabey, D. M., & Ambwani, K. (2003). Dinosaur coprolites from the Late Cretaceous (Maastrichtian) Lameta Formation India: isotopic and other markers suggesting a C_3 plant diet. *Cretaceous Rresearch, 24*, 743–750.

Jaegar, J. J., Courtillet, V., & Tapponier, P. (1989). Palaeontological view of ages of Deccan Traps, the Cretaceous-Tertiary Boundary and India-Asia collision. *Geology, 17*, 316–319.

Kaneoka, I., Iwata, N., Nagao, K., & Deshmukh, S. S. (1996). Period of volcanic activity of the Deccan Plateau.inferred from K-Ar and ^{40}Ar-^{39}Ar ages and problems related to radiometric dating. *Gondwana Geophys, 2*, 311–319.

Karmarkar, B. M. (1978). The Deccan Traps basalt flows of the Borghat sector of Central Railways. *Journal of the Geological Society of India, 19*, 106–114.

Karmarkar, B. M., Kulkarni, S. R., Marathe, S. S., Sowani, P. V., & Peshwa, V. V. (1972). Giant phenocryst basalt in the Deccan Traps. *Bulletin of Volcanology, 35*, 965–974.

Kashyap, M., Shrivastava, J. P., & Kumar, R. (2010). Occurrence of small- scale inflated pahoehoe lava flows in the Mandla lobe of the eastern Deccan Volcanic Province. *Current Science, 98*, 72–76.

Keller, G., Adatte, T., Bajpai, S., Mohabey, D. M., Widdowson, H., Khosla, A., et al. (2009). K-T transition in Deccan Traps of central India marks major marine seaway across India. *Earth & Planetary Science Letters, 282*, 10–23.

Keller, G., Adatte, T., Bhowmick, P. K., Upadhyay, H., Dave, A., Reddy, A. W., & Jaiprakash, B. C. (2012). Nature and timing of extinctions in Cretaceous- Tertiary planktic foraminifera preserved in Deccan intertrappean sediments of Krishna-Godavari Basin, India. *Palaeogeography, Palaeoclimatology, Palaeoecology, 341–344*, 211–221.

Keller, G., Adatte, T., Gardin, S., Bartolini, A., & Bajpai, S. (2008). Main Deccan Volcanism phase end near the K-T boundary : Evidence from Krishna- Godavari basin, SE India. *Earth and Planetary Science Letters, 268*, 293–311.

Kent, R. W., Pringle, M. S., Miller, R. D., Saunders, A. D., & Ghose, N. C. (2002). ^{40}AR-^{39}Ar geochronology of the Rajmahal basalts, India, and their relationship to the Kerguelen plateau. *Journal of Petrology, 43*, 1141–1153.

Khadri, S. F. R. (2003). Occurrence of N-R–N sequence in the Malwa. *Deccan lava flows to the north of Narmada region, Madhya Pradesh, Current Science, 85*, 1126–1129.

Khadri, S. F. R., Subbarao, K. V., & Walsh, J. N. (1999a). Stratigraphy, form and structure of the East Pune basalts, western Deccan basalt province, India. *Journal of the Geological Society of India, 43*, 179–202.

Khadri, S. F. R., Walsh, J. N., & Subbarao, K. V. (1999b). Chemical and magnetostratigraphy of Malwa Traps around Mograba, Dhar District (M.P). *Memoirs-Geological Society of India, 43*, 203–218.

Knight, K. B., Renne, P. R., Halkett, A., & White, N. (2003). ^{40}Ar/^{39}Ar dating of the Rajahmundry Traps, India and their relationship to the Deccan Traps. *Earth & Planetary Science Letters, 208*, 85–99.

Krishnamurthy, P., Pande, K., Gopalan, K., & MacDougal, J. D. (1988). Upper mantle xenoliths in alkaline basalts related to Deccan Traps Volcanism. *Memoirs-Geological Society of India, 10*, 53–68.

Krishnamurthy, P., Pande, K., Gopalan, K., & Macdougal, J. D. (1999). Mineralogical and chemical studies on alkaline basaltic rocks of Kutch, Gujarat, India. *Memoirs-Geological Society of India, 43*, 757–783.

Kumar, A., Dayal, A. M., & Padmakumari, V. M. (2003). Kimberlite from Rajmahal magmatic province: Sr-Nd-Pb isotopic evidence for Kerguelen plume derived magma. *Geophysical Research Letters, 30*, 9–11.

Kumar, A., Gopalan, K., Rao, K. R. P., & Nayak, S. S. (2001a). Rb-Sr age of kimberlites and lamproites from Eastern Dharwar Craton, South India. *Journal of the Geological Society of India, 58*, 135–141.

Kumar, A., Pande, K., Venkatesan, T. R., & Bhaskar Rao, Y. J. (2001b). The Karnataka Late Cretaceous dykes as products of Marion hotspot at the Madagascar-India breakup event: Evidence from ^{40}AR-^{39}Ar geochronology and geochemistry. *Geophysical Research Letters, 28*, 2715–2718.

Lakshminarayana, G., Manikyamba, C., Khanna, Y. C., Kanakdandi, P. P., & Raju, K. (2010). New observations on Rajahmundry Traps of the Krishna-Godavari Basin. *Journal of the Geological Society of India., 75*, 807–819.

Lala, T., Choudhary, A. K., Patil, S. K., & Paul, D. K. (2011). Mafic dykes of Rewa Basin, central India : Implication on magma dispersal and petrogenesis. In R. K. Srivastava (Ed.), *Dyke Swarms : Key for Geodynamic Interpretation* (pp. 140–164). Berlin: Springer-Verlag.

Lehmann, B., Burgess, R., Frei, D., Belyatsky, B., Mainikar, D., Chalapathi Rao, N. V., et al. (2010). Diamondiferous kimberlites in central India synchronous with Deccan flood basalts. *Earth and Planetary Science Letters, 290*, 142–149.

Lightfoot, P. C., Hawkesworth, C. J., & Sethna, S. F. (1987). Petrogenesis of rhyolites and trachytes from the Deccan Traps: Sr, Nd, and Pb isotope and trace element evidence. *Contributions to Mineralogy and Petrology, 95*, 44–54.

Mahoney, J., Macdougal, J. D., Lugmair, G. W., Murali, A. K., Das, M. S., & Gopalan, K. (1982). Origin of the Deccan Traps flows at Mahabaleshwar inferred from Nd and Sr isotopic chemical evidence. *Earth & Planetary Science Letters, 60*, 47–60.

Mathur, U. B., & Pant, S. C. (1986). Sauropod dinosaur from Lameta Group (Upper Cretaceous–Paleocene) of Kheda District, Gujarat. *Journal of Palaeontological Society of India, 31*, 22–25.

Mishra, U. K., & Sen, S. (2004). Dinosaur remains from Dirang, West Khasi Hills district, Meghalaya. *Journal of the Geological Society of India, 63*, 9–14.

Mitchell, C., & Cox, K. G. (1988). A geological sketch map of the southern part of the Deccan Province. *Journal of the Geological Society of India*, *10*, 27–33

Mohabey, D. M. (1984). The study of dinosaurian eggs from Intratrappean limestones in Kheda district, Gujarat. *Journal of the Geological Society of India, 25*, 329–337.

Mohabey, D. M. (1987). Juvenile sauropod dinosaur from Upper Cretaceous Lameta Formation of Panchmahal district, Gujarat, India. *Journal of the Geological Society of India, 30*, 210–216.

Mohabey, D. M. (1996). Depositional environment of Lameta Formation (Late Cretaceous) of Nand-Dongargaon internal basin, Maharashtra: The fossil and lithological evidence. *Memoirs-Geological Society of India, 37*, 363–386.

Mohabey, D. M., & Mathur, U. B. (1989). Upper Cretaceous dinosaur eggs from new localities of Gujarat, India. *Journal of the Geological Society of India, 33*, 32–37.

Mohabey, D. M., & Udhoji, S. G. (2000). Vertebrate fauna of Late Cretaceous dinosaur-bearing Lameta Formation of Nand-Dongargaon inland basin, Maharashtra: Palaeoenvironment and K-T Boundary implications. *Memoirs-Geological Society of India, 46*, 295–322.

Mohabey, D. M., Udhoji, S. G., & Verma, K. K. (1993). Palaeontological and sedimentological observations on non-marine Lameta Formation (Upper Cretaceous) of Maharashtra, India: Their palaeoecological and palaeoenvironmental significance. *Palaeogeography, Palaeoclimatology, Palaeoecology, 105*, 83–94.

Narayandas, G. R., Sharma, C. V., & Navaneetham, K. V. (1982). Carbonate–alkali complex of Mundwara. *Journal of the Geological Society of India, 23*, 604–609.

Negi, J. G., Agarwal, P. K., Singh, A. P., & Pandey, O. P. (1992). Bombay gravity high and eruption of Deccan flood basalts (India) from a shallow secondary plume. *Tectonics, 206*, 341–350.

Pande, K. (2002). Age and duration of the Deccan Traps, India: A review of radiometric and palaeomagnetic constraints. *Proceedings of the Indian Academy of Sciences (Earth & Planetary Sciences)*, *111*, 115–123.

Pande, K., Pattanayak, S. K., Subbarao, K. V., Pavaneetha Krishnan, P., Venkatesan, T. R. (2004). $^{40}Ar/^{39}Ar$ age of a lava flow from the Bhimshankar Formation, Giravali Ghat, Deccan Traps. *Proceedings of the Indian Academy of Sciences (Earth & Planetary Sciences)*, *113*, 755–758.

Pande, K., Sheth, H. C., & Bhutani, R. (2001). $^{40}AR-^{39}Ar$ age of the St. Mary's Islands volcanics, Southern India: Record of India-Madagascar break-up on the Indian subcontinent. *Earth & Planetary Science Letters, 193*, 39–46.

Pande, K., Venkatesh, T. R., Gopalan, K., Krishnamurthy, P., & MacDougal, J. D. (1988). $^{40}Ar–^{39}Ar$ ages of alkali basalts from Kutch, Deccan Volcanic Province, India. *Memoirs-Geological Society of India, 10*, 145–150.

Pandit, M. K., Golani, P. R. (2001). Reappraisal of the petrologic status of Newania 'carbonatite' of Rajasthan, western India. In: Special Issue: Alkaline and Carbonatitic Magmatism and Associated Mineralization, Part II. *Journal of Asian Earth Sciences*, *19*, 305–310.

Parthasarathy, G., Bhandari, N., Vairamani, M., Kunwar, A. C., & Narasaiah, B. (2000). Natural fullerenes from the K-T boundary layer at Anjar, Kutch. *Catastrophic Events and Mass Extinction: Impacts and Beyond* (pp. 12–13). Houston: Lunar & Planetary Institute.

Poornachandra Rao, G. V. S., Mallickarjuna Rao, J., & Subba Rao, M. V. (1996). Palaeomagnetic and geochemical characteristics of the Rajmahal Traps, eastern India. *Journal of Southeast Asian Earth Sciences, 13*, 113–122.

Prasad, G. V. R. (1989). Vertebrate fauna from the Infra– and Intertarppean Beds of Andhra Pradesh: Age implications. *Journal of the Geological Society of India, 34*, 161–173.

Prasad, G. V. R., & Khajuria, C. K. (1995). Implication of the infra- and intertrappean biota from the Deccan, India for the role of volcanism in Cretaceous-Tertiary boundary extinction. *Journal of the Geological Society of London, 152*, 289–296.

Prasad, G. V. R., & Khajuria, C. K. (1996). Palaeoenvironment of the Late Cretaceous mammal–bearing Intertrappean Beds of Naskal, Andhra Pradesh. *Memoirs-Geological Society of India, 37*, 337–362.

Prasad, G. V. R., Verma, B. O., Gheerbrant, E., Goswami, A., Parmar, V., & Sahni, A. (2010). First mammal evidence from the Late Cretaceous of India for biotic dispersal between India and Africa at KT transition. *Comptes Rendus Palaeontology, 9*, 63–71.

Radhakrishna, T., Maluski, H., Mitchell, J. G., & Joseph, M. (1999). $^{40}Ar/^{39}Ar$ and K/Ar geochronology of the dykes from the south Indian granulite terrain. *Tectonophysics, 304*, 109–129.

Raju, D. S. N., Jaiprakash, B. C., Kumar, A., Saxena, R. N., Dave, A., Chatterjee, T. K., & Mishra, C. M. (1995). Age of Deccan volcanism across KTB in Krishna-Godavari basin: New evidence. *Journal of the Geological Society of India, 45*, 229–233.

Rana, R. S. (1990). Palaeontology and palaeoecology of the Intertrappean (Cretaceous–Tertiary transition) beds of the Peninsular India. *Journal of Paleontology Society of India, 35*, 105–120.

Rathore, S. S., Venkatesan, T. R., & Srivastava, R. K. (1996). Mundwara alkali igneous complex, Rajasthan, India: Chronology and strontium isotope systematics. *Journal of the Geological Society of India, 48*, 515–528.

Ray, J. S., & Pande, K. (1999). Carbonatite alkaline magmatism associated with continental flood basalts at stratigraphic boundaries: Cause for mass extinction. *Geophysical Research Letters, 26*, 1917–1920.

Ray, J. S., Pande, K., & Pattanayak, S. K. (2003). Evolution of the Amba Dongar carbonatite complex: constraints from ^{40}Ar-^{39}Ar chronologies of the inner basalt and an alkaline plug. *International Geology Review*, *45*, 857–862.

Ray, J. S., Ramesh, R., Pande, K., Trivedi, J. R., Shukla, P. N., & Patel, P. P. (2000). Isotope and rare earth element chemistry of carbonatite-alkaline complex of Deccan Volcanic Province: Implications to magmatic processes. *Journal of Southeast Asian Earth Sciences, 18*, 177–194.

Ray, R., Sheth, H. C., & Mallik, J. (2007). Structure and emplacement of the Nandurbar-Dhule mafic dyke swarm, Deccan Traps and the tectonomagmatic evaluation of flood basalts. *Bulletin of Volcanology, 69*, 537–557.

Sahni, A. (2003). Indian dinosaurs revisited. *Current Science, 85*, 904–910.

Sahni, A., & Bajpai, S. (1988). Cretaceous-Tertiary boundary events: The vertebrate, palaeomagnetic and radiometric evidence from Peninsular India. *Journal of the Geological Society of India, 32*, 382–396.

Sahni, A., & Bajpai, S. (1991). Eurasiatic elements in the Upper Cretaceous nonmarine biotas of Peninsular India. *Cretaceous Research, 12*, 177–183.

Sahni, A., Tandon, S. K., Jolly, A., Bajpai, S., Sood, A., & Srinivasan, S. (1994). Upper Cretaceous dinosaur eggs and nesting sites from the Deccan Peninsular India. In K. Carpenter, K. Kirsch, & J. Horner (Eds.), *Dinosaur Eggs and Babies* (pp. 204–225). New York: Cambridge University Press.

Salil, M. S., & Shrivastava, J. P. (1996). Trace and REE signatures in the Maastrichtian Lameta Beds for the initiation of Deccan volcanism before KTB. *Current Science, 70*, 399–402.

Sant, D. A., Mathew, G., Khadkikar, A. S., Gogte, V., & Gundurao, T. K. (2003). Co-existent cristobalite and iridium at 65 Ma, Anjar intertrappeans, Kachchh, Western India. *Cretaceous Research, 24*, 105–110.

Sarkar, A., Bhattacharya, S. K., & Mohabey, D. M. (1991). Stable isotope analyses of dinosaur eggshells: Palaeoenvironmental implications. *Geology, 19*, 1068–1971.

Sen, G. (2001). Generation of Deccan Trap magmas. *Proceedings of the Indian Academy of Sciences (Earth & Planetary Sciences), 110*, 409–431.

Sen, A., Pande, K., Hegner, E., Sharma, K. K., Dayal, A. M., Sheth, H. C., & Mistry, H. (2012a). Deccan Volcanism in Rajasthan: ^{40}Ar-^{39}Ar geochronology and geochemistry of the Tavidar volcanic suite. *Journal of Asian Earth Sciences, 59*, 127–140.

Sen, B., Sabale, A. B., & Sukumaran, P. V. (2012b). Lava channel of Khadri Dam, NE of Nasik in Western Deccan Volcanic Province : Detailed morphology and evidence of channel reactivation. *Journal of the Geological Society of India, 80*, 314–328.

Seth, H. C., Choudhary, A. K., Bhattacharya, S., Cucciniello, C., Laishram, R., & Gaurav, T. (2011). The Chogat-Chamardi subvolcanic complex, Saurashtra, northwestern Deccan Traps: Geology, petrochemistry and petrogenetic evolution. *Journal of Asian Earth Sciences, 41*, 307–324.

Sethna, S. F. (1999). Geology of Mumbai and surrounding areas and its position in Deccan Volcanic Stratigraphy, India. *Journal of the Geological Society of India, 53*, 359–365.

Sethna, S. F. (2003). The occurrence of acid and intermediate rocks in the Deccan volcanic province, India, with associated high positive gravity anomalies, and their probable significance. *Journal of the Geological Society of India, 61*, 220–222.

Sethna, S. F., Kothare, P., Sethna, B. S., & Javeri, P. (2001). Geology and petrography of the intrusives in the Deccan Traps of central and southeastern Saurashtra, India. *Journal of the Geological Society of India, 57*, 249–256.

Sethna, S. F., & Sethna, B. S. (1990). Petrology of Deccan Trap basalts of the Western Ghats around Igatpuri and their petrogenetic significance. *Journal of the Geological Society of India, 35*, 631–643.

Sheth, H. C., Mathew, G., Pande, K., Mallick, S., & Jena, B. (2004). Cones and craters on Mount Pavagarh, Deccan Traps, rootless cones? *Proceedings of the Indian Academy of Sciences (Earth & Planetary Sciences)*, *113*, 831–838.

Sheth, H. C., Pande, K., & Bhutani, R. (2001a). ^{40}AR-^{39}Ar Age of a national geological monument: The Gilbert Hill basalt, Deccan Traps, Bombay. *Current Science, 80*, 1437–1440.

Sheth, H. C., Pande, K., & Bhutani, R. (2001b). ^{40}AR-^{39}Ar ages of Bombay trachytes: Evidence for a Paleocene phase of Deccan volcanism. *Geophysical Research Letters, 28*, 3513–3516.

Shrivastava, J. P., & Pattanayak, S. K. (2002). Basalts of Eastern Deccan Volcanic Province, Indias. *Gondwana Research, 5*, 649–665.

Shrivastava, J. P., Salil, M. S., & Pattanayak, S. K. (2000). Clay mineralogy of ir-bearing Anjar intertrappeans, Kutch, Gujarat, India: inferences on palaeoenvironment. *Journal of the Geological Society of India, 55*, 197–206.

Shukla, A. D., Bhandari, N., Kusumgar, S., et al. (2001). Geochemistry and magnetostratigraphy of Deccan flows at Anjar, Kutch. *Proceedings of the Indian Academy of Sciences (Earth & Planetary Sciences)*, *110*, 110–132.

Smith, T., Bast, E. D., & Siege, B. (2010). Euarchontan affinity of Palaeocene Afro-European adiapisoriculid mammals and their origin in the late Cretaceous Deccan Traps of India. *Naturwessenshaften*. doi:10.1007/00114-010-0651-5.

Sreenivasa Rao, M., Reddy, N. R., Subbarao, K. V., Prasad, C. V. R. K., & Radhakrishnamurthy, C. (1985). Chemical and magnetic stratigraphy of parts of Narmada region, Deccan Basalt Province. *Journal of the Geological Society of India, 26*, 617–639.

Srivastava, R. K., Pandit, M. K., & Upadhyay, R. (1988). Petrography and chemical stratigraphy of Deccan basalts from a part of the Malwa Plateau: use of cluster analysis. *Geological Society of India, Memoir, 10*, 181–198.

Subbarao, K. V. (2000). Sr isotopic evidence on the spilitic degradation of the Deccan basalt. *Proceedings of the Indian Academy of Sciences (Earth & Planetary Sciences)*, *109*, 49–55.

Subbarao, K. V., Bodas, M. S., Hooper, P. R., & Walsh, J. N. (1988). Petrogenesis of Jawhar and Igatpuri Formations, Western Deccan Basalt Province. *Memoirs-Geological Society of India, 10*, 253–280.

Subbarao, K. V., Hooper, P. R., Dayal, A. M., Walsh, J. N., & Gopalan, K. (1999). Narmada dykes. *Memoirs-Geological Society of India, 43*, 89–902.

Subbarao, K. V., & Pathak, S. (1993). *Journal of the Geological Society of India, 41*, 71–72.

Subbarao, K. V., Valsangkar, A. B., & Vishwanathan, S. (1993). Mineralogy of the acid volcanics of St. Mary's Islands. *Proceedings of the National Academy of Sciences, 63A*, 97–113.

Subrahmanyam, N. P., & Leelanandam, C. (1991). Geochemistry and petrology of the cumulophyric layered suite of rocks from the Toa pluton of the Mundwara Alkali Igneous Complex, Rajasthan. *Journal of the Geological Society of India, 38*, 397–411.

Sukeshwala, R. N. (1974). Gradation of tholeiitic Deccan basalts into spilite, Bombay, India. *Spilites and Spilitic Rocks* (pp. 229–250). Heidelberg: Springer-Verlag.

Sukeshwala, R. N. (1982). Igneous complex of Mount Girnar, Saurashtra, Gujarat: A reappraisal. *Journal of the Geological Society of India, 23*, 13–18.

Sukeshwala, R. N., & Poldervaart, A. (1958). Deccan basalts of the Bombay area, India. *Geological Society of America Bulletin, 69*, 1475–1494.

Sukeshwala, R. N., & Udas, G. R. (1963). Carbonatite of Ambadongar, Gujarat state and its economic potentialities. *Science & Culture, 29*, 563–568.

Sukheswala, R. N., & Sethna, S. F. (1962). Deccan Traps and associated rocks of the Bassein area. *Journal of the Geological Society of India, 3*, 125–146.

Tandon, S. K. (2002). Records of the influence of Deccan volcanism on contemporaneous sedimentary environment in Central India. *Sedimentary Geology, 147*, 177–192.

Tandon, S. K., Andrews, J. E., Sood, A., & Mittal, S. (1998). Shrinkage and sediment supply control on multiple calcrete profile development: A case study from the Maastrichtian of Central India. *Sedimentary Geology, 119*, 25–45.

Tandon, S. K., Sood, A., Andrews, J. E., & Dennis, P. F. (1995). Palaeoenvironments of the dinosaur-bearing Lameta Beds (Maastrichtian), Narmada Valley, Central India. *Palaeogeography, Palaeoclimatology, Palaeoecology, 117*, 153–184.

Valsangkar, A. B., Radhakrishnamurthy, C., Subbarao, K. V., & Beckinsale, R. D. (1981). Palaeomagnetism and potassium-argon age studies of acid igneous rocks from the St. Mary's Islands. *Memoirs-Geological Society of India, 3*, 265–276.

Venkatachala, B. S. (1977). Fossil floral assemblage in the east coast Gondwana—Critical review. *Journal of the Geological Society of India, 18*, 378–379.

Venkatesan, T. R., Pande, K., & Ghevariya, Z. G. (1996). ^{40}AR-^{39}Ar ages of Anjar Traps, western Deccan Province (India) and its relation to the Cretaceous-Tertiary boundary events. *Current Science, 70*, 990–996.

Vijaya and Bhattacharji. (2002). An Early Cretaceous age for the Rajmahal traps, Panagad area, West Bengal: palynological evidence. *Cretaceous Research, 23*, 789–805.

Viladkar, S. G., Ramesh, R., Avasia, R. K., & Pawaskar, P. B. (2005). Extrusive phase of carbonatite-alkalic activity in Amba Dongar Complex, Chhota Udaipur, Gujarat. *Journal of the Geological Society of India, 66*, 273–276.

Viladkar, S. G., & Schidlowski, M. (2000). Carbon and oxygen isotope geochemistry of the Amba Dongar carbonatite complex, Gujarat, India. *Gondwana Research, 3*, 415–424.

West, W. D. (1958). The Deccan Traps and other flood eruptions—a comparative study. *Proceedings of the Indian National Science Academy, 51A*, 465–494.

West, W. D. (1981). The duration of Deccan Traps volcanicity. *Memoirs-Geological Society of India, 3*, 277–278.

Widdowson, M., Pringle, M. S., & Fernandez, O. A. (2000). A post K-T Boundary (Early Palaeocene) age for Deccan-type feeder dykes, Goa, India. *Journal of Petrology, 41*, 1177–1194.

Yellur, D. D. (1968). Carbonatite complexes as related to the structure of the Narmada Valley. *Journal of the Geological Society of India, 9*, 118–123.

Chapter 15
Pericratonic Basins: The Mesozoic Scenario

15.1 Crustal Extension in Continental Margins

The northward drifting India experienced crustal extension during the Late Triassic to Early Cretaceous period due to India moving and rotating away from Australia and Antarctica and attendant transformation along the Coromandal coast. The leading edge of the Indian continent subsided deeper into the NeoTethys Sea in the north and its western and eastern passive margins started sinking intermittently, giving rise to pericratonic basins. Embracing the whole of the Himalaya domain, the NeoTethys Ocean spread all over the subsiding part of the continental margin in western Rajasthan and Kachchh. The Indian Ocean likewise encroached on the sinking parts of the Kaveri–Palar, the Krishna–Godavari, the Mahanadi, and the Bengal–Meghalaya sectors of the passive continental margin (Fig. 15.1). The sagging of the continental crust took place along faults and lineaments of the Precambrian antiquity. This gave rise to rift-related depressions and ridges in the Late Triassic in the Jaisalmer sector, during the Middle Jurassic in Kachchh, and in the Upper Jurassic in the Coromandal Belt. There was also a seaward tilting of rift basins, leading to formation of embayments and gulfs in the Coromandal Belt and in Kachchh. During the Late Cretaceous, an arm of the sea extended deep into the land along the Narmada rift zone.

The pericratonic basins, it may be recapitulated, formed due to rifting of the continental margin and evolved in stages on the passive margins. The reactivation of subparallel faults and lineaments of considerable antiquity was responsible for their evolution. The sediments that accumulated in these basins bear strong stamp of the oceanic environments with which they were associated. The basins of Kachchh, Jaisalmer and Himalaya belong to the NeoTethys faunal province and the Bengal–Meghalaya, the Krishna–Godavari and the Kaveri–Palar basins had affinity with the Australasian domain of the Indian Ocean. There is preponderance of lamellibranchs, relative poverty of gastropods and corals, richness in

K.S. Valdiya, *The Making of India*, Society of Earth Scientists Series,
DOI 10.1007/978-3-319-25029-8_15

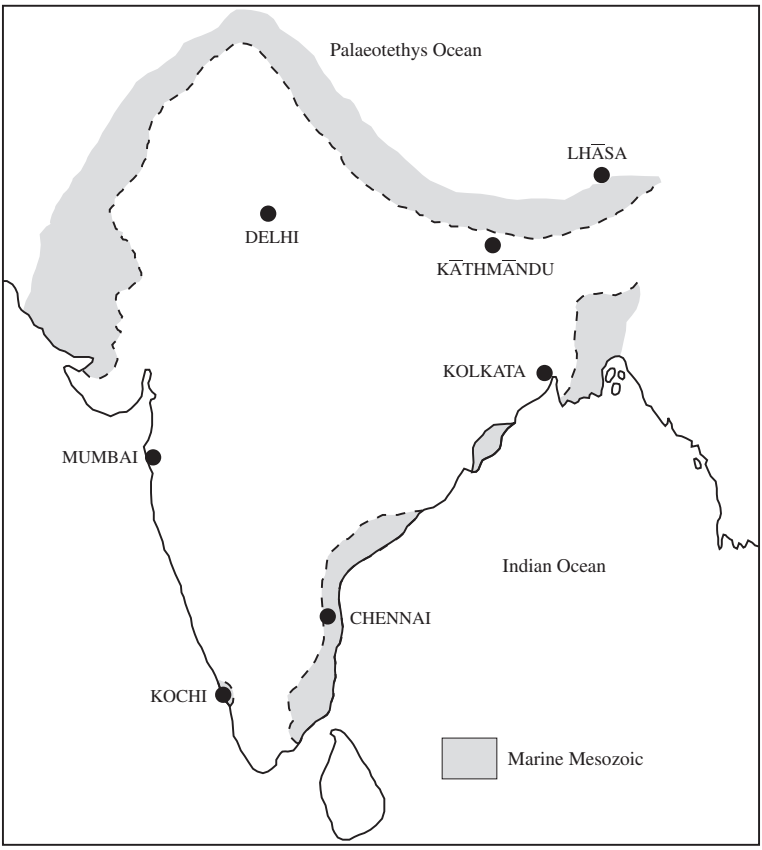

Fig. 15.1 The NeoTethys Ocean in the north and north-west, and the Indian Ocean in the south-east and east overspread the subsiding pericratonic margin of India affected by crustal extension

the assemblage of ammonites, and notable presence of Mediterranean *Hippurites* in the Kachchh, Jaisalmer and Himalaya sectors (Krishna 1987). The Coromandal domain in the south-east is characterized by dominance of cephalopods, notable presence of gastropods and warm-water reef-building corals, and absence of *Hippurites*. Evidently, the NeoTethys Ocean and the Indian Ocean were not mutually connected in the Mesozoic.

15.2 North-eastern Continental Margin

15.2.1 Bengal Basin

During the Mesozoic era on the passive continental margin in the northern part of Bengal and Bangladesh, there was a 100-km-wide shelf that deepened eastwards into the ocean basin (Johnson and Alam 1991). It began to subside in the Lower

Cretaceous (at 127 Ma) when the Indian plate drifted away from Antarctica. The shelf is characterized by transverse Gondwana grabens filled with Late Permian sediments of the Kuchma and Paharpur formations in the Bangladesh grabens and their equivalents in the Gondwana domain of Jharkhand and West Bengal. Unconformably overlying is a pile of volcanic rocks with intertrappean beds constituting the Rajmahal Formation of the earliest Cretaceous age. The Late Cretaceous subsurface succession comprises Sibganj, Dhananjaypur and Bolpur formations (Roybarman 1992; Khan et al. 1994, 1996; Alam 1989; Alam et al. 2003). All these formations lie under the thick pile of Indo-Gangetic sediments. The Early Cretaceous *Sibganj Formation* is an accumulation of trapwash with ferruginous red sandstone and claystone. It grades into the Dhananjaypur/Bolapur successions towards the west. Consisting of dark grey shale, the *Dhananjaypur* Formation represents the earliest marine transgression in this basin. The overlying *Bolpur Formation* comprises a fluvial facies made up of arkosic sandstone.

15.2.2 Meghalaya Region

In the Jaintia and Khasi Hills in southern Meghalaya, the 150- to 200-m Cretaceous succession is exposed as thin strips of outcrops bordering the southern faulted margin of the Meghalaya massif (Figs. 15.2 and 15.3). The rocks dip gently southwards, and in Bangladesh are concealed under an alluvial expanse. Resting unconformably on partly Sylhet Volcanics and partly Precambrian gneisses, the *Jadukata Formation* along the Dauki Fault zone is a Lower Cretaceous fluvial deposits made up of conglomerate–pebbly sandstone alternation. The 150- to 180-m-thick succession of conglomerates intercalated with subarkose and volcanifeldspathic wackes is known as the *Mahadek Formation* (Fig. 15.3). The Mahadek onlaps both the Sylhet Volcanics and the Precambrian gneisses. A characteristic element of the Mahadek in many places is the localized occurrence of pyroclastic beds (Kak and Subrahmanyam 2002). Above a layer of laterite, the *Upper Mahadek* comprises marine sediments containing Companian–Maastrichtian nannofossils (Jafar 1996) and foraminifers *Globotruncana linnaena* and *Globotruncana ventricosa* (Raju and Mishra 1996; Raju et al. 2002). The homotaxial *Sibganj Formation* is characterized by pollen *Aquinopollenites indica*—assemblage of the Upper Cretaceous (Reimann 1993). Near Singrimani in the Garo Hills Gondwana, equivalent rocks are present.

15.2.3 Ultrabasic–Alkaline–Carbonatite Complex

Related to a N/NE–S/SW trending shear zone and to the Sylhet Volcanics (Fig. 15.2) is a 7- to 8-km-wide dyke swarm, made up of peridotite, pyroxenite and meliltolite lamprophyre, constituting the *Jasra Complex* (Mamallan et al.

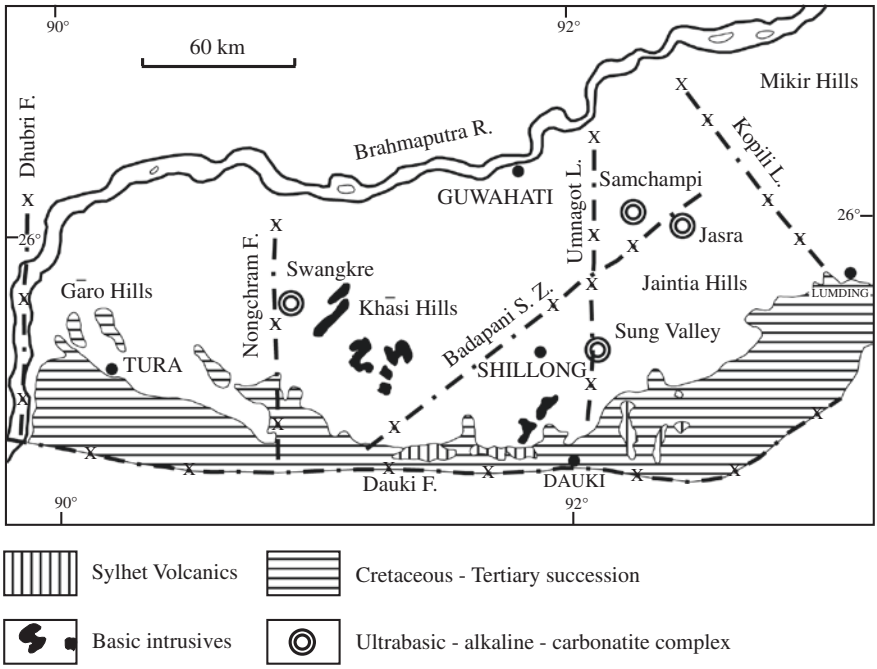

Fig. 15.2 Tectonic framework of the Meghalaya plateau showing occurrence of ultramafic–alkaline–carbonatite complexes in the context of the Sylhet Volcanics and the Cretaceous—Tertiary sedimentary succession (after Srivastava et al. 2004a)

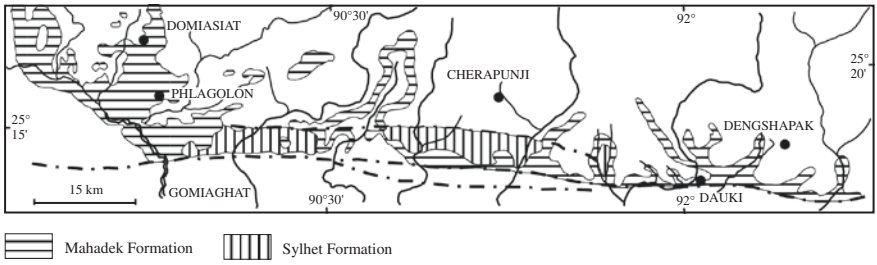

Fig. 15.3 Extent of the exposed Mesozoic, including the Cretaceous formations in eastern continental margin (modified after Mishra and Sen 2004)

1994; Srivastava and Sinha 2004a, b). It is intruded by minor veins of ijolite, tinguite and nepheline syenite. There are two intrusive bodies of carbonatite in the Karbi Along district. Post-dating the main event of the Sylhet flood basalts by about 10 million years, there was emplacement of the carbonatite–alkaline-rock complex in the Sung Valley Jaintia Hills, Samchampi and Barbang (Mikir Hills). Geochemical and isotopic data indicate that the Sung Valley carbonatite was

derived from and interacted with an isotopically heterogeneous mantle and that the carbonatites show εNd values of +0.7 to +1.8, εSr values of +4.7 to +7.0—within the range exhibited by the ocean island basalts of the Kerguelen province in the Indian Ocean, implying linkage of the two (Srivastava et al. 2005). The weighted mean ^{40}Ar–^{39}Ar age of the *Sung Valley Complex* is 107.2 ± 0.8 Ma (Ray and Pande 2001).

15.2.4 Mineral Deposits

In West Khasi district about 140-km SW of Shillong at Domiasiat (Fig. 15.3) and at Phlamgdiloin, rich uranium deposits are associated with sedimentary fills of a braided river characterized by plant litter and biogenic pyrite (Sengupta et al. 1991; Singh 1992; Maithani et al. 1995). Occurring in the Lower Mahadek, the Domiasiat deposit of pitchblende and coffinite is world's largest deposit of its kind.

15.3 South-eastern Continental Margin

The Coromandal coast embraces the Eastern Ghat terrane and the deltaic expanses of the Krishna–Godavari and the Kaveri–Palar rivers and their offshore equivalents (Sastry et al. 1973). The Mesozoic formations are exposed few and far between in the coastal stretch, but their larger parts lie concealed under younger deltaic and marine sediments of coastal and offshore shelf (Figs. 15.4, 15.5, 15.6 and 15.11; Table 15.1). The sediments here were deposited in the grabens. The East Coast, stretching from Athagarh in Odisha to beyond Ramanathapuram in Tamil Nadu, came under the sway of marine waters towards the end of the Jurassic period. Demarcated by an east–west trending boundary fault, the 700-m-thick *Athgarh Sandstone* represents an extensive alluvial fan, the distal part of which grades into the lacustrine deposits in the centre of the basin (Mishra et al. 2004) and into deltaic deposits towards the shelf. The Athagarh succession in the Mahanadi domain comprises sandstone with thin intercalations of claystone and carbonaceous shale. The shale is characterized by Early Cretaceous flora of the Upper Gondwana Rajmahal affinity (Patra 1973). Evidently, there was interfingering of land-derived sediments (with their plant contents) and the marine sediments containing invertebrate fossils, indicating a delta-front environment.

15.3.1 Krishna–Godavari Basin

The coastward extension of the Gondwanic Pranhita–Godavari graben is terminated by the NE–SW trending Barpatla Ridge along the Eastern Ghat

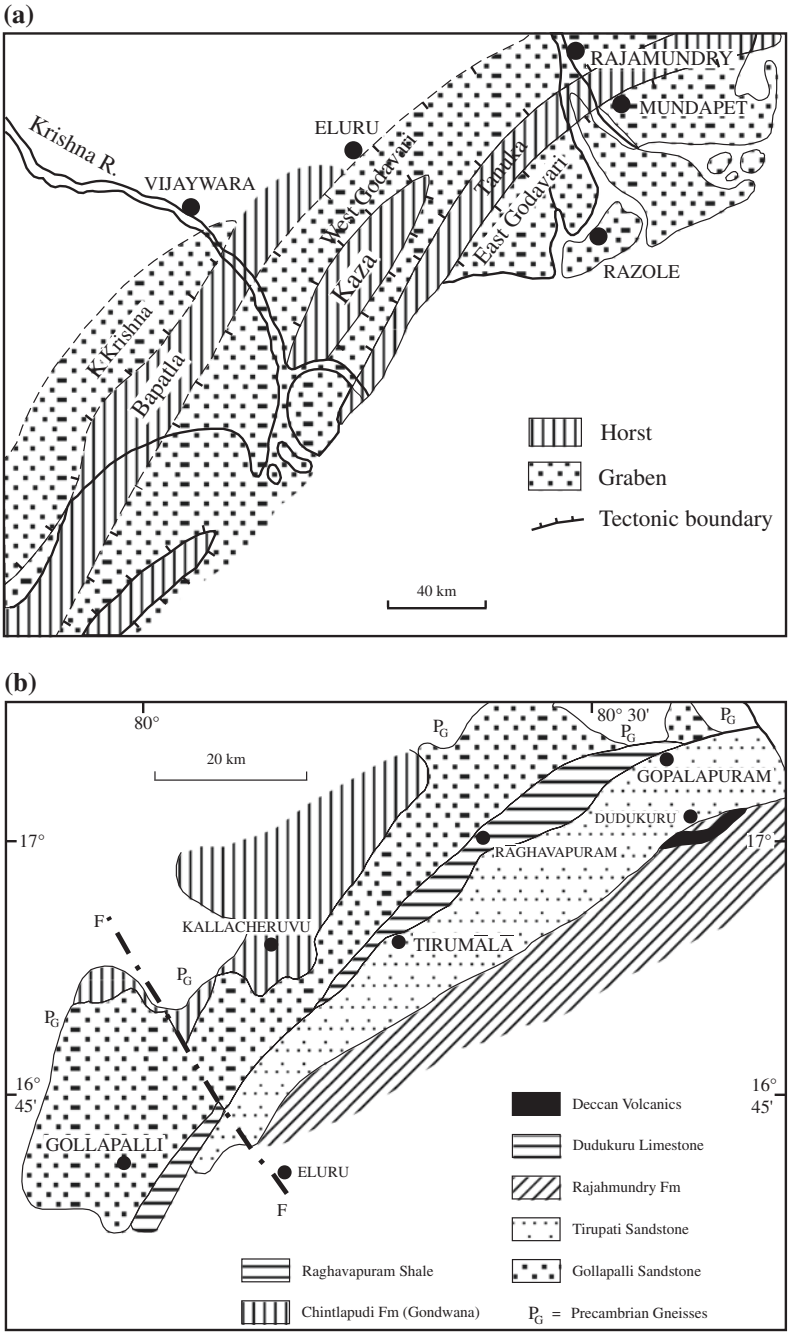

Fig. 15.4 **a** Tectonic setting of the Krishna–Godavari domain (after Majumdar et al. 1995). **b** Exposed Mesozoic formations in the coastal stretch of Andhra Pradesh (after Prasad and Pundir 1999)

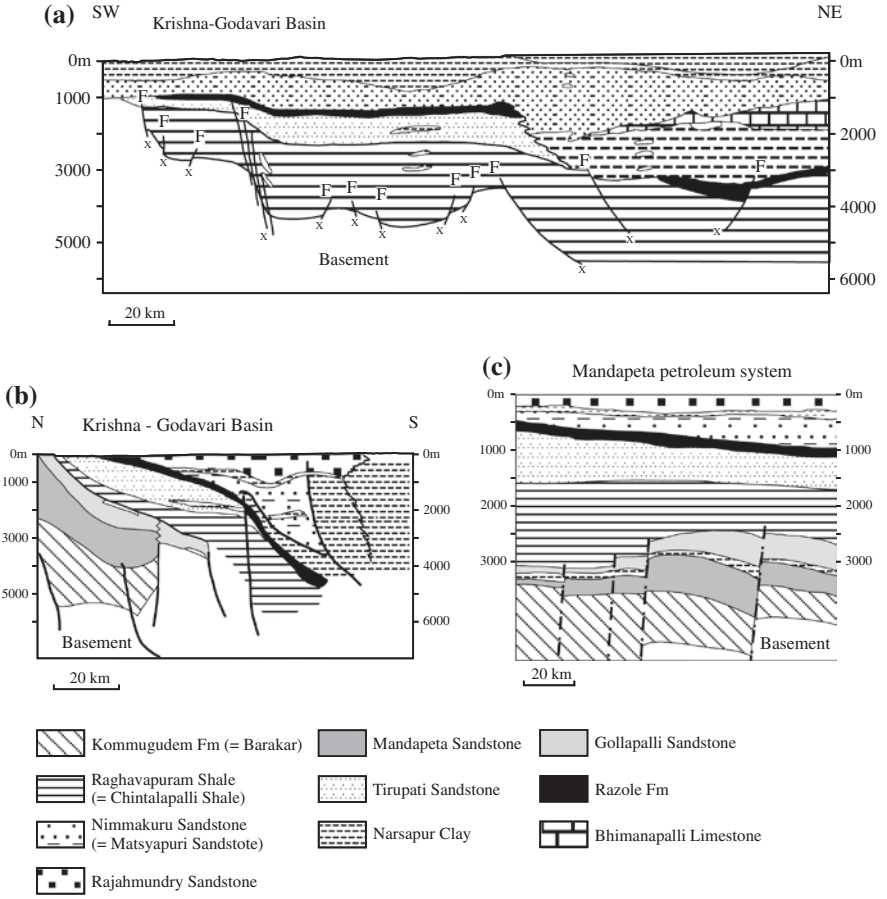

Fig. 15.5 Structural architecture and lithostratigraphic pattern of the Krishna–Godavari Basin. Sections show the sources and the nature of the traps of the hydrocarbon deposits (modified after Majumdar et al. 1995)

characterized by ridges and grabens (Manmohan et al. 2003) that became sites of sedimentation (Figs. 15.4, 15.5 and 15.11). The tilting of later basins southeastwards resulted in drowning of the coastal land. In the lower reaches of the Pranhita–Godavari Valley, towards the delta region, the Gondwana sediments rest on the Archaean basement. The Early Permian *Draksharama Formation* is made up of grey black shale alternating with claystone, sandstone and coal seams. Overlying is the *Mandapeta Sandstone*, comprising intercalations of shale that have yielded Triassic assemblage of palynomorphs. Unconformably overlying is the *Bapatla Sandstone*, characterized by Upper Jurassic assemblage of dinoflagellates and acritarchs (Mehrotra et al. 2002). The Cretaceous starts with the *Gollapalli/Budavada Sandstone* that rests upon the Gondwanic Mandapeta

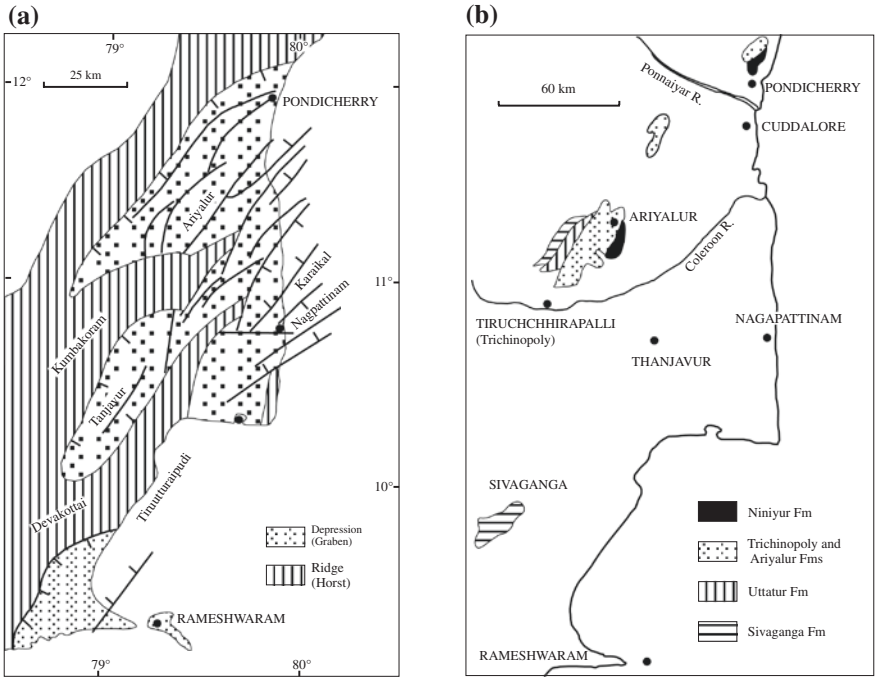

Fig. 15.6 **a** Graben-and-horst structure developed in the Coromandal Coast, on the passive continental margin of India (modified after Sastry et al. 1977). **b** Exposed Jurassic and Cretaceous formations in the Kaveri–Palar Basin in Tamil Nadu (after Pandey and Dave 1998)

Sandstone. In the marine shelf, carbonates and clastic sediments formed a fan-shaped delta along the ridges; and turbidites covered the slopes and the graben floors. By the Campanian epoch, a large delta had emerged and was prograding rapidly (Prabakaran and Ramesh 1995). The Gollapalli/Budavada comprises micaceous ferruginous gritty sandstone and shale containing abundant plant fossils of the Upper Gondwana affinity such as *Williamsonia, Taeneopteris, Cladophlebis, Otozamites, Ptilophyllum, Pterophyllum* and *Elatocladus* of the Neocomanian age. The plant remains imply considerable contribution of terrestrial detritus and plants by rivers draining upland and coastal region. As everywhere in the pericratonic basins of India, the plant fossils along with detritus were washed down into the sea, resulting in the admixture of marine and terrestrial materials. It could also be a large prograding delta lobe over the coastal region where fluvial and marine sediments interfingered (Biswas 2003). The *Raghavapuram Shale* represents the first marine transgression. It comprises a succession of brittle shale and soft claystone, the latter characterized by a rich assemblage of ammonites, lamellibranchs, brachiopods and foraminifers. Dinoflagellete cysts, ammonites and palynofossils indicate Barremian to Early Aptian age of the Raghavapuram Shale (Prasad and

Table 15.1 Cretaceous lithostratigraphy of the Krishna–Godavari Basin (based on Biswas 2003)

Age	Inland		Subsurface and offshore
	Rajahmundry–Ellore Belt	Guntur–Ongole Belt	
Palaeocene	Razole		
Unconformity			
Upper Cretaceous	Tirupati Sandstone	Pavalur Sandstone	Chintalapalli Shale
Disconformity			
Lower Cretaceous	Raghavapuram Shale	Vemavaram Shale	Gajulapadu Shale/Raghavapuram Shale
Unconformity			
	Gollapalli Sandstone	Budavada Sandstone	Krishna Fm/Pennar Fm
Unconformity			
Late Jurassic	Nellore Claystone, Chintalapudi Sandstone		Bapatla Sandstone
Unconformity			
Permo-Triassic			Mandapeta Sandstone, Kommugudem Fm, Draksharama Argillite
Unconformity			
Precambrian basement			

Pundir 1999). The *Tirupati Sandstone* is a formation of coarse- to medium-grained white grey sandstone containing pollens of the Cenomanian angiosperms and gymnosperm plants (Kapoor et al. 1999).

The Tirupati Sandstone and its offshore equivalent to the *Chintalapudi Sandstone* are conformably overlain by the Rajahmundry Volcanics/Razole Volcanics of the Palaeocene age.

15.3.2 Hydrocarbon Deposits of Krishna–Godavari Basin

Rich in organic material, the Raghavapuram Shale is the source rock of oil and gas; and the associated sandstone serves as the reservoir rock *in the offshore zone*. The deposits (Fig. 15.5) are confined to the lower part of the Raghavapuram where high-gamma and high-resistivity anomalies have been detected (Manmohan et al. 2003). The gas-bearing sandstone straddles across the unconformity on top of the high-gamma and high-resistivity horizon at the base of the formation. According to some workers, this part of the Raghavapuram Shale represents the deposit of an estuarine valley fill, deposited in lowstand tract. An incised valley carved out earlier in the underlying unit was filled back by sediments during the Cenomanian–Turonian transgression (Chitra Rao and Asthana 2000). This is the feature which

Table 15.2 Jurassic–Cretaceous lithostratigraphy of the Kaveri–Palar Basin in Tamil Nadu (after ONGC 1993)

Age	Onland unit	Subsurface and offshore formation
Palaeocene	Niniyur Group	
- *Unconformity* -		
Late Upper Cretaceous	Ariyalur Group	Proto Novo Shale, Komarakshi Shale, Nannilam Shale
- *Unconformity* -		
Middle Upper Cretaceous	Trichinopoly Group	Kadavasal Shale
- *Unconformity* -		
Early Upper Cretaceous	Uttatur Group	Bhuvanagiri Formation, Sattapadi Formation
- *Unconformity* -		
Late Lower Cretaceous	Dalmiapuram Formation	Andimadam Formation
- *Unconformity* -		
Upper Jurassic to Earliest Cretaceous	Sivaganga/Therani Formation	Sivaganga
- *Unconformity* -		
Archaean basement		

had a significant bearing in the formation of the hydrocarbon deposits. Over 325-m-deep wells (4600–5200 m) have identified more than 160 structures of hydrocarbon deposition, out of which 48 have been proved hydrocarbon-bearing. The Mandapeta gas field is related to the Permian sandstone, and the Lingala oil field to the Lower Cretaceous Raghavapuram Shale (Rao 2001, 2002). It may be mentioned that besides the Mesozoic deposits of hydrocarbon, there are Tatipaka–Pasarlapudi gas field and Mori oil field related to Lower Eocene and Miocene-connected Ravva oil field (Chandra et al. 1994; Rao 2002) (Table 15.2).

15.3.3 Kaveri–Palar Basin

Like the Krishna–Godavari Basin in Andhra Pradesh, the Palar–Kaveri Basin in Tamil Nadu coast is characterized by horst-and-graben structures beneath a thick cover of Tertiary–Quaternary sediment (Figs. 15.6 and 15.11; Table 15.2). The evolution of the structural depression commenced in the Late Jurassic and continued all through the Cretaceous and the Cenozoic (Banerji 1972; Sastry et al. 1968; Sastry et al. 1977). In the Santonian interval 87.5–84 million years ago, strong faulting caused subsidence of high grounds, leading to development of steeply sloping river

valleys, acceleration of terrestrial erosion, transgression of the sea, and high influx of detrital sediments into the basin (Ramkumar et al. 2005). The basin extends over offshore with an easterly tilt, as is evident from progressive eastward-thickening of the sedimentary succession. The larger basin comprises five subbasins, each representing a graben oriented in the NE–SW direction parallel to the coast (Fig. 15.6a).

Resting on the Archaean gneisses–khondalites or locally on patches of the inland Gondwana sedimentary rocks, the Mesozoic succession begins with the Pre-Albian *Sivaganga Formation* near Ariyalur and its near temporal equivalent the *Therani Formation* near Thanjavur. Characterized by calcareous concretions in feldspathic sandstone and conglomerate at the base, the *Sivaganga Formation* forms isolated hillocks in Ramanathapuram. It comprises fluvial, lacustrine and paludal sediments and is characterized by plant fossils (filicales, cycades, gingkos and conifers) of the Upper Jurassic to lowermost Cretaceous age. The plant assemblages represent terrestrial material washed down by streams into a tide-swept estuary. Or possibly there was interfingering of fluvial and marine environments of deposition. The claystone in the upper part of the Therani Formation contains ammonites and arenaceous foraminifers of Neocomanian–Aptian age (Mamgain et al. 1973; Banerjee 1982). Palynormorph assemblage together with plant *Ptilophyllum* corroborates the Early Cretaceous time span of the Therani–Sivaganga succession (Venkatachala 1977). In the northern Palar Basin, the *Satyavedu Formation* in the north, the *Avadi Formation* in the central part and the *Sriperumbadur Formation* in the south represent the Neocomanian–Aptian succession (Kumaraguru and Trivikram Rao 1994).

The overlying marine formation *Dalmiapuram* comprises coralline-algal reef limestone with black shale. Besides ammonites, there are foraminifers and ostracodes of the Aptian to Albian age (Jain 1968; Bhatia and Jain 1969; Banerji 1970; Banerji et al. 1996). The Dalmiapuram Limestone is intensively used for manufacture of cement.

The *Uttatur Group* comprises reefal limestone, greenish grey gypseous shale and black carbonaceous shale. The bioherms developed during the Middle Aptian to Cenomanian time, along an edge of the block associated with an active fault parallel to the coast, as borne out by breccias and conglomerates intimately associated with the reefs. The bioherm, that grew as high as 150 m, is composed of sponges and a variety of scleractinid corals and algal crust (Steinhoff and Bandel 2000). The Karai claystone with gypseous shales and phosphatic nodules in the Uttatur Group is very rich in planktonic and benthic foraminifers, the $\delta^{18}O$ values of which indicate near-surface sea water temperature of 29 °C and seafloor temperature of 21 °C (Dasgupta et al. 2006). The Late Cretaceous *Trichinopoly Group* is made up of Garudamangalam and Paravay formations, comprising calcareous gritty and conglomeratic sandstone with bands of sandy limestone and gypseous shale and marlite. The *Ariyalur Group* comprises cross-bedded green sandstone (locally conglomeratic) interbedded with grey and purple shale. The biohermal limestone within the succession is known as the Kallankurichchi Limestone (Sundaram et al. 2001). *Phylloceratina, Lytoceratina* and *Ammonitina* found near Pondicherry comprise most diverse Upper Maastrichtian ammonite assemblage

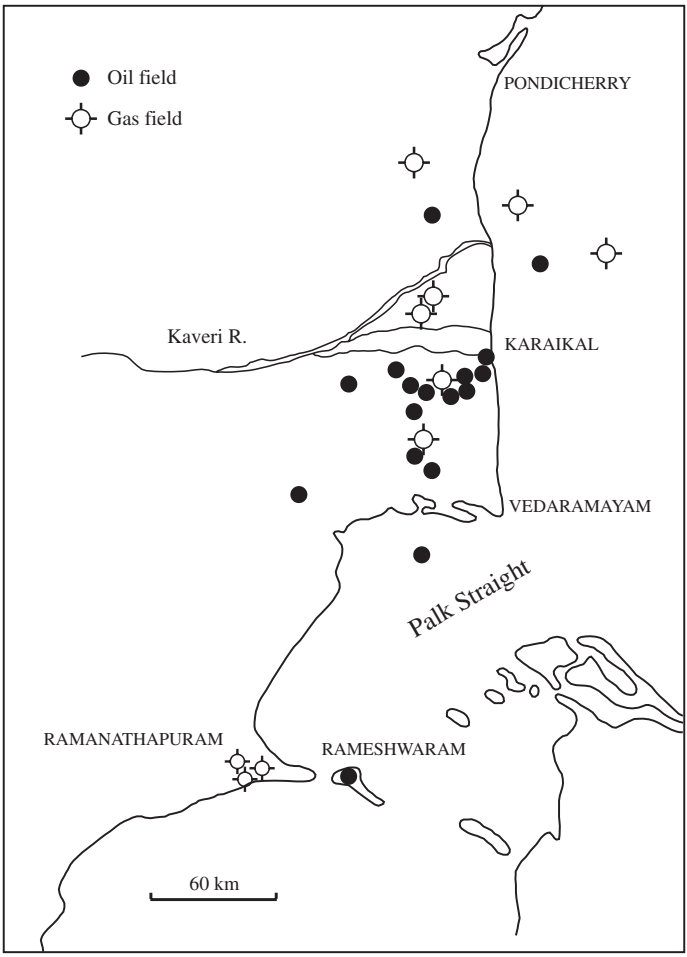

Fig. 15.7 Location of oil and gas fields in the Kaveri–Palar Basin (after Govindan et al. 2000)

anywhere known (Kennedy and Henderson 1992). The Kallakkudi Limestone (Albian–Cenomanian) and the Kallankuruchchi Limestone (Maastrichtian) are composed of packstone and greenstone, representing carbonate shoals. These two horizons have yielded condensate with 49° API gravity and hydrocarbons (Yadagiri and Govindan 2000; Govindan et al. 2000). The Early Cretaceous shale deposits that accumulated in depressions under anoxic conditions are the sources of hydrocarbons (Fig. 15.7) in the Kaveri–Palar Basin (Raju and Mishra 1996; Raju et al. 2002). The petroleum fields of the offshore zone tap these pay horizons. The top part of the Creataceous succession of the Kaveri Basin records gradual change of climate and sea level as reflected in the change in isotope geochemistry of sediments, which received increased influx of detrital material from land (Ramkumar et al. 2004).

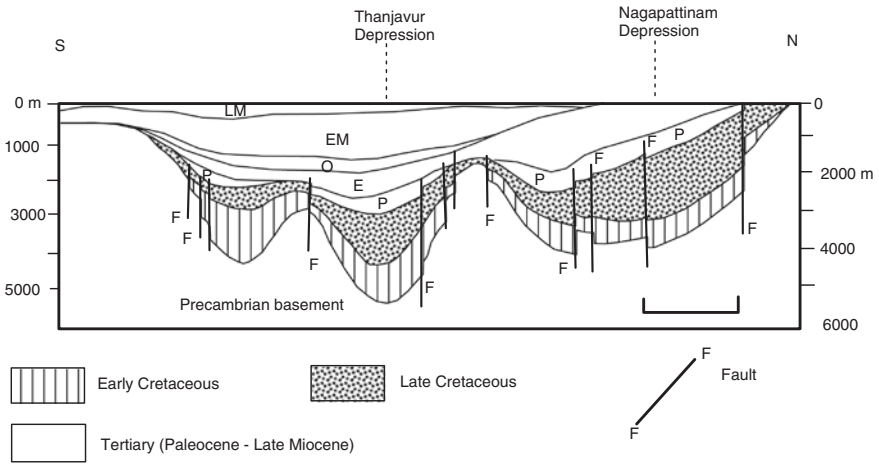

Fig. 15.8 Cross section shows subsurface structure and lithostratigraphy of the Kaveri–Palar Basin (Sastry et al. 1997)

The names Uttaltur, Trichonopoly and Ariyalur were given by H.F. Blanford in 1862. The subsurface Cretaceous succession exhibiting considerable lateral facies variation in the onland part of the basin (Fig. 15.8) extends eastwards over the continental slope. The offshore extension of the Uttattur Group is represented by the *Andimadam Conglomerate* and the *Sattapadi Shale* ranging in age from Pre-Albian to Cenomanian. The Sattapadi Shale is overlain by the *Bhuvanagiri Formation* made up of predominant sandstone with minor shale. The Bhavanagiri contains Cenomanian to Conacian species of *Rotalipora* and *Marginotruncana*. The offshore facies of the Ariyalur Group are described as the *Palk Bay Formation* of calcareous sandstones, the *Kudavasal Shale*, the *Nannilam Shale*, the *Porto Novo Shale* and the *Komarakshi Shale* containing Campanian to Maastrichtian species of foraminifers including *Rosita*, *Globotruncana* and *Abathomphalus* (Raju and Mishra 1996). The faunas indicate the depositional environment varying from outer shelf to bathyal zone.

15.4 North-western Continental Margin

15.4.1 Kachchh Basin

The north-western part of the Indian continental margin experienced lithospheric stretching and rifting in the Late Triassic (Biswas 1982, 1987, 2003, 2005). The resulting depression (rift valleys) is oriented east–west (Figs. 15.9 and 15.11; Table 15.3). The depositional sites were of the nature of embayment between the uplifted Tharad–Nagarparkar Ridge in the north, the raised-up Saurashtra High

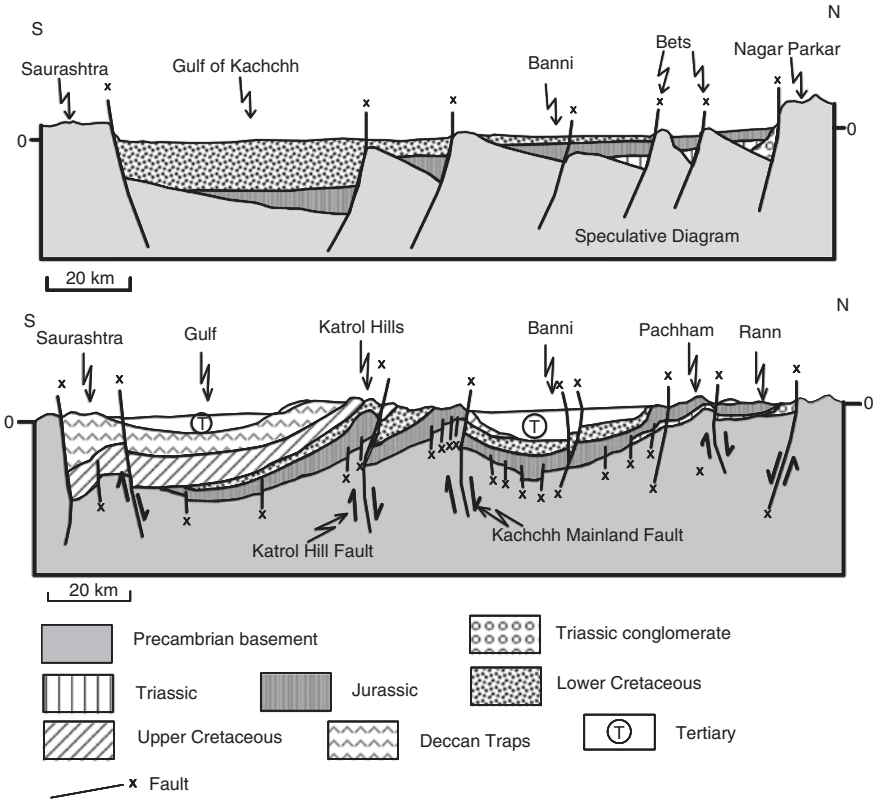

Fig. 15.9 Rifting of the north-western continental margin gave rise to the Kachchh Basin, comprising a series of ridge- and half-graben-oriented east–west (after Biswas 2005)

Table 15.3 Mesozoic lithostratigraphy of the Kachchh and Jaisalmer basins in north-western continental margin of India

Age	Kachchh Basin	Jaisalmer Basin
Late Cretaceous	Deccan traps	Parh Formation
- *Unconformity* -		
Early Cretaceous	Bhuj	Goru
		- - - - - - - - -*Unconformity*- - - - - - - - - -
		Habur
- *Unconformity* -		
Upper Jurassic	Katrol	Pariwar Bhadesar/Baisakhi
	Chari	
Middle Jurassic	Patcham	Jaisalmer
Lower Jurassic		Lathi
Upper Triassic		Shumarwali
- *Unconformity* -		
Precambrian/Proterozoic basement, Permian Karampura		

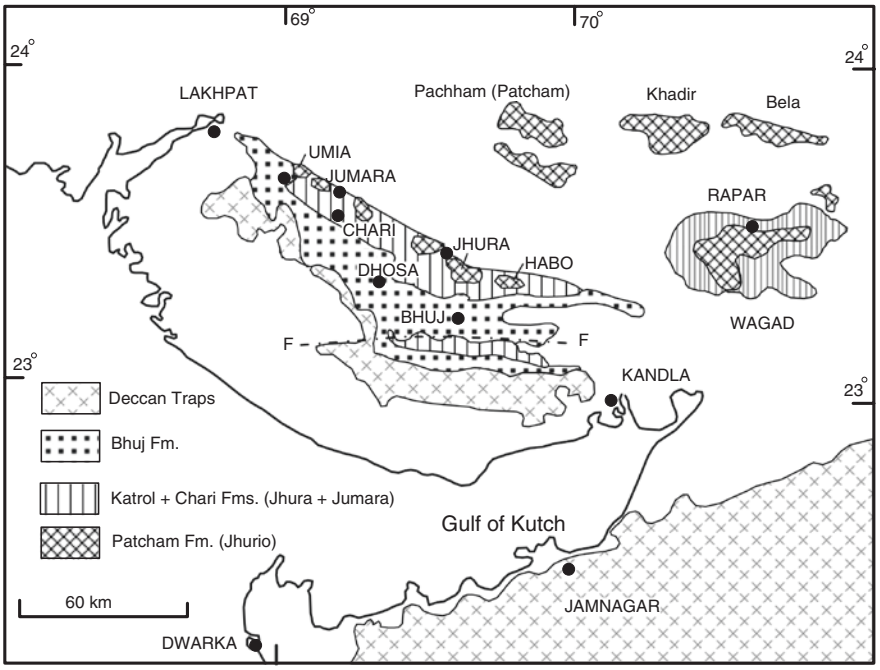

Fig. 15.10 Sketch map showing the Jurassic–Cretaceous formations in the Kachchh Basin (after Biswas 1992)

in the south and the Radhanpur–Barmer High in the east. A NNE–SSW trending high divides the basin into two parts—the western part exhibiting progressive thickening and facies variation of sediments, and the eastern part having shallow-water sediments (Biswas and Deshpande 1983). The sediments, laid down on the Archaean and Proterozoic basements, provide a coherent record of stratigraphy of the Mesozoic (Agrawal 1957, 1977, 1981; Krishna 1987). The lithostratigraphic nomenclature was proposed by W. Waagen in 1873.

The sedimentation in the Kachchh Basin (Figs. 15.9, 15.10 and 15.11; Table 15.3) started in the Middle Jurassic time. The *Patcham Formation* (also described as Jhurio) comprises Bajocian–Early Callovian carbonate–shale association. The bioclastic limestone of the upper part contains rich assemblage of corals, molluscs, brachiopods, ammonites and bryozoans and foraminifers. In the lower part, the shale is interbedded with thick limesone with golden oolites. The overlying *Chari Formation* (Jumara) comprises laminated shales with intercalation of siltstone, marl and bioclastic limestone of deltaic environment. The limestone is oolitic; the characteristically golden coloured oolitic limestone is known as the *Dhosa Oolite*. The sedimentary rocks making the Jhumra, Juma and Habo domes in western Kachchh contain ostracode assemblages indicating their Bathonian to Callovian (Middle and Upper Jurassic) ages, and also pointing to the similar assemblages in Laurasian as well as Indo-East African provinces along

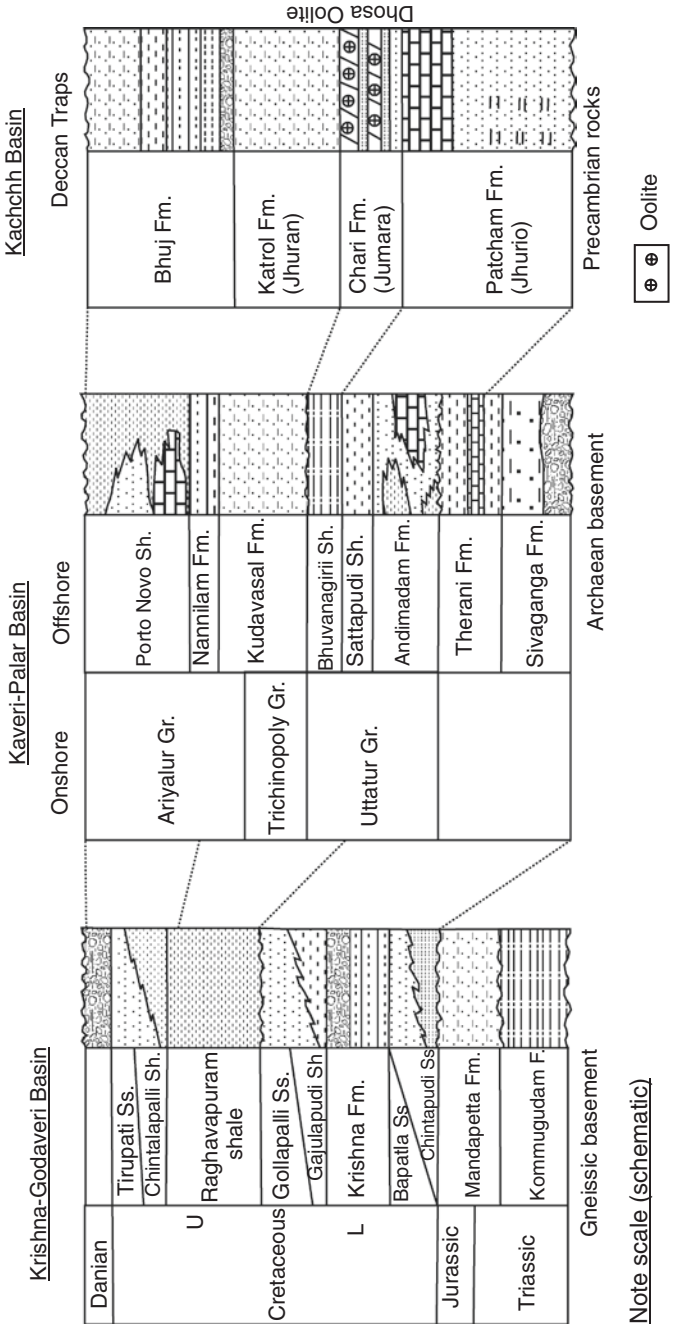

Fig. 15.11 Lithological logs of the Mesozoic formations of the Kachchh and the Jaisalmer basins

the Tethys. Across a paraconformity, the thick coursing upwards succession of cross-bedded sandstone and shale characterized by ferruginous concretions of the *Katrol Formation* (Jhuran) belong to the Upper Jurassic to very Early Cretaceous (Kimmeridgian to Neocomanian) period. It consists of yellow brown cross-bedded feldspathic sandstone with cyclic interbeds of yellow-laminated sandstone, grey carbonaceous shale and locally kaolinitic white shale and dark brown to purple bioturbate siltstone. Even as littoral zone expanded and the delta complex grew into the open sea to the west, the fluvial processes had become active (Krishna et al. 1998).

The Jurassic succession is overlain probably with break by the Cretaceous rocks, 1000–1200 m in thickness (Table 15.3) and ranges in age from Berriasian–Valanginian to Late Turonian–Coniacian (Krishna 1991). Fission-track dating of glauconite from the uppermost horizon (Bhuj Formation) placing it between 112 and 89 Ma (Biswas 2005) confirms the early Upper Cretaceous age of the youngest horizon of the Mesozoic of Kachchh. The *Bhuj Formation* (Table 15.3), made up of Ghuneri, Ukra and Upper Unit, comprises grey silty shale with limonitic parting and locally carbonaceous shale. As elsewhere, there is a rich assemblage of *Ptilophyllum* flora, understandably derived from the land through rivers and streams. The bioturbated sandstone characterized by iron oxide enrichment and leaf impressions contains Middle Albian nannofossils. The *Ghuneri Member* is made up of rhythmic alternation of red and yellow sandstone and shale and with bands of ironstone or ferruginous sandstone and lensoid bodies of coal formed in a deltaic environment. The *Ukra Member* consists of glauconitic sandstone, shale and oolitic limestone and marl that contain abundant ammonites and pelecypods as well as fossil wood. Occurring in the westernmost part of the basin, this horizon represents a short transgressive episode in the delta-front during sea-level high-stand in the Aptian time. Plant fossils *Ptylophyllum, Otozamites, Cladophlebis* and *Williamsonia* recall upper Gondwana flora. It is overlain by Upper Member comprising cross-bedded coarse-grained sandstone with ferruginous bands, limestone and white kaolinitic clays. The hummocky cross-bedding indicates interference of storm waves with ebb-tide currents along a prograding shoreline (Bose et al. 1986). Such features such as wavy lamination, ripple drift lamination and flaser bedding indicate that the sediments of the terminal horizon of the Kachchh Cretaceous were deposited in tidal channels and tide-affected shelf embracing tidal flats and lagoons (Krishna et al. 1983).

In the Wagad–Rapar–Adesar area in north-eastern Kachchh, the feldspathic, locally ferruginous and conglomeratic sandstone with minor shale contain both marine fossils and plant remains of the Lower Cretaceous age. These sediments represent nearshore deposits in a tidal environment where the distributary channels had NW–SE direction (Bandyopadhyay 2004).

It may be stressed that the Jurassic rocks of Kachchh have acquired global importance for their exceptionally rich ammonite assemblages, particularly of the Callovian–Tithonian (Upper Jurassic) time span (Krishna 1987, 1991; Krishna and Cariou 1986; Krishna et al. 1998). The ammonite assemblage, including *Gregoryceras fouguei, Euaspidosa*, *Perisphinctes* and *Epimayaites*, implies

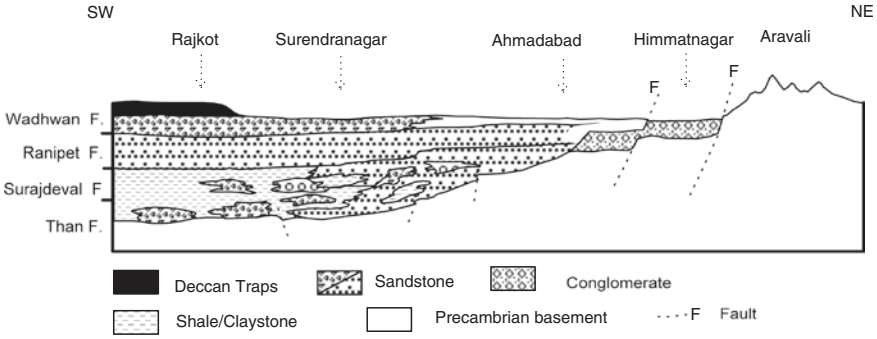

Fig. 15.12 Pattern and environment of deposition of the sediments of the Dhrangadhra succession in north-eastern Saurashtra (after Casshyap and Aslam 1992)

connection of the Kachchh fauna with that of Indo-African faunal province. The horizon of the Dhosa Oolite, an important stratigraphic marker, is characterized by a faunal assemblage that contains elements of both the Indo-African (Mayaitinae) and the Tethyan (Perisphinctinae) faunal provinces.

In north-eastern Saurashtra, there is a 500- to 600-m-thick succession of cross-bedded feldspathic and ferruginous sandstones with intercalations of shale containing leaf impressions of the Gondwana affinity and local layers of conglomerate above the Early Proterozoic basement. The succession is known as the *Dhrangadhra Formation* (named by F. Fedden in 1884). This succession (Fig. 15.12) is time transgressive of the *Wadhwan Beds* in the Surendranagar district. The two formations are regarded as the inland facies of the marine Cretaceous. The upward-coarsening lower part was formed by the distributaries of a delta in the proximity of the shoreline, while the upper part is made up of deposits of subtidal to tidal and beach zones (Casshyap and Aslam 1992; Aslam 1992). At the top is a horizon of fossiliferous limestone interbedded with pebbly sandstone and mudstone deposited in embayments and estuaries. The calcareous upper part interbedded with lava flows of the Wadhwan contains, besides the plant *Cladophlebis*, remains of a fish of the Upper Tithonian to Albian age (Borkar 1973).

The Sadara Sill in the Pachchham area in Kachchh having composition transitional between basalt and basanite, and characterized by Sr, B, Pb and LREE enrichment and Nb, Cr, Y, Cs, Lu depletion, shows magnetic pole in the pre-Deccan Volcanism period in the 85- to 91-Ma interval (Ray et al. 2006). It must have been emplaced along faults resulting from the rifting of the crust in Kachchh.

15.4.2 Jaisalmer Basin

The Jaisalmer Basin is one of the four basins developed in the Rajasthan continental margin—the Bikaner–Nagaur Basin, the Barmer Basin, the Sancher Basin and

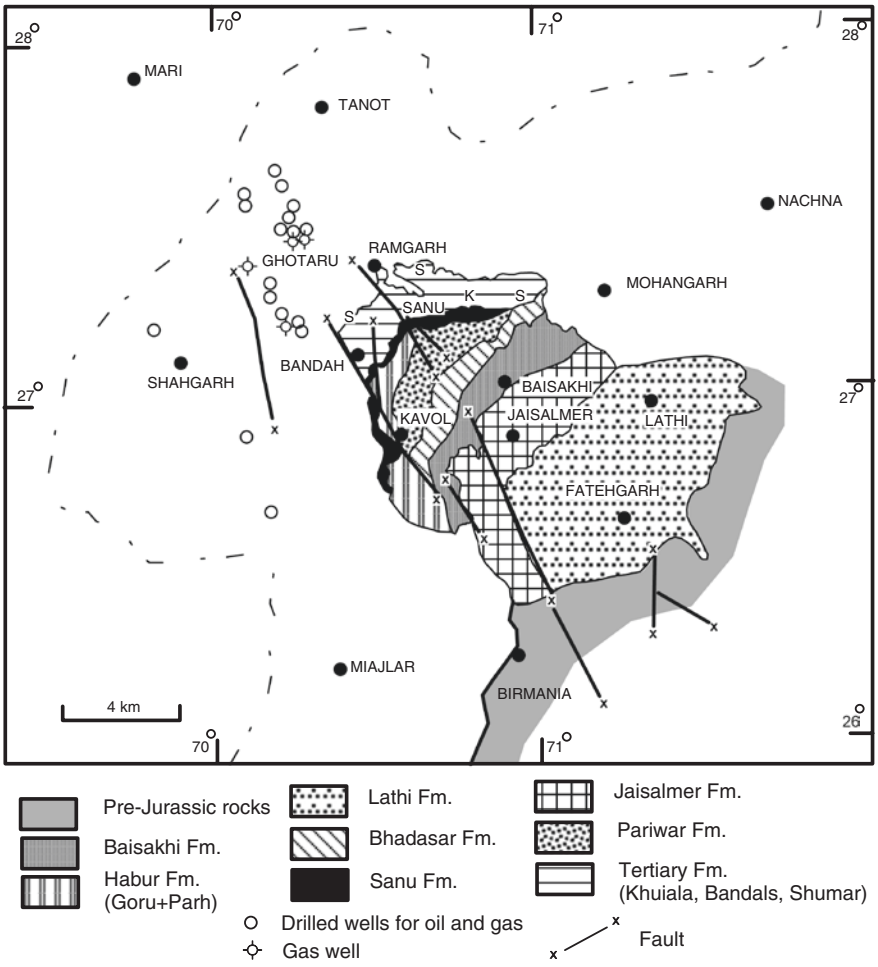

Fig. 15.13 Sketch map showing the Mesozoic formations of the Jaisalmer Basin and adjoining areas in western Rajasthan. Important structural lines delineate the tectonic boundaries (based on Singh 1996 and Sinha-Roy 1984)

the Jaisalmer Basin, the last one being pericratonic (Datta 1983). The Bikaner–Nagaur Basin is a Precambrian–Palaeozoic Basin, and the Barmer and Sancher basins evolved in the Middle Jurassic. In the Jaisalmer Basin (Fig. 15.13; Table 15.3), sedimentation commenced in the Permian time and continued throughout the Mesozoic and the Cenozoic. It may be pointed out that while the Barmer Basin in the south received its sediments dominated by heavy mineral hornblende from this Mewar–Marwar Ridge, the Jaisalmer Basin was fed by rivers draining the Jaipur–Ajabgarh–Alwar region of the central Aravali Range, as testified by staurolite, kyanite and garnet (Siddique 1963). The 1200-m-thick Jaisalmer succession on the continental shelf is characterized by several cycles of carbonate sedimentation.

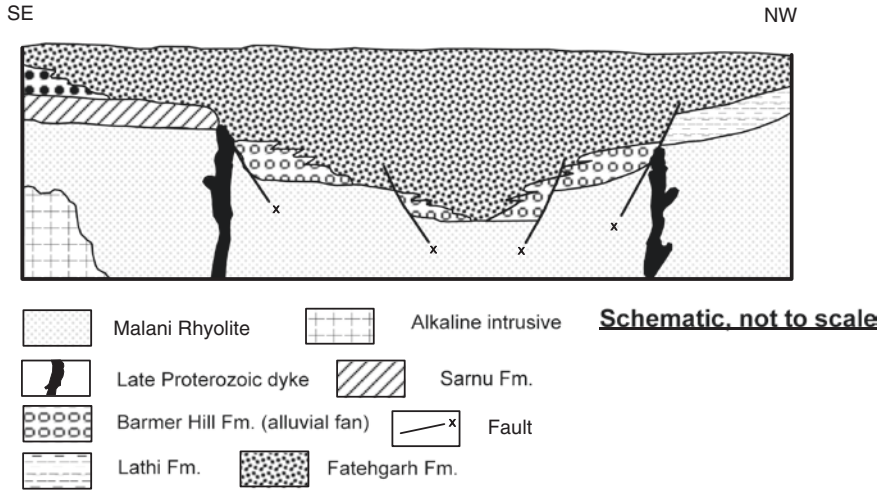

Fig. 15.14 Structure and lithostratigraphy of the Barmer Basin illustrates the pattern and sequence of the Mesozoic sedimentation in Rajasthan (after Sisodia and Singh 2000)

The Barmer Basin (Fig. 15.14) is a narrow N–S-oriented fault-lined depression. In the Barmer Basin, the Lower Cretaceous *Sarnu Formation* is exposed along the western-faulted margin. The horizon consists of dominant fine-grained to pebbly feldspathic sandstone with plant fossils (the Sarnu is unconformably overlain by Palaeocene Fatehgarh Formation). The intertidal to neritic shelf deposit at the base gives way upwards to a fining-upward succession of sandstone, locally ferruginous and phosphatic and containing fossil wood. Its upper part is made up of tidal-flat mud (Sisodia and Singh 2000).

In the Jaisalmer Basin (Fig. 15.13 and Table 15.3) overlying the Permian Karampura Formation, the *Shumarwali Formation* of the Triassic time comprises a sequence of fluvial to deltaic and shallow epineritic clastic sediments. The Early Jurassic *Lathi Formation* represents the continuation of the Triassic sedimentation nearly the same environment on an intertidal to neritic shelf. The sediments of the overlying *Jaisalmer Formation* were laid down on the extensive stable shelf, in which several cycles of carbonate depositions took place. The situation then changed, and sandstone–shale alternation of the *Baisakhi* and *Bhadasar formations* was laid down in the Upper Jurassic time. The Cretaceous period commences with the deposition of yellow brown siltstone–sandstone alternation, calcareous feldspathic sandstone and claystone (with a fossil of tree trunk) making up the *Pariwar Formation*. Palynomorph assemblage and arenaceous foraminifers indicate Neocomanian age of the deltaic sediments of the Pariwar Formation (Das Gupta 1975; Dave and Chatterjee 1996; Mehrotra et al. 2002). The overlying *Habur Formation* comprises alternation of cross-bedded calcareous sandstones and coquinoidal limestone, foraminiferal limestone and shale. This nearshore sequence is characterized by the Lower Aptian to Middle Albian ammonites and foraminifers (Krishna 1987). The succeeding *Goru*

Formation consists of greenish grey locally pyritous shale, and calcareous siltstone with marl. The glauconite grains give Rb–Sr age of 103.3 ± 3.0 Ma (Vijan et al. 2000) confirming the Albian age. The thick succession of argillaceous limestone and marl exposed in the Parh Hill in Sindh (Pakistan) and its subsurface easterly extension in western Rajasthan is known as the *Parh Formation*. The Parh contains Coniacian fossils (Mukherjee et al. 1995). At the top of the Cretaceous formation, the horizon described as "Siliceous Earth" contains volcanic ash made up of glass shards, agglutinates and hollow spheroids at Matti-ka-god and Ni-rich vesicular glass, sanidine spherules, magnesioferrite crystals with soot at Bariyara, implying an event that possibly could be related to the K–T boundary (Sisodia et al. 2005).

15.5 Northern Continental Margin

Even as a large part of the subcontinent including Saurashtra, Kachchh, Marwar, Meghalaya–Bengal and Coromandal coast came under the sway of sea water, the leading edge of the northward-moving India (which had been the site of sedimentation all through the Proterozoic and Palaeozoic) started to subside during the Cretaceous. The sea continued to deepen progressively along the northern periphery. In the deep sea were deposited siliceous and calcareous oozes and pelagic clays, giving rise to chert beds and limestones and shales. Phosphatic nodules and glauconite, occurring locally, indicate deep and cold water that was deficient in oxygen. Simultaneous with the subsidence of the northern edge of India, an oceanic trench started forming along the edge of the Tibetan landmass, and by the end of the Cretaceous the trench had become more than 2000 m deep.

The sinking of the seafloor was followed by its fissuring. Through the fissures came out lavas on a grand scale all along the tract. A chain of volcanic sea mounts and islands developed in front of the sinking continental margin of India. The arc-shape chain of volcanic island stretched from Kohistan in the west to Shigatse in the east. By then, the northward-moving Indian plate had come close to the Tibetan landmass of the Asian plate. In between lay the arcuate chain of volcanic islands and a trench filled with sediments.

This aspect is dealt with in Chaps. 16 and 17.

15.6 An Arm of Sea Inside Central India

Related to the regional Narmada graben, there were a number of linear depressions of the nature of half-graben in central India (Tripathi and Lahiri 2000). These were sites of fluvial sedimentation. Reactivation of faults caused downfaulting in the zone of the Narmada graben, inviting sea water from the west. In the Narmada Valley, the Upper Cretaceous is thus represented by the fluvial horizon succeeded by a marine formation.

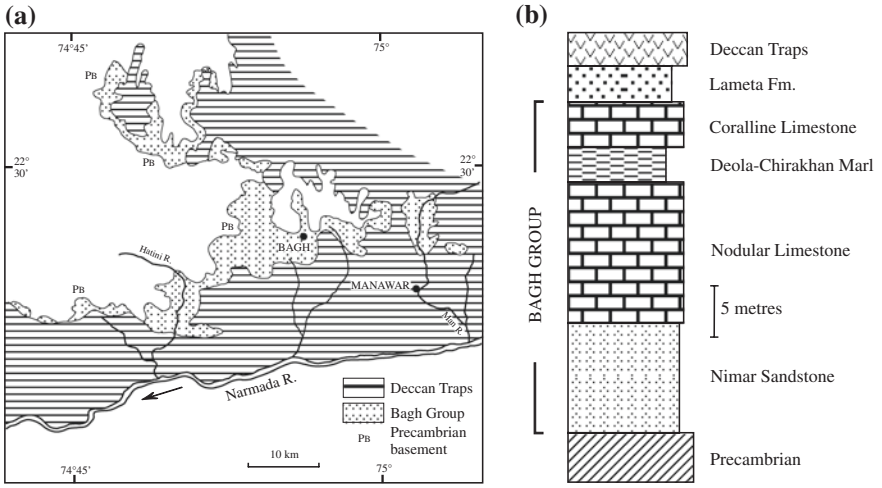

Fig. 15.15 **a** *Sketch map* showing the spread of the Bagh Beds, a Cretaceous formation in the Narmada Valley (after Tripathi and Lahiri 2000). **b** Lithology of the Bagh Beds as seen in the man river section near Deola (after Taylor and Badve 1995)

Outliers of conglomerate and gritty calcareous sandstones measuring a few tens to a few hundred metres in thickness were first described as the *Nimar Sandstone* by P.N. Bose in 1884 in the area of the famous Bagh Caves in the Narmada Valley. In and around Chakrud, polymictic conglomerate, strongly graded pebbly sandstone that is characterized by hummocky cross-bedding, and ripple-marked mudstone with limestone, bear testimony to the influence of alternating fair weather and storm conditions in the site of the Nimar sedimentation (Bose and Das 1986). Possibly tides were also active (Ahmad and Akhtar 1990; Akhtar and Ahmad 1991). The upward-fining sequence of the Nimar was laid down in freshwater, as carbon- and oxygen-isotopic composition of limestone indicates (Bhattacharya et al. 1997a, b). The Nimar Sandstone is succeeded by the *Karondia Limestone* representing a platform deposit formed on the ramp of the shelf dotted with islands in the subtidal zone (Akhtar and Khan 1997). The upper part of the sequence has yielded Cretaceous benthic foraminifers (Rajashekhar 1991) and nannoplankton species *Marthastenites furcatus* of the Turonian age (Jafar 1982).

The marine incursion in the Late Cretaceous is represented by small isolated outcrops of the *Bagh Beds* in the Dhar district, Madhya Pradesh (Fig. 15.15). W.T. Blanford gave the name in 1869. The group extends eastwards as far as Barwaha. The Bagh Beds unit comprises three formations (Fig. 15.15). The *Nodular Limestone* in the lower part is a clastic carbonate characterized by ripple marks formed in shallow-water environment (Singh and Srivastava 1981; Akhtar and Khan 1997), containing rich assemblages of pelecypods and gastropods (Chiplonkar et al. 1977; Chiplonkar 1959, 1987) and benthic foraminifers (Rajashekhar 1991). In the upper part near Kukshi, the Late Turonian marker

ammonite *Prionocyclus germari* occurs in the Hathni Valley (Kennedy et al. 2003). Essentially, a bryozoan carbonate horizon, the *Coralline Limestone* is characterized by the dominant bryozoan *Chiplonkarina dimorphora* of "Lower Cenomanian–Turonian age" (Taylor and Badve 1995).

The Bagh Beds give way upwards to feldspathic arenite and carbonates—recognized as the Lameta Formation of lacustrine origin. The Lameta has been discussed in detail in Chap. 14.

15.7 Mesozoic Panorama of Marine Life

15.7.1 Prolific and Diverse Life

As a consequence of Hercynian tectonic upheaval towards the end of the Permian, the sea withdrew from a large part of the continental margin the resultant reduction of environmental niches caused decline in the population of marine invertebrates and extinction of many. The Late Permian was a time of large-scale extinction of marine life all over the world (Kummel 1961). But the return of the sea in the Jurassic and Cretaceous periods over much larger areas of the Indian continental margin, as already elaborated, enlarged the areal extent of the habitats of the marine communities. Availability of diverse niches promoted vigorous growth and proliferation of life in the Mesozoic. By the Middle Triassic, the marine fauna became extremely prolific and diverse, particularly in the Himalayan domain belonging to the Tethyan faunal province. And this trend continued till the end of Cretaceous.

15.7.2 Age of Ammonites

One among the cephalopods, the ammonites dominated marine fauna of the Triassic time. Not only were they abundant and widespread but also very diverse in spite of three extinctions they suffered before their final disappearance at the end of the Cretaceous. Each time, the surviving stock evolved to more diverse and more abundant forms, far grander in scale than that of the previous period (Kummel 1961). The size of ammonites ranged from 2.7 m to a few millimetres, and the shape varied from flat, globular, loosely coiled to tightly coiled shell. *Turrilites* was an uncoiled ammonite, and *Acanthoceras* developed spines on their shell for self-defence. The Early Triassic ammonites were unoriented forms with rather simple ceratitic sutures. The Middle Triassic forms were highly ornamented with ribs or nodes or both giving rise to ammonite sutures. They persisted towards the end of the Triassic, giving way to those who had more complex pattern of development—the lytoceratids and phylloceratids peopling the Himalayan domain.

The nautiloids evolved slowly and became highly specialized in ornamentation and pattern of suture during the Late Triassic. Only one group of nautiloids survived extinction, and it produced great number of species belonging to *Nautilus* in the Jurassic. In the Jurassic and Cretaceous, the belemnoids became abundantly widespread.

15.7.3 Reef Builders and Associated Invertebrates

The pelecypods became very widespread and diverse in the Mesozoic era. The important forms include *Monotis, Exogyra, Gryphaea, Mytilus, Hippurites, Trigonia, Inoceraus, Pecten* and *Ostrea.* One group of pelecypods—the rudistids—became attached to the bottom and built reefs in shallow warm waters. Likewise, corals built conspicuous reefs. The reef-building corals belonged to the order *Sclerictinia*, which first appeared in the Middle Jurassic and became dominant by the Late Jurassic and in the Cretaceous. Echinoderms became very abundant and diverse in the later part of the Mesozoic. Rare in the Triassic, the bryozoans increased in number appreciably during the Jurassic and Cretaceous times. There was explosive growth of planktonic foraminifers during this period. First appearing in the Triassic, the phytoplankton Coccolithophores (made up of calcareous microscopic plates) proliferated greatly and eventually formed the famous chalk beds of the Cretaceous. The siliceous diatoms and the dinoflagellates evolved and increased in number and varieties in cooler waters during the Cretaceous.

15.7.4 Marine Vertebrates

In the Early Permian seas lived small reptiles having slender long body, small neck, teeth-bearing jaws and paddle-like short legs. The *Mesosaurus* was the oldest aquatic reptile. By the Late Cretaceous, they had grown in size—as much as 25–9 m in length. The *Pleisiosurus* was 3.5–6 m long. And *Ichthyosaurus* measured 3 m in length having a streamlined body, flipper-like forelimbs and powerful tail for propulsion.

Among fish, the lung fish crossopterigians were important. By the Late Cretaceous, the advanced group of fish teleosts became dominant. Shark-like fish *Otodus, Pycnodus* and *Ptychodus* were common in the Trichinopoly Formation.

Labyrinthodonts, represented by *Archegosaurus*, possessed crocodile-like long snout, and their eyes were surrounded by rings of long plates, and the body was covered with overlapping scales. *Archegosaurus* occurs in the Triassic of Kashmir of the Tethyan domain. It was a contemporary of *Gondwanasaurus* which lived in the Panchet Basin near Pachmarhi in Madhya Pradesh.

References

Agrawal, S. K. (1957). Kutch Mesozoic. A study of the Jurassic of Kutch with special reference to Jhura dome. *Journal of the Palaeontological Society of India, 2*, 119–130.

Agrawal, R. K. (1977). Structure and tectonics of Indo-Gangetic plain. In V. L. S. Bhimasankaram (Ed.), *Geophysical Case Histories* (pp. 27–48). Hyderabad: Association of Exploration Geophysicists.

Agrawal, S. K. (1981). Kachchh Mesozoic: Some problems and recent contributions. *Recent Researches in Geology, 4*, 482–492.

Ahmad, A. H. M. & Akhtar, K. (1990). Clastic environments and facies of the Lower Cretaceous Narmada basin, India. *Journal Sedimentary Petroleum*.

Akhtar, K., & Ahmad, A. H. M. (1991). Single cycle cratonic quartzarenites produced by tropical weathering: The Nimar Sandstone (Lower Cretaceous) Narmada Basin, India. *Sedimentary Geology, 71*, 23–32.

Akhtar, K., & Khan, D. A. (1997). A tidal island model for carbonate sedimentation: Karondia limestone of Cretaceous Narmada basin, India. *Journal-Geological Society of India, 50*, 481–489.

Alam, M. (1989). Geology and depositional history of Cenozoic sediments of the Bengal Basin of Bangladesh. *Palaeogeography, Palaeoclimatology, Palaeoecology, 69*, 125–139.

Alam, M., Alam, M. M., Curray, J. R., Chowdhury, M. L. R., & Gani, M. R. (2003). An overview of sedimentary geology of the Bengal basin in relation to the regional framework abd basin-fill history. *Sedimentary Geology, 155*, 179–208.

Aslam, M. (1992). Delta plain coal deposits from the Thar formation of the early Cretaceous Saurashtra basin Gujarat, Western India. *Sedimentary Geology, 81*, 181–193.

Bandyopadhyay, A. (2004). Sedimentation, tectonics and palaeoenvironment in eastern Kachchh, Gujarat. *Journal-Geological Society of India, 63*, 171–182.

Banerji, R. K. (1970). On the stratigraphy and microplaeontology of Dalmiapuram formation (Lower Cretaceous)—a new rock-stratigraphic unit of South India. *Journal of the Palaeontological Society of India, 15*, 32–41.

Banerjee, R. K. (1982). Sivaganga formation, its sedimentology, micropalaeontology and sedimentation history. *Journal-Geological Society of India, 23*, 450–457.

Banerji, R. K. (1972). Stratigraphy and micropalaeontology of the Cauvery basin, part I, exposed area. *Journal of the Palaeontological Society of India, 17*, 7–30.

Banerji, R. K., Ramaswamy, S., Malini, C. S., & Singh, D. (1996). Uttatur group redefined. *Memoirs-Geological Society of India, 37*, 213–299.

Bhatia, S. B., & Jain, S. P. (1969). Dalmiapuram formation: A new Lower Cretaceous horizon in South India. *Bulletin Indian Geologists' Association, 2*, 105–109.

Bhattacharya, S. K., Jani, R. A., Tripathi, S. C., & Lahiri, T. C. (1997a). Carbon and oxygen isotopic composition of Intertrappean limestones from Central and Western India and their depositional environment. *Journal-Geological Society of India, 50*, 289–296.

Bhattacharya, A., Nandi, A., & Dutta, A. (1997b). Triassic mega- and micro-plant fossils from the Kamthi formation of Talchir coalfield, Orissa, with chronological significance. *Special Publication of Geological Survey of India, 54*, 123–126.

Biswas, S. K. (1982). Rift basins in western margin of India and their hydrocarbon prospect, with special reference to Kutch. *Bulletin of American Association Petroleum Geological, 66*, 1497–1513.

Biswas, S. K. (1987). Regional tectonic framework, structure and evolution of the western marginal basins of India. *Tectonophysics, 135*, 307–327.

Biswas, S. K. (1992). Tertiary stratigraphy of Kutch. *Journal of the Palaeontological Society of India, 37*, 1–29.

Biswas, S. K. (2003). Regional tectonic framework of the Pranhita–Godavari basin, India. *Journal of Asian Earth Sciences, 21*, 543–551.

Biswas, S. K. (2005). A review of structure and tectonics of Kutch basin, Western India, with special reference to earthquakes. *Current Science, 88*, 1592–1600.

Biswas, S. K., & Deshpande, S. V. (1983). Geology and hydrocarbon prospects of Kutch, Saurashtra and Narmada basin. In L. L. Bhandari, et al. (Eds.), *Petroliferous Basins of India* (pp. 111–126). Dehradun: KDM Institute of Petroleum Exploration.

Borkar, V. D. (1973). New fossil fishes from the intertrappean beds of Surendranagar District, Gujarat State. *Current Science, 42*, 12.

Bose, P. K., & Das, N. G. (1986). A transgressive storm- and fair-weather wave dominated shelf sequence: Cretaceous Nimar formation Chakrud, Madhya Pradesh, India. *Sedimentary Geology, 46*, 147–167.

Bose, P. K., Shome, S., Bardhan, S., & Ghosh, G. (1986). Facies mosaic in the Ghuneri member (Jurassic) of the Bhuj formation Kutch, Western India. *Sedimentary Geology, 46*, 293–309.

Casshyap, S. M., & Aslam, M. (1992). Deltaic and shoreline sedimentations in Saurashtra basin, Western India: An example of infilling in an early Cretaceous failed rift. *Journal of Sedimentary Petrology, 62*, 972–991.

Chandra, K., Srivastava, D. C., Sharma, R. & Pal, M. (1994). Hydrocarbon prospects and status of exploration in Gondwana basins of India. *Proceedings of the International Gondwana Symposium* (pp. 1177–1197). New Delhi: Oxford-IBH.

Chiplonkar, G. W. (1959). Bryozoa from the Bagh Beds. *Proceedings of the Indian Academy Science* (*Earth and Planet Science*), *10B*, 98–109.

Chiplonkar, G. W. (1987). Three decades of invertebrate palaeontology and biostratigraphy of marine Cretaceous rocks of India. *Special Publication of Geological Survey of India, 2*(1), 305–339.

Chiplonkar, G. W., Ghare, M. A., & Badwe, R. M. (1977). Bagh Beds—their fauna, age and affinities: A retrospect and prospect. *Biovigyanum, 3*, 33–60.

Chitra Rao, A. M., & Asthana, M. (2000). Cretaceous valley fill sandstone of Nandigama area, Krishna–Godavari basin, A.P. *Journal-Geological Society of India, 56*, 27–38.

Das Gupta, S. K. (1975). A revision of the Mesozoic-tertiary stratigraphy of the Jaisalmer basin, Rajasthan. *Indian Journal of Earth Science, 2*, 77–94.

Dasgupta, K., Saraswati, P. K., Kramar, U., Ravindran, C. N., Stuben, D., & Berner, Z. (2006). *Oxygen Isotopic Composition of Albanian–Turonian foraminifera from Cauvery basin, India: Evidence of warm sea surface temperature*. Soc: Journal Geological. 66.

Datta, A. K. (1983). Geological evolution and hydrocarbon prospects of Rajasthan basin. *Petroleum Asia Journal* (pp. 93–100). Dehradun: ONGC.

Dave, A., & Chatterjee, K. (1996). Integrated foraminiferal and ammonoid biostratigraphy of Jurassic sediments in Jaisalmer basin, Rajasthan. *Journal-Geological Society of India, 47*, 477–490.

Govindan, A., Ananthanarayanan, S., & Vijayalakshmi, K. G. (2000). Cretaceous petroleum system in Cauvery basin, India. *Memoirs-Geological Society of India, 46*, 365–382.

Jafar, S. A. (1982). Nannoplankton evidence of Turonian transgression along Narmada valley, India and Turonian–Coniacian boundary problem. *Journal of the Palaeontological Society of India, 27*, 17–30.

Jafar, S. A. (1996). The evolution of marine Cretaceous basins of India: Calibration with nannofossil zones. *Journal-Geological Society of India, 37*, 121–134.

Jain, S. P. (1968). Ostracodes from the pre-Cretaceous grey shales of Dalmiapuram, South India. *Bulletin Industrial Geologists' Association, 2*, 70–71.

Johnson, S. Y., & Alam, A. M. N. (1991). Sedimentation and tectonics of the Sylhet through, Bangladesh. *Geological Society of America Bulletin, 103*, 1513–1527.

Kak, S. N., & Subrahmanyam, A. V. (2002). Depositional environment and age of Mahadek formation of Wahblei river section, West Khasi Hills, Meghalaya. *Journal-Geological Society of India, 60*, 151–162.

Kapoor, P. N., Prasad, B., Swamy, S. N., & Shukla, S. D. (1999). Palynostratigraphy and hydrocarbon source potential of Cretaceous sediments in Krishna subregion India. *Geoscience Journal, 20*, 21–24.

Kennedy, W. J., & Henderson, R. A. (1992). Non-heteromorph ammonites from the upper Maastrichtian of Pondicherry South India. *Palaeontology, 35*, 381–442.

Kennedy, W. J., Phansalkar, V. G., & Walaszczyk, T. (2003). *Prionocyclus germari* (Reuss 1845), a late Turonian marker fossil from the Bagh Beds of Central India. *Cretaceous Research, 24*, 433–438.

Khan, A. A., Sattar, G. S. & Rahman, T. (1994). Tectogenesis of the Gondwana rifted basins of Bangladesh in the so-called Garo–Rajmahal Gap and their pre-drift regional tectonic correlation. *Proceedings of the 9th International Gondwana Symposium* (pp. 647–655). New Delhi: Oxford-IBH.

Khan, A. A., Sattar, G. S. & Rahman, T. (1996). Technogenesis of the Gondwana rifted basins of Bangladesh in the so-called Garo–Rajmahal gap and their pre-drift regional tectonic correlation. *Ninth International Gondwana Symposium* (Vol. 2, pp. 647–656). Hyderabad: Geological Survey of India.

Krishna, J. (1987). An overview of the Mesozoic stratigraphy of Kachchh and Jaisalmer basins. *Journal of the Palaeontological Society of India, 32*, 136–152.

Krishna, J. (1991). Discovery of Lower Berriasian (Lower Cretaceous) ammonoid genus Argentiniceras from Kachchh (India) and its relevance to Jurassic-Cretaceous boundary. *Newsletter Stratigraphy, 23*, 141–150.

Krishna, J., & Cariou, E. (1986). The Callovian of Western India: New data on the biostratigraphy of the ammonites and correlation with Western Europe. *Newsletter Stratigraphy, 17*, 1–8.

Krishna, J., Pathak, D. B., & Pandey, B. (1998). Development of Oxfordian (Early Upper Jurassic) in the most proximately exposed part of the Kachchh Basin at Wagad outside the Kachchh mainland. *Journal-Geological Society of India, 52*, 513–522.

Krishna, J., Singh, I. B., Howard, J. D., & Jafar, S. A. (1983). Implications of new data on Mesozoic rocks of Kachchh Western India. *Nature, 205*, 790–792.

Kummel, B. (1961). *History of the Earth: An introduction to historical geology* (p. 610). Delhi: Eurasia Publishing House.

Kumaraguru, P. & Trivikram Rao, A. (1994). A reappraisal of the geology and tectonics of the Palar basin sediments, Tamilnadu. *Proceedings of the 9th International Gondwana Symposium* (pp. 821–831), New Delhi: Oxford-IBH.

Maithani, P. B., Taneja, P. C., & Singh, R. (1995). A sandstone-type uranium deposit at Phlangdiloin, West Khasi Hills, Meghalaya. *Journal Atomic Minerals Science, 3*, 45–60.

Majumdar, S. K., Basu, B., Shivashankar, J., Arunachalam, A. & Rangaraju, M. K. (1995). Palakollu–Pasarlapudi petroleum system, Krishna–Godavari basin, India. In *Proceedings of the Petrotech-5: Technology Trends in Petroleum Industry* (pp. 495–508). New Delhi: B.R. Publishing Corporation.

Mamallan, R., Kumar, D., & Bajpai, R. K. (1994). Jasra ultramafic–mafic–alkaline complex: A new find in the Shillong Plateau NE India. *Current Science, 66*, 64–65.

Mamgain, V. D., Sastry, M. V. A., & Subbaraman, J. V. (1973). Report of ammonites from Gondwana plant beds at Terani, Tiruchirapalli. *Journal-Geological Society of India, 14*, 198–210.

Manmohan, M., Rao, M. R. R., Kamaraju, A. V. V. S., & Yalamarty, S. S. (2003). Origin and occurrence of Lower Cretaceous high-gamma-high-resistivity Raghavapuram Shale—a key stratigraphic sequence for hydrocarbon exploration in Krishna–Godavari basin, A.P. *Journal-Geological Society of India, 62*, 271–289.

Mehrotra, N. C., Venkatachala, B. S., Swamy, S. N., & Kapoor, P. N. (2002). *Palynology in Hydrocarbon Exploration* (p. 159). Bangalore: Geological Society of India.

Mishra, U. K., & Sen, S. (2004). Dinosaur remains from Dirang, West Khasi Hills district, Meghalaya. *Journal of the Geological Society of India, 63*, 9–14.

Mishra, B., Pandya, K. L., & Maejima, W. (2004). Alluvial fan-lacustrine sedimentation and its tectonic implications in the Cretaceous Athgarh Gondwana basin Orissa, India. *Gondwana Research, 7*, 375–385.

Mukherjee, M. K., Bhandari, S. K. & Purkayastha, D. (1995). Hydrocarbon prospects and evidence of presence of Proterozoic basin in Lunar–Miajlar area, Rajasthan. *Proceedings of the International Petroleum Conference* (pp. 133–164). New Delhi: B.R. Publishing Corporation.

ONGC. (1993). *Lithostratigraphy of Indian Petroliferous Basins*. Dehradun: KDM Institute of Petroleum Exploration. 11.

Pandey, J., & Dave, A. (1998). *Stratigraphy of Indian Petroliferous Basins* (p. 248). Dona Paula: National Institute of Oceanography.

Patra, B. P. (1973). Notes on some Upper Gondwana plants from Athgarh sandstone, District Cuttack Orissa. *Palaeobotanist, 20*, 325–333.

Prabakaran, S. & Ramesh, P. (1995). Basin evolution, stratigraphy and depositional systems in Krishna–Godavari basin, India. In *Proceedings of the Petrotech-5: Technology Trends in Petroleum Industry* (pp. 229–249). New Delhi: B.R. Publishing Corporation.

Prasad, B., & Pundir, B. S. (1999). Biostratigraphy of the exposed Gondwana and Cretaceous rock of Krishna–Godavari basin, India. *Journal of the Palaeontological Society of India, 44*, 91–117.

Rajashekhar, C. (1991). Foraminifera from the Nodular limestone, Bagh Beds, Madhya Pradesh, India. *Journal-Geological Society of India, 38*, 151–168.

Raju, D. S. N. & Mishra, P. K. (1996). Cretaceous stratigraphy of India: A review. In: A. Sahni (Ed.), *Cretaceous Stratigraphy and Palaeoenvironments* (L. Rama Rao volume) (Vol. 37, pp. 1–34). Bangalore: Geological Society of India.

Raju, D. S. N., Ramesh, P., Mohan, S. G. K. & Uppal, S. (2002). Sequence and bio-chronostratigraphic subdividions of the Cretaceous and Cenozoic of India—with notes on Pre-Cretaceous events: An overview. *First Association of Petroleum Geologists Conference, Mussoorie* (pp. 119–129).

Ramkumar, M., Stuben, D., Berner, Z., & Schneider, J. (2004). Geochemical and isotopic anomalies preceding K/T boundary in the Cauvery basin, South India: Implications and Cretaceous events. *Current Science, 87*, 1738–1746.

Ramkumar, M., Subramanian, V., & Stuben, D. (2005). Deltaic sedimentation during Cretaceous period in the northern Cauvery basin, South India: Facies architecture, depositional history and sequence stratigraphy. *Journal-Geological Society of India, 66*, 81–94.

Rao, G. N. (2001). Sedimentation, stratigraphy, and petroleum potential of Krishna–Godavari basins, East Coast of India. *American Association of Petroleum Geologists Bulletin, 85*, 1623–1643.

Rao, G. N. (2002). Petroleum Geology: Krishna–Godavari basin. *Journal-Geological Society of India, 60*, 705–706.

Ray, J. S. & Pande, K. (2001). ^{40}AR–^{39}Ar age of carbonatite–alkaline magmatism in Sung Valley, Meghalaya, India. *Proceedings of the Indian Academic Science* (*Earth and Planetary Science*), *110*, 185–190.

Ray, A., Patil, S. K., Paul, D. K., Biswas, S. K., Das, B., & Pant, N. C. (2006). Petrology, geochemistry and magnetic properties of Sadara Sill: Evidence of rift related magmatism from Kutch basin, Northwestern India. *Journal of Asian Earth Sciences, 27*, 907–921.

Reimann, K.-U. (1993). *Geology of Bangladesh*. Berlin: Gebrüder Borntraeger. 160 p.

Roybarman, A. (1992). Geological history and hydrocarbon exploration in Bengal basin, India. *Journal Geological, 64*, 235–238.

Sastry, M. V. A., Mamgain, V. D., & Rao, B. R. J. (1968). Biostratigraphic zonation of upper Cretaceous formation of Trichinopoly District, South India. *Memoirs Geological Society of India, 2*, 10–17.

Sastry, V. V., Raju, A. T. R., Sinha, R. N., Venkatachala, B. S., & Banerjee, R. K. (1977). Biostratigraphy and evolution of the Cauvery basin, India. *Journal-Geological Society of India, 18*, 355–377.

Sastry, V. V., Sinha, R. N., Singh, G., & Murti, K. (1973). Stratigraphy and tectonics of sedimentary basins of east coast of Peninsular India. *American Association of Petroleum Geology, 74*, 655–678.

Sengupta, B., Bahuguna, R., Kumar, S., Singh, R., & Kaul, R. (1991). Sandstone-type uranium deposit at Domiasiat West Khasi Hills District, Meghalaya, Northeastern Indian. *Current Science, 61*, 46–47.

Siddique, H. N. (1963). The Jodhpur-Malani divide separating the Barmer and Jaisalmer basins. *Journal-Geological Society of India, 4*, 97–108.

Singh, R. (1992). Evolution of exploration concepts for sandstone-type uranium deposits in Meghalaya, India. *Journal Atomic Minerals Science, 5*, 1–11.

Singh, M. P. (1996). Mesozoic–Tertiary biostratigraphy and biogeochronological dalum planes in Jaisalmer Basin, Rajasthan, In: J. Pandey, R. J. Azmi, A. Bhandari, & A. Dave (Eds.) *Contrib. XV Indian Colloquium on Micropalaeontology and Stratigraphy*. Dehradun: KDMIPE, WIHG Publication.

Sinha-Roy, S. (1984). Precambrian crustal interaction in Rajasthan, NW India. *Indian Journal of Earth Sciences,* CISM Volume, 84–91.

Singh, S. K., & Srivastava, H. K. (1981). Lithostratigraphy of Bagh Beds and its correlation with Lameta Beds. *Journal of the Palaeontological Society of India, 26*, 77–85.

Sisodia, M. S., & Singh, U. K. (2000). Depositional environment and hydrocarbon prospects of the Barmer basin Rajasthan. *NAFTA, 9*, 309–326.

Sisodia, M. S., Singh, U. K., Lashkari, G., Shukla, P. N., Shukla, A. D., & Bhandari, N. (2005). Mineralogy and trace element chemistry of the siliceous earth of Barmer basin, Rajasthan: Evidence for a volcanic origin. *Journal Earth System Science, 114*, 111–124.

Srivastava, R. K., Mohan, A., & Filho, C. F. F. (2005). Hot-fluid driven metasomatism of Samalpatti carbonatites South India, evidence for mineral chemistry, trace elements and stable istotope composition. *Gondwana Research, 8*, 77–85.

Srivastava, R. K., & Sinha, A. K. (2004a). Geochemistry of early Cretaceous alkaline ultramafic–mafic complex from Jasra Karbi Aglong District Shillong Plateau, Northern India. *Gondwana Research, 7*, 549–561.

Srivastava, R. K., & Sinha, A. K. (2004b). Early Cretaceous Sung valley ultramafic-alkaline-carbonatite complex, Shillong Plateau, Northeastern India: Petrological and genetic significance. *Contribution Mineralogy and Petrology, 80*, 241–263.

Steinhoff, D., & Bandel, K. (2000). Palaeoenvironmental significance of early to middle Cretaceous bioherm sequences from the Thiruchirapalli District, Tamilnadu, Southeastern India. *Memoirs-Geological Society of India, 46*, 257–271.

Sundaram, R., Handerson, R. A., Ayyaasami, K., & Stilwell, J. D. (2001). A lithostratigraphic revision and palaeoenvironmental assessment of the Cretaceous system exposed in the onshore Cauvery basin, Southern India. *Cretaceous Research, 22*, 743–762.

Taylor, P. D., & Badve, R. M. (1995). A new chelostone bryozoan from the Cretaceous of India and Europe: A cyclostome homeomorph. *Palaeontology, 38*, 627–657.

Tripathi, S. C., & Lahiri, T. C. (2000). Marine oscillation event stratification: An example from Late Cretaceous Bagh carbonate sequence of Narmada valley, India. *Memoirs Geological Society of India, 46*, 15–24.

Venkatachala, B. S. (1977). Fossil floral assemblage in the east coast Gondwana—critical review. *Journal-Geological Society of India, 18*, 378–379.

Vijan, A. R., Rathore, S. S., Vig, K. C., Bansal, M., Singh, M. P., & Prabhu, B. N. (2000). K–Ar and Rb–Sr ages of Cretaceous glauconites from Jaisalmer basin, Rajasthan. *Journal-Geological Society of India, 56*, 15–25.

Yadagiri, K., & Govindan, A. (2000). Cretaceous carbonate platforms in Cauvery basin: Sedimentology, depositional setting and subsurface signatures. *Memoirs-Geological Society of India, 46*, 323–344.

Chapter 16
Northern and North-western Continental Margin: Mesozoic Stratigraphy

16.1 Tectonics

The impact of the breaking of the Gondwanaland Supercontinent in the Lower Permian was the subsidence of the margin of the Indian crust and its stretching and followed by effusion of lavas in many sectors. The culmination of these phenomena was the opening of a new ocean the *NeoTethys* in the latest Upper Permian. Later, the West Gondwanaland separated from the East Gondwanaland during the Middle to Upper Jurassic time. And within the East Gondwanaland assembly, Australia broke away from Antarctica in the Middle Cretaceous time. The reorganization of the East Gondwanaland (Fig. 16.1) from the Upper Jurassic (Kimmeridgian) onwards had profound impact on the nature and extent of sedimentation on the subsiding northern and north-western continental margin. As each time a continental block moved away, there was uplift, presumably due to doming up due to heating (Durr and Gibling 1994) and attendant exhumation and accelerated erosion. More erosion meant more terrestrial detritus that rivers carried to the NeoTethys Sea. The result was frequent inter-banding of terrestrial sediments with marine material in the Tethyan domain.

On the steadily subsiding shelf and slope of the NeoTethys, there was, in general, practically uninterrupted accumulation of sediments all along the periphery of the Indian continental margin—from Kachchh, through Jaisalmer and Ladakh to Kampa–Gyantse in southern Tibet (Fig. 16.2). Latitudinal changes of the northward-moving India exercised strong control on the nature and pattern of sedimentation. Besides, local factors like entry of terrestrial detritus due to accelerated erosion in uplifted belts and volcanism in some sectors had a control on the facies variation of the accumulating sediments on the shelves and slopes. One of the most remarkable features of the Mesozoic stratigraphy of the Tethyan domain

K.S. Valdiya, *The Making of India*, Society of Earth Scientists Series,
DOI 10.1007/978-3-319-25029-8_16

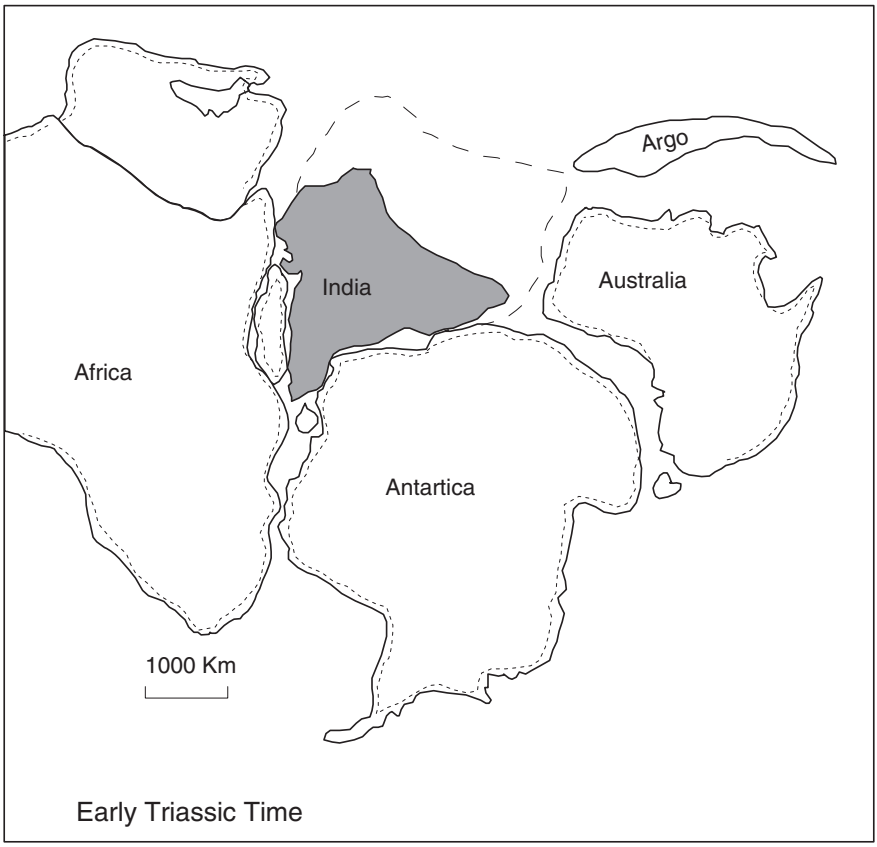

Fig. 16.1 Positions of continents in the East Gondwanaland in the Early Triassic time (Ogg and Rad 1994)

is the near-uniformity of sequence and facies variation (Fig. 16.3), implying similarity of tectonic conditions prevailing over more than 2000 km expanse of the Tethyan domain.

16.2 Biotic Communities: Profound Change

The dawn of the Mesozoic era witnessed a profound change in biotic communities. Towards the end of the Permian (nearly 250 million years ago) something extraordinary happened. High anomalies of europium (11.9) and cerium (1.4) in the

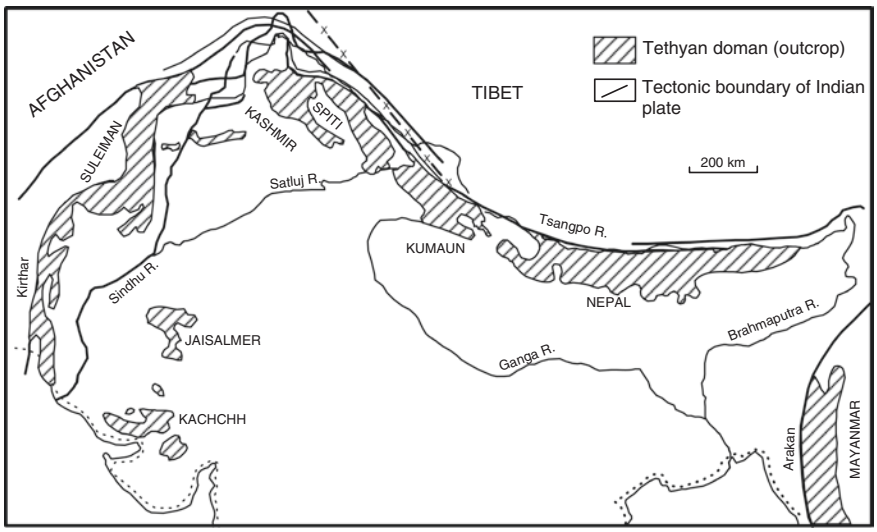

Fig. 16.2 Sketch map of northern and north-western continental margin of India showing the extent of the Tethyan domain encompassing Mesozoic sedimentary succession (based on Gansser 1964)

limonitic sediments at the base of the Triassic succession in the Spiti area (Bhandari et al. 1993) implies that certain unusual event had occurred. Simultaneously, the sea vacated some parts of the continental margin, exposing rocks to erosion and weathering, and allowing formation of red lateritic soil, as seen in the Lilang area in the Spiti Basin (Garzanti 1999). One of the consequences of this worldwide sea-level change was the loss of original niches or places and development of new habitats of life. It was inevitable that the fauna suffered stresses. The brachiopods, which were pre-eminent among the marine fauna in the Permian, were relegated to very insignificant position by the ammonites in the Triassic. And the lamellibranchs became important once again.

There is also a view that the mass extinction in the latest Permian–earliest Triassic interval was associated with a change in climate and resultant oceanic productivity, perhaps due to increase in carbon dioxide level in the atmosphere, and consequent production of warm saline bottom waters poor in oxygen. The excess CO_2 is attributed to stupendous volcanism in Siberia. In the Salt Range (Pakistan), the extinction of marine invertebrates is ascribed to widespread development of inhospitable conditions of deficiency in oxygen and resultant deterioration in the shallow marine shelf during the Griesbachian interval (Wingnall and Hallam 1993).

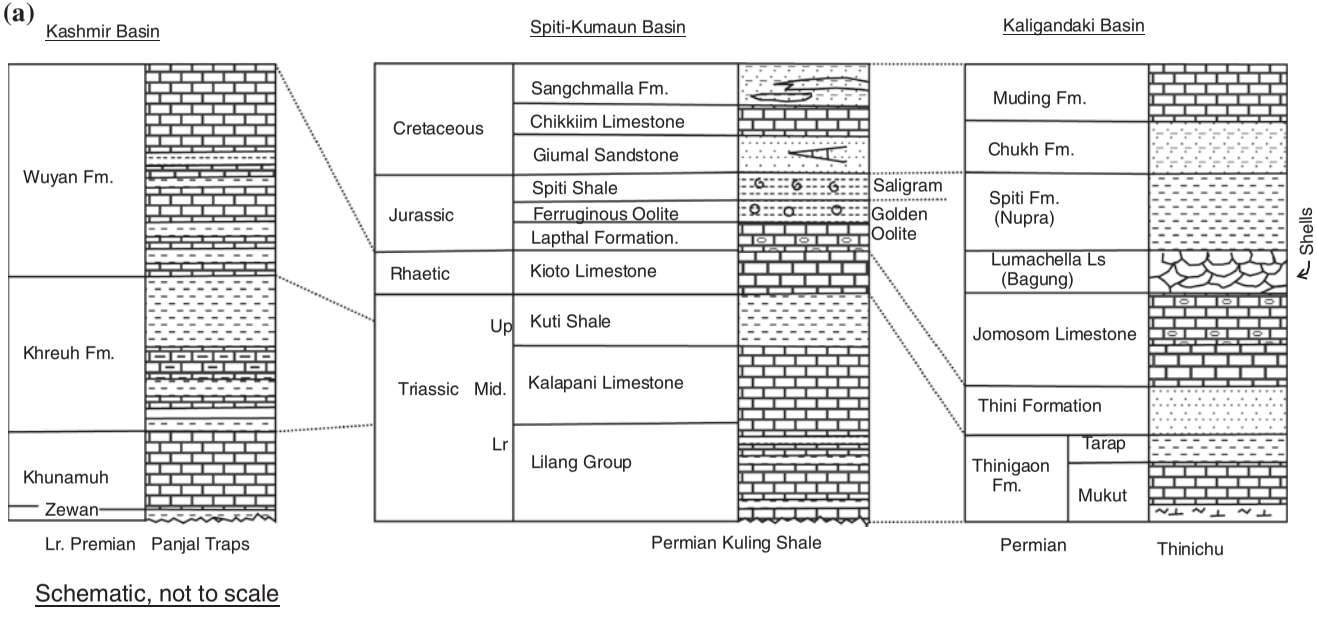

Fig. 16.3 Generalized lithostratigraphic columns of the Mesozoic successions in a northern and north-western continental margin of India. **a** Main Himalayan Belt. **b** The Pakistan Himalaya

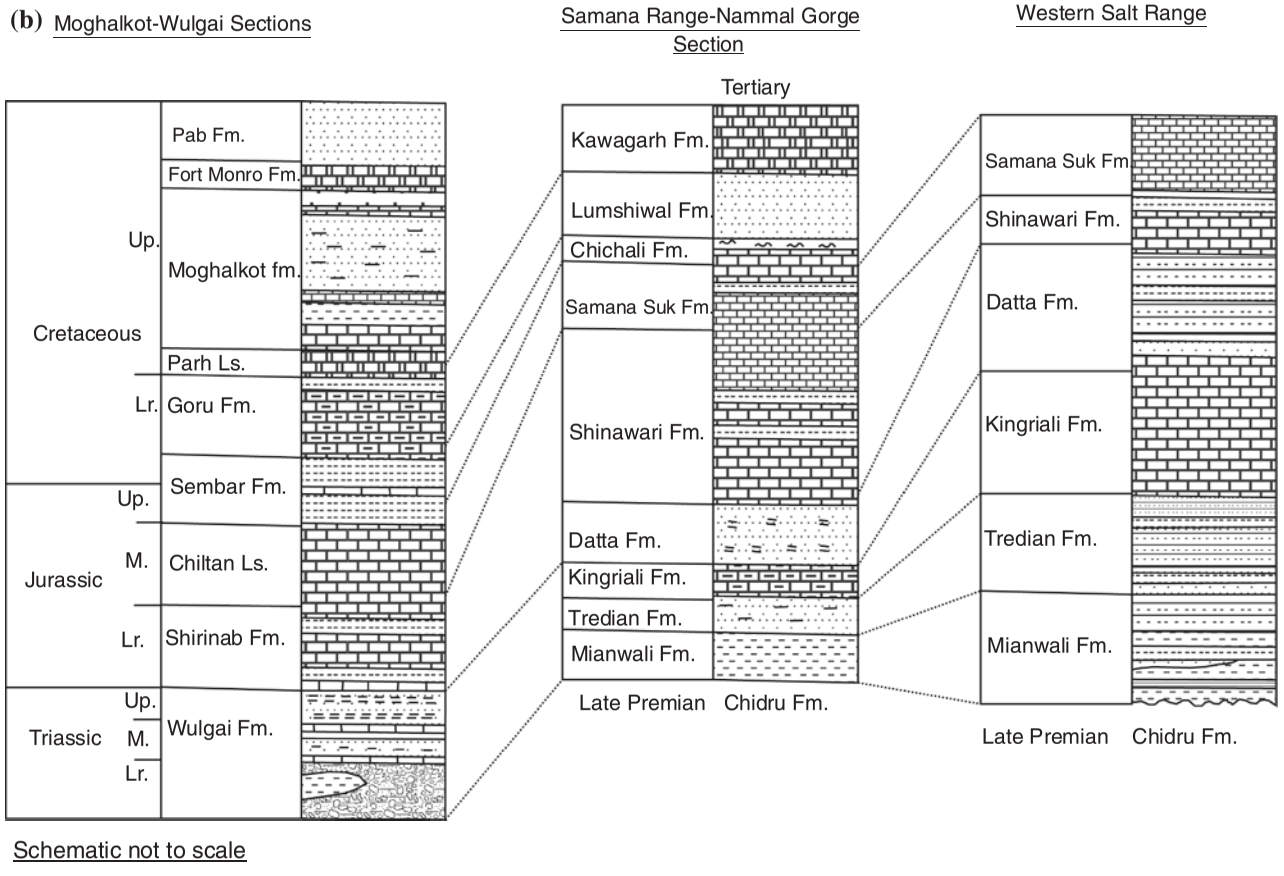

Fig. 16.3 (continued)

16.3 Stratigraphy and Sedimentation

16.3.1 Type Areas

The Mesozoic palaeogeography of the continental margin in north and north-west embraces presently isolated basins of the *NeoTethys* in north-central Nepal, Sikkim, Bhutan and adjoining Tibet, north-eastern Kumaun, Spiti–Lahul–Tandi, southern Zanskar in Himachal Pradesh, central Kashmir, Hazara–Potwar–Kohat in northern Pakistan, the Salt Range in west-central Pakistan and the Sulaiman–Kirthar–Balochistan ranges west of the lower Indus Basin (Fig. 16.3a, b; Table 16.1). The Mesozoic succession resting upon the Permian rocks begins seemingly without break in most of these sectors. However, considering the Hercynian tectonic upheaval, widespread volcanic activity on a big scale and the considerable faunal turnover that is, drastic change and replacement of forms during the interval of the Permian–Triassic transition, the conformable succession of sediments seems to be apparent, not real. This is borne out from the absence of the Lower and Middle Triassic in many areas, and the presence of red soils and/or conglomeratic beds at the base of the Triassic in other places.

There is a remarkable uniformity with regard to faunal assemblages; and in lithologies in a couple of cases, throughout the Mesozoic from one end of the NeoTethys to the other (Fig. 16.3a, b). It seems that near similar tectonic condition existed throughout the expanse of India's north-western and northern continental margin. However, overprinted on this uniformity, there is lateral facies variation—in the nature of sediments and the thicknesses of different lithostratigraphic formations from sector to sector.

We owe our understanding of the geology of the Tethyan domain to the seminal works of the pioneers such as C.L. Griesbach, F. Stoclickza, R. Lydekker, H.H. Hayden, C. Diener, C.S. Middlemiss, D.N. Wadia, and A. Heim and A. Gansser. In recent years, a new scheme of stratigraphic classification has been proposed. However, in this work the traditional classification is followed.

Table 16.1 provides the schemes of subdivision of the Mesozoic succession in different sectors—northern Nepal (Egeler et al. 1964; Bodenhausen and Egeler 1971; Bordet et al. 1971; Bassoullet and Mouterde 1977; Fuchs 1967, 1977; Fuchs et al. 1988); northern Kumaun (Heim and Gansser 1939; Gansser 1964; Mamgain and Mishra 1989; Sinha 1989); Spiti and Lahaul (Srikantia 1981; Bhargava 1991; Bhargava et al. 1998, 2004), south-eastern Zanskar (Gaetani et al. 1983, 1985, 1990; Baud et al. 1984), Kashmir (Wadia 1931, 1934, 1937a; Kapoor 1977; Nakazawa 1985; Nakazawa et al. 1975; Nakazawa and Kapoor 1981; Arora et al. 1996); and Hazara–Potwar–Kohat region in northern Pakistan and Sulaiman–Kirthar–Baluchistan in southern Pakistan (Kummel and Teichert 1966; Ibrahim Shah 1977; Kazmi and Qasim Jan 1997).

Table 16.1 Succession of Mesozoic formations in the major basins of sedimentation in the Tethyan domain (compiled on the basis of a large number of works)

Period	Kashmir	Zanskar-Spiti	Kumaun	Western Nepal	Eastern Nepal–Sikkim	Bhutan
Cretaceous		Chikkim Limestone	Sangchamalla Fm	Muding Fm	Khampa Group	Chebesa Fm
		Giumal Sandstone	Chikkim Limestone	Tangbe Fm		
			Giumal Sandstone	Chuk Fm		
Jurassic	Wumuh	Spiti Shale	Spiti Shale	Saligram Fm		Mochu Fm
			Ferruginous oolite	Ferruginous beds		
			Lapthal Fm	Lumachelle Fm		
			Kioto Limestone	Jomosom Limestone		
Triassic	Wuyan	Kioto Limestone	Kuti Shale	Tarap Shale	TsoLhamo Fm	
	Khreuh	Lilang Fm	Kalapani Limestone	Mukut Limestone		
	Khrunamuh		Chocolate Fm	Thinigaon Fm		
Permian	Zewan	Kuling Shale		Thinichu Shale	Lachi Fm	Shodung Fm

16.3.2 The Triassic

The Triassic succession is developed throughout the Tethyan domain. The typical section is encompassed in the *Lilang Group* in Spiti (Fig. 16.4; Table 16.1). The Lilang section illustrates not only its development in fullness, but also its relation with the underlying and overlying formations. The holy cave of Amarnath shrine—with its exquisite ice stalagmite—is located in the upper part of the Triassic limestones of the Zanskar–Sonmarg Range in north-eastern Kashmir. The Triassic is a predominantly carbonate group, exhibiting marked increase in the influx of terrigenous detritus occurring as deltaic deposits towards the upper part. This is discernible all along the Tethyan domain.

The faunal wealth of the Lilang Group is particularly visible in the upper part of the Middle Triassic. Everywhere the top is marked by the dominant presence of *Megalodon* in limestones. There is striking resemblance of the Himalayan assemblage with the fauna of the contemporary formation in the Alps belonging to the western domain of the Tethys Ocean.

The Lower Triassic in the Spiti–Lahaul region (Table 16.1; Figs. 16.2 and 16.4) is a succession of bioclastic carbonates micritic limestone, intraclastic wackestone and cross-bedded bioclastic packstone (Bhatt and Arora 1984; McElroy et al. 1990; Bhatt et al. 1999). The carbonates are characterized by filamentous and thin-shelled biota and are interbedded with subordinate marl, grey shale and radiolarian siliceous sediments. The sediments of the *Mikkin/Tambakurkur, Kaga* and *Chomule* formations—which encompass biostratigraphic zones characterized severally by *Otoceras woodwardi, Ophioceras sakuntala, Meekoceras ladakhensis, Hedenstroemia, Rhychonella, Keyserlingites, Ptychites, Daonella* and *Halobia*—were laid down in bathyal to subtidal environment (Bhargava et al. 1987). In Kumaun, the *Kalapani Limestone* sediments represent a condensed sequence characterized by orange-brown weathering ankerite and bathyal forms like *Tropites subbulatus* (Heim and Gannser 1939; Mamgain and Mishra 1989). In Himachal Pradesh, the Sanglung horizon (containing *Spiriferina, Dielasma, Juvavites*) comprises sediment deposited on the foreslope, the Hangrang unit represents high-energy back-reef lower part of the slope, and the Alaror sequence is a lagoonal deposit containing *Spiriferina* and *Rhynchonella* among others (Bhargava et al. 1987). The coeval unit in south-eastern Zanskar (Zozar) in Kumaun (*Kuti Shale*), and in north-central Nepal (*Tarap Shale*) formed in an environment similar to that of the Alaror. A remarkable thing about the *Kuti Shale* is the presence of teeth of sharks *Xenacanthus* and *Acrodus* and of reptile *Saurichithys* (Mehrotra et al. 1981). The overlying Rhaetic horizon is one of the very conspicuously persistent successions of quartzose sediments—the Nunluka (≡ *Tsatsa, Thinigaon*) (Table 16.1). It is made up of poorly sorted bioclastic calcarenite with abundant crinoid remains at the base, cross-bedded calcarenite and quatzarenite interbedded with grey micaceous siltstone and marl in the middle, and biosparite with oosparite layers at the top. The moderately sorted arkosic sediments deposited in shallow subtidal beach environment were derived from the continental provenance (Gaetani et al. 1983; Baud et al. 1984; McElroy et al. 1990). The interbeds of this

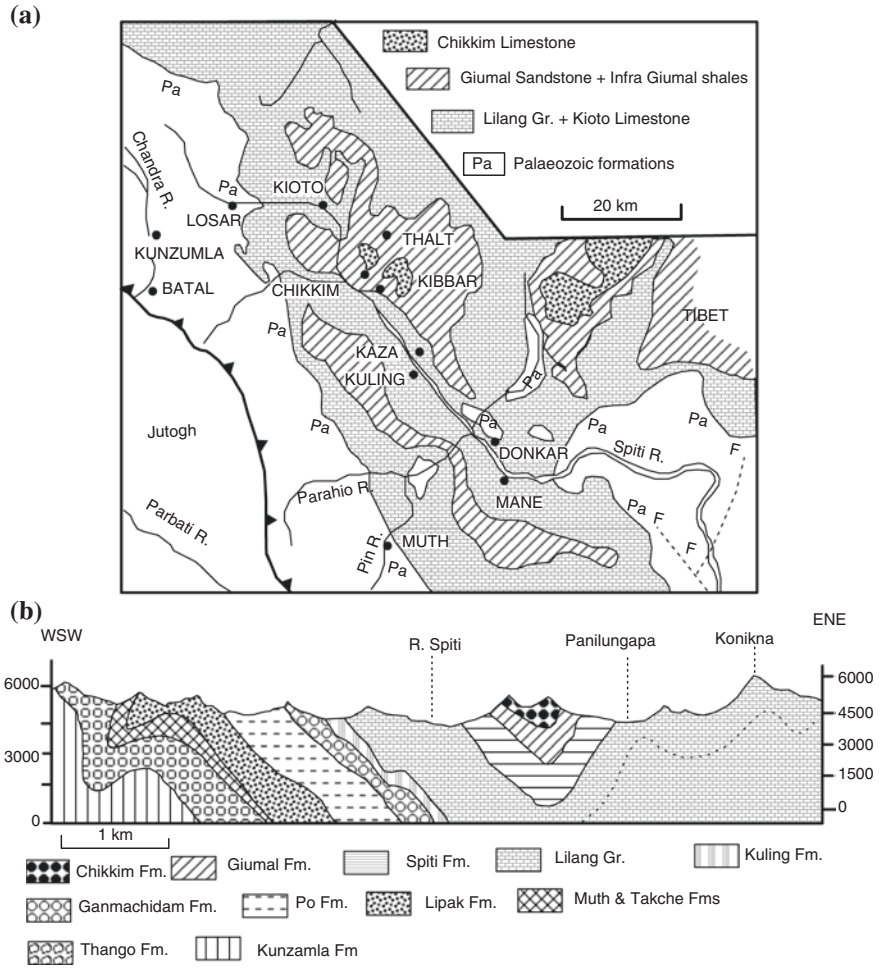

Fig. 16.4 **a** Sketch map showing development of Mesozoic succession on northern Himachal Pradesh and adjoining Kashmir [after Sinha 1989 (Map)]. **b** Section after Fuchs (1987)

horizon contain benthic forms such as *Involina communis* and *I. gaschei* of the Rhaetic age. Undoubtedly, the Nunluka horizon marks a change in the environment of deposition resulting from change in tectonic condition and/or eustatic conditions towards the end of the Triassic.

In the Kashmir Basin, the well-developed richly fossiliferous Triassic succession is divisible, on the basis of conodonts, bivalves and ammonites, into three well-defined formations: the Scythian *Khrunamuh*, the Anisian to Ladinian *Khreuh* and the Carnian to Norian *Wuyan* (Nakazawa et al. 1975; Nakazawa and Kapoor 1981). In lithology and faunal assemblages, the Kashmir Triassic sediments are not different from those of the Zanskar–Spiti Basin. In the Warwan valley in the Kishtwar region to the east–south-east of the Kashmir Basin, thick Triassic succession comprises dark grey shale alternating with grey limestone in the upper part

(Singh et al. 2000; Brookfield et al. 2003). Further, south-east in the Tandi syncline, overlying the Permian Conglomerate occur Triassic limestones characterized by *Konickites* and *Greisbachites* of the Scythian age (Prashra and Raj 1990).

The Triassic group in Pakistan is of restricted thickness and extent. It occurs in tectonized blocks in the Kohat–Hazara region, the Salt Range and the Sulaiman–Kirthar Ranges (Kazmi and Qasim Jan 1997). The Triassic succession on the Kohat–Potwar–Hazara region is divided into Mianwali Formation, Chakjabbi Limestone and Kingriali Formation. In the southern Salt Range, only the Lower Triassic and lowermost Middle Triassic rocks occur, while north of the Sindhu River, a full succession of the Triassic is developed, of course with a hiatus between the Middle and the Upper Trias (Wadia 1975). The Lower Triassic of the Salt Range—the *Mianwali Formation*—is rich in biota and divided into zones. The overlying *Tredian Formation* is an arenaceous unit characterized by terrestrial fauna. The dolomites of the *Kingriali Formation* contain bivalves resembling those of the Kioto Limestone (Kummel and Teichert 1966; Kapoor personal communication 2007). In the Quetta–Zhob Belt, the outcrops of the Upper Triassic appear like inliers. In the Lower Sindhu Basin and Balochistan, the Triassic is described as the *Wulgai Formation*.

In the Thakkhola region in Nepal, there is in general upsection upward increase in the relative importance of the Triassic carbonate rocks, implying that the northward-moving India passed through increasingly warmer latitudinal zones in the tropics. A general megacycle characterizes the Triassic succession (Fig. 16.5). It begins with a major transgression at the base, followed by shallowing upward of facies during the Middle to Upper Triassic times, and climaxing in regression during the latest Triassic (Ogg and Rad 1994). The 20- to 30-m-thick condensed sequence of grey nodular biomicrite and marlite of the *Thinigaon Formation* (≡ Tambakurkur) with its pelagic fauna developed on the starved subsiding basin peopled by Early Triassic conodonts (Wiedmann and Balka 1996). During the Carnian, a 400-m-thick fining-upward succession of filamentous carbonates, greywackes–shale cycle called the *Mukut Limestone* was laid down in the bathyal environment. The succeeding 300-m pile of sandy siltstone and shale with quartz-rich bioclastic intercalations of the Late Carnian to Early Norian *Tarap Shale* is

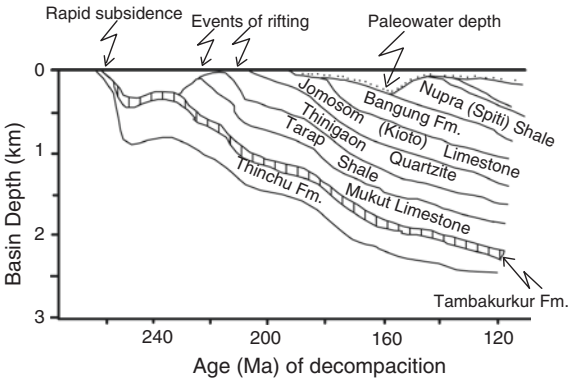

Fig. 16.5 Decompacted burial curves and palaeobathymetry of the Triassic and associated formations in the Thakkhola region, Nepal (after Ogg and Rad 1994)

the homotaxial of the Kuti Shale. The Upper Norian to Rhaetian *Thini Formation* comprises arkosic and quartzose sandstones intercalated with coal-bearing shale and bioclastics of shallow marine environment (Rad et al. 1994). Representing the eastern extension of the Nunluka, the Thini unit comprises continental sediments brought by rivers draining the land that lay to the south of the NeoTethys.

In the Arakan Yoma along the Indo-Myanmar Border Ranges, only uppermost Lower Triassic, characterized by *Halobia* and *Monotis* of Norian/Rhaetian age, is seen.

The Triassic succession in eastern Myanmar (Fig. 16.12) made up of thinly bedded marly limestone intercalated with dolomite north of Lashio contains cephalopod assemblage *Octoceras–Ophiceras–Vishnuites–Owenites* of the Scythian age. In Northern Shan States, the Upper Triassic succession (Bronnimann et al. 1975) comprises anhydrite, gypsum, halite with minor epsomite and bromide and intercalated red shale and calcareous yellow mudstone (*Pango Evaporite*). The famous *Bawgyo Salt Well* draws its mineralized (salt) water from the evaporates of this Upper Triassic formation. The overlying succession of light yellow shale and marlite with thin interbeds of dolomite (*Napeng Formation*) is characterized by Rhaetic fauna. The end of the Napeng saw halt of sedimentation over a large, part of eastern Myanmar due to uplift in the Early Jurassic interval. In Southern Shan States forming the upper part of the so-called Plateau Limestone or Shan Dolomite, a platform carbonate known as the *Thigaungdaung Formation* is intensively dolomitized, resulting in obliteration of its fossils. West of the high scarp of the "Plateau Limestone", the Heho–Kalaw tract comprises the *Kondeik Limestone* characterized by Anisian cephalopods, including *Acanthoceras* and conodonts (Gramann et al. 1972). However, over larger part of eastern Myanmar, the Triassic begins with a regional discordance as seen north of Hsipaw. Known as the *Nwabangyi Dolomite*, the Triassic succession throughout the Shan States is made up of dolomite and platy micritic limestone characterized by layers and nodules of chert. The carbonates are pervasively brecciated. A horizon of siliceous calcarenite the *Natteik Limestone* containing Anisian fauna is overlain by the *Mudstone Formation* constituting the cap on the "Plateau Limestone". It is assigned to the uppermost Triassic.

The Triassic rocks occur sparsely in the region south of the Shan States. Overlying the Permian Moulmein Limestone, there are scattered outcrops of the Lower Triassic *Martaban Beds* of sandstone and calcareous shale. It is overlain by biostromal limestone the *Kamawkala Limestone*, homotaxial with the Natteik Limestone of the Shan States.

16.3.3 The Jurassic

In the Kalemyo area in the Central Myanmar Basin (Fig. 16.12; Table 16.2), a sandstone–shale alternation with subordinate nodular limestone forming a fringe along the foot of the Chin Hills contains *Halobia* and conodonts of the Carnian age (Thein 1973a, b). Almost the same is the situation on the edge of Mount Victoria in the western border of Pakokku district (Gramann 1974).

Period	Indo-Myanmar Range	Central Myanmar Basin	Northern Shan States	Southern Shan States	Karen-Tenasserim Belt
	Arakan Flysch				
Cretaceous	Kyauknimaw Cherts	Kabaw Group			Red Beds of Mergui/ Khorat
			Unconformity		
			Hsipaw Red Beds	Kalaw Red Beds	
				Thigyit Beds	
Jurassic			Tati Limestone	Loi-An Beds	
				Ma-U Bin Beds	
			Unconformity		
			Napeng Fm	Mudstone Fm	
			Pango Evaporites	Natteik Fm	
			Nawbangyi Dolomite	Nawbangyi Dolomite	Kamawkala
			Otoceras Beds	Kondeik Limestone	Limestone
Triassic				Thigaungdaung Limestone	Martaban Beds
Permian			Thitsipin Limestone	Thitsipin Limestone	Moulmein Limestone

Table 16.2 Mesozoic rock formations of Myanmar (after Bender 1983)

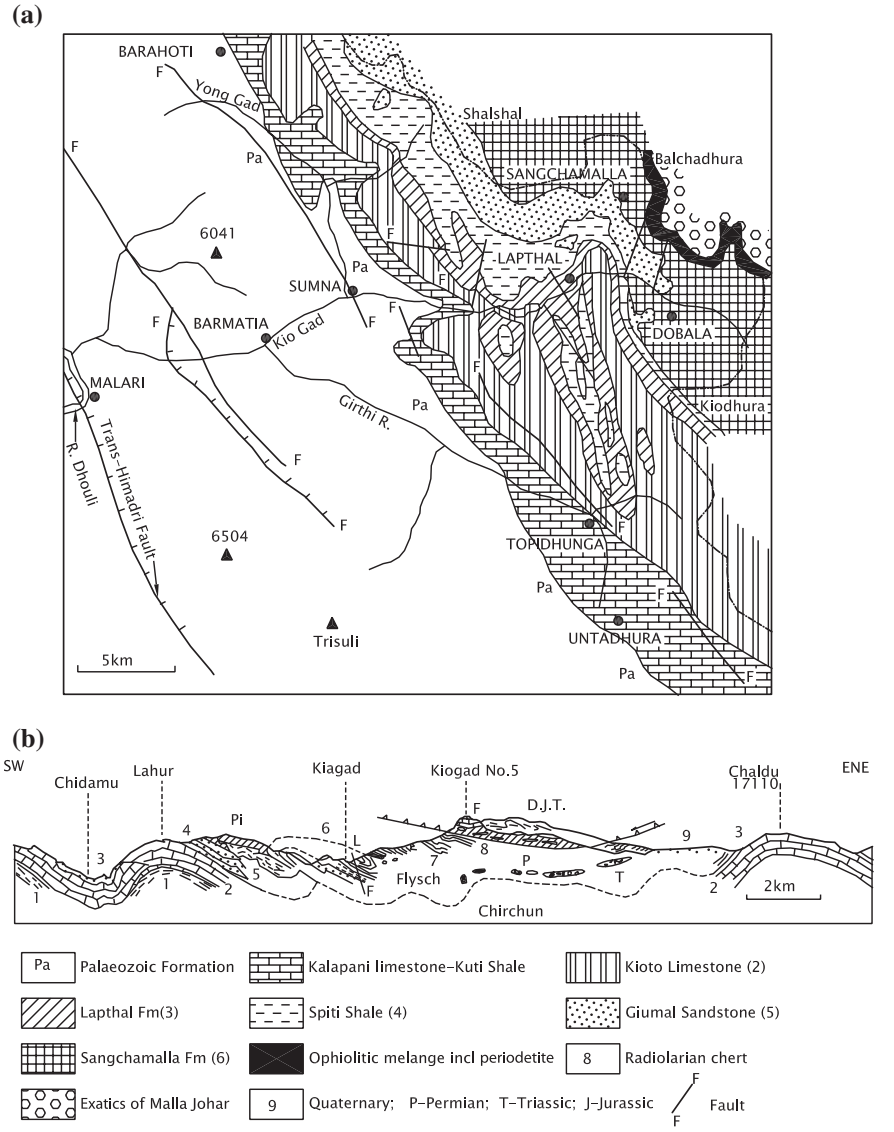

Fig. 16.6 **a** Sketch map of the Tethyan domain in northern Kumaun showing spread of the Mesozoic formations (based on Sinha 1989). **b** Section across Malla Johar in Uttarakhand showing the abducted ophiolites and flysch occurring as nappes (after Heim and Gansser 1939)

Triassic carbonate sedimentation continued into the Early Jurassic time in the Kachin and Shan states in eastern Myanmar. However, there was a big change towards the Middle Jurassic from the marine carbonates to the continental clastic sedimentation. In the Hsipaw–Namtu tract in the Northern Shan States unconformably overlying the Upper Triassic Napeng and overlapping the Permian and

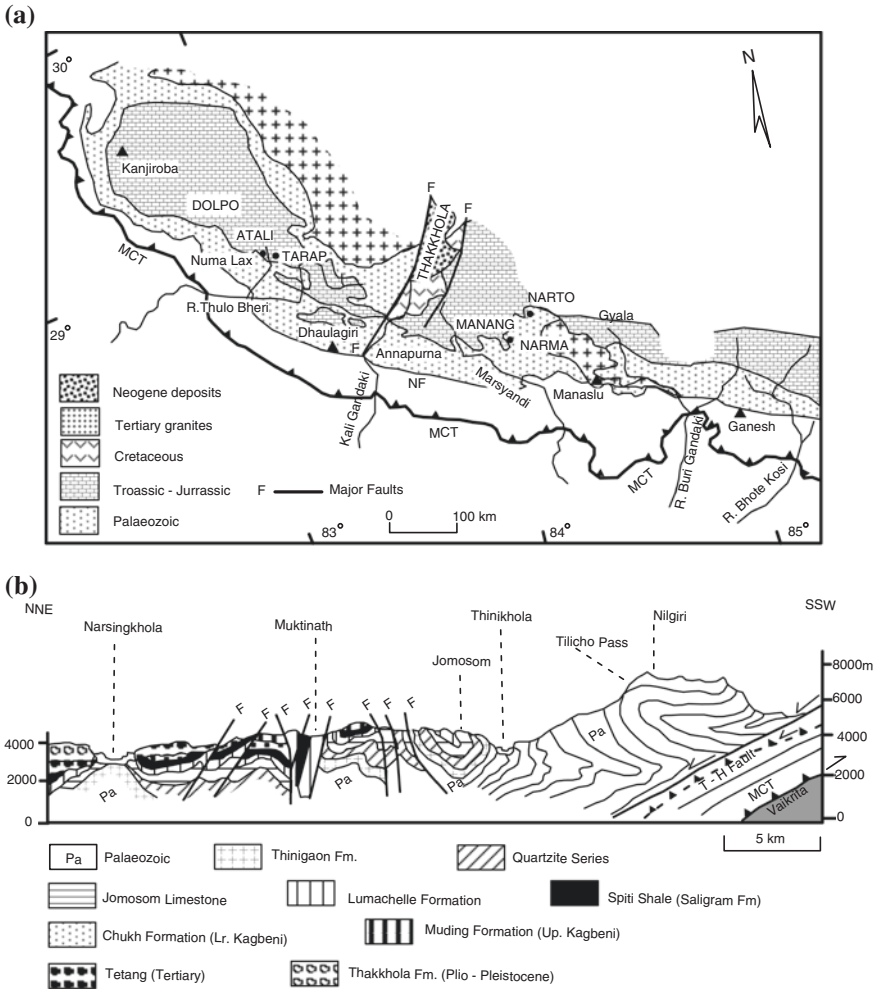

Fig. 16.7 **a** Sketch map of the Tethyan domain in Nepal and adjoining southern Tibet depicting distribution of the Mesozoic sediments (After Garzanti 1999). **b** Cross section across the Mesozoic formations, entangled in the maize of structures of the Nilgiri Massif (after Colchen et al. 1986)

the Devonian rocks, there is a succession of the *Tati Limestone* made up of yellow to buff limestone with yellow to grey marlite (the latter becoming brown towards the top) and characterized by ostreiid brachiopod of the Bathonian–Callovian age. In Southern Shan States, the Mudstone Formation is succeeded by the *Loi–An* sequence containing coal-bearing sandstone and shale that are characterized by Jurassic flora (described by M.R. Sahni in 1937) as well as marine *Alectryonia* in the intercalated limestones. In the Thigyit–Hsikip area, a succession of shale with coal has yielded Upper Jurassic cephalopods. The Tati Limestone is overlain

by the *Hsipaw Red Beds*, first reported in 1900 by P.N. Datta. The 1100- to 1200-m-thick Hsipaw Red Beds (described as the *Kalaw Red Beds* in the Kalaw–Heho tract) is a monotonous succession of fine to medium-grained argillaceous ripple-marked sandstone and shale of conspicuous red and brown colours with thin layers of limestone and conglomerate at various levels in the lower part, and a thick sequence of shale and mudstone in the middle part.

In the Himalaya province, the Jurassic sedimentary succession covers wide areas in Bhutan, southern Tibet, north-central Nepal, northern Kumaun and Spiti–Lahaul region (Figs. 16.6, 16.7 and 16.8).

In the Lingshi Basin in Bhutan, the Jurassic succession comprises greenish grey fine-grained sandstone interbedded with black carbonaceous shale, the latter characterized by plant fossils of the Upper Gondwana (Jabalpur) affinity, occurring in association with marine lamellibranchs, brachiopods and cephalopods (Nautiyal et al. 1964). The Middle to Late Jurassic succession comprises the Moch and the Chebesa formations (Tangri and Pande 1995a, b).

On the northern slope of Nilgiri–Sagarmatha (Everest) range in eastern Nepal (Fig. 16.3; Table 16.1), the Triassic–Jurassic succession is normal without break, as confirmed by gamma ray survey and study of ammonites and palynomorphs across the boundary (Hallam et al. 2000). In the Thakkhola region (Fig. 16.7), the coeval *Jomosom Limestone*, overlying the coastal sediments (Thini) of the Upper Triassic was emplaced as a platform deposit in warm waters of tropical latitudes (Gradstein et al. 1991) in the Liassic or Liassic to Rhaetic time (Rad et al. 1994). A horizon of shell limestone overlying the Jomosom is described as the *Lumachelle Formation* (Bordet et al. 1971; Bodenhausen and Egeler 1971; Bassoullet and Mouterde 1977; Fuchs 1967, 1977; Fuchs et al. 1988).

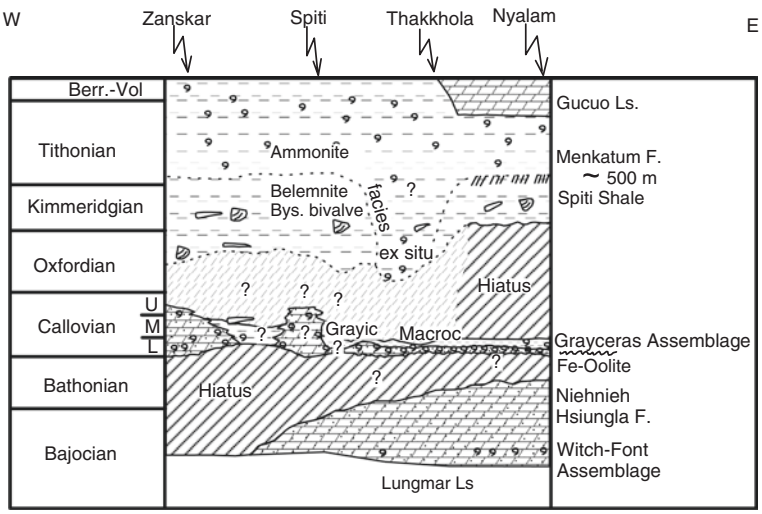

Fig. 16.8 Facies variation in the Spiti Shale and associated formations in southern Tibet (After Westermann and Yi-gang 1988)

In Kumaun, a horizon of multiple layers of broken shells deposited in shallow water stretches west from Kungribingri in Nepal border to Painkhanda in Garhwal (Fig. 16.6). It is known as the *Lapthal Formation* (Heim and Gansser 1939). Then follows a condensed sequence comprising arenite at the base and oolitic limestone forms the bulk of the *Ferruginous Oolite Formation* (Table 16.1). Strikingly golden reddish in colour and formed in warm waters agitated by waves, the oolite horizon forms one of the most conspicuous and persistent stratigraphic units in the Neotethyan domain. Set in iron-rich matrix, the golden oolite and pisolite are seen all along from southern Tibet, through northern Kumaun and Spiti to the Quetta region in Baluohistan and then to the Kachchh region in Gujarat.

In the Spiti Basin on top of the Triassic succession is the *Kioto Limestone*, forming spectacular cliffs in the desolate landscape. It is characterized by *Megalodon ladakhensis, Dicericardium himalayaensis, Strephaenoceras,* and *Spirifer neotlingi*. The massive dolomite and limestone are bioclastic packstone characterized by anhydrite pseudomorph at the base, low-angle cross-stratification and heterolithic channel-fills, presumably of tidal streams active in a storm-affected beach environment. The weight of evidence adduced from various sectors of the NeoTethys favours placing of the Kioto in the Early Jurassic level. The Upper Jurassic *Spiti Shale* shows singular geographic persistence without lithological variation from Hazara in the west to southern Tibet in the east (Table 16.1). It is a shelf environment in which muds were deposited at a very slow rate, and there were mud-flows occasionally and hard-ground formation frequently (Bhargava et al. 1987). A very arresting feature of the Spiti Shale is *Shaligram*, a concretionary ball or nodule with any ammonite forming the nucleus. Among the rich variety of ammonites forming *Shaligrams* are *Macrocephalites, Lytoceras, Phylloceras* and *Hoplites*. Three biostratigraphic zones of ammonite assemblages are recognizable in the Spiti–Lahaul region: (i) *Mayites, Torquatisphinctes and Pachysphinctes* assemblages of the Oxfordian–Kimmeridgian time, (ii) *Aulacosphinctoiodes, Paraboliceras* and *Spiticeras* assemblages of the Lower Tithonian and (iii) *Virgatosphinctes* and *Himalayaites* assemblages of the Upper Tithonian epoch (Pathak 1997). In the deeper shelf-to-slope faunas of the Spiti Shale in southern Tibet, the ammonite assemblages comprise the following: (1) *Witchellia–Fontannesia* assemblage having affinity with the north-western Australian fauna and (2) the Oxfordian *Graiceras* assemblage containing (in addition to endemic forms), the elements of both the India–Madagascar and the Mediterranean provinces (Westermann and Yi-Gang 1988).

The Jurassic rocks occur in much attenuated forms as bands in the synclinal troughs of the much-folded Wuyan Formation in Kashmir. The sequence of limestone, sandstone, brownish- yellow sandy limestone and black shale containing Jurassic fauna including *Macrocephalites* is described as the *Wumuh Formation*, (Nakazawa and Kapoor 1981). There is so far no record of post-Liassic sedimentation in the Kashmir Valley (Arora et al. 2002). In Ladakh, the *Lamayuru Formation* (Gaetani and Garzanti 1991; Sinha and Upadhyay 1993) represents a Jurassic slope-deposit comprising turbiditic sandstone, carbonaceous shale and limestone characterized by predominance of pelagic sediments and by local

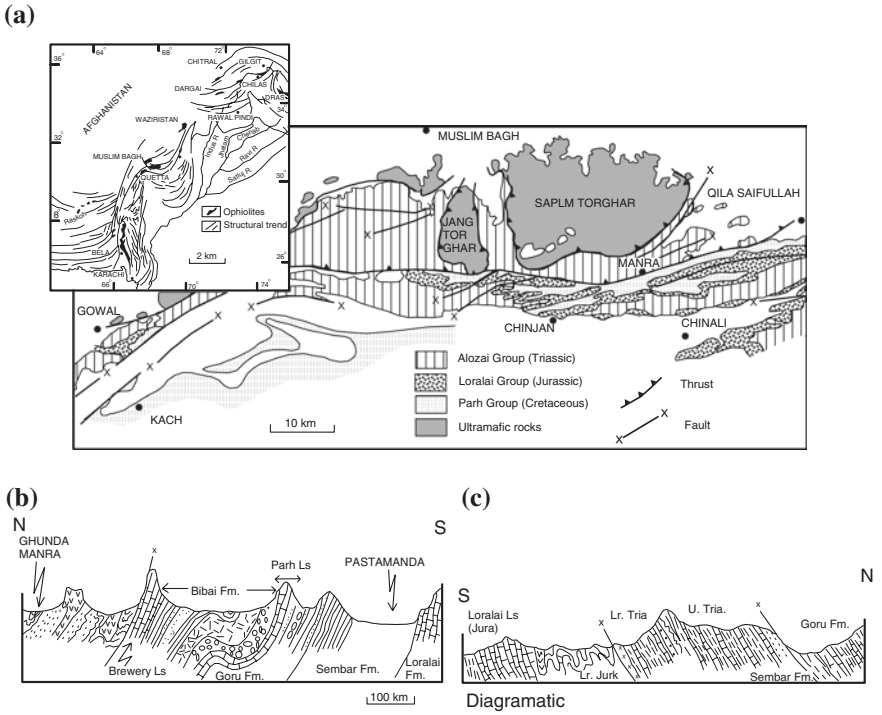

Fig. 16.9 **a** Sketch map of a part of Pakistan depicting the Mesozoic formations (after Okimura and Fatmi 1988). **b** Cross sections bring out the structural design of the Mesozoic formations in the lithotectonic set-up of the above-mentioned belt (based on Kazmi and Qasim Jan 1997)

presence of *olistostromes*. The clasts of the olistostromes were derived from the fore-reef, the basin-margin sedimentary rocks and the shelf itself. Ammonite *Psiloceras planorbis* occurring approximately in the middle of the Lamayuru succession places the horizon in the Hettangian level of the stratigraphic column (Krishna 1997). It is the time when there was eustatic rifting of the continental margin in Kachchh.

The *Bagong* Formation of southern Tibet contains the fauna of latest Middle Jurassic or Early Callovian to Early Oxfordian (Gradstein et al. 1991).

The Jurassic succession in Pakistan, measuring 800–3000 m in thickness, comprises shelf deposits that form a part of the platform cover in the entire Indus Basin, including the Sulaiman–Kirthar Ranges (Kazmi and Qasim Jan 1997). They occur in the latter belt only in the cores of anticlines, but in Balochistan as sheets and blocks. The Lower Jurassic is represented as the *Datta Formation* and *Shinwari Formation* in the Kohat–Hazara region, and as the *Shirinab Formation* in the Sulaiman–Kirthar Ranges. The MazarDrik/Chiltan Formation of the Sulaiman–Kirthar Belt and the *SamanaSuk Formation* of the

Potwar–Besham–Hazara region are made up of Middle Jurassic sedimentary rocks. The Upper Jurassic *Chichali Formation* is a *Belemnites*-rich shale succession characterized by glauconite, phosphatic nodules and seams of ironstone. The upper part is made up of glauconitic siltstone and sandstone, with a cap of oxidized and winnowed glauconitic sandy iron ore of commercial importance. Near Kalabagh in the Salt Range, there are deposits of lignite and coal in the horizon characterized by plant fossils of the Upper Gondwana (the Jabalpur Fm.) affinity. The Chichali ends with *Belemnites*-rich beds of Berriasian to Valanginian age (Hallam and Maynard 1987).

16.3.4 The Cretaceous

As already adumbrated, in northern Pakistan, the Chichali Formation extends upwards without break into the Neocomian. The Lower Cretaceous part is made up of dark grey glauconitic sandstone, siltstone and shale. Among the fauna, the remains of some reptiles and fish occur together with *Exogyra* and *Pholodomya* (Wadia 1975). The *Lumshiwal Formation* comprises, by and large, Aptian–Albian sediments, but in some places, it ranges in age from the earliest Cretaceous and thus is in part coeval with the Chichali. The Lumshiwal is made up of light grey current-bedded glauconitic sandstone with felspathic–ferruginous elements in the lower part and carbonaceous sediments in the upper. This unit developed in a neritic environment of a shallow shelf (Sheikh and Naseem 1996). Isolated lenticular Kawagarh represents a horizon of the Coniacian to Campanian interval (Kazmi and Qasim Jan 1997). In many areas such as Bela and Muslimbagh (Fig. 16.9), the Cretaceous succession contains volcanic rocks, ophiolites and ophiolitic melanges (Okimura and Fatmi 1988). Ranging in age from the Late Tithonian to Maastrichtian, these rocks are the main elements of the obduction complex emplaced tectonically when India docked with the Eurasian plate.

In the Kirthar–Sulaiman Ranges and adjoining belts in the Lower Indus Basin, the Lower Cretaceous is represented by the *Sembar* and the *Goru* formations. The former consists of black shale and siltstone interbedded with argillaceous nodular rusty limestone characterized by glauconite, pyrite and phosphatic nodules. The Goru is latterly made up of light grey and olive-coloured limestone intercalated with shale and siltstone. The Goru is succeeded by porcellaneous and argillaceous limestones of white and cream colours and subordinate olive green and maroon shales of the *Parh Limestone*. The Upper Cretaceous *Moghalkot Formation* comprises dark grey calcareous mudstone, shale and quartzose sandstone, while the overlying *Fort Munroe Formation* is made up of black limestone and shale. The youngest Cretaceous Formation is the *Pab Formation*, embodying white, yellow and brown cross-bedded quartzose sandstone and marl with argillaceous limestone intercalations. Significantly, the Moro unit of limestone, marl and shale of is characterized by volcaniclastic conglomerate (Sheikh and Naseem 1996).

Coming to the central sector of the Tethyan domain, the Cretaceous succession is a flysch assemblage made up of rhythmites—glauconitic greywacke interbedded with shale and bedded chert. Known as the *Giumal Sandstone*, the flysch formation is traceable from Nindam in Ladakh to Kagbeni and to Kampa in southern Tibet (Figs. 16.4, 16.6 and 16.7). The Giumal comprises moderately sorted, graded to cross-bedded calcareous sublitharenite interbedded with *Belemnites*-rich black shale. Deposited in the outer shelf (Baud et al. 1984), the Giumal represents a proximal turbidite formation developed on the upper slope of the continental margin (Bhargava 1991). The basal member of this formation in the Spiti region yielded *Neocosmoceras* and *Odentodiscoceras* of the Berriasian stage (Pathak 1997). In south-eastern Zanskar, the Giumal incorporates ferruginous detritus derived from the continental source that lay in the south-west. The deltaic deposits pass laterally into offshore pelitic sediments (Fuchs 1987). The conformably succeeding *Chikkim Limestone* has yielded *Hedbergella infracretacea* and *Globorotalites aptiensis* of Gargesian stage (Colchen et al. 1986). The Chikkim is a succession of pelagic limestone and marlite developed as a continental slope deposit in a fast subsiding basin.

The coeval of the Giumal Sandstone in Nepal (Fig. 16.10) is the *Kagbeni Group* (Bordet et al. 1971). It comprises three formations—the Chuk (Berriasian), the Tangbe (Valangian to Albian) and the Muding (Cenomanian to Coniacian) (Gibling et al. 1994). The Chuk is a succession of dominant glauconitic quartzarenite. The Tangbe consists of mudstone, greywacke sandstone with volcaniclastic conglomerate. The Chuk–Tangbe succession was formed in deep cold water as testified by glauconite and phosphatic nodules in mudstone and by siliceous limestone interbedded with bedded radiolarian chert. Significantly, the storm-affected sediments of the Chuk contain material including plant debris brought by rivers from the distant land in the south (Gibling et al. 1994).

In the Lingshi Basin in *Bhutan,* the *NigeiLa Formation* consisting of carbonaceous shale, olive-brown nodular slate with thin intercalation of sandstone, is characterized by Valangian to Tithonian fauna including *Callyptychoceras, Odontodicoceras, Hoplites, Venericardita* (Tangri and Pande 1995a, b). The sequence represents the Cretaceous sediments deposited amidst the Precambrian rocks. Along the Tingri–Kampa Belt in southern Tibet, the Zhepure Mountain (Fig. 16.10) is made up of the *Kampa Group* (Wager 1939) of Upper Albian to Eocene age (Willems et al. 1996). It comprises pelagic marl intercalated with foraminiferal limestone characterized by dinoflagellates, and ammonites, indicating transition from open marine environment in the lower part to an outer shelf environment in the upper part during the time span upper Albian to Lower Santonian (Willems et al. 1996). The succeeding part of the sedimentary column consists of limestone containing planktonic foraminifers, dinoflagellates and filaments of the outer shelf environment. A horizon of polymictic pebbles in the upper part is associated with sediment of the continental slope environment containing larger foraminers—*Orbitoides media* and *Omphalocyclus macroporus*.

In the *Arakan Yoma Terrane* of the Indo-Myanmar Border Ranges, the Cretaceous flysch (*Arakan Flysch*) forms the oldest sedimentary

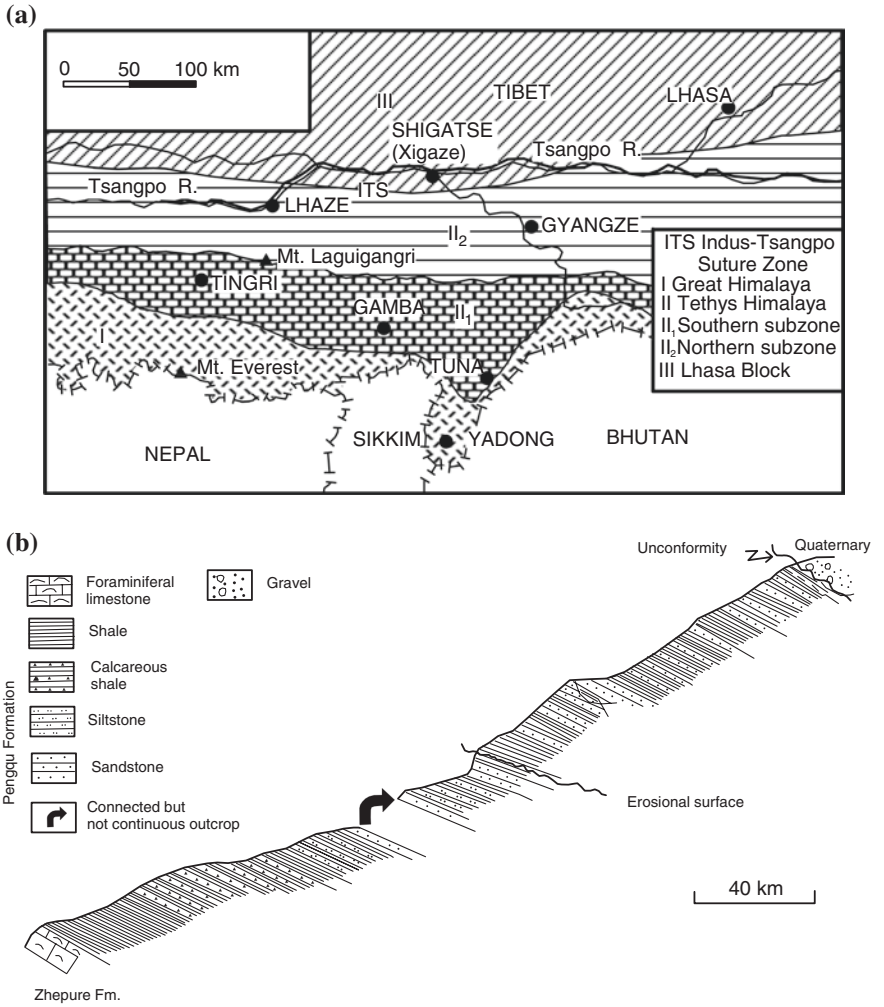

Fig. 16.10 **a** Sketch map of north-central Nepal and adjoining Tibet showing *upper part* of the Tethyan succession. **b** Detailed cross section of a part of the Zhepure Mountain showing stratigraphic range of the youngest marine formation extending up to latest Eocene (after Wang et al. 2002)

formation (Figs. 16.11 and 17.15; Table 16.2). The lower part of the succession (*Kyauknimaw)* consists of volcanic tuffs and chert with Albian–Cenomanian fossils, giving way upwards to limestone and mottled chert with volcanics, turbidite shale and sandstone–shale alternation. There are *exotic blocks* of limestone bearing *Globotruncana* of the Campanian to Maastrichtian age (Brunnschweiller 1966). Interbedded with the sedimentary rocks are sills linked to the dykes and stocks of serpentinized ultrabasics and to the beds of tuffs and agglomerates in the

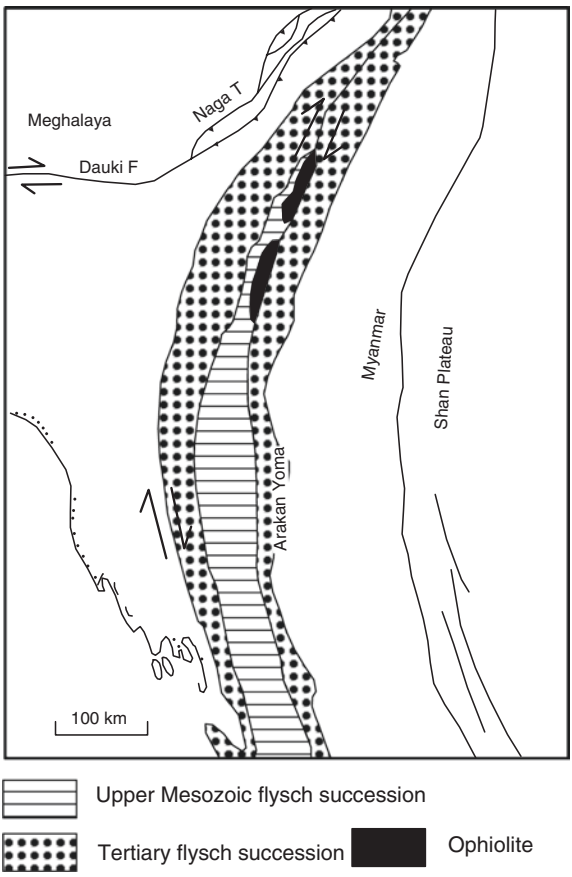

Fig. 16.11 Sketch map of the Indo-Myanmar Border Ranges showing the Mesozoic and Early Tertiary sedimentary rocks involved in the tectonics of plate convergence (based on Gansser 1964)

Chin Hills, the Naga Hills and the Ngapali Hills. West of Minbu near Kalemyo in the Chin Hills the *ophiolites* occur as large and small lenses—70 km in length and 40 km in width—within the 1200-km-long flysch belt but localized in the tectonic boundary between the terranes of Arakan Yoma and Central Myanmar Basin. Characterized by chromite deposits, the ophiolites delineate the eastward-dipping *subduction zone* developed between the Myanmar microplate and the Arakan Yoma Terrane. The coming together of the two resulted in development of the thrust belt of the Indo-Myanmar Border Ranges (Thein 1973b; Fan and Koko 1994).

In the island of Ramree in the Akyab coast, pelagic micritic limestone with subordinate red and green shales is assigned to Campanian to Maastrichtian interval (Nagappa 1959).

From northern *Myanmar* through the Gulf of Martaban (with its Barren and Narcondam volcanic islands) to western Sumatra runs a chain of volcanic assemblages within the belt of flysh-facies sedimentary succession. It represents an

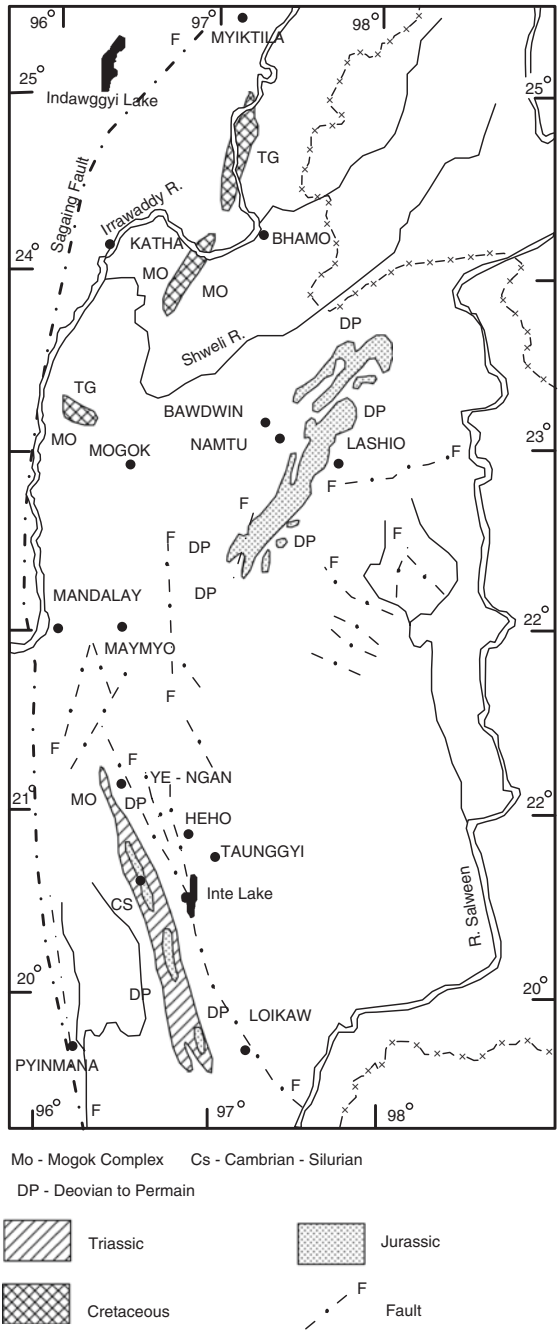

Fig. 16.12 Sketch map showing the Eastern Myanmar Terrane defined against the Irrawaddy plains to the west by the sagging fault. Exposures of Mesozoic formations are shown (modified after Thein 1973a)

arc-trench complex, resulting from India–Myanmar collision. Overlying the Mid-Triassic Thanbaya Formation (Fig. 16.12; Table 16.2) is the *Kabaw Group* spanning the Middle to Upper Cretaceous period. The lower part of the Kabaw comprises cherty limestone and platy bituminous limestone—the *Paungchaung Limestone*—characterized by vertebrates, cephalopods including *Acanthoceras* and foraminifers (including *Hedbergella*) overlain by *Turritella*-bearing limestone (*Ywahaungyi Limestone*). The middle part of the Kabaw is a 200-m-thick sequence of graded volcaniclastics. It is topped by algal reefal bioclastic limestone containing *Globotruncana* and *Siderolites* of the Campanian to Maastrichtian age (Gramann 1974). The volcanic arc is made up of a chain of volcanic rock complexes of basic, intermediate and acidic composition (Figs. 10.13 and 16.12). The 60-km-long and 40-km-wide belt of highly serpentinized dunite, peridotite, pyroxenite and hornblendite in the Indawgyi Lake Belt in the Myiktila district is well known for rich jadeite deposits that are localized in the schists surrounding the ultrabasic bodies (Chhibbar 1934).

Paralleling the Shan Boundary Fault Zone, a N–S trending belt of granitic plutons extends from the estuary of the Sittang River to as far north as Bhamo (Figs. 10.13 and 16.12). The largest *granitic complex*, 310 km long and 30 km across and occurring north-east of Pyinmana, is made up of soda-granite, associated with dykes of hornblende-bearing granophyre and rhyolitic tuffs (Chhibbar 1934). Further north in the Neyaunaga and Ye-ngan areas between Kalaw and Kyaukse, porphyritic rhyolite and dacite are associated with andesitic tuff, and with plugs, sills and dykes of dacite, rhyodacite and rhyolite porphyry. The sills are intercalated with sediments belonging to the Upper Jurassic to Lower Cretaceous age (Garson et al. 1976). West of the domain of the volcanic arc occurs a batholith of granodiorite–adamellite–granite, penetrated by dykes of aplites and wolframite-bearing pegmatites.

Extending north–north-west from the Davis Island in the Gulf of Martaban to Mawchi and beyond (Fig. 10.13), there is another belt of granite plutons, intruding the Mergui succession. The granites are mineralogically similar throughout the belt. Many of the granite bodies are of Triassic age, but the one south of Mae Sariang has yielded a Rb–Sr age of 70–80 Ma.

16.3.5 Transition to Palaeogene

In southern Tibet, unconformably overlying the Kampa rocks (Fig. 16.10b) is a succession of hemipelagic marly sandstone and black marl characterized by profusion of calcispheres, followed upwards by black nodular marl and limonite-rich sandstone. The summit of the Zhepure Mountain is made up of thick-bedded dolomitic skeletal limestone and nodular limestone. The nodular limestone exhibits abundance of foraminifers—*Operculina, Miscellanea, Alveolina, Orbitolina, Assilina, Discocyclina, Astrocyclina* and dominant *Nummulites* testifying to the Danian to Lutetian age (Willems et al. 1996). Recently recognized marine the

Pengau Formation conformably overlying shallow-water carbonate formation comprises shale interbedded with sandstone deposited in a neritic shelf environment and containing nannofossils and foraminifers of the later Early Lutetian to Late Priabonian (Upper Eocene) (Wang et al. 2002). This fact implies that in this part, the NeoTethys was not closed until about the latest Eocene.

In Kumaun, the Chikkim is overlain by the *Sangchamalla Formation* (Shah and Sinha 1974; Sinha 1989). It is a flysch succession comprising dark green and purple shales with greywacke and subordinate limestone. The limestone abounds in foraminifers, including the Upper Cretaceous *Odontochitina cribropoda*. The succeeding dark grey shale associated with radiolarian chert contains foraminifers and dinoflagellates of Eocene age (Sinha 1989). In the Spiti Basin, the Tethyan sedimentation ended with the Chikkim Limestone, but in south-eastern Zanskar it continued through Paleocene up to Lower Eocene. The *Spanboth Formation* of shallow-water limestone is associated with grey quartzose sandstone and grey bioclastic calcarenite containing abundant *Omphalocyclus* and *Daviesina,* and the *Chulungla Slate* of thick-bedded limestone intercalated with maroon green grey slate, siltstone and litharenite represent, respectively, the Paleocene and Lower Eocene horizons (Fuchs 1987; Gaetani and Garzanti 1991; Garzanti and Haver 1988).

16.4 Cycles of Marine Transgression and Regression

Following the break-up of the Gondwanaland, the northward drift of the Indian plate brought about eustatic sea-level changes in its continental margin (Fig. 16.13). The sea level was extremely low in the Permian, high in the Upper Triassic and low again during the Rhaetic–Liassic as clearly witnessed in the Thakkhola region and north of Sagarmatha (Everest) Range (Xiachi and Grant-Mackie 1993; Rad et al. 1994). There is an *apparently* continuous sedimentary succession across the Permian–Triassic boundary in the Salt Range and Kashmir. However, in most of the Tethyan sectors, the transgressive episode at the base of the Triassic is followed by four-to-five events of sea-level oscillation during the Lower Triassic (Kapoor 1992, 1996; Ogg and Rad 1994). In the Thakkhola region, the gap between the Permian and the Triassic successions is quite widespread and conspicuous. The Lower Triassic is represented by a relatively condensed unit of deep-water facies and the uppermost Triassic comprises merely 2-m-thick condensed sequence of deltaic/barrier shoal quartzarenite, ferruginous sandy limestone and reddish-orange dolomite overlain by ammonite-rich nodular limestones (Basoullet and Mouterde 1977; Bassoullet et al. 1986).

Within the Jurassic period, the Early Callovian–Early Oxfordian hiatus, clearly discernible in the Thakkhola succession, corresponds to a global transgression resulting presumably from accelerated seafloor spreading (Gradstein et al. 1991). The Late Jurassic–Early Cretaceous sea-level changes (Fig. 16.13) coupled with the steady subsidence of the basin floor is attributed to the break-up of the

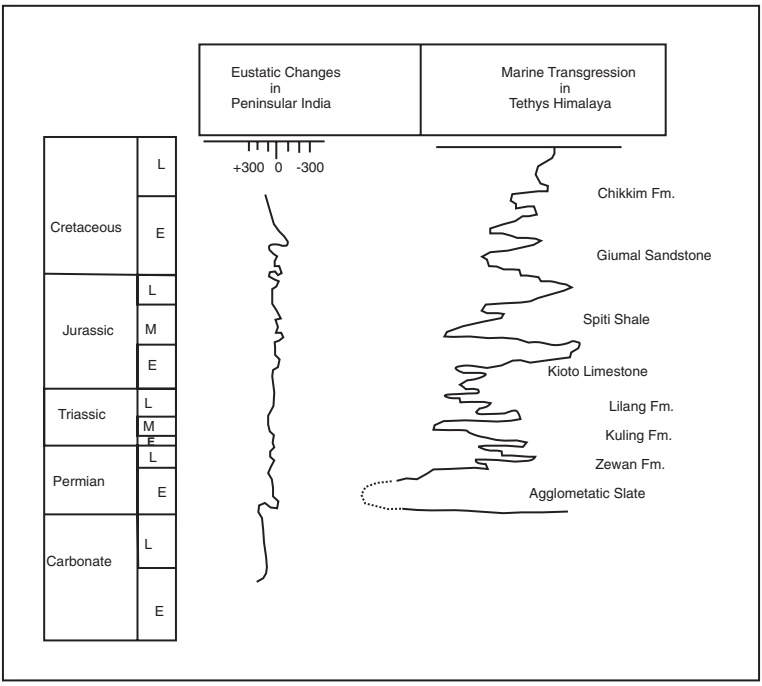

Fig. 16.13 Cycles of marine transgression and regression in Himalaya and Peninsular India (after Shah 1991)

Gondwanaland and attendant volcanism that lasted until the Albian (Gibling et al. 1994).

In the Gyantse–Kampa Belt in southern Tibet, the Early Upper Cretaceous time saw a major event of extinction of foraminifers and calcareous nannoplanktons followed by an interval of low-diversity survival, the latter event straddling the Cenomanian–Turonian boundary. The fauna soon after recovered and proliferated once again. This faunal tragedy is related to the development of reducing conditions in the basin bottom as borne out by occurrence of framboid pyrite.

Later, during the Cretaceous–Tertiary boundary interval, the Gyantse–Kampa region witnessed mass death of 50–70 % planktonic and 90 % benthonic foraminifers due to inhospitable environment following the change in oceanic circulation as India and other microplates moved rapidly towards Eurasia (Wang et al. 2001).

16.5 Influx of Plant Debris and Volcanic Clasts: Provenance Inland

16.5.1 Plant Debris

There was conspicuous influx of plant material, including tree trunks and leaves, from inland forests of the Upper Gondwana time into the near-coast marine sediments of the Cretaceous time (Fig. 16.14). Such occurrences are seen in the Lingshi Basin in Bhutan (Nautiyal et al. 1964; Ganesan and Bose 1982; Bhargava and Tangri 1996), in the Kagbeni and Kampa areas in north-central Nepal and adjoining southern Tibet (Colchen et al. 1986), the Kalabagh area in the Salt Range (Kazmi and Qasim Jan 1997) and the Umia area in Kachchh (Rajnath in 1932; Krishna 1987).

In the Muktinath–Bagong Belt close to the India–Asia tectonic junction, the deltaic sediments characterized by volcanic clasts are intimately associated with deep-sea sediments. The deltaic sediments contain such plant remains as *Taemispteris*, *Ptilophyllum acutifolia* and *Araucarioxylon nepalensis* (Colchen et al. 1986). In the Lingshi Basin, the floral assemblage includes *Ptilophyllum acutifolia, P. cutchenis, Elatocladus jabalpuria* (Ganesan and Bose 1982) in association with marine invertebrates such as *Aucella spitiensis*, *Nucula spitiensis, Rhynchonella, Perisphinctes* and *Hoplites* in Tanchu Basin (Mamgain and Rao 1989).

It will be evident that the floral assemblages occurring in the marine sediments of northern Tethyan domain represent the Upper Gondwana plants that were growing prolifically in the central Indian terranes stretching from Rajmahal Hills in the east to the Aravali Range in the west. The sediments containing plant debris were carried to the shores of the NeoTethys by rivers draining the land northwards and westwards (Fig. 16.14).

16.5.2 Volcaniclastics

Along with plant debris, there was profuse influx of fragments and grains of volcanic rocks and ash into the sediments of the Cretaceous deposits on the shelves and slopes of the passive continental margin. This is discernible practically all along the coast from southern Tibet to Balochistan. Whole-rock analysis of the volcanic fragments in northern Nepal and adjoining southern Tibet shows that those occurring in the lower part of the succession were derived from basaltic parental rocks, and those that characterize the upper part came from dacitic-rhyolitic provenance belonging to the within-plate geotectonic setting (Durr and Gibling 1994). The inland volcanism responsible for profuse generation of clasts may be related to the seafloor spreading that began in the Late Valanginian/Hauterivian to Albian interval. The 117–114 m.y. old Rajmahal

Volcanics in the Jharkhand–Meghalaya Belt (Figs. 14.2 and 16.14) is believed to have served as the source of the volcanic clasts, occurring in the Cretaceous of the Thakkola region (Sakai 1984, 1991). The abundant generation of arkosic sediments associated with terrestrial plant debris and volcanic clasts was carried to the NeoTethys Sea by rivers that flowed northwards from eastern central India. The rivers were very active in eroding rocks of the terranes that must have been rising up due to tectonism towards the close of the Cretaceous. The uplift prompted accelerated erosion.

It may be stressed that a part of the volcanic clasts occurring in the Cretaceous sediments must have been derived from the penecontemporaneous volcanic activity within the Tethyan domain itself. The occurrence of clasts of alkali basalts in the siliciclastic sediments (turbidites) interbedded with radiolarian chert in Ladakh (Figs. 16.15 and 17.5) and southern Tibet (Fig. 16.10) imply that the volcanic activity started as early as Middle Jurassic to Upper Jurassic in some sectors (Wadia 1937a; Robertson and Sharp 1998; Xiachi and Grant-Mackie 1993).

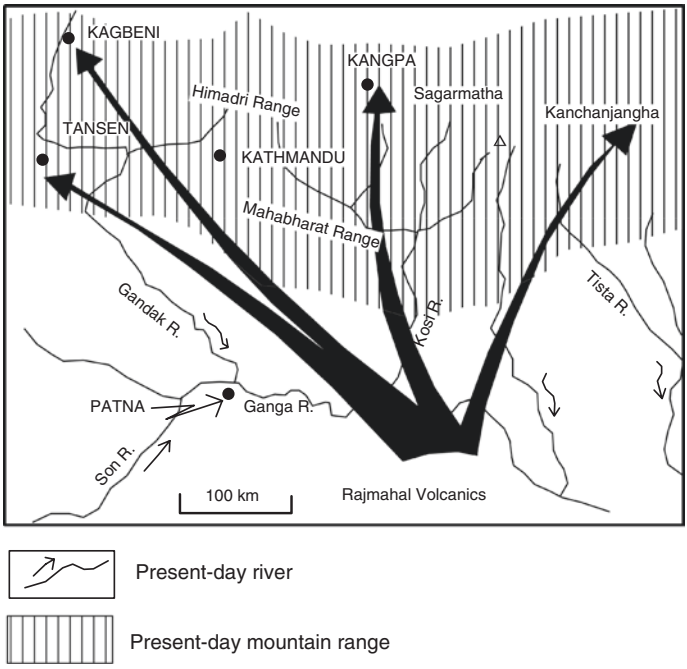

Fig. 16.14 Rivers draining the Rajmahal Hills in the Jharkhand–Meghalaya belt carried plant debris along with sediments and volcanic clasts to the Tethys shore (modified after Sakai 1984)

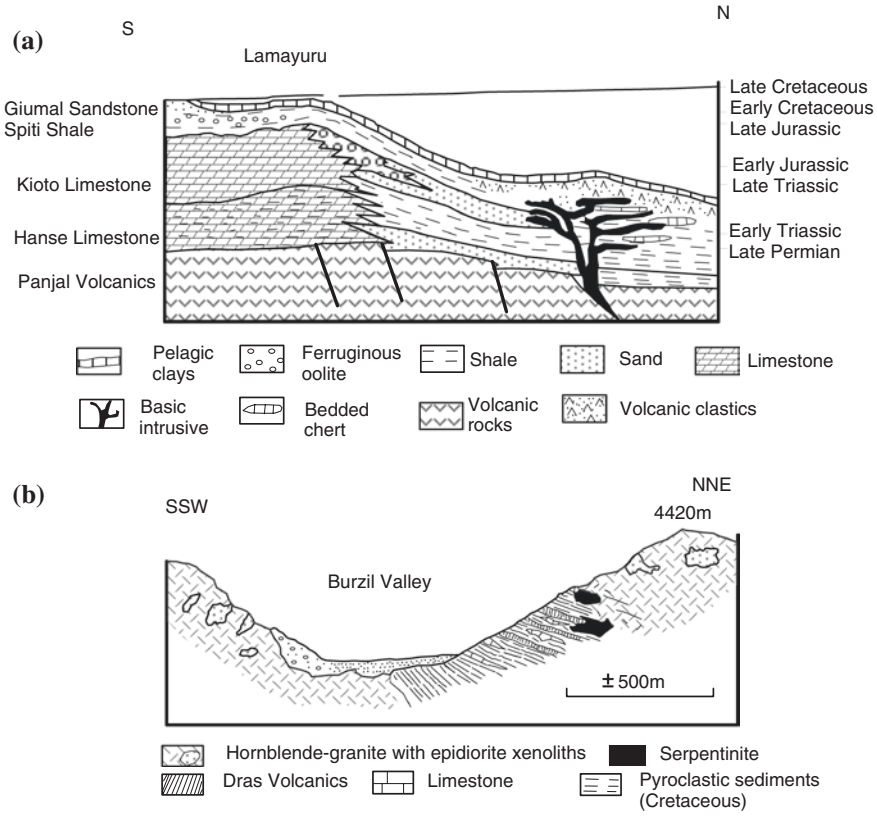

Fig. 16.15 **a** Volcanism in submarine setting had started as early as *Middle to Upper* Jurassic in some sectors. An example is the Lamayuru area (modified after Robertson and Sharp 1998). **b** Dras Volcanics associated with deep marine sediments in the Burzil Pass area (after Wadia 1937a)

16.6 Volcanic Activity Along the Periphery

As already stated, volcanic activity penecontemporaneous with sedimentation in the Tethyan domain had started as early as Middle to Upper Jurassic in some sectors. The volcanism became pronounced in the Middle and Upper Cretaceous, even as the rapidly subsiding Tethyan Basin floor was subjected to extensional renting of the crust.

West of the Chaman Fault, in Balochistan, the carbonate rocks of the Jurassic *Loralai Formation* (Figs. 16.3b and 16.9) are intercalated with the volcanic rocks (Okimura and Fatmi 1988). In a 150-km-long NE–SW trending Spangar–Kozhkach Belt between north-west of Quetta and Zhob, dykes, sills and pipe-like intrusives of kimberlitic lamprophyres intrude the Early Jurassic *Shirina Formation*, but not the overlying Loralai Formation (Ahmad 1991). Related to

horizontal extension and attendant rifting within the plate, these alkaline rocks represent Early Jurassic to Late Cretaceous magmatism in Baluchistan. The *Sinjrani Volcanics* of Baluchistan is made up of porphyritic andesite and agglomerate and the *Bela Volcanics* in the Kirthar Range comprises spilitic pillow lavas of basaltic composition which are associated with agglomerates and tuffs (Sheikh and Naseem 1996). The upper part of the Middle Cretaceous *Parh Formation* shows evidence of penecontemporaneous volcanism in the form of ash and agglomerate intercalated with limestone (Fig. 16.9). North-east of Quetta, in the type area, the *Bibai Formation* overlies the Parh Formation. The Bibai consists of porphyritic and amygdaloidal alkali basalts (showing pillow structures at the base) and agglomerate followed up by conglomerate interbedded with tuffs and tuffaceous sediment. To the south-east of the Muslim Bagh ophiolite complex, there are dykes of soda-dolerite which intrude the Cretaceous calcareous shales and limestones (Shams and Ahmad 1976). On the flank of the Bela ophiolites is the *Porali Volcanics*. The Porali was emplaced before the obduction of the ophiolites (Sarwar 1992). These are related to sills and dykes of ultramafic and mafic rocks. In the Sulaiman Range, the *Tor Ghar* intrusive is a cone-shaped body, 2 km across, having an inner rim of fine-grained basic composition and outer rim of hornfels. It intrudes the very Early Cretaceous *Sembar Formation* (Jadoon and Lawrence 1994). Judging from the distribution of outcrops of lavas and intrusive bodies, it appears that the volcanics formed a 2-km-wide horizon, stretching 1200 km from north-west of Karachi to Waziristan in the north (Siddiqi et al. 1994). In the Hazara region, there is a 30-m-thick unit of felsic lavas of rhyolitic composition succeeded by a poorly fossiliferous Upper Triassic limestone (Wadia 1975). Evidently volcanic activity had started earlier in this part of the continental margin, or else the acid volcanics represents a manifestation of the Permian Panjal Volcanism.

In north-western Ladakh, the *Dras Volcanics* form a 20-km-wide belt extending from Astor through Burzil to Dras, traversing the Zanskar range at the head of the Burzil Valley (Wadia 1937a). Basalt, agglomerates and layered tuffs are associated with marine limestones and shales, the latter characterized by ammonites, corals, gastropods and foraminifers including *Orbitolina*. Related to the basic volcanic arc is a varied group of plutonic intrusives including gabbro and peridotite (Fig. 16.15). In the Sarchu Valley in the Zanskar domain, the Upper Jurassic Spiti Shale contains interbedded volcanics as well as intrusives of mafic rocks (Raina and Bhattacharyya 1977).

It is apparent that as the floor of the NeoTethys subsided, the northern periphery of the Indian plate experienced extensional strain and resultant rifting. Basic and ultrabasic magmas found their ways into the fissures, and lavas poured out into subaqueous environment of active sedimentation. The lavas and volcanic ejectaments formed a linear belt close to the northern edge of the Indian continental margin.

16.7 Active Tectonic Environment in Late Cretaceous

16.7.1 Sinking Basin Floor

While the central Indian terrane was uplifting, the basin of deposition in the Tethyan domain continued to deepen as its floor sank progressively. By the Cretaceous time, the seafloor adjacent to the continental slope had reached the abyssal level. This is documented by glauconite-bearing deep-sea sediments of the Late Albian age and by the succeeding pelagic limestones and shales of the latest Albian (Garzanti 1999). The trend of the deepening of the basin floor is related to seafloor spreading that pushed the Indian plate progressively against the Asian landmass. In the Zhepure Mountain range close to the India–Asia tectonic boundary, the Upper Albian to Eocene succession provides a testimony to stronger subsidence in the Middle Maastrichtian to Early Paleocene time when the convergence had brought India close to Asia.

The stronger subsidence of the basin floor was the precursor to the closure of the NeoTethys Sea following the subduction of the Indian plate beneath Asia.

16.7.2 Submarine Slides

Steepening of the slopes of the Tethyan shelf due to progressive sinking of the basin floor triggered submarine slides in the environment in which turbidity currents were active (Valdiya 1998a). The *submarine slides* and debris flows are represented by deep-sea *olistostromes*, and associated chaotically structured deposits in the succession of turbidites and pelagic sediments (Fig. 16.16). The blocks and fragments are quite extraneous and exotic in comparison with the matrix material, as testified by the contained fossils (Gansser 1977, 1981; Shah 1977; Brookfield and Reynolds 1981; Brookfield and Andrews-Speed 1984; Sinha and Upadhyay 1993, 1997). The olistostromes contain significant proportion of fragments and blocks of distal older rocks of the Indian continental margin and less commonly of the proximal accretionary prism and magmatic volcanic arc of the active margin of Asia (Einsele et al. 1994).

It is quite evident that towards the end of the Cretaceous, the volcanoes were active in the inland as well as offshore belts. Simultaneously, the northern part of the cratonic India was uplifted and its northern margin and adjoining basin floor progressively subsided. The steepening of the shelf slope triggered submarine slides on the slopes of both India and Asia, implying that the two continents had come very close to one another. This development was the precursor to the subduction of the Indian plate—with its prism of sedimentary succession—beneath the Asian plate. The NeoTethys Sea was eventually closed as the two continents touched and were welded together, bringing to the end the long history of Tethyan sedimentation on the passive continental margin of India.

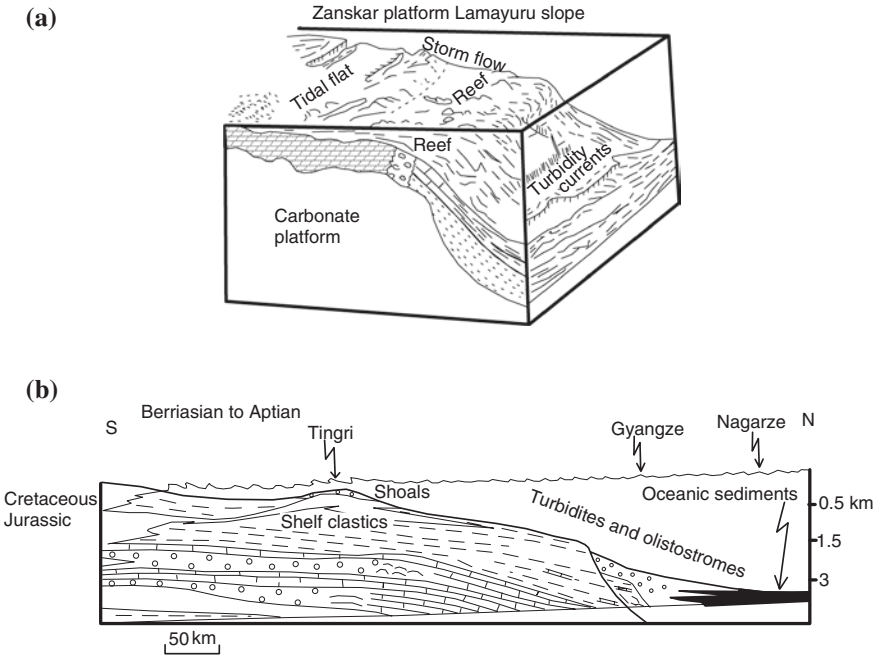

Fig. 16.16 **a** Steepening of slope of the Tethyan shelf (in the Zanskar area) following stronger subsidence of the basin floor, triggering submarine slides and attendant debris flows (after Sinha and Upadhyay 1993). **b** Basin evolution and lithofacies development in the Gyantse–Tingri region, showing initiation of slumping of slope material (after Einsele et al. 1994)

16.8 Mesozoic Stratigraphy of Karakoram

The Late Permian–Middle Triassic period witnessed development of peritidal carbonate flats in the south-western part of the Karakoram terrane (Gaetani 1997). The Triassic *Chhongtash Formation* is made up of fossiliferous limestones. The quartzolithic sandstones, characterized by clasts of serpentinite and mafic volcanic rocks, are overlain *unconformably* by the Upper Liassic red sandstone, documenting EoCimmerian tectonism. The Upper Jurassic and Lower Cretaceous successions are poorly documented, but the post-Barremian (Lower Cretaceous) time saw sedimentation in northern Karakoram which was subsequently deformed into a package of thrust sheets, including a slice of the basement crystalline rocks. The Middle Cretaceous is represented by conglomerates which cover the aforesaid thrust sheets. The Late Cretaceous *Morgo* and *Burtsa* formations are made up of richly fossiliferous limestone-shale alternation (Upadhyay 2002).

16.9 Mesozoic Stratigraphy of Tibet

The *Angui Formation* of the Lhasa area is overlain by a thick succession of limestones of the Triassic age. The limestones abound in brachiopods such as *Spiriferella* and *Neospirifer*. A continuous succession of sedimentary rocks from the Lower Triassic to the Upper Eocene occurs in southern Tibet adjoining the northern tectonic boundary (Indus-Tsangpo Suture) of India. Disconformities in the succession document major and minor hiatuses at ~255, 239, 215, 177, 157, 138, 107, 80, 68 and 50 Ma (Xiaoying et al. 1996). It is surmised that the 239-Ma event is related to the break-up of Tibet from India and the 113-Ma event marks the beginning of India's subduction, while the 80-Ma event is interpreted as the result of India–Asia contact. There was a strong uplift and thrusting in the Late Paleocene. Needless to state, these dates are not compatible with the commonly accepted chronology of events.

Overlying a sequence of the Triassic, Liassic and Middle Jurassic limestones and shales—the shale of the Gyantse and Kampa Dzong areas are correlatable with the Spiti Shale. The Cretaceous succession, known as the *Kampa Group*, covers a large part of central Tibet. In the type area Kampa Dzong, the Kampa succession comprises the following sequence: (i) basal unfossiliferous limestone, (ii) Cenomanian shale and argillaceous limestone containing *Acanthoceras rhotomagense* and *Turrilites costatus*, (iii) Campanian shales characterized by *Hemiaster*, *Gryphaea* and *Inoceramus* and (iv) Maastrichtian limestones containing *Gryphaea, Orbitoloides media* with *Radiolites*, among other taxa. The Kampa is capped by a ferruginous sandstones representing the Cretaceous–Tertiary transition.

References

Ahmad, Z. (1991). Ultramafic–mafic alkaline rocks from Spangar, Pishin district, Pakistan: Magmatism from the waning Gondwanaland. *Acta Mineral Pakistan, 5*, 25–45.

Arora, R. K., Mehra, S., & Misra, V. P. (1996). Stratigraphy of Triassic sequence in central part of Kashmir valley. *Special Publications of Geological Survey of India, 21*, 33–37.

Arora, R. K., Singh, G., Mehra, S., & Mehrotra, S. C. (2002). *Standardization of phanerozoic sequence, Tethyan belt, Northwest himalaya*. Kolkata: Geological Survey India. 110 p.

Bassoullet, J. P., Enay, R., & Mouterde, R. (1986). La marge noid Himalayenne au Jurassique. In P. Le Fort, M. Colchen, & C. Montenant (Eds.), *Orogenic evolution of Southern Asia* (pp. 43–60). Paris: La Foundation Scientifique de la Geologie et de ses Application.

Bassoullet, J. P., & Mouterde, R. (1977). Les formations sedimentaires mesozoiques du domaine tibetain de I' Himalaya due Nepal. In C. Jest (Ed.), *Ecologie et Geologie de l' Himalaya* (pp. 53–60). Paris: CNRS.

Baud, A., Gaetani, M., Garzanti, E., Fois, E., Nicora, A., & Tintori, A. (1984). Geological observation in southeastern Zanskar and adjacent Lahaul area (Northwestern Himalaya). *Eclogae Geologicae Helvetiae, 77*, 171–197.

Bender, F. (1983). *Geology of Burma*. Berlin: Gebruder Borntraeges. 293 p.

Bhandari, N., Shukla, P. N., & Cini Castagnoli, G. (1993). Geochemistry of some K/T sections in India. *Palceogeography Palaeoclimatology Palaeoecology, 104*, 199–211.

Bhargava, O. N., Krystyn, L., Balini, H., Lein, R., & Nicora, A. (2004). Revised litho- and biosequence stratigraphy of the Spiti Triassic. *Albertina, 30*(Supplement), 21–38.

Bhargava, O. N., Singh, I., Hans, S. K., & Bassi, U. K. (1998). Early Cambrian trace and trilobite fossils from the Nigalidhar Syncline (Sirmur District, Himachal Pradesh), lithostratigraphic correlation and fossil contents of the Tal group. *Himalayan Geology, 19*, 89–108.

Bhargava, O. N., Srivastava, R. N., & Gadhoke, S. K. (1987). Jurassic-Cretaceous sedimentation in the Spiti Valley, NW Himalaya. *Journal Indian Association Sedimentologists, 7*, 1–7.

Bhargava, O. N., & Tangri, S. K. (1996). Late Jurassic-Early Cretaceous Lingshi Formation, Bhutan Himalaya. *Journal Geological Society India, 37*, 113–119.

Bhatt, D. K., & Arora, R. K. (1984). Octoceras bed of Himalaya, and Permian-Triassic boundary assessment and elucidation with conodont data. *Journal Geological Society India, 25*, 720–727.

Bhatt, D. K., Joshi, V. K., & Arora, R. K. (1999). Conodont biostratigraphy of the Lower Triassic in Spiti Himalaya. *Journal Geological Society India, 54*, 153–167.

Bodenhausen, J. W. A., & Egeler, C. G. (1971). On the geology of the upper Gandaki valley, Nepalese Himalaya. *Koninklijke Nederlandse Akademie van Westenchappen, 74*, 526–546.

Bordet, P., Colchen, M., Krummenacher, D., Le Fort, P., Mouterde, R., & Remy, M. (1971). *Recherches Geologiques dans l'Himalaya du Nepal Region de la Thakkola*. Scientifique, Paris: Centre Nationale Recher. 279 p.

Bronnimann, P., Whittaker, J. E., & Zaninetti, L. (1975). Triassic foraminiferal biostratigraphy of the Kyaukme–Langtaw-kno area, Northern Shan States, Burma. *Rivista Italiana Paleontologia, 81*, 1–30.

Brookfield, M. E., & Andrews-Speed, C. P. (1984). Sedimentology, petrography and tectonic significance of the shelf-flysch and molasse-clastic deposits across the Indus Suture Zone, Ladakh, NW India. *Sedimentary Geology, 40*, 249–286.

Brookfield, M. E., & Reynolds, P. H. (1981). Late Cretaceous emplacement of the indus suture zone ophiolitic melange and Eocene-Oligocene magmatic arc on the northern edge of the Indian plate. *Earth & Planetary Science Letters, 55*, 157–162.

Brookfield, M. E., Twitchetl, R. J., & Goodings, C. (2003). Palaeoenvironments of the Permian-Triassic transition sections in Kashmir, India. *Palaeogeography Palaeoclimatology Palaeoecology, 198*, 353–371.

Brunnschweiller, R. O. (1966). On the geology of the Indo-Burman Ranges. *Geological Society Australia Journal, 13*, 127–194.

Chhibbar, H. L. (1934). *The Geology of Burma*. London: MacMillan. 538 p.

Colchen, M., Le Fort, P., & Pecher, A. (1986). *Recherches Geologiques dans l' Himalaya due Nepal Annapurna, Manaslu*. Paris: Ganesh Himal, Centre Nationale Recherche Scientifique. 136 p.

Durr, S. B., & Gibling, M. R. (1994). Early Cretaceous volcaniclastic and quartzose sandstones from Northcentral Nepal: Composition, sedimentology and geotectonic significance. *Geologische Rundschau, 83*, 62–75.

Egeler, C. G., Bodenhausen, J. W. A., DeBooy, T., & Nijhuis, H. J. (1964). *On the geology of central west Nepal*. Report 22nd International Geology Congress, Part 10, New Delhi, pp 101–122.

Einsele, G., Liu, B., Durr, S., Frisch, W., Liu, G., Luterbacher, H. P., et al. (1994). The Xigaze forearc basin: evolution and facies architecture (Cretaceous Tibet). *Sedimentary Geology, 90*, 1–32.

Fan, P. F., & Koko, K. (1994). Accreted terranes and mineral deposits of Myanmar. *Journal Asian Earth Sciences, 10*, 95–100.

Fuchs, G. R. (1967). Zum Bau des Himalaya, Denkschr. Obterr. Akad. Wiss., Wien, 211 p.

Fuchs, G. R. (1977). Traverse of Zanskar from the Indus to the valley of Kashmir—a preliminary note. *Jahrbuch der Geolgischen Bundesanstaly, 120*, 219–229.

Fuchs, G. R. (1987). The geology of southern Zanskar (Ladakh)—evidence for the autochthony of the Tethys zone of the Himalaya. *Jarhbuch Geologischen Bundesanstalt, 130*, 465–491.

Fuchs, G. R., Widder, R. W., & Tuladhar, R. (1988). Contributions to the geology of the Annapurna Range (Manang area) Nepal. *Jahrbuch der Geolgischen Bundesanstaly, 131*, 593–607.

Gaetani, M. (1997). The Karakoram block in central Asia, from Ordovician to Cretaceous. *Sedimentary Geology, 109*, 339–359.

Gaetani, M., & Garzanti, E. (1991). Multicyclic history of northern India continental margin (NW Himalaya). *Bulletin American Association Petroleum Geology, 75*, 1427–1446.

Gaetani, M., Garzanti, E., Fois, E., Nicora, A., & Tintori, A. (1983). Upper cretaceous and palaeocene in Zanskar Range (NW Himalaya). *Rivista Italiana Palaeontologia & Stratigraphy, 89*, 81–118.

Gaetani, M., Garzanti, E., & Tintori, (1990). Permo-carboniferous stratigraphy in SE Zanskar and NW Lahaul (NW Himalaya, India). *Eclogae Geologicae Helvetiae, 83*, 143–161.

Gaetani, M., Raffache, C., Fois, E., Garzanti, E., Jadoul, F., Nicora, A., & Tintori, A. (1985). Stratigraphy of the Tethys Himalaya in Zanskar Ladakh. *Rivista Italiana Palaeontologia & Stratigraphy, 91*, 443–478.

Ganesan, T. M., & Bose, M. N. (1982). Plant remains of Mesozoic age from Lingshi basin, Bhutan. *Geophytology, 12*, 279–286.

Gansser, A. (1964). Geology of the himalayas. *Interscience Publishers, London, 289*, 289.

Gansser, A. (1977). The great suture zone between Himalaya and Tibet: A preliminary note. *Himalaya: Science de la Terre* (pp. 181–191). Paris: CNRS.

Gansser, A. (1981). The geodynamic history of the Himalaya. In H. K. Gupta & F. M. Delany (Eds.), *Zagros–Hindukush–Himalaya: Geodynamic evolution, amer* (pp. 111–121). Washington: Geophysical Union.

Garson, M. S., Amos, B. J., & Mitchell, A. H. G. (1976). The geology of the area around Neyaunagga and Yengan, Southern Shan States, Burma. *Overseas Memoir International Geology Science London, 2*, 1–70.

Garzanti, E. (1999). Stratigraphy and sedimentary history of the Nepal Tethys Himalaya passive margin. *Journal Asian Earth Sciences, 17*, 805–827.

Garzanti, E., & Haver, T. V. (1988). The Indus clastics: forearc basin sedimentation in the Ladakh Himalaya (India). *Sedimentary Geology, 59*, 237–249.

Gibling, M. R., Gradstein, F. M., Kristianen, I. L., Nagy, J., Sarti, M., & Wiedmann, J. (1994). Early cretaceous strata of Nepal Himalaya: Conjugate margins and rift volcanism during Gondwana breakup. *Journal Geological Society London, 151*, 269–290.

Gradstein, F. M., Gibling, M. R., Sarti, M., von Rad, U., Thrurow, J. W., Off, J. G., et al. (1991). Mesozoic Tethyan strata of Thakkhola, Nepal: Evidence for the drift and breakup of Gondwana. *Palaeogeography Palaeoclimatology Palaeoecology, 88*, 193–218.

Gramann, F. (1974). Some palaeontological data on the Triassic and Cretaceous of the western part of Burma (Arakan Islands, Arakan Yoma, western outcrops of Central Basin). *Newsletters on Stratigraphy, 34*, 277–290.

Gramann, F., Lain, F., & Stoppel, D. (1972). Paleontological evidence of Triassic age for limestones from the Southern Shan State and Kayah State of Burma. *Geological Jarhbuch Bundes., 115*, 1–33.

Hallam, A., & Maynard, J. B. (1987). The iron ores and associated sediments of the Chichali Formation (Oxfordian to Valanginian) of the Trans-Indus Salt Range, Pakistan. *Journal Geological Society London, 144*, 107–114.

Hallam, A., Wignall, P. B., Jiarun, Y., & Riding, J. B. (2000). An investigation into the possible facies changes across the Triassic-Jurassic boundary in southern Tibet. *Sedimentary Geology, 137*, 101–106.

Heim, A., & Gansser, A. (1939). Central Himalaya: Geological observations of the Swiss expedition 1936. *Denkschr Schweiz Naturf Ges, 32*, 1–245.

Ibrahim Shah, S. M., 1977. (Ed) *Stratigraphy of Pakistan*. Geological Survey of Pakistan, Quetta, 138 p.

Jadoon, I. A. K., & Lawrence, R. D. (1994). Mari-Bugti pop-up zone in the central Sulaiman fold belt, Pakistan. *Journal Structure Geology, 16*, 147–158.

Kapoor, H. M. (1977). Pastannah section of Kashmir with special reference to *Ophiceras* bed of Middlemiss. *Journal Palaeontology Society India, 20*, 339–347.

Kapoor, H. M. (1992). Permo-Triassic boundary of the Indian subcontinent and its intercorrelation. In W. C. Sweet., Y. Zunyi., J. M. Dikins, & H. Yin (Eds.), Permo-Triassic events in the Eastern tethys. Cambridge University Press, pp. 21–36.

Kapoor, H. M. (1996). The Guryul ravine section, Kashmir, In: H. Yin (Ed.), *The Palaeozoic Mesozoic Boundary* (pp. 99–110). China University Geoscience Press, Wuhun.

Kazmi, A. H., & Qasim Jan, M. (1997). *Geology and Tectonics of Pakistan*. Karachi: Graphic Publishers. 554 p.

Krishna, J. (1987). An overview of the Mesozoic stratigraphy of Kachchh and Jaisalmer basins. *Journal Palaeontogical Society India, 32*, 136–152.

Krishna, Jai, Singh, Anshu K., & Upadhyay, R. (1997). First find of the Hettangian Psiloceras (Jurassic Ammonitina) from the Indus-Tsangpo Suture, Ladakh Himalaya, Diverse implications. *Himalayan Geology, 18*, 145–151.

Kummel, B., & Teichert, C. (1966). Relation between the Permian and Triassic formations in the salt range and trans-Indus ranges, West Pakistan. *Neues Jahrbuch Geologie Palaontologie Abhandlungen, 125*, 297–333.

Mamgain, V. D., & Mishra, R. S. (1989). Biostratigraphical studies of the Palaeozoic and Mesozoic sediments of the Tethyan facies in U.P. Himalaya. *Record Geological Survey India, 122*, 296–299.

McElroy, R., Carter, J., Roberts, I., Peckham, A., & Bond, M. (1990). The structure and stratigraphy of SE Zanskar, Ladakh Himalaya. *Journal Geological Society London, 147*, 989–997.

Mehrotra, D. K., Sahgal, A., & Jangpangi, B. S. (1981). On some early Triassic fish microremains from the Shalshal area of Kumaun Himalaya, U.P. *Himalayan Geology, 11*, 433–437.

Nagappa, Y. (1959). Foraminiferal biostratigraphy of the Cretaceous–Eocene succession in the India–Pakistan–Burma region. *Micropalaeontology*, 5, 145–177.

Nakazawa, K. (1985). The Permian and Triassic system in the Tethys—Their palaeography. In K. Nakazawa & J. M. Dickins (Eds.), *The Tethys—Her Palaeogeography and Palaeobiogeography from Palaeozoic to Mesozoic, Tokai University* (pp. 93–111). Tokyo: Press.

Nakazawa, K., & Kapoor, H. M. (1981). The Upper Permian and Lower Triassic fauna of Kashmir. *Palaeontologia Indica, 46*, 1–204.

Nakazawa, K., Kapoor, H. M., Bando, I., Okimura, Y., & Kokuoka, T. (1975). The Upper Permian and Lower Triassic in Kashmir, India. *Memoir Faculty of Science, Kyoto University* (Geology-Mineralogy Series), 42, 1–106.

Nautiyal, S. P., Jangpangi, B. S., Singh, P., Guha Sarkar, T. K., Bhate, V. D., Raghavan, M. R., & Sahai, T. N. (1964). A preliminary note on the geology of Bhutan Himalaya. *Report of 22nd International Geological Congress*, 11, pp. 1–14.

Ogg, J. G., & von Rad, U. (1994). The Triassic of Thakkhola (Nepal): Palaeolatitudes and comparison with other Eastern Tethyan margins of Gondwana. *Geologische Rundschau, 83*, 107–129.

Okimura, Y., & Fatmi, A. N. (1988). Tectonics and sedimentation of the Indo-Eurasian colliding plate boundary region and its influence on the mineral developments in Pakistan. *Journal Overseas Scientific Research, Hiroshima University, 32*, 1–32.

Pathak, D. B. (1997). Ammonoid stratigraphy of the Spiti Shale Formation in Spiti Himalaya, India. *Journal Geological Society India, 50*, 191–200.

Prashra, K. C., & Raj, D. (1990). Permo-Triassic fossils from the Tandi Group of Lahaul Himalaya, Himachal Pradesh: their stratigraphic and palaeogeographic significance. *Journal Geological Society India, 36*, 512–518.

Raina, V. K., & Bhattachayya, D. P. (1977). The geology of a part of the Charap and Sarchu valley, Lahul and Spiti district, Himachal Pradesh. *Quaterly Journal Geology Mining Metallurgical Society India*, Golden Jubilee Volume, pp. 129–142.

Rajnath, R. (1932). A contribution to the stratigraphy of Cutch. *Quaterly Journal Geological Mining Metallurgical Society India, 4*, 161–174.

Robertson, A., & Sharp, I. (1998). Mesozoic deep-water slope/rise sedimentation and volcanism along the North Indian passive margin: evidence from the Karamba Complex, Indus Suture Zone (Western Ladakh Himalaya). *Journal Asian Earth Sciences, 16*, 195–215.

Sakai, H. (1984). Stratigraphy of Tansen area in the Nepal Lesser Himalaya. *Journal Nepal Geological Society, 4*, 41–52.

Sakai, H. (1991). The Gondwanas in Nepal Himalaya. In S. K. Tandon, S. M. Casshyap, & C. C. Pant (Eds.), *Sedimentary Basin of India: Tectonic Context* (pp. 204–217). Nainital: Gyanodaya Prakashan.

Sarwar, G. (1992). Tectonic setting of the Bela ophiolites, southern Pakistan. *Tectonophysics, 207*, 359–381.

Shah, S. K. (1977). Indus ophiolite belt and the tectonic setting of the MallaJohar–Kiogarh exotics in Himalaya, In *Himalaya: Science de la Terra* (Vol. 268, pp. 361–368), CNRS, Paris.

Shah, S. K. (1991). Stratigraphic setting of the Phanerozoic rocks along the northern boundary of the Indian plate. *Physics and Chemistry of the Earth, 18*, 317–328.

Shah, S. K., & Sinha Anshu, K. (1974). Stratigraphy and tectonics of the Tethyan zone in a part of western Kumaun Himalaya. *Himalayan Geology, 4*, 1–27.

Shams, F. A., & Ahmad, S. (1976). Petrology of the Twin Sisters soda dolerite, southeast of Muslimbagh, Zhob district, Baluchistan, Pakistan. *Pakistan Journal Science Research, 28*, 79–84.

Sheikh, S. A., & Naseen, S. (1996). A synthesis of the Cretaceous System of Pakistan. *Memoirs Geological Society India, 37*, 105–112.

Siddiqi, R. H., Aziz, A., Mengal, J. M., Hoshino, K., Sawada, Y., & Nabi, G. (1994). Petrology and mineral chemistry of Muslimbagh ophiolite complex and its tectonic implications. *Proceedings Geoscience Colloquium, 9*, 17–50.

Singh, R., Jamwal, J. S., & Singh, K. (2000). Geology of part of Warwan Valley, Doda district, Kashmir Himalaya. *Journal Geological Society India, 56*, 651–659.

Sinha, Anshu K. (1989). *Geology of Higher Central Himalaya*. Chichester: John Wiley. 236 p.

Sinha, Anshu K., & Upadhyay, R. (1993). Mesozoic Neo-Tethyan pre-orogenic deep marine sediments along the Indus-Yarlung Suture. *Terra Nova, 5*, 271–281.

Sinha, Anshu K., & Upadhyay, R. (1997). Tectonic setting and preorogenic sedimentation in the Indus-Tsangpo Suture Zone of Ladakh Himalaya. *Journal South East Asian Earth Sciences, 9*, 435–450.

Srikantia, S. V. (1981). Lithostratigraphy, sedimentation and structure of Proterozoic–Phanerozoic formations of Spiti basin in Higher Himalaya of Himachal Pradesh. In A. K. Sinha (Ed.), *Contemporary Geoscientific Researches in Himalaya* (Vol. I, pp. 31–48). Bishensingh & Mahenderpalsingh, Dehradun.

Tangri, S. K., & Pande, A. C. (1995a). Tethys sequence. In O. N. Bhargava (Ed.), *The Bhutan Himalaya: A Geological Account* (pp. 109–141). Kolkata: Geological Survey of India.

Tangri, S. K., & Pande, A. C. (1995b). Tectonostratigraphy of Tethyan sequence. *Geological Survey India Special Publications, 39*, 109–142.

Thein, M. (1973a). A preliminary synthesis of the geological evolution of Burma, with special reference to the tectonic development of Southeast Asia. *Geological Society Malaysia Bulletin, 6*, 87–116.

Thein, M. L. (1973b). The Lower Palaeozoic stratigraphy of western part of the Southern Shan States, Burma. *Geological Society of Malaysia, 6*, 143–163.

Upadhyay, R. (2002). Stratigraphy and tectonics of Ladakh, Eastern Karakoram, Western Tibet and Western Kun Lun. *Journal Geological Society India, 59*, 447–467.

Valdiya, K. S. (1998). *Dynamic himalaya*. Hyderabad: Universities Press. 178 p.

von Rad, U., Durr, S. B., Ogg, J. G., & Wiedmann, J. (1994). The Triassic of the Thakkhola (Nepal): Stratigraphy and palaeoenvironment of a northeast Gondwana rifted margin. *Geologische Rundschau, 83*, 76–106.

Wadia, D. N. (1931). The syntaxis of the northwest Himalaya: its rocks, tectonics and orogeny. *Record Geological Survey India, 65*, 189–200.

Wadia, D. N. (1934). The Cambrian-Trias sequence of NW Kashmir. *Record Geological Survey India, 68*, 121–167.

Wadia, D. N. (1937). The Cretaceous volcanic series of Astor-Deosai, Kashmir and its intrusion. *Record Geological Survey India, 72*, 151–161.

Wadia, D. N. (1975). *Geology of India*. New Delhi: Tata McGraw Hill. 508 p.

Wager, L. R. (1939). The Lachi series of N. Sikkim and the age of the rocks forming Mount Everest. *Record Geological Survey India, 74*, 171–188.

Wang, C. S., Hu, X. M., Jansa, L., Wan, X. Q., & Tao, R. (2001). The Cenomanian-Turonian anoxic event in southern Tibet. *Cretaceous Research, 22*, 481–490.

Wang, C., Xianghui, L., Hu, X., & Jansa, L. F. (2002). Latest marine horizon north of Qomolongma (Mt. Everest): implications for closure of Tethys seaway and collision tectonics. *Terra Nova, 14*, 114–120.

Westermann, G. E. G., & Yi-Gang, W. (1988). Middle Jurassic ammonites of Tibet and the age of the lower spiti shales. *Palaeontology, 31*, 295–339.

Wiedmann, J., & Balka, Z. (1996). Conodont stratigraphy of the lower triassic in the Thakkhola region (eastern Himalaya, Nepal). *Newsletter Stratigraphy, 33*, 1–14.

Wingnall, P. B., & Hallman, A. (1993). Griesbachian (Earliest Triassic) palaeoenvironmental changes in the Salt Range, Pakistan, and southeast China and their bearing on the Permo-Triassic mass extinctions. *Palceogeography Palaeoclimatology Palaeoecology, 102*, 215–237.

Willems, H., Zhou, Z., Zhang, B., & Grafe, K.-U. (1996). Stratigraphy of the Upper Cretaceous and Lower Tertiary strata in the Tethyan Himalayas of Tibet (Tingri area, China). *Geologische Rundschau, 85*, 723–754.

Xiachi, L., & Grant-Mackie, J. A. (1993). Jurassic sedimentary cycles and eustatic sealevel changes in southern Tibet. *Palaeogeography Palaeoclimatology Palaeoecology, 101*, 27–48.

Xiaoying, S., Jiarum, Y., & Caiping, J. (1996). Mesozoic to Cenozoic sequence: Stratigraphy and sea level changes in the northern Himalayas, southern Tibet. *Newsletters on Stratigraphy, 33*, 15–61.

Chapter 17
Docking of India with Asia

17.1 India–Asia Convergence

As India converged towards Asia, its leading edge dipped northwards. The floor of the NeoTethys Sea subsided progressively as India approached the active continental margin of Asia. By Early Cretaceous, the seafloor had sunk considerably to form a deep depression. Thick deposits of flysch accumulated all along the periphery of the passive continental margin of India, and in the depression in front of the active margin of Asia. Steepening of the shelf slope sometimes triggered submarine slides and generated debris flows and attendant turbidity currents. These phenomena gave rise to wild flysch characterized by olistostrome of chaotic texture and structure. It appears that by the Late Cretaceous the two continents had come very close to one another (Fig. 17.1) and the sliding of the seafloor under the Asian plate had resulted in the formation of an elongate deep oceanic trench. In this deep depression were deposited material derived from the converging continents, predominantly from the Indian plate.

17.2 Evolution of Volcanic Island Arc

The northward moving and subducting oceanic crust was rent apart offshore of the continental margin of Asia, and lavas welled out to form volcanic islands in the sea. The arcuate chain of submarine volcanoes and seamounts extended more than 2500 km from Chitral in the west through Dras in Ladakh, to Shigatse in southern Tibet (Fig. 17.2). Fragments of volcanic rocks in the continental rise on the margin of the Indian plate and in the oceanic trench indicate that volcanism commenced in the Late Jurassic to Early Cretaceous (Brookfield and Andrews-Speed 1984; Robertson and Degnan 1994) and culminated in the development of island

K.S. Valdiya, *The Making of India*, Society of Earth Scientists Series,
DOI 10.1007/978-3-319-25029-8_17

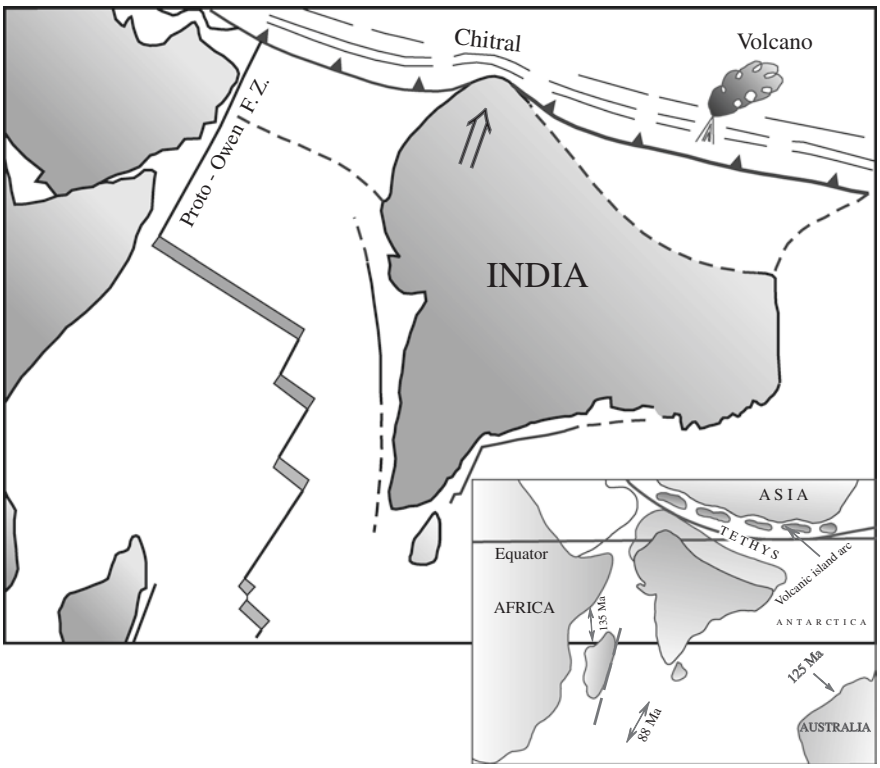

Fig. 17.1 India–Asia convergence at the rate of 180–195 mm per year (Klootwijk et al. 1992) brought India close to the active margin of Asia

arc complexes. The complexes comprise the main body of basic lavas associated with underlying ultrabasic rocks. These were flanked by shallow southern forearc and northern *back-arc basins* of volcanosedimentary assemblages.

17.2.1 Kohistan Island Complex

The *Kohistan Island Complex* comprises three main lithotectonic assemblages (Fig. 17.3). In the southern part, the *Jijal Formation* consists of ophiolitic mantle material—dunite, harzburgite, websterite and basic rocks dated 102 ± 12 Ma (Albian) by the Rb–Sr method (Petterson and Windley 1985). To the north, on the dominantly oceanic ridge basalts occurs a thick pile of ocean-type basalts (*Kamila Formation*) intruded at 85 Ma by multiple plutons of gabbro, norite, dunite, harzburgite, layered cumulates and hornblendite (*Chilas Formation*). The norite plutons not only intrude the Kamila lavas, but also the low-grade metamorphic rocks in the Gilgit area. Turbidite sediments associated with pillow basalts

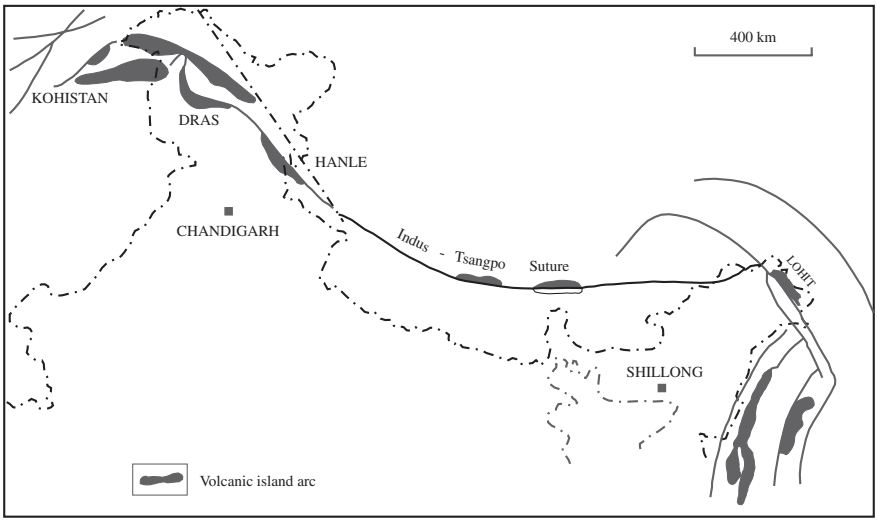

Fig. 17.2 Chain of volcanic islands north of the continental margin of India in relation to the zone of India–Asia docking (Valdiya 1998)

(*Jaglot Formation*) and high-magnesium andesite and boninite lavas (*Chalt-Yasin Formation*) were emplaced, respectively, in the back-arc and forearc basins. The high-boninite *Chalt Volcanics* are characterized by initial strontium ratio of 0.7036–0.7066, εNd of +28 to +7.4 and $^{206}Pb/^{204}Pb$ ratio of 18.0–18.6, a characteristic property of island-arc volcanics (Asif Khan et al. 1997). The Kohistan complex amalgamated to Asia at about 100 Ma. This was accompanied by thickening of the arc and development of intra-arc shear zones and rifting of the crust. This rifting permitted emplacement of voluminous gabbro–norite suite of the *Chilas Complex*. The boninite in the northern part is interpreted as an eruption into a short-lived back-arc basin. In the Dir-Utror area, the volcanics are characterized by enrichment of Ce, La, Ba, Rb and K and by strongly negative Nb and Ti anomalies, implying their affinity with the subduction-related magma derived from LREE-enriched mantle beneath the arc (Shah and Shervais 1999). From the garnet-bearing granulite in the Jijal ultrabasics, it is inferred that the rocks had subducted to the depth of 45 km where they were metamorphosed under pressure of 12–14 kbar (Searle et al. 1999). The Kohistan complex grew downwards through magmatic emplacement in the lower part and upwards through extrusion of lavas over a period 120/125–90 Ma—that is from the Early Aptian to the Turonian/Coniacian (Asif Khan et al. 1998).

The Kohistan Island touched the Karakoram terrane of Asia and was amalgamated with it some time between 102 ± 12 Ma (Petterson and Windley 1985) and 85 Ma (Treloar et al. 1996). Later, the Jijal ophiolite is believed to have been obducted between 75 and 55 Ma (Searle et al. 1999). Following the joining together of continents, the island-arc complex was intruded by granites

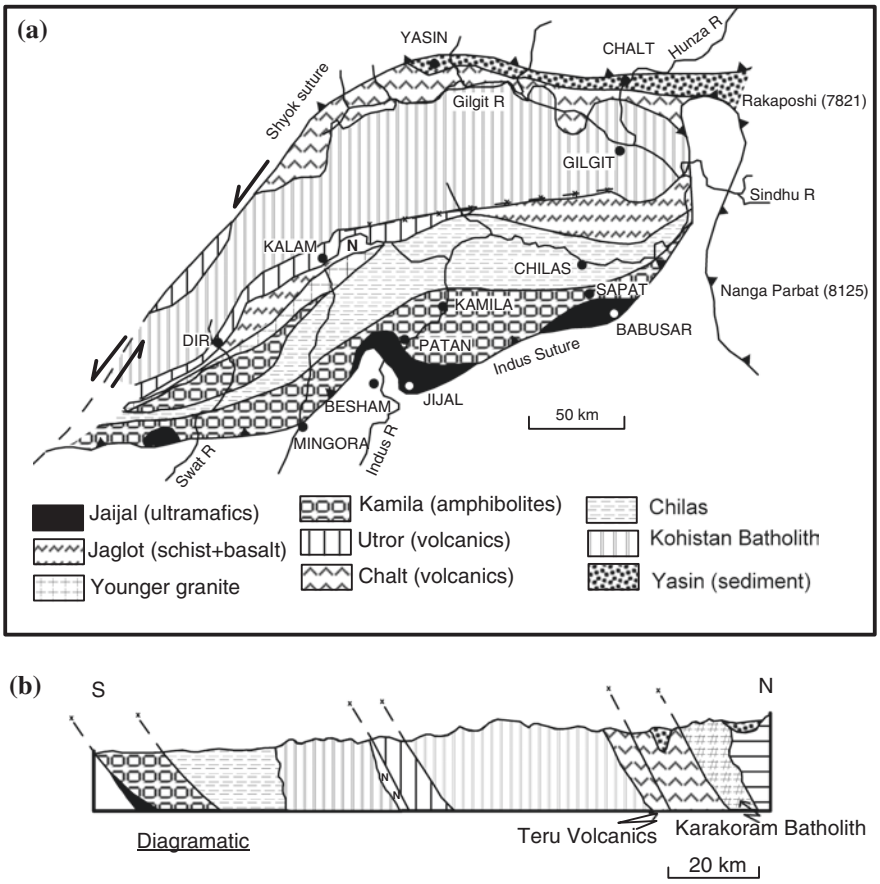

Fig. 17.3 Kohistan island-arc complex in northern Pakistan. **a** Sketch map shows lithological units defined by the Indus–Tsangpo suture (Main Mantle Thrust) and the Shyok suture (Main Karakoram Thrust or Northern suture) (modified after Bignold and Treloar 2003). **b** Simplified schematic section unravels the structural architecture of the Kohistan complex (modified after Danishwar et al. 2001)

of batholithic dimension. The *Kohistan Batholith* includes two plutons dated 54 ± 4 Ma and 40.6 Ma (Petterson and Windley 1985). There are dykes and sheets of aplite and pegmatite cutting across the batholithic mass.

17.2.2 Dras Island Complex

The N–S trending promontary of the Indian plate in the north-western syntaxis or mountain bend the Nanga Parbat–Haramosh massif—separates the Kohistan island arc complex from the Ladakh terrane, another island-arc complex in the

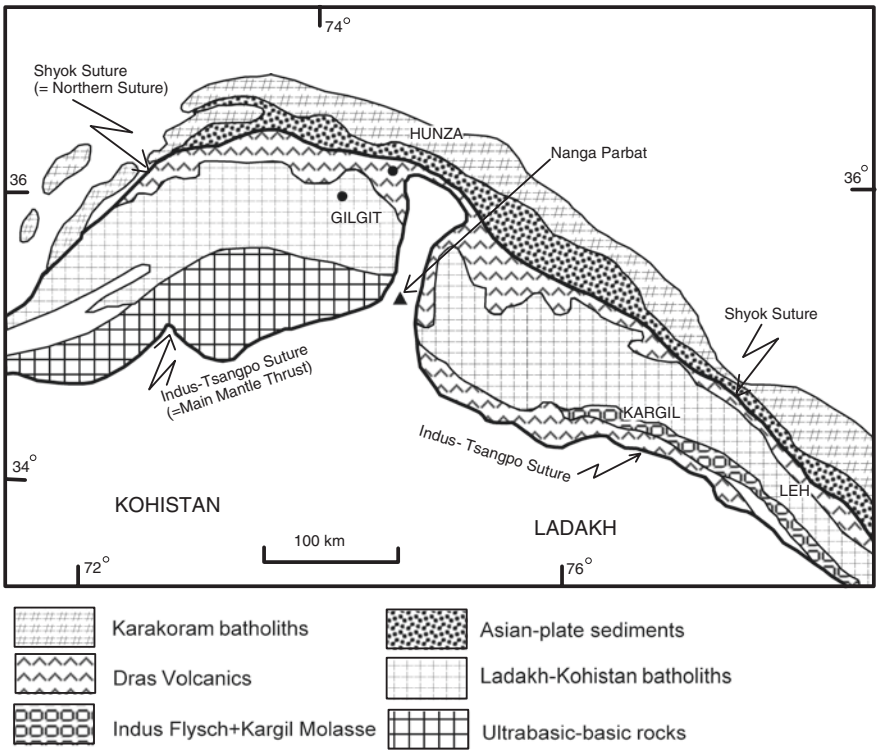

Fig. 17.4 Kohistan and Ladakh terranes, representing island-arc complexes and penetrated by Batholiths of granite, are separated by a N–S trending promontary of the Indian landmass—the Nanga Parbat–Haramosh massif occupying the pivot of the syntaxis (after Robertson and Collins 2002)

east—the *Dras Island Complex*—(Fig. 17.4). The Ladakh terrane represents a Late Cretaceous intra-oceanic volcanic island-arc complex developed on a partly dissected Upper Jurassic oceanic crust, (Shah et al. 1976; Srikantia 1978; Shanker et al. 1976; Frank et al. 1977; Fuchs 1977; Shah 1977; Sharma and Kumar 1978; Srikantia and Razdan 1980; Thakur and Bhat 1983; Sharma and Gupta 1983; Brookfield and Andrews-Speed 1984; Thakur and Misra 1984; Srimal 1986; Srimal et al. 1987; Garzenti and Haver 1988; Reuber 1989; Sharma 1991; Sinha and Upadhyay 1993, 1997; Robertson and Degnan 1994; Rolland et al. 2000; Clift et al. 2000; Robertson and Collins 2002). The complex (Fig. 17.5) comprises three main lithological assemblages: (1) The arc-interior *Dras Formation* made up of serpentinized peridotite, harzburgite, lherzolite and hornblende-gabbro representing modified mantle material and the basalts that are compatible with potential source rocks for mid-oceanic ridge basalt. The volcanic islands and seamounts (Sinha and Mishra 1992a, b) constitute the main body of the arc complex; (2) The proximal forearc apron (*Naktul Formation*) consisting of shallowing-upwards sequence of turbidites, capped by nummulitic limestone in the southern

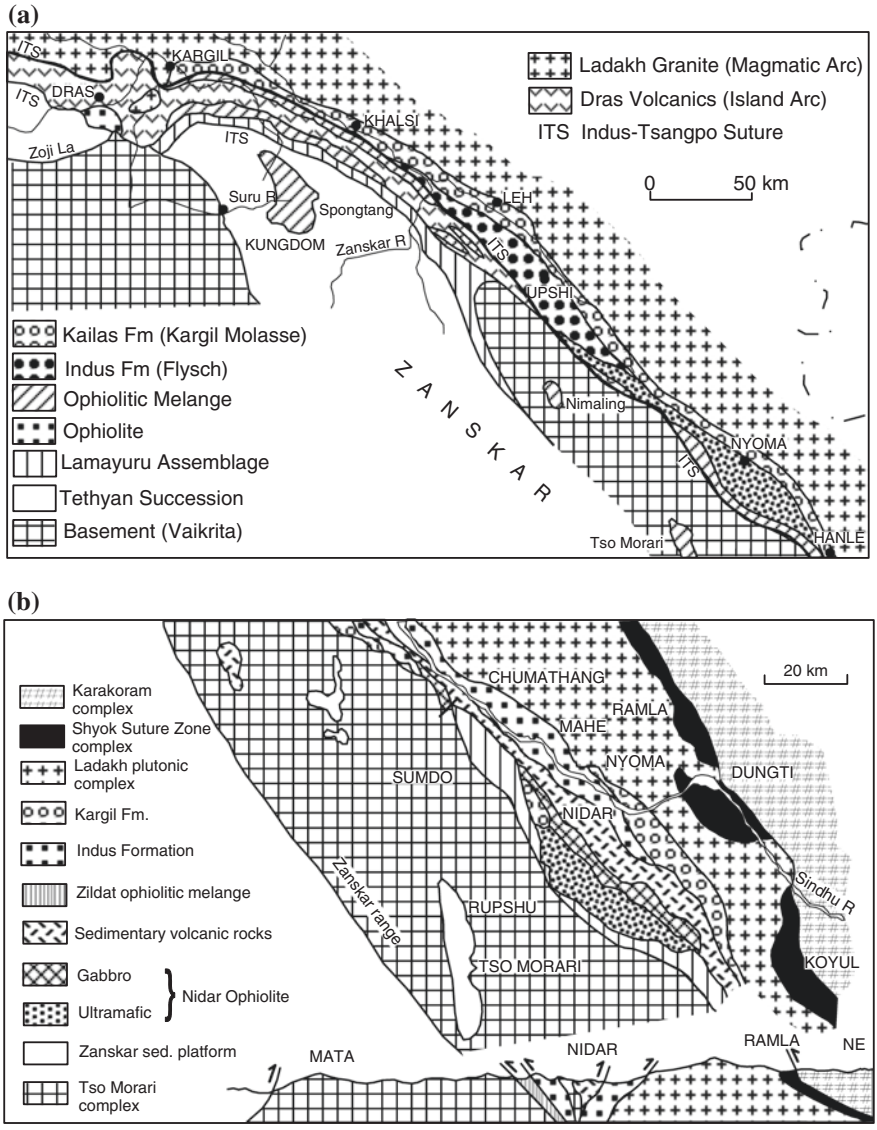

Fig. 17.5 Sketch map depicting the geology of the eastern part of the Ladakh Island Arc Complex (compiled from various sources, Valdiya 1998)

flank of the arc, and fining-upwards deltaic deposits on the northern side; and (3) The distal deep-water volcaniclastic turbiditic flysch with chert beds (*Nindam Formation*) of the forearc basin and its slopes. It is characterized by olistostrome formed due to collapse of the basin slopes (Fig. 17.6).

In the Upper Early Cretaceous time, a platform of carbonates (designated *Khalse Formation*) developed on the fringe of the Dras volcanic island. Its deeper

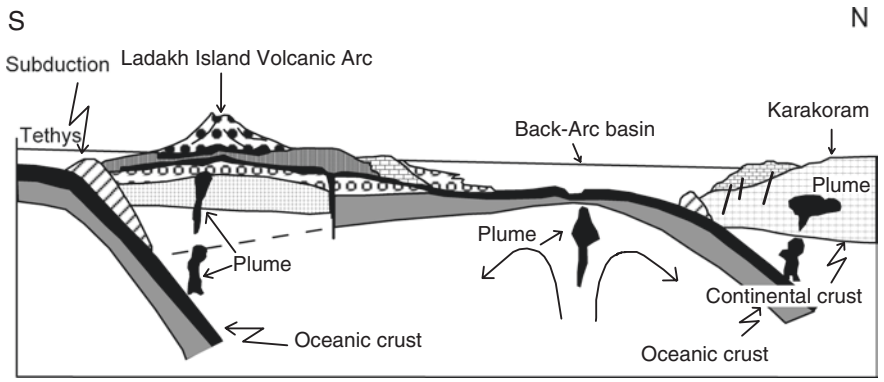

Fig. 17.6 Conceptual model of the evolution of the Dras volcanic island in the Ladakh complex during the Albian to Cenomanian time (after Rolland et al. 2002)

water facies embodies a flysch sequence characterized by clasts derived from the Tethys Himalayan sedimentary domain to the south. In the Burzil area, the limestone intercalations within lava succession contain orbitolines of the Barremian to Aptian age (Mamgain and Jagannath Rao 1965). The Dras volcanoes emerged above the sea water in the Cenomanian–Turonian time and were exposed to subaerial erosion. Large volumes of volcaniclastic detritus thus generated (Fig. 17.6) were carried by turbidity currents to deeper part of the basin where pelagic sediments were accumulating (Robertson and Degnan 1994).

The volcanic island complex was intruded by the *Ladakh Batholith* of great dimension over a long period. It is a calc–alkaline magmatic body comprising predominant granodiorite and biotite–granite, associated with such volcanics as trachyandesite and andesitic rhyolite. The $^{40}Ar/^{39}Ar$ dating indicates that the granitic complex of Ladakh was later subject to partial melting, giving rise at 44.3 ± 0.6 Ma to granodiorite Batholith, and later at 29.8 ± 0.2 Ma to leucogranite (Bhutani et al. 2004). U–Pb zircon ages of granites from different places in the Ladakh batholithic body fall in four distinct group—66.6 ± 2.1 Ma, 57.6 ± 1.4 Ma, 53.4 ± 1.8 Ma to 52.50 ± 0.53 Ma and 45.27 ± 0.5 Ma, indicating that the great plutonic body is a composite of granites of four different ages—67, 58, 53 and 45 Ma spanning the period Palaeocene to Middle Eocene (Upadhyay et al. 2008). In the Indus-Tsangpo Suture Zone, high temperature (>500 °C) lasted nearly 8 million years, until about 38 Ma, as borne out by the basalts of the Sumdo stream. Xenoliths of quartzite and metapelites interbedded with lavas and platform carbonates indicate the lithological composition of the country rock. In the xenoliths of marbles were found *Megalodon* and *Lithiotes* of the Late Triassic to Early Jurassic age.

The convergence of India towards Asia had narrowed the sea considerably. Towards the later stage, the once vast NeoTethys Sea ended up in a remnant basin. The succession of deep-sea clay, calcareous limestone, chert and greywacke, described as the *Indus Flysch* (Tewari 1964), conformably overlies other older

formations of the island complex and the continental margin. In the Chagdo area, the sandstone of the Indus succession Flysch is overlain by a limestone horizon containing Ypressian (Early Eocene) *Nummulites* (Clift et al. 2002). It is the youngest marine horizon in the belt of subduction and seems to represent the end of the NeoTethys Sea in the Ladakh sector.

17.2.3 Shyok (Northern) Suture

In the north, the Kohistan and Ladakh island-arc complexes are separated from the Palaeozoic sedimentary rocks with the Karakoram Batholith (Figs. 17.3, 17.4 and 17.5) of the Asian continental margin by what has been described as the *Main Karakoram Thrust* (Tahirkheli 1982; Tahirkheli et al. 1979) or Northern Suture (Pudsey 1986), and the *Shyok Suture* (Bhandari et al. 1979; Srikantia et al. 1982; Thakur and Misra 1984; Srimal 1986; Upadhyay et al. 1999). This suture developed when the island-arc complexes slammed against the Karakoram terrane of Asia, in the Early Late Cretaceous (Pudsey 1986) or at 78–75 Ma (Searle et al. 1999). The Northern Suture (Fig. 17.3) is marked by a zone of melange, 150 m–4 km in width, and characterized by blocks and fragments of volcanic greenstones, limestones, red shales, conglomerates and quartzites associated with serpentinites held in the matrix of slates. Part of this melange is *olistostrome*, was derived largely from the Kohistan Volcanic Complex itself. The limestone blocks contain the Aptian–Albian fossils, and the plutonic clasts give dates varying from 111 to 62 Ma (Pudsey 1986). Significantly, close to the syntaxis or the acute mountain bend, the high-grade metamorphic rocks of the Asian continental margin are thrust southwards along the Main Karakoram Thrust onto the suture zone formations (Tahirkheli 1970, 1982; Tahirkheli et al. 1979).

Across the N–S Nanga Parbat–Haramosh massif forming the pivot of the north-western syntaxis, the acute mountain bend (Wadia 1931), the suture zone (Robertson and Collins 2002) is characterized by tectonic stacking of five lithounits or assemblages (Fig. 17.7): (1) turbidite sediments and basic volcanics emplaced in a marginal-basin setting which experienced amphibolite facies metamorphism; (2) thick succession of volcaniclastic sandstone, limestone, breccia and subordinate basaltic andesite that shows greenschist facies metamorphism; (3) melange made up of serpentinized ultrabasic and basic volcanic rocks of mid-oceanic ridge suite; and (4) thick succession of carbonate and siliciclastic sediments characterized by clasts derived from Ordovician to Triassic formations of the Karakoram terrane. Felsic lavas and pyroclastics with a sill of porphyritic andesite collectively known as the *Khardung Volcanics* unconformably overlies the Ladakh Granite in the south (Rai 1979, 1997). It is caught in the suture zone tectonics. The SHRIMP U/Pb dating of single zircon grain indicates that the volcanism spans the time between 67.4 and 60.5 Ma (Dunlap and Wysoczenski 2002). This was the time when volcanoes were pouring out stupendous volumes

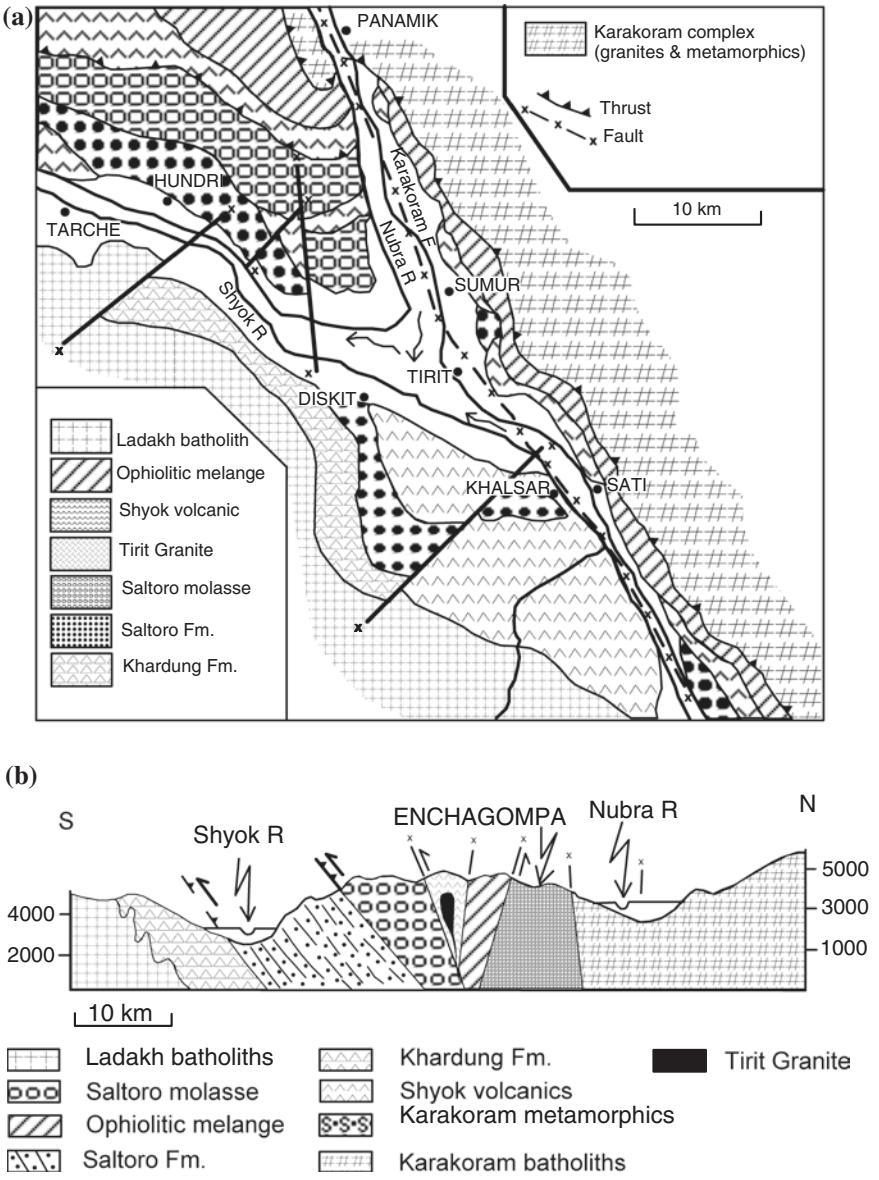

Fig. 17.7 Geological sketch map of and sections across the Shyok Suture Zone in northern Ladakh (modified after Upadhyay et al. 1999)

of lavas in the Deccan Province. Two samples of the Khardung volcanic rocks in tectonic contact rhyolite within the Shyok Suture zone are dated 52.8 ± 0.9 Ma and 56.4 ± 0.4 Ma (^{40}Ar–^{39}Ar whole-rock age) (Bhutani et al. 2009). The Khardung volcanic rocks were later affected by thermal disturbance at ~14 Ma,

implying reactivation of the faults of the suture zone. The metamorphism and deformation took place in the Early Cretaceous, and the suturing of the Ladakh complex with the Karakoram terrane occurred in the Late Cretaceous (Dunlap and Wysoczanski 2002)—at 75 Ma (Robertson and Collins 2002). Associated with tuffs and olistoliths, the basaltic rocks are depleted in LREE, enriched in LILE, and slightly depleted in Nb as characteristic of the volcanics in back-arc basin (Rolland et al. 2000). The dominantly andesitic lavas on the southern side show LREE and LILE enrichment, flat HREE pattern and strong Nb–Ta depletion such as exhibited by island-arc volcanism. Overlying the island-arc rocks is a 200-m-thick succession of reefal limestone containing abundant shallow water rudists, corals, gastropods, algae and orbitolines of the Late Aptian to Early Albian age (Upadhyay 2001). The volcanic arc, by inference, is a Middle Cretaceous creation. In the Nubra–Shyok part, there is predominance of the Albian-to-Cenomanian siliciclastic sediments that must have once formed a large platform on the northern part of the arc. At the top of this succession occurs a band of basalt and andesitic lavas.

The Shyok volcanics, immediately south of the melange zone is intruded by a granite–granodiorite–tonalite body called the *Tirit Granite*. Exposed along the Nubra–Shyok valleys, the Tirit Granite occupies the Shyok Suture. The weakly deformed complex of granodiorite–tonalite plus gabbro–diorite has given U–Pb zircon age of 71.4 ± 0.36 Ma, the date implying that the juxtaposition of the two blocks along the Shyok Suture occurred before 72 Ma and that the subduction-related plutonism persisted until above 68 Ma (Upadhyay 2008). The 5-km-thick Saltoro Granite in the Karakoram domain cuts through the volcanic rocks of the Shyok Suture in the area west of Udamara. The U–Pb zircon age of the Saltoro Granite shows that its crystallization took place at 24.52 ± 0.5 Ma (Upadhyay 2009). That was thus a later or post-plutonic phase of the Karakoram Batholith emplacement. North of the Shyok Suture lies the *Karakoram Batholith*. Its southern margin against the suture is marked by a 50-m-wide zone of mylonites and strongly foliated rocks. The Batholith comprises granites and granodiorites exhibiting enrichment in LREE, depletion in HREE, and a Rb–Sr age of 83 ± 9 Ma (Upadhyay et al. 1999). Both the Muglib pluton made up of Late Cretaceous granodiorite and diorite and the Pangong Metamorphic Complex of the Pangong Lake region were subjected to anatexis accompanying deformation, resulting in the generation of heterogeneous magma emplaced extensively forming networks of intrusive bodies (Reichardt et al. 2010). The initial ^{87}Sr–^{86}Sr ratios and C Nd values of these leucocratic bodies in the Karakoram Shear Zone are similar to those of the Karakoram Batholiths. The suture zone in the Saltoro–Charasa–Skardu belt is fringed by a molasse succession of red-green shales and sandstones interbedded with porphyritic andesite described as the *Saltoro Molasse*. Significantly, the molasse sediments are characterized by desiccation cracks and raindrop prints, indicating subareal exposure in a floodplain (Sinha and Upadhyay 1997; Upadhyay et al. 1999). The Hundiri Saltoro flysch and molasses contain Aptian to Early Albian orbitolinids (Juyal 2006).

17.2.4 Shigatse Island Complex

South of Lhasa in Tibet (Fig. 17.8), the Bainang terrane represents an intra-oceanic island arc caught in the subduction of NeoTethys floor. This seafloor was covered with sediments, including radiolarian chert, ranging in age from the Late Triassic to Middle Cretaceous. It now forms southward thrust imbricated stack of thrust sheets that become younger upwards. Biostratigraphic study based on the testimony of radiolarians demonstrate that the ophiolite was generated within a period less than 10 million years—from the Late Barremian to the Late Aptian—and that the main deposition of the flysch took place in the Late Aptian (Ziabrev et al. 2003). Ammonites *Mortinoceras inflatum* and *Neophlycticeras brottianum* indicate Lower Late Aptian age of the forearc flysch in front of the active Asian margin (Wiedmann and Durr 1995). Pelagic sediment was deposited on the basin floor in the Albian to Cenomanian time, while a carbonate platform formed on the shelf margin. The basin was filled to the crest of the outer ridge by the Late Cretaceous with siliciclastic sediments containing high proportion of volcanic clasts. Interestingly, turbidity currents (Fig. 17.9a) were active in the part west

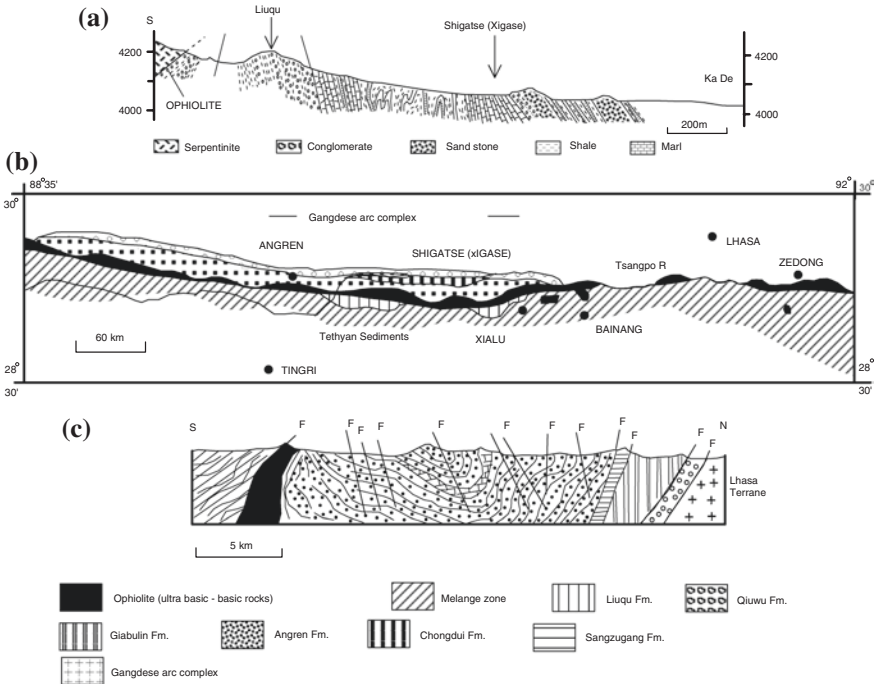

Fig. 17.8 **a** Shigatse Island Arc Complex in southern Tibet in the tectonic zone of India–Asia junction (after Ziabrev et al. 2003). **b** Lithological formations of the junction zone near Shigatse (after Davis et al. 2002). **c** Profile of the I-TSZ showing seven sedimentary units (after Wang et al. 2000)

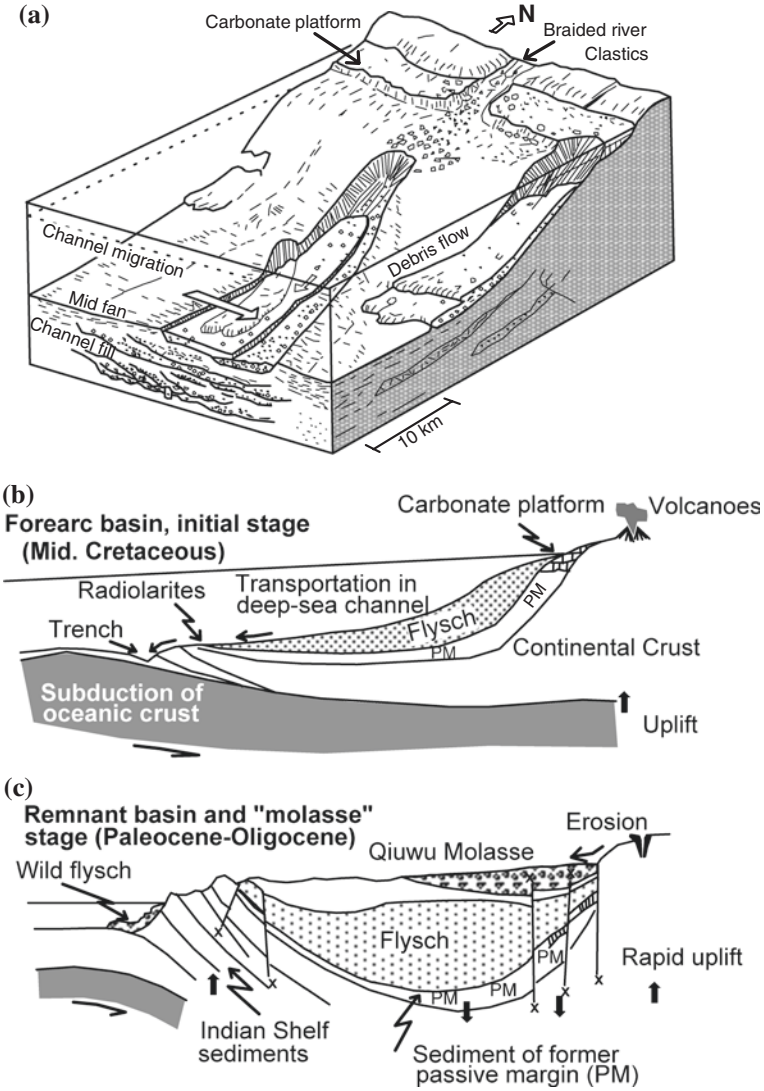

Fig. 17.9 **a** The manner in which the forearc basin related to the Shigatse volcanic island was filled. Channels migrated repeatedly even as fluvial gravels were delivered to the shelf-edge where they were incorporated in debris flows and mud flows. **b** Trapping of ocean crust (with sediments) in the subduction at its initial stage. **c** Uplift of both the island arc and accretionary wedge, followed by subsidence of the basin allowing fluvial deposition (molasse) (after Einsele et al. 1994)

of Shigatse, as borne out by channel fills and laterally migrating channels on the submarine sedimentary fans developed in the setting of deposition of hemipelagic clays and marls (Einsele et al. 1994). The peridotite–harzburgite–gabbro assemblage (ophiolite) involved in the subduction and characterized by serpentinization and foliation represents an oceanic crust with upper mantle substratum.

The Zedong terrane comprises a succession of tholeiite basalts overlain by a 15-m-thick radiolarian red chert of the Bajocian to Callovian age, overlain by a 1000-m sequence of volcaniclastic breccia cut by intrusives of andesite and diorite. The terrane represents a remnant of an intra-oceanic volcanic island (Aitchison et al. 2002). The island complex was subjected to compression in the Palaeocene (60–50 Ma), resulting in development of isoclinal folds and thrusts. There were large-scale gravity-prompted mass movements giving rise to debris flows (Einsele et al. 1994).

17.2.5 Timing of Docking

The convergence of continents culminated in slamming of India against Asia (Figs. 17.1 and 17.10). The north-western edge of India docked with the Kohistan complex, which had already become a part of the Asian landmass. As the pressure grew, the rocks of the Kohistan complex were pushed and thrust onto the continental margin of India. Fossils contained in the sedimentary rocks of the Indian continental margin in the Waziristan–Khurram region indicate that this happened at nearly 65 Ma (Beck et al. 1995). The welding of India with Eurasia was

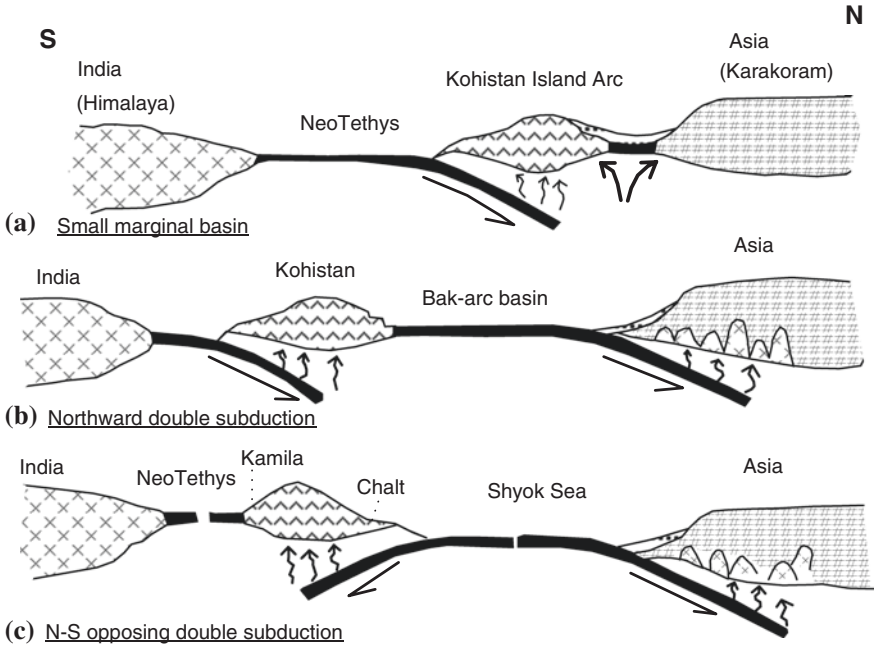

Fig. 17.10 Convergence and collision of India with Asia. Three models explain the manner in which the suturing of the island arc complex with the continents was accomplished (based on Asif Khan et al. 1997; Robertson and Collins 2002; Bignold and Treloar 2003)

accomplished in three phases—(i) joining together or suturing between Kohistan arc and Karakoram microplate of Asia margin in the middle Cretaceous, (ii) docking of north-western tip of the Indian plate with the Kohistan–Karakoram composite in the Palaeocene and (iii) oblique docking between the western margin of Indian plate with Afghanistan and the development of Chaman Fault in the Late Eocene to Early Oligocene (Zaman et al. 1999).

India touched the Cuofiang area in southern Tibet (of Asia) at about 68 Ma (Xiaoying et al. 1996). The Palaeocene *Liuqu Conglomerate*, occupying a tract entirely south of the line of India–Asia junction in southern Tibet, bears testimony to the docking occurring in the Later Cretaceous to Palaeocene time (Aitchison et al. 2002). In south-central Tibet where Upper Cretaceous to Eocene marine sediments occur both to the north and the south of the Indus–Tsangpo Suture, there was a major change in the depositional environment and sedimentary provenance (reflected in the appearance of chromium-rich spinel from the obducted ophiolite) at about 65 Ma implying onset of India–Asia docking during the middle Eocene or earlier (Ding et al. 2005).

Palaeomagnetic study of Early Palaeogene marine sedimentary rocks in the Lhasa sector in southern Tibet suggests that the initial contact between the converging Indian and Asian plates occurred before 60.5 ± 1.5 Ma—very likely near the Cretaceous–Tertiary boundry at 65 Ma (Yi et al. 2011). In order to identify the provenance of the Upper Cretaceous clastic sediments near Gyatse in south-central Tibet, petrographic study of the clastic rocks, in situ detrital zircon U–Pb age, Lu–Hf isotopic composition, whole-rock Nd-isotopes and Cr-spinel electromicroprobe analyses were carried out. The collective data adduced indicate that the detrital zircon in the clastic sediments of the Barriasian to Caniacian (Upper Cretaceous) formations of southern Tibet were all derived from the Archaean to Cambrian rocks of the Indian shield (Cai et al. 2011). In contrast, one of the uncomformably overlying formations of the Late Maastrichtian to Late Palaeocene age in its uppermost horizon records abrupt influx of Cretaceous zircon along with juvenile isotopic composition, arc-related spinel and positive C Nd, suggesting derivation from the arc and subduction-zone rocks (Cai et al. 2011). This means that by Upper Cretaceous to Palaeocene time an arc with subduction zone between the converging continents had been formed. The conclusion that India had touched Asia before this development is inevitable. In other words, the docking took place in the period 70–65 Ma (Cai et al. 2011).

There is another view on the India–Asia docking. In the western Zanskar region, the initiation of the docking started in the Later Ypressian (~52 Ma), while north and east of Sagarmatha in Nepal the start of docking was later than Lutetian (49–41 Ma) (Rowley 1996). In the Zhepure Shan range, the record of the Cretaceous–Early Tertiary shelf carbonates and siliciclastics shows that the Palaeocene clasts at Jidula contain quartzose grains derived from a craton, while the Early Eocene and younger sediments contain immature grains with distinct ophiolitic and volcanic affinity related to a volcanic arc. The sediments were presumably derived from the Gangdese arc and trench system associated with obduction, implying that the onset of docking took place at 50.6 ± 0.2 Ma (Zhu Bin et al. 2005).

Interestingly, the speed of northward moving India at the rate 180–195 mm/year suddenly slowed down to 45 mm/year at 55 Ma, implying resistance that the fast-moving Indian plate had encountered due to its docking with Asia (Klootwijk et al. 1992). Based on global palaeomagnetic data, it is inferred that the rate of northward moving India abruptly decreased at 57 ± 3 Ma, corresponding to the time when India collided with Asia (Acton 1999).

The motion of the northward moving Indian plate dramatically dropped from 15cm/year to 4 cm/year in the interval 50–35 Ma during the onset of mountain-building activity in Tibet and the rearrangement of plate boundaries in the Indian Ocean (Copley et al. 2010). In other words, the abrupt decrease in the rate of movement is not due to docking of India with Asia, but is a consequence of building up of deformational mountains in Tibet and as well as in the Himalayan terrane itself.

Palaeocene palynomorphs, including pollens produced by palm *Nypa fruticans* of the Gondwana (Indian) affinity, found in the Nindam succession in Ladakh arc complex is suggestive of the fact that the forearc basin was still not closed until the Palaeocene (Upadhyay et al. 2004). The Ypressian *Nummulite*-bearing limestone overlying the fluvial sandstone at Chogdo in Ladakh—which rests of lithotectonic units on all the so called collision zone constraints the age of docking to being no younger than the latest Early Eocene, that is not less than 49 Ma (Garzanti and Haver 1988; Clift et al. 2002). Very significant is the recognition of five phases of granite emplacement at approximately 67, 58, 53 and 45 Ma as indicated by U–Pb ages of zircon in the granites of the so called collision zone (Upadhyay 2008, personal communication). It is obvious that the zone of welding was active all through the temporal span from the Palaeocene to the Middle Eocene.

It seems that it took nearly 8–10 million years during the Mesozoic–Tertiary transition period for the complete amalgamation of India with Asia.

17.2.6 Formation of Land Bridge

In the Maastrichtian time (70–65 Ma), a large variety of vertebrate animals such as artiodactyls or even-toed animals such as deers, turtles, crocodiles and fish suddenly made appearance in the Kalakot area in Jammu (Ranga Rao 1971; Sahni and Kumar 1974) and in the Kirthar Hills in Pakistan (Pascoe 1964). They bore remarkably strong similarity with those of China, Mongolia, Siberia and Central Asia in the mainland Eurasia. Their appearance for the first time in India implies that a landbridge permitting animal migration from Asia to India had formed by the Maastrichtian time (Sahni 1984). The landbridge was formed presumably in the north-west where India first docked with Asia. Not only did come migrate in the mammals, but also came frogs—which are highly allergic of saline seawater—and hopped their ways through the land corridor and reached as far south as the Deccan where their remains are found in the Infratrappean and Intertrappean beds (Jaeger et al. 1989; Sahni 1984; Sahni and Bajpai 1991).

17.2.7 Deformation and Metamorphism

The coming together of continents was so strong that the entire assemblage of volcanic island complex together with sediments of the arc basins and deep sea was strongly folded and split into multiple stacks of mutually overlapping slices. These were then squeezed up and pushed out—that is obducted—onto the continental margin. The ophiolites are chaotically admixed with sediments giving rise to *ophiolitic melanges* seen all along the zone of continental welding from Mingora on the Afghan border, through Jijal and Sapat in Kohistan, Zildat and Shergol in Ladakh, Darchen in the Kailas–Mansarovar region, Shigatse in southern Tibet to

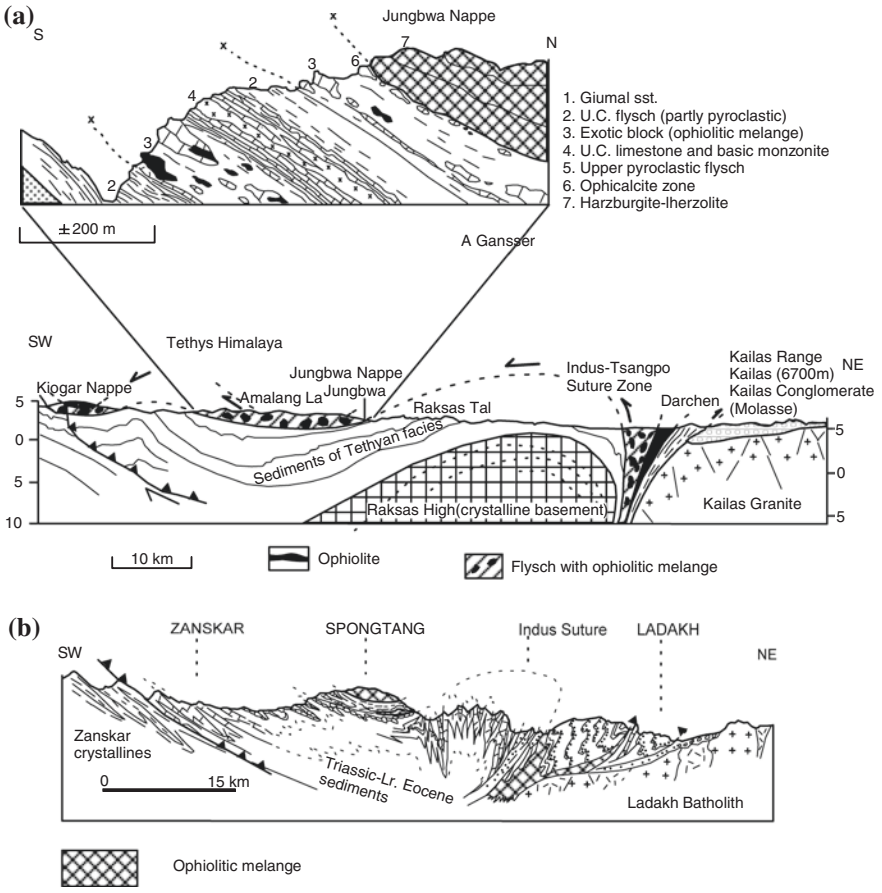

Fig. 17.11 Obducted or pushed up material from the zone of continental docking was thrust southwards onto the Indian continental margin—some travelling very far and forming klippen. Development of domal upwarp in the leading edge of the Indian plate is a result of resistance encountered by the Indian plate as it impacted under the Asian plate. **a** Northern Kumaun (after Gansser 1964). **b** Ladakh (after Colchen et al. 1986)

Tuting–Tidding belt in eastern Arunachal Pradesh. The compression, to which the island arc complexes were subjected, gave rise to isoclinal folds and attendant thrusting. North-verging conjugate faults and thrusts of the Late Cretaceous age along the northern boundary in the Swat area caused upward expulsion of the subducted mass (Anckiewicz et al. 1998).

Most scientists believe that the leading part of the Indian plate plunged down and slid a long distance under the Asian plate. However, the development of domal upwarps all along the junction zone is indicative of the resistance encountered by the Indian plate docking with Asia. There was perhaps plunging down of the lithosphere into the asthenosphere (Fig. 17.11) and resultantly forming domal upwarps (Valdiya 1987, 1998). The upwarps are discernible all along the stretch from Nimaling in Ladakh (Thakur 1981), through Gurla Mandhata in the Kailas–Mansarovar region (Heim and Gansser 1939; Gansser 1964) to Lhagoi–Kangri–Kangmar belt in north-eastern Nepal (Brunel 1986). This aspect is dealt with in Chapter Eighteen.

17.3 Indus-Tsangpo Suture Zone

17.3.1 Structure and Lithology

As already stated, the sedimentary accumulations in the oceanic trench, on the adjoining seafloor, along the shelves of the continental margin, in the interior basins and on the flanks of the intra-oceanic volcanic islands were all severely compressed, tightly folded, and split by multiple thrusts, and then squeezed up when the two continents were welded. Even the pillow lavas of the seafloor and the underlying sheeted swarms of dykes with still deeper ultrabasic heavy rocks were thrust up and implanted within the deformed assemblage of the sedimentary rocks, giving rise to *melanges of rocks* in the zone of docking. The melange-bearing tectonized zone was named *Indus–Tsangpo Suture* (ITS) by Gansser (1966, 1977, 1981, 1991). Rivers Sindhu (Indus) and Tsangpo (Yarlung Zangbo) carved out their courses in this tectonized zone. In Ladakh, the mélange associated with the ITS is known as the Nidar Ophiolite (Thakur and Bhatt 1983). The *Nidar Ophiolite* sequence, which includes oceanic plagiogranite, originated from subalkaline tholeiitic magma by fractional crystallization aided by filter-pressing process.

Skirting parabolically around the transverse Nanga Parbat–Haramosh promontory of the Indian landmass, the ITS (Fig. 17.12) is traced westwards where it is described as *Main Mantle Thrust* by Tahirkheli (1970, 1982), Tahirkheli et al. (1979), and Argeles (2000). It defines the southern boundary of the Kohistan island arc complex and extends further west and links up with the N–S trending transcurrent strike-slip *Chaman Fault* (Figs. 17.12 and 17.14). The Chaman Fault, since its inception, has registered left-lateral aggregate displacement of the order of 200–300 km (Lawrence and Yates 1979). It may be mentioned that coesite-bearing

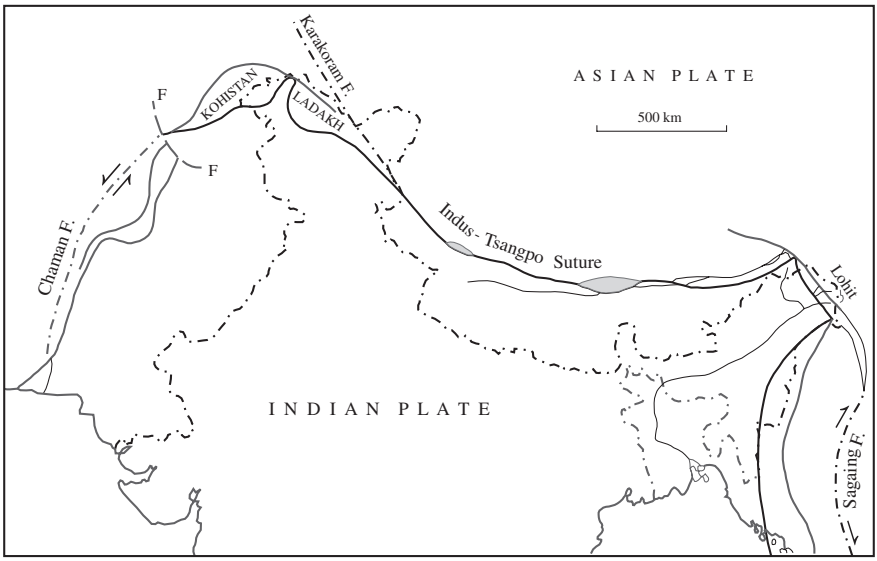

Fig. 17.12 Indus–Tsangpo suture represents the zone of welding of India with Asia. It is linked in the east and west with transcurrent strike-slip faults that have, since their inception, caused 300–500 km of aggregate displacement of the Indian block with respect to the Asian (from Valdiya 1998, based on Gansser 1966, 1991; Garzanti and Haver 1988)

eclogite in the hanging wall of a major south-directed ductile thrust zone in the Kaghan Valley (northern Pakistan) testifies to synchronous thrusting and extensional shearing during the later stage of deformation (Treloar et al. 2003).

The ophiolitic melange characterized by spinel mineral and chromite pods near Luobusa in south-central Tibet comprises lherzolite, harzburgite and dunite of the mantle origin (Dupuis et al. 2005)—the upper mantle in the MORB region (Zhou et al. 2005).

In the Lohit Valley in eastern Arunachal Pradesh, the I-TS is delineated by a thrust-bound melange zone made up of volcanic rocks associated with serpentinized ultrabasics and siliceous limestones along the Tuting–Tidding shear zone (Dhuundial et al. 1976; Acharyya 1982, 2005; Singh 1993; Misra and Singh 2002; Gururajan and Choudhuri 2003). Around the Namcha Barwa anticlinal massif, the Tsangpo–Brahmaputra River reveals a section of the I-TSZ ophiolite comprising narrow slivers of mafic volcanics, the trace-element geochemistry of which indicates their origin in the subduction zone of an intra-oceanic basin (Saha et al. 2012). Extending further south-east into Myanmar, the I-TS is linked with the transcurrent right-lateral strike-slip *Sagaing Fault* (Figs. 16.12 and 17.12). Along this fault, the Myanmar block has right-laterally moved 300–500 km northwards with respect to South-east Asia (Swe 1972; Maung 1987).

17.3.2 Overthrusting of Obducted Units

In many sectors, so severe was the impact of docking of the continents that the squeezed out ophiolites and ophiolitic melanges of the I-TS zone were thrust southwards 30–80 km away from their roots. As discrete sheets or nappes, these thrust masses lie piled up one over another as klippen. The sliding of the thick slabs of heavy rocks must have been aided by gravity—the gravity gliding resulting from steepening of slopes as the leading edge of Indian plate heaved up (Fig. 17.11) and formed domal upwarps (Valdiya 1987). Remnants of such far-travelled sheets are seen 30 km away from the root at Dargai in Kohistan (Tahirkheli et al. 1979), 34 km south of the I-TS in the Spongtang area in Ladakh (Shanker et al. 1976; Frank et al. 1977; Sinha and Upadhyay 1997), and 80 km south of the root in the Kailas–Mansarovar region (Fig. 17.13) in SW Tibet (Heim and Gansser 1939; Gansser 1964, 1966, 1977; Shah 1977; Sinha 1989). This assemblage of rocks of the suture zone, comprising blocks of varied rocks from Asian landmass as well as the Tethyan domain in India, was appropriately described by A. Von Kraft in 1862 from Kumaun as *Exotic Blocks of Malla Johar* (Fig. 17.11a). The Spongtang Klippe is made up of the material from the mantle and oceanic crust thrust onto the Zanskar domain during the Late Cretaceous (Fig. 17.11b). A distant thrust sheet of accretionary complex underlies the ophiolite sheet. It comprises melanges and alkali basalt overlain by a condensed sequence of the Permian to Late Cretaceous limestones and is associated with a seamount rock (Corfield et al. 1999). The U–Pb dating of zircon grains from a dioritic segregate in a gabbro shows that the complex formed at 177 ± 1 Ma—in the latest Early Jurassic time (Pedersen et al. 2001). An andesitic flow overlying the ophiolite sequence gave a Middle Cretaceous date, 88 ± 5 Ma. The klippe material was emplaced in the root zone during the Turonian–Maastrichtian time. Magnesite deposits occurring in the serpentinized ultrabasic rocks owe their formation to CO_2-bearing fluxes of metamorphic origin. Oxygen isotope composition of emerald occurring in quartz–magnesite and talc–magnesite assemblages in the Mingora and Gujarkili areas shows strong enrichment in ^{18}O and remarkable uniformity at +15.6 ± 4 ‰, implying derivation from S-type granitic magma (Jan et al. 1981a, b; Arif et al. 1996).

South of the Indus–Tsangpo Suture Zone, the heat flow is nearly constant all through the width at 146 mW/m^2 over a distance of 30 km and drops to 91 mW/m^2 in less than 25 km (Francheteau et al. 1984). The existence of a heat anomaly is located at a less than 25 km in the Tibetan crust, probably due to recent emplacement of plutonic bodies. The heat transfer is concentrated along 30- to 50-km "heat bands" which are associated with nearly 600 geothermal system (Hochstein and Regenauerlieb 1998).

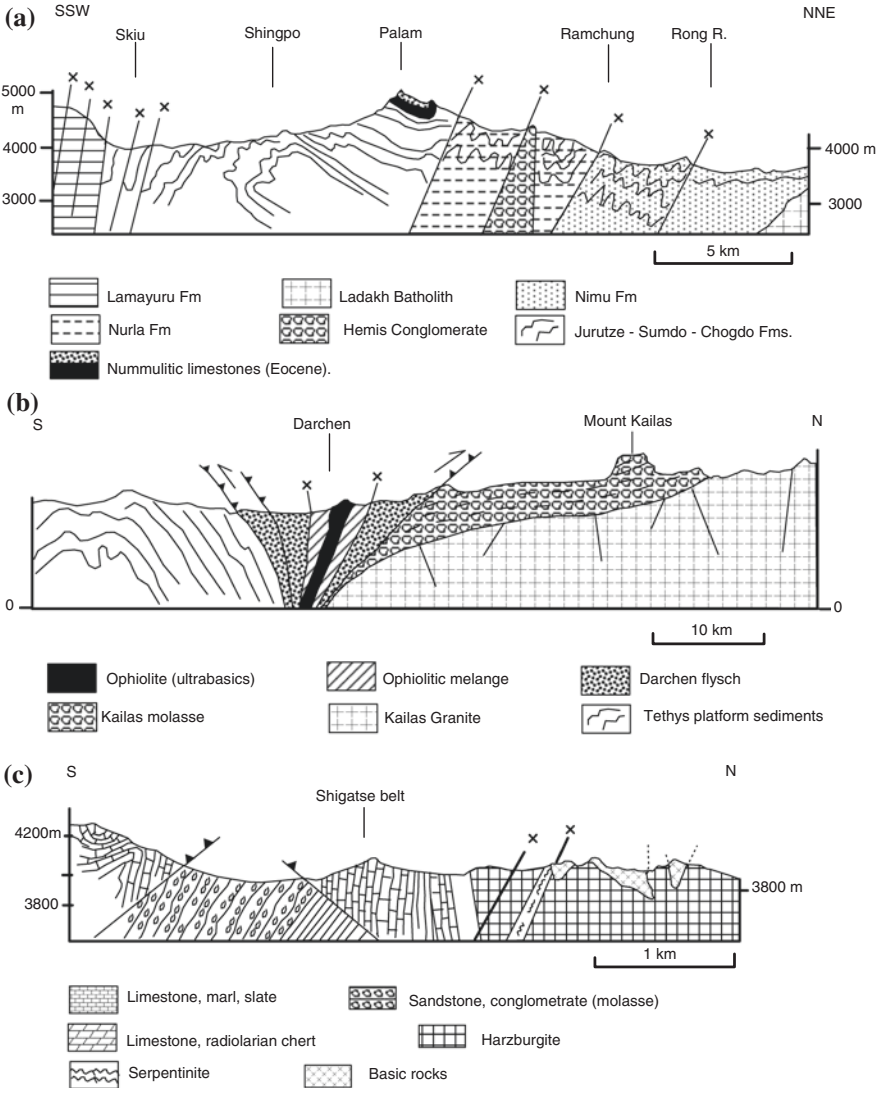

Fig. 17.13 Geological profile sections across the Indus–Tsangpo suture zone, illustrating its structural architecture and lithological units. **a** Ladakh (after Thakur and Bhat 1983). **b** Kailas–Darchen area in south-western Tibet (after Gansser 1964). **c** Shigatse area in southern Tibet (after Bally et al. 1980)

17.4 Magmatic Arc North of Suture Zone

As the leading edge of the Indian plate docked with the Asian plate, there was large-scale differential melting of the crustal rocks, giving rise to an anatectic granitic magma. Emplaced all along the southern margin of Asia as discordant bodies

such as batholiths and stocks, the granite–granodiorite–tonalite plutons form a more than 2700-km-long magmatic arc. It extends from Kohistan in the west, through Karakoram and Kailas to Gangdese in Tibet and then to the eastern part of the Lohit district in Arunachal Pradesh (Fig. 17.14). The magmatic bodies are associated with volcanic rocks—lavas, agglomerates and tuffs of felsic compositions. This *Karakoram–Kailas–Gangdese Magmatic Arc* evolved in the manner of the magmatic arc of the Andes Mountain in South America due to the subduction of the Pacific Ocean floor along the Chile Trench.

The granitic activity of the magmatic arc was spread over a long period of time from about 110 Ma to nearly 42 Ma, the peak being in the 60–45 Ma interval (Gansser 1991; Debon 1995; Copeland et al. 1995). While one pluton was dated 153 ± 6 Ma, the other gave an age of 30.4 ± 0.4 Ma (Murphy et al. 2002). In the Kohistan sector, basalt, andesite and pyroclastics of Teru area were emplaced during the Late Cretaceous to Palaeocene time (Danishwar et al. 2001). Some of the lavas belong to the Early Eocene (45 Ma) (Petterson and Windley 1985). The andesite, rhyolite and ignimbrite volcanics associated with the granites of the Gangdese mountain range in age from 119 to 38 Ma.

Radiometric dating and biostratigraphic data (Fig. 17.14 insets) point to the subduction-related magmatism in the Lhasa sector commencing in the Late Jurassic and lasting until the Middle Oligocene (Ziabrev et al. 2003).

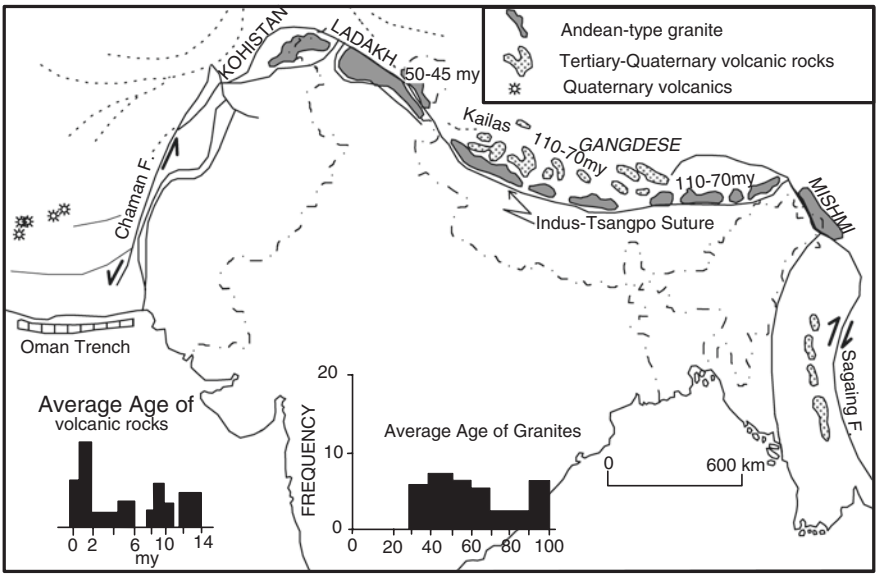

Fig. 17.14 Arcuate belt of granitic Batholiths and related plutons emplaced in the active continental margin of Asia immediately north of the zone of welding of the Indian plate with Asia (from Valdiya 1998, based on Gansser 1991)

17.5 Oblique Convergence: Indo-Myanmar Border Ranges

The NNE–SSW trending Indo-Myanmar Border Ranges (Brunschweiller 1966) abut transversely against the NW- to SE-oriented Tuting–Tidding Zone which represents the I-TS (Figs. 17.11 and 17.2). The Patkai–Naga–Arakan Ranges are made up of predominant flysch of the Late Cretaceous to Eocene ages. The succession is split into multiple thrust sheets, one overlapping another as a consequence of the Indian plate sliding obliquely under the Myanmar block or microplate. These thrust sheets represent the accretion prism of low-grade metamorphic rocks, the lowest sheet comprising pelagic and hemipelagic sediments of the ocean floor underlain by ophiolite and succeeded by terrigenous trench-slope sediments including radiolarian chert and siliceous limestone. Kummeridian to Lower Tithonian (Upper Jurassic) radiolarians have been detected in chert associated with ophiolitic mélange near Salumi in Nagaland (Baxter et al. 2011). Radiometric dating confirms the radiolarian testimony. Characterized by predominant Maastrichtian to Palaeocene foraminifers and coccoliths, this sedimentary sequence (Fig. 17.15) is named *Phokphur Formation* (Acharyya 1991, 2005; Vidyadharan et al. 1989; Sengupta et al. 1990).

Dismembered bodies of ophiolites occur in two parallel belts along the western margin of the Indian plate and adjacent to the magmatic arc of the Central Myanmar Basin. The Manipur Ophiolite Complex comprises peridotite, dunite, harzburgite, lherzolite and wehrlite. Its geochemistry shows that in comparison with the iridium group the palladium group of minerals has higher concentration, implying derivation by partial melting of the residual upper mantle (Dabala Devi and Singh 2011). The gabbros, dolerites and pillow basalts in the ophiolitic mélange, however, suggest their origin to a mid-oceanic ridge setting (Krishnakant Singh et al. 2012). The western belt is characterized by steeply dipping mafic and ultramafic rocks associated with continental metamorphic rocks, and the eastern belt consists of rootless subhorizontal bodies or nappes, overlying the Eocene–Oligocene flyschoid sediments (Acharyya 2006). The ophiolites and metamorphic rocks occurring as nappes in the western flank of the Indo-Myanmar Border Ranges were emplaced during the Late Oligocene docking between the Indian plate and the *Myanmar microplate*. The ophiolite bodies occupy a zone of deep thrusts all along the length of the Indo-Myanmar Border Ranges. A major thrust plane separates the subduction complex (Ghose and Singh 1980) from the continental metamorphic rock (*Naga Metamorphic Complex*) (Fig. 17.15). The Naga Hill complex has a cover of weakly metamorphosed neritic sediments (*Nimi Formation*), of the Middle Cretaceous age and belonging to the margin of the Myanmar microplate. There are a few klippen of the Myanmarese rocks resting on the ophiolites, and some klippen of both the ophiolites and metamorphic rocks sit on the Tertiary sedimentary rocks in the west (Ghose and Agrawal 1989; Roy 1989). These klippen demonstrate the extent of obduction during the Middle Eocene (Acharyya 1993, 2006) and attendant westward thrusting of the

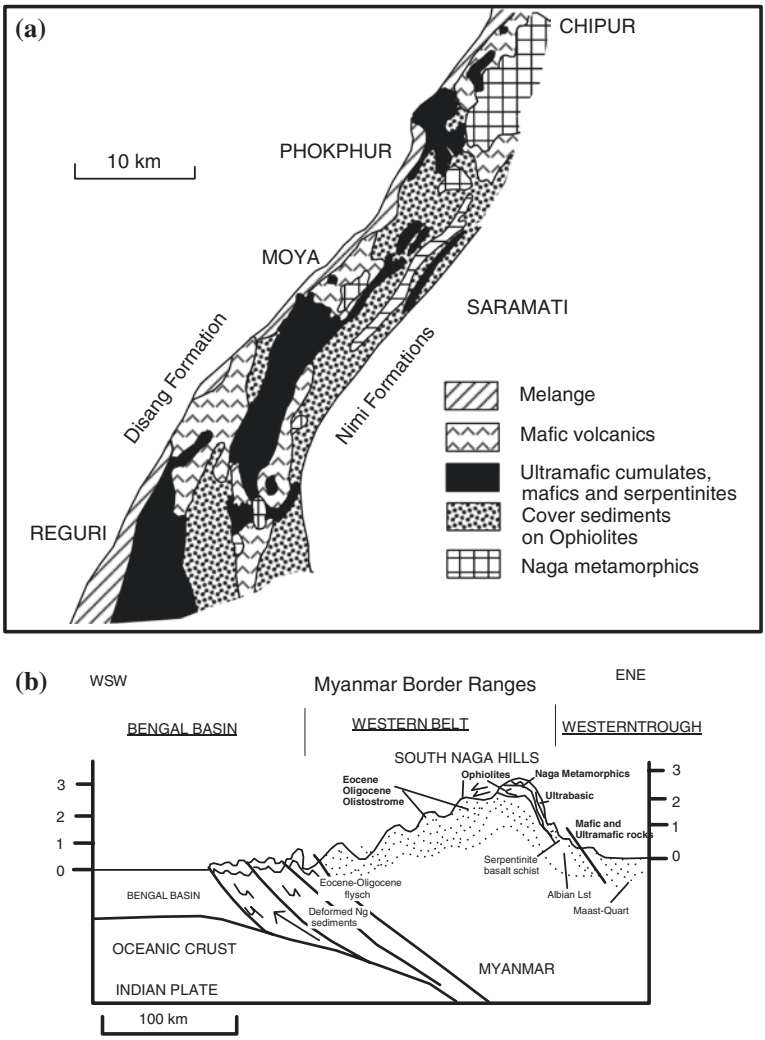

Fig. 17.15 Lithotectonic elements of the subduction zone in the present occur as obducted units in the imbricated succession of the Myanmar Border Ranges. **a** Sketch map of the Naga Hills (Sengupta et al. 1989). **b** Cross section of the Manipur Hills (Vidyadharan et al. 1989)

subduction-zone rocks as a result of oblique convergence of India and Myanmar microplate. The ophiolites comprise serpentinized dunite, harzburgite, lherzolite, wehrlite, pyroxenite, gabbro, plagiogranite and mafic volcanics. The Ti/V ratios and the REE distribution pattern of the low-Ti ophiolites show characteristics of overlapping mid-oceanic ridge basalt and island arc, suggesting a back-arc setting, while the high-Ti ophiolites have similarities with the intraplate basalts erupted as off-axis seamounts and islands (Sengupta et al. 1989).

Significantly, the ophiolites are chromite-bearing and contain minor deposits of platinum associated with garnierite and Cypress-type copper in the central part of the Arakan Yama (Bender 1983).

17.6 Ophiolite Bodies in Sulaiman–Kirthar Ranges

East of the socalled axial zone (Auden 1974), the Sulaiman–Kirthar Ranges are made up of tightly folded Cretaceous flysch with pillow lavas and large bodies of ophiolites (Fig. 17.16) in the Bela, Muslim Bagh, Zhob and Waziristan areas. The ophiolite bodies are tectonic implantations. The *Muslim Bagh Ophiolite* (Asrafullah et al. 1979; Ahmad and Abbas 1979), related to a WSW–ENE trending thrust sequence, occurs in the uppermost part of a pile of nappes accreted onto the Indian continental margin. There are sheeted dykes cross-cutting the ultrabasic rock sequence, and some of them grade into gabbro and pyroxenite. Argon–argon dating of the Muslim Bagh Ophiolite gave plateau age of 70.7 ± 5.0 Ma for the metamorphics and 68.7 ± 1.8 Ma for the amphibolites at the base of the sheeted

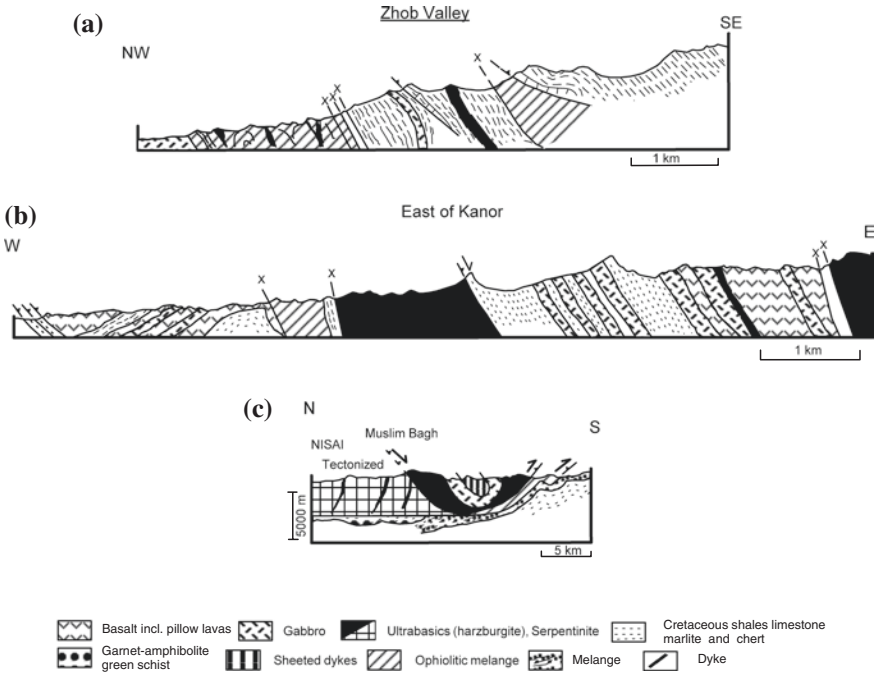

Fig. 17.16 Tectonically emplaced ophiolite bodies in the Kirthar–Sulaiman Ranges (in Pakistan) are associated with the Cretaceous–Eocene flysch formations. **a** Zhob valley through Gwal (after Gansser 1979). **b** East of Kanor (after Gansser 1979). **c** Muslim Bagh (after Ahmad and Abbas 1979)

dykes (Mahmood et al. 1995). It seems that the floor of the NeoTethys Sea was subducted 65–70 million years ago in the Pakistan sector.

17.7 Karakoram Batholith

The *Karakoram Batholith* intrudes the Carboniferous–Permian succession (Upadhyay 2002). The plutonic body rises to the elevation of 8611 m in the Baltoro region, forming the world's second highest peak, the *K-2*. It is made up of plagioclase–hornblende and biotite–hornblende potash feldspar orthogneisses. The orthogneisses are intruded by 120–115 Ma leucogranites, characterized by garnet together with tourmaline and micas. The $^{40}Ar/^{39}Ar$ age of the Karakoram hornblende 90 ± 1.8 Ma indicates Middle Cretaceous phase of magmatism, concomitant with the early subduction-related component of the Karakoram Batholith.

References

Acharyya, S. K. (1982). Structural framework and evolution of the eastern Himalaya. *Himalayan Geology, 10*, 412–439.

Acharyya, S. K. (1991). Late Mesozoic-Early Tertiary basin evolution along the Indo-Burmese range and Andaman island arc. In S. K. Tandon, et al. (Eds.), *Sedimentary Basins of India: Tectonic Context* (pp. 104–130). Nainital: Gyanodaya Prakashan.

Acharyya, S. K. (1993). Greenstones from Singhbhum Craton, their Archaean character, oceanic crustal affinity and tectonics. *Proceedings of the National Academy Science of India, 63*, 211–222.

Acharyya, S. K. (2005). Geology and tectonics of NE India. *Journal of Geophysics, 26*, 35–49.

Acharyya, S. K. (2006). Collisional emplacement history of the Naga–Andaman ophiolites and the position of the eastern-Indian suture. *Journal of Asian Earth Sciences*.

Acton, G. D. (1999). Apparent polar wander of India since the Cretaceous, with implications for regional tectonics and true polar wonder. *Memoires Geological Society of India, 44*, 125–129.

Ahmad, Z., & Abbas, S. G. (1979). The Muslim Bagh ophiolites. In A. Farah & K. A. Dejong (Eds.), *Geodynamics of Pakistan* (pp. 243–249). Quetta: Geological Survey of Pakistan.

Aitchison, J. C., Davis, A. M., & Badengzhu, Luo H. (2002). New constraints on the India-Asia collision: the Lower Miocene Gangrinboche conglomerates, Yarlung-Tsangpo suture zone, SE Tibet. *Journal of Asian Earth Sciences, 21*, 251–263.

Anczkiewicz, R., Burg, J. P., Hussain, S. S., Dawood, H., Ghazanfar, M., & Chaudhry, M. N. (1998). Stratigraphy and structure of Indus suture in the Lower Swat, Pakistan, NW Himalaya. *Journal of Asian Earth Sciences, 16*, 225–237.

Argles, T. W. (2000). The evolution of the main central thrust in the western syntaxis, northern Pakistan. In M. A. Khan, P. J. Treloar, M. P. Searle, & M. Q. Jan (Eds.), *Tectonics of the Nanga Parbat Syntaxis and the Western Himalaya* (pp. 101–122). London: Geological Society.

Arif, M., Fallick, A. E., & Mim, C. J. (1996). The geneses of cumulus and their rocks from Swat, northwestern Pakistan. *Mineral Deposita, 31*, 255–268.

Asif Khan, M., Stern, R. J., Gribble, R. F., & Windley, B. F. (1997). Geochemical and isotopic constraints on subduction polarity, magma sources, and palaeogeography of the Kohistan intra-oceanic arc, northerm Pakistan Himalaya. *Journal of Geological Society of London, 154*, 935–946.

Asif Khan, M., Treloar, P. J., Khan, M. A., Khan, T., Qazi, M. S., & Jan, M. Q. (1998). Geology of Chalt-Babusar transect, Kohistan terrane, N. Pakistan: implications for the constitution and thickening of island-arc crust. *Journal of Asian Earth Sciences, 16*, 253–268.

Asrarullah, A. Z., & Abbas, S. G. (1979). Ophiolites in Pakistan: Introduction. In A. Farah & K. A. Dejong (Eds.), *Geodynamics of Pakistan* (pp. 181–192). Quetta: Geological Survey of Pakistan.

Auden, J. B. (1974). Afghanistan-West Pakistan. In A. M. Spencer (Ed.), *Mesozoic orogenic belts: Data from orogenic Studies* (pp. 235–253). London: Geological Society.

Bally, A. W., Allen, R. E., Geyer, W. B., Hamilton, C. A., Hopson, P. H., Molnar, P., et al. (1980). Notes on the geology of Tibet and adjacent Nepal. *United States of the Geological Survey Open File Report*, 80–501.

Baxter, A. T., Aitchison, J. C., Zyabrev, S. V., & Ali, J. R. (2011). Upper Jurassic radiolarian from the Naga Ophiolite, Nagaland, northeast India. *Gondwana Research, 20*, 638–644.

Beck, R. A., Burbank, D. W., Sercombe, W. J., Riley, G. W., Barndt, J. K., Berry, J. R., et al. (1995). Stratigraphic evidence for an early collision between northwest India and Asia. *Nature, 373*, 55–58.

Bender, F. (1983). *Geology of Burma*. Berlin: Gebruder Borntraeges. (293 p).

Bhandari, A. K., Srimal, N., Radclif, R. P., & Srivastava, D. K. (1979). Geology of a part of Shyok and Nubra valleys, Ladakh District, J & K, India: A preliminary note. *Himalayan Geology, 9*, 158–171.

Bhutani, R., Pande, K., & Venkatesan, T. R. (2004). Tectonothermal evolution of the India–Asia collision zone based on $^{40}Ar/^{39}Ar$ thermochronology in Ladakh, India. *Proceedings of the Indian Academic Sciences (Earth & Planetary Sciences), 113*, 737–754.

Bhutani, R., Pande, K., & Venkateshan, T. R. (2009). The ^{40}Ar–^{39}Ar dating of volcanic rocks of the Shyok suture zone in northwest trans-Himalaya: Implication for the post-collision evolution of the Shyok suture zone. *Journal of Asian Earth Sciences, 34*, 168–177.

Bignold, S. M., & Treloar, P. J. (2003). Northward subduction of the Indian Plate beneath the Kohistan island arc, Pakistan Himalaya: New evidence from isotopic data. *Journal of Geological Society of London, 160*, 377–384.

Brookfield, M. E., & Andrews-Speed, C. P. (1984). Sedimentology, petrography and tectonic significance of the shelf-flysch and molasse-clastic deposits across the Indus Suture Zone, Ladakh, NW India. *Sedimentary Geology, 40*, 249–286.

Brunel, M. (1986). Ductile thrusting in the Himalaya: Shear sense criteria and stretching lineation. *Tectonics, 5*, 247–265.

Brunnschweiller, R. O. (1966). On the geology of the Indo-Burman ranges. *Geological Society of Australian Journal, 13*, 127–194.

Cai, F., Ding, L., & Yue, Y. (2011). Provenance analysis of Upper Cretaceous strata in the Tethys Himalaya, southern Tibet: Implications for timing of India-Asia collision. *Earth and Planetary Science Letters, 305*, 195–206.

Clift, P. D., Degnan, P. J., Hannigan, R., & Blusztajn, J. (2000). Sedimentary and geochemical evolution of the Dras forearc basin, Indus Suture Zone, Ladakh Himalaya, India. *Geological Society of American Bulletin, 112*, 450–466.

Clift, P. D. Carter, A., Krol, M., & Kirby, E. (2002). Constraints on India–Eurasia collision in the Arabian Sea region taken from the Indus Group, Ladakh Himalaya, India. In P. D. Clift, D. Droon, C. Gaedicke & J. Craig (Eds.), *The Tectonic and Climatic Evolution of the Arabian Sea Region* (Vol. 195, pp. 97–116). London: Geological Society.

Colchen, M., Le Fort, P., & Pecher, A. (1986). *Recherches Geologiques dans l' Himalaya due Nepal Annapurna, Manaslu, Ganesh Himal*. Paris: Centre Nationale Recherche Scientifique. (136 p).

Copeland, P., Harrison, T. M., Yun, P., Kidd, W. S. F., Roden, M., & Yuquan, Z. (1995). Thermal evolution of the Gangdese batholith, southern Tibet: A history of episodic unroofing. *Tectonics, 14*, 223–236.

Copley, Alex, Avouac, J.-P., & Royer, J.-Y. (2010). India–Asia collision and the Cenozoic slowdown of the Indian plate: Implications for the forces driving plate motion. *Journal of Geophysics Research, 115*, B03410. doi:10.1029/2009JB006634.

Corfield, R. I., Searle, M. P., & Green, O. R. (1999). Photang thrust sheet: An accretionary complex structurally below the Spongtang ophiolite, constraining timing and tectonic environment of ophiolite obduction, Ladakh Himalaya, NW India. *Journal of Geological Society of London, 156*, 1031–1044.

Danishwar, S., Stern, R. J., & Khan, M. A. (2001). Field relations and structural constraints for the Teru volcanic formation, northern Kohistan terrane, Pakistan Himalayas. *Journal of Asian Earth Sciences, 19*, 683–695.

Davis, A. M., Aitchison, J. C., Badengzhu, L. H., & Zyabrev, S. (2002). Paleogene island arc collision-related conglomerates, Yarlung-Tsangpo suture zone, Tibet. *Sedimentary Geology, 150*, 247–273.

Debala Devi, L., & Singh, I. (2011). Geochemical study of peridotites from the Manipur ophiolite complex, northeast India with special reference to their PGE concentration. *Journal of Geological Society of India, 77*, 273–279.

Debon, F. (1995). Incipient India-Eurasia collision and plutonism: The lower Cenozoic Batura granites (Hunza Karakoram, North Pakistan). *Journal of Geological Society of London, 152*, 785–795.

Dhaundial, D. P., Santra, D. K., & Dange, M. N. (1976). A new look at the stratigraphic and tectonic importance of Tidding limestone and serpentinite in Lohit District. *Miscellaneous Publications of Geological Survey of India, 24*(II), 368–378.

Ding, L., Kapp, P., & Wan, X. (2005). Paleocene-Eocene record of ophiolite obduction and initial India-Asia collision, southcentral Tibet. *Tectonics, 24*(TC3001), 1–18.

Dunlap, W. J., & Wysoczanski, R. (2002). Thermal evidence for early Cretaceous metamorphism in the Shyok suture zone and age of the Khardung volcanic rocks, Ladakh, India. *Journal of Asian Earth Sciences, 20*, 481–490.

Dupuis, C., Herbert, R., Dubois-Cote, V., Guilmette, C., Wang, C. S., Li, Y. L., et al. (2005). The Yarlung-Zangbo Suture Zone ophiolitic mélange (southern Tibet): New insights from geochemistry of ultramafic rocks. *Journal of Asian Earth Sciences, 25*, 937–960.

Einsele, G., Liu, B., Durr, S., Frisch, W., Liu, G., Luterbacher, H. P., et al. (1994). The Xigaze forearc basin: Evolution and facies architecture (Cretaceous Tibet). *Sedimentary Geology, 90*, 1–32.

Francheteau, J., Jaupart, C., Jie, S. X., WenHua, K., Delu, L., JaiChi, B., et al. (1984). High heat flow in southern Tibet. *Nature, 307*, 32–34.

Frank, W., Gansser, A., & Trommsdorff, V. (1977). Geological observations in the Ladakh area, a preliminary report. *Schweizerische Mineralogische und Petrographische Mitteilungen, 57*, 89–113.

Fuchs, G. R. (1977). Traverse of Zanskar from the Indus to the valley of Kashmir—A preliminary note. *Jahrbuch Geologische Bundesanstalt, 120*, 219–229.

Gansser, A. (1964). *Geology of the Himalayas* (p. 289). London: Interscience Publishers.

Gansser, A. (1966). The Indian Ocean and the Himalaya: A geological interpretations. *Eclogae Geologicae Helvetiae, 59*, 831–848.

Gansser, A. (1977). The great suture zone between Himalaya and Tibet: A preliminary note. *Himalaya: Science de la Terre* (pp. 181–191). Paris: CNRS.

Gansser, A. (1979). Reconnaissance visit to the ophiolites in Baluchistan and the Himalaya. In A. Farah & K. A. Dejong (Eds.), *Geodynamics of Pakistan* (pp. 193–213). Quetta: Geological Survey of Pakistan.

Gansser, A. (1991). Facts and theories on the Himalayas. *Eclogae Geologicae Helvetiae, 84*, 33–59.

Garzanti, E., & Haver, T. V. (1988). The Indus clastics: Forearc basin sedimentation in the Ladakh Himalaya (India). *Sedimentary Geology, 59*, 237–249.

Ghose, N. C., & Agrawal, O. P. (1989). Geological framework of the central part of Naga Hills ophiolites, Nagaland. In N. C. Ghose (Ed.), *Phanerozoic Ophiolites of India* (pp. 165–188). Patna: Sumna Publication.

Ghose, N. C., & Singh, R. N. (1980). Occurrence of blueschist facies in the ophiolite belt of Naga Hills, east of Kiphire, NE India. *Sounds of Geologische Rundschau, 69*, 41–48.

Gururajan, N. S., & Choudhuri, B. K. (2003). Geology and tectonic history of the Lohit valley, eastern Arunachal Pradesh, India. *Journal of Asian Earth Sciences, 21*, 731–741.

Heim, A., & Gansser, A. (1939). Central Himalaya: Geological observations of the Swiss expedition 1936. *Denkschriften der Schweizerischen Naturforschenden Gesellschaft, 32*, 1–245.

Hochstein, M. P., & Regenauerlieb, K. (1998). Heat generation associated with collision of two plates: The Himalayan geothermal belt. *Journal of Volcanology and Geothermal Research, 83*, 75–72.

Jaegar, J. J., Courtillet, V., & Tapponier, P. (1989). Palaeontological view of ages of Deccan Traps, the Cretaceous-Tertiary Boundary and India–Asia collision. *Geology, 17*, 316–319.

Jan, M. Q., Asif, M., & Tahirkheli, T. (1981a). The geology and petrography of the Tarbela "alkaline" complex. *Geological Bulletin University of Peshawar, 14*, 1–28.

Jan, M. Q., Kamal, M., & Khan, M. I. (1981b). Tectonic control over emerald mineralization in Swat. *Geological Bulletin University of Peshawar, 14*, 101–109.

Juyal, K. P. (2006). Foraminiferal biostratigraphy of the Early Cretaceous Hundriri Formation, lower Shyok area, eastern Karakoram India. *Current Science, 91*, 1096–1101.

Klootwijk, C. T., Gee, J. S., Pierce, J. W., Smith, F. M., & McFaddan, P. L. (1992). An early India–Asia contact: Palaeomagnetic constraint from Ninety-east Ridge, ODG Leg 121. *Geology, 20*, 395–398.

Krishnakant Singh, A., Ibotombi Singh, N., Debala devi, L., & Bikramaditya Singh, R. K. (2012). Geochemistry of Mid-Oceanic ridge mafic intrusive from the Manipur ophiolitic complex, Indo-Myanmar orogenic belt, NE India. *Journal of Geological Society of India, 80*, 231–240.

Lawrence, R. D., & Yeats, R. S. (1979). Geological reconnaissance of the Chaman fault in Pakistan. In A. Farah & K. A. Dejong (Eds.), *Geodynamics of Pakistan* (pp. 353–361). Quetta: Geological Survey of Pakistan.

Mahmood, K., Boudier, F., Gnos, E., Monie, P., & Nicolas, A. (1995). $^{40}Ar/^{39}Ar$ dating of the emplacement of the Muslim Bagh ophiolite, Pakistan. *Tectonophysics, 250*, 169–181.

Mamgain, V. D., & Jagannath Rao, B. R. (1965). Orbitolines from limestone intercalations of Dras volcanics, J & K State. *Journal of Geological Society of India, 6*, 122–129.

Maung, H. (1987). Transcurrent movements in the Burma-Andaman Sea region. *Geology, 15*, 911–912.

Misra, D. K., & Singh, T. (2002). Tectonic setting and neotectonic features along the eastern Syntaxial bend (Lohit and Dihang), Arunachal Himalaya. In C. C. Pant & A. K. Sharma (Eds.), *Aspects of geology and environment of Himalaya* (pp. 19–40). Nainital: Gyanodaya Prakashan.

Murphy, M. A., Yin, A., Kapp, P., Harrison, T. M., Manning, C. E., Ryerson, F. J., et al. (2002). Structural evolution of the Gurla Mandhata detachment system, southwest Tibet: Implications for the eastward extention of the Karakoram Fault system. *Geological Society of American Bulletin, 114*, 428–447.

Pascoe, E. H. (1964). *A Manual of the Geology of India and Burma* (Vol. III, pp. 1345–2131). Kolkata: Government of India Press.

Pedersen, R. B., Searle, M. P., & Corfield, R. I. (2001). U–Pb zircon ages from the Spongtang ophiolite, Ladakh Himalaya. *Journal of Geological Society of London, 158*, 513–520.

Petterson, M. G., & Windley, B. F. (1985). Rb–Sr dating of the Kohistan arc-batholith in the trans-Himalaya of north Pakistan, and tectonic implications. *Earth & Planetary Science Letters, 74*, 45–57.

Pudsey, C. J. (1986). The Northern suture, Pakistan: Margins of a Cretaceous island arc. *Geological Magazine, 123*, 405–423.

Ranga Rao, A. (1971). New mammals from Murree (Kalakot zone) of the Himalayan foothills near Kalakot, J&K State. *Journal of Geological Society of India, 12*, 125–134.

Reichardt, H., Weinberg, R. F., Anderson, U. B., & Fanning, C. M. (2010). Hybridization of granitic magmas in the source: The origin of the Karakoram Batholith, Ladakh, NW India. *Lithos*. doi:10.1016/j.lithos.2009.11.013.

Reuber, I. (1989). The Dras arc: Two successive volcanic events on eroded oceanic crust. *Tectonophysics, 161*, 93–106.

Robertson, A. H. F., & Collins, A. S. (2002). Shyok suture zone, N. Pakistan: Late Mesozoic-Tertiary evolution of a critical suture separating the oceanic Ladakh Arc from the Asian continental margin. *Journal of Asian Earth Sciences, 20*, 309–351.

Robertson, A., & Degnan, P. (1994). The Dras arc complex: Lithofacies and reconstruction of a late Cretaceous oceanic volcanic arc in the Indus Suture Zone, Ladakh Himalaya. *Sedimentary Geology, 92*, 117–145.

Rolland, Y., Pecher, A., & Picard, C. (2000). Middle Cretaceous back-arc formation and arc evolution along the Asian margin: Shyok suture zone in northern Ladakh (NW Himlaya). *Tectonophysics, 325*, 145–173.

Rowley, D. B. (1996). Age of initiation of collision between India and Asia: A review of stratigraphic data. *Earth Planetary Science Letters, 1945*, 1–13.

Roy, R. K. (1989). Mesozoic accretionary prism on the margin of Indo-Burman Range ophiolite and its implication. In N. C. Ghose (Ed.), *Phanerozoic Ophiolites of India* (pp. 145–164). Patna: Sumna Publications.

Saha, P., Archaryya, S. K., Balaram, V., & Roy, P. (2012). Geochemistry and tectonic setting of Tuting metavolcanic rocks of possible ophiolitic affinity from Eastern Himalayan Syntaxis. *Journal of Geological Society of India, 80*, 167–176.

Sahni, A. (1984). Cretaceous-Paleocene terrestrial faunas of India: Lack of endemism during drifting of Indian plate. *Science, 226*, 441–443.

Sahni, A., & Bajpai, S. (1991). Eurasiatic elements in the Upper Cretaceous nonmarine biotas of Peninsular India. *Cretaceous Research, 12*, 177–183.

Sahni, A., & Kumar, K. (1974). Palaeogene palaeobiogeography of the Indian subcondtinent. *Palaeogeography, Palaeoclimatology, Palaeoecology, 15*, 209–226.

Searle, M. P., Asif Khan, M., Fraser, J. E., & Gough, S. J. (1999). Tectonic evolution of the Kohistan-Karakoram collision belt along the Karakoram Highway, north Pakistan. *Tectonics, 18*, 929–949.

Sengupta, S., Acharyya, S. K., Hul, H. J. V. D., & Chattopadhyay, B. (1989). Geochemistry of volcanic rocks from the Naga Hills ophiolites, northeast India and their inferred tectonic setting. *Journal of Geological Society of London, 146*, 491–498.

Sengupta, S., Ray, K. K., Acharyya, S. K., & de Smith, J. B. (1990). Nature of ophiolite occurrences along the eastern margin of the Indian plate and their tectonic significance. *Geology, 18*, 439–442.

Shah, S. K. (1977). Indus ophiolite belt and the tectonic setting of the MallaJohar–Kiogarh exotics in Himalaya. In *Himalaya: Science de la Terra* (Vol. 268, pp. 361–368). Paris: CNRS.

Shah, S. K., Sharma, M. L., Gergan, J. T., & Tara, C. S. (1976). Stratigraphy and structure of the western part of the Indus suture belt, Ladakh, NW Himalaya. *Himalayan Geology, 6*, 534–556.

Shah, M. T., & Shervais, J. W. (1999). The Dir-Utror metavolcanic sequence, Kohistan arc terrane, northern Pakistan. *Journal of Asian Earth Sciences, 17*, 459–475.

Shanker, R., Padhi, R. N., Prakash, G., Thussu, J. L., & Wangdus, C. (1976). Recent geological studies in the upper Indus valley and the plate tectonics. *Miscellaneous Publications of Geological Survey of India, 34*, 217–236.

Sharma, K. K. (1991). Tectonomagmatic and sedimentation history of Ladakh collision zone: A synthesis. *Physics & Chemistry of Earth, 17*, 115–132.

Sharma, K. K., & Gupta, K. R. (1983). Calc alkaline island arc volcanism in Indus-Tsangpo suture zone. In V. C. Thakur & K. K. Sharma (Eds.), *Geology of Indus Suture Zone in Ladakh* (pp. 71–78). Dehradun: Wadia Institute of Himalayan Geology.

Sharma, K. K., & Kumar, S. (1978). Contributions to the geology of Ladakh, northwestern Himalaya. *Himalayan Geology, 8*, 252–287.

Singh, S. (1993). Geology and tectonics of the eastern Syntaxis, Arunachal Pradesh. *Journal of Himalayan Geology, 4*, 149–164.

Sinha, A. K. (1989). *Geology of higher central Himalaya*. Chichester: Wiley. (236 p).

Sinha, A. K., & Mishra, M. (1992a). Plume activity and sea mounts in the Neo-Tethys: Evidence supported by geochemical and geochronological data. *Journal of Himalayan Geology, 3*, 91–96.

Sinha, A. K., & Mishra, M. (1992b). Emplacement of the ophiolitic melange along continental collision zone of Indus Suture Zone in Ladakh Himalaya, India. *Journal of Himalayan Geology, 3*, 179–189.

Sinha, A. K., & Upadhyay, R. (1993). Mesozoic Neo-Tethyan pre-orogenic deep marine sediments along the Indus-Yarlung suture. *Terra Nova, 5*, 271–281.

Sinha, A. K., & Upadhyay, R. (1997). Tectonic setting and preorogenic sedimentation in the Indus-Tsangpo suture zone of Ladakh Himalaya. *Journal of South East Asian Earth Sciences, 9*, 435–450.

Srikantia, S. V. (1978). The Indus tectonic belt of Ladakh Himalaya: Its geology, significance and evolution. In P. S. Saklani (Ed.), *Tectonic geology of Himalaya* (pp. 43–62). New Delhi: Today & Tommorrow.

Srikantia, S. V., Ganesan, T. M., & Wangdus, W. C. (1982). A note on the tectonic framework and geological setup of the Pangong Tso-Chusul sector, Ladakh Himalaya. *Journal of Geological Society of India, 23*, 354–357.

Srikantia, S. V., & Razdan, M. L. (1980). Geology of a part of central Ladakh Himalaya with particular reference to Indus Tectonic zone. *Journal of Geological Society of India, 21*, 523–545.

Srimal, N. (1986). India–Asia collision: Implications from the geology of eastern Karakoram. *Geology, 14*, 523–527.

Srimal, N., Basu, A. R., & Kyser, T. K. (1987). Tectonic inferences from oxygen isotopes in volcanic-plutonic complexes of the India–Asia collision zone. *Tectonics, 6*, 261–273.

Swe, W. (1972). Strike-slip faulting in central Burma. In N. H. Haile (Ed.), *Regional conference on geology of Southeast Asia* (pp. 59–61). Kuala Lumpur: Geological Society of Malaysia.

Tahirkheli, R. A. K. (1970). The geology of the Attock-Cherat Range, West Pakistan. *Geological Bulletin University of Peshawar, 5*, 1–26.

Tahirkheli, R. A. K. (1982). Geology of the Himalaya, Karakoram and Hindukush in Pakistan. *Geological Bulletin Peshawar University, 15*, 1–51.

Tahirkheli, R. A. K., Mattauer, M., Proust, F., & Tapponier, P. (1979). The India-Eurasia suture zone in northern Pakistan: Synthesis and interpretation of recent data at plate scale. In A. Farah & K. A. Dejong (Eds.), *Geodynamics of Pakistan* (pp. 125–130). Quetta: Geological Survey of Pakistan.

Tewari, A. P. (1964). On the Upper Tertiary deposits of Ladakh Himalaya and correlation of various geotectonic units of Ladakh with those of Kumaun–Tibet region. *Report 22nd International Geological Congress* (Vol. 11, pp. 37–58). Kolkata: Geological Survey of India.

Thakur, V. C. (1981). Regional framework and geodynamic evolution of the Indus-Tsangpo suture zone in Ladakh Himalaya. *Transactional Royal Society of Edinburgh (ES), 72*, 89–97.

Thakur, V. C., & Bhat, M. I. (1983). Interpretation of tectonic environment of Nidar ophiolite: A geochemical aproach. In V. C. Thakur & K. K. Sharma (Eds.), *Geology of Indus Suture Zone* (pp. 21–31). Dehradun: Wadia Institute of Himalayan Geology.

Thakur, V. C., & Misra, D. K. (1984). Tectonic framework of Indus and Shyok suture zones in eastern Ladakh, NW Himalaya. *Tectonophysics, 101*, 207–220.

Treloar, P. J., O'Brien, P. J., Parrish, R. R., & Khan, M. A. (2003). Exhumation of early Tertiary coesite-bearing eclogites from the Pakistan Himalaya. *Journal of Geological Society of London, 160*, 367–376.

Treloar, P. J., Petterson, M. G., Jan, M. Q., & Sullivan, M. A. (1996). A re-evaluation of the stratigraphy and evolution of the Kohistan arc sequence, Pakistan Himalaya: implications for magmatic and tectonic arc-building processes. *Journal of Geological Society of London, 153*, 681–693.

Upadhyay, R. (2001). Middle Cretaceous carbonate buildups and volcanic seamount in the Shyok suture, northern Ladakh, India. *Current Science, 81*, 695–699.

Upadhyay, R. (2002). Stratigraphy and tectonics of Ladakh, eastern Karakoram, western Tibet and western Kun Lun. *Journal of Geological Society of India, 59*, 447–467.

Upadhyay, R. (2008). Implications of U–Pb zircon ages of the Tirit granitoids on the closure of the Shyok suture zone, Ladakh, India. *Current Science, 94*, 1635–1639.

Upadhyay, R. (2009). U–Pb zircon age for a granite intrusion within the Shyok suture zone, Saltoro Hills, northern Ladakh. *Current Science, 97*, 1234–1238.

Upadhyay, R., Awatar, R., Kar, R. K., & Sinha, A. K. (2004). Palynological evidence for Paleocene evolution of the fore-arc basin, Indus Suture Zone, Ladakh, India. *Terra Nova, 16*, 1–10.

Upadhyay, R., Frisch, W., & Siebel, W. (2008). Tectonic implications of new U–Pb zircon ages of the Ladakh batholith, Indus Suture Zone, NW Himalaya, India. *Terra Nova, 20*, 309–317.

Upadhyay, R., Sinha, A. K., Chandra, R., & Rai, H. (1999). Tectonic and magmatic evolution of the eastern Karakoram, India. *Geodynamica Acta, 12*, 341–358.

Valdiya, K. S. (1987). Trans-Himadri fault and domal upwarps immediately south of the collision zone: tectonic implications. *Currrent Science, 56*, 200–209.

Valdiya, K. S. (1998). *Dynamic Himalaya*. Hyderabad: Universities Press. 178 p.

Vidyadharan, K. T., Joshi, A., Ghosh, S., Gaur, M. P., & Shukla, R. (1989). Manipur ophiolite: Its geology, tectonic setting and metallogeny. In N. C. Ghose (Ed.), *Phanerozoic Ophiolites of India* (pp. 197–212). Patna: Sumna Publications.

Wadia, D. N. (1931). The syntaxis of the northwest Himalaya: Its rocks, tectonics and orogeny. *Records of Geological Survey of India, 65*, 189–200.

Wang, C., Liu, Z., & Hebert, R. (2000). The Yarlung-Zangbo palaeo-ophiolite, southern Tibet: Implications for the dynamic evolution of the Yarlung-Zangbo suture zone. *Journal of Asian Earth Sciences, 18*, 651–661.

Wiedmann, J., & Durr, S. B. (1995). First ammonites from the Mid- to Upper-Cretaceous Xigaze Group, South Tibet, and their significance. *Newsletter Stratigraphy, 32*, 17–26.

Xiaoying, S., Jiarum, Y., & Caiping, J. (1996). Mesozoic to Cenozoic sequence: Stratigraphy and sea level changes in the northern Himalayas, southern Tibet. *Newsletters on Stratigraphy, 33*, 15–61.

Yi, Z., Huang, B., Chen, J., Chen, L., & Wang, H. (2011). Palaeomagnetism of early Palaeocene marine sediment in southern Tibet, China: Implications to onset of the India-Asia collision and size of Greater India. *Earth & Planetary Science Letters, 309*, 153–165.

Zaman, H., Yoshida, M., Khadim, I. M., Ahmad, M. N., & Akram, H. (1999). Palaeomagnetism of the Himalaya-Karakoram belt and surrounding terranes since the Jurassic: Implications for three-phase collision. *Memoires Geological Society of India, 44*, 177–207.

Zhou, M.-F., Robinson, P. T., Malpas, J., Edwards, S. J., & Qi, L. (2005). REE and PGE geochemical constraints on the formation of dunites in the Luobusa ophiolite, southern Tibet. *Journal of Petrology, 46*, 615–639.

Zhu, B., Kidd, S. F., Rowley, D. B., Currie, B. S., & Shafique, N. (2005). Age of initiation of the India–Asia collision in the east-central Himalaya. *Journal of Geology, 113*, 265–285.

Ziabrev, S. V., Aitchison, J. C., Abrajevitch, A. V., Badengzhu, Davis A. M., & Luo, H. (2003). Precise radiolarian age constraints on the timing of ophiolite generation and sedimentation in the Dazhuqu terrane, Yarlung-Tsangpo suture zone, Tibet. *Journal of Geological Society of London, 160*, 591–599.

Chapter 18
Emergence and Evolution of Himalaya

18.1 Amalgamation of India with Eurasia

The Kohistan island arc in the frontal part of the Indian plate docked with mainland Asia, as already stated, around 65 Ma, and the suturing or welcing of the two continents was complete by 50–55 Ma. The frontal part of the Indian plate bent—the continental margin—down, was cut by deep steep faults and compressed into a series of folds, giving rise to a huge synclinorium in the terrane known as the *Tethys Himalaya*. The sediments of the trench in front of the Asian landmass and adjoining seafloor, it may be recapitulated, were compressed into very tight folds and later thrust up and pushed southwards onto the Tethys Himalaya. Even the pillow lavas and underlying dyke swarms along with the substratum of basic–ultrabasic rocks were squeezed up or abducted and implanted within the strongly deformed mass of sediments. The mixed suite of rocks—the melange—was sheared, shattered and uprooted in the zone of welding of the two continents. This zone of welding is known as *Indus–Tsangpo Suture* (Figs. 17.2, 17.12 and 17.14).

18.2 Bending and Bulging up of Leading Edge

18.2.1 Deformation

Most scientists believe that the leading edge of the northward-moving Indian plate plunged and slid under the Eurasian plate. There is another view. After the docking and resultant amalgamation of continents, there being no scope for further northward movement, the northern edge of Indian plate simply bent down (Fig. 18.1) and plunged partially into the asthenosphere (Valdiya 1987; 1998). This implies that the part of Indian crust that subducted or went down south of

K.S. Valdiya, *The Making of India*, Society of Earth Scientists Series,
DOI 10.1007/978-3-319-25029-8_18

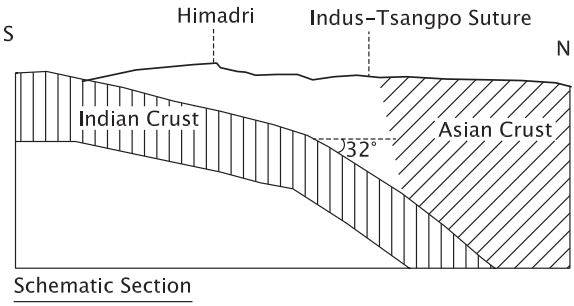

Fig. 18.1 A model depicting the leading edge of the Indian plate bending against the Asian crust and plunging into the asthenosphere (after Makovsky et al. 1996)

the Indus–Tsangpo Suture does not extend north beneath, and form a part of, the Tibetan crust (Molnar and Grey 1979; Hirn et al. 1984; Makovsky et al. 1996). The Indian mass being about 20 % less dense than the underlying mantle and therefore comparatively buoyant with respect to the mantle, there was resistance to its sliding under the Asian plate. Consequently, the leading edge of India buckled up into a domal upwarp against the zone of continental docking (Figs. 18.2 and 17.11). The upwarp is discernible all along its length between Nimaling in Ladakh, through Gurla Mandhata in the Kailas–Mansarovar region, to Lhagoi Kangri belt in Nepal.

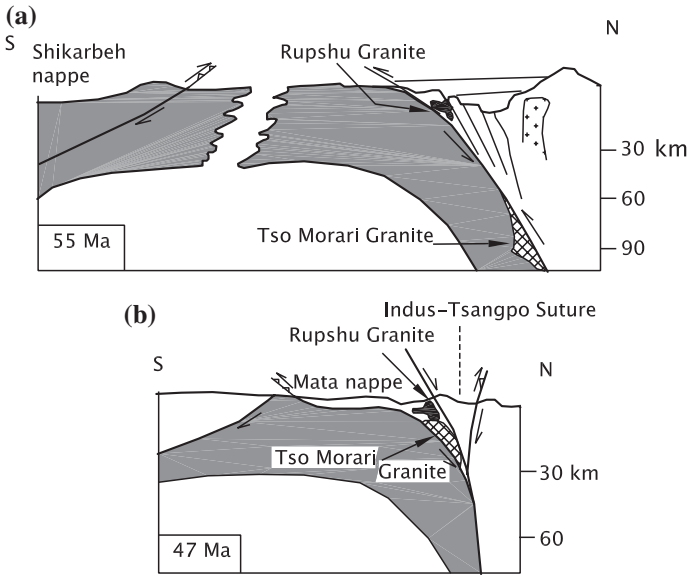

Fig. 18.2 Bulging up of leading edge of the Indian crust and attendant metamorphism and southward thrusting of the abducted material. In the deeper part of the suture zone, high pressures under low-temperature condition gave rise to blue schists of the eclogite facies (based on Schlup et al. 2003)

The warping up of the crust resulted in the exhumation and brought up to the surface even the basement complex with its 500 ± 25 Ma porphyritic granite, immediately south of the Indus–Tsangpo Suture Zone. In Kohistan, the development was somewhat different. Slices of broken-up crust popped up and were emplaced in the form of imbricated stacks. While in the northern part, the structures bent northwards above the thick zone of ductile decoupling of the suture zone, in the south, these are quite upright (Coward et al. 1988). Even the huge batholithic bodies of the Kohistan Granite was deformed and thrust and propelled southwards on the shear planes related to the Indus–Tsangpo Suture.

18.2.2 Metamorphism

Shortly after the docking, the rocks of the junction zone were deformed and metamorphosed. Pressures locally as strong as 11–9 kbar and the temperatures rather as low as (420–350 °C) converted the ophiolites in many places into *blue schists* which are made up of glaucophane, jadeite, lawsonite with or without phengite (Jan and Seymour 1977; Frank et al. 1977; Shams 1980a, b; Honnegger et al. 1982; Jan 1985; Virdi et al. 1977). Coesite-bearing eclogite in the Kaghan Valley in northern Pakistan indicates ultrahigh-pressure metamorphism at 46 Ma (Treloar et al. 2003). The blue schist of the Shangla area in Kohistan testified to the metamorphism and deformation at 80 Ma taking place at the depth ≥10 km, where the pressure must have been 400–700 Mpa (Anczkiewicz et al. 2000). After the peak metamorphism, the blue schist became part of the arc and finally emplaced along the zone of India–Asia docking. There a greenschist facies metamorphism was superimposed on the blue schists. In the Swat–Nayan belt in northwestern Pakistan, greenschist to amphibolite facies metamorphism in the Late Eocene time indicates a temperature in the range of 600–700 °C and pressure in the range of 9–11 kbar (DiPietro 1991). Locally, the temperature was high enough to cause partial melting and generating leucogranite in the Early Eocene (Zeitler et al. 1995). In the Nanga Parbat massif, high temperature above 500 °C was attained in the Middle Eocene time (Treloar et al. 1991).

The eclogite intrusives intercalated with pelitic schists of the Tso Morari complex are characterized by coesite, coexisting with 130 ± 39 Ma years of age phengite and paragonite (Gouzu et al. 2006). The phengite and coesite occurring in the pelitic schists are indistinguishable from those of the eclogite.

18.3 Sagging of ITS Zone

18.3.1 Sedimentation

Even as the northern edge of the Indian plate bulged up, the zone of welding of India and Asia sagged down. This happened in the Late Eocene time, 34–30 million years ago. A 2000-km-long and 60–100-km-wide depression (Figs. 18.2a and 18.3a) was

formed along what is today occupied by the valleys of the Sindhu and Tsangpo rivers. The depression is described as the *Sindhu Basin* (Valdiya 1998). In this basin were deposited a varied assemblage of sediments, comprising alternation of clays, calcareous–siliceous oozes, cherty limestones and greywackes, constituting the *Indus Flysch* (Tewari 1964; Sharma and Kumar 1978; Brookfield and Andrews-Speed 1984). The flysch comprises, among other things, limestones containing Middle Eocene marine foraminifers (Mathur 1983).

The flysch passes upwards into a very thick succession of molasse—ungraded softer conglomerates, arkosic sandstones, siltstones and muds deposited in the channels, their overbanks and floodplains of the rivers that alternately meandered and flowed swiftly as braided systems in their nearly 30-km-wide floodplain (Brookfield and Andrews-Speed 1984). The conglomerates of this molasse succession rest *also* on the floor of the Ladakh–Kailas Granite, as discernible on the scarps of Mount Kailas—the holiest of the holy mountains of the world. The molasse succession, described as the *Kargil Conglomerate* (Heim and Gansser 1939; Gansser 1964, 1977, 1981), covers a vast stretch of tract from Kargil in the west, through Hemis in south-eastern Ladakh and Kailas region north of Uttarakhand, to Liuquu in southern Tibet.

18.3.2 Life and Time

The shale within the upper part of the Kailas succession in the Liyan area (in Ladakh) contains entombed remains of palms—*Sabal major* and *Trachycarpus* together with *Livistona Prunus* rosewood and charophytes. These plants indicate warm and moist climate conditions and altitudes not higher than 2100 m in the Oligocene time (Lakhanpal et al. 1983). Remains of such vertebrates as goats, deers, rodents, pythons and small-sized mammals (Nanda and Sahni 1990) indicate that these animals were able to immigrate from Asia during the Oligocene time. Belonging to the Rhinoceratoid mammals, the taxa *Juxia* indicates Late Eocene time of the molasse emplacement (Tiwari 2005). Upper molar of anthracothere *Hyoboops palaeindicus* in the Kargil molasses establishes the correlation of the Kargil molasses with the Lower Miocene Dera Bugti succession of the Laki Hills. The Kargil molasse has yielded vertebrate fossils (Dixit et al. 1971). A cricetid rodent *Democricetodon* from the basal part of the Kargil molasse, 3 km west of Taruche in the Leh district, indicates Early to Middle Miocene age of the succession (Prasad et al. 2005).

The homotaxial basin in the Pakistan is known as the *Katawaz Basin*. In this basin, the molasse sedimentation started around Late Palaeocene, with the deposition of protodelta clays, passing upsection into delta-front sandstones and shales, and ending up with delta-top sandstone of a more non-marine character (Qayyum et al. 1997).

It seems that the sinking of the Indus–Tsangpo zone started in the Middle Eocene time and continued into the Oligocene epoch. Similar sinking of the Indian crust occurred along the southern margin of the nascent Himalaya. Various aspects of this (southern) basin are dealt with in Chapter 19.

18.4 Breaking of Himalayan Crust

18.4.1 Main Central Thrust

The revival of tectonic movements in the Early Miocene time accentuated the deformation of synclinorial Tethys Himalaya terrane and its basement the Himadri complex. Earlier formed folds were further tightened and overturned, some of them toppling over southwards. Many of the tightened folds were split by faults along their axial planes and subsequently displaced or thrust southwards as much as 30–80 km (Figs. 18.2b and 17.11). There was continuous build-up of compressive strain, and the buckled-up Himalayan crust broke up at 21 ± 2 Ma along what was to become the *Main Central Thrust* (MCT), first recognized by A. Heim and A. Gansser in 1939 in the Uttarakhand sector.

The broken-up crustal block (Fig. 18.3) moved up and southwards along gently (30°–45°) inclined thrust plane all along its 2000 km stretch—from the Kishtwar in the north-west to the Siang valley in the east. Eventually emerged the *Great Himalayan* or *Himadri terrane*, delimited at the base by the Main Central Thrust (MCT). The MCT has been described as the Vaikrita Thrust in Uttarakhand and Himachal Pradesh (Valdiya 1980a, b, 1988). The MCT is a wide zone of shearing characterized by mutually overlapping masses of highly mylonitized and deformed rocks, piled up one upon another as imbricated stacks (Fig. 18.4). The deformation took place along many planes of gliding and sliding and was accompanied by retrograde metamorphism. Pervasive and conspicuously strong lineation indicates strong and repeated movements in the northerly direction on multiple planes of dislocation. The rocks of the MCT zone in Kumaun have thus undergone marked superimposition of homogenous ductile strain as it was involved in vertical displacement of about 18 km (Bhattacharya 1987). The MCT brought the basement rocks from the depth of ductile deformation to the level of brittle deformation. The MCT is thus a terrane-defining tectonic plane bringing the Great Himalayan high-grade metamorphic rocks that are intruded by Miocene granites, onto and over the Lesser Himalayan lower-grade metamorphic rocks intimately associated with the Proterozoic granites.

The Vaikrita pile of the Himadri in Garhwal shows deformation one phase more than the underlying Lesser Himalayan Munsiyari rocks (Bhakuni 1995). Between Baragaon and Luhri in the Satluj valley in Himachal Pradesh, the 1.5–6.3-km-wide MCT zone of brittle–ductile deformation shows pure shear component of deformation. The deformation started close to simple shear flow at high temperatures, becoming progressively more general shear during cooling and ended up in a pure shear-dominated flow during the final stage of brittle deformation (Grasemann et al. 1999). Beyond the Kishtwar region in the west, the MCT is concealed under the Chamba Nappe. West of the Sindhu valley, the nearly parallel Laut and Batal faults of the megashear zone in the Neelam and Kaghan valleys in northern Pakistan represent the Main Central Thrust. For, these faults are associated with separation and dislocation of two lithological regimes and with, a break in pressure-temperature condition,

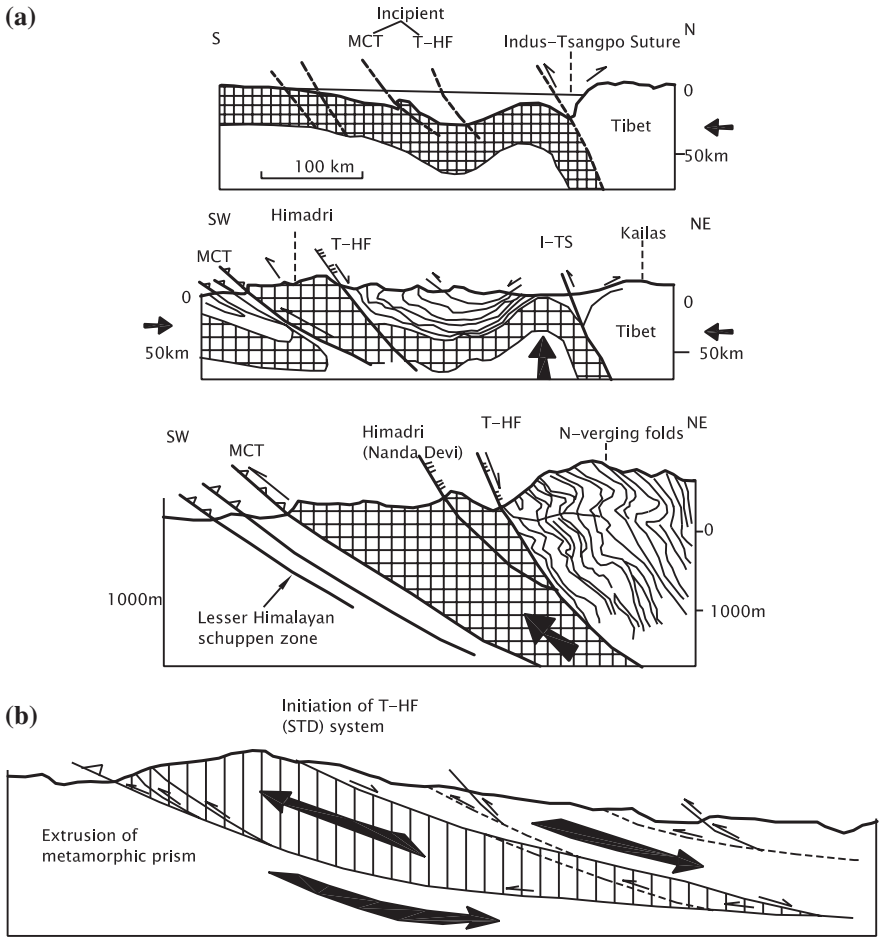

Fig. 18.3 **a** Following the docking of the Indian plate with mainland Asia and their amalgamation, the Indian plate buckled up and was faulted, leading to the development of a frontal upwarp and eventually to the formation of terrane-defining thrusts faults (after Valdiya 2005). **b** The pile of the Tethyan sedimentary rocks slipped northward on the plane of the Trans-Himadri Detachment Fault (Hodges et al. 1992)

and different tectonic styles (Fig. 18.4). There is also more than one-kilometre wide zone of mylonitization (Chaudhry and Ghazanfar 1987). The MCT ends against the Indus–Tsangpo Suture which is in Pakistan, where it is described as the *Main Mantle Thrust* (Tahirkheli et al. 1979; Tahirkheli 1982).

In Nepal, the MCT zone is a 2- to 3-km-thick zone of strain that developed during two or more episodes of movement (Pecher 1977). The earlier movement, occurring at 22.5 Ma, was concentrated along Chomrong Thrust, which represents—like the Vaikrita Thrust in Uttarakhand—a sharp metamorphic discontinuity between the middle and upper amphibolite facies metamorphic rocks of the

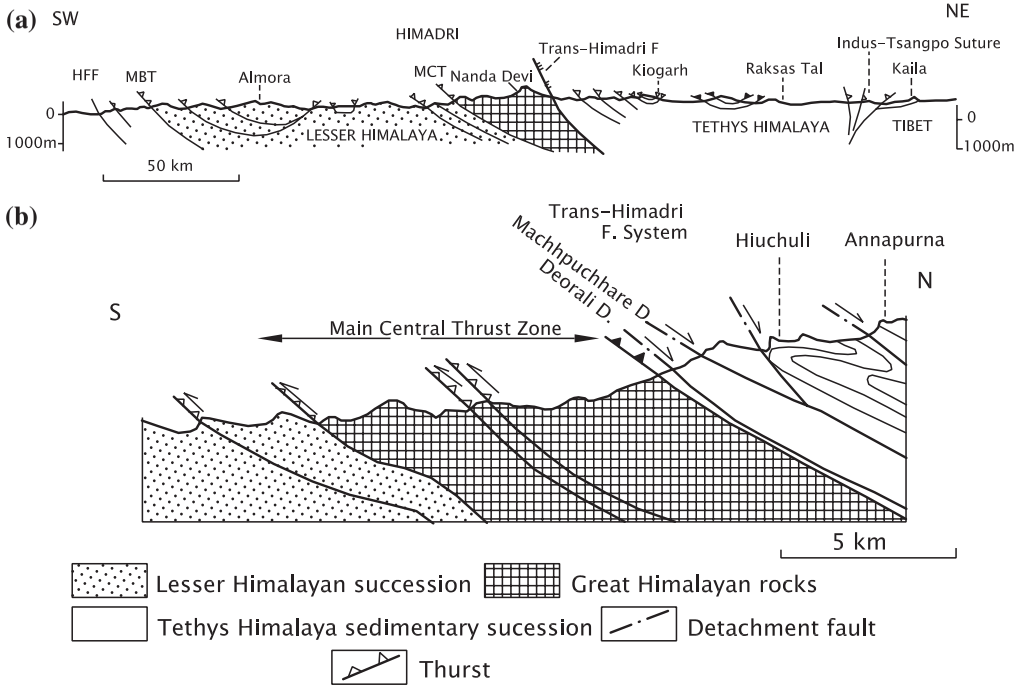

Fig. 18.4 **a** Generalized schematic cross section through the Uttarakhand Himalaya showing terrane-defining thrusts, including the Main Central Thrust (based on Gansser 1964). **b** Imbricated stack of various lithotectonic units beneath the Main Central Thrust in north-central Nepal. Also shown are detachment planes at the top of the sequence of Great Himalayan crystalline rocks (Hodges et al. 1996)

Great Himalaya and the greenschist facies rocks of the Lesser Himalayan successions (Hodges et al. 1996). The emplacement of higher-grade Himadri rocks upon the Lesser Himalayan low-grade metamorphics took place at 21 ± 0.2 Ma, as testified by Ar–Ar data from hornblende (Hubbard et al. 1991). In the Langtang region, asymmetric deformation features such as mica fish and shear bands below the kyanite-bearing pelitic metamorphic assemblage show the parts thrusting westwards on the MCT (Takagi et al. 2003). East of the Langtang area in the Dudh Kosi sector, the MCT has been interpreted as a thrust which has not moved in a normal sequence. It represents post-metamorphic compressional phase, which began during 40–35 Ma and ended in thrusting at 21 Ma (Carosi et al. 1999). As elsewhere, in Nepal also there were two distinct periods of movement on the MCT—the Early Miocene ductile motion and the later shear zone movement that took place after 5.8 Ma (Macfarlane 1993). Shearing movement with attendant intense mylonitization within a wide zone occurred on both sides of the MCT, in the footwall and in the hanging wall, resulting in the development of inverted metamorphism (Meier and Hiltner 1993).

In Bhutan, the Tashigang section reveals sliding and consensing of several packages of rocks in the MCT zone (Stuve and Foster 2001). In eastern Arunachal Pradesh, the *Sela Thrust,* representing the MCT, is a megashear ending up against the Indus–Tsangpo Suture (Singh 1993a).

18.4.2 Trans-Himadri Detachment Fault

Nearly, at the same time, when the Himalayan crust broke along the MCT and the Himadri pile advanced southwards onto the Lesser Himalayan terrane, the thick Tethyan sedimentary cover was detached from the hard unyielding crystalline basement making the Great Himalaya (Figs. 18.5, 18.6, 18.7 and 18.8). The plane of detachment represents normal gravity fault (whose inclination varies from sector to sector) which was first described as the *Malari Fault Thrust* in the valleys of Dhauli, Gori and Kali (Valdiya 1976, Valdiya 1981) and later named the *Trans-Himadri Detachment Fault* (Valdiya 1987). In the type area, the strongly NNE–SSW-lineated Vaikrita metamorphics having NE-plunging folds give way to sedimentary strata that lack reclined, isoclinal folds and so characteristics of the Vaikrita. Instead, there are NNE-verging backfolds, sigmoidal in shape and characterized by subhorizontal cleavage as spectacularly developed along the Gori valley over more than 20 km width. The Trans-Himadri Fault is associated with a number of sympathetic and antithetic faults. In the Kali valley, even the Vaikrita complex is split by faults into two unequally dipping slabs and the overlying Middle Ordovician Garbyang strata are faulted against the upper slab of the Budhi Schist of the Vaikrita succession. In the Western Dhauli valley, the hanging wall is cut by both south-hading and northward-inclined faults that dismember the north-verging backfolds. At Malari, the Vaikrita granite and migmatite with pegmatite dykes of the footwall are highly sheared and locally brecciated, implying movement later than the emplacement

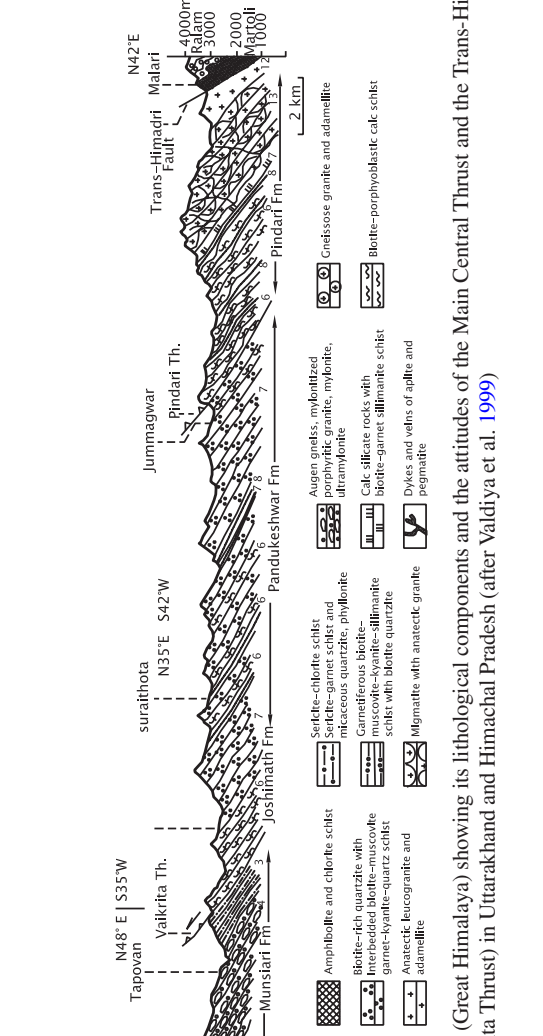

Fig. 18.5 Section across the Himadri (Great Himalaya) showing its lithological components and the attitudes of the Main Central Thrust and the Trans-Himadri Detachment Fault (described as Vaikrita Thrust) in Uttarakhand and Himachal Pradesh (after Valdiya et al. 1999)

during the Early Miocene time. The movements of the Trans-Himadri Fault in Uttaranchal are dominantly dip slip (Valdiya 1987, 2005). The remarkable feature associated with the T-HF is the complex backfolds on the hanging wall discernible all along its extent. Moreover, in addition to down-dip slip of rocks, there is strike-slip movement due to extension as seen in the Gangotri area, where microstructures indicate dextral sense of movement (Gururajan and Choudhuri 1999). In the Gori valley, the drainage is disturbed over the vertical fault—the hanging wall characterized by spread and splaying out of drainage lines in contrast to straight lines in the footwall, implying reduction of the river gradient due to uplift of the footwall (Gupta et al. 2006). The formation of huge lakes upstream of the T-HF in valleys of Western Dhauli, Gori, Eastern Dhauli and Kali corroborates this inference (Valdiya 2001, 2005). The detachment fault is discernible in Lahaul, and Spiti and Kullu valleys in Himachal Pradesh (Choudhuri et al. 1992) (Fig. 18.6).

In the Zanskar Range the 2.25–6.75-km-wide ductile shear zone, is described as the *Zanskar Shear Zone* (Herren 1987). It is traceable as a prominent morphological feature for 80 km. The displacement took place along closely spaced infinitesimal shear planes, resulting in inversion of metamorphic grades across the 15–20-km-thick south-verging pile (Jain and Manickavasagam 1993; Jain et al. 2003). The south-westward-overturned folds of the shear zone are believed to be contemporaneous with the SW-directed thrusting along the MCT in the Late Oligocene to Early Miocene time, while the later phase of deformation resulted in the development of a dextral shear zone along the Chandra valley between the Tethys cover and Great Himalayan basement (Vanny and Steck 1995). The

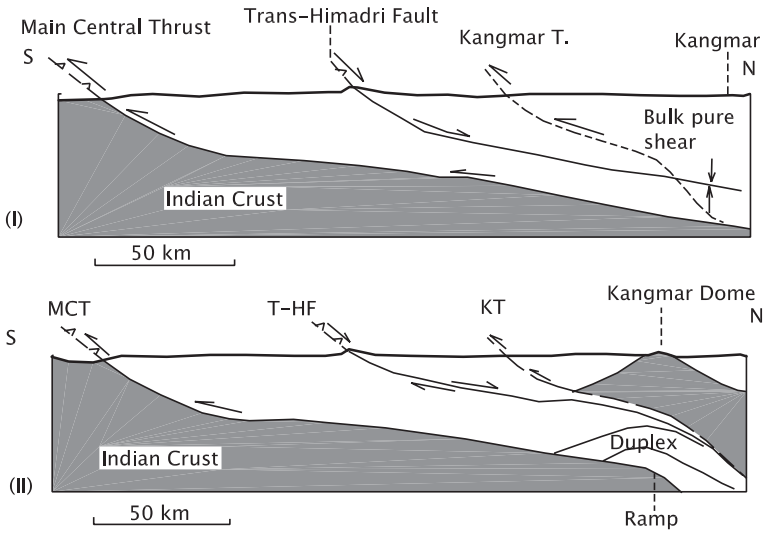

Fig. 18.6 Interpretive, schematic section across Himalaya showing the relationship of the evolution of structural domes in the Tethys terrane with the detachment of the Tethyan cover from its basement (after Lee et al. 2000)

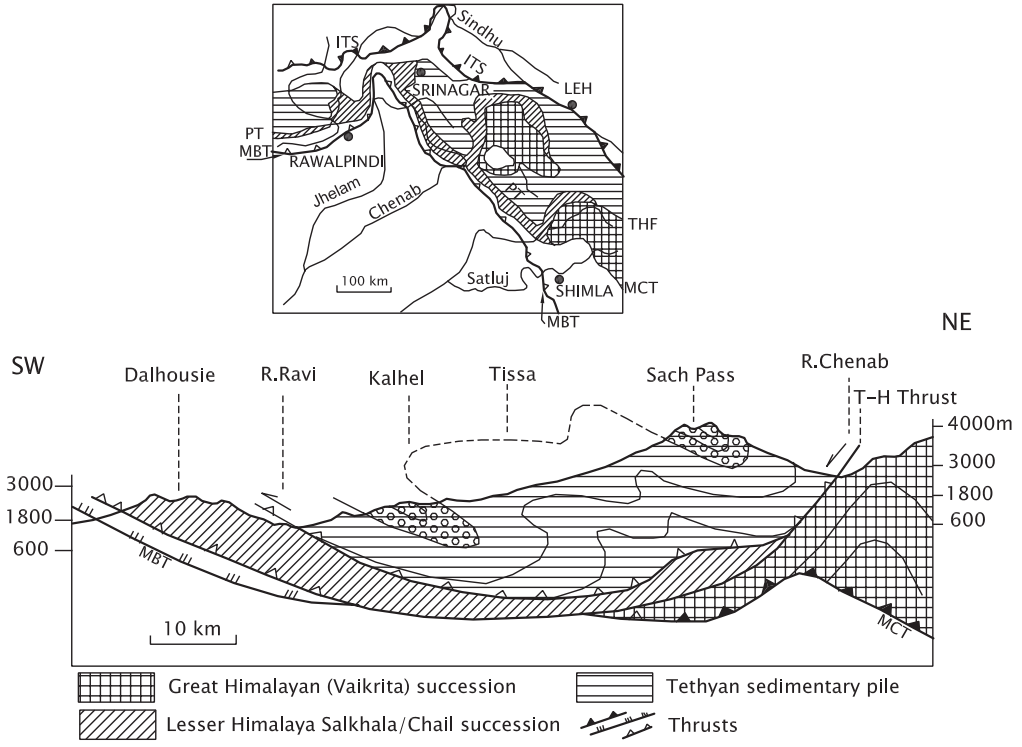

Fig. 18.7 Sketch map and section of NW Himalaya showing south-westward turning of the Trans-Himadri Detachment Fault system and emplacement of the basal Tethyan sedimentary rocks (the Haimanta) as the Chamba Nappe of low-grade metamorphic rocks (based on Thakur 1993, 1998. *Inset* after Valdiya 1988)

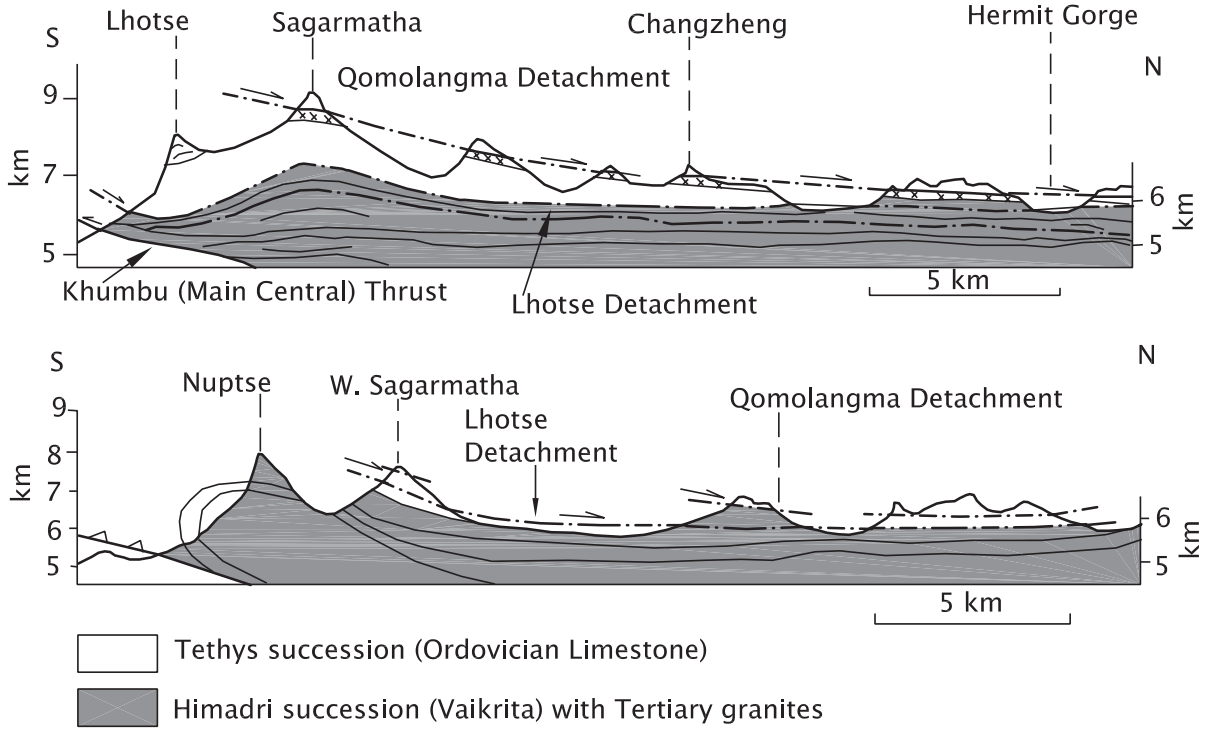

Fig. 18.8 T-HDF system, described as the Qomolangma Detachment and the South Tibet Detachment, split the top of the Sagarmatha massif and separated the high-grade Great Himalayan metamorphic rocks (Barun Gneiss) from the Tethyan sedimentary pile (after Searle et al. 2003)

north-east-directed backfolds were produced probably during gravitational collapse of the thrust stack along the Zanskar Shear Zone (Wyss et al. 1999). The deformation on the ZSZ was ongoing at 26 Ma and continued intermittently up to 16 Ma in some sectors (Inger 1998). In the Baralacha Pass area, low-angle conjugate normal faults represent the more brittle equivalent of the ductile Zanskar Shear Zone, accommodating both vertical extrusion and horizontal extension related to doming up and backfolding (Epard and Steck 2004).

In the Kishtwar region, a NE-dipping normal fault of the ductile shear zone at the top of the Himadri slab was severely deformed in the period between 22 and 16 Ma (Stephenson et al. 2001). The Haimanta succession of the Tethyan terrane was detached from the basement and displaced 30 km southwards as a thrust sheet designated as the *Chandra Nappe* (Thakur 1998). In the northern flank, this terrane-defining thrust is described as the Chenab Fault, and in the southern flank, it is known as the *Panjal Thrust* (Fig. 18.7). In the northern flank there was gravity collapse, resulting from northward translation of faulted rocks, whereas in the southern flank, there was southward propagation of nappes, the translation being dominated by compressional strain in the frontal fault zone and shear strain in the oblique zone of the Chamba Thrust (Singh 1993b; Sharma and Bhola 2004). The culmination of this development is that in the Kishtwar window in north-eastern Jammu adjoining Himachal Pradesh, the Tethyan rock pile has advanced considerably southwards (Fig. 18.7), surrounding not only the Great Himalayan rocks but also overriding the Lesser Himalayan thrust sheets (Singh 2010).

In the Kali Gandaki sector in central Nepal, northward-overturned gravity-driven folds of the ductile normal faulting are accompanied by structures indicating dextral shearing related to eastward extrusion of Tibet in the period 25–15 Ma (Pecher 1991). Described as the *Annapurna Detachment* (Fig. 18.4b), the T-HDF in north-central Nepal records two stages of normal-sense shearing. The first-stage ductile deformation occurred at mid-crustal depth and formed southward-overturning isoclinal folds, and the second-phase deformation caused detachment of the basement from cover rocks, the latter giving rise to north-eastward-overturned backfolds along with extrusion parallel to the trend of the orogen (Brown and Nazarchuk 1993).

In the Sagarmatha massif, the Great Himalayan crystalline rock complex is split by a number of gently dipping thrusts (Fig. 18.8), the upper thrust plane dipping 5–15°N—and traceable to the border of Tibet. It shows northward displacement of the Tethyan sedimentary pile, and gravity collapse of the Miocene topographical front (Wang and Zheng, 1975) has been described as the *South Tibetan Detachment* (Burchfield and Royden 1985; Carosi et al. 1998) or the *Qomolangma Detachment* (Searle 1999). A brittle deformation has affected and cut all older leucogranites of the footwall, while the ductile southward tectonic extrusion of the footwall rocks is of the order of 200 km (Searle et al. 2003). The development of the ductile extensional shear zone took place in the period 24–16 Ma (Carosi et al. 1998). In Bhutan, erosional remnants of Tethyan metasediment resting atop the Himadri high-grade metamorphics and granites (Chasilakha–Takhtasang Gneiss) represent klippen of the T-HDF nappe. This thrust is described as the *DontoLa Detachment* (Grujic et al. 2002). There

was exhumation or bringing up of metamorphic rocks that evolved at 6–4 kbar pressure, followed by northward thrusting of Tethyan sediments along the detachment fault and along an out-of-sequence thrust.

18.4.3 Timing of Detachment

Most workers believe that the T-HDF (STD) and MCT movements were broadly contemporaneous (albeit episodically) and continued long after their commencement at about 21 Ma (Hodges et al. 1992; Valdiya 2005). It is possible that the detachment took place due to slowing down or periodic blocking of movements on the MCT (Valdiya 1987, 1998).

The times of the detachment of the basement from its cover and the revival of movement on this plane of decoupling have been determined from the radioactive minerals present in granitic bodies that predate and post-date the fault movements and occur within the zone of the T-HDF system. In the Rongbuk valley in southern Tibet, the extensional movements related to the detachment occurred between 19.5 and 23.5 Ma (Burchfiel and Royden 1985), in the Khula Kangri area at ~12 Ma (Wu et al. 1998), in the Sagarmatha region between 16.37 and 16.67 Ma (Hodges 2000) and in Bhutan simultaneously with the movements on the MCT between 16 and 22 Ma (Grujic et al. 2002). The movements seem to have been distributed over a long period (~10 million years) on this "long-lived crustal-scale decoupling horizon between the upper crust and the middle-lower crust" (Hodges 2000). The common view is that the T-HF system was formed around 20.9 Ma, nearly at the same time when the Main Central Thrust was formed (Royden and Burchfiel 1987; Hodges et al. 1992; Hodges 2000). In the north-western Himalaya, the initial decoupling occurred at 26.5 ± 0.7 to 26.1 ± 1.3 Ma in the central part of the Zanskar Shear Zone and between 26 Ma and 15 Ma in its western part (Walker 1999; Jain et al. 2003).

There is another view, it was the T-HDF that first evolved between the rigid basement complex and sedimentary cover. And as the deformation front propagated southwards, other detachment planes and faults were formed, culminating eventually in the formation of the Main Central Thrust during the climactic phase of the Himalayan orogen at 21–22 Ma. It seems that the T-HDF system was active during the period when large-scale crustal thickening took place. There was simultaneous E–W extension attributed to collapse of the Tibetan plateau as a result of body forces arising from crustal thickness contrast between Himalaya and Tibet (Hodges et al. 1992).

18.5 Domal Structures in Tethys Terrane

All along the northern zone of the Himalaya province, high points or domal structures of large dimension occur within the sedimentary expanse of the Tethys terrane. In south-eastern Ladakh, the *Tso Morari Dome* in the surrounding of Later

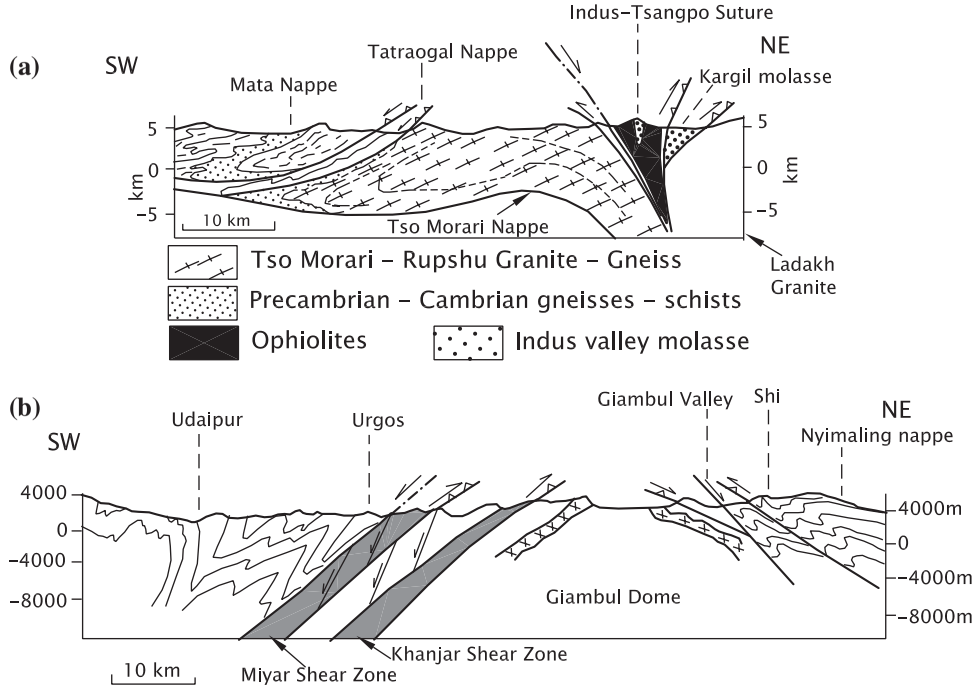

Fig. 18.9 **a** Structural architecture of the Tso Morari Dome in the context of the subduction of Indian plate along the Indus–Tsangpo Suture and general tectonics of the Himalaya (modified after Schlup et al. 2003). **b** Structural design of the Gianbul Dome along the Miyar and Gianbul valleys showing the Shikar Beh and Nyimaling–Tsarap nappes (after Robyr et al. 2002)

Precambrian to Cretaceous succession (Fuchs 1986) is characterized by imbricated stack of the three south-west-directed recumbent nappes (Fig. 18.9a). These were formed by shearing of the upper crust metamorphic rocks and emplaced 50 million years ago and brought up to shallow levels of 10 km along a high-angle fault at 40–45 Ma, followed by rapid cooling and backfolding (Steck et al. 1999; Schlup et al. 2003). Mineral phengite in the eclogite of the Tso Morari complex indicates a pressure range of 11–14 kbar, and the garnet–omphacite mineralogy suggests 530°–580° temperature (Sachan et al. 1999). In the Miyar and Gianbul valleys, a 180-km-long and 60-km-wide dome is made up of gneisses and migmatites

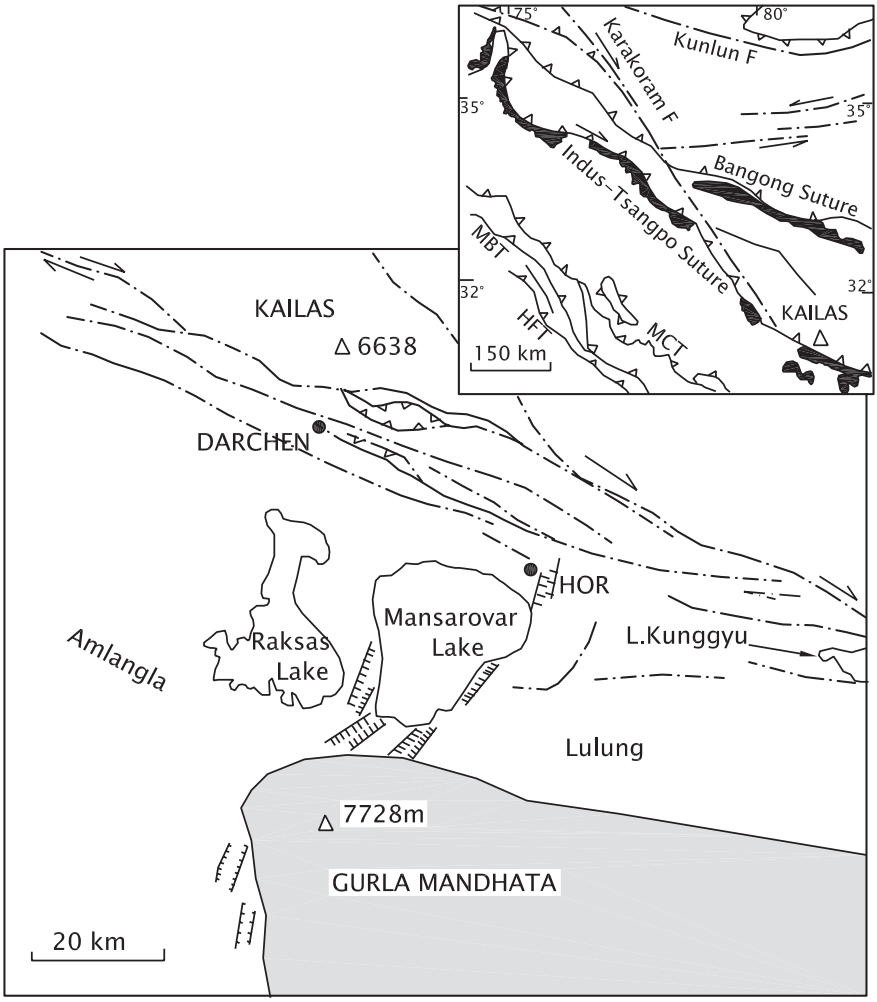

Fig. 18.10 Location of the domal Gurla Mandhata massif in the tectonic framework of Hundesh (south-western Tibet), the type area of the Indus-Tsangpo Suture (Laccasin et al. 2004)

in the core, surrounded by metamorphic rocks successively of the sillimanite, kyanite, staurolite, garnet, biotite and chlorite zones (Robyr et al. 2002). The earlier NE-directed thrusting gave rise to the formation of two nappes (Fig. 18.9b). This was followed by extension along the frontal part of the younger nappe as well as along the south-dipping shear zone in the southern limb of the Gianbul dome, leading to its coming up to the surface (Robyr et al. 2002). Significant is the intimate association of exhumed eclogite (Sachan et al. 1999). The uplift was broadly synchronous with the formation of anatectic leucogranites around 25 Ma (Gapais et al. 1992). Later phase of deformation caused dextral shearing along the Chandra valley resulting in the development of a large-scale strike-slip ductile shear zone between the basement crystallines of the Himadri and the Tethyan sedimentary cover (Vannay and Steck 1995). Further deformation induced large-scale doming up and NE-verging backfolds.

South of Mount Kailas is the gneissic Gurla Mandhata Dome, the development of which is related to the tectonics of the Indus–Tsangpo Suture (Heim and Gansser 1939; Gansser 1964; Lacassin et al. 2004). The WNW–ESE-trending fault occupied by terraced valley of Humla Karnali (which cuts through the Tethys Great Himalayan and Lesser Himalayan terranes is a normal fault that registers right-lateral net strike slip of 21 km on the southern side (Murphy et al. 2005). Th–Pb ion microprobe monazite age for leucogranite bodies indicates that the movement occurred *after* 15 Ma (Fig. 18.10).

There are large dome and basin structures trending NNE–SSW and NW–SE in northern Nepal. These were formed after the extrusion of the Himadri complex at the top (Carosi et al. 1999). Relatively small domes of earlier generation and oriented conformable to the Himalayan trend (like the Kangmar dome) are cored by orthogneiss and covered successively by staurolite, kyanite, garnet and chloritoid zones resulting from contraction and thermal re-equilibration manifest in moderate-pressure high-temperature metamorphism and subsequent vertical thinning

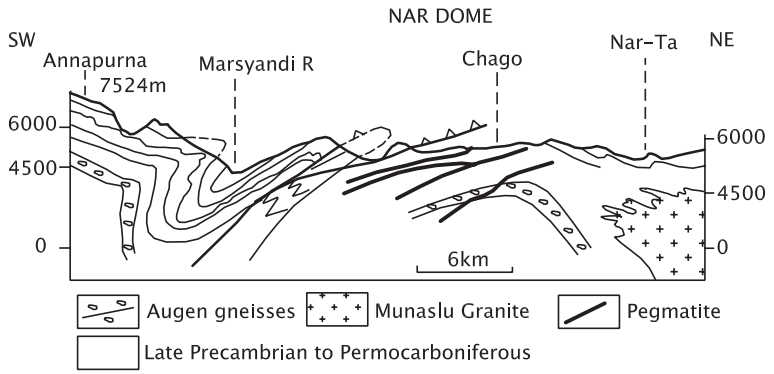

Fig. 18.11 Structure of the Nar Dome north of the Annapurna massif characterized by spectacular backfolding and backthrusting resulting from gravitational collapse as the Himadri complex was squeezed up and thrust southwards (after Bordet et al. 1975)

and horizontal extension (Lee et al. 2000). The domal structure was formed in the Middle Miocene as the rock pile moved up and over a north-dipping thrust fault ramp or transverse ridge. One such example is the Nar Dome, north of the Annapurna massif (Fig. 18.11).

18.6 Metamorphism in Himadri (Great Himalaya) Terrane

18.6.1 P-T Conditions

Metamorphic mineral assemblages characterized by staurolite, kyanite and sillimanite indicate that the Himadri metamorphic rocks evolved at the depth of 30–35 km where the temperature was higher than 600 °C and the pressure more than 7–8 kbar. The P-T conditions in south-eastern Kashmir including Kishtwar were 8.5–10 kbar at the depth of the 33–37 km (Stephenson et al. 2001), in the Padar–Zanskar belt 700 °C and 10 kbar at the depth of 28–30 km, and 550 °C and 8.5 kbar in the upper structural level (Searle et al. 1992; Vance and Harris 1999; Manickavasagam et al. 1999) in the eastern Garhwal sector 645 ± 50 °C and 7.5 ± 0.5 kbar to 900 K and 317–323 Mpa at the depth of 12–19 km (Gairola and Ackermann 1988; Hodges and Silverberg 1988), in the Kumaun sector at 600–650 °C and over 5 kbar (Valdiya and Goel 1983), and in the Dhaulagiri massif in central Nepal 610 °C and 9.4 kbar at a depth more than 35 km (Vanna and Hodges 1996). In the upper part of the Himadri succession, the later phase of deformation was accompanied by excessive heat production.

18.6.2 Inverted Metamorphism

First noticed in the Darjeeling Hills, the abnormal succession of metamorphic grades was described by F.R. Mallet in 1884, by P.N. Bose in 1891 and by Ray (1947) and Mohan et al. (1989) as a case of inverted metamorphism.

The Barrovian metamorphism was overprinted by lower-pressure and/or high-temperature metamorphism due to quick and quasi-adiabatic uplift by transportation along the MCT ramp, resulting in inverted zonation of metamorphic rocks (Pecher 1989). The inversion of metamorphism is only apparent and is related to repeated thrusting (Fig. 18.12). Metamorphic index minerals preserved in Lower to Upper Siwalik succession of the Himalayan Foreland Basin suggest differential denudation of the metamorphic zones over the past 18 million years, implying that inverted metamorphic zoning is a consequence of imbricated thrusting and ductile shearing (Sorkhabi and Arita 1997). Deformation of two right-way-up or normal sequences, involving splitting of the overturned limb in the broad shear zone by faults, results in inversion of this kind (Harrison et al. 1998). Another view is that intracontinental underthrusting along the MCT and bowing down of the isotherms

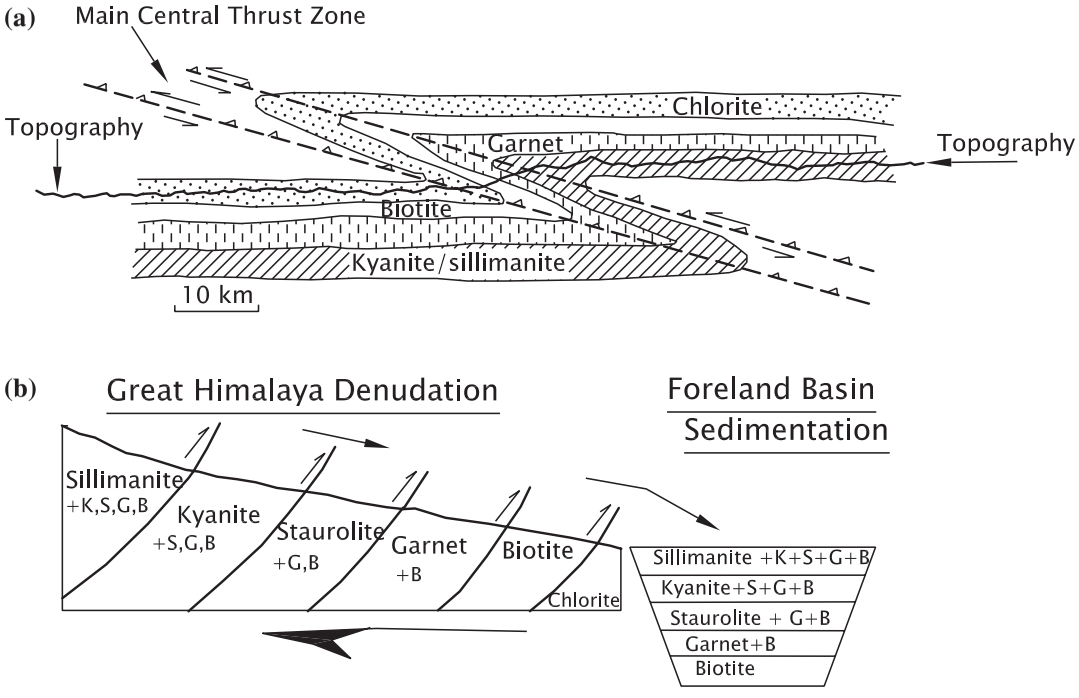

Fig. 18.12 Apparent inversion of metamorphic grades is interpreted in different ways. Two acceptable models are as follows: **a** effect of deformation of a normal metamorphic sequence across a broad shear zone (after Harrison et al. 1998) and **b** differential denudation of the metamorphic zones as a consequence of imbricated thrusting (modified after Sorkhabi and Arita 1997)

resulted in the inversion of metamorphic grades (Sinha-Roy, 1982). There is also a postulation that an exceptionally hot granite slab thrust over cold sedimentary pile is responsible for this abnormality (Le Fort 1988).

18.6.3 Date of Metamorphism

The peak metamorphism preceding ductile shearing occurred at 37.7 ± 2 Ma in the Zanskar Range (Jain et al. 2003). In the Dhaulagiri massif, the acme of metamorphism taking place at 37.2 ± 2.8 Ma was followed by retrograde metamorphism at 22.5–21.5 Ma (Vannay and Hodges 1996). In north-eastern Nepal, the hanging wall rocks above the MCT were metamorphosed during the thrust movement at 21 Ma (Catlos et al. 2002). Argon–argon data from a profile across rocks in the immediate hanging wall of the MCT zone in eastern Bhutan indicate muscovite cooling age of 14.1 ± 0.2 Ma, where the temperature at 6.5 kbar was 600–650 °C (Stuve and Foster 2001). Apparently, there was revival of movements on the MCT.

18.7 Anatexis and Emplacement of Leucogranites

18.7.1 Mode of Occurrence

In the Himadri domain, the pressure and temperature had risen so high in the Early Miocene that susceptible parts of the metamorphic rocks melted differentially or partially, giving rise to molten material of granitic composition. Minerals such as sillimanite, cordierite and garnet, so common in metamorphic rocks, occur profusely in these *anatectic granites*. The granites are leucocratic all along the Himadri expanse. The anatectic magmas were emplaced in the form of batholiths, stocks, laccoliths, sills, dykes and veins. The highly mobile material also pervasively penetrated layer after layer the schists and gneisses in the upper part of the Himadri sequence, giving rise to migmatites throughout the length of the Great Himalayan terrane. Thus, the leucogranite plutonic bodies are commonly intimately associated with zones of *migmatites* of the same age. Even the Tethyan sedimentary sequence resting on the high-grade metamorphic rocks of the Himadri basement was intruded by anatectic granites formed in the period 24–22 Ma, the peak time being at 21 ± 0.5 Ma (Lefort 1988; Trivedi 1990; Gapais et al. 1992). The holy massif of Badrinath and Kedarnath in Garhwal (Fig. 18.13) is made up of 1.5–2.0-km-thick laccoliths associated with feeder dykes of leucogranites, characterized by enrichment in Rb, Sn, U, B and F and depletion of Sr, Ba, Za, Th and REE, implying fractional crystallization of the magma in the early phase (Scaillet et al. 1990, 1995). The Shivling Granite is a plutonic body of tourmaline-bearing leucogranite in the Badrinath massif emplaced around 20.0 ± 0.2 Ma as a foliation

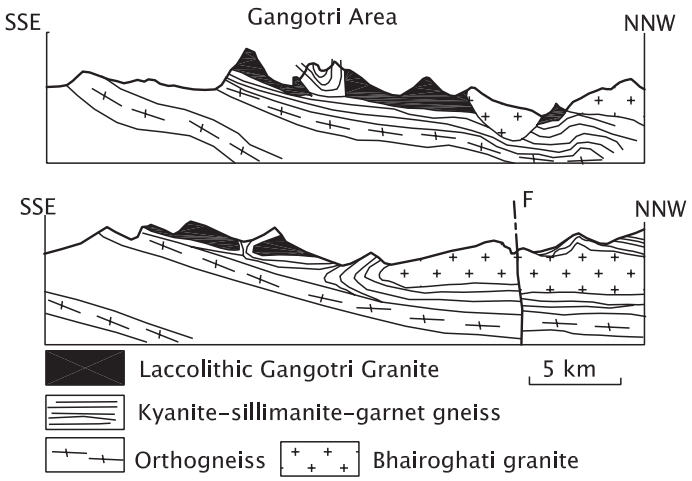

Fig. 18.13 Cross section of the Badrinath massif in the Gangotri area shows the mode of occurrence of the 20–21-million-year-old leucogranite (after Scaillet et al. 1995)

parallel laccolith, via a dyke network in the Vaikrita succession of the Gangotri region (Searle et al. 1993). The leucogranites of the Beas-Parbati valleys (H.P.) belong to this phase of granitic activity (Jain et al. 1999)

18.7.2 Causes of Anatexis

The cause of *anatexis* or differential melting of metamorphic rocks giving rise to the anatectic leucogranite is a matter of debate. The shear zone stress on thrusts and faults at the base and at the top of the Himadri succession must have decreased, resulting in decompression melting (England and Molnar 1993; Harris and Massey 1994). In the southern part of the Nanga Parbat massif, the 22–16 Ma leucogranites occur adjacent to the Rupal Shear Zone (Schneider et al. 1999a, b). In the Kishtwar region, it was formed due to frictional heating along the MCT (Stephenson et al. 2001). In the Annapurna massif, the 21.5–22.5 Ma granite dykes resulted from in situ partial melting during metamorphism (Hodges et al. 1996). In the Langtang National Park, the anatexis in extensional regime was synchronous with movements on both the MCT and the STD (Harris and Massey 1994). In the Sagarmatha massif, the exhumation that allowed isotherms to rise resulted in the partial melting of the thickened crust at 650–700 °C and 2.4 kbar even as metamorphic fluids released during the exhumation coming up permeated surrounding rocks (Pognante and Benna 1993). In the Shishapangma massif, the 20.2 ± 0.2 Ma granite bodies, characterized by strontium ratio in the range of 0.738 and 0.750, imply origin of the granite magma due to crustal extension (Searle et al. 1997), entailing shear heating on a continuously active thrust and attendant partial melting (Harrison et al. 1998).

The U–Pb monazite dating of leucogranites across the Himalaya province reveals northward younging of magma crystallization. The emplaced magmas became younger northwards from 23 Ma in the south to 12 Ma in the north, suggesting a connection of the magma generation with southward extension (thrusting) of the Himadri slab (Wu et al. 1998).

18.8 Development of Lesser Himalayan Terrane

18.8.1 Northern Duplex Zone

Repeated translation or thrusting of the Himadri rock pile threw more than 7000-m-thick Lesser Himalayan sedimentary and metasedimentary successions into a series of folds. Close to the MCT, the squeezing and tightening of folds resulted in southward overturning and toppling over of folds, accompanied by their splitting by a multiplicity of faults along axial planes (Figs. 18.4b and 18.14). This gave rise to a *duplex* or *schuppen zone* comprising imbricating lithotectonic stacks as seen in the tract between Alaknanda and Yamuna in Uttarakhand (Valdiya 1978, 1980b, 1988; Saklani 1972a, b, 1983, 1993; Bahuguna and Saklani 1988; Saklani et al. 1991; Bist and Sinha 1980). There was southward progression of thrusting (Table 18.1) with some reactivation of thrusts in the duplex zone and breakback thrusting with respect to the Munsiyari Thrust in the footwall of the MCT, resulting in the shortening of more than 65 % (Srivastava and Mitra 1994). Across the MCT, both the Himadri and Lesser Himalayan rocks were affected by late-stage retrograde metamorphism during exhumation (Valdiya 1988; Paudel and Arita 2000). The Lesser Himalaya acquired inverted zonation of metamorphic rocks during a one-stage prograde metamorphism, its origin attributed to thrusting along the MCT and the heat supplied from the overlying Himadri succession (Pecher 1989).

The metamorphism of the Munsiari unit below the MCT in Uttarakhand took place at 450 °C and 4 kbar (Valdiya and Goel 1983). In central Nepal, the Kathmandu succession (Bhimphedi Group) beneath the MCT is characterized by metamorphic rocks that evolved at 754–588 °C and 8.9–5.8 kbar pressure (Rai 2001).

18.8.2 Far-Travelled Nappes

Increasing compression resulted in the uprooting of the entire folded pile under the MCT and their 80 to 125 km displacement southwards in the form of thrust sheets or nappes. Their detached pieces or erosional remnants form klippen atop the Lesser Himalayan sedimentary pile. The nappes and klippen are preserved in the synclinal cores of the sequence with which they were concordantly folded after the thrusting.

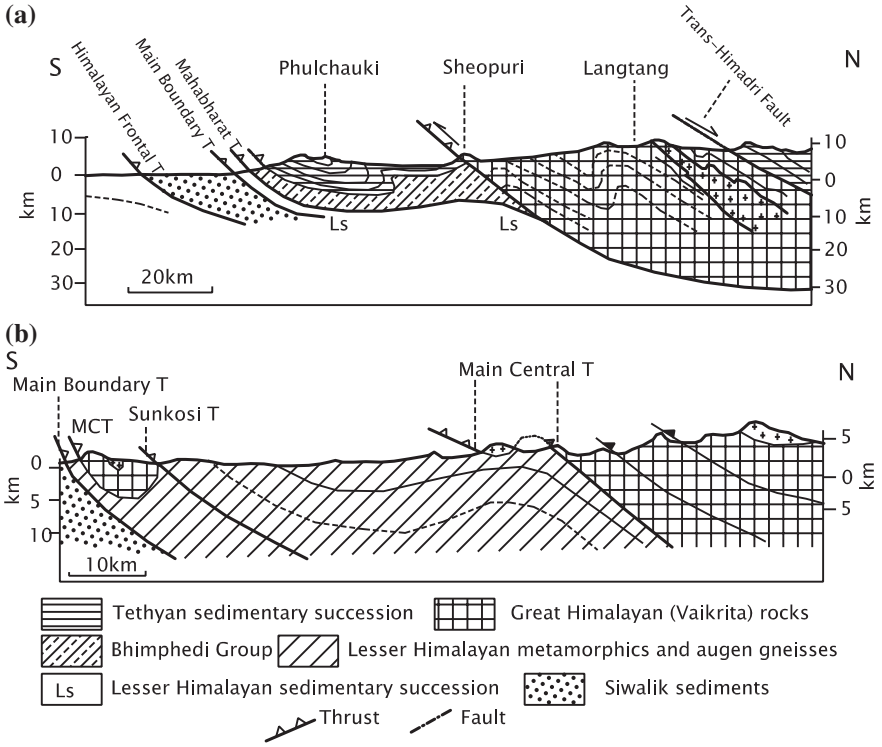

Fig. 18.14 **a** In central Nepal, the Lesser Himalayan Kathmandu Nappe, made up of the Bhimphedi metamorphics, is separated from the Himadri succession of the Gusainkund massif by the MCT. The Kathmandu nappe stretches south nearly up to the border of the Lesser Himalaya (after Rai 2001). **b** Thrust along the MCT, the Himadri complex of high-grade metamorphic rocks (Barun/Darjeeling Gneiss) in eastern Nepal reaches the Siwalik–Lesser Himalayan boundary (the Main Boundary Thrust) (after Schelling 1992)

There are two principal lithologically and structurally distinctive nappes (Table 18.1). The structurally lower *Ramgarh–Chail Nappe* is made up of low-grade metamorphic rocks integrally associated with 1900 ± 100 Ma mylonitized porphyritic granite and porphyry. In western Nepal, the Ramgarh thrust sheet—0.2 to 2.0 km in thickness—registers nearly 120 km of initial south-verging dislocation (Robinson et al. 2001; Pearson and DeCelles 2005) and more in eastern Nepal (Schelling and Arita 1991) compared to 85 km in Kumaun (Heim and Gansser 1939; Valdiya 1980b). The structurally upper *Almora/Munsiari–Jutogh Nappe* comprises medium-grade metamorphic rocks intruded by 500 ± 25 Ma granite–granodiorite plutons. Known by different names (Table 18.1), these two nappes extend all over the Lesser Himalayan subprovince from northern Pakistan to eastern Arunachal Pradesh (Figs. 10.1 and 11.1).

The original place (root) of these two nappes of crystalline rocks is a matter of speculation. Most workers show them rooted under the MCT. Another view is

Table 18.1 Tectonic succession in the Himalaya

Kashmir	Himachal	Kumaun	Nepal	Darjiling	Bhutan	Kameng
Tethys sediment	Tethys sediment	Tethys sediment	Tethys sediment		Tethys sediment	
_____ T-HDF _____						
Nanga Parbat Gneiss	Central Gneiss	Vaikrita	Up crystalline Tibetan slab	Darjeeling	Thimpu (Chasilakha)	Sela
_____	*MC (Vakrita) T*_	*MC (Vaikrita) T* _____	*MCT* _____	*T* _____	*T* _____	*T* _____
Salkhala	Jutogh	Musiari (+Almora)	Lr crystalline Up midland	Paro	Paro	Bomdila
___ *Panjal T* ___	*Jutogh T* _____	*Munsiari T* _____	*Thrust* _____	*T* _____	*T* _____	*T* _____
Ramsu	Chail	Ramgarh (Bhatwari Unit)	Chail-2/ Lr midland	Daling	Samchi (Shumar)	Tenga
__ *Duldhar T* __	*Chail T* _____ Jaunsar *Jaunsar T*	*Ramgarh-Bhatwari T*_ Berinag *Berinag T*	*Thrust* _____ Chail-3/ Birethanti *Thrust*	*T* _____	*T* _____	*T* _____
Parautochthon	Parautochthon –autochtnon	Autochthon	Parautochthon–autochthon	Parautochthon	Parautochthon	Autochthon
__	*Tons T* _____	*Shrinagar T* _____				
	Krol	Krol		Tansen		
__ *Murree T* __	*Krol T* _____	*Krol T* _____	*K–Thrust–MBT*_	*MBT* _____	*MBT* _____	*MBT* (*Garu*) __
Muree	Dharmsala	Siwalik	Siwalik	Siwalik	Siwalik	Siwalik

that they represent exotic slabs comprising sediments that were deposited at the northern edge of continental marginal sea in an intermediate position between the Lesser Himalayan sediments and the Great Himalayan facies in the north (Upreti and Le Fort 1999). It was the MCT that brought the Great Himalayan rocks over these rocks of the root, and the two in turn were subsequently thrust over the Lesser Himalayan sediments.

In the Champawat area in eastern Kumaun, the Almora succession indicates metamorphism at temperatures 500 ± 50 °C to 600 °C and pressures 2–3 kbar and the intrusion of the Champawat Granodiorite causing thermal metamorphism which manifested itself in the formation of hornfels characterized by fibrolite and andalusite, besides garnet (Valdiya 1962; Das 1985; Joshi et al. 1994). In central Kumaun, the 2.5-km-thick mylonite zone defining the basal limit of the northern flank of the Almora Nappe in the Takula area developed at temperature 500–600 °C near the top and 400 °C near the base of the thrust zone, suggesting a thermal profile resulting from gradual cooling (Srivastava and Mitra 1994, 1996). Significantly, the middle part of the basal lithological unit (described as Saryu Formation) of the Almora Nappe somehow escaped pervasive mylonitization in the Chaunsali–Hawalbagh section near Almora, as borne out by lattice-preferred orientation of quartz axes and preservation of original lithological banding and tight isoclinal folding of quartzite, presumably related to a pre-Himalayan tectonism (Joshi and Tiwari 2004). The flattening strain in the ductile deformation, estimated from minor folds, varies from 0.12 to 0.65, and the buckle shortening of the Almora Nappe amounts to 40–90 % (Bhattacharya and Agarwal 1989).

The Kathmandu Nappe in central Nepal, made up of the low-grade Bhimphedi metamorphics, (Fig. 18.14) is separated from the Gusainkund unit of the Himadri succession of high-grade metamorphic rocks—by what has been described as an out-of-sequence thrust (Arita et al. 1983). The Kathmandu Nappe stretches southward from its root to the southern border of the Lesser Himalaya (Rai 2001) and forms practically the bulk of the Mahabharat Range, overlooking the Siwalik (Fig. 18.14b).

In southern Bhutan, the gneissic succession (Thimpu Group) was involved in repeated thrusting at several levels (Ray et al. 1989). The southern frontal segment of the folded thrust mass forms outward-jutting salients and sharp inward-pointing re-entrants, defining a multiple lobate pattern of deformation (Ray 1995) (Fig. 18.15).

The Lesser Himalayan terrane in southern Kashmir–Jammu region is a narrow schuppen zone exhibiting a duplex geometry and characterized by inclined slabs lying one upon the other (Rautela and Thakur 1992). This development took place owing to the terrane-defining thrust planes coming close together in the proximity of the Siwalik–Lesser Himalaya boundary which is the Main Boundary Thrust (Fig. 18.16).

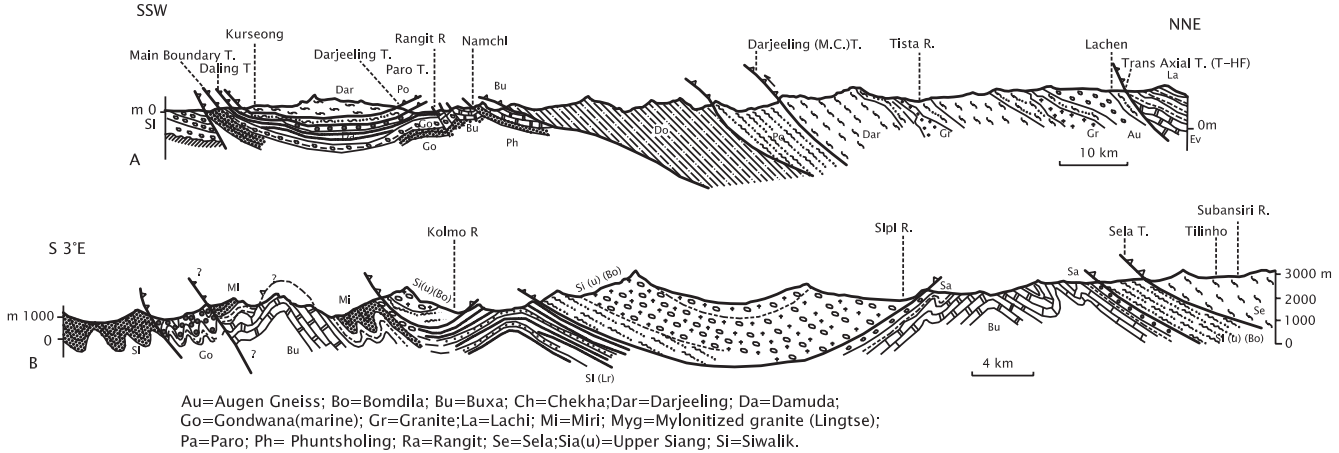

Fig. 18.15 **a** Structural architecture and lithological composition of the nappes in the Darjeeling–Sikkim Himalaya (after Acharyya 1975). **b** Section across eastern Arunachal Pradesh showing its tectonic design (after Kumar and Singh 1980)

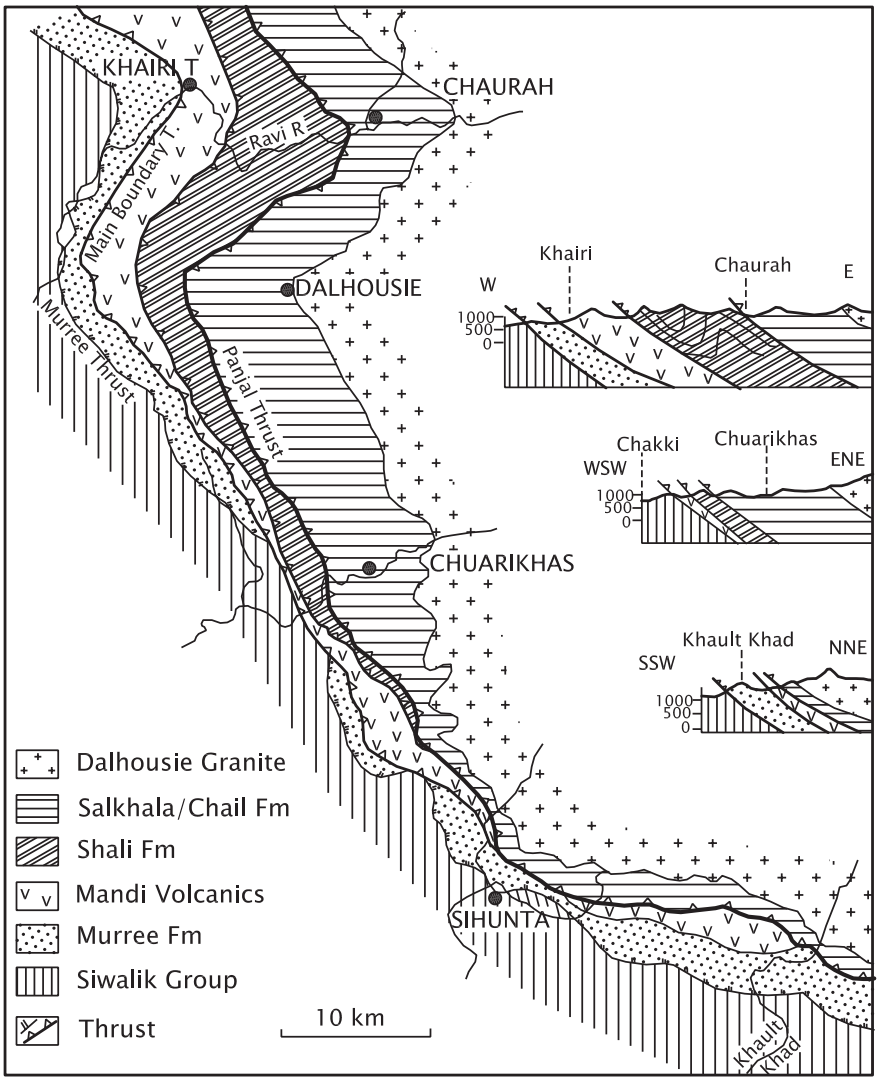

Fig. 18.16 Geological sketch map and cross section of NW Himachal Pradesh and adjoining southern Kashmir showing the duplex geometry of the terrane-defining thrust planes—Main Boundary Thrust and Panjal Thrust (after Rautela and Thakur 1992)

18.9 Evolution of Syntaxial Bends

18.9.1 Impact of Projecting Promontories

The WNW–ENE-oriented Himalaya mountain arc, with all its rock formations and structures including fold belts and thrust systems, abruptly bends southwards, making acute angles, at its two extremities (Figs. 18.17, 18.20, 17.12 and 10.5). These

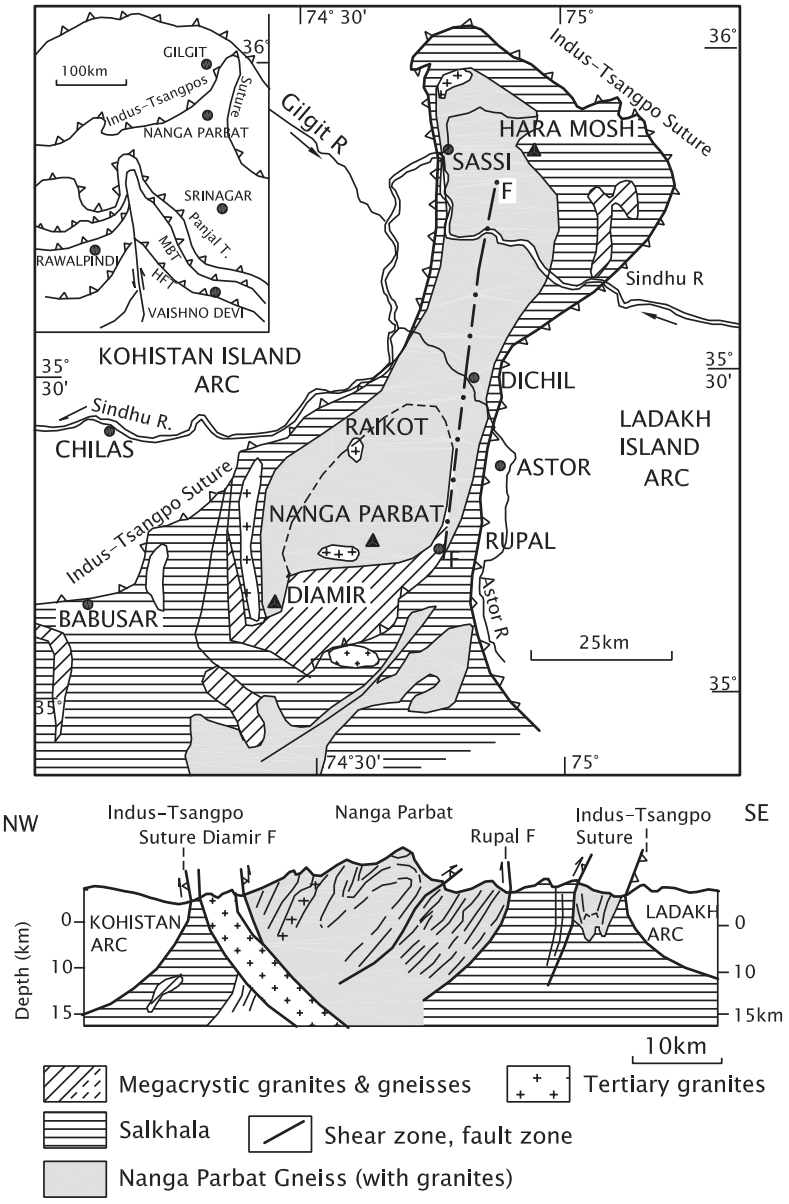

Fig. 18.17 Sketch map shows the lithological units and tectonic boundaries in the Nanga Parbat syntaxial antiform. The nearly north–south cross section elucidates the structural design of the massif (after Schneider et al. 1999a). *Inset* shows the tectonic setting of the syntaxial bends

spectacular features, resembling knee bends, are known as the *syntaxial bends*. D.N. Wadia in 1931 postulated that the north-western syntaxial bends were formed due to strong impact of the projecting promontories—points of highland jutting of the Indian Shield. The docking of India with Asia made very profound dent in the southern margin of the Asian plate, more severely on the Himalaya province that lays between the two continents. The projecting parts of the Indian Shield jut out boldly into the Himalaya province. Folds after folds developed around the projecting promontories. Continued pushing resulted in these folds breaking along strike-slip faults that subsequently merged with the N–S-trending long transcurrent *Chaman Fault* in the west and the *Sagaing Fault* in the east (Fig. 17.12). These transcurrent tear faults register considerable cumulative northward movements of the order of 300 km or more of the Indian block between them.

18.9.2 Nanga Parbat Syntaxial Bend

The *Nanga Parbat Syntaxis* is a northwardly plunging antiformal structure (Fig. 18.17), in the core of which occur Proterozoic gneisses. The gneisses give way outwardly to mylonitized and sheared rocks of marginal shear zones, thrusts, and dextral faults, particularly in the west (Coward et al. 1986, 1988; Treloar et al. 1991, 2003). The Rupal shear zone carried southwards the migmatitic gneisses of the core onto the non-migmatitic metasedimentary rocks of the Tarshing belt. This shear zone passes northwards into a steep and narrow belt elongated N–S due to constriction (Butler et al. 2000). The Nanga Parbat massif is thus a pop-up structure that provided a mechanism for crustal accommodation by upward extrusion along bounding shear zones (Winslow et al. 1996; Schneider et al. 1999b). It has also been interpreted as a feature that resulted from interference of structures of two thrust systems. First, there was clockwise rotation and then dextral marginal displacement. The structures that developed within the south-verging Pakistani thrust stack were reworked by later structures (Treloar et al. 1991). Microstructures in the N–S-trending, steeply dipping gneisses betray evidence of dextral as well as sinistral shear in discrete layers within the footwall of the Indus–Tsangpo Suture here known as Main Mantle Thrust (Argles and Edwards 2002). The rocks of the structure have since been rising rapidly, resulting in near-isothermal decompression with clockwise pressure–temperature histories towards the margin (Zeitler et al. 1995) (Fig. 18.18).

18.9.3 Hazara Syntaxis

In the *Hazara Syntaxis,* the entire succession of NW–SE-trending rock formations with intervening thrust zones bends around southwards, making an angle of 40°. The western flank of the syntaxis behaved differently. There was appreciable amount of salt—which acts as a lubricant—in the basal part of the succession in

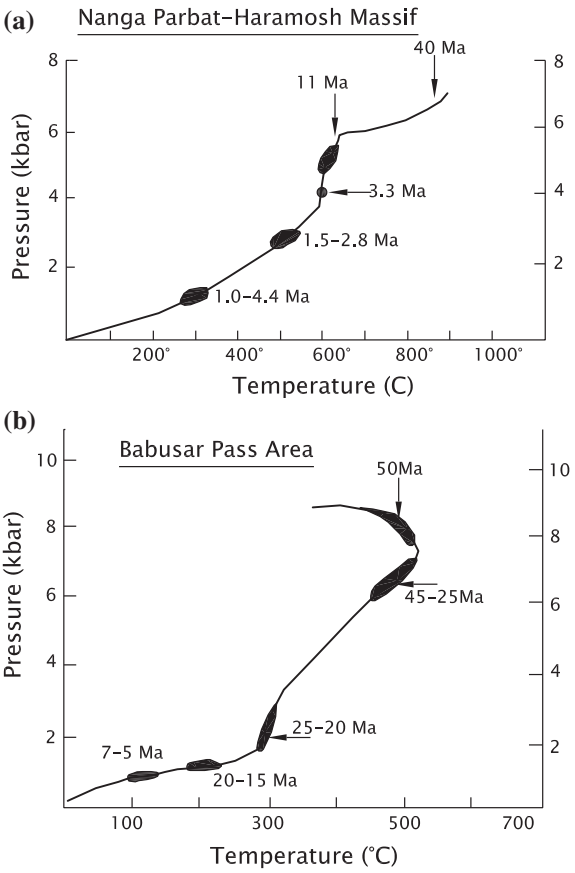

Fig. 18.18 Pressure–temperature–time histories: **a** Nanga Parbat massif; **b** footwall of the Main Mantle Thrust (Indus–Tsangpo Suture) in northern Pakistan (after Zeitler and Chamberlain 1999)

the west. Consequently, the rock masses involved slid smoothly as far south as the Salt Range and onto the Indian platform sediments without much folding and related deformation (Fig. 18.19). In contrast, the Pir Panjal flank with little salt in the succession was severely folded and split repeatedly by thrusts along the axes of folds. The syntaxis thus resulted from an early set of nappe units thrust southwards, followed by the formation of large shear zones and finally transportation of overthrust units southwards (Bossart et al. 1988). North-east of Islamabad, the sinistral strike-slip movements associated with south-eastward thrusting and folding in an essentially transpressional regime indicate two palaeostress tensor directions—a dominant NW–SE compression and a minor E–W compression compatible with buckling around the N–S axis of Hazara Syntaxis (Burg et al. 2005).

18.9.4 Siang Syntaxis

In the eastern Himalaya, the *Siang Syntaxis* (Fig. 18.20) was formed due to compressive movements on continental conjunction which led to northward displacement

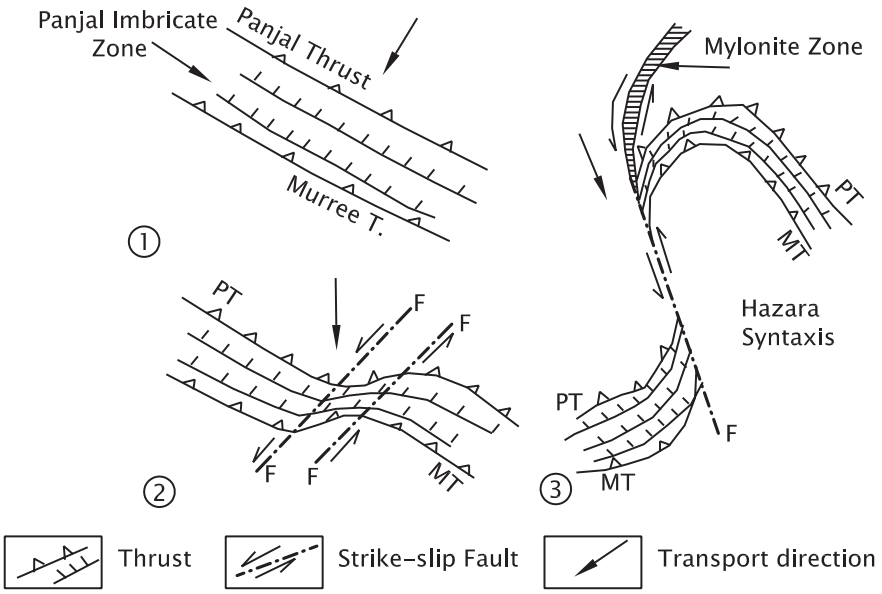

Fig. 18.19 Formation of the Hazara–Kashmir syntaxis: **a** initial overthrust geometry, **b** rotation of overthrust units and formation of shear zones and **c** further rotation of overthrust units, leading to present-day geometry of the syntaxis (after Bossart et al. 1988)

of the Arunachal block and Myanmar landmass relative to the Tibet–Shan States–Malaysia block of the Asian plate. The Patkari–Naga–Arakan Ranges link up this syntaxis with the Andaman–Nicobar Island Arc delimited by the very active subduction zone of the Indian Ocean floor. The ocean floor is descending under the Malaysian plate (Fig. 21.1).

The orogenic structures of the eastern Himalaya, along with the Indus–Tsangpo Suture Zone, are bent around Namcha Barwa (7756 m) massif and continue into Myanmar. Characterized by a youthful geomorphology, the Namcha Barwa is a large antiform, the core of which is formed of biotite gneiss and migmatite. The antiformal massif is made up of felsic gneisses with sporadic boudins of high-pressure granulites in the lower part and marble and calc silicate rocks with interlayered felsic gneisses in the upper part. Together with the Nyaingentanglha. The Namcha Barwa complex represents the basement rock which was deformed, metamorphosed and intruded by granites at the end of the Proterozoic period (Quanru et al. 2006). A few 73-million-year-old dykes and associated plutons of gabbroic to granodioritic composition intrude the gneissic migmatite. The high-grade metamorphic rocks that envelope the core were formed at the depth of 30 km, but now brought up to the surface due to uplift, which continues since about 4 Ma at a rapid rate (Burg et al. 1998). A NW–SE-trending tectonic zone—the *Tidding–Tuting Shear Zone*—characterized by isolated bodies of serpentinites and related ultrabasic rocks separates the Mishmi Hills made up of an imbricated pile of metasedimentary rocks from the complex of hornblende- and biotite-bearing granite–granodioritic belonging to the Tibetan plate (Dhaundial

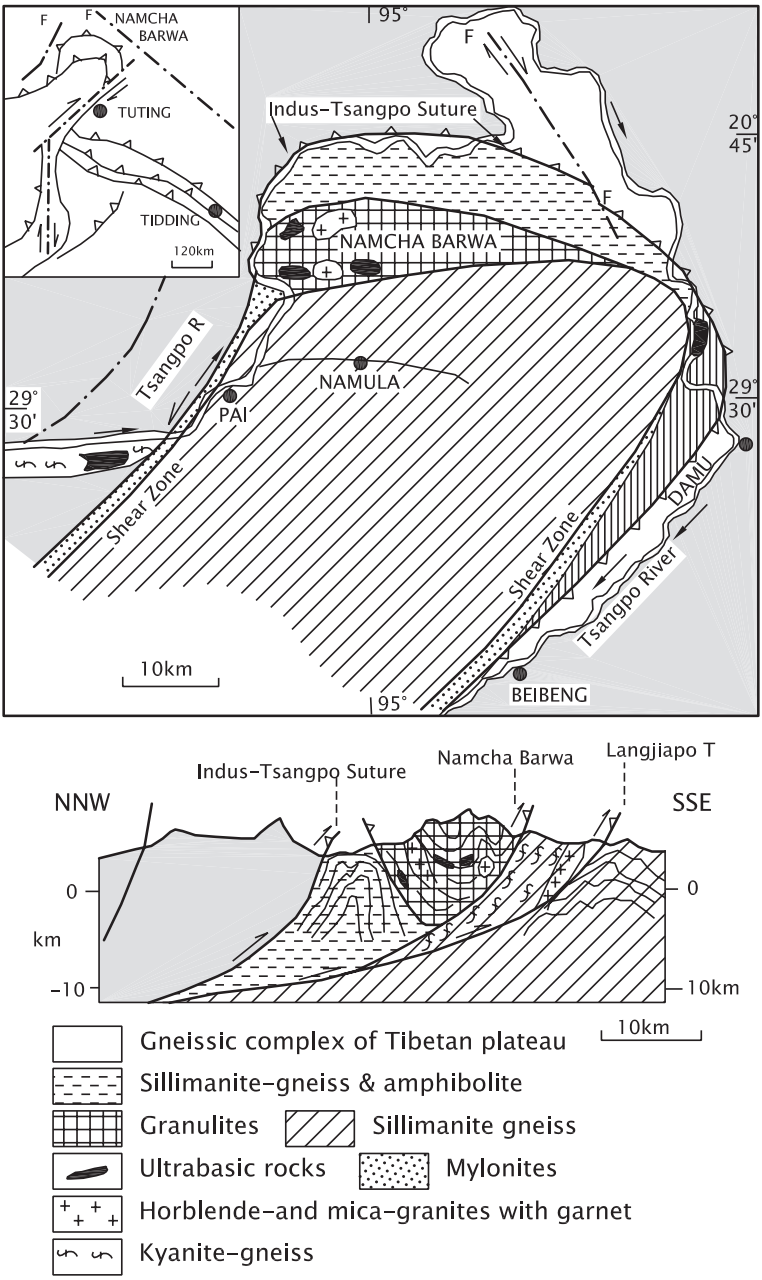

Fig. 18.20 Siang syntaxis in eastern Himalaya. The eastern Arunachal Pradesh flank is delimited by the NW–SE-trending Tidding–Tuting Shear Zone, representing the Indus–Tsangpo Suture. The cross section portrays its unique structural design (after Ding et al. 2001)

et al. 1976; Thakur and Jain 1974. The Tidding–Tuting Shear Zone is the continuation of the Indus–Tsangpo Suture zone. This zone of brittle deformation, resulting from compression by the Myanmar block, shows evidence of sinistral fault movements (Ding et al. 2001), and the massif continues to rise as evident from very fast rate of erosion (Burbank et al. 1996).

18.10 Oblique Thrust Ramps

The Himalaya province is cut by *wrench faults* trending transverse to the general trend of the Himalaya, forming NNW–SSE- and N/NNE–S/SSW-oriented conjugate fault systems (Valdiya 1976; Nandy and Dasgupta 1991). In quite many regions, the tear faults coincide with the thrust planes defining the base of nappes and klippen of crystalline rocks, as seen in Kumaun and western Nepal.

Some of these faults, coinciding with the older thrusts, have been interpreted as *oblique thrust ramps* or transverse ridges of Precambrian antiquity in which inhomogeneous strain during late-stage deformation resulted in the formation of extensional faults on hanging walls (Dubey and Bhakuni 2004). The Kaurik–Chango fault system, defining the Leopargial horst in the Himadri terrane in north-eastern Himachal Pradesh, provides an example of the oblique ramp thrusts. The N–S-oriented Thakhola Graben in the Tethyan Himalaya in north-central Nepal is possibly related to a similar oblique ramp in the basin floor (Fig. 18.21).

The *Karakoram Fault*, developed sometime after 17 Ma, accommodated the evolution of the Tibetan Plateau (especially its westward extension). It cuts the 17 Ma leucocratic granite at Tangtse. The fault registered dextral oblique thrusting, resulting in the exhumation of amphibolite facies rocks. The Karakoram Shear Zone is characterized by mylonitic rocks, the structural features of which indicate dextral movement along the shear zone. The consequence of mylonitization is the development of amphibolites facies and locally greenschist facies. In the footwall of the Karakoram Fault occurs SE plunging isoclinal to recumbent folds and north-directed thrust, the latter exhuming the anatectic rocks of the Pangong Range (McCarthy and Weinberg 2010). The latter development took place at 700–300 °C and 18–15 kbar. Towards the south-east, close to the Pangong Lake, a large fold is rotated from NE–SE trend to E–W orientation (McCarthy and Weinberg 2010). The NE–SE-trending Karakoram Fault is responsible for 50–54 km offsetting of the Indus-Tsangpo Suture Zone and the adjoining batholith, implying strike-slip movement rate of 4.5 ± 0.1 mm/year since about 12 Ma (Wang et al. 2012). There is variation of opinion on its south-eastern termination. Some workers believe that it merges with the Indus-Tsangpo Suture near Mount Kailas (Dunlop et al. 1998). Others think that it joins up with the detachment fault of the Gurla Mandhata dome (Fig. 18.10) even though there is no evidence of dextral offsetting and no linear connection of Murphy et al. 2002. The third view is that the Karakoram Fault extends beyond the Gurla Mandhata, splaying out into several branches along the Indus-Tsangpo Suture (Lacassin et al. 2004).

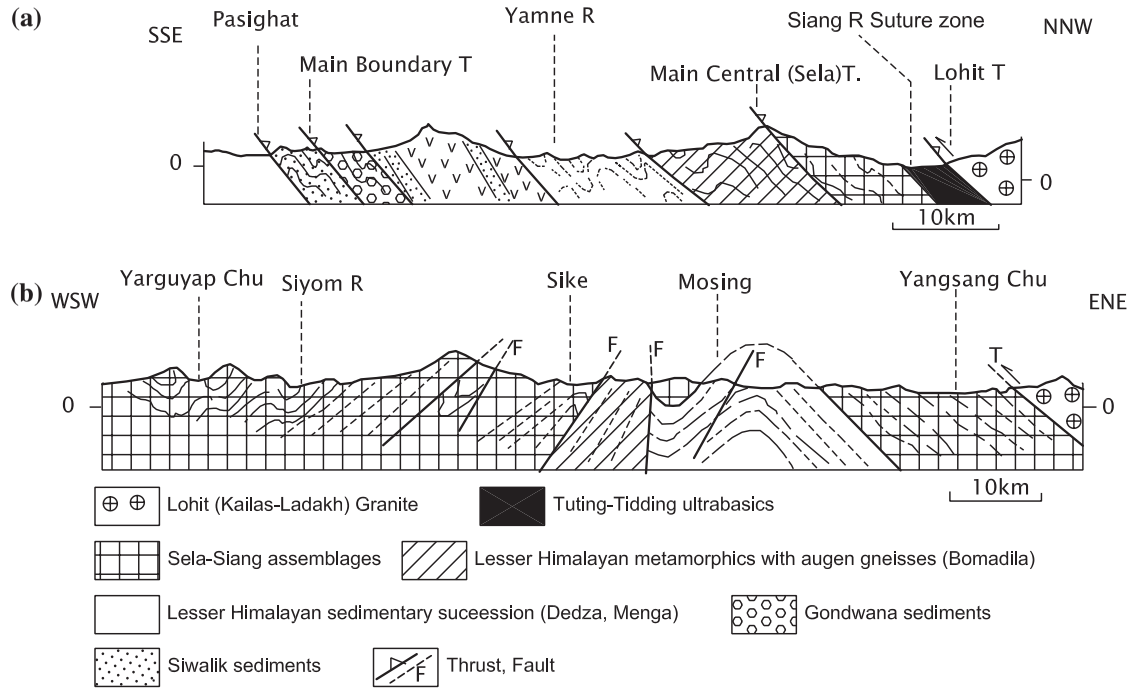

Fig. 18.21 Cross sections illustrate the structure and lithology of the Arunachal Himalaya and of the Mishmi terrane, forming the two eastern flanks of the Siang Syntaxis (after Singh and Chowdhary 1990, 1993)

References

Acharyya, S. K. (1975). Structure and stratigraphy of the Darjeeling frontal zone, Eastern Himalaya [miscellaneous publication]. *Geological Survey* of *India*, *24*(II), 71–90.

Anczkiewicz, R., Burg, J. P., Villa, I. M., & Meier, M. (2000). Late Cretaceous blueschist metamorphism in the Indus Suture Zone, Shangla region, Pakistan Himalaya. *Tectonophysics*, *324*, 111–134.

Argles, T. W., & Edward, M. A. (2002). First evidence for high-grade Himalayan-age synconvergent extension recognized within the western syntaxis—Nanga Parbat, Pakistan. *Journal of Structural Geology, 24*, 1327–1344.

Bahuguna, V. K., & Saklani, P. S. (1988). Tectonics of the Main Central Thrust in Garhwal Himalaya. *Journal of the Geological Society of London, 31*, 197–209.

Bhakuni, S. S. (1995). The structure of the Great Himalaya in Chamoli and Uttarkashi districts, Kumaun Himalaya. *Geoscience Journal, 16*, 1–7.

Bhattacharya, A. R. (1987). A "ductile thrust" in the Himalaya. *Tectonophysics, 135*, 37–45.

Bhattacharya, A. R., & Agarwal, K. K. (1989). Strain analysis and fold shape modification in crystalline complex of the Lesser Himalaya. *Krystalinikum*, *20*, 7–25.

Bist, K. S., & Sinha, A. K. (1980). Some observations on the geological and structural setup of Okhimath area in Garhwal Himalaya. *Himalayan Geology, 10*, 467–475.

Bordet, P., Colchen, M., & Le Fort, P. (1975). *Recherches Geologiques dans l'Himalaya du Nepal, Region du Nyi-Shang*. Paris: Centre National de la Recherche Scientifique. 138 p.

Bossart, P., Dietrich, D., Greco, A., Ottiger, R., & Ramsay, J. G. (1988). The tectonic structure of the Hazara-Kashmir syntaxis, southern Himalaya, Pakistan. *Tectonics, 7*, 273–297.

Brookfield, M. E., & Andrews-Speed, C. P. (1984). Sedimentology, petrography and tectonic significance of the shelf-flysch and molasse-clastic deposits across the Indus Suture Zone, Ladakh, NW India. *Sedimentary Geology, 40*, 249–286.

Brown, R. L., & Nazarchuk, J. H. (1993). Annapurna detachment fault in the Greater Himalaya of central Nepal. In P. J. Treloar & M. P. Searle (Eds.), *Himalayan tectonics* (pp. 461–473). London: Geological Society.

Burbank, D. W., Beck, R. A., & Mulder, T. (1996). The Himalayan foreland basin. In A. Yin & T. M. Harrison (Eds.), *The tectonic evolution of Asia* (pp. 149–188). Cambridge: Cambridge University Press.

Burchfiel, B. C., & Royden, L. H. (1985). North-south extension within the convergent Himalayan region. *Geology, 13*, 679–682.

Burg, J.-P., Celerier, B., Chaudhry, N. M., Ghazanfar, M., Gnehm, F., & Schnellmann, M. (2005). Fault analysis and palaeostress evolution in large strain region: Methodological and geological discussions of the southeastern Himalayan fold-and-thrust belt in Pakistan. *Journal of Earth Sciences, 24*, 445–465.

Burg, J.-P., Nievergelt, P., Oberli, F., Seward, D., Davy, P., Maurin, J.-C., et al. (1998). The Namche Barwa syntaxis: Evidence for exhumation related to compressional crustal folding. *Journal of Asian Earth Sciences, 16*, 239–252.

Butler, R. W. H., Wheeler, J., Treloar, P. J., & Jones, C. (2000). Geological structure of the southern part of the Nanga Parbat massif, Pakistan Himalaya and its tectonic implications. In M. A. Khan, P. J. Treloar, M. P. Searle, & M. Q. Jan (Eds.), *Tectonics of the Nanga Parbat Syntaxis and the Western Himalaya* (pp. 123–136). London: Geological Society.

Carosi, R., Lombardo, B., Molli, G., Musumeci, G., & Pertusati, P. C. (1998). The South Tibetan detachment system in the Rongbuk valley, Everest region: Deformation features and geological implications. *Journal of Asian Earth Sciences, 16*, 299–311.

Carosi, R., Lombardo, B., Musumeci, G., & Pertusati, P. C. (1999). Geology of the Higher Himalayan Crystallines in Khumbu Himal (Eastern Nepal). *Journal of Asian Earth Sciences, 17*, 785–803.

Catlos, E. J., Harrison, T. M., Manning, C. E., Grove, H., Rai, S. M., Hubbard, M. S., & Upreti, B. N. (2002). Records of the evolution of the Himalayan orogen from in situ Th-Pb ion microprobe dating of monazite: Eastern Nepal and western Garhwal. *Journal of Asian Earth Sciences, 20*, 459–479.

Chaudhry, M. N., & Ghazanfar, M. (1987). Geology, structure and geomorphology of upper Bhaghan valley, northwest Himalaya, Pakistan. *Geological Bulletin of the Punjab University, 22*, 13–57.

Choudhuri, B. K., Bist, K. S., & Rawat, B. S. (1992). Evidence for thrusting between the Higher Himalayan crystallines and Tethyan metasediments in Lahaul and Kullu valleys, Himachal Pradesh. *Journal of Himalayan Geology*, *3*, 191–194.

Coward, M. P., Butler, R. W. H., Khan, M. A., & Knipe, R. J. (1988). Folding and imbrication of the Indian crust during Himalayan collision. *Philosophical Transactions of the Royal Society of London, A326*, 89–114.

Coward, M. P., Windley, B. F., Broughton, R., Luff, I. W., Petterson, M. G., Pudsey, C., et al. (1986). Collision tectonics in the NW Himalaya. In M. P. Coward & A. Ries (Eds.), *Collision tectonics* (pp. 203–219). London: Geological Society.

Das, B. K. (1985). Petrology of thermally metamorphosed peltic rocks in the Champawat area, Kumaun Himalaya. *Proceedings of the Indian Academy* of *Sciences* (*Earth & Plant Sciences*), *94*, 57–70.

Dhaundial, D. P., Santra, D. K., & Dange, M. N. (1976). A new look at the stratigraphic and tectonic importance of Tidding Limestone and serpentinite in Lohit District [miscellaneous publication]. *Geological Survey* of *India*, *24*(II), 368–378.

Ding, L., Zhong, D., An, Y., Kapp, P., & Harrison, T. M. (2001). Cenozoic structural and metamorphic evolution of the eastern Himalayan syntaxis, Namche Barwa. *Earth and Planetary Science Letters, 192*, 423–438.

DiPietro, J. A. (1991). Metamorphic pressure-temperature conditions of Indian plate rocks south of the Main Mantle Thrust, Lower Swat, Pakistan. *Tectonics, 10*, 742–757.

Dixit, P. C., Kachroo, R. K., Rai, H., & Sharma, N. L. (1971). Discovery of vertebrate fossils from the Kargil basin, Ladakh J&K. *Current Science, 42*, 633–634.

Dubey, A. K., & Bhakuni, S. S. (2004). Development of extension faults in the oblique thrust ramp hanging wall: Example from the Tethys Himalaya. *Journal of Asian Earth Sciences, 23*, 427–434.

Dunlap, W. J., Weinberg, R. F., & Searle, M. P. (1998). Karakoram fault zone rocks cool in two phases. *Journal of Geological Society of London, 155*, 903–912.

England, P., & Molnar, P. (1993). Cause and effect among thrust and normal faulting anatectic melting and exhumation in the Himalaya. In P. J. Treloar & M. P. Searle (Eds.), *Himalayan Tectonics* (pp. 401–411). London: Geological Society.

Epard, J.-L., & Steck, A. (2004). The eastern prolongation of the Zanskar Shear Zone (Western Himalaya). *Eclogae Geologicae Helvetiae, 97*, 193–212.

Frank, W., Gansser, A., & Trommsdorff, V. (1977). Geological observations in the Ladakh area, a preliminary report. *Schweizerische Mineralogische und Petrographische Mitteilungen, 57*, 89–113.

Fuchs, G. R. (1986). The geology of the Markha-Nimalang area in Ladakh (India). *Jarhbuch der Geologischen Bundesanstalt, 128*, 403–437.

Gairola, V. K., & Ackermann, D. (1988). Geothermobarometry of the Central Crystallines of the Garhwal Himalaya, U.P. *Journal of the Geological Society of London, 31*, 230–242.

Gansser, A. (1964). *Geology of the Himalayas* (p. 289). London: Interscience Publishers.

Gansser, A. (1977). The great suture zone between Himalaya and Tibet: A preliminary note. *Himalaya: Science de la Terre* (pp. 181–191). Paris: CNRS.

Gansser, A. (1981). The geodynamic history of the Himalaya. In H. K. Gupta & F. M. Delany (Eds.), *Zagros–Hindukush–Himalaya: Geodynamic evolution* (pp. 111–121). Washington: American Geophysical Union.

Gapais, D., Pecher, A., Gilbert, E., & Ballevre, M. (1992). Synconvergence spreading of the Higher Himalaya Crystalline in Ladakh. *Tectonics, 11*, 1045–1056.

Gouzu, C., Itaya, T., Hyodo, H., & Ahmad, T. (2006). Cretaceous isochron ages from K-Ar and $^{40}Ar/^{39}Ar$ dating of eclogitic rocks in the Tso Morari Complex, western Himalaya, India. *Gondwana Research, 9*, 426–440.

Grasemann, B., Fritz, H., & Vannay, J. C. (1999). Quantitative kinematic flow analysis from the Main Central Thrust zone (NW Himalaya, India): Implications for a decelerating strain path and the extrusion of orogenic wedge. *The Journal of Structural Geology, 21*, 837–853.

Grujic, D., Hollister, L. S., & Parrish, R. R. (2002). Himalayan metamorphic sequence as an orogenic channel; insight from Bhutan. *Earth and Planetary Science Letters, 198*, 177–191.

Gupta, R. P., Fritz, H., & Bojar, A. V. (2006). On the nature of the South Tibetan Detachment Zone, Kumaun Himalaya. *International Journal of Remote Sensing, 27*, 455–458.

Gururajan, N. S., & Choudhuri, B. K. (1999). Ductile thrusting metamorphism and normal faulting in Dhauliganga valley, Garhwal Himalaya. *Himalayan Geology, 20*, 19–29.

Harris, N., & Massey, J. (1994). Decompression and anatexis of Himalayan metapelites. *Tectonics, 13*, 1537–1546.

Harrison, T. M., Grove, M., Lovera, O. M., & Catlos, E. J. (1998). A model for the origin of Himalayan anatacxis and inverted metamorphism. *Journal of Geophysical Research, 103*, 27017–27032.

Heim, A., & Gansser, A. (1939). Central Himalaya: Geological observations of the Swiss Expedition 1936. *Denkschriften der Schweizerischen Naturforschenden Gesellschaft, 32*, 1–245.

Herren, E. (1987). Zanskar shear zone: Northeast–southwest extension within the Higher Himalayas (Ladakh). *Geology, 15*, 409–413.

Hirn, A., Lepine, J. C., Jobert, G., Sapin, M., Wittlinger, G., Xin, X. Z., et al. (1984). Crustal structure and variability of the Himalayan border of Tibet. *Nature, 307*, 23–30.

Hodges, K. V. (2000). Tectonics of the Himalaya and southern Tibet from two perspectives. *GSA Bulletin, 112*(3), 324–350.

Hodges, K. V., Parish, R., Housh, T., Lux, D., Burchfiel, B. C., Royden, L., & Chen, Z. (1992). Simultaneous Miocene extension and shortening in the Himalayan orogen. *Science, 258*, 1466–1470.

Hodges, K. V., Parish, R. R., & Searle, M. P. (1996). Tectonic evolution of the central Annapurna range, Nepalese Himalaya. *Tectonics, 15*, 1264–1291.

Hodges, K. V., & Silverberg, D. S. (1988). Thermal evolution of the Great Himalaya, Garhwal, India. *Philosophical Transactions of the Royal Society of London, A326*, 257–280.

Honegger, K., Dietrich, V., Frank, W., Gansser, A., Thoni, M., & Trommsdroff, W. (1982). Magmatism and metamorphism in the Ladakh Himalaya (The Indus Tsangpo Suture Zone). *Earth and Planetary Science Letters, 60*, 253–292.

Hubbard, M., Royden, L., & Hodges, K. (1991). Constraints on unroofing rates in the High Himalaya, Eastern Nepal. *Tectonics*, *10*, 287–298.

Inger, S. (1998). Timing of an extensional detachment during convergence orogeny: New Rb-Sr geochronological data from the Zanskar Shear Zone, northwestern Himalaya. *Geology, 26*, 223–226.

Jain, A. K., & Manickavasagam, R. M. (1993). Inverted metamorphism in the intra-continental ductile shear zone during Himalayan collision tectonics. *Geology, 21*, 407–410.

Jain, A. K., Manickavasagam, R. M., & Singh, S. (1999). Collision tectonics in the NW Himalaya: Deformation, metamorphism, emplacement of leucogranite along Beas–Parbati Valleys, Himachal Pradesh, In A. K. Jain & R. M. Manickavasagam (Eds.), *Geodynamics of the NW Himalaya* (Vol. 6, pp. 3–37), Gondwana Research Group, Memoirs.

Jain, A. K., Singh, Sandeep, & Manickavasagam, R. M. (2003). Intercontinental shear zones in the Southern Granulite Terrain, their kinematics and evolution. *Memoir of the Geological Society of India, 50*, 225–253.

Jain, A. K., Thakur, V. C., & Tandon, S. K. (1974). Stratigraphy and structure of the Siang district, Arunachal Pradesh (NEFA). *Himalayan Geology, 4*, 28–60.

Jan, M. Q. (1985). High-P rocks along the suture zones around Indo-Pakistan plate and phase chemistry of blueschists from eastern Ladakh. *Geological Bulletin University of Peshawar, 18*, 1–40.

Jan, M. Qasim, & Seymour, R. F. (1977). Piedmontite schist from upper Swat, northwest Pakistan. *Mineralogical Magazine, 41*, 537–540.

Joshi, M., & Tiwari, A. N. (2004). Quartz C-axes and metastable phases in the metamorphic rocks of Almora Nappe: Evidence of pre-Himalayan signatures. *Current Science, 87*, 995–999.

Joshi, M., Singh, B. N., & Goel, O. P. (1994). Metamorphic conditions of the aureole rocks from Dhunaghat area, Kumaun Lesser Himalaya. *Current Science, 67*, 185–188.

Kumar, S., & Singh, T. (1980). Tectono-stratigraphic setup of the Subansiri District, Arunachal Pradesh. In K. S. Valdiya & S. B. Bhatia (Eds.), *Stratigraphy and Correlations of the Lesser Himalayan Formations* (pp. 267–282). Delhi: Hindustan Publishing Corporation.

Lacassin, R., Valli, F., Arnaud, N., et al. (2004). Large-scale geometry, offset and kinematic evolution of the Karakoram fault, Tibet. Earth and Planetary Science Letters, *219*, 255–269.

Lakhanpal, R. N., Sah, S. C. D., Sharma, K. K., & Guleria, J. S. (1983). Occurrence of *Livistona* in the Hemis conglomerate horizon of Ladakh. In V. C. Thakur & K. K. Sharma (Eds.), *Geology of Indus Suture Zone of Ladakh* (pp. 179–183). Dehradun: Wadia Institute of Himalayan Geology.

Lee, J., Hacker, B. R., Dinklage, W. S., Wang, Yu., Gani, P., Calvert, A., et al. (2000). Evolution of the Kangmar dome, southern Tibet: Structural, petrologic and thermochronologic constraints. *Tectonics, 19*, 872–895.

Lefort, P. (1988). Granites in the tectonic evolution of the Himalaya—a model for its genesis and emplacement. *American Journal of Geophysical Research, 86*, 10545–10568.

Macfarlane, A. M. (1993). Chronology of tectonic events in the crystalline core of the Himalaya, Langtang National Park, central Nepal. *Tectonics, 12*, 1004–1025.

Makovsky, Y., et al. (1996). Structural elements of the southern Tethys Himalayan crust from wide-angle seismic data. *Tectonics*, *15*, 997–1005.

Manickavasagam, R. M., Jain, A. K., Singh, S., & Asokan, A. (1999). Metamorphic evolution of the northwest Himalaya, India: Pressure-temperature data, inverted metamorphism and exhumation in the Kashmir, Himachal and Garhwal Himalaya [special paper]. *Geological Society of America, 328*, 179–197.

Mathur, N. S. (1983). The Indus Formation of the Ladakh Himalaya: Its biozonation, correlation and faunal provincialism. In V. C. Thakur & K. K. Sharma (Eds.), *Geology of the Indus Suture Zone in Ladakh* (pp. 127–144). Dehradun: Wadia Institute.

McCarthy, M. R., & Weinberg, R. F. (2010). Structural complexity resulting from pervasive ductile deformation in Karakoram Shear Zone, Ladakh, NW India. *Tectonics*, *29*, TC 3004. doi: 10.1029/2008.TC002354.

Meier, K., & Hiltner, E. (1993). Deformation and metamorphism within the Main Central Thrust zone, Arun tectonic window, eastern Nepal. In P. J. Treloar & M. P. Searle (Eds.), *Himalayan Tectonics* (pp. 511–523). London: Geological Society.

Mohan, A., Windley, B. F., & Searle, M. P. (1989). Geothermobarometry and development of inverted metamorphism in the Darjeeling-Sikkim region of the eastern Himalaya. *Journal of Metamorphic Geology, 7*, 95–110.

Molnar, P., & Grey, D. (1979). Subduction of continental lithosphere: Some constraints and uncertainties. *Geology, 7*, 58–62.

Murphy, M. A., & Copeland, P. (2005). Translational deformation in the central Himalaya and its role in accommodating growth of the Himalayan orogen. *Tectonics*, *24*, TC 4012, 1–19.

Murphy, M. A., Yin, A., Kapp, P., Harrison, T. M., Manning, C. E., Ryerson, F. J., et al. (2002). Structural evolution of the Gurla Mandhata detachment system, southwest Tibet: Implications for the eastward extention of the Karakoram Fault system. *Bulletin of the Geological Society of America, 114*, 428–447.

Nanda, A. C., & Sahni, A. (1990). Oligocene vertebrates from the Ladakh molasses group, Ladakh Himalaya: Palaeogeographic implications. *Journal of Himalayan Geology*, *1*, 1–10.

Nandy, D. R., & Dasgupta, S. (1991). Tectonic patterns in northeast India. In K. K. Sharma (Ed.), *Geological and geodynamic evolution of collision zone* (pp. 371–384). Oxford: Pergamon.

Paudel, L. P., & Arita, K. (2000). Tectonic and polymetamorphic history of Lesser Himalaya in central Nepal. *Journal of Asian Earth Sciences, 18*, 561–584.

Pearson, O. N., & DeCelles, P. G. (2005). Structural geology and regional tectonic significance of the Ramgarh Thrust, Himalayan fold-thrust belt of Nepal. *Tectonics*, *24*, TC 4008, 1–26.

Pecher, A. (1977). Geology of the Nepal Himalaya: Deformation and petrography of the MCT zone. In *Himalaya Science de Terre* (Vol. 268, pp. 301–318). Paris: CNRS.

Pecher, A. (1989). The metamorphism in the central Himalaya. *Journal of Metamorphic Geology, 7*, 31–41.

Pecher, A. (1991). The contact between the Higher Himalaya Crystallines and the Tibetan sedimentary series: Miocene large-scale dextral shearing. *Tectonics, 10*, 587–598.

Pognante, U., & Benna, P. (1993). Metamorphic zonation, migmatization and leucogranites along the Everetst transect of Eastern Nepal and Tibet: Record of an exhumation history. In P. J. Treloar & M. P. Searle (Eds.), *Himalayan tectonics* (pp. 323–340). London: Geological Society.

Prasad, G. V. R., Bajpai, S., Singh, S., & Parmar, V. (2005). First cricetid rodent (Mammalia) from the Ladakh mollasse, NW Himalaya, India: Age implications. *Himalayan Geology, 26*, 85–92.

Qayyum, M., Lawrence, R. D., & Niem, A. R. (1997). Molasse-delta flysch continuum of the Himalayan orogeny and closure of the Palaeogene Kataway remnant ocean, Pakistan. *International Geology Review, 39*, 861–875.

Quanru, G., Guitang, P., Zheng, L., Chen, Z., Fisher, R. D., Sun, Z., et al. (2006). The Eastern Himalayan Syntaxis: Major tectonic domains, ophiolitic melanges and geological evolution. *Journal of Asian Earth Sciences, 27*, 265–285.

Rai, S. M. (2001). Geology, geochemistry and radio-chronology of the Kathmandu and Gosainkund Crystalline nappes, central Nepal Himalaya. *Journal of the Nepal Geological Society, 25*, 135–155.

Rautela, P., & Thakur, V. C. (1992). Structural analysis of the Panjal Thrust zone Himachal Himalaya. Journal of Himalayan Geology, *3*, 195–207.

Ray, S. (1947). Zonal metamorphism in the Eastern Himalaya and some aspects of local geology. *Quarterly Journal Geological, Mining and Metallurgical Society (India), 19*, 117–140.

Ray, S. K. (1995). Lateral variation in geometry of thrust planes and its significance as studied in the Shumar allochthon, Lesser Himalayas, eastern Bhutan. *Tectonophysics, 249*, 125–139.

Ray, S. K., Bandyopadhyay, B. K., & Razdan, R. K. (1989). Tectonics of a part of the Shumar allochthon in eastern Bhutan. *Tectonophysics, 169*, 51–58.

Robinson, D. M., DeCelles, P. G., Patchet, P. J., & Garzione, C. N. (2001). The kinematic evolution of the Nepalese Himalaya interpreted from Nd isotopes. *Earth and Planetary Science Letters, 192*, 507–521.

Robyr, M., Vannay, J.-C., Epard, J.-L., & Steck, A. (2002). Thrusting, extension and doming during the polyphase tectonometamorphic evolution of the High Himalayan Crystalline Zone in NW India. *Journal of Asian Earth Sciences, 21*, 221–239.

Royden, L. H., & Burchfiel, B. C. (1987). Thin-skinned N–S extension within the convergent Himalayan region: Gravitational collapse of a Miocene topographic front. In M. P. Coward et al. (Ed.), *Continental extensional tectonics* (pp. 611–612). Washington: Geological Society of America.

Sachan, H. K., Bodnar, R., Islam, R., Szabo, C. S., & Law, R. D. (1999). Exhumation history of Eclogites from the Tso-Morari crystalline complex in Eastern Ladakh: Mineralogical and fluid inclusion constraints. *Journal of the Geological Society of London, 53*, 181–190.

Saklani, P. S. (1972). Metamorphic petrology of the area south of Mukhem, Garhwal Himalaya. In *Recent researches in geology* (pp. 82–106). India: Hindustan Publishing Corporation.

Saklani, P. S. (1972b). Lithostratigraphy and structure of the area between the Bhagirathi and Bhilangana rivers, Garhwal Himalaya. *Himalayan Geology, 2*, 342–355.

Saklani, P. S. (Ed.). (1983). *Himalayan Shears* (p. 113p). New Delhi: Himalayan Books.

Saklani, P. S. (1993). *Geology of the Lower Himalaya (Garhwal)* (p. 246p). Delhi: International Books.

Saklani, P. S., Nainwal, D. C., & Singh, V. K. (1991). Geometry of composite Main Central Thrust in the Yamuna valley, Garhwal. *Neues Jahrbuch fur Geologie und Palaontologie Monatshefte, 6*, 364–380.

Scaillet, B., France-Lanord, C., & LeFort, P. (1990). Badrinath-Gangotri plutons (Garhwal, India): Petrological and geochemical evidence of fractionation processes in a High Himalayan leucogranite. *Journal of Volcanology and Geothermal Research, 44*, 163–188.

Scaillet, B., Pecher, A., Rochette, P., & Champenois, M. (1995). The Gangotri Granite (Garhwal Himalaya): Laccolithic emplacement in an extending collisional belt. *Journal of Geophysical Research, 100*, 585–607.

Schelling, D. (1992). The tectonostratigraphy and structure of the Eastern Nepal Himalaya. *Tectonics, 11*, 925–943.

Schelling, D., & Arita, D. (1991). Thrust tectonics, crustal shortening and the structure of the far-eastern Nepal Himalaya. *Tectonics*, *10*, 851–862.

Schlup, M., Carter, A., Cosca, M., & Stech, A. (2003). Exhumation history of eastern Ladakh revealed by 40Ar/39Ar and fission-track ages: The Indus River-Tso Morari transect, NW Himalaya. *Journal of the Geological Society of London, 160*, 385–399.

Schneider, D. A., Edwards, M. A., Kidd, W. S. F., Asif Khan, M., Seeber, L., & Zeitler, P. K. (1999a). Tectonics of Nanga Parbat, Western Himalaya: Synkinematic plutonism within the doubly vergent shear zones of a crustal-scale pop-up structure. *Geology, 27*, 999–1002.

Schneider, D. A., Edwards, M. A., Kidd, W. S. F., Zeitler, P. K., & Coath, C. D. (1999b). Early Miocene anatexis identified in the western syntaxis, Pakistan. *Earth and Planetary Science Letters, 167*, 121–129.

Searle, M. P. (1999). Extensional and compressional faults in the Everest-Lhotse massif, Khumbu Himalaya, Nepal. *Journal of the Geological Society of London*, *156*, 227–240.

Searle, M. P., Metcalfe, R. P., Rex, A. J., & Norry, M. J. (1993). Field relations, petrogenesis and emplacement of the Bhagirathi leucogranite, Garhwal Himalaya. In P. J. Treloar & M. P. Searle (Eds.), *Himalayan tectonics* (pp. 429–444). London: Geological Society.

Searle, M. P., Parrish, R. R., Hodges, K. V., Hurford, H., Ayres, M. W., & Whitehouse, M. J. (1997). Shisha Pagma (8027 m) leucogranite, South Tibetan Himalaya: Field relations, geochemistry, age, origin and emplacement. *Journal of Geology, 105*, 295–317.

Searle, M. P., Simpson, R. L., Law, R. D., Parrish, R. P., & Waters, D. J. (2003). The structural geometry, metamorphic and magmatic evolution of the Everest massif, High Himalaya of Nepal–South Tibet. *Journal of the Geological Society of London*, *160*, 345–366.

Searle, M. P., Waters, D. J., Rex, D. C., & Wilson, R. N. (1992). Pressure, temperature and time constraints on Himalayan metamorphism from eastern Kashmir and western Zanskar. *Journal of the Geological Society of London, 149*, 753–775.

Shams, F. A. (1980a). Origin of the Shangla blue schist, Swat Himalaya, Pakistan. *Geological Bulletin of University of Peshawar, 13*, 67–70.

Shams, F. A. (1980b). An anatectic liquid of granitic composition from the Hazara Himalaya, Pakistan, its petrogenetic importance. *Atti della Accademia Nazionale dei Lincei, Classe di Scienze Fisiche, Matematiche e Naturali, Rendiconti, 68*, 207–215.

Sharma, B. K., & Bhola, A. M. (2004). Kink bands in the Chamba region, Himalaya, India. *Journal of Asian Earth Sciences*, 1–16.

Sharma, K. K., & Kumar, S. (1978). Contributions to the geology of Ladakh, northwestern Himalaya. *Himalayan Geology, 8*, 252–287.

Singh, S. (1993a). Geology and tectonics of the eastern Syntaxis, Arunachal Pradesh. *Journal of Himalayan Geology, 4*, 149–164.

Singh, K. (1993b). Reverse and oblique-slip movement along the Chamba Thrust, NW Himalaya: Implications for tectonic evolution. *Journal of Himalayan Geology, 4*, 143–148.

Singh, K. (2010). Tectonic evolution of Kishtwar Window with respect to the Main Central Thrust, northwest Himalaya, India. *Journal of Asian Earth Sciences, 39*, 125–135.

Singh, S., & Chowdhary, P. K. (1990). An outline of the geological framework of the Arunachal Pradesh. *Journal of Himalayan Geology*, *1*, 189–197.

Sinha-Roy, S. (1982). Himalayan Main Central Thrust and its impliciations for Himalayan inverted metamorphism. *Tectonophysics, 84*, 197–224.

Sorkhabi, R. B., & Arita, K. (1997). Towards a solution for the Himlayan puzzle: Mechanism of inverted metamorphism constrained by the Siwalik sedimentary record. *Current Science, 72*, 862–867.

Srivastava, P., & Mitra, G. (1994). Thrust geometries and deep structure of the Outer and Lesser Himalaya, Kumaun and Garhwal (India): Implications for evolution of the Himalayan fold and thrust belts. *Tectonics, 13*, 89–109.

Srivastava, P., & Mitra, G. (1996) Deformation mechanisms and inverted thermal profile in the North Amora Thrust mylonite zone, Kumaun Lesser Himalaya, India. *Journal* of *Structural Geology*, *18*, 27–39.

Steck, A., Epard, J.-L., & Robyr, M. (1999). The NE-directed Shikar Beh nappe: A major structure of the Higher Himalaya. *Eclogae Geologicae Helvetiae, 92*, 239–250.

Stephenson, B. J., Searle, M. P., Waters, D. J., & Rex, D. C. (2001). Structure of the Main Central Thrust zone and extrusion of the High Himalayan deep crustal wedge, Kishtwar-Zanskar Himalaya. *Journal of the Geological Society of London, 158*, 637–652.

Stuwe, K., & Foster, D. (2001). $^{40}Ar/^{39}Ar$, pressure temperature and fission track constraints on the age and nature of metamorphism around the Main Central Thrust in the eastern Bhutan Himalaya. *Journal of Asian Earth Sciences, 19*, 85–95.

Tahirkheli, R. A. K. (1982). Geology of the Himalaya, Karakoram and Hindukush in Pakistan. *Geological Bulletin of the Peshawar University, 15*, 1–51.

Tahirkheli, R. A. K., Mattauer, M., Proust, F., & Tapponier, P. (1979). The India-Eurasia Suture Zone in northern Pakistan: synthesis and interpretation of recent data at plate scale. In A. Farah & K. A. Dejong (Eds.), *Geodynamics of Pakistan* (pp. 125–130). Quetta: Geological Survey of Pakistan.

Takagi, H., Arita, K., Sawaguchi, T., Kobayashi, K., & Awaji, D. (2003). Kinematic history of the Main Central Thrust zone in the Langtang area, Nepal. *Tectonophysics, 366*, 151–163.

Tewari, A. P. (1964). *On the Upper Tertiary deposits of Ladakh Himalaya and correlation of various geotectonic units of Ladakh with those of Kumaun-Tibet region, Report 22nd International Geological Congress* (Vol. 11, pp. 37–58). Kolkata: Geological Survey of India.

Thakur, V. C. (1993). *Geology of Western Himalaya* (366p). Oxford: Pergamon Press.

Thakur, V. C. (1998). Structure of the Chamba nappe and position of the Main Central Thrust in Kashmir Himalaya. *Journal of Asian Earth Sciences, 16*, 269–282.

Thakur, V. C., & Jain, A. K. (1974). Tectonics of the region of Eastern Himalaya Syntaxis. *Current Science, 43*, 783–785.

Tiwari, B. N. (2005). Tertiary vertebrates from the Himalayan foreland of India: An explanation of Late Eocene-Oligocene faunal gap [special publication]. *Paleontological Society of Korea, 2*, 141–153.

Treloar, P. J., O'Brien, P. J., Parrish, R. R., & Khan, M. A. (2003). Exhumation of early Tertiary coesite-bearing eclogites from the Pakistan Himalaya. *Journal of the Geological Society of London, 160*, 367–376.

Treloar, P. J., Potts, G. J., Wheeler, J., & Rex, D. C. (1991). Structural evolution and asymmetric uplift of the Nanga Parbat syntaxis, Pakistan Himalaya. *Geologische Rundschau, 80*, 411–428.

Trivedi, J. R. (1990). Geochronological studies of Himalayan Granites (Unpublished Ph.D. Thesis). Physical Research Laboratory, Ahmadabad, 170p.

Upreti, B. N., & Le Fort, P. (1999). Lesser Himalayan crystalline nappes of Nepal: Problems of their origin [special papers]. *Geological Society of America*, *328*, 225–238.

Valdiya, K. S. (1962). A study of the Champawat Granodiorite and associated metamorphics of the Lohaghat subdivision, district Almora, U.P., with special reference to petrography and petrogenesis. *Indian Mineralogist, 3*, 6–37.

Valdiya, K. S. (1976). Himalayan transverse faults and folds and their parallelism with subsurface structures of North Indian plains. *Tectonophysics, 32*, 353–386.

Valdiya, K. S. (1978). Extension and analogues of the Chail Nappe in the Kumaun Himalaya. *Indian Journal of Earth Sciences, 5*, 1–19.

Valdiya, K. S. (1980a). The two intracrustal boundary thrusts of the Himalaya. *Tectonophysics, 66*, 323–348.

Valdiya, K. S. (1980b). *Geology of Kumaun Lesser Himalaya* (p. 291p). Dehradun: Wadia Institute of Himalayan Geology.

Valdiya, K. S. (1981). Tectonics of central sector of the Himalaya. In H. K. Gupta & F. M. Delancy (Eds.), *Geodynamics Series: Vol. 3. Zagor–Hindukush Himalaya, geodynamic evolution* (pp. 87–110). Washington D.C.: American Geophysical Union.

Valdiya, K. S. (1987). Trans-Himadri fault and domal upwarps immediately south of the collision zone: Tectonic implications. *Currrent Science, 56*, 200–209.

Valdiya, K. S. (1988). Tectonic evolution of the central sector of Himalaya. *Philosophical Transactions of the Royal Society of London, A326*, 151–175.

Valdiya, K. S. (1998). *Dynamic Himalaya* (p. 178p). Hyderabad: Universities Press.

Valdiya, K. S. (1999). Rising Himalaya: Advent and intensification of monsoon. *Current Science, 76*, 514–524.

Valdiya, K. S. (2001). Reactivation of terrane-defining boundary thrusts in central sector of the Himalaya: Implications. *Current Science, 81*, 1418–1431.

Valdiya, K. S. (2005). Trans-Himadri Fault: Tectonics of a detachment system in central sector of Himalaya, India. *Journal of the Geological Society of London, 65*, 537–552.

Valdiya, K. S., & Goel, O. P. (1983). Lithological subdivision and petrology of the Great Himalayan Vaikrita Group in Kumaun. *Proceedings of the Indian Academy* of *Sciences* (*Earth & Plant Sciences*), *92*, 141–163.

Vance, D., & Harris, N. (1999). Timing of prograde metamorphism in the Zanskar Himalaya. *Geology, 27*, 395–398.

Vannay, J.-C., & Hodges, K. V. (1996). Tectonometamorphic evolution of the Himalayan metamorphic core between the Annapurna and Dhaulagiri, central Nepal. *Journal of Metamorphic Geology, 14*, 635–656.

Vannay, J.-C., & Steck, A. (1995). Tectonic evolution of the High Himalaya in Upper Lahaul (NW Himalaya, India). *Tectonics, 14*, 253–263.

Virdi, N. S., Thakur, V. C., & Kumar, S. (1977). Blue-schist facies metamorphism in the Indus Suture Zone of Ladakh and its significance. *Himalayan Geology, 7*, 479–487.

Wang, Y., & Zheng, X. (1975). Imbricate structure in the northern slope of Jomolungma and discussion on the uplift of the Himalaya. *Scientific Exploration on Jomolungma* (pp. 199–221). Beijing: Science Publication House.

Winslow, D. M., Zeitler, P. K., Chamberlain, C. P., & Williams, I. S. (1996). Geochronological constraints on syntaxial development in the Nanga Parbat region, Pakistan. *Tectonics, 15*, 1292–1308.

Wu, C., Nelson, K. D., Wortman, G., Sampson, S. D., Yue, Y., Li, J., et al. (1998). Yadong cross structure on South Tibetan Detachment in the east central Himalaya. *Tectonics, 17*, 28–45.

Wyss, M., Hermann, J., & Steck, A. (1999). Structural and metamorphic evolution of the northern Himachal Himalaya, NW India. *Eclogae Geologicae Helvetiae, 92*, 3–44.

Wang, S., Wang, C., Phillips, R. J., Murphy, M. A., Fang, X., & Yue, Y. (2012). Displacement along the Karakoram Fault, NW Himalaya estimated from LA -ICP-MS U-Pb dating of offset geological markers. *Earth and Planetary Science Letters*, *337–338*, 156–163.

Zeitler, P. K., & Chamberlain, C. P. (1999). Petrogenetic and tectonic significance of young leucogranites from the northwestern Himalaya, Pakistan. *Tectonics, 10*, 729–741.

Zeitler, P. K., Chamberlain, C. P., & Smith, H. (1995). Synchronous anatexis, metamorphism and rapid denudation at Nanga Parbat (Pakistan). *Geology, 21*, 247–250.

Chapter 19
Himalayan Foreland Basin

19.1 Origin and Development

Following crustal thickening in the Lesser Himalaya subprovince, particularly along its southern margin due to bending down of the crust, a flexural depression developed immediately south of the emerging young mountain. This was a consequence of tectonic loading. It was a basin that deepened away from the Indian Shield (Fig. 19.1). The formation of this peripheral basin was almost synchronous with the development in the north of the Sindhu Basin due to sagging of the zone of India–Asia collision, dealt with in Chap. 18. The depression was soon invaded by the oceanic water, giving rise to what has been described as the Sirmaur Basin (Valdiya 1998), named after the district in south-eastern Himachal Pradesh. Eroded material from the nascent, growing orogen filled the basin progressively even as its floor sank due to growing load of the accumulated detritus. The development of the *Sirmaur Foreland Basin* had commenced in the Early Palaeocene time, as testified by, among other things, the Ranikot Formation in Sindh (Pakistan), the Kakara Formation in Himachal Pradesh and the Amile Formation in Nepal.

The shallow Sirmaur Basin stretched from the Ranikot–Laki Belt in Sindh in the west to Meghalaya and beyond. In the east, it was linked with the Bay of Bengal through the Bengal Basin. In the west, the *Himalayan Foreland Basin* (HFB) was connected with the Arabian Sea through western Rajasthan and Kachchh (Fig. 19.2a). The HFB covered Jaisalmer–Palana–Barmer Belt in western Rajasthan; the Salt Range–Hazara region in central, western and northern Pakistan; the Kakara–Subathu Belt in Himachal Pradesh; the Phart–Singtali–Satpuli area in Garhwal; the Amile–Bhainskati–Dumri sector in Nepal, the Yinkiong–Dalbuing area in eastern Arunachal Pradesh; the Kopili area in Assam; and the Jaintia Hills in Meghalaya and the Indo-Myanmar Border Ranges

K.S. Valdiya, *The Making of India*, Society of Earth Scientists Series,
DOI 10.1007/978-3-319-25029-8_19

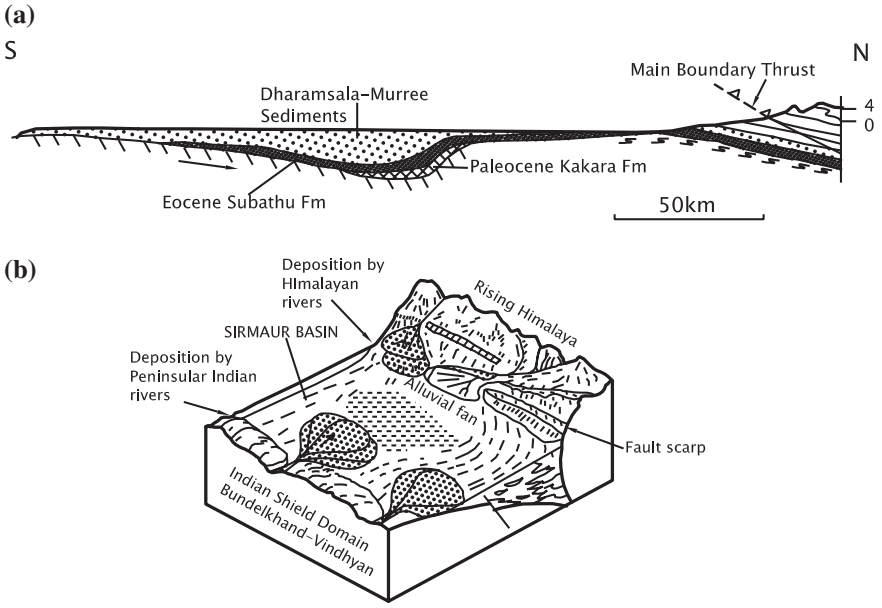

Fig. 19.1 **a** Foreland basin formed due to sagging of the Indian crust immediately south of the margin of the Himalaya province. It was a wedge-shaped depression that deepened towards the mountain. **b** The block diagram shows rivers building fans of sediments (deltas) at their mouths (Valdiya 1998)

(Fig. 19.2b). Although the foreland succession has a widespread distribution, its basal part is exposed in limited areas such as Ranikot and Rakhashani in Balochistan, Kalakot in Jammu, Kakara in Himachal and Theria in Meghalaya.

19.2 Paleogene Sedimentation and Stratigraphy

19.2.1 North-western and Western Himalaya

The *Sirmaur Basin* became the site of marine sedimentation. It was quite shallow, and its shores were agitated by waves and currents as borne out by oolites and pisolites and certain sedimentary structures in the basal horizons. In warmer waters flourished a variety of algae, bryozoans and foraminifers, besides dense populations of gastropods, lamellibranchs and echinoids.

South-west of Shimla in the Gambhar Valley (Himachal Pradesh), the Early Palaeocene succession (Fig. 19.3; Table 19.1) made up of pisolitic bauxite at the base and green brown, purple and yellow shales with carbonaceous–phosphatic nodules and characterized by foraminifers *Ranikothalia, Globigerina* and *Lockhartia conditi* is known as the *Kakara Formation* (Srikantiah and Bhargava

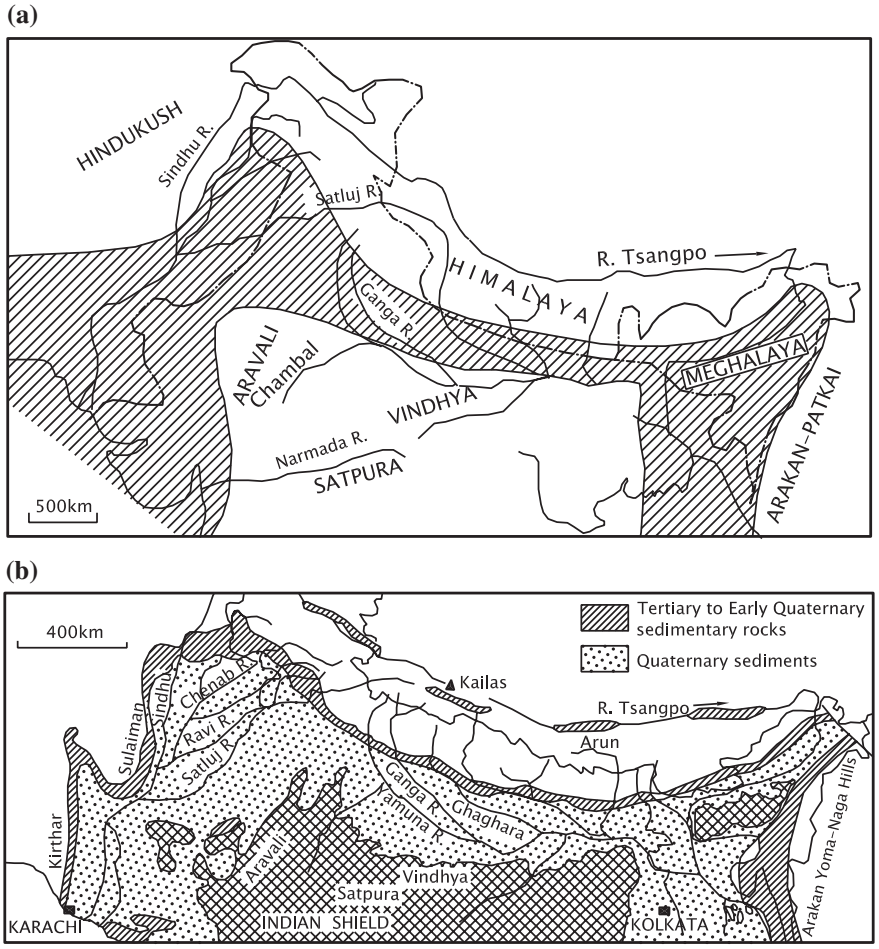

Fig. 19.2 **a** Extent of the original Himalayan Foreland Basin encompassing both Sirmaur and Siwalik basins (after Valdiya 2002). **b** Exposed Tertiary and Early Quaternary sedimentary rocks of the Himalayan Foreland Basin (after Brookfield 1993)

1967; Juyal and Mathur 1990). In the Ganga Valley in Garhwal, the Kakara has been described as the Singtali and the Bansi (Valdiya 1980). The Kakara is succeeded by the *Subathu Formation*, named after a town Sapatu, south-west of Shimla. The *Subathu Formation* was given its name by H.B. Medlicott in 1865. It represents a lagoonal deposit comprising carbonaceous shale, intercalated with oyster-bearing limestone and yellow marl with purple shale. The limestone contains lamellibranchs and foraminifers of Late Thanetian (Upper Palaeocene) to Middle Lutetian (Lower Eocene) (Bhatia and Mathur 1965; Bhatia 1982, 2000, 2003; Bhatia and Bhargava 2006). In a locality, rich remains of rodents have been found (Kumar et al. 1997a, b). At Jumma, near Parwanu in the Solan area

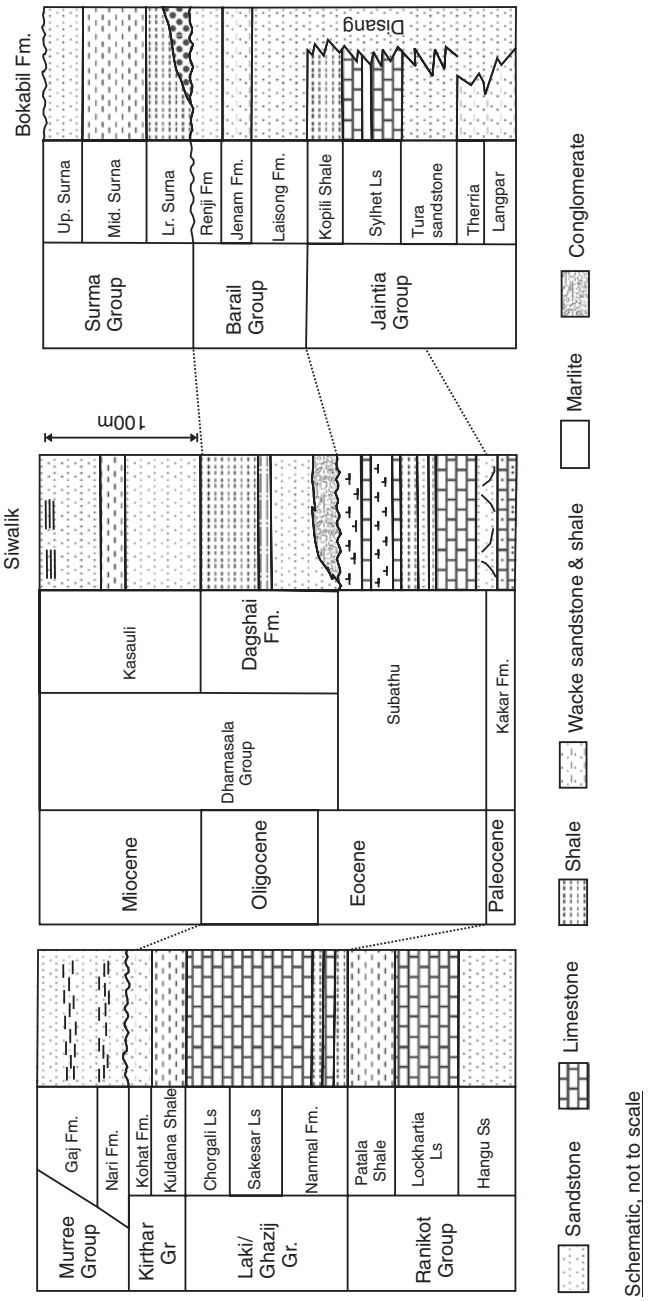

Fig. 19.3 Columns showing the lithologies of the Paleogene Formations in the respective type areas and their correlation (compiled from various sources)

Epoch/Age	Sindh–Salt Range	Potwar–Jammu	Himachal–Kumaun	Nepal	Arunachal Pradesh	Assam	Indo-Myanmar Border Range
—— 16.2 m.y. ——							Bokabil
Early Miocene	Gaj	Murree	Kasauli	Dumri		Surma	Bhuban
—— 23 m.y.——							
	Nari		Dagshai				Renji
Oligocene							Jenam
—— 30.5 m.y. ——	----------		*Unconformity*	----------		Barail	
Later Eocene	Kirthar	Chharat Ls.	Subathu	Bhainskati	Yinkiong		Laisong
Middle Eocene	Laki Ghazij						Kopili
Early Eo cene							
—— 53 m.y. ——		Hill Limestone.	----------	*Unconformity*	----------	Jaintia/ Disang	Sylhet
Paleocene							Lakadong (Langpar) Therria
—— 65 m.y. ——	Ranikot		Kakara-Bansi	Amile			

Table 19.1 Correlation of the Palaeogene–Neogene formations of the Sirmaur Basin (after Valdiya 1998)

(Himachal Pradesh), the Late Palaeocene to Middle Eocene Subathu Formation includes a clastic limestone characterized by sole marks, intraformational conglomerate and cross-laminations—all indicating effect of storm activity (Singh and Srivastava 2011). Sedimentological and palaeontological studies have established its precise stratigraphic position (Saluja et al. 1969; Raiverman and Raman 1971; Raiverman 1979; Mathur 1969; Juyal and Mathur 1992). In the Tons Valley, it was subjected to low-grade metamorphism which occurred at temperatures below 200 °C under very low pressure (Johanson and Oliver 1990).

In the Kalakot area in Jammu, the Kakara is represented by 4–5 m of breccia below a 6–10-cm-thick horizon of reworked bauxite. And at Salal, an angular unconformity defines its base against the Proterozoic Jammu Limestone. The succession of the Kalakot–Salal Belt indicates deposition of the Palaeocene sediments in a fault-formed depression adjacent to a forebulge in the Peninsular shield (Singh and Andotra 2000; Singh 2003). The presence of *Ranikothalia nuttali* in the basal beds indicates that it commenced in the Late Palaeocene. In the Hazara and Potwar–Kohat regions in northern Pakistan, the Palaeocene is represented by the *Patala Shale* and the *Hangu Shale*. The Hangu contains an iron-rich horizon that is mined for iron ore at Langrial, and the Patala is characterized by selenite-bearing horizon and marcasite nodules with coal seams in shales in the Surghar Range. The limestones in the Fort Lockhart and Dhak Pass areas in the Salt Range are characterized by Palaeocene foraminifers including *Lokhartia conditi, Miscellanea miscella* and *Operculina patalaensis*. The Dungan Hill in the Sulaiman Range is made up of dominant nodular and massive limestones of this age. In the Kirthar Range (Fig. 19.3), the same limestone was named by W.T. Blanford in 1876 as the *Ranikot Formation*, after the fort in northern Laki Hills. There are basalt flows within the Ranikot succession at Khadro, and volcanic debris occurs with oyster-bearing dark limestone and *Cardita beaumonti* shale of the Danian age in the Bara area. In Balochistan, the proportion of volcanic component is high, as seen in the *Rakhashani* succession, particularly in the Chagai region where andesite and basalt flows are associated with agglomerates in the sedimentary succession containing *C. beaumonti*, among others.

The coeval lithounit of the Subathu in northern Pakistan is known as the *Kuldana* and *Chorgali* formations, named after the Chorgali Pass in the Khair-e-Murat Hills in the Salt Range. Forming an integral part of the Eocene succession, rock salt occurs as stringers and in bedded form at Bahadurkhel in the Kohat region. Overlying the salt horizon at Jatta is a thick sequence of variegated shale, marl and limestone, which is locally gypsiferous and characterized by rich assemblage of Early to Middle Eocene bivalves and vertebrates. In the Salt Range, the limestone grading into massive gypsum at Daudkhel is known as *Sakesar Limestone*. In the southern part of the Kirthar Range and in the Bugti–Masri Belt of the Sulaiman Range, the succession of yellowish to greyish limestone, marl and calcareous shale with sandstone—and local laterite beds—was designated by F. Noetling in 1903 as the *Laki Series*. The Laki contains typical Ypresian foraminifers, such as *Assilina granulosa, Lockhartia hunti, Flosculina globosa* and *Dictyoconoides*

vredenburgi. Its horizon, the *Sui Main Limestone* hosts a very rich deposit of petroleum gas. Overlying the Laki is the *Kirthar Formation* of limestones, marls and shales, characterized by Middle to Late Eocene foraminifers—*Pellatispira madrasi, Actinocyclina alticosteta, Assilina cancillata, Nummulites beaumonti and Dictyoconoides cooki*, along with Early Oligocene *Lepidocyclina dilata, Nummulites fichteli* and *N. intermedius* (Cheema et al. 1977). A dominant shale–claystone succession with subordinate sandstone, conglomerate and limestone with gypsum and coal deposits in some places was described as the *Ghazij* by R.D. Oldham in 1890. In Balochistan, the Eocene is represented by the *Saindak* succession which includes agglomerates with clasts of mottled maroon and green andesite and basalt interbedded with grey shale, calcareous sandstone and limestone characterized by Eocene foraminifers.

Across the Indus Basin in western Rajasthan, the Early Palaeocene succession forms an unconformable cover on the Triassic-to-Cretaceous shelf sediments resting on the Proterozoic basement. The basement gently dips west-north-westwards, giving way to more than 10,000-m-deep Shahgarh depression. The basement is differentiated into Jaisalmer, Bikaner–Nagaur and Barmer subbasins by structural highs such as the NW–SE trending Jaisalmer–Mari High delimited by the Fatehgarh Fault (Figs. 15.13 and 19.2). The Jaisalmer subbasin is connected to the Cambay Basin of Gujarat through the narrow N–S-oriented Barmer graben and the Sancher subbasin (Eremenko and Negi 1968). The Sanchor seems to be the northerly extension of the Cambay Basin. The Early Paleogene shallow marine deposits of the Ranikot, Laki and Kirthar formations bear local names in the Jaisalmer, Bikaner–Nagaur and Barmer subbasins. The Ranikot is described as *Sanu*, *Palana* and *Akli* in the three subbasin; the Laki as *Khuila*, *Marh*, *Mandal*; and the Kirthar as *Bandah*, *Jogira* and *Kapurdi*, respectively (Datta 1983).

Down to the south-west in the Kachchh Island, there is a thick cover of Tertiary rocks, characterized by lateral continuity of lithological units, vertical discontinuities marked by laterized undulating surfaces or bioturbated cut-and-fill structures, and regional overlaps. This succession has been subdivided into four units—Matonmadh, Naredi, Harudi, Fulra and Maniyara Fort formations, each characterized by distinctive foraminiferal assemblages including *Nummulites, Assilina, Discocyclina* and *Lepidocyclina* (Biswas 1973, 1992; Biswas and Raju 1973). The Tertiary successions of Rajasthan and Kachchh are discussed in Chap. 20.

19.2.2 Eastern India

As already stated, the HFB was linked with the Bay of Bengal through the Bengal Basin, which was overtaken by a major marine transgression in the beginning of the Paleogene. Various lithostratigraphic names were given by F.R. Mallet in 1876. Percy Evans in 1932 provided comprehensive sedimentary stratigraphic history of the Assam Basin during the Tertiary period (Bhandari et al. 1973). The

Tura Sandstone in the Bengal Basin is equivalent of the Kakara, and the *Jaintia Formation* is the coeval of the Subathu. It turns out that the Bengal Basin had become a site of carbonate sedimentation on the shelf by the Middle Eocene time, giving rise to the *Sylhet Limestone* Formation characterized by foraminiferal assemblages *Nummulites thalicus, Lokhartia haimei, M. miscella, Nummulites obtusus, N. beaumonti* and *Assilina papillata* in its two units, thus establishing the contemporaneity of the Sylhet with the Ranikot–Kirthar succession in Pakistan. The Sylhet Limestone is biostratigraphically correlatable also with the Early Paleogene sediments on the floor of the Indian Ocean (Jauhari and Agrawal 2001). The *Kopili Shale*, characterized by Upper Eocene *Discocyclina, Heterostigina* and *Pellatispira,* represents clastic sedimentation that had started by the Upper Eocene time on a progressively subsiding shelf of the Bengal Basin (Alam 1989).

19.3 Paleogene Sedimentation North of I-T Zone

The fluvial *Qazil Langer Formation* in eastern Karakoram is a 600–700 m of fining-upward sequence, developed in a foreland basin (Kumar et al. 1997). The sediments, deposited by debris flows and a braided river system, contain post-Maastrichtian, possibly Palaeocene fossils.

The Tertiary succession of central Tibet encompasses limestones with shales and intercalations of ferruginous or micaceous sandstones that range in age from Danian to Lower Eocene. Presence of gastropod *Velates schmideliana* and foraminifers *Numulites, Operculina, Orbitolites, Alveolina* and *Miliolina* suggests correlation with the Ranikot–Laki succession in south-western Pakistan.

19.4 Beginning of Fluvial Sedimentation

19.4.1 Drainage Reversal

One of the very momentous developments recorded in the foreland basin succession is the drastic reversal of drainage in the Early Palaeocene time. All through the nearly 2000 million years long history of the Indian subcontinent, rivers draining the northern part of the Peninsular India flowed in the northwards and northwestward directions. Abruptly, there was a reversal of the pattern of palaeocurrents and sediment dispersal. The rivers started draining and denuding a highland that had just emerged. They were flowing southwards in the central sector (Srivastava and Casshyap 1983) and eastwards in the Pakistan sector (Waheed and Wells 1990).

The reversal of drainage took place as a consequence of the emergence of the Himalaya as a highland.

19.4.2 North-western Himalaya

Another development of great significance was the final withdrawal of the sea from the Himalaya province and beginning of the fluvial sedimentation in a terrestrial setting (Table 19.1). The beginning of the fluvial sedimentation is dated at about 31 Ma—on the basis of fission-track dating of detrital zircon and monazite from basal Dagshai succession (Najman et al. 1993, 1994, 1997). In the Koshalya Valley, SE of Kasauli in Himachal Pradesh, a 280-m-thick succession of sedimentary rocks reveals a distinct erosional hiatus or break between the marine Subathu and the succeeding fluvial Dagshai–Kasauli sequence (Kumar et al. 2008, 2011). The whole of the Himalaya province had risen up as a highland and subjected to denudation. Acceleration of erosion resulted in the generation of enormous volumes of detritus, which the rivers and streams carried to the Sirmaur Basin (Fig. 19.4). As deltas advanced at the river mouths, the sea retreated progressively, and the foreland basin was converted into vast floodplains. The floodplains of the meandering rivers extended from the Nari–Gaj areas in Sindh, through Marwar in western Rajasthan, the Murree Hills in northern Pakistan and Jammu, the Dharamsala–Dagshai–Kasauli Belt in Himachal Pradesh, the Dumri Hills in Nepal to the Surma Valley and Barail Hills in eastern India (Fig. 19.2).

In the Hazara region in northern Pakistan and adjoining Jammu sector, the 6000-m-thick succession of deltaic–alluvial sediments is known as the *Murree Formation* (Fig. 19.3). In the Balakot area, the Murree comprises multiple cycles of sediments, each cycle commencing with typical channel-fill sediments passing upwards into tidal-flat deposits and ending up with red clayey siltstones with calcareous concretion or fossil caliche (Bossart and Ottiger 1989; Khan et al. 1997). In the southern Sulaiman region, the meandering rivers of the Early Murree time were succeeded by the braided rivers of the later epoch. They flowed in the SSW direction (Waheed and Wills 1990). Layers of conglomerate at the base of the Murree Formation in the Potwar and Kohat plateaus indicate that the beginning of the fluvial sedimentation was marked by a hiatus. In the Poonch area in Jammu–Kashmir, the passage is transitional or slightly disconformable. The sediments were deposited by SSE to SSW-flowing rivers (Singh 2000).

In the Himachal sector (Fig. 19.4), meandering rivers in the early stage laid down maroon and red sandstones, shales and mudstones in their floodplains. These sediments are represented by the *Dagshai Formation*. In the later stage, the sediments are preponderantly grey lithic sandstone with subordinate mudstone deposited principally in their channels represented by the *Kasauli Formation* (Raiverman 1979; Raiverman and Raman 1971). The Dagshai–Kasauli succession is a handiwork of a river system that flowed in the SE as well as SW directions in different parts of the basin (Srivastava and Casshyap 1983). This combined Dagshai–Kasauli succession, also known as the *Dharamsala Formation* in western Himachal Pradesh, represents the filled or overfilled stage of the foreland basin sedimentation. There is a strong perception among paleontologists and stratigraphers that there is biochronological continuity from the marine Subathu

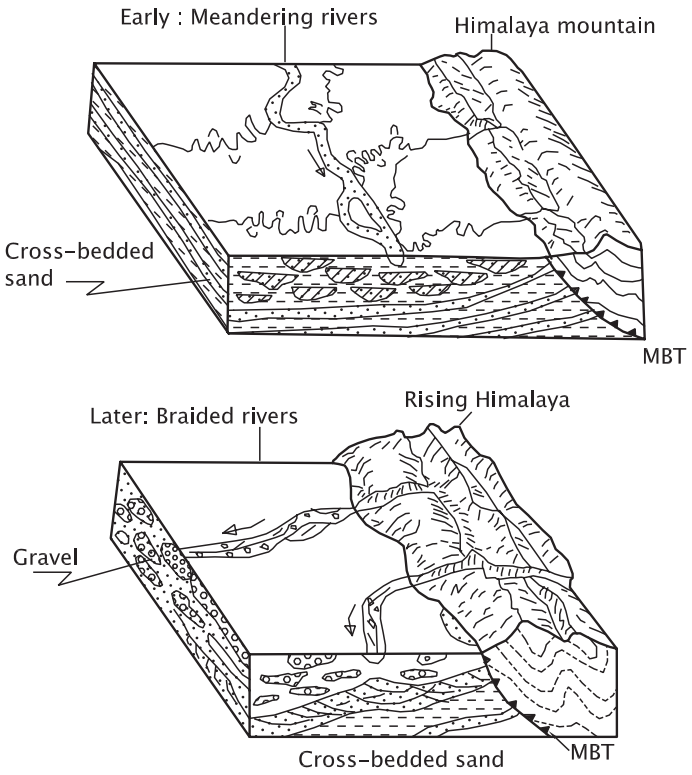

Fig. 19.4 While the Dagshai and coeval sediments were deposited principally by meandering rivers, the Kasauli succession and homotaxial formations were the products of braided rivers (based on Waheed and Wells 1990; from Valdiya 1998)

of Late Thanetian to Middle Lutetian—Palaeocene to Lower Eocene age through the passage beds represented by the Kasauli Formation (Late Lutetian to Middle Bartonian) to the Dagshai Formation (Late Bartonian to Rupelian of the Upper Eocene–Lower Oligocene age) as seen all along the foreland basin east of the Hazara syntaxial bend (Bhatia and Bhargava 2006). There is thus no long hiatus between the Subathu and the Dharamsala successions in the Indian sector.

Significantly, while the Subathu is made up predominantly of recycled detritus derived from the ophiolites and basic volcanic rocks of the Indus Tsangpo Suture Zone, the Dagshai–Kasauli sediments are characterized by clastics of metamorphic rocks of Himalayan terranes (Najman et al. 2004). Mineral spinel is characteristic of the Subathu, and the clastic fragments of metamorphic rocks in the Dagshai–Kasauli sediments show progressive increase in the grade of metamorphism, implying exhumation or experse to surface of progressively higher grade rocks through the time in the provenances.

19.4.3 Sindh and Baluchistan

The equivalents of the Dagshai and the Kasauli formations in Sindh are known as the *Nari* and the *Gaj*, respectively (Table 19.1). In the Gaj River section in the Kirthar Range, the Nari succession comprises sandstones and shales with subordinate limestones characterized by Oligocene foraminifers (*Nummulites fetchteli*, *N. intermediu* and *L. dilata*), corals, molluscs and echinoids. In the Balochistan region, sandstones, shales and volcanic ash with agglomerates and andesitic lavas form the *Amalaf* succession. In the Makran coast, the Oligocene Formation comprises sediments deposited in estuarine and deltaic environments (Cheema et al. 1977). The sea withdrew from a large part of the foreland basin in Pakistan in the Miocene period. This is evident from widespread deposits of deltaic–fluvial deposits of the Middle Miocene time in the Kohat–Potwar region, the so-called Axial Belt, and the Indus Basin. The Gaj Formation, typically exposed in the section of the Gaj River flowing across the Kirthar Range, comprises green-grey and variegated shales, locally gypsiferous, sandstone with limestones containing Aquitanian to Burdigalian fauna. In the Balochistan region, the Miocene sediments form the Hinglaj Mountain. The Makran Range is the emergent part of the E–W trending accretionary wedge formed where the oceanic floor was (and is) subducted beneath the southern margin of the Asian plate. Extending from Hormuz in the west to the Kirthar–Sulaiman Ranges in the east, the accretionary wedge comprises abyssal-plain turbidites and slope and shelf sediments of the Oligocene to Early Miocene age (Critelli et al. 1990). The *Makran Group* thus represents the top of an evolving accretionary wedge (Table 19.1).

19.4.4 Nepal

In the Nepal sector (Table 19.1), the succession that unconformably overlies the Bhainskati Formation and begins with an oxisol at the base and comprises sediments that were deposited in the time span of 27 to 17 Ma is described as the *Dumri Formation* (Sakai et al. 1999). The Dumri sediments were laid down by rivers that flowed in the WSW direction (DeCelles et al. 1998). Fission-track date 31 ± 1.6 Ma of detrital zircons from the base of the Dumri succession in Nepal establishes its correlation with the Dagshai of Himachal Pradesh (Najman et al. 2004). The Dumri was subjected to mild metamorphism during the time 17–16 Ma.

19.4.5 Eastern India

The influx of clastic sediments that began in the Middle Eocene time, on the progressively subsiding shelf of the Bengal Basin (Fig. 19.5; Table 19.1), manifested itself in the deposition of more than 1100-m-thick sediments known as the *Barail*

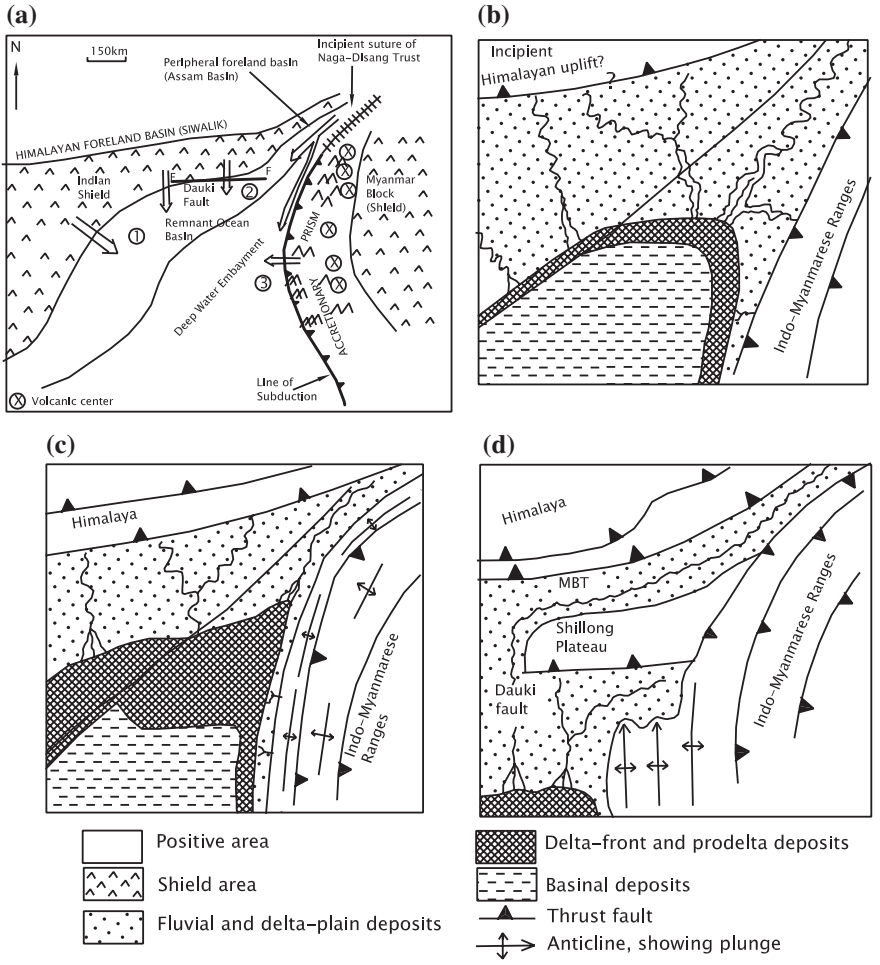

Fig. 19.5 Schematic maps showing the changing geography of eastern India as fluvial sedimentation advanced and the sea withdrew (after **a** Gani and Alam 2003; **b**, **c**, **d** Johnson and Alam 1991)

(contemporaneous with the Dagshai and the Nari) and culminated in the emplacement of the *Surma* (the coeval of the Kasauli and Gaj). At Aizawl in Mizoram, the Bhuban Formation—which is the uppermost unit of the Surma Group—is found to contain rich assemblage of selachian fish of Aquitanian to Burdigalian (Lower Miocene) age (Ralte et al. 2011). The fish remains indicate warm shallow near-shore water. The upper part of the Bhuban Formation contains planktic and benthic foraminifers including Early to Middle Miocene uvigerinids, testifying to middle–upper parts of the neritic sites (Lokho et al. 2011). The lower part of the *Surma* in the Rangamati–Sitapahar Belt represents an apron of debris deposited on the slope of continental margin adjoining a bathyal environment in the Sylhet

subbasin. The stratigraphic span of the Barail Formation in Bangladesh is Lower Eocene to Early Miocene, the major inputs of sediments occurring at 38 Ma in the Bengal Basin when >1000-m-thick body of the Barail was formed (Najman et al. 2008). In Assam–Arakan Range, the middle member of the Barail Formation—the Jenam—consists of deep-water submarine fan deposit emplaced in the proximal parts of the basin by turbidity currents and debris flows, as borne out by olistostromes characterized by clasts of volcanic rocks (Biswas and Mukhopadhyay 2011). The overall Surma succession displays basinward progradation from deep marine through coastal marine to deltaic environment. There was thus westward migration of accretionary prism complex within the active margin of the Indo-Myanmar plate convergence. In the Early Miocene, it was wholly fluvial sedimentation—the Surma succession by braided streams with channel bars gradually passing upsequence into meandering river deposits (Gani and Alam 1999, 2003).

19.4.6 Provenance of Sirmaur Sediments

Tiny fragments of phyllite, ophiolite and volcanic rocks in the Murree litharenite show that the detritus was derived from the rocks of the Indus–Tsangpo Suture Zone (Critelli and Garzanti 1994). Chrome spinel recovered from a basal bed of the Murree at Balkot in northern Pakistan indicates its derivation from a source in the Kohistan island arc (Bossart and Ottiger 1989).

Abundance of very small fragments of medium-grade metamorphic rocks, together with detrital garnet, staurolite, muscovite and monazite in the Lower Dharamsala sedimentary rocks, and the presence of fragments of low-grade metamorphic rocks in the upper Dharamsala strata demonstrate that the sources lay, respectively, in the Himadri Complex and the Tethyan Haimanta rocks, subordinately in the Lesser Himalaya (Johnson and Oliver 1990). It seems that the overthrust sheet—the Chamba Nappe—was already emplaced by about 17 Ma. The Dumri sediments of Nepal likewise received its detritus from the source that rested upon the Himadri Complex (DeCelles et al. 1998). By the Kasauli time, the Himadri Complex was exhumed and exposed to denudation. This is inferred from the presence of microliths of high-grade metamorphic rocks and heavy minerals in the Kasauli sediments (Chaudhari 1972; Najman et al. 1993).

19.4.7 Palaeoclimate Variation

In the Dagshai time, semi-arid conditions prevailed on the floodplains as testified by caliche occurring in sediments. By the Kasauli epoch, warmer humid climate had returned. The floodplains were covered by such plants as *Sabal major*, a palm of the Late Oligocene to Early Miocene time.

However in Assam, the area from where the Barail sediments were scraped by streams, there were thick forests which eventually contributed organic matter for the formation of coal and lignite occurring as seams within the Upper Barail succession.

19.5 Life in the Paleogene Period

Foraminifers were the pre-eminent members of the invertebrate marine communities that included ostracodes, corals, gastropods, lamellibranchs and echinoids. Only those taxa are dealt with that have bearing on the evolution of life in the HFB. While the lower part of the Subathu in the Kalakot area contains colonies of oil-forming green alga *Botryococcus* (Prasad and Sarkar 2000), the upper part of the Subathu in the Jammu region and at Kuldana in Pakistan yielded Middle Eocene rodents and a variety of other animals (Srivastava et al. 1996; Kumar et al. 1997a, b). And the Subathu in Himachal Pradesh is characterized by Late Ypresian nannofossils (Jafar and Singh, 1992) and Middle Eocene rodents (Kumar et al. 1997a).

19.5.1 Palaeocene–Eocene Vertebrates

Near Dera Bugti in Baluchistan, a rich assemblage of micromammals, reptiles and fish includes the most primitive of rhinocerotidae—*Bugtirhynus precursor*—found in the Chitarwata succession (Antoine and Welcomme 2000). In the Bozmar Valley in the Zinda Pir area (Sulaiman Range), the shelf-margin sediment revealed a 46.5-million-year-old archaeocete *Rodhocetus,* an animal intermediate between land mammal and marine whale (Gingerich et al. 1994). The Subathu in the Kalakot, Metka and Moghla inliers in Jammu region contain raoellid rodents, perissodactyls, creodonts, anthracobunds and the ratellid artiodactyls and a cetacean protocetid whale *Ichthyolestes pinfoldi* (Kumar et al. 1985). Similar taxa are found in the Kuldana Shale in northern Pakistan. A creature named *Himalayacetus subathuensis* found in Kuther Valley near Subathu, (in the Shimla Hills) is believed to be the oldest known pakicetid archaeocete (Fig. 19.6) which lived both in freshwater and marine environments 58–54 million years ago (Bajpai and Gingerich 1998).

19.5.2 Oligocene–Lower Miocene Fauna

A mixed faunal assemblage comprising terrestrial and aquatic vertebrates, marine and non-marine molluscs, ostracodes, smaller foraminifers and charophytes implies transitional passage of the Subathu to the Dagshai (Bhatia 2000, 2003;

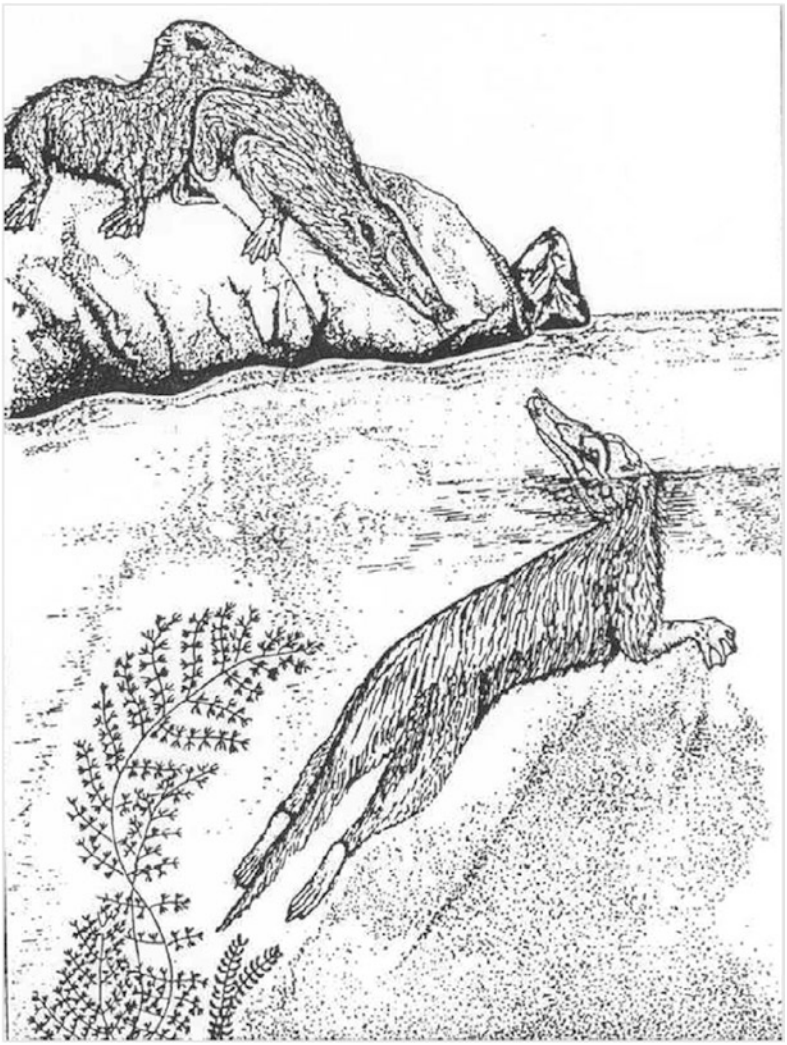

Fig. 19.6 A land-living mammal that took to living permanently in the sea became a marine whale—*Ambulocetus* (*Courtesy* Ashok Sahni)

Tiwari 2005). The lowermost unit of the Murree in the Kalakot area shows terrestrial vertebrate fauna, including varanids, lizards, testudines and crocodiles among the lower vertebrates and artiodactyls, perissodactyls and Early Miocene cricetid rodent *Primus microps* among the mammals (Sahni and Kumar 1974). Significantly, the Murree mammalian fauna is dominated by an exotic taxa related to Eurasia, Africa and North America (Kumar and Kad 2003). In the marshy

woods of the Barail and Surma valleys in Assam roamed *Rhinoceros sivalensis, Paraceratherium* and *Dinotherium* (Wadia 1975).

The Kasauli succession is characterized by the plant remains that indicate mixed lowland forests comprising moist deciduous to evergreen elements. They include palm leaves showing affinity with tropical fanpalm, *Dipterocarpus, Amoora, Bambusa, Bauhinia* and *Cassia* (Guleria et al. 2000).

19.6 Momentous Tectonic Events

19.6.1 Formation of Main Boundary Fault

As the Lesser Himalayan thrust sheets advanced southwards, they encountered resistance, which was maximum on the southern front. Consequently, the Himalayan crust broke along the 2500 km length of the Himalaya province in a series of faults (Fig. 19.7). These thrust faults are collectively known as the *Main Boundary Thrust* (MBT), a name given in 1864 by H.B. Medlicott to one of the faults of the boundary zone. The MBT is steep (>50º) near the surface, but flattens to <20º in deeper levels. The Indian plate, carrying the prism of Cenozoic sediments (including those of the foreland basin), slid under the Himalaya along the MBT (Fig. 19.7b). There was simultaneous shortening of the basin. Results obtained from balancing a few sections of the 85-km-wide western segment of the foreland basin indicate that the shortening amounts reported by various workers vary from 22 to 71.3 %, implying that shortening rates do not provide reliable idea of the basin evolution (Dubey et al. 2004).

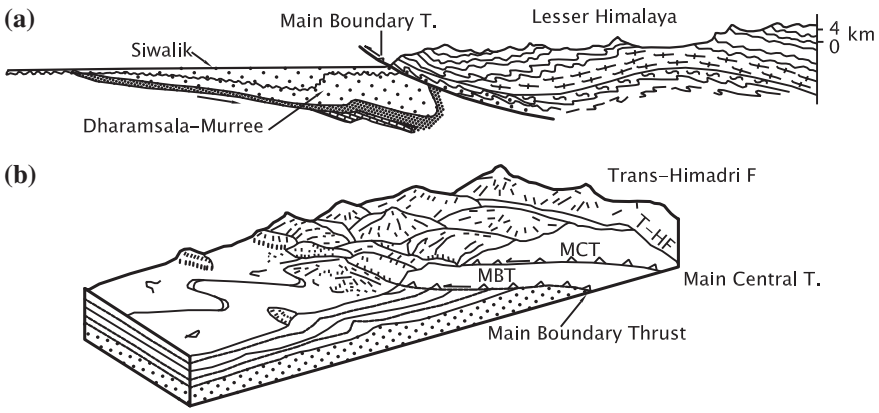

Fig. 19.7 Formation of the Main Boundary Thrust and evolution of the Neogene foreland basin known as the Siwalik Basin (section based on Colchen et al. 1986; block diagram after Tokuoka et al. 1990)

The Bibai Thrust has brought south-eastwards the succession of deep-water Early Tertiary sedimentary rocks of the north-western part of the Sulaiman domain over the succession of shallow water marine sedimentary rocks with associated volcanics and "local submarine edifice" and broken by many disconformities in the fold and thrust belt of the south-eastern part (Kassi et al. 2009).

19.6.2 Southward Relocation of Foreland Basin

This development in the northern margin of the Sirmaur Foreland Basin induced its southward relocation, with a consequence that the Murree/Dharamsala deposition prograded onto the northern margin of the Indian craton.

The initial displacement along the MBT occurred at about 11 Ma, the time when the rate of sediment accumulation, the sandstone–shale ratio, and formation of amalgamated sandstone bodies all substantially increased and there was rapid cooling (10–8 million years ago). These developments occurred after bedrock uplift, and erosion began 1–2 million years earlier at the leading edge of the MBT in the Kohat region (Meig et al. 1995).

19.6.3 Formation of Siwalik Basin

As the crust broke along the MBT, it sagged immediately south of the line of breaking (Fig. 19.7). An elongated depression—the second in succession of the Paleogene Sirmur Basin—came into existence upon and overlapping onto the shield. It is known as the *Siwalik Basin*, a great repository of detritus brought down from the fast rising youthful Himalaya mountain (Fig. 19.8; Table 19.2). The total thickness of the sediments accumulated amounts to about 7000 m. In the course of digging for the Ganga canal near Haridwar, Captain P.T. Cautley had found some vertebrate fossils near a Shiva (Siwa) temple. R.D. Oldham in 1893 gave the name Siwalik to the sediments containing these fossils. In 1913, G.E. Pilgrim subdivided the Siwalik succession and identified formations such as the *Kamlial, Chinji, Nagri, Dhok Pathan* and *Tatrot*, after the localities in the Campbell district in the Potwar plateau and the *Pinjor* and the *Boulder Conglomerate* in Haryana–Punjab sector, primarily on the basis of vertebrate assemblages.

Embracing what has been described as the *Manchhar* in Baluchistan and Sindh (Table 19.2), the Siwalik succession forms the outermost hill ranges of the north-western Himalaya stretching from Potwar through Jammu to Tanakpur, the Churia Range of Nepal, the Dafla–Subansiri–Kimin sedimentary sequences of Arunachal Pradesh, the Namsang–Dihing domain in Assam and the Tipam–Dupitila area in Cachar and Tripura. It embraces the Irrawaddy Valley of Myanmar.

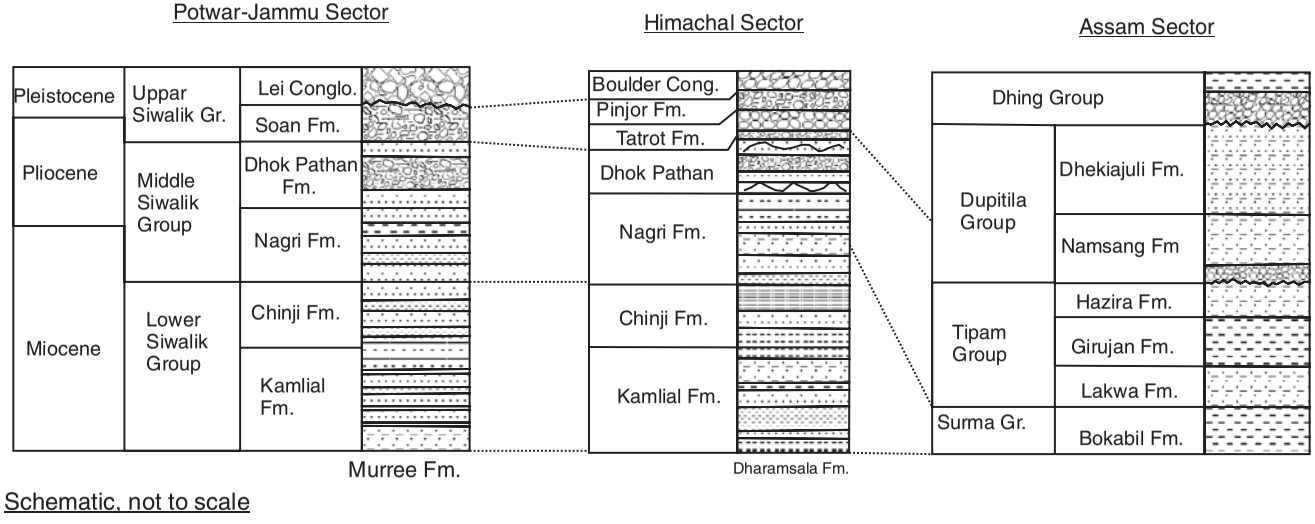

Fig. 19.8 Columns illustrating the lithological associations and subdivisions of the Siwalik succession

Table 19.2 Neogene and Pleistocene formations of the Outer Himalaya (Valdiya 1998)

	Potwar–Jammu		Himachal–Kumaun	Nepal	Arunachal Pradesh
	Lei Conglomerate		Siwalik Boulder Conglomerate	Deorali Boulder Beds	
	Upper Siwalik	Pinjor Tatrot	Upper Siwalik	Chitwan	Kimin
har	Middle Siwalik	Dhokpathan Nagri	Middle Siwalik	Binaikhola	Subansiri
har	Lower Siwalik	Chinji Kamlial	Lower Siwalik	Arungkhola	Dafla
	Muree		Kasauli	Dumri	––

19.7 Siwalik Sedimentation

19.7.1 Lithology

In the Middle Miocene time, high-grade metamorphic rocks with their granitic bodies were thrust southwards along the Main Central Thrust, giving rise to the mountain ranges that rose to a great height. Huge amounts of detritus eroded from these fast rising mountain ranges were delivered to the Siwalik Basin. The amounts of sediments were so large that quite a part of them spilled over the basin and spread into the Bengal Basin and beyond in the Bay of Bengal and onto the Arabian Sea. Emptying their abundant load of sediments, the Himalayan rivers eventually converted the Siwalik Basin into a vast floodplain.

The Siwalik succession of sediments is divisible into three major units (Table 19.2; Fig. 19.8). The *Lower Siwalik*, known as the *Lower Manchhar*, in Sindh, the *Dafla* in Arunachal Pradesh and the *Tipam–Girujan* in Assam comprise alternation of muddy sandstones and maroon mudstone and shale with occasional beds of pebbly conglomerate in the lower part. The *Middle Siwalik* and the coeval of the *Upper Manchhar* in Sindh, the *Subansiri* in Arunachal Pradesh and the *Dupitila/Namsang* in eastern India are made up of micaceous, calcareous lithic arenite and sublitharenite with subordinate grey and maroon shales. The Upper Siwalik, described as the *Kimin* in Arunachal Pradesh and the *Dihing* in Assam and adjoining region, consists of coarse sandstones becoming increasingly pebbly and locally conglomeratic towards the upper part, as typically seen in the Dehra Dun and Pinjor duns (Fig. 19.9). The top of the Upper Siwalik is a thick sheet of boulder conglomerate of vast lateral spread.

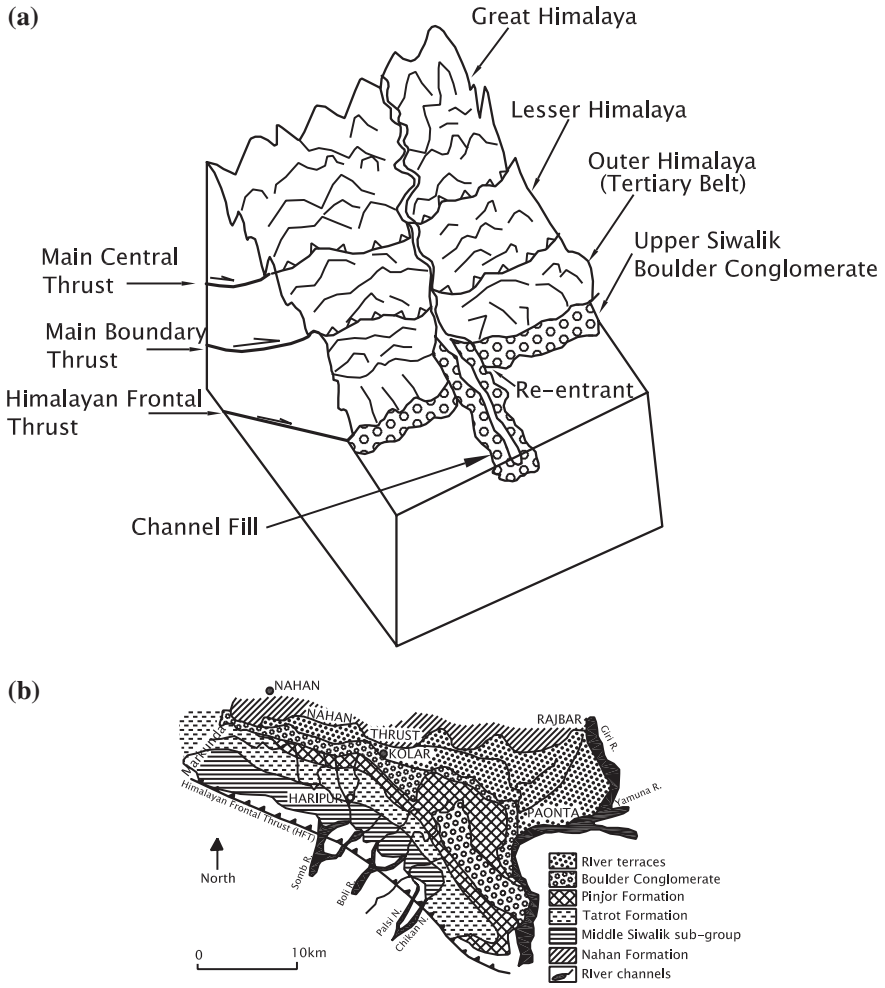

Fig. 19.9 **a** During the Upper Siwalik time, accelerated erosion in the rising orogen brought influx of enormous volume of gravelly detritus, emplaced along the foothills and in channels of the braided rivers (after Abbasi and Friend 2000). **b** Distribution of boulder conglomerate of the Upper Siwalik in the Dehra Dun subbasin (Sangode and Bloemendal 2004)

19.7.2 Temporal Span

Palaeomagnetic studies demonstrate that the Siwalik succession between Sukhidhang and Tanakpur in south-eastern Kumaun correlates with the geomagnetic polarity time scale of 12.5 Ma to 4.0 Ma (Kotlia et al. 2008). Magnetostratigraphic data show that the 325-m-thick succession of the Siwalik in south-western Arunachal Pradesh was deposited in the period 25 Ma to 13 Ma, the transition between the Lower and Middle Siwalik occurring at 10 Ma (Chirouze

et al. 2012). Coupled with the study of sedimentary structures, the palaeomagnetic data clearly demonstrate that the chronostratigraphic record of the Eastern Himalayan Siwalik is the same all over the sub-Himalaya.

19.7.3 Environment of Deposition

The silty-heterolithic association of the Lower Siwalik in the Jammu region represents an upland interfluve ("doab") deposit of meandering rivers (Sharma et al. 2001).

The Middle Siwalik in the Jammu region is characterized by multiple storeys of sandstone bodies representing channel fills (Fig. 19.1; Table 19.2) of rivers that drained in the SSE direction (Sharma et al. 2002). Obviously, the meandering rivers of the Lower Siwalik time had turned into braided rivers during the Middle Siwalik. The Potwar–Khaur sector in northern Pakistan provides the type of drainage system that was responsible for emplacement of the multistoreyed sand bodies (channel bars and fills) of the Chinji and Nagri units. The channels within 1- to 2-km-wide flood belt were 80–200 m wide and 4–13 m deep with channel-bank discharge of the order of 400–800 m^3/s (the full flood-belt discharge being 1500–2000 m^3/s) during the Chinji time, becoming 200–400 m wide and 15–30 m deep with channel-bank discharge of 3000–5000 m^3/s and full flood-belt discharge of 10,000 m^3/s in the Nagri time (Wills 1993; Zaleha 1997). These rivers flowed south-east. The Dhok Pathan succession exhibits nearly the same situation (Khan et al. 1997). Large channel-belt complex constitutes the main feature of the Chinji River network as inferred from megasheets of coarse sandstones in northern Pakistan (Friend et al. 2001).

The Upper Siwalik sediments were deposited by northward-flowing streams in the basin in the backside of and attached to the Potwar subbasin on the hanging wall of the Salt Range, following uplift of the Shinghar Range (Pivnick and Khan 1996). The 2800 m Upper Siwalik of the Haripur–Kolar Belt in Himachal Pradesh is the making of a braided river system, occupying the plain characterized by calcrete nodules in alfisol soil (Tandon et al. 2002; Thomas et al. 2002). In the Kangar area in Jammu, the various facies of the Boulder Conglomerate Formation represent sediments deposited rapidly in an environment recurrently affected by high-energy flows of braided rivers (Pandita et al. 2011). In the Suraikhola Belt in westcentral Nepal, flooding increased dramatically in the interval 10.5 to 9.5 Ma, and the fluvial style changed from the meandering to the braided system between 9.0 and 6.5 Ma and again to the gravelly braided system after 3.0–2.5 Ma (Nakayama and Ulak 1999). The Siwalik succession of the Arungkhola–Binaikhola represents deposits laid down in the early stage by low-discharge, low-relief meandering rivers which became flood-dominated at 9.9 Ma and braided sandy after 8.2 Ma, primarily due to intensification of rainfall. The gravel deposits in the braided rivers are attributed to the tectonic resurgence at 2.5 Ma related to movements on the MBT. Evidently, the ground slope had

steepened, and there was profuse influx of very coarse detritus, presumably due to accelerated erosion in the uplifted and rising Himadri domain. Significantly, the Pinjore succession shows what looks like tectonically induced structure (Ravindra et al. 2005).

Intensification of monsoon rainfall may also be responsible for the emplacement of boulder deposits, represented by the *Upper Siwalik Boulder Beds*, described as the *Lei Conglomerate* in the Potwar region. By the Middle Miocene time, there was huge influx of clastic sediments from the west as well as from north-east and east into the greater Bengal Basin (Fig. 19.5). From now onwards, the *Barail* Basin started receiving sediments from the west and north-west also (Alam et al. 2003). With increasing load of sediments, the floor of the basin subsided progressively, and the rate of subsidence increased dramatically 3–8 times from Middle Miocene to Pliocene–Pleistocene (Johnson and Alam 1991).

The *Tipam–Dupitila–Dihing/Namsang* succession (Fig. 19.8; Table 19.2), spanning the time from the Middle Miocene to the Early Pleistocene (Roy et al. 2004), is the coeval to the Lower–Middle–Upper Siwalik. The Dupitila of the foothills of the Shillong massif comprises an upward-fining sequence of trough cross-bedded sandstone, ripple cross-laminated sandstone, finely laminated mudstone with ripple marks and massive mudstone characterized by rootlets. It represents a deposit of meandering river, the channel of which was 5–30 m deep (Roy et al. 2004; Gani and Alam 2004). In a part, it is an alluvial fan that had channels directed towards SSE, S and SSW, and their depth varying from 87 to 185 m (Roy et al. 2004). The Tipam Formation in the Chittagong Hills, Bangladesh, exhibits sedimentary features indicating deposition of sediments in tidal marsh (Roy et al. 2008). In the Lalmai Hills (Chittagong), in Bangladesh, the Dupitila Formation comprises piedmont alluvial deposits. In its lower part, the sedimentary features of the deposits indicate south-westward palaeoflow of braided rivers, while the middle and upper parts are made up of deposits in the estuarine tidal flat (Ray et al. 2012).

19.7.4 Rates of Sediment Accumulation

The rate of sediment accumulation in the Siwalik Basin in northern Pakistan increased over the time during the Middle Siwalik. It became three times faster than what it was in the Lower Siwalik period (Johnson et al. 1983). There was a notable rise of sedimentation rate in the Himachal–Uttarakhand sector in the period 10.8–9.5 Ma, when the Nagri sediments were laid down. But the largest fluctuation of sedimentation occurred after 1.7 Ma, when the boulder conglomerate was emplaced over very extensive belt at the top of the Siwalik succession. The Upper Siwalik gravelly sediments were deposited at the rate of 70 cm/1000 years in the Dehra Dun subbasin and 39 cm/1000 years in the Subathu subbasin (Kumar et al. 2003). And in the Haripur sector, the rate of accumulation of gravelly sediments increased from 45 cm/1000 years to 54 cm/1000 year after 2.6 Ma (Sangode and Kumar 2003). In westcentral Nepal, the average rate of sedimentation

varied from 20–150 cm/1000 years to 32–50 cm/1000 years (Tokuoka et al. 1990; Gautam and Rosler 1999).

19.7.5 Extensive Debris Flows

Towards the close of the Pliocene and beginning of the Pleistocene about 1.5–1.7 million years ago, the entire Siwalik subprovince, extending from the Potwar region in the west to the Dihing Valley in the east, was overwhelmed by sudden excessive influx (Fig. 19.9) of gravelly detritus and avalanches of muddy debris as already stated (Valdiya 1998). The gravelly debris was derived principally from the outer ranges of the Lesser Himalaya and from the older rocks of the Siwalik itself. Understandably, both the outer Lesser Himalaya and the Siwalik Belt were affected by very strong tectonic movements that triggered massive landslides and debris flows on the slopes of the destabilized mountain ranges. The collapse and erosion of the uplifted hanging walls of fault blocks within the Siwalik generated sediments of the Upper Siwalik (Raiverman et al. 1983; Kumar and Tandon 1985; Tandon 1991). Stupendous volumes of debris comprising boulders, cobbles and pebbles gave rise to the 2800- to 1800-m-thick *Boulder Conglomerate* horizon which is known as the *Lei Conglomerate* in northern Pakistan. The conglomerates are intercalated with brown to yellow muds and earthy clays emplaced by debris flows. Some of these layers of yellow earthy mud are bentonitic in composition. The bentonitic represent altered volcanic ashes. The volcanic ash suggests the timing of the conglomerate emplacement from 1.7 to 1.5 Ma.

19.7.6 Episodes of Contemporary Volcanism and Tectonism

While rivers were depositing detritus in their channels and floodplain in the Siwalik foreland basin, volcanoes in Afghanistan and central Myanmar were active, emitting fume and ash. Wind carried the volcanic ash and dust and shed them on the Siwalik floodplains. As stated above, the ashes have since altered to bentonitic clays. Their age ranges from 9.46 ± 0.59 Ma to 1.61 ± 0.1 Ma (Johnson et al. 1983; Ranga et al. 1995). There was a notable increase in the volcanic activity in the interval 3–1.5 Ma, particularly in the valley of the Irrawaddy River in Myanmar, where active volcanoes follow a tectonic–volcanic line.

The sedimentary succession of the Siwalik in the Kangra subbasin was affected by the major tectonic disturbance at 10 and 5.5 Ma, the earlier event causing intrabasinal overriding of sedimentary pile, as borne out by abrupt change of palaeodrainage pattern from meandering to braided river system at 10 Ma (Ghosh et al. 2009). The disturbance at 5.5 Ma initiated emplacements of fluvial sediments. Significantly, there was also variation between 10 and 9 Ma in the influx of detrital material dominated by those derived from metamorphic rocks of the chaill thrust

sheet (Ghosh et al. 2009). The 325-m-thick Middle Siwalik sedimentary succession in the Darjiling sector has inverted occurrence of soft-sediment deformation structures such as convolute lamination and flame structure, resulting from increased pore-water pressure developed due to strong seismic shock (Kundu et al. 2011). In the Itanagar–Golipur section in Arunachal Pradesh, the Middle Siwalik sediments show soft-sediment deformation structures such as flame structure, pseudonodules, diapirs detached folds, pinch-and-swell bedding, and bulged sand bodies identified as seismites (Bhakuni et al. 2012).

19.7.7 Provenance of Siwalik Sediments

Study of heavy mineral distribution in the Siwalik Sandstones reveals predominance of staurolite in the Lower Siwalik (as it is the case in the Murree), of kyanite in the Middle Siwalik, and of sillimanite with hornblende in the Upper Siwalik (Raju 1967; Chaudhari 1972). Excessive delivery of kyanite with garnet, staurolite and epidote during the Middle Siwalik period in the temporal span of 11.5–5.1 Ma implies exhumation or exposure at higher elevation and attendant denudation of the Himadri Complex at about 11 Ma. This was indeed the time of a strong and momentous tectonic movement. The detrital material in the Siwalik of the Ramnagar sector in south-western Kumaun points to their derivation as early as 7 Ma from metamorphic rocks, presumably of the Ramgarh thrust sheet made up of low-grade metamorphic rocks with porphyritic granites and mylonites and of the Almora thrust sheet consisting of medium-grade metamorphic and granites (Jalal et al. 2011). This is very significant finding, for it shows that by 7 Ma, the two sheets of crystalline rocks had been emplaced—that these rock successions had been overthrust southwards from their roots. In the Late Miocene to Pliocene Siwalik sediments in Arunachal Pradesh, some heavy minerals and other detrital minerals including quartz and feldspars suggest derivation from the batholiths of the Gangdese Range in southern Tibet (Cina et al. 2009). If this finding is established beyond doubt, it will imply that the such trans-Himalayan river systems as Subansiri and Disang (Brahmaputra) have been in existence since about 10 million years, for these rivers carried 75–31 % of the residual zircon found in the Siwaliks of Arunachal Pradesh (Cina et al. 2009).

19.8 The Siwalik Life

19.8.1 Favourable Conditions

Warm and humid climate conditions prevailed during the Siwalik time. In the Miocene–Pliocene Tipam Formation in Mizoram, a petrified forest has been identified at Zawinuam and Buchang indicating presence of plant precursors to the

modern *Marginifera, Terminalia, Shorea* and *Dalbergia* (Tiwari et al. 2012). The plant fossils indicate warm–humid climate with heavy rainfalls during the Tipam time. The floodplains were clothed with thick rain forests, particularly in the Early Siwalik time. This is evident from plant fossils. With abundance of food available from forests, and water being aplenty in the land of rivers, lakes and swamps, a rich and varied life grew and flourished dramatically. In the streams lived reptiles, including crocodiles and turtles, and the swamps were populated by rhinos and hippos. In the forests lived mammals such as tigers, elephants, buffaloes, cows, deers, goats and tree-climbing primates.

Attracted by the abundance of food, water and living places, herd after herd of quadrupeds came to this land of plenty from as far as northern Eurasia, Africa and North America (Fig. 19.10).

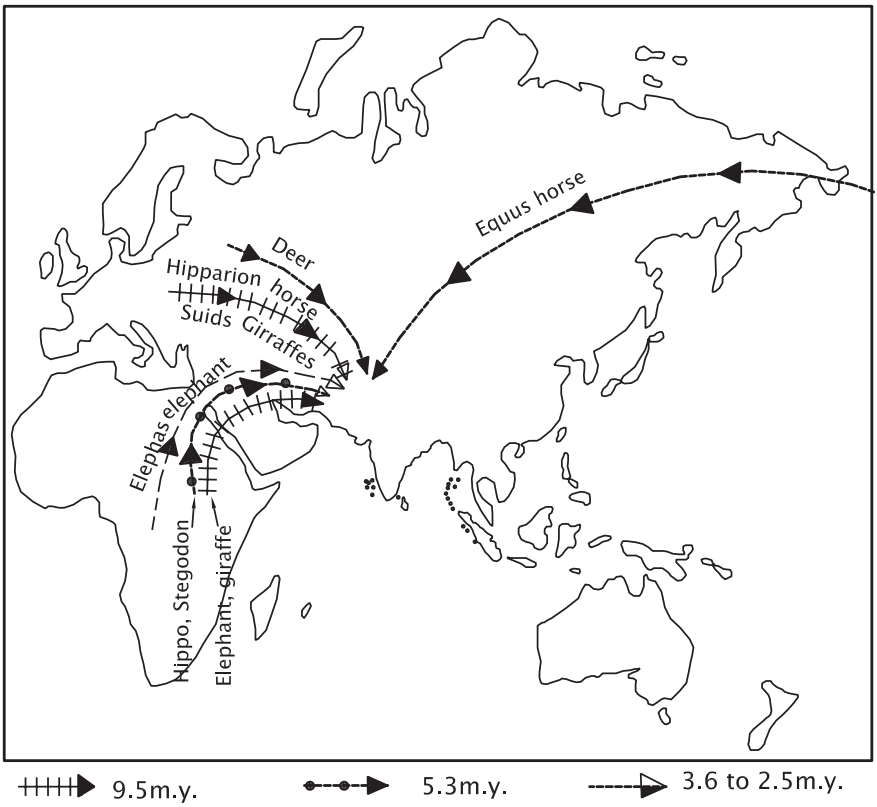

Fig. 19.10 Attracted by abundant food and water, quadrupeds immigrated to this land of plenty from northern Eurasia, Africa and North America. They came in several waves of migration. (From Valdiya 2002)

19.8.2 Faunal Assemblages

The rich and varied faunal assemblages have been studied in detail in a number of type areas in various parts of the Siwalik terrane (Nanda 2004; Nanda and Sehgal 1993; Corvinus 1995; Nanda and Corvinus 2000; Nanda and Shukla 2001).

During the *Lower Siwalik* time in the rain forests, pigs such as *Listriodon, Conohyus* and *Dicoryphochoerus* were abundant in the marshy tracts along with mammals with long mobile nose-like head proboscids *Dinotherium, Anthracotherium* and *Gomphotherium*, the carnivores *Dissopsalis* and *Vishnufelis*, the anthracotherids *Hemimeryx* and *Hyaboops,* and giraffids *Giraffa* and *Giraffokeryx*. Primates such as *Sivapithecus* (Fig. 19.11a) lived on forest trees dominated by *Dipterocarpus* and *Calophyllum*. A variety of reptiles including a giant turtle *Colossochelys atlas* lived in water bodies of the marshy land.

By the *Middle Siwalik* time, climate had become drier and the pine (*Pinus*) succeeded in securing a foothold, and patches of grassland appeared in the forests.

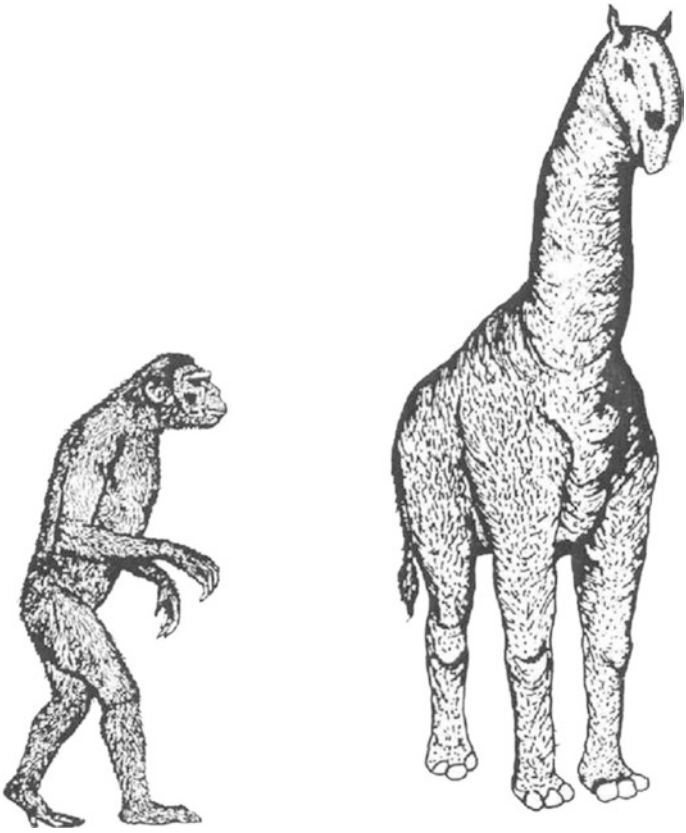

Fig. 19.11 **a** Primate *Sivapithecus*, also known as *Ramapithecus*, resembling modern orang-utan in south-eastern Asia. **b** Hornless giant *Baluchitherium* was a treetop brouser that lived in the Siwalik terrain of Baluchistan (Pakistan) (*Courtesy* A.C. Nanda)

In the communities of above-mentioned animals appeared the three-toed horse *Hipparion* with *Vishnutherium* and *Brahmatherium* (Fig. 19.11b), the proboscids such as *Stegodon*, the carnivores such as *Amphicyon* and *Sivanasua*, the giraffids such as *Hydaspitherium megacephalum* and *Giraffa punjabiens,* and the pigs such as *Dicoryphochoerus vinayaki and Dorcabune nagrii*. There were Late Miocene bivalves, charophyte *Nitellopsis* and ostracode *Ilyocypris*, testifying to the existence of permanent lakes of cool water (Bhatia 2003) in the Middle Siwalik flood plain. In certain parts of forests in Panjab lived a *Macacus* monkey with apes such as *Sivapithecus*.

In the *Upper Siwalik* time, the terrain was covered by savannah-type grassy plains dotted sparsely with trees. Grazing and browsing animals became preponderant in the forests dominated by trees such as *Terminalia* ("sain"), *Mangifera* ("aam"), *Bauhinia* ("kachnaar"), *Albizzia* ("siris") and *Acacia* ("khair") (Awasthi 1982; Vishnu-Mitre 1984). In the forests and grasslands lived the primates such as *Pongo, Presbytes and Procynocephalus*; the proboscids such as *Mastodon sivalensis, Gomphotherium, Stegodon bombifrons, Stegodon insignis and Elephas hysudricus*; the hoofed mammals ungulate such as *Rhinoceros, Equus sivalensis and Hexaprotodon sivalensis* (hippo); the three-toed horses such as *Hipparion antilopium* and *Cormohipparion*; the giraffids such as *Indratherium* and *Sivatherium*; the pig (*Sus*); the camel (*Camelus*); the carnivores such as *Sivafelis, Canis, Hyaena, Panthera* and *Felis*; the bovids or mammals of cattle family such as *Bubalus* (buffalo), *Bos* (cow), *Leptobos, Hemibos* and *Bison*; and the deer (*Cervus*).

19.8.3 Faunal Turnover

In the Siwalik fauna, the bovids—mammals of catter family—were the most common of larger mammals, and the murids and cricetid rodents occupied a dominant position in the small mammal assemblages. The number of species of artiodactyls (even-toed hoofed animals) and rodents increased considerably, reaching peaks at 13.5 and 8.5 Ma, respectively, and then declined (Barry et al. 1995). In the communities of small mammals, including insectivores and rodents, it was a turnover on a massive scale all over the Siwalik world. There was a change in the nature of the vegetation also (Quade and Cerling 1995). Within a short interval of two million years, a completely different fauna replaced the archaic ctenodactyloid rodents of the Early Miocene times. However, one lineage *Fallomous-Diatomys* of the ctenodactyloid group survived (Flynn 2000).

It may be stressed that all newcomers were immigrants, and they came to the Siwalik subprovince from northern Eurasia, Africa and North America (Fig. 19.10).

There was another drastic change in the composition of the faunal communities in the Upper Siwalik time. The cricetid microvertebrates living in ponds, wooded grasslands, bushland and sandy plains in the Pinjor area were replaced by murid rodents—the non-grazers gave way to the grazers. The modern form

of rodents such as *Hadromys* made appearance around 2.5 Ma (Patnaik 1995, 2003). The change is attributed to intensification of monsoon. The extinction—or possibly outmigration—of the Pinjor mammals in the interval 1.72 and 0.60 Ma (Nanda 2004) must have been due to emplacement of Boulder (Lei) Conglomerate resulting from stupendous debris flows and associated floods that engulfed the whole of the Siwalik subprovince. The rapid disappearance of mammalian fauna in the post-Pinjor period may also be due to severe cold in the Himalaya province (Sahni and Khan 1964). This development is reflected in the disappearance of *Globigerinoides extremus* on the western shelf of the ocean (Ramanathan and Pandey 1988).

19.8.4 Immigration of Exotic Quadrupeds

The great faunal turnover in the Siwalik world was brought about, as already stated, by immigration of exotic quadrupeds, as witnessed 9.5–7.4 Ma ago in the Potwar region in northern Pakistan. Of the animals that came to the Siwalik (Fig. 19.10), the three-toed horse *Hipparion* was possibly the pioneer immigrant. It came from Europe via central Asia about 9.5 Ma ago. The long mobile nosed proboscid elephant *Stegodon* and the hippo *Hexaprotodon* arrived around 5.3 Ma along with the "langur" *Presbytis*, the carnivore *Dinofelis* and the giraffid *Vishnutherium* from central Africa. Quite sometime later, about 3.6 Ma came the elephant *Elephas planifrons* from Africa, and still later at 2.5 Ma arrived the one-toed horse *Equus*, coming all the way from Alaska in North America via the Bering Straight—almost at the same time when the deer *Cervus* arrived from central Africa (Nanda 2004).

The rhino (*Rhinoceros*), the buffaloe (*Bubalus*) and the cow (*Bos*) are purely indigenous animals.

The movement of the big-bodied heavy-footed quadrupeds across the Himalaya province in the Late Miocene indicates that despite the mountain ranges having risen high, they still were not high enough in some sectors to prevent the passage of herds of heavy and big animals (Valdiya 1993, 2002). A few corridors could have been enough for immigration. However, considering the wide distribution of the bulky animals in Tibet, Outer Lesser Himalaya (in Kashmir and Nepal) and the Siwalik, more than just corridors were needed to allow heavy traffic and widespread dispersal of these quadrupeds.

19.9 Climate Change and Intensification of Monsoon

The fast rising Himadri must have become a lofty barrier—high enough to cause disruption in the west-to-east flow of air currents, bringing low-pressure area southwards over northern India (Fig. 19.10a). The low-pressure area attracted

moist summer winds from the Indian Ocean and caused spells of heavy rainfall. The sudden appearance of endemic or native upwelling species in the Indian Ocean planktonic assemblages between 8.5 and 7.5 Ma (Prell et al. 1992) indicates activation of upwelling currents, which must have been set in motion at 8 Ma by the south-west monsoon winds. The monsoon climate is characterized by alternating long dry and short wet seasons. It was initiated in the Late Miocene when the Himalaya attained its critical height (Molnar et al. 1993; Valdiya 1999). The ^{13}C values of soil carbonate in the Siwalik succession imply that 10.5–6 Ma ago, the floodplain was covered by C_3 type of vegetation, and in the period 6–1.8 Ma, the C_4 type of vegetation appeared (Sanyal et al. 2004). The $^{18}O/^{16}O$ ratio of the soil-forming clays within the Siwalik sedimentary succession indicates intensification of rainfall at 11, 6 and 3 Ma (Sanyal et al. 2010). This deduction is in agreement with the findings of a study of carbonates in the soil-forming clays in a 54 km stretch of the Ramnagar area in south-western Kumaun, which showed that the $\delta^{16}O$ value varying from -122 ‰ to -5.9 ‰ in the older part increased to nearly $+2$ ‰ in the younger—implying increase in rainfall at 10, 5 and 1.8 Ma (Singh et al. 2012).

Increased rainfall caused acceleration of erosion. There was nearly sudden two-and-half-fold increase of sediment accumulation in the Potwar subbasin at 11 Ma (Burbank et al. 1986) and at about 10 Ma in the Nepalese Arungkhola (Tokuoka et al. 1990) and at 9 Ma in the Tinaukhola (Gautam and Appel 1994). This event implies that the Great Himalaya (Himadri) suddenly became a high mountain and exposed to brisk erosion. The first appearance of kyanite in the heavy mineral assemblage along with sand-sized gneiss fragments in the Middle Siwalik at 9.2 Ma (Hisatomi 1996) corroborates the postulation that the Himadri rose up as a high barrier 9–10 Ma ago. Neodymium–strontium and oxygen isotope compositional similarities demonstrate derivation of the Indian Ocean sediments from the Himalayan crystalline terranes (France-Lanord et al. 1993). Abundance of calcic amphibole at 10.9 Ma and of other heavy minerals between 10.9 and 7.5 Ma in the Bengal Fan deposits in the Bay of Bengal (Amano and Taira 1992) coupled with the manifold increase in the sediment influx into the northern Indian Ocean (Fig. 19.12b) corroborates the deduction that the Himadri was uplifted rapidly in the Late Miocene time (Rea 1992). The intensity of sediment influx into the ocean is further borne out by an abrupt increase of land-derived organic matter from 0.5 to 2 % in Arabian Sea at 9 Ma (Meyers and Dickens 1992). The organic matter was transported with clayey material derived from denudation of the vegetation-covered Lesser Himalaya that was exposed to denudation in the Late Miocene. Not only the organic matter but also the phosphorus content and the Ce/Si ratio in opaline silica of the diatoms and the strontium ratio in the sea water increased perceptively during this time (Filippeli 1997).

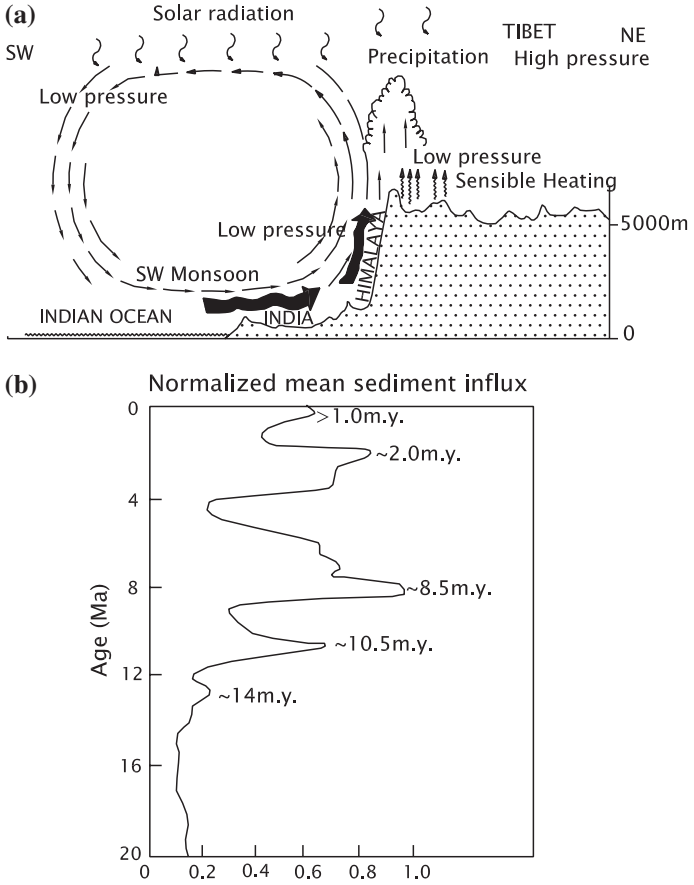

Fig. 19.12 **a** Change in wind circulation due to dramatic rise of the Himalayan barrier, initiating the monsoon cycle. **b** Increased rainfall as a result of intensification of monsoon resulted in larger discharge of sediments to the sea (after Rea 1992)

19.10 Structural Development in Siwalik Terrane

19.10.1 Reactivation of MBT

The revival of tectonic movement towards the end of the Pleistocene at about 1.6 Ma on the MBT and associated faults brought the Lesser Himalayan rocks riding over and trampling upon the Siwalik. In the Amritpur area in southern Kumaun, just north of Haldwani, ~100-m-thick fault damage zone comprises imbricated sheets, and the thrust registers sinistral wrench movement accompanying NNE–SSW-directed horizontal stretching in the fault damage zone (Shah et al. 2012). Deformation of the Siwalik sedimentary pile gave rise to range after range

of hills, many of which were latitudinally cut by faults and thrusts along the strike (Figs. 19.13 and 19.14). The intensity of deformation was strongest and close to the MBT zone. In this zone, folds were tightened and split along axial planes and squeezed out as imbricated stacks. Away from the MBT, the structural architecture varies from tight to open upright folds affected by reverse faults in the middle zone to gentle broad folds in the south. West of the 79° longitude, open synclines alternate with tight anticlines, commonly faulted along their axial planes. Some of the synclines were later filled with subrecent to recent gravel deposits, giving rise to flat intermontane plains called "*duns*" (Fig. 19.15). And east of 87° longitude, the Siwalik terrane is represented only by imbricating stacks of the Siwalik rocks that were involved in duplex tectonics (Fig. 19.14b).

19.10.2 Structural Design in SW Nepal

The structural architecture of the Siwalik in south-western Nepal (Fig. 19.14) is portrayed as simple folds cut by faults, branching off from an underlying decollement—the plane making the boundary between the two different rock successions. The thrust sheets laterally relayed and simultaneously emplaced, resulting in the evolution of a basin on the backside of and attached to another (Chalaron et al. 1995; Mugnier et al. 1999). The north-dipping thrusts delineate tectonic boundaries of the Siwalik units. The Main Dun Thrust—also described as *Central Churia Thrust* (Tokuoka et al. 1986, 1990)—is formed by a succession of laterally relayed thrusts. The Main Frontal Fault, representing the regional *Himalayan Frontal Thrust* (Nakata 1972), is formed of three segments that die out laterally in the propagating folds, or they branch off as relay faults along the lateral transfer zones (Mugnier et al. 1999). These NE–SW trending transfer zones, characterized by sigmoidal folds and strike-slip faults, are one of those *tear* or *wrench faults* that have affected not only the entire Siwalik terrane but also the Lesser Himalaya (Valdiya 1976). Their origin is related to basement scarps or transverse ridge that controls the geometry of the basement decollement.

19.10.3 South-western Uttarakhand

Seismic reflection data show that the Siwalik terrane in the Dehra Dun region comprises anticlines associated with a southward overturned thrust that is rooted in a 6° north-dipping decollement, and the fault-propagation folds have steep limbs in the north and fold propagation and fault-bend folds in the southern limb that gently dips northwards (Powers et al. 1998). The southern boundary of the Dehra Dun Siwalik is demarcated by a series of discontinuous reverse faults and imbrication structures in a 0.5- to 1-km-wide zone of brittle deformation of the *Himalayan Frontal Thrust*, first ever recognized by Nakata (1972). The fault-related folds,

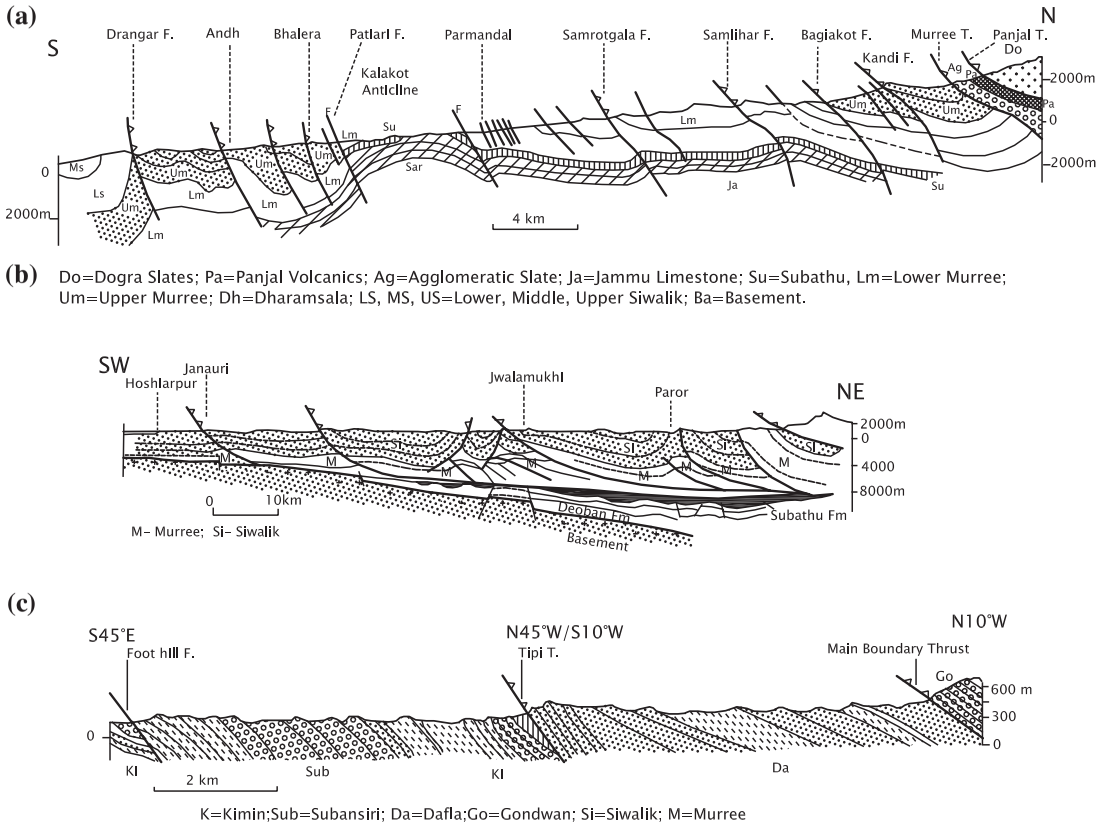

Fig. 19.13 Siwalik structural architecture **a** Jammu region **b** Southcentral Himachal Pradesh (**a** after Karunakaran and Ranga Rao 1979; **b** after Raiverman et al. 1993)

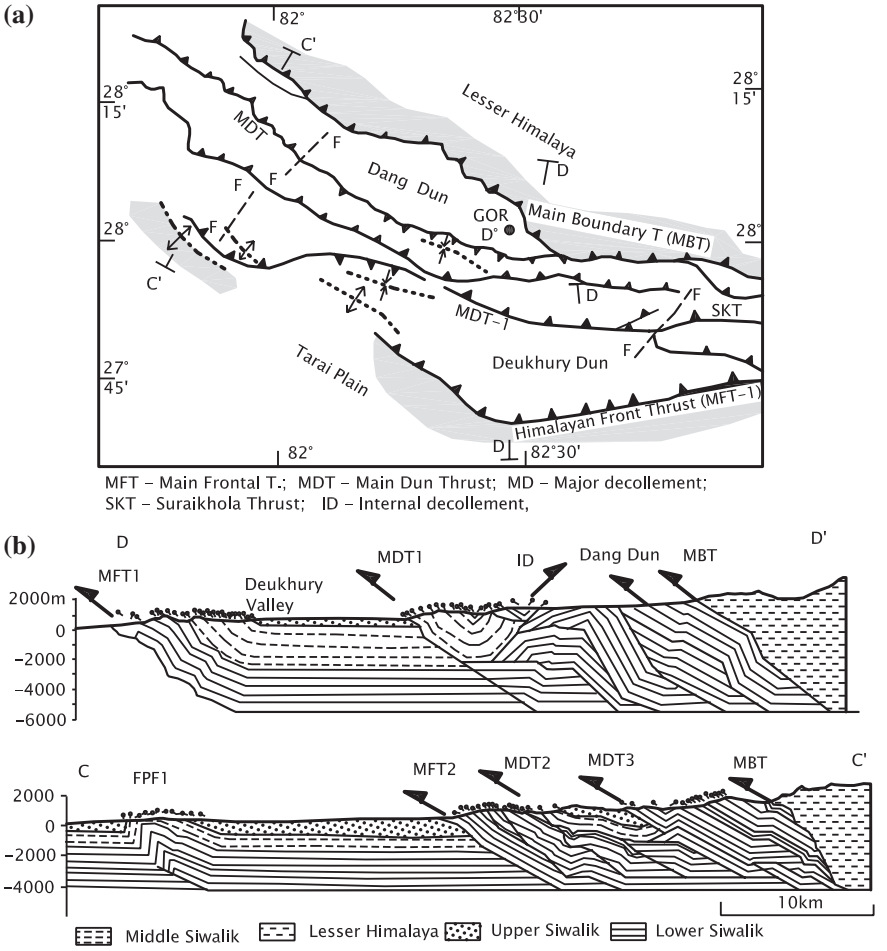

Fig. 19.14 **a** Structural map of the Siwalik domain in south-western Nepal. **b** Cross sections of the Siwalik east and west of the West Dang "transfer zone", a wrench fault system (after Mugnier et al. 1999)

such as the Mohand anticline, have non-cylindrical geometry resulting from climbing of thrust sheets over the frontal and oblique ramps (Srivastava and John 1999). At certain locations, the Himalayan Frontal Thrust is a blind thrust beneath the anticlines (Yeats and Lillie 1991).

North-west of the Dehra Dun re-entrant, the Kangra re-entrant is a south-vergent homoclinal imbricated thrust stacks and associated piggyback basin and antiformal linear thrust stacks (Kak et al. 1999). It was formed as a result of combined frontal and oblique thrust ramps or transverse ridges which were initiated as listric normal faults during a pre-Himalayan tensional phase and were later reactivated as listric thrust during the Himalayan orogeny (Dubey et al. 2004).

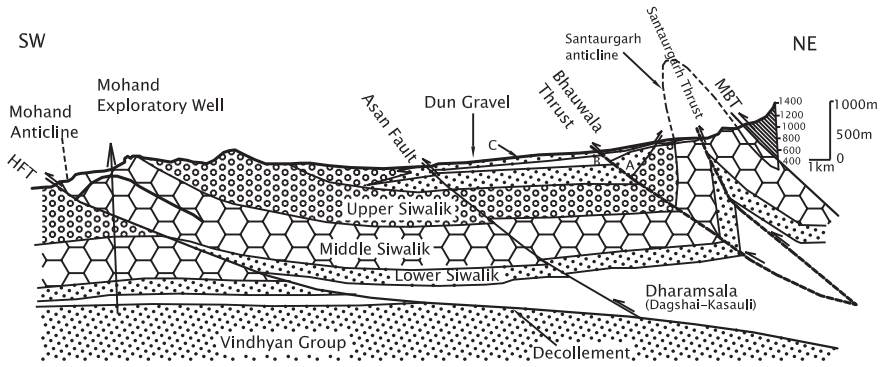

Fig. 19.15 Cross section of the Siwalik in south-western Uttarakhand showing the Dun at the top (after Thakur and Pandey 2004)

19.10.4 Salt Range–Potwar Plateau

A gentle upward convexity of the basement related to formation of a ramp is responsible for the decollement within the Eocambrian evaporite sequence of the Salt Range (Lillie et al. 1987). North of the Salt Range evolved an asymmetric *Soan Syncline*, the northern limb of which is characterized by intense folding, faulting and imbricated stacking of rock units (Fig. 19.16). The 100-km-wide Soan–Salt Range unit moved southwards as a coherent slab over the thick succession of evaporates that covered the basement surface. Strike-slip movements along the decollement surface gave rise to folds that have cores of both blind thrusts and pop-up structures which are overturned both towards the hinterland and the foreland (Pennock et al. 1989; Jadoon et al. 1997). Located not far from the intersection of the E–W trending faults of the Himalayan and the N–S trending sinistral transcurrent *Chaman Fault* (Fig. 19.17), the Kohat plateau is a product of transpressional tectonics. The southward-directed thrusting affected the Precambrian basement and involved it in the deformation that culminated in the formation of positive flower structure (Sercombe et al. 1998). The structures are offset by high-angle oblique-slip reverse faults. The Kohat plateau is separated from the Potwar plateau by the *Kalabagh Fault*, a right-lateral wrench fault trending N15ºW–S15ºE. Its southern boundary is defined by the Surghar Range Thrust, and the northern limit is delineated by the MBT. It exhibits passive-roof duplex geometry (Abbasi and McElroy 1991). The E–W trending thrusts that split the rock successions branch out from the Kalabagh Fault, a wrench fault. While the lower detachment is common to both the Kohat and the Potwar plateaus, the upper level is restricted to the Kohat region.

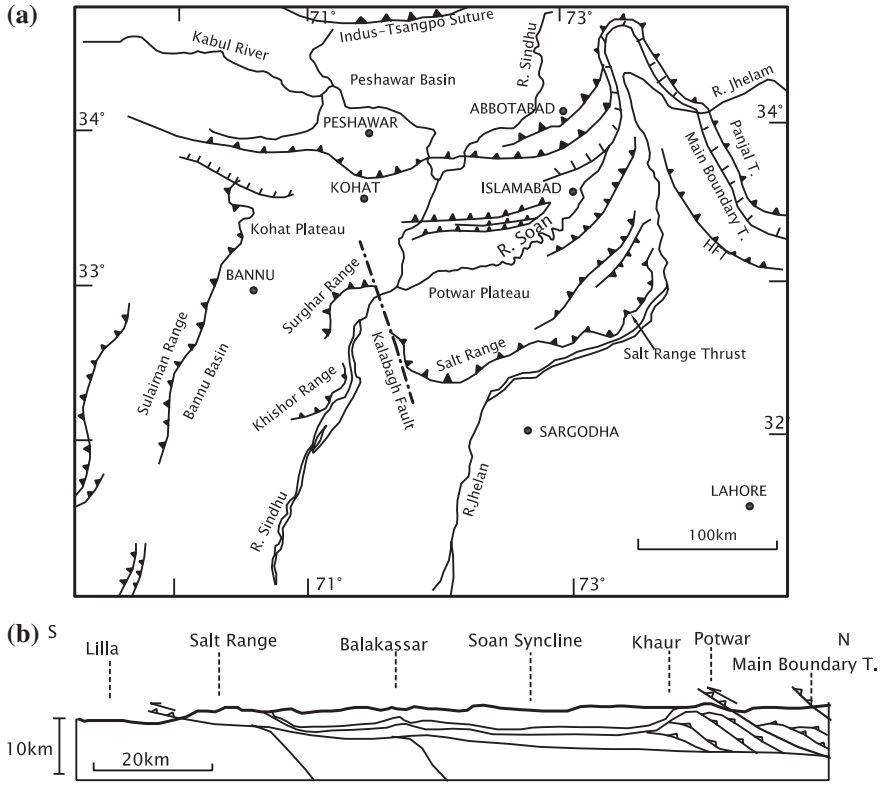

Fig. 19.16 **a** Sketch map shows major thrusts of the Kohat–Potwar region. **b** Cross sections of western Potwar and Kohat plateaus exhibiting the style of deformation (after Abbasi and McElroy 1991)

19.10.5 Sulaiman Fold Belt

The structural design of the Sulaiman Fold Belt (Fig. 19.17), like that of the Salt Range, is characterized by a basal decollement lying within the Eocambrian salt beds, or still deeper older material showing ductile behaviour. Immediately to the west of the frontal folds, a steep and highly elevated zone is underlain by a passive-roof duplex. The roof thrust is really back thrust in relation to the duplex that developed towards the foreland (Humayon et al. 1991). East of the Kangri Fault—a tear fault—crustal shortening amounts to about 108 km. Duplex style of deformation persists throughout the central Sulaiman Belt. High-angle faults that are inclined towards both the hinterland and foreland juxtapose the Cretaceous rocks in the cores of tight symmetrical anticlines against Eocene rocks (Jadoon and Lawrence 1994).

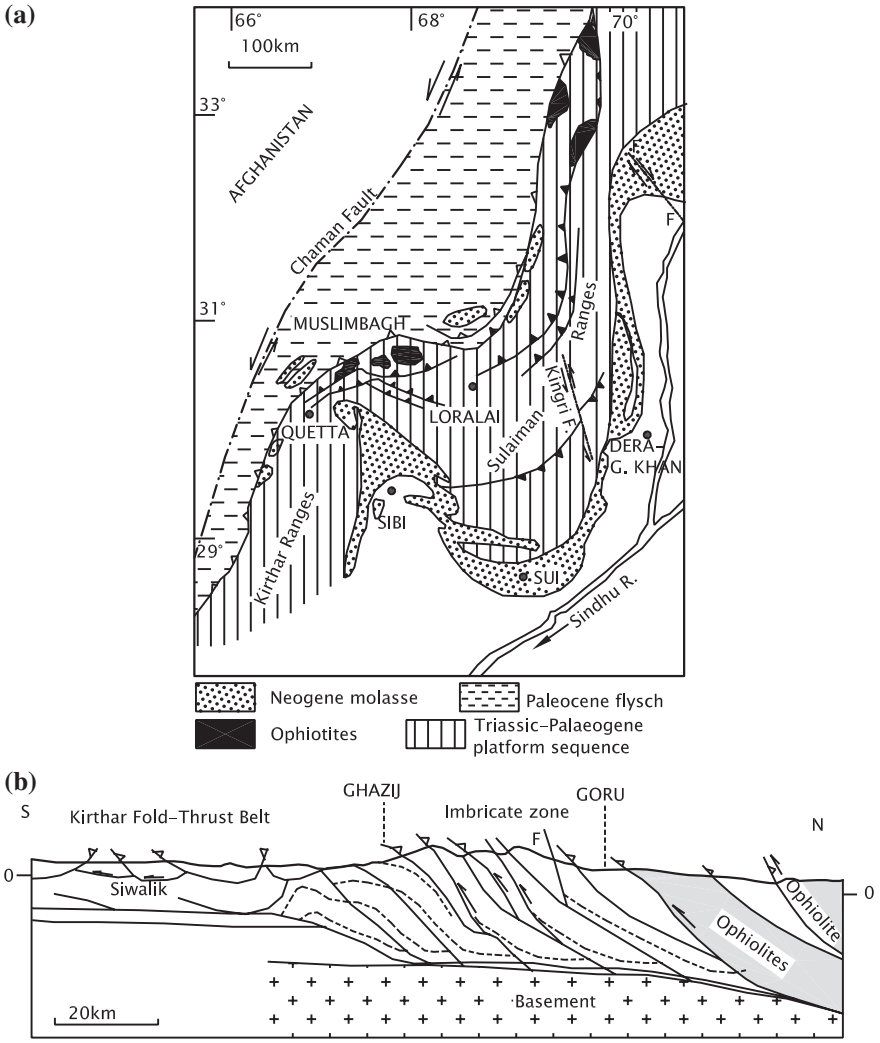

Fig. 19.17 **a** Sketch map of the Sulaiman fold and thrust belt in Pakistan (after Jadoon and Lawrence 1994). **b** Cross section of the western segment of the Sulaiman arc showing passive-roof duplex geometry. The roof sequence has been removed by erosion along passive back thrust (after Banks and Warburton 1986)

19.11 The Tertiary in Myanmar

The Tertiary sedimentary successions occur in three belts: (i) in the west along the Indo-Myanmar Border Ranges including the Arakan Coast with the islands of Ramree and Cheduba; (ii) in the Central Myanmar Belt, associated with the Miocene volcanic arc to its east; and (iii) the mountainous tract in the far east. As

was the case in the HFB and in the pericratonic coastal Tertiary Basins, the marine sedimentation during the Palaeocene to Lower Miocene period gave way to deltaic-to-fluvial sedimentation in the Upper Miocene and Pliocene time (Bender 1983).

19.11.1 Tectonics

In the Central Myanmar Belt (Fig. 19.18), the origin of the Salin Basin is related to right-lateral strike-slip movements along the transcurrent *Sagaing Fault* (Figs. 16.12 and 19.20). There was NW-directed extensional deformation in the Miocene time, followed by transpressional deformation manifested in thrusting and faulting in the Pliocene and continuing into the Pleistocene. It was during the Miocene time that the Myanmar microplate obliquely impacted the Indian plate as it moved northwards along the Sagaing Fault (Pivnik et al. 1998). The Myanmar microplate collided with Asia in the Pliocene, causing transpressional deformation along the Central Myanmar Belt, as clearly discernible in the Salin Basin.

19.11.2 Palaeocene–Eocene Time

Dominantly, Eocene flysch constitutes the larger bulk of the Indo-Myanmar Border Ranges, attaining a maximum thickness of nearly 9000 m in the Arakan sector (Table 19.3). Within this succession occur ophiolites and lentiform horizons of *olistoliths* or *exotic blocks* of shallow water limestones characterized by Palaeocene foraminifer *Ranikotalia* and algae (Nagappa 1959). The Eocene flysch, known as the *Chunsung*, *Ngapali* and *Kyaukkale* formations in the Arakan coastal islands, comprises turbidites, chert beds and limestones that contain Middle Eocene *Nummulites*.

In the Minbu district in the Central Myanmar Belt, a sequence of volcaniclastics and tuffs interbedded with clay (*Kyauktusaw* Formation) represents the Palaeocene epoch. The Eocene succession comprises Laungshe Shale, Paunggyi Conglomerate, Tilin Sandstone, Tabyn Claystone and Pondaung Sandstone. In the Thyetmo area, the *Laungshe Shale* contains *Nummulites atacicus* of Lower to the Middle Eocene. The *Paunggyi Conglomerate* is associated with lithothamnian algal limestone. More than 500-m-thick red beds of the *Tilin Sandstone* form the hill ranges along the Pokoku–Tilin road. The bluish grey clay associated with platy limestone and lignite lenses of the *Tabyn* succession are characterized by typical Kirthar foraminifer *N. atacicus*. The imposing hill ranges in the Minbu district are made up of Middle to Upper Eocene, the *Pondaung Sandstone*, comprising sandstone with intercalations of conglomerate and claystone and red beds in upper part. The succession is characterized by the remains of an Anthracotheriidae vertebrate—*Amphipithecus mogaunggensis*—a lemuroid primate (Szalay 1970) and the earliest known anthropoid primate *Pondaungia cotteri* (BaMaw et al. 1979).

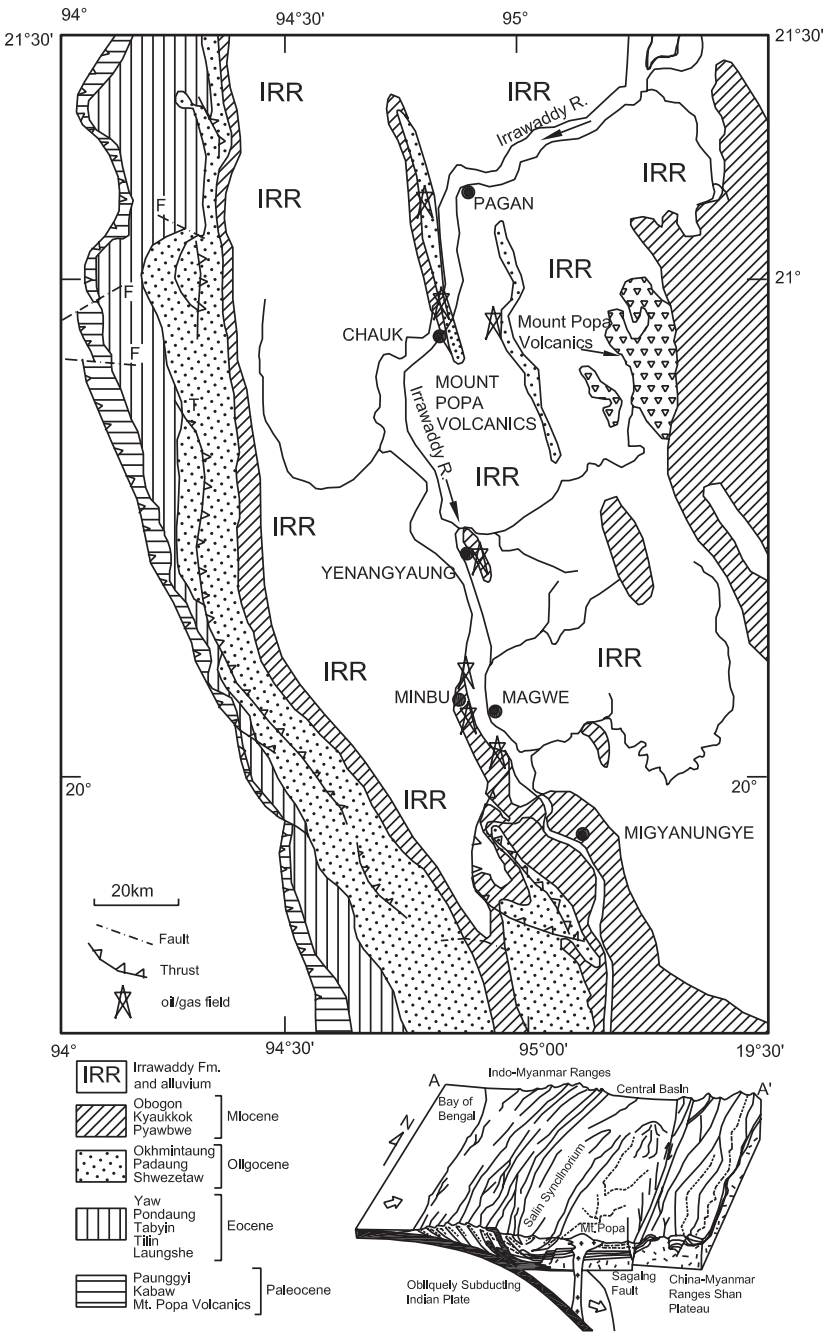

Fig. 19.18 **a** Reconstruction of structure of the Jwalamukhi gas field in southcentral IRR-Irrawaddy Plains Himachal Pradesh (Powers et al. 1998). **b** Khairpur–Jacobabad cross section elucidates the structure of the Sui gas reservoir containing more than 20 tcf of recoverable gas (Siddiqui 2004)

Table 19.3 Tertiary Formations occurring in two belts of Myanmar (after Bender 1983)

	Arakan coast and Indo-Myanmar Border ranges	Central Myanmar Basin
Miocene	Leikkanaw Formation	Obogon Formation
	Sane Formation	Kyaukkok Formation
	Ngo-Ok Formation	Pyawbwe Formation
Oligocene	Kalangyan Formation	Okhmintaung Formation
	Yechangi Formation	Padaung Formation
		Schwezetaw Sandstone
Eocene	Kyaukkale/Chunsung	Pondaung Formation/Yaw Formation
		Tilin/Tabyin Formation
		Laungshe Shale
Palaeocene		Paunggyi Formation

The disconformably succeeding *Yaw Shale* characterized by bituminous coal west of Kalewa contains *Nummulites striatus, Discocyclina sella and Operculina canalifera* of the Upper Eocene age (Table 19.3).

19.11.3 Oligocene Epoch

The *Shwezetaw Sandstone*, the *Padaung Formation* and the *Okhimintaung Formation* of the synclinal Salin Basin represent the Oligocene in the Central Myanmar Belt. Made up of fine-grained sandstones, siltstones and shales, the Oligocene succession is characterized by *Globularia birmanica* and *Globorotalia* in the lower level; corals and gastrapods *Lyria varicosa and Turricula birmanica* and foraminifer *Globorotalia opima* with *Ammonia* and *Florilus* of the Upper Oligocene age in the middle part (Kyi 1970); and *Heterostegina* and *Lepidocyclina* in the limestone within the upper horizon at Thayetmyo on the bank of the Irrawaddy.

In the Arakan sector of the Indo-Myanmar Border Ranges, the Oligocene planktonic foraminifers such as *Globigerina suturalis* and *Globorotalia opima* occur in the successions described as the *Yechangi* and the *Kalangyan* formations of the flysch facies.

19.11.4 Miocene Successions

In the Arakan coastal sector, including the islands of Ramree and Cheduba, the Miocene is represented by another flysch succession that is divisible into three units. The *Ngo-Ok Formation* in the lower part is made up of conglomerate and

greywacke with claystone, containing benthic foraminifers *Orbulina suturalis* and *Globorotalia peripheronda* of the Lower Miocene age (Helmecke and Ritzkowski in Bender 1983). The overlying *Sane Formation* is characterized by *Globigerinoides primordius* and *Globorotalia kugleri*. The *Leikkanaw Sandstone* contains Upper Miocene ichnofauna.

In the Minbu area in the Central Myanmar Belt, the Okhmintaung is unconformably overlain by a succession of Pyawbwe, Kyaukkok and Obogon formations assigned to the Miocene epoch. The *Pyawbwe* Shales contain coral *Callistoma singuense* and the lamellibranchs *Anadara pethensis*, *Dosinia protojuvenitis, Indoplacuna birmanica* and *Paphia protolirata* (Eames 1950). In the Prome area of the Irrawaddy delta, *Miogypsina*-bearing limestone also contains ostracodes of the Miocene age. The *Kyaukkok* Formation is very sandy and characterized by rich assemblage of molluscs including *Conus bonneti, Loxocardium minbuense* and *Trachycardium subrugosa*. The *Obogon* Formation is a sequence of alternation of fine-grained sandstone and claystone containing the Middle Miocene fauna (Kyi 1970). In the delta of the Irrawaddy River, the Miocene strata are interbedded with volcaniclastic sediments (Bender 1983). Evidently, volcanoes of the Cental Myanmar Belt had become active during the Miocene sedimentation (Fig. 19.18).

19.12 Mineral Assets of Foreland Basins

The Early Palaeocene was a time of formation of *lignite* and *coal*, as seen in the Palana area in western Rajasthan, the Kalakot Belt in Jammu, the Mikir Hills in Assam and the southern flank of the Meghalaya massif. In the Lakhpat area in western Kachchh, the lignite deposits occur in the deltaic deposits of Lower to Middle Eocene (Mukhopadhyay and Shome 1996). Vegetable debris derived from lush forests accumulated in lakes, estuaries and riverine pools and were eventually converted into coal, passing through the stages of peat and lignite. Workable deposits of the Palaeocene lignite and subbituminous coal occur in the Makeral, Khushah–Dandot, Quetta, Hyderabad and Chhoi (Kalachitta) areas in Pakistan. The Salt Range coal seams are parts of the Patala Shale; the Quetta coal reserve is constituted of three lenticular seams in the middle of the Ghazij Formation of the Eocene age; and the Hyderabad coal deposits at Jatta, Bahadurkhel and Karak in Kohat and Upper Indus Basin occur in the Laki (Early Eocene) succession (Raza and Iqbal 1977).

Constituting merely 0.43 % of the total coal reserve of India, the 887 million tonnes of Tertiary coal occur in the Palaeocene—Lower Eocene horizons in the Garo Hills (Meghalaya), Mikir Hills (Assam) and Jammu Hills (J & K) in the Palana area (Rajasthan); and in the Upper Tertiary Formations in Upper Assam, Namchik and Namphul areas in Arunachal Pradesh, South Arcot (Tamil Nadu), and Varkala and Quilon (Kerala) (Table 19.4).

Table 19.4 Tertiary coal reserve (Chandra et al. 2000)

State	Total reserve (million tonnes)	Proven reserve (million tonnes)
Assam	317	228
Arunachal Pradesh	90	31
Meghalaya	459	118
Nagaland	3	20

At the Jwalamukhi temple in southcentral Himachal (Fig. 19.16a), methane gas has been coming out uninterruptedly since time immemorial. The source is believed to be the Palaeocene–Lower Eocene sediments. Made up of olive green, grey and black shales, and prominent beds of shelly and foraminiferal limestones, the Subathu Formation and its coevals are the horizons in which *petroleum oil* and *gas* were formed from organic matter deposited in an environment deficient in oxygen. Bacterial activity in the upper 30–40 cm depth of sediments broke down plant and animal debris—algae, fungi, diatoms, foraminifers, radiolarians and possibly sponges and jelly fish—and converted chemically through different stages like fats, amino acids, lignins and lipids to finally oil and gas. Some clays and metallic elements were possibly active as catalyzing agents. The Middle Palaeocene Lokhartia Limestone, the Early Eocene Sakesar Limestone and the Chorgali Formation in Pakistan provided the right conditions for the formation of hydrocarbon deposits (Raza and Iqbal 1977).

The Kohat–Potwar depression (Fig. 19.19) comprises more than 5000-m-thick pile of marine sediments ranging in age from the Proterozoic to the Eocene and more than 10,000 m of Miocene to Pleistocene alluvial sedimentary deposits. There are ten oil fields, with a total ultimately recoverable hydrocarbon reserve of nearly 2.4 billion bbl of oil equivalents, of which 200 million bbl form a recoverable reserve (Khan et al. 1986). The Paleogene horizons are the source of the hydrocarbons. A recoverable reserve of more than 20 tcf of gas in 14 fields occurs in porous reservoir contained in the Ypresian *Sui Main Limestone* (Fig. 19.18b), the underground extension of the Laki Formation (Siddiqui 2004). Sandwiched between impervious shales, this porous limestone forms a trap at the apex of a mound. A deep-seated N–S trending rift, comprising horst and grabens at great depth in the southern Sindhu Basin, holds prospects of discoveries of oil and gas (Zaigham and Mallick 2000).

Since the first discovery of oil in 1889 at Digboi in Upper Assam, more than 310 oil and gas fields have been discovered in the Tertiary Basins of the Indian subcontinent, thirty of them in Assam alone. These include the giant fields of Bombay High, Vasai, Ankleshwar, Gandhar, Lakwa–Lakhmani, South and Middle Tapti and Nahorkatiya. The Andaman and Nicobar and Kachchh basins are known to have accumulations of hydrocarbons but without commercial production. The hydrocarbon resource of India is estimated to be of the order of 32 billion tonnes, of which the proven reserve is only 7.57 billion tonnes (Chandra 2004).

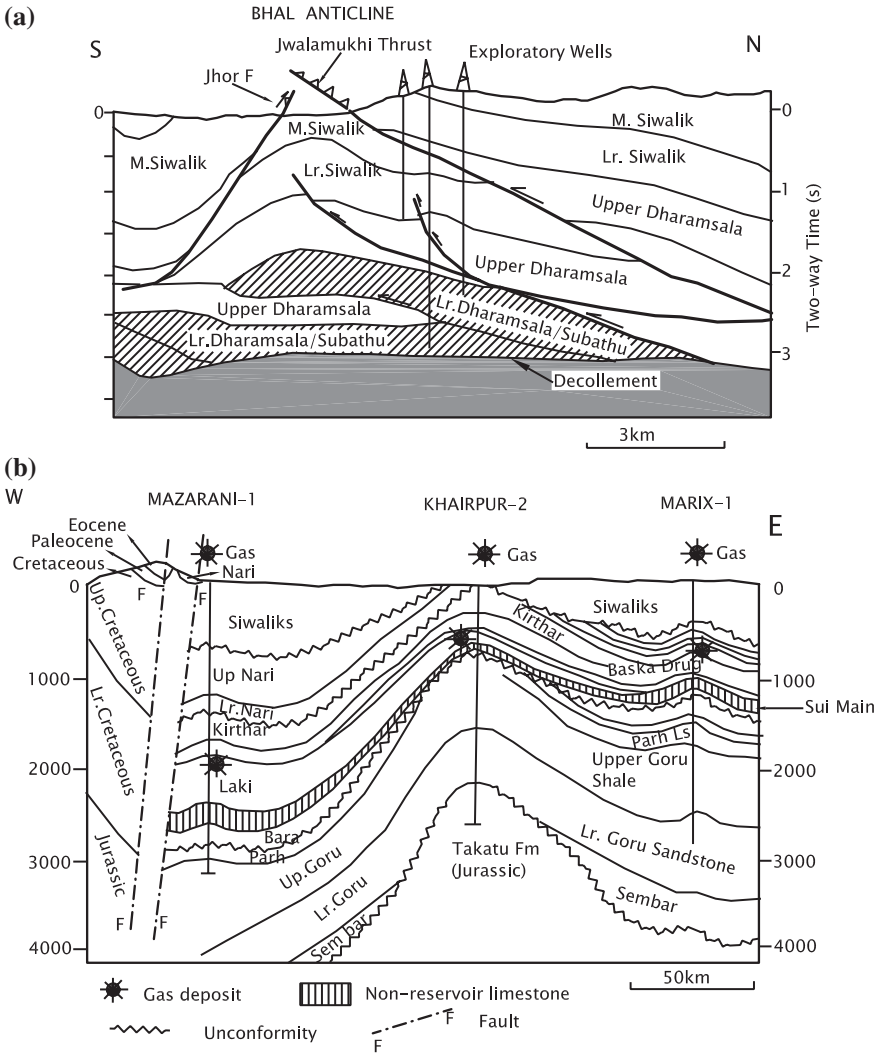

Fig. 19.19 Location of oil and gas fields in the Kohat–Potwar depression in the context of tectonic setting (**a** after Sercumbe et al. 1998; **b** after Khan et al. 1986)

In Upper Assam, the sandstone of the middle part of the Lakadong succession (of the Sylhet Formation) forms the reservoirs of hydrocarbons (Bharali et al. 1995). It is seen that in Assam, there are two petroleum systems—(i) the organic-rich carbonaceous shales, coals and subordinate limestone of the Upper Eocene to Lower Eocene Sylhet Limestone and the Upper Palaeocene Langpar Formation (Handique and Bharali 1981), and (ii) the Oligocene Barail Formation including

the carbonaceous shale of the Moran horizon (Fig. 19.20). In both systems, the source rocks are interbedded with reservoir rocks (Kent et al. 2002), the source rock being deposited in fresh to brackish water under turbid conditions (Saikia and Dutta 1980). The fluvial–paralic character of reservoir units in both the petroleum systems is exhibited in many local intraformational scales, the Girujan Clay providing the regional top seal (Kent et al. 2002).

The Nahorkatiya, Jorjan and associated satellite fields are located along the crest of a structural nose that plunges beneath the *Naga Thrust* (Figs. 19.20 and 19.21) and forms a focus for migration. Except for the Borholla–Champang field, which occurs immediately in front of and under the leading edge of the Naga Thrust, all other fields extending beneath the Naga Thrust are located where the mountain front is oriented E–W at nearly 90º to its normal NE–SW trend (Krishna Rao and Prasad 1982).

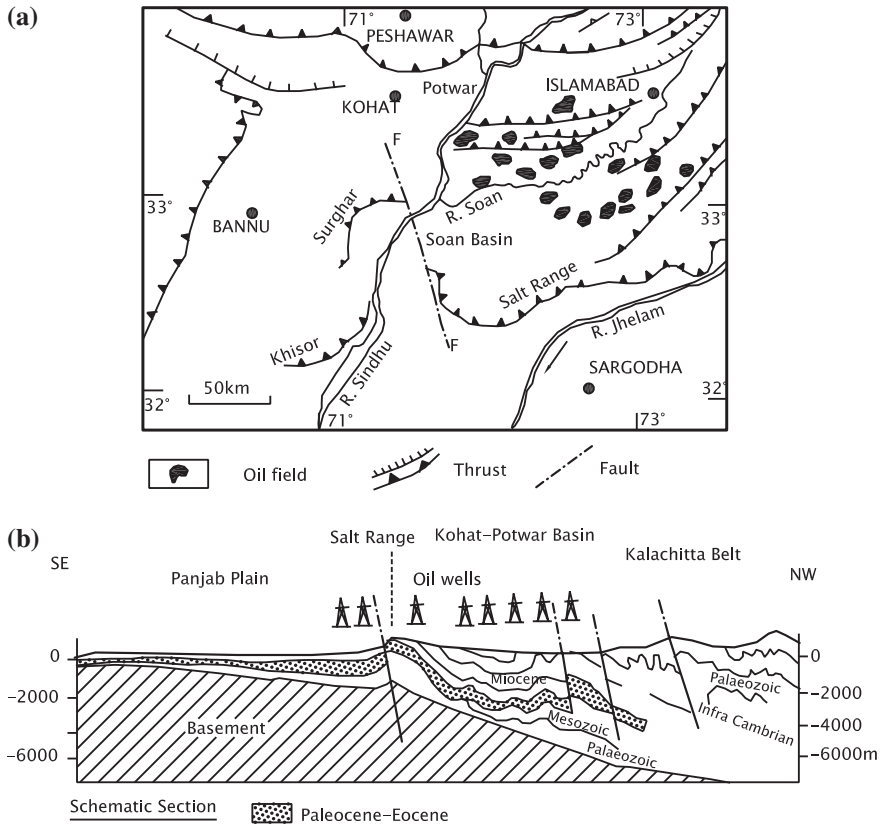

Fig. 19.20 Geological sketch map of Assam showing the location of oil fields (based on Desikachar 1984; Dasgupta 1977; Viswanath 1997 and Kent et al. 2002)

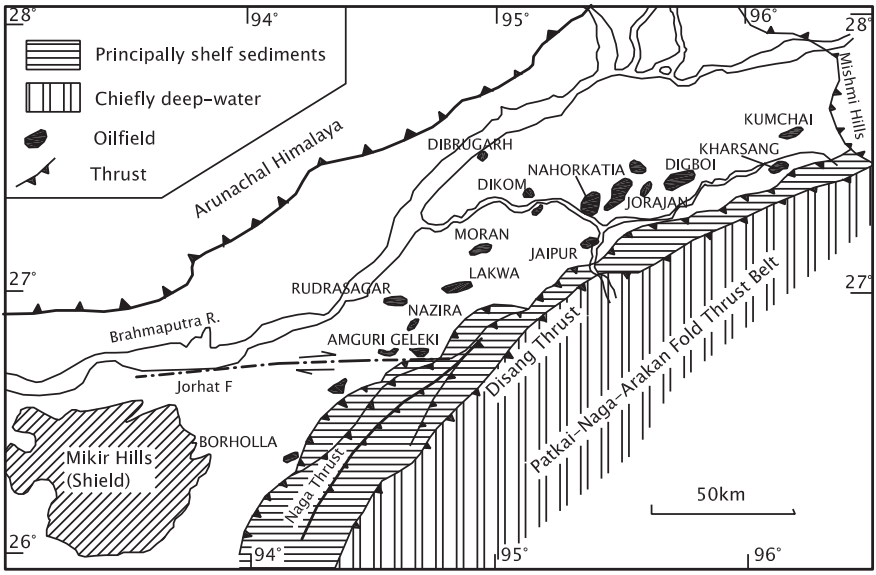

Fig. 19.21 **a** Schematic section of the Assam Basin, showing the location of the reservoirs of hydrocarbon deposits (Desikachar 1984). **b** Cross sections showing the structure of the Digboi oil field and the location of reservoirs in structural traps (Kent et al. 2002)

Evaporite deposits of great economic value occur at Jatta, Bahadurkhel and Karak in Kohat and upper Sindhu Basin. At Jatta, a 100-m-thick salt bed underlies a horizon of gypsum, dolomite and claystone. The Bahadurkhel salt deposit is more than 500 m thick. Associated with dolomite and organic laminate, the gypsum and anhydrite beds form a Sabka-type cyclic sequence in the Ghazij Formation in the Lower Indus Basin and all along the Sulaiman–Kirthar Belt in the Marri–Bugti Hills at Jatta in Kohat and in the Sakesar Limestone of the Salt Range.

Between Poonch by the Jhelum River in the west and Tanakpur on the bank of River Kali in the east, *uranium mineralization* of importance has been recorded in 350-odd places. The mineralization is restricted to horizons in the upper part of the Lower Siwalik, the upper part of the Middle Siwalik and the lower part of the Upper Siwalik. The uranium minerals such as uraninite, pitchblende, coffinite and a variety of secondary minerals such as uranophane occur in small lensoid bodies ranging in length from a few tens of metres to 1700 m, their thickness varying from less than a metre to 4 m (Kaul et al. 1993). The raw material contains 0.02–0.06 % of U_3O_8.

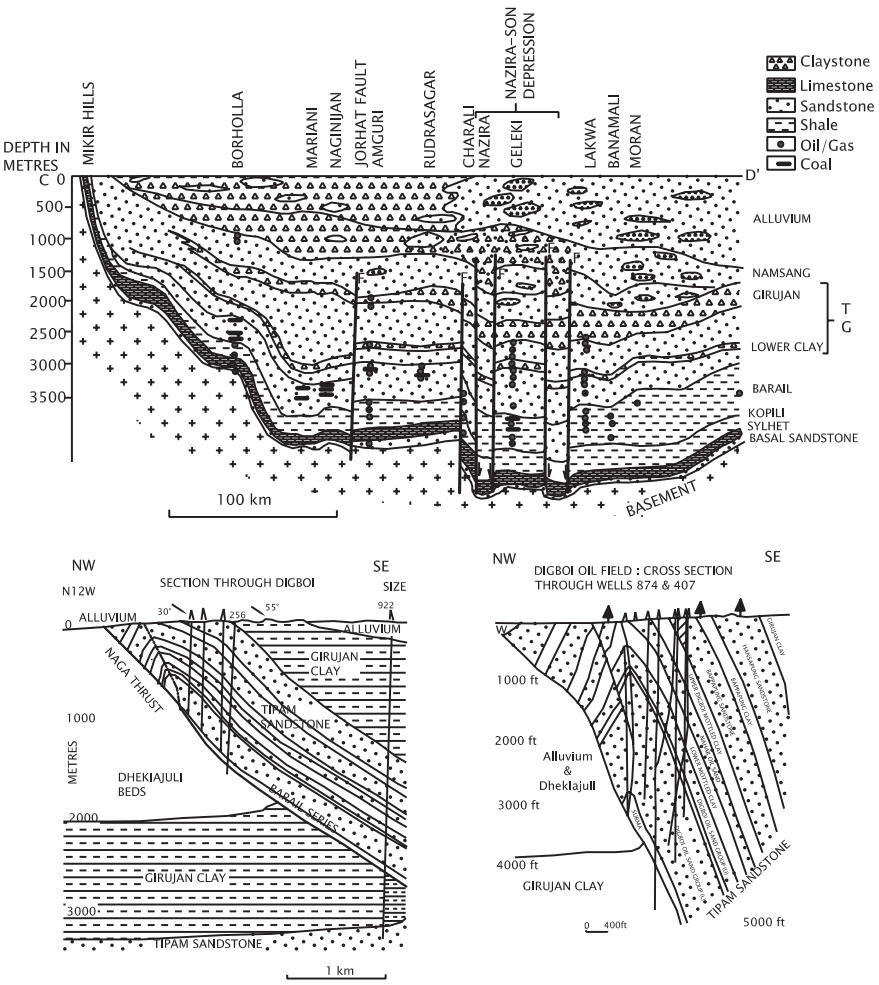

Fig. 19.21 (continued)

References

Abbasi, I. A., & Friend, P. F. (2000). Exotic conglomerates of the Neogene Siwalik succession and their implications for the tectonic and topographic evolution of the Western Himalaya, In M. A. Khan et al (Eds.), Tectonics of the Nanga Parbat syntaxis and the Western Himalaya (pp. 455–466). London: Geological Society.

Abbasi, I. A., & McElroy, R. (1991). Thrust kinematics in the Kohat Plateau, Trans-Indus Range, Pakistan. *Journal of Structural Geology, 13*, 319–327.

Alam, M. (1989). Geology and depositional history of Cenozoic sediments of the Bengal Basin of Bangladesh. *Palaeogeography, Palaeoclimatology, Palaeoecology, 69*, 125–139.

Alam, M., Alam, M. M., Curray, J. R., Chowdhury, M. L. R., & Gani, M. R. (2003). An overview of sedimentary geology of the Bengal Basin in relation to the regional framework abd basin-fill history. *Sedimentary Geology, 155*, 179–208.

Amano, K., & Taira, A. (1992). Two-phase uplift of Higher Himalayas since 17 Ma. *Geology, 20*, 391–394.

Antoine, P. O., & Welcomme, J. L. (2000). A new *Rhinocerosus* from the Lower Miocene of the Bugti Hills, Baluchistan, Pakistan. *Palaeontology, 43,* 795–816.

Awasthi, N. (1982). Tertiary plant megafossils from the Himalaya: A review. *Palaeobotanist, 30*, 254–267.

Bajpai, S., & Gingerich, P. D. (1998). A new Eocene archaeocete (*Mammalia, Cetacea*) from India and the time of origin of whales. *Proceedings of the National Academy of Sciences of the United States of America, 95*, 15464–15468.

BaMaw, R. L., & Savage, D. E. (1979). Late Eocene of Burma yields earliest anthropoid primate, Pondaungia cotteri. *Nature, 282*(5734), 65–67.

Banks, C. J., & Warburton, J. (1986). 'Passive-roof' duplex geometry in the frontal structures of the Kirthar and Sulaiman mountain belt, Pakistan. *Journal of Structural Geology, 8*, 229–237.

Barry, J. C., Morgan, M. E., Flynn, L. J., Pilbeam, D., Jacobs, L. L., Lindsay, E. H., et al. (1995). Patterns of faunal turnover and diversity in the Neogene Siwaliks of Northern Pakistan. *Palaeogeography, Palaeoclimatology, Palaeoecology, 115*, 209–226.

Bender, F. (1983). *Geology of Burma* (p. 293). Berlin: Gebruder Borntraeges.

Bhakuni, S. S., Luive, K., & Mrilanee Devi, R. K. (2012). Soft-sediment deformation structures (seismites) in Middle Siwalik sediments of Arunachal Pradesh, NE Himalaya. *Himalayan Geology, 33*, 139–145.

Bhandari, L. L., Fuloria, R. C., & Sastri, V. V. (1973). Stratigraphy of Assam Valley, India. *Bulletin American Association of Petroleum Geologists, 57*, 642–656.

Bharali, B., Rath, S., Mallick, R. K., & Saikia, B. (1995). Depositional systems and their relation to habitat of oil in Paleocene—Lower Eocene rocks in parts of Assam basin. In *Proceedings of First International Petroleum Conferences* (pp. 165–174). Delhi: B.R. Publishing Corporation.

Bhatia, S. B. (1982). Facies, flora, fauna of the Lower Tertiary formations of the Himalaya: A synthesis. *Journal of Palaeontology Society India, 31*, 8–20.

Bhatia, S. B. (2000). Faunal and floral diversity in the Subathu-Dagshai passage beds: A review. *Himalayan Geology, 21*, 87–97.

Bhatia, S. B. (2003). Facies, fossils and correlation of Late Miocene fluvial sequences of the Himalayan foreland basin. *Current Science, 84*, 1002–1005.

Bhatia, S. B., & Bhargava, O. N. (2006). Biochronological continuity of the Paleogene sediments of the Himalaya-Foreland Basin: Palaeontological and other evidences. *Journal of Asian Earth Sciences, 26*, 477–487.

Bhatia, S. B., & Mathur, N. S. (1965). On the occurrence of pulmonate gastropods in the Subathu-Dagshai passage beds near Dharampur, Simla Hills. *Bulletin Geology Social India, 2*, 33–36.

Biswas, S. K. (1973). Time stratigraphic classification of the Tertiary rocks of Kutch—A revision and amendments. India: *Quaternary Journal of Geology, Mineral, Metal Society, 44*.

Biswas, S. K. (1992). Tertiary stratigraphy of Kutch. *Journal of Palaeontology Society India, 37*, 1–29.

Biswas, A., & Mukhopadhyay, B. P. (2011). Signature of Paleogene submarine fan from the Jenam Formation, Barail Group, Assam-Arakan Orogen, Northeastern India. *Journal of Geological Society of India, 78*, 510–522.

Biswas, S. K., & Raju, D. S. N. (1973). The rock stratigraphic classification of the Tertiary sediments of Kutch. *Bulletin ONGC, 10*, 37–46.

Bossart, P., & Ottiger, R. (1989). Rocks of the Murree formation in northern Pakistan: Indicators of a descending foreland basin of Late Palaeocene to Middle Eocene age. *Eclogae Geologicae Helvetiae, 82*, 133–165.

Brookfield, M. E. (1993). The Himalayan passive margin from Precambrian to Cretaceous times. *Sedimentary Geology, 84*, 1–35.

Burbank, D. W., Raynold, R. G. H., & Johnson, G. D. (1986). Late Cenozoic tectonics and sedimentation in the southwestern Himalayan foredeep. In C. Paola & K. Kleinspehn (Eds.), *New Perspective in Basin Analysis* (pp. 331–351). New York: Springer.

Chalaron, E., Mugnier, J. L., & Marsle, G. (1995). Control on thrust tectonics in the Himalayan foothills: A view. *Tectonophysics, 248*, 139–163.

Chandra, A. (2004). Emerging trend in oil and gas exploration in India—A bright future ahead. *Journal of Geophysical, 25*, 3–11.

Chandra, D., Singh, R. M., & Singh, M. P. (2000). *Text book of coal (Indian context)* (p. 402). Varanasi: Tata Book Agency.

Chaudhari, R. S. (1972). Heavy minerals from the Siwalik formations of northwest Himalaya. *Sedimentary Geology, 8*, 72–82.

Cheema, M. R., Raza, S. M., & Ahmad, H. (1977). Cainozoic. In S. M. I. Shah (Ed.), *Stratigraphy of Pakistan* (pp. 56–101). Quetta: Geological Survey of Pakistan.

Chirouze, F., Dupont-Nivet, G., Huyghe, P., vander Beek, P., Chakraborti, T., Bernet, M., & Erens, V. (2012). Magnetostratigraphy of the Neogene Siwalik Group in far-eastern Himalayan: Kameang section, Arunachal Pradesh, India. *Journal of Asian Earth Sciences, 44*, 113–117.

Cina Sara, E., Yin Grove, M., Dubey, S. C., Shukla, D. P., Lovera, O. M., Kelty, T. K., et al. (2009). Gangdese arc detritus within the Eastern Himalayan Neogene foreland basin: Implications for the Neogene evolution of the Yalu-Brahmaputra River System. *Earth & Planetary Sciences Letters, 285*, 150–162.

Colchen, M., Marcle, G., & Van Haver, T. (1986). Some aspects of collision tectonics in the Indus Suture Zone, Ladakh. *Geological Society of London, Special Publication, 19,* 173–174.30.

Cornivus, G. (1995). Quaternary stratigraphy of the intermontane Dun Valley of Dang-Deokhuri and associated pre-historic settlements in western Nepal. *Memoir. Geological Society of India, 32*, 124–149.

Critelli, S., & Garzanti, E. (1994). Provenance of the Lower Tertiary Murree redbeds (Hazara–Kashmir Syntaxis, Pakistan) and initial rising of the Himalayas. *Sedimentary Geology, 89*, 265–284.

Critelli, S., Rosa, R. D., & Platt, J. P. (1990). Sandstone detrital modes in the Makran accretionary wedge, SW Pakistan: Implications for tectonic settling and long-distance turbidite transportation. *Sedimentary Geology, 68*, 241–260.

Dasgupta, A. B. (1977). Geology of Assam-Arakan region. *Quarterly Journal Geological Mining & Metallurgical Society of India, 49*, 1–57.

Datta, A. K. (1983). Geological evolution and hydrocarbon prospects of Rajasthan basin. *Petroleum Asia Journal* (pp. 93–100). Dehradun: ONGC.

DeCelles, P. G., Gehrels, G. E., Quade, J., & Ojha, T. P. (1998). Eocene-Early Miocene foreland basin development and the history of Himalayan thrusting, western and central Nepal. *Tectonics, 7*, 741–765.

Desikachar, S. V. (1984). Oil-gas deposits in the deltaic sequence of sediments in Cambay Basin and Upper Assam valley. *Journal of Geological Society of India, 25*, 200–220.

Dubey, A. K., Bhakuni, S. S., & Selokar, A. D. (2004). Structural evolution of the Kangra recess, Himachal Himalaya: A model based on magnetic and petrobaric strains. *Journal of Asian Earth Sciences, 24*, 245–258.

Eames, F. E. (1950). The Pegu system of central Burma. *Record Geological Survey of India, 81*, 377–388.

Eremenko, N. A., & Negi, B. S. (1968). *Tectonic Map of India*. Dehradun: 1:20,00,000 scale ONGC.

Filippeli, G. M. (1997). Intensification of the Asian monsoon and chemical weathering event in the Late Miocene-Early Pliocene: Implications for a Late Neogene climate change. *Geology, 25*, 27–30.

Flynn, L. J. (2000). The great small-mammal revolution. *Himalayan Geology, 21*, 39–42.
France-Lanord, C., Cerry, L., & Michard, A. (1993). Evolution of the Himalaya since Miocene time: Isotopic and sedimentologic evidence from the Bengal Fan. In P. J. Treloar & M. P. Searle (Eds.), *Himalayan Tectonics* (pp. 603–621). London: Geological Society of London.
Friend, P. E., Raza, S. M., Geehan, G., & Sheikh, K. A. (2001). Intermediate-scale architectural features of the fluvial Chinji Formation (Miocene) Siwalik Group, northern Pakistan. *Journal of Geological Society of London, 158*, 163–177.
Gani, M. R., & Alam, M. M. (1999). Trench-slope controlled deep-sea clastics in the exposed Lower Surma Group in the southeastern fold-belt of the Bengal Basin, Bangladesh. *Sedimentary Geology, 127*, 221–231.
Gani, M. R., & Alam, M. M. (2003). Sedimentation and basin-fill history of the Neogene clastic succession exposed in the southeastern fold-belt of the Bengal Basin, Bangladesh: A high resolution sequence stratigraphic approach. *Sedimentary Geology, 155*, 227–270.
Gani, M. R., Royhan, & Alam, M. M. (2004). Fluvial facies architecture in small-scale river systems in the Upper Dupitila Formation, northeast Bengal Basin, Bangladesh. *Journal of Earth Sciences, 24*, 225–236.
Gautam, P., & Appel, E. (1994). Magnetic polarity stratigraphy of the Siwalik Group sediments of Tinaukhola section in westcentral Nepal. *International Geophysical Journal, 117*, 223–234.
Gautam, P., & Rosler, W. (1999). Depositional chronology and fabric of Siwalik Group sediments in central Nepal from magnetostratigraphy and magnetic anisostropy. *Journal of Asian Earth Sciences, 17*, 659–682.
Ghosh, S. K., Sinha, S., & Kumar, Rohtash. (2009). Response to 10-Ma thrusting event in the Himalayan foreland sediments, Kangra sub-basin, Himachal-Pradesh. *Himalayan Geology, 30*, 1–15.
Gingerich, P. D., Raza, S. M., Arif, M., Anwar, M., & Zhou, X. (1994). New whale from the Eocene of Pakistan and the origin of cetacean. *Nature, 368*, 844–848.
Guleria, J. S., Srivastava, R., & Prasad, M. (2000). Some fossil leaves from the Kasauli Formation of Himachal Pradesh, NW India. *Himalayan Geology, 21*, 43–52.
Handique, G. K., & Bharali, B. (1981). Temperature distribution and its relation to hydrocarbon accumulation in Upper Assam Valley, India. *American Association of Petroleum Geologists, 65*, 1633–1641.
Hisatomi, K. (1996). The sandstone petrography of the Churia (Siwalik) Group in the Arung Khola-Binai Khola area, westcentral Nepal. *Bulletin Faculty of Education, Wakayama University, Japan, 39*, 5–29.
Humayon, M., Lillie, R. J., & Lawrence, R. D. (1991). Structural interpretation of the eastern Sulaiman Fold Belt and foredeep, Pakistan. *Tectonics, 10*, 299–324.
Jadoon, I. A. K., Frisch, W., Kamal, A., & Jaswal, T. M. (1997). Thrust geometries and kinematics in the Himalayan foreland (North Potwar deformed zone), North Pakistan. *Geologische Rundschau, 86*, 120–131.
Jadoon, I. A. K., & Lawrence, R. D. (1994). Mari-Bugti pop-up zone in the central Sulaiman fold belt, Pakistan. *Journal of Structural Geology, 16*, 147–158.
Jafar, S. A., & Singh, O. P. (1992). K/T boundary species with Early Eocene nannofossils discovered from Subathu Formation, Shimla Himalaya. *Current Science, 62*, 409–413.
Jalal, P., Ghosh, S. K., & Sundriyal, Y. P. (2011). Detrital modes of Neogene Siwalik sandstone of the Ramganga sub-basin, Kumaun sub-Himalaya: Implication for the source area tectonic history. *Himalayan Geology, 32*, 123–135.
Jauhari, A., & Agarwal, K. K. (2001). Early Paleogene in south Shillong Plateau, NE India: Local biostratigraphic signals of global tectonic and oceanic changes. *Palaeogeography, Palaeoclimatology, Palaeoecology, 168*, 187–203.
Johnson, S. Y., & Alam, A. M. N. (1991). Sedimentation and tectonics of the Sylhet through, Bangladesh. *Geological Society of America Bulletin, 103*, 1513–1527.
Johnson, M. R. W., & Oliver, G. J. H. (1990). Pre-collision and post-collision thermal events in the Himalaya. *Geology, 18*, 753–756.

Johnson, G. D., Opdyke, N. M., Tandon, S. K., & Nanda, A. C. (1983). The Magnetic polarity stratigraphy of the Siwalik Group at Haritalyanagar, District Bilaspur, H.P. *Himalayan Geology, 12*, 118–144.

Juyal, K. P., & Mathur, N. S. (1990). Ostracoda from the Kakara and Subathu formations of Himachal Pradesh and Garhwal Himalaya. *Journal of Himalayan Geology, 1*, 209–223.

Juyal, K. P., & Mathur, N. S. (1992). Ostracodes from the Subathu Formation of Jammu region, J & K State. *Journal of Himalayan Geology, 3*, 21–35.

Kak, H. L., Kar, B. K., & Shukla, K. M. (1999). Structural style of frontal thrust-fold belt of northwestern Himalaya. *Bulletin ONGC, 36*, 89–96.

Karunakaran, C., & Ranga Rao, A. (1979). Status of exploration of hydrocarbons in the Himalaya: Contributions to stratigraphy and structure. *Miscellaneous Publication Geological Survey of India, 41*(5), 1–66.

Kassi, A. M., Kelling, G., Kasi, A. K., Umar, M., & Khan, A. S. (2009). Contrastic late cretaceous palaeocene lithostratigraphic succession across the Bibai thrust, western Sulaiman fold-thrust belt, Pakistan: Their significance in deciphering the early collisional history of the NW Indian plate margin. *Journal of Asian Earth Sciences, 35*, 435–444.

Kaul, R., Umamaheshwar, K., Chandrasekaran, S., Deshmukh, R. D., & Swarnakar, B. M. (1993). Uranium mineralization in the Siwaliks of NW Himalaya, India. *Journal of Geological Society of India, 41*, 243–258.

Kent, W. N., Hickam, R. G., & Dasgupta, U. (2002). Application of a ramp flat-fault model to interpretation of the Naga thrust and possible implications for petroleum exploration along the Naga thrust front. *American Association Petroleum Geology, 86*, 2023–2045.

Khan, M. A., Ahmed, R., Raza, H. A., & Kamal, A. (1986). Geology and petroleum in Kohat-Potwar depression, Pakistan. *American Association Petrology Geologists Bulletin, 70*, 396–414.

Khan, I. A., Bridge, J. S., Kappelman, J., & Wilson, R. (1997). Evolution of Miocene fluvial environments eastern Potwar plateau, Northern Pakistan. *Sedimentology, 44*, 221–251.

Kotlia, B. S., Partiyal, B., Kosaka, T., & Bohra, Archana. (2008). Magneto-stratigraphy and lithology of Miocene-Pliocene Siwalik deposits between Tanakpur and Suikhidhang, south-eastern Uttarakhand Himalaya. *Himalayan Geology, 29*, 127–136.

Krishna Rao, V. V., & Prasad, K. L. (1982). Exploration in the "schuppen belt" of Nagaland. *Bulletin ONGC, 19*, 213–220.

Kumar, R., Ghosh, S. K., Mazari, R. K., & Sangode, S. J. (2003). Tectonic impact on the fluvial deposits of Plio-Pleistocene Himalayan foreland basin, India. *Sedimentary Geology, 158*, 209–234.

Kumar, R., Ghosh, S. K., & Sangode, S. J. (2011). Sedimentary architecture of Late Cenozoic Himalayan Foreland Basin fill: An overview. *Memoir Geological Society of India, 78*, 245–280.

Kumar, R., Gill, G. S., & Gupta, L. N. (2005). Earthquake-induced structures in Pinjor Formation of Nadah area, Haryana. *Journal of Geological Society of India, 65*, 346–352.

Kumar, K., Loyal, R. S., & Srivastava, R. (1997a). Eocene rodents from new localities in Himachal Pradesh, Northwest Himalaya, India: Biochronologic implications. *Journal of Geological Society of India, 50*, 461–474.

Kumar, K., Srivastava, R., & Sahni, A. (1997b). Middle Eocene rodents from the Subathu Group, Northwest Himalaya. *Palaeovertebrata, 26*, 83–128.

Kumar, R., & Rai, Hakim. (1997). Post-Cretaceous molasses deposits of the intermontane foreland basin in eastern Karakoram. *Tertiary Geology, 18*, 23–30.

Kumar, K., & Sahni, A. (1985). Eocene mammals from the Upper Subathu Group, Kashmir Himalaya. *Journal Vertebrate Palaeontology, 5*, 153–168.

Kumar, R., Sangode, S. J., Ghosh, S. K., & Sinha, S. (2008). Marine to fluvial transition and erosion hiatus in the Paleogene sediments of NW Himalayan Foreland Basin. *Himalayan Geology, 29*, 147–160.

Kumar, K., & Shashi, Kad. (2003). Early Miocene vertebrates from the Murree Group, NW Himalaya: Affinities and age implications. *Himalayan Geology, 24*, 29–53.

Kumar, R., & Tandon, S. K. (1985). Sedimentology of Plio-Pleistocene late orogenic deposits associated with intraplate subduction—the Upper Siwalik subgroup of a part of Panjab sub-Himalaya, India. *Sedimentary Geology, 42*, 105–158.

Kundu, A., Matin, A., Mukul, M., & Eriksson, P. G. (2011). Sedimentary facies and soft-sediment deformation structures in the Late-Miocene-Pliocene Middle Siwalik subgroup, Eastern Himalaya, Darjiling district, India. *Journal of Geological Society of India, 78*, 321–331.

Kyi, M., (1970). Biostratigraphy of the Central Burma Basin with special reference to the depositional conditions during Late Oligocene and Early Miocene times. *Union of Barma Journal of Sciences and Technology* (3rd Burma Research Congress, 1968), 3, 1, 75–90, 4 pls., Rangoon.

Lillie, R. J., Johnson, G. D., Yousuf, M., Zaman, A. S. H., & Yeats, R. S. (1987). Structural development within the Himalayan foreland fold-and-thrust belt of Pakistan. In C. Beaumont & A. J. Tankard (Eds.), *Sedimentary Basins and Basin-Forming Mechanisms* (pp. 379–392). Ottawa: Canadian Society of Petroleum Geologists.

Lokho, K., Raju, D. S. N., & Azmi, R. J. (2011). Palaeoenvironmental and biostratigraphic significance of uvigerinidi and other foraminifera from the Bhuban Foration, Assam-Arakan basin, Mizoram. *Journal of Geological Society of India, 77*, 252–260.

Mathur, N. S. (1969). Fauna of the red beds of the Subathu (Eocene) near Garkhal, Simla Hills. *Publication of the Centre of Advance Studies in Geology, Panjab University, Chandigarh, 6*, 34–42.

Meigs, A. J., Burbank, D. W., & Beck, R. R. (1995). Middle-Late Miocene (>10 Ma) formation of the main boundary thrust in the western Himalayan. *Geology, 23*, 423–426.

Meyers, P. A., & Dickens, G. R. (1992). Accumulation of organic matter in sediments of the Indian Ocean: A synthesis of results from scientific deep sea drilling. In R. A. Duncan (Ed.), *Synthesis of Results from Scientific Drilling in the Indian Ocean* (pp. 295–308). Washington: American Geophysical Union.

Molnar, P., England, P., & Martinod, J. (1993). Mantle dynamics uplift of the Tibetan plateau and the Indian Ocean. *Review of Geophysics, 31*, 357–391.

Mugnier, J. L., Leturmy, P., Mascle, G., Huyghe, P., Chalaron, E., Vidal, G., et al. (1999). The Siwaliks of western Nepal: Geometry and kinematics. *Journal of Asian Earth Sciences, 17*, 629–642.

Mukhopadhyay, S. K., & Shome, S. (1996). Depositional environment and basin development during Early Paleogene lignite deposition, western Kutch, Gujarat. *Journal of Geological Society of India, 47*, 579–592.

Nagappa, Y. (1959). Foraminiferal biostratigraphy of the Cretaceous-Eocene succession in the India–Pakistan–Burma region. *Micropalaeontology, 5*, 145–177. New York.

Najman, Y., Bickle, M., BouDagher-Fadal, M., Carter, A., Garzanti, E., Paul, M., et al. (2008). The Palaogene record of Himalayan erosion: Bengal Basin, Bangladesh. *Earth & Planetary Sciences Letters, 273*, 1–14.

Najman, Y. M. R., Clift, P., Johnson, M. R. W., & Robertson, A. H. F. (1993). Early stages of foreland basin evolution in the Lesser Himalaya, N. India. In P. J. Treloar & M. P. Searle (Eds.), *Himalayan Tectonics* (pp. 541–558). London: Geological Society of London.

Najman, Y. M. R., Enkin, R. J., Johnson, M. R. W., Robertson, A. H. F., & Baker, J. (1994). Palaeomagnetic dating of the earliest continental Himalayan foredeep sediments: Implications for Himalayan evolution. *Earth & Planetary Sciences Letters, 128*, 713–718.

Najman, Y. M. R., Johnson, K., White, N., & Oliver, G. (2004). Evolution of the Himalayan foreland basin, NW India. *Basin Research, 16*, 1–24.

Najman, Y. M. R., Pringle, M. S., Johnson, M. R. W., Robertson, A. H. F., & Wijbrans, J. R. (1997). Laser $^{39}Ar/^{40}Ar$ dating of single detrital muscovite grains from early foreland-basin sedimentary deposits in India: Implications for early Himalayan evolution. *Geology, 25*, 535–538.

Nakata, T. (1972). *Geomorphic History of Crustal Movements of the Himalaya* (p. 77). Sendai: Institute of Geography, Tohuku University.

Nakayama, K., & Ulak, P. D. (1999). Evolution of fluvial style in the Siwalik Group in the foothills of the Nepal Himalaya. *Sedimentary Geology, 125*, 205–224.

Nanda, A. C. (2004). Upper Siwalik mammalian faunas of India and associated events. *Journal of Asian Earth Sciences, 21*, 47–58.

Nanda, A. C., & Corvinus, G. (2000). Skull characteristics of two proboscideans from the Upper Siwalik subgroup of Nepal. *Neues Jahrbuch fur Geologie und Palaontologie-Abhandlungen, 217*, 89–110.

Nanda, A. C., & Sehgal, R. K. (1993). Siwalik mammalian faunas from Ramnagar (J & K) and Nurpur (H.P) and lower limit of Hipparion. *Journal of Geological Society of India, 42*, 115–134.

Nanda, A. C., & Shukla, S. D. (2001). Fossil Giraffid from the Middle Siwalik subgroup near Dehradun. *Himalayan Geology, 22*, 121–125.

Oldham, R. D. (1893). *A Manual of the Geology of India*. Kolkata: Government of India Press. 553 p.

Pandit, S. K., Bhat, S. K., & Kotwal, S. (2011). Facies evaluation of boulder conglomerate formation, Upper Siwalik, Jammu Himalaya. *Himalayan Geology, 32*, 63–65.

Patnaik, R. (1995). Micromammal-based palaeo-environment of Upper Siwaliks exposed near village Saketi, H.P. *Journal of Geological Society of India, 46*, 429–437.

Patnaik, R. (2003). Reconstruction of Upper Siwalik palaeoecology and palaeoclimatology using microfossil palaeocommunities. *Palaeogeography, Palaeoclimatology, Palaeoecology, 197*, 133–150.

Pennock, E. S., Lillie, R. J., Zaman, A. S. H., & Yousaf, M. (1989). Structural interpretation of seismic reflection data from eastern Salt Range and Potwar Plateau, Pakistan. *American Association of Petroleum Geologists Bulletin, 73*, 841–857.

Pivnik, D. A., & Khan, M. J. (1996). Transition from foreland-to-piggyback-basin deposition, Plio-Pleistocene Upper Siwalik, Shinghar Range, NW Pakistan. *Sedimentology, 43*, 631–646.

Pivnik, D. A., Nahm, J., Tucker, R. S., Smith, G. O., Nyein, K., Nyunt, M., & Maung, P. H. (1998). Polyphase deformation in a forearc/backarc basin, Salin subbasin, Myanmar (Burma). *American Association of Petroleum Geologists Bulletin, 82*, 1837–1856.

Powers, P. M., Lillie, R. J., & Yeats, R. S. (1998). Structure and shortening of the Kangra and Dehradun re-entrants, subHimalayan India. *Geological Society of America Bulletin, 110*, 1010–1027.

Prasad, V., & Sarkar, S. (2000). Palaeoenrivonmental significance of *Botryococcus* (Chlorococcules) in the Subathu Formation of Jammu and Kashmir, India. *Current Science, 78*, 682–685.

Prell, W. L., Murray, D. W., & Clemens, S. C. (1992). Evolution and variability of the Indian Ocean summer monsoon: Evidence from the western Arabian Sea Drilling Programme. In R. A. Duncan (Ed.), *Synthesis of Results from Scientific Drilling in the Indian Ocean* (pp. 447–469). Washington: American Geophysical Union.

Raiverman, V. (1979). Stratigraphy and facies distribution of Subathu sediments, Simla Hills, northwest Himalaya. *Geological Survey of India Miscellaneous Publications, 41*, 111–126.

Raiverman, V., Kuntle, S. V., & Mukherjee, A. (1983). Basin geometry, Cenozoic sedimentation and hydrocarbon in northwestern Himalaya and Indo–Genetic Plains. *Petroleum Asia Journal, 6*, 67–92.

Raiverman, V., & Raman, K. S. (1971). Facies relation in the Subathu sediments, Simla Hills, northwestern Himalaya. *Geological Magazine, 108*, 329–341.

Raiverman, V., Srivastava, A. K., & Prasad, D. N. (1993). On the foothill thrust of northwestern Himalaya. *Journal of Himalayan Geology, 4*, 237–256.

Raju, A. T. R. (1967). Observation on the petrography of tertiary clastic sediments of the Himalayan foothills of North India. *Bulletin ONGC, 4*, 5–15.

Ralte, V. Z., Tiwari, R. P., Lalchawimawii, & Malsawma, J. (2011). Selachian fishes from Bhuban Formation Surma Group, Aizawi, Mizoram. *Journal of Geological Society of India, 78*, 328–348.

Ramanathan, S., & Pandey, J. (1988). Neogene/Quaternary boundary in Indian basins. *Journal of Palaeontology Society India, 33*, 21–45.

Ranga Rao, A., Nanda, A. C., Sharma, U. N., & Bhalla, M. S. (1995). Magnetic polarity stratigraphy of the Pinjor Formation (Upper Siwalik) near Pinjore, Haryana. *Current Science, 68*, 1231–1236.

Raza, H. A., & Iqbal, M. W. A. (1977). Mineral deposits. In S. M. I. Shah (Ed.), *Stratigraphy of Pakistan* (pp. 98–120). Quetta: Geological Survey of Pakistan.

Rea, D. K. (1992). Delivery of Himalaya sediments to the northern Indian Ocean and its relation to global climate, sea-level, uplift and seawater strontium. *Synthesis from Scientific Drilling in the Indian Ocean* (pp. 387–402). Washington: American Geophysical Union.

Roy, M. K., Ahmad, S. S., Bhattacharjee, T. K., Mahmud, S., Moniruzzaman, Md, Haque, Md M, et al. (2012). Palaeoenvironment of deposition of the Dupi Tila Formation, Lalmai Hills, Comilla, Bangladesh. *Journal of Geological Society of India, 80*, 409–419.

Roy, M. K., Karmarkar, B. C., Saha, S., & Chaudhuri, S. (2004). Facies and depositional environment of the Dupitila Formation, Dupitila Hill Range, Jaintipur, Sylhet, Bangladesh. *Journal of Geological Society of India, 63*, 139–157.

Roy, A., Sengupta, A., & Mandal, A. (2008). Synchronous development of mylonite and pseudotachytite: An example from the Chitradurga eastern margin shear zone, Karnataka. *Journal of Geological Society of India, 72*, 447–457.

Sahni, M. R., & Khan, E. (1964). Stratigraphy, structure and correlation of the Upper Siwaliks, East of Chandigarh. *Journal of Palaeontology Society India, 4*, 61–74.

Sahni, A., & Kumar, K. (1974). Paleogene palaeobiogeography of the Indian subcondtinent. *Palaeogeography, Palaeoclimatology, Palaeoecology, 15*, 209–226.

Sakai, H., Takigami, Y., Nakamuta, Y., & Nomura, H. (1999). Inverted metamorphism in the Pre-Siwalik foreland-basin sediments beneath the crystalline nappe, western Nepal Himalaya. *Journal of Asian Earth Sciences, 17*, 727–739.

Saluja, S. K., Srivastava, N. C., & Rawat, M. S. (1969). Microfloral assemblages from Subathu sediments of Simla Hills. *Journal of Palaeontology Society India, 12*, 25–40.

Sangode, S. J., & Bloemendal, J. (2004). Pedogenic transformation of magnetic minerals in Pliocene-Pleistocene palaeosols of the Siwalik Group, NW Himalaya, India. *Palaeogeography, Palaeoclimatology, Palaeoecology, 212*, 95–118.

Sangode, S. J., & Kumar, R. (2003). Magnetostratigraphic correlation of the Late Cenozoic fluvial sequences from NW Himalaya, India. *Current Science, 84*, 1014–1017.

Sanyal, P., Bhattacharya, S. K., Kumar, R., Ghosh, S. K., & Sangode, S. J. (2004). Mio-Plliocene monsoonal record from Himalayan foreland basin (Indian Siwalik) and its relation to vegetational change. *Palaeogeography, Palaeoclimatology, Palaeoecology, 205*, 23–41.

Sanyal, P., Sarkar, A., Bhattacharya, S. K., Kumar, Rohtash, Ghosh, S. K., & Agrawal, S. (2010). Intensification of monsoon, microclimate and asynchronous C_4 appearance: Isotopic evidence from the Indian Siwalik sediments. *Palaeogeography, Palaeoclimatology, Palaeoecology, 296*, 165–173.

Seracumbe, W. J., Pivnik, D. A., Wilson, W. P., Albertin, M. L., Beck, R. A., & Stratton, M. A. (1998). Wrench-faulting in the northern Pakistan foreland. *American Association of Petroleum Geologists Bulletin, 82*, 2003–2030.

Shah, J., Srivastava, D. C., & Joshi, Suman. (2012). Sinistral transpression along the Main Boundary Thrust in Amritpur area, southeastern Kumaun Himalaya. *Tectonophysics, 532–535*, 258–270.

Sharma, M., Sharma, S., Shukla, U. K., & Singh, I. B. (2002). Sandstone-body architecture and stratigraphic trends in the Middle Siwalik succession of the Jammu area, India. *Journal of Asian Earth Sciences, 20*, 817–828.

Sharma, S., Sharma, M., & Singh, I. B. (2001). Facies characteristics and cyclicity of Lower Siwalik sediments, Jammu area: A new perspective. *Geological Magazine, 138*, 455–470.

Siddiqui, N. K. (2004). Sui Main Limestone: Regional geology and the analysis of original pressures of a closed-system reservoir in central Pakistan. *American Association of Petroleum Geologists Bulletin, 88*, 1007–1035.

Singh, B. P. (2000). Sediment dispersal pattern in the Murree Group of the Jammu area, NW Himalaya, India. *Himalayan Geology, 21*, 189–200.

Singh, B. P. (2003). Evidence of growth fault and forebulge in the Late Paleocene (~57.9–54.7 Ma), western Himalayan foreland basin, India. *Earth & Planetary Sciences Letters, 216*, 717–724.

Singh, B. P., & Andotra, D. S. (2000). Barrier-lagoon and tidal cycles in Paleocene to Middle Eocene Subathu Formation, NW Himalaya. *Tertiary Research, 20*, 65–78.

Singh, S., Parkash, B., Awasthi, A. K., & Singh, T. (2012). Palaeoprecepitationrecord using O-isotope studies of the Himalayan Foreland Basin sediments, NW India. *Palaeogeography, Palaeoclimatology, Palaeoecology, 331–332*, 39–49.

Singh, B. P., & Srivastava, A. K. (2011). Storm activities during the sedimentation of Late Palaeocene-Middle Eocene Subathu Formation, Western Himalaya foreland basin. *Journal of Geological Society of India, 77*, 130–136.

Srikantiah, S. V., & Bhargava, O. N. (1967). Kakra series, a new Palaeocene formation in Simla Hills. *Bulletin Geology Social India, 4*, 114–116.

Srivastava, V. K., & Casshyap, S. M. (1983). Evolution of the pre-Siwalik Tertiary Basin of Himachal Himalaya. *Journal of Geological Society of India, 24*, 134–147.

Srivastava, D., & John, G. (1999). Deformation in Himalayan Frontal Fault zone: Evidence from small-scale structures in Mohand-Khara area, NW Himalaya. In A. K. Jain & R. M. Manickavasagam (Eds.), *Geodynamics of the NW Himalaya* (pp. 273–284). Japan: Gondwana Research Group.

Srivastava, R., & Kumar, Kishor. (1996). Taphonomy and palaeoenvironment of the Middle Eocene rodent localities of NW Himalaya. *Palaeogeography, Palaeoclimatology, Palaeoecology, 122*, 185–211.

Szalay, F. S. (1970). Late Eocene Amphipithecus and the origin of catarrhine primates. *Nature, 227*, 355–357.

Tandon, S. K. (1991). The Himalayan foreland: Focus on Siwalik Basin. In S. K. Tandon, C. C. Pant, & S. M. Casshyap (Eds.), *Sedimentary Basins of India* (pp. 171–201). Nainital: Gyanodaya Prakashan.

Tandon, S. K., Thomas, J. V., Parkash, B., & Mohindra, R. (2002). Lithofacies and palaeosol analysis of the Middle and Upper Siwalik Group (Plio-Pleistocene) Haripur-Kolar section, Himachal Pradesh. *Sedimentary Geology, 150*, 343–366.

Thakur, V. C., & Pandey, A. K. (2004). Active deformation of Himalayan frontal thrust and piedmont zone south of Dehra Dun in respect of seismotectonics of Garhwal Himalaya. *Himalayan Geology, 25*, 23–31.

Thomas, J. V., Parkash, B., & Mohindra, R. (2002). Lithofacies and palaeosol analysis of the Middle and Upper Siwalik Groups (Plio–Pleistocene), Haripur-Kolar section, Himachal Pradesh, India. *Sedimentary Geology, 150*, 343–366.

Tiwari, B. N. (2005). Tertiary vertebrates from the Himalayan foreland of India: An explanation of Late Eocene-Oligocene faunal gap. *Special Publication Palaeontology Society India, 2*, 141–153.

Tiwari, R. C., Hota, R. N., & Maejima, W. (2012). Fluvial architecture of Early Permian Barakar rocks of Korba, Gondwana basin, eastern-central India. *Journal of Asian Earth Sciences, 52*, 43–52.

Tokuoka, T., Takayasu, K., Hisatomi, K., Yamasaki, H., Tanaka, S., Konomatsu, M., et al. (1990). Stratigraphy and geological structures of the Churia (Siwalik) Group in the TinauKhola–BinaiKhola area, west-central Nepal. *Memoir Faculty Sciences, Shimane University, 24*, 71–88.

Tokuoka, T., Takayasu, K., Yoshida, M., & Hisatomi, K. (1986). The Churia (Siwalik Group of the Arungkhola area, West Nepal. *Memoir Faulty Science, Shimane, University, 20*, 135–210.

Valdiya, K. S. (1976). Himalayan transverse faults and folds and their parallelism with subsurface structures of North Indian plains. *Tectonophysics, 32,* 353–386.

Valdiya, K. S. (1980). *Geology of Kumaun Lesser Himalaya*. Dehradun: Wadia Institute of Himalayan Geology. 291.

Valdiya, K. S. (1999). Rising Himalaya: Advent and intensification of monsoon. *Current Science, 76,* 514–524.

Valdiya, K. S. (1993). Evidence for Pan-African–Cadomian tectonic upheaval in Himalaya. *Journal of Palaeontology Society India, 38*, 51–62.

Valdiya, K. S. (1998). *Dynamic himalaya* (p. 178). Hyderabad: Universities Press.

Valdiya, K. S. (2002). *Saraswati: The River that Disappeared* (p. 116). Hyderabad: Universities Press.

Vishnu, M. (1984). Floristic change in Himalaya at southern slope of Siwalik from Middle Tertiary to Recent. In R. O. White (Ed.), *The Evolution of East Mian Environment* (pp. 483–503). Hong Kong: University of Hong Kong.

Viswanath, S. N. (1997). *A Hundred Years of Oil*. New Delhi: Vikas Publishing House. 175 p.

Wadia, D. N. (1975). *Geology of India*. New Delhi: Tata McGraw Hill. 508 p.

Waheed, A., & Wells, N. A. (1990). Changes in palaeocurrents during the development of an obliquely convergent plate boundary (Sulaiman fold belt, southwestern Himalaya), west-central Pakistan. *Sedimentary Geology, 67*, 237–261.

White, N. M., Pringle, M., Garzanti, E., Bickle, M., Najman, Y., Chapman, H., & Friend, P. (2002). Constraints of the exhumation and erosion of the High Himalayan slab, NW India from foreland basin deposits. *Earth & Planetary Sciences Letters, 195*, 29–44.

Willis, B. (1993). Ancient river systems in the Himalayan foredeep, Chinji village area, northern Pakistan. *Sedimentary Geology, 86*, 1–76.

Yeats, R. S., & Lilie, R. J. (1991). Contemporary tectonics of the Himalayan Frontal Fault system: Folds, blind thrusts and the 1905 Kangra earthquake. *Journal of Structural Geology, 13*, 215–225.

Zaigham, N. A., & Mallick, K. A. (2000). Prospect of hydrocarbon associated with fossil-rift structures of the southern Indus basin, Pakistan. *American Association of Petroleum Geologists, 84*, 1833–1848.

Zaleha, M. J. (1997). Fluvial and lacustrine palaeoenvironments of the Miocene Siwalik Group, Khaur area, northern Pakistan. *Sedimentology, 44*, 349–368.

Chapter 20
Tertiary Basins: Along Coasts and Offshore

20.1 Continental Margin

The beginning of the Tertiary era witnessed submergence of the entire margin of the Peninsular India under water of a transgressive sea that also engulfed the foreland of the young Himalaya (Chap. 19). As a matter of fact, the Himalayan Foreland Basin (Sirmaur Basin) extended southwards through the Bengal Basin in the east and the Makran depression in the west. The sediments deposited in these extended pericratonic Tertiary basins make the continental shelves in the eastern and western seaboards of the Peninsular India (Figs. 20.1 and 20.2).

The continental margin along the eastern Coast is 25–210 km wide and dissected by a number of submarine canyons in the continuity of rivers discharging into the Bay of Bengal. Rivers such as the Ganga, the Mahanadi, the Krishna, the Godavari, the Palar and the Kaveri have been building prograding deltas since the Late Mesozoic time, and the present-day deltas conceal larger basins of Tertiary sedimentation. The greater parts of these basins lie under water in the offshore zone. The western continental margin is 100 km wide near Kanyakumari and about 300 km offshore Mumbai.

The offshore Tertiary basins grew in size and deepened due to growing loads of sediments, which accumulated during the rifting and sideway extension of the grabens. The subsidence was differential and controlled by faults of Precambrian antiquity, oriented NE–SW and ENE–WSW in the eastern margin and NNW–SSE and ESE–WNW in the western margin. The reactivation of older faults and lineaments is related to the collision of India with Asia. While the land in front of the growing Himalaya sank to give rise to the Sirmaur Foreland Basin, the eastern and western margins of the Peninsular India experienced extensional tectonism, resulting in the rifting along pre-existing faults in some sectors and differential vertical movements giving rise to horsts and grabens in other parts of the continental shelf. The depressions understandably trapped greater thickness of sediments, while the

K.S. Valdiya, *The Making of India*, Society of Earth Scientists Series,
DOI 10.1007/978-3-319-25029-8_20

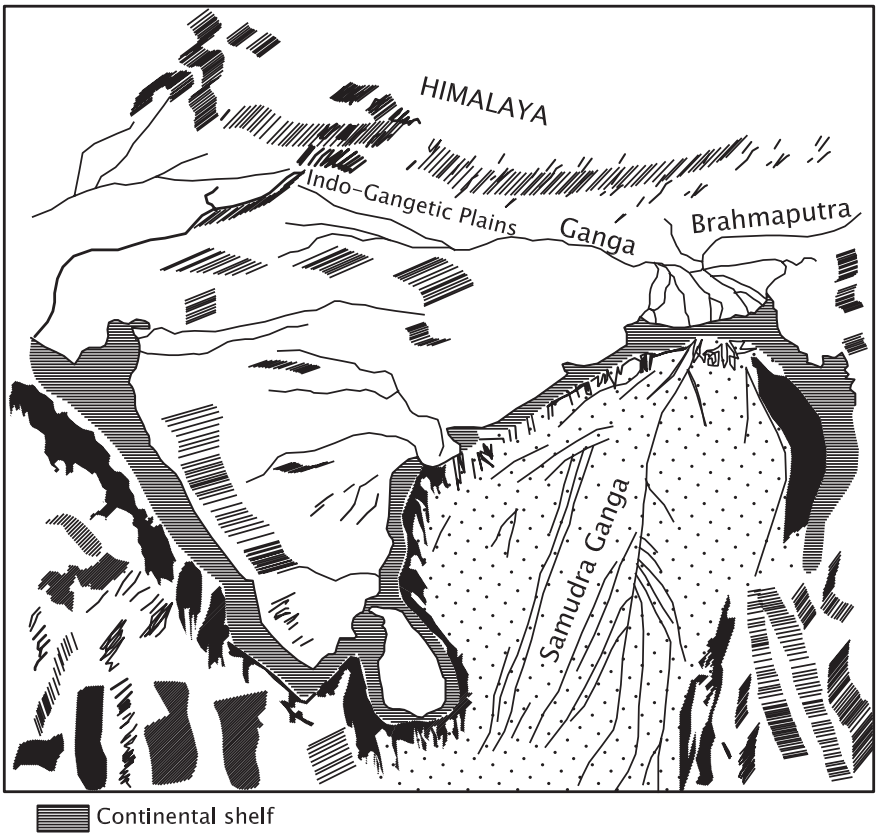

Fig. 20.1 Continental margin of the Peninsular India is made up of the shelves that suddenly drop to abyssal level onwards from the depth of 90 m

ridges were capped by comparatively thinner piles. Sedimentation in the offshore basins proceeded synchronously with the stepwise growth of the *down-to-basin* faults (Figs. 20.9, 20.10, 20.11 and 20.12).

The Tertiary basins of the continental margin, including the gulfs related to it, are of great importance as they host commercially productive petroleum fields.

20.2 Dual-Facies Sedimentation

As was the case in the Himalayan Foreland Basin, the sedimentation in the peri-cratonic Tertiary basins of the Peninsular India was dual-facies (Wadia 1975). The marine conditions continued up to the Early Miocene in Kachchh and Saurashtra. The Palaeogene sedimentation in marine environment gave way to accumulation

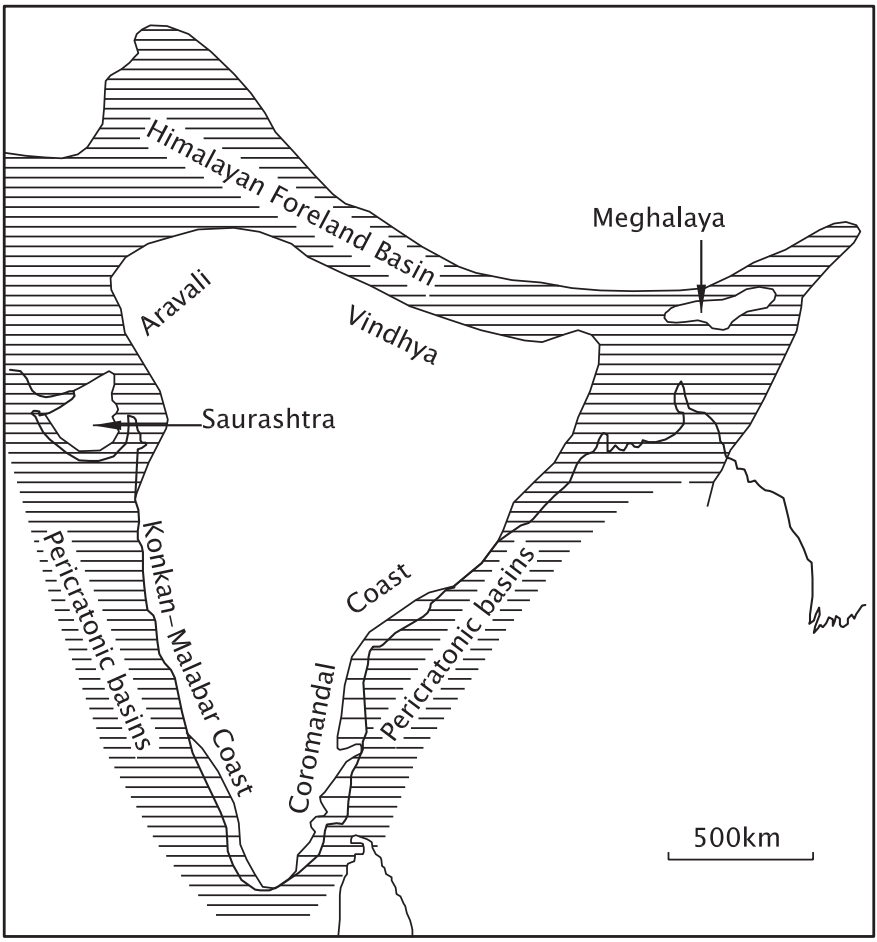

Fig. 20.2 Engulfing eastern and western margins of the Peninsular India, the Tertiary sea also occupied the depression that developed in front of the growing young Himalaya, following docking of India with Asia

of sediments in deltaic and fluvial settings during the Neogene when larger part of coastal land came under the sway of sea. The Palaeogene sediments are largely concealed under the younger sediments, both in onland and in offshore belts. The Neogene formations occur as discontinuous patches on land along the Coromandal and Malabar Coasts as well as along the Kachchh and Saurashtra Coastal stretches. It may be recalled that similar development took place also in the Himalayan Foreland Basin, where the sea retreated towards the end of the Oligocene. It was a gradual retreat, earlier in the Himalayan realm and later in the pericratonic Peninsular province.

20.3 Link with Himalayan Foreland Basin

20.3.1 Kachchh Tertiary Succession

Soon after the Deccan lavas were emplaced, the Kachchh Mobile Belt sank once again, inviting fresh marine transgression along the E–W depression that was formed. It was the reactivation of older faults that had prompted earlier sedimentation during the Jurassic and Cretaceous periods.

The Tertiary succession in Kachchh (Figs. 20.3 and 20.4) begins with the *Matonmadh Formation*, the coeval of the Ranikot Formation of Sindh (Biswas and Deshpande 1983; Biswas and Raju 1973; Biswas 1973, 1992). It comprises lateritic conglomerate, ferruginous and bentonitic claystones with coarse sandstone and tuffaceous shale, the last one representing a trap wash. The detritus was derived obviously from the denuding Deccan country. The presence of the tuffs in the sedimentary sequence of the Matonmadh implies that the volcanic ash from the Balochistan volcanoes of the Palaeocene time spread far beyond the Balochistan region. And the occurrence of dicot leaves with polypores in shales indicates that the hinterland was covered with vegetation.

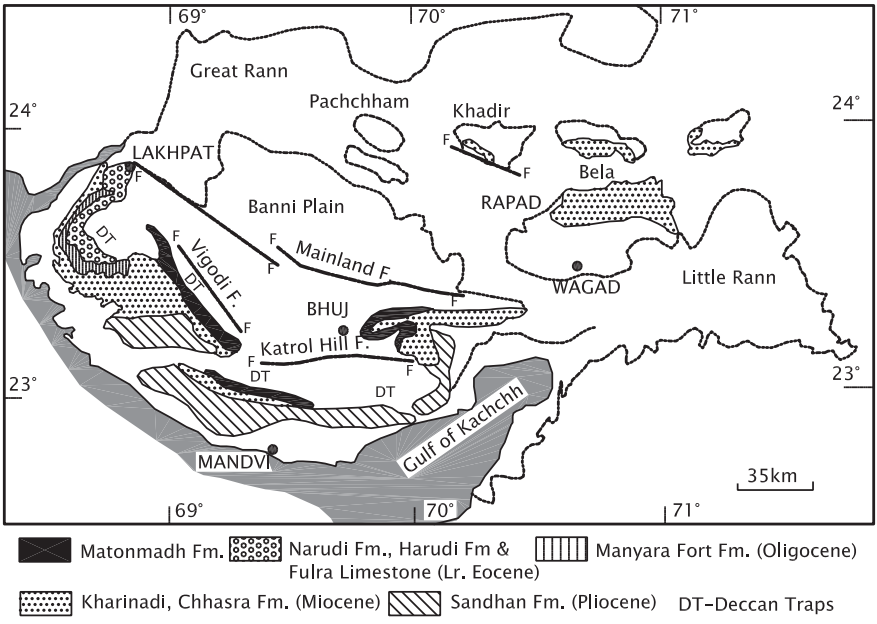

Fig. 20.3 Geological Sketch map shows areal extent of the Tertiary formations of Kachchh. The sediments rest on the foundation of the Deccan lavas (Based on Biswas and Deshpande 1983; Merh 1995; Biswas 1987)

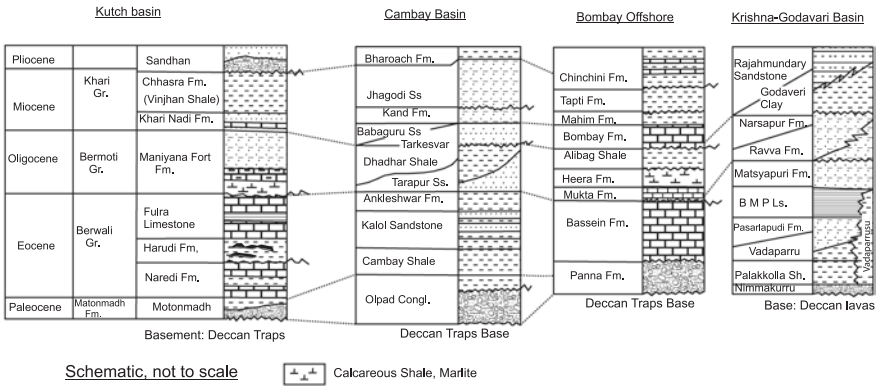

Fig. 20.4 Columns illustrate the lithological succession of the Tertiary formations of coastal and offshore belts in the Peninsular India

The homotaxial of the Laki Formation, described as the *Naredi Formation* in Kachchh, is made up of gypseous brown shales, glauconitic green shale and fossiliferous marlite. It contains foraminifers *Nummulites atacicus, Assilina granulosa* and *A. leymerie*, and plant fossils *Potamogetan* and *Botryoceus* and *Micropinus* on the basis of which a Ypresian age is assigned to the Naredi Fm. This horizon in south-western Kachchh revealed a rich assemblage of benthonic and some plankonic foraminifers of Palaeocene to Early Eocene age (Tandon et al. 1980). Between Beranda and Beranana, occurs the carbonate formation that contains planktonic foraminifers including *Catapsydrax unicavus* and *Hantkenina aragonensis* (Mohan and Soodan 1970).

The Naredi is disconformably overlain by the *Harudi Formation* that is made up of calcareous shale. This sequence is followed upsection by a pile of limestones described as the *Fulra Limestone*. This is coeval of the Kirthar. The Fulra Limestone, consisting of thickly bedded micrites and biosparites (Hardas and Biswas 1973; Biswas and Raju 1973), is characterized by Middle Eocene foraminifers *Discocyclina sowerbii* and *Fasciolites elliptica, Assilina exponens* and *Discoconoides cooki* (Mohan and Soodan 1970) and by the presence of bones of whales, sea cow and fish (Sahni and Mishra 1975). In the Lakhpat area, calcareous nannoplanktons assign a Late Middle Eocene age to the Fulra Limestone (Pratap and Singh 1986). The stable oxygen- and carbon-isotope analyses of foraminifers indicate that the δ^{18} O and δ^{13} C variations correspond to the chronostratigraphic units of the Lakhpat–Naliya area (Saraswati and Ramesh 1992). This fact implies that Eocene climatic stresses brought about decline in oceanic productivity, eventually causing extinction of larger benthic foraminifers (Sarangi et al. 1998; Sarkar et al. 2003a). Around Jhadwan and Harudi in south-western Kachchh, the Middle Eocene Fulra Limestone is replete with foraminifers and Chlorophyceae-Rhodophyceae algae which clearly indicate that the sediment deposition took

place in deeper inner to mud-ramp environments at depths of 40–80 m (Singh et al. 2010). Larger benthic foraminifers of the carbonates at the boundary of the Eocene and Oligocene horizons show LREE depletion, HREE enrichment, low average La/Lu and La/Yb and high Er/Nd ratios implying prevalence of oxygen deficiency in water column at the time when the sea level had gone down, and there was cooling of the ocean water (Sarkar et al. 2003a, b).

Disconformably overlying is the *Maniyara Fort Formation*, coeval of the Nari Formation. The Maniyara Fort sequence comprises alternating foraminiferal and glauconitic siltstones and gypseous claystone with intercalations of biomicrite and biosparite (Hardas and Biswas 1973). The sediments contain Rupelian to Chattian (Oligocene) foraminifers including *Nummulites intermedius fichteli, Lepidocyclina, Spiroclypeus ranjanae* and *Miogypsina complanata*, besides ostracodes, echinoids, gastropods, corals and reptilian bones. The equivalent of the Gaj Formation are represented by the *Kharinadi Fm.* and *Chhasra Formation* comprising variegated siltstones, grey and khaki claystones and fossiliferous marlite characterized by *Miogypsina globulina, M. droogeri, Austrotrillina howchini* and *Nephrolepidina* of Aquitanian to Burdigalian (Early Miocene) age (Pandey and Dave 1996, 1998).

The unconformably overlying *Sandhan Formation* succession, equated with the Manchhar Formation, comprises grey sandstone, pink fossiliferous calcareous sandstone and conglomerate with subordinate shale, containing Pliocene foraminifers and plants such as *Dipterocarpoxylon*. Significantly, the foraminiferal assemblage *Pararotalia nipponica—Laxostomum lobatum* in the Lakhpat–Naliya area indicates that the Miocene succession (Figs. 15.13 and 20.2) comprises lagoonal and high intertidal deposits in the lower part and beach ridge-tidal inlet sequence in the upper part (Wahi et al. 1991).

The Kachchh shelf is a sloping platform with E–W-oriented Kachchh Mainland Hill Range and NW–SE-trending "high" or bulge. A number of step faults subdivide the basement into blocks. Movements on these faults resulted in progressive thickening of sediments from onshore to the shelf area and beyond. Thus, more than 4500 m of Tertiary sequence is present in the offshore belt (Raju 1975).

20.3.2 Rajasthan Tertiary Basin

The Rajasthan Tertiary succession (Figs. 15.13 and 20.2) comprises alternating sequence of fine clastics, marls and carbonates of shallow marine environment. The rocks are characterized by foraminiferal assemblages comprising (i) *Nummulites atacius, Assilina granulosa, A. leymerei and Lokhartia tipperi* in the lower part and (ii) *Nummulites mammilatus, D. sowerbii, Dictyoconoides cooki, Heterostigina and Flosculina* in the upper part, equating them with, respectively, the Laki and the Kirthar fauna (Singhal et al. 1971; Singh 1951, 1953). Deposited on a wide stable shelf, the carbonate build-ups in the Jaisalmer Basin provided the source, the reservoirs and the caps of oil and gas deposits in the Indus Basin and in the western Rajasthan region along the Indo-Pak border.

The *Sanu*, *Khuliala* and *Bandah* formations of the Jaisalmer Basin are characterized by Late Palaeocene to early Late Eocene foraminiferal assemblages—*Planorotalites pussila, P. pseudomenardii, Assilina dandotica, Morozovella velascoensis, A. granulosa, Fasciolites globosa, Assilina daviesi, A. spira, F. elliptica, Nummulites bagelensis* and *Baculogypsinoides* (Singh 1996). Near Kolayat, fullers earth is intercalated with marlite and grey carbonaceous shale comprising lignite seams (Khosla 1973), which unconformably overlie the *Palana* Formation and contain Ypresian *Morozovella*, *Assilina* and *Econoides parvulus* and *Econoides wellsi* (Kalia 1978; Kalia and Banerjee 1995). The holothurian sclerite-bearing limestone of Marh in the Kolayat area contains Ypresian (Lower Eocene) *A. daviesi* (Soodan 1980). The disconformably overlying succession in the Bikaner Basin contains Lutetian foraminifers. About 145 km NW of Jaisalmer, the well at Tanot struck Late Eocene strata containing *Pellatispira, Nummulites fabiani, N. striata and Asterotrillina stellata* (Kalia and Banerjee 1991). The *Man* succession of the Kolayat area contains remains of such plants as *Ficus*, *Kayea* and *Grewia* that grew in moist evergreen deciduous forests (Mathur and Mathur 1998). These plants resemble the Kasauli flora of the Himalayan Foreland Basin. The *Bandah* succession comprises bentonitic clays, argillaceous limestone, chalky to crystalline limestone containing foraminifers and gypseous shales. The foraminiferal assemblage includes Lutetian to Pribonian *N. atacicus, N. beaumonti, Discocyclina javana, Fasciolites ellipticus, A. spira* and *Dictyoconoides* (Singh 1951, 1996).

In the *Barmer Basin,* the Tertiary succession begins with the *Akli Formation*. It is made up of bentonites, variegated clays and carbonaceous-bituminous claystone intercalated locally with lignite seams (Siddique and Bahal 1965). The Akli has revealed remains of vertebrates, including crocodiles, snakes and fish of the Lower Eocene age (Rana et al. 2005).

20.4 Saurashtra Coast and Offshore

From Bhavnagar–Gogha area in the east to Okhamandal in the north-west (Fig. 20.5) occurs in isolated small patches a succession of grey to bluish grey gypseous clays with intercalations of yellow limestone (*Ratanpur*), fossiliferous conglomerate, grit, argillaceous sandstone with minor clays (*Bhumbli*) and grey argillaceous sandstone with clay and calcareous layers (*Kuda*), representing the coeval of the Gaj Formation. It is 600 m thick in the Bhavnagar area, but attenuates to less than 15 m in Okhamandal. The presence of *Ostrea latimarginata*, *Austrotrillina*, *Miogypsina*, *Spiroloculina* and *Nephrolepidina* indicates Lower Miocene age of the Ratanpur–Bhumbli–Kuda succession.

In the Okhamandal area in north-western Saurashtra, the Dwarka succession rests conformably on them and on the Deccan lavas. The lower part of the Neogene succession (*Ashapura*) of variegated claystone, gypseous marl and yellow limestone is characterized by the Lower to Middle Miocene *Miogypsina* and

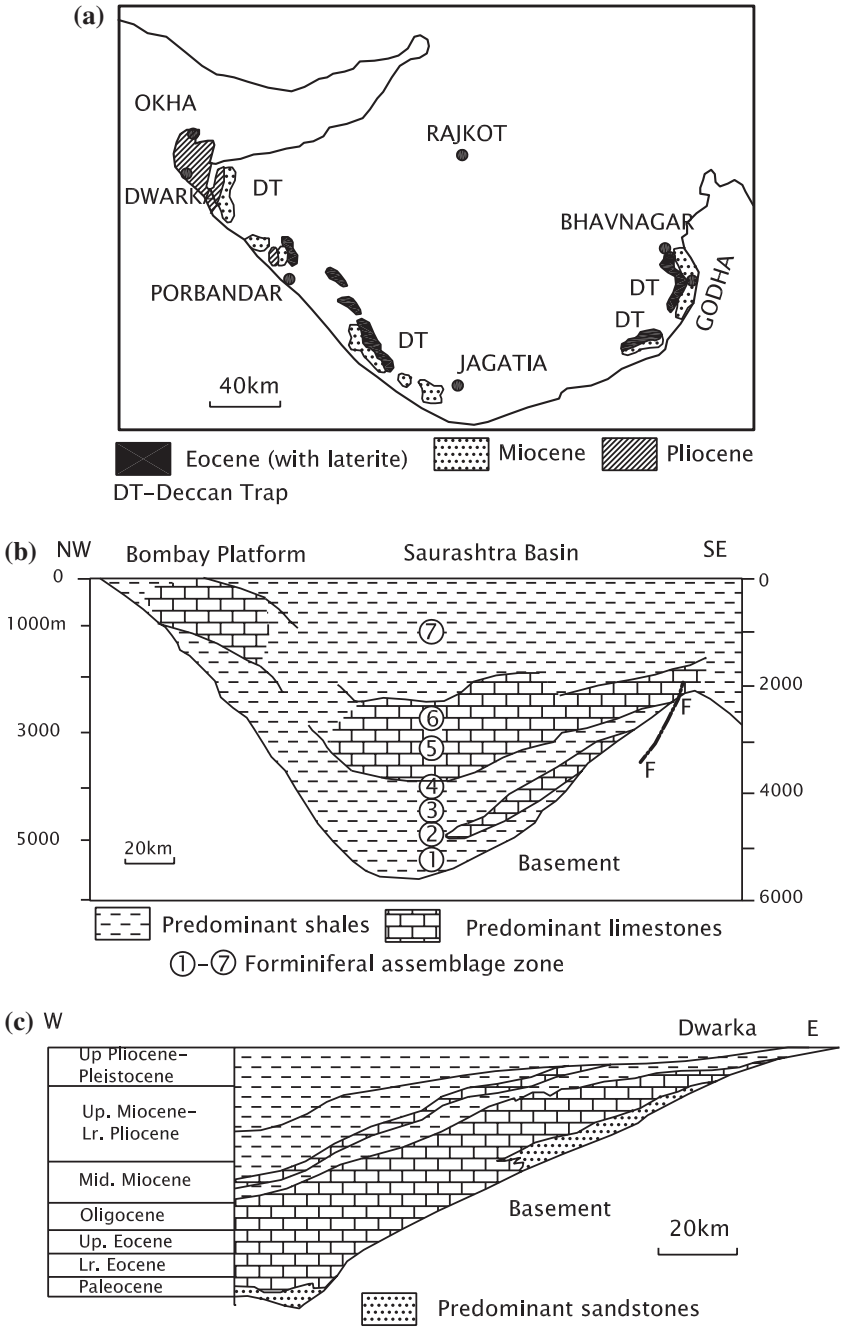

Fig. 20.5 Sketch map shows the outcrops of the Tertiary formations along the Saurashtra Coast, and the cross sections illustrate the structure and stratigraphic succession of the Saurashtra offshore (**a** and **c** after Biswas and Deshpande 1983, and **b** after Nair et al. 1992)

Cyclorubiculina. The disconformably overlying thick succession of bioclastic, pelloid limestone and coralline Limestone with bands of dolomite is known as the *Dwarka Formation*. The top of the Dwarka comprises beds containing *Pecten pascoe* of the Late Miocene to Pliocene age (Bhatt 2000).

The offshore basin, characterized by down-to-basin faults and a well-defined graben structure, comprises more than 4600-m-thick shelf carbonates, ranging in age from the Palaeocene to the Middle Miocene (Mitra et al. 1983).

20.5 Sabarmati–Cambay Basin

20.5.1 Gravity Condition

A NNW–SSE- to N–S-trending linear belt of positive Bouguer gravity anomaly delineates the rift valley presently occupied by the Gulf of Khambhat (Cambay) and the valley of the Sabarmati River (Fig. 20.6). Extending north of Sanchore through the narrow Barmer Graben, it is linked with the Himalayan Foreland Basin (Fig. 20.2). Deep seismic sounding (Tewari et al. 1995) revealed that the basement of this basin consists of 1000–3200-m-thick Deccan Volcanics forming subsurface ridges and depressions resulting from differential subsidence along a multiplicity of listric faults. The aggregate subsidence is of the order of 2000–3000 m in the northern (Sabarmati) part and 4000–5000 m in the southern (Khambhat) sector (Mathur et al. 1968; Raju 1968, 1975).

20.5.2 Structure and Tectonics

The N–S- to NNW–SSE-trending *Sabarmati–Cambay Basin* is bound along east and west by discontinuous *en echelon* step faults. The subsidence of the Deccan terrane along these faults commenced in the Late Palaeocene and continued through the Tertiary period. The result was a large graben with a number of subsidiary depressions and ridges (uplifts) within the larger rift basin (Fig. 20.7). And this rift basin comprises one of the most hydrocarbon-productive sedimentary piles of the Indian subcontinent. The elongated Cambay Basin with its internal ridges and depressions is subdivided into four major tectonic blocks by ENE–WSW- to NE–SW-oriented oblique tear faults, described as transfer faults. The basin is separated from the Bombay Offshore Basin to the south by the seaward extension of the Son–Narmada faults (Rao and Talukdar 1980). The evolution of this basin took place (Figs. 20.6 and 20.7) in three stages—extension of the crust and formation of horsts and grabens during the Late Palaeocene to Early Eocene time, thermal subsidence in the Early to Middle Eocene period and structural inversion due to reactivation of older faults in the post-Miocene time (Raju and Srinivasan 1983; Wani and Kundu 1995; Lal et al. 1995).

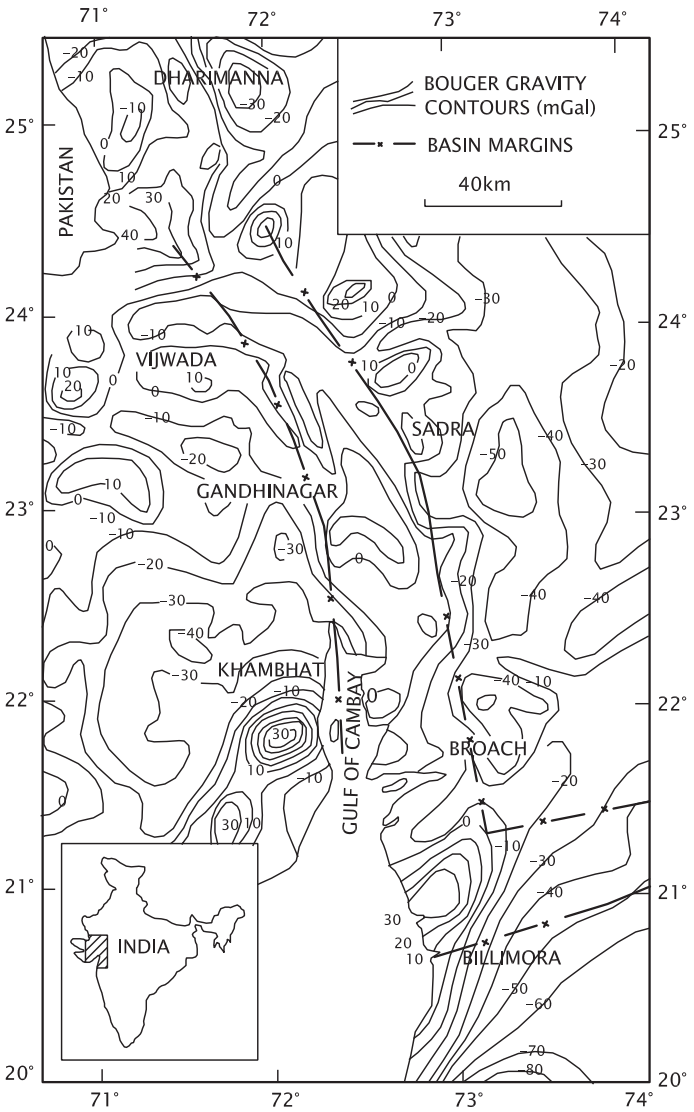

Fig. 20.6 Bouguer gravity anomaly (mGal) of the Sabarmati–Cambay Basin indicating existence of a linear rift structure (Tewari et al. 1995)

20.5.3 Sedimentation and Stratigraphy

In a preliminary attempt at stratigraphic classification of the Tertiary succession in the Cambay rift basin (Fig. 20.4), names such as *Cambay*, *Kalol*, *Tarapur*, (Zuvov et al. 1966), *Bharoach* (Chandra and Chowdhary 1969), *Ankaleshwar* and *Tarakeswar* (Rao 1969; Sudhakar and Basu 1973; Mohan 1982) were suggested

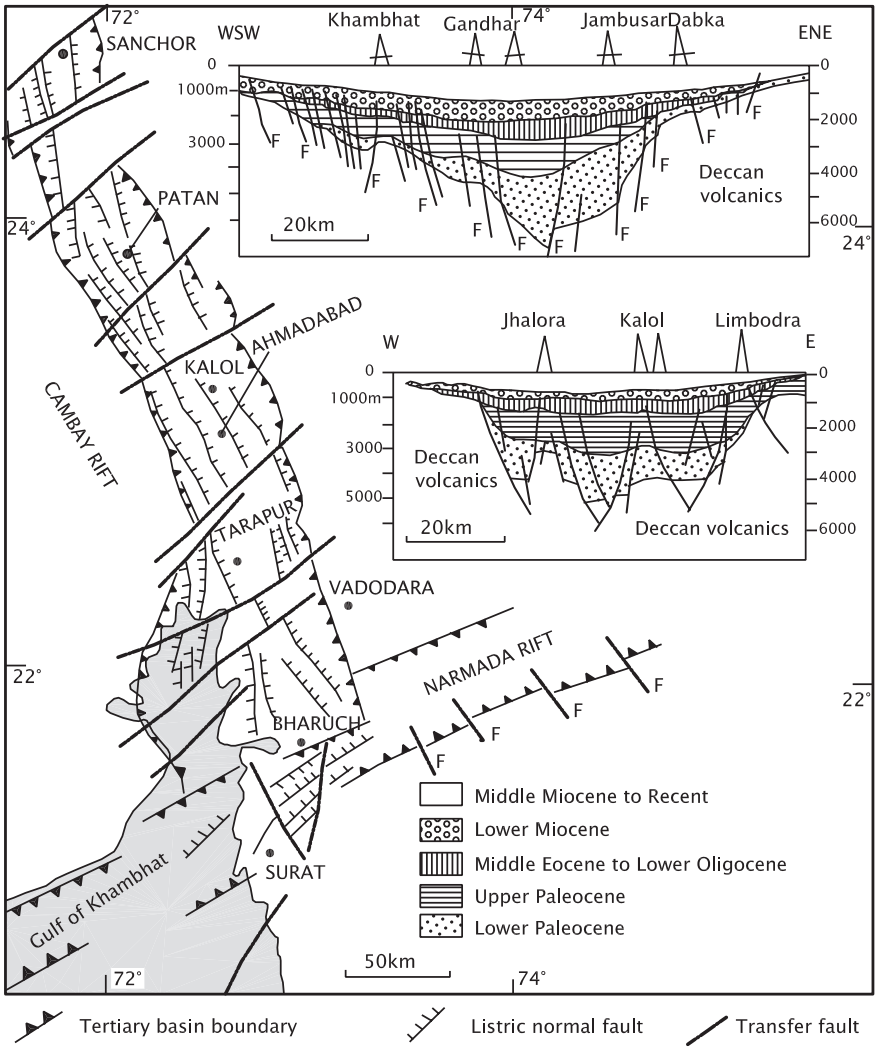

Fig. 20.7 Sketch map showing structural setting of the Sabarmati–Cambay Basin, delineated by discontinuous en echelon faults. *Upper* section shows the Sabarmati Graben in the Bharuch sector. *Lower* section shows the structure and lithostratigraphy in the Ahmadabad Block of the Sabarmati–Cambay Basin (Wani and Kundu 1995)

and later standardized through comprehensive sedimentological and micropalaeontological studies (Bhandari and Chowdhary 1975).

More than 2000-m-thick pile of conglomerates with sandstones and claystones of the Late Palaeocene to Early Eocene age represents a fan-shaped sedimentary fill in the marginal part of the depression (Fig. 20.8) adjacent to an uplifted terrain (Raju and Srinivasan 1983). The basal horizon—*Olpad Formation*—is a trap

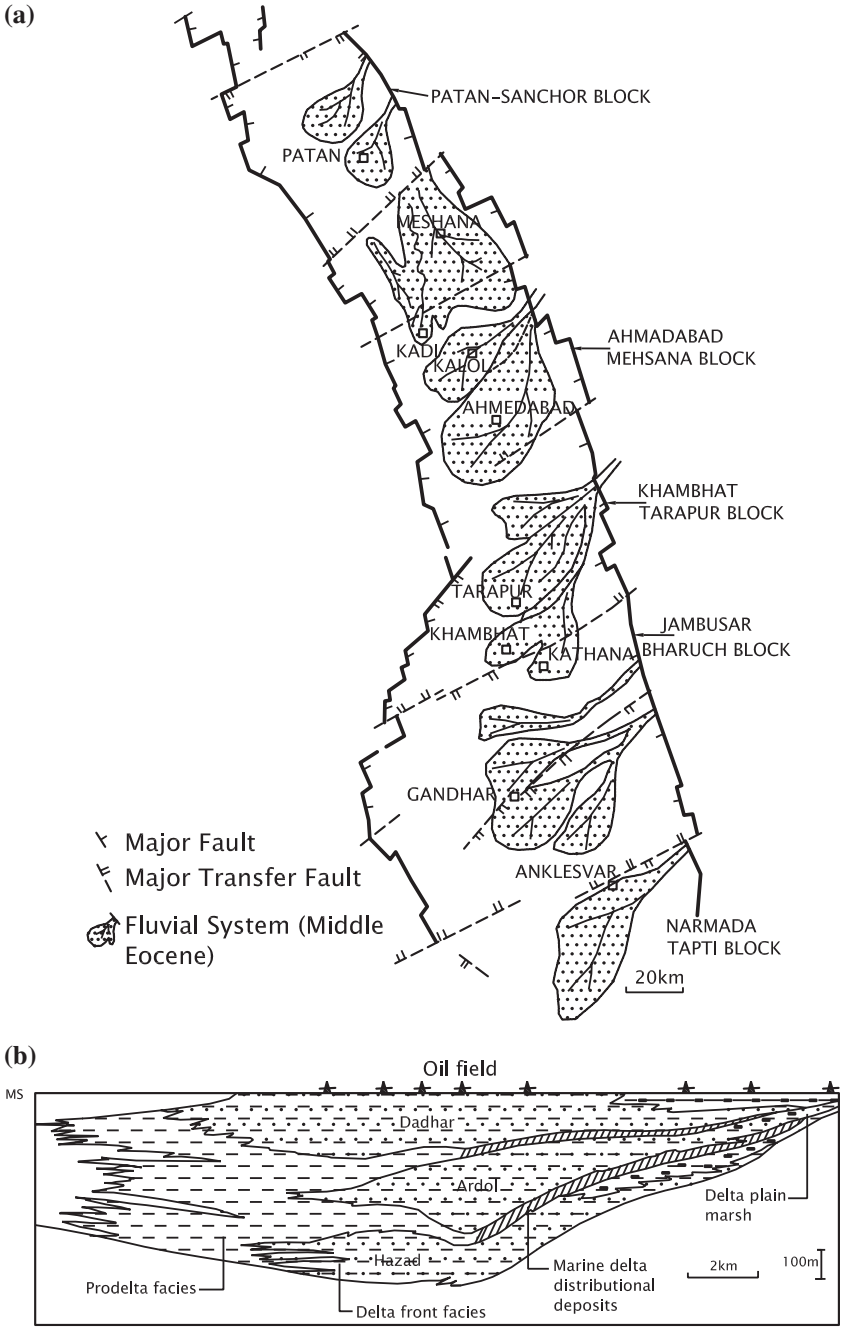

Fig. 20.8 **a** Filling of the Sabarmati–Cambay Basin by rivers and streams by building progressively prograding deltas in different blocks. **b** Cross section shows the history of sedimentation in the Bharuch Block—one of the most productive domains of the petroliferous basins of India (after Mohan 1995)

wash detritus, swept down from the Deccan Volcanics of the upland. This detritus contains remains of chelonian fish of Palaeocene–Early Eocene age. This horizon is succeeded by lagoonal shales with siltstone intercalation extraordinarily rich in organic matter (the *Cambay Shale*), laterally grading eastwards into Vagadkhol Sandstone. The hinterland drainage supplied a large amount of terrigenous claystone forming delta plains and delta fronts, the former embodying intertidal marshes backshore lagoons, tidal flats and gulfs (Mohan 1995) in an environment resulting from marine transgression. The occurrence of *Nummulites burdigalensis* in the Cambay Shale of the Vastan Lignite Mine suggests Ypresian age. In the Vastan sequence is manifest the Palaeocene–Eocene transition when there was pronounced global warming. In the Cambay Basin, climate warming gave rise to prolific formation of petroleum hydrocarbon-forming flora and fauna leading to the development near shore of low-energy euxinic lagoonal environment. The Vastan seems to exhibit similar condition and environment (Sahni et al. 2006). The shallow benthic foraminifers such as *N. burdigalensis* of Early Eocene age place the Vastan Lignite in the basal Cuisian time (Punekar and Saraswati 2010).

The *Ankaleshwar* Fm is a sequence of grey claystone and deltaic sandstone alternating with carbonaceous shale containing Middle to Upper Eocene foraminifers—*N. atacicus* and *Pseudohastigerina* of the delta front environment (Pandey and Dave 1996). The deltaic sandstones of this formation hold significant oil deposits in the Ankleshwar oilfield. The *Kadi* unit, representing a lagoonal facies in the north, consists of grey shale and coal layers with sideritic concretions. Corals, ostacodes and palynomorphs place it in the Lower to Middle Eocene time. The *Kalol* succession consists of sandstone/siltstone–carbonaceous shale alternations with coal beds. In the upper part, the presence of *Discocyclina*, *Pellatispira* and *N. atacicus* indicates its Middle to Upper Eocene age (Fig. 20.11).

There was a hiatus following marine transgression during the Oligocene, as was the case in Kachchh (Biswas and Raju 1973; Mohan 1995). The Neogene begins with predominant fluvial–alluvial sedimentation, continuing through Miocene and Pliocene to the present. The Miocene comprises the *Babaguru Sandstones*, the *Kand Formation* and the *Jhagadia Sandstone* (Fig. 20.4). In the western margin of the Khambhat gulf, there is a horizon of conglomeratic sandstone and siltstone that forms the island of Piram.

South-east of Bharuch in the Tapi Valley, in Tarakeshwar area, calcareous nannoplanktons including *Coccolithus* of shallow marine environment occur along with larger benthonic foraminifers of inner neritic shelf (Singh et al. 1978).

20.5.4 Life in the Sabarmati Domain

Located thirty kilometres south-west of Surat, the *Vastan Lignite Mine* reveals a rich assemblage of fauna and flora of the Early Eocene time. Dark grey shale with siltstone intercalations above the lignite bed contains Ypresian amphibians, lizards, crocodiles, turtles, snakes and birds living in association with perissodactyls,

artiodactyls, proteutherians, apatotherians, insectivores, rodents, bats and marsupials (Bajpai et al. 2005). Dispersed nodules of amber in the lignite seams contain well-preserved remains of exceptionally diverse amaebae (*Phryganella*), spiders, insects, fungi and degraded leaf and flower material, including *Proxaperites,* indicating the kind of life that flourished in the subtropical rainforests of the coastal lagoons, swamps and freshwater bodies in the Sabarmati domain (Alimohammadian et al. 2005).

Apart from gastropods, lamellibranchs, echinoids and corals, the foraminifers were the most common among the invertebrate fauna. The important taxa from the Eocene sections include *Assilina, Asterocyclina, Baculogypsinoides, Dictyoconoides, Discocyclina, Fasciolites, Linderina, Lockhartia, Nummulites* and *Pellatispira*. Among these, the only genus that continued into the Oligocene is *Nummulites* joined by *Heterostigina, Lepidocyclina, Miogypsinoides and Spiroclypeus*. The larger foraminifers show greater latitudinal distribution and high diversity during the Middle and Upper Eocene time but had restricted occurrence and lesser diversity in the Early to Middle Oligocene period (Saraswati et al. 1993).

20.5.5 Climate Change

Oxygen isotopic measurements of larger foraminifers such as *Nummulites* and *Lepidocyclina* indicate that the temperature of the sea water was around 32 °C in the Palaeocene and Early Eocene time, dropped by 6 °C towards the end of the Middle Eocene, became 22 °C in the Late Eocene and then rose to 25 °C towards the close of the Oligocene (Saraswati et al. 1993).

20.6 Bombay Offshore Basin

20.6.1 Basin Structure

The Bombay Offshore Basin (Fig. 20.9) developed in the belt of transitional type thinned crust characterized by perceptibly high heat flow and greater thermal gradient (Pandey and Agrawal 2000). The slope of the 300-km-wide continental shelf breaks at the depth of 90 m below the sea level (Narain et al. 1968). Located in the line of the Sabarmati–Cambay rift basin, the Bombay Offshore Basin (Figs. 20.4 and 20.9) also exhibits NNW/NW–SSE/SE trending graben-and-horst structure between the Surat depression in the north and Vengurla arc in the south. The oil-bearing giant structure, known as the *Bombay High*, is the most productive oilfields of India (Rao and Talukdar 1980).

The commencement of rifting of the Bombay Offshore Basin was synchronous with the outpouring of the Deccan lavas in the Palaeocene time. An

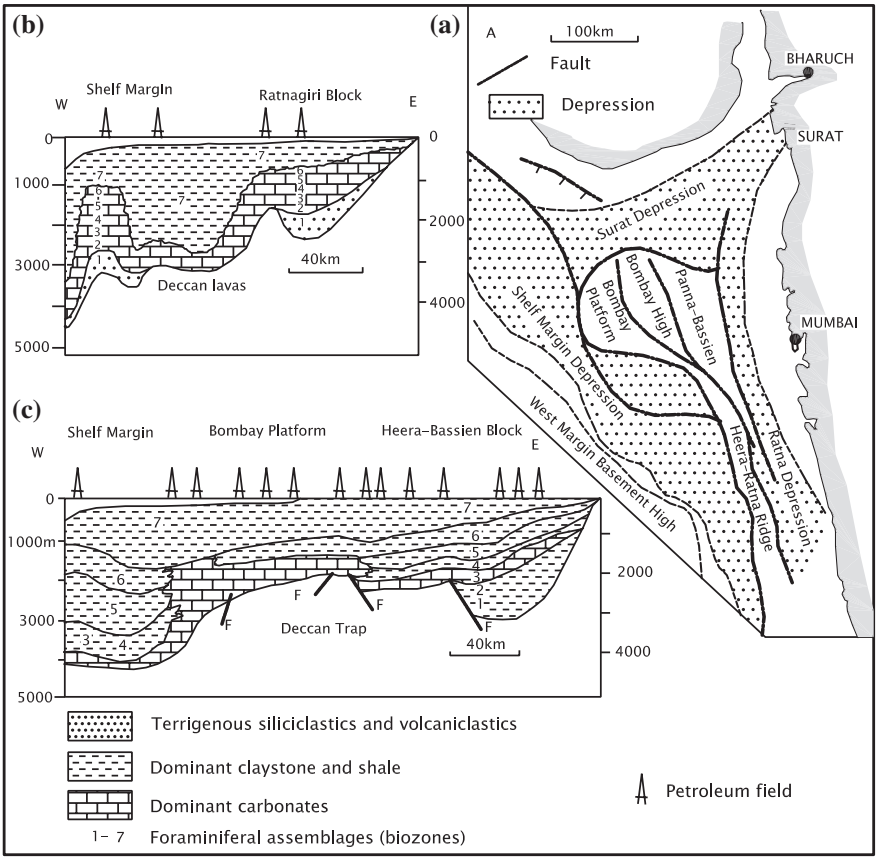

Fig. 20.9 **a** Sketch map shows the main structures of the Bombay Offshore Basin comprising horsts and grabens (after Lal et al. 1995). **b** and **c** Cross sections of the Ratnagiri and the Bombay platform and Heera–Bassein blocks, showing the structure and lithostratigraphy (after Nair et al. 1992)

extensional deformation resulted in the formation of a series of step faults of the rift and graben structures that grew with time as brisk sedimentation proceeded in the shelf zone.

20.6.2 Sedimentation History

Beginning with the accumulation of terrestrial clastic sediments, including a trap wash (Basu et al. 1982; Mitra et al. 1983) in the lagoonal environment in the Late Palaeocene to Early Eocene time (*Panna Formation*), there was carbonate sedimentation of platform facies in the Middle Eocene time (Figs. 20.4 and 20.9).

The *Bassien Formation* is made up of algal and foraminiferal limestones characterized by peloids, peloid–biospaiite and biomicrite textures. Separated by an unconformity, the Panna and Bassien successions are important reservoirs of petroleum oil and gas. Excepting the attenuated *Mukta* and *Heera* sequences, the Late Oligocene was a period of no deposition and then followed a regression that laid down thick deposits of shales (*Alibagh Formation*) in the Upper Oligocene and huge carbonates (*Bombay Formation*) during the Lower Miocene time under alternating transgressive and regressive cycles. The Bombay Formation is the main oil-bearing sequence in the Bombay High. The later part of the Lower Miocene and the Middle Miocene epochs was the time of emplacement of claystones with siltstones (*Mahim* and *Tapti* formations).

The *Bassein Formation* is made up of a sequence of micrite and biomicrite with intercalations of shale, and is characterized by Lower Miocene *Miogypsina tani, M. globulina, Ammonia papillosus* and *Globigerinoides primordius*. The *Bassein* unit comprises a monotonous sequence of packstone and wackestone carbonates characterized by Middle to Upper Eocene *Fasciolites, Coskinolina, Pellatispira* and *N. fabiani*. The *Mahim* succession is dominated by dark grey calcareous shale with subordinate limestone and siltstone in the upper part containing *Miolepidocyclina excentrica* and *Anmosia papillosus* of the Lower Miocene age (Pandey and Dave 1998). The *Kand* sequence is dominantly grey claystone with local sandstone and calcarenite containing *Miogypsina, Globoquadrina altispira, Asterotrillina howchini and A. papillosus* of Lower to Middle Miocene age. The *Chinchini* sequence is greenish and bluish grey claystone intercalated with shelly Limestone. The limestone is characterized by Upper Miocene *Globigerna nepenthes* and *Globigerinoides fistula*.

20.6.3 Faunal Turnover

Taking into account the history of the whole north-western part of the Tertiary province including the basins of Kachchh, Saurashtra, Sabarmati–Cambay and Bombay Offshore, it is realized that there were three notable events in the faunal history (Pandey 1982; Pandey and Dave 1998). Marine *A. papillosus* disappeared at 15.5 Ma, even as terrestrial *Dinotherium* appeared among the vertebrate fauna of the Gaj beds in Kachchh. Primitive land mammal *Dicoryphochoerus* appeared in the Fatehgarh beds in Kachchh, while the marine *Anomalinella rostrata* vanished at 14.5 Ma. A rich assemblage of vertebrates appeared in the Late Miocene sediments of the Piram Island, while the marine assemblage of *Ammonia annectens* disappeared at 8.5 Ma from the Cambay Basin.

20.7 Kerala Basin

20.7.1 Outcrops Along Coast

The Tertiary strata occur in two onland belts along the Malabar Coast in Kerala—between Kasaragod and Kannur in the north and between Ponnani and Thiruvananthapuram in the south (Figs. 20.2 and 20.10). The Tertiary sedimentary belt is widest (16 km) between Kundam and Kollam (Quilon) (Menon 1967; Paulose and Narayanswami 1968; Varadarajan and Madhavan Nair 1978).

The succession begins with coarse-grained sandstone interbedded with claystone and lignite of the basin-margin fluvial facies (*Mayyanad Formation*). The Mayyanad, comprising coarse-grained sandstone and subordinate of claystone and lignite, is characterized by Early Oligocene to Early Miocene foraminifers including *Nummulites fichteli* and *Nummulites vacus*. The overlying succession is known

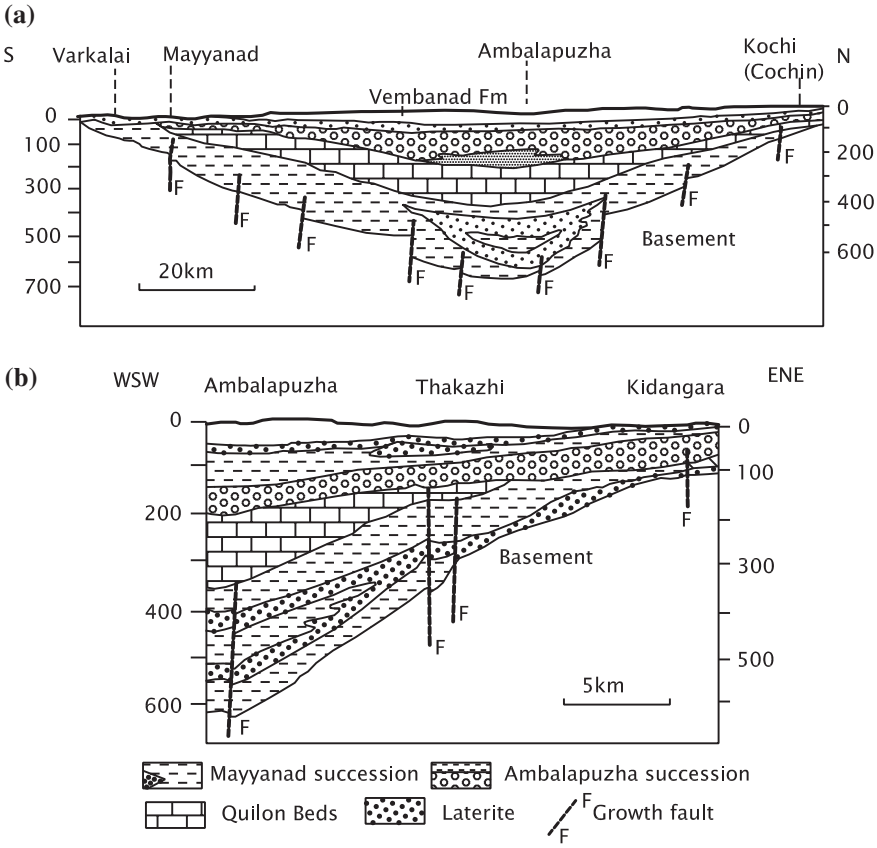

Fig. 20.10 Cross sections show the structural design and the lithostratigraphy of the Kerala Basin (after Raha et al. 1986)

as the *Quilon Beds*. It is a 130-m-thick sequence of brownish white, buff to grey foraminiferal and algal wackestone and packstone carbonates first described and named by W. King in 1882 as Quilon Beds. Partially dolomitized, it is characterized by the Late Oligocene to Middle Miocene foraminifers—*Miogypsinoides complanatus, S. ranjanae, Miogypsina droogeri* and *Cycloclypeus indopacifica* (Pandey and Dave 1998). This carbonate succession tapers eastwards towards the basin margin to less than one metre (Raha et al. 1986) so that the overlying horizon appears to rest directly on the Mayyanad sequence. In the cliff section along the Ashtamudi estuary, the Quilon Limestones contain besides lamellibranchs, pelecypods, ostracodes and corals, such foraminifers as *Taberina malabarica, Lepidocyclina, A. howchini* and *Miogypsina malabarica* of Miocene age (Jacob and Sastry 1952; Pandey and Dave 1998).

The 140-m-thick *Warkalli Formation* at the top of the Tertiary succession—named in 1883 by W. King—comprises coarse-grained sandstone interbedded with variegated to mottled claystones. Some of the clays are alum-bearing, some containing lithomargic material and others rich in carbonaceous matter (Menon 1967). There are also intercalations of peat and lignite beds. Sedimentary structures such as cross-bedding, convolute lamination, water-escape structures and clay galls show that this upward-fining sequence was deposited by a meandering river (Padmalal 1996). Typically exposed at Ambalapuzha and well exposed on the cliff of Varkala, the Warkalli wears nearly 8-m-thick cap of laterite. The upper part of the succession contains Late Miocene to Pliocene foraminifers including *Ammonia beccardi* (Pandey and Dave 1998). Carbonaceous clays and peat within the Warkalli yielded pteridophytic spores, fungal remains and angiospermous pollens, indicating low-land swamp conditions during the Miocene time (Kumaran et al. 1995).

20.7.2 Offshore Zone

Five kilometres offshore from the shoreline (Fig. 26.9), the sedimentary sequence below the depth of 11 m is the same as in the onland outcrops—the Late Palaeocene to Early Eocene sediments resting upon basement and becoming young upwards through the Oligocene to Miocene (Mohan and Kumar 1980). Significantly, this submarine succession is simultaneously conformable with the crest of the Lakshadweep–Chagos Ridge made up of rhyolitic lavas and tuffs interbedded with penecontemporaneous Palaeocene carbonates and overlain by the Eocene Limestones (Siddiqui and Sukeshwala 1976). The Early Oligocene is represented by sandy clay within the sequence of limestone containing *N. fichteli*, among other foraminifers. The overlying sandstone, claystone and limestone are characterized by *Lepidocyclina sumatraensis* and *M. droogeri* of the Early to Late Miocene age (Mohan and Kumar 1980; Mohan 1982).

20.8 Kaveri Basin

The Cretaceous succession of the Kaveri delta domain (Figs. 20.2 and 20.11) passes upsection to the *Niniyur Formation* of limestones characterized by exceptionally rich assemblage of algae, of which the dominant elements is coralline algae *Sporolithon* and *Lithothamnian* of the Palaeocene age (Prabhakar and Zutshi 1993). In the subsurface, the Cretaceous–Tertiary boundary is marked by an unconformity. In the Pondicherry area occurs a marlite horizon at the base of the Tertiary succession which contains *Globorotalia angulata, Globorotalia*

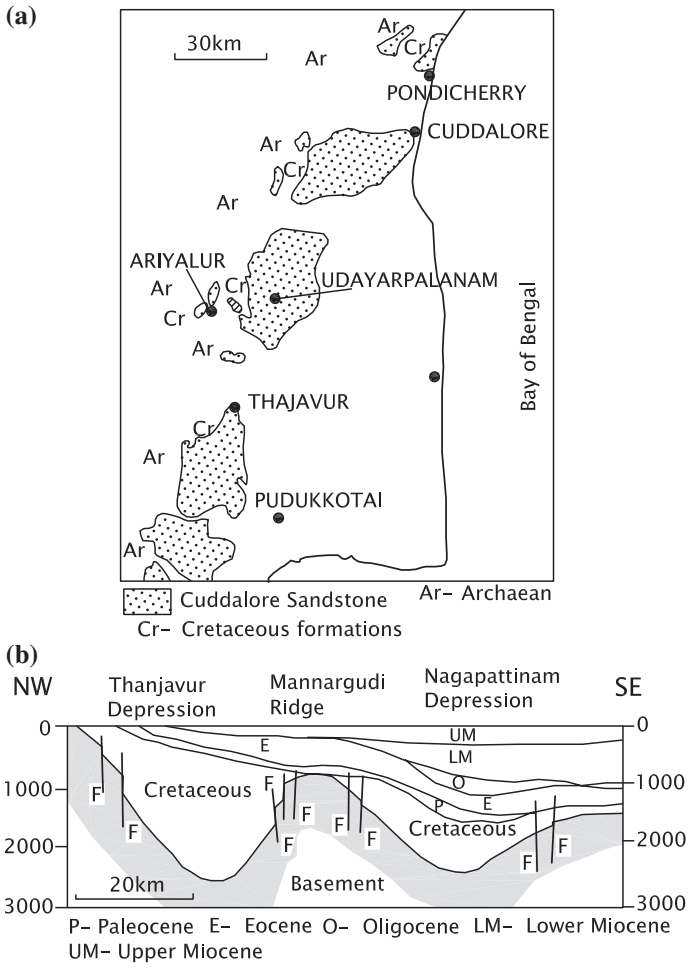

Fig. 20.11 **a** Sketch map shows the geographical distribution of the Tertiary formations along the Coromandal Coast (after Mohan et al. 1977). **b** Cross section shows foraminiferal zones in the distal offshore part of the Kaveri Basin (after Mohan et al. 1977)

velascoensis and *Globorotalia aequa* of the Palaeocene time. The succeeding sequence of limestone described as the *Karikal Beds* is characterized by Ypresian *Discocyclina* (Samanta 1973).

The Neogene is represented by patches of paralic sediments all along the Coromandal Coast from Kanyakumari to Odisha. Resting unconformably on the basement is made up of Precambrian crystallines, the Gondwana and the Cretaceous sedimentary rocks, the 400-m succession of the *Cuddalore Sandstone* is well developed in the tract between Sivaganga and Pondicherry (Fig. 20.4a). The formation was given this name by W. King in 1870. It comprises cross-bedded brown to yellow and mottled soft friable sandstones intercalated with pebble beds and claystone layers. At places, there are thick beds of lignite of considerable economic value. The lignite deposit of Neyveli is commercially mined. In addition to the remains of algae, foraminifers and molluscs, there are spectacular petrified tree trunks in the Cuddalore Sandstones as seen at *Tiruvakkarai Petrified Forest*. These fossils place the Cuddalore in the Miocene–Pliocene time span.

Down south at Kudankulam between Kanyakumari and Tiruchendur, the Cuddalore succession of arkose, subarkose, litharenite and sublitharenite shows LREE enrichment, flat HREE and negative europium anomaly, indicating derivation of detritus from the felsic sources in the proximity of the basin, presumably the Proterozoic gneisses and charnockites of the Kerala Khondalite Belt. The implication is significant. The Kerala Khondalite Belt must have been exhumed and exposed to denudation by the Cuddalore time (Armstrong-Altrin et al. 2004).

20.9 Krishna–Godavari Basin

Resting unconformably on the older rocks, including the Proterozoic khondalites and charnockites, the 600-m-thick succession of the *Rajahmundry Sandstone* forms small hills in the coastal belt of the Krishna–Godavari delta domain (Figs. 20.4 and 20.12). Like its homotaxial Cuddalore Sandstone, the Rajahmundry Formation is made up of coarse-grained sandstone with subordinate claystone and pebble beds. The Rajahmundry Sandstone was given its name by W. King in 1870. Its Thittachery section contains *A. papillosus* of the Mid Miocene to Pliocene age.

In the larger offshore zone underlying the seaward extension of the Rajahmundry Sandstone, there is a 1100-m-thick succession of Tertiary strata (Fig. 20.5b) ranging in age from the Palaeocene to the Pliocene (Majumdar et al. 1995; Rao 2001, 2002). It begins with the *Razole Formation* of the earliest lower Palaeocene, comprising dark grey to variegated shales, micaceous siltstone, sandstone and three units of lava flows. The volcanics are related presumably to the Deccan Trap. The claystone contains Early Palaeocene foraminifers. It seems that the Razole is the drowned or underwater part of the Deccan Inertrappean Beds. In the near-shore belt, the Razole strata are overlain by the *Nimmakuru Sandstone* of the Lower–Upper Palaeocene time and the distal offshore belt shows the Razole

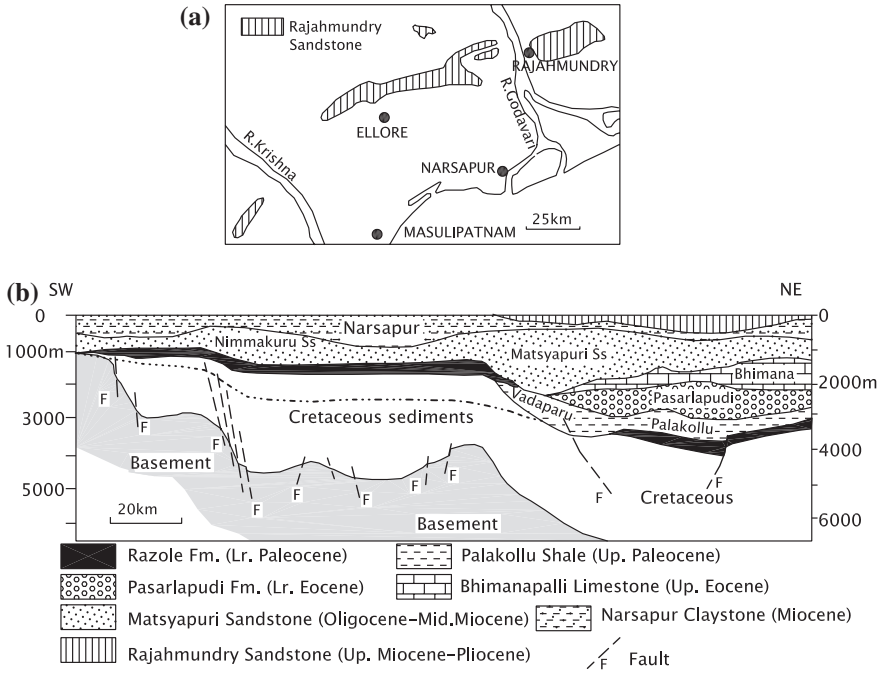

Fig. 20.12 **a** Sketch map shows outcrops of the Rajahmundry Sandstone of the Miocene–Pliocene age straddling across the delta domain of the Krishna and Godavari rivers (based on Prasad and Pundir 1999). **b** Lithostratigraphic succession and structure of the Krishna–Godavari Basin (after Majumdar et al. 1995)

succeeded by penecontemporaneous thick accumulation of the *Palakollu Shale* (Jaiprakash et al. 1993).

The Eocene is represented in the distal offshore belt by a thick succession of shale (*Vadaparru Shale*) and in the near-shore zone by a succession comprising grey-white sandstone with subordinate dark grey shale in the lower part (*Pasarlapudi Sandstone*), fossilliferous buff limestone with subordinate shale and sandstone in the upper part (*Bhimanapalli Limestone*). The *Pasarlapudi* succession comprises alternating grey dark sandstone and limestone containing *Lockhartia hunti*, *N. atacicus* and *N. globulus* of the Late Palaeocene to Early Eocene age. The unconformably overlying *Matsyapuri Formation* belongs to the Eocene to Early Oligocene time. The Oligocene *Narsapur Claystone* is an attenuated horizon sandwiched between two unconformities. Its distal offshore equivalent has been described as the *Ravva Formation*. The Ravva is made up of sandstone alternating with thick-bedded claystone and locally pebbly, pyritic and glauconitic clays. Foraminiferal assemblage comprising *Globigerinoides sicanus, Globigerina altispira, Miogypsina excentrica* and *Lepidocyclina* assigns the Ravva to the Miocene–Pliocene interval (Rao 2001). The seaward extension of the *Rajahmundry Sandstone*, unconformably covering the Narsapur, belongs to the Miocene to Pliocene temporal span.

In the offshore regime, the Mio–Pliocene equivalent of the Rajahmundri Sandstone is the *Godavari Claystone* containing layers of sandstones.

20.10 Mahanadi Delta Domain

The Quaternary sediments completely conceal the Tertiary succession in the Mahanadi delta domain (Fig. 20.13a). There is rapid seaward thickening of sediments. The disposition and quantity of sediments controlled by penecontemporaneous growth of normal faults are compatible with the Precambrian

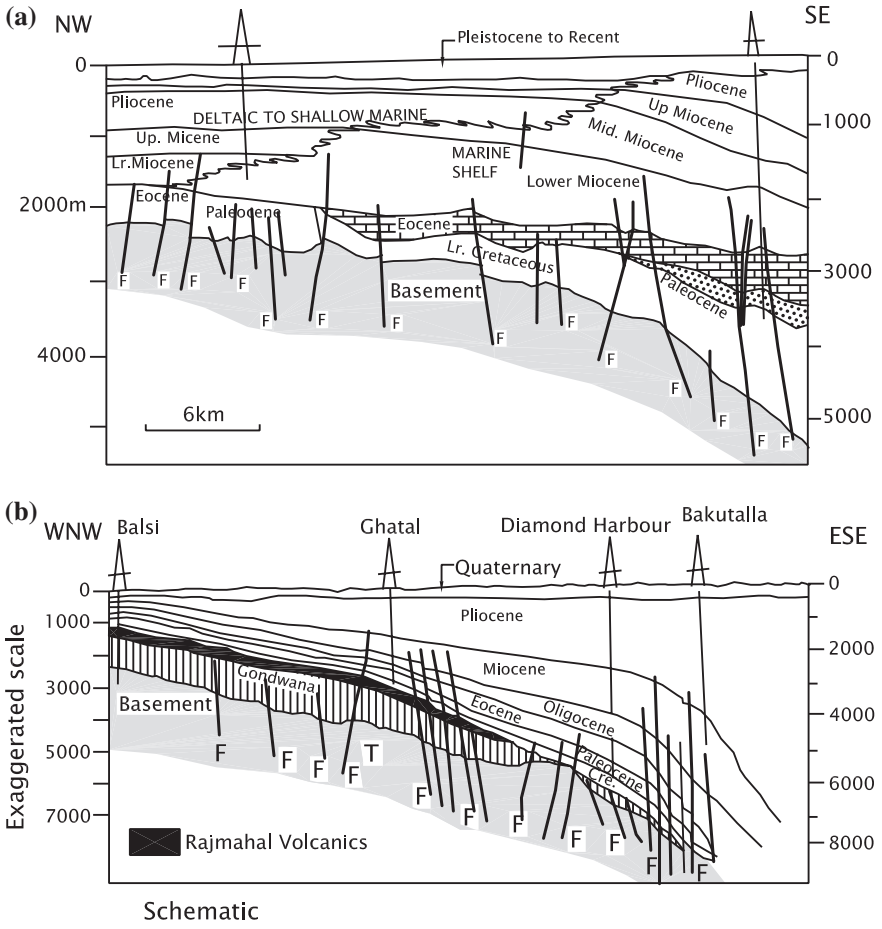

Fig. 20.13 **a** Generalized cross section of the Mahanadi offshore basin showing its structure and lithostratigraphy (after Jagannathan et al. 1983). **b** Schematic cross section of western flank of the Bengal Basin elucidating its structure and sedimentary succession (after Roybarman 1983)

structural trends. The offshore belt is believed to be a pull-apart basin developed parallel to the Coast (Jagannathan et al. 1983). Unconformably overlying the Lower Cretaceous in the underwater setting, the Palaeocene sequence comprises fine-grained sandstone, siltstone and claystone deposited in a delta environment. The succeeding Eocene carbonates, including lenticular horizons of biostromes and bioherms, cover a much larger area. The carbonates are overlain by claystone grading into siltstone with subordinate fine-grained sandstone assigned to the Lower–Middle Miocene. In the Upper Miocene–Pliocene time, the Mahanadi shelf was occupied by prograding deltas.

20.11 Bengal Basin

In the larger Bengal Basin, the Tertiary succession (Fig. 20.13b) occurs under a thick cover of the Quaternary sediments. It begins with arkose, with carbonaceous shale and coal–shale alternation locally characterized by pyritic or microspherulitic siderites. The succession represents a deltaic–estuarine deposit interdigitating with marine carbonates consisting of oolitic foraminiferal and algal limestones (Roybarman 1992). While the Lower Palaeocene sequence is described as the *Ghatal Formation*, the Upper Palaeocene to Middle Eocene succession is embodied in the *Jalangi Formation*. The *Kalighat* horizon comprises alternation of glauconitic sandstone and limestone, possibly the coeval of the Eocene Sylhet Limestone of the Meghalaya region.

Grey to dark grey calcareous shale and arkosic sandstone with dark grey siltstone, coal–shale and coal beds belonging to the Oligocene (Fig. 20.13b) are divisible into the *Hooghli*, *Burdwan* and *Diamond Harbour* formations. The Diamond Harbour succession testifies to the prevalence of marshy condition towards the end of the Oligocene and beginning of the Miocene. The Miocene *Pandua Formation* comprises very thick succession of sandstones with subordinate shales. Its lateral variant is dominated by shale (*Matla Formation*). During the Pliocene, the sediments were deposited on the shelf and deeper part of the basin. The *Debagram/Ranaghat Formation* is made up of siltstone and claystone with minor proportion of sandstone (Roybarman 1983).

20.12 Evolution of Life During the Tertiary Time

The Cenozoic era is described as the *Age of Mammals*. The beginning of the Tertiary saw rapid diversification of mammals which soon became the most abundant land-dwelling animals even as the land was dominated by flowering plants, the angiosperms. Adapting to many styles of flying, the birds became the most successful vertebrates in the sky.

20.12.1 Marine Invertebrates

Foraminifers were among the major components of the Cenozoic marine invertebrates. Corals once again became the dominant reef builders in warm waters. Echinoids and bryozoans proliferated. Among the cephalopods, the nautiloids and the shell-less forms such as squids and octopus were abundant.

The phytoplanktons were represented by diatoms, dinoflagellates and coccolithosphores, the diatoms being particularly abundant during the Miocene.

20.12.2 Terrestrial Mammals

There were two crucial developments in the bodies of the mammals: (i) development of chewing teeth, molars and premolars and (ii) the fusion of amnion of the amniote egg with the walls of uterus to form a placenta that carried nutrients and oxygen from mother to embryo. This permitted the young to develop much more fully before birth. These two developments gave the mammals tremendous advantage to develop and proliferate on land. Several new orders of mammals made their first appearance during the Palaeocene—rodents, rabbits and primitive carnivores, among others (Wicander and Monroe 2000). Many of the early mammals such as shrews, moles and hedgehogs were insectivores although quite many were plant eaters.

During the Eocene time, there was diversification of the mammals, some of the groups became extinct in the Oligocene epoch when dry climate prevailed. In the group that survived, there were ancestors of horses, camels, elephants, rhinoceros, and a variety of hoofed animals. These ancestral animals bear little resemblance with their descendents. Through their extraordinary capability of adaptation, the rodents that first appeared in the Palaeocene became very diverse and dominant, constituting more than 40 % of mammals species (Wicander and Monroe 2000). By the Miocene and Pliocene times, three-toed horses, sabre-tooth cats and deer-like animals with forked horns on their snouts had become prolific.

Primitive primates of the Early Palaeocene time were of the size of mice and had long-snouted animals (like shrews). But by the Eocene time, large primates had evolved. They had the looks of the present-day lemurs and tarsiers. The humanoid group containing apes and humans evolved in the Miocene epoch.

Development of canine teeth and special shearing teeth invested a the carnivores with the ability to kill other animals. The carnivores first appeared in the Palaeocene. Of the two branches that evolved, one became extinct in the Miocene and the other that grew and proliferated included cats and hyenas. They were able to develop better shearing teeth and longer limbs for faster movements.

Appearing in the Early Eocene, the even-toed hoofed animals, artiodactyls, soon became very diverse and included species of cattle, sheep, goat, pig, antelope, deer, giraffe, hippopotamus, and camel. The odd-toed hoofed animals (perissodactyls) were less diversified and included species of horse, rhinoceros and tapir.

They evolved during the Eocene, increased in number and diversified through the Oligocene. Being herbivores, their chewing teeth were modified for the diet of vegetation—high-crown chewing teeth resistant to abrasion in grazing animals, and sharper teeth in browsing animals. In order to gain speed in running, they developed longer and slender limbs. However, some even-toed hoofed mammals (ungulates) like rhinoceros remained large bodied, with massive limbs to support their weight. Appearing in the Eocene, the camels were two-toed during the Miocene time and soon diversified into several distinct types.

The bovids (cattle, bison, sheep, goat and antelope) evolved during the Miocene and diversified in the Pliocene.

Elephants of one kind or another lived through the entire Cenozoic era. By the Oligocene time, they showed a trend to larger size and the development of long snout (proboscis) and modification of incisors to large tusks. In some of them, the tusks were curved downwards (deinotheres); in others, the teeth adapted were to browsing (*mastodon*); and in some others, the teeth were modified for grazing (*mammoth*). The mammoths and the present-day elephants diversified during the Pliocene and Pleistocene time.

In the Early Eocene, a terrestrial wolf-size carnivore animal mesonychids took to the sea. It underwent modification—the front limbs gradually became fin-like flippers, there was development of a large horizontal fluke for propulsion, and the nostril was relocated at the top of the head. The Early Eocene whale *Ambulocetus* still preserved limbs capable of bearing the weight of the animal on land (Fig. 19.20). By the Oligocene time, the whale had evolved fully.

20.13 Important Mineral Deposits

The Tertiary sediments are among the most productive geological formations of India so far as the economically valuable petroleum deposits are concerned. The other important deposits are of clays, lignite and beach sands with several detrital minerals.

Organic-rich marine clays and sands of deltaic environment are the source and good reservoir of *petroleum oil and gas*. Shales constitute the top seals that trap the petroleum fluids. As already explained, the hydrocarbon deposits were formed under oxygen-deficient or anoxic conditions in rapidly subsiding depressions of marine realm and later during the Miocene time migrated updip within various play types where there was structural inversion. In the Sabarmati–Cambay Basin (Fig. 20.14a), the source rocks occur at the top of Lower Palaeocene Olpad Formation, in the middle of the Upper Palaeocene to the Middle Eocene Cambay Shale and at the base of Middle Eocene Kalol Formation (Banerjee et al. 2002). Excluding the Gandhar deposit (near Bharuch), the estimated reserves are 820 million tonnes of oil and 200 million tonnes of oil equivalents of gas (Merh 1995). In the Bombay Offshore Basin (Fig. 20.14b), the principal source of hydrocarbons is the Palaeocene–Eocene sediments deposited in restricted marine and paralic environments. Associated with unconformities, the Miocene Limestones make

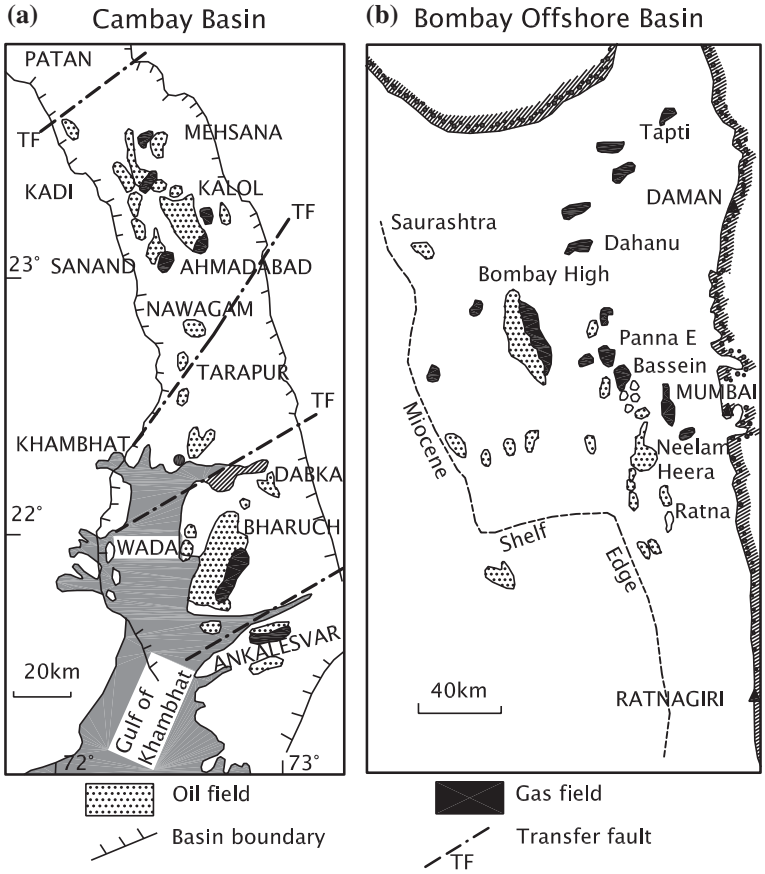

Fig. 20.14 **a** Main petroleum fields in the Sabarmati–Cambay Basin (based on Banerji et al. 1991; Viswanath 1997). **b** Oil and gas fields in the Offshore Bombay Basin (after Viswanath 1997)

the main reservoir rocks in the Bombay High and the Middle Eocene to Lower Oligocene limestones in other areas. The Oligocene sandstones form the main reservoir in the Daman–Tapi area (Banerjee et al. 1991).

In the Krishna–Godavari Offshore Basin (Figs. 20.12 and 20.15) the Palakollu/Vadaparru Shale of the Late Palaeocene to Early Eocene age are the source of hydrocarbons. The Palakollu has the potential of 1700 MMT oil and 1700 MMT of gas, but the established reserve is of the order of only 24 MMT (Majumdar et al. 1995). There are more than two dozen small- and medium-size wells of oil and gas fields on land and a little more than 8 fields in the offshore belt. Hydrocarbon accumulations are found in the Matsyapuri, the Ravva and the Godavari formations in addition to several small fields ranging in age from Permo–Triassic to Cretaceous.

In Bangladesh, the hydrocarbon condensates occurring within organic-rich shales of the Miocene Bhuban Formation in the Surma Basin are waxy and

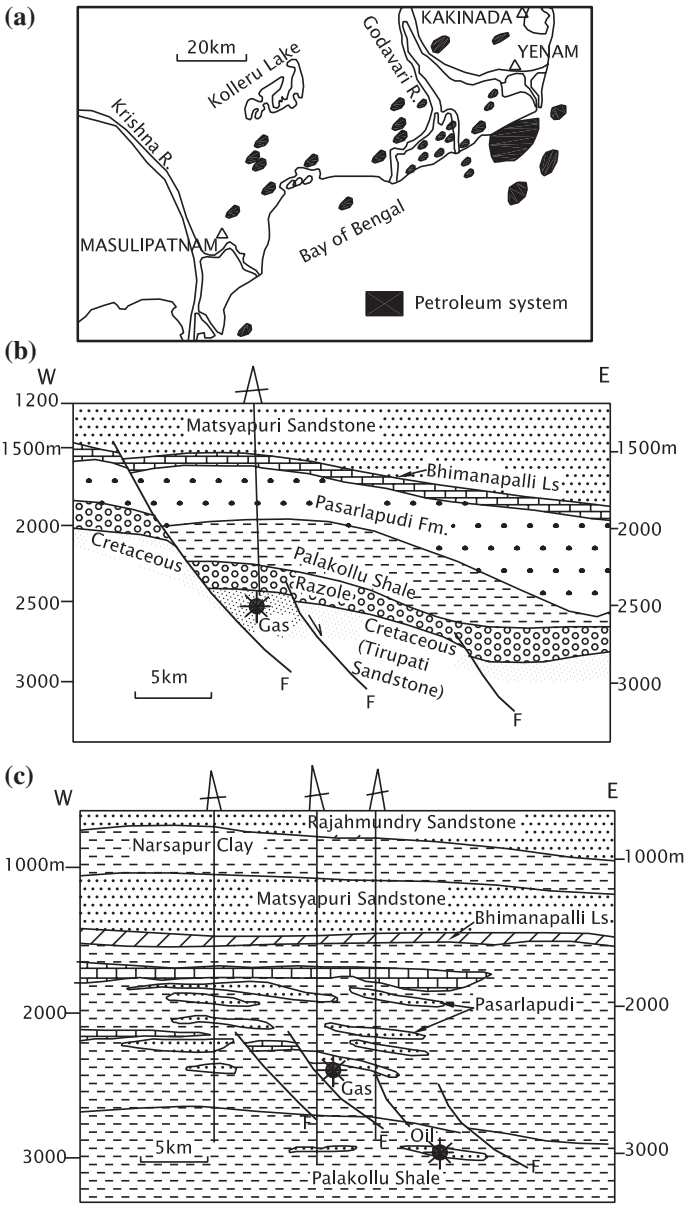

Fig. 20.15 Krishna–Godavari Offshore Basin

isotopically enriched in C^{13} and characterized by large amount of bicadinanes with a high ratio of pristane–phytane, implying genesis from angiospermous plants (Curiale et al. 2002). It may be mentioned that the petroleum deposits are of the order of 61 tcf in the Surma Basin.

As of 2010, the position of hydrocarbon (oil and gas) deposits in various petroliferous basins in India is summarized below (Singh 2000; Biswas 2012; Aron 2010).

Bombay offshore Basin	
Total estimated resource base	9190 MMT
In-place reserve of oil and oil-equivalent gas	3390 MMT
Bombay high alone	2122 MMT
Cambay Basin	
Total estimated resource	2050 MMT
In-place reserve	1140 MMT
Rajasthan Basin	
Prognosticated oil and oil-equivalent gas resource	380 MMT
Estimated in-place reserve of oil	94 MMT
Estimated in-place oil and oil-equivalent gas	116 MMT
Assam Basin	
Prognosticated resource	3180 MMT
Total in-place estimated reserve of oil	1000 MMT
Gas	121 BCM
Tripura–Mizoram Basin	
Total estimated reserve of oil and oil-equivalent gas	1860 MMT
In-place estimated reserve of gas	20 BCM
Mahanadi Basin	
Prognosticated onshore resource	45 MMT
Prognosticated offshore reserve	100 MMT
Krishna–Godavari Basin	
Prognosticated reserve	1130 MMT
Total estimated in-place reserve	185 MMT
Kaveri Basin	
Prognosticated resource	700 MMT
Total estimated in-place reserve	92 MMT

The reserve of Tertiary *coal* is larger than that of the Gondwana successions. However, out of the re-estimated 254 billion tonnes of Tertiary coal reserve (down to the depth of 1500 m), only about 12 billion tonnes occurring at shallow depths can be mined, and the deeper deposits amounting to 242 billion tonnes (123 billion tonnes in Gujarat, 100 billion tonnes in Rajasthan and 19 billion tonnes in Tamil Nadu) are not amenable to mining (Sharma 2003). The *lignite* horizon in the Cuddalore Sandstone succession occurs in a N–S, 40-km-long and 10-km-wide Neyveli belt. Under the 55-m-thick overburden, the lignite seams vary in thickness from 8 to 22 m. Huge reserve of coal—50 m in thickness—at the depth of 700–1000 m below the ground surface in the Mehsana area in northern Gujarat opens a possibility of underground gasification for energy resource.

In the Tertiary of Kachchh, there are quite a few workable deposits of *clays*. More than 6 million tonnes of *bentonite clay* is mined profitably. In the Bhavnagar

area, nearly 40 million tonnes of clays are associated with bauxite at the base of the Tertiary, resting atop the Deccan lavas (Merh 1993).

Known as ball clay in Kerala, the *kaolin* deposits occur in parts of Kannur and Kollam districts, the reserve being of the order of 0.41–1.31 million tonnes (Soman 2002).

References

Alimohammadian, H., Sahai, H., Patnaik, R., Rana, R. S., & Singh, H. (2005). First record of an exceptionally diverse and well-preserved amber-bedded biota from lower Eocene (~52 Ma) lignites, Vastan, Gujarat. *Current Science, 89*, 1328–1330.

Armstrong-Altrin, J. S., Lee, Y. I., Verma, S. P., & Ramasamy, S. (2004). Geochemistry of sandstones from the Upper Miocene Kundankulam Formation, southern India: Implication for provenance, weathering and tectonic setting. *Journal of Sedimentary Research, 74*, 285–297.

Bajpai, S., Kapur, V. V., Das, D. P., Tiwari, B. N., Saravanan, N., & Sharma, R. (2005). Early Eocene land mammals from Vastan lignite mine, district Surat (Gujarat, West India). *Journal of Palaeontological Society of India, 50*(101–113), 147–151.

Banerji, V., Mittal, A. K., Gupta, A. K., Balyan, A. K., & Chaudhary, D. R. (1991). On the origin of hydrocarbon reservoired in Bombay High: Stable isotopic studies of natural gases. *Journal of Southeast Asian Earth Science, 5*, 339–343.

Banerjee, A., Pahari, S., Jha, M., Sinha, A. K., Jain, A. K., Kumar, N., et al. (2002). The effective source rocks in the Cambay Basin, India. *Bulletin American Association of Petroleum Geologists, 86*, 433–456.

Basu, D. N., Banerjee, A., & Tamhane, D. M. (1982). Facies distribution and petroleum geology of Bombay Offshore Basin, India. *Journal of Petroleum Geologists, 5*, 57–75.

Bhandari, L. L., & Chowdhary, L. R. (1975). Stratigraphic analysis of Khadi and Kalol Formations, Cambay Basin, India. *Bulletin American Association of Petroleum Geologists, 59*, 856–871.

Bhatt, N. (2000). Lithostratigraphy of the Neogene-Quaternary deposits of Dwarka-Okha area, Gujarat. *Journal of the Geological Society of India, 55*, 139–148.

Biswas, S.K. (1973). Time stratigraphic classification of the Tertiary rocks of Kutch—A revision and amendments. *Quaternary Journal of Geological Mining Metallurgical Society India, 44.*

Biswas, S. K. (1987). Regional tectonic framework, structure and evolution of the western marginal basins of India. *Tectonophysics, 135*, 307–327.

Biswas, S. K. (1992). Tertiary stratigraphy of Kutch. *Journal of Palaeontological Society of India, 37*, 1–29.

Biswas, S. K., & Deshpande, S. V. (1983). Geology and hydrocarbon prospects of Kutch, Saurashtra and Narmada basin. In: L. L. Bhandari, et al. (Eds.), *Petroliferous Basins of India* (pp. 111–126). Dehradun: KDM Institute of Petroleum Exploration.

Biswas, S. K., & Raju, D. S. N. (1973). The rock stratigraphic classification of the Tertiary sediments of Kutch. *Bulletin ONGC, 10*, 37–46.

Chandra, P. K., & Chowdhary, L. R. (1969). Stratigraphy of the Cambay Basin. *Bulletin ONGC, 6*, 37–50.

Curiale, J. A., Covington, G. C., Shamsuddin, A. H. K., Morelos, J. A., & Shamsuddin, A. K. (2002). Origin of petroleum in Bangladesh. *American Association of Petroleum Geologists, 86*, 625–652.

Hardas, M. G., & Biswas, S. K. (1973). Palaeogene sediments from southwestern Kutch, Gujarat. *Bulletin ONGC, 10*, 47–54.

Jacob, K., & Sastry, V. V. (1952). Miocene foraminifers from Chavara, near Quilon, Travancore. *Record Geological Survey of India, 82*, 342–353.

Jagannathan, C. R., Ratnam, C., Baishya, N. C., & Dasgupta, U. (1983). Geology of the offshore Mahanadi Basin. In: L. L. Bhandari, et al. (Eds.), *Petroliferous Basins of India* (pp. 101–104). Dehradun: KDM Institute of Petroleum Explortion.

Jaiprakash, B. C., Singh, J., & Raju, D. S. N. (1993). Foraminiferal events across K/T boundary and age of Deccan volcanism in Palakollu area, Krishna-Godavari Basin, India. *Journal of the Geological Society of India, 41*, 105–118.

Kalia, P. (1978). Buliminids from Middle Eocene of Rajasthan, India. *Journal of Palaeontological Society of India, 21–22*, 44–48.

Kalia, P., & Banerjee, A. (1991). *Pellatispira*-bearing Upper Eocene subcrops in Tanot-I well, northwest of Jaisalmer, Rajasthan, and their significance. *Journal of the Geological Society of India, 38*, 76–81.

Kalia, P., & Banerjee, A. (1995). Occurrence of the genus *Eoconuloides* Cole and Bermudez 1944 in Rajasthan, India and its palaeobiogeographic significance. *Micropalaeontology, 41*, 187–194.

Khosla, S. C. (1973). Stratigraphy and microfauna of the Eocene beds of Rajasthan. *Journal of the Geological Society of India, 14*, 142–152.

Kumaran, K. P. N., Soman, K., Kamble, C. V., & Joseph, A. (1995). Palynological analysis of sections from Bharathi and Kundara clay mines, Kerala Basin: Palaeoecological and tectonic perspective. *Current Science, 69*, 1023–1027.

Lal, N. K., Garg, A., Harinder, P., Rawat, S., & Dirghangi, R. S. (1995). Rifting and drifting of Indian plate, its effect on tectonics and sedimentation in the eastern part of the Bombay Offshore Basin, India. In *Proceedings of the 1st International Petroleum Conference*. Delhi: B.R. Publishing Corporation, pp. 485–495.

Majumdar, S. K., Basu, B., Shivashankar, J., Arunachalam, A., & Rangaraju, M. K. (1995). Palakollu–Pasarlapudi petroleum system, Krishna–Godavari basin, India. In *Proceedings of the Petrotech-5: Technology Trends in Petroleum Industry*. New Delhi: B.R. Publishing Corporation, pp. 495–508.

Mathur, U. B., & Mathur, A. K. (1998). A Neogene flora from Bikaner, Rajasthan. *Journal of Geoscience, 19*, 129–142.

Mathur, L. P., Rao, K. L. N., & Chaube, A. N. (1968). Tectonic framework of Cambay Basin. *Bulletin ONGC, 5*, 7–28.

Menon, K. K. (1967). The lithology and sequence of Quilon Beds. *Proceedings of the Indian Academy of Science, 65*, 20–25.

Merh, S. S. (1993). Neogene-Quaternary sequence in Gujarat: A review. *Journal of the Geological Society of India, 41*, 259–276.

Merh, S. S. (1995). *Geology of Gujarat*. Bangalore: Geological Society of India. 222 p.

Mitra, P., Zutshi, P. L., Chaurasia, R. A., Chugh, M. L., Ananthanarayanan, S., & Shukla, B. (1983). Exploration in western offshore basins. In: L. L. Bhandari, et al. (Eds.), *Petroliferous Basins of India* (pp. 15–24). Dehradun: K.D.M. Institute of Petrolleum Exploration.

Mohan, M. (1982). Palaeogene stratigraphy of western India. In: *Special Publication of the Palaeontological Society of India, 1*, 21–36.

Mohan, M. (1995). Cambay Basin—a promise of oil and gas potential. *Journal of Palaeontological Society of India, 40*, 41–47.

Mohan, M., & Kumar, P. (1980). Biostratigraphy of Kerala Offshore. *Journal of Geoscience, 1*, 1–9.

Mohan, M., & Soodan, K. S. (1970). Middle Eocene planktonic foraminiferal zonation of Kutch, India. *Micropalaeontology, 16*, 37–46.

Mohan, M., Kumar, P., & Narayanan, V. (1977). Palaeocene-Eocene boundary in Cauvery Basin. *Journal of the Geological Society of India, 18*, 401–411.

Nair, K. M., Singh, N. K., Ram, J., Gavarshetty, L. P., & Balamuralikrishnan, B. (1992). Stratigraphy and sedimentation of Bombay Offshore basin. *Journal of the Geological Society of India, 40*, 415–442.

Narain, H., Kaila, K. L., & Verma, R. K. (1968). Continental margin of India. *Canadian Journal of Earth Science, 5*, 1051–1065.

Padmalal, D. (1996). Sedimentary structures and textures of the Warkalli sandstone (Mio-Pliocene) at Cherunniyoor, Kerala. *Journal of the Geological Society of India, 48*, 403–407.

Pandey, J. (1982). Chronostratigraphic correlation of the Neogene sedimentaries of western Indian shelf, Himalayas and Upper Assam. In: *Special Publication of Palaeontological Society of India, 1*, 95–129.

Pandey, O. P., & Agrawal, P. K. (2000). Thermal regime, hydrocarbon maturation and geodynamic events along the western margin of India since Cretaceous. *Journal of Geodynamics, 30*, 439–459.

Pandey, J., & Dave, A. (1996). Early Palaeogene smaller benthic foraminifera of Indian basins. In *Proceedings of 15th Colloquialism Micropalaentology stratigraphy*. Dehradun, pp. 99–110.

Pandey, J., & Dave, Alok. (1998). *Stratigraphy of Indian Petroliferous Basins* (p. 248). Dona Paula: National Institute of Oceanography.

Paulose, K. V., & Narayanaswami, S. (1968). The Tertiaries of Kerala coast. *Memoirs of the Geological Society of India, 2*, 300–308.

Prabhakar, K. N., & Zutshi, P. L. (1993). Evolution of southern part of Indian East Coast basins. *Journal of the Geological Society of India, 41*, 215–230.

Prasad, B., & Pundir, B. S. (1999). Biostratigraphy of the exposed Gondwana and Cretaceous rock of Krishna-Godavari basin, India. *Journal of Palaeontological Society of India, 44*, 91–117.

Punekar, J., & Saraswati, P. K. (2010). Age of the Vatsan Lignite in context of some oldest Cenozoic fossil mammals from India. *Journal of the Geological Society of India, 76*, 63–68.

Raha, P. K., Rajendran, C. P., & Kar, R. K. (1986). Eocene palynofossils from the subcrop of Kerala. *Bulletin of the Geological Mining Metallurgical Society of India, 54*, 227–232.

Raju, A. T. R. (1968). Geological evolution of Assam and Cambay Tertiary basins of India. *Bulletin American Association of Petroleum Geologists, 12*, 2422–2437.

Raju, A. T. R. (1975). Depositional environments of the oil-bearing Eocene sands on Ankaleshwar field, Cambay Basin. *Journal of the Geological Society of India, 18*, 165–176.

Raju, A. T. R., & Srinivasan, S. (1983). More hydrocarbon from well-explored Cambay Basin. In: L. L. Bhandari, et al. (Eds.), *Petroliferous Basins of India* (pp. 25–35). Dehradun: K.D.M. Institute of Petroleum Exploration.

Rana, R. S., Kumar, K., Singh, H., & Rose, K. D. (2005). Lower vertebrates from the Late Palaeocene-Earliest Eocene Akli Formation, Giral Lignite Mine, Barmer district, western India. *Current Science, 89*, 1606–1612.

Rao, K. L. N. (1969). Lithostratigraphy of the Palaeogene succession of southern Cambay Basin. *Bulletin ONGC, 6*, 24–37.

Rao, G. N. (2001). Sedimentation, stratigraphy, and petroleum potential of Krishna-Godavari basins, East Coast of India. *Bulletin American Association of Petroleum Geologists, 85*, 1623–1643.

Rao, G. N. (2002). Petroleum geology: Krishna-Godavari Basin. *Journal of the Geological Society of India, 60*, 705–706.

Rao, R. P., & Talukdar, S. N. (1980). Petroleum geology of Bombay High Field, India. In: M. T. Halbouty (Ed.), *Giant Oil And Gas Fields of the Decade* (pp. 1968–1978). Tulsa: American Association of Petroleum Geologists.

Roybarman, A. (1983). Geology and hydrocarbon prospects of West Bengal. *Journal of the Petroleum Asia, 6*, 51–56.

Roybarman, A. (1992). Geological history and hydrocarbon exploration in Bengal Basin, India. *Journal of Geology, 64*, 235–238.

Sahni, A., & Mishra, V. P. (1975). Lower Tertiary vertebrates from western India. *Monograph Palaeontological Society of India, 3*, 1–48.

Sahni, A., Saraswati, P. K., Rana, R. S., Kumar, K., Singh, H., Alimohammadian, H., et al. (2006). Temporal constraints and depositional palaeoenvironments of the Vastan Lignite sequence, Gujarat: Analogy for the Cambay Shale hydrocarbon source rocks. *Indian Journal of Petroleum Geologists, 15*, 1–20.

Samanta, B. K. (1973). On the age of the Pondicherry Formation of Madras, S. India. *Journal of the Geological Society of India, 14*, 289–295.

Sarangi, S., Sarkar, A., Bhattacharya, S. K., & Ray, A. K. (1998). Isotopic evidence of a rapid cooling and continuous sedimentation across the Eocene-Oligocene boundary of Wagapadhar and Waior, Kutch. *Journal of the Geological Society of India, 51*, 245–248.

Saraswati, P. K., & Ramesh, R. (1992). Eocene-Oligocene stable isotope stratigraphy of Kutch. *Journal of the Geological Society of India, 39*, 427–432.

Saraswati, P. K., Ramesh, R., & Navada, S. V. (1993). Palaeogene isotopic temperature of western India. *Letheia, 26*, 89–98.

Sarkar, A., Sarangi, S., Bhattacharya, S. K., & Ray, A. K. (2003a). Carbon isotope across the Eocene-Oligocene boundary sequence of Kutch, western India: Implications to oceanic productivity and CO_2 change. *Geophysical Reseach Letters, 30*, 1–4.

Sarkar, A., Yoshioka, H., Ebihara, M., & Naraoka, H. (2003b). Geochemical and organic carbon isotope studies across the continental Permo-Triassic boundary of Raniganj basin, eastern India. *Palaeogeography Palaeoclimatology Palaeoecology, 191*, 1–14.

Sharma, D. D. (2003). Review of Coal resources in India and their exploitation stratigraphy. *Journal of the Geological Society of India, 61*, 387–402.

Siddique, H. N., & Bahl, D. P. (1965). Geology of the bentonite deposits of Barmer district, Rajasthan. *Memoirs of the Geological Survey of India, 96*, 1–96.

Siddique, H. N., & Sukeshwala, R. N. (1976). Occurrence of rhyolitic tuff at deep sea drilling project site 219 on the Laccadive Ridge. *Journal of the Geological Society of India, 17*, 539–546.

Singh, S. N. (1951). Kirthar foraminifera from Rajasthan. *Current Science, 20*, 230–232.

Singh, S. N. (1953). Geology of the area WSW of Marh village near Kolyat, Bikaner, Rajasthan. *Proceedings of the National Academy of Sciences, 23*, 13–20.

Singh, M. P. (1996). Mesozoic–Tertiary biostratigraphy and biogeochronological dalum planes in Jaisalmer Basin, Rajasthan. In: J. Pandey, R. J. Azmi, A. Bhandari & A. Dave (Eds.), *Contrs XV Indian Colloq Micropal Strat*. Dehradun: KDMIPE and WIHG Publication.

Singh, B. P. (2000). Sediment dispersal pattern in the Murree Group of the Jammu area, NW Himalaya, India. *Himalayan Geology, 21*, 189–200.

Singh, P., & Singh, M. P. (1986). Late Middle Eocene calcareous nannoplanktons from Babia Hill, Kutch, Gujarat. *Journal of Geoscience, 8*, 145–162.

Singh, P., Rastogi, K. K., & Vimal, K. P. (1978). Late Eocene calcareous nanoplanktons from Tarkeshwar, Surat-Bharoach area, Gujarat. *Journal of Palaeontological Society of India, 21–22*, 1–12.

Singh, S. K., Kishore, S., Misra, P. K., Jauhari, A. K., & Gupta, A. (2010). Middle Eocene calcarious algae from southwestern Kachchh, Gujarat. *Journal of the Geological Society of India, 75*, 749–759.

Singhal, J., Singh, N. P., & Lys, M. (1971). Paleocene-Eocene boundary in the Jaisalmer area. *Journal of Foraminiferal Research, 1*, 190–194.

Soodan, K. S. (1980). Fossil Holothuroidea from the Eocene rocks of Bikaner, Rajasthan. *Journal of Geoscience, 1*, 11–12.

Sudhakar, R., & Basu, D. N. (1973). A reappraisal of the Palaeogene stratigraphy of southern Cambay Basin. *Bulletin ONGC, 10*, 55–76.

Tandon, K. K., Mathur, V. K., & Saxena, R. K. (1980). Paleocene-Early Eocene biostratigraphy in Nareda, southwestern Kutch, western India. *Journal of the Palaeontological Society of India, 23–24*, 86–91.

Tewari, H. C., Dixit, M. M., & Sarkar, D. (1995). Relationship of the Cambay rift basin to the Deccan volcanism. *Journal of Geodynamics, 20*, 85–95.

Varadarajan, K., & Madhavan Nair, K. (1978). Stratigraphy and structure of Kerala Tertiary basin. *Journal of the Geological Society of India, 19*, 217–220.

Viswanath, S. N. (1997). *A Hundred Years of OIL*. New Delhi: Vikas Publishing House. 175 p.

Wadia, D. N. (1975). *Geology of India* (p. 508). New Delhi: Tata McGraw Hill.

Wahi, S., Tandon, S. K., & Sharma, U. (1991). Lithofacies analysis, benthic foraminifers and depositional environments of the Chhasra Member: A transgressive tide and storm-affected Early Miocene sequence in Kachchh, India. *Journal of the Geological Society of India, 38*, 119–149.

Wani, M. R., & Kundu, J. (1995). Tectonostratigraphic analysis in Cambay rift basin: Leads for future exploration. In *Proceedings of the 1st International Petroleum Conference*. Delhi: B.R. Publishing Corporation, pp. 147–174.

Wicander, R., & Monroe, J. S. (2000). *Historical geology: Evolution of earth and life through time* (4th ed., p. 427 p). Thompson, USA: Books/Cole.

Zubov, I. P., Naugolny, I. K., Zapivalov, N. P., & Chandra, P. K. (1966). Problem of correlation and distribution of hydrocarbon-bearing horizons in the Eocene of Cambay Basin. *Bulletin ONGC, 3*, 9–13.

Chapter 21
Andaman Island Arc and Back-Arc Sea

21.1 Configuration

The 850-km-long chain of islands between the Bay of Bengal and the Andaman Sea constitutes the central part of the 5000-km-long Myanmar–Indonesia Mobile Belt related to an *active subduction zone*. The Andaman Island Arc comprises two nearly parallel arcuate belts. The western arc is represented by more than 300 islands of the Andaman, Nicobar and Mentawai groups. It is made up of Upper Cretaceous–Tertiary flysch, implanted with ophiolites at various structural levels. This belt is the southern extension of the Patkai–Naga–Arakan Orogenic Belt of the India–Myanmar border and stretches south-eastwards into a festoon of islands and associated subduction zone, offshore Sumatra (Fig. 21.1). The eastern arc embodies seamounts and dormant and active volcanoes extends northwards through the central sedimentary basins of Myanmar, characterized by Miocene to Quaternary volcanoes. South-eastwards, it continues into the island of Sumatra. West of the Andaman Island Arc, the seafloor of the Bay of Bengal is subducting eastwards. This is evident from pronounced seismicity and deformation of Pleistocene and younger sediments at the base of the landward wall of the sediment-filled Java Trench that continues north-westward past the Andaman Island Arc. And east of this arc lies the *back-arc basin*, the Andaman Sea, resulting from splitting apart of the ocean floor due to its spreading.

The island arc is divided by the Ten Degree Channel into the Andaman group and the Nicobar cluster of islands. The highest point in the Andaman Island is the 732-m-high Saddle Peak, and the tallest island in the Nicobar group is the 642-m Thulier Point. The larger number of islands shows very low relief and is commonly surrounded by coral reefs.

Among the pioneers whose contributions form the basis of constructing the framework of the geological history of the Andaman geotectonic unit are V. Ball (in 1870), R.D. Oldham (in 1885), F.R. Mallet (in 1888), G.H. Tipper (in 1911) and E.R. Eames (in 1926).

K.S. Valdiya, *The Making of India*, Society of Earth Scientists Series,
DOI 10.1007/978-3-319-25029-8_21

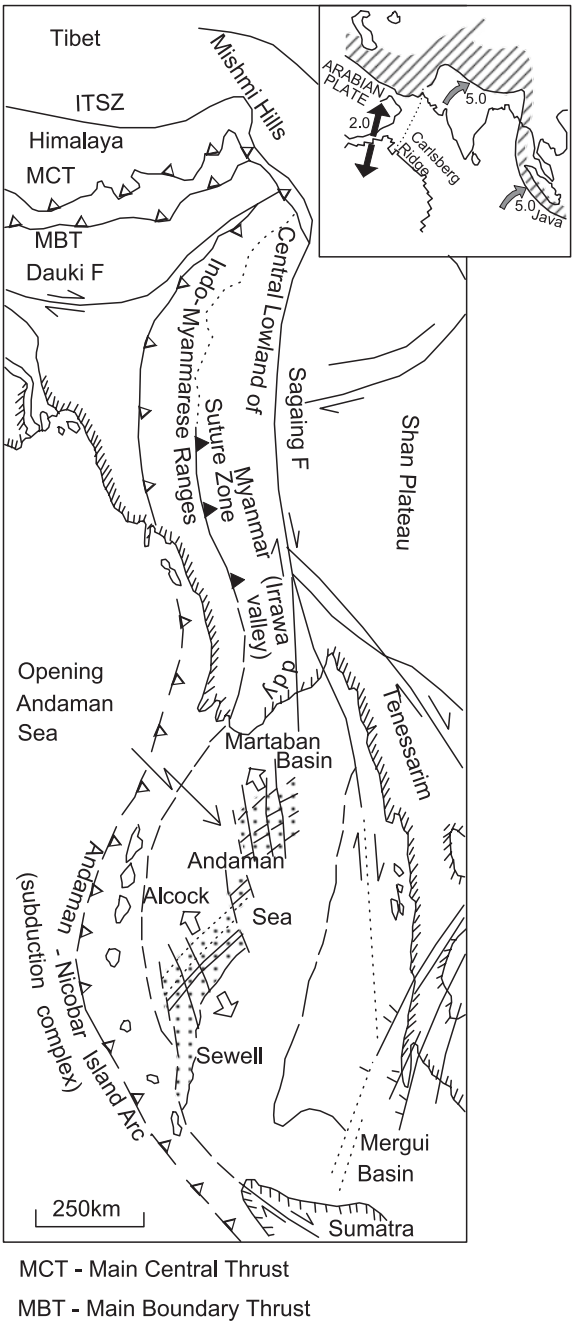

MCT - Main Central Thrust

MBT - Main Boundary Thrust

Fig. 21.1 Andaman Island Arc forms the central part of the Myanmar–Indonesia Mobile Belt. It is a young subduction complex. *Inset* shows the tectonic setting of the island arc (based on Curray et al. 1978 and Curray 2005)

21.2 Geophysical Characteristics

West of the island arc, the gravity anomaly is pronouncedly negative varying from −20 mGal in the northern part close to Myanmar to −100 mGal in the south near Nicobar (Mukhopadhyay 1988), implying mass deficiency usually associated with sinking down of the crust. Seismic data define an eastward-dipping (45º–55º) *Benioff Zone* (Fig. 21.2) with shallow intermediate and deep (up to 200 km) hypocentres (Dasgupta and Mukhopadhyay 1993).

East of the island arc, the central belt of the Andaman Sea is characterized by anomalously high heat flow—of the order of 5.27–5.9 HFU compared to mere 1.9–3.3 HFU of the surrounding floor of the sea (Curray et al. 1978; Eguchi et al. 1980).

21.3 Structural Layout

The structural design of the western sedimentary belt of the Andaman Island Arc (Figs. 21.3, 21.4 and 21.5) is very similar to that of the Arakan–Naga–Patkai Range. Bordered along the west by a sediment-filled oceanic trench—the extension of the *Java Trench*—the Andaman ridge is made up of a chain of islands. Within a distance of just 30 km, the steep western slope goes down to the depth of 1500–2000 m, while the outer flank is 5–15 km wide and compresses a series of faulted anticlines and synclines of the amplitude 100–1000 m (Cochran 2010). The West Andaman Fault forms the boundary between the Burman and the Sunda plates and divides the sea into forearc and back-arc basins. The islands are formed of a series of narrow parallel folds split longitudinally by a multitude of faults (Figs. 21.3, 21.4 and 21.5) that dip eastwards such as listric faults (Roy 1983, 1987). This has given rise to a stack of imbricating slices, each made up of sedimentary and ophiolitic rocks (Roy 1992) (Fig. 21.4). Some of the folds have diapiric cores of mudstones, presumably related to mud volcanoes. The older folds and strike faults are superimposed by a younger set of cross-folds and wrench faults, oriented ENE–WSW to NE–SW (Fig. 21.3). As a result of wrench faulting and segmentation, the

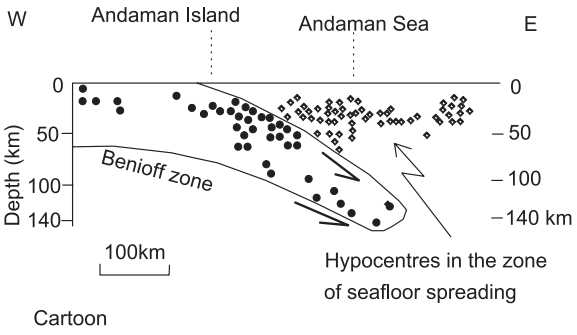

Fig. 21.2 Benioff Zone defined by hypocentres (after Dasgutpa and Mukhopadhyay 1993)

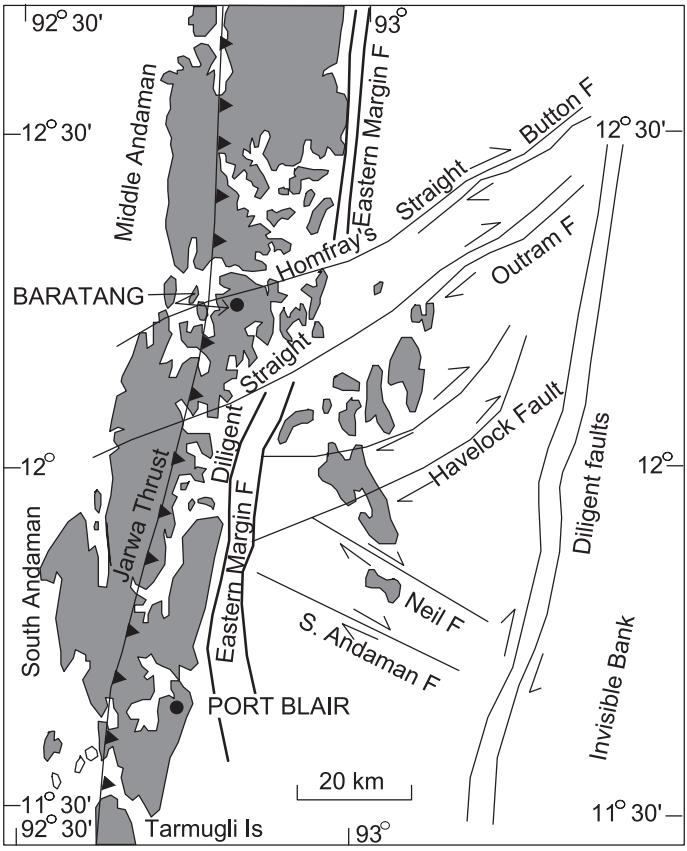

Fig. 21.3 Tectonic map of the Andaman Island Arc showing major faults with associated sharp folds. Note the ENE- to WNW-oriented wrench faults that have segmented the island arc (after Roy 1983)

island arc itself is dextrally shifted away from the mainland Myanmar in the north, and from the Indonesian Island Arc in the south-east. The deformation is particularly intense in the Nicobar sector (Fig. 21.4c).

The eastern margin of the Andaman Ridge is characterized by a 60-km by 20-km shallow platform known as the *Invisible Bank*. It is demarcated by a fault that has downthrown the eastern block to the depth of −3000 m and formed a deep rift (Figs. 21.3 and 21.4b). Close to the Invisible Bank Fault occurs a festoon of seamounts (Alcock and Sewell) and dormant (Narcondam) and active (Barren) volcanoes. The rift extends southwards into the Semenko rift valley in Sumatra.

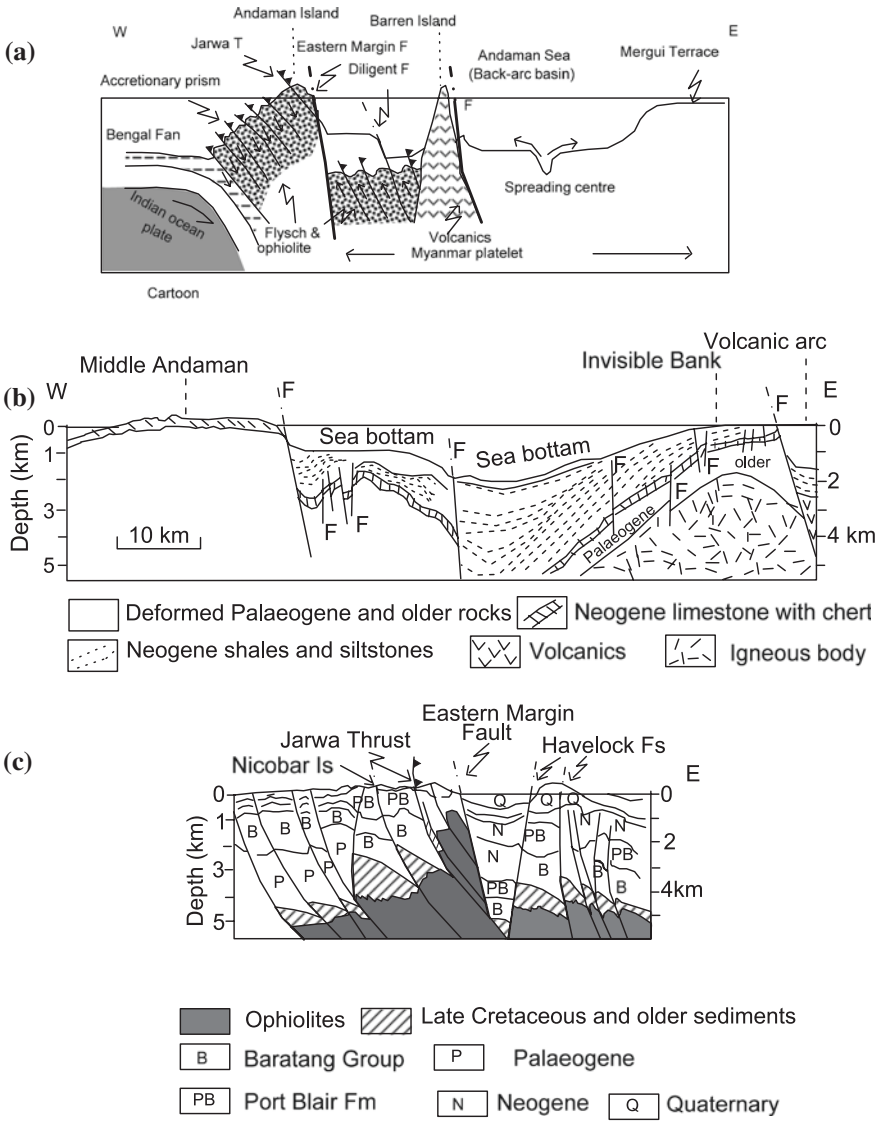

Fig. 21.4 **a** and **b** Sections show the rift basin between the forearc basin and the Invisible Bank, defined by a fault and a chain of volcanoes (after Roy 1983). **c** Profile of the Great Nicobar island, showing less disturbed Neogene sedimentary rocks unconformably resting on the strongly folded Upper Cretaceous–Palaeogene sedimentary assemblage (after Roy 1992)

On the back (eastern) side of this volcanic arc lies the ~4000-m-deep *Andaman Sea*. The floor of this sea is characterized by a NNE–SSW trending rift valley cut by a series of N–S to NNW–SSE trending right-lateral strike-slip faults (Fig. 21.1). The offset is of the order of 5–8 km and the downthrow of ~1500 m. New oceanic material has been forming in this Andaman rift since the Miocene

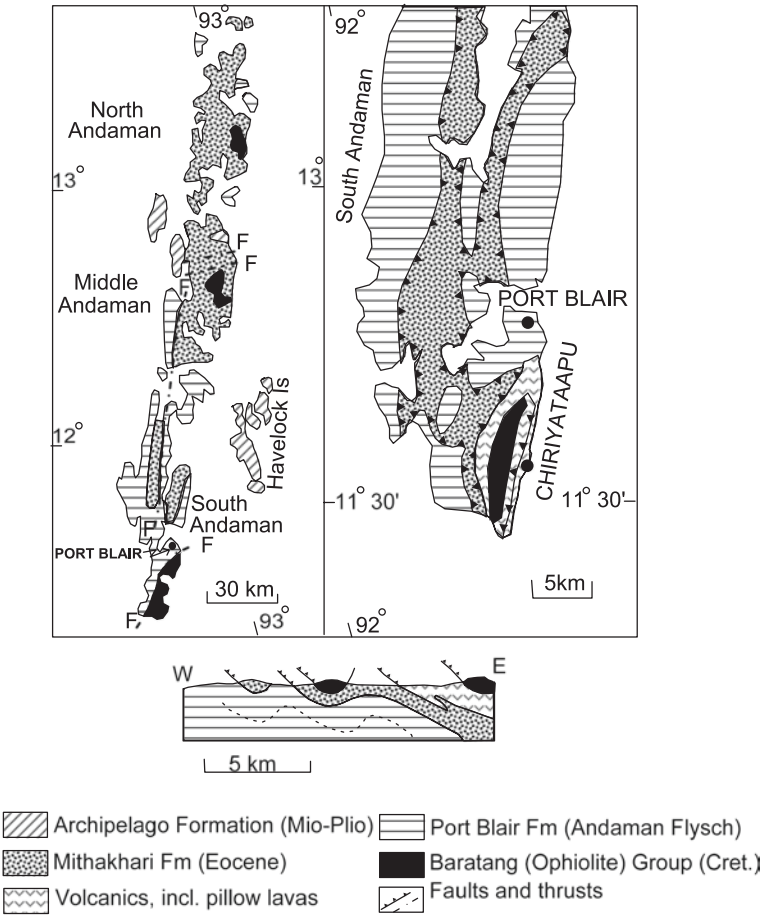

Fig. 21.5 **a** Generalized geological map of the Andaman Island Arc (after Pal et al. 2003). **b** Geological sketch map of a part of the South Andaman Island showing disposition of different geological units. **c** Section across the South Andaman (**b** and **c** after Ray et al. 1988)

time (Curray et al. 1978), resulting in the spreading of the seafloor. Its northerly extension is being filled vigorously with the sediments brought by the Irrawaddy, Sittang and Salween rivers. And the northernmost part was completely filled up during the Tertiary period by the precursors of the Irrawaddy and converted into the central Myanmar Plains.

East of the Andaman Sea, the sediments of the shelf on the continental slope of the Myanmar–Thailand–Malayasia landmass are folded and faulted.

Very significant is the presence of a pronounced regional unconformity in the Andaman–Nicobar Islands between the highly folded Palaeogene and the less-deformed Neogene sedimentary rocks (Roy 1983; Roy and Das Sharma 1993).

21.4 Stratigraphy and Sedimentation

The construction of regional stratigraphic framework of the Andaman Island Arc (Fig. 21.6) is based on the works of Karunakaran et al. (1964, 1968), Srinivasan and Sharma (1973), Srinivasan (1978, 1988), Roy (1983) and Pal et al. (2003). The following stratigraphic units are recognized (Fig. 21.6).

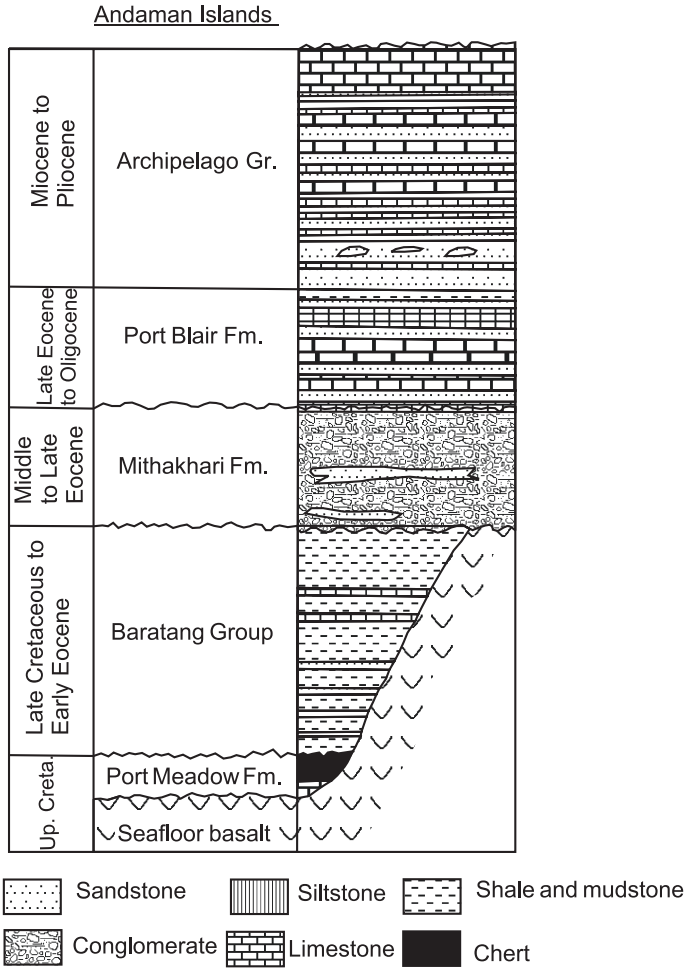

Fig. 21.6 Lithological sequences and compositions of the Tertiary formations of the Andaman Arc (based on Srinivasan and Sharma 1973; Roy 1983 and Chakraborty et al. 1999)

21.4.1 Port Meadow Formation

In the western arc of the Andaman Island Arc, the oldest lithostratigraphic unit, known as the *Port Meadow Formation* (Roy 1983) or Prolob Group (Srinivasan 1988), is made up of pink chert, jaspillite, dark shale, marlites and white siliceous limestones. The cherts contain Cretaceous radiolarians (Jacob 1954), and the limestones are characterized by Late Cretaceous globigerinids. In some areas, the sedimentary rocks are locally metamorphosed to quartzite, quartz–mica schist and phyllite. The associated basic-ultrabasic rocks of the ophiolites suite are likewise converted to amphibole–epidote–carbonate–chlorite assemblage of green schist to lower amphibolite facies.

21.4.2 Baratang Group

Two lithological units are distinguishable within the gamut of the *Baratang Group*. Directly in contact with the Port Meadow Formation rocks is a *suite of ophiolites* with intercalations of deep-sea sediments. The *ophiolites* commonly occur as broken up bodies at different structural levels, forming parts of disparate tectonic slices of the *accretionary prism* (Roy 1992) all along the zone of subduction of the Indian Ocean floor. In the topmost slice, the ultrabasic components include serpentinized harzburgite, lherzolite, wehrlite, pyroxenite and gabbro with stringers of chromite (Vohra et al. 1989). The ophiolites also occupy high ground as discernible on the Saddle Peak in the Andaman Island. The cumulates of the ophiolite suite are overlain by non-cumulate gabbro and intrusives of plagiogranite. And the top of the sequence comprises dacite and andesitic basalt showing pillow structure (Ray 1985; Ray et al. 1988). Plagiogranite in the southern margin of South Andaman section (Fig. 21.5) is characterized by vermicular micrographic intergrowth of quartz and plagioclase. Bearing chemical similarity with the ophiolites, the plagiogranite, however, exhibits Rb, Yb, Nb, Ta and Y abundances like those of volcanic-arc granite. This implies its crystal fractionation origin under low pressure from a potassic tholeiitic magma derived from a mantle source in the tectonic setting above the subduction zone (Jafri et al. 1995). The FeO- to TiO_2-enriched basic rocks of the Port Blair–Chiriyatapu area are associated with plagiogranite intrusives that represent the end product of magmatic differentiation (Shastry et al. 2001). High strength element geochemistry suggests derivation of the high TiO_2 basalt from the magma similar to the mid-oceanic ridge basalts (Srivastava et al. 2004).

The second component of the Baratang Group is a succession of deep-sea pelagic sediments including ribbon chert, variegated and dark grey shales, greywackes, impure limestones and volcanics. Thin layers of red clay and red

chert yielded the radiolarian *Nassellaria spumellarian*, and the planktonic foraminifers *Globigerina eugubina, Globorotalia compressa*, *Globotruncana arca* and *Globigerinelloides* of Late Cretaceous to Palaeocene age (Roy et al. 1988).

The Late Cretaceous to Early Eocene Baratang assemblage of deep-sea sediments implanted with ophiolites represent a seafloor material (crustal layer and covering sedimentary) scraped off the oceanic plate that is underthrusting the south-east Asian plate (Curray and Moore 1971; Curray et al. 1978).

21.4.3 Mithakhari Formation

Disconformably overlying the oceanic basement and made up of ophiolites, the 1400-m-thick succession of the *Mithakhari Formation* (Fig. 21.6) comprises conglomerates, sandstones and mudstones with black pyritic shales (Karunakaran et al. 1968; Bandyopadhyay et al. 1973). The polymictic conglomerates, best seen at Hope Town, are interpreted as deposits of debris flows. The clasts of the conglomerates were derived from the ophiolites. Characterized by frequent facies variation, the Mithakhari Formation represents deposits of isolated basins on the tectonically resurgent slope of the *Andaman Trench* (Pal et al. 2002, 2003). There is evidence in the form of desiccation cracks and gypsum crystals of tectonic shoaling during the filling of these basins. The mudstones are associated with crystal-rich tuffs of basic and intermediate composition, indicating advanced stage of magma differentiation. The pyroclastics are interpreted as deposits of debris flows in submarine channels and of ash falls (Bandyopadhyay and Ghosh 1998). Imbrication of clasts and orientation of such sedimentary structures are sole marks and wave ripple marks indicate that the detritus was derived from the provenance that lay NE of the Middle Andaman Island (Chakraborty et al. 1999).

The Mithakhari shales contain Middle to Late Eocene foraminifers—*Cumulates atacicus, Assilina papillata, Pelatispira* and *Biplanispira* (Roy et al. 1988).

21.4.4 Port Blair Formation

The 300- to 400-m-thick succession of siliciclastic turbidites (quartzwacke–shale rhythmite) of the *Port Blair Formation*, also described as *Andaman Flysch*, covers greater part of the Andaman Islands. The maximum thickness is over 1100 m (Pandey et al. 1992). The flysch assemblage represents a proximal turbidites formed by a combination of processes—deposition by sandy debris flows in a mud-fan environment and by pelagic sedimentation in a forearc setting (Bandyopadhyay and Ghosh 1998). Significantly, there are scattered exotic blocks of older rocks in a melange horizon within the Port Blair succession.

The shales of the Port Blair have yielded some broken lamellibranch shells with *Rotalia, Nummulites, Assilina, Globorotalia* and *Globigerina,* suggesting Lower Eocene to Oligocene age (Pawde and Ray 1963; Pandey et al. 1992). In the cherts occur Hagistrids (Jafri 1986).

21.4.5 Archipelago Formation

Unconformably overlying the Port Blair Formation, the 1650–2450-m-thick succession of the Archipelago Group is divisible into five formations (Fig. 21.6), ranging in age from Early Miocene to Plio–Pleistocene (Srinivasan and Sharma 1973). The sediments were deposited under fluctuating shallow and deep marine conditions (Srinivasan and Chatterjee 1981). The *Archipelago Formation*, named after the Richtie's Archipelago, consists of alternation of siliciclastic turbidites and subaqueous pyroclastic debris-flow deposits in the lower part and carbonate turbidites in the upper part (Pal et al. 2003). Like the Mithakhari and the Port Blair, the Archipelago Formation is a deposit of a *forearc basin*. The turbidites are characterized by the Bouma cycle of sedimentary structures including graded bedding and parallel lamination. The small proportion of carbonates in the flysch succession are of biostromal and biohermal origin. In the lower part of the succession, the sediments are characterized by abundant glass shards, suggesting explosive volcanism during that interval.

The Archipelago sediments contain rich assemblage of nannofossils and pelagic foraminifers including *Lepidocyclina* and *Miogypsina* and bryozoans and algae of the Lower Miocene to Pliocene age (Ray 1982). The biota exhibits affinity with the Indo-Pacific fauna (Srinivasan 1978, 1988).

On the basis of recognition of clearly defined zones of planktic foraminifers, particularly the species of *Globigerinatella,* the broad-spectrum Archipelago Group has been reclassified into seven formations, each formation named after the island (Fig. 21.6) where the type section is Straight Fm (Early Miocene), Round Fm (Early Miocene), Inglis Fm (Late early Miocene to Early middle Miocene), Long Fm (Early middle Miocene to Late Miocene), Sawai Fm (Late Miocene to Late early Pliocene), Guitar Fm (Late Miocene to Late Pliocene) and Neill West Coast Fm (Late Pliocene to Pleistocene) (Sharma and Srinivasan 2007).

21.4.6 Sawai Bay Formation

In the Great Nicobar, the *Sawai Bay Formation* (Srinivasan and Sharma 1973) consists of mudstone and limestone. The limestone is characterized by planktonic foraminifers including *Globorotalia tumidaflexuosa, Globigerina nepenthes, Globorotalia multicamerata* and *Pulleniatina obliquiloculata* of the Early

to Middle Pliocene age. In the Neill Island, the Sawai Bay sediment is characterized by the Late Miocene calcareous nannofossil *Discoaster berggrentii* (Jafar and Singh 1996).

It may be mentioned that the Sawai Bay Formation and the younger Neill Formation have been here separated from the larger Archipelago Group of Srinivasan and Sharma (1973) and Srinivasan (1988).

21.4.7 Neill Formation

Developed in the southern Andaman Island, the *Neill Formation* comprises silty mudstone and limestone, as discernible in the Chidyatapu–Wandoor area. The benthic foraminifers assign it to the Pliocene–Pleistocene temporal span (Srinivasan and Azmi 1979).

The Neill Formation is succeeded by the Holocene biocalcarenites characterized by the presence of coralline alga *Corallina* (Rajashekhar and Reddy 2003).

21.5 Volcanics of Eastern Arc

The eastern arc of volcanic rocks extends south-east from central Myanmar to the Barisan volcanic ridge in Sumatra. It embodies the Alcock and Sewell seamounts and the Narcondam and Barren volcanoes in the Andaman Sea. The *Barren Island* rises 2300 m above the sea floor, the height of its summit being 335 m above the mean sea level. It has exhibited resurgent volcanism in the historical time, as evident from eruption in A.D. 1787, 1789, 1795, 1803–1804, 1852, 1991, 1994–1995 and 2005 (Haldar and Luhr 2003). Currently, it is in the fumarolic stage. There is piling up of lava flows and emplacement of scoria around the caldera (Fig. 21.7). It exhibits strombolian-type activities, including collapse of the main cone.

Enriched in LREE and LILE and depleted in HFSE, the Barren lavas of the Pleistocene age and of the year 1994 are olivine-basalt, while those of the year 1991 are andesitic basalt with olivines (Haldar and Luhr 2003). A 5-m-wide NNE–SSW-oriented dyke in the south-eastern side of the caldera rim is petrologically indistinguishable from the lava flows (Alam et al. 2004). Multiple depressions formed in A.D. 2005 are aligned in the N–S direction, and the phenocryst-rich fragments in the ejected material indicate advanced stage of magma crystallization (Bandyopadhyay et al. 2006).

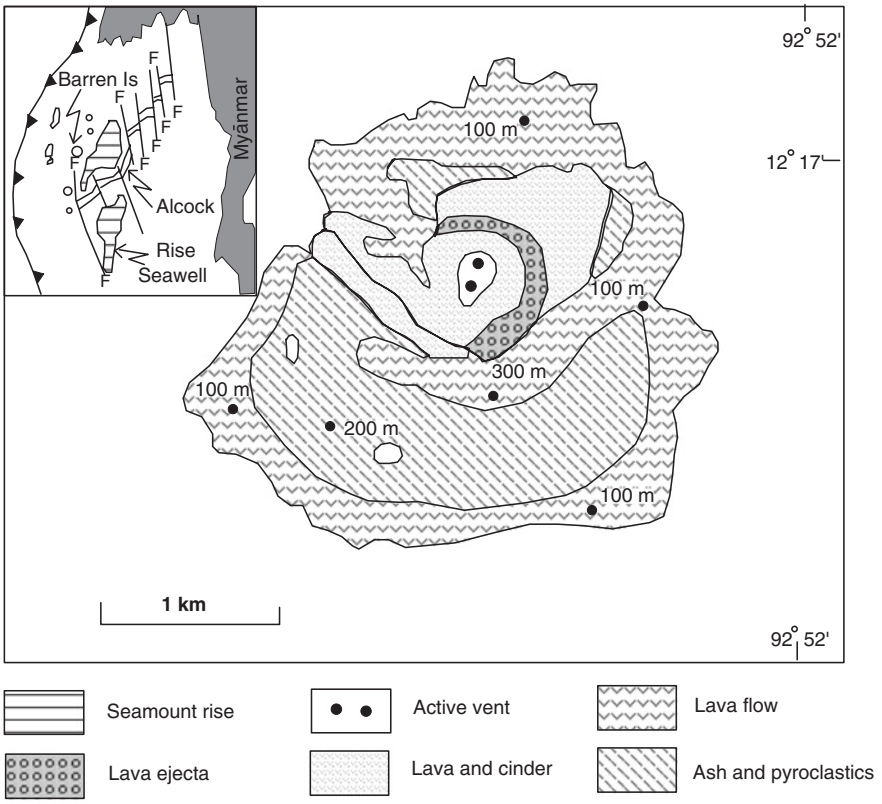

Fig. 21.7 Lava flows and pyroclastic deposits of the Barren Island in the Andaman Sea (after Haldar and Luhr 2003). *Inset* shows the location of the active Barren volcano, the dormant Narcondam volcano and the seamounts Alcock and Sewell (after Bandypadhyay et al. 2006)

21.6 Evolution of Andaman Mobile Belt

As a result of oblique subduction of the Indian Ocean plate under the Myanmar microplate of the South-east Asian continental plate (Eguchi et al. 1980; Curray 1989; Roy 1992), the oceanic crust along with its sedimentary cover was scraped off and piled up as multiple thrust sheets or slices, forming an *accretionary prism* (Fig. 21.4a). This prism forms the western sedimentary arc of the Andaman–Nicobar–Mentawai islands chain. The subduction started in the Late Cretaceous, and since then has been going on intermittently.

Some workers believe that the Indian Ocean floor is subducting along the Diligent Straight, east of the Andaman Island chain, and not on the north-western extension of the Java Trench along the western margin of island chain (Sengupta et al. 1990; Avasthi 2005). An accretionary prism, the Andaman Island Arc is perceived to have been built around the Narcondam–Barren volcanoes.

Following differential movements on the imbricating faults of the accretionary prism, small isolated basins in the prism were formed. These basins became sites of forearc sedimentation during the Cenozoic era. The forearc-basin sediments are represented by the Baratang, Mithakhari, Port Blair and Archipelago successions.

Dextral movements along the Sagaing–Semenko fault systems of the Myanmar–Indonesia Mobile Belt resulted in the opening up of the Andaman Sea behind the Andaman sedimentary arc (Curray 1989, 2005; Curray et al. 1978; Pal et al. 2003). The opening of the sea in the Early Miocene time was accompanied and followed by explosive volcanic activity all along the belt immediately east of the chain of the sedimentary islands (Srinivasan 1988).

The Andaman Sea is thus a *back-arc basin* formed as the seafloor spread after splitting apart along the NNE–SSW trending rift. *Oblique convergence* entailed rotation of oceanic subplates and increased rate of strike-slip motion. The result was the evolution of an extensional basin. The opening up of the Andaman Sea began at about 32 Ma and the present-day plate edge was formed nearly 4 million years ago when major stratigraphic changes occurred in the chain of islands as described in the Andaman ridge, and in the Mergui basin to the east. As stated above, there was submarine volcanism along the eastern faulted margin of sedimentary arc, which culminated in the evolution of the eastern volcanic arc, represented by the Narcondam–Barren volcanic chain. A NNE–SSW trending underwater *spreading ridge* running through the middle of the Andaman Sea was offset by 13 km at 94°21E-longitude, dividing it into two segments (Kamesh Raju et al. 2004, 2007). The northeastern segment is a well-defined rift (Fig. 21.8).

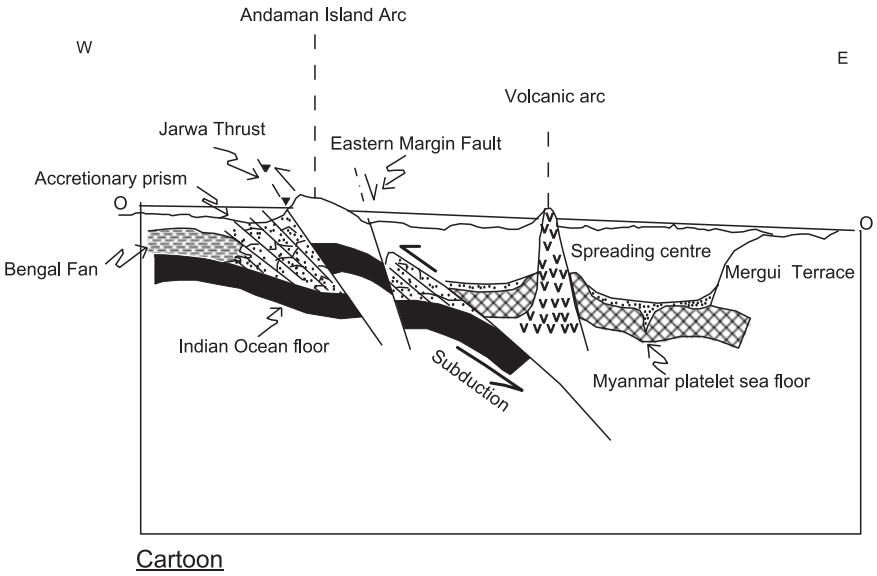

Fig. 21.8 There is a view that the subduction of the Indian Ocean floor occurred east of the island chain along the Diligent Straight and that the whole of the island arc is an accretionary prism (modified after Avasthi 2005)

It is a site of heavy sedimentation, but the south-western segment wears only a thin cover of sediments.

Magnetic anomalies in the seafloor suggests very slow initial rate of the opening of the Andaman Sea. The initial rate of 1.6 cm/year later increased to 3.8 cm/year (Kamesh Raju et al. 2004). The opening occurred in three phases—(i) spreading centre jumped during the Late Oligocene, (ii) extension and rifting occurred during the Middle Miocene to Early Pliocene period, and since then (iii) there was westward propagation of the spreading centre (Kamesh Raju et al. 2005, 2007).

21.7 Mineral Asset

Even though the northern extension of the Andaman Basin in central Myanmar and its south-eastern continuation in Sumatra host productive petroleum deposits, the Andaman Sea has so far not revealed the presence of any hydrocarbon deposit. However, an exploration well-drilled east of Port Blair by the Oil and Natural Gas Commission revealed the presence of gas in the Andaman Basin.

Hydrothermal activity in the Andaman back-arc basin resulted in the formation of heavy encrustation of sulphides of Cu, Pb, Zn and Fe (Rao et al. 1996).

References

Alam, M. A., Chandrasekharam, D., Vaselli, O., Capaccioni, B., Manetti, P. & Santo, P. B. (2004). Petrology of the prehistoric lavas and dyke of the Barren Island, Andaman Sea, Indian Ocean. *Proceedings of Indian Academy Sciences (Earth & Planetary Sciences)*, *113*, 715–721.

Avasthi, D. N. (2005). The Sunda Trench and the Andaman-Nicobar Islands. *Journal of Geological Society of India, 66*, 519–520.

Bandypadhyay, P. C., & Ghosh, M. (1998). Facies, petrology and depositional environment of the Tertiary sedimentary rocks around Port Blair, South Andaman. *Journal of Geological Society of India, 52*, 53–66.

Bandypadhyay, P. C., Mitra, S. K., Pal, T., & Raghav, S. (2006). The 2005 eruption on Barren Island, Andaman Sea. *Current Science, 90*, 620–622.

Bandypadhyay, S., Subramanyam, M. R., & Sharma, P. N. (1973). The geology and mineral resources of the Andaman and Nicobar Islands. *Records of Geological Survey of India, 105*, 25–68.

Chakraborty, P. P., Pal, T., Dutta-Gupta, T. P., & Gupta, K. S. (1999). Facies pattern and depositional motif in an immature trench-slope basin, Eocene Mithakhari Group, Middle Andaman, India. *Journal of Geological Society of India, 53*, 271–284.

Cochran, J. R. (2010). Morphology and tectonics of the Andaman Forearc, northeastern Indian Ocean. *Geophysical Journal of International, 182*, 631–651.

Curray, J. R. (1989). The Sunda Arc: A model for oblique plate convergence. *Netherlands Journal of Sea Research, 24*, 131–140.

Curray, J. R. (2005). Tectonics and history of the Andaman Sea region. *Journal of Asian Earth Sciences, 25*, 187–232.

Curray, J. R., & Moore, D. G. (1971). Growth of the Bengal deep sea fan and denudation in the Himalaya. *Geological Society of American Bulletin, 82*, 563–572.

Curray, J. R., Moore, D. G., Lawker, L. A., Emmel, F. J., Raitt, R. W., Henry, M., & Kieckhefer, R. (1978). Tectonics of the Andaman Sea and Burma. *Geological and Geophysical Investigations of Continental Margins* (pp. 189–198). A Tulsa: American Association of Petroleum Geology.

Dasgupta, S., & Mukhopadhyay, M. (1993). Seismicity and plate deformation below the Andaman arc, Northeastern Indian Ocean. *Tectonophysics, 225*, 529–542.

Eguchi, T., Uyeda, S., & Maki, T. (1980). Seismotectonics and tectonic history of the Andaman sea. *Tectonophysics, 57*, 35–51.

Haldar, D., & Luhr, J. F. (2003). The Barren Island volcanism during 1991 and 1994-1995: Eruptive style and lava petrology. *Memoires Geological Society of India, 52*, 313–338.

Jacob, K. (1954). The occurrence of radiolarian cherts in association with ultramafic intrusives in the Andaman Islands and its significance in sedimentary tectonics. *Record Geological Survey of India, 83*, 398–422.

Jafar, S. A., & Singh, O. P. (1996). Late Miocene calcareous nannofossils from Sawai Bay Formation, Neill Island, Andaman Sea, India (pp. 733–738). *Dehradun: Proceedings of Fifteenth Colloquium Micropalaeontology Strati*.

Jafri, S. H. (1986). Occurrence of Hagistrids in chert associated with Port Blair Series, South Andaman, India. *Journal of Geological Society of India, 28*, 41–43.

Jafri, S. H., Charan, S. N., & Govil, P. K. (1995). Plagiogranite from the Andaman ophiolite belt, Bay of Bengal, India. *Journal of Geological Society of London, 152*, 681–688.

Kamesh Raju, K. A. (2005). Three-phase tectonic evolution of the Andaman backarc basin. *Current Science, 89*, 1932–1936.

Kamesh Raju, K. A., Ramprasad, T., Rao, P. S., Ramalingeswara Rao, B., & Varghese, J. (2004). New insights into the tectonic evolution of the Andaman basin, northeast Indian Ocean. *Earth & Planetary Sciences Letters, 221*, 145–162.

Kamesh, Raju, K. A., Murty, G. P. S., Amarnath, D. & Mohan, Kumar, M. L. (2007). The West Andaman Fault and its influence on the aftershock pattern of the recent megathrust earthquakes in the Andaman–Sumatra region. *Geophysical Research Letters*, *34*, doi:10.1029.

Karunakaran, C., Pawde, M. B., Raina, V. K. & Ray, K. K. (1964). Geology of the South Andaman Islands (Vol. 11, pp. 79–100). *Proceedings of 22nd International Geological Congress*, New Delhi.

Karunakaran, C., Ray, K. K., & Saha, S. S. (1968). Tertiary sedimentation in the Andaman-Nicobar geosyncline. *Journal of Geological Society of India, 9*, 32–39.

Mukhopadhyay, M. (1988). Gravity anomalies and deep structure of the Andaman Arc. *Marine Geophysical Research, 9*, 197–210.

Pal, T., Charakborty, P. P., Duttagupta, T., & Singh, C. D. (2003). Geodynamic evolution of the outer arc–forearc belt in the Andaman Islands, the central part of the Burma-Java subduction complex. *Geological Magazine, 140*, 289–307.

Pal, T., Duttagupta, T., & Dasgupta, S. C. (2002). Vitric tuffs from Archipelago Group of rock (Mio-Pliocene) of South Andaman. *Journal of Geological Society of India, 59*, 111–114.

Pandey, J., Agarwal, R. P., Dave, A., Maithani, A., Trivedi, K. B., Srivastava, A. K., & Singh, D. N. (1992). Geology of Andaman. *Bulletin ONGC, 29*, 19–103.

Pawde, M. P., & Ray, R. K. (1963). Sedimentary structures in greywackes of South Andaman. *Science and Culture, 30*, 279–280.

Rajashekhar, C., & Reddy, P. P. (2003). Quaternary stratigraphy and micropalaeontology of rocks of South Andaman, Bay of Bengal. *Gondwana Geological Magazine, 6*, 33–38.

Rao, P. S., Kamesh Raju, K. A., Ramprasad, T., Nagender Nath, B., Ramalingeswara Rao, B., Rao, Ch M, & Nair, R. R. (1996). Evidence for hydrothermal activity in the Andaman Back-arc basin. *Current Science, 70*, 379–385.

Ray, K. K. (1982). A review of the geology of Andaman and Nicobar islands. *Miscellaneous Publication Geological Survey of India*, *42*(II), 110–125.

Ray, K. K. (1985). East coast volcanics—New suite in the ophiolites of Andaman Islands. *Record Geological Survey of India, 116*(2), 83–87.

Ray, K. K., Sengupta, S., & van Den Hul, H. J. (1988). Chemical characters of volcanic rocks from Andaman ophiolite assemblage, India. *Journal of Geological Society of London, 145*, 393–400.

Roy, T. K. (1983). Geology and hydrocarbon prospects of Andaman-Nicobar Basin. *Petroliferous Basins of India* (pp. 37–50). Dehradun: ONGC.

Roy, S. K. (1992). Accretionary prism in Andaman forearc. *Special Publication, Geological Survey of India, 29*, 273–278.

Roy, D. K., Acharyya, S. K., Ray, K. K., Lahiri, T. C., & Sen, M. K. (1988). Nature of occurrence and depositional environment of the oceanic pelagic sediment associated with ophiolite assemblage, South Andaman Island. *Indian Minerals, 42*, 31–56.

Roy, A. K., & Bhattacharya, A. (1982). Regional geomorphology of Vindhyachal. *Geology of Vindhyachal* (pp. 9–22). Delhi: Hindustan Publishing Corporation.

Roy, S. K., & Das Sharma, S. (1993). Evolution of Andaman forearc basin and its hydrocarbon potential. In S. K. Biswas (Ed.), *Petroliferous basins of India* (pp. 407–428). Dehradun: Indian Petroleum Publishers.

Sengupta, S., Ray, K. K., Acharyya, S. K., & de Smith, J. B. (1990). Nature of ophiolite occurrences along the eastern margin of the Indian plate and their tectonic significance. *Geology, 18*, 439–442.

Sharma, V., & Srinivasan, M. S. (2007). *Geology of Andaman-Nicobar: The Neogene*. New Delhi: Capital Publishing Co. 163 p.

Shastry, A., Srivastava, R. K., Chandra, R., & Jenner, G. A. (2001). Fe-Ti-eriched mafic rocks from South Andaman ophiolite suite: Implication of late stage liquid immisibility. *Current Science, 80*, 453–454.

Srinivasan, M. S. (1978). New chronostratigraphic division of the Andaman-Nicobar Late Cenozoic rocks. *Recent researches in Geology* (pp. 22–36). Delhi: Hindustan Publishing Corporation.

Srinivasan, M. S. (1988). Late Cenozoic sequences of Andaman-Nicobar Island: Their regional significance and correlation. *Indian Journal of Geology, 60*, 11–34.

Srinivasan, M. S., & Azmi, R. J. (1979). Correlation of Late Cenozoic marine sections in Andaman-Nicobar, Northern Indian Ocean and equatorial Pacific. *Journal of Palaeontology, 53*, 1401–1415.

Srinivasan, M. S., & Chatterjee, B. K. (1981). Stratigraphy and depositional environments of Neogene limestones of Andaman Nicobar Islands, Northern Indian Ocean. *Journal of Geological Society of India, 22*, 536–546.

Srinivasan, M. S., & Sharma, V. (1973). Stratigraphy and microfauna of Car Nicobar Island, Bay of Bengal. *Journal of Geological Society of India, 14*, 1–11.

Srivastava, R, K., Chandra, R., & Shastry, A. (2004). High-Ti type N-MORB parentage of basalts from the South Andaman ophiolite suite, India, (Vol. 113, pp. 605–618). In *Proceedings of Indian Academy of Sciences (Earth & Planetary Sciences)*.

Vohra, C. P., Haldar, D., & Ghosh-Roy, A. K. (1989). The Andaman-Nicobar ophiolite complex and associated mineral resources. In N. C. Ghose (Ed.), *Phanerozoic Ophiolites of India* (pp. 281–315). Patna: Summay Publication.

Chapter 22
Indo-Gangetic Plains: Evolution and Later Developments

22.1 Formation of Foredeep

The Indo-Gangetic Plains evolved as a consequence of filling up of a *foredeep basin* in front of the rising Siwalik Ranges. Earlier, the Siwalik foredeep had come into existence due to the flexing down of Indian plate following the collision of India with Asia (Lyon-Caen and Molnar 1985). This foredeep expanded and deepened as sedimentation proceeded progressively until the Late Quaternary 1.5–1.7 million years ago. This was the time when it broke up into two unequal parts along the fault known as the *Himalayan Frontal Thrust* (Fig. 22.1). The northern 25–45-km-wide part evolved to the rising Siwalik Ranges, and the southern 200–450-km-wide part became the subsiding basin (Valdiya 1998, 2001). This depression was filled up rapidly with sediments derived predominantly from the Himalaya and partly from the hills of the northern Peninsular India, eventually transforming the basin into vast plains known as the *Indo-Gangetic Plains*. It is 150–500 km wide and covers about 300,000 km^2 area (Fig. 22.2) in northern India.

The *Indo-Gangetic Basin* (I-GB) expanded and became progressively deeper as sediments accumulated through the time. The result of combined processes of floor subsidence and voluminous sedimentation was the formation of the world's largest alluvial plain (Fig. 22.2), now 30–100 m above the mean sea level. The thickness of sediments varies from a few tens of metres in the southern margin to as much 1500–2500 m in the northern margin in northeastern Uttar Pradesh and adjoining Bihar—along the foot of the mountain ranges. The easterly extension of the I-GP in Assam is 80–100 km wide. The surface of this plain is 120 m above the sea level at Kobo, 50 m at Guwahati and 28 m at Dhubri (Goswami 1985). It is an area of subsidence between the foothills of the Arunachal Himalaya and the Meghalaya–Mikir massifs in the south (Das 1992).

K.S. Valdiya, *The Making of India*, Society of Earth Scientists Series,
DOI 10.1007/978-3-319-25029-8_22

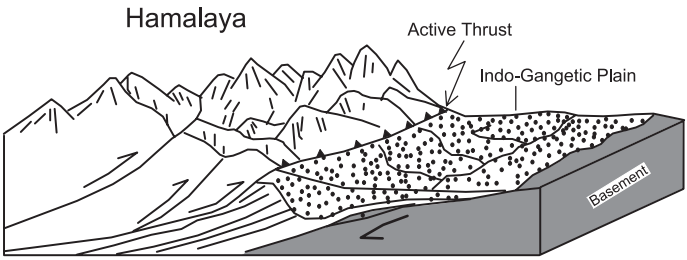

Fig. 22.1 Siwalik foredeep basin broke up into two unequal parts along the Himalayan Frontal Thrust. The southern part became the subsiding basin—the Indo-Gangetic Basin (after Valdiya 1998)

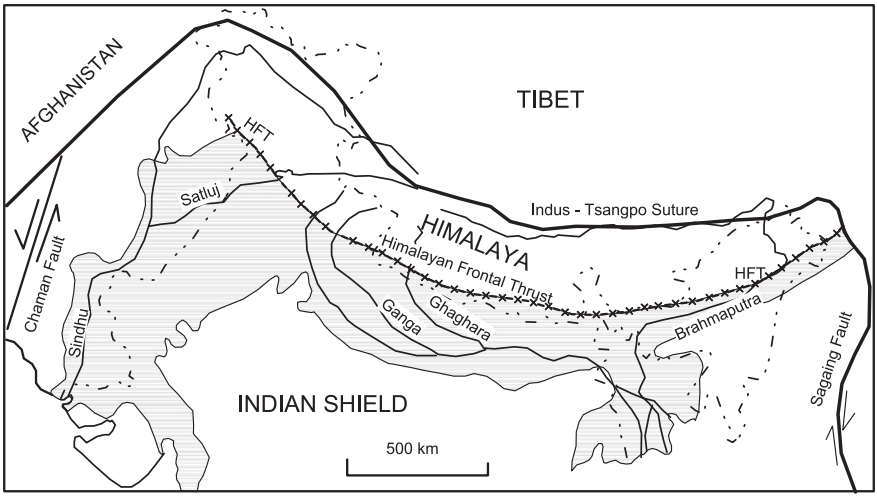

Fig. 22.2 Extent of the Indo-Gangetic Plains between the Himalaya mountain and the northern hilly margin of the Peninsular India (after Burbank 1992)

22.2 Floor of Indo-Gangetic Basin

22.2.1 Ganga Basin

Aeromagnetic, ground magnetic, gravity and seismic surveys coupled with deep drilling have shown that the floor of the I-GB is very uneven and dissected by faults (Sastry et al. 1971; Fuloria 1996). There are large depressions or "lows" separated by ridges or "highs". They trend NE–SW in the central sector, and NW–SE in the western (Pakistan) sector (Fig. 22.3). The transverse structures are closely associated with faults of considerable extent. In addition, there are many broad E–W- to ESE–WNW-oriented upwarps and depressions of lesser

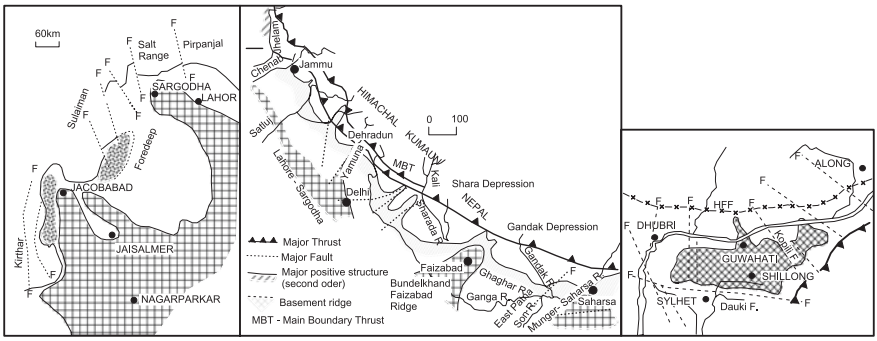

Fig. 22.3 **a** Ridges (or "highs") and depressions (or "lows") oriented transverse to the ESE–WNW layout of the Ganga Basin characterize its floor (Raiverman et al. 1993). **b** In the western sector, the Sindhu Basin floor is characterized by NW–SE-trending "lows" and "highs" (Modified after Kazmi and Qasim Jan 1997 and Pandey and Dave 1998). **c** In the east, a promontory of the Meghalaya–Mikir massif extends transversely under the Brahmaputra sediments

amplitude (Raiverman et al. 1993). The transverse structures are the continuation of the structures of the Peninsular India (Valdiya 1976). The basement of the Ganga Basin is made up of the Precambrian Bundelkhand gneisses overlain successively by the Proterozoic Vindhyan, the Permian Gondwana and the Tertiary Siwalik formations. In the Madhubani and Purnea depressions in Bihar, deep drill holes struck the Bundelkhand gneisses at depths of respectively 5954 and 2445 m (Singh and Singh 1997).

The depressions deepen towards the mountain front (Fig. 22.4). The *Sharada Depression* and the *Gandak Depression* account for 6000–7000-m-thick sedimentary pile, of which the upper 1500–2500-m part is made up of the Late Pleistocene–Holocene sediments. The depressions developed due to progressive sinking of the basin floor as the Indian lithosphere slid under the Himalaya. Reactivation of older faults provided stimulus for heavy sedimentation. For example, in the Haryana Plain, which is 191–200 m above the sea level, tectonic movements on N/NNE–S/SSW-trending faults gave rise to the Sohna depression, which is 75 km long and 20 km wide. Progressive subsidence of the floor took it to the level below the mean sea level, giving rise to a 40–318-m-thick prism of sedimentary fill (Thussu 2001) (Fig. 22.4).

22.2.2 Sindhu Basin

In the western sector of the I-GP, a branch of the Aravali orogen extends WNW/NW as the *Lahore–Sargodha Ridge* (Fig. 22.3). Inliers of Precambrian rocks in the Kirana Hills in Panjab (Pakistan) represent the summits of this ridge. The *Barwani–Jaisalmer Ridge* passing through Pokaran in western Rajasthan is

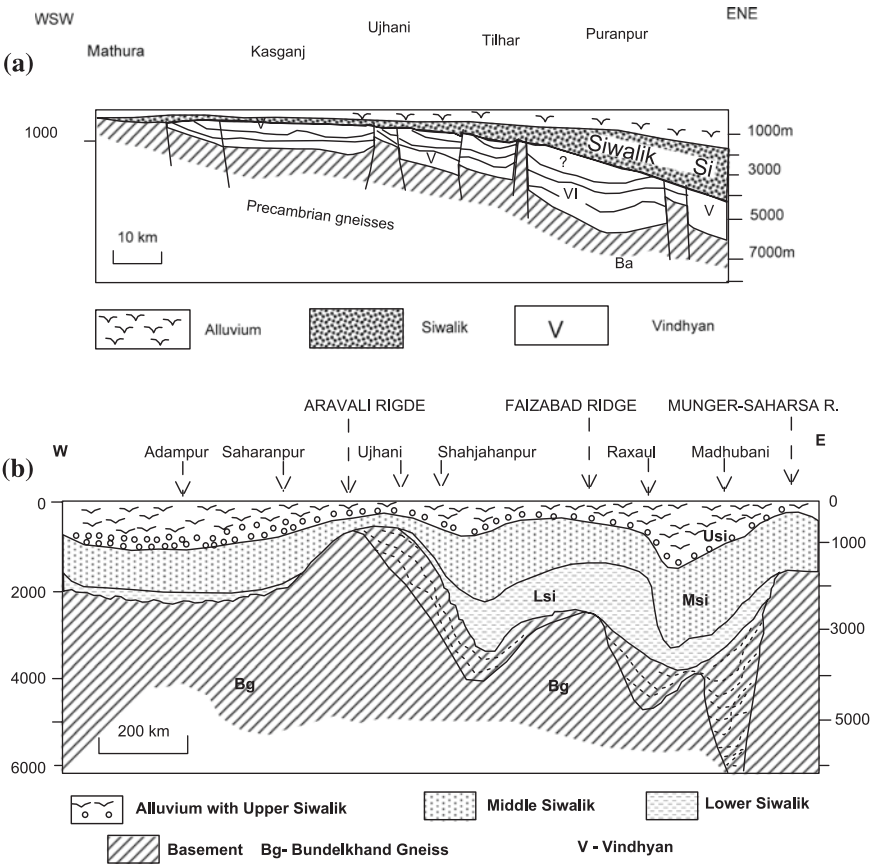

Fig. 22.4 Profiles across the Ganga Basin illustrate its structural framework and lithostratigraphy. **a** NE–SW section (after Agrawal 1977). **b** E–W section (after Pandey and Dave 1998)

delimited by a fault. Further westnorthwest, there are monadnocks of Precambrian rocks between Shahkot and Chiniot and small hillocks near Khairpur, Hyderabad and Thatte in the alluvial plain. They represent exposed tops of the hidden ranges. Interestingly, one of the monadnocks rises 250 m above the mean sea level. The NagarParkar Ridge in the extreme south of the Sindhu Basin is flanked by depressions and upwarps (Kazmi and Qasim Jan 1997). The basin deepens westward Fig. (22.5c), giving rise to the *Sulaiman Depression* and *Kirthar Depressions* comprising, respectively, 10,000- and 15,000-m-thick sediments, the Quaternary amounting to more than 500 m.

The Quaternary sediments are underlain by the Siwalik sedimentary successions in the northern part, and by the Eocene rocks south of the Lahore–Sargodha Ridge. The Precambrian and Palaeozoic rocks forming the basin floor are restricted to the Panjab part and to the Sulaiman Depression, thinning out in the

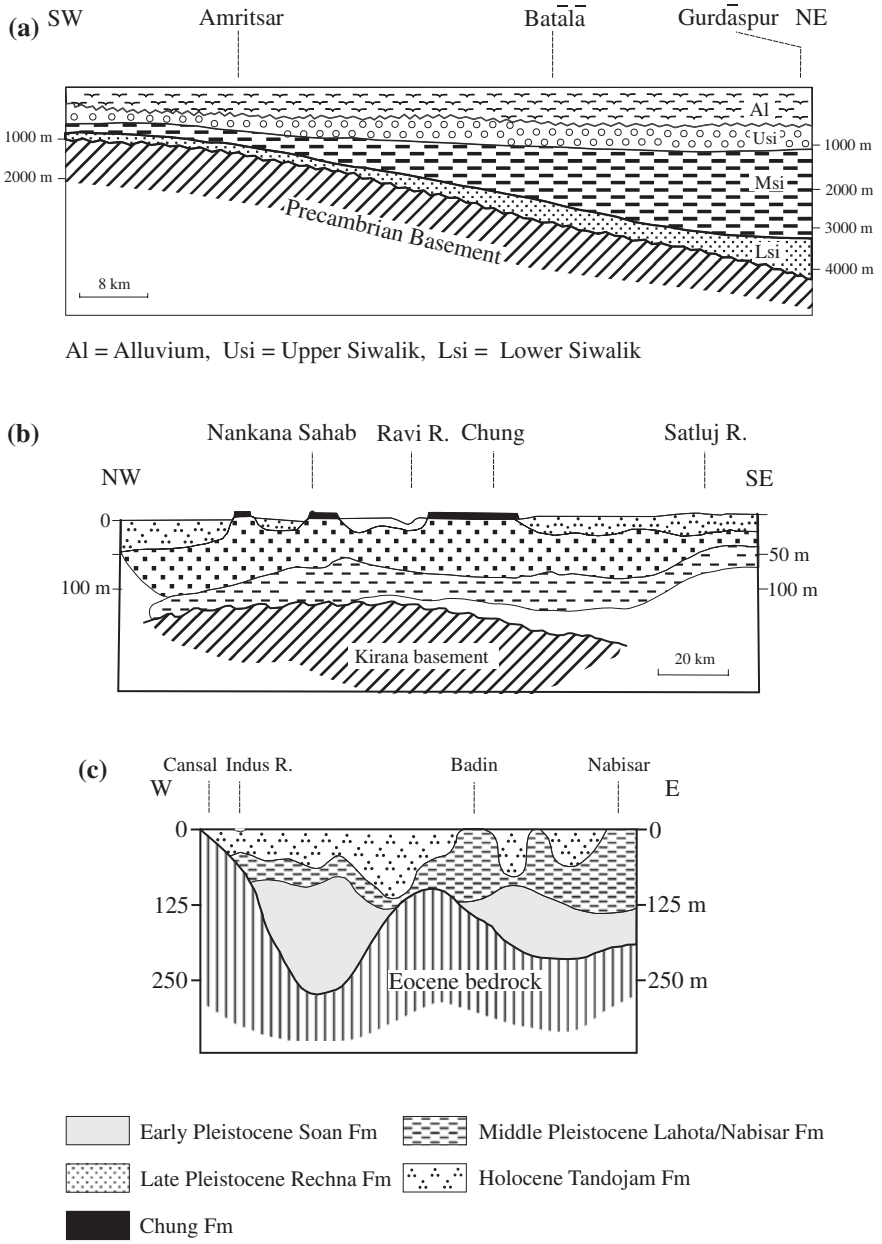

Fig. 22.5 Subsurface structures and pattern of sediment deposition in the Sindhu Basin. **a** NE–SW section in Indian Panjab (after Agrawal 1977). **b** NW–SE section in Pakistani Panjab. **c** E–W section in southern Sindh (**b**, **c** after Kazmi and Qasim Jan 1997)

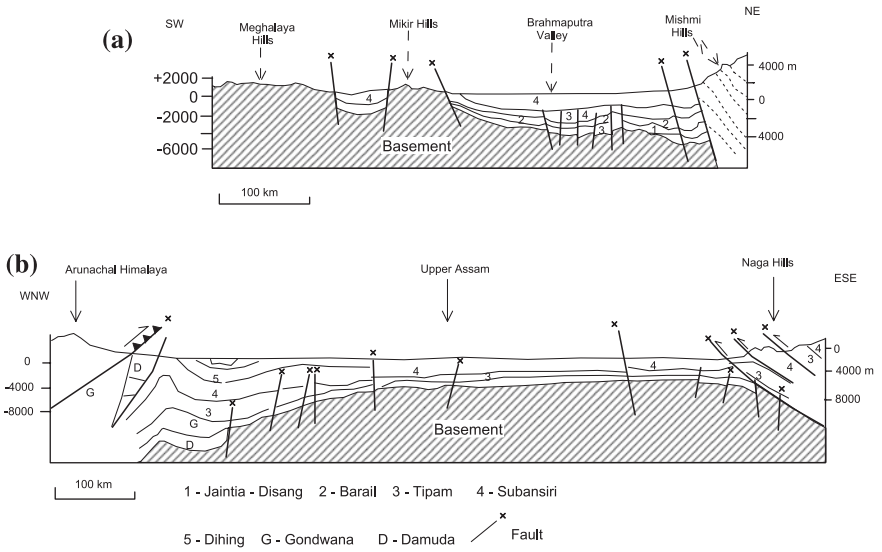

Fig. 22.6 Structural framework and lithostratigraphy of the Brahmaputra Basin. **a** NE–SW profile of the southern part (after Ranga Rao 1983). **b** WNW–ESE-oriented regional diagrammatic section (after Das 1992)

Jacobabad–Khairpur region and absent in the Sindhu region. The basement is characterized by several large but gentle anticlinal flexures and faults. Some of these structures contain pools of oil and gas (Kazmi and Qasim Jan 1997).

22.2.3 Brahmaputra Basin

In the 80–100-km-wide Brahmaputra Basin, the Meghalaya massif extends north beyond the river course in the form of isolated inliers of Precambrian rocks amidst alluvial sediments of the river (Fig. 22.3). In Upper Assam, the Brahmaputra sediments are underlain by 7000-m-thick pile of the Upper Cretaceous-to-Pleistocene formations (Das 1992). The basement is faulted, the fault blocks dipping and the basin floor deepening southeastwards (Fig. 22.6).

22.2.4 Bengal Basin

In northern Bengal and Bangladesh (Sengupta 1966), the NE–SW-oriented zone of gravity high occurs in the *Bengal Basin*. Characterized by linear distribution of epicentres of earthquakes resulting from strike-slip movements, it represents

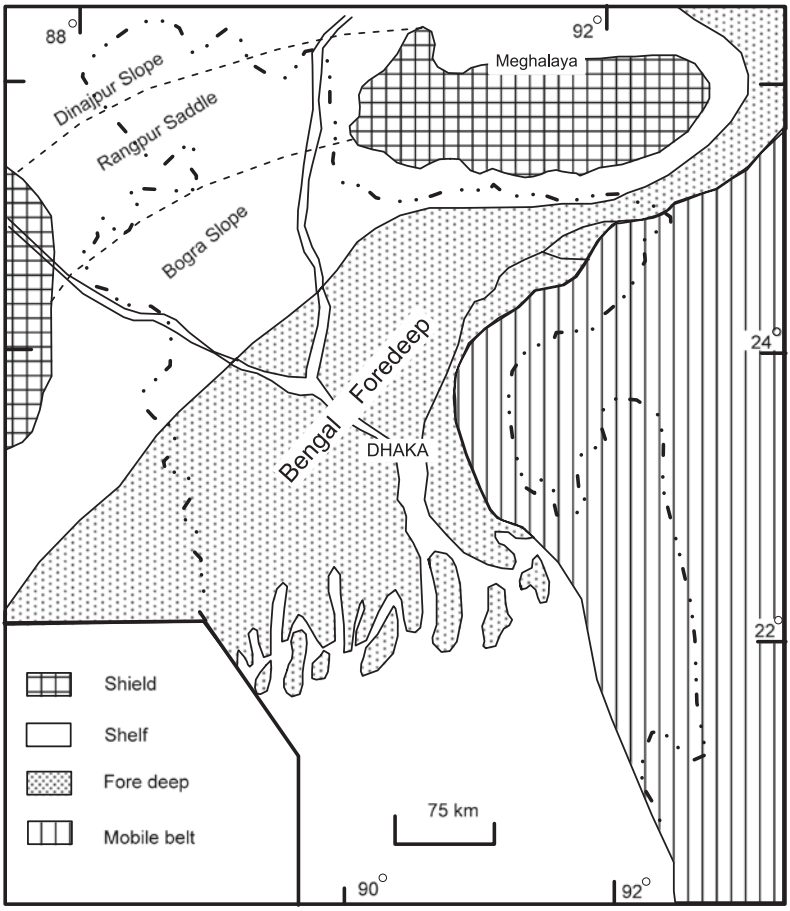

Fig. 22.7 Tectonic framework of the *Bengal Basin*. The sketch map shows major structural elements of the floor of the basin (modified after Alam 1996)

a 12–60-km-wide upwarp developed on the northern continental shelf of India. Known as the *Rangpur Saddle* (Reimann 1993), it connects the main Indian Shield in Jharkhand with the Meghalaya–Mikir massifs in the east (Fig. 22.7). The Rangpur Saddle is covered thickly by the recent to subrecent sediments. There are several N–S-oriented Gondwana grabens on the two slopes of this upwarp. North of the crest of the Rangpur Saddle, the Dinajpur slope descends to the depth of 4000 m and is covered with sediments of the Middle Miocene to Pleistocene ages. The southern slope dips gently southeastwards. The Archaean floor is overlain successively by the Gondwana, the Rajmahal and the Upper Cretaceous-to-Neogene formations. It deepens eastwards considerably, culminating in the *Sylhet Trough* (Fig. 22.7). This depression contains 12–16-km-thick pile of sediments deposited on the continental shelf. The Sylhet Trough has been sinking since its inception in

the Upper Cretaceous (Morgan and McIntyre 1959; Johnson and Alam 1991; Alam 1996). The subsidence is related to reactivation of the E–W-trending *Dauki Fault* (Fig. 22.3c) as evident from the clustering of swamps and lakes in great number in the immediate proximity of the Dauki Fault. The Sylhet Trough is one among the many subsurface structures—Faridpur Trough, Hatiya Trough, Madhupur High, Barind High, etc.

22.3 Sedimentation in Ganga Basin

The Indo-Gangetic sedimentary succession represents the continuation of the Siwalik sedimentation. This is evident from the Sindhu River sediments succeeding the Upper Siwalik rocks in a normal order at Kharian Hill, southeast of Jhelam in Pakistan (Pascoe 1964). Deep drilling in the Ganga Basin has shown the presence of the Siwalik everywhere beneath the Ganga sediments (Fig. 22.5). In the proximity of the subsurface Munger–Saharsa Ridge (Fig. 22.3a) at Barasiaghat near Bhagalpur in Bihar, fossil-bearing Siwalik rocks were encountered at a depth of 30 m in an excavation for bridge piers (Sinha 1999).

The sedimentation in the *Ganga Basin* began when the climate was humid and the rainfall copious. There were lakes and swamps in the flood plains of rivers characterized by high discharges of water and sediments. The sediments accumulated on the floor that was subsiding. In the marginal parts of the basin, rivers and streams built lobes and fans as they shed their loads of coarse detritus. In the central part, larger rivers that had longer residence time in their channels built multistorey sandbodies, while the interfluves were formed of fine-grained sediments in floodplains (Singh 1996).

After the initial phase of heavy rainfall and high river discharges, there was a short spell of arid climate when streams had little or no water and sediments to carry. Blowing wind piled up fine-grained sands of yellow-brown colour as heaps 6–7 m in height. These aeolian sand mounds in the vicinity of stream channels are called *Bhur* (Joshi 2001). Not only the Bhur, but also the soils of the Ganga–Gandak interfluve bear testimony to the prevalence of dry climate at about 18,000 years B.P. (Mohindra and Prakash 1994; Mohindra 1995). As a matter of fact, south of the I-GP, the Son and the Balan valleys wear blankets of Late Pleistocene loess, the wind-borne sediments. Around 8000 years B.P., the climate became wet and warm once again. The rainfall was more than what it is at present, as testified by anomalously wide channel, for example, a rivulet named Chhoti Sarju (Joshi 2001). Naturally there was vigorous fluvial activity, the rivers had wide channels, and they developed meandering loops, oxbow lakes and swamps. In the Ghaghara–Gandak interfluve (Fig. 22.8), the older part of the soil shows concentration of salts at the surface, and also the effects of decalcification and illuviation due to higher rainfall (Mohindra 1995).

Determination of ^{10}Be concentration in quartz grains in the sediments of the Indo-Gangetic Plains revealed that its basin is being filled by rivers draining the

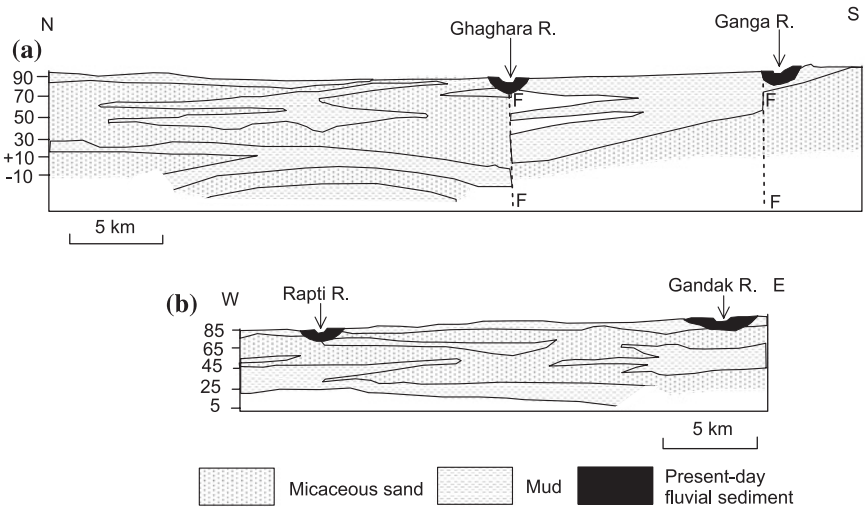

Fig. 22.8 Subsurface lithofacies of the middle part of the Ganga Basin in eastern Uttar Pradesh (after Dwivedi et al. 1997)

Peninsular India and eroding at a rate of 0.007 mm/year and by the rivers draining the Himalaya and eroding their terrains at the rate of varying from 0.5 to 1.4 mm/year, the total sediment delivery being of the order of 610 ± 230 million tonnes per year (Lupker et al. 2012). In the Assam part of the Indo-Gangetic Plains, the sediments were delivered at much faster rate, for the rivers draining the mountains were eroding at much faster rate. Detrital zircon cooling ages from 19 samples along the Brahmaputra and its tributaries showed that the Namcha Barwa massif—the major source (69.70 %) of the sediments—is being eroded at the rate 5–9 mm/year (Enkelmann et al. 2011).

22.4 Growth of Deltas

22.4.1 Ganga–Brahmaputra Delta

Increased influx of sediments brought by the Himalayan-born rivers made the sedimentary lobes to grow seawards in the form of deltas. During the time of the *Last Glacial Maximum*, when the sealevel was low, there was strong dissection of the upland surfaces. Sediments were deposited between 12,000 and 10,000 years B.P. in the Bengal Basin, which was then a part of the sea (Fig. 22.9). By the Late Holocene, broad peatland and marshland had formed even as rivers deposited their loads vigorously in their channels. And mangrove-vegetated islands and peninsulas grew in front of the prograding deltas (Umitsu 1993; Allison et al. 2003).

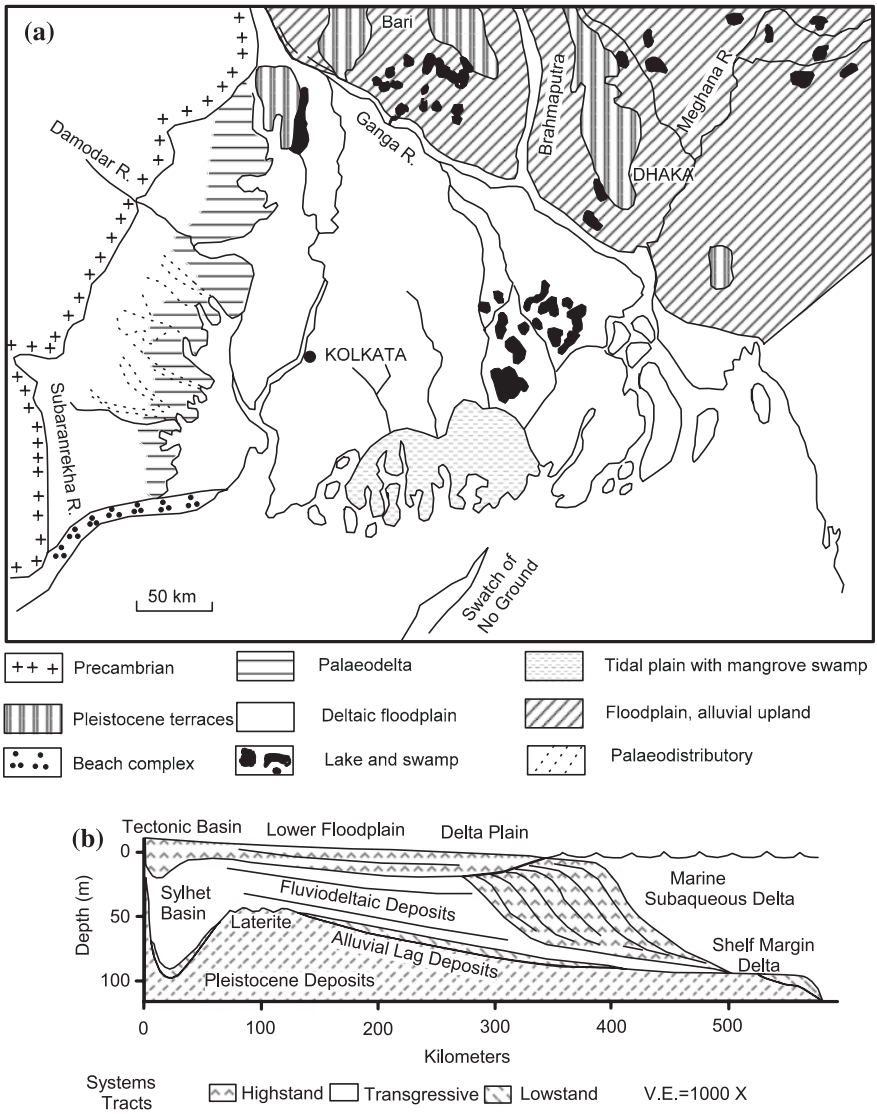

Fig. 22.9 **a** Shoreline of emergence shifted progressively southeastwards in the Bengal Basin. The map shows various geomorphological elements of the Sundarban Delta (after Agrawal and Mitra 1991). **b** Deltas grew progressively seawards in the Late Quaternary time (after Goodbred and Kuehl 2000)

The present delta—the *Sundarban Delta*—in the Bengal Basin has been growing for the last 7000 years (Figs. 22.9 and 22.10). It is a product of five cycles of development (Roybarman 1983). Located as it is in a tectonically active setting, the Sundarban Delta grew under control of tectonics, high marine and fluvial

energy and high influx of sediments (Goodbred and Kuehl 2000; Goodbred et al. 2003). This is clearly reflected in the varied lithologies of the delta. The lateritic uplands on the western margin of the basin are followed successively by palaeodelta plain, younger fluviodelta plain and recent tidal flat with beach ridges. On the western palaeodelta plain, the Damodar, the Dwarkeshwar and the Karai rivers show sharp inflexion and then break into distributories—with their channels filled with sands, and the levees making their flanks. The younger fluviodelta plain is characterized by abandoned channels, lakes, swamps and tidal levees. Within the tidal flat occurs intricate network of creeks and islands (Agrawal and Mitra 1991). Marking the delta front, the shoreline of emergence has been shifting progressively southwards and eastwards through the time (Niyogi 1975).

The delta complex formed in this manner as a result of combined contributions of the Ganga and the Brahmaputra is the world's largest delta (Fig. 20.10). It covers 60,000 km^2 area and rises 1.5–20 m above the mean sea level. The sediment contribution of the Ganga is characterized by higher proportion of smectite among

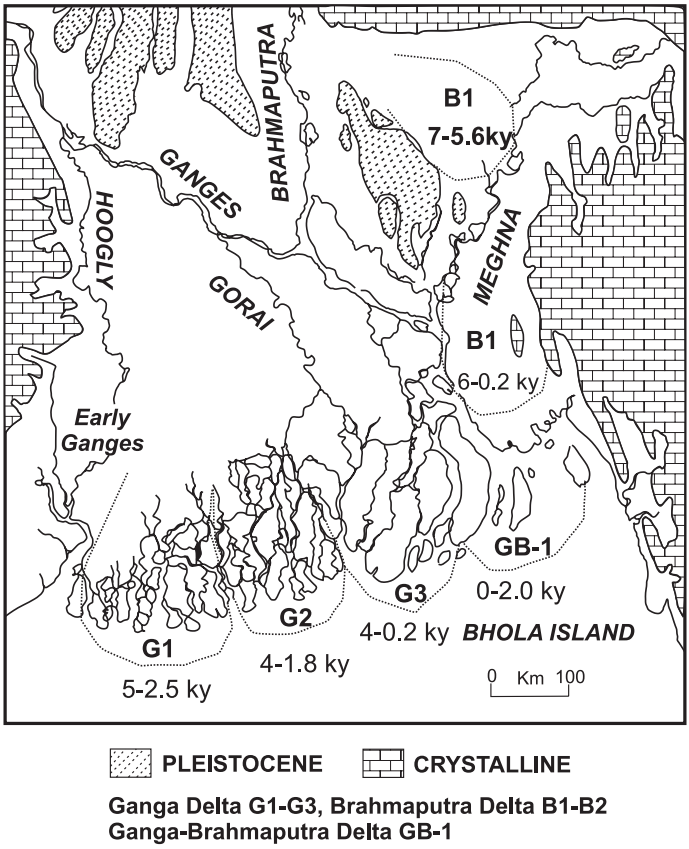

Fig. 22.10 Pathways and timing of the phases of growth of the lower delta plains associated with the Ganga (*G1*, *G2*, *G3*) and the Brahmaputra (*B1*, *B2*) (after Allison et al. 2003)

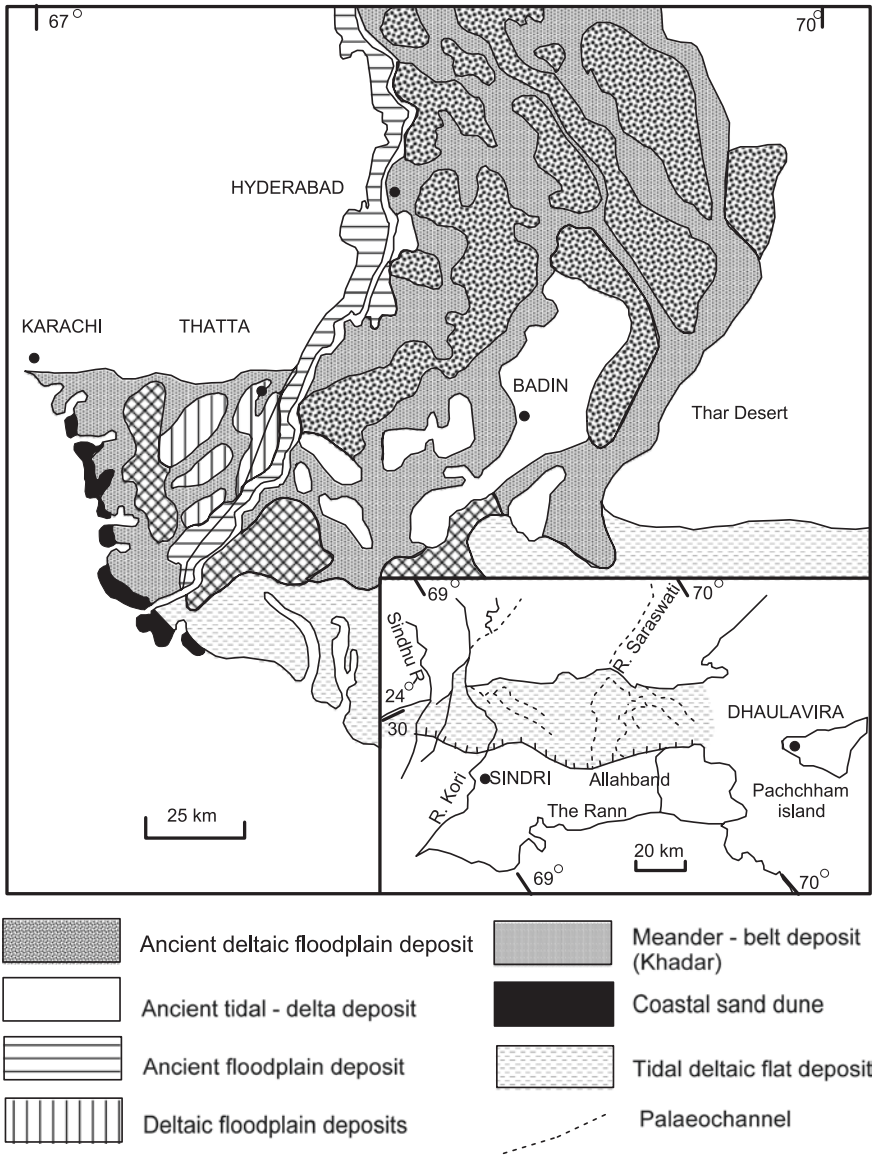

Fig. 22.11 Indus Delta with its varied lithological units and landforms (modified after Kazmi and Qasim Jan 1997). *Inset* shows the palaeodelta built by the Saraswati River that disappeared some time in the Late Holocene (after Malik et al. 1999)

clays and lower epidote–garnet ratio in the sand-silt fraction. And the Brahmaputra brought sediments rich in illite, kaolinite and chlorite clays (Heroy et al. 2003).

The subaerial extension of the Sundarban Delta feeds the world's largest submarine fan—the *Bengal Fan*—extending south more than 3000 km into the Indian

Ocean (Curray and Moore 1971). Quite a proportion of sediments is carried to the sea through a submarine canyon known as Swatch of No Ground (Fig. 22.10).

22.4.2 Sindhu Delta

In the west, the Sindhu River was building its delta throughout the Late Quaternary. The present-day delta complex comprises deltaic floodplain and tidal flats. There is an arcuate zone of older tidal deposits formed as a result of distributories along the margin of the deltaic floodplain (Fig. 22.11). Much of the coarse sediment is delivered to the Arabian Sea through a submarine canyon. The *Indus Delta* extends south of Thatta, covering 2600 km^2 area. Before the construction of dams in the Sindhu River System, the delta was growing at the rate of 34 m/year, even as the Sindhu was annually transporting 300 million tonnes of sediments (Kazmi and Qasim Jan 1997).

To the southeast of the Indus Delta is the *Rann of Kachchh*, a 350-km-long and 150-km-wide tidal flat. Once connected with the Gulf of Khambhat (Cambay) through the Nal Sarovar (a brackish water marsh), the Rann is a salt-encrusted plain, inundated by marine waters during the monsoon months. This gulf was converted into a delta plain by the rivers of the Sindhu Basin.

22.5 Physiographic Developments

22.5.1 Ganga Plain

Nearly 30–100 m above the mean sea level, the *Ganga Plain* in the centre of the Indo-Gangetic domain comprises six distinct physiographic units, each characterized by its own lithology. These are the Banda, the Varanasi, the Bhangar, the Bhur, the Khadar and the Bhabhar (Table 22.1, Fig. 22.12). The first three units were earlier described as parts of the *Older Alluvium*, and the Bhur and the Khadar constituted the *Newer Alluvium*.

Fringing the Bundelkhand–Vindhyan uplands in the south, the elevated tract of the Pleistocene deposits is called the *Banda Formation* and the *Varanasi Formation* (Joshi and Bhartiya 1991; Bhartiya et al. 1995; Dwivedi et al. 1997). The Banda is made up of variegated clays and quartzofelspathic sands with local beds of gravels. The Varanasi is a 70–240-m-thick fan deposit laid down by braided to meandering rivers associated with lakes and swamps in the upper part of the sequence.

The *Bhangar* Formation is composed of beds of clays of yellow and brownish red colours and commonly characterized by calcareous concretions or calcrete (*kankar*) and ferruginous concretions. Owing to the variegated colours of its soil, the Bhangar is known as *Rangmati Formation* in Bengal and Assam. Dating of shells from the superficial part of the Bhangar gave an age of

Table 22.1 Lithostratigraphic succession in the Ganga Basin (based on Pascoe 1964; Bhartiya et al. 1995; Dwivedi et al. 1997)

Bhabhar	Fans and cones of gravels coalesced to form an apron along the foothills
Khadar (Newer Alluvium)	*Recent Alluvium* (4–10 m): grey micaceous, fine to medium grained sand with intercalations of clay
	Terrace Alluvium (3–15 m): grey and light brown quartzo-felspathic, fine-grained sand with intercalations of silt and clay
	Bhur Fm. (3–10 m): fine grained aeolian sand with oxidized red brown surface
	——— *Disconformity* ———
Bhangar (Older Alluvium)	*Varanasi Fm.* (34–40 m): polycyclic sequence of buff to brown clays with minor silt and clays. Intercalated horizons of clays are characterized by calcrete, locally ferruginous concretions
	Banda Fm. (64–88 m): lateritic gravel with variegated clay in lower part and felspathic medium-to-coarse sand in upper part
	——— *Unconformity* ———
	Bundelkhand Gneiss in south/Upper Siwalik in north

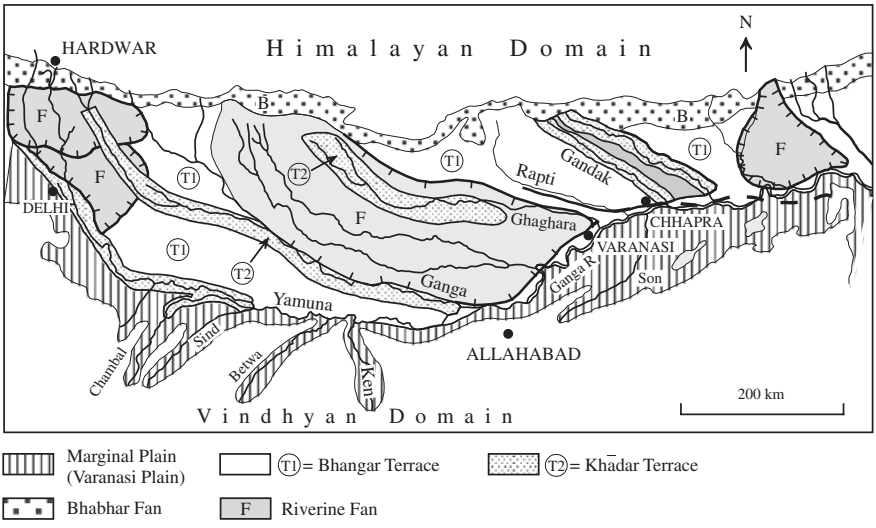

Fig. 22.12 Physiographical cum lithological units of the Ganga Plain (modified after Dwivedi et al. 1997; Bhartiya et al. 1995; Singh 1996)

11,040 ± 190 years B.P. (Joshi and Bhartiya 1991). The Bhangar succession is best seen in cliffs along the valleys of the Yamuna and the Ganga in southwestern Uttar Pradesh. There is a chain of upland with 14-m-high escarpment on the southern bank of the Ganga, possibly related to an active fault oriented broadly

east–west (Bajpai 1989). Conjugate pairs of fractures affect the 2–3°-dipping calcrete-rich conglomerate beds containing 9960 ± 80 year old bivalve shells. These beds make 20–60-m-high cliffs in the Sengar Valley, and the Yamuna River has cut deep incision into its valley. All these features indicate uplift of the belt in the Middle–Upper Holocene time (Singh et al. 1997; Agarwal et al. 2002). At Kalpi, a 20-m-high cliff exposes about 33-m-thick succession of the Bhangar, comprising red-brown mud with rhyzocretions. The formation of cliffs is attributed also to climate-induced incision (Gibling et al. 2005; Sinha et al. 2002, 2005; Tandon et al. 2006). In response to climate forcing, particularly during the Holocene, there were repetitive aggradation and degradation, and valleys migrated during the intensifications of monsoon in the last 6000 years.

A very distinctive feature of the Bhangar is the concretionary nodule of carbonates called *kankar* (calcretes) and in some places alkali salts. The alkali salts consisting of chlorides, nitrates and carbonates of calcium and potassium are known as *reh, kallar* or *usar*. The concretionary carbonates and alkali salts were formed due to capillary rise of groundwater during hot dry climate in the 6000–10,000 years B.P. period. Another consequence of the spell of aridity was the accumulation, locally, of fine-grained aeolian sands in heaps and mounds called *Bhur* in western U.P., Haryana and Panjab. In the Ravi–Beas interfluve, 0.5–5-m-thick aeolian sand representing the Bhur is intercalated with more than 150-m-thick multicyclic sequence of the Bhangar, which is the Older Alluvium (Ruby and Punj 1999).

Cutting 15–60 m deep into the Bhangar Formation, the rivers of the Ganga Plain have formed 5–20-km-wide floodway. These are the valleys subsequently covered with alluvial–fluvial deposits (Fig. 22.13a). These are known as the *Khadar* (or *Newer Alluvium*). The Khadar flats are characterized by tight meandering loops in streams, oxbow lakes and abandoned channels, as best seen in the Ganga–Ghaghara interfluve.

In the northern margin of the I-GP, adjoining the foothills of the Himalaya there is a fringe of coalescing fans of gravel deposits known as the *Bhabhar*. This apron of gravels is the youngest unit of the Indo-Gangetic domain (Table 22.1, Fig. 22.12). It was formed in the last few thousand years by the mountain-born rivers and torrents. The Yamuna, the Ganga, the Sharada, the Gandak and the Kosi continue to build large fans of very coarse detritus, predominantly gravels. In the foothills of the Kumaun Himalaya, the Bhabhar surface is characterized by uneven topography, low drainage density, subparallel to radial pattern of drainage, disparate fan cycles of sediments and deep incision by the Gaula River (Shukla and Bora 2003). This deposit is growing in thickness due to continuing mass wasting and sheet flow processes. Development of four levels of fluvial terraces in the Piedmont zone of the Darjiling–Sikkim Himalaya is linked with regional uplift and consequent incision and related to the coalescing and migrating alluvial fans of the Tista and Jaldhaka rivers. While the oldest first and the upstream segment of the second terraces were formed in the straight channel, the downstream segment of the second, the third and the fourth tiers of terraces accreted as point bars in meandering channels (Sinha-Roy 1980).

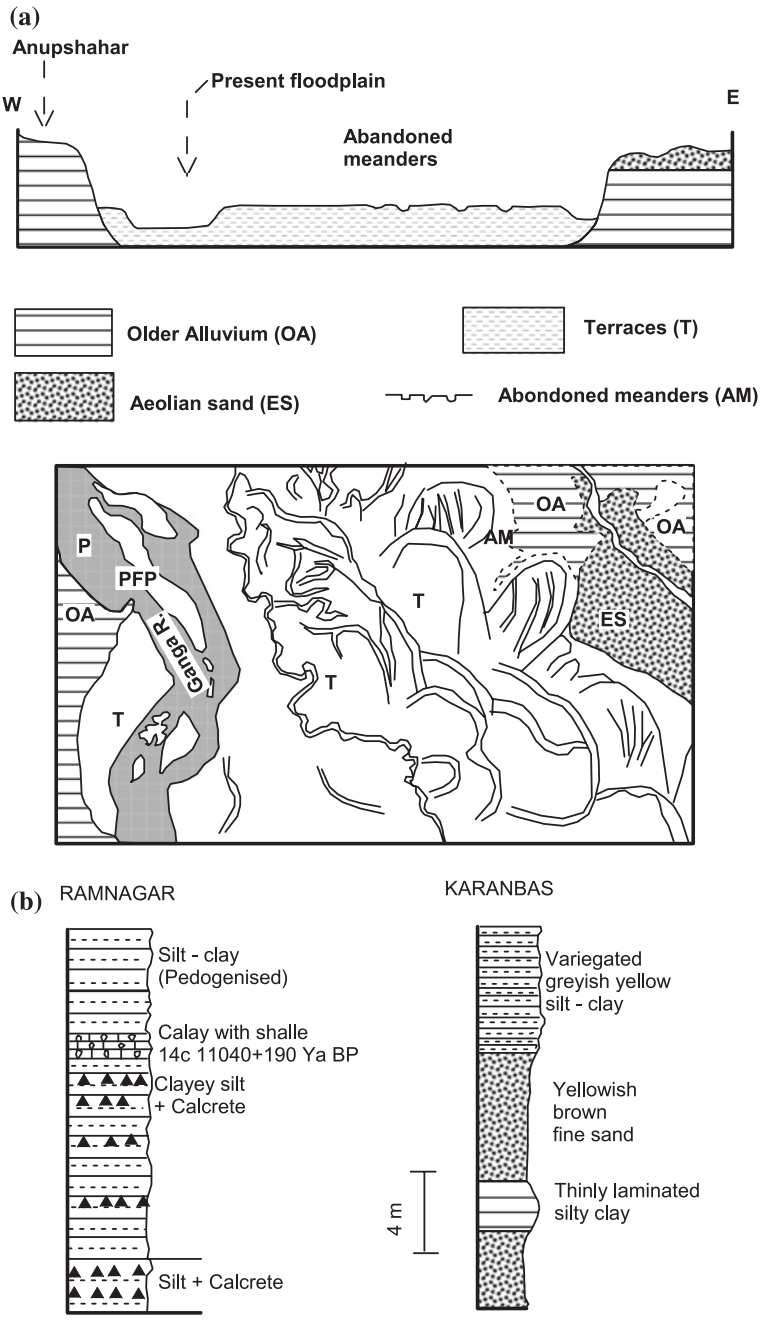

Fig. 22.13 **a** Khadar surface of the Ganga Plain in the Ganga–Ghaghara interfluve area characterized by abandoned channels, oxbow lakes, cut-off meanders, etc. The Khadar was formed as a consequence of rivers cutting deep, wide valleys into the Bhangar, and laying down their sediments, now forming terraces T_2. **b** Lithology of the Khadar in two sections (**a**, **b** modified after Joshi 2001)

The TL dating (Srivastava et al. 2003) suggests that the marginal plain in the southern part and the nearly contemporary upland interfluve surfaces were formed in the period, respectively 76–32 and 48–7 Ka. The Ganga megafan was built in the interval 26–22 ka. The younger Piedmont fans in the northern margin were emplaced 8000–3000 years B.P. And the river valley terraces developed in the last 3000–1100 years. As already stated, the 11000–8500 years B.P. period witnessed cold arid to semiarid climate when pedogenic calcrete developed over large areas in the Ganga Plain. On the other hand, the eastern part of the Ganga Plain in northern Bihar is much younger and continuously aggrading. The near-surface sediments are 1100–2100 years old (Sinha and Friend 1994).

22.5.2 Sindhu Plain

In the Panjab sector, alluvial fans extend nearly 9–15 km south from the immediate Piedmont, and 30–100-m-high vertical cliff characterizes the river valleys, as they debouch into the Panjab Plain. There is no doubt that there was uplift south of the Piedmont belt. In the Sindhu Plain, the Bhabhar is known as the *Piedmont Zone*. It stretches in the form of a 16–24-km-wide apron of coalescing fans of gravel all along the foot of the Sulaiman and Kithar ranges. The relatively steeper upper part of the Indus Piedmont is made up of coalescing fans of gravels, and the lower gently sloping part comprises relatively finer detritus. Badland topography and braided streams characterize this zone (Kazmi and Qasim Jan 1997; Kazmi and Shah 1998). The 16–50-km-wide central alluvial plain is 180–210 m above the mean sea level in the north and 3–4 m at the delta. It is largely a Khadar expanse and terminates against low terraces, alluvial ridges and levees (Fig. 22.14). Streams are moderately entrenched in the floodplain and are confined to their well-defined shallow 6–25-km-wide meandering belts. The banks are vertical or marked by alluvial terraces.

In the Panjab part of the Sindhu Basin (Fig. 22.14 *inset*), the interfluve terrace deposits are known as the *Chung*. They are homotaxial with the Terrace Alluvium (Table 22.1) of the Ganga Khadar (Ruby and Punj 1999).

22.5.3 Brahmaputra–Ganga Plain

The Bengal Plain of the Brahmaputra and Ganga systems (Fig. 22.15a) is the extension of the Ganga Plain. Its western and northern margins are made up of the Pleistocene terraces. In the eastern side, the *Lalmai Terrace* is 30 m above the sea level. In the western side, the upland is covered by the Lower to Middle Pleistocene terraces made up of red soil. In the north lies the *Barind Terrace*, characterized by three topographical levels. In the midst of the floodplains of the Ganga and Brahmaputra, the *Madhupur Terrace* is made up of typically reddish

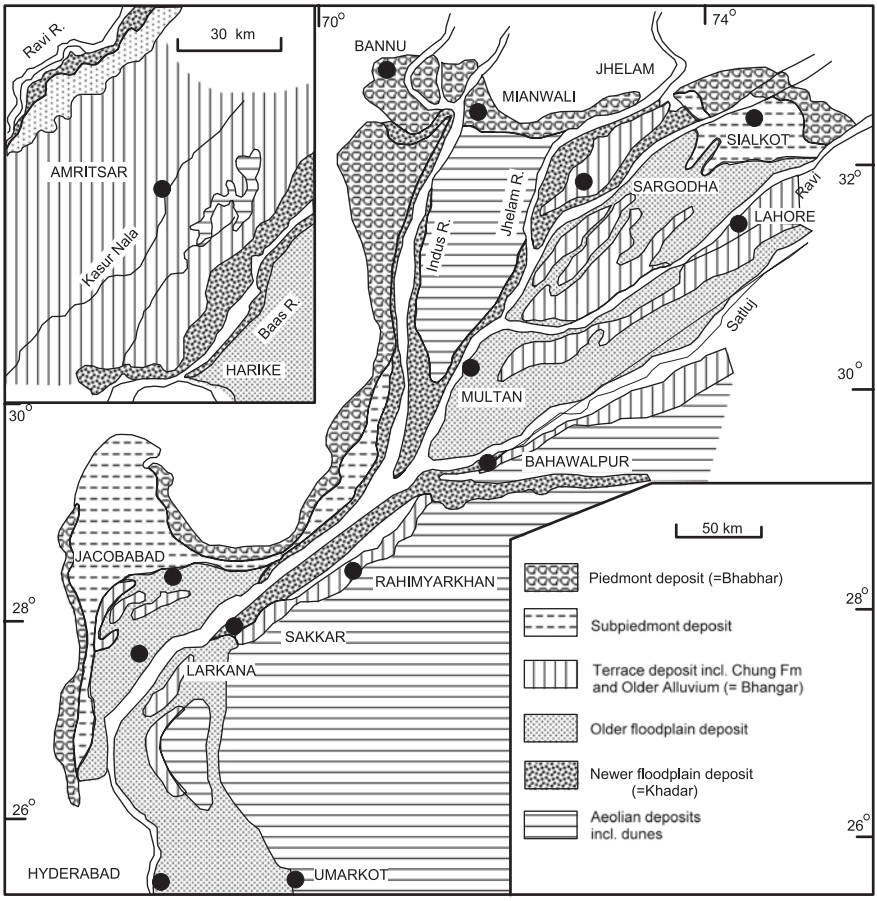

Fig. 22.14 Physiography and lithological units of the Sindhu Plain in Pakistan (modified after Kazmi and Qasim Jan 1997). *Inset* Lithogratigraphic and geomorphological features in the northern part of the Sindhu Plain (modified after Ruby and Punj 1999)

brown and mottled sediments with ferruginous and calcareous concretions typical of the Bhangar in the Ganga Plain. Both the Barind and the Madhupur terraces are dramatically modified by faulting up and resultant profound erosion (Morgan and McIntyre 1959; Alam 1996). The Madhupur Terrace is uplifted 30 m above the mean sea level in the western side forming an escarpment, but slopes down to only 6 m in the northern and eastern sides. The surface slopes beneath the recent flood plain (Fig. 22.15b). There was domal uplift in the Barind region as evident from high elevation of the central part and its surface sloping northwards and southwards (Khandeker 1987). The Atrai and Purnabhaba rivers have entrenched valleys in the Barind tract, which is defined in the east by a 40-km-long NE–SW-trending fault.

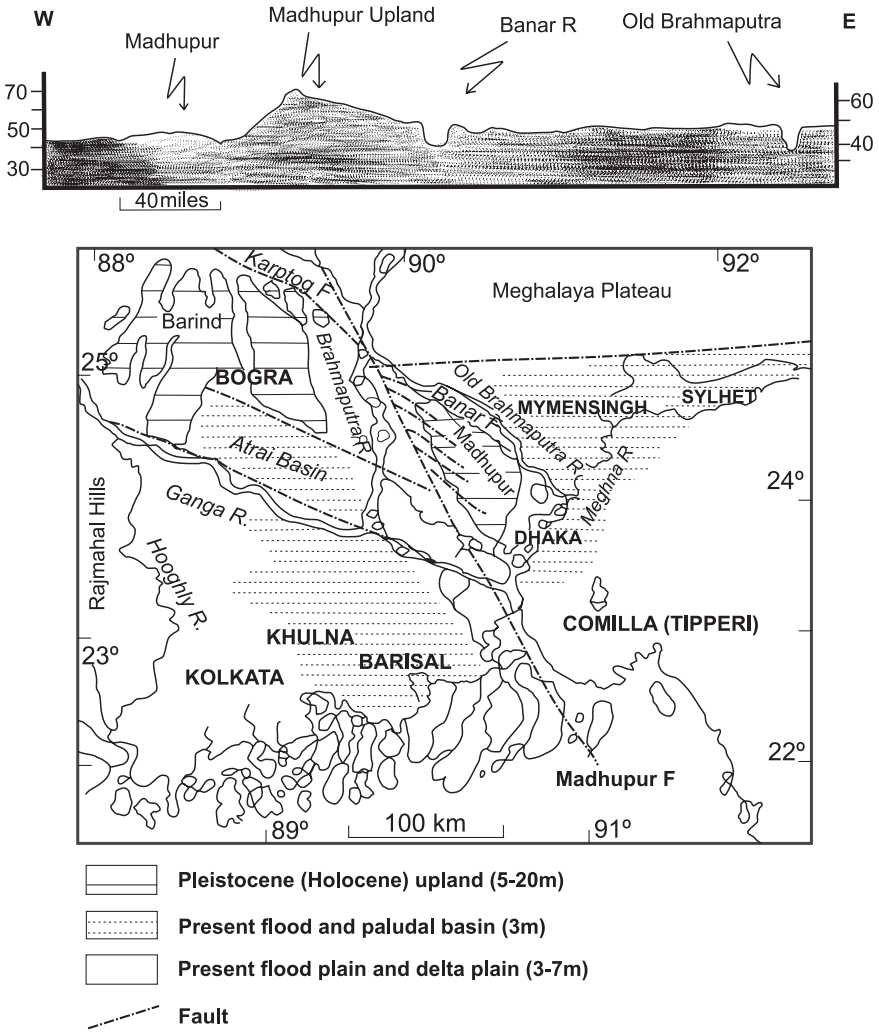

Fig. 22.15 **a** Profile across the Pleistocene and recent surface in the Bengal Plain (after Morgan and McIntyre 1959). **b** Physiography and lithological units of the Bengal Plain built in the Later Quaternary time (based on Morgan and McIntyre 1959; Alam 1996; Goodbred et al. 2003)

The flood plain of the Ganga, the Brahmaputra and the Meghna are homotaxial and with the Khadar of the Ganga Plain. They are low-lying flats, not more than a few metres above the mean sea level—the lowest point being merely 3 metres (Alam 1996). The floodplains are characterized by innumerable lakes and swamps called *hoar* or *bil*. They occur in clusters. One of the clusters occurs close to the scarp of the Meghalaya Plain defined by the active Dauki Fault.

22.6 Drainage: Pattern and Changes

The line joining Mount Kailas in Tibet through Mount Abu in the Aravali Range with Mount Girnar in Saurashtra seems to have served like a watershed (Fig. 22.16 *inset*). All rivers to the east of this axis of sorts flow eastwards and southeastwards and empty themselves in the Bay of Bengal, and the rivers to the west flow southwestwards and southwards and discharge into the Arabian Sea. While the eastern and western parts of the I-GP (Fig. 22.16) are well watered by dense systems of rivers and streams, the axial part embracing eastern Haryana and adjoining northwestern Rajasthan region is bereft of the bounty of rivers (Valdiya 2002).

One of the very conspicuous features of the Ganga drainage is that the Himalayan-born rivers flow 200–300 km away from the mountain front (Fig. 22.16). Rapid growth of megafans of sediments deposited by these rivers seems to have pushed them southwards (Burbank 1992). The southwards migration of the Yamuna in the Kalpi area took place during the time of active tectonism (Singh et al. 1997) or when there was greater discharge in the river following intensification of monsoon 6000–8000 years B.P. (Tandon et al. 2003).

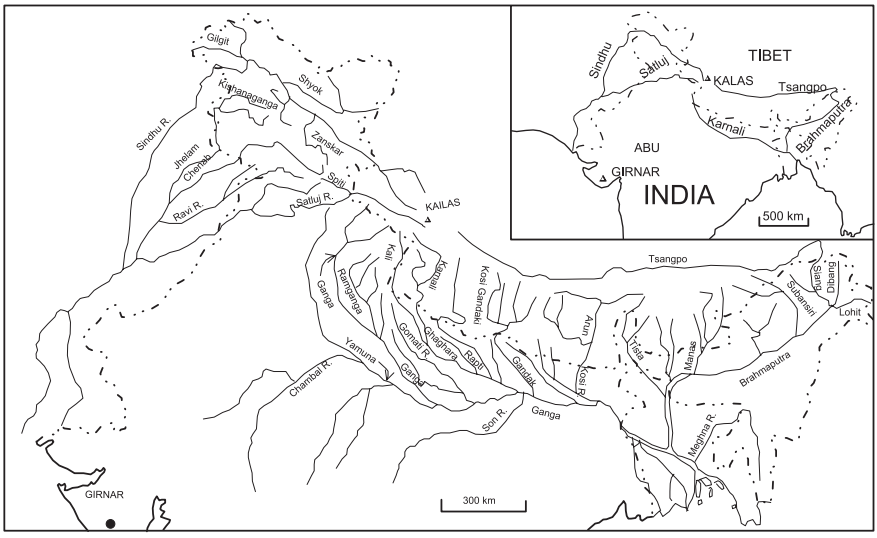

Fig. 22.16 Drainage pattern of the Indo-Gangetic Plains. Note that rivers east of the Kailas–Girnar line flow eastwards and southeastwards to empty themselves in the Bay of Bengal; the rivers to the west of the line flow southwestwards to join the Arabian Sea. And eastern Haryana and northwestern Rajasthan remain undrained by any river of consequence (after Valdiya 1998)

22.7 Life in the Early Indo-Gangetic Time

The remains of animals found in the Banda and Varanasi formations demonstrate that the animal life in the Bhangar time was not much different from what it is today. There were elephants, horses, pigs, antilopes, buffaloes, cows and rats. Among others, *Stegodon* roamed the Varanasi Plain in the early time.

Some animals have become extinct since then. These include *Stegodon*, the hippopotami *Tetraprotodon palaeindicus* and *Hexaprotodon*, the elephant *Elephas namadicus*, the primate *Semnopithecus* and the cow *Bos namadicus*. Their extinction is attributed to a drastic change in the climate 5000–6000 years ago. Skeletal remains of primates and of early man have not been found so far anywhere in the I-GP, despite the fact that an ape *Sivapithecus* (Fig. 19.21) lived in the woods of the Lower Siwalik time in the Hartalyangar–Jammu Belt of the adjoining Siwalik domain, and stone implements have been found from sediments as old as 540,000 years B.P. This fact has prompted the speculation that humans evolved outside the Indian subcontinent and came only as an evolved species—the *Homo sapiens*. The subject is discussed in Chap. 24.

References

Agarwal, K.K., Singh, I.B., Sharma, M., & Sharma, S. (2002). Extensional tectonic activity in the cratonward parts (peripheral bulge) of the Ganga Plain foreland basin, India, *Internation Journal of Earth Science (Geological Rundschau), 91*, 879–905.

Agrawal, R. K. (1977). Structure and tectonics of Indo-Gangetic plain. In V. L. S. Bhimasankaram (Ed.), *Geophysical Case Histories* (pp. 27–48). Hyderabad: Association of Exploration Geophysicists.

Agrawal, R. P., & Mitra, D. S. (1991). Palaeogeographic reconstruction of Bengal delta during Quaternary period. *Memoirs of the Geological Society of India, 22*, 13–24.

Alam, Mahmood. (1996). Subsidence of the Ganges-Brahmaputra delta of Bangladesh and associated drainage, sedimentation and salinity problems. In J. D. Milliman & B. U. Haq (Eds.), *Sea Level Rise and Coastal Subsidence* (pp. 169–192). Amsterdam: Kluwer Academic Publishers.

Allison, M. A., Khan, S. R., Goodbred, S. L., & Kuehl, S. A. (2003). Stratigraphic evolution of the Late Holocene Ganges-Brahmaputra lower delta plain. *Sedimentary Geology, 155*, 317–342.

Bajpai, V. N. (1989). Surface and subsurface evidence of neotectonics and the aquifer disposition in central Gangetic alluvial terrain of Kanpur-Unnao region in Uttar Pradesh. *Photonirvachak, 17*, 47–53.

Bhartiya, S. P., Narayan, S., & Nigam, A. C. (1995). Lithostratigraphy and alluviation history of Quaternary deposits of southern part of Gangetic plains, U.P. *Journal of Geological Society of India, 46*, 393–399.

Burbank, D. W. (1992). Causes of recent Himalayan uplift deduced from deposited patterns in the Ganges Basin. *Nature, 357*, 680–682.

Curray, J. R., & Moore, D. G. (1971). Growth of the Bengal deep sea fan and denudation in the Himalaya. *Geological Society of American Bulletin, 82*, 563–572.

Das, J. D. (1992). The Assam Basin: Tectonic relation to the surrounding structural features and Shillong Plateau. *Journal of the Geological Society of India, 39*, 303–311.

Dwivedi, G. N., Sharma, S. K., Prasad, S., & Rai, R. P. (1997). Quaternary geology and geomorphology of a part of Ghaghara–Rapti–Gandak sub-basins of IndoGangetic plain, U.P. *Journal of Geological Society of India, 49*, 193–202.

Enkelmann, E., Eheler, T. A., Zeitler, P. K., & Hallet, B. (2011). Denudation of the Namche Barwa antiform, eastern Himalaya. *Earth & Planetary of Science Letters, 307*, 323–333.

Fuloria, R. C. (1996). Geology and hydrocarbon prospects of the Vindhyan sediments in Ganga valley. *Memoirs of the Geological Society of India, 36*, 235–256.

Gibling, M. R., Tandon, S. K., Sinha, R., & Jain, M. (2005). Discontinuity-bounded alluvial sequences of the southern granulite plains, India: Aggradation and degradation in response to monsoon strength. *Journal of Sedimentary Research, 75*, 369–385.

Goodbred, S. L., & Kuehl, S. A. (2000). The significance of large sediment supply, active tectonism, and estuary on margin sequence development: Late Quaternary stratigraphy and evolution of the Ganges-Brahmaputra delta. *Sedimentary Geology, 133*, 227–248.

Goodbred, S. L., Kuehl, S. A., Steckler, M. S., & Sarker, M. H. (2003). Controls on facies distribution and stratigraphic preservation in the Ganges-Brahmaputra delta sequence. *Sedimentary Geology, 155*, 301–316.

Goswami, D. C. (1985). Brahmaputra River in Assam: Physiography, basin denudation and channel aggradation. *Water Resources Research, 27*, 959–978.

Heroy, D. C., Kuehl, S. A., & Goodbred, S. L. (2003). Mineralogy of the Ganges and Brahmaputra rivers: implications for river switching and Late Quaternary climate change. *Sedimentary Geology, 155*, 343–359.

Johnson, S. Y., & Alam, A. M. N. (1991). Sedimentation and tectonics of the Sylhet through, Bangladesh. *Geological Society of America, Bulletin, 103*, 1513–1527.

Joshi, D. D. (2001). Late Quaternary climate events of the Gangetic plain. *Special Publication, Geological Survey of India, 65*(111), 101–107.

Joshi, D. D., & Bhartiya, S. P. (1991). Geomorphic history and lithostratigraphy of a part of eastern Gangetic plains, U.P. *Journal of Geological Society of India, 37*, 569–576.

Kazmi, A. H., & Qasim Jan, M. (1997). *Geology and Tectonics of Pakistan*. Karachi: Graphic Publishers. 554 p.

Kazmi, A. H., & Shah, A. A. (1998). The Indus fluvial system and the Quaternary geology of the Indus Plain. In M. I. Ghazanavi, S. M. Raza, & M. T. Hasan (Eds.), *Siwaliks of South Asia* (pp. 99–110). Islamabad: Geological Survey of Pakistan.

Khandeker, R. A. (1987). Origin of elevated Barind-Madhupur areas, Bengal basin, results of neotectonic activities, Bangladesh. *Journal of Geology, 6*, 1–9.

Lupker, Maarten, Blard, P.-H., Lave, J., France-Lanord, C., Leanni, L., Puchol, N., et al. (2012). ^{10}Be-derived Himalayan denudation rates and sediment budgets in the Ganga basin. *Earth & Planetary of Science Letters, 333–334*, 146–156.

Lyon-Caean, H., & Molnar, P. (1985). Gravity anomalies, flexure of the Indian plate and the evolution of the Himalaya and Ganga Basin. *Tectonics, 4*, 513–538.

Malik, J., Merh, S.S., & Sridhar, V. (1999). Palaeodelta complex of Vedic Saraswati and other ancient rivers of northwestern India, *Memoirs of Geological Society of India*, 163–174.

Mohinder, R., & Parkash, B. (1994). Geomorphology and neotectonic activity of the Gandak Megafan and adjoining areas, Middle Gangetic Plain. *Journal of Geological Society of India, 43*, 149–158.

Mohindra, R. (1995). Holocene soil chronoassociation in part of the middle Gangetic Plain: morphological and micromorphological characteristics. *Terra Nova, 7*, 305–314.

Morgan, J. P., & McIntire, W. G. (1959). Quaternary geology of the Bengal basin, East Pakisthan and India. *Geological Society of America, Bulletin, 70*, 319–342.

Niyogi, D. (1975). Quaternary geology of the coastal plain in West Bengal and Orissa. *Indian Journal of Earth Science, 2*, 51–61.

Pandey, Jagadish, & Dave, Alok. (1998). *Stratigraphy of Indian Petroliferous Basins*. Dona Paula: National Institute of Oceanography. 248 p.

Pascoe, E. H. (1964). *A Manual of the Geology of India and Burma* (Vol. III, pp. 1345–2131). Kolkata: Government of India Press.

Raiverman, V., Srivastava, A. K., & Prasad, D. N. (1993). On the Foothill Thrust of northwestern Himalaya. *Journal of Himalyan Geology, 4*, 237–256.

Ranga Rao, A. (1983). *Geology and Hydrocarbon Potential of a Part of Assam-Arakan Basin and Adjacent Region* (pp. 130–133). November issue: Petroleum Asia Journal.

Reimann, K.-U. (1993). *Geology of Bangladesh*. Berlin: Gebrüder Borntraeger. 160 p.

Roybarman, A. (1983). Geology and hydrocarbon prospects of West Bengal. *Petroleum Asia Journal, 6*, 51–56.

Ruby, B. S., & Punj, N. K. (1999). Quaternary geological studies in Amritsar district, Punjab. *Gondwana Geological Magazine, 4*, 33–42.

Sastry, V. V., Bhandari, L. L., Raju, A. T. R., & Datta, A. K. (1971). Tectonic framework and subsurface stratigraphy of the Ganga Basin. *Journal of the Geological Society of India, 12*, 222–233.

Sengupta, S. (1966). Geological and geophysical studies in western part of Bengal Basin, India. *American Association of Petroleum Geologists Bulletin, 40*, 1001–1018.

Shukla, U. K., & Bora, D. S. (2003). Geomorphology and sedimentology of piedmont zone. *Ganga Plain, India, Current Science, 84*, 1034–1040.

Singh, I. B. (1996). Geological evolution of Ganga plain—an overview. *Journal of Palaeontological Society of India, 41*, 99–137.

Singh, A. K., & Singh, J. N. (1997). Sequence stratigraphic analysis of pre-Tertiary succession in Ganga basin. *Journal of the Geological Society of India, 49*, 629–646.

Singh, I. B., Rajagopalan, G., Agrawal, K. K., Srivastava, P., Sharma, M., & Sharma, S. (1997). Evidence of middle to late Holocene neotectonic activity in the Ganga Plain. *Current Science, 73*, 1114–1117.

Sinha-Roy, S. (1980). Terrace systems in the Tista valley of Sikkim-Darjeeling Himalayas and the adjoining piedmont region. *Indian Journal of Earth Science, 7*, 146–161.

Sinha, K. Ravindra. (1999). Neotectonics in the vicinity of Munger-Sahara Ridge on the Ganga Plain, Bihar. *Gondwana Geological Magazine, 4*, 117–129.

Sinha, R., & Friend, P. F. (1994). River systems and their sediment flux, Indo Gangetic plains, northern Bihar, India. *Sedimentology, 41*, 825–845.

Sinha, R., Khanna, M., Jain, V., & Tandon, S. K. (2002). Mega-geomorphology and sedimentation of parts of the Ganga-Yamuna plains. *Current Science, 82*, 562–566.

Sinha, R., Gibling, M. R., Tandon, S. K., Jain, V., & Dasgupta, A. S. (2005). Quaternary stratigraphy and sedimentology of the Kotra section of the Betwa river, southern Gangetic plains, Uttar Pradesh. *Journal of Geological Society of India, 65*, 441–450.

Srivastava, Pradeep, Singh, I. B., Sharma, S., Shukla, U. K., & Singhvi, A. K. (2003). Late Pleistocene-Holocene hydrologic changes in the interfluve areas of the central Ganga Plain, India. *Geomorphology, 54*, 279–292.

Tandon, S. K., Sinha, R., Gibling, M. R., Jain, V., & Ghazanfar, A. A. (2003). Quaternary stratigraphy of southern Gangetic Plains: The Kalpi section, U.P., *Geological Magazine.*

Tandon, S. K., Ginling, M. R., Sinha, R., Singh, V., Ghazanfari, P., Dasgupta, P., et al. (2006). Alluvial valleys of the Gangetic plains, India: Causes and timing of incision. In *Incised valleys in Time and Space* (Vol. 85, pp. 15–35), SEPM Special Publication.

Thussu, J. L. (2001). Origin of Quaternary basin of Sohna valley, southeastern Haryana. *Journal of the Geological Society of India, 58*, 457–464.

Umitsu, M. O. (1993). Late Quaternary sedimentary environments and landforms in Ganges delta. *Sedimentary Geology, 83*, 177–186.

Valdiya, K. S. (1976). Himalayan transverse faults and folds and their parallelism with subsurface structures of North Indian plains. *Tectonophysics*, *32*, 353–386.

Valdiya, K. S. (1998). *Dynamic Himalaya*. Hyderabad: Universities Press. 178 p.

Valdiya, K. S. (2001). Reactivation of terrane-defining boundary thrusts in central sector of the Himalaya: Implications. *Current Science, 81*, 1418–1431.

Valdiya, K. S. (2002). *Saraswati: The River that Disappeared* (p. 116). Hyderabad: Universities Press.

Chapter 23
Quaternary Cover and Tectonism: Peninsular India

The Quaternary stratigraphy and sedimentation in the Indo-Gangetic Plains has been dealt with comprehensively in Chap. 22. In this chapter are discussed the tectonic developments in the Indo-Gangetic Plains, the formation of sedimentary successions and neotectonic movements in the western continental margin and the central Indian rift valleys and in the coastal belts of the Peninsular India. The rest of the Indian Shield was an elevated landmass exposed to unrelenting activities of weathering and formation of lateritic soils. Changes of climate conditions, fluctuation of sea level and reactivation of older faults due to revival of crustal stresses played important roles in the making of the Quaternary cover of the Peninsular India. Some of the developments that took place in the Quaternary period were witnessed by primitive Stone-Age people who had by then found habitats in riverine tracts.

23.1 Drainage Disruption in Indo-Gangetic Plains

A notable feature of the Ganga Plain is the stream disruption, especially of the smaller tributaries of large rivers, resulting in the formation of swamps, ponds and lakes. Increasing aridity during the Middle to Late Holocene time is believed to have been responsible for reduced discharges in rivers of the Ganga Plain (Srivastava et al. 2003). However, ground subsidence offers more plausible explanation for this kind of drainage disruption. In north-eastern Uttar Pradesh and adjoining Bihar, the ground has been sinking at the rate of 0.2–0.3 mm/year as evident from progressive subsidence of the Survey of India benchmarks (Sinha and Jain 1998). The ground subsidence is responsible for impeded flow and the resultant waterlogging and development of swamps and lakes (Mohinder and Parkash 1994).

K.S. Valdiya, *The Making of India*, Society of Earth Scientists Series,
DOI 10.1007/978-3-319-25029-8_23

The Brahmaputra Plain in Assam is also subsiding as testified by a large number of wetlands (*bil*). In a stretch of 260 km between Kaziranga and Majuli, the areal extent of water bodies has expanded from 93.7 km^2 (with 529 lakes) in 1914 to 183 km^2 (with 780 lakes) in 1998 (Bezbaruah et al. 2003).

23.1.1 Shifting Courses

Many of the rivers of the Indo-Gangetic Plains have been shifting their courses laterally. The Yamuna, for example, has moved eastwards 10 km near Kiraoli to 40 km at Kaman (Bakliwal and Sharma 1980). Abandoned channels, cut-off meanders and levees bear testimony to the shifting courses. Numerous sites of prehistoric Ochre Coloured Pottery and Painted Greyware periods as well as remains of pre-Harappa settlements at Noh were located along the old courses abandoned by the Yamuna (Fig. 23.1). Like the Yamuna, the Ganga River has also migrated

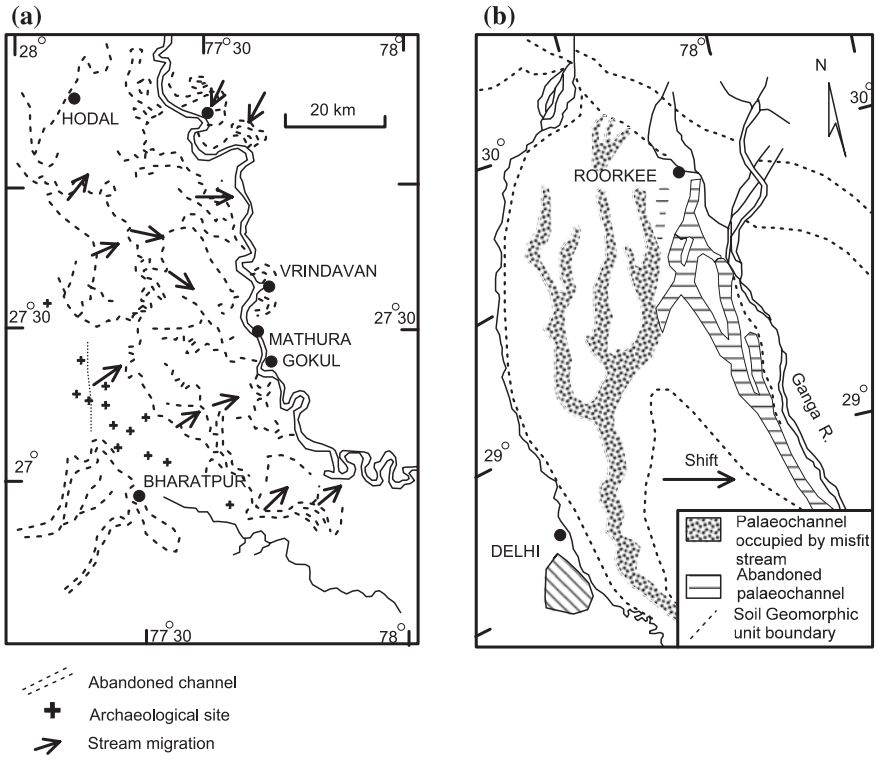

Fig. 23.1 **a** The Yamuna has been migrating eastwards as testified by abandoned channels, cut-off meanders and levees, and also existence of archaeological sites (after Bakliwal and Sharma 1980). **b** The Ganga likewise has been moving eastwards as evident from the abandoned channels (Parkash et al. 2000)

eastwards (Fig. 23.1), presumably due to the eastward tilting of the ground since 2500 yr B.P. (Parkash et al. 2000). Significantly, the adjoining Ramganga Block has tilted westwards. In the western part of the Ganga Basin the topography is degradational. For the soil mantles occur in interfluve areas and the channels are incised and the badlands are quite common, particularly in the south-western part of the Gangetic domain (Gibling et al. 2005). It could be the manifestation of neotectonic uplift.

The Gandak and Kosi rivers in Bihar (Fig. 23.2) migrated far more frequently—the Kosi moved 112 km between AD 1736 and 1964 and the Gandak moved 105 km over its own megafan from west to east in about a hundred years (1735–1975) (Mohinder and Parkash 1994). The abandoned channel of the Gandak, known as Budhi Gandaki, indicates that the River Gandak flowed past Kushinagar (now called Kasia) during the time when Gautam Buddha lived there about 550 B.C. Existence of many abandoned channels, now occupied by seasonal rivers like the Punpun, the Kao and the Banas of the Son River between Bhojpur and Fatwa in Bihar indicates that the Son has also been changing its course (Tomar and Tomar 1995). There is a view that in the interfluve area characterized by shallow aggradational channels which were subjected to extensive flooding, the channels have been migrating through avulsion and cut-off in response to continuing tectonic movements as well as sedimentological readjustment (Sinha and Friend 1994; Sinha et al. 2005).

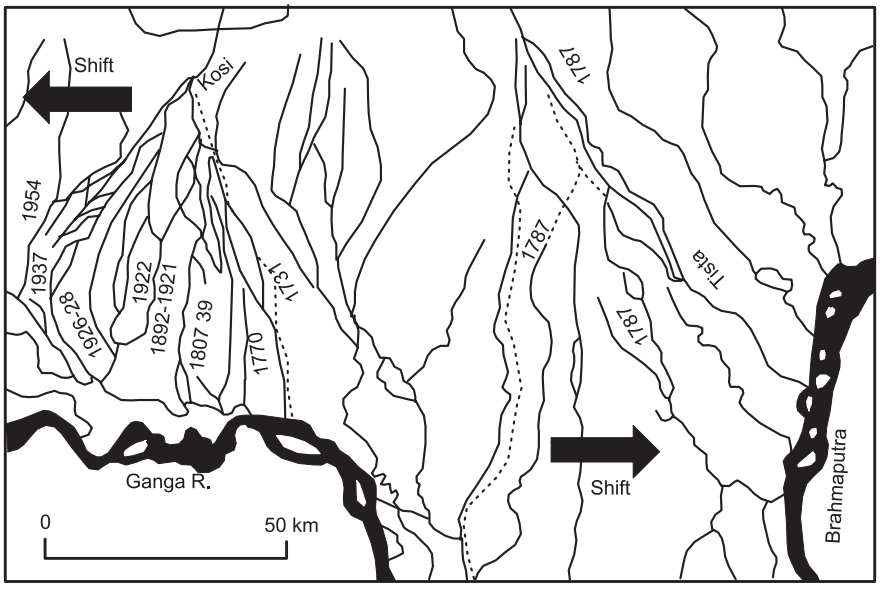

Fig. 23.2 The Kosi migrated 105 km in about a hundred years over its own megafan. The Tista changed its course in 1787 from its southerly flow to the south-eastern direction

The Tista suddenly deflected in 1787 AD from its original southerly course meeting the Ganga to a south-easterly course to join the Brahmaputra (Fig. 23.2). The migration of the Brahmaputra in Assam has been rather erratic. Historical records point to its flowing 20 km north of the present course about 200 years ago (Gilfellon et al. 2003).

The rivers in Bangladesh have also been shifting their courses, primarily due to uplift and sinking of the land. In the interval AD 1720 and 1830, the Brahmaputra abandoned its easterly course past Mymensingh and through the Meghna River to flow southwards to join the Ganga. The new course is called the Jamuna. The uplift by 20 m of the Madhupur tract along a series of six *en echelon* faults (Fig. 22.15) must have been the cause of this development. In some areas, streams migrated at the rate of 100 m/year (Barua 1997). Moving south-eastwards, the Jamuna (i.e. new channel of the Brahmaputra) is eroding its bank at the rate of 50 m/year, even as the Ganga is shifting north-eastwards (Barua 1997).

In the early part of the Sindhu Basin sedimentation, especially during the Tertiary period, the detritus came predominantly from the Indus–Tsangpo Suture Zone and from the terrane north of it. In the later part, rivers draining the Himalayan terranes (south of the I–TSZ) contributed sediments substantially. This change of sediment characters is attributed by some investigators to rerouting of the major rivers of Panjab into the Sindhu River, which until then flowed eastwards into the Ganga. However, there is no evidence of eastward flow of the tributaries of the Sindhu, except the Saraswati, which abandoned the Satluj sometime in 3500–4000 yr B.P. and joined the Ganga through a tributary of the Chambal (Valdiya 2002). The new course of the Saraswati is now known as the Yamuna, also called Jamuna.

23.1.2 River Piracy

A major river known as the Saraswati formed by the confluence of the Shatadru (≡Satluj) and the Tons–Yamuna (of the past) flowed through Haryana, southern Panjab, north-western Rajasthan and eastern Sindh and emptied itself in the Gulf of Kachchh (Fig. 23.3). This river was much revered by the Rigvedic scholars. It nurtured the Harappa Civilization until it disappeared in the Late Holocene time (Valdiya 2002; Pal et al. 1980). The disappearance of the Saraswati is a case of river piracy by branches of the Ganga and the Sindhu rivers.

Weaving together various threads of evidence adduced from archaeological, geomorphological and drainage-related studies, and gleaning relevant information from satellite imageries, it is surmised that the *Saraswati River* rose in the snowy realm of the Himadri in north-western Uttarakhand. It flowed south-west through one of the tributaries of the present-day Ghaghgar River of the foothills and met the south-east flowing Shatadru (Satluj) at Shatrana, about 15 km south of Patiala. At the confluence, the channel was 6–8 km wide, implying very high discharge of the Saraswati. The Ghaghgar is known as the Hakra in its middle reaches and as

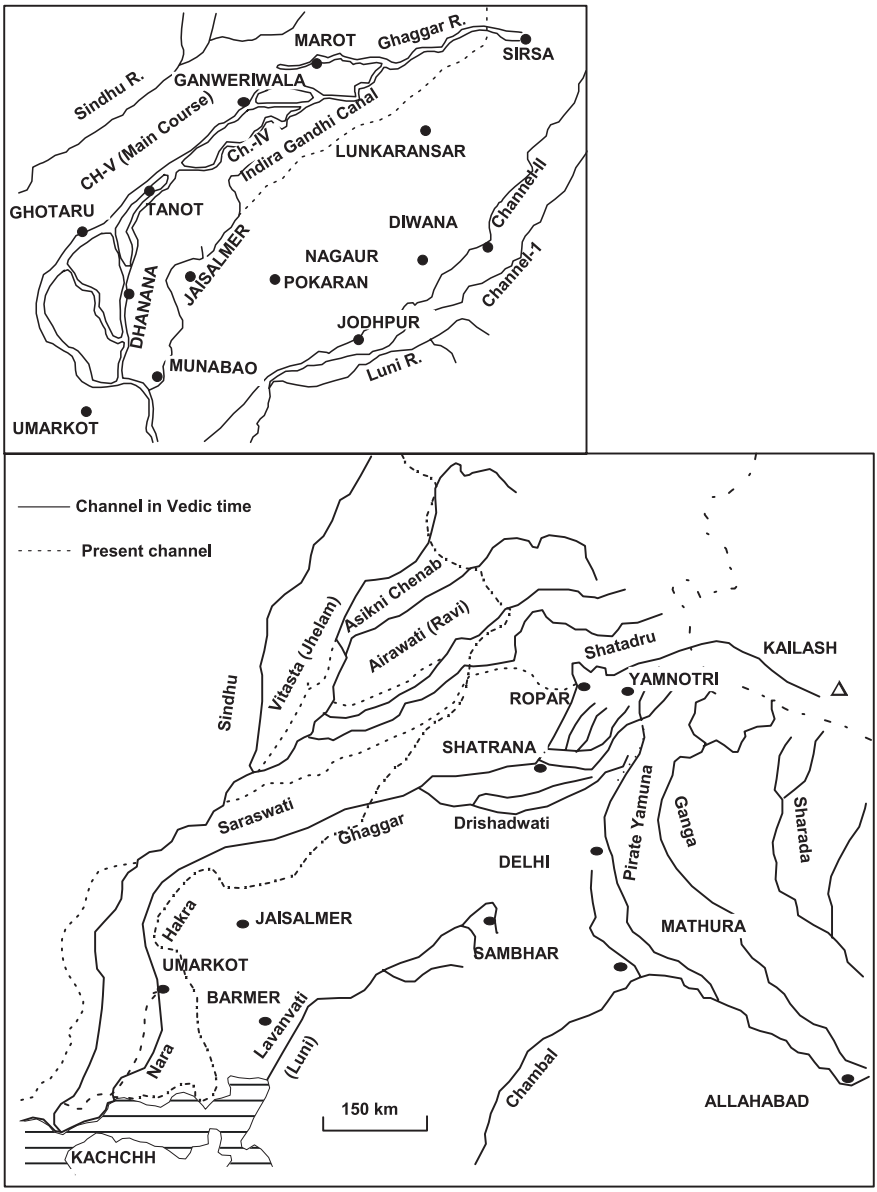

Fig. 23.3 Course of the legendary Saraswati River of the Harappan and Vedic times (Valdiya 1996, 2002). *Inset* in the *upper right* shows the Saraswati course delineated on the basis of latest techniques of remote sensing (Gupta et al. 2004)

the Nara in the lower reaches. Recent comprehensive works by Saini et al. (2009), Kshetrimayum and Bajpai (2011) and Sinha et al. (2012) in the Haryana reach of the Saraswati from the foothills of the Siwalik to the border of Pakistan show not

only the great thickness but also the great areal extent of the fluvial deposits of this mighty river. Vertical Resistivity Sounding applying Wenner configuration technique with maximum electrode spacing up to one kilometre together with study of IRS 1D L ISS-IV (scale 1:25,000) imagery by Kshetrimayum and Bajpai (2011) in the upper reaches of the Ghagghar system just south of the Siwalik front brought out a number of facts. The buried sand bodies are aquifer (water-bearing) horizons composed of coarse sand with gravel at the depth between 10 and 100 m, having an average thickness of 90 m and lateral extent of 12 km. Another aquifer horizon at the depth of 45–148 m connects the Markanda and the Sarsuti (corruption of Saraswati) rivers. The lower course of the Markanda is hydraulically connected with the palaeochannels of the Saraswati Nadi. The archaeological sites found in the study area belong to the *Late Harappan period*, suggesting that the buried sand bodies at different places have the same historical time in terms of age (Kshetrimayum and Bajpai 2011). It is obvious from the study that only a large perennial river could have filled the channel with so thick deposits of sands with gravels of the Sarsuti and the Markanda in the Late Harappan time (3900–3300 yr B.P.).

Saini et al. (2009) carried out extensive geological fieldwork, analysis of subsurface lithological data collected from exploratory boreholes dug by the Central Ground Water Board, together with the geophysical investigation and the OSL dating of sediments in the central reach of the Ghagghar within the state of Haryana done by the Geological Survey of India. This comprehensive work demonstrated that (i) more than 80 % of the thickness (varying between 10 and 30 m and in some places more than 50 m) of the channel fills is made up of alluvial deposits in spite of the fact that presently no large perennial river exists in the terrain, (ii) recognition of the major palaeochannel belt in the surface provides definite proof of the presence of a strong fluvial regime sometime in the past, (iii) the subsurface architecture of the palaeochannels and their floodplains in the Sirsa–Phaggu sector is approximately 10–25 km wide, the palaeochannel with 9- to 29-m-thick sediments being oblique to the present-day Ghagghar River. This fact points to the existence of multichannel, multilateral systems (Saini et al. 2009). The grey fine-grained micaceous sands occupy different depths that are *similar to modern-day sediments of mountain-fed rivers such as the Yamuna and the Ganga* (Saini et al. 2009).

The OSL dating shows that the older sediments are 26.0 $\pm$ 2 ka to 21 $\pm$ 2 ka old, and the younger fluvial activity was recognized in the limited part of the region between 5.9 $\pm$ 0.3 ka and 2.9 $\pm$ 0.2 ka (Saini et al. 2009)—between 6000 and 2900 yr B.P. The period of the Harappa Civilization is 5000–4600 yr B.P. (Early Harappa), 4600–3900 yr B.P. (Mature Harappa) and 3900–3300 yr B.P. (Late Harappa).

Very recent comprehensive geoelectrical study by Sinha et al. (2012) across very crucial reaches of palaeochannels—including the valley abandoned by the Satluj River when it swung west to join the Beas River of the Sindhu (Indus) System—has unravelled the large-scale geometry and architecture of the palaeochannel system adjacent to the Harappan sites and also proved the presence of a

thick and extensive band of sand body more than 12 km long and 30 m thick in the subsurface part of northern Haryana, Punjab and NW Rajasthan. They have demonstrated that the dimension of palaeochannel bodies *represents deposits of a large river system*. Significant is the finding that the channel abandoned by the Satluj River is filled with 40- to 50-m-thick sedimentary succession overlying a gravel bed (Sinha et al. 2012). The authors emphasize that "first-order relationship" between the postulated surface trace of a palaeochannel belt in satellite imagery and the subsurface sand body has been established beyond doubt "the dimension of the palaeochannel complex of a large *long-lived fluvial system.* Significantly, the groundwater recovered in the middle reaches from tube wells deeper than 160 m was found to be 22,000–6000 years old, whereas in the shallow well water, carbon has been dated at 5000–1800 years (Nair et al. 1999). The age of the water increased downstream from Kishangarh. Since the tritium value is negligible, these waters do not represent the rainwater fed through contemporary recharge by rainwater. The deeper—and older—water must be attributed to the ancient river that flowed in the time earlier than 5000 yr B.P.

Western Rajasthan was dotted with the settlements of the Stone-Age people. Parts of Rajasthan, Gujarat and Sindh were inhabited by the people of the Harappa culture (7000–3300 yr B.P.). More than 2000 settlements, including those of the Harappa culture (Fig. 23.4) and the *ashrams* of sages of the Vedic time, lay on the banks of the River Saraswati that discharged into the Gulf of Kachchh. This is the Saraswati River that the *Rigved* describes in glowing terms—"Breaking through the mountain barrier" this "swift-flowing tempestuous river surpasses in majesty and might all rivers of the land".

Tectonic movement, including the uplift of the NE–SW trending fault-delimited blocks of the Aravali Range, must have caused the deflection of the headwaters of the Yamuna and the Shatadru, leading to the disappearance of this mighty river (Valdiya 2002). The eastern branch deviated southwards around 3700 yr B.P., flowed through the channel of a tributary of the Chambal—what is now the Yamuna—and joined the Ganga at Triveni or Allahabad. The consequent dwindling of the river discharge propelled the migration of the Late Harappa (3900–3300 yr B.P.) people upstream from the Ganganagar–Bahawalpur areas to the upper reaches in the Siwalik. This is evident from a dramatic increase of the Late Harappa settlements in the Siwalik Belt in south-eastern Himachal Pradesh and the adjoining Haryana and Uttar Pradesh. As a matter of fact, this foothill region became populated for the first time.

Later, during the time of Gautam Buddha (who lived in the east about 2600 yr B.P.), the Shatadru River also betrayed the Saraswati. It abruptly swerved westwards to join the Beas of the Sindhu system. Deprived of the waters of these two major rivers, the Saraswati became a dry channel. The collapse of the Harappan civilization seems to be wholly due to the disappearance of the Saraswati and its associated rivers.

As tectonic activity continued to afflict the region, there were frequent disruptions, including changes in the river courses (Ramasamy 1999; Valdiya 2002). It

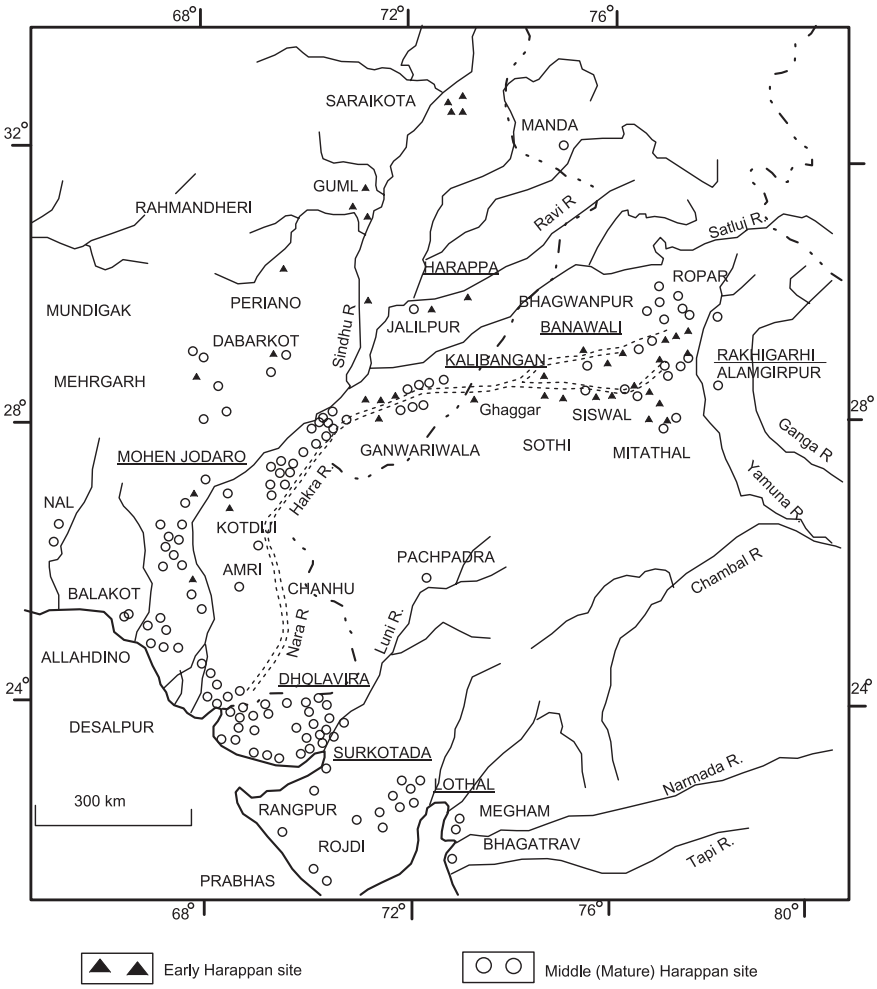

Fig. 23.4 Pre-Harappa, Early Harappa and Mature Harappa settlements in north-west India. There are concentrations of sites along the course of the Saraswati (from Valdiya 2002)

seems that some water of the Himalayan rivers continued to flow into the Hakra–Nara Channel until about 1245 AD. At that time, there was a great migration of the desert people out of the region. The Satluj finally ceased to contribute water in 1593 AD when it finally changed its course. It was not only the Satluj that was moving westwards. All rivers of the Sindhu system, including the Sindhu itself—have been shifting westwards. The Sindhu is known to have migrated 160 km westwards in the historical times.

23.2 Western Continental Margin

23.2.1 Tectonism

Tectonic resurgence of the Aravali Mobile Belt in the Late Tertiary and Quaternary times manifested itself in the uplift of the Aravali in the form of a horst mountain and in slow intermittent rise of the land to the north-west and west of the mountain domain (Ahmad 1986). The secular uplift affected the entire terrane stretching from Delhi to Saurashtra (Fig. 23.5). Reactivation of faults such as the 300-km-long Sardarshahar Fault, the 750-km-long Luni–Suki Fault and the 1000-km-long Jaisalmer–Barwani Fault (Bakliwal and Ramasamy 1987; Sinha-Roy et al. 1993) brought about change in the pattern of sedimentation in what was until then a part of the southern Himalayan Foreland Basin. There was reorganization of the drainage system, resulting in deviation, deflection and disruption, culminating in a few cases in the disappearance of rivers and the development of a desert. This tract of Indian land may be described as the *Thar Domain*, embracing western Rajasthan, adjoining Haryana northern Gujarat, Kachchh and Saurashtra (Figs. 23.5 and 23.6). In the old Sanskrit literature, this vast tract of arid land, where the monotony of sand is broken by isolated exposures of Precambrian, Mesozoic and Tertiary rocks, was described as *Marusthali* and is now known as *Marwar*. It was the NE–SW trending stepped graben-like depression with westward downthrown blocks that hosted Quaternary sediments in western Rajasthan and northern Gujarat (Kar 1988; Bakliwal and Wadhawan 2003). In the south-eastern part of the Aravali Mobile Belt, the neotectonic resurgence is manifested in 25–30 km shifting of the Banas watershed from its initial position along the Vindhya Hills, capturing of the Banas catchment by the Chambal (Sinha-Roy 2001).

23.2.2 Sedimentation

Quite a part of Haryana is covered with pile of Quaternary sediments (Thussu 1995). The sedimentary succession of the Thar Domain (embracing western Rajasthan and northern Gujarat) comprises two major components—(i) the lower fluvial and fluvio-lacustrine sediments, with local colluvial components in the Aravali foothill belt and (ii) the upper aeolian sediments representing reworked fluvial material (Fig. 23.6). During the larger part of the Pleistocene time, the Thar Domain witnessed widespread alluvial sedimentation, implying that the land was well-watered by mostly Himalayan-born rivers, even though the climate was predominantly semi-arid (Singhvi and Kar 1992; Dhir et al. 1994). In the basin north of the Jaisalmer–Barwani ridges (Fig. 23.5 inset), the thickness of the sedimentary succession varies from less than 5 m to more than 30 m, and in some places up to 90 m (Fig. 23.7). The sediments were deposited by a large river, which later degenerated into a misfit stream characterized by marshes and lakes

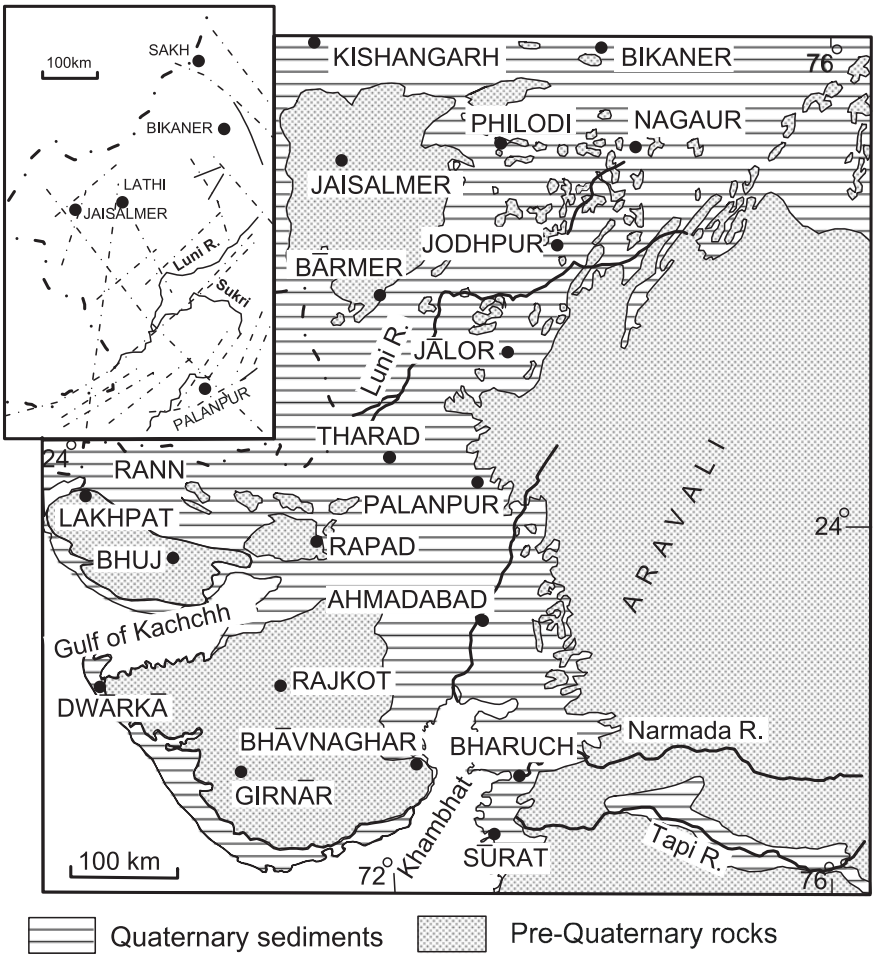

Fig. 23.5 Sketch map shows the Quaternary sedimentary cover on the western continental margin of the Peninsular India. (based on Geological Survey of India Map 1993). *Inset* shows faults and lineaments in western Rajasthan and adjoining areas (based on Bakliwal and Ramasamy 1987)

in its floodway. This phase ended with the sifting and dumping of finer sediments by dry winds, marking the onset of desertification. The large river that deposited sediments of the Late Pleistocene time followed a NNE–SSW trend—the channel of the present-day Ghaghgar, the Hakra and the Nara rivers—forming part of the *River Saraswati* of the Vedic time (Valdiya 2002). The ENE–WSW oriented faults controlled the accumulation of sediments in lakes developed in the fluvial regime (Raghav 1999). The earlier drainage was drastically changed by later landforms shaped by desert winds. At a number of places, fan-shaped or conical masses of

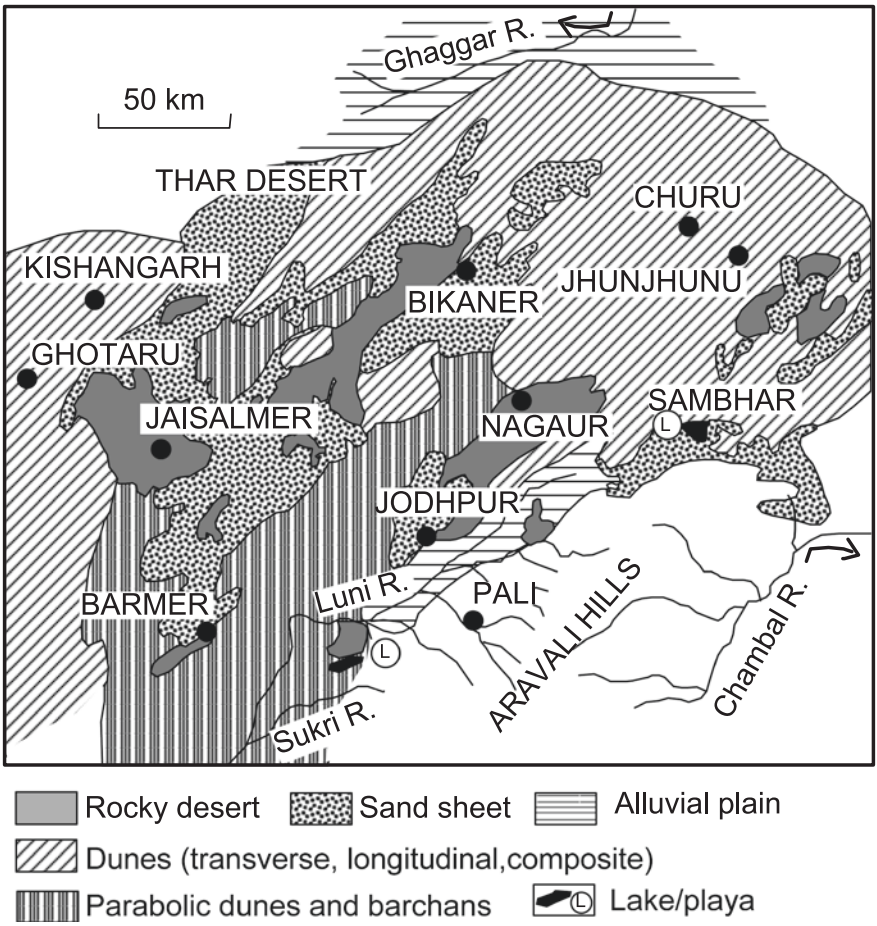

Fig. 23.6 Quaternary sedimentary cover and geomorphology of western Rajasthan (based on Bakliwal and Wadhawan 2003)

debris deposits caused stream blockage, resulting in the formation of lakes that eventually turned saline and formed playas (Singhvi and Kar 1992; Kar 1995; Raghav 1999).

Upstream of Sirsa, the sediment fill of the Ghaghgar channel contains Himalayan-derived sands characterized by rich suite of micas and deficiency in smectite clay (Courty 1995). Six stages of development are recorded by this riverine succession (Fig. 23.7): (i) accumulation of more than 10 m of sediments derived from a provenance in the Himalaya by a river which had heavy discharges prior to about 40,000 yr B.P.; (ii) decrease in discharge of this river, which had degenerated into a seasonal stream but prone to floods during rains; (iii) formation of nearly 2-m-thick extensive cover of wind-blown sands and silts in the

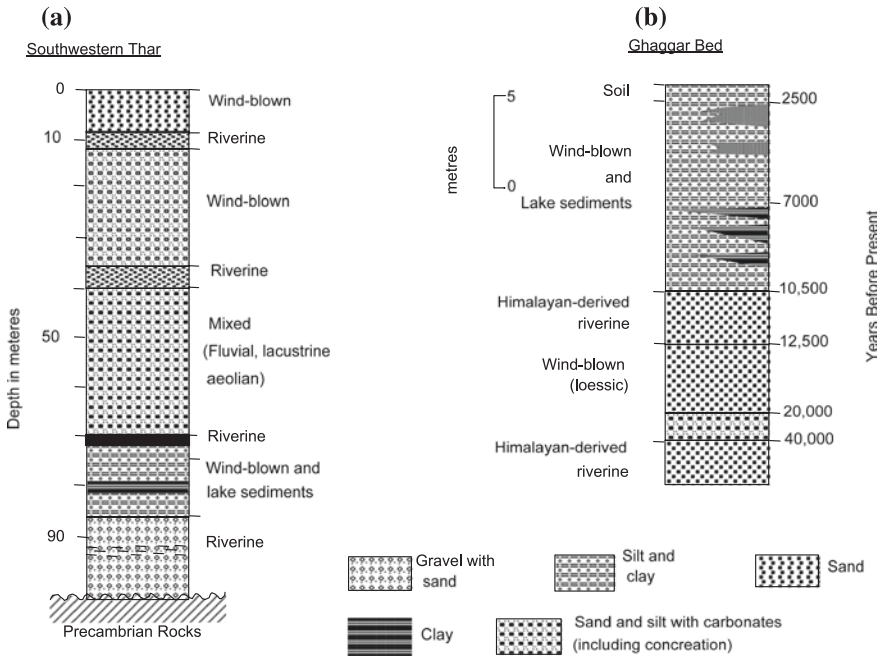

Fig. 23.7 Succession of sediments in the floodplain of the Ghaghgar River—the Himalayan-born *Saraswati* of the Vedic time—shows positions of Himalayan-derived sediments and lacustrine and paludal clays (based on Singhvi and Kar 1992; from Valdiya 2002)

period 20,000–12,000 yr B.P.; (iv) increase in the discharge of the Himalayan river, which laid down typically Himalayan sediments; (v) progressive reduction in fluvial sedimentation and simultaneous increase in wind activity resulting in the emplacement of loess deposits, the generation of concretionary carbonates and the formation of lakes and marshes in the period 7000–5000 yr B.P; and (vi) formation of localized sand sheets and dunes in the floodplain and reduction in river discharge, but seasonal flooding of channels in the interval 5000–2500 yr B.P. (Courty 1995).

In the Luni Basin, close to the Aravali Range, 300-m-thick succession occurs in a restricted reach upstream of an E–W fault provides testimony to the control of E–W, NE–SW and NW–SE faults in fashioning the drainage of the Luni River. The succession comprises (i) bedload gravels with sands and slackwater silts, characterized by products of floodplain pedogenesis, (ii) pebbly sand with gravel lenses emplaced by semistable episodic flows that had significant lateral spread during the early to middle Late Pleistocene, and (iii) pebbly coarse sands and overbank silts deposited during the Middle Holocene time when the climate had become wet again (Jain et al. 1999). The upper part of this succession betrays strong impact of aridity and wind action, culminating in the development of desert dunes. The aeolian sands are intercalated with sediments formed under wetter condition around 5000 yr B.P. The fluvio-lacustrine sediment succession in

the Khudal area provides a record of a period of more than 100,000 yr B.P.—the aeolian phase followed by a phase of channel reactivation in the period 70,000–30,000 yr B.P. and an interlude of climate instability during 13,000–8000 yr B.P. (Kar 1995; Kar et al. 2001).

Between the Luni and the Sabarmati rivers in northern Gujarat, the partly consolidated 300-m sediments of the Pleistocene to Holocene age are dominantly alluvial and partly aeolian in character. Burried channels, oxbow lakes and discontinuous abandoned channels indicate existence of two major river systems draining into the Rann of Kachchh—different from the present-day drainage pattern (Sridhar et al. 1994). In the Sabarmati Basin, the Late Quaternary succession comprises (i) conglomerates and sands forming NE–SW trending alluvial fans developed during semi-arid to arid conditions and (ii) heterolithic deposits of ephemeral streams reworked by wind (Tandon et al. 1997). Thermoluminescence dating shows that the age of the sediments range from ≥300,000 yr B.P. to nearly 5000 yr B.P. Pedogenesis occurred during the interval 58,000–39,000 yr B.P.

The variable thickness of the Quaternary sedimentary cover of the Gujarat plains (Fig. 23.8) suggests sedimentation in fault-bound subbasins within the

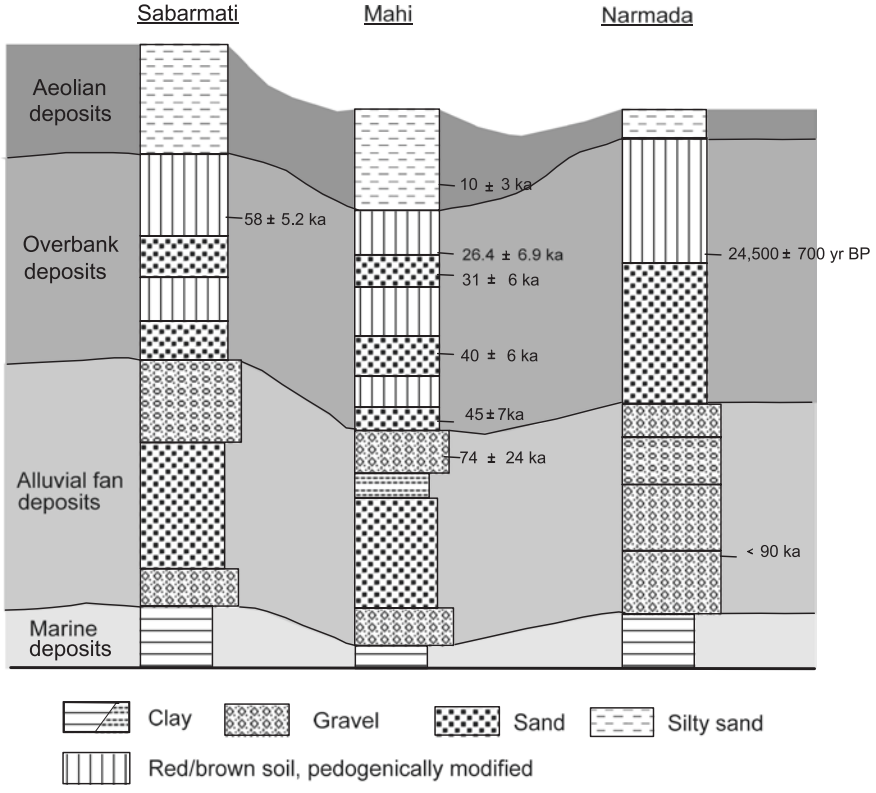

Fig. 23.8 *Columns* show the Quaternary lithology in the basins of three rivers of the western continental margin of India (after Chamyal et al. 2003)

larger Cambay Basin (Merh and Chamyal 1997; Maurya et al. 2000; Chamyal et al. 2003). The Mahi Basin represents the southern margin of the Thar Domain. It comprises sediments deposited in a downfaulted block within the Cambay Basin. As elsewhere, pedogenesis affected the Quaternary succession (Fig. 23.8) which comprises alternation of clays and gravels in the lower part and aeolian silts and dune sands in the upper part (Pant and Chamyal 1990). At the base is a sequence of marine sediments dating back to 125 ka and representing a marine transgression. The overlying alluvial sediments were emplaced by ephemeral rivers in a time of semi-aridity. There was intense pedogenesis in times of aridity during this period. The fluvial sediments are buried under the thick blanket of aeolian deposits which occur as poorly organized dunes of the time span 26,000–5000 yr B.P. (Juyal et al. 2003). It may be pointed out that while the aeolian accretion continued up to about 600 yr ago in the Thar Desert, it ended around 5000 yr B.P. in the Sabarmati Basin and about 10,000 yr B.P. in the Mahi Domain.

The post-aeolian period witnessed tectonic uplift and revival of the fluvial activity, which manifested itself in severe erosion of the Late Pleistocene sediments and formation of 40–50-m-deep incised meandering valleys and ravines—the badlands of the Mahi Valley (Chamyal et al. 2003).

23.2.3 Fluctuation of Climate Condition

The climate condition during the larger part of the Quaternary was dry, the aridity setting on with the beginning of Quaternary period. This is evident from profuse carbonate concretions and hardpan (Khadkikar et al. 2000). The $\delta^{13}C$ value in the calcretes varies from −0.3 to −1.5 ‰, and the $\delta^{18}C$ from −1.5 to −5.9 ‰, indicating their formation in the capillary zone near the surface (Achyuthan 2003). The TL dating of the dune sands suggests prevalence of hot dry condition since about 200,000 yr B.P. (Singhvi and Kar 1992; Dhir et al. 1994). The aeolian activity in the Thar Desert occurred in a cyclic fashion in the intervals 115–100, ~75, ~55, 30–25, ~16, 14–10, ~5–3.5, ~2, ~0.8 and ~0.6 ka during the times of strong south-western monsoon winds—that is during the transition from arid to wet phase or vice versa. In other words, the aeolian activity was not strong during the periods of high aridity such as the LGM. The rise and fall of groundwater in the piedmont deposits, interdune sands and sheet wash sediments was responsible for the formation of calcrete horizon at ~150, ~100, ~60 and 27–14 ka. Overlying a bed of gravel (representing an ephemeral stream), a 12-m-thick pile of dune sand contains calcrete in substantial measure. The analysis of calcrete of six litho units showed that rainfall increased at 60,000 B.P., and in the interval 10,000–20,000 yr B.P., as also borne out by the presence of C_4 vegetation implying wet climate (Dhir et al. 2010).

The Bap–Malar and Kanod playas with their, respectively, 7- and 2.5–3-m-thick sediments containing 15 ka-old pollens indicate that in the heart of the Thar, the 8–5.5 ka period was a time of appreciable rainfall when the

lakes were full of water and vegetation grew around the lakes (Deotare et al. 2004).

The long periods of dryness were broken by spells of high rainfall and humidity in the intervals 40,000–20,000, 18,000–13,000 and 10,000–4000 yr B.P. (Fig. 23.9) (Singhvi and Kar 1992). Those were the times when vegetation grew and proliferated and the land was occupied by hominids—the Stone-Age people. This is borne out by stone artefacts found in the sedimentary succession. During the Holocene interlude of wetness (Fig. 23.9), the rainfall was nearly 500 mm more than that of the present, as testified by pollens of *Pinus*, *Artemesia* and *Syzygium* that grew in and around the *Lunkaransar Lake* and the *Didwana Lake* (Singh et al. 1974; Bryson and Swain 1981). Radiocarbon dating of carbonaceous matter of the Lunkaransar Lake sediments indicate that the water rose abruptly at 6300 yr cal B.P. and the lake dried up by 4800 yr cal B.P. (Enzel et al. 1999). This means that the *Harappa Civilization* of the Sindhu–Saraswati basins began and flourished in the time about a thousand years after the desiccation of the land. The presence of cutigens in pollen rains and of charcoal fragments from the burning of stubbles implies that agriculture had begun around 9400 yr cal B.P. in the Lunkaransar Basin and at about 8000 yr cal B.P. in the Sambhar Lake area (Singh et al. 1974).

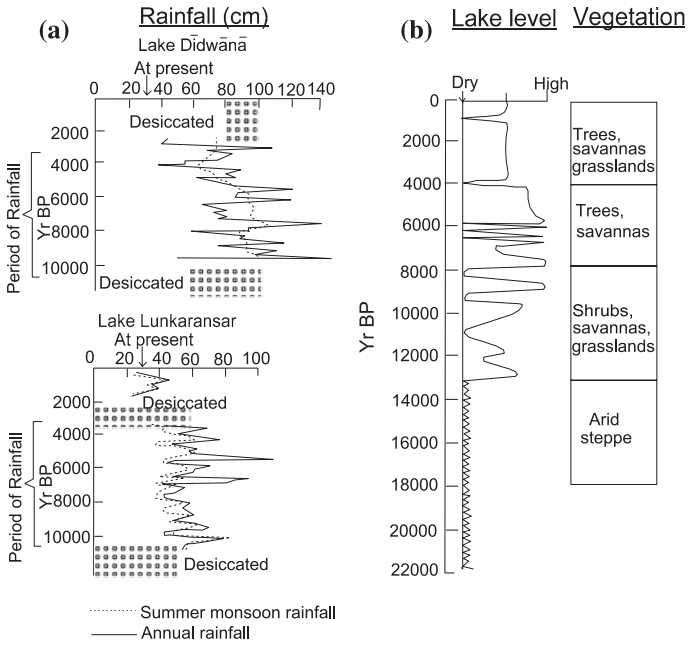

Fig. 23.9 In the period 8500–4000 yr B.P., the climate was very wet in Rajasthan. This is evident from high rainfall in the two lake areas and the growth of shrubs and trees in a savanna environment (**a** after Bryson and Swain 1981 and **b** after Wasson 1995)

Sedimentary architecture and textural attributes of the sediments of the Gujarat rivers bear testimony to fluctuation of climate—a period of reduced precipitation 120–100 ka, followed by a time 100–70 ka of heavy rainfall when bedded calcretes were formed, then an interval of weak monsoon 70–60 ka, followed by the return of the time of heavy rainfall 60–30 ka, and finally the onset of dry desertic condition at 30 ka (Juyal et al. 2000, 2003).

23.2.4 Lake Testimony

A dense network of drainage in the *Sambhar Lake* Basin indicates abundant water supply during the wetter phase of the climate in the Thar Domain. The 23-m-thick succession of lake sediments is characterized by alternation of clastics and evaporites, and a change in mineralogy at a depth of 5 m from the dominance of gypsum in the lower part to the absence of gypsum and the presence of thenardite, kieserite and polyhalite in the upper part (Sinha et al. 2004; Sinha and Raymahashay 2004).

The *Nal Sarovar* in the southern margin of the Thar Domain occupies a depression between the Rann of Kachchh and the Gulf of Khambhat (Fig. 23.10 *inset*). Fed by run-off from the monsoon rains, the Nal Sarovar records sedimentary history of the past 6600 years (Prasad et al. 1997). The silty clays and clayey silts of the lower part contain dominant smectite and illite clays derived from the weathering of the Deccan basalts, while the upper part of the lake sediments is characterized by illite and heavy minerals derived from the granite and metamorphic rocks of the Aravali Domain (Pandarinath et al. 1999). The mineralogy of the Nal Sarovar is not much different from that of the Sabarmati alluvial succession (Jain and Tandon 2003).

23.2.5 Drainage Deviation and Disruption

As a consequence of continuing tectonic activity, drainage changes took place in western Rajasthan and adjoining regions. This is borne out by rivers and streams abandoning their old courses and their piracy and degenerating into lakes and marshes in the sea of sands (Ghose et al. 1979; Pal et al. 1980; Kar and Ghose 1984; Ramasamy et al. 1991; Kar 1988; Kar et al. 2001; Sahai 1999; Valdiya 2002).

This topic has been dealt with in the beginning of the chapter. Suffice it would be to state that the Ghaghgar–Chautang system (the Saraswati–Drishadwati of the Vedic time) migrated north-westwards and westwards to occupy the present Ghaghgar–Hakra–Nara course (Fig. 23.3). Across the Jaisalmer–Barwani ridges, the Luni in the Barmer Basin shifted southwards. It may be pointed out that the

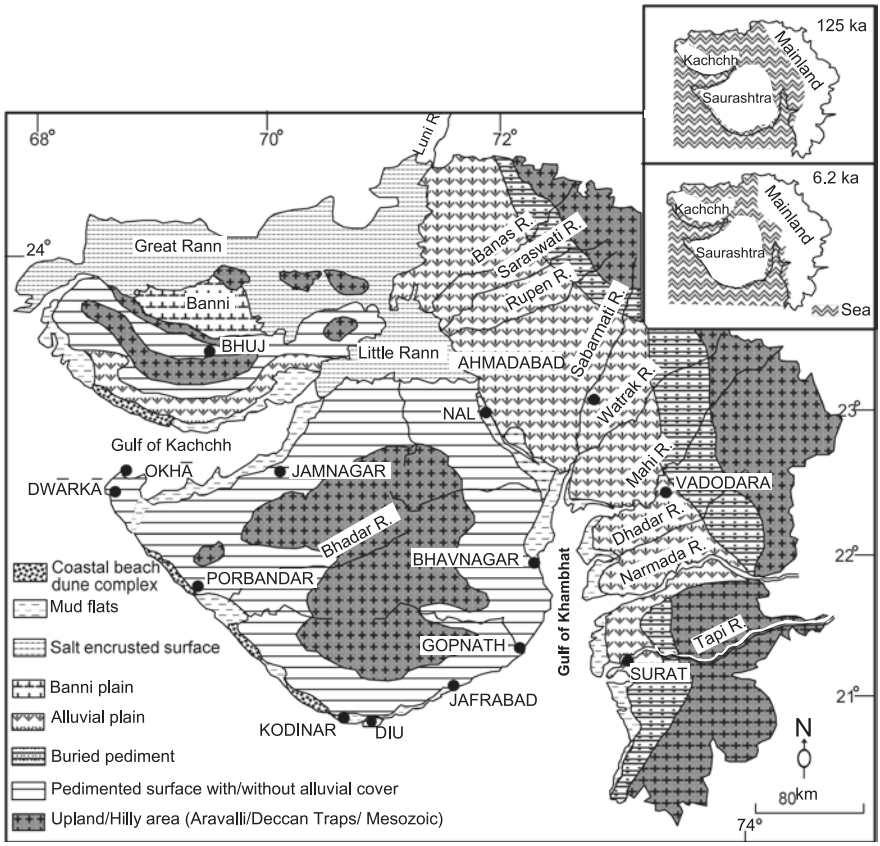

Fig. 23.10 Sketch map shows the distribution of the Quaternary sediments along the Gujarat coast. *Inset* shows the extent of marine transgression around 125,000 yr B.P. and during the 6000–2000 yr B.P. interval (after Chamyal et al. 2003)

Ghaghgar and the Luni remained independent of one another throughout the geological history of that land (Valdiya 2002). Recent studies (Gupta et al. 2004) corroborate the deduction that the Saraswati of the Vedic time flowed through the Ghaghgar course (Fig. 23.3 *inset*).

In northern Gujarat, the Sabarmati River earlier flowed through the channel of the Rupen River and discharged into the Great Rann of Kachchh. Subsequently, it changed its course southwards and emptied itself into the gulf of Khambhat (Sridhar et al. 1994; Ramasamy et al. 1991). In the southern part of the Mahi Basin, the Orsang River used to flow through the channel of the Dhadar River during the Late Pleistocene, but tectonic uplift deflected it southwards to join the Narmada River (Raj 2004).

23.3 Gujarat Coastal Belt

23.3.1 Marine Transgression

A very large part of the Gujarat Plain comprises Quaternary sediments of great thickness (Merh and Chamyal 1997). Embracing Kachchh and Saurashtra, the Gujarat coastal belt continued to remain under the sway of sea during the Quaternary time (Fig. 23.10). In the Okhamandal of the Saurashtra peninsula, the *Chaya Formation* of the Middle to Late Pleistocene age unconformably overlies the Middle Miocene Dwarka Formation. It consists of 10–12-m-thick succession of bioclastic limestones, including cross-bedded pelloidal limestone, succeeded by 4-m-thick reefal carbonate of the Late Pleistocene to Holocene age (Bhatt and Patel 1998; Bhatt 2000). The reefal limestone is characterized by Scleractina and Hexacoralline corals that at present build barrier reefs. Resting on the Deccan basalts with a basal horizon of palaeosol, the reefal limestones are exposed in cliffs of riverbanks in southern Saurashtra. This implies that there was marine transgression up to the elevation of 10–15 m in the Late Pleistocene time.

23.3.2 WindSwept Coast

Forming ridges with cliff faces as high as 4.0 m, parallel to the coast, the *Miliolite Limestone* of the Middle Pleistocene age is a prominent lithostratigraphic horizon in the Saurashtra coast (Bruckner et al. 1987; Chakrabarti et al. 1993; Merh 1993, 2005). It is a pelsparite biointrasparite to pelmicrite Limestone made up of broken shells of miliolid and rotalid foraminifers. Inland it occurs as parabolic or obstacle dunes characterized by large-scale trough cross-bedding or as sheets of aeolinite, bearing the stamp of strong wind action (Patel and Bhatt 1995). In Kachchh, the Miliolite Limestone occurs as thin horizontal sheets occupying topographical depressions or as obstacle dunes resting against slopes of high hills (Desai et al. 1982).

23.3.3 Neotectonic Development

The southern coastal belt of Kachchh is segmented—cut by NNE–SSW-trending tear faults. The faulting has resulted in drowning of the western sector, emergence of the eastern part and formation of straight and split cuspate foreland in the central sector (Kar 1993). Along the foot of the Northern Hill Range (Fig. 23.11), immediately north of the *Kachchh Mainland Fault*, there are transverse colluvial

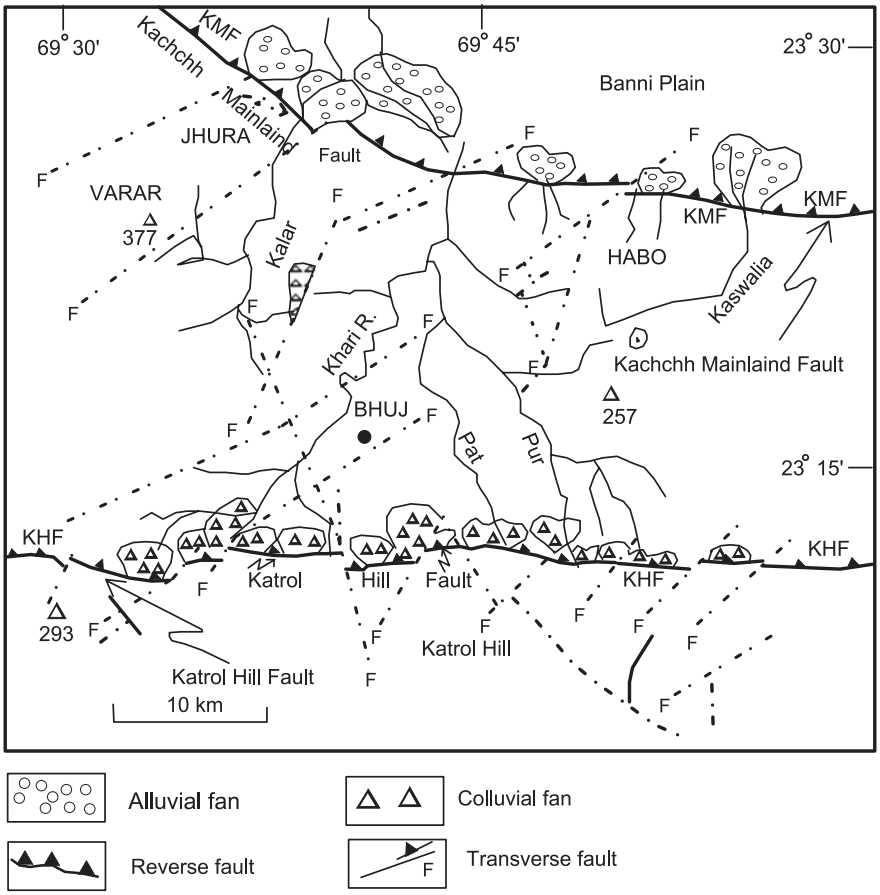

Fig. 23.11 Sketch map of Kachchh showing colluvial fans formed of deposits of debris flows generated due to reactivation of the E–W-trending faults cut transversely by tear faults (based on Thakkar et al. 1999; Malik et al. 2001)

fans of debris-flow deposits resulting from reactivation of and uplift along the Kachchh Mainland Fault (Malik et al. 2001). The fans extend northwards over the Banni plain and onto the Rann flat. The E–W faults are displaced by NNW–SSE- and NNE–SSW-oriented tear faults. Very youthful streams have cut deep incisions into these fans (Thakkar et al. 2006). Characterized by large potholes and fluting features in its bed, the Khari River has cut during the Early Holocene, a deep gorge along rather straight NE–SW direction, testifying to ongoing movements on the Katrol Hill Fault.

23.3.4 The Rann

The salt-encrusted mudflats that remain under marine water during the period of the rainy season are known as the *Rann*, meaning a playa of sorts. It was a part of the sea until about the time of the Harappa Civilization when the River Saraswati of Himalayan origin and the Aravali-born Sabarmati River emptied themselves into it. Archaeological evidence corroborates oceanographic inferences (Hashimi et al. 1995) that 6000 yr B.P. the sea level was approximately 6 m higher than at present (Gaur and Vora 1999). Preserving the records of the Late Pleistocene and Holocene sea-level fluctuation, the Rann sedimentary succession was repeatedly shaken by earthquakes as borne out by seismites at different stratigraphic levels. The lithostratigraphical succession of the Rann (Merh 1993, 2005) is as follows:

Late Holocene	- Brown silty clay with organic matter ($\leq$2 m) - Sand and silt with salt encrustation and gypsum nodules making Banni Plain and islands (*Bets*) (2.5–10 m)
Middle Holocene	Blue-green clay with foraminifers (1–9 m)
Early Holocene to Late Pleistocene	Coarse sand intercalated with silt and clay and characterized by nodules of carbonates and gypsum (45–50 m)

Underwater archaeological finds of various stone implements together with pieces of hearth, charcoal, animal bones and teeth, embedded in fluvial sand and silt at the depth of 5–30 m in the Gulf of Khambhat 20 km west of Hazira, indicate that Man had appeared on the scene about 9500 yr cal B.P. (Kathiroli et al. 2002).

23.4 Narmada–Tapi Valleys, Central India

23.4.1 Tectonic Setting

The Satpura Range, a horst mountain, is flanked by the *Narmada Graben* in the north and the *Tapi Graben* in the south (Fig. 23.12a). Seismic refraction and wide-angle reflection data across the Son–Narmada "Lineament" clearly bring out its graben character underneath the Deccan lavas in the west (Kaila et al. 1987). These demonstrate the presence of a horst-like feature between the North Narmada Fault and South Narmada Fault in the eastern part (Tewari et al. 2001). This horst-like feature is associated with a mid-crustal and Moho upwarp, implying its formation as a result of deep-seated tectonics in the Precambrian time. The grabens exhibit high heat flow—it is 290 $\pm$ 50 mW per square metre in the Tattapani–Jhor area in the Narmada rift and 97–135 mW/m^2 at Salbardi in the Tapi Valley (Shanker 1991). The grabens continue to subside along their delimiting faults. At Salbardi, the vertical throw is of the order of about 1000 m, of which nearly 425 m was during the Quaternary period. A multitude of transverse tear faults offset the Tapi–Narmada grabens (Fig. 23.12). Recent activity on the faults

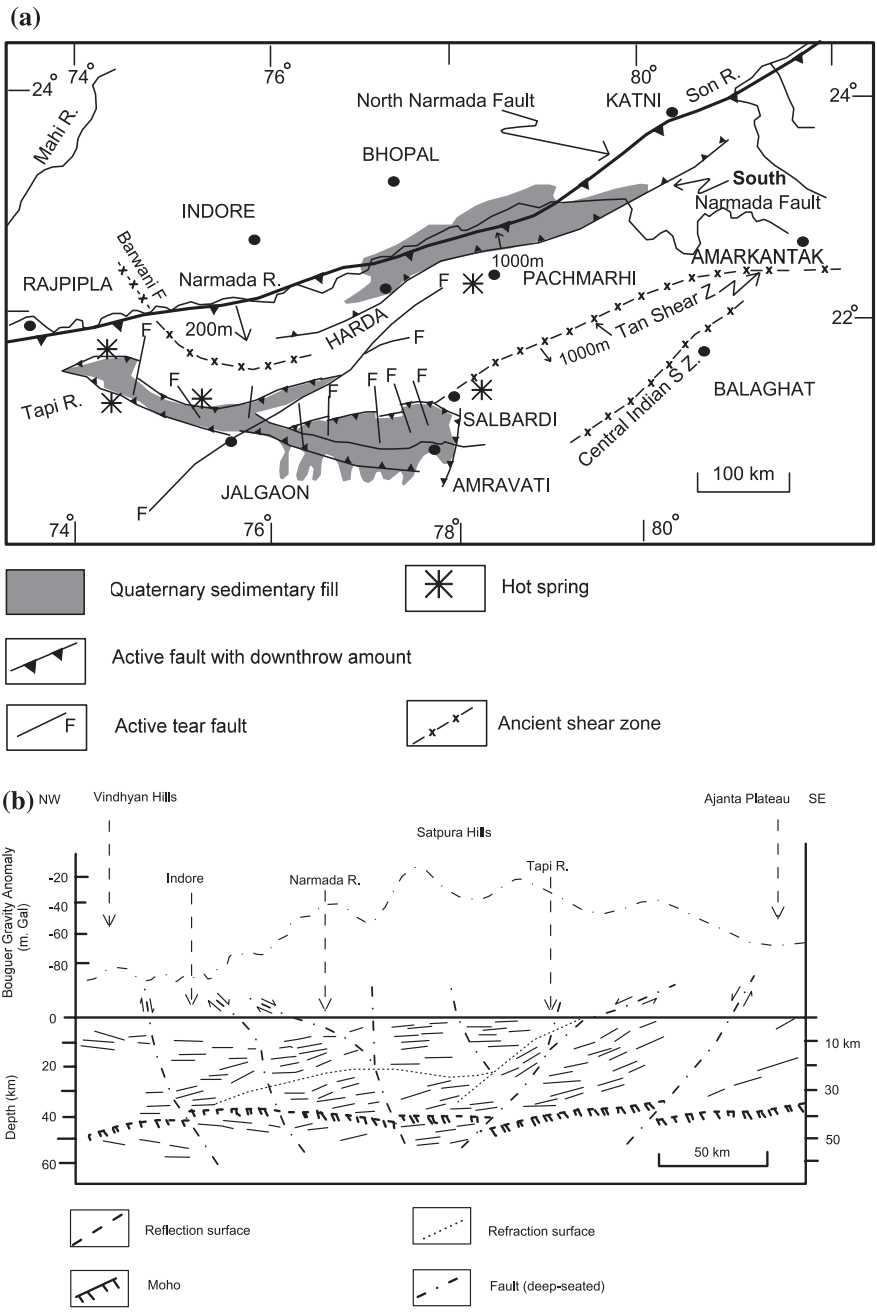

Fig. 23.12 **a** The Satpura horst mountain is flanked by active grabens—the Narmada Graben in the north and the Tapi Rift in the south (after Krishnaswamy and Raghunandan 2005).**b** Deep seismic sounding across the Satpura Range and the Narmada Valley shows existence of deep-seated faults that have offset the Moho (after Tewari et al. 2001)

defining the graben is evident from abrupt eastward swerving for short reaches of northerly flowing tributaries of the Narmada along the foot of the alluvial scarp parallel to the graben fault. The various fault blocks and their alluvial cones are consequently sunk, and tilted as much as 30º. And there is an abrupt change in the depth of the basement–sediment contact from a couple of metres below the ground surface to over 200 m below the mean sea level.

Epeirogenic rise of the Satpura Range and the adjacent area during the Upper Pleistocene was followed by Holocene uplift of the order of 1000 m of the horst block along faults (Krishnaswamy and Raghunandan 2005). The Narmada–Tapi domain is thus a belt of tectonic resurgence where streams show derangement and have dissected deep channels, and their longitudinal profiles are marked by abrupt changes. In the lower reaches of the Narmada, there was slow subsidence of the basin during the Late Pleistocene time, followed by inversion of the movement in the Holocene (Chamyal et al. 2002). The rift zone of the Narmada near the Dardi Fall registers intense bedrock erosion, resulting in the formation of a gorge, dated 40,000 years as terrestrial cosmogenic radionuclide dating indicates (Gupta et al. 2007). Obviously, the increase in the intensity of erosion is a consequence of rapid uplift of this part of the Narmada rift zone.

23.4.2 Sedimentation

In the Tilakwara area in its lower reaches, the Narmada crosses an active ENE–WSW- and N–S-oriented faults and suddenly becomes an unconfined river, building 23-km-long fan made up dominantly of debris-flow deposits during the Late Pleistocene (Chamyal et al. 1997, 2002). The Narmada fan has been correlated with the *Older Alluvium* of Gujarat. Near Rajpipla, a number of Early Holocene alluvial fans of gravel deposits and sand sheet form an uplifted terrace (Bhandari et al. 2001, 2005). The 30- to-50-m-high cliffs of the deep ravines which cut the terrace bear eloquent testimony to recent uplift along the fault bounding the Narmada Graben.

In the middle reaches of the Narmada (Fig. 23.13), the Late Pleistocene to Early Holocene deposits form three terraces (Ganjoo 1995; Tiwari and Bhai 1997a, b). Resting unconformably on the basement, the lower unit of the valley fill consists of red clay with lenses of boulders. The horizon is characterized by the presence of a variety of mammals—*Hexaprotodon namadicus, Equus namadicus, Bos namadicus, Elephas, Stegodon*, *Babulus* and *Sus* (Biswas 1989, 1997; Badam 1979; Badam et al. 1986). Significantly, the vertebrate animals occur along with Palaeolithic stone artefacts. Made up of sandy–pebbly gravels, the middle terrace containing the remains of vertebrate animals together with stone artefacts is assigned a Late Pleistocene age. The youngest terrace (Fig. 23.13) comprising yellow and brown silts characterized by calcretes belongs to the Late Pleistocene to Holocene time (Ganjoo 1995). The upper 70–90 m sequence of sediments of the Narmada Valley was emplaced in a single aggradational episode with minor

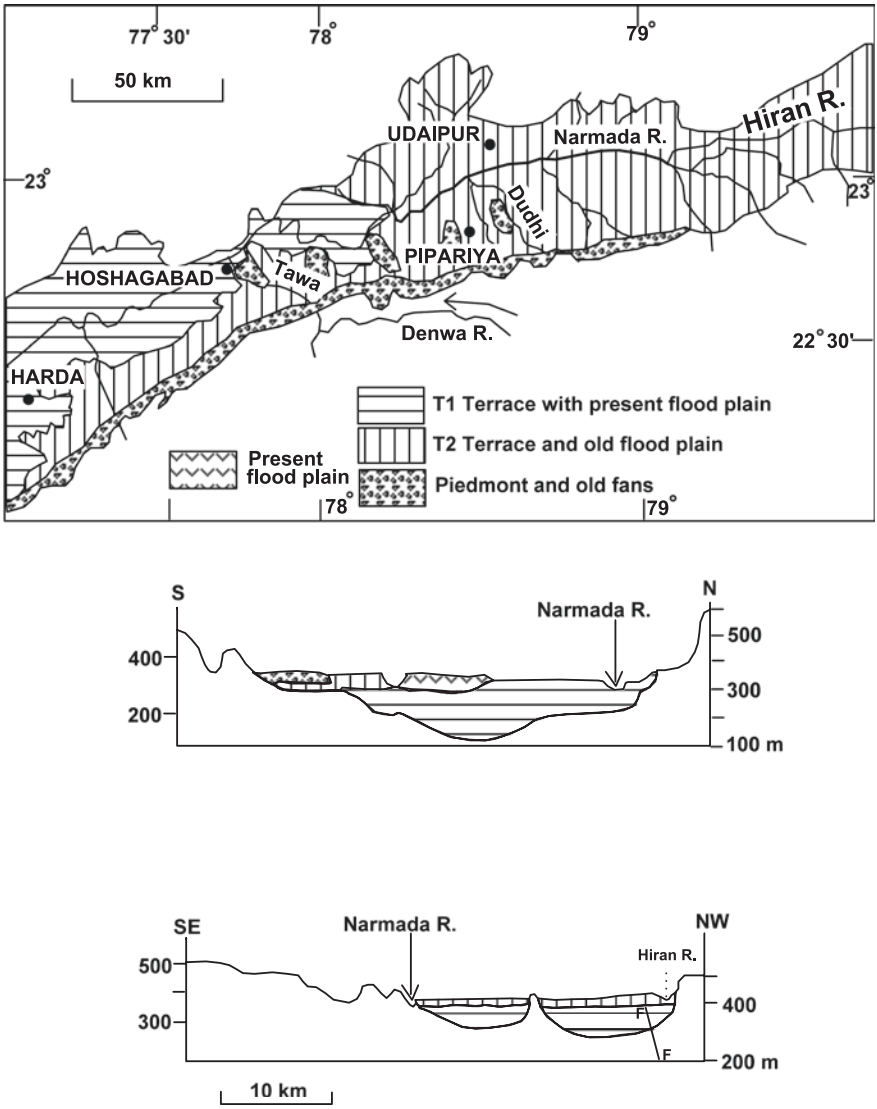

Fig. 23.13 Map shows fluvial terraces in the Narmada Valley in its central reach. Cross sections show the relationship of various terraces with the basement (after Tiwari and Bhai 1997a)

pauses. The dissection of the deposit produced two older terraces, each 15–16 m in height (Khan and Sonakia 1992).

Magnetic polarity study of the Narmada Valley sediments containing, among others, Toba volcanic ash and artefacts of the Acheulian age at Bori, Morgaon, Gandhidham, Andera and Nevasi in central and western parts shows that the

deposition of the sediments took place within the Brunhes Chron, beginning more than >0.78 Ma (Sangode et al. 2007).

23.4.3 Episode of Volcanism

In the Madhumati tributary of the Narmada and also in the middle of the Narmada succession at Baneta, a layer of tuff is intercalated with red-grey-mottled silt and sand belonging to the middle Brunhes magnetostratigraphic level of the Upper Pleistocene (Tiwari and Bhai 1997b). The tuff bed is attributed to the rain of volcanic ash (Basu et al. 1987) from the Toba Volcano in Indonesia which erupted 75,000 years ago (Westgate et al. 1998).

Interestingly, not far away at Lonar in the Buldhana district of Maharashtra is a circular depression, 2000 m across and 135 m deep. It is now represented by a saline Lake with a raised (up to 15 m) rim formed of outwardly dipping basalt layers (Venkatesh 1967). The presence of high-pressure deformation features in plagioclase, of shatter cones in the 300–400-m-thick powdery basaltic material showing no stratigraphic consistency, and the occurrence at a depth of 350 m of spherules under the breccia Zone has been interpreted as indicating the *Lonar Crater* originated as a result of either impact of a meteorite or due to cryptovolcanism—steam explosion diatreme action—and caldera subsidence (Subrahmanyam 1985) about 35,000 years ago during the Pleistocene time.

23.4.4 Hominid Presence

On the right bank of the Narmada at Hathnora (Fig. 23.14) where a rich assemblage of mammalian fauna is present, the basal red clays with gravel lenses yielded partial skull (calvaria) of a hominid, younger in age than the Indonesian and Chinese *Homo erectus* (Sonakia 1984). A right part of the skull cap (calvarium) and a complete right collar bone, partial left clavicle and ninth left rib found in the same locality show that it was a female pygmy belonging to a robust, short and stocky archaic *Homo erectus* who made the Acheulian tools found in the Narmada Valley (Sankhyan 2005).

The central Indian Hathnora *Homo erectus namadicus* comes after the apeman *Ramapithecus* (=*Sivapithecus*) *sivalensis* of the Siwalik Domain in northern India.

About 3 km upstream of Hathnora at Netankhari, bones representing femur and humerus of hominin identified as archaic *Homo erectus* and archaic *Homo sapiens* have been found (Sankhyan et al. 2012). In this place also, the human bones are associated with Acheulian-age artefacts of the temporal span 20,000–25,000 years, that is Middle and Upper Pleistocene.

Blessed with ample resources of water, wild plants and mammalian animal foods, and availability of a variety of raw materials for making stools and

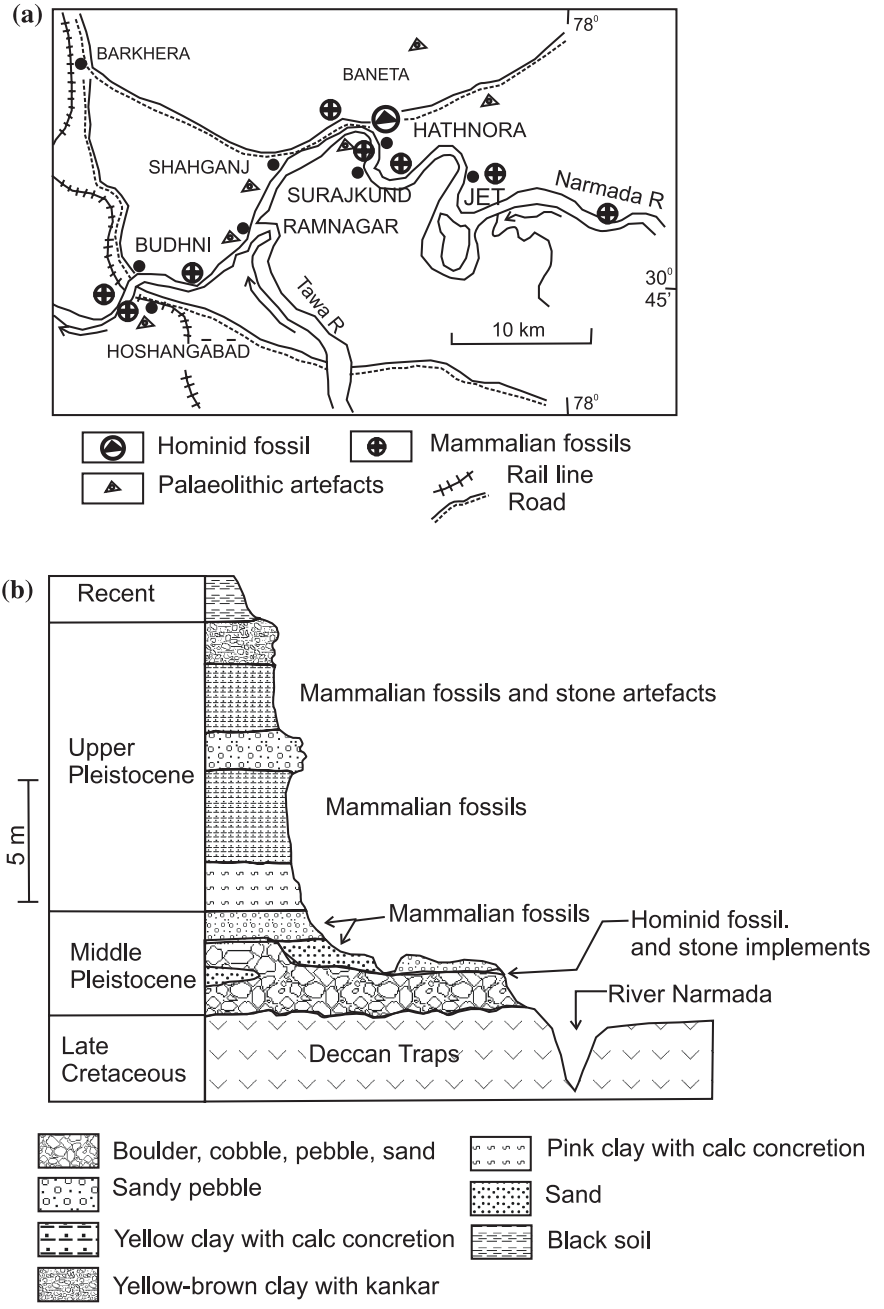

Fig. 23.14 **a** Position of the locality Hathnora where body parts of a hominid were found along with the Acheulian stone tools remains of contemporary mammalian fauna (Sonakia 1984). **b** Lithological column showing the horizon in which the remains of *Homo erectus namadicus* was found (after Khan and Sonakia 1992)

thousands of rock shelters, the central Indian region provided an ideal environment for hunting–gathering people of the Stone Age and after. As already stated, the mammalian animals lived in the valleys of Narmada, Son and Belan, where congenial conditions of climate prevailed. Understandably, these valleys were intensively inhabited by human groups since earliest time. About 4500 years ago, agriculture was introduced in the region (Misra 1997) and the hunter-gatherers gradually adopted a settled way of life.

Some of the human groups did not completely give up hunting and gathering. These groups are today represented by the forest-dwelling tribals of the land, such as the Bhils, Gonds, Baigas, Korwas, Santhals and Mundas.

23.5 Konkan–Kanara Coastal Belt

23.5.1 Structure and Geomorphology

Mumbai is situated on a downthrown block west of the N–S- to NNW–SSE-trending *Mahim Fault*, and Thane is located close to it on the eastern upthrown block (Srinivasan 2002). The Mahim Fault is one of the many N–S-trending step faults in the Raigarh–Thane region of Maharashtra (Fig. 25.18). The fault-related throw increases progressively southwards where it is expressed in the high escarpment of the Western Ghat. The belt of the *Konkan–Kanara–Malabar Coast* is affected by very prominent NNW–SSE lineaments or faults which are locally displaced by ESE–WNW- to E–W-oriented shear zones (Nair 1990; Sukhtankar 1995; Kundu and Matan 2000; Valdiya 2001a; Valdiya and Narayana 2007). Less prominent are the NW–SE, N–S, NNE–SSW and ENE–WSW lineaments. In the northern (Mumbai) part, a multiplicity of faults dipping eastwards and fault blocks tilting westwards has given rise to the *Panvel Flexure* (Auden 1949; Dessai and Bertrand 1995). Buried forests off the dockyards of Mumbai at the depth of 6–12 m indicate sinking of the fault blocks (Sukhtankar 1995). The occurrence at the elevation of 100 m above the mean sea level in the Velas–Bankot belts of beds of more than 40,000 years old lignites formed from the organic matters of coastal marsh and containing nearshore foraminifers implies that the landward fault blocks have risen up in the Late Quaternary time (Powar 1993; Rajashekhar and Kumaran 1998). In one locality, low-level laterite with bauxite is drowned in the Arabian Sea (Bhoskar et al. 2001).

Rising high in the Sahyadri Range, the Konkan–Kanara rivers flow westwards across the 50–60 km wide coastal belt through a series of deeply incised and meandering channels. There is a series of steep-sided spurs 300–600 m in elevation that extend WNW towards the shore from the main Western Ghat (Widdowson and Cox 1996; Valdiya 2001a). One of the peculiarities of the Konkan drainage is that whereas the main rivers are graded and are without floodplains or even broad valleys and deltas, the tributary streams are ungraded and flowing through a landscape in a youthful stage (Dikshit 1976). Incised meanders

and development of terraces in the Konkan coastal lowland indicate discrete uplift events (Widdowson and Cox 1996). In the Kanara coastal belt, the rivers show anomalous behaviour—they deflect abruptly, there is hairpin geometry of drainage, and they have cut deep channels across raised NNW–SSE- to WNW–ESE-oriented ridges in the coastal belt and exhibit ponding or blockage represented by palaeolakes of the past and stagnant bodies of water in the present upstream of their crossing the faults (Fig. 23.15). These features provide compelling evidence of continuing reactivation of the faults (Valdiya 2001a).

Significantly, there are no basins with Quaternary sediments anywhere in the Konkan, Kanara and northern Kerala coastal belts. This suggests that this stretch of the west coast belt of the Peninsular India has been differentially rising up continually or intermittently all through the Quaternary period.

23.5.2 Evolution of Western Ghat

East of the undulating terrain of the coastal belt characterized by low ridges and shallow depressions trending NNW–SSE to WNW–ESE, the land rises to great height of the Sahyadri mountain range. The change in elevation from 40–120 to 700–1800 m is quite abrupt, and the contrast of topographic relief is pronounced. However, the lithological composition including laterite capping and structural design is much the same—the NNW–SSE-trending *en echelon* faults cut the Sahyadri into elongate linear blocks in the manner of horsts, and the WNW–ESE shear zones break these horsts into blocks. The Western Ghat escarpment in Karnataka is characterized by an *en echelon* pattern of slope breaks (Fig. 23.15 *inset*), step-like small terraces and smaller scarps (Valdiya 2001a). The seaward face of the Sahyadri is more than 700-m-high escarpment. The escarpment is known as the *Western Ghat (Paschimi Ghat)*. Meandering rivers and streams flowing in their wide valleys with gentle slopes and low gradient in the mountainous Sahyadri Domain progressively deepen their channel downstream and cut gorges before dropping as cascades, rapids or waterfalls across the multiple escarpment representing different fault blocks. It seems that the fault-defined blocks of the central Sahyadri in Karnataka rose more than 700 to nearly 1800 m elevation, while the coastal belt could not rise beyond 40–120 m (Valdiya 2001a). (Recent geophysical investigations over the entire length of the West Coast strongly corroborate this postulation (Singh et al. 2007). Following oblique-slip displacement along the NNW–SSE-trending faults, the linear blocks when pushed northwards broke along the ESE–WNW- to E–W-oriented southwardly inclined reverse faults or shear zones (Fig. 23.15 *inset*). The north-western edges of the broken blocks eventually became steep slope breaks, and the fault-delimited west-facing sides formed the scarps. Significantly, the elevation of the fault blocks diminishes progressively northwards—from 2695 m Elaimalai in Kerala to 2620 m Nilgiri in Tamil Nadu, to 1820 m Kudremukh, and to 810 m Sira–Talaguppa in Karnataka. It seems that the dip-slip movements on the ESE–WNW-oriented faults progressively decreased from south to north.

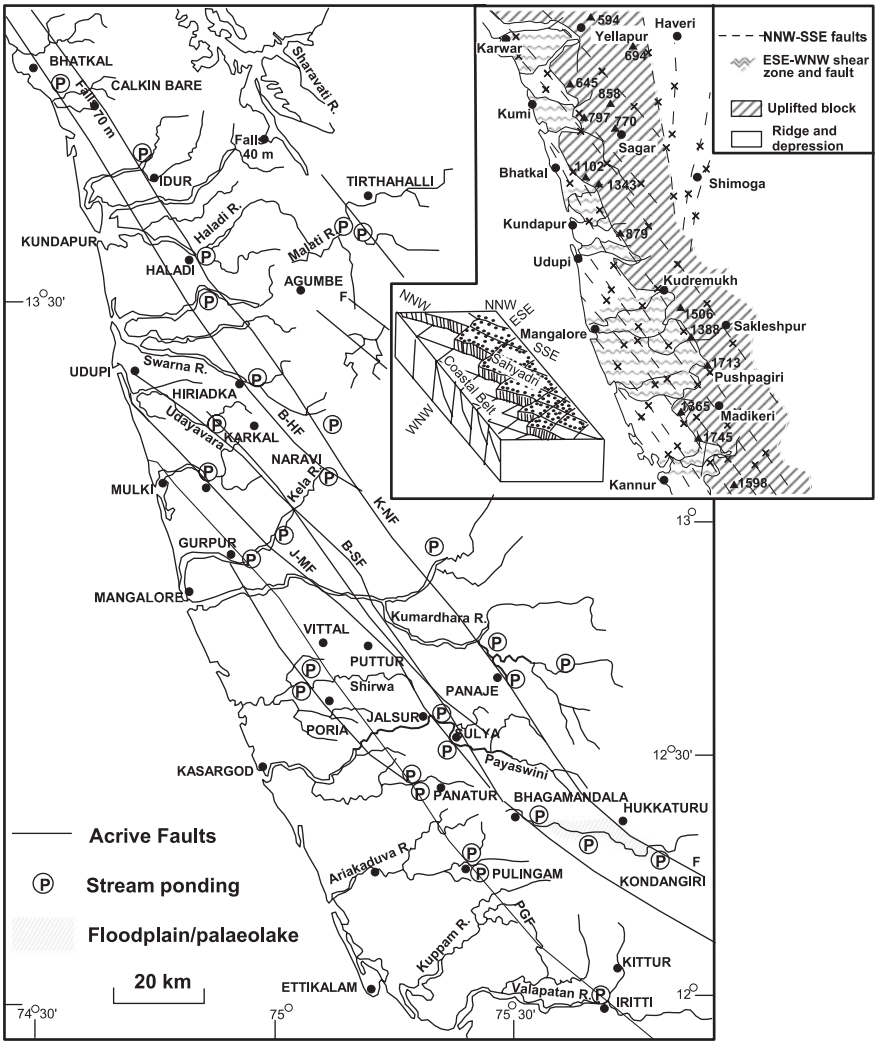

Fig. 23.15 Active NNW–SSE(and WNW–ESE)-oriented faults of the Kanara coastal belt and the Sahyadri Domain. The reactivation of faults caused past ponding of rivers (represented by palaeolakes) and present-day stagnation of river water upstream of their crossings. *Inset* Cartoon shows *en echelon* NNW–SSE-trending fault blocks breaking along the WNW–ESE reverse faults or shear zones due to strike-slip and oblique-slip movements on the NNW–SSE-trending faults and giving rise to the peculiar configuration and shape of the Western Ghat escarpment (after Valdiya 2001a)

However, the majority view is that the Western Ghat is a product of protracted *scarp recession* (Fig. 23.16) which started with the Gondwana break-up accompanied by uplift of the western edge of the Indian landmass (Ollier and Powar 1985;

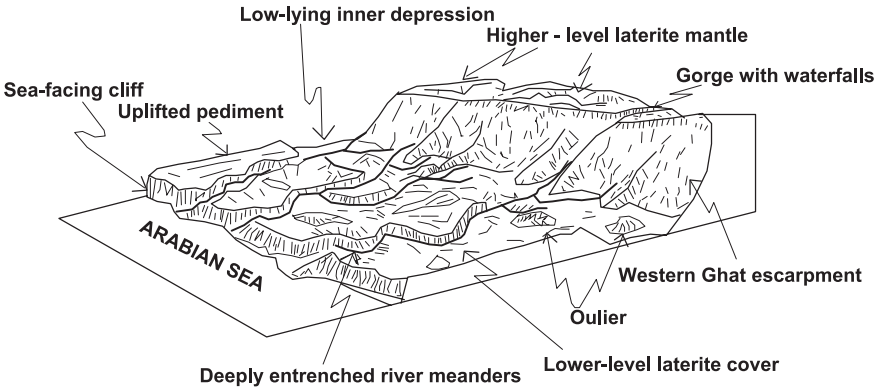

Fig. 23.16 The majority view on the development of the Western Ghat escarpment is that protracted recession of scarp due to erosion since the break-up of the Gondwanaland and attendant uplift of the western margin of Peninsular India gave rise to the peculiar topography of the Konkan–Kanara coastal belt and the Sahyadri (after Widdowson 1977)

Widdowson and Cox 1996; Gunnel et al. 2003). The uplift and extensive erosion in the Lower to Middle Tertiary time gave rise to low-relief coastal terrain developed through eastward recession of the scarpline.

23.5.3 Laterization of Pediplain

The low-level, low-relief undulating tract of the Konkan–Kanara belts is characterized by thick mantle of laterites resulting from in situ weathering of the Deccan basalts and Archaean gneisses with metamorphic rocks. In addition to the *primary (in situ) laterites*, there are accumulations of *secondary (transported) laterites*. The latter is characterized by clasts of older laterites and has a profile different from the typical one. The transported laterites occupy limited extents of topographic depressions (Widdowson 1997). The laterite cap does not always form the highest topography. In some places, unaltered basement rocks rise above the general level of coastal laterites without eroded laterite blocks or detrital deposits upon flanks of ridges (Widdowson 1997; Valdiya 2001a).

On the Paduvari Plateau in the Dakshin Kannada district (Fig. 23.17), the laterite profile consists of a lower zone of lithomarge clays, the middle zone of laterite–aluminous laterite–bauxite sequence and the upper zone of enriched laterite cap (Khandali and Devaraju 1987). The bauxite deposits normally underlie the enriched laterite that forms ferruginous crust and do not extend beyond the depth of 6–8 m from the surface. The laterites and bauxites show excessive depletion of Ca, Na, K, Sr, Li and Rb, low mobility of Mg and Be, retention of Na:K, and Li:Rb ratios of the parental gneisses. These characteristics demonstrate that there was leaching out of alkalies and alkali earths during *laterization*.

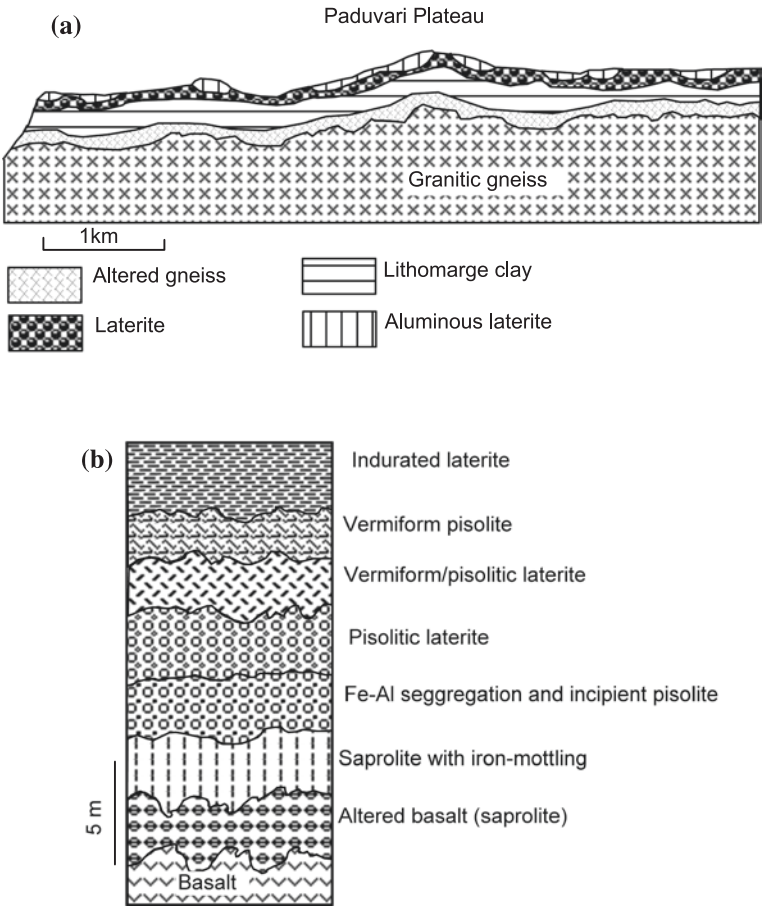

Fig. 23.17 **a** Laterization on the Paduvari Plateau made up of gneissic granites in Dakshin Kannada district, showing different zones of the laterite profile (Khandali and Devaraju 1987). **b** Compositional details of the laterite profile of the Deccan Lava

The mineralogy of the laterite profile is dominated by gibbsite with kaolinite, compared to lithomarge and goethite–haematite in the ferruginous laterite horizon (Khandali and Devaraju 1987).

23.6 Malabar Coast

23.6.1 Structural Layout

Like the Konkan–Kanara coastal belt, the *Malabar Coast* in Kerala is affected by five sets of lineaments of Precambrian antiquity, the most prominent being the

NNW–SSE-, N–S- and WNW–ESE-oriented ones (Nair 1990). The WNW–ESE lineaments control the present drainage pattern which earlier in the Precambrian time served as locales of plutonic bodies. Significantly, the WNW–ESE-trending faults truncate all other lineaments.

23.6.2 Sedimentary Cover

After a long stretch of several hundred kilometres from Gujarat, the depositional basin of Quaternary coastal sediments has developed only in the tract between Kollam and Kodungallur in central Kerala. The 80-km-long *Vembanad Lagoon* with its sedimentary accumulation is linked with the Kollam–Kodungallur basins. The Vembanad floor deposits comprise sandy clays and clayey sands with silts, intercalated with peat as old as 40,000 yr B.P. (Narayana et al. 2002). A 80-m-thick succession of the Pleistocene to Holocene sediments is coeval with, if not extension of, the Vembanad deposits (Nair et al. 2006). The fluvial sediments are underlain by littoral–lagoonal sediments emplaced during the Early Holocene marine transgression.

23.6.3 Gold-Bearing Laterite

One of the unique things of the laterite profile of the Kerala coast is the occurrence of exceedingly pure gold, occurring as fine grains and nuggets in the highly ferruginous nodular laterite in the Nilambur area, northern Kerala (Omana and Santosh 1998). Dissolution followed by precipitation of elemental gold during weathering of parental rocks under acidic condition gave rise to the placer gold in the laterites.

23.7 Coromandal Coast

23.7.1 Kanyakumari–Rameswaram Tract

In the 125-km-long stretch of the east coast between Kanyakumari and Rameswaram, the strandline occurs not higher than 4 m above the mean sea level. The Holocene transgression reached just one metre above the sea level, implying near stability of the coast. At Kanyakumari (Fig. 23.18), the sea transgressed inland into inselberg landscape, laying down conglomerate and sand characterized by gastropods and shells dated 12,000–4600 yr B.P. The horizon is overlain by aeolinite made up of calcrete and red shells (called *teri*) belonging to the last interglacial epoch (Bruckner 1989).

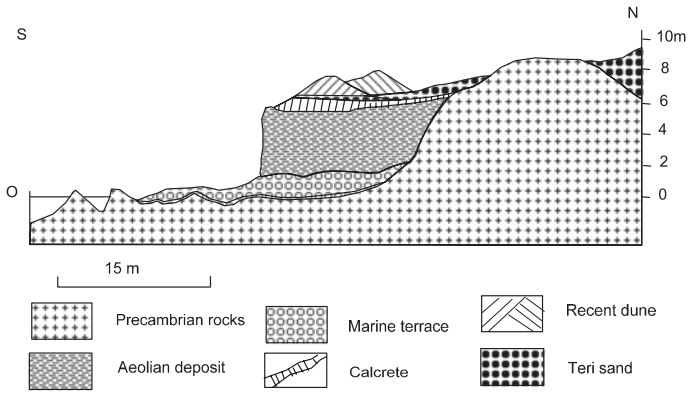

Fig. 23.18 Marine terrace at Kanyakumari formed due to the transgression of the sea (after Bruckner 1989)

In the coastal stretch off the Palk Bay, the occurrence of thermal springs implies deep-seated nature of the E–W-trending faults (Vaz et al. 2006). The faults developed on the Kochi–Ramanathapuram tectonic arc of ongoing movement, as borne out by progressive shift of the courses of the Kaveri, Palar and Ponnaiyer rivers. The sinuosity and arcuate coastline of Tamil Nadu are attributed to E–W-oriented structural arch (Ramasamy 2006).

The beach sands between Kanyakumari and Mandapam show selective concentration of heavy minerals including zircon, garnet and kyanite, such as seen in the Kallam–Vaippar tract (Angusamy and Rajamanickam 2000). There are buried placer deposits just south of Chennai (Mohan 1995; Angusamy et al. 2000; Mohan and Rajamanickam 2000). The concentration of heavy minerals in the sands is attributed to arcuate nature of the coastline.

23.7.2 Evolution of Jaffna Peninsula

Separated from the Tamil Nadu coast by a shallow sea embracing the Gulf of Mannar and the Palk Strait, the northern part of the island of Sri Lanka is made up of shelf sandstones and limestones of the Oligocene to Pleistocene ages. The Miocene *Jaffna Limestone* builds the bulk of the *Jaffna Peninsula* (Fig. 23.19) and extends underwater to the Tamil Nadu coastal belt (Senaratne and Dissanayake 1982). Overlying the Jaffna unit in Sri Lanka occur recent sand dunes and coral reefs. In Tamil Nadu, the Quaternary is represented by red earth, gravels and alluvial sediments covering the Jaffna Limestone.

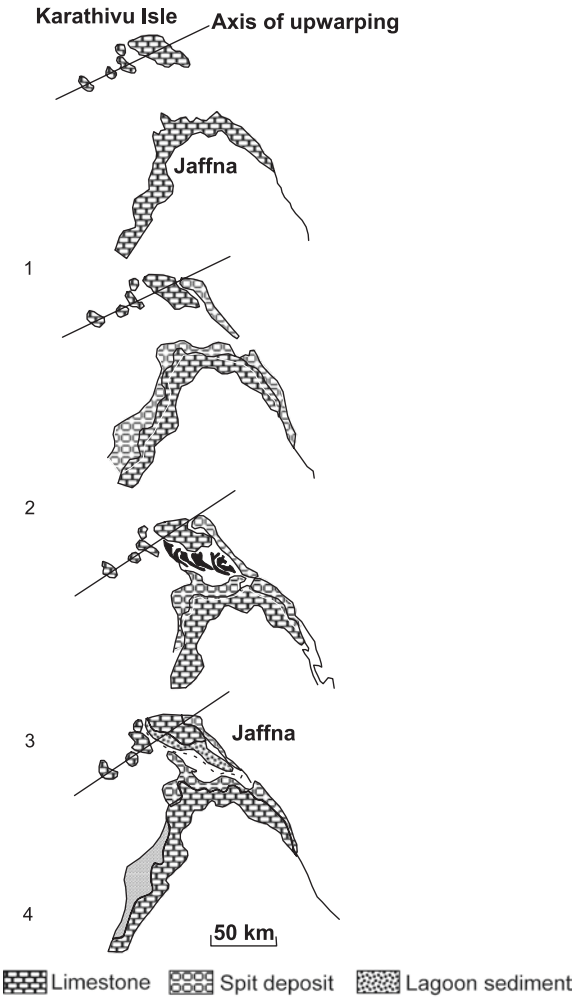

Fig. 23.19 Development of the Jaffna Peninsula took place by progressive growth of spits and hooked spits that enclose lagoonal inlets in the island of Sri Lanka (after Senaratne and Dissanayake 1982)

23.7.3 Growth of Kaveri Delta

Straddling across the faulted basement, the delta of the Kaveri has been building for a long period of time (Fig. 15.6). Much of the 6000–8000-m-thick pile of sediments represents prodeltas of the time span Late Cretaceous to the end of the Tertiary. The Quaternary delta comprises three geomorphic units—upland degradational plain, central fluviomarine plain and coastal marine plain (Babu 1991). The constituents of the delta plains include fluvial channel sands and interdistributary silts and muds, as well as sand ridges alternating with silty mudflats, beach

sands and estuarine or lagoonal muds. Quaternary movements resulted in the uplift of the delta domain and resultant cessation of the delta build-up. The morphology of the Kaveri Delta and the pattern of palaeochannel distributories point to neotectonic activity (Ramasamy 2006).

In the Palar delta, the estuaries and tidal flats between Muttukadu and Marakkam testify to a rapid sea-level rise after 3500 yr B.P. (Achyuthan and Baker 2002).

23.7.4 Human Remains

The ferricrete cover of a stratified fluvial–aeolian sediment succession about 2 km south of Pondicherry at Odai revealed remains of a baby human skull with the braincase capacity of 312 cc, 1- to 2-mm-thick cranial bone and maxilla and mandible with milk teeth (Rajendran et al. 2003). The skull occurs with artefacts of Palaeolithic and Mesolithic ages.

The palynospores in the sediments of Pachivaram area indicate amelioration of climate conditions during the Late Holocene (Farooqui and Sekhar 2002; Farooqui and Achuthan 2006). It seems that while the Quaternary sedimentary cover was building up, the humans found foothold along the east coast of India.

23.7.5 Development of Deltas of Godavari and Mahanadi

In the East Coast, the Quaternary sedimentary successions are covered by large fluvial deposits (Vaidyanadhan and Ghosh 1993). Three major rivers, the Krishna, the Godavari and the Mahanadi, have been building deltas along the east coast for a long period of time. The Krishna and Godavari deltas (Fig. 15.4) evolved in four stages. The oldest strand line of marine environment dates back to 6500 yr B.P. (Rengamannar and Pradhan 1991).

The Mahanadi delta (Fig. 23.20) is the product of activities of three rivers—the Mahanadi, the Brahmani and the Baitarani. The delta formation commenced after a major marine transgression in the Middle Miocene time. The youngest progradational delta, comprising beach ridges, sand dunes and tidal flats, is growing in the northerly direction as evident from the development of barrier spits. The presence of abandoned delta distributaries show more than one stage of the delta development—all controlled by former strand lines (Bharali et al. 1991). In Odisha, the spit of the Chilka Lake comprises shells of *Ostrea virginiana* dated 3750 ± 200 yr B.P. The Chilka lagoon is a result of sea-level rise between 6000 and 8000 yr B.P.

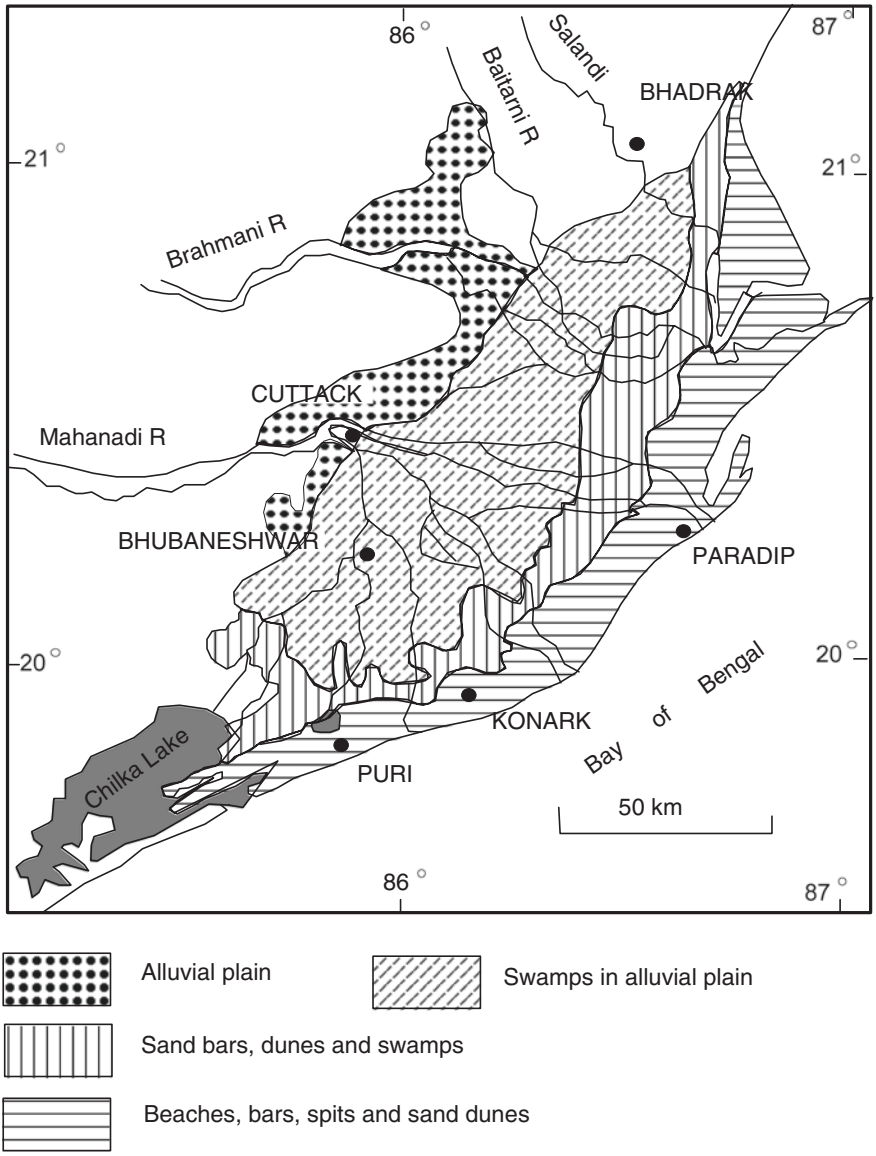

Fig. 23.20 Geomorphological features of the Mahanadi delta (after Bharali et al. 1991)

23.8 Mysore and Maharashtra Plateaus

23.8.1 Laterite Cap of Sahyadri

Forming in the Late Cretaceous to Early Tertiary time, the laterite mantle now occurs in a series of mesas—isolated plateaus—along the Sahyadri Range. These are high-level soil mantle comprising vermicular and massive forms of laterites with bauxites, as seen in the Boknur–Navage plateaus in the Belgaum district. This laterite–bauxite cap formed as a consequence of actions of slightly acidic meteoric water (Krishna Rao et al. 1989).

23.8.2 Multiple Planation Surfaces

The Nilgiri massif in the high Sahyadri Ranges testify to repeated spurts of uplift in the Quaternary period (Wadia 1942). Two planation surfaces in the upper part of the *Nilgiri Hills* are represented by the 2620 m Dodabetta and the 2120 m Udagamandalam (Ooty) surfaces that developed when the climate was warm and wet (Pardasaradhi and Vaidyanadhan 1974). The gentle slopes of mounds and streams that had reached high degree of geomorphic maturity drop as rapids and cascades at the edge of the Udagamandalam surface. In many places, the streams drop as waterfalls across high scarp faces. The Nilgiri is surrounded by 880–940-m-high Wayanad Plateau in the northwest, the 380–400-m-high Coimbatore upland to the south and 0–90-m-high Kerala plain to the west. The various peneplanation surfaces imply a cycle of erosion that affected the Sahyadri Domain. Taking the whole of the Southern Indian Shield, four base levels of erosion are recognizable (Fig. 23.21 profile)—the Mysore–Kollimalai Plane (270 m), the Kolar–Manantody Surface (180 m), the Palani–Tirupattur Level (90 m) and the Madurai–Palghat Plane (45 m). These planes or surfaces represent, respectively, the last stages of the Mesozoic, the Early Tertiary, the Late Tertiary and the Pleistocene cycles of erosion (Babu 1975).

Close to the Palghat–Cauvery Shear Zone in the Wadakkancherry area (Palghat region), a WNW–ESE-oriented south-dipping reverse fault traceable over 30 km is response for sharp deflection of the Bharathapuzha stream and formation of a waterfall (John and Rajendran 2008). The EST dating of the fault gouge characterized by cross-cutting fractures indicates that on this fault there were at least four episodes of movement in the Middle Quaternary time, the aggregate dip-slip displacement being 2.1 m (John and Rajendran 2009).

The NNE–SSW- to N–S-trending lineament traceable from Kanyakumari to Tirupati seems to represent an active fault, as borne out by a deep gorge between the Chitteri and Shevaroy hills, landslides on the high fault scarp, drainage deflection, occurrence of earthquake at Vaniyambadi, Salem and Tirupattur and eruption of brown mud as seen on 28 January 1997 at Attanavur (Ramasamy 2006).

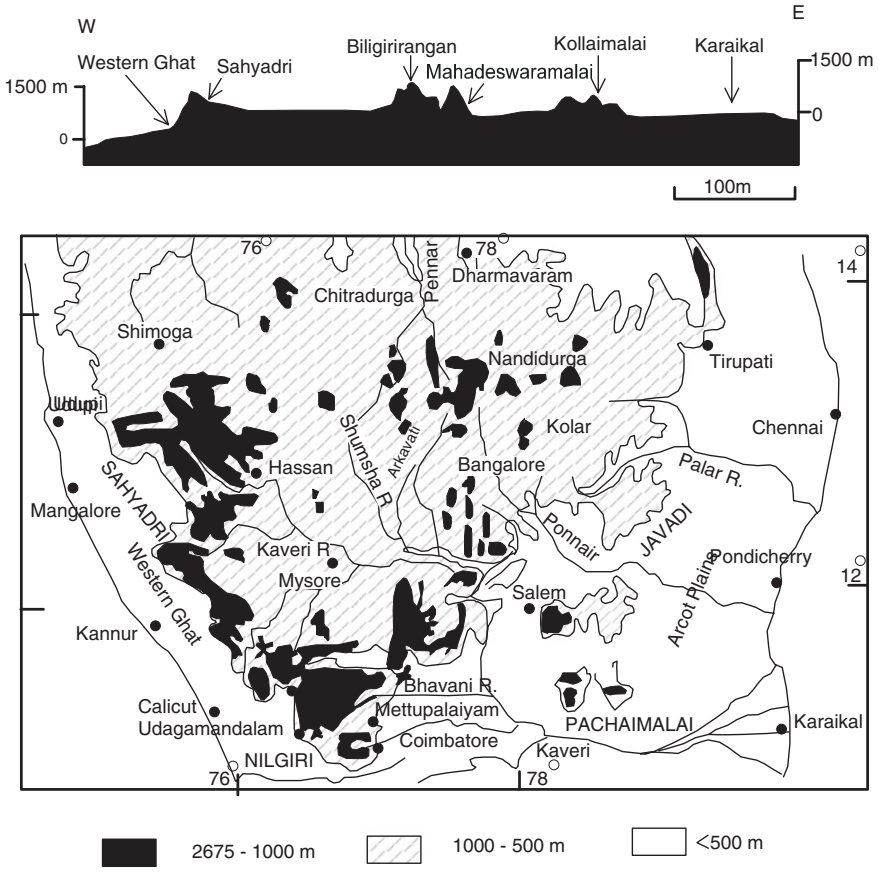

Fig. 23.21 Southern Indian Shield encompassing the Mysore Plateau having an average elevation of 800 m above sea level is bordered on three sides by high mountains that rise 300 to more than 1000 m above the undulating terrain of the plateau. The profile at the *top* shows several levels of plantations (Valdiya 2001b)

23.8.3 Tectonically Resurgent Mysore Plateau

The whole of Southern Indian Shield, as already stated, has been rising epeirogenically (Kailasam 1975, 1979; Radhakrishna 1964, 1993; Powar 1993). The tectonic resurgence has been attributed to buoyancy of the crust related to hot spot activity (Raval 1995) or to continued northward movement of the Indian plate (Valdiya 1998b, 2001b). The Mulki–Pulicat line along the 13° parallel is a zone of buckling of the Indian crust (Subrahmanya 1994, 2002) as evident from (i) the line marking the water divide of the northward-flowing and southward-flowing rivers, (ii) mild seismicity, (iii) seaward protrusion of landmass near Mangalore along the west coast and near Chennai in the east coast, (iv) tide-gauge data showing

fall of sea level north of Mangalore, (v) the presence of beach ridges, dead oyster colonies a few metres above the highest high-water level and (vi) dessicated nature of the laterite plateaus south of Mangalore. All of these imply uplift of the Mulki–Pulicat belt of the Karnataka Plateau.

Cut by NNW–SSE-, N–S- and NNE–SSW- and ESE–WNW- to E–W-oriented fractures and shear zones or faults, the *Mysore Plateau* is characterized by a dynamic landscape. The capturing of an eastward-flowing stream by the west-flowing Sharavati River along the western edge of the plateau (Radhakrishna 1964) bears testimony to the tectonic resurgence of the region. In the Bangalore region, the N–S- and NNE–SSW-trending faults demarcate the flanks of long linear hills and linear series of isolated hillocks characterized by high scarps and peneplaned laterite-capped tops. These hills are northward extensions of the 1000–1700-m-high horst blocks of the *Biligirirangan–Mahadeswaramalai Ranges* south of Bangalore. Most of these faults are associated with stream and river deflections, palaeolakes and present-day stagnant bodies of water in the channels of rivers upstream of fault crossings (Valdiya 1998b). The narrow passages of the rivers that have cut through the downstream blocks bear testimony to entrenchment due to the uplift of the downstream foothill (Fig. 23.22).

Oblique-slip movements along the N–S *Kollegal Fault* that demarcates the west-facing high scarp of the Biligirirangan Hill are responsible for the ponding of the Kaveri and its tributaries, the Shimsha, the Kabini and the Suvarnavati. The *Kollegal Palaeolake* is represented by 6–10-m-thick black clay deposits dated more than 26,000 to less than 4900 yr B.P. (Valdiya 1998b; Valdiya and Rajagopalan 2000). Significantly, the clay flat has been vertically displaced 10 m by a fault passing by Talakad and Malavalli, implying a Late Holocene movement affecting the Kaveri Basin.

23.8.4 Uplift of the Deccan Plateau

The rivers of Maharashtra show five phases of fluvial activity (Fig. 23.23). The dominantly aggradational activity during the Late Pleistocene (until 12,000–10,000 yr B.P.) was followed by strong incision during the major part of the Holocene when rivers cut their own deposits and formed deep channels (Kale and Rajaguru 1987; Rajaguru and Koriesettar 1987). After a phase of aggradation, there was yet another phase of intense incision in the Late Holocene. And this phase continues to the present.

In particular, the *Upland Maharashtra* in the Sahyadri Domain, many rivers are incised 20–25 m deep, cutting through their own deposits into the basalt basement. Together with knick points entrenched meanders, there are high waterfalls close to the sources of rivers such as the Venna (180 m), the Pravara (50 m), the Adhala (50 m) and the Ulhas (330 m). The rivers of upland Maharashtra are thus rejuvenating as a consequence of uplift of the terrane

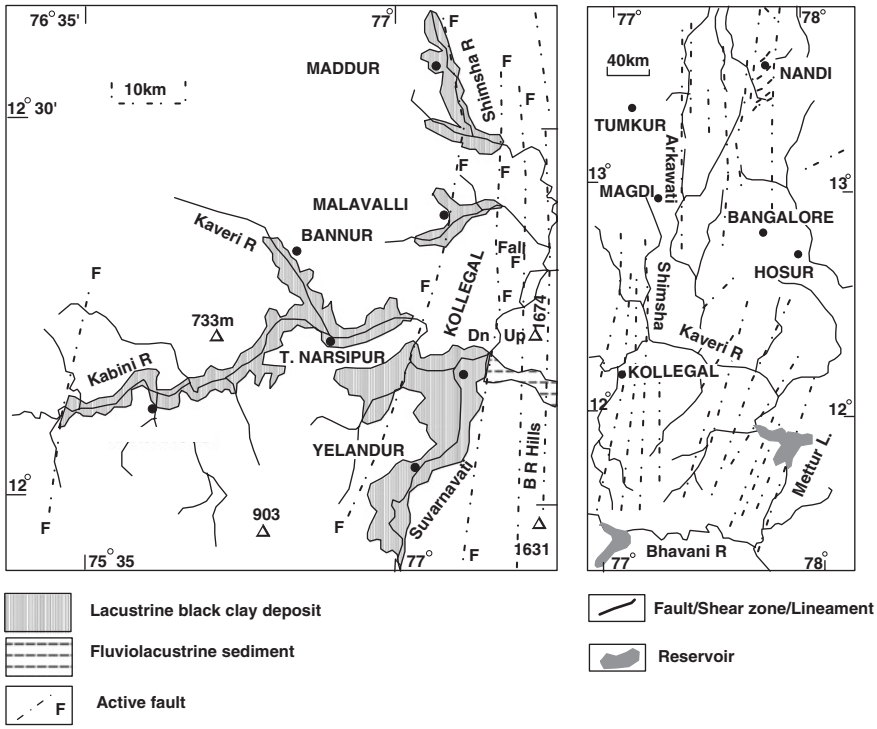

Fig. 23.22 **a** Long linear hills and isolated hillocks rising abruptly 300–600 m above the nearly 900-m planation surface of the Bangalore region are delineated by NNE–SSW- to N–S-trending *en echelon* faults. These linear hills extend southwards as 1000–1700–m-high Biligirirangan–Mahadeswaramalai Hills, a horst of sorts. **b** Reactivation of the Kollegal Fault that demarcates the western escarpment of the Biligirirangan Hill is responsible for the development of a palaeo-lake that spreads along valleys of the Shimsha, the Kaveri, the Kabini and the Suvarnavati (after Valdiya 2001b)

(Gupta and Rajaguru 1971). Colluvial deposits 1–10 m in thickness made up of the material stripped off the hills are dumped along the foot of the rising high hills (Joshi and Kale 1997).

The Indian crust has been under compressive stress ever since India collided with Asia. The reactivation of the Palghat–Cauvery Shear Zone and the crustal buckling along the Mulki–Pulicat axis are responses to the growing stresses in the crust of the Peninsular India. The strong deformation that the Indian Ocean crust experienced at 0.8 Ma (Krishna et al. 1998) may be related to the intense fluvial erosion in upland Maharashtra at about 0.5 Ma (Kale and Rajaguru 1987). The Mysore Plateau did not escape from these tectonic phenomena, as manifest in the reactivation of ancient faults and resultant landscape development, and in ponding of rivers (Valdiya 2001b).

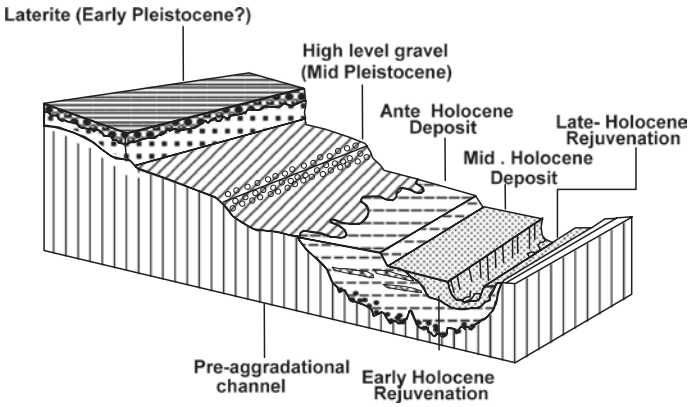

Fig. 23.23 Rivers of upland Maharashtra are characterized by thick valley fills of aggradational phases and of terraces formed during the phases of incision (Rajaguru and Kale 1985). **b** Composite lithostratigraphic profile of the Kukadi River at Bori in the Pune district (Korisettar et al. 1989)

23.8.5 Volcanism and Life

The sediments of the Kukadi River at Bori in the Pune district contain 20-cm to 2-m-thick intercalations of vitric rhyolitic tuffs within 2–8-m-thick succession of clay with occasional lenses of basaltic rubbles and calcrete and characterized by Acheulian (Palaeolithic) stone implements (Korisettar et al. 1989). Middle Palaeolithic archaeological assemblages at Jwalapuram in Kurnool district, Andhra Pradesh, are associated with 2.55-m-thick layer of volcanic ash with glass shards representing the 74 ka B.P. Youngest Toba Tuff indicates that humans were present in the Indian subcontinent 74,000 years ago (Petroglia et al. 2007). The Stone-Age people must have braved the rains of volcanic dust that fell in Maharashtra, adjoining Andhra Pradesh and in the Narmada and Son valleys in Madhya Pradesh.

In a southerly tributary (Majra) of the Godavari River, a 10–12-m-thick Late Pleistocene sequence of fluvial sediments at Gaurwadi in district Ahmadnagar comprises calcretized pebbly sand and silty–sandy clays. Within this sediment succession occur remains of *Hippopotamus*, *Cervus unicolour, Bos indicus, Babulus, Sus, Equus namadicus, Elephas hysudricus, Elephas maximus, Stegodon insignis, Stegodon ganesa* and *Crocodylus* along with Mesolithic tools made of chert and chalcedony (Badam 1984). At Kokur in the Bhima Valley (Gulbarga district), a nearly complete skull of *Hippopotamus* along with remains of *Equus namadicus* and artefacts of Palaeolithic time indicates the humans living in the company of Pleistocene mammalian animals (Anantharaman et al. 2005). The sediments of the Hunsgi and Baichbal valleys in the Islamabad area of district Gulbarga (dated 174,000 to >350,000 yr B.P.) contain the Acheulian (Lower Palaeolithic) to Iron-Age tools occurring along with the bones of cattle, horses, elephants and deers (Paddayya et al. 2002).

23.9 Mineral Assets

Deposits of *placer minerals* such as ilmenite, rutile, zircon and monazite together with garnet and sillimanite occur in the Ratnagiri coast in Maharashtra, the Kollam coast in Kerala, the Kanyakumari–Tuticorin coast in Tamil Nadu, the Srikurmam coast in Andhra Pradesh and the Gopalpur coast in Odisha. The aggregate deposit is of the order of 340 million tonnes, of which 20.71 million tonnes occurring in Srikurmam stretch alone (Mohan and Rajamanickam 2000). The location of the sites of concentration of the heavy minerals in the sands is strongly controlled by the structures of the ground as discernible in the deposits of Mandapam–Kanyakumari, Kanyakumari–Kuttankutti and the Wada–Vetye, Ambolgarh, Rajapur and Vijaydurg bays along the Konkan coast (Angusamy et al. 2000).

Concentration of sufficient merit of ilmenite, rutile, zircon and monazite occurs in the coastal dune sand 6–12 km inland at Brahmagiri, Sultana, Konark, Baulpur, Ramnagar, etc., in the Bengal–Odisha coast (Jagannadha Rao et al. 2008).

In the playa deposits characterized by abundant calcrete at Lachhri in Nagaur district (Rajasthan), surface deposits of uranium, estimated to amount 14 tonnes, have been recognized (Misra et al. 2011).

References

Achyuthan, H. (2003). Petrologic analysis and geochemistry of the Late Neogene-Early Quaternary hardpan calcretes of western Rajasthan, India. *Quaternary International, 107*, 3–10.

Achyuthan, Hema, & Baker, V. R. (2002). Coastal response to changes in sea level since the last 4500 yr B.P., on the east coast of Tamil Nadu India. *Radiocarbon, 44*, 137–144.

Ahmad, F. (1986). Geological evidence bearing on the origin of Rajasthan desert. *Proceedings of the Indian National Science Academy, 52A*, 1285–1306.

Anantharaman, S., Das Sarma, D. C., & Ashok Kumar, P. (2005). A new species of Quaternary hippopotamid from Bhima valley, Karnataka. *Journal-Geological Society of India, 66*, 209–216.

Angusamy, N., Loveson, V. J., & Rajamanickam, G. V. (2000). Shoreline configuration and the distribution of Quaternary coastal placers of Southern Tamil Nadu, India. In G. V. Rajamanickam & M. J. Toley (Eds.), *Quaternary sea level variation shoreline displacement and coastal environment* (pp. 132–139). Delhi: New Academic Publishers.

Angusamy, N., & Rajamanickam, G. V. (2000). Distribution of heavy minerals along the beach from Mandapam to Kanyakumari, Tamil Nadu. *Journal-Geological Society of India, 56*, 199–211.

Auden, J. B. (1949). Dykes in western India—a discussion of their relationship with the Deccan Traps. *Transactions National Institute of Science India, 3*, 123–157.

Babu, P. V. L. P. (1975). A study of cyclic erosion sufaces and sedimentary unconformities in the Cauvery basin, South India. *Journal-Geological Society of India, 16*, 349–353.

Babu, P. V. L. P. (1991). Cauvery delta—its past and present. *Memoirs Geologist Society India, 22*, 91–101.

Badam, G. L. (1979). *Pleistocene fauna of India*. Pune: Deccan College.

Badam, G. L. (1984). Pleistocene faunal succession of India. In R. O. Whyte (Ed.), *The evolution of East Asian environment* (pp. 746–775). Hongkong: University of Hongon.

Badam, G. L., Ganjoo, R. K., & Salahuddin, (1986). Preliminary taphonomical studies of some Pleistocene fauna from the Central Narmada Valley, M.P., India. *Palaeogeography, Palaeoclimatology, Palaeoecology, 53*, 335–348.

Bakliwal, P. C., & Ramasamy, S. M. (1987). Lineament fabric of Rajasthan and Gujarat. *Record Geology Survey of India, 113*, 54–65.

Bakliwal, P. C., & Sharma, S. B. (1980). On the migration of the Yamuna River. *Journal-Geological Society of India, 21*, 461–463.

Bakliwal, P. C., & Wadhawan, S. K. (2003). Geological evolution of Thar desert in India—issues and prospects. *Proceedings of the Indian National Science Academy, 69A*, 151–165.

Barua, D. K. (1997). The characteristics and mobility of some major rivers in Bangladesh. *Water Nepal, 5*, 109–127.

Basu, P. K., Biswas, S., & Acharyya, S. K. (1987). Quaternary ash beds from Son and Narmada basins, Madhya Pradesh. *Indian Minerals, 34*, 66–72.

Bezbaruah, D., Kotosky, P., Baruah, J., & Sarma, J. N. (2003). Geomorphological explanation of swamps along the Brahmaputra river channel, Assam. *Journal-Geological Society of India, 62*, 605–613.

Bhandari, S., Maurya, D. M., & Chamyal, L. S. (2005). Late Pleistocene alluvial plain sedimentation in Lower Narmada valley, western India, Palaeoenvironmental implications. *Journal of Asian Earth Sciences, 24*, 433–444.

Bhandari, S., Raj, R., Maurya, D. M., & Chamyal, L. S. (2001). Formation and erosion of Holocene alluvial fans along the Narmada basin, western India. *Journal-Geological Society of India, 58*, 519–531.

Bharali, B., Rath, S., & Sarma, R. (1991). A brief review of Mahanadi delta and the deltaic sediments in Mahanadi basin. In R. Vaidyanadhan (Ed.), *Quaternary deltas of India* (pp. 31–47). Bangalore: Geological Society of India.

Bhatt, Nilesh. (2000). Lithostratigraphy of the Neogene-Quaternary deposits of Dwarka-Okha area, Gujarat. *Journal-Geological Society of India, 55*, 139–148.

Bhatt, N., & Patel, M. P. (1998). Bioclastic shore deposits: Indicators of Late Quaternary high sea in Saurashtra, Western India. *Journal-Geological Society of India, 52*, 537–542.

Bhoskar, K. G., Bhatia, S. K., Gupta, A., & Saha, A. K. (2001). Geomorphology of the Konkan region along the west coast of Maharashtra: Related lateritic bauxite profiles and their potential. *Special Publication Geological Survey of India, 65*, 265–269.

Biswas, S. (1989). Fossils of *Equus* from central Narmada valley in M.P. *Records Geological Survey of India, 118*(2), 53–62.

Biswas, S. (1997). Fossil mammals of the Quaternary sequence of the Narmada valley, their affinity, age and ecology. *Special Publication Geological Survey of India, 46*, 91–104.

Bruckner, H. (1989). Later Quaternary shorelines in India. In D. B. Scott (Ed.), *Late Quaternary sea level correlation and application* (pp. 169–194). Dordrecht: Kluwer Academic Publication.

Bruckner, H., Mangini, A., Montaggioni, L. & Rescher, K. (1987). Miliolite occurrences of Kathiawar peninsula (Gujarat), India, Berliner geographishe—studien, band 25, seite, (pp. 343–361).

Bryson, R. A., & Swain, A. M. (1981). Holocene variations of monsoon rainfall in Rajasthan. *Quaternary Research, 16*, 135–145.

Chakrabarti, A., Somayajulu, B. L. K., Baskaran, A., & Kumar, B. (1993). Quaternary miliolites of Kutch and Saurashtra, western India: Development and environments in the light of physical sedimentary structures, biogenic and structures and geochronological silty Kutch. *Senckenbergiana maritima, 23*, 7–28.

Chamyal, L. S., Khadkikar, A. S., Malik, J. N., & Maurya, D. M. (1997). Sedimentology of the Narmada alluvial fan, western India. *Sedimentary Geology, 107*, 263–279.

Chamyal, L. S., Maurya, D. M., Bhandari, S., & Raj, R. (2002). Late Quaternary geomorphic evolution of the Lower Narmada valley, western India: Implications for neotectonic activity along the Narmada-Son Fault. *Geomorphology, 46*, 177–202.

Chamyal, L. S., Maurya, D. M., & Raj, R. (2003). Fluvial systems of the drylands of western India: A synthesis of Late Quaternary environmental and tectonic changes. *Quaternary International, 104*, 69–86.

Courty, M. A. (1995). Late Quaternary environmental changes and natural constraints to ancient landuse (Northwest India). In E. Johnson (Ed.), *Ancient people and landscapes* (pp. 106–126). Lubbock, Texas: Museum of Technical University.

Deotare, B. C., Kajab, M. D., Rajaguru, S. N., Kusumgar, S., Jull, A. J. T., & Donahue, J. D. (2004). Palaeoenvironmental history of Bap-Malar and Kanod playas of western Rajasthan, Thar desert. *Proceedings of Indian National Science Academy (Earth and Planetary Science), 113*, 403–425.

Desai, G., Hardas, M. G., Patel, M. P., & Merh, S. S. (1982). Origin of Miliolite rocks of Kutch—microfaunal evidence. *Journal-Geological Society of India, 23*, 246–252.

Dessai, A. G., & Bertrand, H. (1995). The Panvel Flexure along the western Indian continental margin: An extensional fault structure related to Deccan magmatism. *Tectonophysics, 241*, 165–178.

Dhir, R. P., Rajaguru, S. N., & Singhvi, A. K. (1994). Desert Quaternary formations and their morphostratigraphy: Implications for the evolutionary history of the Thar. *Journal-Geological Society of India, 43*, 435–447.

Dhir, R. P., Singhvi, A. K., Andrews, J. E., Kar, A., Sareen, B. K., Tandon, S. K., et al. (2010). Multiple episodes of aggradations and calcrete formation in Late Quaternary aeolian sands, central Thar Desert, Rajasthan, India. *Journal of Asian Earth Sciences, 37*, 10–16.

Dikshit, K. R. (1976). Drainage basins of Konkan: Forms and characteristics. *National Geographical Journal India, 22*, 152–169.

Enzel, Y., Ely, L. L., Mishra, S., Ramesh, R., Amit, R., Lazar, B., et al. (1999). High-resolution Holocene environmental changes in the Thar desert, northwestern India. *Science, 284*, 125–126.

Farooqui, A., & Achuthan, H. (2006). Middle to Late Holocene palaeoenvironment changes: Evidence from the sediments, pollens and radiocarbon dates, Adyar, Chennai. *Journal-Geological Society of India, 68*, 230–238.

Farooqui, A., & Sekhar, B. (2002). Holocene sea level/climatic changes evidenced by palynostratigraphical and geochemical studies. *Memoirs Geologist Society India, 49*, 41–50.

Ganjoo, R. K. (1995). Late Quaternary stratigraphy of central Narmada valley, M.P: Response to tectonics and basin morphology. *Journal of the Palaeontological Society of India, 40*, 1–8.

Gaur, A. S., & Vora, K. H. (1999). Ancient shoreline of Gujarat, India during the Indus civilization (Late Mid-Holocene): A study based on archaeological evidences. *Current Science, 77*, 183–185.

Ghose, B., Kar, A., & Hussain, Z. (1979). The lost courses of the Saraswati River in the great Indian desert—new evidence from Landsat imagery. *Geographical Journal, 145*(3), 446–451.

Gibling, M. R., Tandon, S. K., Sinha, R., & Jain, M. (2005). Discontinuity-bounded alluvial sequences of the southern granulite plains, India: Aggradation and degradation in response to monsoon strength. *Journal of Sedimentary Research, 75*, 369–385.

Gilfellon, G. B., Sarma, J. N., & Gohain, K. (2003). Channel and bed morphology of a part of Brahmaputra River in Assam. *Journal-Geological Society of India, 62*, 227–235.

Gunnell, Y., Gallagher, K., Carter, A., Widdowson, M., & Hurford, A. J. (2003). Denudation history of the continental margin of western Peninsular India since the early Mesozoic—reconciling apatite-fision-track data with geomorphology. *Earth and Planetary Science Letters, 215*, 187–201.

Gupta, A., Kale, V. S., Owen, L. A., & Singhvi, A. K. (2007). Late Quaternary bedrock incision in the Narmada River at Dardi Falls. *Current Science, 93*, 564–567.

Gupta, R. B., & Rajaguru, S. N. (1971). Late Pleistocene geomorphological history of rivers of western Maharashtra. *Bulletin Volcanologique, 35*, 686–695.

Gupta, A. K., Sharma, J. R., Sreenivasan, G., & Srivastava, K. S. (2004). New findings on the course of River Saraswati. *Photonirvachak, 32*, 1–24.

Hashimi, N. H., Nigam, R., Nair, R. R., & Rajagopalan, G. (1995). Holocene sea level fluctuations on western Indian continental margin: An update. *Journal-Geological Society of India, 46*, 157–162.

Jagannadha Rao, K., Subramanyam, A. V., Kumar, Ahinav, Sunil, T. C., & Chaturvedi, A. K. (2008). Discovery of heavy mineral-rich sand dunes along the Orissa-Bengal coast of India, using remote sensing techniques. *Current Science, 99*, 983–985.

Jain, M., Tandon, S. K., Bhatt, S. C., Singhvi, A. K., & Mishra, S. (1999). Alluvial and aeolian sequences along the River Luni, Barmer District: Physical stratigraphy and feasibility of luminescence chronology methods. *Memoirs-Geological Society of India, 42*, 273–295.

John, B., & Rajendran, C. P. (2008). Geomorphic indications of neotectonism from the Precambrian terrain of the Peninsular India: A study from Bharathapuzha basin, Karala. *Journal-Geological Society of India, 71*, 827–840.

Joshi, Veena U., & Kale, Viswas S. (1997). Colluvial deposits in northwest Deccan, India: Their significance in interpretation of Late Quaternary history. *Journal of Quaternary Science, 12*, 391–403.

Juyal, N., Kar, A., Rajaguru, S. N., & Singhvi, A. K. (2003). Luminescence chronology of aeolian deposition during the Late Quaternary on the southern margin of Thar desert India. *Quaternary International, 104*, 87–98.

Kaila, K. L., Murthy, P. R. K., Mall, D. M., Dixit, M. M., & Sarkar, D. (1987). A deep sceismic sounding along Hirapur-Mandla profile, Central India. *Geophysical Journal International, 89*, 399–404.

Kailasam, L. N. (1975). Epeirogenic studies in India with reference to recent vertical movements. *Tectonophysics, 29*, 505–521.

Kailasam, L. N. (1979). Plateau uplift in Peninsular India. *Tectonophysics, 61*, 243–265.

Kale, V. S., & Rajaguru, S. N. (1987). Late Quaternary alluvial history of the northwestern Deccan upland region. *Nature, 325*, 612–614.

Kar, A. (1988). Possible neotectonic activities in the Luni-Jawai Plains, Rajasthan. *Journal-Geological Society of India, 32*, 522–526.

Kar, Amal. (1993). Neotectonic influences on morphological variations along the coast line of Kachchh India. *Geomorphology, 8*, 199–219.

Kar, A. (1995). Geomorphology of arid western India. *Memoirs-Geological Society of India, 32*, 168–190.

Kar, A., & Ghose, B. (1984). Drishadvati River System in India—an assessment and new findings. *Geographical Journal, 150*, 221–229.

Kar, A., Singhvi, A. K., Rajaguru, S. N., Juyal, N., Thomas, J. N., Banerjee, D., & Dhir, R. P. (2001). Reconstruction of the Late Quaternary environment of lower Luni plains, Thar desert, India. *Journal of Quaternary Science, 16*, 61–68.

Kathiroli, S., Badarinarayan, S., Venkata Rao, D., Rajaguru, S. N., Sivakholundu, K. M., & Sasisekaran, B. (2002). A new archeological find in the Gulf of Cambay, Gujarat. *Journal-Geological Society of India, 60*, 419–428.

Khadkikar, A. S., Chamyal, L. S., & Ramesh, R. (2000). The character and genesis of calcrete in Late Quaternary alluvial deposits, Gujarat, India and its bearing on the interpretation of ancient climates. *Palaeogeography, Palaeoclimatology, Palaeoecology, 162*, 239–261.

Khan, A. A., & Sonakia, A. (1992). Quaternary deposits of Narmada with special reference to the Homminid fossils. *Journal-Geological Society of India, 39*, 147–154.

Khandali, S. D., & Devaraju, T. C. (1987). Laterite-bauxite of Paduvari plateau, South Kanara, Karnataka State. *Journal-Geological Society of India, 30*, 255–266.

Korisettar, R., Venkatesan, T. R., Mishra, S., Rajaguru, S. N., Somayajulu, B. L. K., Tandon, S. K., et al. (1989). Discovery of tephra bed in the Quaternary alluvial sediment of Pune district (Maharashtra) Peninsular India. *Current Science, 58*, 564–576.

Krishna, J., Pathak, D. B., & Pandey, B. (1998). Development of Oxfordian (Early Upper Jurassic) in the most proximately exposed part of the Kachchh Basin at Wagad outside the Kachchh mainland. *Journal-Geological Society of India, 52*, 513–522.

Krishna Rao, B., Satish, P. N., & Sethumadhav, M. S. (1989). Syngenetic and epigenetic features and genesis of the bauxite-bearing laterite of Boknur-Navge plateau, Belgaum District, Karnataka. *Journal-Geological Society of India, 34*, 46–60.

Krishnaswamy, V. S., & Raghunandan, K. R. (2005). The Satpura uplift and the palaeoclimate of the Holocene and auxiliary evidence from the Valmiki Ramayana. *Journal-Geological Society of India, 66*, 161–170.

Kshetrimayum, K. S., & Bajpai, V. N. (2011). Establishment of missing stream link between the Markanda river and Vedic Saraswati river in Himalaya, India—geoelectrical resistivity approach. *Current Science, 100*, 1719–1724.

Kundu, B., & Matan, A. (2000). Identifical of proble faults in the vicinity of Harnai-Ratnagiri region of the Konkan Coast, Maharashtra. *Current Science, 78*, 1556–1560.

Malik, J. N., Sohoni, P., Merh, S. S., & Karanth, R. V. (2001). Active tectonic control on alluvial fan architecture along Kachchh mainland hill range western India. *Zeitschrift für Geomorphologie, NF, 45*, 81–100.

Maurya, D. M., Raj, R., & Chamyal, L. S. (2000). History of tectonic evolution of Gujarat alluvial plains, western India, during Quaternary: A review. *Journal-Geological Society of India, 55*, 343–366.

Merh, S. S. (1993). Neogene-Quaternary sequence in Gujarat: A review. *Journal-Geological Society of India, 41*, 259–276.

Merh, S. S., & Chamyal, L. S. (1997). *The Quaternary geology of Gujarat alluvial plains* (pp. 63–98). New Delhi: Indian National Science Academy.

Misra, V. N. (1997). Early man and his environment in central India. *Journal Palaeontology Society of India, 42*, 1–18.

Misra, A., Pande, D., Ramesh Kumar, K., Nanda, L. K., Maithani, P. B., & Chaki, A. (2011). Calcrete-hosted surfacial uranium occurrence in playa-lake environment at Lachhri Nagaur district, Rajasthan, India. *Current Science, 101*, 84–88.

Mohan, M. (1995). Cambay basin—a promise of oil and gas potential. *Journal of the Palaeontological Society of India, 40*, 41–47.

Mohan, P. M., & Rajamanickam, G. V. (2000). Indian beach placers—a review. In G. V. Rajamanickam & M. J. Toley (Eds.), *Quaternary sea level variation, shoreline displacement and coastal environment* (pp. 23–52). Delhi: New Academic Publishers.

Mohinder, R., & Parkash, B. (1994). Geomorphology and neotectonic activity of the Gandak Megafan and adjoining areas, Middle Gangetic Plain. *Journal of the Geological Society of India, 43*, 149–158.

Nair, M. M. (1990). Structural trendline patterns and lineaments of the Western Ghats, south of 13º lattitude. *Journal-Geological Society of India, 35*, 99–105.

Nair, A. R., Navada, S. V. & Rao, S. M. (1999). Isotope study to investigate the origin and age of groundwater along palaeochannels in Jaisalmer and Ganganagar districts of Rajasthan. *Memoirs-Geological Society of India*, 315–319.

Nair, K. M., Padmalal, D., & Kumaran, K. P. N. (2006). Quaternary geology of South Kerala sedimentary basin—an outline. *Journal-Geological Society of India, 67*, 165–179.

Narayana, A. C., Priju, C. P., & Rajagopalan, G. (2002). Later Quaternary peat deposits from Vembanad Lake (lagoon), Kerala, SW coast of India. *Current Science, 83*, 318–321.

Ollier, C. D., & Powar, K. B. (1985). The Western Ghats and the morphotectonics of peninsular India. *Zeitschrift für Geomorphologie N.F., 54*, 57–69.

Omana, P. K., & Santosh, M. (1998). Gold in laterites: Combined field and laboratory experimental investigations on the dissolution and precipitation mechanisms. *Indian Mineral, 32*, 61–62.

Paddayya, K., Blackwell, B. A. B., Jhaldiyal, R., Petraglia, M. D., Fevrier, S., Chaderton, D. A., et al. (2002). Recent findings on the Acheulian of the Hunsgi and Baichbal valleys Karnataka with special reference to the Islampur excavation and its dating. *Current Science, 83*, 641–645.

Pal, Y., Sahai, B., Sood, R. K., & Agrawal, D. P. (1980). Remote sensing of the lost Saraswati river. *Proceedings Indian Academy Science (Earth & Planetary Science), 89*, 317–337.

Pandarinath, K., Prasad, S., Deshpande, R. P., & Gupta, S. K. (1999). Late Quaternary sediments from Nal Sarovar, Gujarat: Distribution and provenance. *Proceedings of the Indian Academy of Sciences (Earth and Planetary Sciences), 108*, 107–116.

Pant, R. K., & Chamyal, L. S. (1990). Quaternary sedimentation pattern and terrain evolution in the Mahi River basin, Gujarat. *Proceedings of Indian National Science Academy, 56A*, 501–511.

Pardasaradhi, Y. J., & Vaidyanadhan, R. (1974). Evolution of landforms over the Nilgiri, South India. *Journal-Geological Society of India, 15*, 182–188.

Parkash, B., Kumar, S., Rao, M. S., Giri, S. C., Kumar, C. S., Gupta, S., & Srivastava, P. (2000). Holocene tectonic movements and stress field in the western Gangetic plains. *Current Science, 79*, 438–449.

Patel, M. P., & Bhatt, N. (1995). Evidence of palaeoclimatic fluctuation in miliolitic rocks of Saurashtra, western India. *Journal-Geological Society of India, 45*, 191–200.

Petroglia, M., Korisettar, R., et al. (2007). Middle Palaeolithic assemblages from the Indian subcontinent before and after the Toba super-eruptions. *Science, 317*, 114–116.

Powar, K. B. (1993). Geomorphological evolution of the Konkan coastal belt and adjoining Sahyadri upland with reference to Quaternary uplift. *Current Science, 64*, 793–796.

Prasad, Sushma, Kusumgar, S., & Gupta, S. K. (1997). A mid to late Holocene record of palaeoclimatic changes from Nal Sarovar: A palaeodesert margin lake in western India. *Journal of Quaternary Science, 12*, 153–159.

Sinha, R. Yadav, G. S., Gupta, S., Singh, A. & Lahiri, S. K. (2012). Geoelectric resistivity evidence for subsurface palaeochannel system adjacent to Harappan sites in NW India. *Quaternary International*. doi:10.1016/J.Quart.2012.08.002

Radhakrishna, B. P. (1964). Evolution of the Sharavati drainage, Mysore State, South India. *Journal-Geological Society of India, 5*, 72–79.

Radhakrishna, B. P. (1993). Neogene uplift and geomorphic evolution of the Indian Peninsula. *Current Science, 64*, 787–792.

Raghav, K. S. (1999). Evolution of drainage basin in parts of northern and western Rajasthan. *Memoirs-Geological Society of India, 42*, 175–185.

Raj, R. (2004). Fluvial response to Later Quaternary tectonic changes in the Dhadhar River basin, Mainland Gujarat. *Journal of the Geological Society of India, 64*, 666–676.

Rajaguru, S. N., & Kale, V. S. (1985). Changes in the fluvial regime of western Maharashtra upland rivers during Later Quaternary. *Journal-Geological Society of India, 26*, 16–27.

Rajaguru, S. N., & Korisettar, R. (1987). Quaternary geomorphic environment and cultural succession in Western India. *Indian Journal of Earth Sciences, 14*, 349–361.

Rajashekhar, C., & Kumaran, K. P. N. (1998). Micropalaeontological evidence for tectonic uplift of near-shore deposits around Bankot–Velas–Ratnagiri District, Maharashtra. *Current Science, 74*, 705–708.

Rajendran, P., Bharath Kumar, P., & Bhanu, B. V. (2003). Fossilized hominid baby skull from the ferricrete at Odai, Bommayarpalayam, Villupuram District, Tamil Nadu, South India. *Current Science, 84*, 754–756.

Ramasamy, S. M. (1999). Neotectonic controls on the migration of Sarasvati River of the Great Indian desert. *Memoirs Geological Society India, 42*, 153–162.

Ramasamy, S. M. (2006). Remote sensing and active tectonics of South India. *International Journal of Remote Sensing, 27*, 4397–4431.

Ramasamy, S. M., Bakliwal, P. C., & Verma, R. P. (1991). Remote sensing and river migration in western India. *Internal Journal Remote Sensing, 12*, 2597–2609.

Raval, U. (1995). Geodynamics of the tectonomagmatic and geophysical signatures within mobile parts of the transect. *Memoirs-Geological Society of India, 31*, 37–61.

Rengamannar, V., & Pradhan, P. K. (1991). Geomorphology and evolution of Godavari delta. *Memoirs Geologist Society India, 22*, 51–56.

Sahai, B. (1999). Unravelling of the lost Vedic Saraswati. Memoirs-Geological Society of India, 121–141.

Saini, H. S., Tandon, S. K., Mujtalia, S. A. I., Pant, N. C., & Khorana, R. K. (2009). Reconstruction of buried channel-floodplain system of northwestern Haryana Plains and their relation to the Vedic Saraswati. *Current Science, 97*, 1634–1693.

Sangode, S. J., Mishra, S., Naik, S., & Deo, S. (2007). Magnetostratigraphy of the Quaternary sediments associated with some Toba tepha and Acheulian artefacts-bearing localities in the western and central India. *Gondwana Geological Magazine, 10*, 111–121.

Sankhyan, A. R., Dewangan, L. N., Chakraborty, S., Kundu, S., Prabha, S., Chakrabarty, R., & Badam, G. L. (2012). New human fossils and associated findings from the Central Narmada Valley India. *Current Science, 103*, 1461–1469.

Senaratne, A., & Dissanayake, C. B. (1982). Palaeogeographic reconstruction of the Jaffna Peninsula, Sri Lanka. *Journal-Geological Society of India, 23*, 545–550.

Shanker, R. (1991). *Geothermal atlas of India*. Kolkata: Geological Survey of India.

Singh, G., Joshi, R. D., Chopra, S. K., & Singh, A. B. (1974). Late Quaternary history of vegetation and climate of the Rajasthan desert, India. *Philosophical Transactions of the Royal Society of London, 267B*, 467–501.

Singh, Kharak, Radhakrishna, M., & Pant, A. P. (2007). Geophysical structure of the western offshore basins of India and its implications to the evolution of the Western Ghats. *Journal-Geological Society of India, 70*, 445–458.

Singhvi, A. K., & Kar, A. (1992). *Thar desert in Rajasthan: Land man and environment* (p. 186). Bangalore: Geological Society of India.

Sinha, R., & Friend, P. F. (1994). River systems and their sediment flux Indo-Gangetic plains, Northern Bihar, India. *Sedimentology, 41*, 825–845.

Sinha, R., Gibling, M. R., Tandon, S. K., Jain, V., & Dasgupta, A. S. (2005). Quaternary stratigraphy and sedimentology of the Kotra section of the Betwa river, Southern Gangetic plains, Uttar Pradesh. *Journal of the Geological Society of India, 65*, 441–450.

Sinha, R., & Jain, K. (1998). Flood hazards of north Bihar rivers, Indo-Gangetic Plains. *Memoirs-Geological Society of India, 41*, 27–52.

Sinha, R., & Raymahashay, B. C. (2004). Evaporite mineralogy and geochemical evolution of the Sambhar Salt Lake Rajasthan. *Sedimentary Geology, 166*, 59–71.

Sinha, R., Stueben, P., & Berner, Z. (2004). Palaeohydrology of the Sambhar playa, Thar desert, India, using geomorphological and sedimentological evidences. *Journal-Geological Society of India, 64*, 419–430.

Sinha-Roy, S. (2001). Neotectonically controlled catchment capture: An example from the Banas and Chambal drainage basins, Rajasthan. *Current Science, 80*, 293–298.

Sinha-Roy, S., Mohanty, M., & Guha, D. B. (1993). Banas dislocation zone in Nathadwara-Khannor area Udaipur District, Rajasthan and its significance on the basement-cover relations in the Aravali fold belt. *Current Science, 65*, 68–72.

Sonakia, A. (1984). The skull cap of Early man and associated mammalian fauna from Narmada valley alluvium, Hoshangabad area, M.P. (India). *Record Geological Survey of India, 113*, 159–172.

Sridhar, V., Chamyal, L. S., & Merh, S. S. (1994). North Gujarat rivers: Remnants of super fluvial system. *Journal-Geological Society of India, 44*, 427–434.

Srivastava, P., Singh, I. B., Sharma, S., Shukla, U. K., & Singhvi, A. K. (2003). Late Pleistocene-Holocene hydrologic changes in the interfluve areas of the central Ganga Plain India. *Geomorphology, 54*, 279–292.

Subrahmanya, K. R. (1994). Post-Gondwana tectonics of Indian Peninsula. *Current Science, 67*, 527–530.

Subrahmanya, K. R. (2002). Deformation-related lineaments in the Indian Peninsula near 13º N. *Indian Journal of geophysics, 23*, 59–68.

Subrahmanyam, B. (1985). Lonar crater: A crypto-volcanic origin. *Journal-Geological Society of India, 26*, 326–335.

Tandon, S. K., Sareen, B. K., Someshwar Rao, M., & Singhvi, A. K. (1997). Aggradation history and luminescence chronology of Late Quaternary semi-arid sequences of the Sabarmati basin, Gujarat, Western India. *Palaeogeography, Palaeoclimatology, Palaeoecology, 128*, 339–357.

Tewari, H. C., Murty, A. S. N., Kumar, P., & Sridhar, A. R. (2001). A tectonic model of Narmada region. *Current Science, 80*, 873–878.

Thakkar, M. G., Goyal, B., Patidar, A. K., Maurya, D. M., & Chamyal, L. S. (2006). Bedrock gorges in the central mainland Kachchh: Implications for landscape evolution. *Journal of Earth System Science, 115*, 249–256.

Thakkar, M. G., Maurya, D. M., Rau, Rachna, & Chamyal, L. S. (1999). Quaternary tectonic history and terrain evolution of the area around Bhuj, Mainland Kachchh. *Journal-Geological Society of India, 53*, 601–610.

Thussu, J. L. (1995). Quaternary stratigraphy and sedimentation of the Indo-Gangetic plains, Haryana. *Journal-Geological Society of India, 46*, 533–544.

Tiwari, M. P., & Bhai, H. Y. (1997a). Geomorphology of the alluvial fill of the Narmada valley. *Special Publication Geological Survey of India, 46*, 9–18.

Tiwari, M. P., & Bhai, H. Y. (1997b). Quaternary stratigraphy of the Narmada valley. *Special Publication Geological Survey of India, 46*, 33–63.

Tomar, S., & Tomar, A. (1995). Identification and mapping of the changing course of the Son River from the epic time to present time, using remote sensing techniques. *Asian Pacific Remote Sensing Journal, 7*, 62–65.

Vaidyanadhan, R., & Ghosh, R. N. (1993). Quaternary of the East Coast of India. *Current Science, 64*, 804–816.

Valdiya, K. S. (1998). Late Quarternary movements on landscape rejuvenation in southeastern Karnataka and adjoining Tamil Nadu in Southern Indian shield. *Journal-Geological Society of India, 51*, 139–166.

Valdiya, K. S. (2001a). River response to continuing movements and scarp development in central Sahyadri and adjoining coastal belt. *Journal-Geological Society of India, 57*, 13–30.

Valdiya, K. S. (2001b). Tectonic resurgence of the Mysore plateau and surrounding regions in cratonic Southen India. *Current Science, 81*, 1068–1089.

Valdiya, K. S. (2002). *Saraswati: The River that Disappeared* (p. 116). Hyderabad: Universities Press.

Valdiya, K. S., & Narayana, A. C. (2007). River response to neotectonic activity: Example from Kerala, India. *Journal-Geological Society of India, 70*, 427–443.

Valdiya, K. S., & Rajagopalan, G. (2000). Large palaeolakes in Kaveri basin in Mysore Plateau: Late Quaternary fault reaction. *Current Science, 78*, 1138–1142.

Vaz, G. G., Subba Rao, V., & Ravi Kumar, V. (2006). Thermal springs in Indian coastal areas of the Palk Bay: Their implications in relation to lineaments, coastal morphology and seismicity. *Journal-Geological Society of India, 68*, 593–596.

Venkatesh, V. (1967). The Lonar Crater—some geochemical data. *Journal-Geological Society of India, 8*, 29–37.

Wadia, D. N. (1942). *The making of India, presidential address*, *Proceedings of the 29th Indian Science Congress, Part II, Kolkata* (pp. 91–118).

Widdowson, M. (1977). Tertiary palaeosutures of SW Deccan, Western India: Implications for passive margin uplift. *Geological Society of London, Special Publications, 120*, 221–248.

Wasson, R. J. (1995). The Asian monsoon during the Late Quaternary: Test of orbital forcing. In S. Wadia, et al. (Eds.), *Quaternary environments and geoarchealogy of India* (pp. 22–35). Bangalore: Geological Society of India.

Widdowson, M., & Cox, K. G. (1996). Uplift and erossional history of the Deccan Traps, India: Evidence from laterites and drainage patterns of the Western Ghats and Konkan Coast. *Earth and Planetary Science Letters, 137*, 57–69.

Chapter 24
Quaternary Developments in Himalaya

24.1 Morphogenic Phase

24.1.1 Rapid Uplift

The Quaternary period represents morphogenic phase of the evolution of the Himalaya (Gansser 1964, 1991). It was during this period that the Himalaya rose up to attain its present spectacular height and form (Valdiya 1993b). There is an overwhelming evidence of acceleration of erosion due to uplift in the temporal interval 0.8–0.9 Ma in Tibet, in the Himalaya and in the Indo-Gangetic Plains. The uplift of the Himalaya was five times faster than that of the Alps. Testimonies of vertebrates including rhinos, hippos and elephants and of spores and pollens support the postulation that the Tibetan landmass raised rapidly to the elevation above 5000 m in the Quaternary time (Shackleton and Chang 1988).

24.1.2 Rugged Youthful Himadri

The Nanga Parbat–Haramosh Massif in north-western Kashmir is rising at the rate of 3–4 mm/year (Whittington 1996). The rate of uplift of the Karakoram terrane north of the Indus–Tsangpo Suture is about 2 mm/year (Zeitler et al. 1982). The consequence of this fast rate of uplift is the faster rate of erosion. The Sindhu River has carved a deep valley parallel to the active thrust boundary creating extreme local relief in the Nanga Parbat Massif. Constrained on the basis of the bedrock incision made by the Sindhu River in the Nanga Parbat region, the rate of erosion is computed at 2–12 mm/year (Burbank et al. 1996). In situ cosmogenic ^{10}Be and ^{26}Al exposure age dating of straths abandoned by progressive

K.S. Valdiya, *The Making of India*, Society of Earth Scientists Series,
DOI 10.1007/978-3-319-25029-8_24

incision of the Sindhu River in northern Pakistan showed that the rate of erosion increased from 1–6 mm/year before 7000 yr B.P. to 9–12 mm/year after that time (Leland et al. 1998). Upstream in the Leh–Upshi Belt in the Ladakh region, the rate of incision came down from 2 mm/year in the period 22,000–15,000 yr B.P. to 0.3–0.4 mm/year after 15,000 yr B.P. (Sharma et al. 1998). In the Nubra Valley, the Shyok volcanics and the Baltoro Granite bear evidence of reactivation of the *Karakoram Fault* in the period 20–10 Ma and 13.9 ± 0.1 Ma (Bhutani et al. 2003). Significantly, the block of the 21.05-Ma-old Baltora Granite has been rotated clockwise into a NW–SE alignment east of the Siachin Glacier with a maximum offset along the 90-km-long fault (Searle 1986). The course of the Sindhu River was offset dextrally by 120 km south of the Pangong Lake in the last 4 million years, possibly during the time of the origin of the Karakoram Fault. The displacement of a debris-flow deposit dated 11–14 ka by the ^{10}Be method, and the offsetting of a 1–2 km fan indicates that the average rate of slip on the Karakoram Fault is 4 ± 1 mm/year (Brown et al. 2002). It is obvious that the erosion rate varies from belt to belt, understandably due to the variable degree of activeness of the faults dissecting the terrain as well as variation in climate conditions. The dissection by rivers is highest in the region of the two syntaxial bends.

The entire *Himadri (Great Himalaya)* domain is rising at very fast rate. The rapid rise has resulted in development of a very lofty mountain barrier characterized by formidable scarps, soaringly high peaks and pronounced incisions in river valleys. The channel pattern of the rivers Brahmaputra, Kosi, Karnali, Ganga, Satluj and Sindhu is remarkably independent of the tectonic trend which is controlled by intracrustal faults and thrusts. Without deflecting, these rivers cross the Great Himalayan mountain barrier and enter the relatively gentler terrain of the Lesser Himalaya through deep canyons. In the northern margin defined by the Trans-Himadri Detachment Fault, the antecedent rivers have carved slit canyons (Valdiya 2005). In the southern zone related to the Main Central Thrust (MCT), the rivers are characterized by gorges that have convex to nearly vertical walls and steep riverbed gradients marked by knickpoints. These features imply that between the very active Trans-Himadri Detachment Fault and the Main Central Thrust, the Himadri is rising up at a very fast rate—being squeezed up like a lithotectonic slab. In the Nepal sector, the erosion rate all through the zone of nearly 20 km length between the Main Central Thrust and the Trans-Himadri Fault is the same, implying nearly uniform upward tectonic transport—thrusting up—of the Great Himalayan rocks. This has caused extraordinary ruggedness of the mountain ranges and youthfulness of its landforms.

24.1.3 Milder, Mature Lesser Himalaya

Sprawling between the Himadri and the Siwalik, the *Lesser Himalaya* subprovince has a topography that is comparatively gentle. The geomorphically mature terrain is characterized by rounded mountains having strikingly even summits, gentler

mountain slopes and extraordinarily wide valleys associated with short stretches of undulating plains and flats. The tributary streams flow windingly or even tortuously before descending into deep valleys of trunk rivers. This is commonly discernible in the middle belt of the central sector of the Himalaya. Striking changes are seen in the behaviour of the windingly flowing or meandering streams as they approach active faults. They become progressively entrenched in their channels and cut deep gorges or simply plummet down through chasms—as much as 200–300 m. This is seen on the sides of the Nainital Massif involved in the active tectonics of the Main Boundary Thrust (Valdiya 1988b). In many sections, regional thrusts that have emplaced crystalline nappes upon sedimentary autochthon are associated with huge fans or cones of debris deposits, presumably resulting from mass-movements triggered by movements on the thrust planes. At the crossings of these thrusts, rivers and streams have carved narrow valleys or gorges, adding to the topographic splendour and ruggedness of the terrain. The gentler mountain slopes and the undulating plains wear thick covers of soils. These features are indicative of an advanced stage of the peneplanation the Lesser Himalaya went through during the Early Pleistocene when climatic conditions were warm and wet.

In central Nepal, the rate of uplift of the Lesser Himalayan terrain is 3 mm/year (Jackson and Bilham 1994). The situation is nearly the same throughout the central sector. The consequence of the secular uplift is the superposition of a youthful topography on the matured relief of the Early Pleistocene time (Valdiya 1993b). Practically all rivers and major streams are characterized by paired or unpaired depositional terraces. Commonly there are three levels of terraces and locally six (Khan et al. 1982), invariably upstream of the points where the faults cross the valleys. Where faults are active, the number of terraces is more than three. Upstream of the Tehri Dam between Chham and Bhaldiyana where the active Srinagar Thrust follows the Bhagirathi River, there are six terraces, implying three more pulses of uplift in the post-Upper Pleistocene–Lower Holocene period of the formation of the common three terraces.

24.1.4 Resurgent Siwalik

South of the Main Boundary Thrust, the *Siwalik terrane* comprises rugged youthful ranges rising to the elevation of 1700–1800 m above the sea level in southern Kumaun. Immediately to the north of the Main Boundary Thrust, the Lesser Himalayan ranges also are ruggedly high (more than 2100 m), such as the Dhauladhar in western Himachal, the Mussoorie–Nainital Range in Uttarakhand and the Mahabharat Range in central Nepal. The ruggedness of the Siwalik mountain barriers is broken by high scarps. Northward-hurrying streams descend on steep slopes which are covered in many places by colluvial fans and cones. Rivers cross this mountain barrier through gorges and narrow valleys. These valleys have raised point-bar deposits. Obviously, the northern belt of the Siwalik rose up recently at a rate much faster than that of the southern belt, owing to

subrecent–recent movements on active faults that cut the Siwalik terrane longitudinally. One such active thrust fault is seen north of Paonta Sahab in Himachal Pradesh, where the Lower Siwalik sandstone has moved southwards along the Markanda Thrust to ride over the Dun Gravel (Joshi et al. 2005).

In the Darjeeling sector, the Main Boundary Thrust is folded into a faulted synform-antiform pair by neotectonic activity along a younger thrust in the footwall (Siwalik). The younger fault cuts through the fault-propagation structure of the hanging wall (Mukul 2000). In this sector, the footwall imbrication stretches southwards over a width more than 30 km. The imbrication of fault blocks has raised the riverbed and arrested the flow of the Tista, resulting in the formation of a bar upstream of the MBT trace.

In many sectors, the middle belt of the Siwalik has a remarkably gentle topography characterized by aggradational flat expanses called *duns*. The *duns* represent synclinal valleys filled up thickly by gravel deposits during the Later Pleistocene to Early Holocene time. These deposits are known as the *Dun Gravel* (Nakata 1972). In some area, the Dun gravels are covered partially by younger debris fans.

24.2 River Ponding and Lake Formation

24.2.1 Fault Reactivation

Movements on active faults entailing uplift or strike-slip displacement of the footwall caused blockage of flows of rivers and streams, resulting in the formation of lakes upstream of the fault crossings. Where the rivers and streams carried larger quantities of sediment load and the ponding or blockage lasted longer time, the lakes were filled up and converted into flat stretches of sediments. These represent the *palaeolakes* comprising predominant clays and muds with lenses or interfingering of gravels of fluvial and/or colluvial origin. In the areas where the sediment discharges were smaller and the blockage occurred not long ago, the ponding is represented by lakes in an essentially fluvial regime, such as the *Nainital* and *Bhimtal* (*tal* = lake) in Kumaun, and the *Rara* and *Pokhara lakes* in Nepal. Thermoluminescence dating of fault gouges, coupled with radiocarbon dating of basal sediments of lakes in Ladakh, Himachal and Kumaun, shows that the lakes formed sometime in the period 60,000 and 40,000 yr B.P., (Singhvi et al. 1994; Banerjee et al. 1999). Bathymetric survey of the Naini Lake, unravelling deformation of lake-bottom sediments, shows that tectonic movement continues to take place in the present on the NW–SE trending tear fault (Hashimi et al. 1988).

24.2.2 Palaeolakes in Tethys Terrane

Nestling at the altitude of 1700–1800 m above the sea level between the 3000–3200 m Pir Panjal and more than 4000-m-high Zanskar ranges, the Dal and Wular

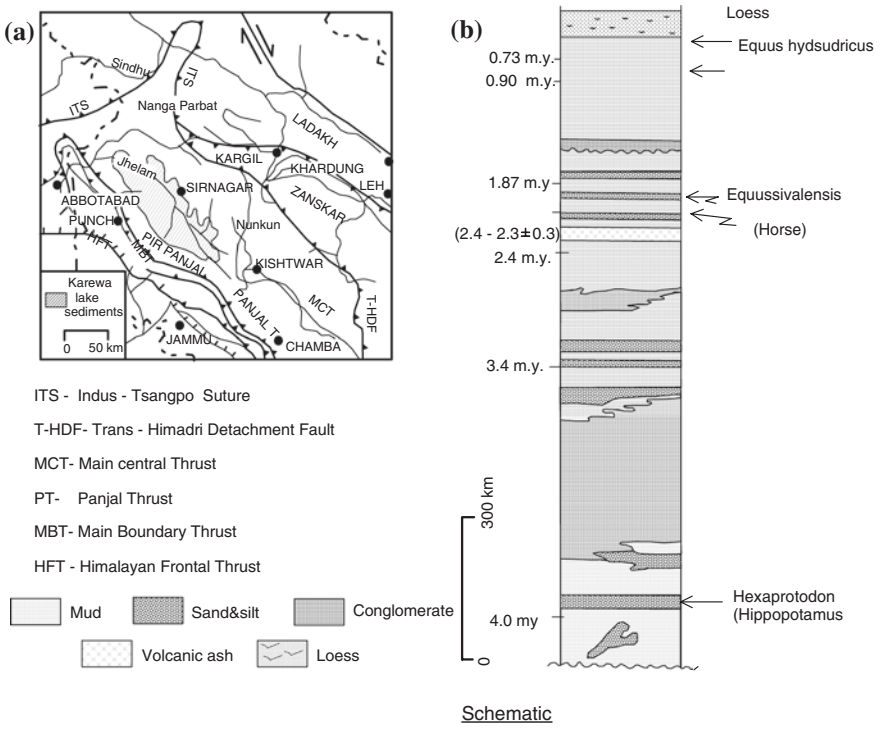

Fig. 24.1 **a** Location of the Karewa palaeolake in the tectonic framework of NW Himalaya (after Thakur 1987). **b** Lithological column of the Karewa Group showing positions of the gravel lenses of tectonic origin and of the vertebrate-bearing horizons (after Kotlia 1990)

lakes in Kashmir are remnants of a once large lake (Fig. 24.1a) formed due to ponding of the Jhelam. It was the uplift nearly 4 million years ago of the Pir Panjal along one of the thrusts of the Main Boundary Thrust–Panjal Thrust system that was responsible for the formation of the *Karewa Palaeolake*. The lake is represented by a 1300-m-thick sedimentary succession described comprehensively by H. DeTerra and T.T. Paterson in 1939. The *Karewa Group* (Bhatt 1976; Agrawal et al. 1989) of dominant clays and muds contains at different levels several big and small lenses of gravels generated by landslides or debris flows triggered by tectonic movements on active faults (Burbank and Johnson 1983). At the top is a 10- to 20-m-thick mantle of *loess* formed by strong wind action during dry spells of climate. Within the loess sequence, there are several horizons of *palaeosols* formed during warm–wet interludes between 80,000 yr B.P. and 50,000 yr B.P. (Pant et al. 1985; Bronger et al. 1987) and some in the last 25,000 years (Kusumgar et al. 1985, 1992).

The Karewa sediments contain at various levels remains of large-sized heavy vertebrate animals such as *Hexaprotodon* (hippopotamus), *Rhinoceros* (rhino) and *Elephas hysudricus* (elephant) in addition to *Equus sivalensis* (horse), *Cervus*

punjabiensis (deer), *C. sivalensis*, *Canis vitastensis* and the rodents *Kilarkola* and *Microtus* (Kotlia 1990, 1991). The faunal assemblages point to the existence of a marshland in a terrain that must have been gentle, possibly not a few hundred metres above the sea level. Plant remains in the middle level indicate prevalence of temperate to warm climate (Awasthi 1982).

The southern part of the Karewa on the Pir Panjal flank with fingers of terraces was faulted up to the elevation of 2700–3000 m, giving rise to what is known as *margs*. The *margs* are lacustrine–eolian terraces occurring high up on the mountain slopes (Bhatt 1978), such as Gulmarg and Khillanmarg. Continuing movements on faults culminated in the opening of the Baramula Gorge and substantial draining out of the Karewa palaeolake around 20,000 yr B.P. (Agrawal et al. 1989). The remnants of that palaeolake are the present Wular and Dal lakes.

Uplift rate of the Pir Panjal in the post-Karewa time is estimated to be 3.5–10.0 mm/year (Burbank and Johnson 1983). Its south-easterly extension, the Dhauadhar Range, likewise rose up on a NW–SE trending active fault along which the Ravi has carved its course. The reactivation of this fault caused blockage in the Ravi and emplacement of 250-m-thick deposit over a length of 20 km in the 3-km-wide valley (Joshi and Tandon 1987; Tandon and Josh 1991; Joshi 2004).

West of Leh in Ladakh, a tectonically induced landslide built a debris dam across the Lamayuru River, sometime during the 35,000–45,000 yr B.P. period (Fort et al. 1989; Bagati et al. 1996; Phartiyal et al. 2005). The 110-m-thick *Lamayuru succession* comprises turbidites, laminated muds and lenses of debris-flow deposits along the margin of the lake. Bivalves, gastropods and ostracods occurring in the basal horizon indicate that the sedimentation alternated between fluvial and lacustrine environments and ended up in the formation of a delta (Mathur and Kotlia 1999).

In northern Uttarakhand, the Tethyan succession of sedimentary rocks is detached from its basement along the Trans-Himadri Detachment Fault. Reactivation of this active terrane-boundary fault resulted in the ponding of the rivers Western Dhauli, Gori, the Eastern Dhauli and Kali (Valdiya 2005). The resulting lakes (Fig. 24.2) stretched 7–15 km upstream of the dam formed by the uplift of the footwall (made up of Vaikrita crystalline rocks) and attendant massive landslide debris and movement of moraines in the terrain of glaciers. Soft-sediment deformation structures, including *seismites* at various levels including at the base indicate that movement on the T-HDF continued during the sediment-filling of the lakes (Valdiya 2001c). The *Goting Palaeolake* was formed earlier than 40,000 yr B.P. (Pant et al. 1998), and in the *Garbyang Palaeolake* tectonic movements occurred in the intervals 20,000–17,000 yr B.P. and 14,000–13,000 yr B.P. (Juyal et al. 2004). The seismites show that the T-HDF was active in the interval 16,000–11,000 yr B.P. at Burphu in the Gori Valley (Pant et al. 2006). These movements eventually led to the breaking of the debris dams and draining out of the lakes. As the lakes drained out, the rushing waters cut spectacular slit canyons downstream of the fault crossings.

In north-central Nepal, the Thakkhola half graben (Fig. 16.7) resulting from dextral strike-slip movement on a NNE–SSW trending fault in the Later Pliocene time was the site of a large lake that continued to exist until the Pleistocene (Fort et al. 1982).

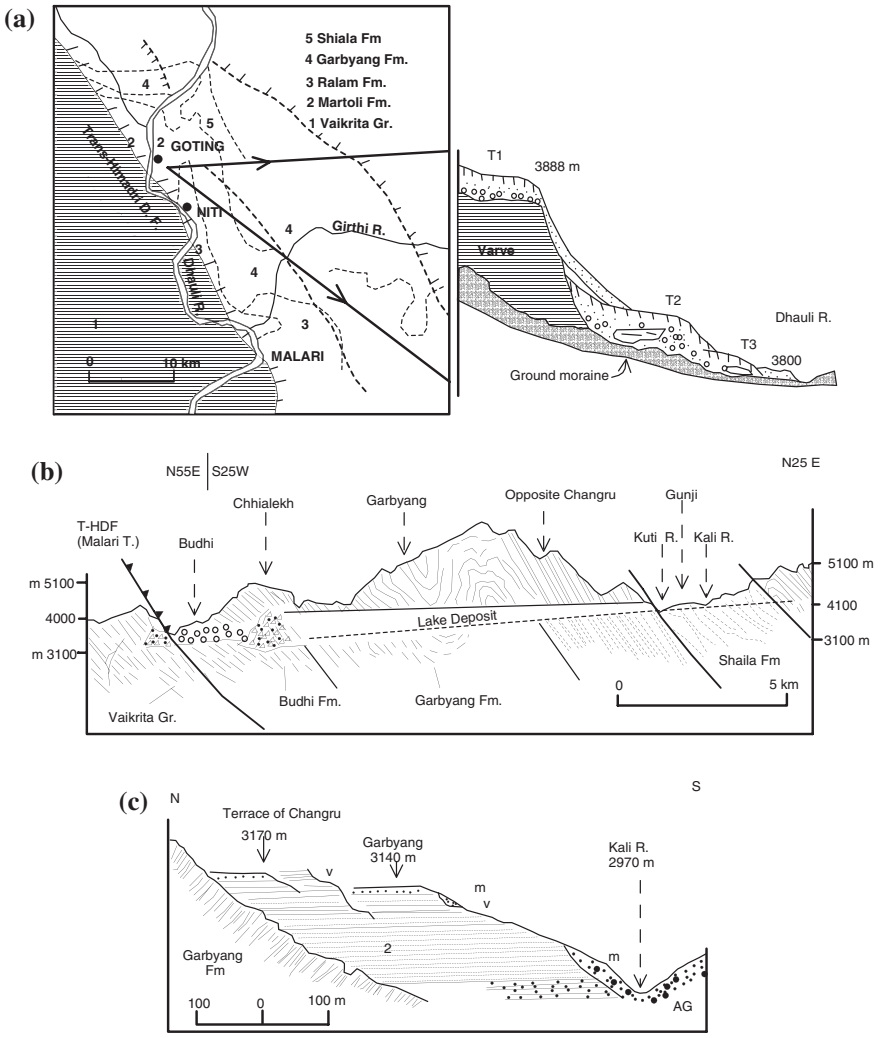

Fig. 24.2 Ponding or blockage of the rivers Western Dhauli, Eastern Dhauli and Kali in northern Kumaun gave rise to large lakes in the Tethys Himalaya. **a** Simplified geological map showing the active Trans-Himadri Fault crossing the Western Dhauli, and causing formation of slit canyons at Malari, south and north of Niti and of a lake at Goting (modified after Pant et al. 1998). **b** The Kali River was ponded near Garbyang due to movement on the T-HDF (after Valdiya 2005). **c** Sedimentary succession of the Garbyang palaeolake (after Heim and Gansser 1964)

24.2.3 River Ponding in Lesser Himalaya

In the Kathmandu Basin at the elevation of 1360–1550 m between the Sheopuri Range in the north and the Mahabharat Range in the south, there is a 284-m succession of fluviolacustrine sediments representing the *Kathmandu Palaeolake*.

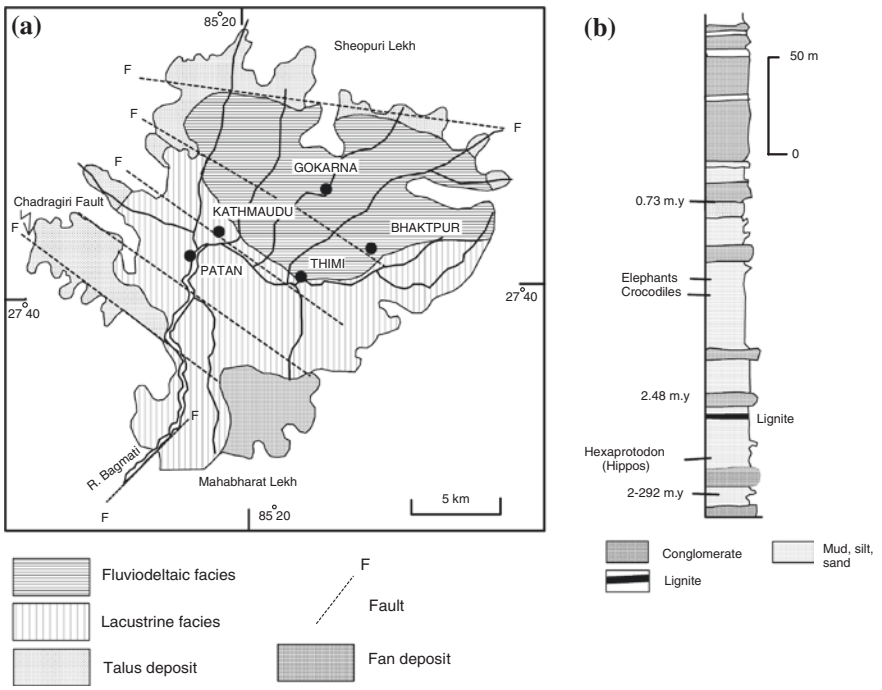

Fig. 24.3 **a** Environment of deposition of sediments in the Kathmandu Palaeolake, 2.8 Ma–1.1 Ka in age (after Sakai 2001). **b** *Column* shows the lithology of the Kathmandu Group and locations of fossiliferous horizons (after Yoshida and Gautam 1988)

The formation of the lake commenced 2.8 million years ago (Yoshida and Gautam 1988; Sakai 2001). It was a consequence of reactivation of an east–west fault that caused uplift of the Chandragiri Hills and attendant ponding of the Bagmati River. Movements on a NE–SW oriented 80–90° west dipping tear fault triggered the draining out of the lake at 11,000 yr B.P.

The initial fluvial regime subsequently became lacustrine. Later, the axial dispersal of sediments gave way to fluvial deltaic accumulation, mainly from the limbs of the Kathmandu synclinorium (Figs. 24.3 and 24.4). Ongoing compression with attendant uplift gave rise to a water-divide within the lake basin, and its subdivision into two sub-basins (Dill et al. 2001, 2003). Wedges of debris-flow deposits interfinger with floodplain sediments. Three highstands of water level dated >30,000 yr B.P., 28,000–19,000 yr B.P. and 11,000–4000 yr B.P. are recognizable in the sedimentary record of the Kathmandu palaeolake.

Early Pleistocene vertebrate fauna consisting of *Elephas planifrons, E. hysudricus, Stegodon ganesa, Hexaprotodon sivalensis, Crocodylus* and *Rhinoceros* together with cervids, bovids and suids in the lower part of the *Kathmandu Group* (Yoshida and Gautam 1988; Gautam et al. 2001) recalls very similar fauna of the Karewa Lake in Kashmir and of the Upper Siwalik vertebrate life in the Jammu

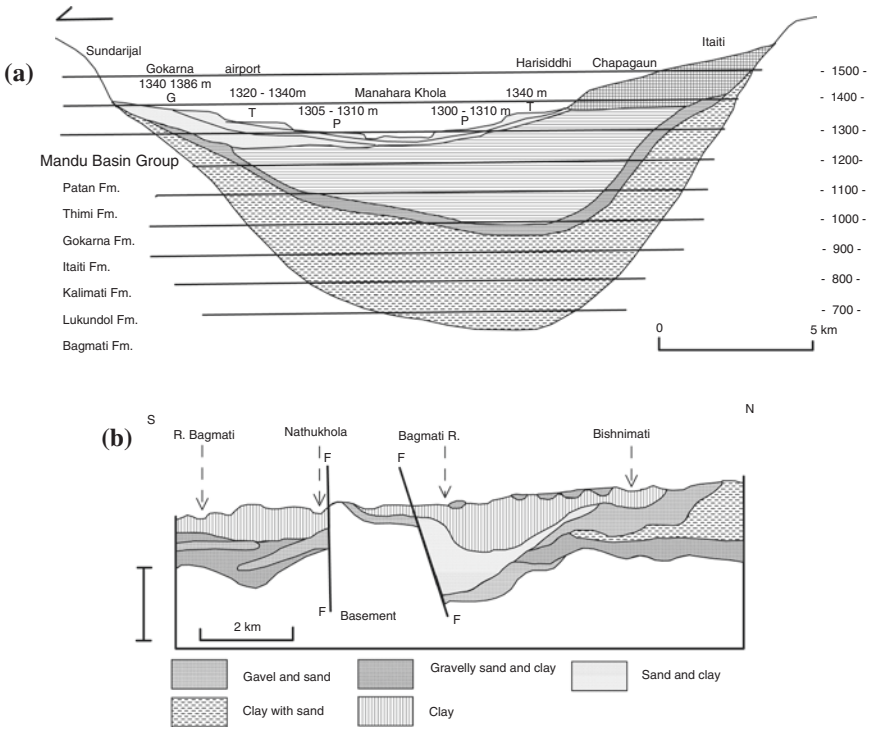

Fig. 24.4 Schematic cross sections of the Kathmandu Palaeolake basin portray two different perceptions of the sedimentary tectonics of the Kathmandu Basin **a** after (Sakai 2001); **b** after (Dill et al. 2001)

Basin. The striking resemblance of the fauna in the three widely separated areas belonging to three different lithotectonic terranes is very significant.

In south-central Kumaun, there are a number of lakes related to the dynamics of the faults of the Main Boundary Thrust zone. The *Naini Tal* and *Bhim Tal* (*tal* = lake), among others, owe their origin to movements on the faults that constitute conjugate pairs of the NW–SE and NE/N–SW/S trending faults. While the NW–SE faults show right-lateral strike-slip displacement, the NE/N- to SW/S-oriented faults are characterized by left-lateral movement (Valdiya 1988b). One of these lakes—the once continuous Bhimtal–Naukuchiatal Basin—contains 52-m-thick deposits with remains of the Soricidae and Muridae families of rodents together with spores and pollens of *Quercus, Pinus, Alnus* and *Betula* (Kotlia 1995; Kotlia et al. 1997).

At the foot of the Himadri in the northern belt of the Lesser Himalaya, the ponding of the Saryu River is represented by the *Dulam Palaeolake* characterized by 30,000-year-old murid rodents (*Soriculus, Mus, Golunda*), bovids, cyprinidae fish, lizard, ostracodes and gastropods, testifying to the existence of savanna, grassland and bushland in the lake basin (Kotlia and Jayshri Sanwal 2004).

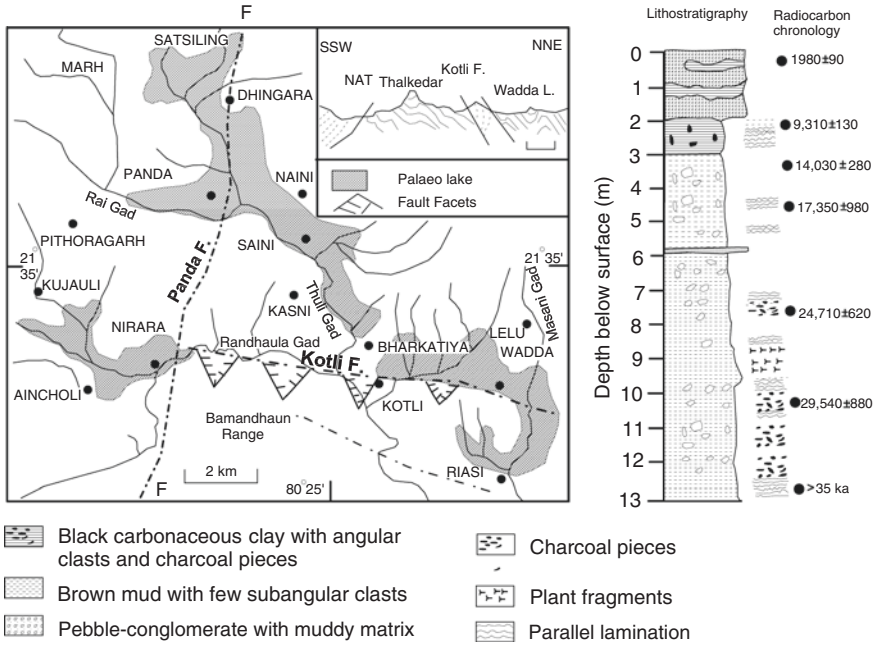

Fig. 24.5 Ponding of the Thuli Gad and its tributaries due to uplift along the Kotli Fault was responsible for the formation of the Late Pleistocene Wadda Palaeolake around Pithoragarh (in the Sor Valley) in eastern Kumaun (after Valdiya and Kotlia 2001)

In eastern Kumaun, the township of Pithoragarh is surrounded on three sides by black clay deposits of the lake that was formed as a result of the footwall rising up along an E–W trending fault (Fig. 24.5). The Thuli Gad and its tributary streams were ponded, giving rise to the *Wadda Palaeolake*, represented by 7- to 13-m-thick deposits of black clays (Valdiya and Kotlia 2001). The upper part of the lacustrine succession interfingers with lenticular beds of flat-pebble conglomerate and is covered by fans of finer gravel representing sheet wash. The lake that was formed more than 35,000 yr B.P., drained out by 10,000 yr B.P. (Kotlia et al. 2000) although some remnants existed until about 2000 yr B.P.

24.2.4 Developments in Siwalik Domain

1. Tectonic movements along intra-basinal faults west of the Gaula River in south-central Kumaun decreased the gradients of streams and rivers in the Siwalik terrane. This leads to dumping of their sediment load and accumulation of thick piles of very coarse detrital deposits during the Late Pleistocene–Early Holocene period. The gravel deposits are described as the *Dun Gravel* (Fig. 24.6). At places in the distal part, the Dun Gravel contains

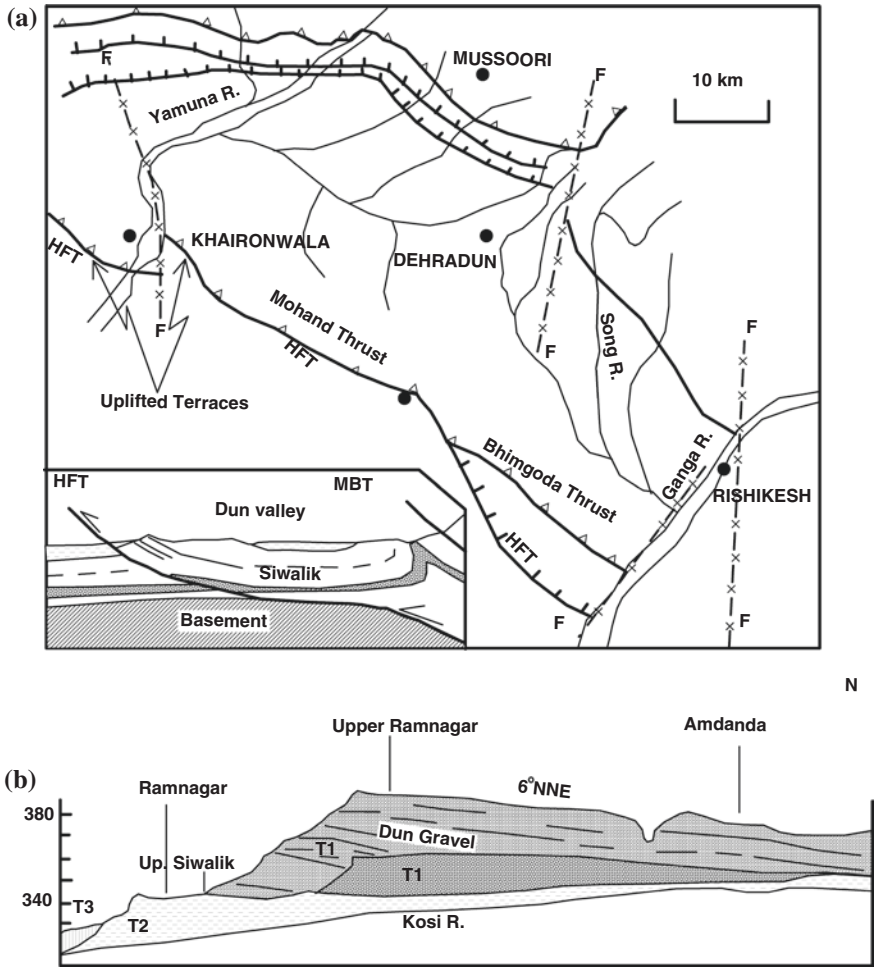

Fig. 24.6 **a** Siwalik domain in the Dehradun region is left-laterally offset by a tear fault along the Yamuna River. A 20–30 m uplift of a fluvial terrace immediately south of the Himalayan Frontal Thrust (HFT) in the section (*Inset*) containing 3663 ± 215 year old organic matter indicates uplift along the Himalayan Frontal Thrust. The part between MBT and HFT is made up of the Dun Gravel (after Valdiya 2005). **b** Tilted Dun Gravel in the Kosi Valley in south-central Kumaun is overlain by the New Dun deposits forming two fluvial terraces (after Valdiya et al. 1992)

laminated clays, indicating deposition in lakes and ponds—or ponded streams. Reactivation of these faults not only caused tilting (15–20°) and deformation of the Dun Gravel (Nakata 1972; Valdiya et al. 1992; Rautela and Sati 1996; Thakur and Pandey 2004) but also subsequent development of the *Newer Dun* (Rao 1977) representing large debris fans formed after the decrease in stream gradients in the Later Holocene time. These developments are related to the

neotectonics of the *Himalayan Frontal Thrust* that delimits the Siwalik against the Ganga Plain. There are clear signatures of Quaternary tectonic activities in parts of the Dehra Dun (Kandpal et al. 2006). In south-central Kumaun, a 60- to 90-m-high scarp on the northward-tilted Dun Gravel, and the streams breaking through this hill front showing deep incised meanders indicate uplift on the Himalayan frontal Fault (Valdiya 1992; Valdiya et al. 1992). Significantly, a 20–30 m uplift of fluvial terrace containing 3663 ± 215 year old organic matter near the Yamuna Gorge (Wesnousky et al. 1999) points to the Holocene movements that have taken place along the Himalayan Frontal Thrust. A WNW–ESE trending 5- to 25-km-high fault scarp discernible between Nangal and Jhandian across the Pinjaur Dune is related to an echelon fault system (Philip and Virdi 2007). Alluvial fans dated (OSL) 85.83 ± 7.7 ka to 67.05 ± 8.4 ka are cut by faults close to Nalagarh Thrust, showing displacement of 1.6 m and slip of 2.5 m in the 30° ENE direction of the fault (Philip et al. 2011).

2. In Pakistan, the older rocks of the Salt Range have advanced over the recent Jhelam sediments, and the Kalagarh Conglomerate (that unconformably succeeds the Upper Siwalik sediments) is folded along a NW- to SE-oriented fault (Yeats et al. 1984). A lateral ramp developed along the Kalabagh Fault links the Salt Range with the Surghar Range in the west. It is an oblique ramp with respect to the Main Frontal Thrust (Khan et al. 2012). Down south along the Makran Coastal Belt, active mud volcanoes form a chain of mud mounds in the NE–SW direction extending from Chandragup to Malan Island in the sea (Delisle et al. 2002).

It is obvious that the Siwalik terrain, including its southern front, is going through processes of geomorphological modification and considerable landscape changes.

24.3 Climate Change and Advent of Ice Age

24.3.1 Cold Climate

Colder condition precursor to glaciation had set in as early as the Late Pliocene. This is evident from the appearance in the Karewa succession of rodents such as *Kilarkola* and *Microtus* which were very prolific in the cooler regions of contemporary Europe (Kotlia 1990, 1991). The 0.8–0.9 Ma event of rapid uplift made the Himalaya even higher than it was earlier. Naturally, cooler conditions conducive to glaciation developed in the higher realm. The glaciers spread far and wide in Potwar, Kashmir, Ladakh and Tibet. There were four successive advances of the glaciers as comprehensively described in 1939 by H. DeTerra and T.T. Paterson. The Uttarakhand domain was affected by three phases of glacial advance (Pant et al. 2006). In the Kashmir Himalaya, the oldest glaciers descended to the level of 1675 m above the sea level, and the youngest reached down to the elevation

of 2400 m (Wadia 1975). New data show that the *Pleistocene Glaciation* was not synchronous throughout the region: In some areas, they were most extensive during the period 60,000–30,000 yr B.P. and in other places during the global maxima interval 20,000–18,000 yr B.P. (Benn and Owens 1998).

24.3.2 Dry Desertic Climate

Following the period of glaciation, the south-west monsoon slackened and drier climate prevailed all over the Indian subcontinent including the mountain world. Even during the periods of glaciation, there were relatively shorter intervals of dry climatic condition, i.e. aridity. The glaciers had left behind large volumes of gravels and fine sediments in the Kashmir Valley. The dry, cold winds blew away the finer sediments and spread far and wide as *loess*. The Karewa Lake deposit was covered by a 10- to 20-m-thick blanket of eolian sediments. The Quaternary eolian sediments cover wide areas of Tibet. Layers of silt on top of the Pleistocene moraines from central and southern Tibet provide evidence of Early Holocene ages of the eolian deposits (Lehmkuhl et al. 2000). The eolian dust accumulated at a faster rate in the interval between 1.1 and 0.9 ka (Sun and Liu 2000). This was the time when there was volcanism in the marginal parts of the Plateau.

In the Pindar Valley in the Kumaun Himalaya, three events of loess depositions are recognizable—the first two between 20,000 and 9000 yr B.P., and the third one between 4000 and more than 1000 yr B.P. (Pant et al. 2005). The *loess* sequences contain quite a few horizons of *palaeosols* indicating interglacial intervals of stronger monsoon rains. In the lacustrine sediments, there are lenses of lignite in the Kashmir Valley at various levels. These horizons represent short intervals of warm and wet climate within an otherwise long period of cold desertic climate (Pant et al. 1985; Bronger et al. 1987). The prolonged period of Pleistocene cold dryness persisted until about 11,000 yr B.P., as records preserved in the deposits of a large number of lakes all over the Himalaya indicate. For example, in the Kathmandu Valley, the pollens of *Quercus, Cyclobalanopsis, Pinus, Alnus, Gramineae* show that cool climate during the time 2.5–2.1 ka changed to warm and relatively dry climate in the interval 2.1–1.0 ka, followed by seven cycles of warm–wet and cold–dry conditions during the temporal period 1.0 ka to the present (Fujii and Sakai 2001). In the Kali Valley in north-eastern Kumaun, the records in the Garbyang palaeolake sediments show high-amplitude, low-frequency, climate changes in the interval between 20,000 $\pm$ 3000 yr B.P. and 13,000 $\pm$ 2000 and low-amplitude, high-frequency changes from 13,000 $\pm$ 2000 yr B.P. to 11,000 $\pm$ 1000 yr B.P. (Juyal et al. 2004). The palaeolakes around Pithoragarh and the Bhimtal–Naukuchiatal Basin in the Lesser Himalaya record similar pattern of climate changes (Kotlia et al. 1997, 2000).

24.4 The Coming of Man

24.4.1 Human Settlements

A variety of stone implements found in the Quaternary sediments indicate that the tool-making humans have been living in India since about 540,000 years ago. They lived mostly alongside lakes and rivers. The earliest were the people of the *Palaeolithic Culture* of the Lower Pleistocene time who had settlements in extreme north-western Kashmir, in western Rajasthan, Gujarat and adjoining parts of Madhya Pradesh and Maharashtra. The duns in the Siwalik subprovince provided ideal situation for habitation to the early humans. The topography was gentle, and there was abundance of vegetation, animal life and water. Stone artefacts as old as Palaeolithic are found (Fig. 24.7) in the valleys of rivers Soan in Potwar, Kathua in Jammu, Tarnah, Ben, Chenab, Beas, Ravi, Banganga, Markanda and Ghaghgar in Himachal Pradesh (Sahni and Khan 1964; Verma 1975; Verma and Gupta 1997). In the Dang–Deochauri duns in south-western Nepal, Early Pleistocene lacustrine succession contains Palaeolithic to Neolithic tools (Cornivus 1995).

The gentle terrain of the Lesser Himalaya with its productive soil cover and bracing climate was peopled by humans all along its expanse from Swat–Dardistan in the west to western Nepal in the east. Significantly, the settlements were located preferentially in the meander loops of rivers and streams where the water front ensured safety from wild animals on three sides. In Kumaun rock,

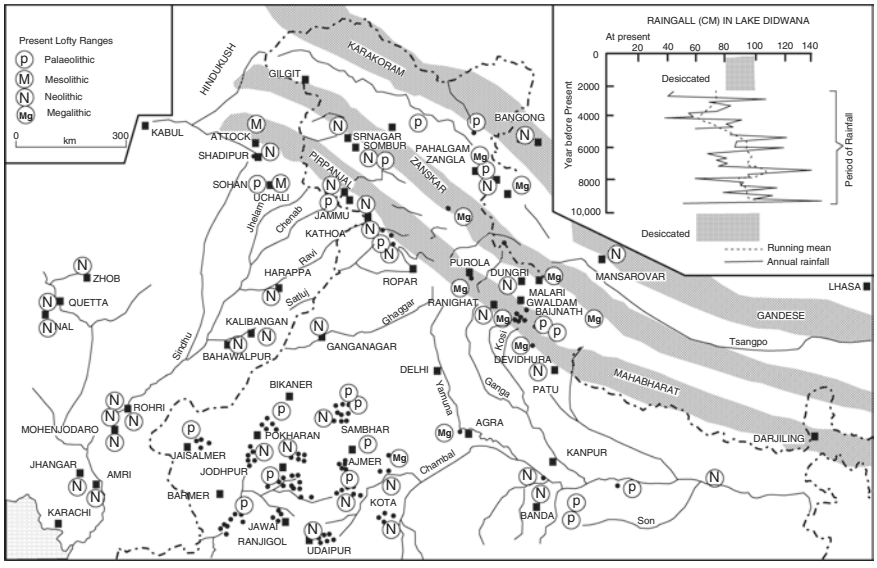

Fig. 24.7 Stone-Age settlements (*in solid circles*) in north-western India (From various sources, references in Valdiya 2002). *Inset* shows high rainfall in the Didwana Lake region in western Rajasthan in the period 8500 to 3500 yr B.P. (after Bryson and Swain 1981)

shelters with wall paintings such as at LakhuUdyar, Dalband and Kimni together with burial cists at Gwaldam, Baijnath, Devidhura, Ladyuna, Koormand and Bechandhar bear testimony to human occupation of the Lesser Himalayan land (Nautiyal and Khanduri 1985).

Across the mountain barrier of the Himadri, many ritualistic funerary remains are found at Malari in the Western Dhauli Valley, and in Lahaul and the Kashmir Valley of the Tethys subprovince. The locations of settlements in far-flung and presently forbiddingly high (1600–3900 m) places suggest that the mountain ranges at that time were not as formidable and difficult to cross as they are today. In the Kashmir Valley, atop the Karewa succession, a number of *Neolithic settlements* existed at Burzahom, Pampur and near Pahalgam. They lived in dwelling pits and buried their deads in crouching position with pet animals, using ash, lime and potsherd as burial material. Charcoal from a stone hearth was dated 4325 ± 115 yr B.P. (Kusumgar et al. 1985, 1992). Funerary remains are found in the Leh–Gaik area in Ladakh in the backdrop of caves with the uplifted terraces. The location at Gaik of stone hearth with 6710 ± 130 year old charcoal pieces along with unburnt wood and animal bones (Sharma et al. 1989) is extremely significant.

24.4.2 Free Migration

The Burzahom burials are strikingly similar to those of the contemporary sites in central Asia, north-west China, and Swat and Dardistan in Pakistan. It seems that the stone-age people moved freely in the Siwalik, the Lesser Himalaya and the Tethyan domains. They possibly had contacts and perhaps sociocultural intercourse with their contemporaries in central Asia, Dardistan and Rajasthan. As stated above, the mountain ranges were perhaps not so high and formidable as they are at present as pointed out by Birbal Sahni in 1936. Indeed, the Tibetan plateau was a peneplaned surface of low relief, only a few hundred metres above the sea level, until major fault movements during the Pleistocene elevated the landmass to the altitude above 5000 m (Shackleton and Chang 1988).

The Rajasthan part of the Peninsular India was a land clothed in a green carpet of vegetation and the valleys were verdant in the time interval between 11,000 and 10,000 yr B.P. when the Indian subcontinent was once again under the sway of rains, and the climate was wet and warm. Going by the evidence provided by spores and pollens recovered from the sediments of the Lunkaransar and Didwana lakes in western Rajasthan, the rainfall had become very heavy in the period 4000–6500 yr B.P. (Fig. 24.7 Inset). Carbon dating shows that the Lunkaran Lake was brimming with water from 6300 yr B.P. to 4800 yr B.P. and that humans were in occupation of the lake basin about 4230 ± 55 yr B.P. (Enzel et al. 1999).

Significantly, among the vegetal remains recovered from the sediments of the Lunkaransar and Sambhar lakes are cutigens, pollens and charcoal of the stubbles of cereal plants. The charcoal is dated 8000–9400 yr B.P. Clearly, the people

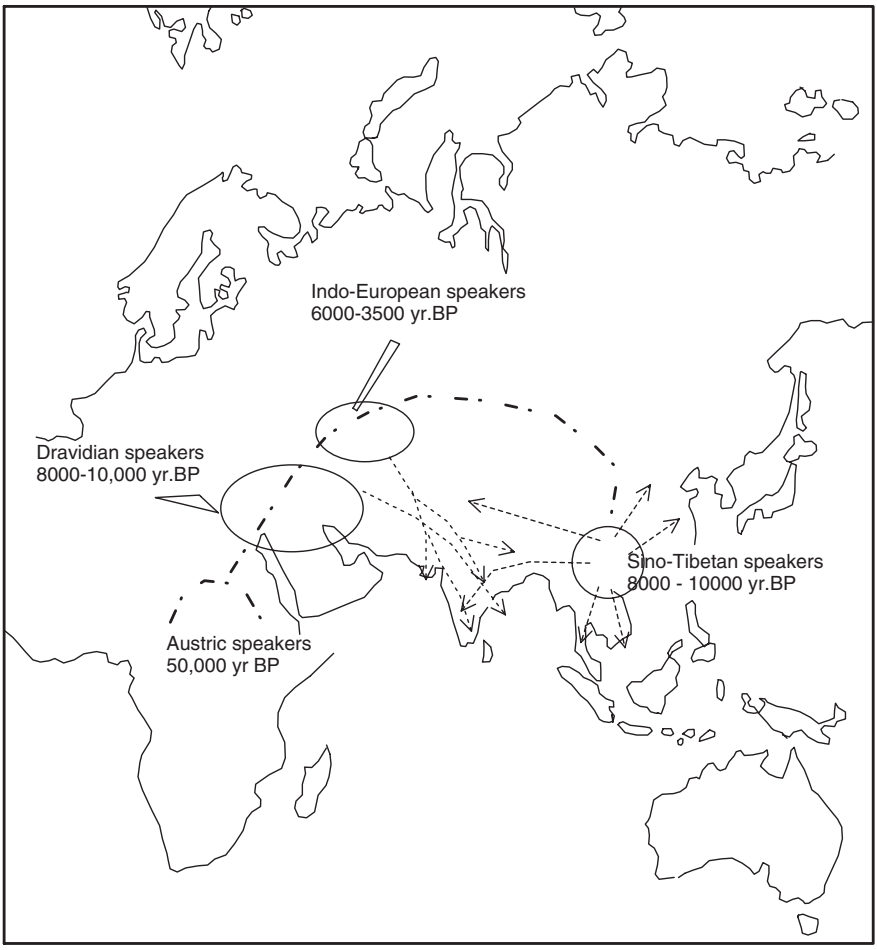

Fig. 24.8 There were four major waves of emigration of people, coming from different centres of evolutionary expansion (based on Gadgil et al. 1998; Valdiya 2002)

who lived around these lakes had started harvesting food crops (Singh et al. 1974; Bryson and Swain 1981.) In the Indo-Gangetic Plain, the Neolithic revolution took place rather early. Occurrence of Cerealia pollens along with tiny pieces of charcoal representing slash-and-burn agriculture testifies the occupation of the Ganga Plain by humans. The charcoal gives a date of 15,000 yr B.P., and the cultivated rice in the Ganga Plain is about 8400 yr B.P. (Singh 2005). Stone implements testifying to Palaeolithic culture confirm this deduction.

The domestication of plants, such as the domestication of animals, marks a crucial development—the beginning of a new mode of life. The hunter-gatherer had become a produce-herder. His life became relatively sedentary. This led eventually to the emergence of urban culture—the culture of the Harappa people who lived

in their urban centres in the floodplains of the Sindhu and Saraswati rivers in the early to Middle Holocene time (Figs. 24.3 and 24.7).

24.4.3 Immigration

Since fossils of the human skeleton appear only after 45,000–50,000 yr B.P. in the Narmada Valley, it is speculated that the humans originated outside India and came in four successive waves and settled in different parts of India (Gadgil et al. 1998). Those who speak Austric languages migrated from Africa and entered India via north-eastern India about 50,000 years ago and settled down in western and central India between 8000 and 10,000 yr B.P. People of the Sino-Tibetan stock, who cultivated rice and reared buffaloes, came from South-east Asia between 8000 and 10,000 yr B.P. and settled down in the northern territories of the Himalaya and the hills along the border with Myanmar (Fig. 24.8). The speakers of the Dravidian languages—who knew the art of cultivating wheat and domesticating cattle—came from West Asia and occupied lands in western and southern India. The people of the Indo-European stock came in several waves of migration between 3500 and 6000 yr B.P. from Central Asia. They rode horses and used iron technology. These immigrants made northern India, including the Himalaya province, their home.

References

Agrawal, D. P., Dodia, R., Kotlia, B. S., Razdan, H., & Sahni, A. (1989). The Plio-Pleistocene geologic and climatic record of the Kashmir Valley, A review and new data. *Palaeogeography, Palaeoclimatology, Palaeoecology, 73*, 267–286.

Awasthi, N. (1982). Tertiary plant megafossils from the himalaya: A review. *Palaeobotanist, 30*, 254–267.

Bagati, T. N., Mazari, R. K., & Rajagopalan, G. (1996). Palaeotectonic implication of Lamayuru Lake (Ladakh). *Current Science, 71*, 479–482.

Banerjee, D., Singhvi, A. K., Pande, K., Gogte, V. D., & Chandra, B. P. (1999). Towards a direct dating of fault gouges using luminescence dating techniques. *Current Science, 77*, 256–268.

Benn, D. I., & Owens, L. A. (1998). The role of the Indian summer monsoon and the mid-latitude westerlies in Himalayan glaciation: Review and speculative discussion. *Journal Geological Society London, 155*, 353–363.

Bhatt, D. K. (1976). Stratigraphical status of Karewa Group of Kashmir. *Himalayan Geology, 6*, 197–208.

Bhatt, D. K. (1978). Geological observation on the "Margs" of Kashmir valley. *Himalayan Geology, 8*(II), 208–269.

Bhutani, R., Pande, K., Desai, N., & Nikhil, L. (2003). Age of the Karakoram fault reactivation: ^{40}Ar–^{39}Ar geochronological study of Shyok suture zone in northern Ladakh, India. *Current Science, 84*, 1454–1455.

Bronger, A., Pant, R. K., & Singhvi, A. K. (1987). Pleistocene climatic changes and landscape evolution in Kashmir Basin, India: Palaeopedologic and chronostratigraphic studies. *Quaternary Research, 27*, 167–181.

Brown, E. T., Benedick, R., Bourles, D. L., Gaur, V. K., Molnar, P., Raisbeck, G. M., et al. (2002). Slip rates of the Karakoram Fault, Ladakh, India, determined using cosmic ray exposure dating of debris flows and moraines. *Journal Geophysics Research, 107*(9), 1–7.

Bryson, R. A., & Swain, A. M. (1981). Holocene variations of monsoon rainfall in Rajasthan. *Quaternary Research, 16*, 135–145.

Burbank, D. W., Beck, R. A., & Mulder, T. (1996). The himalayan foreland basin. In A. Yin & T. M. Harrison (Eds.), *The tectonic evolution of Asia* (pp. 149–188). Cambridge: Cambridge University Press.

Burbank, D. W., & Johnson, G. D. (1983). The late cenozoic chronologic and statigraphic development of the Kashmir intermontane basin, NW Himalaya. *Palaeogeography, Palaeoclimatology, Palaeoecology, 43*, 205–235.

Cornivus, G. (1995). Quaternary stratigraphy of the intermontane dun valley of Dang-Deokhuri and associated pre-historic settlements in western Nepal. *Memoirs Geological Society India, 32*, 124–149.

Delisle, G., von Rad, U., Andruleit, H., Daniels, C. H., Tabrez, A.-R., & Inam, A. (2002). Active mud volcanoes on- and off-shore eastern Makran Pakistan. *International Journal Earth Science (Geological Runds), 91*, 93–110.

Dill, H. G., Khadka, D. R., Khanal, R., Dohrmann, R., Melcher, F., & Busch, K. (2003). Infilling of the young Kathmandu-Banepa intermontane lake basin during the late Quaternary (Lesser Himalaya, Nepal): A sedimentological study. *Journal Quaternary Science, 18*, 41–60.

Dill, H. G., Kharel, B. D., Singh, V. K., Piya, B., Busch, K., & Geyh, M. (2001). Sedimentology and palaeogeographic evolution of the intermontane Kathmandu basin, Nepal. *Journal Asian Earth Science, 19*, 777–804.

Enzel, Y., Ely, L. L., Mishra, S., Ramesh, R., Amit, R., Lazar, B., et al. (1999). High-resolution Holocene environmental changes in the Thar desert, northwestern India. *Science, 284*, 125–126.

Fort, M., Burbank, D. W., & Freytet, P. (1989). Lacustrine sedimentation in semiarid alpine setting: An example from Ladakh, NW Himalaya. *Quaternary Research, 31*, 332–350.

Fort, M., Freytet, P., & Colchen, M. (1982). Structural and sedimentological evolution of the Thakkhola Mustang Graben (Nepal). *Zeitschrift Geomorphologie N F, 42*, 75–98.

Fujii, R., & Sakai, H. (2001). Palynological study of the drilled sediments from the Kathmandu Basin and its palaeoclimatic and sedimentological significance. *Journal Nepal Geological Society, 25*, 53–61.

Gadgil, M., Joshi, N. V., Manoharan, S., Patil, S., & Prasad, Shambhu. (1998). Peopling of India. In D. Balasubramanian & N. Appaji Rao (Eds.), *The Indian human heritage* (pp. 100–129). Hyderabad: Universities Press.

Gansser, A. (1964). *Geology of the himalayas* (p. 289). London: Interscience Publishers.

Gansser, A. (1991). Facts and theories on the himalayas. *Eclogae Geologicae Helvetiae, 84*, 33–59.

Gautam, P., Hosoi, A., Sakai, T., & Arita, K. (2001). Magnetostratigraphic evidence for the occurrence of pre-Brunhes (>780 k yr) sediments in the northwestern part of the Kathmandu Valley, Nepal. *Journal Nepal Geological Society, 25*, 99–109.

Hashimi, N. H., Pathak, M. C., Jauhari, P., Sharma, A. K., Bhakuni, S. S., Bisht, M. K. S., et al. (1988). Bathymetric study of the neotectonic Naini Lake in Outer Kumaun Himalaya. *Journal Geological Society India, 41*, 91–104.

Jackson, M., & Bilham, R. (1994). Constraints on Himalayan deformation inferred from vertical velocity fields in Nepal and Tibet. *Journal Geophysics Research, 99*, 13897–13912.

Joshi, D. D. (2004). A seismogenic active fault in the western himalaya. *Current Science, 87*, 863–864.

Joshi, D. D., Kandpal, G. C., John, Biju, & Pande, Prabhas. (2005). Morphotectonic and palaeoseismic studies along the Yamuna tear zone, Himalayan frontal belt. *Special Publications Geological Survey India, 85*, 225–236.

Joshi, D. D., & Tandon, S. K. (1987). Quaternary valley-fill deposits of the Ravi drainage basin in Chamba, western himalaya: Definition, lithostratigraphy and depositional framework. *Journal Geological Society India, 29*, 540–553.

Juyal, N., Pant, R. K., Basavaiah, N., Yadava, M. G., Saini, N. K., & Singhvi, A. K. (2004). Climate and seismicity in the higher central Himalaya during 20–10 ka: Evidence from the Garbyang basin, Uttaranchal, India. *Palaeogeography Palaeoclimatology Palaeoecology, 213*, 315–330.

Kandpal, G. C., Joshi, K. C., Joshi, D. D., Singh, B. K., & Singh, Jaya. (2006). Signature of quaternary tectonics in a part of Dehradun valley, Uttaranchal. *Journal Geological Society India, 67*, 147–152.

Khan, S. D., Chen, L., Ahmad, S., Ahmed, I., & Ali, F. (2012). Lateral structural variation along the Kalabagh Fault zone, NW Himalayan foreland fold-and- thrust belt, Pakistan. *Journal Asian Earth Science, 50*, 79–87.

Khan, A. A., Dubey, U. S., Sehgal, M. N., & Awasthi, S. C. (1982). Terraces in the Himalayan tributaries of the Ganga in Uttar Pradesh. *Journal Geological Society India, 23*, 392–401.

Kotlia, B. S. (1990). Large mammals from the Pleo-Pleistocene of Kashmir intermontane basin, India, with reference to their status in magnetic polarity time scale. *Eiszeitalter u Gengenwart, 40*, 38–52.

Kotlia, B. S. (1991). Pliocene Soricidae (Insectivora Mammalia) from Kashmir intermontane basin, northwestern India. *Journal Geological Society India, 38*, 253–275.

Kotlia, B. S. (1995). Upper Pleistocene Soricidae and Muridae from Bhimtal-Bilaspur deposits, Kumaun himalaya. *Journal Geological Society India, 46*, 177–190.

Kotlia, B. S., Bhalla, M. S., Sharma, C., Rajagopalan, G., Ramesh, R., Chauhan, M. S., et al. (1997). Palaeoclimatic conditions in the upper Pleistocene and Holocene Bhimtal-Naukuchiatal lake basin in southentral Kumaun, India. *Palaeogeography Palaeoclimatology Palaeoecology, 130*, 307–322.

Kotlia, B. S., & Jaishri, Sanwal. (2004). Fauna and palaeoenvironment of a late Quaternary fluviolacustrine basin in central Kumaun Himalaya. *Current Science, 87*, 1295–1299.

Kotlia, B. S., Sharma, C., Bhalla, M. S., Rajagopalan, G., Subrahmanyam, K., Bhattacharya, A., et al. (2000). Palaeoclimatic conditions in the late Pleistocene Wadda Lake (Pithoragarh), Kumaun Himalaya. *Palaeogeography Palaeoclimatology Palaeoecology, 162*, 105–118.

Kusumagar, S., Agrawal, D. P., Bhandari, N., Deshpande, R. P., Raina, A., Sharma, C., & Yadava, M. G. (1992). Lake sedimentation from Kashmir Himalaya: Inverted ^{14}C chronology and its implications. *Radiocarbon, 34*, 561–565.

Kusumgar, S., Agrawal, D. P., & Kotlia, B. S. (1985). Magnetic stratigraphy of the Karewas of the Kashmir Valley. In *Current trends in geology* (Vol. 6, pp. 13–17). Today & Tomorrow's, New Delhi.

Lehmkuhl, F., Klinge, F., Rees-Jones, J., & Rhodes, E. J. (2000). Late Quaternary aeolian sedimentation in central and southeastern Tibet. *Quaternary International, 68–71*, 117–132.

Leland, J., Reid, M. R., Burbank, D. W., Finkel, R., & Caffee, M. (1998). Incision and differential bedrock uplift along the Indus River near Nanga Parbat, Pakistan Himalaya, from ^{10}Be and ^{26}Al exposure age dating of bedrock straths. *Earth & Planetary Science Letters, 154*, 93–107.

Mathur, P. P., & Kotlia, B. S. (1999). Late Quaternary microvertebrate assemblage from glaciolacustrine sediments of the Lamayuru basin, Ladakh Himalaya. *Journal Geological Society India, 53*, 173–180.

Mukul, M. (2000). The geometry and kinematics of the main boundary thrust and related neotectonics in the Darjiling Himalaya fold-and-thrust belt, West Bengal, India. *Journal Structure Geology, 22*, 1261–1283.

Nakata, T. (1972). *Geomorphic history of crustal movements of the himalaya* (p. 77). Sendai: Institute of Geography, Tohuku University.

Nautiyal, K. P., & Khanduri, N. M. (1985). New cultural dimension in central Himalayan region of Uttarakhand: An archaeological assessment. *Annali Institute Universite Orientale, 101*, 30–31.

Pant, R. K., Basavaiah, N., Juyal, N., Saini, N. K., Yadava, M. G., Appel, E., et al. (2005). A 20-ka climate record from central Himalayan loess deposits. *Journal Quaternary Science, 20*, 485–492.

Pant, R. K., Juyal, N., Basavaiah, N., & Singhvi, A. K. (2006). Late Quaternary glaciation and seismicity in the higher himalaya: Evidence from Shalang basin (Goriganga), Uttaranchal. *Current Science, 90*, 1500–1505.

Pant, R. K., Juyal, N., Rautela, P., Yadav, M. G., & Sangode, S. J. (1998). Climatic instability during last glacial stage: Evidence from varve deposits at Goting, District Chamoli, Garhwal himalaya. *Current Science, 75*, 850–855.

Pant, R. K., Krishnamurthy, R. V., Tandon, S. K., & Bisht, V. (1985). Loess stratigraphy of the Kashmir Basin. *Current trends in geology* (Vol. 6, pp. 123–129). New Delhi: Today & Tomorrow's.

Phartiyal, B., Sharma, A., Upadhyay, R., Awatar, R., & Sinha, A. K. (2005). Quaternary geology, tectonics and determination of palaeo- and present fluvioglacio-lacustrine deposits in Ladakh, NW Indian Himalaya—A study based on field observations. *Geomorphology, 65*, 241–256.

Philip, G., Suresh, N., Bhakuni, S. S., & Gupta, V. (2011). Palaeoseismic investigation along Nalagarh thrust : Evidence of late pleistocene earthquake in Pinjaur Dun, northwestern subhimalaya. *Journal Asian Earth Science, 40*, 1056–1067.

Philip, G., & Virdi, N. S. (2007). Active faults and neotectonic activity in the Pinjaur Dun, northwestern frontal himalaya. *Current Science, 92*, 532–542.

Rao, D. P. (1977). A note on recent movements and origin of some piedment deposits of Dehradun valley. *Photonirvachak, 5*, 5–40.

Rautela, P., & Sati, D. (1996). Recent crustal adjustments in Dehradun Valley, western Uttar Pradesh, India. *Current Science, 71*, 776–780.

Sahni, M. R., & Khan, E. (1964). Stratigraphy, structure and correlation of the Upper Siwaliks, East of Chandigarh. *Journal Palaeontological Society India, 4*, 61–74.

Sakai, H. (2001). Stratigraphic division and sedimentary facies of the Kathmandu Basin Group, central Nepal. *Journal Nepal Geological Society, 25*, 19–32.

Searle, M. P. (1986). Structural evolution and sequence of thrusting in the high himalayan Tibetan-Tethys and Indus Suture Zones of Zanskar and Ladakh, Western Himalaya. *Journal Structural Geology, 8*, 923–936.

Shackleton, R. M., & Chang, C. (1988). Cenozoic uplift and deformation of the Tibetan Plateau: The geomorphic evidence. *Philosophical Transactions of the Royal Society of London, A327*, 365–377.

Sharma, K. K., Gu, Z. Y., Pal, D., Caffe, M. W., & Southon, J. (1998). Late Quaternary morphotectonic evolution of Upper Indus valley: A cosmogenic radionuclide study of river polished sufaces. *Current Science, 75*, 366–369.

Sharma, K. K., Rajagopalan, G., & Choubey, V. M. (1989). Radiocarbon dating of charcoal from pre-Indus civilization fireplace, Upper Indus Valldy, Ladakh. *Current Science, 58*, 306–308.

Singh, I. B. (2005). Quaternary palaeoenvironments of the Ganga plain and anthropogenic activity. *Man & Environment, 30*, 1–35.

Singh, G., Joshi, R. D., Chopra, S. K., & Singh, A. B. (1974). Late quaternary history of vegetation and climate of the Rajasthan desert, India. *Philosiphical Transactions Royal Society London, 267B*, 467–501.

Singhvi, A. K., Banerjee, D., Pande, K., Gogte, V., & Valdiya, K. S. (1994). Luminiscence studies on neotectonic events in southcentral Kumaun himalaya—A feasibility study. *Quaterly Geochronology, 13*, 595–600.

Sun, J., & Liu, T. (2000). Stratigraphic evidence for the uplift of the Tibetan plateau between ~1.1 and 0.9 myr ago. *Quaternary Research, 54*, 309–320.

Tandon, S. K., & Joshi, D. D. (1991). A high valley-width stretch of the Ravi River—evidence for strike-slip related neotectonic activity in the western Himalaya. *Zeitschrift Geomorphologie N F, 35*, 269–282.

Thakur, V. C. (1987). Development of major structures across northwestern himalaya. *Tectonophysics, 135*, 1–13.

Thakur, V. C., & Pandey, A. K. (2004). Active deformation of Himalayan frontal thrust and piedmont zone south of Dehra Dun in respect of seismotectonics of Garhwal himalaya. *Himalayan Geology, 25*, 23–31.

Valdiya, K. S. (1988). *Geology and Natural Environment of Nainital Hills* (p. 155). Nainital: Gyanodaya Prakashan.

Valdiya, K. S. (1993). Uplift and geomorphic rejuvenation of the himalaya: In the Quaternary period. *Current Science, 64*, 873–885.

Valdiya, K. S. (2001). Reactivation of terrane-defining boundary thrusts in central sector of the himalaya: implications. *Current Science, 81*, 1418–1431.

Valdiya, K. S. (2002). *Saraswati: The River that Disappeared* (p. 116). Hyderabad: Universities Press.

Valdiya, K. S. (2005). Trans-Himadri fault: Tectonics of a detachment system in central sector of Himalaya, India. *Journal Geological Society India, 65*, 537–552.

Valdiya, K. S., & Kotlia, B. S. (2001). Fluvial geomorphic evidence for late quaternary reactivation of a synclinally folded nappe in Kumaun Lesser Himalaya. *Journal Geological Society India, 58*, 303–313.

Valdiya, K. S., Rana, R. S., Sharma, P. K., & Dey, P. (1992). Active himalayan frontal fault, main boundary thrust and Ramgarh thrust in southern Kumaun. *Journal Geological Society India, 40*, 509–528.

Verma, B. C. (1975). Occurrence of Lower Palaeolithic artefacts in the Pinjor Member (Lower Pleistocene), Himachal Pradesh. *Journal Geological Society India, 16*, 518–521.

Verma, B. C., & Gupta, S. S. (1997). New light on the antiquity of Siwalik great apes. *Current Science, 72*, 302–303.

Wadia, D. N. (1975). *Geology of India* (p. 508). New Delhi: Tata McGraw Hill.

Wesnousky, S. G., Kumar, S., Mohindra, R., & Thakur, V. C. (1999). Uplift and convergence along the himalayan frontal thrust. *Tectonics, 18*, 967–976.

Whittington, A. G. (1996). Exhumation over-reted at Nangpa Parbat northern Pakistan. *Tectonophysics, 206*, 215–226.

Yeats, R. S., Khan, S. H., & Akhtar, M. (1984). Late quaternary deformation of the salt range of Pakistan. *Geological Society American Bullettin, 95*, 958–966.

Yoshida, M., & Gautam, P. (1988). Magnetostratigraphy of Plio-Pleistocene lacustrine deposits in the Kathmandu Valley, central Nepal. *Palaeoclimatic and Palaeoenvironmental Changes in Asia During the Last 4 Million Years* (pp. 78–85). New Delhi: Indian National Science Academy.

Zeitler, P. K., Johnson, N. M., Naeser, C. W., & Tahirkheli, R. A. K. (1982). Fission-track evidence for Quaternary uplift of the Nanga Parbat region, Pakistan. *Nature, 298*, 255–257.

Chapter 25
Holocene Tectonic Movements and Earthquakes

25.1 Strain Build-up and Relaxation

25.1.1 Convergence of Continents

The Indian plate is moving towards mainland Asia at a rate of 58 ± 4 mm/year (Freymueller et al. 1996). A recent analysis of the velocity of a GPS station at Bangalore relative to Asia (Fig. 25.1) suggests 5–7 mm/year (14 %) slower rate (Paul et al. 2001) than the rates inferred from NUVEL-IA (DeMets et al. 1994). Along the eastern mountain range, the rate of oblique convergence of the Shillong massif with respect to the Sundaland is 34 ± 6 mm/year (Sahu et al. 2006). A large part of the Indian plate convergence is stored as elastic strain in the structural frameworks of the Himalaya, the Indo-Myanmar Border Ranges and the Andaman Island Arc. The strain is particularly strong where the leading edge of the Indian plate impinges against the Asian plate and also where the tail end of crustal framework is fractured.

Periodic acceleration of continental convergence results in forward lurch of India and reactivation of long, deep ancient faults, particularly those that define the terrane boundaries, the horsts and the grabens (Fig. 25.2). This manifests itself in the occurrence of earthquakes (Plate 25.1), with attendant geomorphic changes and drainage aberration including changing of courses and ponding of rivers. The elastic strain accumulates for longer periods on deeper and longer active faults. Consequently, there is aseismic ductile deformation of rocks at depths followed by sudden fault slip accompanied by earthquakes. The coseismic slip, that is, earthquakes accompanying slip of rock masses, is not distributed uniformly, the asperities or rough edges of moving blocks bringing out release of most of the stored stresses.

K.S. Valdiya, *The Making of India*, Society of Earth Scientists Series,
DOI 10.1007/978-3-319-25029-8_25

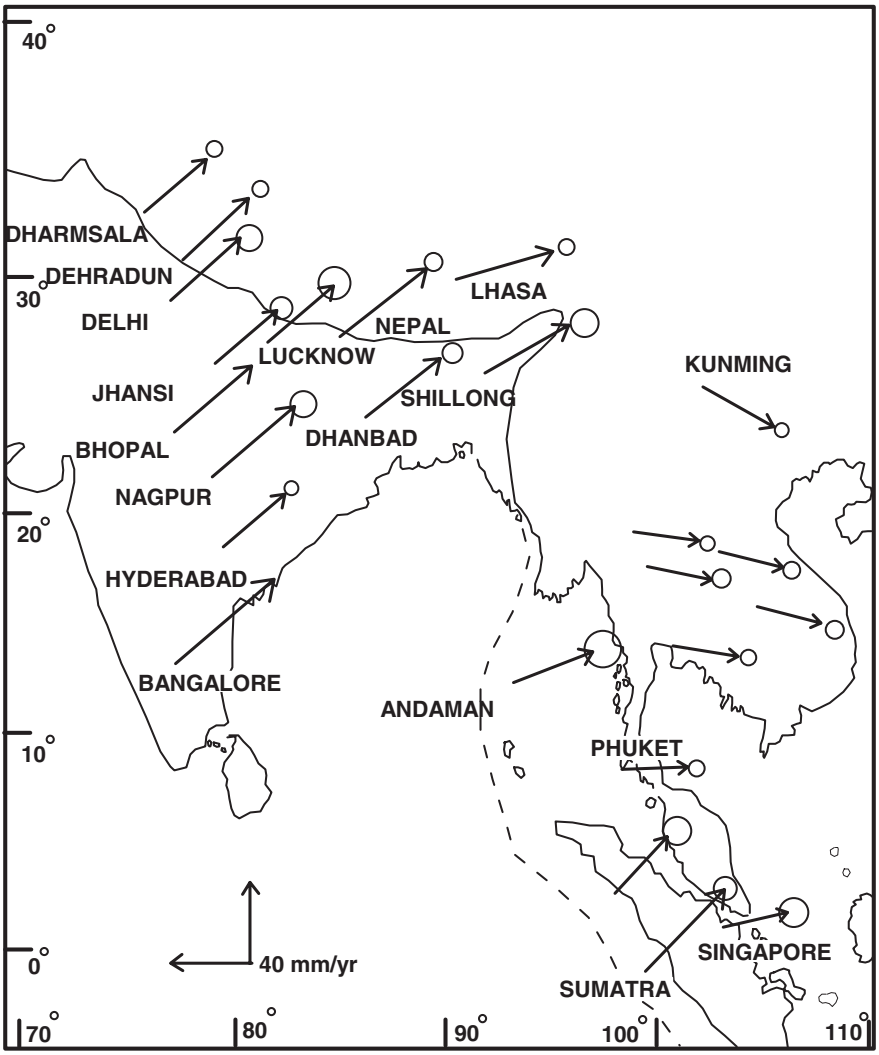

Fig. 25.1 Global Positioning System (GPS) measurements indicate north-eastward and eastward velocities of the Indian plate towards mainland Asia. The GPS velocities are given in the International Terrestrial Reference Frame (after Banerjee 2005)

25.1.2 Uplift of Fault-Bound Blocks

Levelling observations across central Nepal Himalaya and in the Siwalik terrane in south-western Uttarakhand showed that the recoverable elastic strains are accumulating in the upper crust. These strains manifest themselves in the uplift of the

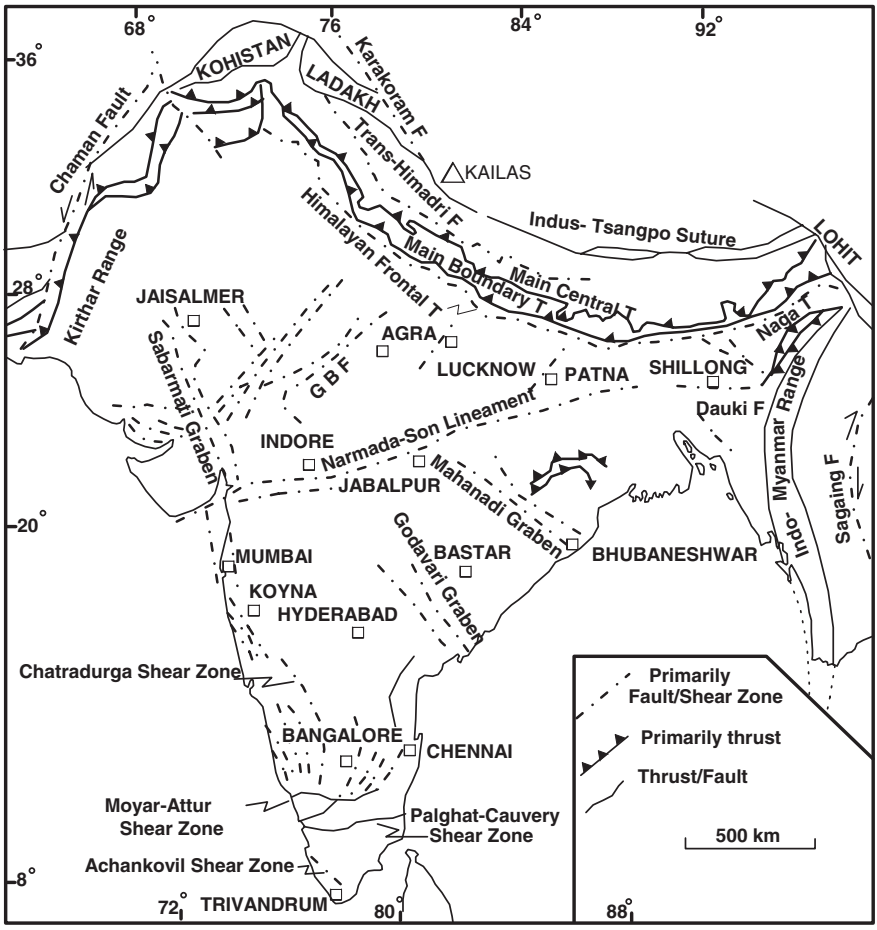

Fig. 25.2 Generalized tectonic map of India showing terrane-defining thrusts, faults and shear zones. Some segments of these tectonic planes are currently active, and some others were active in the Early Quaternary period (compiled from various sources)

fault-bound blocks at a rate varying from 1 to 0.8 mm/year (Chander and Gahlaut 1994). The GPS measurements at Delhi and Shillong indicated that the Meghalaya block is rising up (Paul et al. 2001). A difference in the rate of convergence of points at Hyderabad (37.04 ± 1.4 mm/year) and Bangalore (35.68 ± 1.7 mm/year) with respect to Kathmandu (Catherine 2004) is suggestive of neotectonic resurgence of the Mysore Plateau riven with active faults (Valdiya 1998, 2001b).

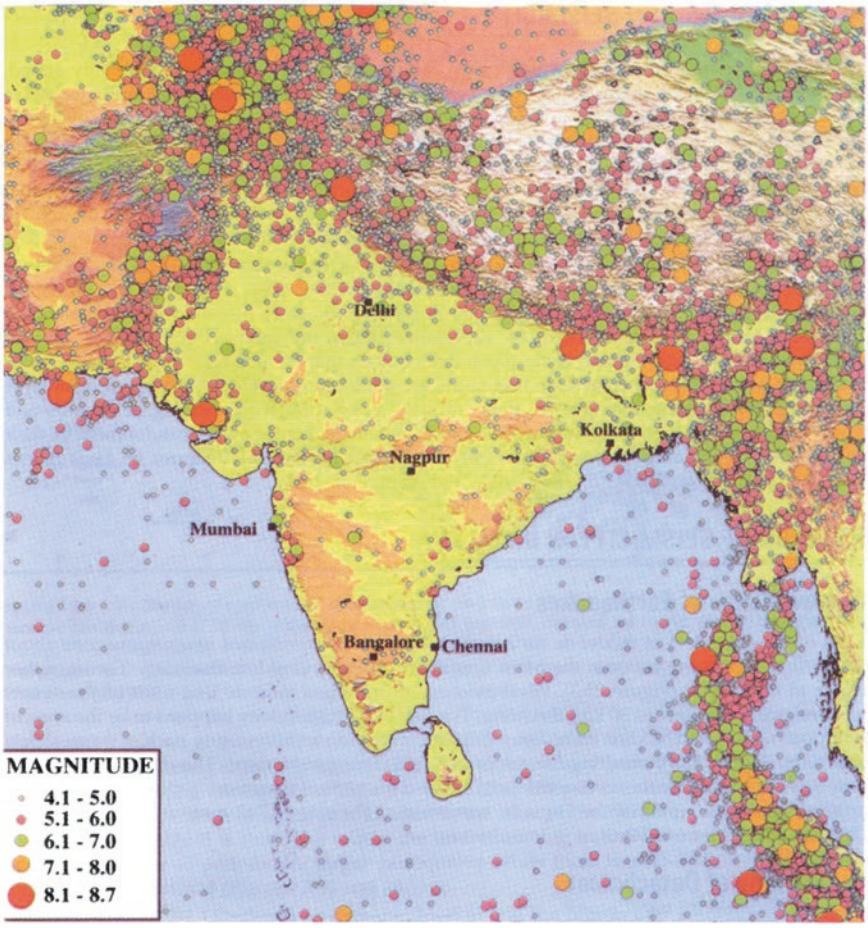

Plate 25.1 Distribution of epicentres of earthquakes in India and surrounding regions in southern Asia (Courtesy Gangan Prathap. Cover of Annual Report of 2001–200- of Centre for Mathematical Modelling and Computer Simulation, Bengaluru)

25.1.3 Slip Along Himalayan Border

The Indian plate bends down as it underthrusts the Himalaya. The rate of slip determined from seismic movements of great earthquakes is 17.7 mm/year (18 ± 5 mm/year) (Molnar and Lyon-Caean 1989; Molnar 1990). This rate is consistent with the rate determined from geological evidence—20 ± 3 mm/year in the central Himalayan sector (Wesnousky et al. 1999; Lave and Avouac 2000) to 10 mm/year in the Salt Range, Pakistan (Peltier and Saucier 1996). The GPS measurements confirm variation of slip rate from east to west (Fig. 25.1). It is 10–12 mm/year in the Sikkim Himalaya, 10–18 mm/year in the Uttarakhand sector and 14–20 mm/year in the western Himalaya (Banerjee and Burgmann 2001; Jade 2005).

The slip manifests in itself in seismic as well as aseismic displacement along active faults. Nearly, 80 % of the 20 mm/year slip rate is absorbed along the 50-km-wide belt of the Himalaya which is closer towards the Main Central Thrust (Pandey 1995; Bilham and Gaur 2000). The southern edge of the Himalaya is moving up rapidly onto the sedimentary piles of the Siwalik and Indo-Gangetic domains, causing crustal shortening at a rate of 5 mm/year (Molnar 1990). It should be obvious that only one-third of the India–Asia convergence (58 ± 4 mm/year) is absorbed across the Himalaya. The remaining portion is accommodated in part possibly by the faulted belts in the Peninsular India and in Tibet (Fig. 25.2). A part is stored as strains in the fault zones.

Convergence rates determined on the basis of GPS measurements vary considerably with time or perhaps location of stations. Compared to India–Lhasa Block convergence at a rate of 16 ± 0.5 mm/year to 16 ± 0.5 mm/year, the India–Myanmar convergence varies from 8 to 1.5 mm/year—8 mm/year in the Nagaland Salient, 6 mm/year in the Manipur Recess, and 1.5 mm/year in the Tripura–Mizoram Salient (Jade et al. 2007). Another measurement demonstrated that the Indo-Myanmar Belt convergence rate is nearly 20 mm/year, while the movement is propagated southwards at a rate of nearly 50 mm/year (Steckler et al. 2008). Recent investigation shows that the rate of India–Asia convergence is approximately 15 mm/year, the compressional strain being higher near the Main Central Thrust in the north than in the southern faulted zones (Ponraj et al. 2010). In the Darjeeling–Sikkim sector, the convergence rate is 12 mm/year, of which 4 mm/year is taken by Lesser Himalayan thrusts of the duplex zone (Mukul 2010). In the Arunachal Himalaya, the rate is nearly 16–22 mm/year in the north–south direction, of which 1.5–3.5 mm/year is taken eastward convergence between Meghalaya Plateau and Indo-Myanmar Orogenic Belt (Mukul et al. 2010). Using the age and geometry of upliftment of river terraces along the zone of Himalayan Frontal Thrust in eastern Arunachal Pradesh, the convergence rate is estimated at 23 ± 6.2 mm/year (Burgess et al. 2012). It is more than obvious that the India–Asia convergence is taking place at much faster rate in the eastern Himalaya.

Monitoring over a period from 1995 to 2007 in 29 continuous GPS stations and 41 survey-mode GPS stations all over India indicates that the *convergence within the Peninsular India* is 1–3 mm/year, while in the Meghalaya Plateau, it is 4–7 mm/year southwards (Banerjee et al. 2008).

GPS measurements over a period of six years show that the Godavari Graben has experienced compressive deformation at a rate more than 1.5 mm/year—locally as high as 3.3 ± 0.5 mm/year (Mahesh et al. 2012). It is the steep faults of the southern margin of the rift valley that are showing continuing movement.

25.2 Extension and Uplift of Tibetan Plateau

The high plateau is riven by normal faults trending N–S. Some of these faults in many areas are associated with grabens. The grabens and faults imply extension of the Tibetan Plateau at a rate of 19 ± 9 mm/year beginning at 8 ± 3 Ma

(Molnar et al. 1993). The extension is corroborated by dextral strike-slip movements on a multiplicity of E–W-trending faults. The movement is taking place at a rate of 1–5 mm/year in southern Tibet. The GPS velocities from 553 control points show that there is deformation throughout the Tibetan Plateau interior by ESE–WNW extension and slightly slower NNE–SSW shortening. Relative to Eurasia, the Tibetan fault blocks are moving eastwards with a speed that increases towards the east and then towards south around the eastern end of the Himalaya (Zhang et al. 2004). As the Plateau stretched in the east–west direction, it grew higher and higher by crustal thickening and shortening perpendicular to the margin (Molnar and Lyon-Caen 1989; Molnar et al. 1993).

The southward migration of the locus of thrust faulting enabled the southern margin of the Plateau to extend beyond the Indus–Tsangpo Suture onto the Tethys domain. Tight folding of the Pliocene to Quaternary sedimentary rocks about 100–150 km from the edge of the Plateau bears testimony to this fact (Molnar and Lyon-Caen 1989). It may be mentioned that in southern Tibet, the Gangdese Range is characterized by both north-dipping thrust faults and south-dipping younger thrusts. One of the thrusts (the Rengbu–Zedong Thrust) brought the Late Cretaceous fore-arc basin deposits (Xigaze Group) onto and over the Tethyan sedimentary succession (Yin et al. 1994).

The Miocene uplift of Eastern Tibet and attendant tectonism resulted in change of the courses of modern rivers (Clark et al. 2004). The Red River system brought about that once drained into the South China Sea, was disrupted due to river capture and reversal (Clark et al. 2004). The Tsangpo, which earlier flowed south-east into Myanmar and joined the Irrawaddy River, was forced to go south to the Bay of Bengal, earlier through the Lohit tributary and later through the Siang branch. Extensive and strong deformation on the Siang Syntaxis brought the Salween, Mekong and Yangtze rivers (now flowing through incised valleys) into exceptionally close proximity—they are only tens of kilometres apart for over 300 kilometres reach (Hallet and Molnar 2001). The situation points to large crustal strain due to NE–SW shortening followed by dextral shear strain along a north-trending zone.

25.3 Historical Earthquakes

There are numerous references to earthquakes and related terrestrial phenomena in *Vedas, Puranas, Mahabharat* and *Ramayan*. Among the many works on history, Varahmihir's *Brihat Samhita* (5–6 century AD), Ballal Sen's *Adbhut Sagar* (10–11 century AD), Chamunda Raya's *Lokopakarakam* (1025 AD), Kalhana's *Rajatarangini* (twelfth century AD) and Hasan Shah's *Tarikh-i-Hasan* (nineteenth century AD) describe earthquakes from different parts of India, even in terms of extent of ground shaking and causes of origin (Iyengar 1999; Iyengar and Sharma 1999). In the *Shalya Parva* of the *Mahabharat*, it is stated that three aftershocks after the main shock were felt at Kurukshetra, the site of the epic battle, and in

the *Mausal Parva*, it is stated that 36th year after the war was over, precursory anomalous signs and bizarre behaviour of animals and birds were noticed by the Pandavas in their capital and the Yadavas in Dwarika, which finally sank into the sea due to an earthquake nearly 3700 yr B.P. (Valdiya 2002).

In the recent historical past (Bapat et al. 1983), among the larger earthquakes are those that occurred on 6 June 1505 (M_S 8.2) in western Tibet–NW Nepal; in September 1555 (M_S 7.6) in the east of Srinagar in Kashmir; in September 1713 somewhere in Bhutan–Arunachal border; in 1751 (M_S 7.0) in the upper reaches of the Satluj; in September 1803 (M_S 7.5) in the Badrinath area in Uttarakhand; and in 1806 (M_S 7.7) in the Bhutan–Tibet border (Ambraseys and Jackson 2003).

25.4 Movements on Active Faults and Thrusts

The continuing underthrusting of the Indian plate beneath the Himalaya as already stated results in the development of two kinds. Some segments of the crust buckle up and fault blocks rise up, the rate varying from sector to sector and situation to situation. Elsewhere the movements get stuck, leading to progressive stress build-up. This is followed by periodic relaxation of strain in sudden bursts in the form of earthquakes. The relaxation of strain takes place along faults that have been active in the Quaternary period, particularly in the Holocene time. It is noticeable that all the major earthquakes were associated with one or the other of the active faults in the mobile belts, both in the Himalaya province and in the shield region of the Peninsular India (Fig. 25.2).

In the Leh–Spituk belt along the Shyok Suture Zone, there is a palaeolake at Khalsar characterized by multiple lenses of palaeoseismites, implying recurrent earthquakes in the suture zone (Phartiyal and Sharma 2009). The OSL dating of the uplifted and incised fluvial sediments in Seko–Nascong palaeolake in the upper reaches of the Spiti River showed that the age of the sediments ranged from 12,000 to 8000 yr B.P. and that palaeoseismic events occurred at ~12,000 year and 7000 yr B.P. (Phartiyal et al. 2009). In the southern part of the Kashmir Valley, just north of the Pir Panjal Range, the valley of the Rambiasa River has unpaired fluvial terraces and the basin is cut by three NE-dipping faults—one of them traceable for over 10 km and causing stratigraphic separation of 13 m (Ahmad and Bhat 2012). Needless to say, the faults have considerably affected the recent deposits. There was the southward propagation of deformation causing exhumation of rock units of the south-westerly overturned synclinal nappe embodying the Chhiplakot crystalline rocks, and the fission-track dating of apatite and zircon indicates that the movement presently is taking place on the Vaikrita Thrust and the Main Central Thrust at a rate of 1.2–3 mm/year (Patel et al. 2011). Nestling on the southern flank of the Great Himalaya in Kumaun, the Pindari Glacier has carved out a valley showing telltale signs of neotectonic activity (Bali et al. 2013). The anisotropy of magnetic susceptibility further testify to continued activity—at least two phases of rejuvenation—one prior to 25,000 year and another after 3000 year

(Bali et al. 2011). In eastern Kumaun region, neotectonic activity is manifest in the tilting of the ground north-eastwards and south-westwards, across the North Almora Thrust. In the Someshwar-Lodh-Gagas in western Kumaun, uplifted terraces, wide and straight course of streams suddenly narrowing into gorges and cutting of unconsolidated sediments imply that the North Almora Thrust is registering ongoing movement (Kothyari and Pant 2008).

In the south-eastern Garhwal, there are four riverine terraces in the Yamuna valley at different elevations as much as 65 to 80 m—that are dated by the OSL method at approximately 24–35 ka, 11–5 ka, 7–4 ka, 3–2 ka and less than 2 ka (Dutta et al. 2012). The fact clearly demonstrates that the Siwalik through which the Yamuna flows was lifted up four times in the Late Pleistocene to Holocene times.

A low-angle 19-km-long thrust passing through Bhawuwala in the Dehradun Valley, which has given rise to an upwarp on the Dehradun surface and tilts the ground, has been dated by the OSL method at 2619 $\pm$ 225 year and by a radiometric method at 2570 $\pm$ 220 year, indicating deformation in the Late Holocene time (Jayangondaperumal et al. 2008).

Close to the Himalayan Frontal Thrust at Kalaam, repeated rupturing has given rise to a 15–38-m-high fault scarp. The trench investigations showed seismites resulting from earthquakes sometime between 1300 and 1400 A.D. (Malik et al. 2008). Another trenching excavation survey here showed the presence of large-size injection of sand bodies induced by earthquake shocks, the earthquakes of $M \geq 7.5$ occurring at 29.3 and 17 ka, and of $M \geq 7.2$ at 5.8 and 2.0 ka (Philip et al. 2012). On the ground, stream strath is not only uplifted but also upwarped, and an alluvial fan is truncated. In the Nahan Salient, tilted fluvial terraces are faulted at a number of places (Singh et al. 2011), recalling similar development in the Ramnagar area in Kumaun (Valdiya 1992). Movement on the Himalayan Frontal Thrust is believed to be responsible for the formation of an asymmetric anticlinal ridge representing a fault bend overthrust in the Chandigarh area (Thakur et al. 2009). The drainage pattern, the incision of landforms, and the geometry of structures indicate that it is a blind back-thrust, which is clearly manifest in the fold scarp on the northern margin of the ridge. At Ropar in the Satluj Valley, there is a transverse westward-inclined tear fault registering lateral strike-slip movement (Singh et al. 2008). The fault at Hajipur in the Himalayan Frontal Thrust zone is responsible for palaeoseismic events, attendant modification of the ground landscape (Malik et al. 2010a). Not far from the Himalayan Frontal Thrust, the frontal foreland anticlinal fold of Janauri exhibits fault growth and segment linkages related to the active fault (Malik et al. 2010b).

A case of slick-slip-advance of rock pile is witnessed in the Potwar Plateau, Pakistan. In this sector, the rock piles commonly slide smoothly at a rate of 3 mm/year due to the presence of unduly viscous salt in the basal horizon. However, where there is a loss of lubricating salt in the decollement, an earthquake of M_w 6.0 occurred in 1992 (Satyabala et al. 2012).

The south-flowing Singra, Kimin and Ranga rivers in Arunachal Pradesh are abruptly deflected northwards along fault lines or due to impediments of shatter ridges and fault scarps along their paths implying that the faults are active (Mrinalini Devi 2008). Almost similar phenomenon, including ground tilting

and river migration westwards, is discernible in the valley of the Silgi River in the Likhabari area in the frontal part of the mountain (Luireis and Bhakuni 2008). There is a N–S oriented 15 km long and 5 km wide across lake in the Kale River, a tributary of the Subansiri, the lake having 22–25-m-thick sediments deposited in the period 22–20 ka with seismites in one of its horizons. The lake was formed as a result of ponding of the Kale by movement on a fault. At its southern end, lake is cut by a transverse fault, and the life of the lake was terminated at 21 ka, due to reactivation of this fault (Srivastava et al. 2009).

Ground-penetrating radar study of the sediments of the area between the Kosi and Gandaki rivers revealed that the thick sediments beneath the megafans of these rivers are thrust up northward, resulting in the development of a bulge on the ground with attendant northward tilting of the ground (Pati et al. 2011). To the west, as the river Gomati joins the Ganga, its flow is broken by breaks and then through an incised 6–15-m-deep valley with convex wall—all indicating bulging up of the terrain, presumably related to the active subsurface Faizabad Ridge.

Parallel to the Katrol Hill Fault, there are a number of active faults. One of them about 1 km north of the Banni Plain is associated with a 10-m-thick shear zone and has displaced Quaternary sediments in the gorge of the Khari River (Morino et al. 2008). Along the Kachchh Mainland Fault, there is a east–west-trending north-facing 10–15-m-high fault scarp at Lodai, where the recent alluvial fan surface is appreciably displaced (Malik et al. 2008). It is also noticed that there is a progressive northward shifting of tectonic activity along the imbricate reverse faults, resulting in the displacement of young Quaternary sediments characterized by seismites underground.

Earthquakes commonly occur at the intersections of the active faults, where oblique to transverse faults cut the longitudinal faults (Valdiya 1976, 1981, 2001c). In the Himalaya province as the nappes (thrust sheets) advanced southwards onto the underthrusting slab, the transverse faults were reactivated. In the Peninsular India, the intersections are the sites of earthquakes (Kayal 2000; Kayal et al. 2006). It is obvious that the transverse tear faults serve as strain transfer zones. The transverse tear faults are particularly active, as borne out from river response to neotectonic movements, their intimate association with ponding of streams and rivers in the past as well as in the present, the anomalous deflection or even abandonment of channels by rivers, and from the development of very young geomorphic features on fault planes (Valdiya 1992, 1998, 2001a, b; Valdiya and Narayana 2007).

25.5 Pattern of Seismicity in Himalaya

25.5.1 Narrow Zone of Earthquakes

Most of the epicentres of moderate earthquakes ($M \geq 5$) are concentrated in a narrow zone about 50 km in width, lying between the Main Central Thrust and the Main Boundary Thrust, rather closer to the former (Fig. 25.3). Focal mechanism

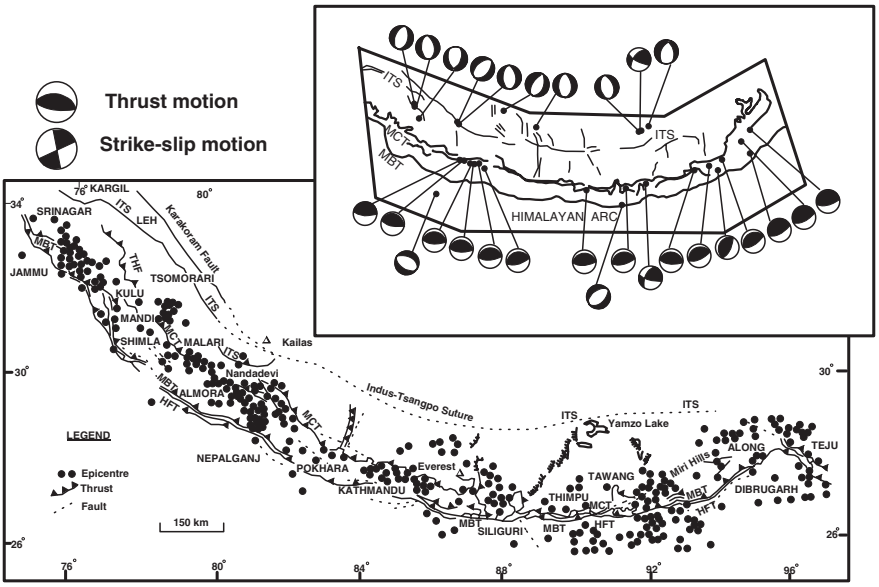

Fig. 25.3 Distribution of epicentres of earthquakes of magnitude $M \geq 5$ in the Himalaya shows that most of them are concentrated in a 50-km-wide zone between MCT and MBT, closer to the former (based on data from Chandra (1978) and Valdiya (1992)). *Inset* shows focal mechanism solutions, indicating that most of the events were related to shallow thrusting (after Rastogi 1974)

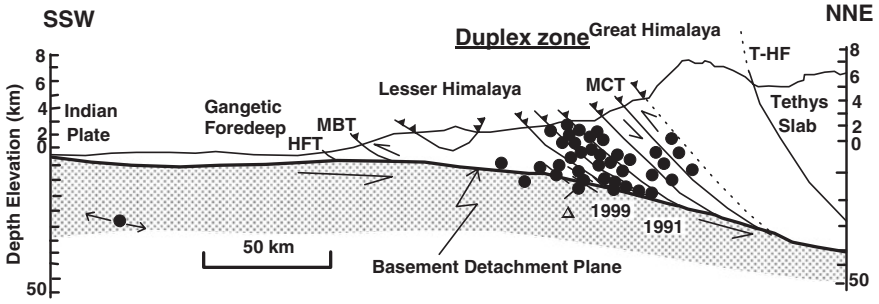

Fig. 25.4 Zone of imbricating pack of thrust sheets and slabs constituting a duplex zone resulting from repeated and strong movement along the Main Central Thrust. The lower limit of hypocentres defines a plane of movement related to India sliding under the Himalaya. This is believed by most workers to be the plane of decoupling of the basement and superincumbent sedimentary pile

solutions indicate that most of the events were related to shallow ($\leq$30 km) thrusting. The belt of high seismicity happens to be the zone of schuppen structure. The zone embodies duplex comprising imbricating pack of thrust sheets and slabs (Fig. 25.4), resulting from repeated and strong movement. The duplex zone is not

only seismotectonically the most active belt, but also the zone of maximum strain build-up. This is apparent from the uplift of the Himadri mountain at a rate of 7 ± 2 mm/year in central Nepal (Jackson and Bilham 1994).

25.5.2 *Basal Plane of Detachment*

The focal mechanisms give thrusting solutions (Rastogi 1974). The pattern of vertical distribution shows confinement of the hypocentres in the depth levels of 15–16 km which define a plane that has an apparent dip of 15°. This simple planar zone has been interpreted by most workers as a plane of detachment or decoupling (Fig. 25.5) between the underthrusting Indian plate and the Himalaya crustal block (Seeber and Armbruster 1981; Ni and Barazangi 1984; Baronowski et al. 1984). Significantly, the underthrusting Indian plate is flexed down 10–15° by the weight of the Great Himalaya (Fig. 18.1) and has given rise to a ramp at the MCT (Lyon-Caean and Molnar 1983). The ramp is the location of strong stress and strain build-up and serves as a geometric asperity—a rough edge of the advancing crustal blocks. This is evident from intense microseismicity and frequent occurrence of moderate-magnitude earthquakes in the zone of the ramping of the Indian plate (Pandey et al. 1999). It is this ramp where the underthrusting Indian plate often gets stuck or locked, giving rise to periodically larger earthquakes when there is unlocking and the Indian plate lurches northward (Figs. 25.4 and 25.5).

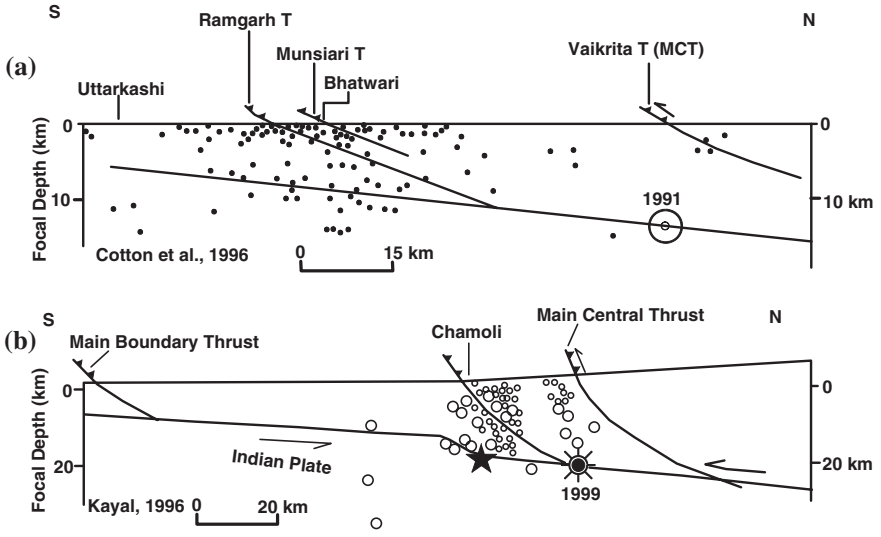

Fig. 25.5 Hypocentres of the Uttarkashi and Chamoli earthquakes and their aftershocks were confined to the 15–25 km depth level, defining a plane of detachment and displacement (**a** after Cotton et al. 1996; **b** after Kayal 1996, 2003)

The October 1991 Uttarkashi earthquake (M_b 6.6) and the March 1999 Chamoli earthquake (M_b 6.3) originated at a depth of 12–15 km and their aftershocks occurred all over the duplex zone. The two earthquakes of the central sector of the Himalayan arc seem to testify to the reactivation of the basal detachment plane (Fig. 25.5) in the duplex zone of the MCT (Kayal 1996, 2003; Sarkar et al. 2001).

25.5.3 Clustering of Epicentres

Significant lateral variation in ongoing deformation due to change in structure and composition of the crust is evident from the concentration of epicentres of earthquakes of $M \geq 5$ in limited areas and the pattern of seismicity (Kaila et al. 1972; Pandey et al. 1999). These are the areas that are affected by tear faults oriented orthogonally to the Himalayan trend (Valdiya 1976, 1981). Trending NNW/NW–SSE/SE and NNE/N–SSW/S and forming conjugate pairs, the tear faults (Figs. 25.6 and 25.7) are related to the wrenching or violent twisting of

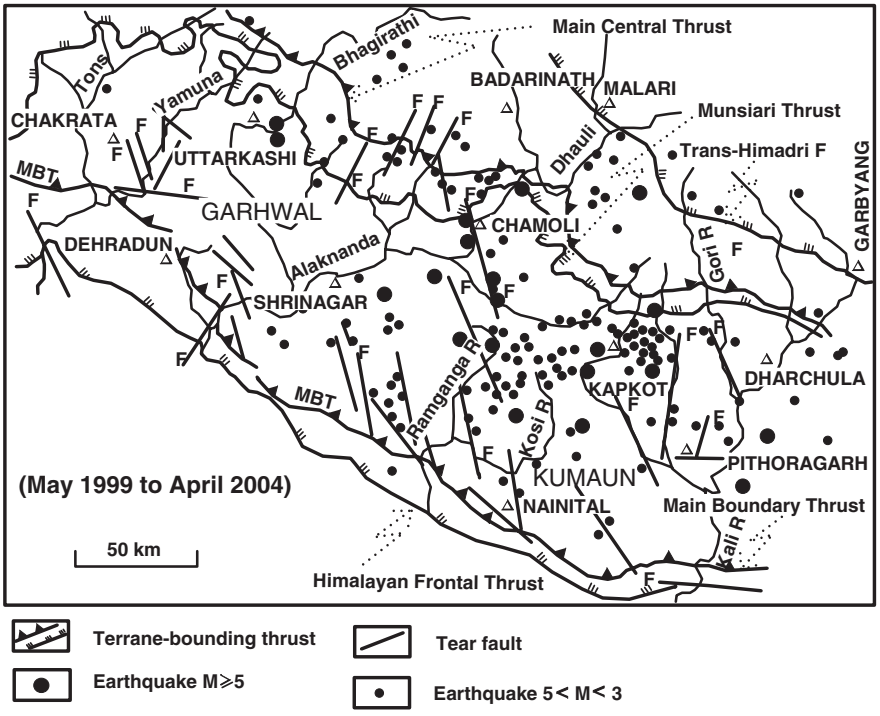

Fig. 25.6 Microseismicity in the period 1999–2004 in Uttarakhand (Paul et al. 2005) is related to the reactivation of thrusts in the duplex zone immediately south of the Main Central Thrust and to the tear faults that are oriented transversely. The Dharchula area in the north-eastern part is enigmatically quiet so far as the larger earthquakes are concerned (Valdiya 1981)

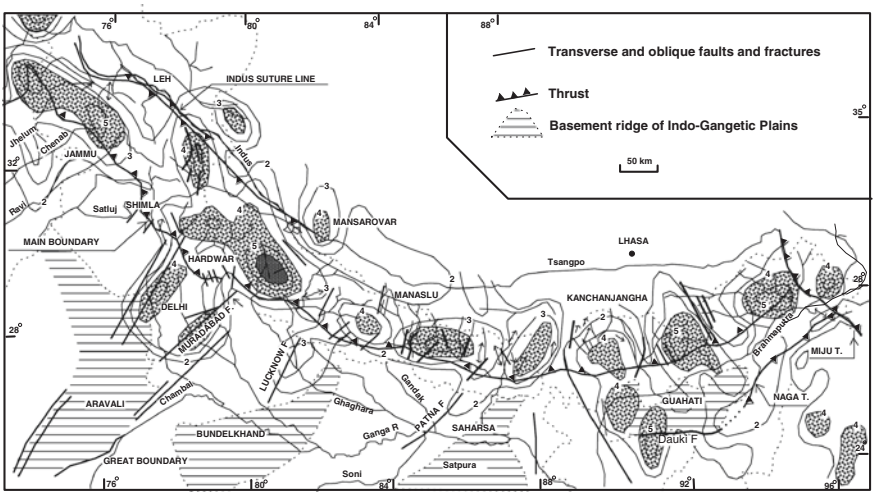

Fig. 25.7 Quantitative seismicity map (based on distribution of epicentres of $M \geq 5$ earthquakes) bring out areas or pockets of high seismicity (Kaila et al. 1972) which are riven with transverse tear faults (from Valdiya 1981)

the differentially overthrusting piles of rocks. In a large number of cases, the tear faults extend across the terrane boundaries. Strong and persistent compression of the fold mountains caused the rock masses or nappes to move bodily along the thrust planes, and also their tearing apart at bends. This phenomenon resulted in differential horizontal advance and attendant wrenching of the thrust sheets accompanied by earthquakes. Reactivation of the basal detachment plane may also have been responsible for tear faulting and the generation of earth tremors.

In the duplex zone in north-eastern Kumaun, the tear faults and strike-slip faults are quite active (Pant et al. 1992; Luirei et al. 2006). The July 1980 Bajang earthquake of M_s 6.5 (Fig. 25.3) in the adjoining area of Nepal (occurring at a depth of 20 ± 5 km) showed a small component of right-lateral slip along a 62°-W dipping nodal plane (Khanal 1997). Analysis of 312 events out of 2000-odd earthquakes of $M \leq 4.5$ during the period 1999–2004 in Kumaun (Fig. 25.6) indicated that the strain was released by the NNW–SSE- and N–S-trending faults (Paul et al. 2005). In the Garhwal region, many of the small earthquakes that were confined to the depth of 6–8 km showed strike-slip motion (Gaur et al. 1985). The main shock of 29 March 1999 Chamoli earthquake (M_b 6.3) showing thrust–fault–plane solution was located in the line of the most active NW–SE-trending Nandprayag Fault (Valdiya 1976, 1980). This fault generated aftershock by strike-slip mechanism (Kayal 2003). Soft sediment deformation features in the fluvial sediments (Pandey and Pandey 2004) testify to recurrent movement in this tectonically most sensitive area of the Uttarakhand Himalaya. In the Bhagirathi valley near Uttarkashi, soft sediment deformation in the fluvial terraces indicates ongoing movements on the N–S-trending transverse Hinna Fault (Pandey and Pandey 2006).

It is evident that although thrust movements are predominant, the strike-slip displacements are also responsible for the high seismicity in the Himalaya province. This is particularly pronounced in the eastern sector of the mountain arc where NW–SE-trending faults are very common (Fig. 25.7). Earthquakes that occurred in the period 1937–2003 in Bhutan provide mostly strike-slip focal mechanism solutions with mid- to deep crustal depths (Drupka et al. 2006). The seismicity occurs along conjugate sets of NE–SW- and NNW–SSE-trending faults by strike-slip and normal faulting, implying E–W extension and N–S shortening (Meyer et al. 2006). The Yadong–Gulu, the Bomdila Fault and the Kopili Fault, for example, have right-laterally offset the mountain ranges (Nandy 1980, 2005; Nandy and Dasgupta 1991). In this sector, microseismicity is pronounced not in the zone closer to the MCT, but in the zone related to the transverse faults that cut across the Main Boundary Thrust (Figs. 25.7 and 25.13) (Mukhopadhyay 1984; Kayal and De 1991; Kayal et al. 1993).

The recent occurrence of earthquakes in Sikkim, Bhutan and adjoining parts of the Indo-Gangetic Plain testifies the activity along the many faults that cut the land in NNW–SSE and N–S directions. The earthquakes in the plains of 1869 (M 7.7), 1943 (M 7.2), and 2006, 2009 and 2012 (magnitude $M_w > 5$) and the Bhutan earthquake (M_w 6.3) were all generated in the 300-km-long and 100-km-wide zone of the Kopili Fault trending NNW–SSE (Hazarika et al. 2010; Kayal et al. 2012). The 18 September 2011 Sikkim earthquake of M_w 6.9 (with loci at a depth of 60 km) and tight clustering of its coevents, and the 20 August 1988 earthquake at Udepur in Nepal of M_w 6.6 are all attributed to strike-slip movement on the NNW–SSE- or NNE–SSW-trending "lineaments" or faults (Ravikumar et al. 2012; Dasgupta et al. 2013). It has been speculated that the so-called lineaments define the promontories of the northward-advancing Indian Craton, producing conjugate shear faults and the strike-slip movements on which generated earthquakes (Dasgupta et al. 2012).

In the eastern syntaxial bend of the mountain arc, the compression is so strong that practically all thrusts and faults are active. This is evident from the advance of the Mishmi metamorphic rocks onto the Brahmaputra sediments (Thakur and Jain 1974) and the development of very youthful geomorphic features including abrupt narrowing of otherwise wide valleys to gorges (such as of the Lohit), the 20–25-m uplift of fluvial gravel terraces and the slumping down of mountain slopes (Misra and Singh 2002).

In the western Himalaya, the same pattern of transverse pockets or areas of high seismicity related to tear faults is observed. The earthquakes triggered landslides and liquefaction of soft sediments. In the Dehradun area, the NNE–SSW-trending Raipur–Tunwala fault caused 1.5-m vertical uplift of the Late Quaternary to Early Holocene Dun Gravel Fan (Rao 1977). The sediments exhibit many events of liquefaction of sediments (Mohindra and Thakur 1998). The N–S- to NNW–SSE-oriented Yamuna Fault—the tear fault that provided passage to the river Yamuna onto the plains—demonstrates evidence of left-lateral strike movement in the Late Quaternary and the occurrence of an earthquake 800 yr B.P. (Joshi et al. 2005). Recent sediments to the north-west of the Yamuna, close to Chandigarh in the Nandah Nala, show contortions and diapiric intrusion of mud into silt due to an

earthquake of subrecent origin. The deformation is related to a transverse tear fault (Kumar et al. 2005). In the Spiti valley in north-eastern Himachal Pradesh, the N–S-trending Sumdo Fault is among the very active transverse faults. This is evident from geomorphic features of recent origin, displacement of fluvial and lacustrine sediments (Sah and Virdi 1997) and the occurrence of seismites at eight levels in a 120-m-thick column of sediments dated 90–26 ka (Mohindra and Bagati 1996; Banerjee et al., 1997). The 19 January 1975 earthquake of magnitude 6.8 occurred on this fault. In the region of 1905 Kangra earthquake, the active Chamba Fault, along the Ravi river, was the source of earthquake in 1945 (M 6.5), 1968 (M 4.9), 1986 (M 5.5) and 21 March 1995 (Joshi 2004) (Fig. 25.8).

25.5.4 Great Earthquakes

The great earthquakes ($M \geq 8$) occurred where the underthrusting-related movements were stored as elastic strain for long periods of time—spanning a few hundred years. Earthquakes of magnitude 8 or higher occurred in 1803, 1833, 1905,

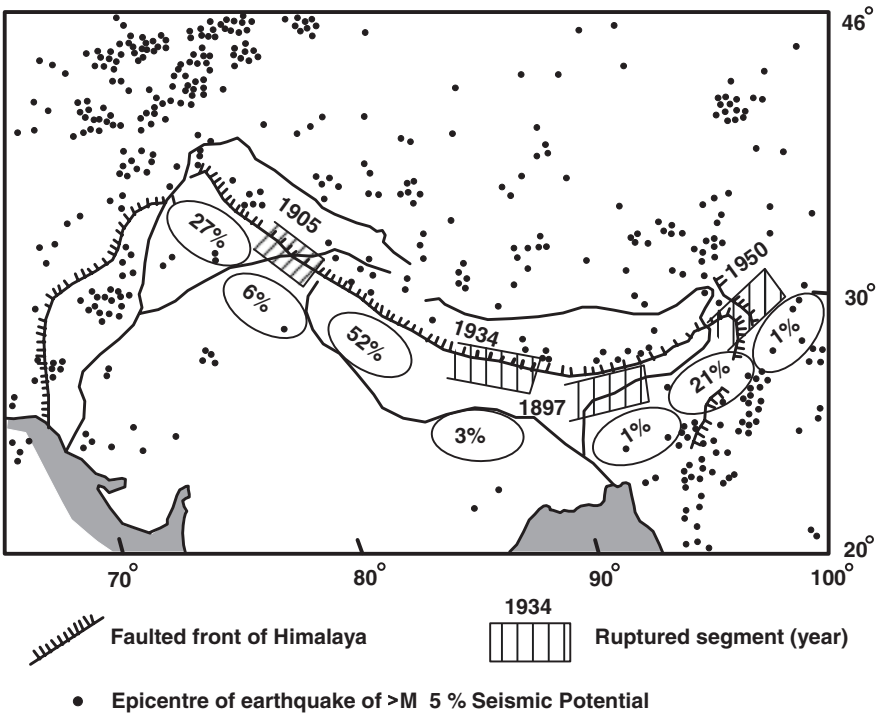

Fig. 25.8 The tectonic front of the Himalaya was ruptured during great earthquakes ($M \geq 8$). The unruptured parts are the seismic gaps where chances of occurrence of great earthquakes (given in percentage) are very high (Khattri 1999)

1934 and 1950 in different sectors, rupturing the crust extensively. The Kangra event of 1905 was associated with >120-km-long rupture and 8-m slip, the 1934 northern Bihar–Nepal earthquake ruptured 200–300-km-long crustal segment with 4-m slip, and the 1950 earthquake in eastern Arunachal Pradesh was related to a 200-km-long rupture and 8-m slip (Khattri 1987, 1998; Molnar 1990). Some of the great earthquakes have been downgraded in magnitude and their location shifted (Ambraseys and Bilham 2000)—the Kangra earthquake to M_s 7.83, the 1883 Nepal event to M_w 7.7, the 1934 north Bihar earthquake to M_w 8.2 and the 26 August 1833 Nepal earthquake to $7.5 < M_l < 7.9$ (Bilham 1995).

Palaeoseismic studies indicate that the movements on the Himalayan Frontal Thrust (HFT) generated great earthquakes in the geologically recent past. In a 250-km-long sector of the *dun* valleys, six sites in the canyons of the Ghaghgar Markanda, Shahjahanpur and Kosi rivers show evidence of uplift of the bed rock at a rate of 4–6 mm/year, resulting from slip at a rate of 4–16 mm/year on a 20–45°N dipping thrust related to the Himalayan Frontal Thrust (Kumar et al. 2006). Radiocarbon ages of the material in the displaced sediments indicate very large surface rupture that occurred sometime between 1200 and 1700 AD. In the meizoseismal area of the 1934 earthquake in the northern Indo-Gangetic plains, great earthquakes occurred earlier than 25,000 yr B.P. and during the period 1700–5300 yr B.P. (Sukhija et al. 2002). In the Mahakhola area in Nepal, a single event of M_w 8.8 at about AD 1100 ruptured the HFT over a length of 240 km with attendant slip of nearly 17 (+5/−3) m (Lave et al. 2005). In south-central Kumaun, where the MBT and the HFT are extremely active (Valdiya 1992; Valdiya et al. 1984, 1992), palaeoseismites testify to the occurrence of a megaevent near Ramnagar around AD 1500, the coseismic slip being 18–28 m (Thakur 2006). In the Markanda valley near Kala Am, palaeoseismites indicate the occurrence of great earthquakes at AD 260, 1294 and 1423, entailing displacement of 4.6 and 2.4 to 4 m, respectively (Kumar et al. 2001). In the Pinjore Garden, an earthquake occurred before 400 yr B.P. causing 2-m displacement over a length of 45 km, thus giving rise to the 2–16-m-high escarpment in the garden area (Malik and Mathews 2005).

25.5.5 Seismicity at North-western Terminal

The Himalaya makes a spectacular bend at its north-western terminal—the Hazara–Kashmir syntaxial bend. A zone of extremely high compression (Fig. 25.9) experiences frequent and very strong earthquakes, many of which originating at greater depth. The 8 October 2005 event of M_w 7.6 and its aftershocks lie north-west of the syntaxial bend—in the Indus–Kohistan Seismic Zone between the Hazara Thrust system and the Kohistan mountain range. The Tangdhar–Uri belt provided evidence of oblique slip movement along a NW–SE-trending fault extending from Balakot to Muzaffarabad and beyond (Thakur et al. 2006). This is the zone of very high microseismicity (Armbruster et al. 1978). The

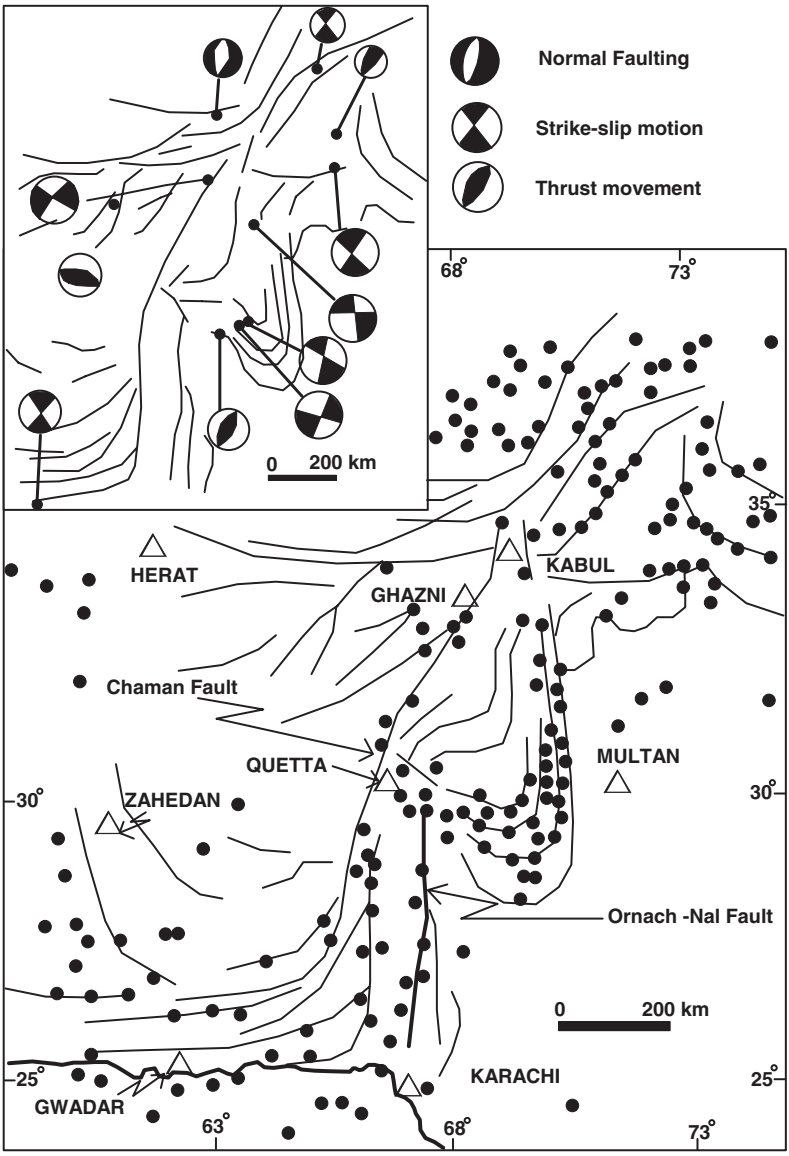

Fig. 25.9 Seismicity in the Pakistan sector of the mountain arc is related to active thrusts and faults, including the 800-km-long strike-slip Chaman Fault and the Nal–Ornach Fault system (Quittmeyer and Jacob 1979). *Inset* shows focal mechanism solutions of some earthquakes (Verma et al. 1980)

strain relaxation in the upper 25 km of the crust correlates with the pronounced topographical step, while the deeper (down to the depths of 70 km) is related to another tectonic plane which is 100 km south of the Indus–Kohistan Seismic Zone. Fault plane solutions showed either reverse or strike-slip faulting (Fig. 25.9 *inset*). Comprehensive documentation of earthquakes of the period 1914–1965 demonstrated that left-lateral movements gave rise to earthquakes including the 1935 Quetta event of M_w 7.6 along the Chaman and Herat faults (Quittmeyer and Jacob 1979). It may be mentioned that the Chaman Fault is in the line of the active Owen Fracture in the Arabian Sea. Making the boundary between the Arabian and Indian plates, the Owen Fracture is a right-lateral transform fault system. The great earthquake of 27 November 1945 (M_s 8), which was accompanied by tsunami, is attributed to the subduction of the Indian Ocean plate along the Makran Subduction Zone.

25.6 Seismicity in the Eastern Flank

25.6.1 Segmented Plate Margin

The Indian plate is underthrusting the Myanmar microplate of the Asian Plate at a rate of 35 mm/year. It is an oblique convergence entailing clockwise motion of India. This has resulted in the segmentation of the eastern margin of the Indian plate encompassing Assam and Bangladesh (Alam 2004). Significantly, several tracts of the Bengal Basin are subsiding due to movements on active faults such as the Dauki and the Madhupur. The rate of subsidence varies from sector to sector—3.9 mm/year in Sirajpur–Rangpur area, 2.04 mm/year in the Sylhet Plain, 4.00 mm/year in the Khulna region and more than 5.00 mm/year in the Sundarban–Hatiya deltaic tract (Umitsu 1993; Alam 1996).

Seismic data coupled with fractal analysis show that the Indo-Myanmar fold belt (Fig. 25.10) in Tripura is seismically more active than the Bengal Basin (Sonmonu and Dimri 1995). Epicentral distribution in Assam shows two distinct trends—the NE–SW to N–S arcuate trend parallel to the border ranges, and the ENE–WSW to NW–SE trend transverse to this orientation. The NW–SE trend extends into Bangladesh, as is evident from the 27 July 2003 Kolabari earthquake of M_s 5.6 which originated at a depth of 11 km, in the Rangamati district. This earthquake was related to thrusting with a strike-slip component (Alam 2004).

25.6.2 Myanmar Belts

The distribution of intermediate-depth hypocentres defines a Benioff Zone (Fig. 25.10c) dipping eastward under the Myanmar platelet (Verma et al. 1976). A critical analysis of hypocentres of earthquakes, restricted to the depth of 180 km,

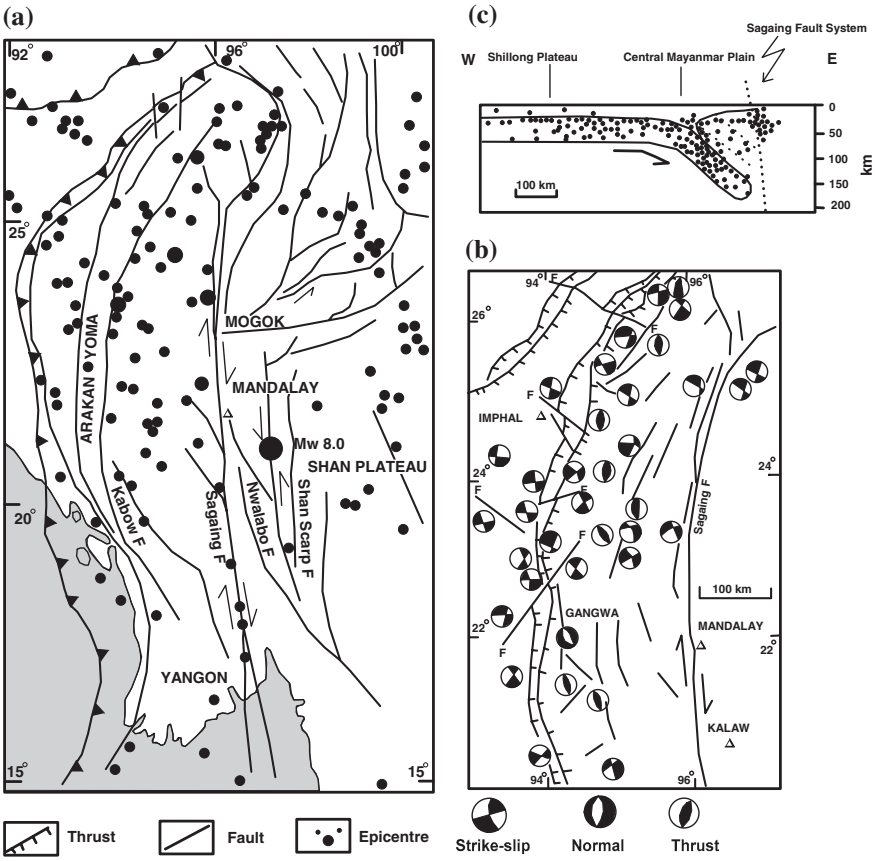

Fig. 25.10 **a** Epicentres of earthquakes in the context of tectonic framework of Myanmar (after Vigny et al. 2003). **b** Focal mechanism solutions of some earthquakes shown in a very generalized tectonic map (after Mukhopadhyay and Dasgupta 1988). **c** Myanmar Benioff Zone defined by hypocentres under Myanmar (after Verma et al. 1976)

suggests that the Benioff zone is not uniform and it terminates beyond the latitude 26°N. Focal mechanism solutions (Fig. 25.10b) indicate shallow-angle thrusting at the upper edge of the slab and down-dip tensional faulting in the lower edge (Mukhopadhyay and Dasgupta 1988). There is a clear segregation of events of the strike-slip type down to the depth of nearly 90 km and of the thrust-type earthquakes occurring exclusively below this depth (Ravi Kumar et al. 1996).

In the eastern margin of Myanmar, the earthquakes are attributed to strike-slip movement on the Sagaing Fault and to normal faulting along the Shan Scarp Fault. GPS survey in the Mandalay area during 1998–2000 unequivocally establishes the deduction that these two fault systems absorb <20 mm/year of the 35 mm/year India–Sundaland strike-slip motion (Vigny et al. 2003). Obviously, the Indo-Myanmar Ranges accommodate the remaining (>10 mm/year) convergence.

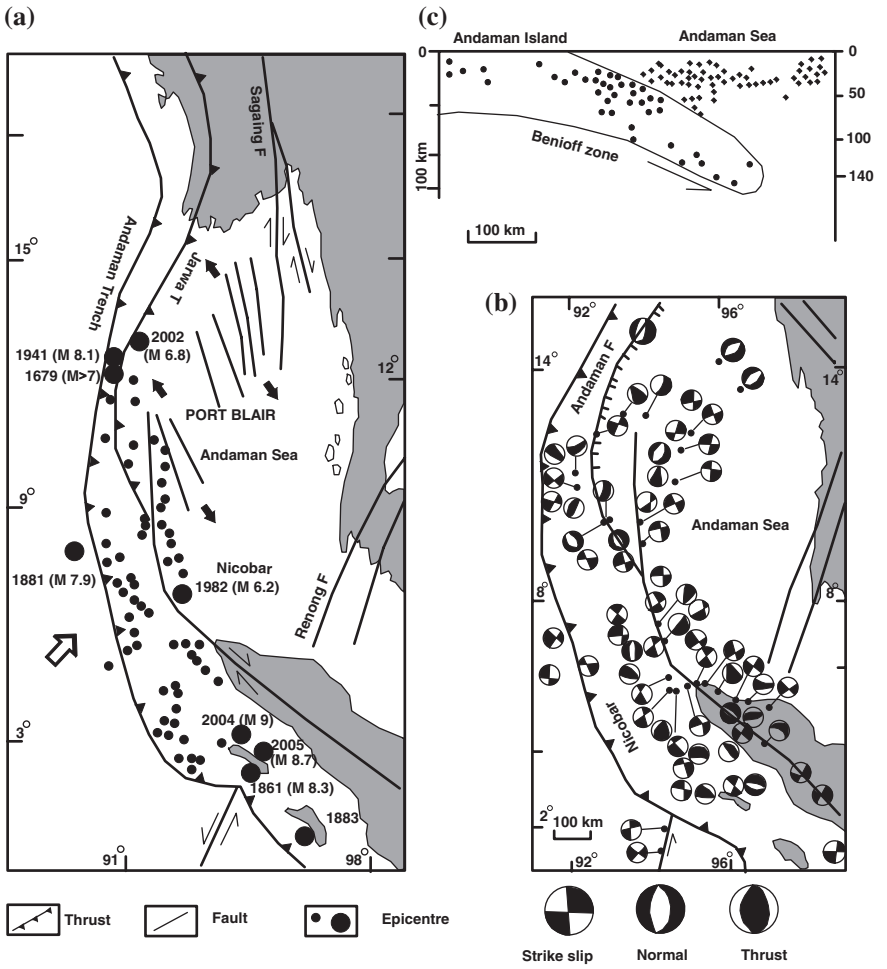

Fig. 25.11 **a** Epicentral distribution in the domain of the Andaman Island Arc and the Andaman Sea (based on Curray 2005 and Purnachandra Rao and Chary 2005). **b** Focal mechanism solutions of some earthquakes shown in the very generalized tectonic map. **c** Hypocentres define the Andaman Benioff Zone (**b** and **c** modified after Dasgupta and Mukhopadhyay 1993)

However, there is also a suggestion that no subduction is taking place along the India–Myanmar border mountain because the north-eastward motion of the Indian plate is compensated by the eastward motion of the South China plate (Sahu et al. 2006) (Fig. 25.11).

25.6.3 Andaman Island Arc and Back-Arc Sea

1. Representing the southward extension of the Indo-Myanmar Ranges and the central Myanmar Plains, the belts of the Andaman Island Arc and the Andaman Sea exhibit nearly the same pattern of seismicity. The Indian Ocean plate is converging towards Sundaland at a rate more than 30 mm/year (Curray 2005) and underthrusting along the Andaman Trench. The GPS investigations demonstrate that the convergence is taking place through thrusting normal to the arc (Banerjee 2005). The earthquake foci define a Benioff Zone dipping 40°–55° eastward down to a depth of nearly 200 km below the Andaman Islands. The oblique Benioff Zone is developed down to the depth of 200 km. Gravity models provide evidence that there was structural control in the propagation of rupture within the lithosphere (Radhakrishna et al. 2008). Focal mechanism solutions of 68 earthquakes showed low-angle thrusting along the upper edge of the descending Indian Ocean plate and down-dip tensional events on steeply (>60°) dipping nodal planes in the lower edge. The seismicity in the back-arc part—the Andaman Ridge—is restricted to the depth level of 40–46 km (Dasgupta and Mukhopadhyay 1993).

The 31 December 1881 Car Nicobar earthquake of M_w 7.9 ± 0.1, which ruptured two segments of the island arc—40 km in the north and 150 km in the south—was associated with a mean slip of 2.7 m and the ground uplift of 10–60 cm (Ortiz and Bilham 2003). It generated a tsunami, having wave height less than one metre along the Indian coast. The 13 September 2002 Diglipur event of M_s 6.8 represented a peak in the progressive strike-slip deformation of the island. It was a renewal of stress build-up after the 26 June 1941 great earthquake of M_s 8.1, which had ruptured nearly 800 km of the island arc (Rajendran et al. 2003). The megaevent of the magnitude M_w 9.3 that originated in the Andaman–Java Trench off Sumatra on 26 December 2004 formed a 1200-km-long rupture and caused 10–15-m slip (Purnachandra Rao and Chary 2005). The 800-km rupture in the Andaman Island Arc was accompanied by subsidence and elevation—(i) 1–1.5-m subsidence of both margins of the North Andaman island (north of 10°N), (ii) <1-m emergence of the western margin and equal subsidence of the eastern margin of the Middle Andaman and (iii) >1-m emergence of both margins of the South Andaman island (Rajendran et al. 2007). The 28 March 2005 earthquake of M 8.7 occurred 250 km south-east of the 26 December 2004 earthquake at a same depth, causing 350-km-long rupture. The location of the earthquake was the triple junction of the Indian Ocean, Asian and Australian plates. Unlike the 26 December event, this earthquake did not generate any large tsunami.

Analysis of GPS data shows that the 26 December 2004 event caused eastward shifting of the Southern Indian Shield by 10–16 mm, decrease by 30 mm of the interstation distance between Bangalore and Singapore, and 16-mm eastward shifting of Bangalore with respect to Dehradun. These developments indicate an average slip of more than 5 m along the full length of the rupture in the

Andaman Island Arc (Banerjee 2005). Coseismic surface displacement vectors were as follows—Car Nicobar 6.49 ± 0.009 m towards WSW with a significant 1.1-m subsidence, Chatham island near Port Blair 3.53 ± 0.010 m towards WSW with reduced subsidence and Diglipur in North Andaman 4.78 ± 0.008 m to the SW with significant uplift of 0.6 m (Jade et al. 2005).

25.7 Stable Continental Seismicity: Northern Peninsular India

25.7.1 Reactivation of Ancient Faults

Made up of four cratonic blocks, the Peninsular India is a shield that remained unaffected by compressional deformation for very long geological time. However, in this stable continental region, tension-generated rift valleys and horst mountains mostly of the Precambrian antiquity are experiencing discernible deformation since the later Quaternary period. Whenever there is a spurt of northward lurch of the Indian plate, old faults and shear zones are reactivated, giving rise to earthquakes of moderate and smaller magnitudes. Mobile belts in between the cratonic blocks are particularly prone to seismicity of this kind. One of the mobile belts is the Aravali. It extends towards the Himalaya in the form of the hidden Delhi–Haridwar Ridge under the cover of the sediments of the Indo-Gangetic Plains (Fig. 22.3).

25.7.2 Delhi–Haridwar Ridge

Delineated and cut by NE–SW-trending faults, the Aravali Mobile Belt (Figs. 25.2 and 22.3) extends towards Haridwar at the foot of the Himalaya. It is a hidden range under the cover of sediments of the Indo-Gangetic Plains. Persistent microseismicity (M 1–4.2) of the belt is related to reactivation of faults that especially pass by Rohtak, Sohna, Sonipat and Bijnaur (Fig. 25.12). Spatial distribution of epicentres shows that the NW–SE-trending subsurface Delhi–Lahore–Sargodha Ridge is also quite seismogenic, as borne out by the clustering of two-third numbers of epicentres. In the period 1983–1995, there was nearly uniform cycle of stress accumulation and relaxation of strain through small and moderate earthquakes (Bhadauria et al. 1998). Occurrence of moderately high-intensity events indicates that in the Aravali–Delhi–Haridwar belt, there is potential for large earthquakes (Verma 1985; Verma et al. 1995). This is testified by the 15 July 1720 earthquake of Delhi (intensity IX), the 1 September 1803 event of Mathura (intensity IX), the 10 October 1956 earthquake of Bulandshahr (M 6.5), the 27 August 1960 event of Delhi (M 6.0) and the 15 August 1966 earthquake of Moradabad (M 5.8).

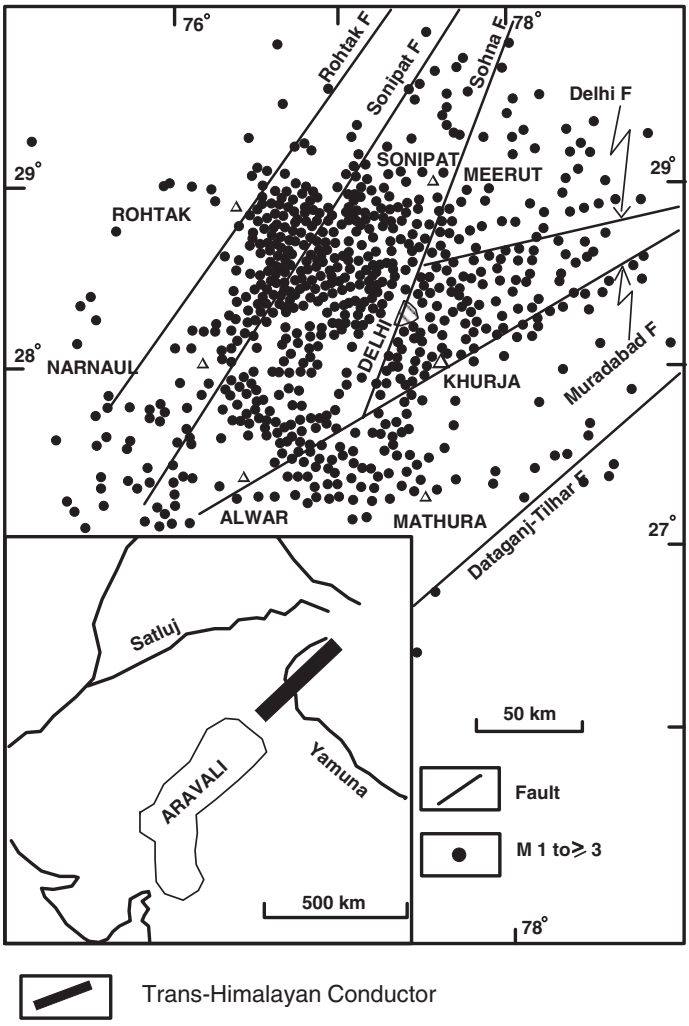

Fig. 25.12 The faulted terrain of the northerly extension of the Aravali, known as the Delhi–Haridwar Ridge, showing very high microseismicity as evident from the distribution of events ($M \geq 3$) during the period 1983–1995 (modified after Bhadauria et al. 1998). *Inset* shows existence of a transconductor, a mid-crustal electrical feature believed to be responsible for higher seismicity in this part of the Himalaya and the Indo-Gangetic Plains (based on Arora 1993)

Significantly, the top of an electric transconductor detected in the mid-crustal level and extending into the interior of the Himalaya and bending down at the Himalayan Frontal Thrust correlates with the plane of hypocentres of moderate earthquakes and defines the cut-off depth of the microseismicity (Arora and Mahashabde 1987; Arora 1993; Arora and Reddy 1995). This transconductor seems to be responsible in some way for higher seismicity in the Aravali Mobile

Belt and in the adjacent Himalayan domain. For, there is a build-up of stresses in front of this ridge and there is the release of fluids from rocks which triggers earthquake at the junction of the Himalaya with the Aravali (Arora 1993; Raval 1995).

Another subsurface branch of the Aravali trending in the NNW–SSE direction and lined by the Barmer–Konai Fault (Fig. 22.3) is believed to be responsible for the 8 November 1991 Jaisalmer earthquake of M_b 5.6 (Joshi et al. 1997).

25.7.3 Meghalaya Massif

Constituted of the dismembered and laterally offset block of the Singhbhum Craton, the Meghalaya massif is delineated in the south by the strike-slip Dauki Fault. It lies very close to the zone of underthrusting of the Indian plate under the Myanmar microplate beneath the Indo-Myanmar Ranges (Fig. 25.13). It is nearly 200 km away from the zone of underthrusting beneath the Arunachal Himalaya. The earthquakes that shake the massif are thus related to the seismicity of a stable continental region (SCR).

The Meghalaya plateau witnessed the most powerful historical earthquake of the Indian subcontinent on 12 June 1897. The M 8.7 event was described very comprehensively in 1889 by R.D. Oldham. The rupture must have been 200 km long (Molnar 1987), and the earthquake originated at a depth of 15–23 km on a steep (50°–60°) dipping fault that follows the Brahmaputra River between Hathimora and Kholband (Gahalaut and Chander 1992). Extensive development of swamp in the Chaulkhowa basin to the north of the Brahmaputra, the eastward migration of the Pagladia and Puthimari rivers and the 4–5-m uplift of the alluvial deposit of the Brahmaputra collectively indicate that it was the subsidence of the crust on a south-dipping fault—the Brahmaputra Fault—that gave rise to the 1897 megaevent (Rajendran et al. 2004). Palaeoseismites of the belt of the NW–SE-oriented Chedrung Fault show that there were three more great earthquakes in the region—around 500 ± 150 yr B.P., 1100 ± 200 yr B.P. and >1500 ± 200 yr B.P. (Sukhija et al. 1999).

The present level of microseismicity (Fig. 25.13) is very high beneath the Tura Hills cut by the Dapsi Thrust—a low-angle north-dipping reverse fault showing a component of strike-slip motion (Kayal and De 1991; Kayal 2003; Kayal et al. 2006). Focal mechanism solutions indicate both strike-slip and thrust movements at a depth of 20–40 km (Barua et al. 1997). The Dapsi Thrust and the Brahmaputra Fault are responsible for the higher seismicity of the region.

It may be mentioned that great and large earthquakes ($M \geq 7.5$) in north-eastern India were preceded by swarms of anomalous seismic activity, occurring for the duration of 11–17 years before the event of M 7.5–8.0 and 23–27 years prior to the earthquake of M 8.7 (Singh et al. 2005).

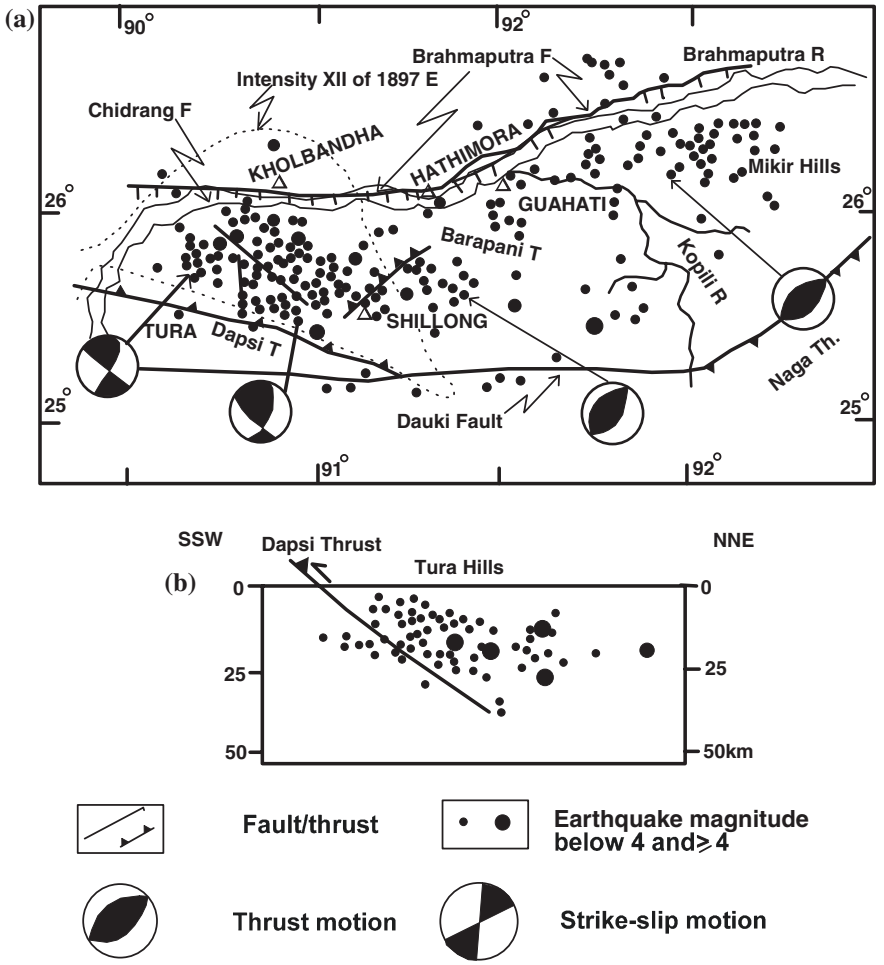

Fig. 25.13 Microseismicity in the Meghalaya massif is probably related to the reactivation of the Dapsi Thrust and the Brahmaputra Fault. Focal mechanism solutions indicate predominance of faulting-related earthquakes (based on Kayal and De 1991; Gahlaut and Chander 1992). *Section* shows distribution of hypocentres in relation to the Dapsi Thrust (after Kayal 2003; Kayal et al. 2006)

25.7.4 Kachchh Domain

Kachchh is a domain of horst hills and graben depressions. These are by a multiplicity of E–W and transverse faults (Fig. 15.9 and 25.14). The Katrol Hill represents one of the two hill ranges, and the *Ranns* occupy depressions. Reactivation of delimiting faults is responsible for the high seismicity of this region located not far from the active Owen Fracture and Laxmi Basin in the Arabian Sea. The Sabarmati Graben forms the eastern boundary of this extraordinarily active

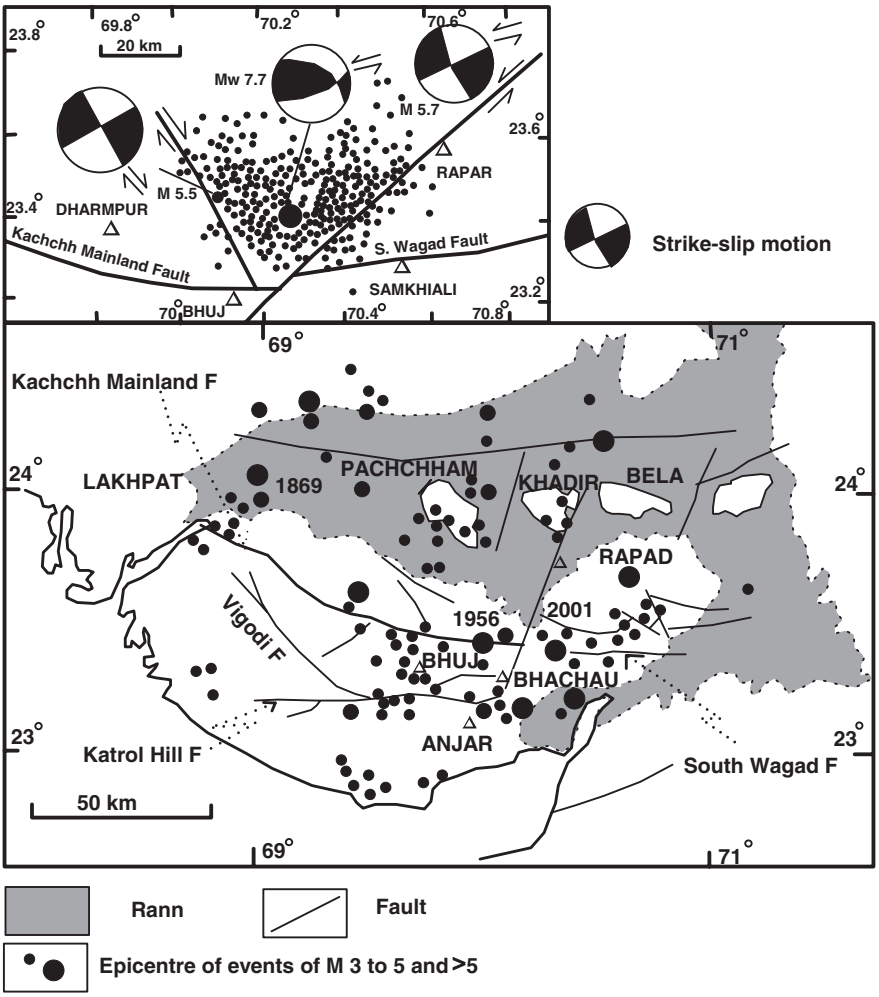

Fig. 25.14 Major faults of the Kachchh terrane in western India and the location of epicentres of larger earthquakes (after Biswas and Khattri 2002). *Inset* shows two clear trends of aftershocks of the 2001 Bhuj earthquake of M_w 7.7). All aftershocks were due to strike-slip movements (after Kayal and Mukhopadhyay 2006)

region in the stable continental margin. The E–W-oriented reverse faults and the transverse tear faults provided places to the moderate to large events. Soft sediment liquefaction features in the north-western part of Kachchh indicate the occurrence of earthquake at nearly 3000 yr B.P. and about 1000 yr B.P. in addition to the 1819 earthquake of M_w 7.5 (Rajendran et al. 2002). The 80-km-long Allahabad escarpment is a product of cumulative slip on the rupture plane.

The 1956 earthquake of M_w 7.0 at Anjar and the 26 January 2001 event of M_w 7.7 at Bhuj seem to be related to tear faults that have left-laterally offset the

Kachchh Main Fault (which extends eastwards as the South Wagad Fault). The epicentres of the aftershocks of the 2001 Bhuj earthquake show two major trends (Fig. 25.14 *inset*)—in the NE–SW and NW–SE directions. The focal mechanism solutions of the main shock and of the best located and selected aftershock clusters indicate strike-slip motion of reverse faulting (Talwani and Gangopadhyay 2001; De et al. 2003; Kayal and Mukhopadhyay 2006). The main shock also generated right-lateral N–S tear faults, and many aftershocks were associated with these tear faults.

Nearly, 48 % of the total slip occurred on the primary fault (Dimri et al. 2005).

The N–S- to NNW–SSE-trending Sabarmati Graben of the Gujarat plains likewise experiences earthquakes, but less frequently. This is also evident from the palaeoseismites dated 3320 ± 90 yr B.P. and 2850 ± 90 yr B.P. in the Kothiyakhad–Majpur area in the lower Mahi valley (Maurya et al., 1998) and at Itola in the Dhadhar valley dated 5570 ± 30 yr B.P. (Raj et al. 2003) and the 23 March 1970 Bharuch earthquake of M 5.2 (Fig. 25.15) that occurred due to strike-slip motion on a reverse fault (Chung 1993).

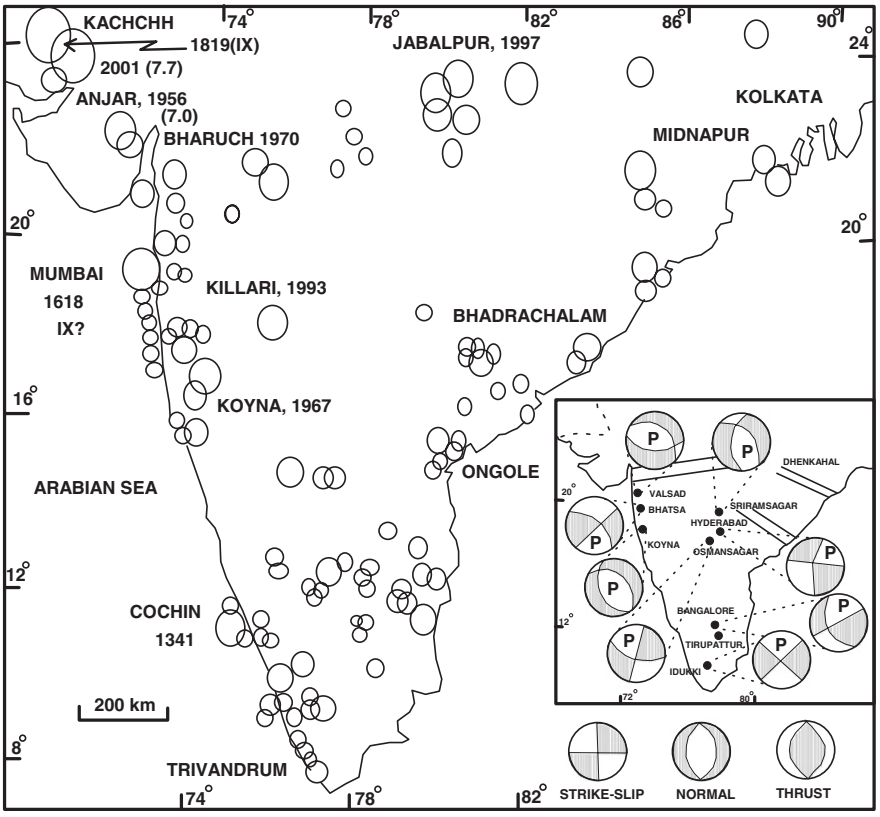

Fig. 25.15 Epicentres of known historical earthquakes of moderate and low magnitudes in central and southern parts of the Peninsular India (after Rajendran 2001). *Inset* shows focal mechanism solutions of a few important events (after Rastogi 1992)

In the Mumbai arc east of the Thane Creek, two N–S-oriented faults related to the Panvel Flexure are associated with recent earthquakes of magnitude less than 4.2 M—at Ambe on 31 May 1998, at Khairna on 16 November 2001 and at Kalyan on 14 June 2005.

25.7.5 Narmada and Tapi Grabens

In the line of the Dauki Fault, the Son–Narmada "lineament" extends WSW to the shore of the Arabian Sea. Represented by a fault pair, it defines Narmada rift valley and Satpura horst mountain of Precambrian antiquity (Fig. 25.16). The faults dip steeply 70°–80° (Shanker 1987). The throw of the faults is of the order of 1500–1800 m (Mishra and Kumar 1998; Tewari et al. 2001). The Narmada graben is offset 20–30 m by a multiplicity of transverse tear faults (Fig. 25.16). Not only are the Pleistocene sedimentary terraces tilted 20°–25° in the tract Hardi–Jabalpur but also they are displaced 10–15 m near Navagam. Ongoing movements are manifest in recurrent seismicity. There were six events in the period 1876–1993, including the 23 March 1970 Bharuch earthquake of M 5.2, the 1945 earthquake M 5.7 of Navagam, the 1938 earthquake of M 6.3 near Khandwa, the 1997 Jabalpur earthquake of M_w 6.1, and the 1927 event of M 6.5 that occurred southwest of Rewa (Figs. 25.15 and 25.16). The 22 May 1997 Jabalpur earthquake occurred at a depth of 36 ± 4 km along an ENE–WSW-trending fault (Rajendran

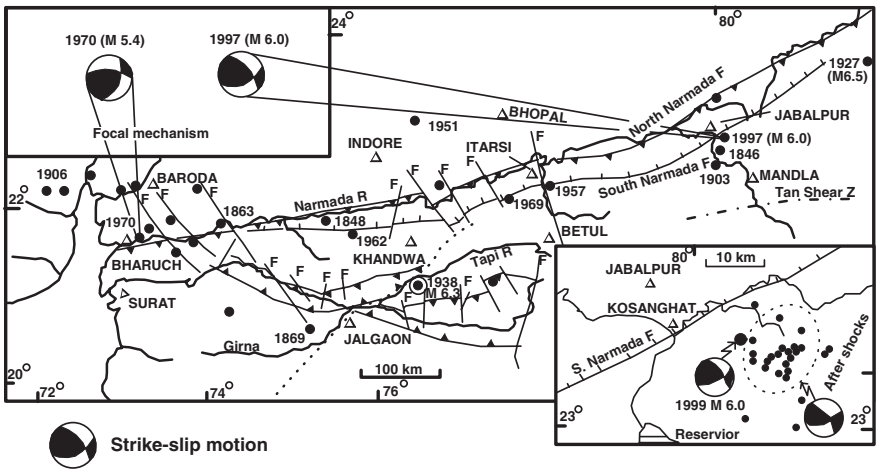

Fig. 25.16 Son–Narmada and the Tapi grabens, cut and offset by tear faults, is an active zone in central India (tectonic map based on Krishnaswamy and Raghunandan 2005 and epicentral distribution after Rajendran and Rajendran 1998). *Upper inset* fault plane solutions of Bharuch and Jabalpur earthquakes (after Rajendran and Rajendran 1998). *Lower inset* fault plane solutions of the main shock and aftershocks of the Jabalpur event (after Kayal 2000)

and Rajendran 1998). Fault plane solutions indicate reverse faulting with a component of left-lateral strike-slip motion (Kayal 2000). It is obvious that the earthquake was associated with a well-defined tectonic feature—the Narmada rift—and was of deep crustal source.

25.8 SCR Seismicity: Southern Indian Shield

25.8.1 Deccan Plateau

Historical earthquakes of many places, including Dhule in 1869 and 1872, Bhorvadi in 1896, Ahmednagar in 1938, Appegaon in 1201 and 1970, Beed in 1953, Nanded in 1942, Toka in 1757, Ujani in 1955, Ter in AD 450, Lonand in 1764 and Sholapur in 1865 and 1934 (Chandra 1978; Srivastava and Dube 1996; Ramalingeswara Rao 2000), bear testimony to the seismicity in the stable continental region (SCR) of the Deccan Plateau. Palaeoseismites in the Chandanpur valley in upland Maharashtra show that a great earthquake had shaken the subsurface Kurduvadi rift belt sometime between 5000 and 7000 yr B.P. (Dole et al. 2000). In the Killari area in district Osmanabad, soft sediment liquefaction features indicate occurrence of earthquakes sometime between 190 B.C. and A.D. 410 along an east–west-trending fault zone (Sukhija et al. 2006). Deep drilling in another place in the same area revealed a cumulative slip of 6 m which must have been caused by at least six moderate earthquakes (1977). There is also an evidence for at least one moderate earthquake about 1500 yr B.P. at Ter, 40 km northwest of Killari (Rajendran and Rajendran 1999). The 30 September 1993 event at Killari was of the magnitude M_w 6.1 (M_b 6.3) and occurred at a depth less than 10 km (Fig. 25.17a). Focal mechanism solutions show that the main shock and the deeper (6–15 km) aftershocks were caused by reverse faulting, while the shallow aftershocks resulted from strike-slip movement (Kayal 2000). It was possibly the intersection of an E–W thrust and a NW–SE-trending fault that provided the locale for the Killari events. It may be recapitulated that earthquakes occur due to reactivation of pre-existing faults. Due to slow strain build-up, they recur after long intervals of time. The heat flow is also not normal (Roy and Rao 1999).

The pattern of epicentral distribution of earthquakes of $M \geq 3$ in the Koyna–Warna valleys characterized by low background seismicity (Fig. 25.17b) implies reactivation of a N/NNE–S/SSW-oriented shear zone (Rajendran and Harish 2000), the reactivation being triggered by increased load of impounded reservoir water (Gupta et al. 1982; Gupta 1983). Fault plane solution of the 13 April 1969 Bhadrachalam earthquake of M_w 5.7 (Fig. 25.15), which originated at a depth of 10 km, showed strike-slip motion on a fault (Chung 1993) of the Godavari graben.

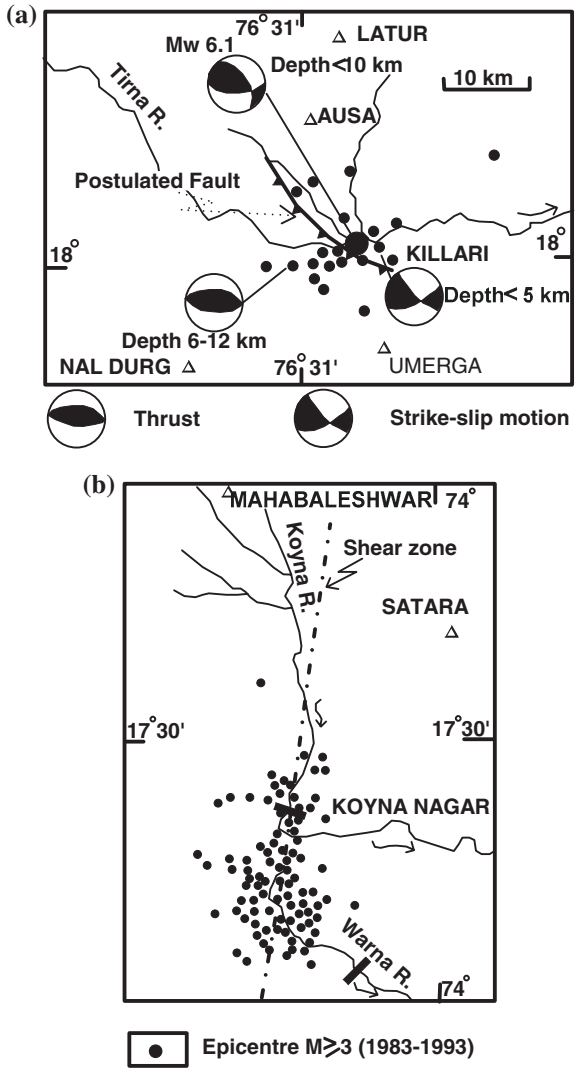

Fig. 25.17 **a** 1993 Killari earthquake and its deeper aftershocks were related to thrusting movement, while shallow aftershocks resulted from strike-slip faulting (after Kayal 2000). **b** Relocated earthquakes of $M \geq 3$ of the period 1983–1993 in the Koyna–Warna basin suggest existence of a N/NNE–S/SSW-trending active shear zone (after Rajendran and Harish 2000)

25.8.2 Mysore Plateau

Most of the earthquakes of the Deccan and Mysore plateaus give strike-slip fault plane solutions, such as the 14 January 1982 Osman Sagar (Md 3.5, depth 2 km) earthquake, the 30 June 1983 Hyderabad event (Md 4.5, depth 13 km), the 20 March, 1984 Bangalore earthquake (Md 4.6, depth 12 km) and so on (Rastogi 1992). About 25 earthquakes (Fig. 25.15 *inset*) occurring since 1828 in the Karnataka Plateau were associated with eight major lineaments that have length more than 100 km, of which eight events of M 3.7–4.3 were close to the

Mandya–Bangalore line (Ganesh and Nijagunappa 2002). Most of the lineaments are active faults (Fig. 23.22) as borne out by topographical peculiarities developed in recent time, anomalous deflection and ponding of rivers and streams and existence of zones of shearing (Valdiya 1998, 2001b). Regional measurement of strain revealed negligible changes of dilatational strain—+11.210 microstrain and of shear strain 0.661.2 mμ radian (Paul et al. 1995). This is because the active faults continue to relax the accumulated strain through earthquakes and slow imperceptible movements along faults (Valdiya 2001b).

In the Sahyadri domain in western Karnataka, which is cut by a multiplicity of NNW–SSE- and N–S-oriented active faults and ESE–WNW shear zones (Valdiya 2001a), moderate- to low-magnitude earthquakes occur, particularly at the intersection of faults (Fig. 25.18c) as seen in the Kudremukh region (Sambandam et al. 1994). The association with some of these faults of thermal springs such as Rajapura and Puttur implies that they are possibly deep-seated in nature (Ramanathan and Chandrasekharam 1997).

On the eastern flank of the Dharwar Craton, one of the NE–SW- to NNE–SSW-trending faults in the basement of the Cauvery deltaic sediments was responsible for the September 2001 earthquake of M 5.6 (Subramanian and Gopalakrishnan 2002).

25.8.3 Kerala Region

The Palghat–Cauvery Shear Zone that separates the Dharwar Craton from the Southern Granulite Terrane experiences low to moderate seismicity. Among the many earthquakes, mention may be made of the events of 1865, 1900, 1972 and 1992. The Coimbatore earthquake of AD 1900 was of the magnitude 5.8 and the 12 December 1994 Wadakkanchery event of M_l 4.3 (Rajendran and Rajendran 1996).

In the central part of Kerala (Fig. 25.18d), the June 1988 earthquakes of M 4.5–3.4 were confined to a small area cut by WNW–ESE- and NE–SW-oriented faults (Singh et al. 1989) and the 12 December 2000 Erattupetta earthquake of M_l 5 at a depth of 6 km, occurred at the intersection of WNW–ESE-oriented fault (paralleling the Periyar Fault) with the NW–SE-oriented Thekkady Fault (Rastogi 2001). The earthquakes give strike-slip fault plane solutions.

25.8.4 Tectonics of the Tail End

The Indian crust has been under compression ever since India collided with Asia. The E–W-oriented shear zones of Precambrian origin are characterized by anastomosing system of reverse faults and hence are particularly weak. The shear zones provided planes of breaking of the Indian crust in the geological past. This resulted in the northward thrusting and even popping up of the deeper part

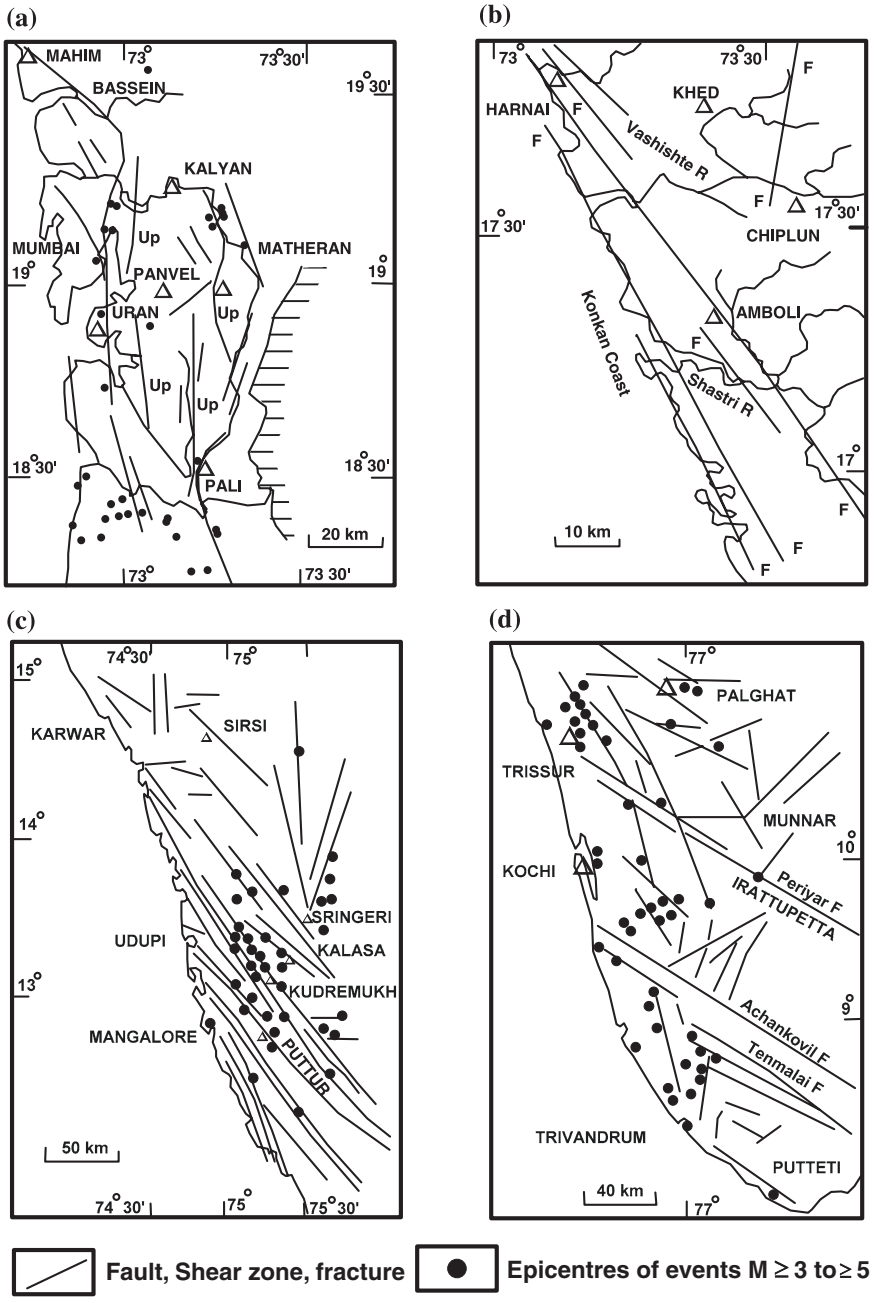

Fig. 25.18 Major faults, shear zones and lineaments in the west coast belt. Many of these are quite active (in the Mumbai belt). **a** Mumbai sector (based on Srinivasan 2002; Raghukanth and Iyer 2006). **b** Konkan sector (based on Kundu and Matam 2000). **c** Kanara sector (based on Sambandam et al. 1994; Valdiya 2001b). **d** Malabar sector (based on Singh and Mathai 2004; Valdiya and Narayana 2007)

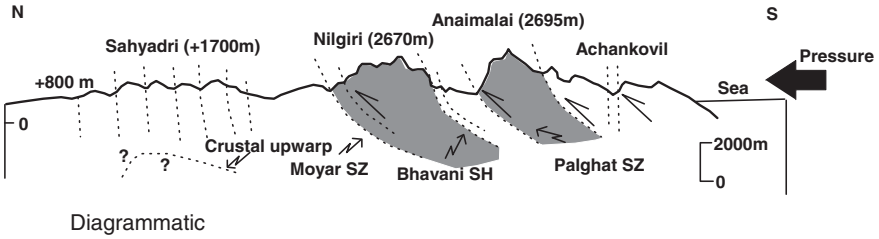

Fig. 25.19 Overstressed crust of the Indian Shield in southern India broke along the reactivated reverse faults of the E–W-trending Palghat–Cauvery and Moyar–Bhavani Shear Zones of Precambrian antiquity (after Valdiya 2001a). The southern part (Southern Granulite Terrane) was thrust up as high mountains, culminating eventually in the emergence of the Nilgiri and the Anaimalai–Elaimalai Hills. The northward-directed thrust movement was transferred partially as strike-slip displacement along the reactivated N–S-trending tear faults of the Dharwar Craton, thus giving rise to the two horst mountains on its margins, the Biligirirangan–Mahadeswaramalai Range in the east and the Sahyadri Mountain in the west

of the crust and giving rise to the Anaimalai–Elaimalai and the Nilgiri massifs (Fig. 25.19). Continuing push of the northward-moving Indian plate reactivates these steeply dipping fault planes, giving rise to earthquakes periodically (Valdiya 1998, 2001b).

References

Ahmad, S., & Bhat, M. I. (2012). Tectonic geomorphology of the Rambiasa basin, SW of Kashmir valley reveals emergent out-of-sequence active fault system. *Himalayan Geology, 33*, 162–172.

Alam, M. (1996). Subsidence of the Ganges-Brahmaputra delta of Bangladesh and associated drainage, sedimentation and salinity problems. In J. D. Milliman & B. U. Haq (Eds.), *Sea level rise and coastal subsidence* (pp. 169–192). Amsterdam: Kluwer Academic Publishers.

Alam Khan, A. (2004). Tectonoics of collision margin and nature of seismicity in Eastern Folded Belt of Bengal Basin. *Journal of Nepal Geological Society*, *30*, 31–38.

Ambraseys, N., & Bilham, R. (2000). A note on the Kangra M_s 7.8 earthquake of 4 April 1905. *Current Science, 79*, 45–50.

Ambraseys, N., & Jackson, D. (2003). A note on early earthquakes in northern India and southern Tibet. *Current Science, 84*, 570–582.

Armbruster, J., Seeber, L., & Jacob, K. A. (1978). Northwestern termination of the Himalayan mountain front: Active tectonics from microearthquakes. *Journal of Geophysical Research, 83*, 269–282.

Arora, B. R. (1993). Implication of electrical conductivity structures in the tectonic framework of northwest India. *Current Science, 64*, 848–855.

Arora, B. R., & Mahashabde, M. V. (1987). A transverse conductive structure in the northwest Himalaya. *Physics of the Earth & Planetary Interiors, 45*, 119–127.

Arora, B. R., & Reddy, C. D. (1995). Deep crustal conductive structures of the frontal belt of the Garhwal Himalaya and their seismotectonic significance. *Memoirs of the Geological Society of India, 30*, 109–124.

Bali, R., Agarwal, K. K., Patil, S. K., Nawaz Ali, S., Rastogi, S. K., & Krishna, Kalyan. (2011). Record or neotectonic activity in the Pindari Glacier Valley: Study based on glacio-geomorphic and AMS fabric evidences. *Earth Science India, 40*, 1–14.

Bali, R., Nawaz Ali, S., Agarwal, K. K., Rastogi, S. K., Krishna, K., & Srivastava, P. (2013). Chronology of late Quaternary glaciations in the Pindar valley, Alaknanda basin, Central Himalaya, India. *Journal of Asian Earth Sciences, 66*, 224–233

Banerjee, P. (2005). Interseismic geodetic motion and far-field coseismic surface displacements caused by the 26 December 2004 Sumatra earthquake observed from GPS data. *Current Science, 88*, 1491–1496.

Banerjee, P., & Burgmann, R. (2001). Convergence across the northwest Himalaya from GPS measurements. *Geophysical Research Letters*, *29*. doi:10.1029/2002

Banerjee, P., Burgmann, R., Nagarajan, B., & Apel, E. (2008). Intraplate deformation of the Indian subcontinent. *Geophysical Research Letters*, *35*, L. 18301.

Banerjee, D., Singhvi, A. K., Bagati, T. N., & Mohindra, R. (1997). Luminescence chronology of seismites at Sumdo (Spiti valley) near Kaurik-Chango fault, NW Himalaya. *Current Science, 73*, 276–281.

Bapat, A., Kulkarni, R. C., & Guha, S. K. (1983). *Catalogue of Earthquakes in India and Neighbourhood*. Roorkee: Indian Society of Earthquake Technology.

Baronowski, J., Armbruster, J., Seeber, L., & Molnar, P. (1984). Focal depths and fault-plane solutions of earthquakes and active tectonics of the Himalaya. *Journal of Geophysical Research, 89*, 6918–6928.

Barua, S., Duarah, R., & Yadav, D. K. (1997). Pattern of seismicity in Shillong-Mikir Plateau and the orientation of compressional axis. *Journal of the Geological Society of India, 49*, 533–538.

Bhadauria, Y. S., Arora, S. K., & Singh, M. (1998). Seismicity of Delhi region from local earthquake data of the Delhi seismic array. *Journal of Indian Geophysical Union, 2*, 7–21.

Bilham, R. (1995). Location and magnitude of the 1833 Nepal earthquake and its relation to the rupture zones of contiguous great Himalayan earthquake. *Current Science, 69*, 101–128.

Bilham, R., & Gaur, V. K. (2000). Geodetic contributions to the study of seismotectonics in India. *Current Science, 79*, 1259–1269.

Biswas, S. K., & Khattri, K. N. (2002). A geological study of earthquakes in Kutch, Gujarat, India. *Journal of the Geological Society of India, 60*, 131–142.

Burgess, W. P., Yin, A., Dubey, S. C., Shen, Z.-K., & Kelty, T. K. (2012). Holocene shortening across the Main Frontal Thrust zone in the eastern Himalaya. *Earth & Planetary Science Letters*, *357–358*, 152–167.

Catherine, J. K. (2004). A preliminary assessment of internal deformation in the Indian plate from GPS measurements, *Journal of Asian Earth Sciences, 23*, 461–465.

Chander, R., & Gahalaut, V. K. (1994). Preparations for future great earthquakes seen in levelling observations along two lines across the Outer Himalaya. *Current Science, 67*, 531–534.

Chandra, U. (1978). Seismicity, earthquake mechanisms and tectonics along the Himalaya mountain range and vicinity. *Physics of the Earth & Planetary Interiors, 16*, 109–131.

Chung, W.-Y. (1993). Source parameters of two rift-associated intraplate earthquakes in Peninsular India: The Bhadrachalam earthquake of April 13, 1969 and the Broach earthquake of March 23, 1970. *Tectonophysics, 225*, 219–230.

Clark, M. K., Schoenbohm, L. M., Royden, L. H., Whipple, K. X., Burchfiel, B. C., Zhang, X., et al. (2004). Surface uplift, tectonics and erosion of eastern Tibet from large-scale drainage patterns. *Tectonics*, *23*, TC 1006. doi:10.1029/2–002TC001402

Cotton, F., Campillo, M., Deschamps, A., & Rastogi, B. K. (1996). Rupture history and seismotectonics of the 1991 Uttarkashi Himalaya earthquake. *Tectonophysics, 258*, 35–51.

Curray, J. R. (2005). Tectonics and history of the Andaman Sea region. *Journal of Asian Earth Sciences, 25*, 187–232.

Dasgupta, S., & Mukhopadhyay, M. (1993). Seismicity and plate deformation below the Andaman arc, northeastern Indian Ocean. *Tectonophysics, 225*, 529–542.

Dasgupta, S., Mukhopadhyay, B., Mukhopadhyay, M., & Nandi, D. R. (2013). Role of transverse tectonics in the Himalayan collision: further evidence from two contemporary earthquakes. *Journal of the Geological Society of India*, *81*, 241–247.

De, R., Gaokar, S. G., Srirama, B. V., Ram, S., & Kayal, J. R. (2003). Fault plane solutions of the January 26, 2001 Bhuj earthquake sequence. *Proceedings of the Indian Academy of Sciences (Earth & Planetary Sciences)*, *112*, 413–419.

DeMets, C., Gordon, R. G., Argus, D. F., & Stein, D. (1994). Effect of recent revision of the geomagnetic reversal time-scale and estimates of current plate motion. *Geophysical Reseach Letters, 21*, 2191–2194.

Dimri, V. P., Vedanti, N., & Chattopadhyay, S. (2005). Fractal analysis of aftershock sequence of the Bhuj earthquake. A wavelength-based approach. *Current Science, 88*, 1617–1620.

Dole, G., Peshwa, V. V., & Kale, Vivek. (2000). Evidence of a palaeoseismic event from the Deccan Plateau upland. *Journal of the Geological Society of India, 56*, 547–555.

Drupka, D., Velasco, A. A., & Doser, D. I. (2006). Seismicity in the Kingdom of Bhutan (1937–2003): Evidence for crustal transcurrent deformation. *Journal of Geophysical Research*, *111*. doi:10.1029/2004JB003087

Dutta, S., Suresh, N., & Kumar, R. (2012). Climatically controlled Late Quaternary terrace staircase development in the fold-and-thrust belt of sub-Himalaya. *Palaeogeography, Palaeoclimatology, Palaeoecology, 356–357*, 16–26.

Freymueller, J., Bilham, R., Burgmann, R., Larson, K. M., Paul, J., Jade, S., et al. (1996). Global positioning system measurements of Indian plate motion and convergence across the Lesser Himalaya. *Geophysical Reseach Letters*, *23*, 3107–3110.

Gahalaut, V. K., & Chander, R. (1992). A rupture model for the great earthquake of 1897, northeast India. *Tectonophysics, 204*, 163–174.

Ganesh, R. K., & Nijagunappa, R. (2002). Major lineaments of Karnataka state and their relation to seismicity: Remote sensing based analysis. *Journal of the Geological Society of India, 63*, 430–439.

Gaur, V. K., Chander, R., Sarkar, I., Khattri, K. N., & Sinvhal, H. (1985). Seismicity and the state of stress from investigations of local earthquakes in Kumaun Himalaya. *Tectonophysics, 118*, 243–251.

Gupta, H. K. (1983). Induced seismicity hazard mitigation through water level manipulation at Koyna, India. *The Bulletin of the Seismological Society of America, 73*, 679–682.

Gupta, H. K., Rastogi, B. K., & Mohan, I. (1982). Studies on reservoir-induced seismicity and earthquakes in Peninsular India. *Bulletin of Glaciological Research, 20*, 127–139.

Hallet, B., & Molnar, P. (2001). Distorted drainage basins as markers of crustal strain east of Himalaya. *Journal of Geophysical Research, 106*, 13697–13709.

Hazarika, P., Kumar, M. R., Srijayanthi, G., Raju, P. S., Rao, N. P., & Srinagesh, D. (2010). Transverse tectonics in Sikkim Himalaya: Evidence from seismicity and focal mechanism data. *The Bulletin of the Seismological Society of America, 100*, 1816–1822.

Iyengar, R. N. (1999). Earthquakes in ancient India. *Current Science, 77*, 827–829.

Iyengar, R. N., & Sharma, D. (1999). Some earthquakes of the Himalayan region from historical sources. *Himalayan Geology, 20*, 81–85.

Jackson, M., & Bilham, R. (1994). Constraints on Himalayan deformation inferred from vertical velocity fields in Nepal and Tibet. *Journal of Geophysical Research, 99*, 13897–13912.

Jade, S. (2005). Estimates of plate velocity and crustal deformation in the Indian subcontinent using GPS geodesy. *Current Science, 86*, 1443–1448.

Jade, S., Anand, M. B., Dileep Kumar, P., & Banerjee, S. (2005). Co-seismic and post-seismic displacements in Andaman and Nicobar Islands from GPS measurements. *Current Science, 88*, 1980–1984.

Jade, S., Mukul, M., Bhattacharya, A. K., Vijayan, M. S. M., Jagannathan, S., Kumar, A., et al. (2007). Estimates of interseismic deformation in northeast India from GPS measurements. *Earth & Planetary Science Letters, 263*, 221–234.

Jayangondaperumal, R., Kumar, S., Wisnousky, S. G., Mahajan, A. K., Gupta, V., Arora, B. R., & Suresh, N. (2008). Late Pleistocene activity of intrabasinal Bhauwala thrust, Dehradun, NW Himalaya. *Himalayan Geology, 29*, 1–142.

Joshi, D. D. (2004). A seismogenic active fault in the western Himalaya. *Current Science, 87*, 863–864.

Joshi, V. U., & Kale, V. S. (1997). Colluvial deposits in northwest Deccan, India: Their significance in the interpretation of late Quaternary history. *Journal of Quaternary Science*, *12*, 391–403.

Joshi, D. D., Dharman, R., Saxena, A. K., & Mulkraj, (1997). Jaisalmer earthquake of 1991: Its effects and tectonic implications. *Journal of the Geological Society of India*, *49*, 433–436.

Joshi, D. D., Kandpal, G. C., John, Biju, & Pande, P. (2005). Morphotectonic and palaeoseismic studies along the Yamuna tear zone, Himalayan frontal belt [special publication]. *Geological Survey of India, 85*, 225–236.

Kaila, K. L., Gaur, V. K., & Narain, Hari. (1972). Quantitative seismicity map of India. *The Bulletin of the Seismological Society of America, 62*, 1119–1132.

Kayal, J. R. (1996). Precursor seismicity, foreshocks and aftershocks of the Uttarkashi earthquake of October 20, 1991 in Garhwal Himalaya. *Tectonophysics, 263*, 339–345.

Kayal, J. R. (2000). Seismotectonic study of the two recent SCR earthquakes in central India. *Journal of the Geological Society of India, 55*, 123–138.

Kayal, J. R. (2003). Seismotectonic structures of western and eastern Himalayas: constraints from microearthquake data. *Memoirs of the Geological Society of India, 53*, 279–311.

Kayal, J. R., Arefiev, S. S., Barua, S., Hazarika, D., Gogoi, N., Kumar, A., et al. (2006). Shillong plateau earthquakes in northeast Indian region: Complex tectonic model. *Current Science, 91*, 109–114.

Kayal, J. R., Barua, S., Baruah, S., & Tatevossian, R. (2012). Is the Kopilis fault vulnerable for impending large earthquake in northeast India? *DCS-DST News*, August Issue, 2–5.

Kayal, J. R., & De, R. (1991). Microseismicity and tectonics in northeast India. *The Bulletin of the Seismological Society of America, 81*, 131–138.

Kayal, J. R., De, R., & Chakraborty, P. (1993). Microearthquakes at the Main Boundary Thrust in eastern Himalaya and the present-day tectonic model. *Tectonophysics, 218*, 375–381.

Kayal, J. R., & Mukhopadhyay, S. (2006). Seismotectonics of the 2001 Bhuj earthquake (Mw 7.7) in western India: Constraints from aftershocks. *Journal of Indian Geophysical Union, 10*, 45–57.

Khanal, K. N. (1997). Source parameters estimation of the 1980 Bajang earthquake, farwestern Nepal. *Journal of Nepal Geological Society, 15*, 45–51.

Khattri, K. N. (1987). Great earthquake gaps and potential for earthquake disaster along the Himalaya plate boundary. *Tectonophysics, 138*, 79–92.

Khattri, K. N. (1998). A seismic hazard and risk scenario for Himalaya and Ganga plains due to a future great earthquake. *National Academy of Science Letters, 21*, 193–220.

Khattri, K. N. (1999). Probabilities of occurrence of great earthquakes in Himalaya. *Current Science, 77*, 967–972.

Kothyari, G. C., & Pant, P. D. (2008). Evidence of active deformation in northwest part of Almora in Kumaun Lesser Himalaya: A geomorphic perspective. *Journal of the Geological Society of India*, *72*, 353–304.

Krishnaswamy, V. S., & Raghunandan, K. R. (2005). The Satpura uplift and the palaeoclimate of the Holocene and auxiliary evidence from the Valmiki Ramayana. *Journal of the Geological Society of India, 66*, 161–170.

Kumar, R., Gill, G. S., & Gupta, L. N. (2005). Earthquake-induced structures in Pinjor Formation of Nadah area, Haryana. *Journal of the Geological Society of India, 65*, 346–352.

Kumar, S., Wesnousky, S. G., Rockwell, T. K., Ragona, D., Thakur, V. C., & Seitz, G. G. (2001). Earthquake recurrence and rupture dynamics of Himalayan Frontal Thrust, India. *Science, 294*, 2328–2331.

Kundu, B., & Matan, A. (2000). Identifical of proble faults in the vicinity of Harnai-Ratnagiri region of the Konkan Coast, Maharashtra. *Current Science, 78*, 1556–1560.

Lave, J., & Aouac, J. P. (2000). Active folding of fluvial terraces across the Siwalik Hills, Himalayas of central Nepal. *Journal of Geophysical Research, 105*, 5735–5770.

Lave, J., Yule, D., Sapkota, S., Basant, K., Maddan, C., Attal, M., & Pandey, M. R. (2005). Evidence for a great medieval earthquake (~1100 AD) in the central Himalaya, Nepal. *Science, 307*, 1302–1305.

Luirei, K., & Bhakuni, S. S. (2008). Ground tilling in Likhabari area along the frontal part of Arunachal Himalaya: Evidence from neotectonics. *Journal of the Geological Society of India, 71*, 780–786.

Luirei, K., Pant, P. D., & Kothyari, G. C. (2006). Geomorphic evidence of neotectonic movements in Dharchula area, northeast Kumaun: A perspective of recent tectonic activity. *Journal of the Geological Society of India, 67*, 92–100.

Lyon-Caean, H., & Molnar, P. (1983). Constaints on the structure of the Himalaya from an analysis of gravity anomalies and a flexural model of the lithosphere. *Journal of Geophysical Research, 88*, 8171–8191.

Mahesh, P., Gahlaut, V. K., Catherine, J. K., Ambikapathy, A., Kundu, B., Bansal, A., et al. (2012). Localized crustal deformation in the Godavari failed rift, India. *Earth & Planetary Science Letters, 333–334*, 46–51.

Malik, J. N., & Mathew, G. (2005). Evidence of palaeoearthquakes from trench investigations across Pinjore Garden fault in Pinjore Dun, NW Himalaya. *Journal of Earth System Science, 114*, 387–400.

Malik, J. N., Morino, M., Mishra, P., Bhuiyan, C., & Kaneko, F. (2008a). First active fault exposure identified along Kachchh Mainland Fault : Evidence from trench excavation near Lodai village, Gujarat, northern India. *Journal of the Geological Society of India, 71*, 201–208.

Malik, J. N., Nakata, T., Philip, G., Suresh, N., & Virdi, N. S. (2008b). Active fault and palaeoseismic investigations : evidence of a historic earthquake along Chandigarh Fault in the Frontal Himalaya Zone, NW India. *Himalayan Geology, 29*, 109–113.

Malik, J. N., Sahoo, A. K., Shah, A. A., Shinde, D. P., Juyal, N. & Singhvi, A. V. (2010a). Palaeoseismic evidence from trench investigation along Hajipur fault, Himalaya Frontal Thrust, NW Himalaya: Implications of the faulting pattern on landscape evolution and seismic hazard. *Journal of Structural Geology*, *32*, 350–361.

Malik, J. N., Shah, A. A., Sahoo, A. K., Puhan, B., Banerjee, C., Shinde D. P., et al. (2010b). Active fault, fault growth and segment linkage along the Janauri anticline (front foreland fold), Northwest Himalaya, India. *Tectonophysics*, *483*, 327–343.

Maurya, D. M., Rachna, R., & Chamyal, L. S. (1998). Seismically induced deformational structures (seismites) from the Mid-Late Holocene terraces, lower Mahi valley, Gujarat. *Journal of the Geological Society of India, 51*, 755–758.

Meyer, M. C., Miesmyr, G., Brauner, M., Haisler, H., & Wangda, D. (2006). Active tectonics in eastern Lunana (NW Bhutan): Implication for the seismic and glacial hazard potential. *Tectonics*, *25*, doi:10.1029/2005TC001858

Mishra, D. C., & Ravi Kumar, S. (1998). Characteristics of faults associated with the Narmada–Son Lineament and rock types of Jabalpur section. *Current Science*, *75*, 308–310.

Mishra, D. C., & Ravi Kumar, S. (1998b). Characteristics of faults associated with the Narmada-Son Lineament and rock types of Jabalpur section. *Current Science, 75*, 308–310.

Misra, D. K., & Singh, T. (2002). Tectonic setting and neotectonic features along the Eastern Syntaxial Bend (Lohit and Dihang), Arunachal Himalaya. In C. C. Pant & A. K. Sharma (Eds.), *Aspects of Geology and Environment of Himalaya* (pp. 19–40). Nainital: Gyanodaya Prakashan.

Mohindra, R., & Bagati, T. N. (1996). Seismically induced soft-sediment deformation structures (seismites) around Sumdo in the Lower Spiti valley (Tethys Himalaya). *Sedimentary Geology, 101*, 69–83.

Mohindra, R., & Thakur, V. C. (1998). Historic large earthquake-induced soft sediment deformation features in the sub-Himalayan Doon Valley. *Geological Magazine, 133*, 269–281.

Molnar, P. (1987). The distribution of intensity associated with the great 1897 Assam earthquake and bounds on the extent of the rupture zone. *Journal of the Geological Society of India, 30*, 13–27.

Molnar, P. (1990). A review of the seismicity and the rates of active underthrusting and deformation at the Himalaya. *Journal of Himalayan Geology, 1*, 131–154.
Molnar, P., England, P., & Martinod, J. (1993). Mantle dynamics uplift of the Tibetan plateau and the Indian Ocean. *Review of Geophysics, 31*, 357–391.
Molnar, P., & Lyon-Caean, H. (1989). Fault-plane solution of earthquakes and active tectonics of the Tibetan plateau and its margin. *Geophysical Journal International, 99*, 123–133.
Morino, M., Malik, J. N., Mishra, P., Bhuiyan, C., & Kaneko, F. (2008). Active fault traces along Bhuj Fault and Katrol Hill Fault, and trenching survey at Wandhay, Kachchh, Gujarat, India. *Journal of Earth System Science, 117*, 181–188.
Mrinalini Devi, R. K. (2008). Tectono-geomorphic forcing of the frontal sub-Himalayan streams along the Kimin section of Arunachal Himalaya. *Journal of the Geological Society of India, 72*, 253–262.
Mukhopadhyay, D. (1984). The Singhbhum Shear Zone and its place in the evolution of the Precambrian mobile belt, North Singhbhum. *Indian Journal of Earth Sciences*, *CEISM* Volume, 205–212.
Mukhopadhyay, M., & Dasgupta, S. (1988). Deep structure and tectonics of the Burmese arc: Constraints from earthquake and gravity data. *Tectonophysics, 149*, 299–322.
Mukul, M. (2010). First-order kinematics of wedge-scale active Himalayan deformation: Insights from Darjiling-Sikkim-Tibet wedge. *Journal of Asian Earth Sciences, 39*, 645–657.
Mukul, M., Jade, S., Bhattacharya, A. K., & Bhushan, K. (2010). Crustal shortening in convergent orogens: Insight from Global Positioning System (GPS) measurements in northeast India. *Journal of the Geological Society of India, 75*, 302–312.
Nandy, D. R. (1980). Tectonic pattern of northeast India. *Indian Journal of Earth Sciences, 7*, 103–107.
Nandy, D. R. (2005). Geodynamics and seismicity of northeastern India and its adjoining areas [special publication]. *Geological Survey of India, 85*, 49–59.
Nandy, D. R., & Dasgupta, S. (1991). Tectonic patterns in northeast India. In K. K. Sharma (Ed.), *Geological and Geodynamic Evolution of Collision Zone* (pp. 371–384). Oxford: Pergamon.
Ni, J., & Barazangi, M. (1984). Seismotectonics of Himalayan collision zone: Geometry of the underthrusting Indian plate beneath the Himalaya. *Journal of Geophysical Research, 89*, 1147–1163.
Ortiz, M., & Bilham, R. (2003). Source area and rupture parameters of the 31 December 1881 Mw 7.9 Car Nocobar earthquake estimated from tsunamis recorded in the Bay of Bengal. *Journal of Geophysical Research*, *108*, B4, 2215. doi:10.1029/2002JB001941.
Pandey, M. R. (1995). Interseismic strain accumulation on the Himalayan crust. *Geophysical Reseach Letters, 22*, 751–754.
Pandey, P., & Pandey, A. K. (2004). Soft sediment deformation features in the meizoseismal region of 1999 Chamoli earthquake of Garhwal Himalaya and their significance. *Himalayan Geology, 25*, 79–87.
Pandey, P., & Pandey, A. K. (2006). Active deformation along the Hinna Fault in Uttarkashi region of Garhwal Himalaya. *Journal of the Geological Society of India, 68*, 657–665.
Pandey, M. R., Tandukar, R. P., Avouac, J. P., Vergne, J., & Heritier, Th. (1999). Seismotectonics of the Nepal Himalaya from a local seismic network. *Journal of Asian Earth Sciences, 17*, 703–712.
Pant, P. D., Geol, O. P., & Joshi, M. (1992). Neotectonic movement in the Loharkhet area, district Almora, Kumaun Himalaya. *Journal of the Geological Society of India, 40*, 245–252.
Pati, P., Parkash, B., Awasthi, A. K., Acharya, V., & Singh, S. (2011). Concealed thrusts in the middle Gangetic plains—a ground penetrating radar study proved the truth against the geomorphic features supporting normal faulting. *Journal of Asian Earth Sciences, 40*, 315–325.
Paul, J., Blume, F., Jade, S., Kumar, V., Swathi, P. S., Ananda, M. B., et al. (1995). Microstrain stability of Peninsular India. *Proceedings of the Indian Academy of Sciences (Earth & Planetary Sciences)*, *104*, 131–146.

Paul, J., Burgmann, R., Gaur, V. K., Bilham, R., Larson, K. M., Ananda, M. B., et al. (2001). The motion and active deformation of India. *Geophysical Reseach Letters, 28*, 647–650.

Paul, A., Pant, C. C., Darmwal, G. S., Pathak, U., & Joshi, K. K. (2005). Seismicity pattern of Uttaranchal (1999–2004) as recorded by DTSN in Kumaun Himalaya [special publication]. *Geological Survey of India, 85*, 89–96.

Phartiyal, B., & Sharma, A. (2009). Soft sediment deformation structures in the Late Quaternary sediments of Ladakh: Evidence for multiple phases of seismic tremours in northwestern Himalayan region. *Journal of Asian Earth Sciences, 34*, 761–770.

Phartiyal, B., Srivastava, P., & Sharma, A. (2009). Tectono-climate signatures during the Quaternary period from upper Spiti Valley, NW Himalaya, India. *Himalayan Geology, 30*, 167–174.

Philip, G., Bhakuni, S. S., & Suresh, N. (2012). Late Pleistocene and Holocene large—magnitude earthquakes along Himalayan Frontal Thrust in the central seismic gap in NW Himalaya, Kala Am, India. *Tectonophysics, 580*, 162–177.

Ponraj, M., Misra, S., Reddy, C. P., Prajapati, S. K., Amritraj, S., & Mahajan, S. H. (2010). Estimation of strain distribution using GPS measurement in the Kumaun region of Lesser Himalaya. *Journal of Asian Earth Sciences, 39*, 658–667.

Purnachandra Rao, N., & Chary, A. H. (2005). What caused the great Sumatran earthquake of 26 December 2004 and 28 March 2005. *Current Science, 89*, 449–452.

Quittmeyer, R. C., & Jacob, K. H. (1979). Historical and modern seismicity of Pakistan, Afghanistan, northwestern India and southeastern Iran. *The Bulletin of the Seismological Society of America, 69*, 773–823.

Rajendran, R. K., Rajendran, C. P., Thakkar, M., & Gartia, R. K. (2002). Sand blows from the 2001 Bhuj earthquake reveal clues on past seismicity. *Current Science, 83*, 603–610.

Radhakrishna, M., Lasitha, S., & Mukhopadhyay, M. (2008). Seismicity, gravity anomalies and lithospheric structure of the Andaman arc, NE Indian Ocean. *Tectonophysics, 460*, 248–262.

Raghukanth, S. T. G., & Iyengar, R. N. (2006). Seizonic hazard estimation or Mumbai. *Current Science*, *91*, 1486–1494.

Raj, R., Mulchandani, N., Bhandari, S., Maurya, D. M., & Chamyal, L. S. (2003). Evidence of a mid-Late Holocene seismic event from Dhadhar river basin, Gujarat alluvial plain, western India. *Current Science, 85*, 812–815.

Rajendran, C. P. (2001). Using geological data for earthquake studies—A perspective from Peninsular India. *Current Science, 79*, 1251–1258.

Rajendran, K., & Harish, C. M. (2000). Mechanism of triggered seismiity at Koyna: An evaluation based on relocated earthquakes. *Current Science, 79*, 358–363.

Rajendran, C. P., & Rajendran, K. (1996). Low–moderate seismicity in the vicinity of Palghat Gap, south India and its implications. *Current Science, 70*, 304–307.

Rajendran, K., & Rajendran, C. P. (1998). Characteristics of the 1997 Jabalpur earthquake and their bearing in its mechanism. *Current Science, 74*, 168–174.

Rajendran, C. P., & Rajendran, K. (1999). Geological invesitigations at Killari and Ter, central India and implications for palaeoseismicity in the shield region. *Tectonophysics, 308*, 67–81.

Rajendran, C. P., Earnest, A., Rajendran, K., Devi Das, R., & Kesavan, S. (2003). The 13 September 2002 North Andaman (Diglipur) earthquake: An analysis in the context of regional seismicity. *Current Science, 84*, 191–924.

Rajendran, C. P., Rajendran, K., Duarah, B. P., Baruah, S., & Earnest, A. (2004). Interpreting the style of faulting and palaeoseismicity associated with the 1897 Shillong, NE Indian earthquake: Implications for regional tectonism. *Tectonics*, *23*, TC2009. doi:10.1029/2003TC001605.

Rajendran, C. P., Rajendran, K., Anu, P., Earnest, A., Machado, T., Mohan, P. M., & Freymueller, J. (2007). Crustal deformation and seismic history associated with the 2004 Indian Ocean earthquake: A perspective from the Andaman-Nicobar Islands. *Bulletin of the Seismological Society of America, 97*, S174–S191.

Ramalingeswara Rao, B. (2000). Historical seismicity and deformation rates in the Indian Peninsular Shield. *Journal of Seismology, 4*, 247–258.

Ramanathan, A., & Chandrasekharam, D. (1997). Geochemistry of Rajapur and Puttur thermal springs of the West Coast, India. *Journal of the Geological Society of India, 49*, 559–565.

Rao, D. P. (1977). A note on recent movements and origin of some piedment deposits of Dehradun Valley. *Photonirvachak, 5*, 5–40.

Rastogi, B. K. (1974). Earthquake mechanism and plate tectonics in the Himalayan region. *Tectonophysics, 21*, 47–56.

Rastogi, B. K. (1992). Seismotectonics inferred from earthquakes and earthquake sequences in India during the 1980s. *Current Science, 62*, 101–108.

Rastogi, B. K. (2001). Erattupetta earthquake of 12 December 2000 and seismicity of Kerala. *Journal of the Geological Society of India, 57*, 273–275.

Raval, U. (1995). Geodynamics of the tectonomagmatic and geophysical signatures within mobile parts of the transect. *Memoirs of the Geological Society of India, 31*, 37–61.

Ravi Kumar, M., Purnachandra Rao, N., & Chalam, S. V. (1996). A seismotectonic study of the Burma and Andaman arc regions using centroid moment tensor data. *Tectonophysics, 253*, 155–165.

Ravikumar, M., Hazarika, P., Srihari Prasad, G., Arun, S., & Saha, S. (2012). Tectonic implication of the September 2011 earthquake and its aftershocks. *Current Science, 102*, 788–796.

Roy, S., & Rao, R. U. M. (1999). Geothermal investigations in the 1993 Latur earthquake area, Deccan Volcanic Province, India. *Tectonophysics, 306*, 237–252.

Sah, M. P., & Virdi, N. S. (1997). Geomorphic signatures of neotectonic activity along the Sumdo Fault, Spiti valley, district Kinnaur, H.P. *Himalayan Geology, 18*, 81–92.

Sahu, V. K., Gahalaut, V. K., Rajput, S., Chadha, R. K., Laishram, S. S., & Kumar, A. (2006). Crustal deformation in the Indo-Burmese arc region: Implications from the Myanmar and southeast Asia GPS measurements. *Current Science, 90*, 1688–1693.

Sambandam, S. T., Devaprasad, C., Srinivasan, R., & Raghunandan, K. R. (1994). *Seismotectonic Map (Scale 1 cm = 20 km), Project Vasundhara* (73 p.). Bangalore: Geological Survey of India.

Sarkar, I., Pachauri, A. K., & Israil, M. (2001). On the damage caused by the Chamoli earthquake of 9 March 1999. *Journal of Asian Earth Sciences, 19*, 129–134.

Satyabala, S. P., Yang, Z., & Bilham, R. (2012). Stick-slip advance of the Kohat plateau in Pakistan. *Nature Geoscience*, 1–4. doi:10.1038/NGE1373.

Seeber, L., & Armbruster, J. G. (1981). Great detachment earthquakes along the Himalayan arc and long-time forecasting. In D. W. Simpson & P. G. Richards (Eds.), *Earthquake Prediction: An International Review* (pp. 259–277). Washington: American Geophysical Union.

Senthil, K., Wesnousky, S. G., Rockwell, T. K., Briggs, R. W., Thakur, V.C., & Jayangondaperumal, R. (2006). Palaeoseismic evidence of great surface rupture earthquakes along the Indian Himalaya. *Journal of Geophysical Research*, *111*. doi:10.1029/2004JB003309.

Shanker, R. (1987). Neotectonic activity along the Tapti-Satpura lineament in central India. *Indian Minerals, 41*(1), 19–30.

Singh, R. J., Joshi, D. D., & Pande, P. (2008). Geological signatures of the Ropar tear in Ropar-Nalagarh sector of the northwestern Himalaya, India. *Himalayan Geology*, *29*, 105–108.

Singh, B., & Kumar, S. (2005). Petrogenetic appraisal of Early Palaeozoic granitoids of Kinnaur district, High Himachal Himalaya. *Gondwana Research, 8*, 67–76.

Singh, H. N., & Mathai, J. (2004). *Field Investigation for Collection of Macroscopic and Geological Data on Ground Deformation, Fluctuation in Water Level and Other Related Incidents in Kerala*. Technical Report, CESS-PR-13-2004, Centre for Earth Science Studies, Trivandrum, 96 p.

Singh, H. N., Raghavan, V., & Varma, A. K. (1989). Investigations of Iddukki earthquake sequence of 7–8th June 1988. *Journal of the Geological Society of India, 34*, 133–146.

Singh, H. N., Shankar, D., & Singh, V. P. (2005). Occurrence of anomalous seismic activity proceeding large to great earthquakes in northeast India region, with special reference to 6 August 1988. *Physics of the Earth & Planetary Interiors, 148*, 261–284.

Singh, T., Sharma, U., Awasthi, A. K., Virdi, N. S., & Kumar, R. (2011). Geomorphic and structural evidences of neotectonic activity in the sub- Himalayan belt of Nahan Salient, NW India. *Journal of the Geological Society of India, 77*, 175–182.

Singh, A. K., Singh, N. I., Devi, L. D., & Singh, R. K. (2008). Pillow basalts from the Manipur Ophiolitic Complex (MOC), Indo-Myanmar Range, Northeast India. *Journal of the Geological Society of India*, *72*, 168–174.

Srinivasan, V. (2002). Post-Deccan Trap faulting in Raigad and Thane districts of Maharashtra. *Journal of the Geological Society of India*, *59*, 23–31.

Srivastava, H. N., & Dube, R. K. (1996). Comparison of precursory and non-precursory swarm activity in Peninsular India. *Tectonophysics, 265*, 327–339.

Srivastava, P., Misra, D. K., Agrawal, K. K., Bhakuni, S. S., & Luiri, K. (2009). Late Quaternary evolution of Ziro intermontane lake basin, NE Himalaya. *Himalayan Geology, 30*, 175–185.

Steckler, M., Akhter, S. H., Seeber, L. (2008). Collision of Ganges-Brahmaputra Delta with the Burma Arc: Implications for earthquake hazard. *Earth & Planetary Science Letters*, *332*, 367–378.

Subramanian, K. S., & Gopalakrishnan, K. (2002). Earth tremors in the coastal belt of Tamil Nadu and Pondicherry in Setpember 2001—A geolocal analysis. *Journal of the Geological Society of India, 60*, 691–693.

Sukhija, B. S., Lakshmi, B. V., Rao, M. N., Reddy, D. V., Nagbhushanam, P. V., Hussain, S., & Gupta, H. K. (2006). Widespread geologic evidence of a large palaeoseismic event near meizoseimal area of the 1993 Latur earthquake, Deccan Shield, India. *Journal of Indian Geophysical Union, 10*, 1–14.

Sukhija, B. S., Rao, M. N., Reddy, D. V., Nagabhushanam, P., Kumar, D., Lakshmi, B. V., & Sharma, P. (2002). Palaeoliquifaction evidence of prehistoric large/great earthquakes in North Bihar, India. *Current Science, 83*, 1019–1025.

Sukhija, B. S., Rao, M. N., Reddy, P. V., Nagaghushanam, P., Hussain, S., & Chadha, R. K. (1999). Palaeoseismic studies of the Shillong Plateau, Northeast India. *Himalayan Geology, 20*, 105–112.

Talwani, P., & Gangopadhyay, A. (2001). Tectonic framework of the Kachchh earthquake of 26 January 2001. *Seismological Research Letters, 72*, 336–345.

Tewari, H. C., Murty, A. S. N., Kumar, P., & Sridhar, A. R. (2001). A tectonic model of Narmada region. *Current Science, 80*, 873–878.

Thakur, V. C. (2006). Reassessment of earthquake hazard in the Himalaya and implications from the 2004 Sumatra-Andaman earthquake. *Current Science, 90*, 1070–1072.

Thakur, V. C., & Jain, A. K. (1974). Tectonics of the region of Eastern Himalaya Syntaxis. *Current Science, 43*, 783–785.

Thakur, V. C., Jayangonda Perumal, R., & Suresh, N. (2009). Late Quaternary- Holocene fold and landform generated morphogenic earthquakes in Chandigarh anticlinal ridge in Punjab sub-Himalaya. *Himalayan Geology, 30*, 103–113.

Thakur, V. C., Jayangondaperumal, R., Champatiray, P. K., Bhatt, M. I., & Malik, M. A. (2006). 8 October, 2005 Muzaffarabad earthquake and seismic hazard assessment of Kashmir gap in northwestern Himalaya. *Journal of the Geological Society of India, 68*, 187–200.

Umitsu, M. O. (1993). Late Quaternary sedimentary environments and landforms in Ganges delta. *Sedimentary Geology, 83*, 177–186.

Valdiya, K. S. (1976). Himalayan transverse faults and folds and their parallelism with subsurface structures of North Indian plains. *Tectonophysics*, *32*, 353–386.

Valdiya, K. S. (1980). *Geology of Kumaun Lesser Himalaya*. Dehradun: Wadia Institute of Himalayan Geology. 291 p.

Valdiya, K. S. (1992). The Main Boundary Thrust Zone of Himalaya, India. Annales Tectonicae, 6, 54–84.

Valdiya, K. S. (1981). Tectonics of central sector of the Himalaya. In H. K. Gupta & F. M. Delancy (Eds.), *Zagros–Hindukush Himalaya, Geodynamic Evolution,* Geodynamics series (Vol. 3, pp. 87–110). Washington D.C.: Publication of American Geophysical Union.

Valdiya, K. S. (1998). Late Quarternary movements on landscape rejuvenation in southeastern Karnataka and adjoining Tamil Nadu in Southern Indian Shield. *Journal of the Geological Society of India, 51*, 139–166.

Valdiya, K. S. (2001a). Tectonic resurgence of the Mysore Plateau and surrounding regions in cratonic southen India. *Current Sci., 81*, 1068–1089.

Valdiya, K. S. (2001b). Reactivation of terrane-defining boundary thrusts in central sector of the Himalaya: Implications. *Current Science, 81*, 1418–1431.

Valdiya, K. S. (2001c). River response to continuing movements and scarp development in central Sahyadri and adjoining coastal belt. *Journal of the Geological Society of India, 57*, 13–30.

Valdiya, K. S. (2002). *Saraswati: The River that Disappeared* (116 p.). Hyderabad: Universities Press.

Valdiya, K. S., Joshi, D. D., Sanwal, R., & Tandon, S. K. (1984). Geomorphic development across the active Main Boundary Thrust, an example from the Nainital Hill in Kumaun Himalaya. *Journal of the Geological Society of India, 25*, 761–774.

Valdiya, K. S., & Narayana, A. C. (2007). River response to neotectonic activity: Example from Kerala, India. *Journal of the Geological Society of India, 70*, 427–443.

Valdiya, K. S., Rana, R. S., Sharma, P. K., & Dey, P. (1992). Active Himalayan Frontal Fault, Main Boundary Thrust and Ramgarh Thrust in Southern Kumaun. *Journal of the Geological Society of India, 40*, 509–528.

Verma, R. K. (1985). *Gravity field, seismicity and tectonics of the Indian Peninsula and the Himalaya*. New Delhi: Allied Publishers.

Verma, R. K., Mukhopadhyay, M., & Ahluwalia, M. S. (1976). Earthquake Mechanisms and Tectonic Features of Northern Burma. *Tectonophysics, 32*, 387–399.

Verma, R. K., Mukhopadhyay, M., & Bhanja, A. K. (1980). Seismotectonics of the Hindukush and Baluchistan arc. *Tectonophysics, 66*, 301–322.

Verma, R. K., Roonwal, G. S., Kamble, V. P., Dutta, U., Kumar, N., Gupta, Y., & Sood, S. (1995). Seismicity of northwestern part of the Himalayan arc, Delhi-Hardwar Ridge and Garhwal-Kumaun Himalaya region: A synthesis of existing data. *Memoirs of the Geological Society of India, 30*, 83–99.

Vigny, C., Socquet, A., Rangin, C., Chamot-Rook, N., Pubellier, M., Bouin, M-N., Bertrand, G., & Becker, M. (2003). Present-day crustal deformation around Sagaing Fault, Myanmar. *Journal of Geophysical Research*, *108*, B112533. doi:10.1029/2002JB001999.

Wesnousky, S. G., Kumar, S., Mohindra, R., & Thakur, V. C. (1999). Uplift and convergence along the Himalayan Frontal Thrust. *Tectonics, 18*, 967–976.

Yin, A., Harrisson, T. M., Ryerson, F. J., Wenji, C., Kidd, W. S. F., & Copeland, P. (1994). Tertiary structural evolution of the Gangdese thrust system, southeastern Tibet. *Journal of Geophysical Research, 99*, 18175–18291.

Zhang, P.-Z., Shen, Z., Wang, M., Gan, W., Burgmann, R., Molnar, P., et al. (2004). Continuous deformation of the Tibetan plateau from global positioning system data. *Geology, 32*, 809–812.

Chapter 26
Ocean Around Peninsular India

26.1 Seafloor Structure and Morphology

26.1.1 Origin

The thin carpet of sediments and the youthful seamounts demonstrate that the floor of the Indian Ocean is probably not older than Early Cretaceous. It formed as a consequence of India, Australia and Antarctica moving away from the supercontinent Gondwanaland in the southern hemisphere. The separation of India from Australia and Antarctica created the floor of the Bay of Bengal, and the breaking away of India–Madagascar from Africa produced the Arabian Sea. The Seychelles separated from India nearly at the same time. The separation of India from the Gondwanaland was initiated around 120 million years ago. This is evidenced by the presence of Mesozoic magnetic anomalies in the Bay of Bengal and its conjugate the Enderby margin of Antarctica; and by the volcanic activity in the Rajmahal area in Jharkhand and the Garo Hills in Meghalaya. India drifted northwards rapidly at the rate of 18–20 cm/year in the period 95 to 35 Ma and 10 cm/year in the Later Tertiary time. Converging towards Eurasia, India ploughed through the Kohistan–Ladakh–Shigatse island arc of volcanic rocks, and collided with Asia, resulting in the reduction of its speed, which at present is 5 cm/year.

26.1.2 Characteristic Features

Dividing the Indian Ocean floor into a number of discrete plates, there are three *mid-oceanic ridges* that are actively spreading. It is along these spreading centres where new oceanic crust is forming since the inception. These are the

K.S. Valdiya, *The Making of India*, Society of Earth Scientists Series,
DOI 10.1007/978-3-319-25029-8_26

N–S-trending *Central Indian Ridge*, the NW–SE-oriented *South eastern Indian Ridge* and the NE–SW-trending *South western Indian Ridge* (Figs. 26.1 and Plate 25.1). These three underwater mountain ranges meet at 25°S latitude and 70°E longitude, forming the *Rodriguez Triple Junction*. In the north-western part of the Indian Ocean, the Central Indian Ridge extends in the NW–SE direction as the *Carlsberg Ridge*.

The relief of these ridges varies from 2000 to 4000 m *above the adjoining ocean floor*. Made up of almost wholly olivine basalts, the mid-oceanic ridges are characterized by rift valleys along their axes. The Central Indian Ridge graben is 500–600 km long and 10–15 km wide. Its nearly flat floor lies at the water depth of 2700–3200 m. Intermittent volcanism in the axial grabens makes them the *zone of plate construction* in which new crust is generated as a result of *accretion* or addition, that is, emplacement of basaltic material by pushing aside the older part of the lithosphere. This is accomplished by upwelling convection currents in the mantle. There are alternating stripes of magnetic anomalies caused by polarity reversals, and there is progressive increase in age of the rocks in these stripes away from the central graben. These facts corroborate the inference that the new ocean floor is being generated across the Carlsberg Ridge at the half spreading rate of

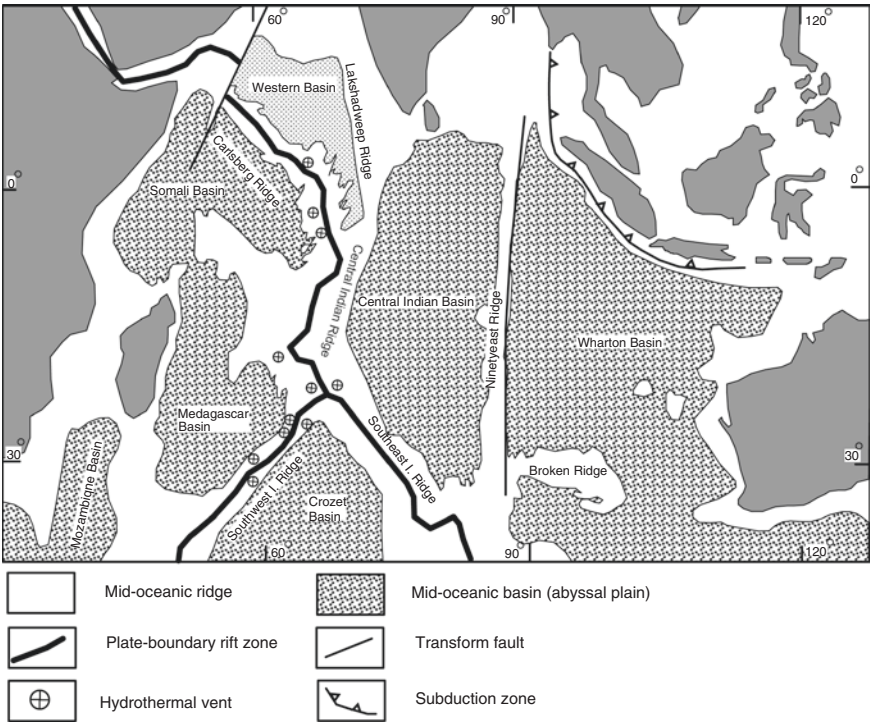

Fig. 26.1 Indian Ocean around the Peninsular India comprises mid-oceanic ridges with axial rift valleys (shown by *serrated lines*), transform faults that segment and offset these ridges, and oceanic basins represented by abyssal plains (based on Srinivasan and Chaturvedi 1992)

Plate 26.1 Physiography of the Indian Ocean, showing underwater ridges, transform faults, trenches and submarine sedimentary fans built by the Sindhu and Ganga–Brahmaputra river systems (from K.V. Subbarao and R. Shankar, Story of the Oceans, Geological Society of India, Bangalore, 36 p, 2003)

5–6 cm/year, the Southwest Indian Ridge at 3 cm/year, the Central Indian Ridge at 1.8–2.4 cm/year and South-east Indian Ridge at 0.8 cm/year.

There are two long-lived hotpots—the *Kerguelen Hotspot* and the *Reunion Hotspot* (Plate 26.1). These have been active since 116 and 66 Ma, respectively, and have played very crucial role in the evolution of Indian Ocean and the volcanism in the Peninsular India. The Kerguelen Hotspot activity is represented by the 116–90 Ma southern and central Kerguelen Plateau and 38 to 0 Ma-old cluster of volcanic islands on the northern edge of the Plateau. It is also responsible for the formation of the *NinetyEast Ridge* in the eastern part of the Indian Ocean during the period 90–38 Ma. To the Reunion Hotspot is attributed the formation of the Chagos–Lakshadweep Ridge. The plumes are believed to have originated as a consequence of partial melting at the base of the mantle. Volcanism started synchronous with rifting of the belt offshore Seychelles Islands. Volcanism started during 28 Chron—marking the first organized spreading at the Carlsberg Ridge. The separation of Seychelles started at 27 Chron approximately at 62 Ma and was completed in about 3.5 Ma (Collier et al. 2008). The Deccan Volcanism is associated with the breaking of India and Seychelles.

Recently, a continental fragment comprising at the top of a pile of lavas was discovered between Madagascar and India. This fragment is believed to be a piece detached from India when it drifted away from Madagascar (*The Hindu*, February 28, 2013).

The mid-oceanic ridges are torn apart and offset by several regularly spaced, remarkably straight, strike-slip *transform faults*. Some of these faults link the spreading centres (axial grabens). At some locations, they link mid-oceanic ridges,

with the subduction zones along the margin of the Arabian Sea and the Bay of Bengal (Plate 26.1). These faults thus convert or transform the spreading motion along the ridge crests into the underthrusting in the subduction zones. Continued horizontal movements along these faults have brought about segmentation of the mid-oceanic ridges. Shallow seismicity testifies to their activeness. This is also manifest in volcanism represented by underwater volcanoes and *seamounts* emplaced along fractures zones. One of the N–S-trending transform faults gave rise to the *NinetyEast Ridge* that stretches north into the Bay of Bengal. Another active fault is represented by the *Chagos–Lakshadweep Ridge* in the eastern part of the Arabian Sea. The *Owen Fracture* in the north-western part of the Arabian Sea has dextrally offset the Carlsberg Ridge. The NinetyEast and the Chagos–Lakshadweep faults together took up the northward movement of the Indian Ocean that caused India to move northwards and eventually collide with Asia.

The third important feature is the *oceanic trench*. Along the trenches, the oceanic plate is plunging (*subducting*) deep into the mantle. There are two oceanic trenches in the Indian Ocean—the *Java Trench* along the western margin of the Andaman–Nicobar–Indonesia Island Arc and the *Oman Trench* south of the Makran Coast in Pakistan. Both the trenches are filled with sediments brought by rivers draining the continent. The subduction zones are generally characterized by negative gravity anomaly and by shallow, medium and deep seismicity. These are the zones *of plate destruction*. In the zones of subduction, the ocean floor along with its sedimentary cover is scarped off, compressed into folds-and-fault belts and welded to the continent (as along the Makran coast) or to form an island arc such as the Andaman–Nicobar archipelago.

The average seafloor depth of the Indian Ocean is 5100 m. Presence of mid-oceanic ridges, transform faults and fractures (Plate 26.1), volcanic cones and seamounts (one of them 24 km wide at the base, 1275 m high) make the ocean floor extremely rugged. The basins between the ridges have nearly flat topography.

26.1.3 Diffuse India–Australia Plate Boundary

1. In the equatorial belt lies the boundary of the Indian plate against the Australian plate (Fig. 26.2a). Related to ongoing motion of the oceanic plate, the boundary is very diffuse and characterized by wide zone of folding of the oceanic lithosphere along with its sedimentary cover (Drolia et al. 2003; Drolia and Dematts 2005). The deformation events occurred in the Miocene (8.0–7.5 Ma), the Pliocene (5–4 Ma) and the Pleistocene at 0.8 Ma (Krishna et al. 1998a, b). Seismic reflection profile indicates that the zone of diffused deformation in the Central Indian Ocean is characterized by reverse faults spaced 5 km apart and long-wave folds (Krishna et al. 2001). The compressional activity started in the period 15.4 to 13.9 Ma—much earlier than previously deduced (Krishna et al. 2009). The deformation is seen in the formation

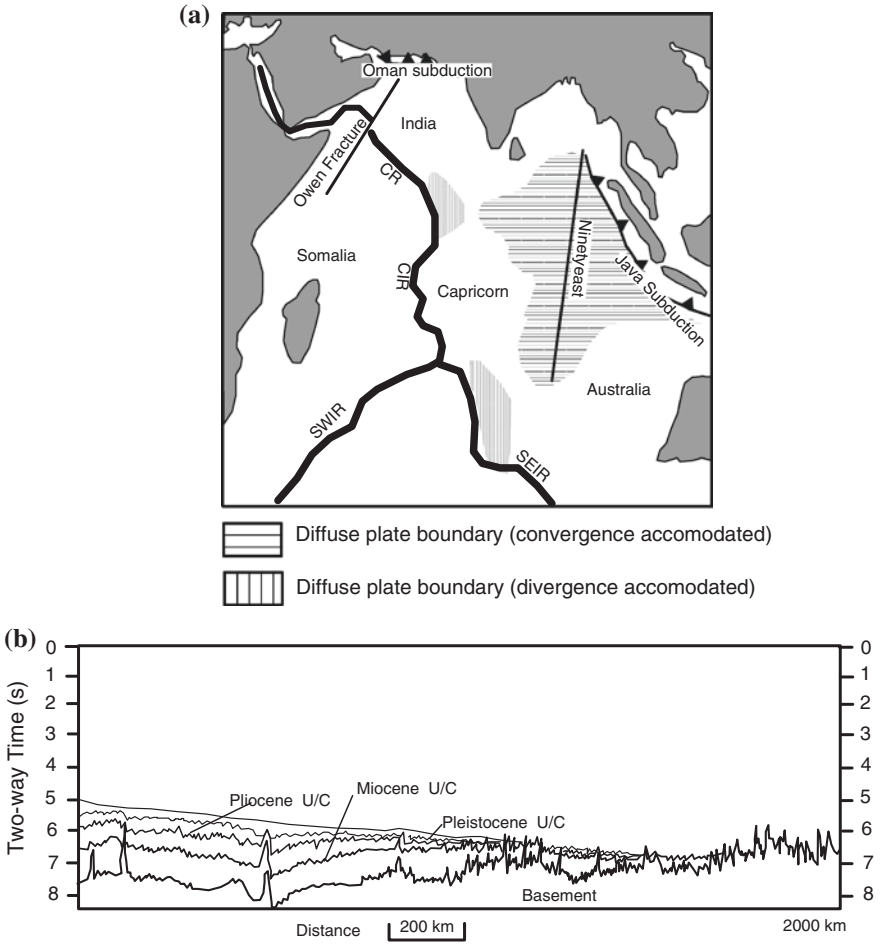

Fig. 26.2 **a** Diffuse India–Australia plate boundary in the Indian Ocean. *Vertically striped regions* represent zones of divergence, and *horizontal stripes* show diffuse plate boundary across which convergence is accommodated (after DeMets and Royer 2003). **b** N–S profile along 87°E longitude shows long-wave folding of basement and overlying sedimentary strata of three different ages (Krishna et al. 1998a, b)

of long folds having wavelength of 150–300 km, involving the basement also (Fig. 26.2b). It has caused 1–2 km vertical offsets and a series of tight folds and high-angle 5–20 km deep faults, as seen between the Afanasy Nikitin Seamount and the NinetyEast Ridge (Fig. 26.2). The diffuse zone extends west up to the Central Indian Ridge and isolates the Indian plate from the Capricorn Plate.

26.2 Tectonics of the Bay of Bengal

26.2.1 Plate Movement

The north-eastern part of the Indian Ocean, known as the *Bay of Bengal*, wears a mantle of sediments as much as 22 km in thickness in some areas. In the proximal part of the *Bengal Fan,* the sediment thickness is 18 km (Curray and Moore 1971), whereas in the middle part of the Fan, it is 7–8 km. These sediments rest over the basement of the Cretaceous rocks. In the distal part of the Bengal Fan, the sediment thickness is 2–3 km. The Mesozoic sequence of magnetic anomaly of the floor of the Bay reveals that the initial motion of the Indian plate from the Australia–Antarctica Plate commenced immediately after the Gondwanaland break-up at about 133 Ma in the Early Cretaceous (Ramana et al. 1994, 2001). In the time span 118 to 84 Ma, the direction of plate movement changed from NW–SE to N–S. It was during this period that the trace of the NinetyEast Ridge evolved as the Indian plate moved over the Kerguelen Hotspot (Ramana et al. 1997). The 84–40 Ma period witnessed acceleration of India's northward motion, resulting in the development of the Central Indian Basin.

26.2.2 Evolution of Ninety East Ridge

Extending north from 34°S to 10°N latitude, approximately 4800-km-long *NinetyEast Ridge* rises from 3500 to 2000 m above the ocean floor at 5000 m water depth (Figs. 26.2 and 26.3). The ridge top becomes progressively deeper northwards until it is wholly concealed under the cover of the Bengal Fan. The

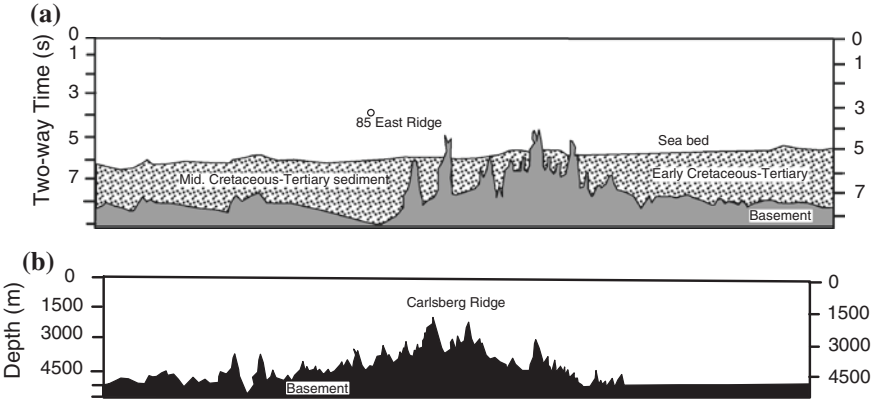

Fig. 26.3 Cross sections of the ocean floor show underwater topography of the basement. **a** In the distal part of the Bengal Fan in the Bay of Bengal (after Ramana et al. 1997). **b** In the Arabian Sea (after Chaubey et al. 1993)

sediments delivered to the Bay of Bengal by the Ganga–Brahmaputra river system. This Ridge was formed due to basaltic volcanism of the Kerguelen Hotpot. It was formed when the spreading centres of the Wharton Ridge were moving, with multiple southward ridge jumps relative to the stationary Kerguelen Hotspot (Krishna et al. 1999).

The nearly 200-km-wide ridge is cut longitudinally by a number of faults, including the one that defines its eastern flank. In the belt of the ridge, the crustal thickness is nearly 22 km, in sharp contrast to the average 7-km-thick crust of the Central Indian Basin. It is inferred that steep downward faulting (by 2 km) along the eastern flank of the ridge is responsible for this extraordinary situation—attributed to compressional and extensional stresses applied along the 89°E fracture zone (Krishna et al. 1999, 2001, 2002).

Magnetic lineations, abandoned spreading centres and seismic structure collectively indicate the interaction of hot spot volcanism with the spreading axis during the period 60 to 54 Ma. This is supported by the emplacement of isotopically heterogenous basalts and oceanic and e sites at 59–58 Ma (Krishna et al. 1999).

Seismic reflection data and bathymetric analysis indicate that the NinetyEast Ridge is now close to the Andaman–Java Trench—it is at the starting stage of touching the island arc (Subrahmanyam et al. 2008a). The Ridge may be going down the trench and simultaneously slipping northwards, but still away from the overriding Burmese plate. The NinetyEast Ridge is believed to have been formed by a hot spot volcanism on the northward-moving plate (Sager et al. 2010). The gravity data show that it is characterized by a series of nearly E-W-trending lineaments, each nearly 45 km apart. This fact correlates with the horst-and-graben structure formed probably at the time close to emplacement of lavas near the spreading ridge that separated the Indian plate from the Antarctica Plate (Sager et al. 2010).

Satellite gravity data taken in conjunction with magnetic anomaly structure demonstrate that cut by N5°E-trending fractures, the NinetyEast Ridge increased in length at the rate of nearly 118 km/Ma between 77 and 13 Ma—which is two times faster than the rate at which the crust adjoining the Ridge accreted (Krishna et al. 2012). The magnetic anomalies document "spreading ridge jumps" in the ocean immediately west of the NinetyEast Ridge.

26.2.3 Structure and Origin of Eighty Five East Ridge

The 100- to 180-km-wide *Eighty Five East Ridge* trending broadly N–S between 19 and 6°N and NE–SW towards offshore Sri Lanka abuts against the northern extension of the *Afanasy Nikitin Seamount* chain (Fig. 26.3b). It is associated with negative gravity anomaly and positive magnetic anomaly (Ramana et al. 1997). The Afanasy Nikitin Seamount is underlain by an 8-km-thick crustal body of magmatic rocks, while the other structure of the seafloor indicates flexing down of the crust up to the depth of 2.5 km. These facts imply the origin of the Eighty

Five East Ridge due to a hot spot in the intraplate position 35 million years ago (Krishna 2003). It evolved as a result of shearing of the lithosphere caused by stretching and compressional forces. The forces are related to a major plate reorganization immediately after the crustal formation at 118 Ma. Sagging followed by buckling deformation might have generated horizontal compressional forces, bring about this development (Ramana et al. 1997).

The seafloor south of Sri Lanka, created during the Early Cretaceous, evolved with half spreading rate varying from 5.5 cm/year to 11.53 cm/year. Around 50 Ma, the direction of spreading changed from NW–SE to N–S even as the half spreading rate came down drastically (Desa et al. 2006). That was the time when India collided with Asia.

The *Andaman Basin* is believed to have formed due to the initiation of the seafloor spreading within the Central Andaman. High-resolution swath bathymetry in conjunction with gravity and magnetic surveys indicate that the evolution of the Andaman Sea occurred around 4 Ma (Kamesh Raju et al. 2004).

26.3 Geodynamics of the Arabian Sea

26.3.1 Origin of Carlsberg Ridge and Owen Fracture

The Arabian Sea evolved as a consequence of India–Madagascar break-up. After a phase of strike-slip movement between Madagascar and India, there was spreading of the ocean floor during the time 84–64 Ma, giving rise to the Mascarene Basin (Gaedicke et al. 2002) and the West Arabian Basin (Chaubey et al. 1993).

The north-westerly extension of the Central Indian Ridge is known as the *Carlsberg Ridge* in the Arabian Sea (Fig. 26.3b). This ridge extends into the Gulf of Aden and the Red Sea as the Sheba Ridge (Merkouriev and Sotchevanova 2003). The *Owen Fracture* offsets the Carlsberg Ridge before it enters the Gulf of Aden (Figs. 26.2 and 26.4a). The western flank of the Owen Fracture forming the boundary between the Arabian and Indian plates is marked by a more than 800-km-long submarine fault scarp comprising a series of segments of strike-slip faults with several bends (Fournier et al. 2011). From 6 to 3 Ma, the total displacement along these faults was 10–12 km.

The Somali–Arabia Basin to the west of the Owen Fracture originated during the Palaeogene (Royer et al. 2002). There is a depression—the Dalrymple Trough over a thinned continental crust west of the huge Indus Fan—beyond which extends oceanic crust. The continent–ocean transition is less than 10-km-wide belt of oblique extension and manifest in a 3000-m-high steep scarp in the south-east and a series of small en echelon scarps in the north-east (Edwards et al. 2008). The Carlsberg Ridge is characterized by a well-defined 3500-m-deep axial valley bordered by steep walls that rise up to nearly 2500 m above the valley floor. The valley resembles a graben that contains a sequence of sediments and intrusive bodies of serpentinite and peridotite (Mudholkar et al. 2002). The oceanic crust

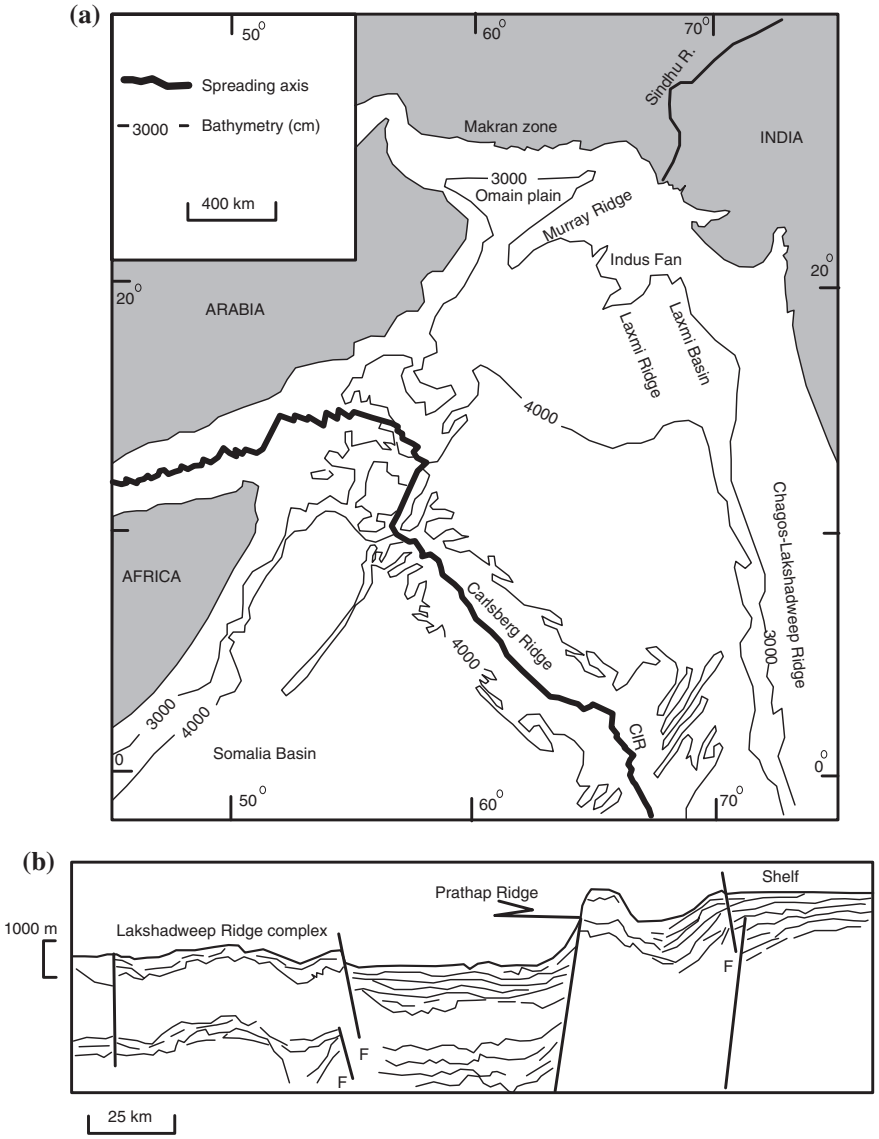

Fig. 26.4 **a** Bathymetric contours (in metres) of northern Arabian Sea and the location of the Laxmi Basin with respect to the Carlsberg and Chagos–Lakshadweep ridges (after Gaedicke et al. 2002). **b** Multichannel seismic reflection structure of the Lakshadweep and Prathap ridges and the intervening basin (after Subrahmanyam et al. 1993b)

across the Carlsberg Ridge was created with a half spreading rate of 1.2–1.6 cm/year (Ramana et al. 1993; Kamesh Raju 1993). The spreading rate accelerated in the post-Cretaceous–pre-Eocene time.

26.3.2 Evolution of Laxmi Basin

Through the eastern Arabian Sea run in the north–south direction, the *Chagos–Lakshadweep Ridge* and the *en echelon* positioned NNW–SSE-oriented *Laxmi Ridge* (Fig. 26.4a). The 100-km-wide Laxmi Ridge is characterized by prominent negative gravity anomaly (Bhattacharya et al. 1994) and 11-km-thick oceanic crust. This apparent crustal thickening is also attributed to emplacement of an anomalously low-density layer below 19 km depth. The thickened crust is believed to be representing an asthenospheric upwarp (Pandey et al. 1995).

The floor of the Laxmi Basin is uneven and characterized by a broad gravity high and a narrower prominent gravity low within it. It is a crust that stretched in the east–west direction and magmatic bodies were emplaced along the fractures (Krishna et al. 2006). The Laxmi Basin floor was created as a result of symmetric seafloor spreading, and the half spreading rates vary from 0.7 cm/year to the present 1.2 cm/year (Chaubey et al. 1993, 1998, 2000). The opening of the Basin started shortly before 84 Ma and stopped around 65 Ma (Bhattacharyya et al. 1994). The Laxmi Ridge, the Seychelles Plateau and the Saya de Malha Bank remained parts of the Indian plate until about 63 Ma. This was the time when the seafloor spreading centre jumped northwards by about 200 km into the crust of the Indian continental margin. This phenomenon separated the Indian plate from the Seychelles–Saya de Malha Bank microplate (Gaedicke et al. 2002). Significantly, there was widespread volcanism on the Indian continent—the Deccan Volcanism—in the period 63–68 Ma.

Using wavelength analysis and considering the fractal dimension, it is surmised that the spectral behaviour of the crust of the Laxmi Basin near the continental shelf of India is of the continental nature (Chamoli and Dimri 2007). This surmise is strongly corroborated by the fact now known that there is a continental sliver in the form of Laxmi Ridge (Yatheesh et al. 2009). The Gop Basin, in contrast, has a oceanic crust with an extinct spreading centre represented by the Palitana Ridge.

26.4 Magmatic Rocks of the Indian Ocean

The basalts that constitute the overwhelmingly large proportion of rocks of the ridges and the floor are characterized by high $^{208}Pb/^{204}Pb$ and $^{87}Sr/^{86}Sr$ and low $^{143}Nd/^{144}Nd$ and $^{206}Pb/^{204}Pb$ ratios. Underneath the cover of basalt layer occur in great abundance lherzolite in the form of sills, pods and crudely to well-structured dykes. And harzburgite, orthopyroxenite, olivine gabbro, norite and anorthosite

constitute minor components of the plutonic bodies. There are dykes of dolerite and dykelets of quartz-monzonite. Sodium-trondhjemite occurs locally indicating lower crustal and upper mantle origin (Iyer and Ray 2003). The overlying basalts are characterized by pillow structures, low-potassium chemistry and high-plagioclase and olivine mineralogy. Isotopic and REE characteristics of the rocks of the ridges and the floor point to their generation from diverse magma- and magma-mixing processes.

26.5 Deep-Sea Sedimentation: Faunal Record

26.5.1 Western Part

The deposits of ooze comprising tests of planktonic foraminifers and pteropods generally accumulated at slower pace over limited areas during the Palaeogene period and at faster rate over wide areas in the Neogene times (Davies et al. 1995). The Middle Miocene carbonate sedimentation occurred over shallow ridges and plateaus in the western part of the Indian Ocean, including the Arabian Sea (Fig. 26.5).

The oxygen-isotope measurements indicate that larger benthic foraminifers grew in temperature condition of 33 °C during the Palaeocene and Early Eocene, 26 °C in the Late Middle Eocene, 22 °C during the Early Oligocene and 25 °C in the Late Oligocene (Saraswati et al. 1993). In the Middle Miocene time, there was dramatic increase (1–2 %) in the content of organic matter in the submarine sediments off Somalia, Oman and Pakistan, indicating higher productivity related to upwelling of ocean currents (Meyers and Dickens 1992). Among the planktonic foraminifers, the presence of a particular taxon *Globigerinoides ruber* demonstrates that the surface water of the equatorial Central Indian Ocean during the Last Glacial Maximum was 2.1 °C colder than at the present (28.5 °C) (Saraswati et al. 2005). The water of the Arabian Sea during that time (Last Glacial Maximum) was more saline (by 1.5 psu) than it was during the Holocene epoch, presumably due to reduction in the influx of fresh water from the melting of Himalayan ice (Banakar et al. 2003).

Oxygen isotopic composition of the tests of *Orbulina universa* in the carbonate capping of the Carlsberg Ridge indicates that there was freshwater influx due to the melting of Himalayan ice in the post-Last Glacial Maximum time (Nigam et al. 1994). Along with the melt water came illite and smectite clays, underscoring the important role played by the Sindhu River in bringing detritus and water from the Himalaya province. The benthic foraminifers of the Arabian Sea indicate a perceptible change in the pattern of precipitation at 3500 yr B.P. (Naidu 1996).

According to the testimony of planktonic foraminifers, the eastern part of the Arabian Sea off Kerala experienced minimum upwelling, presumably due to weakened monsoon in the period 23,000–18,000 yr B.P. There was gradual increase in the upwelling intensity during the 18,000–15,000 yr B.P. interval reaching the maximum in the temporal span 12,000 to 10,000 yr B.P. (Singh 1998).

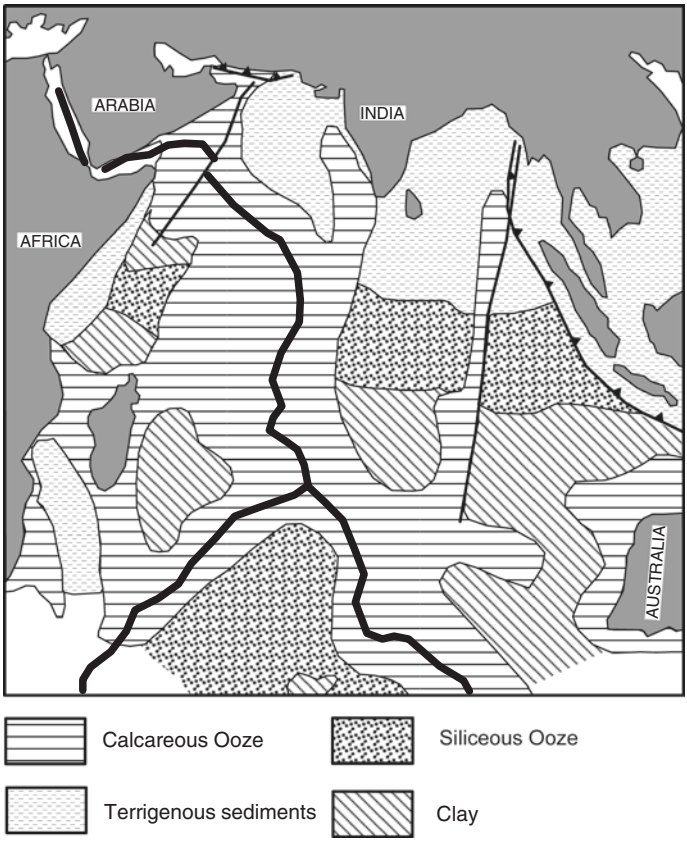

Fig. 26.5 Present-day distribution of various types of sediments in the Indian Ocean (after Davies et al. 1995)

26.5.2 Eastern Part

The planktonic foraminiferal assemblages of the tropical Indian Ocean document major changes at 22, 14, 12–10, 6.2–5.2 and 1.8 Ma (Srinivasan 1996). Interestingly, there is a remarkable similarity of the foraminiferal succession of the tropical Indian Ocean and the tropical Pacific Ocean, except with respect to the Early Pliocene taxon *Pulleniatina spectabilis*, so common in the Pacific but absolutely absent in the Indian Ocean. This situation developed due to breaking off of the connection of the two oceans after the closing of the Indonesian seaway during the earliest Pliocene (Srinivasan and Chaturvedi 1992; Srinivasan and Sinha 1998). The close of the Indonesian seaway is attributed to northward movement of the Australian plate and attendant evolution of the Indonesian archipelago.

In the tropical Indian Ocean, the deeper benthic assemblages of foraminifers show significant increase during the intervals 8.5 to 7.5 Ma and 6.2 to 5.2 Ma of *Uvigerina proboscidea* and decrease of *Bulimina alazarensis, Cibicides kullenbergi* and *Cibicides wullerstorfi*. The change is related to a shift caused by the excessive input of organic carbon and the high rate of productivity due to increased upwelling (Gupta and Srinivasan 1992). In the south-eastern part of the Indian Ocean, these taxa document environmental change at 8.3 Ma. This change is from cold and well-oxygenated water with low organic carbon influx to oxygen-poor water having sustained influx of organic matter presumably resulting from intensification of monsoon system (Singh and Gupta 2004). Isotopic data of planktonic foraminifers *Globigerinoides sacculifer, Globorotalia menardii* and *Orbulina universa* in the surface water of the eastern part of the Indian Ocean point to the formation of a thick mixed layer of water during the period 2000 to 900 ka. This was followed by weakening of surface water stratification, shallowing of the mixed layer and continuous cool climate with increased surface productivity in the last 900 ka (Gupta and Dhingra 2004).

From the temporal variation of $\delta^{18}O$ in the foraminifers *Globigerinoides ruber* and *G. sacculifer* as well as geochemical indices of weathering, it is inferred that there was decline in the input of sediments into south-western Arabian Sea in the period 2200–1800 yr B.P.—primarily due to deterioration of south-western monsoon (Chauhan et al. 2010).

26.6 Evolution of Mid-Oceanic Island Chains

26.6.1 Maldive Coral Islands

More than 1200 coral islands, 22 of them atolls, make up the Maldive archipelago (Fig. 26.6a). On the foundation of lagoonal sediments, the *Maldive coral islands* grew initially during 5500 to 4000 yr B.P., the growth taking place 2.5 to 1.0 m below the present sea level (Kench et al. 2005). It seems that the level of the sea was rising, and it stabilized about 2000 yr B.P. Stratigraphically distinguishable three main facies constitute the edifice of the Maldive islands: (i) peripheral reef facies comprising layered framework of *Porites, Acropora* and *Heliopora* sands and gravels, (ii) lagoon facies (*Velu*) of shallow depressions consisting of horizontally bedded sands of primarily *Halimeda* and overlying hummocky layer of fractured *Halimeda* and algal particles, and (iii) sandbank (*Finolhu*) facies made up of gently dipping beds that extend above and across the inner reef and constituted of coral and algal sand grains.

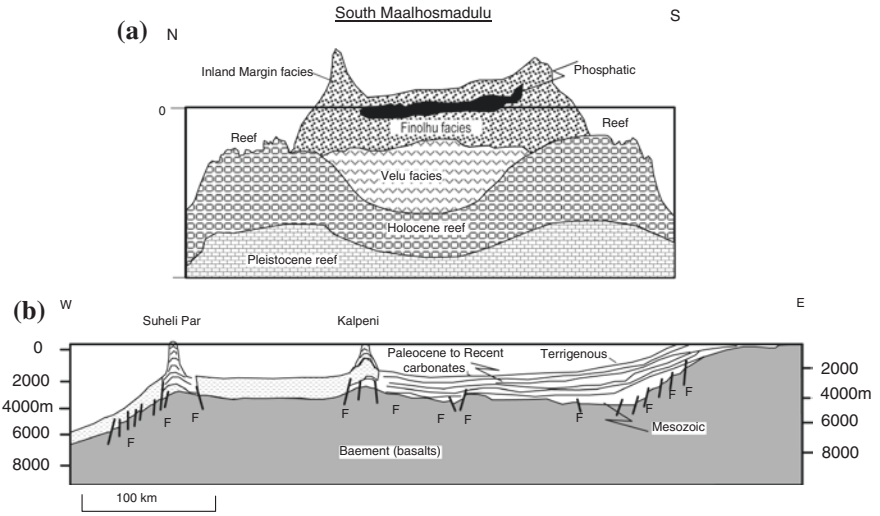

Fig. 26.6 **a** Morphology and stratigraphy of the South Maalhosmadula Atoll in the Maldive island chain (modified after Kench et al. 2005). **b** Coral island of the Lakshadweep chain is built on the foundation of volcanic rocks on the outer side of the continental margin, which is characterized by horsts and grabens (after Eremenko and Datta 1968)

26.6.2 Lakshadweep Islands

The *Lakshadweep coral islands* forming a chain atop the Chagos–Lakshadweep Ridge are built west of the continental margin, which is split into horsts and grabens off Kerala (Fig. 26.7b). The top of the ridge is constituted of rhyolitic lavas and tuffs, penecontemporaneous with the Palaeocene carbonate sediments overlain by the Lower Eocene limestones (Siddique and Sukeshwala 1976). The culmination of volcanic activity was followed by subsidence of the ridge by about 200 m and deposition of biogenic sediments.

Three submerged terraces at depths 10–15, 21–36 and 43–47 m below the sea surface off the islands of Kadamat and Bangaram testify to as many phases of subsidence of the Lakshadweep island chain (Siddique 1975).

26.7 Submarine Sediment Fans

26.7.1 Bengal Fan

Nearly thirty per cent of the sediment load of the Ganga–Brahmaputra river system is carried to the Bay of Bengal and deposited as a fan (Fig. 26.7)—the *Bengal Fan* (Goodbread and Kuehl 1998). The accumulation of more than

Fig. 26.7 Bengal Fan and Indus Fan grew as a consequence of voluminous discharge of Himalayan-born rivers, respectively, the Ganga–Brahmaputra and the Sindhu. The tectonic map underscores the control of tectonic movement in the extraordinary development of the submarine fans (Qayyum et al. 1997)

200 million km^3 volume of sediment spread over 2 million km^2 area was deposited at the rate of 50 m per million years (Curray and Moore 1971), giving rise to the world's largest submarine fan. Stretching between 20°N and 10°S latitudes, the Bengal Fan is 2800–3000 km long and 1430 km wide at its widest part. It is dissected by a number of channels, tens of kilometres wide and hundreds of metres deep. In the channels, bound by levees flow turbidity currents and sheet flows for over 450 km distance.

Multibeam bathymetric, seismic, gravity and magnetic investigation show that the NNE-SSW-trending 300-km-long underwater Swatch-of-No-Ground canyon is 18 km wide with step like microterraces and levee deposits 100–150 m in thickness on both sides (of the canyon), implying that the canyon was formed by the flow of a major river with its underwater currents (Subrahmanyum et al. 2008b).

Analysis of multichannel seismic reflection record across the Bengal Fan north of 13°N revealed eight seismic sequence boundaries—corresponding to Early Cretaceous to Recent—and 85°E serving as a boundary between the western and eastern basins (Gopala Roa et al. 1994).

In the distal part of the Bengal Fan, the lower lithostratigraphic unit consists of older than 13,000 yr B.P. turbidites comprising olivegrey and black clays and silts, the clays being dominated by illite and chlorite. The upper unit is made up of 12,000 yr B.P. old and younger calcareous pelagic clays of yellow-brown colour with enriched smectite and kaolinite and appreciable contents of organic carbon and biogenic calcium carbonate (Kessarkar et al. 2005). While the sediments of the lower unit were derived predominantly from the Himalaya provenances, the detritus of the upper unit was delivered by the rivers draining both the Himalaya and the eastern part of the Peninsular India.

During the Pleistocene, there were two major pulses of fluvial sediment influx—at 11.5 and 9.5 ka, related to intensification of the monsoon which set in around 9.5 ka and paused at 5 and 2.2 ka (Chauhan et al. 2004).

The excessively lower values of $\delta^{18}O$ in the foraminifers *Globigerinoides ruber* and *G. sacculifer* occurring in the sediments in the Bay of Bengal indicate that the sediments were brought from a terrain experiencing heavy rainfall at the beginning of the Holocene ~9500 yr B.P., the condition persisting through the Holocene but with short spells of aridity during 5000–4300 yr B.P. and at 2000 yr B.P. (Chauhan 2003). Across the great Bengal Fan in the northern part of the Bay of Bengal, there is marked difference in the clay assemblages in the temporal span 18,000 to 12,600 yr B.P.—abundance of smectite clay in sediments in the western side delivered by rivers draining the Peninsular India and dominance of illite–chlorite in the sediments of the eastern part of the Bay brought by the rivers draining the Himalayan (Chauhan and Vogelsang 2006).

26.7.2 Indus Fan

The sediment discharge of the River Sindhu has resulted in the deposition of 2500-m-thick pile of detritus (Fig. 26.7) forming a 1500-km-long and 960-km-wide fan (Qayyum et al. 1997). Before the Sindhu was dammed for irrigation, it used to deliver sediments at the rate of 450 million tonnes per year to the Arabian Sea. The *Indus Fan* (Fig. 26.7) is characterized by five 20- to 30-m-deep submarine sinuous channels, extending to the water depth of 4200 m at the 12°N latitude (Kodagali and Jauhari 1999). The channels were formed predominantly by

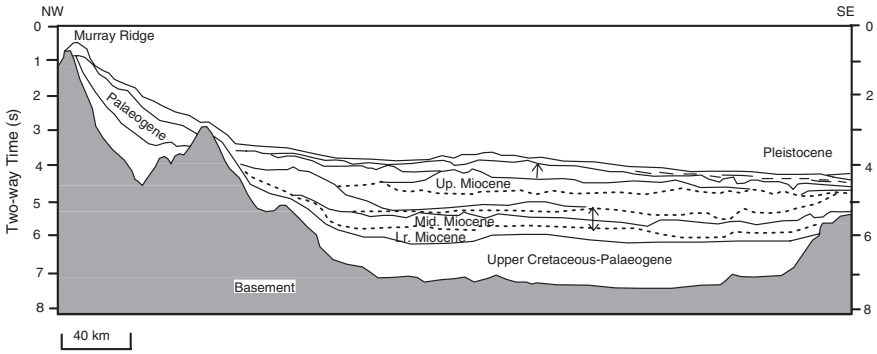

Fig. 26.8 Multichannel seismic profile of the Indus Fan–Murray Ridge region shows large thickness of Palaeogene strata that predate uplift of the Murray Ridge and the sequence of the Neogene sediments (after Clift et al. 2001)

turbidity currents that originated at the mouth of the Sindhu and have been active since the Early Miocene (Qayyum et al. 1997).

Nearly thirty-five per cent of the sediments of the Indus Fan and the adjoining Arabian Seafloor (including the Murray Ridge) are older than the Early Miocene and about forty per cent older than the Middle Miocene. The fact implies that the Arabian Sea has been an important repository of sediments during the Palaeogene period (Fig 26.8). The occurrence in the Middle Eocene sandstones of potash feldspar having Pb-isotope composition very similar to those of the Indus–Tsangpo Suture Zone and beyond indicates that India had collided with Asia well before the Middle Eocene time (Clift et al. 2001). The Pleistocene provenance of detritus was similar to that during the Eocene, but there were greater contributions from the Karakoram domain.

The uppermost layer of sediments of the northern Indus Fan consists of the 'channel-levee complex' of the Middle Miocene to Recent age. This unit overlies a layer of hemipelagic to pelagic sediments deposited during the drift phase after the Seychelles–India Plate broke away from Africa (Gaedicke et al. 2002).

26.8 Structure of and Sedimentation on Continental Margin

26.8.1 Western Continental Margin

The depth of the *continental shelf* off Kachchh, Saurashtra and Mumbai is between 80 and 154 m, while the upper boundary of the *continental slope* lies at the depth of 1450 m in the vicinity of the Indus Fan and of 2900 m in the southern part (Chauhan and Almeida 1993). The gradient of the continental slope is steep

off Karachi but gentler and characterized by benches off the coasts of Mumbai and Karnataka. The shelf break in general occurs between 90 and 180 m along the western margin.

All along the Konkan–Kanara offshore belt, (Fig. 26.9) the continental margin is characterized by a series of ridges and depressions representing horsts and grabens corresponding to and in the line of the Precambrian structural trends manifest in lineations, shear zones and fold axes in the Peninsular India (Chandrasekharam 1985; Subrahmanyam et al. 1993a, b). One of the topographic highs of the offshore belt comprises St. Mary's chain of 93-million-year-old volcanic islands.

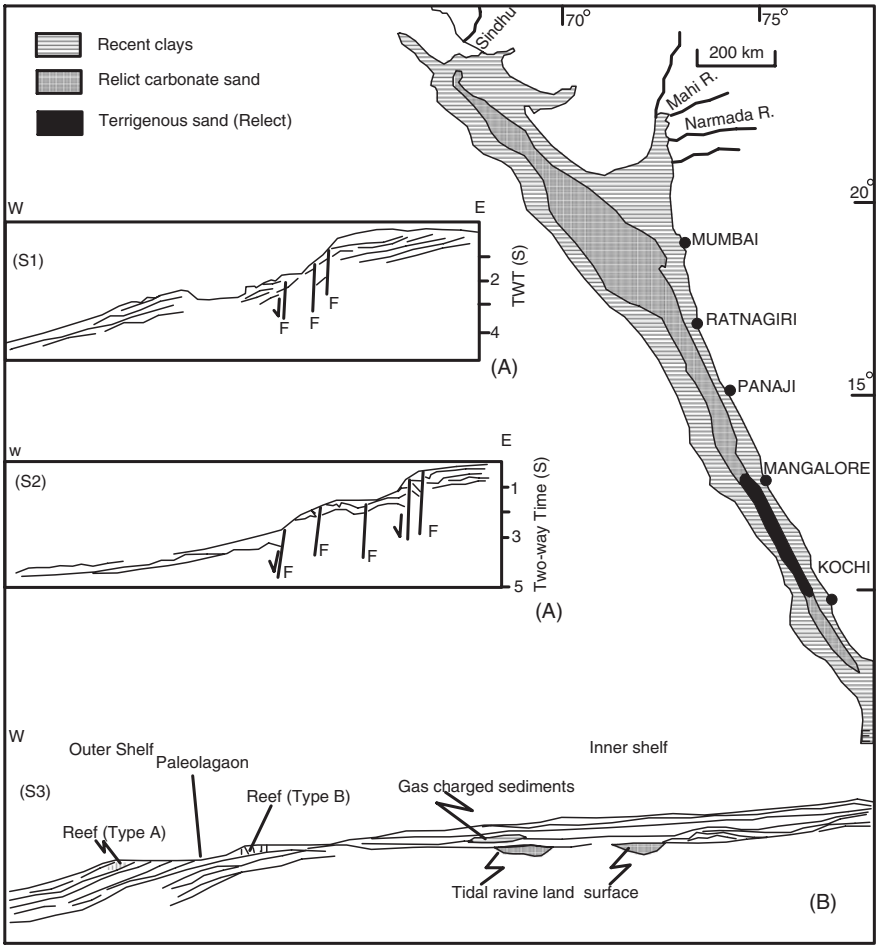

Fig. 26.9 Distribution of sediments on the western continental margin. **a** Generalized schematic profiles and sequence stratigraphy of the central sector of the continental shelf. (Map and A based on Karisiddaiah et al. 2005). **b** Seismic section of the offshore belt, northern continental margin (after Chauhan and Almeida 1993)

Comprehensive geophysical investigation of the entire western offshore belt from the coast to shelf margin reveals that underlying the thick pile of Tertiary sediment, the basement is characterized by a number of NW–SE- and N–S-oriented horst-and-graben structure, and the NNW–SSE-oriented ridges of the Lakshadweep and Kori-Comorin which are separated by depressions (Singh et al. 2007). It is seen that the basin is more differentiated in the Eocene–Oligocene section where N–S-trending horsts and grabens are present. The seismic data demonstrate strike-slip movements particularly associated with flower structure. *The onshore Western Ghat may therefore be a result of rifting and severe faulting with uplift and tilting to the east* (Singh et al. 2007). This finding strongly corroborates the deduction of Valdiya (2001a, b).

Similar investigations in the sector 12°40′N and 15°N revealed existence of several flat-topped NNW-SSE-trending bathymetric highs of considerable areal extent (256–1165 km^3) separated by bathymetric lows, the two forming horst-and-graben structures related to deep faults belonging to a rifted framework (Gopala Rao et al. 2010). The faults were formed presumably during the initial movement of the Indian plate.

On the shelf of the continental margin occurs a sedimentary sequence (Fig. 26.9) ranging in age from 9000 yr B.P. to 14,000 yr B.P. and embodying glacial–interglacial boundary at 10,200 yr B.P. (Hashimi and Nair 1981). Off Karnataka coast, the fine-grained sediments occur between the water depth of 15 and 50 m, and the calcareous sand comprising tests of foraminifers, pelecypods and gastropods is confined to the inner shelf between the water depth of 15–50 m and shelf edge (Hashimi and Nair 1981). Sand ridges 0.5–10 km in width and 1.5–18 m in height occur in the outer shelf off Mumbai at a water depth of 75 and 100 m (Wagle and Veerayya 1996).

The shelf edge is covered with relicts of carbonate facies and partially buried bioherms of the Holocene age, particularly off Mumbai and Saurashtra (Chauhan and Almeida 1993). Forming prominent shelf edge facies at the water depth of 85–136 m all along the 1000-km-long coast, the 1–2-m-high and 0.1–2.6-km-wide coral-algal reefs grew during the Holocene transgression (Vora et al. 1996). The sand ridges and coral-algal reefs occurring along the outer shelf indicate drowning of the continental shelf due to either rise of the sea level or neotectonic subsidence of the faulted underwater terrane (Fig. 26.9) as discernible off Mumbai–Saurashtra coasts (Purnachandra Rao et al. 1996; Chauhan and Almeida 1993).

The present rate of sedimentation in the Mangalore sector varies from 0.72 mm/year to 0.56 mm/year for the depths of 35 and 45 m, respectively (Manjunath and Shankar 1992).

Seismic stratigraphic analysis defining nine units in the belt off Kundapur and Mangalore demonstrates Late Quaternary regression–transgression cycle together with the sedimentary processes changing from siliciclastic to carbonate sedimentation and back to siliciclastic sediment deposition (Karisiddaiah and Subba Raju 2002). Off Goa, the inner-shelf sediments are characterized by dominant presence of kaolinite, illite and gibbsite (Thamban et al. 2002). Offshore Karwar, the clay sediments contain palynological evidence of the change at about 3500 yr B.P.

of evergreen forests to savannah forests on land and reduction of mangrove flora (Cartini et al. 1994).

In the Konkan–Kerala sector, the volume of Cenozoic sediments amounts to about 1,090,000 km^3. This huge amount could not have been delivered by but an "elevated rift-flank of flexure" which is an important component in the development of western Indian continental margin (Campanile et al. 2008). Multichannel seismic reflection profile in the south-western continental margin reveals the presence of westerly dipping reflector beneath the pile of sediments, inferred to be made of volcanic rocks (Ajay et al. 2010).

26.8.2 Eastern Continental Margin

In the sectors where no sediment deposition is taking place, the shelf bottom at the water depth of 70–116 m shows pinnacles and domes related to a karstic topography that is now drowned. The shelf break and upper slope belts are characterized by V-shaped canyons, as seen off the Mahanadi, the Krishna and the Godavari and Pondicherry (Purnachandra Rao and Kessarkar 2001). There are submarine canyons and various types of valleys (Fig. 26.10). The canyons and valleys coalesce downstream to form a broad drainage fan on the continental slope. This fan extends beyond the *continental rise* and occupies the abysmal plain.

Interpretation of gravity, magnetic and multichannel seismic reflection data show existence in the basement of prominent ENE-WSE-trending horst-and-graben structure, the structure resulting from rifting of the offshore belt (Bastia et al. 2010a). There is also a suggestion for the presence of canyon fills and channel-levee deposits in the study area. Needless to state, all these features are pointers to the presence of requisite basic framework for formation and accumulation of petroleum deposits. High-resolution and close-grid two-dimensional reflection seismic data of the Mahanadi shelf show existence of N–S-trending broad morphological highs and equally broad continuous ridge and also a chain of linearly oriented volcanic cones, implying continuation of the 83°E Ridge of the Bay of Bengal on to the Mahanadi shelf (Bastia et al. 2010b). It is significant that in the line of this trend lies the Rajmahal Volcanics Province. The magnetization pattern of the Eightythree East Ridge correlates with the geomagnetic polarity timescale, indicating start of volcanism in the Mahanadi Basin by short-lived hot spot activity at anomaly 33 r (nearly 80 Ma) which continued towards south and finally ended at the vicinity of Mount Afanasi Seamount at about 55 Ma (Michael and Krishna 2011).

The continental slope and beyond show three stratigraphic sequences. The shallow seismic records depict three to five prominent reflectors, corresponding probably to the Late Miocene to the Recent. Below the seabed, the imprints of marking of rising gas are a common feature, particularly off the Krishna–Godavari delta. Nearly half the continental slope deposits exhibit slumping and sliding as seen off Puri, Machalipatnam and Pondicherry (Purnachandra Rao and Kessarkar 2001).

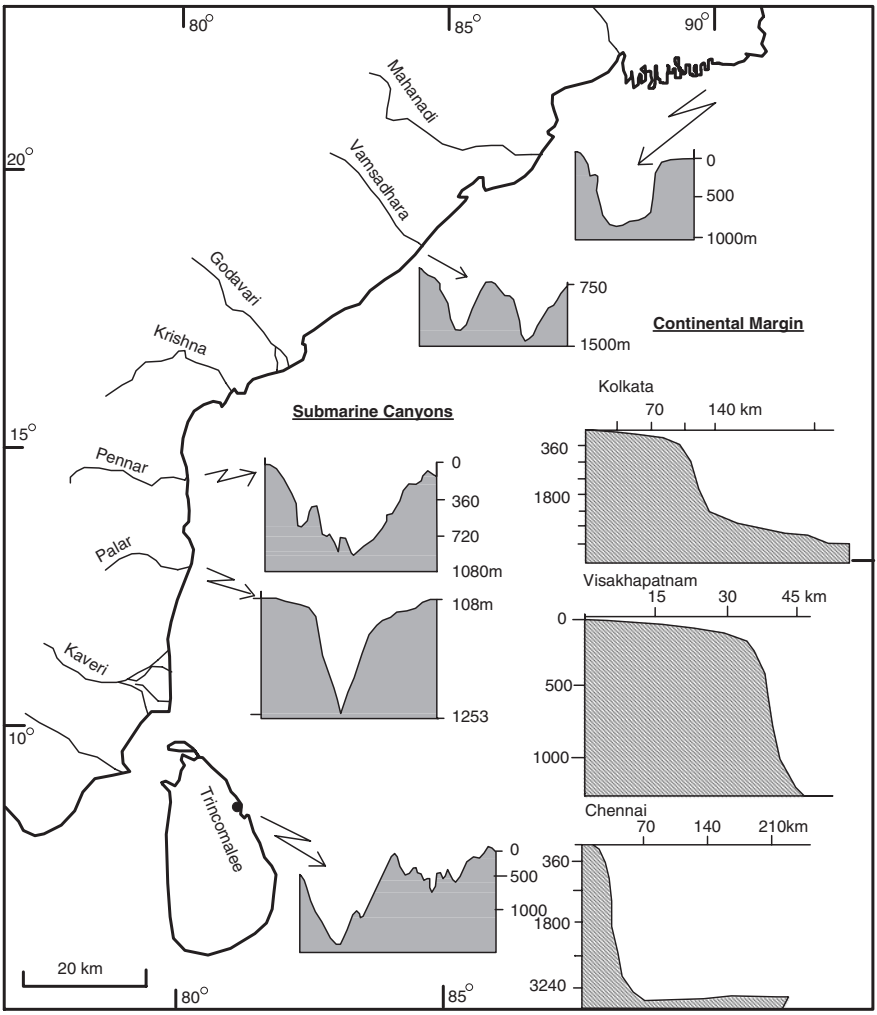

Fig. 26.10 Bathymetric profiles along the eastern continental margin showing the shelf, the slope and the rise, and the shape of submarine canyons (based on Purnachandra Rao and Kessarkar 2001)

26.8.3 Sedimentation off Irrawaddy Delta

The Irrawaddy, the Sittang and the Salween rivers of Myanmar together discharge more than 360 million tonnes of sediments annually. The result is more than 176-km-wide sedimentary shelf incised by the Martaban canyon. The shelf deposit is made up of mud in the near-shore belt, relict sand in the outer shelf and mixed sediments in the Gulf of Martaban (Rao et al. 2005). In the Gulf, the bulk of the sediments is being displaced eastwards by tidal current aided by monsoon currents that flow clockwise.

26.9 Sea-Level Change

Related to the glaciation on continents that caused withdrawal of water and the deglaciation resulting in influx of melt water, the sea level has been changing through the time. There is also neotectonic subsidence and uplift of the fault blocks along the coasts. This change is well documented by sediments, faunal assemblages and coastal geomorphic features.

The *sea water level* stood nearly 100 m below the present level around 14500 yr B.P., then rose rapidly at the rate of 10 m/1000 years to the water depth of 80 m around 12,000 yr B.P. and remained still in the next 2000 years (Nigam et al. 1992, 1994; Hashimi et al. 1995). Significantly, from the beginning of the Holocene until about 7000 yr B.P., the rate of the rise of the sea level was 20 m/1000 yr. Discovery at the depths of 30–40 m of the Neolithic settlements (nearly 9500 yr B.P.) along with fluvial gravel deposit in the Gulf of Khambhat off Hazira corroborates the deduction of the rapid rise of the sea level (Nigam and Hashimi 2002).

Occurrence of 10760 ± 130 year and 9280 ± 150 year old carbonized wood and peat of mangrove origin on the continental shelf off Kerala implies change of the sea level during Late Pleistocene to Early Holocene period (Pandarinath et al. 2001). The sea level stabilized after 6000 yr B.P.

In the Visakhapatnam–Gopalpur stretch along the Andhra–Odisha coast, submarine terraces, reefs and pinnacles at the water depth of 80–100, 50–70 and 25–30 m testify to the sea-level change in the Late Pleistocene–Early Holocene interval (Mohan Rao et al. 2000). From the faulting of the coastal belt, it has been surmised that neotectonic activity played an important role in the change of the sea level (Purnachandra Rao et al. 1996) (Figure 26.11).

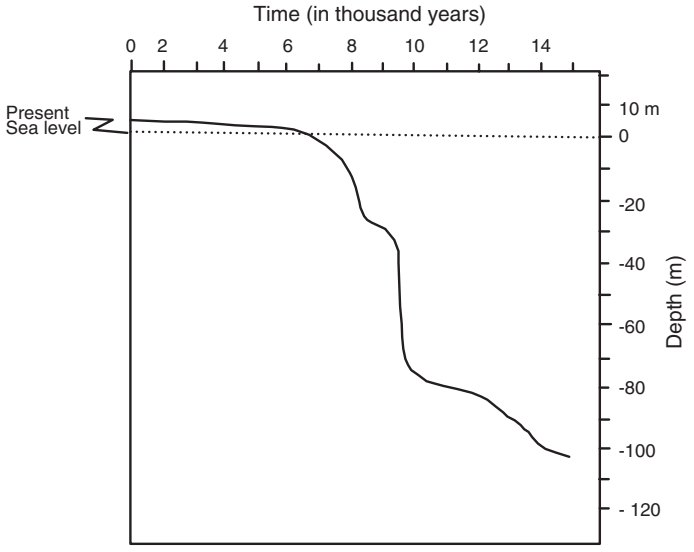

Fig. 26.11 Holocene sea level relative to the present sea level. The position of Neolithic settlement in the Gulf of Khambhat is shown by an *arrow* (Hashimi et al. 1995)

26.10 Ongoing Movements and Seismicity

Dense distribution of epicentres along the axial valleys of the mid-oceanic ridges and subduction zones—and in the zones of transform faults—demonstrates that the Indian Ocean is under tectonic stress. It is due to north–south compression and east–west extension.

Vertical compression has brought about crustal thinning in the western part of the Indian Ocean and crustal extension in the eastern part (Singh 1988). Movement tensor solutions of earthquakes indicate combination of thrust- and strike-slip faulting in the Bay of Bengal and thrust and normal faulting or strike-slip faulting in the Arabian Sea. The compressive stresses are changing from N–S to E–W and the resultant tensional stress direction from E–W to N–S in different parts of the Indian Ocean. This fact implies that there is counterclockwise movement of the region defined by the equator and 35°S and 64°E and 94°E latitudes. This is responsible for the stretching of the crust in the region of Rodriguez Triple Junction, intense compressional deformation in the Central Indian Ocean and formation of a new subduction zone beneath the intensely deformed zone in the Central Indian Ocean (Singh 1997).

Benioff zones off Makran Coast in northern Arabian Sea and beneath the Andaman–Indonesia Island Arc in the Bay of Bengal allow plunging down or subduction of the Indian floor into the mantle (Jacob and Quittmeyer 1979; Mukhopadhyay 1984).

26.11 Mineral Assets

Geological and geophysical studies indicate the presence of *placer deposits* in the near-shore and inner shore belts of both the West Coast and the East Coast.

In the inner shelf occur gas-charged sediments and deposits of gas hydrates. The *gas hydrate* is a crystalline substance composed of cages of water molecules hosting gases under low temperature and high pressure. Unconformably overlying the Pleistocene–Holocene sediments, a 5–35-m-thick horizon of weakly stratified clays at water depth of less than 60 m along the western shelf is believed to contain gas-charged sediment (Veerayya et al. 1998). Significant gas seepages occur in the outer shelf and middle continental slope, and there are indications of the presence of gas hydrates in the middle–lower continental slope and continental rise region, probably trapped in folds, diapiric structures and fault zones (Ramana et al. 2006). Indication of the presence of gas hydrates occurs over 1400 km^2 and a potential gas province in Krishna–Godavari delta off Narasapur in Andhra Pradesh and off Chilka Lake in Odisha (Purnachandra Rao and Kessarkar 2001). There is indication of presence of significantly large volume of gas hydrates in Middle Miocene to Upper Miocene west of the Andaman Island.

Base metal deposits in minor quantities are associated with hydrothermal vents in the mid-oceanic ridges. In the south-western part of the Andaman Sea, the active part of the rifted ridge and the crater of a seamount show vein-type sulphide mineralization including pyrite and chalcopyrite (Rao et al. 1996). Massive sulphide deposits occur north of the Rodriguez Triple Junction in the Central Indian Ocean—in the fourth ridge segment close to the rift axis and associated with hydrothermal chimney structure (Halbach et al. 1998). Sulphide encrustation indicates appreciable metallogenesis along the Indian Ocean Ridge System (Banerjee and Raj 2003).

Ferromanganese nodules and *cobalt-rich encrustations* occur in deep ocean floor over large areas and on topographic highs like the Afanasy Nikitin Seamount in the Central Indian Basin. The Rodriquez trijunction has an encrustation of ferromagnetic minerals (Nagendernath et al. 1997). Scattered biogenic remains and mineral grains in addition to the main nuclei acted as accessory seeds for growth of oxide layers. Laminations alternately dominated by todorokite and vernadite are a characteristic feature of these nodules. Showing dendritic, laminated and microglobular structures, the ferromanganese nodules occur in a variety of host sediments—terrigenous clay, siliceous ooze, calcareous ooze and red clay east of the Chagos–Lakshadweep island chain (Banerjee et al. 1999). Manganese micronodules occur in the middle fan region of the Bay of Bengal—abundantly in the areas of relatively low sedimentation in the eastern part (Chauhan et al. 1993). More than 2700 million tonnes of nodules occur in the Central Indian Ocean. Ferromanganese crust in a layer of carbonate fluorapatite on the summit of the Afanasy Nikitin Seamount is enriched in cobalt (Banakar et al. 1997).

Phosphorite deposits of the Pleistocene age occur on the continental margin at water depths of 380–390 m off Goa and 186–293 m off Chennai. Associated with outer-shelf glauconite and shells of molluscs and rhodoliths and phosphorite off Chennai are similar to phosphatized stromatolites. Microbial processes played a major role in the phosphatization of the stromatolitic carbonates (Purnachandra Rao et al. 2000). The off Goa phosphorite crust is made up of carbonate fluorapatite, occurring as globules. It is believed that the initial substrate for the phosphorite crust was a fish coprolite, which was phosphatized under lower rates of terrigenous sedimentation during the Pleistocene (Purnachanra Rao et al. 1995).

References

Ajay, K. K., Chaubey, A. K., Krishna, K. S., Gopala Rao, D., & Sar, D. (2010). Seaward dipping reflectors along the SW continental margin of India: Evidence for volcanic passive margin. *Journal Earth System Science, 119*, 803–813.

Banakar, V. K., Galy, A., Sukumaran, N. P., Parthiban, G., & Volvaiker, A. Y. (2003). Himalayan sedimentary pulses recorded by silicate detritus within a ferromagnetic crust from the central Indian Ocean. *Earth & Planetary Science Letters, 205*, 337–348.

Banakar, V. K., Pattan, J. N., & Mudholkar, A. V. (1997). Paleocenographic conditions during the formation of a ferromanganese crust from the Afanasity-Nikitin seamount, north Central Indian Ocean: Geochemical evidence. *Marine Geology, 136*, 299–315.

Banerjee, R., & Raj, D. (2003). Metallogenesis along the Indian Ocean ridge system. *Current Science, 85*, 41–47.

Banerjee, R., Roy, S., Dasgupta, S., Mukhopadhyay, S., & Miura, H. (1999). Petrogenesis of ferromanganese nodules from east of the Chagos archipelago, central Indian Ocean. *Marine Geology, 157*, 145–158.

Bastia, R., Radhakrishna, M., Das, Suman, Kale, A. S., & Catuneanu, O. (2010a). Delineation of the 85^0E ridge and its structure in the Mahanadi offshore basin, Eastern Continental Margin of India, from seismic reflection imagery. *Marine & Petroleum Geology, 27*, 1841–1848.

Bastia, R., Radhakrishna, M., Srinivas, T., Nayak, S., Nathanid, D. M., & Biswal, T. K. (2010b). Structural and tectonic interpretations of geophysical data along the Eastern Continental Margin of India with special reference to the deep water petroliferous basins. *Journal Asian Earth Science, 39*, 608–619.

Bhattacharya, G. C., Chaubey, A. K., Murty, G. P. S., Srinivas, K., Sarma, K. V. L. N. S., Subrahmanyam, V., et al. (1994). Evidence for seafloor spreading in the Laxmi Basin, northeastern Arabian Sea. *Earth & Planetary Science Letters, 125*, 211–220.

Campanile, D., Nambiar, C. G., Bishop, P., Widdowson, M., & Brown, R. (2008). Sedimentations record in the Konkan-Kerala Basin: Implication for the evolution of the Western Ghats and western Indian passive margins. *Basin Research, 20*, 3–20.

Cartini, C., Bentaleb, I., Fontugne, I. M., Morzadek-Kerfourn, M. T., Pascal, J. P., & Tissot, C. (1994). A less humid climate since ca 3500 yr BP from marine cores off Karwar, western India. *Palaeogeography, Palaeoclimatology, Palaeoecology, 109*, 371–384.

Chamoli, A., & Dimri, V. P. (2007). Continental crust in Laxmi Basin (Arabian Sea) using wavelet analysis. *Indian Journal Marine Science*, *36*, 117–121.

Chandrasekharam, D. (1985). Structure and evolution of the western continental margin of India deduced from gravity, seismic, geomagnetic and geochronological studies. *Physics, Earth & Planetary Interiors, 41*, 186–198.

Chaubey, A. K., Bhattacharya, G. C., Murty, G. P. S., & Desa, Maria. (1993). Spreading history of the Arabian Sea: Some new constraints. *Marine Geol., 112*, 343–352.

Chaubey, A. K., Bhattacharya, G. C., Murty, G. P. S., Srinivas, K., Ramprasad, T., & Gopala Rao, D. (1998). Early Tertiary seafloor spreading magnetic anomalies and palaeopropagators in the northern Arabian Sea. *Earth & Planetary Science Letters, 154*, 41–52.

Chaubey, A. K., Dyment, J., Bhattacharya, G. C., Royer, J.-Y., Srinivas, K., & Yatheesh, V. (2000). Paleogene magnetic isochrones and palaeo-propogators in the Arabian and Eastern Somali basins, NW Indian Ocean. In P. D. Clift, D. Karoon, C. Gaedicke, & J. Craig (Eds.), *The Tectonic and Climatic Evolution of the Arabian Sea Region* (Vol. 195, pp. 71–85). Geological Society of London, Special Publications.

Chauhan, O. S. (2003). Past 20,000-year history of Himalayan aridity: Evidence from oxygen isotope records in the Bay of Bengal. *Current Science, 84*, 90–93.

Chauhan, O. S., & Almeida, F. (1993). Influence of Holocene sea level, regional tectonics and fluvial, gravity and slope current induced sedimentation on the regional geomorphology of the continental slope off northwestern India. *Marine Geology, 112*, 313–328.

Chauhan, O. S., Patil, S. K., & Suneetha, J. (2004). Fluvial influx and weathering history of the Himalayas since last glacial maximum—Isotopic, sedimentological and magnetic records from the Bay of Bengal. *Current Science, 87*, 509–514.

Chauhan, O. S., & Vogelsang, E. (2006). Climate induced changes in the circulation and dispersal pattern of the fluvial sources during the Late Quaternary in the middle Bengal Fan. *Journal Earth System Science, 115*, 379–386.

Chauhan, O. S., Vogelsang, E., Basavaiah, N. & Kader, U.S.A. (2010). Reconstruction of variability of the southwest monsoon during the period 3 ka from the continental margin of southwestern Arabia Sea, *Journal Quarternary Science*, *25*, 798–807.

Clift, P. P., Shimizu, N., Layne, G. D., Blusztajn, J. S., Gaedicke, C., Schluter, H. U., et al. (2001). Development of Indus Fan and its significance for the erosional history of the western Himalaya and Karakoram. *Bulletin Geological Society American, 113*, 1039–1051.

Collier, J. S., Sansom, V., Ishizuka, O., Taylor, R. N., Minshull, T. A., & Whitmarsh, R. B. (2008). Age of Seycheles-India breakup. *Earth & Planetary Science Letters, 272*, 264–277.

Curray, J. R., & Moore, D. G. (1971). Growth of the Bengal deep sea fan and denudation in the Himalaya. *Geological Society American Bulletin, 82*, 563–572.

Davies, T. A., Kidd, R. B., & Ramsay, A. T. S. (1995). A time-slice approach to history of Cenozoic sedimentation in the Indian Ocean. *Sedimentary Geology, 96*, 157–179.

DeMets, C., & Royer, J.-Y. (2003). A new high-resolution model for India-Capricorn motion since 20 Ma: Implications for the chronology and magnitude of distributed crustal deformation in the Central Indian Basin. *Current Science, 85*, 339–345.

Desa, M., Ramana, M. V., & Ramaprasad, T. (2006). Seafloor spreading magnetic anomalies south of Sri Lanka. *Marine Geol., 229*, 227–240.

Drolia, R. K., & DeMets, C. (2005). Deformation in the diffuse India–Capricorn–Somalia triple junction from a multibeam and magnetic survey of the northern Central Indian Ridge, 3˚S–10˚S. *Geochemistry Geophysics Geosystems, 6*, 393–415.

Drolia, R. K., Iyer, S. D., Chakraborty, B., Kodagali, V. N., Ray, D., Misra, S., et al. (2003). The Northern and Central Indian ridge: Geology, tectonics of fracture zones-dominated spreading ridge segments. *Current Science, 85*, 415–423.

Edwards, R. A., Minshull, T. A., Flueh, E. R., & Kopp, C. (2008). Dalrymple Trough: An active oblique-slip ocean-continent boundary in the northwest Indian Ocean. *Earth & Planetary Science Letters, 272*, 437–445.

Eremenko, N. A., & Datta, A. K. (1968). Regional geological framework and evolution of the petroleum basins: Prospects of Laccadive-Archipelago and offshore Tertiary basins. *Bulletin ONGC, 5*, 65–73.

Fournier, M., Chamot-Rooke, N., Rodriquez, M., Huchson, P., Petit, C., Besliar, Ju-O, et al. (2011). Owen fracture zone: The Arabia-Asia plate boundary unveiled. *Earth & Planetary Science Letters, 333–334*, 247–252.

Gaedicke, C., Schluter, H.-U., Roeser, H. A., Prexl, A., Schrekenperger, B., Meyer, H., et al. (2002). Origin of the northern Indus fan and Murray ridge, northern Arabian Sea: Interpretations from seismic and magnetic imaging. *Tectonophysics, 355*, 123–143.

Goodbred, S. L., & Kuehl, S. A. (1998). Floodplain processes in the Bengal Basin and the storage of Ganges-Brahmaputra river sediment: An accretion study using 137Cs and 210Pb geochronology. *Sedimentary Geology, 121*, 239–258.

Gopala Rao, D., Bhattacharya, G. C., & Ramana, M. V. (1994). Analysis of multi-channel seismic reflection and magnetic data along 13ºN latitude across the Bay of Bengal. *Marine Journal Geophysics Research, 16*, 225–236.

Gopala Rao, D., Paropkari, A. L., Krishna, K. S., Chaubey, A. K., Ajay, K. K., & Kodagali, V. N. (2010). Bathymetric highs in the mid-slope regions of the western continental margin of India—Structure and mode of origin. *Marine Geology, 276*, 58–70.

Gupta, A. K., & Dhingra, H. (2004). Middle Pleistocene transition (MPT) in eastern Indian Ocean: A 2000-kyr planktonic and isotope record from DSDP Site 214. *Memoir Geological Society India, 63*, 29–38.

Gupta, A. K., & Srinivasan, M. S. (1992). Deep-sea benthic foraminiferal changes and terminal Miocene event at tropical Indian Ocean DSDP Site 214. *Journal Geological Society India, 40*, 262–278.

Halbach, P., Blum, N., Munch, U., Pluger, W., Schonberg, D. G., & Zimmer, M. (1998). Formation and decay of a modern massive sulphide deposit in the Indian Ocean. *Mineralium Deposita, 33*, 302–309.

Hashimi, N. H., & Nair, R. R. (1981). Surfacial sediments of the continental shelf off Karnataka. *Journal Geological Society India, 22*, 266–273.

Hashimi, N. H., Nigam, Rajiv, Nair, R. R., & Rajagopalan, G. (1995). Holocene sea level fluctuations on western Indian continental margin: An update. *Journal Geological Society India, 46*, 157–162.

Iyer, S. D., & Ray, Dwijesh. (2003). Structure, tectonic and petrology of mid-oceanic ridges and the Indian scenario. *Current Science, 85*, 277–289.

Jacob, K. H., & Quittmeyer, R. C. (1979). The Makran region of Pakistan and Iran: Trench-arc system with active plate subduction. In H. Farah & K. A. Dejong (Eds.), *Geodynamics of Pakistan* (pp. 305–315). Quetta: Geological Survey of Pakistan.

Kamesh Raju, K. A. (1993). Magnetic lineations, fracture zones and seamounts in the Central Indian Basin. *Marine Geology, 109*, 195–201.

Kamesh Raju, K. A., Ramprasad, T., Rao, P. S., Ramalingeswara Rao, B., & Varghese, J. (2004). New insights into the tectonic evolution of the Andaman basin, northeast Indian Ocean. *Earth & Planetary Science Letters, 221*, 145–162.

Kench, P. S., McLean, R. F., & Nichol, S. L. (2005). New model of reef-island evolution: Maldives. *Indian Ocean, Geology, 33*, 145–148.

Karisiddaiah, S. M., & Subba Raju, L. V. (2002). Scenario of gas-charged sediments and gas hydrates in the western continental margin of India. *Journal of Geophysics, 23*, 33–41.

Kessarkar, P. M., Rao, P. V., Ahmed, S. M., Patil, S. K., Anil Kumar, A., Babu, G. A., et al. (2005). Changing sedimentary environment during the Later Quaternary: Sedimentological and isotopic evidence from the distal Bengal Fan. *Deep Sea Research, I52*, 1591–1615.

Kodagali, V. N., & Jauhari, Pratima. (1999). The meandering Indus channels: Study in a small area by the multibeam swath bathymetry system Hydrosweep. *Current Science, 76*, 240–242.

Krishna, K. S. (2003). Structure and evolution of the Afanasy Nikitin Seamount, buried hills and 85ºE Ridge in the northeastern Indian Ocean, *Earth & Planetary Science Letters*, *209*, 379–394. (Corrigendum to this article is published in *Earth Planetary Science Letters*, *210* (3–4), pp. 587).

Krishna, K. S., Abraham, H., Sager, W. W., Pringle, M. S., Frey F., Gopala Rao, D., & Levchenko, M. S. (2012). Tectonics of the NinetyEast Ridge derived from spreading records in adjacent oceanic basin and age constraints of the ridge. *Journal Geophysics Research, 117*, Bo4101.

Krishna, K. S., Bull, J. M., & Scrutton, R. A. (2009). Early (pre-8 Ma) fault activity and temporal strain accumulation in Central Indian Ocean. *Geology, 37*, 227–230.

Krishna, K. S., Gopala Rao, D., & Sar, D. (2006). Nature of the crust in the Laxmi Basin (14°–20°N), western continental margin of India. *Tectonics*, 25, TC 1006.

Krishna, K. S., Gopala Rao, D., Subbaraju, L. V., Chaubey, A. K., Schherbakov, V. S., Pilipenko, A. T., & Murthy I. V. R. (1999). Paleocene on-spreading axis hotspot volcanism along the Ninety-East Ridge: An interaction between the Kerguelen hotspot and the Wharton spreading centre, *Proceedings Indian Academy Science (Earth & Planetary Science)*, *108*, 255–267.

Krishna, K. S., Neprochnov, Y. P., Gopala Rao, D., & Grinko, B. N. (2001). Crustal structure and tectonics of the Ninety-East Ridge from seismic and gravity studies. *Tectonics, 20*, 416–433.

Krishna, J., Pathak, D. B., & Pandey, B. (1998a). Development of Oxfordian (Early Upper Jurassic) in the most proximately exposed part of the Kachchh Basin at Wagad outside the Kachchh mainland. *Journal Geological Society India, 52*, 513–522.

Krishna, K. S., Ramana, M. V., Gopala Rao, D., Murthy, K. S. R., Malleswara Rao, M. M., Subrahmanyam, V., & Sarma, K. V. L. N. S. (1998b). Periodic deformation of oceanic crust in the Central Indian Ocean. *Journal Geophysics Research, 103*, 17859–17875.

Krishna, K. S., Rao, D. G., & Neprochnov, Y. P., (2002). Formation of diapiric structure in the deformation zone, central Indian Ocean: A model from gravity and seismic reflection data, *Proceedings Indian Academy Science (Earth and Planetary Science*, *111*, 17–28.

Manjunatha, B. R., & Shankar, R. (1992). A note on the factors controlling the sedimentation rate along the western continental shelf of India. *Marine Geol., 104*, 219–224.

Merkouriev, S. A., & Sotchevanova, N. A. (2003). Structure and evolution of the Carlsberg Ridge: Evidence for non-stationary spreading on old and modern spreading centres. *Current Science, 85*, 334–338.

Meyers, P. A., & Dickens, G. R. (1992). Accumulation of organic matter in sediments of the Indian Ocean: A synthesis of results from scientific deep sea drilling. In R. A. Duncan (Ed.), *Synthesis of Results from Scientific Drilling in the Indian Ocean* (pp. 295–308). Washington: American Geophysical Union.

Michael, L., & Krishna, K. S. (2011). Dating of the 85°E Ridge (NE Indian Ocean) using marine magnetic anomalies. *Current Science, 100*, 1314–1322.

Mohan Rao, K., Reddy, N. P. C., Kumar, P., Raju, M. K., Venkateswarulu, Y. S. N., & Muthy, K. S. R. (2000). Signatures of Late Quaternary sea level changes and neotectonic activity in Visakhapatnam-Gopalpura Shelf, East Coast of India. In G. V. Rajamanickam & M. J. Toley (Eds.), *Quaternary Sea Level Variation, Shoreline Displacement and Coastal Environment* (pp. 116–124). Delhi: New Academic Publishers.

Mudholkar, A. V., Kodagali, V. N., Kamesh Raju, K. A., Valsangkar, A. B., Ranade, G. H., & Ambre, N. V. (2002). Geomorphological and petrological observations along a segment of slow-spreading Carlsberg Ridge. *Current Science, 82*, 982–989.

Mukhopadhyay, M. (1984). Seismotectonics of subduction and back-arc rifting under the Andaman Sea. *Tectonophysics, 108*, 229–239.

Naidu, P. D. (1996). Onset of an arid climate at 3.5 ka in the tropics: Evidence from monsoon upwelling. *Current Science, 71*, 715–718.

Nigam, R., Borole, D. V., & Hashimi, N. H. (1994). Study of subsurface sediments from northern Indian Ocean: Oceanic responses to climatic changes. *Journal Palaeontology Society India, 39*, 1–4.

Nigam, R., & Hashimi, N. H. (2002). Has sea level fluctuation modulated human settlements in Gulf of Khambhat? *Journal Geological Society India, 59*, 583–585.

Nigam, R., Hashimi, N. H., Eileen, T. M., & Wagh, A. B. (1992). Fluctuating sea levels off Bombay (India) between 14500–10000 years before present. *Current Science, 62*, 309–313.

Pandarinath, K., Shankar, R., & Yadava, M. G. (2001). Late Quaternary changes in sea level and sedimentation rate along the SW coast of India: Evidence from radiocarbon dates. *Current Science, 81*, 594–596.

Pandey, O. P., Agrawal, P. K., & Negi, J. G. (1995). Lithospheric structure beneath Laxmi Ridge and late Cretaceous geodynamic events. *Geomarine Letters, 15*, 85–91.

Purnachandra Rao, V., & Kessarkar, P. M. (2001). Geomorphology and geology of the Bay of Bengal and the Andaman sea, In R. Sen Gupta, E. Desa (Eds.), *The Indian Ocean* (Vol. 2, 817–868), Oxford & IBH.

Purnachandra Rao, V., Mohan Rao, K., & Raju, D. S. N. (2000). Quaternary phosphorites from the continental margin off Chennai, southeast India: analogs of ancient phosphatic stromatolites. *Journal Sedimentary Research, 70*, 1197–1209.

Purnachandra Rao, V., Rao, Ch M, Thamban, M., Natarajan, R., & Rao, B. R. (1995). Origin and significance of high-grade phosphorite in a sediment core from the continental slope off Goa, India. *Current Science, 69*, 1017–1019.

Purnachandra Rao, V., Veerayya, M., Thamban, M., & Wagle, B. G. (1996). Evidence of Late Quaternary neotectonic activity and sea-level changes along the western continental margin of India. *Current Science, 71*, 36–40.

Qayyum, M., Lawrence, R. D., & Niem, A. R. (1997). Discoverry of the palaeo-Indus delta-fan complex. *Journal Geological Society London, 154*, 753–756.

Ramana, M. V., Ramprasad, T., Kamesh Raju, K. A., & Desa, M. (1993). Geophysical studies over a segment of the Carlsberg Ridge, Indian Ocean. *Marine Geology, 115*, 21–28.

Ramana, M. V., Nair, R. R., Sarma, K. V. L. N. S., Ramprasad, T., Krishna, K. S., Subrahmanyam, V., et al. (1994). Mesozoic anomalies in the Bay of Bengal. *Earth Planetary Science Letters, 121*, 469–475.

Ramana, M. V., Ramprasad, T., & Desa, M. (2001). Seafloor spreading magnetic anomalies in the Enderby Basin, East Antarctica. *Earth Planetary Science Letters, 191*, 241–255.

Ramana, M. V., Subrahmanyam, V., Chaubey, A. K., Ramprasad, T., Sarma, K. V. L. N. S., Krishna, K. S., et al. (1997). Structure and origin of the 85ºE Ridge. *Journal Geophysics Research, 102*, 17995–18102.

Rao, P. S., Kamesh Raju, K. A., Ramprasad, T., Nagender Nath, B., Ramalingeswara Rao, B., Rao, Ch M, et al. (1996). Evidence for hydrothermal activity in the Andaman Back-arc basin. *Current Science, 70*, 379–385.

Rao, P. S., Ramasamy, V., & Thwin, Swe. (2005). Sediment texture, distribution and transport on the Ayeyarwady continental shelf, Andaman Sea. *Marine Geology, 216*, 239–247.

Royer, J.-Y., Chaubey, A. K., Dyment, J., Bhattacharya, G. C., Srinivas, K., Yatheesh, V., & Ramprasad, T. (2002). Palaeogene plate tectonic evolution of the Arabian and Eastern Somali basins, In: P. D. Clift et al. (Eds.), *The Tectonic and Climate Evolution of the Arabian Sea region* (Vol. 195, pp. 7–23). Special Publications, Geological Society London.

Sager, W. W., Paul, C. F., Krishna, K. S., Pride, M., Eisin, A. E., Frey, F. A., Gopala Rao, D., & Levchenko, O. (2010). Large fault failure of the Ninetyeast Ridge implies near-spreading ridge formation, *Geophysical Research Letters*, *37*, L17304.

Saraswati, P. K., Nigam, R., Weldeap, S., Mackensen A., & Naidu, P. D. (2005). A first look at past sea surface temperatures in the equatorian Indian Ocean from Mg/Ca in foraminifera. *Geophysics Research Letters*, *32*. doi:10.1029/2005GL024093.

Saraswati, P. K., Ramesh, R., & Navada, S. V. (1993). Palaeogene isotopic temperature of western India. *Letheia, 26*, 89–98.

Siddique, H. N., & Sukeshwala, R. N. (1976). Occurrence of rhyolitic tuff at deep sea drilling project site 219 on the Laccadive ridge. *Journal Geological Society India, 17*, 539–546.

Singh, D. D. (1988). Strain deformation in the Northern Indian Ocean. *Marine Geology, 79*, 105–118.

Singh, D. D. (1997). Moment tensor solutions of earthquakes in the Indian Ocean from surface waves and their tectonic implications. *Pure & Applied Geophysics, 150*, 53–73.

Singh, A. D. (1998). Late Quaternary oceanographic changes on the eastern Arabian Sea: Evidence from planktonic foraminifera and pteropods. *Journal Geological Society India, 52*, 203–212.

Singh, R. K., & Gupta, A. K. (2004). Late Oligocene-Miocene palaeooceanographic evolution of the southeastern Indian Ocean: Evidence from deep-sea benthic foraminifera (ODP site 757). *Marine Micropalaeontology, 51*, 153–170.

Singh, K., Radhakrishna, M., & Pant, A. P. (2007). Geophysical structure of the western offshore basins of India and its implications to the evolution of the western Ghats. *Journal Geological Society India, 70*, 445–458.

Srinivasan, M. S. (1996). *Oceanic Micropalaeontology—Major Advances Since the Beginning of DSDP*. Dehradun: KDMIPE. 34 p.

Srinivasan, M. S., & Chaturvedi, S. N. (1992). Neogene planktonic foraminiferal biochronology of the DSDP sites along the Ninetyeast Ridge, northern Indian Ocean. In K. Ishizaki & T. Saito (Eds.), *Centenary of Japanese Micropalaeonoloty* (pp. 175–188). Tokyo: Terra Publications Co.

Srinivasan, M. S., & Sinha, D. K. (1998). Early Pliocene closing of the Indonesian seaway: Evidence from northeast Indian Ocean and tropical Pacific deep sea. *Journal Asian Earth Science, 16*, 29–44.

Subrahmanyam, V., Gangadhara Rao, M., & Subbaraju, L. V. (1993a). Subsurface Precambrian ridge on the continental shelf of western India between Coondapoor and Kasaragod. *Marine Geology, 112*, 329–341.

Subrahmanyam, C., Gireesh, R., Chand, Shyam, Karmesh Raju, K. A., & gopal Rao, D. (2008a). Geophysical characteristics of the Ninetyeast Ridge—Andaman Island arc trench convergent zone. *Earth Planetary Science Letters, 266*, 29–45.

Subrahmanyam, V., Krishna, K. S., Ramana, M. V., & Murthy, K. S. R. (2008b). Marine geophysical investigations across the submarine canyon (Swatch-of-No- Ground), northern Bay of Bengal, *Current Science,*

Subrahmanyam, V., Ramana, M. V., & Gopala Rao, D. (1993b). Reactivation of Precambrian faults in the southwestern continental margin of India: Evidence from gravity. *Tectonophysics, 219*, 327–339.

Thamban, M., Purnachandra Rao, V., & Schneider, R. R. (2002). Reconstruction of late Quaternary monsoon oscillations based on clay mineral proxies using sediment cores from the western margin of India. *Marine Geology, 186*, 527–539.

Valdiya, K. S. (2001a). River response to continuing movements and scarp development in central Sahyadri and adjoining coastal belt. *Journal Geological Society India, 57*, 13–30.

Valdiya, K. S. (2001b). Tectonic resurgence of the Mysore Plateau and surrounding regions in cratonic southern India. *Current Science, 81*, 1068–1089.

Veerayya, M., Karisiddaiah, S. M., Vora, K. H., Wagle, B. G., & Almeida, F. (1998). Detection of gas-charged sediments and gas hydrate horizons along the western continental margin of India. In J. P. Henriet & J. Mienert (Eds.), *Gas Hydrates: Relevance to world margin and Climate Change* (pp. 239–253). London: Geological Society.

Vora, K. H., Wagle, B. G., Veerayya, M., Almeida, F., & Karisiddaiah, S. M. (1996). 1300-km long late Pleistocene-Holecene shelf-edge barrier reef system along the western continental shelf of India: Occurrence and significance. *Marine Geology, 134*, 145–162.

Wagle, B. G., & Veerayya, M. (1996). Submerged sand ridges on the western continental shelf off Bombay, India: Evidence for late Pleistocene-Holocene sea-level changes. *Marine Geology, 136*, 79–95.

Yatheesh, V., Bhattacharya, G. C., & Dyment, J. (2009). Early opening off Western India-Pakistan margin: The gop basin revisited. *Earth & Planetary Science Letters*, *284*, 399–408.

Chapter 27
The Evolving Indian Continent

27.1 India, a Collage of Many Terranes

The Indian subcontinent consists of five structurally and lithologically contrasted and physiographically distinctive geomorphic provinces, each having altogether different evolutionary history (Fig. 1.1). These units are: the mountain province of Himalaya girdling the northern border (Fig. 1.2), the flat expanse of the Indo-Gangetic Plains in the middle, the uplands and plateaus of the Peninsular India and the coastal plains along the seaboards (Fig. 1.3). The sixth terrane is the alluvial plain of the Irrawaddy River flanked eastwards by the Shan–Karen plateaus in Myanmar. They make what the ancient literature describes as *Bharatvarsh* belonging to a mega-island or continent called *Jambudweep*.

27.2 Formation of Continental Nucleii

27.2.1 Indian Shield

South of the Himalayan mountain arc, the Peninsular India is a shield, comprising composite, consolidated and rigid crustal blocks of Archaean antiquity. These crustal blocks, called cratons, that remained undeformed by tectonism for very long geological periods, are separated from each other by rifts or shear zones (Fig. 3.1). The four well-defined cratons are the Dharwar Craton in southern India (Fig. 3.2), the Bastar Craton in central India (Fig. 4.1), the Singhbhum Craton in eastern India (Fig. 4.7) and the Bundelkhand Craton in northwestern India (Fig. 4.14). The cratons contain the oldest granitic rocks of the Indian subcontinent—3.31 Ga in the Bundelkhand Craton, 3.56 Ga in the Singhbhum Craton, 3.01 Ga in the Bastar Craton and 3.20–3.40 Ga in the Dharwar Craton. It

K.S. Valdiya, *The Making of India*, Society of Earth Scientists Series,
DOI 10.1007/978-3-319-25029-8_27

is therefore inferred that these cratonic blocks have oldest major components of 3.3 Ga and experienced widespread cratonization events at 3.0 and 2.5 Ga. Each of these four cratons have witnessed events of crustal rifting and sagging or sinking of dismembered blocks, attendant volcanism, followed by transpressional deformation, pervasive metamorphism and granitization or charnockitization. The result of these processes was the welding together of the crustal blocks into composite rigid cratons. The mosaic of these cratons makes the Indian Shield.

27.2.2 Developments in Dharwar Craton

The history of the evolution of the Dharwar Craton (Fig. 3.5) begins with the formation of the *Gorur Gneiss*, representing a part of the earliest Palaeoarchaean sialic crust. The intimately associated assemblage of ultrabasic–basic magmatic–volcanic rocks with intercalations of pelitic–siliceous sediments constituting the *Sargur Group* is assumed to be a product of an accretionary process involving addition of new crustal material probably in an intracratonic rift basin. The Gorur and the Sargur together formed the 3300–3200 million years old nucleus of the Dharwar Craton. It was extensively invaded by granitic magmas, giving rise to the *Peninsular Gneiss* around 3000 Ma. After the gneissic terrane had stabilized, the craton was affected by sagging and rifting along structural grains. The consequence was the formation of elongate basins of the *Dharwar* sedimentation represented by the *Dharwar Supergroup*. Synsedimentary volcanism dominated the crustal processes in basins, which had attained the nature and shape of intracratonic grabens. Towards the close of the Neoarchaean era, there was westward but oblique convergence of the crustal blocks, manifesting itself in sinistral transpression along the N–S line passing by Chitradurga and also in the westward thrusting up of the rocks of the eastern block along steep shears parallel to the Chitradurga Boundary Fault. Possibly, mantle-related plumes had become active towards the end of the Neoarchaean time, bringing up mantle material through deep shear zones and faults, culminating in the emplacement at 2550 Ma of the *Closepet Granite* and the *Dharwar Batholith* in the northern part of the Dharwar Province. This high temperature–high pressure granulite metamorphism leads to the formation of *charnockites* in the southern part of the Dharwar domain.

Stromatolites with algal filaments, coccoid and rod-shaped bacteria in the carbonate rocks of the Chitradurga Succession in the Dharwar Basin reveal existence and development of cyanobacterial life, marking the appearance of life in the Indian subcontinent.

Within the granite–gneissic terrane in the eastern block of the Dharwar Craton, there are long linear belts of green schists comprising predominant basic volcanics including pillow lavas, felsic rocks and subordinate clastic sediments. The important *schist belts* are the Sandur, the Hutti, the Kolar and the Nellor. East of the Closepet Granite the eastern block comprises 2750–2710 Ma gneisses of granitic to granodioritic composition, collectively known as the *Dharwar Batholith*.

27.2.3 Bastar Craton

The Bastar Craton (Figs. 4.1 and 4.2), covering southern Chhattisgarh, north-eastern Maharashtra, south-western Odisha and north-western Andhra Pradesh, comprises widespread and preponderant quartzofelspathic gneisses and granites of batholithic dimension, with volcanosedimentary covers (supracrustals) forming linear belts and islands known as the *Sukma–Bengpal complexes*. Later involved in strong Proterozoic tectonism, both the basement gneisses and the covering volcanosedimentary units are highly deformed and metamorphosed to generally moderate grade but reaching granulite grade in the Bhopalpatnam Belt in the south-western part. The vestige of 3010-Ma tonalite–trondhjemite–granodiorite—the *Markampara Gneiss*—in the southern part of the Bastar Craton and vestige of 3000-Ma orthogneisses enclaves within the vast expanse of the 2600–2500 million years old *Amgaon Gneiss* imply that the craton grew around a protocontinental nucleus. The temporal span of the growth must have been of the order of 1000 million years Unconformably overlying the Sukma and Bengpal complexes is the 1300- to 2700-m-thick succession of mildly metamorphosed overwhelmingly ferruginous sedimentary rocks with predominant component of banded haematite–quartzite. Known as the *Bailadila Group*, this succession bears striking lithological similarity with the upper part of the Dharwar Supergroup. The combined Sukma–Bengpal–Bailadila assemblages represent a deposit of a continental margin setting or a back-arc basin within the continent, in the regime of transpressional tectonism resulting from stretching of the Archaean sialic crust.

27.2.4 Singhbhum Craton

Covering Jharkhand, Odisha and adjoining areas in the eastern part of the Indian Shield, the Singhbhum Craton (Fig. 4.7) is characterized by relics of the oldest rocks of the Indian subcontinent and Mesoarchaean Gneisses and granites tonalites and granodiorites in composition, and by abundant occurrence of banded iron formation closely associated with basic volcanics and ultrabasic intrusives. All these rocks have undergone pervasive metamorphism of the amphibolite facies.

There was a protocontinent, and a deep basin in the Palaeoarchaean time (Fig. 4.8). The sediments that accumulated in this basin are represented by the *Champua Group* (*Old Metamorphic Group*). Partial melting of the protocontinental and basinal crust due to impact of hot plumes generated predominant tonalitic magma, which by accretion contributed to synkinematic growth of the *Saraikela Gneiss* (*Older Metamorphic Tonalite Gneiss*) by about 3300 Ma (Fig. 4.9). Continuation of granite magmatism in two phases in the period 3300–3200 Ma resulted in the emplacement of the *Besoi Granite* (*Singhbhum Granite Type A Phases I and II*). By about 2800 Ma, a stable microcontinent had evolved in the eastern part of the Indian Shield. There was thermal perturbation in the subcrustal level. Consequently, the microcontinent stretched apart, giving rise to an elongate

NNE- to SSW-oriented basin between the separated granitic bodies. In the shallow water of this basin accumulated dominantly ferruginous and siliceous sediments, much of them are as chemical precipitates. The evolution of the banded iron formation in the rift basin was accompanied at one stage by voluminous extrusion of basic lavas and the intrusion of gabbro and related ultrabasic magmas. A period of deformation and attendant metamorphism was followed, and the structural design of the *Iron Ore domain* was established in the period 3200–3100 Ma (Fig. 4.10). Further sinking of the sialic crust culminated in more differential melting at lower levels and emplacement of granites on a massive scale, giving rise to the *Singhbhum Granite* (Type B of Phase III). Renewal of subsidence in the western part of the Singhbhum terrane created a shallow basin of the Darjin sedimentation. And the emplacement of pink alkali felspar dominant *Tamperkola Granite* at 2800-Ma marks the last thermal disturbances of the Neoarchaean era in the eastern part of the Indian Shield.

27.2.5 Bundelkhand Craton

Constituting the core of north-western expanse of the Indian Shield, the Archaean *Bundelkhand Craton*, also described as *Aravali Craton* (Fig. 4.14), lies in the tight embrace of the Early Proterozoic fold-and-fault belts of the NE- to SW-oriented Aravali Range and the ENE–WSW trending Satpura Range.

A product of fractionated magma derived from the upper mantle, the tonalitic *Mawli Gneiss* of the Mawli–Jhamarkotra areas in the Mewar block and equivalent gneisses of the Mahoba and Baghora areas in the Bundelkhand block, constitutes the nuclei of the north-western Indian Shield formed 3300 million years ago. Due to stretching of the sialic crust was emplaced in the depression, a rift basin came into existence and the volcanosedimentary material forming the *Mangalwar* and *Mehroni complexes* (Fig. 4.18). At a greater depth, where the temperature–pressure conditions were of the order 850–820 °C and 9–8 kbar, high-grade metamorphism of parts of the volcanosedimentary assemblage gave rise to what is known as the *Sandmata Complex* (Fig. 4.17). There may have been intrusion of enderbite and norite subsequent to metamorphism. There was thickening of the crust due to either underplating of granitic magma or multiple thrusting and stacking of slabs. It was during the second phase of deformation roughly around 2900 Ma that the *Untala Granite* and the *Gingla Granite* were emplaced into the complex of older granitic, volcanic and metamorphic rocks. The crust was rifted apart again and the greater Bundelkhand Craton broke into eastern (Bundelkhand) and western (Mewar) blocks. The intervening trough became the site of emplacement of material represented by the *Hindoli Complex*. Following the closing of this trough, the Hindoli pile underwent metamorphism and the Mewar and Bundelkhand blocks were welded together. The geodynamic evolution of the Bundelkhand Craton was complete with the emplacement of 2550-million years-old granite—the *Bundelkhand Granite*—in the Berach and Bundelkhand regions.

27.3 Aravali–Satpura Orogeny: Evolution of Palaeoproterozoic Mobile Belts

27.3.1 Rifting of Sialic Crust

The beginning of the Early Proterozoic era heralded rifting of the southern and central parts of cratonic India, and formation of elongate basins of sedimentation and volcanism. It was ductile extension of the sialic crust of Archaean antiquity. This led to invasion of sea water along the depressions formed in the NNE–SSW direction in eastern Rajasthan and adjoining Haryana, in the ENE–WSW direction in central India and Singhbhum region of southern Jharkhand and in the NNE–SSW direction in north-eastern Maharashtra and adjoining central Chhattisgarh (Figs. 5.1 and 5.3). The culmination of the diastrophic movements was the evolution of Palaeoproterozoic mobile belts which have an almost common history of tectonism, igneous activities, metamorphism and sedimentation. The early rift phase was followed by bimodal volcanism, and penecontemporaneous deposition of arkose and conglomerate. The subsequent sedimentation phase is represented by accumulation of thick sequences of turbidite–greywacke and shale. In the third phase, there was compressional deformation with attendant low- to moderate-grade metamorphism, which in some areas rose high enough to cause differential melting of deeper rocks and generation of granitic melt. In all these basins, two facies in three packages are discernible: one metamorphosed to moderate grade, the other practically unmetamorphosed. Resurgent tectonism invested all these rift-basin successions with the characteristics of mobile belts—the *Aravali* in western India, the *Satpura* in central India, the *Singhbhum* in eastern India and the *Bhandara Triangle* in northern South Indian Shield.

27.3.2 Aravali Domain

The Aravali Mobile Belt is made up of two lithotectonic packages known as the *Aravali Supergroup* and the *Delhi Supergroup*, unconformably overlying the Archaean complex of gneisses and granites (Fig. 5.3). These occur in several belts separated by intervening outcrops of basement rocks. The Aravali succession together with the rocks of the underlying basement complex was involved in three phases of compressional deformation. In some areas, the early-phase deformation with attendant mobilization of basement rocks resulted in differential melting of rocks and generation of granitic melt and formation of migmatite. The 2000-million years-old *Darwal* and *Amet Granites* represent this phenomenon related to the *Aravali Orogeny* around 1900 ± 100 Ma.

The lower Aravali assemblage of volcanosedimentary rocks was deposited in a number of fault-controlled rifts and basins in the sialic crust. Deep-seated marginal faults evolved during initial stage of basin formation. These faults provided

passage to the mafic magma which came out as lavas and was emplaced as mafic and ultramafic bodies during the deepening of the basin mainly along the margins of the shelf (Fig. 5.6). Separated from the Lower group by an unconformity, the upper group of the Aravali succession comprises diamictite (at base), greywacke–shale sequence and the carbonate with thin horizon of phosphorite intimately associated with columnar-branching stromatolites. The stromatolites were formed in protected tidal flats under intertidal to supratidal conditions.

Following the tectonic upheaval that terminated the Aravali sedimentation, the Delhi Basin opened up as a system of grabens and half-grabens. The 10,000-m-thick Delhi succession (divisible into the *Raialo*, the *Alwar* and the *Ajabgarh* groups) is made up of dominant quartzite and phyllite with dolomite and oligomictic conglomerate. These sediments are associated lavas, agglomerates and tuffs, which represent contemporaneous volcanism in the beginning of the Delhi sedimentation. The outpouring of the lavas and ejection of volcaniclastics occupied belts along deep faults demarcating the boundaries of the basin.

Ultramafic and mafic and syenitic bodies occupy the marginal faults which were reactivated towards the close of the Aravali period. It was an ensialic orogeny that gave rise to the Aravali Mobile Belt. The initial rifting and formation of basins of sedimentation (in which the Aravali and Delhi sediments accumulated) is attributed to a thermal plume underneath the Bundelkhand Craton.

27.3.3 Bijawar Basin

The Archaean Bundelkhand Gneiss is fringed along its southern periphery by a narrow impersistent group of flyschoid assemblage characterized by extensive deposits of ferruginous phosphorites known as the *Bijawar* in the Chhatarpur district (Fig. 4.14). The Bijawar Succession developed in an elongate depression formed as a consequence of sagging of the crust made up of Bundelkhand Gneissic Complex and its equivalents. The sagging of the sialic crust is related to rifting of sorts, as evident from early outpouring of 2460- to 2510-million-year-old lavas contemporaneous with basal terrigenous sedimentation.

27.3.4 Singhbhum Domain

The Palaeoproterozoic in eastern India is represented by the *Singhbhum Mobile Belt* which abuts against the Chhotanagpur Gneiss in the north. Its boundary in the south is demarcated by a deep-seated fracture described as the *Copper Belt Thrust* or *Singhbhum Shear Zone* (Fig. 5.18). The rifting of the Archaean sialic crust underneath the belt of the *Dalma Volcanics* followed by widening of the graben invited sea water that inundated the belts peripheral to the Singhbhum Granite and Chhotanagpur Gneiss. The deposits of the depression are represented

by *Chaibasa–Dhalbhum* successions. Towards the later stage of the Singhbhum sedimentation, there was melting of the simatic part of the crust. The molten basic material came out as lavas, accompanied by explosive volcanism. After the renewal of sedimentation (*Kolhan Group*), the basin was subjected to compression due to the southern continental plate going down along the Singhbhum Shear Zone. This caused deformation and metamorphism of the rock succession, and eventually brought about differential melting of the sialic crust and emplacement of 1655 ± 8 Ma granitic plutons. Subsequently, there was extension of the crust, allowing emplacement of basic and ultrabasic magmas along the fractures, particularly along the eastern margin of the Singhbhum Cratonic Block.

27.3.5 Bhandara Triangle

Resting on the Archaean basement made up of the Amgaon Gneiss, the Palaeoproterozoic *Sausar*, *Sakoli* and *Dongargarh* basins form a triangle of sorts in the Bastar Craton in central India embracing the Nagpur, Bhandara and Durg districts (Fig. 5.21). These basins resulted from the Satpura–Singhbhum orogenic cycle. The 6000-m Sakoli Succession consists predominantly of metapelitic rocks with banded iron quartzite, arkose and conglomerate, and lavas and tuffs resting on the basement of the Archaean Amgaon Gneiss. The Dongargarh succession comprises volcanosedimentary rocks—arkosic and arenitic quartzites interbedded with basalt and agglomerate including 2180 ± 25 Ma to 2503 ± 35 Ma rhyolite (Bijli). The volcanics are intruded by the 2270 ± 90 Ma old *Dongargarh Granite* that is characterized by enclaves of rhyolites and basalts. The lavas were erupted in a continental setting along rifts. An E–W oriented arcuate synclinorium, the *Sausar* Belt, comprises a succession of thrust sheets and is faulted against the Tirodi Gneiss. The Sausar Group consists of regionally metamorphosed sandstone, shale and carbonate rock which were deposited on a stable shelf, in an environment of near-offshore platform.

27.4 Crustal Accretion During Mesoproterozoic Time

The Eastern Ghat terrane (Fig. 6.1) of highly deformed rocks that experienced ultra-high temperature granulite-facies metamorphism and invasion of several generations of magmas of varied compositional type. It represents a convergent orogen evolved under NW–SE directed subhorizontal compression resulting from oblique collision of continental plates. The western boundary of the Eastern Ghat Mobile Belt against the cratonic blocks of Archaean Bastar and Dharwar is defined by a prominent shear zone related to a plane of detachment (Fig. 6.4). The northern border of the Proterozoic terrane is delimited against the Singhbhum cratonic block by a wide zone of shearing, running E–W to ESE–WNW, and covered by

the Mahanadi deposits. The exposed Charnockite–Khondalite succession building the bulk of the EGMB represents the upthrust lower crustal material (Fig. 6.7). The basement Archaean rocks are seen nowhere, but the material forming them occur in the framework of the mobile belt in drastically remobilized and reconstituted forms—as integral parts of the rocks that underwent exceptionally high temperature–high pressure metamorphism and attendant partial melting.

Occurring throughout the length and breadth of the EGMB, there are about thirty plutonic bodies of anorthosite and alkaline rocks arranged in echelon in the margin of the terrane. The magmas were emplaced in a rift-related environment. Together with the alkaline plutons, the massif-type anorthosite rocks represent intrusions that have syntectonic to post-tectonic status with respect to the last phase of penetrative deformation. The generation of charnockite suite under granulite–facies conditions took place nearly 3000 Ma ago. There was incorporation of 3200 and 3300 Ma old Archaean continental material in the making of the EGMB lithology. The new crust comprising gneisses ranging in age from 2800 to 1800 Ma was accreted onto or added to the terrane of the Eastern Ghat. The 1600 Ma date of hornblende from rocks of all over the Western Charnockite Zone indicates that there was indeed an extensive thermal event towards the close of the Mesoproterozoic era. It was during the Pan-African orogeny that the EGMB was amalgamated with the cratons.

27.5 Pan-African Rejuvenation of Southern Indian Shield

27.5.1 Dynamothermal Events

South and south-east of the Archaean Dharwar cratonic block, across a prominent terrane-defining shear zone, the southern part of the Peninsular India is known as the *Southern Granulite Terrane* (Fig. 7.1). It embodies two lithotectonically contrasted domains or subprovinces that have undergone different tectonothermal upheavals. The larger southern part, embracing Tamil Nadu and central and southern Kerala, is made up of high-grade metamorphic rocks and predominant charnockites. Two blocks—Madurai and Trivandrum—separated by the Achankovil Shear Zone make up this part of the SGT (Fig. 7.2).

The Madurai Block comprises predominant charnockite of intermediate composition—of tonalitic to granitic affinity. The Rajapalaiyam sapphirine-bearing quartzofelspathic and pelitic gneisses of the block indicate temperature as high as 1040–1060 °C and pressure of 8–12 kbar. The Trivandrum Block embodies what is known as the *Kerala Khondalite Belt* and the *Nagercoil Block*. It is made up of gneisses of varied kind, principally *khondalite*, *leptynite* and *arrested charnockite*. The charnockite resulted from partial isochemical in situ conversion of many or most of the quartzofelspathic gneisses. The transformation has been prompted by influx or entry of CO_2-rich fluids.

The Kodaikanal charnockites indicate that initial crustal formation occurred at 2118 ± 8 Ma, and the peak metamorphism took place at 553 ± 15 Ma. Indeed there is clear evidence for Pan-African metamorphism throughout the Madurai Block. Overwhelmingly large part of magmatic bodies of granitic composition was emplaced in the period 520–590 million years. The ultrabasic and alkaline rocks, such as the *Oddanchatram Anorthosite*, the Tirupattur *Carbonatite*, the Bhavani Layered Anorthosite, the Sittampundi Complex and the *Sivamalai Syenite*, occur in the form of complexes, located preferentially along faults of Precambrian age.

This Shear Zone seems to have developed in a brittle environment of near-surface conditions during Neoproterozoic uplift of the Southern Sahyadri. It is believed to have resulted from crustal extension followed by collapse. The latest imprint at 515 ± 15 Ma Pathanapuram Granite in the Achankovil Shear Zone indicates that the rocks were affected by the Pan-African tectonothermal upheaval.

27.5.2 Proterozoic Terranes of Sri Lanka

Nearly ninety per cent of the landmass of Sri Lanka is made up of Proterozoic rocks developed under high temperature–high pressure conditions. Four complexes—Highland, Wanni, Vijayan and Kadugannawa—constitute the Sri Lankan terranes of the Proterozoic antiquity (Fig. 7.14). The metasediments of the Highland Complex represent sedimentary deposits of rifted continental margin that later evolved into a stable shelf region. The Wanni Complex consists of migmatized gneisses of both igneous and sedimentary parentage. The migmatites and gneisses (2000 Ma) are similar to those of the Achankovil Shear Zone, both having a common Pan-African evolutionary history. The V*ijayan Complex*, forming the eastern flank of the island, consists of mainly granitic and basic gneisses (1800–1100 Ma). These rocks exhibit metamorphism of the amphibolite facies and are locally affected by late-stage development, culminating in the charnockitization of gneisses. The *Kadugannawa Complex* comprises metamorphosed gabbro, diorite and granite.

27.6 Continent-Interior Proterozoic Sedimentary Basins

27.6.1 Configuration and Origin

In the wake of the Eastern Ghat orogenic movements at 1600 ± 100 Ma, when a large part of India was affected by tectonic upheaval and attendant crustal accretion, a number of shallow but subsiding basins developed in the active parts in front of orogenic belts (Fig. 8.1). The Cuddapah Basin in Andhra Pradesh evolved immediately west of the Eastern Ghat Mobile Belt, and the Vindhyan

Basin developed in front of the parabolic Satpura–Aravali orogenic belts. The continental margin in the north likewise subsided progressively to give rise to the Himalayan Basin of the Precambrian time. The Mesoproterozoic–Neoproterozoic sedimentary basins are known as the *Purana*. The Purana succession is broadly contemporaneous with what the Russians call Riphean and Vendian, spanning the temporal period from 1650 ± 50 Ma to 570 Ma. The Purana successions are divided into two major groupings (Fig. 8.2). The successions in various basins preserve records of two major cycles of sedimentation, each punctuated by multiple transgression and recession of marine water, volcanic and magmatic activities, and episodes of tectonic disturbance. The earlier tectonic disturbance coincides broadly with the end of the Mesoproterozoic era 1050 ± 50 Ma and the later one marks the termination of the protracted Purana sedimentation sometime between 500 and 600 Ma. The unconformity at the base represents a tectonic upheaval at 1600 ± 100 Ma. Later tectonic movements contemporaneous with the Pan-African orogeny of Africa and the Adelaide orogeny of Australia brought about the end of sedimentation in all the Purana basins.

27.6.2 Cuddapah Basin

In the *Cuddapah Basin,* a great pile of Precambrian sedimentary rocks rests on the foundation of Archaean gneisses and granulites (Figs. 8.2 and 8.3). Its western limb dips gently with little disturbance. But the eastern flank is intensely deformed, making up the *Nallamalai Range* and culminating in the thrusting over of the Eastern Ghat basement rocks upon the Cuddapah sedimentary rocks. The sediments were deposited in shallow-water environment along the shore and the shelf, the latter deepening eastwards. The carbonates represent platform deposits on the shelf of the Proterozoic sea. A sequence of seven lava flows associated with agglomerates and tuffs, described as Kuppalapalle Volcanics, represents volcanism that commenced towards the close of the Lower Cuddapah epoch. Lavas of andesite and basalt, together with ignimbrite and crystal tuff, were emplaced subaerially. Two horizons are characterized by rich development of Lower to Late Riphean stromatolites of cyanobacterial origin. There are intrusive bodies of lamproite penetrating the succession in the Chelima–Giddaluru area.

In northern Karnataka and adjoining Maharashtra, the *Kaladgi Basin* evolved as a consequence of crustal extension (Fig. 8.6). Resting on the basement of the Archaean gneisses, the 4500-m-thick Kaladgi Succession is folded into a series of anticlines and synclines on E–W to ESE–WNW axes. The Kaladgi Succession is divided into two groups belonging to the Mesoproterozoic and the Neoproterozoic, an angular unconformity separating the two assemblages. A horizon of Middle Riphean stromatolitic limestone testifies to the prolific growth of cyanobacteria.

27.6.3 Godavari Basin

The Indian Shield was dismembered or cut into blocks by rifting into the Dharwar and the Bastar cratons along a NW–SE trending, presumably pre-existing weak zones. Rivers Godavari and Pranhita now occupy the terrain over the graben that was formed in the Mesoproterozoic time (Fig. 8.7). The sedimentary succession of the Godavari Basin, the *Pakhal* and the *Penganga*, occurs independently in different fault-controlled sub-basins characterized by varying degree of tectonism. The Pakhal succession was laid down in settings varying from alluvial fan, braided plain, foreshore and shoreface to offshore environments. The Somanpalli region witnessed volcanic activity, testified by volcanic cones and felsic ash beds with pyroclastics occurring within sedimentary succession at different stratigraphic levels.

The Pakhal and Penganga groups are both overlain unconformably by the *Sullavai* Succession belonging to the Neoproterozoic era. Tectonic convergence of the Eastern Ghat Mobile Belt against the Godavari Succession caused considerable deformation of the Mesoproterozoic Succession.

27.6.4 Semri (Lower Vindhyan) Basin

Parabolically enclosing the Archaean domain of the Bundelkhand Granite, the Vindhyan Basin lies in the embrace of the Satpura and Aravali orogenic mobile belts (Figs. 8.11 and 9.1). It was an intracratonic continent-interior basin. The western, south-western and southern margins of the Vindhyan Basin are demarcated by arcuate faults, forming a parabolic system of thrusts against the Aravali and Satpura orogenic belts. The Vindhyan Basin is segmented into smaller elongate sub-basins by a multiplicity of faults, some of which are wrench faults. The sub-basins are of the nature of half-graben tilting northwards.

The Mesoproterozoic sedimentary rocks in the Vindhyan Basin are represented by the *Semri Group*, beginning with diamictite intimately associated with an assemblage of flysch rocks formed by debris flows. These sediments point to tectonic instability of the terrain during the commencement of the Semri sedimentation. Some parts of the Semri Basin subsided rapidly, accumulating immature sediments as fan-deltas and slope-edge clastic fans, other parts remained a shallow shelf where sedimentation took place slowly, giving rise to carbonate ramps on the seaward side (Figs. 8.13 and 8.14). The carbonates exhibit development of stromatolites of Lower Riphean (1650–1350 Ma) age. Carbonaceous discs and filaments identified as *Grypaenia spiralis* represent eukaryote that grew 1590 ± 50 million years ago. The Semri sedimentation thus started sometime in the temporal span of 1600–1700 Ma. The Semri time witnessed volcanic activity at a number of places and at least twice during the Mesoproterozoic time span. It is represented in andesitic lavas and accretionary lapilli-tuff and acidic volcanics of rhyolitic tuff, vesiculated and accretionary lapilli, ignimbrite and agglomerate and volcanic bombs.

27.6.5 Beginning of Neoproterozoic Era

There was a pronounced interruption of sedimentation in the Purana basins of Cuddapah, Kaladgi, Godavari and Vindhyan in the period 1000 ± 50 Ma. This interruption is represented by a regional unconformity above the sedimentary successions in these basins, dating to an interval 1050 ± 50 Ma. Much larger areas came under the sway of sedimentation as new regions sank, giving rise to the *Chhattisgarh*, *Indravati*, *Sullavai*, *Bhima*, *Badami* and *Kurnool* basins of sedimentation (Figs. 9.7, 9.8, 9.9 and 9.10). In the north, the sedimentation extended beyond the limits of the Vindhyan and encompassed parts of the Indo-Gangetic domain (Figs. 8.1 and 9.1). There was a marked change in the environment of sedimentation. The marine environment of the Mesoproterozoic gave way to dominantly terrestrial environment in the Neoproterozoic. In the terrestrial domain, rivers played very dominant role and wind reworking the fluvial sediments in some regions. In the Vindhyan basin towards the close of the Vindhyan era, deposition took place in a shallow basin embracing lagoons, tidal flats with channels and beaches along which longshore and storm currents were active (Fig. 9.2). Finely laminated algal mats and cyanobacterial stromatolites formed bioherms in the supratidal to subtidal environment. The stromatolites belong to a period transitional between Middle Riphean to Vendian (680–570 Ma). The 1067 ± 31 Ma old lamproite plug, which possibly contributed diamond to the conglomerates in the Rewa Succession, indicates that the Upper Vindhyan sedimentation commenced well before 1100 Ma.

27.6.6 Trans-Aravali Igneous Activities

Towards the later part of the Neoproterozoic era, the south-western flank of the Aravali Mobile Belt and the terrane west of it witnessed emplacement of granites and felsic volcanism on a grand scale over large part of the continental margin (Fig. 9.4). The plutonic bodies (*Erinpura Granite*) give nearly concordant dates between 750 and 900 Ma. The peraluminous anorogenic granite indicates derivation of the magma from an anhydrous granitic source. The volcanic rocks (*Malani Rhyolite*) testify to extensive magmatic activities towards the later part of the Neoproterozoic period.

27.7 Proterozoic Continental-Margin Himalaya Basin

27.7.1 Lesser Himalaya

In the Early Proterozoic era, a large part of the northern continental margin of the Indian Shield—now represented by the Himalaya province—subsided to give rise to more than 2400-km-long basin of sedimentation (Figs. 10.1 and 11.1).

The Lesser Himalayan terrane comprises autochthonous sedimentary succession thrust over by sheets or nappes of metamorphic rocks associated with granites. The granites occur as prominent components all through the length and breadth of the thrust sheets (Figs. 10.2 and 10.3). In the Lesser Himalaya (Fig. 11.1), there are thus three packages or units:

(1) Flysch and flyschoid assemblages of sedimentary rocks including turbidites making the lower part of the autochthonous succession comprising the *Damtha* and the *Tejam* Groups. The basement of the succession is nowhere seen.
(2) Low-grade (epimetamorphic) rocks comprising metaflysch, almost invariably associated with 1900 ± 100 million years old porphyritic granites and quartz porphyries which have overwhelming presence through the length and breadth of the tectonic sheet known as *Chail–Ramgarh*. This tectonic unit is characterized by pronounced facies variation—from predominant sublitharenite to subgreywacke and shale to quartzarenite interbedded with 1487 ± 45 Ma-old to ~1800 Ma basic volcanics.
(3) Medium-grade or mesometamorphic rocks intruded by 500 ± 25 million years-old granodiorite–granite bodies and associated impersistently at the base by 1900 ± 100 million years old augen gneisses forming the *Munsiari–Almora–Jutogh* nappe.

There are many points of commonality between the Early Proterozoic rocks of the Peninsular India and the Lesser Himalaya. In the initial stage of sedimentations, there was deposition of turbiditic flysch in rift-related basins. This was followed by outpouring of basic lavas and emplacement of tuffs and agglomerates, contemporaneous with sedimentation as seen in the Lesser Himalaya, the Aravali, the Bijawar and the Chaibasa domains. In both the provinces, metamorphism has affected the sedimentary successions variably so that different parts of the same lithological unit evince different grades of metamorphism. The metamorphism is related to the earliest phase of deformation. The deformation gave rise to ENE–WSW trending isoclinal folds in the Aravali, Bijawar and Singhbhum mobile belts, as well as in the two thrust sheets of the Lesser Himalaya. The early deformation and attendant metamorphism in many parts of the Peninsular India culminated in the generation and emplacement of granites, exemplified by the nearly 2000 million years old Amet and Darwal granites in the Aravali Mobile Belt, the Rihand Granite in the Bijawar Basin, and the Chakradharpur–Mayurbhanj granites in the Singhbhum Domain. In the Lesser Himalayan terrane, the 1900 ± 100 million years porphyritic granites and quartz porphyries have predominant presence in the two metamorphic thrust sheets.

The quartzites of the epimetamorphic assemblage are intimately associated with basalts and tuffs, representing volcanism penecontemporaneous with sedimentation in shallow-shelf platform. The lava eruption is related to rifting of the sialic crust. The most striking feature of the Chail–Rampur Nappe and its klippen, as already stated, is the predominant occurrence of porphyritic granites and quartz porphyries within the epimetamorphic succession. The porphyritic granites

and porphyries which have undergone wholesale mylonitization cover large areas and make overwhelming presence with phyllonites, belong to the temporal interval 1900 ± 100 Ma.

Likewise granites occur as concordant bodies of batholithic dimension, synclinally folded with the mesometamorphic rock succession (Fig. 10.7). The examples are the *Champawat Granodiorite* in the Almora Nappe, the *Mandi Granite* in the Dhauladhar Range, the *Mansehra Granite*, the *Ambela Granite* and the *Swat Granite* in northern Pakistan. The quartzdiorite–granodiorite–quartzadamellite–granite suite was emplaced 500 ± 25 million years ago, marking a magmatic event that occurred all through the Alpine–Southern Asia belt on the Gondwana scale.

27.7.2 Himadri (Great Himalaya)

In the Great Himalaya or Himadri terrane, the 6000- to 10,000-m-thick lithotectonic slab is made up of high-grade metamorphic rocks known as the *Vaikrita Group* in the central sector of the orogen (Figs. 10.3 and 10.11). The thick homoclinal terrane is split up by a number of intraformational thrust planes. The metamorphism took place under amphibolite to locally lower granulite facies conditions. The Vaikrita succession is intruded by Early Miocene granites of anatectic origin. The granitic bodies occur in all sizes including of batholithic dimension, such as the *Badrinath Granite* in Uttarakhand. They have thrown out a network of dykes and veins of adamellite, aplite and pegmatite. There was a large-scale permissive *lit-par-lit* or leaf-by-leaf injection of granitic melt formed at depth of 15–20 km due to differential melting of high-grade metamorphics. This resulted in the formation of migmatites around the granitic bodies on an extensive scale.

In eastern Himachal Pradesh, the *Kinnar Kailas Granite* contains xenoliths of paragneiss characterized by deformational features developed under amphibolite facies conditions, implying that the deformation suffered by the Vaikrita occurred prior to the emplacement of the 488-Ma-old Kinnar Kailas Granite.

27.8 Neoproterozoic Developments in the Himalaya Province

27.8.1 Tectonic Layout

In the Lesser Himalaya province, the tectonic windows and half windows carved out by rivers in the thrust sheets of epimetamorphic and mesometamorphic rocks expose Proterozoic sedimentary succession, and the larger part of these sedimentary rocks belongs to the upper Mesoproterozoic–Neoproterozoic and extends up to Lower Cambrian (Fig. 11.1). It may be mentioned that in the central sector of

the Himalaya province, the outer Lesser Himalayan part was uprooted and thrust 4–23 km southward during *Tertiary tectonic revolution*, forming parautochthonous *Krol Belt* which is made up of preponderant Neoproterozoic to Early Cambrian rocks (Fig. 11.5). The Proterozoic rocks of the Himalaya represent a thick and extensive deposit on the distal part of the passive continental margin of the Indian plate.

27.8.2 Carbonate Sedimentation

The Palaeoproterozoic to Early Mesoproterozoic argilloarenaceous sediments pass upwards to preponderant calcareous and argillocalcareous sediments laid down in shallow-shelf platforms and lagoons under tectonically quiet conditions (Fig. 11.4). The carbonates form an extensive succession of cherty, siliceous dolomites intercalated with bands and beds of blue limestone and grey slates. The carbonate horizon is associated with stromatolitic bioherms and large and small lentiform deposits of crystalline magnesite between the Kali and Mandakini rivers. The origin of magnesite is attributed to synsedimentary diagenetic replacement of dolomite by $MgCO_3$, under singularly penesaline conditions developed behind biohermal barriers within the barred basins. The stromatolites place the carbonate formation in the transitional period between Middle Riphean and Upper Riphean, that is around 1100–900 Ma. Galena occurring in the top quartzite bed at Garan and Sarsenda in the Vaishnodevi Hills gives a Pb/Pb age of 967 Ma.

The dominant carbonate sediments gave way to a very thick argillocalcareous succession, represented by black carbonaceous shale and in the Krol Belt, phosphatic shales and lense-shaped units of diamictites occurring at several levels. The diamictites represent debris flows, presumably triggered by tectonic disturbances. These tectonic movements were precursors of the impending tectonic upheaval that terminated protracted Proterozoic sedimentation.

27.8.3 Appearance of Shelly Fauna

In the Krol Nappe, the uppermost horizon of the argillocalcareous succession is characterized by the occurrence of small shelly fossils indicating the first appearance of preservable life-forms. The first appearance of small shelly fossils heralded the coming of a variety of organism that had preservable body parts, such as conodonts, trilobites, brachiopods hexactinellid and siliceous sponge spicules and a variety of microscopic biota of Lower Cambrian epoch. This biological event of great moment is attributed to a burst of voluminous methane and/or emplacement of flood basalts, particularly in submarine environment which provided nutrients and materials for building of preservable skeletons of the organism.

27.9 Pan-African Tectonic Upheaval and After

After life had diversified in various forms and proliferated in the Himalaya province, and sedimentation proceeded in environments varying from open shelf to anoxic lagoons, there was a tectonic upheaval. The tectonic movements resulted in the end of sedimentation in the entire Lesser Himalaya subprovince and in the whole of Peninsular India, and caused pronounced interruption in basin-filling in the Tethys domain (Fig. 12.1). This interlude of non-deposition varied in temporal span from sector to sector. The tectonism manifested itself not only in the deformation of rocks but also widespread granitic activity. Strikingly leucocratic 500 ± 25-million-year-old granites occur extensively in the upper part of the low- and medium-grade metamorphic nappes of the Lesser Himalaya and in the lower part of the high-grade metamorphic rocks of the Great Himalayan succession. The granites are the products of anatexis of the continental crust that was rifted and attenuated. The thermal events were not restricted to the Himalaya province. The south-western part of Rajasthan witnessed the granitic activity during nearly the same period, as testified by the 510 ± 10 Ma Sendra Granite. The 550 ± 15 Ma Pondi Charnockite represents widespread charnockitization in the Southern Granulite Terrane during the Pan-African cycle. This tectonic event was not an isolated occurrence, but global in dimension. This is evident from the dramatic change in the palaeogeography world over, related possibly to the reorganization of continental plates, and making and unmaking of a supercontinent. Simultaneously, there was a profound change in the climate during the Late Precambrian–Cambrian interval, and the world witnessed explosive evolution of the biosphere. This biological event was manifest in biomineralization of skeletons—formation of phosphatic and silicious shells of invertebrate organisms in the initial stage of their diversification into different forms, which adapted themselves to different ecological conditions. This implies that the sea water had become enriched in nutrients, at least in some niches of its environment. In the central sector embracing Kumaun and Nepal, the Cambrian is intriguingly absent.

Among the many crucial developments (Figs. 12.4, 12.5 and 12.6), one phenomenon is related to the emplacement of the *Muth* formation. Strikingly snow-white quartzite succession of the Muth Quartzite with intercalations of brown-weathering dolomite extends from the Zanskar to north-central Nepal. The Muth sediments represent elongate offshore bars and shoal complex developed during the Silurian time. The formation marks an epoch of tectonic stability in the period when practically the whole of the Tethyan domain stretching from Tanawal in the west to northern Nepal became a site of shallow-water deposition of well-sorted clean sands.

The Carboniferous time witnessed restriction of water circulation in the sea causing development of anoxic- or oxygen-deficient conditions. This is reflected in the accumulation of thick black carbonaceous shales and black limestone, all through the extent of the Tethys terrane.

27.10 Hercynian Revolution and Gondwana Time

27.10.1 Marine Transgression

Towards the end of the Palaeozoic era, the southern part peripheral to the Lesser Himalaya–Siwalik boundary came under the sway of sea waters, for the first time after the Middle Cambrian retreat. The return of the sea water in the Lesser Himalaya is linked to marine transgression along sunken tracts in the Peninsular India—the Bap–Badhaura arm in Rajasthan and the Rajahara–Umaria course in Jharkhand–Madhya Pradesh (Fig. 13.4). The sedimentary assemblages with Gondwanic elements of southern Garhwal, south-central Nepal, southern Sikkim and southern Arunachal Pradesh represent the transgression of the Gondwanic sea (Figs. 12.13, 12.14 and 13.4). Significantly, the outer Lesser Himalayan Permian units are associated intimately with the volcanics—lavas and pyroclastics. It seems that the deposition of sediments in the new cycle took place in an elongate basin formed due to sagging or rifting down of the crust along the southern periphery of the Lesser Himalaya subprovince. The basin extended from the Salt Range in Pakistan to Garu and beyond in Arunachal Pradesh.

27.10.2 Widespread Volcanism

All along the southern part of the Himalaya from the Sindhu Valley in the west to the Brahmaputra Valley in the east, volcanoes became very active, pouring out lavas and ejecting pyroclastics. The volcanics are represented by the *Panjal Trap* (Figs. 12.11 and 12.12) in the north-west and by the *Abor Volcanics* in eastern Arunachal Pradesh. Across the Sindhu in northern Pakistan, contemporary igneous activity is represented by Shewa–Shahbazganj suite of intrusives. Some of the volcanic islands were covered with forests of *Glossopteris*, *Gangamopteris*, *Waagenophyllum,* etc. that grew luxuriantly in the main Gondwanaland.

The fissuring of the Indian continental margin (within the Himalaya province) with attendant volcanism and marine incursion along a depression implies that the Gondwanic India was overtaken by a powerful crustal movement—the Hercynian diastrophism. The impact of this tectonic movement attained an exciting climax in the northern part of the continental margin, and manifested itself in the breaking away in the late Permian of the Tibetan landmass along with Iran and Turkey and formed Cimmerian microcontinent. A new seaway known as the *NeoTethys Ocean* was formed between the Indian plate and the Cimmerian microcontinent that drifted away. The newly formed sea was connected to the Mediterranean Tethys that extended west up to Portugal in the periphery of Europe. As a consequence of widespread volcanism, there was substantial change in chemistry of the atmosphere and of the oceans (Fig. 12.19). There was also considerable modification in the landscape following plate reorganization. As a result of the Permian

period witnessed worst ever decline and death of marine fauna. Nearly 90 % of the marine species (80 % vertebrates and more than 30 % invertebrates) vanished from the earth, and land plants were drastically decimated.

27.10.3 Formation of Grabens

As the supercontinent *Gondwanaland* was split into smaller cratonic blocks, and the Indian plate started moving northwards, the shear zones, faults and rift valleys of the Precambrian antiquity were reactivated. Consequently, a number of elongate depressions were formed due to ground, subsidence and downfaulting of the cratonic crust. These depressions were subsequently filled up with sediments brought by rivers, giving rise to elongate Gondwana basins (Figs. 13.1 and 13.2). The elongate Gondwana basins trending ENE–WSW and NW–SE are at present occupied by the rivers Damodar, Son and Narmada, Mahanadi and Pranhita and Godavari. The depressions formed in the subsurface Rangpur Saddle in northern Bangladesh and adjacent Bengal lie concealed under thick pile of the Indo-Gangetic sediments. Waters of the surrounding seas rushed in along some of the grabens and inundated the floodplains and lakes that had formed in the depressions. In the northern margins of the Indian landmass, as stated above, lavas came out through deep faults, forming a chain of volcanoes that stretched from the Siang Valley in Arunachal Pradesh to the Pir Panjal and beyond in Kashmir.

27.10.4 Gondwana Palaeogeography

In the early Gondwana time, a large part of the land was in the grip of severe refrigeration and under thick cover of ice (Fig. 13.4). Glaciers descended down the valleys and deposited their loads in depressions and in their water bodies. These deposits are known in the Peninsular India as *Talchir Boulder Beds*.

The Gondwanic India had north-westward slopes and rivers and streams flowed in the northwardly directions (Fig. 13.5). This is evident from sediment dispersal pattern unravelled from palaeocurrent directions and isopach maps of various Gondwana basins. Even in the Pranhita–Godavari domain in Andhra Pradesh the rivers flowed in the north-westerly direction all through the Triassic and Early Jurassic times, but changed eastward in the Middle Jurassic, following tilting of the ground closer to the coast.

27.10.5 Sedimentation

At the base, the Gondwana succession has a glacigene unit recognizable in all the basins. The time of glaciation was followed by a prolonged period by deposition

by rivers in their channels and floodplains (Fig. 13.8). The floodplains were characterized by marshes and lakes. The basin of deposition grew in size and soon became broad, as evident from overlaps and onlaps of younger sediments on older ones and their resting directly on Precambrian basement. Then the climate became dry and semi-arid as testified by red sediments of the alluvial plains. There was a spell of non-deposition before fluvial–alluvial sedimentation gave way to deltaic deposition in the Late Jurassic time.

27.10.6 Formation of Coal Beds

The wetter parts of floodplains of the Gondwanic India were covered by forests of seedless vascular vegetation in the Early Permian but were reduced to creeping forms by the end of the Permian (Fig. 13.12). The Permian flora included *Glossopteris*, *Gangamopteris*, *Schizoneura* and *Noeggerathiopsis*. By the Late Permian time, the climate had become warm, and there was abundance of water and manifold increase in the diversity in species of pteridophytes or flowerless plants and gymnosperms or primitive seed-bearing plants. The numerous thick coal seams testify to rich growth of plants on the floodplains during the Permian period. The climate became dry and warm in the Triassic time. Only a few pools of water were left in the floodplain which had become a waste land. The vegetation impoverished. New floral assemblage comprised ferns, horstails, rushes and clubmosses. Large trees of seed ferns became extensive by the end of the Triassic. The Late Jurassic witnessed a marked change in the plant community. The primitive seed-bearing gymnosperms gave way to the flowering *angiosperms*, marking the most significant development in the evolution of the plant life. The angiosperms proliferated very rapidly. Relegating and other plants, they became the most abundant during the Cretaceous. The Rajmahal flora in the Jharkhand–Bihar border represents the Cretaceous plant assemblage of the Gondwanic India.

Making the hill range at the Jharkhand–Bengal border, the Rajmahal Formation is essentially a pile of 114–118 million years old basaltic lavas with intertrappean plant-bearing sedimentary strata. The Rajmahal volcanism represents the end of the Gondwana time.

27.10.7 Animal Communities

The evolutionary process in the reptiles culminated in the development of mammals in the Triassic and of birds in the Jurassic. The dinosaurs were the most spectacular of the reptiles that reigned supreme until their demise towards the close of the Cretaceous. The fast-moving therapods that leaped into the air with their arms outstretched to catch insects, or to avoid predators, evolved into birds during the Triassic. Taking adaptive line of existence, the thecodonts became a very

important group of animals in the Mesozoic and gave rise to dinosaurs which showed strong tendency of general increase in size, culminating in the evolution of formidable dinosaurs (Fig. 13.13).

27.11 Stupendous Volcanism in the Cretaceous Period

27.11.1 Three Phases of Volcanism

The beginning and end of the Cretaceous period in India witnessed voluminous outpouring of lavas and volcanic explosions. In the early Lower Cretaceous 114–118 million years ago, eastern India, embracing the Rajmahal Hills in Jharkhand and the Sylhet region in Meghalaya, was overwhelmed by volcanism. And towards the close of the Cretaceous 61–69 million years ago, very large part of western and central India was inundated by extensive floods of lavas of tholeiitic basalt. The eastern theatre of volcanism is known as the *Rajmahal Volcanic Province* (Fig. 14.2) and the western domain as the *Deccan Volcanic Province* (Fig. 14.1). The Deccan Volcanism was preceded by eruption nearly 86 million years ago of lavas offshore north-western Karnataka, giving rise to the *Saint Mary's Islands* (Fig. 14.4). The Deccan eruption commenced 69 million years ago and lasted until about 61 million years, the bulk of the lavas having erupted around 65.5 million years ago. The Deccan lavas are believed to have flowed 100–300 km from their sources along the Western Ghat and in the Narmada Valley before they froze to form stepped plateaus. Evidently, the lavas must have been very mobile and therefore spread far and wide. The lava flows overcame topographic impediments, filled depressions and valleys, dammed rivers and streams and buried forests and grasslands. The result of the lava floods was the evolution of flat-topped plateaus, with step-like landform called the *Deccan Traps* (Fig. 14.6). The hot floods of lavas must have taken heavy toll of animals that could not run away from their preferred habitats. Blockages in rivers due to lava dams gave rise to multitudes of shallow lakes and swamps, which became sanctuaries of aquatic fauna and habitats for dinosaurs, mammals and plants. The lakes and swamps were eventually filled up with sediments (Figs. 14.16 and 14.19).

27.11.2 Geodynamics of Deccan Volcanism

The alkaline olivine–basalt and olivine–nephelinite of Saurashtra show close compositional similarly with the rock types associated with the *Reunion Hotspot* or mantle plume in the Indian Ocean (Fig. 14.3). As the northward-moving India rode over the hot spot, lavas came out along its western margin.

The dyke swarms of the Konkan coast and the Narmada–Tapi valleys are considered to have served as feeders of the Deccan lava flows. It was rifting and reactivation of faults of ancient rifts or crustal weak lines that caused the emplacement

of the dykes. This implies that the emplacement took place from a shallow crustal magma chamber. The last phase of the Deccan Volcanism is represented by nepheline syenite, alkali trachyte and carbonatite. They occur as intrusive bodies in the form of dykes, sheets and plugs, cutting across the Deccan lavas of the main phase.

27.11.3 Age of Dinosaurs

Around the lakes and swamps in the floodplains of rivers in the lava world, lived a variety of animals amidst profusion of vegetation. The biota was dominated by dinosaurs (Fig. 14.19) such as *Titanosaurs indicus* and *Indosuchus raptorius* of the Upper Santonian to Maastrichtian age. Layers of sediments interbedded with or underlying lava flows and ash beds bearing dinosaur remains (*Lameta Formation*) are known from several places in the periphery of the Deccan Volcanic Province. It was during the Lameta time that the dinosaurs diversified and spread far and wide.

The Deccan Volcanic activities contributed excessive amount of CO_2 to the atmosphere, leading to temperature rise. Large quantities of CO_2 and other noxious volatiles released by Deccan volcanoes must have caused deterioration of the biosphere, proving fatal to most of the dinosaurs and other animals. Towards the end of the Cretaceous, many plants and animals suddenly disappeared. Over 65–70 % species of animals, including the dinosaurs, perished. Two-thirds of marine species also vanished. However, the disappearance was a gradual phenomenon.

27.12 Subsidence of Continental-Margin During Mesozoic Era

27.12.1 Peninsular India

The northward-drifting India experienced crustal extension during the Jurassic and very Early Cretaceous due to India drifting away from Australia and Antarctica and attendant transformation along the Coromandal Coast in the interval 132–96 Ma. The leading edge of the Indian subcontinent subsided deeper into the Tethys Sea in the north even as its western and eastern flanks started sinking intermittently (Fig. 15.1). Embracing the whole of the Himalayan domain, the Tethys Ocean spread all over the subsiding part of the continental margin in western Rajasthan and Kachchh. The Indian Ocean, likewise, encroached on the sinking parts of the Kaveri–Palar, the Krishna–Godavari, the Mahanadi and the Bengal–Meghalaya sectors of the passive continental margin. The sagging of the continental crust took place along faults and lineaments of Precambrian antiquity. This development gave rise to depressions and ridges in the Late Permian in the Jaisalmer sector, in the Middle Jurassic in Kachchh, and in the Upper Jurassic in the Coromandal

belt. These pericratonic basins had formed due to rifting of the continental margin. There was also a seaward tilting of rift basins, giving rise to embayments and gulfs in the Coromandal belt. An arm of the sea extended deep into the land along the Narmada rift zone, leaving behind its trace in the form of Upper Cretaceous *Bagh Beds* (Fig. 15.15). The Kachchh, Jaisalmer and Himalaya basins belong to the NeoTethys faunal province, and the Bengal–Meghalaya, Krishna–Godavari and the Kaveri–Palar basins bear affinity with the Indian Ocean.

27.12.2 Northern Continental-Margin

A large part of the continental margin of the Peninsular India came under the sway of sea water. Simultaneously, the leading edge—the Himalayan domain—of the northward-moving India (which had been the site of sedimentation all through the Proterozoic and Palaeozoic) started subsiding (Fig. 16.2). The sea continued to deepen progressively along the northern periphery. In the deep sea, siliceous and calcareous oozes and pelagic clays, giving rise to chert beds, limestones and shales, were deposited. The phosphatic modules and glauconite occurring locally indicate deep cold-water that was deficient in oxygen. Simultaneous with the subsidence of the northern edge of India, an oceanic trench started forming along the edge of the Tibetan landmass. On the steadily subsiding shelf and slope of the NeoTethys, there was, in general, practically uninterrupted accumulation of sediments all along the periphery of the Indian continental margin, from Kachchh through Jaisalmer and Ladakh to Kampa–Gyantse in southern Tibet. One of the most remarkable features of the Mesozoic stratigraphy of the Tethyan domain is the near-uniformity of sequence and facies variation and faunal assemblages, implying similarity of tectonic conditions prevailing over more than 2000 km expanse of the Tethyan domain.

A unique horizon of the Jurassic time consists of strikingly golden reddish ferruginous oolite—within the *Spiti Shale* and contemporary formations. The oolite horizon is the most conspicuous and persistent stratigraphic unit in the NeoteThyan domain seen all along from southern Tibet, through northern Kumaun and Spiti to the Quetta region in Baluchistan and then to the Kachchh region in Gujarat.

27.12.3 Influx of Plant Debris and Volcanic Clasts

Yet another peculiarity of the Mesozoic stratigraphy of the Himalaya province is the occurrence of plant remains. The floral assemblages represent the Upper Gondwana plants that were growing prolifically in the central Indian terranes stretching from Rajmahal Hills in the east to the Aravali Range in the west. The sediments containing plant debris were carried to the shores of the NeoteThyan from rivers draining the land northwards and westwards (Fig. 16.14). Along with

plant debris, there was profuse influx of fragments and grains of volcanic rocks and ash into the sediments of Cretaceous deposits on the shelves and slopes of the passive continental margin. This is seen practically all along the coast from southern Tibet to Balochistan. The volcaniclastic debris occurring in the lower part of the succession was derived from basaltic parental rocks. Those that characterize the upper part of the succession came from dacitic–rhyolitic provenance belonging to the within-plate geotectonic setting. The inland volcanism responsible for profuse generation of clasts may be related to seafloor spreading that began in the Late Valanginian/Hauterivian to Albian interval during the Lower Cretaceous.

27.12.4 Volcanic Activity Along Periphery

The occurrence of clasts of alkali basalts in the siliciclastic sediments (turbidites) interbedded with radiolarian chert in Ladakh and southern Tibet implies that the volcanic activity started as early as Middle Jurassic to Upper Jurassic in some sectors. The volcanism became pronounced in the Middle and Upper Cretaceous, even as the rapidly subsiding Tethyan basin floor was subjected to extensional renting of the crust.

27.13 Docking of India with Asia

As India converged towards Asia, its leading edge dipped northwards. The floor of the NeoTethys Sea subsided progressively as India approached the active continental margin of Asia. By Early Cretaceous, the seafloor had sunk considerably to form a deep depression. Thick deposits of flysch accumulated all along the periphery of the passive continental margin of India, and in the depression in front of the active margin of Asia. Steepening of the shelf slope occasionally triggered submarine slides and generated debris flows and attendant turbidity currents (Fig. 16.14). The result was the emplacement of a wild flysch characterized by olistostrome of chaotic texture and structure. It appears that by the Late Cretaceous the two continents had come very close to one another and the dipping of the seafloor under the Asian plate had resulted in the formation of an elongate deep oceanic trench. In this deep depression was deposited material derived from the converging continents, predominantly from the Indian.

27.13.1 Evolution of Volcanic Island Arc

The northward moving and subducting oceanic crust was rent apart offshore of the continental margin of Asia, and lavas welled out to form volcanic islands in

the sea (Fig. 17.2). The arcuate chain of submarine volcanoes and seamounts extended more than 2500 km from Chitral in the west through Dras in Ladakh to Shigatse in southern Tibet. The volcanism commenced in the latest Jurassic to Early Cretaceous and culminated in the development of island arc complexes. The geochemistry of volcanic rocks indicates their affinity with the subduction-related magma derived from LREE-enriched mantle beneath the arc.

27.13.2 Amalgamation of Continents

The convergence of continents culminated in slamming of Asia against India (Fig. 17.1). The Kohistan Island touched the Karakoram terrane of Asia and was amalgamated with it some time between 102 ± 12 Ma and 85 Ma. The north-western edge of Asia first docked with the Kohistan Complex, which had already become a part of the Asian landmass. This happened at about 65 Ma. In the east, India touched the Cuofiang area in southern Tibet (of Asia) at about 68 Ma. However, the speed of northward-moving India at the rate 180–195 mm/yr suddenly slowed down to 45 mm/yr at 55 Ma, implying resistance the fast-moving Indian plate had encountered due to its collision with Asia. It is inferred that the closure of the zone of collision took place in the interval 55–50 Ma—the diachronous collision—occurring in two different periods—commencing in the west in the Later Ypresian time (50–48 Ma) and progressing through the Later Lutetian (48–40 Ma) in the east. In other words, it took 8–10 million years in the Early Eocene for the complete amalgamation of India with Asia. A land-bridge was formed presumably in the north-west where India first docked with Asia. The bridge permitted migration from Asia to India of such animals as even-toed animals such as deers, turtle, crocodiles and fish from Asia to India by the Maastrichtian time.

Following the suturing or joining together of continents, the island arc complex was intruded by granites of batholithic dimension, the *Kohistan Batholith* includes two plutons dated 54 ± 4 Ma and 40.6 Ma (Fig. 17.4). Likewise, the Ladakh island arc complex was intruded by a batholith of great dimension in the Late Cretaceous to Tertiary period.

27.13.3 Deformation and Metamorphism

The docking of continents was so strong and persistent that the entire assemblage of volcanic islands, sediments of the arc basins and deep sea were strongly folded and split into multiple stacks of mutually overlapping slices. These were then squeezed up and thrown out—obducted—onto the continental margin. Pressure as high as 9–11 kbar under temperature of 350–420 °C converted the ophiolites in many places into *blue schist*. Most scientists believe that the leading part of the Indian plate

plunged down and slid a long distance under the Asian plate. However, the development of domal upwarps all along the junction zone is indicative of the resistance encountered by the Indian plate sliding under Asia and resultantly forming domal upwarps. The upwarps are discernible all along the stretch from Nimalang in Ladakh, through Gurla Mandhata in the Kailas–Mansarovar region to Lhagoi–Kangri–Kangmar belt in north-eastern Nepal. The zone of amalgamation, made up of tectonized melange-bearing zone, is known as *Indus–Tsangpo Suture* (ITS).

27.13.4 Magmatic Arc North of Suture Zone

As the leading edge of the Indian plate went down beneath the Asian plate, there was a large-scale differential melting of the crustal rocks, giving rise to an anatectic granitic magma. Emplaced all along the southern margin of Asia as discordant bodies such as batholiths and stocks, the granite–granodiorite–tonalite plutons form a more than 2700-km-long magmatic arc (Fig. 17.14). It extends from Kohistan in the west, through Karakoram and Kailas to Gangdese in Tibet and then to the eastern part of the Lohit district in eastern Arunachal Pradesh. Granitic activity occurred in the period 110 Ma to nearly 42 Ma, the peak being in the 60–45 Ma interval.

27.14 Emergence and Making of Himalaya Orogen

27.14.1 Sagging of ITS Zone

Even as the northern edge of the Indian plate bulged up, the zone of welding of India and Asia sagged down (Fig. 18.1). This happened in the Middle Eocene time, 34–30 Ma ago. A 2000-km-long and 60- to 100-km-wide depression was formed along what is today occupied by the valleys of the Sindhu and Tsangpo rivers. In this basin were deposited a varied assemblages of sediments, constituting the *Indus Flysch* (Figs. 17.5, 17.8 and 17.9). The flysch passes upwards into a very thick succession of fluvial deposits—the *Kargil Molasse*. The Kargil covers a vast stretch of tract from Kargil in the west, through Kailas region north of Uttarakhand to Liuquu in southern Tibet. It seems that the sinking of the Indus–Tsangpo zone started in the Middle Eocene time and continued into the Oligocene epoch.

27.14.2 Breaking of Himalayan Crust

The revival of tectonic movements in the Early Miocene time accentuated the deformation of synclinorial Tethys Himalayan terrane and its basement,

the Himadri complex. Many of the tightened folds were split by faults along their axial planes and subsequently displaced or thrust southwards as much as 30–80 km (Fig. 18.3). The buckled up Himalayan crust broke up at 21 ± 2 Ma along what was to become the *Main Central Thrust*. The broken-up crustal block moved up and southwards along the gently (30–45°) inclined thrust all along its 2000-km stretch—from Kishtwar in the north-west to the Siang Valley in the east. Eventually emerged the *Great Himalaya* or *Himadri* terrane delimited at the base by the Main Central Thrust. Nearly at the same time when the Himalayan crust broke along the Main Central Thrust and the Himadri (Great Himalaya) pile advanced southwards onto the Lesser Himalayan terrane, the thick Tethyan sedimentary cover was detached from the hard unyielding crystalline basement, the Himadri Complex. The plane of detachment is described as *Trans-Himadri Detachment Fault* or *South Tibetan Detachment System* (Figs. 18.3, 18.4, 18.6 and 18.8). The fault zone is characterized by northeast-directed backfolds and back thrusts produced probably during gravitational collapse of the thrust stack.

27.14.3 Metamorphism and Anatectic Granites in Himadri

The Himadri (Great Himalaya) metamorphic rocks evolved at the depth of 30–35 km where the temperature was higher than 600 °C and the pressure more than 7–8 kbar. The Barrovian metamorphism was overprinted by lower pressure and/or high temperature metamorphism due to quick and quasiadiabatic uplift by transportation along the MCT ramp, resulting in inverted zonation of metamorphic rocks (Fig. 18.12). The inversion of metamorphism is only apparent and is related to repeated thrusting. The pressure and temperature had risen so high in the early Miocene time that some parts of the metamorphic rocks melted differentially or partially (anataxis), giving rise to molten material of granitic composition. The anatectic magmas were emplaced in the form of batholiths, stocks, laccoliths, sills, dykes and veins (Fig. 18.13). The highly mobile material also pervasively penetrated layer-after-layer the schists and gneisses in the upper part of the Himadri sequence, giving rise to migmatites throughout the length of the Great Himalayan terrane. Thus, the leucogranite plutonic bodies are commonly intimately associated with zones of migmatites of the same age. The anatectic granitic rocks formed in the period 24–22 Ma, the peak time being 21 ± 0.5 Ma.

27.14.4 Development of Lesser Himalayan Terrane

Repeated translation or thrusting of the Himadri rockpile threw the more than 7000-m-thick Lesser Himalayan sedimentary and metasedimentary successions into a series of folds (Figs. 18.4a and 18.15). Close to the MCT, the squeezing and tightening of folds resulted in southward overturning and toppling over of folds.

This was accompanied by their splitting by a multiplicity of faults along axial planes, giving rise to a duplex or schuppen zone of imbricating lithotectonic stacks. Increasing compression resulted in the uprooting of the entire folded pile under the MCT, and their 80- to 125-km displacement southwards in the form of thrust sheets or nappes. There are two principal lithologically and structurally distinctive nappes. The structurally lower epimetamorphic nappe is made up of low-grade metamorphics integrally associated with 1900 ± 100 Ma mylonitized porphyritic granite and porphyry. The structurally upper mesometamorphic nappe comprises medium-grade metamorphics intruded by 500 ± 25 Ma granite–granodiorite plutons. Known by different names, these two nappes extend all over the Lesser Himalaya subprovince from northern Pakistan to eastern Arunachal Pradesh.

27.14.5 Formation of Syntaxial Bends

The WNW–ENE oriented Himalaya mountain arc, with all its rock formations and structures including fold belts and thrust systems, abruptly bends southwards, making acute angles at its two extremities (Figs. 18.17 and 18.20). These spectacular features, resembling knee bends, are known as *syntaxial bends*. These were formed due to strong impact of the projecting promontories or pointed edges of the Indian shield. Simultaneously fold after fold developed around the promontories. Continued pushing resulted in these folds breaking along strike-slip faults (Fig. 18.19). The Nanga Parbat Massif in the north-west is a pop-up structure that provides a mechanism for accommodation of upwards extrusion along bounding shear zones. In the eastern Himalaya, the Siang Syntaxis was formed due to compressive movements on continental docking which led to northward movement of the Arunachal block and Myanmar landmass relative to the Tibet–Shan States–Malaysia block of the Asian plate.

The Himalaya province is cut by tear faults trending transverse to the general trend of the Himalaya, forming NNW–SSE and N/NNE–S/SSW oriented conjugate fault systems. Some of these faults, coinciding with the older thrusts, have been interpreted as oblique thrust ramps of Precambrian antiquity in which inhomogeneous strain at late-stage deformation resulted in the formation of extensional faults on hanging walls.

27.15 Himalayan Foreland Basin

27.15.1 Origin

Following crustal thickening in the Lesser Himalaya subprovince, particularly along its southern margin, a flexural depression developed immediately south of the emerging young Himalaya. The *Sirmaur Basin* was soon invaded by oceanic

water, giving rise to a foreland basin (Figs. 19.1 and 19.2). The development of the basin commenced in the Early Palaeocene. It stretched from the Ranikot–Laki belt in Sindh (Pakistan) to Meghalaya and beyond in the east. In the east, it was linked with the Bay of Bengal through the Bengal Basin, and in the west, the Himalayan Foreland Basin was connected with the Arabian Sea through western Rajasthan and Kachchh.

27.15.2 Beginning of Fluvial Sedimentation

One of the very momentous developments recorded in the foreland-basin succession is the drastic reversal of drainage in the Early Palaeogene time. All through the nearly 2000 million years long history of the Indian subcontinent, rivers draining the Peninsular India flowed in the northward and north-westward directions. Abruptly, there was a reversal of the pattern of palaeocurrents and sediment dispersal. The rivers started draining and denuding a highland—the Himalaya—that had just emerged. The rivers and stream started flowing southwards in the main Himalaya province and eastwards in the Pakistan sector.

Another development of great significance was the final withdrawal of the sea from the Himalaya province and beginning of fluvial-allivial sedimentation in the terrestrial setting towards the Late Eocene time (Fig. 19.4). The beginning of the fluvial sedimentation is dated at about 31 Ma. The whole of the Himalaya province had risen up as a highland and subjected to denudation. Acceleration of erosion resulted in the generation of enormous volumes of detritus, which the rivers and streams carried to the foreland basin.

27.15.3 Formation of Main Boundary Fault

As the Lesser Himalayan thrust sheets advanced southwards, they encountered resistance. Consequently, the Himalayan crust broke at about 11 Ma along the 2400-km length of the Himalaya province in a series of faults. These thrust faults are collectively known as the Main Boundary Thrust (Fig. 19.6). As the crust broke along the Main Boundary Thrust, it sagged immediately south of the line of breaking. An elongate depression overlapping onto the shield came into existence. It is known as the *Siwalik Basin*, a great repository of detritus brought down from the fast-rising youthful Himalaya mountain. The total thickness of the sediments accumulated amounts to about 7000 m.

Emptying their abundant load of sediments, the Himalayan rivers eventually converted the Siwalik Basin—like its predecessor the Sirmaur Basin—into a vast floodplain. Towards the close of the Pliocene and the beginning of the Pleistocene about 1.5–1.7 Ma ago, the entire Siwalik Subprovince, extending from Potwar in the west to the Dihing Valley in the east, was overwhelmed by sudden excessive

influx of gravelly detritus and avalanches of muddy debris (Fig. 19.8). The resultant deposits are represented by the 2800- to 1800-m-thick Boulder Conglomerate. While rivers were depositing detritus in their channels and flood plain in the Siwalik foreland-basin, volcanoes in Afghanistan and central Myanmar were emitting fume and ash. Wind carried the volcanic ash and dust and shed them on the Siwalik floodplains. The ashes have since altered to bentonitic clays.

The floodplains were clothed with thick rainforests, particularly in the Early Siwalik time. With abundance of food available from forests, and water being aplenty in the land of rivers, lakes and swamps, a rich and varied life grew and flourished dramatically. In the streams lived reptiles, including crocodiles and turtles, and the swamps were populated by rhinos and hippos. In the forests lived mammals like tigers, elephants, buffaloes, cows, deers, goats and tree-climbing primates. Attracted by the abundance of food, water and living places, herd after herd of quadrupeds came to this land of plenty from as far as northern Eurasia, Africa and North America (Fig. 19.9).

Much later towards the end of the Pleistocene at about 1.6 Ma, revival of tectonic movement on the Main Boundary Thrust and associated faults brought the Lesser Himalayan rocks riding over and trampling upon the Siwalik. The intensity of deformation was strongest close to the Main Boundary Thrust zone where the folds were tightened and split along axial planes and squeezed out as imbricated stacks. The southern boundary of the Siwalik is demarcated by a series of discontinuous reverse faults and imbrication structures in a 0.5- to 1-km-wide zone of brittle deformation of the *Himalayan Frontal Thrust*. It is the tectonic boundary of the Siwalik against the Indo-Gangetic Plains (Figs. 19.11 and 19.12).

27.16 Tertiary Marine Transgression of Peninsular Indian Coast

The beginning of the Tertiary era witnessed submergence of the entire margin of Peninsular India under water of a transgressive sea that also engulfed the foreland of the young Himalaya (Figs. 20.10, 20.11, 20.12, 20.13). As a matter of fact, the Himalayan Foreland Basin (Sirmaur Basin) extended southwards through the Bengal Basin in the east and the Makran Depression in the west. The sediments deposited in these extended pericratonic Tertiary basins form the continental shelves in the eastern and western seaboards of Peninsular India (Fig. 20.1). Rivers such as Ganga, Mahanadi, Krishna, Godavari, Palar and Kaveri have been building prograding deltas since the Late Mesozoic time and the present-day deltas conceal larger basins of the Tertiary sedimentation. The larger parts of these basins lie under water in the offshore zone. The offshore Tertiary basins grew in size and deepened due to growing volume and load of sediments. The subsidence was differential and controlled by faults of Precambrian antiquity, oriented NE–SW and ENE–WSW in the eastern margin and NNW–SSE and ESE–WNW

in the western margin. Sedimentation in offshore basins proceeded synchronous with the step-wise growth of the *down-to-basin* faults. The Tertiary basins of the continental margin, including the gulfs related to it, are of great importance as they host commercially productive petroleum fields.

As in the Himalayan Foreland Basin, the sedimentation in the pericratonic Tertiary basins of Peninsular India was dual-facies. The Palaeogene sedimentation in the marine environment gave way to accumulation of sediments in the deltaic and fluvial settings during the Neogene period when larger part of coastal land came under the sway of sea. The Palaeogene sediments are largely concealed under the younger sediments, both on land and in offshore belts. The Neogene formations occur as discontinuous patches on land along the Coromandal and Malabar coasts.

27.16.1 Inland Sabarmati–Cambay Basin

The N–S to NNW–SSE trending Sabarmati–Cambay Basin is bound along east and west by discontinuous *en echelon* step faults (Figs. 20.7 and 20.8). The subsidence of the Deccan terrane along these faults commenced in the Late Palaeocene and continued through the Tertiary period. The result was a large graben with a number of subsidiary depressions and ridges within the rift basin. This basin comprises one of the most hydrocarbon-productive sedimentary piles of the Indian subcontinent.

27.16.2 Bombay Offshore Basin

Located in the line of the Sabarmati–Cambay rift basin, the Bombay offshore Basin also exhibits NNW/NW–SSE/SE graben-and-horst structure (Fig. 20.9). One of the structures is known as the *Bombay High*, containing most productive oilfields of India. The commencement of rifting of the Bombay Offshore Basin was synchronous with the outpouring of the Deccan lavas in the Palaeocene time. An extensional deformation resulted in the formation of a series of step faults that grew with time as brisk sedimentation proceeded in the shelf zone.

27.17 Formation of Andaman Island Arc

The Andaman Island Arc is a 850-km-long chain of islands between the Bay of Bengal and the Andaman Sea. It constitutes the central part of the 5000-km-long Myanmar–Indonesia Mobile Belt related to an *active subduction zone* (Fig. 21.1).

The island arc comprises two nearly parallel arcuate belts. The western arc is represented by more than 300 islands of the Andaman, Nicobar and Mentawai groups. It is made up of Upper Cretaceous–Tertiary flysch, implanted with ophiolites at various structural levels (Fig. 12.4). It is the southern extension of the Patkai–Naga–Arakan Orogenic Belt of the India–Myanmar border and stretches south-eastwards into a festoon of islands and associated subduction zone offshore Sumatra. The eastern arc embodies seamounts and dormant and active volcanoes. It extends northwards through the central sedimentary basins of Myanmar characterized by Miocene-to-Quaternary volcanoes including Mount Pegu and Mount Popa and south-eastwards into the island of Sumatra. West of the Andaman Island Arc, the seafloor of the Bay of Bengal is subducting eastwards. And east of this arc lies the back-arc basin, the Andaman Sea, resulting from splitting apart of the ocean floor due to its spreading.

The Andaman ridge is bordered along the west by a sediment-filled oceanic trench—the extension of the *Java Trench*. The ridge is made up of a chain of islands consisting of a stack of imbricating slices, each made up of sedimentary and ophiolitic rocks (Fig. 21.4). Close to the Invisible Bank Fault along the eastern margin occurs a festoon of seamounts (Alcock and Sewell) and dormant (Narcondam) and active (Barren) volcanoes. On the back (eastern) side of this volcanic arc lies the ~4000-m-deep *Andaman Sea* (Figs. 21.4 and 21.8). The floor of this sea is characterized by a NNE–SSW trending rift valley cut by a series of N–S to NNW–SSE trending strike-slip faults. In this Andaman rift, new oceanic material has been forming since the Miocene time, resulting in the spreading of the seafloor. Its northerly extension is being filled vigorously with sediments brought by the Irrawaddy, Sittang and Salween rivers.

As a result of oblique subduction of the Indian Ocean plate under the split-up narrow Myanmar piece of the South-east Asian continental plate, the oceanic crust along with its sedimentary cover was scraped off and piled up as multiple thrust sheets or slices, forming an accretionary prism (Figs. 21.3, 21.4 and 21.5). This prism forms the western sedimentary arc of the Andaman–Nicobar–Mentawai islands chain. The subduction started in the Late Cretaceous, and since then has been going on intermittently. Following differential movements on the imbricating faults of the accretionary prism, small isolated basins in the prism were formed. These basins became sites of forearc sedimentation during the Tertiary period. Dextral movements along the Sagaing–Semenko fault (Fig. 21.1) systems of the Myanmar–Indonesia Mobile Belt manifested themselves in the opening up in the Lower Miocene time of the Andaman Sea behind the Andaman sedimentary arc. The opening of the sea was accompanied and followed by volcanic activity all along the belt immediately east of the chain of sedimentary islands. This belt is represented by the Narcondam Barren volcanic chain.

27.18 Origin and Development of Indo-Gangetic Plains

27.18.1 Formation of Depression

The Indo-Gangetic Plains evolved as a consequence of filling up of a foredeep basin in front of the rising Himalaya: Earlier, the Siwalik foredeep had come into existence due to flexing down of the Indian plate (Fig. 22.1). This foredeep expanded and deepened as sedimentation proceeded progressively until the very early Quaternary 1.5–1.7 million years ago, when it broke up into two unequal parts along the *Himalayan Frontal Thrust*. The northern 25–45 km wide part evolved to the rising Siwalik Ranges, and the southern 200–450 km wide part became the subsiding basin. This depression was filled up rapidly with sediments derived predominantly from the Himalaya and partly from the hills of the northern Peninsular India. Eventually, it was transformed into vast plains known as the *Indo-Gangetic Plains* (Figs. 22.2 and 22.14). The *Indo-Gangetic Basin* expanded and became progressively deeper as the sediments accumulated through the time. The result of combined processes of floor subsidence and voluminous sedimentation was the formation of one of the world's largest fluvial plains, now 30–100 m above the mean sea level. The thickness of sediments varies from a few tens of metres in the southern margin to as much 1500–2500 m in the northern margin in north-eastern Uttar Pradesh and adjoining Bihar—along the foot of the mountain ranges.

27.18.2 Sedimentation in Ganga Basin

The Indo-Gangetic sediment succession represents the continuation of the Siwalik sedimentation (Fig. 22.4 and 22.5). The sedimentation in the Ganga Basin began when the climate was humid and the rainfall copious. There were lakes, swamps and pools in the floodplains characterized by overbank sediments and lobes and fans built by rivers and streams. There was a short spell of arid climate when streams had little or no water and sediments to carry. Blowing wind piled up fine-grained sands of yellowish-brown colour into heaps 6–7 m in height. Around 8000 yr B.P., the climate became warm and wet. The rainfall was more than what it is at present. Naturally, there was vigorous fluvial activity, the rivers had wide channels and developed meandering loops, oxbow lakes and swamps. Increased influx of Himalayan-borne rivers made big sedimentary lobes and fans. There was fast deposition of sediments between 12,000 and 10,000 yr B.P. in the Bengal Basin (Figs. 22.9 and 22.10), which was then a part of the sea. By the Late Holocene, broad peatland and marshland had formed even as rivers deposited their loads vigorously in their channels. The present Sundarban Delta in the Bengal Basin has been growing for the last 7,000 years. The subaerial extension of the Sunderban Delta feeds the world's largest submarine fan—the *Bengal*

Fan—extending south more than 3,000 km into the Indian Ocean. The Sindhu Delta Complex comprises deltaic floodplain and tidal flats (Fig. 22.11). To the south-east of the Indus Delta is the Rann of Kachchh, a 350-km-long and 150-km-wide tidal flat.

27.19 Tectonic Resurgence and Geomorphic Developments in Quaternary Period

27.19.1 Western India

Tectonic resurgence of the Aravali Mobile Belt in the Late Tertiary and Quaternary times manifested itself in the uplift of the Aravali in the form of a horst mountain, and in slow intermittent rise of the land to the north-west and west of the mountain domain. There was reorganization of the drainage system, resulting in deviation, deflection (Fig. 23.1) and disruption, culminating in a few cases in the disappearance of rivers and development of a desert (Figs. 23.5 and 23.6). This tract of Indian land may be described as the *Thar Domain*, embracing western Rajasthan, adjoining Haryana, northern Gujarat, Kuchchh and Saurashtra. During the larger part of the Pleistocene time, the Thar domain witnessed widespread alluvial sedimentation, implying that the land was well-watered by mostly Himalayan-borne rivers even though the climate was predominantly semi-arid. In the Later Holocene, these rivers degenerated into a misfit stream characterized by marshes and lakes in its floodway. This phase ended with silting and dumping of finer sediments by dry winds, marking the onset of desertification. The Ghaghgar–Chautang system (the Saraswati–Drishadwati of the Vedic time) migrated north-westwards and westwards to occupy the present Ghaghgar–Hakra–Nara course (Fig. 23.3). Recent studies including the dating of fossil waters in the abandoned channels now deep underground corroborate the deduction that the Saraswati of the Vedic time flowed through the Ghaghgar course.

The fluvial sediments in the Gujarat Plain are buried under the thick blanket of aeolian deposits, occurring as poorly organized dunes of the time span 26,000–5000 yr BP. While aeolian accretion continued up to about 600 yr ago in the Thar desert, it ended around 5000 yr B.P. in the Sabarmati Basin and about 10,000 yr B.P., in the Mahi domain.

27.19.2 Central India

The Satpura Range is flanked by the Narmada Graben in the north and the Tapi Graben in the south (Fig. 23.12). The grabens continue to subside along their delimiting faults. The Narmada–Tapi domain is a belt of tectonic resurgence

where streams show deviations, have dissected deep channels, and their longitudinal profiles are marked by abrupt changes. In the middle reaches of the Narmada, the Late Pleistocene to Early Holocene deposits form three terraces (Fig. 23.13). The lower horizon is characterized by the presence of a variety of forms of mammals along with Palaeolithic stone artefacts. And at Hathnora was unearthed a partial skull (calvaria) of a hominid younger in age than the Indonesian and Chinese *Homo erectus* (Fig. 23.14).

27.19.3 Evolution of Western Ghat

The Konkan–Kanara–Malabar coastal belt is affected by very prominent NNW–SSE faults cut and locally displaced by ESE–WNW to E–W oriented shear zones (Fig. 23.15). A variety of features provide compelling evidence for ongoing reactivation of the faults. One of the consequences of continuing fault reactivation is the evolution of the spectacular >700 m high escarpment known as the *Western Ghat*, sharply defining the western flank of the 700–1800 m high Sahyadri Mountain Range.

In the Malabar Belt in Kerala, in the tract between Kollam and Kodungallur occur a depositional basin of Quaternary sediments and a 80-km-long Vembanad lagoon with its sediment accumulation linked with this basin. In the 125-km-long stretch of the east coast between Kanyakumari and Rameswaram, the strandline of the Coromandal Coast occurs not higher than 4 m above the mean sea level. The Quaternary movements resulted in the uplift of the Kaveri delta domain and resultant cessation of built-up of the delta. The Krishna and Godavari deltas evolved in four stages, the oldest strandline of marine environment dating back to 6500 yr B.P.

27.19.4 Plateaus of Southern Peninsular India

A laterite mantle of variable thickness occurs in a series of isolated plateaus along the Sahyadri Range. There are high-level covers comprising vermicular and massive forms of laterites with bauxites. The Nilgiri Massif in the high Sahyadri Ranges testifies to repeated spurts of uplift in the Quaternary period. The various peneplanation surfaces imply a cycle of erosion that affected the Sahyadri domain. The whole of Southern Indian Shield has been rising gradually. Cut by NNW–SSE, N–S and NNE–SSW and ESE–WNW to E–W oriented fractures and shear zones or faults, the Mysore Plateau is characterized by a dynamic landscape (Fig. 23.22). In the Bangalore region, the N–S and NNE–SSW trending faults demarcate the flanks of long linear hills and linear series of isolated hillocks characterized by high scarps and peneplaned laterite-capped tops. Most of these faults

are associated with stream and river deflections, palaeolakes and present-day stagnant bodies of water in the channels of rivers upstream of fault crossings. In the upland of Maharashtra rivers are incised 20–25 m deep, cutting through their own deposits into the basalt basement. Together with entrenched meanders, there are high waterfalls close to the sources of rivers, implying rejuvenation due to uplift of the terrane.

27.19.5 Faster Uplift of Himalayan Terranes

The Quaternary period represents morphogenic phase of evolution of the Himalaya. It was during this period that the Himalaya rose up to attain its present spectacular height and acquired its geomorphic form. There is an overwhelming evidence for acceleration of erosion in the temporal interval 0.8–0.9 Ma in Tibet, in the Himalaya and in the Indo-Gangetic Plains. The rapid rise resulted in the development of a very lofty mountain barrier characterized by formidable scarps, soaring peaks and pronounced incisions in river valleys. The northern belt of the Siwalik rose up recently at a rate much faster than the southern belt of the Lesser Himalayan terrane owing to subrecent–recent movements on active faults that dissect the Siwalik Terrane longitudinally. In many sectors, the middle belt of the Siwalik has a remarkably gentle topography characterized by aggradational flat expanses called *duns*. The *duns* represent wide synclinal valleys filled up thickly by gravel deposits during the Later Pleistocene to Early Holocene time.

27.19.6 Formation of Lakes

Movements on active faults entailing uplift or strike-slip displacement of the footwall caused damming or blockage of river and stream flows, resulting in the formation of lakes upstream of the fault crossings. Where the rivers and streams carried larger quantities of sediment load and the ponding or blockage lasted longer temporal period, the lakes were filled up and converted into flat stretches of sediments. These represent the palaeolakes, comprising represented by predominant clays and muds with lenses of gravels of fluvial and/or colluvial origin. The *Karewa palaeolake* in Kashmir (Fig. 24.1) and the *Kathmandu palaeolake* in Nepal (Fig. 24.3) are the examples. Significantly, the Karewa and the Kathmandu palaeolake sediments contain, at various levels, remains of large-size heavy vertebrate animals such as hippopotamus, rhino, elephant, horse and crocodile. The faunal assemblages point to existence during their time of marshland in a terrain that must have been gentle, possibly not a few hundred metres above the sea level.

27.19.7 Advent of Ice Age

The 0.8–0.9 Ma event of rapid uplift made the Himalaya even higher than it was earlier. Naturally, cooler conditions conducive to glaciation developed in the higher realm of the Himalaya. The glaciers spread far and wide in the Potwar, Kashmir, Ladakh and Tibet regions. There were four successive advances of the glaciers during the Pleistocene period. Following the period of glaciation, the south-west monsoon slackened and drier climate prevailed all over the Indian subcontinent including the mountain world. The glaciers had left behind large volumes of gravels and fine sediments in the Kashmir Valley. The dry, cold winds blew away the finer sediments and spread far and wide as loess. The Karewa lake deposit was covered by a 10- to 20-m-thick blanket of aeolian sediments.

27.19.8 Strain Build-up and Holocene Movements

The Indian plate is moving towards mainland Asia (Fig. 25.1) at the rate 58 $\pm$ 4 mm/yr. Along the eastern mountain range, the rate of oblique convergence of the Shillong Massif with respect to the Sundaland is 34 $\pm$ 6 mm/yr. A larger part of the Indian plate convergence is stored as elastic strain in the structural frameworks of the Himalaya, the Indo-Myanmarese Border Ranges and the Andaman Island Arc. The strain is particularly strong where the leading edge of the Indian plate impinges against the Asian plate and also where the crustal framework of its tail end is fractured. Periodic acceleration of continental convergence results in forward lurch of India and reactivation of long, deep ancient faults, particularly those that define the terrane boundaries, the horsts and the grabens (Fig. 25.2). This manifests itself in the occurrence of earthquakes (Figs. 25.3 and 25.15), with attendant geomorphic changes and drainage aberration including change of courses and ponding of rivers.

It is noticeable that all the major earthquakes were associated with one or the other of the *active faults* in the mobile belts, both in the Himalaya province and in the shield region of the Peninsular India.